

Volume 9 Issue 3

March 2018



ISSN 2156-5570(Online)

ISSN 2158-107X(Print)



Editorial Preface

From the Desk of Managing Editor...

It may be difficult to imagine that almost half a century ago we used computers far less sophisticated than current home desktop computers to put a man on the moon. In that 50 year span, the field of computer science has exploded.

Computer science has opened new avenues for thought and experimentation. What began as a way to simplify the calculation process has given birth to technology once only imagined by the human mind. The ability to communicate and share ideas even though collaborators are half a world away and exploration of not just the stars above but the internal workings of the human genome are some of the ways that this field has moved at an exponential pace.

At the International Journal of Advanced Computer Science and Applications it is our mission to provide an outlet for quality research. We want to promote universal access and opportunities for the international scientific community to share and disseminate scientific and technical information.

We believe in spreading knowledge of computer science and its applications to all classes of audiences. That is why we deliver up-to-date, authoritative coverage and offer open access of all our articles. Our archives have served as a place to provoke philosophical, theoretical, and empirical ideas from some of the finest minds in the field.

We utilize the talents and experience of editor and reviewers working at Universities and Institutions from around the world. We would like to express our gratitude to all authors, whose research results have been published in our journal, as well as our referees for their in-depth evaluations. Our high standards are maintained through a double blind review process.

We hope that this edition of IJACSA inspires and entices you to submit your own contributions in upcoming issues. Thank you for sharing wisdom.

Thank you for Sharing Wisdom!

Managing Editor
IJACSA
Volume 9 Issue 3 March 2018
ISSN 2156-5570 (Online)
ISSN 2158-107X (Print)
©2013 The Science and Information (SAI) Organization

Editorial Board

Editor-in-Chief

Dr. Kohei Arai - Saga University

Domains of Research: Technology Trends, Computer Vision, Decision Making, Information Retrieval, Networking, Simulation

Associate Editors

Chao-Tung Yang

Department of Computer Science, Tunghai University, Taiwan

Domain of Research: Software Engineering and Quality, High Performance Computing, Parallel and Distributed Computing, Parallel Computing

Elena SCUTELNICU

"Dunarea de Jos" University of Galati, Romania

Domain of Research: e-Learning, e-Learning Tools, Simulation

Krassen Stefanov

Professor at Sofia University St. Kliment Ohridski, Bulgaria

Domains of Research: e-Learning, Agents and Multi-agent Systems, Artificial Intelligence, Big Data, Cloud Computing, Data Retrieval and Data Mining, Distributed Systems, e-Learning Organisational Issues, e-Learning Tools, Educational Systems Design, Human Computer Interaction, Internet Security, Knowledge Engineering and Mining, Knowledge Representation, Ontology Engineering, Social Computing, Web-based Learning Communities, Wireless/ Mobile Applications

Maria-Angeles Grado-Caffaro

Scientific Consultant, Italy

Domain of Research: Electronics, Sensing and Sensor Networks

Mohd Helmy Abd Wahab

Universiti Tun Hussein Onn Malaysia

Domain of Research: Intelligent Systems, Data Mining, Databases

T. V. Prasad

Lingaya's University, India

Domain of Research: Intelligent Systems, Bioinformatics, Image Processing, Knowledge Representation, Natural Language Processing, Robotics

Reviewer Board Members

- **Aamir Shaikh**
- **Abbas Al-Ghaili**
Mendeley
- **Abbas Karimi**
Islamic Azad University Arak Branch
- **Abdelghni Lakehal**
Université Abdelmalek Essaadi Faculté
Polydisciplinaire de Larache Route de Rabat, Km 2 -
Larache BP. 745 - Larache 92004. Maroc.
- **Abdul Razak**
- **Abdul Karim ABED**
- **Abdur Rashid Khan**
Gomal University
- **Abeer Elkorany**
Faculty of computers and information, Cairo
- **ADEMOLA ADESINA**
University of the Western Cape
- **Aderemi A. Atayero**
Covenant University
- **Adi Maaita**
ISRA UNIVERSITY
- **Adnan Ahmad**
- **Adrian Branga**
Department of Mathematics and Informatics,
Lucian Blaga University of Sibiu
- **agana Becejski-Vujaklija**
University of Belgrade, Faculty of organizational
- **Ahmad Saifan**
yarmouk university
- **Ahmed Boutejdar**
- **Ahmed AL-Jumaily**
Ahlia University
- **Ahmed Nabih Zaki Rashed**
Menoufia University
- **Ajantha Herath**
Stockton University Galloway
- **Akbar Hossain**
- **Akram Belghith**
University Of California, San Diego
- **Albert S**
Kongu Engineering College
- **Alcinia Zita Sampaio**
Technical University of Lisbon
- **Alexane Bouënard**
Sensopia
- **ALI ALWAN**
International Islamic University Malaysia
- **Ali Ismail Awad**
Luleå University of Technology
- **Alicia Valdez**
- **Amin Shaqrah**
Taibah University
- **Amirrudin Kamsin**
- **Amitava Biswas**
Cisco Systems
- **Anand Nayyar**
KCL Institute of Management and Technology,
Jalandhar
- **Andi Wahyu Rahardjo Emanuel**
Maranatha Christian University
- **Anews Samraj**
Mahendra Engineering College
- **Anirban Sarkar**
National Institute of Technology, Durgapur
- **Anthony Isizoh**
Nnamdi Azikiwe University, Awka, Nigeria
- **Antonio Formisano**
University of Naples Federico II
- **Anuj Gupta**
IKG Punjab Technical University
- **Anuranjan misra**
Bhagwant Institute of Technology, Ghaziabad, India
- **Appasami Govindasamy**
- **Arash Habibi Lashkari**
University Technology Malaysia(UTM)
- **Aree Mohammed**
Directorate of IT/ University of Sulaimani
- **ARINDAM SARKAR**
University of Kalyani, DST INSPIRE Fellow
- **Aris Skander**
Constantine 1 University
- **Ashok Matani**
Government College of Engg, Amravati
- **Ashraf Owis**
Cairo University
- **Asoke Nath**

St. Xaviers College(Autonomous), 30 Park Street,
Kolkata-700 016

- **Athanasios Koutras**
- **Ayad Ismaeel**
Department of Information Systems Engineering-
Technical Engineering College-Erbil Polytechnic
University, Erbil-Kurdistan Region- IRAQ
- **Ayman Shehata**
Department of Mathematics, Faculty of Science,
Assiut University, Assiut 71516, Egypt.
- **Ayman EL-SAYED**
Computer Science and Eng. Dept., Faculty of
Electronic Engineering, Menofia University
- **Babatunde Opeoluwa Akinkunmi**
University of Ibadan
- **Bae Bossoufi**
University of Liege
- **BALAMURUGAN RAJAMANICKAM**
Anna university
- **Balasubramanie Palanisamy**
- **BASANT VERMA**
RAJEEV GANDHI MEMORIAL COLLEGE, HYDERABAD
- **Basil Hamed**
Islamic University of Gaza
- **Basil Hamed**
Islamic University of Gaza
- **Bhanu Prasad Pinnamaneni**
Rajalakshmi Engineering College; Matrix Vision
GmbH
- **Bharti Waman Gawali**
Department of Computer Science & information T
- **Bilian Song**
LinkedIn
- **Binod Kumar**
JSPM's Jayawant Technical Campus, Pune, India
- **Bogdan Belean**
- **Bohumil Brtnik**
University of Pardubice, Department of Electrical
Engineering
- **Bouchaib CHERRADI**
CRMEF
- **Brahim Raouyane**
FSAC
- **Branko Karan**
- **Bright Keswani**
Department of Computer Applications, Suresh Gyan
Vihar University, Jaipur (Rajasthan) INDIA
- **Brij Gupta**

University of New Brunswick

- **C Venkateswarlu Sonagiri**
JNTU
- **Chanashekhhar Meshram**
Chhattisgarh Swami Vivekananda Technical
University
- **Chao Wang**
- **Chao-Tung Yang**
Department of Computer Science, Tunghai
University
- **Charlie Obimbo**
University of Guelph
- **Chee Hon Lew**
- **Chien-Peng Ho**
Information and Communications Research
Laboratories, Industrial Technology Research
Institute of Taiwan
- **Chun-Kit (Ben) Ngan**
The Pennsylvania State University
- **Ciprian Dobre**
University Politehnica of Bucharest
- **Constantin POPESCU**
Department of Mathematics and Computer
Science, University of Oradea
- **Constantin Filote**
Stefan cel Mare University of Suceava
- **CORNELIA AURORA Gyorödi**
University of Oradea
- **Cosmina Ivan**
- **Cristina Turcu**
- **Dana PETCU**
West University of Timisoara
- **Daniel Albuquerque**
- **Dariusz Jakóbczak**
Technical University of Koszalin
- **Deepak Garg**
Thapar University
- **Devena Prasad**
- **DHAYA R**
- **Dheyaa Kadhim**
University of Baghdad
- **Djilali IDOUGH**
University A.. Mira of Bejaia
- **Dong-Han Ham**
Chonnam National University
- **Dr. Arvind Sharma**

- Aryan College of Technology, Rajasthan Technology University, Kota
- **Duck Hee Lee**
Medical Engineering R&D Center/Asan Institute for Life Sciences/Asan Medical Center
 - **Elena SCUTELNICU**
"Dunarea de Jos" University of Galati
 - **Elena Camossi**
Joint Research Centre
 - **Eui Lee**
Sangmyung University
 - **Evgeny Nikulchev**
Moscow Technological Institute
 - **Ezekiel OKIKE**
UNIVERSITY OF BOTSWANA, GABORONE
 - **Fahim Akhter**
King Saud University
 - **FANGYONG HOU**
School of IT, Deakin University
 - **Faris Al-Salem**
GCET
 - **Firkhan Ali Hamid Ali**
UTHM
 - **Fokrul Alom Mazarbhuiya**
King Khalid University
 - **Frank Ibikunle**
Botswana Int'l University of Science & Technology (BIUST), Botswana
 - **Fu-Chien Kao**
Da-Y eh University
 - **Gamil Abdel Azim**
Suez Canal University
 - **Ganesh Sahoo**
RMRIMS
 - **Gaurav Kumar**
Manav Bharti University, Solan Himachal Pradesh
 - **George Pecherle**
University of Oradea
 - **George Mastorakis**
Technological Educational Institute of Crete
 - **Georgios Galatas**
The University of Texas at Arlington
 - **Gerard Dumancas**
Oklahoma Baptist University
 - **Ghalem Belalem**
University of Oran 1, Ahmed Ben Bella
 - **gherabi noreddine**
 - **Giacomo Veneri**
University of Siena
 - **Giri Babu**
Indian Space Research Organisation
 - **Govindarajulu Salendra**
 - **Grebenisan Gavril**
University of Oradea
 - **Gufan Ahmad Ansari**
Qassim University
 - **Gunaseelan Devaraj**
Jazan University, Kingdom of Saudi Arabia
 - **GYÖRÖDI ROBERT STEFAN**
University of Oradea
 - **Hadj Tadjine**
IAV GmbH
 - **Haewon Byeon**
Nambu University
 - **Haiguang Chen**
ShangHai Normal University
 - **Hamid Alinejad-Rokny**
The University of New South Wales
 - **Hamid AL-Asadi**
Department of Computer Science, Faculty of Education for Pure Science, Basra University
 - **Hamid Mukhtar**
National University of Sciences and Technology
 - **Hany Hassan**
EPF
 - **Harco Leslie Henic SPITS WARNARS**
Bina Nusantara University
 - **Hariharan Shanmugasundaram**
Associate Professor, SRM
 - **Harish Garg**
Thapar University Patiala
 - **Hazem I. El Shekh Ahmed**
Pure mathematics
 - **Hemalatha SenthilMahesh**
 - **Hesham Ibrahim**
Faculty of Marine Resources, Al-Mergheb University
 - **Himanshu Aggarwal**
Department of Computer Engineering
 - **Hongda Mao**
Hossam Faris
 - **Huda K. AL-Jobori**
Ahlia University
 - **Imed JABRI**

- **iss EL OUADGHIRI**
- **Iwan Setyawan**
Satya Wacana Christian University
- **Jacek M. Czerniak**
Casimir the Great University in Bydgoszcz
- **Jai Singh W**
- **JAMAIAH HAJI YAHAYA**
NORTHERN UNIVERSITY OF MALAYSIA (UUM)
- **James Coleman**
Edge Hill University
- **Jatinderkumar Saini**
Narmada College of Computer Application, Bharuch
- **Javed Sheikh**
University of Lahore, Pakistan
- **Jayaram A**
Siddaganga Institute of Technology
- **Ji Zhu**
University of Illinois at Urbana Champaign
- **Jia Uddin Jia**
Assistant Professor
- **Jim Wang**
The State University of New York at Buffalo,
Buffalo, NY
- **John Sahlin**
George Washington University
- **JOHN MANOHAR**
VTU, Belgaum
- **JOSE PASTRANA**
University of Malaga
- **Jui-Pin Yang**
Shih Chien University
- **Jyoti Chaudhary**
high performance computing research lab
- **K V.L.N.Acharyulu**
Bapatla Engineering college
- **Ka-Chun Wong**
- **Kamatchi R**
- **Kamran Kowsari**
The George Washington University
- **KANNADHASAN SURIYAN**
- **Kashif Nisar**
Universiti Utara Malaysia
- **Kato Mivule**
- **Kayhan Zrar Ghafoor**
University Technology Malaysia
- **Kennedy Okafor**
Federal University of Technology, Owerri
- **Khalid Mahmood**
IEEE
- **Khalid Sattar Abdul**
Assistant Professor
- **Khin Wee Lai**
Biomedical Engineering Department, University
Malaya
- **Khurram Khurshid**
Institute of Space Technology
- **KIRAN SREE POKKULURI**
Professor, Sri Vishnu Engineering College for
Women
- **KITIMAPORN CHOOCHOTE**
Prince of Songkla University, Phuket Campus
- **Krasimir Yordzhev**
South-West University, Faculty of Mathematics and
Natural Sciences, Blagoevgrad, Bulgaria
- **Krassen Stefanov**
Professor at Sofia University St. Kliment Ohridski
- **Labib Gergis**
Misr Academy for Engineering and Technology
- **LATHA RAJAGOPAL**
- **Lazar Stošić**
College for professional studies educators
Aleksinac, Serbia
- **Leanos Maglaras**
De Montfort University
- **Leon Abdillah**
Bina Darma University
- **Lijian Sun**
Chinese Academy of Surveying and
- **Ljubomir Jerinic**
University of Novi Sad, Faculty of Sciences,
Department of Mathematics and Computer Science
- **Lokesh Sharma**
Indian Council of Medical Research
- **Long Chen**
Qualcomm Incorporated
- **M. Reza Mashinchi**
Research Fellow
- **M. Tariq Banday**
University of Kashmir
- **madjid khalilian**
- **majzoob omer**
- **Mallikarjuna Doodipala**
Department of Engineering Mathematics, GITAM
University, Hyderabad Campus, Telangana, INDIA

- **Manas deep**
Masters in Cyber Law & Information Security
- **Manju Kaushik**
- **Manoharan P.S.**
Associate Professor
- **Manoj Wadhwa**
Echelon Institute of Technology Faridabad
- **Manpreet Manna**
Director, All India Council for Technical Education,
Ministry of HRD, Govt. of India
- **Manuj Darbari**
BBD University
- **Marcellin Julius Nkenlifack**
University of Dschang
- **Maria-Angeles Grado-Caffaro**
Scientific Consultant
- **Marwan Alseid**
Applied Science Private University
- **Mazin Al-Hakeem**
LFU (Lebanese French University) - Erbil, IRAQ
- **Md Islam**
sikkim manipal university
- **Md. Bhuiyan**
King Faisal University
- **Md. Zia Ur Rahman**
Narasaraopeta Engg. College, Narasaraopeta
- **Mehdi Bahrami**
University of California, Merced
- **Messaouda AZZOUZI**
Ziane Achour University of Djelfa
- **Milena Bogdanovic**
University of Nis, Teacher Training Faculty in Vranje
- **Miriampally Venkata Raghavendra**
Adama Science & Technology University, Ethiopia
- **Mirjana Popovic**
School of Electrical Engineering, Belgrade University
- **Miroslav Baca**
University of Zagreb, Faculty of organization and
informatics / Center for biometrics
- **Moeiz Miraoui**
University of Gafsa
- **Mohamed Eldosoky**
- **Mohamed Ali Mahjoub**
Preparatory Institute of Engineer of Monastir
- **Mohamed Kaloup**
- **Mohamed El-Sayed**
Faculty of Science, Fayoum University, Egypt
- **Mohamed Najeh LAKHOUA**
ESTI, University of Carthage
- **Mohammad Ali Badamchizadeh**
University of Tabriz
- **Mohammad Jannati**
- **Mohammad Alomari**
Applied Science University
- **Mohammad Haghighat**
University of Miami
- **Mohammad Azzeh**
Applied Science university
- **Mohammed Akour**
Yarmouk University
- **Mohammed Sadgal**
Cadi Ayyad University
- **Mohammed Al-shabi**
Associate Professor
- **Mohammed Hussein**
- **Mohammed Kaiser**
Institute of Information Technology
- **Mohammed Ali Hussain**
Sri Sai Madhavi Institute of Science & Technology
- **Mohd Helmy Abd Wahab**
University Tun Hussein Onn Malaysia
- **Mokhtar Beldjehem**
University of Ottawa
- **Mona Elshinawy**
Howard University
- **Mostafa Ezziyani**
FSTT
- **Mouhammd sharari alkasassbeh**
- **Mourad Amad**
Laboratory LAMOS, Bejaia University
- **Mueen Uddin**
University Malaysia Pahang
- **MUNTASIR AL-ASFOOR**
University of Al-Qadisiyah
- **Murphy Choy**
- **Murthy Dasika**
Geethanjali College of Engineering & Technology
- **Mustapha OUJAOURA**
Faculty of Science and Technology Béni-Mellal
- **MUTHUKUMAR SUBRAMANYAM**
DGCT, ANNA UNIVERSITY
- **N.Ch. Iyengar**
VIT University
- **Nagy Darwish**

Department of Computer and Information Sciences,
Institute of Statistical Studies and Researches, Cairo
University

- **Najib Kofahi**
Yarmouk University
- **Nan Wang**
LinkedIn
- **Natarajan Subramanyam**
PES Institute of Technology
- **Natheer Gharaibeh**
College of Computer Science & Engineering at
Yanbu - Taibah University
- **Nazeeh Ghatasheh**
The University of Jordan
- **Nazeeruddin Mohammad**
Prince Mohammad Bin Fahd University
- **NEERAJ SHUKLA**
ITM UNiversity, Gurgaon, (Haryana) Inida
- **Neeraj Tiwari**
- **Nestor Velasco-Bermeo**
UPFIM, Mexican Society of Artificial Intelligence
- **Nidhi Arora**
M.C.A. Institute, Ganpat University
- **Nilanjan Dey**
- **Ning Cai**
Northwest University for Nationalities
- **Nithyanandam Subramanian**
Professor & Dean
- **Noura Aknin**
University Abdelamlek Essaadi
- **Obaida Al-Hazaimeh**
Al- Balqa' Applied University (BAU)
- **Oliviu Matei**
Technical University of Cluj-Napoca
- **Om Sangwan**
- **Omaima Al-Allaf**
Asesstant Professor
- **Osama Omer**
Aswan University
- **Ouchtati Salim**
- **Ousmane THIARE**
Associate Professor University Gaston Berger of
Saint-Louis SENEGAL
- **Paresh V Virparia**
Sardar Patel University
- **Peng Xia**
Microsoft

- **Ping Zhang**
IBM
- **Poonam Garg**
Institute of Management Technology, Ghaziabad
- **Prabhat K Mahanti**
UNIVERSITY OF NEW BRUNSWICK
- **PROF DURGA SHARMA (PHD)**
AMUIT, MOEFDRE & External Consultant (IT) &
Technology Tansfer Research under ILO & UNDP,
Academic Ambassador for Cloud Offering IBM-USA
- **Purwanto Purwanto**
Faculty of Computer Science, Dian Nuswantoro
University
- **Qifeng Qiao**
University of Virginia
- **Rachid Saadane**
EE departement EHTP
- **Radwan Tahboub**
Palestine Polytechnic University
- **raed Kanaan**
Amman Arab University
- **Raghuraj Singh**
Harcourt Butler Technological Institute
- **Rahul Malik**
- **raja boddu**
LENORA COLLEGE OF ENGINEERNG
- **Raja Ramachandran**
- **Rajesh Kumar**
National University of Singapore
- **Rakesh Dr.**
Madan Mohan Malviya University of Technology
- **Rakesh Balabantaray**
IIIT Bhubaneswar
- **Ramani Kannan**
Universiti Teknologi PETRONAS, Bandar Seri
Iskandar, 31750, Tronoh, Perak, Malaysia
- **Rashad Al-Jawfi**
Ibb university
- **Rashid Sheikh**
Shri Aurobindo Institute of Technology, Indore
- **Ravi Prakash**
University of Mumbai
- **RAVINA CHANGALA**
- **Ravisankar Hari**
CENTRAL TOBACCO RESEARCH INSTITUE
- **Rawya Rizk**
Port Said University

- **Reshmy Krishnan**
Muscat College affiliated to Stirling University.U
- **Ricardo Vardasca**
Faculty of Engineering of University of Porto
- **Ritaban Dutta**
ISSL, CSIRO, Tasmania, Australia
- **Rowayda Sadek**
- **Ruchika Malhotra**
Delhi Technological University
- **Rutvij Jhaveri**
Gujarat
- **SAADI Slami**
University of Djelfa
- **Sachin Kumar Agrawal**
University of Limerick
- **Sagarmay Deb**
Central Queensland University, Australia
- **Said Ghoniemy**
Taif University
- **Sandeep Reddivari**
University of North Florida
- **Sanskriti Patel**
Charotar University of Science & Technology,
Changa, Gujarat, India
- **Santosh Kumar**
Graphic Era University, Dehradun (UK)
- **Sasan Adibi**
Research In Motion (RIM)
- **Satyena Singh**
Professor
- **Sebastian Marius Rosu**
Special Telecommunications Service
- **Seema Shah**
Vidyalankar Institute of Technology Mumbai
- **Seifedine Kadry**
American University of the Middle East
- **Selem Charfi**
HD Technology
- **SENGOTTUVELAN P**
Anna University, Chennai
- **Senol Piskin**
Istanbul Technical University, Informatics Institute
- **Sérgio Ferreira**
School of Education and Psychology, Portuguese
Catholic University
- **Seyed Hamidreza Mohades Kasaei**
University of Isfahan
- **Shafiqul Abidin**
HMR Institute of Technology & Management
(Affiliated to GGS Indraprastha University), Hamidpur, Delhi -
110036
- **Shahanawaj Ahamad**
The University of Al-Kharj
- **Shaidah Jusoh**
- **Shaiful Bakri Ismail**
- **Shakir Khan**
Al-Imam Muhammad Ibn Saud Islamic University
- **Shawki Al-Dubae**
Assistant Professor
- **Sherif Hussein**
Mansoura University
- **Shriram Vasudevan**
Amrita University
- **Siddhartha Jonnalagadda**
Mayo Clinic
- **Sim-Hui Tee**
Multimedia University
- **Simon Ewedafe**
The University of the West Indies
- **Siniša Opic**
University of Zagreb, Faculty of Teacher Education
- **Sivakumar Poruran**
SKP ENGINEERING COLLEGE
- **Slim BEN SAOUD**
National Institute of Applied Sciences and
Technology
- **Sofien Mhatli**
- **sofyan Hayajneh**
- **Sohail Jabbar**
Bahria University
- **Sri Devi Ravana**
University of Malaya
- **Sudarson Jena**
GITAM University, Hyderabad
- **Suhail Sami Owais Owais**
- **Suhas J Manangi**
Microsoft
- **SUKUMAR SENTHILKUMAR**
Universiti Sains Malaysia
- **Süleyman Eken**
Kocaeli University
- **Sumazly Sulaiman**
Institute of Space Science (ANGKASA), Universiti
Kebangsaan Malaysia

- **Sumit Goyal**
National Dairy Research Institute
- **Supareerk Janjarasjitt**
Ubon Ratchathani University
- **Suresh Sankaranarayanan**
Institut Teknologi Brunei
- **Susarla Sastry**
JNTUK, Kakinada
- **Suseendran G**
Vels University, Chennai
- **Suxing Liu**
Arkansas State University
- **Syed Ali**
SMI University Karachi Pakistan
- **T C.Manjunath**
HKBK College of Engg
- **T V Narayana rao Rao**
SNIST
- **T. V. Prasad**
Lingaya's University
- **Taiwo Ayodele**
Infonetmedia/University of Portsmouth
- **Talal Bonny**
Department of Electrical and Computer Engineering, Sharjah University, UAE
- **Tamara Zhukabayeva**
- **Tarek Gharib**
Ain Shams University
- **thabet slimani**
College of Computer Science and Information Technology
- **Totok Biyanto**
Engineering Physics, ITS Surabaya
- **Touati Youcef**
Computer sce Lab LIASD - University of Paris 8
- **Tran Sang**
IT Faculty - Vinh University - Vietnam
- **Tsvetanka Georgieva-Trifonova**
University of Veliko Tarnovo
- **Uchechukwu Awada**
Dalian University of Technology
- **Udai Pratap Rao**
- **Urmila Shrawankar**
GHRCE, Nagpur, India
- **Vaka MOHAN**
TRR COLLEGE OF ENGINEERING
- **VENKATESH JAGANATHAN**
- **ANNA UNIVERSITY**
- **Vinayak Bairagi**
AISSMS Institute of Information Technology, Pune
- **Vishnu Mishra**
SVNIT, Surat
- **Vitus Lam**
The University of Hong Kong
- **VUDA SREENIVASARAO**
PROFESSOR AND DEAN, St.Mary's Integrated Campus, Hyderabad
- **Wali Mashwani**
Kohat University of Science & Technology (KUST)
- **Wei Wei**
Xi'an Univ. of Tech.
- **Wenbin Chen**
360Fly
- **Xi Zhang**
illinois Institute of Technology
- **Xiaojing Xiang**
AT&T Labs
- **Xiaolong Wang**
University of Delaware
- **Yanping Huang**
- **Yao-Chin Wang**
- **Yasser Albagory**
College of Computers and Information Technology, Taif University, Saudi Arabia
- **Yasser Alginahi**
- **Yi Fei Wang**
The University of British Columbia
- **Yihong Yuan**
University of California Santa Barbara
- **Yilun Shang**
Tongji University
- **Yu Qi**
Mesh Capital LLC
- **Zacchaeus Omogbadegun**
Covenant University
- **Zairi Rizman**
Universiti Teknologi MARA
- **Zarul Zaaba**
Universiti Sains Malaysia
- **Zenzo Ncube**
North West University
- **Zhao Zhang**
Deptment of EE, City University of Hong Kong
- **Zhihan Lv**

Chinese Academy of Science

- **Zhixin Chen**
ILX Lightwave Corporation
- **Ziyue Xu**
National Institutes of Health, Bethesda, MD

- **Zlatko Stacic**
University of Zagreb, Faculty of Organization and
Informatics Varazdin
- **Zuraini Ismail**
Universiti Teknologi Malaysia

CONTENTS

Paper 1: Bitter Melon Crop Yield Prediction using Machine Learning Algorithm

Authors: Marizel B. Villanueva, Ma. Louella M. Salenga

PAGE 1 – 6

Paper 2: Evaluating X-Ray based Medical Imaging Devices with Fuzzy Preference Ranking Organization Method for Enrichment Evaluations

Authors: Dilber Uzun Ozsahin, Berna Uzun, Musa Sani Musa, Ilker Ozsahin

PAGE 7 – 10

Paper 3: Challenges in Designing Ethical Rules for Infrastructures in Internet of Vehicles

Authors: Razi Iqbal

PAGE 11 – 15

Paper 4: Analysis of the Impact of Different Parameter Settings on Wireless Sensor Network Lifetime

Authors: Muhammad Usman Younus

PAGE 16 – 21

Paper 5: Day-Ahead Load Forecasting using Support Vector Regression Machines

Authors: Lemuel Clark P. Velasco, Daisy Lou L. Polestico, Dominique Michelle M. Abella, Genesis T. Alegata, Gabrielle C. Luna

PAGE 22 – 27

Paper 6: Online Estimation of Wind Turbine Tip Speed Ratio by Adaptive Neuro-Fuzzy Algorithm

Authors: Amer Bilal Asghar, Xiaodong Liu

PAGE 28 – 33

Paper 7: Techniques for Improving the Labelling Process of Sentiment Analysis in the Saudi Stock Market

Authors: Hamed AL-Rubaiee, Renxi Qiu, Khalid Alomar, Dayou Li

PAGE 34 – 43

Paper 8: Designing of Cell Coverage in Light Fidelity

Authors: Rabia Riaz, Sanam Shahla Rizvi, Farina Riaz, Sana Shokat, Naveed Akbar Mughal

PAGE 44 – 53

Paper 9: A Collective Neurodynamic Approach to Survivable Virtual Network Embedding

Authors: Ashraf A. Shahin

PAGE 54 – 63

Paper 10: Breast Cancer Classification in Histopathological Images using Convolutional Neural Network

Authors: Mohamad Mahmoud Al Rahhal

PAGE 64 – 68

Paper 11: A Portable Natural Language Interface to Arabic Ontologies

Authors: Aimad Hakkoum, Hamza Kharrazi, Said Raghay

PAGE 69 – 76

Paper 12: Online Incremental Rough Set Learning in Intelligent Traffic System

Authors: Amal Bentaher, Yasser Fouad, Khaled Mahar

PAGE 77 – 82

Paper 13: Permanent Relocation and Self-Route Recovery in Wireless Sensor and Actor Networks

Authors: Khalid Mahmood, Muhammad Amir Khan, Mahmood ul Hassan, Ansar Munir Shah, Muhammad Kashif

Saeed

PAGE 83 – 89

Paper 14: Optimization based Approach for Content Distribution in Hybrid Mobile Social Networks

Authors: Rizwan Akhtar, Imran Memon, Zuhaib Ashfaq Khan, Changda Wang

PAGE 90 – 94

Paper 15: Distributed Energy Efficient Node Relocation Algorithm (DEENR)

Authors: Mahmood ul Hassan, Muhammad Amir Khan, Shahzad Ali, Khalid Mahmood, Ansar Munir Shah

PAGE 95 – 100

Paper 16: Secure and Privacy Preserving Mail Servers using Modified Homomorphic Encryption (MHE) Scheme

Authors: Lija Mohan, Sudheep Elayidon M

PAGE 101 – 110

Paper 17: Strategic Framework and Maturity Index for Measuring Knowledge Management Practices in Government Organizations

Authors: Shilpa Vijaivargia, Hemant Kumar Garg

PAGE 111 – 114

Paper 18: Smart Card ID: An Evolving and Viable Technology

Authors: Praveen Kumar Singh, Neeraj Kumar, Bineet Kumar Gupta

PAGE 115 – 124

Paper 19: A Smart Under-Frequency Load Shedding Scheme based on Takagi-Sugeno Fuzzy Inference System and Flexible Load Priority

Authors: J. A. Laghari, Suhail Ahmed Almani, Jagdesh Kumar, Hazlie Mokhlis, Ab Halim Abu Bakar

PAGE 125 – 131

Paper 20: Fuzzy Gains-Scheduling of an Integral Sliding Mode Controller for a Quadrotor Unmanned Aerial Vehicle

Authors: Nour Ben Ammar, Soufiene Bouallègue, Joseph Haggège

PAGE 132 – 141

Paper 21: Interactive Hypermedia Programs and its Impact on the Achievement of University Students Academically Defaulting in Computer Sciences

Authors: Mohamed Desoky Rabeh

PAGE 142 – 147

Paper 22: Mobile Phone Operations using Human Eyes Only and its Applications

Authors: Kohei Arai

PAGE 148 – 154

Paper 23: Computerized Steganographic Technique using Fuzzy Logic

Authors: Abdulrahman Abdullah Alghamdi

PAGE 155 – 159

Paper 24: An Efficient Algorithm for Load Balancing in Multiprocessor Systems

Authors: Saleh A. Khawatreh

PAGE 160 – 164

Paper 25: Performance Evaluation of a Deployed 4G LTE Network

Authors: E.T. Tchao, J.D. Gadze, Jonathan Obeng Agyapong

PAGE 165 – 178

Paper 26: Automatic Detection Technique for Speech Recognition based on Neural Networks Inter-Disciplinary

Authors: Mohamad A. A. Al- Rababah, Abdusamad Al-Marghilani, Akram Aref Hamarshi

PAGE 179 – 184

Paper 27: Image based Arabic Sign Language Recognition System

Authors: Reema Alzohairi, Raghad Alghonaim, Waad Alshehri, Shahad Aloqeely, Munera Alzaidan, Ouiem Bchir

PAGE 185 – 194

Paper 28: The Adoption of Software Process Improvement in Saudi Arabian Small and Medium Size Software Organizations: An Exploratory Study

Authors: Mohammed Ateeq Alanezi

PAGE 195 – 201

Paper 29: Ant Colony Optimization for a Plan Guide Course Registration Sequence

Authors: Wael Waheed Al-Qassas, Mohammad Said El-Bashir, Rabah Al-Shboul, Anwar Ali Yahya

PAGE 202 – 206

Paper 30: Continuous Path Planning of Kinematically Redundant Manipulator using Particle Swarm Optimization

Authors: Affiani Machmudah, Setyamartana Parman, M.B. Baharom

PAGE 207 – 217

Paper 31: On the Sampling and the Performance Comparison of Controlled LTI Systems

Authors: Sirine FEKIH, Boutheina SFAIHI, Mohamed BENREJEB

PAGE 218 – 225

Paper 32: Arabic Text Categorization using Machine Learning Approaches

Authors: Riyadh Alshammari

PAGE 226 – 230

Paper 33: 2-D Object Recognition Approach using Wavelet Transform

Authors: Kamelsh Kumar, Riaz Ahmed Shaikh, Razaq Hussain Arain, Safdar Ali Shah, Hidayatullah Shaikh

PAGE 231 – 235

Paper 34: Evaluation for Feature Driven Development Paradigm in Context of Architecture Design Augmentation and Perspective Implications

Authors: Shahbaz Ahmed Khan Gahyyur, Abdul Razzaq, Syed Zeeshan Hasan, Salman Ahmed, Rafi Ullah

PAGE 236 – 247

Paper 35: A High Gain MIMO Antenna for Fixed Satellite and Radar Applications

Authors: Ahsan Altaf, Khalid Mahmood, Mehre Munir, Saad Hassan Kiani

PAGE 248 – 251

Paper 36: Circular Calibration of Depth Extraction in Stereo Configuration

Authors: Zulfiqar Ibrahim, Zulfiqar Ali Bangash, Muhammad Zeeshan

PAGE 252 – 262

Paper 37: An Automatic Arabic Essay Grading System based on Text Similarity Algorithms

Authors: Abdulaziz Shehab, Mahmoud Faroun, Magdi Rashad

PAGE 263 – 268

Paper 38: An Effective Automatic Image Annotation Model Via Attention Model and Data Equilibrium

Authors: Amir Vatani, Milad Taleby Ahvanooy, Mostafa Rahimi

PAGE 269 – 277

Paper 39: A Systematic Literature Review of Success Factors and Barriers of Agile Software Development

Authors: Shahbaz Ahmed Khan Ghayyur, Salman Ahmed, Mukhtar Ali, Adnan Naseem, Abdul Razzaq, Naveed Ahmed

PAGE 278 – 291

Paper 40: Standardization of Cloud Security using Mamdani Fuzzifier

Authors: Shan e Zahra, Muhammad Adnan Khan, Muhammad Nadeem Ali, Sabir Abbas

PAGE 292 – 297

Paper 41: Evolutionary Design of a Carbon Dioxide Emission Prediction Model using Genetic Programming

Authors: Abdel Karim Baareh

PAGE 298 – 303

Paper 42: Understanding the Factors Affecting the Adoption of Green Computing in the Gulf Universities

Authors: ARWA IBRAHIM AHMED

PAGE 304 – 311

Paper 43: The use of Harmonic Balance in Wave Concept Iterative Method for Nonlinear Radio Frequency Circuit Simulation

Authors: Hicham MEGNAFI, Nouredine BOUKLI-HACENE, Nathalie RAVUE, Henri BAUDRAND

PAGE 312 – 318

Paper 44: A Solution for the Uniform Integration of Field Devices in an Industrial Supervisory Control and Data Acquisition System

Authors: Simona-Anda TCACIUC(GHERASIM)

PAGE 319 – 323

Paper 45: An Efficient Mechanism Protocol for Wireless Sensor Networks by using Grids

Authors: Emad Ibbini, Kweh Yeah Lun, Mohamed Othman, Zurina Mohd Hanapi

PAGE 324 – 330

Paper 46: Double Authentication Model using Smartphones to Enhance Student on-Campus Network Access

Authors: Zakaria Saleh, Ahmed Mashhour

PAGE 331 – 336

Paper 47: A User-Based Trust Model for Cloud Computing Environment

Authors: Othman Saeed, Riaz Ahmed Shaikh

PAGE 337 – 346

Paper 48: Synthetic Loads Analysis of Directed Acyclic Graphs for Scheduling Tasks

Authors: Apolinar Velarde Martinez

PAGE 347 – 354

Paper 49: A Comprehensive IoT Attacks Survey based on a Building-blocked Reference Model

Authors: Hezam Akram Abdul-Ghani, Dimitri Konstantas, Mohammed Mahyoub

PAGE 355 – 373

Paper 50: Enhanced Detection and Elimination Mechanism from Cooperative Black Hole Threats in MANETs

Authors: Samiullah Khan, Faqir Usman, Matiullah, Fahim Khan Khalil

PAGE 374 – 384

Paper 51: QTID: Quran Text Image Dataset

Authors: Mahmoud Badry, Hesham Hassan, Hanaa Bayomi, Hussien Oakasha

PAGE 385 – 391

Paper 52: Analysis of Biometric Technology Adaption and Acceptance in Canada

Authors: Eesa Al Solami

PAGE 392 – 396

Paper 53: Enhancing Quality of Lossy Compressed Images using Minimum Decreasing Technique

Authors: Ahmed L. Alshami, Mohammed Otair

PAGE 397 – 404

Paper 54: The Impact of Quantum Computing on Present Cryptography

Authors: Vasileios Mavroeidis, Kamer Vishi, Mateusz D. Zych, Audun Jøsang

PAGE 405 – 414

Paper 55: Media Content Access: Image-based Filtering

Authors: Rehan Ullah Khan, Ali Alkhalifah

PAGE 415 – 419

Paper 56: Half Mode Substrate Integrated Waveguide Cavity based RFID Chipless Tag

Authors: Soumaya Sakouhi, Hedi Ragad, Mohamed Latrach, Ali Gharsallah

PAGE 420 – 425

Bitter Melon Crop Yield Prediction using Machine Learning Algorithm

Marizel B. Villanueva

College of Informatics and Computing Sciences
Batangas State University
Batangas, Philippines

Ma. Louella M. Salenga

College of Information and Communication Technology
Holy Angel University
Pampanga, Philippines

Abstract—This research paper aimed to determine the crop bearing capability of bitter melon or bitter gourd more commonly called “Ampalaya” in the Filipino language. Images of bitter melon leaves were gathered from Ampalaya farms and these were used as main data of the research. The leaves were classified as good and bad through their description. The research used Machine Learning Algorithm through Convolutional Neural Network. Training of data was through the capabilities of Keras, Tensor Flow and Python worked together. In conclusion, increasing number of images could enable a machine to learn the difference between a good and a bad Ampalaya plant when presented an image for prediction.

Keywords—Agriculture; Artificial Intelligence; Keras; machine learning algorithm; machine learning; neural network; convolutional neural network; prediction; Python; tensor flow

I. INTRODUCTION

Machines have been very useful to humans from time immemorial. It has been proven that in the pursuit of man to make life easier he has found means to create new things which has helped him achieved progress. Machines vary from each other upon their inception. Their use to man is determined by the need that arises. In this paper, the authors will be able to explain its use specifically the computer in determining crop bearing capabilities of bitter melon or bitter gourd. The researchers will utilize the capabilities of computers for machine learning. Since machines are mostly used for mechanical work and to effectively use them, these are data that need to be trained, to give artificial intelligence.

Artificial Intelligence the ability of a digital computer or robot to perform tasks usually associated with human intelligence. It is frequently applied to the development of systems equipped with the intellectual processes and characteristics of humans, such as the ability to reason out, discover meaning, and generalize, or learn from experience [1]. The application of this in agriculture would be helpful a lot of researchers in this area making it easier to determine decisions for crop production. The researchers thought of creating this project since the Philippines is an agricultural country, with a land area of 30 million hectares, where 47 percent of it is agricultural land. Growing crops is one of the major bread and butter of the rural areas focusing on the development of agricultural studies to help crop management as a step to rural livelihood development [2].

“Ampalaya” the common name as it is called in the Philippines is better known as bitter melon. Production of bitter melon is profitable when grown in small or large scale either in lowland or upland rice-based areas [3]. Essentially, growing bitter melon does not need to have a big area of land, which makes it more attractive to Filipinos who do not have a large lot for growing crops. Aside from this, according to the Philippine Herbal Medicine Organization, Bitter Melon has been endorsed by Department of Health through its Traditional Health Program. It is most known as a treatment of diabetes (diabetes mellitus), for the non-insulin dependent patients [4].

Excerpts of reference researches below show how the sciences of Machine Learning, specifically Neural Networks have been utilized in the field of Agriculture.

A. Rice Blast Prediction based on Gray Ant Colony and RBF Neural Network Combination Model

This agricultural study made was in China was Rice Blast Prediction (RBF) where gray ant colony RBF learning algorithm was used. The RBF is movable and can determine its position by self-organization learning. Self-organizing learning part allocates the network resource in a sense; the purpose is to enable the RBF center to locate in the important region of the input space. The conclusion, the prediction model during 2002-2011 years, has accuracy of up to 96.77 per cent, compared with two the other single prediction models, this scheme has better feasibility and can be applied in rice blast prediction [5].

B. Statistics and Neural Networks for Approaching Nonlinear Relations between Wheat Plantation and Production in Queensland of Australia

This research dealt with treating the historical wheat data in Queensland over 130 years as non-temporal collection of mappings between wheat plantation area and production. Correlation analysis and neural network techniques to reveal whether significant nonlinear relations exist between the two factors were used. The simulation of the Neural Network process involved two phases: 1) training the network with known datasets; and 2) testing the trained network for model generalization. If the testing is conducted using some data selected from the training datasets, it is called the in-sample testing. If different known datasets are used for testing, it is then called the out-sample testing. The study made use of the Levenberg-Marquardt algorithm, chosen to train the selected Multilayer Perceptron (MLP) because this algorithm has been

reported to be the fastest method for training moderate-sized feedforward neural networks. Their MLP models are built using the NN tools in MATLAB. As concluded, their analysis demonstrated that a power correlation, a third-order polynomial correlation, and a three-layer multilayer perceptron model are all of significance, but it is the multilayer perceptron model that can produce accurate prediction [6].

II. METHOD

Focused on the objective of being able to predict crop yield of bitter melon using images, there are two fields of Artificial Intelligence that could be used for this purpose.

Traditionally, when images are a focal point to achieve a goal, Computer Vision is an obvious choice. To define, Computer Vision is a field of Artificial Intelligence and Computer Science that aims to give a computer the similar, if not better capability of humans to use their eyes and their brains to see and visually sense the world around them [7].

Computer vision algorithms their general functions extracts feature vectors from images and utilize these feature vectors to classify images. To be able to make a machine predict, and aside from classifying and grouping together images to be able to identify them, it must learn what they are when the image is presented to it. Based on the Fields of Artificial Intelligence shown in the figure below, the field of machine learning is not directly connected to vision, though they can work together to make a more intelligent machine, wherein machine learning is the focus [8].

Deep Learning is a field of Artificial Intelligence that makes use of Deep Neural Networks It is a subfield of Machine Learning concerned with algorithms inspired by the structure and function of the brain called artificial neural networks [9]. Then again, what is a Neural Network? Why is it needed in this research?

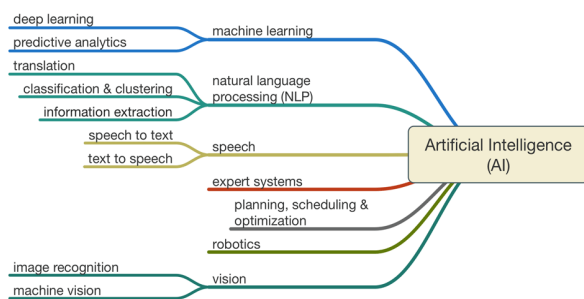


Fig. 1. Fields of artificial intelligence [10].

As seen in Fig. 1, in a white paper by Mills in 2016, all algorithms explained before in this section fall under the classification of Artificial Intelligence but to make a model and the main algorithm must be identified. This is where the Artificial Neural Network has been chosen, that describes the function [10], [11].

A Neural Network, or ‘artificial neural network’ known as ANN is a computing system made up of several simple, highly interconnected processing elements, which process information with dynamic state response to external in-puts. The research aimed to teach the machine to recognize a number of images

and to understand what type of plant they will be, good or bad – fruit bearing or not. These images when trained will create the so- called neurons. This process can increase the accuracy of predicting image samples being fed to a computer [12].

According to the research of Andy Lee from Swarthmore College, he found out that Deep Neural Networks had greater accuracy in identification of images. His study compared Traditional Computer Vision Algorithms with that of Convolutional Neural Networks, made a parallel implementation of both and concluded that with the investment in time and training, Convolutional Neural Networks were more accurate and performed better when applied whereas Traditional Computer Vision worked better in crude on-the-fly mobile robotic applications [13]. Based on another research from University of Toronto, the study used Convolutionary Neural Network to train data which is numerous in size. It enabled a network to increase its layers, learning more, increasing in accuracy and decreasing in error [14].

To accurately describe how a Neural Network has a better efficiency rating, the computational process is described here as a process of finding the best set of weights for the neural network which is referred to as training or learning. The approach used by most software to estimate the weights is backpropagation. Each time the network cycles through the training data, it produces a predicted value for the target variable, which is compared to the actual target value, and an error is computed for each observation. The errors are fed back through the network and new weights are computed to reduce the overall error. Despite the neural network terminology, the training process is actually a statistical optimization procedure. Typically, the procedure minimizes the sum of the squared residuals. Fig. 2 shows the interval activity of the neuron can be computed using the formula [15].

$$v_k = \sum_{j=1}^p w_{kj} x_j$$

Fig. 2. Internal neuron activity formula [15].

An activation function is then applied to the resulting value of v_k to produce the output value y_k . In this study, the activation function used is the sigmoid function. An example of the sigmoid function is using the hyperbolic tangent function is shown in Fig. 3.

$$\varphi(v) = \tanh\left(\frac{v}{2}\right) = \frac{1 - \exp(-v)}{1 + \exp(-v)}$$

Fig. 3. Sample hyperbolic tangent function [15].

This sigmoid function can range between 0 and 1, but it is also sometimes useful to use the -1 to 1 range.

For an artificial neuron, the weight is a number, and represents the synapse. A negative weight reflects an inhibitory connection, while positive values designate excitatory connections. The following components of the model represent the actual activity of the neuron cell. All inputs are summed altogether and modified by the weights. This activity is referred as a linear combination. Finally, an activation function controls

the amplitude of the output. For example, an acceptable range of output is usually between 0 and 1, or it could be -1 and 1 [15].

Mathematically, this method is described in Fig. 4 below.

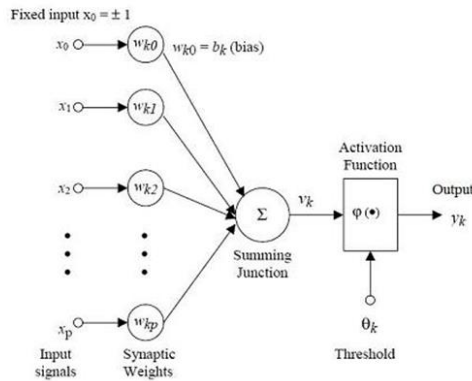


Fig. 4. Artificial neural network [15].

Since the input images are to return only two values for output, which is a good or bad Ampalaya plant, the process of the mathematical solution discussed earlier helps in the determination that the activation function will be effective in making a machine decide between an acceptable range of output which may be between 0 and 1, representing good and bad.

Having established the background of research and understanding the method that will be used, the researchers finalized their procedure to use Convolutionary Neural Networks for Deep Learning to train images of bitter melon or Ampalaya leaves from local farms within the Philippines.

III. DATA ACQUISITION

The need to identify which type of bitter melon plant the research should focus on led to the use of judgmental sampling technique to narrow down the choices of samples that will be gathered.

According to the Production Guide on Ampalaya and by the EntrePinoys and the compilation paper written by Kishore Hemlani (2012), there are the different varieties of the Bitter Melon or Bitter Gourd; these are shown in Table I [16], [17].

TABLE I. AMPALAYA VARIETY TABLE

Variety	Maturity (days)
Sta. Rita	70-75
Makiling	65-70
Sta. Isabel	70-75
Jade Star (A)	70-75
Mayon	65-70
Million Green	65-75
Galaxy (Galactica)	70-75

Among the varieties identified in Table I, the study concentrated on the bitter melon called Galaxy or locally known as “Galactica”, according to the Gazette magazine, this type was one of the most high-yielding varieties until recent studies [17]. With the restriction in accessibility, this was also chosen due to the demographic component whereby sampling needed to be done. The researchers have more accessibility to the plantation areas where this variety was being planted, to be specific, Region IV– A, Batangas City.

A. Data Acquisition Process

1) Interview with the Local Ampalaya farmer

In gathering data for the research, interviews were made with Local Ampalaya farmers in Batangas City. The respondents were Felix Morcilla and Virgilio Villanueva. Mr. Felix Morcilla has been farming bitter melon for 15 years while Mr. Virgilio Villanueva has been farming for 5 years. It was asked from these experts on the field of Ampalaya farming how their crops were determined to have good crops. Both noted that leaves alone could already identify the ability of an Ampalaya plant to bear good or bad crops.

2) Sample Collection Procedure

Since the main object of the research deals with the images of the bitter melon plant, the authors went Ampalaya Farm Lands in Batangas City, Philippines to gather these samples from the actual bitter melon plants. The authors, together with the Farm Land owners went around analyzing the plants. Each vine of the bitter melon would be analyzed for its fruit bearing capacity, and a string of leaves of this plant was taken, and there were only one to two samples per string or vine. This is to ensure the spread and variety of the samples. In the analysis of the plants, only the leaves were the focus. Soil type, irrigation, season of planting, age of the plant, temperature and the use of fertilizer was not covered in the research.

3) Sample Image Capture Procedure

After each plant was identified as fruit bearing or not, from the string of leaves taken, one leaf is placed on top of a white piece of paper then taken a picture of. Each leaf was placed in at least three angles to make sure that the leaf can be identified properly.

It might be a wonder why use Ampalaya leaves? Why not the full vine? The full vine is made up of a string of leaves, and that alone is enough to say that they all belong to the same plant. To identify the fruit bearing capacity using a vine is too big a scope, its analysis of this will also takes time, since the machine will have to deal with multiple leaves and the vine itself just to say, if it will bear fruit or not.

According to the guidelines in growing this plant, most Agricultural authors of the government pamphlets [18], [19] mentioned the analysis of its leaves as a determination of the plant’s health and ability to bear fruit. Together with the interview with the Ampalaya farm owners strengthened the claim that leaves of Ampalaya alone could determine the ability of the plant to bear fruit or not bear fruit at all. Essentially, the colors and description of the Ampalaya leaves, can be classified into the following Table II:

TABLE. II. AMPALAYA LEAF DESCRIPTION [19], [20]

Leaf Description	Fruit Equivalent
Small Dark Green	Bad Class, No Fruits
Normal or DeformedDark Green	Bad Class, No Fruits
Normal Sized Green	Good Class, Good Fruits
Normal Sized Light Green	Good Class, Good Fruits
Irregular-sized Yellow Green	Bad Class, Small or Diseased Fruits
Deformed Brown	Bad Class, Small or Diseased Fruits

Throughout the multiple days of image gathering, there were a total of 293 leaves taken account for. A total of 131 leaves classified as Bad and 162 classified as Good. These images were used to test the model for determining an Ampalaya leaf whether the actual vine will give a good or bad fruit.

The following images show examples of good and bad Ampalaya leaves:



Fig. 5. Good Ampalaya Leaf.



Fig. 6. Bad Ampalaya Leaf.

Fig. 5 and 6 were actual images that were taken by the researchers. These are only two of the 293 images trained to be recognized by the Convolutionary Neural Network.

IV. RESULTS AND DISCUSSION

The research used Experimental Method in doing the research. Multiple samples were tested, trained and processed to be able to meet the objectives. To test the samples of images, the Machine Learning Algorithm used in creating the model was Neural Networks through the media discussed in the subsections below. The aim is to prepare the machine for Sequential, Convolutional Neural Networks.

A. Testing Resources

1) MATLAB

It is a high-performance language for technical computing. It integrates computation, visualization, and programming in an easy-to-use environment where problems and solutions are expressed in familiar mathematical notation. Typical uses include: Data analysis, exploration, and visualization [20].

Initial Testing of the Data was tested in MATLAB. Since the actual machine requirement for MATLAB cannot be supported by the researcher's machines, it was not used as the implementing model for the project. The model created here was used as comparison of the accuracy that will be generated using Tensor Flow and Keras.

After running the model on a single GPU processing machine, the following are the results were attained:

TABLE. III. TRAINING RESULTS

Epoch	Iteration	Time Elapsed	Loss	Accuracy	Rate
1	1	0.62	0.9297	56.25	0.001
17	50	74.24	0.0003	100	0.001
34	100	151.11	0.0023	100	0.001
50	150	225.24	0.0002	100	0.001
67	200	298.99	0.0001	100	0.001
84	250	372.68	0.0001	100	0.001
100	300	447.02	0.0000	100	0.001

Table III yielded a 56.25 per cent on the first run and 100 on the second run of the model. This was based on the 293 leaves taken account for. With A total of 131 leaves classified at Bad and 162 classified as Good.

2) TensorFlow and Keras

Tensor Flow is an open-source software library for machine learning across a range of tasks and developed by Google to meet their needs for systems capable of building and training neural networks to detect and decipher patterns and correlations, analogous to the learning and reasoning which humans were used. It is currently used for both research and production at Google, while Keras is a high-level Python neural networks library that runs on top of either TensorFlow or Theano [21].

These were used by the researchers for the identification of single item input to test if the image is a good or bad Ampalaya. Training of the data was separated into 60-40 sets. 60% of the images that were used to train the machine's neural network and 40% was used to test it. The authors used supervised training to make sure that images are classified and identified with higher accuracy.

Each image was treated with the following algorithm for image uniformity, so when new data is presented even if taken from different devices, they can still be learned since they must be pre-processed before training.

```
if K.image_data_format() == 'channels_first':  
    input_shape = (3, img_width, img_height)  
else:  
    input_shape = (img_width, img_height, 3)
```

In detail, the algorithm above means:

data_format: A string, one of channels_last (default) or channels_first. The ordering of the dimensions in the inputs. channels_last corresponds to inputs with shape (batch, height, width, channels) while channels_first corresponds to inputs with shape (batch, channels, height, width).

In Keras, the image in Fig. 7 describes how the 2D convolutional layers were created.

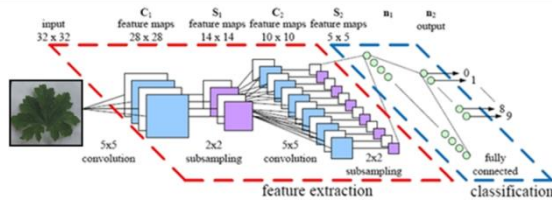


Fig. 7. Convolutional 2d Process [22].

In a research by Y LeCun, et al, it indicated that a network can be fed with the pixels in raw images. These images create patterns, whereby disregarding the image itself but concentrate local nearby pixels, forming layers upon layers of highly correlated ones [22].

In Convolutional Network Architectures, layer patterns are created. In the architecture, stacks of layers are called CONV-RELU, which are followed with POOL layers and repeats this pattern until the image has been merged spatially to a small size. At some point, it is common to transition to fully-connected layers. The last fully-connected layer holds the output, such as the class scores. In other words, the most common ConvNet architecture follows the pattern:

INPUT -> [[CONV ->RELU]*N -> POOL?]*M -> [FC -> RELU]*K -> FC

where the * indicates repetition, and the POOL? indicates an optional pooling layer. Moreover, N >= 0 (and usually N <= 3), M >= 0, K >= 0 (and usually K < 3). For example, here are some common ConvNet architectures you may see that follow this pattern:

- INPUT -> FC, implements a linear classifier. Here N=M=K = 0.
- INPUT -> CONV -> RELU -> FC
- INPUT -> [CONV -> RELU ->POOL]*2 -> FC -> RELU -> FC. Here we see that there is a single CONV layer between every POOL layer.
- INPUT -> [CONV -> RELU -> CONV -> RELU ->POOL]*3 -> [FC -> RELU]*2 -> FC. Here we see two CONV layers stacked before every POOL layer. This is generally a good idea for larger and deeper networks, because multiple stacked CONV layers can develop more complex features of the input volume before the destructive pooling operation [23].

The algorithm that shows how this is done in Python code is shown in Fig. 8, which is the actual code used by the researchers in the study.

```

from keras.models import Sequential
from keras.layers import Conv2D, MaxPooling2D
from keras.layers import Activation, Dropout, Flatten, Dense

model = Sequential()
model.add(Conv2D(32, (3, 3), input_shape=(3, 150, 150)))
model.add(Activation('relu'))
model.add(MaxPooling2D(pool_size=(2, 2)))

model.add(Conv2D(32, (3, 3)))
model.add(Activation('relu'))
model.add(MaxPooling2D(pool_size=(2, 2)))

model.add(Conv2D(64, (3, 3)))
model.add(Activation('relu'))
model.add(MaxPooling2D(pool_size=(2, 2)))

# the model so far outputs 3D feature maps (height, width, features)
    
```

Fig. 8. Conv2d Python code.

To train the data, the actual code used by the researchers is shown in Fig. 9.

```

batch_size = 16

# this is the augmentation configuration we will use for training
train_datagen = ImageDataGenerator(
    rescale=1./255,
    shear_range=0.2,
    zoom_range=0.2,
    horizontal_flip=True)

# this is the augmentation configuration we will use for testing:
# only rescaling
test_datagen = ImageDataGenerator(rescale=1./255)

# this is a generator that will read pictures found in
# subfolders of 'data/train', and indefinitely generate
# batches of augmented image data
train_generator = train_datagen.flow_from_directory(
    'data/train', # this is the target directory
    target_size=(150, 150), # all images will be resized to 150x150
    batch_size=batch_size,
    class_mode='binary') # since we use binary_crossentropy loss, we need binary labels

# this is a similar generator, for validation data
validation_generator = test_datagen.flow_from_directory(
    'data/validation',
    target_size=(150, 150),
    batch_size=batch_size,
    class_mode='binary')
    
```

Fig. 9. Model training Python code.

After identifying the code to treat the data, training was made, the images shown in Fig. 10 to 12 below are the actual outputs of testing. They were single input images from the Python Shell run time window.

Fig. 10. Model creation in Python using 125 epochs.

```

Using TensorFlow backend.
1/1 [=====] - 0s
[[1]]
Good
    
```

Fig. 11. Good Ampalaya predicted output.

Evaluating X-Ray based Medical Imaging Devices with Fuzzy Preference Ranking Organization Method for Enrichment Evaluations

Dilber Uzun Ozsahin¹

Department of Biomedical Engineering, Near East University
Nicosia / TRNC Mersin 10 – Turkey, Gordon Center for Medical Imaging
Massachusetts General Hospital & Harvard Medical School, Boston, U.S.A

Berna Uzun²

Department of Mathematics
Near East University
Nicosia / TRNC Mersin 10 – Turkey

Musa Sani Musa³, Ilker Ozsahin⁴

Department of Biomedical Engineering
Near East University
Nicosia / TRNC Mersin 10 – Turkey

Abstract—X-rays are ionizing radiation of very high energy, which are used in the medical imaging field to produce images of diagnostic importance. X-ray-based imaging devices are machines that send ionizing radiation to the patient's body, and obtain an image which can be used to effectively diagnose the patient. These devices serve the same purpose, only that some are the advanced form of the others and are used for specialized radiological exams. These devices have image quality parameters which need to be assessed in order to portray the efficiency, potentiality and negativity of each. The parameters include sensitivity and specificity, radiation dose delivered to the patient, cost of treatment and machine. The parameters are important in that they affect the patient, the hospital management and the radiation worker. Therefore, this paper incorporates these parameters into fuzzy PROMETHEE (Preference Ranking Organization Method for Enrichment Evaluation) multi-criteria decision theory in order to help the decision makers to improve the efficiency of their decision processes, so that they will arrive at the best solution in due course.

Keywords—X-ray-based imaging devices; medical imaging; fuzzy PROMETHEE

I. INTRODUCTION

Medical imaging refers to the use of ionizing and non-ionizing radiation to produce images of the internal parts of the body for diagnostic purposes [1]. X-ray, which is the origin of medical imaging, was discovered in 1895 by Wilhelm Conrad Rontgen. Many medical imaging devices use X-rays to produce images of diagnostic value. The imaging devices include Computed Tomography (CT), Fluoroscopy, Conventional X-ray Machine, Mammography and Angiography [1]. These devices are similar because they all use X-ray radiation, but they differ in the type of radiological examination to be carried out. The devices have certain parameters like effective dose delivered to the patient, sensitivity, specificity, duration of scan, radiation dose, and cost. These parameters affect the patient directly, and it will be very important if they are analyzed in order for the parties

concerned to have a good understanding of the procedures, their benefits and risks.

Making decision of using which technique for a specific patient or buying an x-ray based machine for a hospital can be difficult because of the high number of criteria and the range of their possible values. Fuzzy PROMETHEE is a method which gives the ability to compare selected alternatives according to some given criteria.

In this paper, Fuzzy PROMETHEE was used to evaluate the mostly used radiological equipment utilizing X-ray by using their parameters including radiation dose and scan time.

Section 1 of this paper introduces the paper while Section 2 introduces the various X-ray based medical imaging devices. In Section 3, the methodology and application is explained, Section 4 shows the result, and lastly Section 5 concludes the study.

II. X-RAY BASED MEDICAL IMAGING DEVICES

A. Conventional X-Ray Machine

This is the main device in most radiology departments, used to image internal structures. It is mainly dedicated to extremities, head, neck and abdominal region examinations. Indications include fractures of the limbs and skull, cervical spine and lumbar vertebra exams, and abdomino-pelvic examinations. The main component of the X-ray machine is the Tube. The Tube consists of the anode, cathode, filament, glass envelope etc. The X-ray is produced when a current is passed through the filament, which results in heating the filament and electron production. These electrons are then accelerated to the anode target, where they become converted to X-ray and pass through a window to the object to be X-rayed. As the X-ray pass through the object, they hit a fluorescent cassette, which converts the X-ray into light, and a final image is produced after processing the cassette. X-ray imaging relies on the attenuation coefficient of the tissues and

organs in the body. This is the reason why some parts appear bright while others appear dark [2].

B. Angiography

This is a specialized radiological examination that employs a contrast medium to outline the blood vessels, such as the arteries and the veins. It is mainly used to check the arterial or venous supply to the head, upper and lower limbs and thorax. Typical example of the procedure includes cerebral angiogram, pulmonary angiogram, coronary angiogram, etc.

The contrast is injected via a catheter into the femoral artery or vein, or into the brachial artery or vein. Several X-ray images of the area of interest are acquired and stored in films or digital format on computers. The procedure is usually indicated for aneurysm, stenosis and coronary artery disease [3].

C. Computed Tomography (CT)

This is a technique in which tomographic images are produced by transmitting X-rays from an external source at several projection angles. This procedure is mostly used for anatomical localization and attenuation correction. CT uses a gantry containing the X-ray source and set of detectors, and also a bed where the patient lies during the examination. Axial images obtained from CT can be reformatted into coronal and sagittal, resulting to a 3D image set. CT is mostly used for tumors, brain and nervous system examination, urinary tract examination, and abdominal tumor [4].

D. Fluoroscopy

This imaging technique is used to obtain real-time images of a patient with the aid of a fluoroscope. It uses X-rays to obtain real-time (moving images) of the interval part of the body. Fluoroscope consists of a fluorescent screen with an X-ray source between which the patient is placed. In modern fluoroscopes, the screen is connected to an X-ray beam condenser and a Charge - coupled device (CCD) video camera, which allows viewing or recording on an image monitor. Indications for fluoroscopy exams include special examinations like Hysterosalpingography (HSG), Intra-venous Urethrography (IVU), Barium studies, etc. Patient is exposed to a large amount of radiation, even if the dose used is minimal [5].

E. Mammography

This is a special device used to image the breast. It has been very effective in the diagnosis of breast and axillary tumors. They use low energy X-ray to create images of the breast in both Medio-lateral and Cranio-caudal projections. These images are analyzed for any abnormal findings. Components include the tube, compression plate, cassette, breast support with grid, exposure button etc. Mammography has a limitation when it comes to women below the age of 30. It is suggested that women between the ages of 35-40 should undergo screening mammography at least once a year. During mammography procedure, the breast is slightly compressed between the two plates of the device for a few seconds. By so doing, all breast tissues are evaluated in 2 dimensions. 3D image can be obtained with digital breast tomosynthesis [6].

III. METHODOLOGY AND APPLICATION

The PROMETHEE method alone was proposed by [7] and [8]. The fuzzy PROMETHEE method allow the decision maker using fuzzy input data, which gives more flexibility to the decision maker while they compare alternatives in vague conditions. Application of this method was done by [9]-[15].

In the study conducted by [16], a detailed description of the fuzzy PROMETHEE method was given. In this study, we applied the same methodology for the evaluation of X-Ray based devices.

The most important parameters of the X-ray based medical imaging devices which include specificity, radiation dose, sensitivity, cost of devices and scan time are given in Table I as low bound, medium and upper. Choosing the parameters into three classes of low bound, medium and upper was done in order to apply triangular fuzzy numbers since the parameters of the alternatives are not crisp.

TABLE I. PARAMETERS OF THE DEVICES

Unit	k\$	Min.	%	%	mSv
	Cost	Time	Specificity	Sensitivity	Radiation Dose
Fluoroscopy	10	30	81	65	1,5
	50	40	85	70	3
	120	45	90	75	7
CT	155	15	78	85	2
	182.5	20	80	90	7
	210	25	87	95	10
Mammography	50	8	69	79	0,2
	80	10	91	82	0,4
	105	15	97	95	0,7
X-Ray	99	5	63	90	0,04
	113	10	70	93	0,1
	125	15	75	95	1,5
Angiography	140	58	94	94	4
	170	60	95	95	9,9
	200	62	96	96	15,8

We used normalization and then we transform them to the triangular fuzzy numbers (N, a, b) as shown in Table II.

TABLE II. TRIANGULAR FUZZY NUMBERS

Unit	\$	Min.	%	%	mSv
	Cost	Time	Specificity	Sensitivity	Rad. Dose
	N a b	N a b	N a b	N a b	N a b
Fluoroscopy	0,084	0,29	0,20	0,16	0,15
	0,06	0,03	0,01	0,01	0,05
	0,07	0,01	0,00	0,00	0,05
CT	0,306	0,14	0,19	0,21	0,34
	0,03	0,01	0,01	0,00	0,08
	0,03	0,01	0,01	0,00	0,06
Mammography	0,134	0,07	0,22	0,19	0,02
	0,02	0,00	0,04	0,00	0,01
	0,00	0,02	0,00	0,02	0,00
X-Ray	0,190	0,07	0,17	0,22	0,00
	0,03	0,03	0,00	0,00	0,00
	0,03	0,02	0,00	0,01	0,04
Angiography	0,285	0,43	0,226	0,22	0,485
	0,023	0,071	0,018	0,007	0,03
	0,022	0,046	0,01	0,01	0,033

And then we used Yager index to see the magnitude of the parameters of the alternatives, which are fuzzy numbers. The linguistic scale of the importance rating of the parameters used for this application can be seen in Table III. It gives us information about the most important parameters to be compared among the alternatives. This information was obtained from expert in the medical imaging field.

TABLE III. LINGUISTIC SCALE FOR IMPORTANCE

Linguistic scale for evaluation	Triangular fuzzy scale	Importance ratings of criteria
Very high (VH)	(0.75, 1, 1)	Specificity, Radiation dose, Sensitivity
Important (H)	(0.50, 0.75, 1)	Cost
Medium (M)	(0.25, 0.50, 0.75)	Scan Time
Low (L)	(0, 0.25, 0.50)	
Very low(VL)	(0, 0, 0.25)	

Furthermore, we used Yager index one more time in order to count the weight of the parameters. Lastly, we applied to the visual PROMETHEE program and used Gaussian preference function for the selected criteria (see Table IV). The best alternatives are expected to be of lower cost, have minimum radiation dose and scan time. They are also expected to have maximum specificity and sensitivity for the performance of the devices.

TABLE IV. VISUAL PROMETHEE APPLICATION

Criteria	Cost of Dev.	Scan Time	Specificity	Sensitivity	Rad. dose
Unit	\$	Min.	%	%	mSv
Preferences					
(min/max)	min	min	max	max	min
Weight	0,75	0,50	0,92	0,92	0,92
Preference Fn.	Gauss	Gauss	Gauss	Gauss	Gauss
Evaluations					
Fluoroscopy	0,088	0,279	0,1992	0,1615	0,15
CT	0,305	0,142	0,1877	0,2085	0,33
Mammography	0,128	0,078	0,2045	0,1964	0,02
X-Ray	0,189	0,069	0,1661	0,2184	0,02
Angiography	0,285	0,42	0,2228	0,2222	0,49

IV. RESULTS AND DISCUSSION

Table V shows the complete ranking of the X-ray based medical imaging devices when they were compared without including the cost of the machine. This is done in order to include parameters that are specific to the patient, being the receiver of the treatment. The total raking shows us that X-ray and mammography which gives less dose of radiation have relatively the same ranking. They are followed by fluoroscopy which all has a positive Net Flow. On the other hand, Computed Tomography and Angiography both having negative Net Flow came second to the last and last respectively on the total ranking table. It can be seen that this is due to the high dose of radiation they give to the patient.

TABLE V. COMPLETE RANKING OF THE IMAGING DEVICES WITH COST OF DEVICE DE-ACTIVATED

Complete Ranking	X-Ray Based Devices	Positive outranking flow	Negative outranking flow	Net Flow
1	X-Ray	0,0017	0,0000	0,0017
2	Mammography	0,0017	0,0000	0,0017
3	Fluoroscopy	0,0006	0,0004	0,0002
4	CT	0,0003	0,0009	-0,0006
5	Angiography	0,0000	0,0030	-0,0030

Table VI shows the complete ranking of the devices with cost of device activated. As it can be seen, there is no difference from the ranking while the cost was de-activated. But a slight change is noticed in the Net flow of Mammography and Conventional X-ray device. The idea to include the cost in Table VI was to produce a ranking table which will be useful for the hospital management, because price of device largely affects their selection process.

TABLE VI. COMPLETE RANKING OF THE IMAGING DEVICES WITH COST OF DEVICE ACTIVATED

Complete Ranking	X-Ray Based Devices	Positive outranking flow	Negative outranking flow	Net Flow
1	Mammography	0,0015	0,0000	0,0015
2	X-Ray	0,0014	0,0001	0,0014
3	Fluoroscopy	0,0008	0,0003	0,0004
4	CT	0,0003	0,0010	-0,0007
5	Angiography	0,0000	0,0026	-0,0026

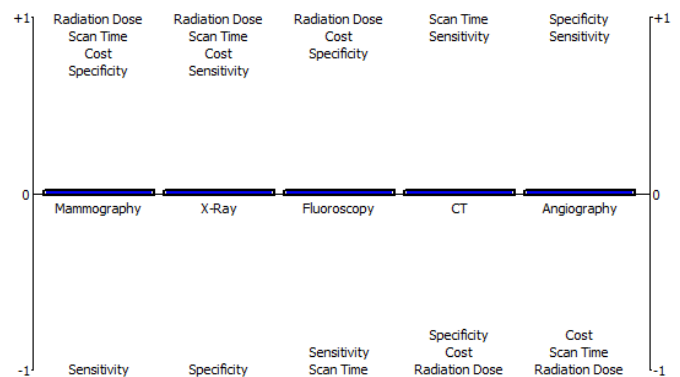


Fig. 1. PROMETHEE evaluation result.

The advantages and disadvantages according to the parameters of the devices are given in Fig. 1. These results also give very important information about the properties of the devices should incase the manufacturer needs to make any improvement for the specific property. This was obtained from the Decision Lab visual PROMETHEE program. The program gives the user the ability to manipulate the parameters and make further comparisons according to the decision maker preferences.

V. CONCLUSION

Utilizing multi-criteria decision methods like fuzzy PROMETHEE gives the possibility to accomplish great outcomes by incorporating fuzzy data. This method was applied on various X-ray based medical imaging devices and a useful result was obtained as shown in Section 4. The method has been tested and validated in previous studies, and it provides useful information when used in the present study. It is good and provides alternative solutions to decision maker. The concerned parties can rely on the outcome of this study to make the necessary decision in due course. The study can be improved by adding more criteria to the alternatives.

Furthermore, compared to other decision-making methods, the PROMETHEE method has proven to be efficient in many fields. The patients and the hospital management are the beneficiary of the outcomes of this study. This method can be applied to other decision-making problems that exist in medical imaging or other field of study.

REFERENCES

- [1] Medical imaging. (2018). World Health Organization. Retrieved 22 March 2018.
- [2] S. Nie, Z. Wang, W. Liu, and X. Liang, (2013). "Clinical Applications of X-ray, B-scan, and CT in the Diagnosis of Ocular Foreign Bodies," *Eye Sciences*. Vol. 28, no. 1, pp. 11-14, 2013.
- [3] J. Yu, and J. Cockburn, "Angiography". Retrieved 22 December 2017.
- [4] C. Garvey, "Computed tomography in clinical practice," *BMJ*, vol. 324, no. 7345, pp. 1077-1080, 2002.
- [5] S. Balter, J.W. Hopewell, J. D.L. Miller, L.K. Wagner, and M.J. Zelefsky, "Fluoroscopically Guided Interventional Procedures: A Review of Radiation Effects on Patients' Skin and Hair," *Radiology*, vol. 254, no. 2, pp. 326-341, 2010.
- [6] F. Gilbert, S. Astley, A. Dibden, A. Seth, J. Morel, S. Bundred, et al., "Does Reader Performance with Digital Breast Tomosynthesis Vary according to Experience with Two-dimensional Mammography?," *Radiology*, vol. 283, no. 2, pp. 371-380, 2017.
- [7] J.P. Brans, and P. Vincke, "A preference ranking organization method", *Management Science*, vol. 31, no. 6, pp. 647-656, 1985.
- [8] J.P. Brans, P. Vincke, and B. Mareschal, "How to select and how to rank projects: the PROMETHEE method," *European Journal of Operational Research*, vol. 24, pp. 228-238, 1986.
- [9] M., Goumas, and V. Lygerou, "An extension of the PROMETHEE method for decision making in fuzzy environment: ranking of alternative energy exploitation projects," *European Journal of Operational Research*, vol. 123, pp. 606-613, 2000.
- [10] J. Geldermann, T. Spengler, O. Rentz, "Fuzzy outranking for environmental assessment. Case study: iron and steel making industry," *Fuzzy Sets and Systems*, vol. 115, no. 1, pp. 45-65, 2000.
- [11] R.U. Bilsel, G. Buyukozkan, D. Ruan, "A fuzzy preference ranking model for a quality evaluation of hospital web sites," *International Journal of Intelligent System*, vol. 21, no. 11, pp. 1181-1197, 2006.
- [12] W.C. Chou, W.T. Lin, C.Y. Lin, "Application of fuzzy theory and PROMETHEE technique to evaluate suitable eco-technology method: a case study in Shimen reservoir watershed," *Ecological Engineering*, vol. 31, pp. 269-280, 2007.
- [13] G. Tuzkaya, B., Gülsün, C. Kahraman, D. Özgen, "An integrated fuzzy multi-criteria decision making methodology for material handling equipment selection problem and an application," *Expert Systems Applications*, vol. 37, no. 4, pp. 2853-2863, 2010.
- [14] A. Ozgen, G. Tuzkaya, U.R. Tuzkaya, D. Ozgen, "A Multi-Criteria Decision Making Approach for Machine Tool Selection Problem in a Fuzzy Environment," *International Journal of Computer Intelligence System*, vol. 4, no. 4, pp. 431-445, 2011.
- [15] D. Ozsahin, B. Uzun, M. Musa, N. Şentürk, F. Nurçin, and I. Ozsahin, "Evaluating nuclear medicine imaging devices using fuzzy PROMETHEE method," *Procedia Computer Science*, vol. 120, pp. 699-705, 2017.
- [16] D. Uzun, B. Uzun, M. Sani, A. Helwan, C. Nwekwo, and F. Veysel, F. et al., "Evaluating Cancer Treatment Alternatives using Fuzzy PROMETHEE Method," *International Journal of Advanced Computer Science and Applications*, vol. 8, no. 10, pp. 177-182, 2017.

Challenges in Designing Ethical Rules for Infrastructures in Internet of Vehicles

Razi Iqbal

College of Computer Information Technology
American University in the Emirates
Dubai, United Arab Emirates

Abstract—Vehicular Ad-hoc Networks (VANETs) have seen significant advancements in technology. Innovation in connectivity and communication has brought substantial capabilities to various components of VANETs such as vehicles, infrastructures, passengers, drivers and affiliated environmental sensors. Internet of Things (IoT) has brought the notion of Internet of Vehicles (IoV) to VANETs where each component of VANET is connected directly or indirectly to the Internet. Vehicles and infrastructures are the key components of a VANET system that can greatly augment the overall experience of the network by integrating the competencies of Vehicle to Vehicle (V2V), Vehicle to Pedestrian (V2P), Vehicle to Sensor (V2S), Vehicle to Infrastructure (V2I) and Infrastructure to Infrastructure (I2I). Internet connectivity in Vehicles and Infrastructures has immensely expanded the potential of developing applications for VANETs under the broad spectrum of IoV. Advent in the use of technology in VANETs requires considerable efforts in scheming the ethical rules for autonomous systems. Currently, there is a gap in literature that focuses on the challenges involved in designing ethical rules or policies for infrastructures, sometimes referred to as Road Side Units (RSUs) for IoVs. This paper highlights the key challenges entailing the design of ethical rules for RSUs in IoV systems. Furthermore, the article also proposes major ethical principles for RSUs in IoV systems that would set foundation for modeling future IoV architectures.

Keywords—Ethics; road side units; vehicular ad-hoc networks; internet of vehicles; intelligent transportation systems

I. INTRODUCTION

Intelligent Transportation Systems (ITS) have been transforming the traditional transportation systems into intelligent systems for decades now. ITS have seen tremendous advancements throughout their life time and have become an essential part of transportation in developed and developing countries. VANETs have played a significant role in transmuting the notion of connected vehicles and infrastructures in ITS. Introduction of autonomous vehicles and drone RSUs are bringing dynamicity with more independence and decentralization to the transportation systems [1]. VANETs have been key area of research for both academicians and industry professionals for years that has reshaped the overall perception of ITS for concepts like smart cities.

IoV is an adherent of VANET where each unit of the system is Internet enabled. This Internet connectivity provides system with greater capabilities of sharing information of common interests besides providing more opportunities of

medium of communication [2]. Recent advancements in computing and communication technologies, like EDGE Computing, Grid Computing, Parallel Processing, Big Data Analysis, Web Semantics and Artificial Intelligence has opened horizons of opportunities for developing and deploying safety and infotainment applications for IoV systems.

One of the key advantages of Internet connectivity in IoV is socializing of objects of systems, e.g., vehicles, infrastructure, passengers, drivers and environmental sensors, etc. Sharing of information on roads through Internet provides ease of driving, safety, awareness, warnings, traffic updates and special services like discount coupons, vacant car parking information and alternate routes etc. [3].

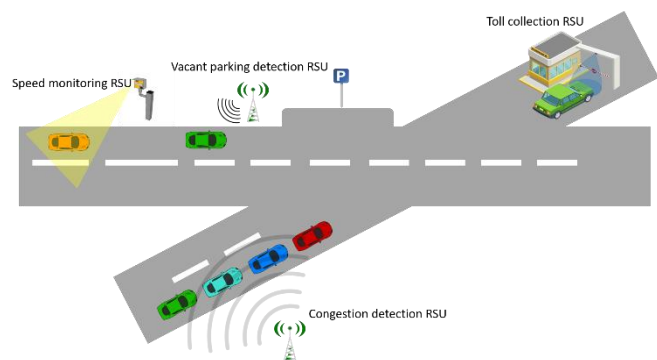


Fig. 1. Distinct types of RSUs in IoV System.

Infrastructure sometimes referred to as Road Side Units (RSUs) are considered key component of IoV systems. RSUs are essential for IoV systems in a way that they provide sensing, communication, processing and computing capabilities. One of the most common RSUs these days are speed checking RSUs that are equipped with cameras for measuring the speed of vehicles on roads. Besides speed checking RSUs, other examples are toll collection RSUs, smart bus stops, digital billboards and motion detecting RSUs. Majority of the RSUs mentioned are connected directly or indirectly to the cloud (Internet) to store, process, compute and communicate information [4]. Moreover, multifaceted RSUs are also gaining popularity in a way that they are capable of multitasking and multiprocessing. Fig. 1 illustrates distinct types of RSUs in IoVs systems.

Growing autonomy in IoV systems brings the concern of ethics. IoV systems will be challenged with ethical dilemmas

and anticipated to operate in an ethically responsible way. Self-governed operations of IoV systems require setting ethical rules and policies before these systems can take an autonomous decision [5]. However, currently, no ethical guidelines are available for components of IoV systems that results in lack of applications and services. This article is an effort towards setting the foundation for designing ethical rules for one of the key components of IoV systems, the RSUs. Below are the contributions of this article:

- Highlight the key challenges involved in designing ethical rules for RSUs in IoV systems.
- Propose major ethical principles for RSUs in IoV systems that would set foundation for modeling future IoV architectures.

The rest of the article is organized as follows: Section II provides more details of RSUs and their types currently available in literature and their applications in real world. Section III focuses on the challenges of designing ethical principles for RSUs in IoV environment. Section IV proposes four major ethical rules for RSUs in IoV systems that are expected to set foundation for future ethical IoV architectures. Finally, the conclusion section concludes the article.

II. ROAD SIDE UNITS IN IOV SYSTEMS

RSUs are considered one of the key components of IoV systems. RSUs perform several activities like traffic monitoring, speed checking, congestion detection, toll collection, identifying vacant car parkings, surveillance, traffic jams, warnings and safety and security on roads. Such activities fall under sensing capabilities of RSUs. In order to realize sensing, RSUs are equipped with additional integrant like cameras and environmental sensors [6].

Besides sensing, RSUs are capable of computing and processing of information as well. In IoVs, RSUs can process and compute information locally to save time and provide quick access to information on request from peer entities of the network, or it can leverage the capabilities of the cloud for data processing if local resources are not sufficient.

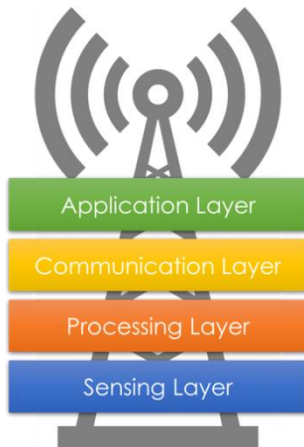


Fig. 2. Traditional RSU layered architecture.

In VANETs, RSUs normally use a dedicated communication technology, Dedicated Short Range Communication (DSRC) to communicate with peer RSUs and vehicles on roads. In IoVs, RSUs are connected directly or indirectly to the Internet. In case of indirect connection to the Internet, RSUs utilize DSRC or wired connection with other Internet enabled RSUs. Furthermore, in IoVs, RSUs can be multifaceted to incorporate multiple communication technologies like Cellular, Wi-Fi, DSRC, 6LowPAN and Wi-Max, etc.

RSUs provide diverse applications based on the context. In IoVs, application layer is anticipated as the most comprehensive layer of RSU architecture as it can provide local and cloud based applications and services. Some of the applications and services provided by RSUs in IoV are warning and safety messages, information about nearby restaurants, maps for navigation within close vicinity, infotainment applications like media sharing and Internet sharing etc. Fig. 2 illustrates the traditional RSU layered architecture.

This section highlights different categories of RSUs currently available in literature along with their real world applications.

A. Data Collection RSUs

One of the most popular RSUs these days are data collection RSUs. These are the units that are equipped with several types of sensors to collect information [7]. One of the commonly used data collection RSUs are speed monitoring RSUs that are equipped with high definition cameras that measure the speed of the vehicle based on images captured at two distinct locations. Fig. 3 illustrates the working of such RSUs.

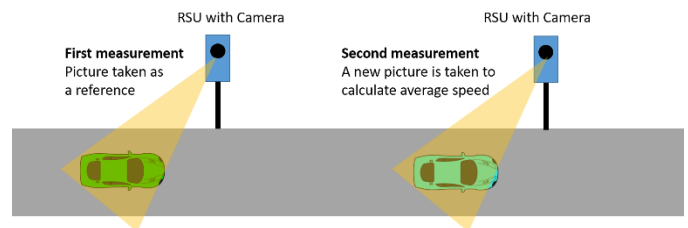


Fig. 3. Speed measuring RSUs.

As illustrated in the figure, in order to measure the exact speed of the vehicle, an image is captured for the vehicle at two stages. The first image is captured as a reference and the second image is captured to calculate the average speed of the vehicle. Based on the speed calculated by the camera, fines are issued by the law enforcement agencies.

B. Toll Collection RSUs

Another popular type of RSUs is toll collection RSUs that are normally installed at highways to collect highway charges. Current state-of-the-art technology used in such RSUs is Radio Frequency Identification (RFID) that operates through an initiator (reader) and responder (passive tag) installed at collection booth (toll gate) and vehicle, respectively.

As illustrated in Fig. 4, as soon as the vehicle enters the communication range of the RFID initiator (approx.10m), an

electromagnetic field is generated around the vicinity that powers up the passive tag installed in the vehicle. Based on the information stored in the tag which is bundled with the account details of the driver, charges are deducted from the account.

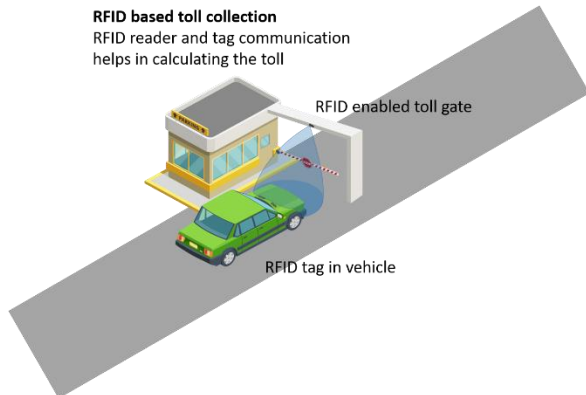


Fig. 4. Toll collecting RSUs.

C. Information Dissemination RSUs

A new form of RSUs emerging these days is information dissemination RSUs. These RSUs are connected to each other through wired or wireless communication medium to form a network in order to shared information [8]. As soon as an event occurs near a RSU, this information is disseminated to the other RSUs in the network based on the context. Fig. 5 highlights the working of information dissemination RSUs.

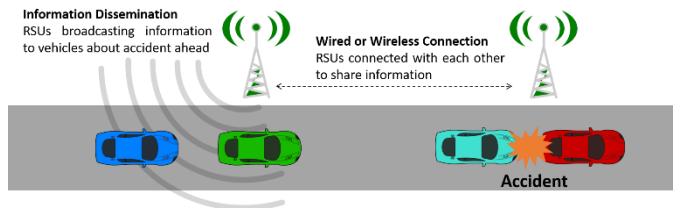


Fig. 5. Information disseminating RSUs.

As illustrated in Fig. 5, two RSUs are connected to each other through a wired or wireless connection. As soon as an accident occurs near one of the RSUs, this information is transmitted to the other RSU in the network which ultimately broadcasts this information to nearby vehicles. This information dissemination helps in avoiding traffic jams due to unfortunate incidents on roads.

D. Special Services RSUs

Surge in Internet connectivity on roads have conceptualized several new forms of services to facilitate vehicles, drivers and passengers. RSU is one of the components of IoV system that can provide special services to other components of the system based on demand. Such RSUs are categorized as special services RSUs [9]. The special services provided by these RSUs are internet sharing, discount coupons of restaurants, vacant car parking detection, upcoming gas station information, alternate routes, media sharing, chatting groups and many other social networking services.

Fig. 6 illustrates the working of two cases of special services RSUs. In first case, a restaurant is providing a discount

coupon of 50% to the passing vehicles. This information is transmitted to passing vehicles through the Internet since both restaurant (considered as a RSU since it can transmit and receive information) and vehicle are Internet enabled. Similarly, in the second case, RSU communicates with a passing vehicle to inform it about upcoming vacant car parking.

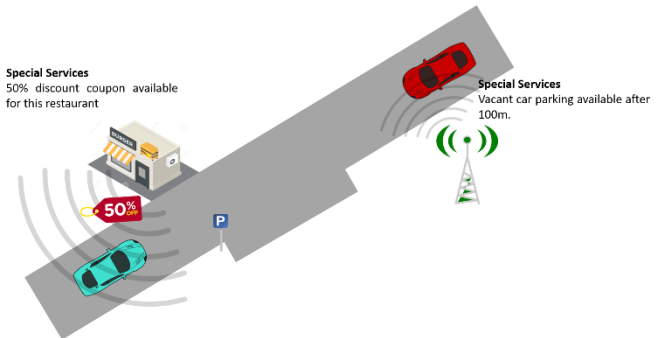


Fig. 6. Special services RSUs.

III. CHALLENGES FOR ETHICAL RULES FOR RSUs IN IOV

RSUs are smart sensing, computing, processing, communicating and storing devices that provide required services without human interferences. However, these self-operational capabilities of RSUs bring ethical concerns when it comes to information gathering, information dissemination and decision making. Currently, no significant efforts have been made to design ethical guidelines for RSUs in IoV systems because of several challenges. This section highlights the major challenges involved in designing ethical guidelines (rules or policies) for RSUs in current state-of-the-art IoV systems.

A. Architectural Design for RSUs

IoV is a relatively new concept; however, RSUs have been around for decades. Besides their availability for years, there is no standard architectural design available for RSUs [10]. In various parts of the world, different types of RSUs are used based on distinct architecture. Several architectural design choices are available for RSUs, e.g., RSUs with sensing and communicating layers, RSUs with sensing, processing and communicating layers and RSUs with only application layer. For example, congestion detection RSUs rely on sensing and communication layers, speed monitoring RSUs rely on sensing, processing and communicating layers and digital billboards on highways rely on application layer only.

The architecture of some RSUs is very complicated as they include security, privacy, trust management, gateway, EDGE computing and web services layers besides traditional layers presented in Fig. 2. Lack of standard architectural design encompasses the challenge of designing ethical rules for RSUs. Scheming generic ethical rules for all kinds of RSUs appears unrealistic unless a global standard for RSU architecture is defined.

B. Decentralization and Scalability

Internet connectivity in IoV has enabled different components of the system to communicate with each other without relying on other units. The concept of decentralization

holds importance as it allows each component of the system to sense, process, communicate and react to events associated with it. Independent operations of IoV components provide flexibility, context-awareness, localization and less dependability on other units. Decentralization provides heterogeneity to the system as each component of IoV system can be different from the other component depending upon the type of the component [11]. IoV system incorporates several vehicles and each vehicle can be different from its peer vehicle in make, kind, size and color, etc. If RSUs have to communicate with these different vehicles, ethical rules should be defined on communication, sensing, processing and information storage at RSU level. For example, if a vehicle does not want to share its information and still RSUs are collecting vehicle information like car type, color, make, registration number plate and driver information, etc. It would be an ethical concern for the driver of the vehicle. Defining an ethical rule for each vehicle, driver and passenger is extremely difficult in IoV environment as the network is very large and probability of predicting the scalability of the network is almost impossible in large area networks.

C. Communication Technologies

In IoV systems, information is transmitted using long range and short range wireless technologies except the communication between RSUs which is sometimes wired. However, the latest trend in RSU communication is wireless transmission as it provides flexibility, cost effectiveness, less hassle and scalable networks. Commonly used communication technologies in IoV systems are Cellular (2G, 3G, 4G etc.), Wi-Max, Wi-Fi, DSRC and some other 6LowPAN [12].

As illustrated in traditional RSU architecture presented in Fig. 2, communication layer is responsible for all the wired and wireless communications between RSUs and other components of IoV systems. However, due to diverse use of technologies in RSU communication, it is hard to define ethical rules for communication technologies since they operate on different frequencies in various parts of the world and are handled by different service providers. Each service provider (vendor) has its own rules for use of technology, security, privacy and data accessibility, which brings complication in the process of defining ethical guidelines of communication technologies. For example, a 6LowPAN technology, ZigBee (IEEE 802.15.4) operates on different frequencies throughout the world, e.g., 868 MHz in Europe, 915MHz in Americas and 2.4GHz elsewhere. ZigBee is used to create an IoV network to ensure cost effectiveness and less power consumption; however, due to its operation on different frequencies and multiple vendors, it becomes immensely difficult to establish ethical rules for communication that apply for all the vendors, across different operating frequencies throughout the world.

D. Diverse Sensors

IoV systems encompass the use of diverse sensors, e.g., speed cameras, motion detection, temperature sensors, congestion detection, vehicle detection, traffic signal monitoring and pedestrian detection etc. Each of these sensors installed in RSU perform different operations based on the context [13]. Different sensors need different rules for their

operation. For example, ethical rules defined for motion detection sensors might not work for temperature sensors. Similarly, besides defining ethical rules for sensors based on their operation, sometimes, ethical rules might differ for the same sensor in different context. For example, if a vehicle detection sensor installed on a busy road has an ethical rule of capturing only the number plate of the vehicle, in normal scenarios, the rule works fine, however a fugitive with a stolen vehicle might not be captured on the road with this ethical rule and might require capturing a snapshot of driver along with the number plate as well. Diverse sensors with different context, distinct road conditions, discrete vehicles and drivers would result in substantially enormous number of scenarios each requiring an ethical rule. Such situations pose momentous challenge of stipulating ethical rules for RSUs.

E. Dynamicity

IoV systems are highly dynamic in nature as the topology of the network is changing rapidly due to fast moving vehicles. RSUs must be efficient and resourceful enough to respond to the requests of the vehicles in their vicinity [14]. Due to vibrant change in the network nodes, the whole network needs to be revised instantaneously to avoid delays in information transmission. In order for the requests to be acknowledged by RSUs, high processing, computing and communication is obligatory as a small delay in the information might result in serious inconvenience for the vehicles on road. For example, if a vehicle requests a RSU for traffic status on upcoming junction and RSU takes a while to gather, process and communicate this information to the vehicle; the information might not be of any use to the vehicle because by that time vehicle might reach the junction. Dynamicity poses a consequential challenge in laying the ethical rules for RSUs as the number of nodes, their locations and context changes expeditiously. The ethical rules set for RSUs based on context, number of nodes, location and type of vehicles might require processing before applying on a fleet of vehicles near the concerned RSU. By the time, the processing is done, fleet of vehicles might change because of their high speed and dynamic nature that results in waste of processing time and resources.

F. Security and Privacy

Security and privacy play crucial role in design and deployment of IoV systems. Due to open environment, IoV systems are exposed to several security attacks like eavesdropping, masquerading, social engineering and Denial of Service etc. These attacks can result in breach of privacy, modification of data and denial of services provided by the systems. RSUs being essential units of the IoV systems hold a lot of information including personal details of drivers and passengers. A breach in the security can seriously affect the way rules are implemented on RSUs, vehicles, drivers and passengers by law enforcing agencies [15]. Similarly, ethical rules implemented through RSUs can be modified through an attack on the system. For example, if an ethical rule of reading vehicles' number plates to calculate the toll is implemented through an RSUs and a network attacker modifies this ethical rule to take the pictures of drivers and start sending them to his server; a serious breach of driver privacy will occur that might result in unfortunate circumstances.

G. Extensive Applications

Employment of Internet in Vehicular Systems has unleashed voluminous opportunities of developing applications for IoVs. Vehicle manufacturers, third party RSU vendors and governmental agencies have already developed several safety and non-safety applications for VANETs and IoVs, e.g., Toll collection, navigation apps and law enforcement applications. Diverse applications for IoV are improving the experience on roads, however, encompasses a challenge of setting ethical rules for app developers. Due to varied number of developers from governmental and non-governmental sector, an ethical framework for app development and deployment specifically for RSUs is lacking that incorporates the challenge of bringing all the developer under the same ethical framework.

IV. PROPOSED ETHICAL PRINCIPLES FOR RSUS IN IOV

Based on the review of literature, a clear gap in defining the ethical rules or framework for RSUs has been identified. Furthermore, it is evident from the literature that several challenges are faced by the ethicist to define clear rules for infrastructures (RSUs) due to dynamic nature of IoV systems, lack of architectural designs for RSUs, decentralization and scalability in IoVs, communication technologies used by RSUs to transmit information, use of diverse sensors and exposure to security and privacy attacks in IoVs. This section provides four general ethical rules for RSUs in IoVs that are expected to set foundation for designing detailed ethical rules for different scenarios:

- Information to and from RSUs can only be monitored, modified and updated by law enforcing agencies.
- Third party hardware (sensors, etc.) and software (applications, etc.) for RSUs should be licensed by law enforcing agencies.
- Information of any component of IoV (vehicles, drivers, passengers and pedestrians, etc.) collected through RSUs should be clearly announced before collection.
- Procedures for processing, computing, communication and information collection should be regularly monitored by law enforcing agencies.

V. CONCLUSION

IoV systems are emerging in the realm of VANETs by providing additional functionality of Internet connectivity to traditional VANETs. Components of IoV are connected directly or indirectly to the Internet. The components of IoV that are not directly connected to Internet require infrastructures like RSUs to assist them in Internet connectivity. All time connected environment of RSUs brings a concern of machine ethics. This article highlighted the importance of RSUs by categorizing them into Data Collection RSUs, Toll Collection RSUs, Information Dissemination RSUs

and Special Services RSUs. Considering the high importance of RSUs in IoV systems, the article focused on underpinning the challenges involved in designing the ethical rules for RSUs. Several challenges like dynamism, lack of architectural design, decentralization and scalability, diversity of sensors, extensive applications and security and privacy have been highlighted to set a solid foundation of proposing general ethical rules for RSUs in IoV systems. Finally, the article proposed four general ethical rules for RSUs that are expected to lay a strong structure for designing ethical principles for different layers of RSU architecture.

REFERENCES

- [1] D. B. Rawat, B. B. Bista, and G. Yan, "CoR-VANETs: Game Theoretic Approach for Channel and Rate Selection in Cognitive Radio VANETs," 2012 Seventh International Conference on Broadband, Wireless Computing, Communication and Applications, 2012.
- [2] K. M. Alam, M. Saini, and A. E. Saddik, "tNote: A Social Network of Vehicles under Internet of Things," Lecture Notes in Computer Science Internet of Vehicles – Technologies and Services, pp. 227–236, 2014.
- [3] W. Wu, Z. Yang, and K. Li, "Internet of Vehicles and applications," Internet of Things, pp. 299–317, 2016.
- [4] A. B. Reis, S. Sargento, and O. K. Tonguz, "On the Performance of Sparse Vehicular Networks with Road Side Units," 2011 IEEE 73rd Vehicular Technology Conference (VTC Spring), 2011.
- [5] H.-Y. Liu, "Irresponsibilities, inequalities and injustice for autonomous vehicles," Ethics and Information Technology, vol. 19, no. 3, pp. 193–207, 2017.
- [6] V. Fux, P. Maillé, and M. Cesana, "Road-side units operators in competition: A game-theoretical approach," Computer Networks, vol. 88, pp. 103–120, 2015.
- [7] M. Rashidi, I. Batros, T. K. Madsen, M. T. Riaz, and T. Paulin, "Placement of Road Side Units for floating car data collection in highway scenario," 2012 IV International Congress on Ultra Modern Telecommunications and Control Systems, 2012.
- [8] H. Duan and Y. Li, "Road-Side Units Based Data Forwarding Framework in Vehicular Ad Hoc Networks," Ictis 2013, Nov. 2013.
- [9] N. Kumar, L. N. Alves, and R. L. Aguiar, "Employing Traffic Lights as Road Side Units for Road Safety Information Broadcast," Transportation Systems and Engineering, pp. 143–159.
- [10] C. Silva and W. Meira, "An architecture integrating stationary and mobile roadside units for providing communication on intelligent transportation systems," Network Operations and Management Symposium (NOMS), IEEE/IFIP, 2016.
- [11] J. G. R. Junior, M. E. M. Campista, and L. H. M. K. Costa, "A Decentralized Traffic Monitoring System based on vehicle-to-infrastructure communications," 2013 IFIP Wireless Days (WD), 2013.
- [12] S. Chen, "Dynamic spectrum access and cognitive radio for vehicular communication networks," Vehicular Communications and Networks, pp. 127–150, 2015.
- [13] Q. Ibrahim, "Design, implementation and optimisation of an energy harvesting system for vehicular ad hoc networks' road side units," IET Intelligent Transport Systems, vol. 8, no. 3, pp. 298–307, Jan. 2014.
- [14] T. P. Van and V. D. Nguyen, "Location-aware and load-balanced data delivery at road-side units in vehicular Ad hoc networks," IEEE International Symposium on Consumer Electronics (ISCE 2010), 2010.
- [15] Y. Kim and J. Lee, "A secure analysis of vehicular authentication security scheme of RSUs in VANET," Journal of Computer Virology and Hacking Techniques, vol. 12, no. 3, pp. 145–150, 2016.

Analysis of the Impact of Different Parameter Settings on Wireless Sensor Network Lifetime

Muhammad Usman Younus

Institut de Recherche en Informatique de Toulouse (IRIT)
Université Paul Sabatier, Toulouse, France

Abstract—The importance of wireless sensors is increasing day by day due to their large demand. Sensor networks are facing some issues in which battery lifetime of sensor node is critical. It depends on the nature and application of the wireless sensor network and its different parameters (sampling frequency, transmission frequency, processing power and transmission power). In this paper, we propose a new and realistic model to show the effect of energy consumption on a lifetime of wireless sensor nodes. After analyzing the model behavior, we are able to find out the sensitive parameters that are highly effective for lifetime of sensor nodes.

Keywords—Wireless sensor network; energy consumption; lifetime; WSN parameters; transmission frequency; sampling frequency

I. INTRODUCTION

The low cost, the low implementation complexity, and the flexibility of wireless sensor networks (WSNs) account for them who are employed in industrial, residential and commercial sectors. Since the last twenty years, there has been a widespread growth in wireless communication technology. Thus, it became a significant part of our lives. The applicability of WSNs extends from telephony and data transfer to non-sensing monitoring approaches. In spite of being a successful and vast field, there exist certain complications like battery lifetime and reliability that need to be sorted. An important parameter to measure the performance of a wireless network is its battery life [1] because wireless sensors have limited battery capacity. In some applications, after the deployment of a sensor, the battery cannot be replaced. So, the problem of high energy consumption is very critical in WSN for continuity of the network communication.

A long battery life is a plus point for wireless local area network (WLAN) cards or cell phones, while it is an obligation for large-scale sensor networks. It is more difficult to replace a battery with hundreds of sensor nodes all the time [2]. This was the main reason which attracted researchers to study a way out to devise a lifetime network for WSNs.

The energy is the main limiting factor for a battery life. The power consumption of transceivers is taken as energy with respect to time. The circuit power is vital determinant for the analysis of battery life as RF of short-range that has a carrier frequency in Giga Hertz. In addition to the aforementioned, other parameters like sensing duration, transmission duration, receiving duration, transmitting frequency, sampling frequency, channel condition, modulation, and data rate must be considered as this effect

transmits power of RF, architecture and operating time of the transceiver [3].

A lot of work has already been done in the field of WSN to reduce the energy consumption of sensor nodes and enhance the lifetime with different ways which are discussed in section II. To the best of our knowledge, no one is focusing on whole WSN energy consumption parameters. In this paper, we are presenting a new and realistic model, in which WSN energy consumption parameters are discussed in detail that will help to enhance the lifetime of the wireless sensor node.

Following is a general layout of our paper: in Section II the literature review is being discussed; in Section III the mathematical formulation of energy consumption of wireless sensor nodes are described; Model analysis, its performance, and discussion are explained in Section IV, while concluding remarks are given in Section V.

II. LITERATURE REVIEW

This section provides the state-of-art in various fields of research regarding battery lifetime of WSNs. Many studies have been focused on the estimation and the issue of battery lifetime regarding different types of applications such as data networks, commercial sector, personal area network, free internet connection sharing, etc. Many researchers are working in this field for the last few decades. Some of the remarkable works are discussed below.

In [4], the researchers carried out a study on modeling the lifetime of wireless sensors. According to this paper, energy consumption and Remaining Lifetime of Individual Sensor (RLIS), Remaining Lifetime of whole Sensor Network (RLSN) and Lifetime of Sensor Network (LSN) were formerly designed. On considering these models, two query protocols were introduced. These two models had two approaches: Firstly, it provides the most usable model for every type of energy consumption such as sleep/active dynamics. Secondly, it provides the efficient protocols. This paper reveals that load balancing causes the extension of the lifetime for a network.

In [5], the researchers investigated the energy consumption of wireless transceivers. According to this study, battery lifetime was considered the vital parameter to evaluate the overall performance of wireless sensor networks (WSNs). Researchers found that energy cost of transceiver electronic systems complicates the situation by putting its impact on battery lifetime. This paper basically aims at the development of energy cost for both electronic circuit and communication protocols.

Followed by the previous work, the others tried to overcome the lapses left by them. Moreover, in [6], the authors suggested a study on the trade-off between utility and lifetime in WSNs using a cross-layer optimization approach. The trade-off model depends on optimization decomposition.

Furthermore, many researchers have demonstrated the packet transmission policies for enhancing the lifetime of WSNs. In [7], they proposed battery friendly packet transmission policies for WSNs. Their work focused on maximizing battery lifetime for those networks that are affected by delayed constraints. In their study, these packets were introduced to reach their goal.

The problem of reducing the energy consumption and enhancing battery lifetime for WSNs attracted the attention of researchers in most applications where sensors are irreplaceable. So, the researchers in [8] studied Hierarchy Energy Driven Architecture (HEDA). This approach targeted overall energy consumption cost for enhancing battery life for WSNs. Many researchers had defined the lifetime of a sensor node and that of a network differently based on nature and applicability of WSN. They had illustrated lifetime being a function of energy consumption that depends on a function of transmitting distance [9]. Additionally, some other parameters like a total number of nodes and area of sensor fields within a network account for the lifetime of WSN. Different parameters like transmission radius, number of nodes in an area and coverage area of sensor network collectively have an impact on a lifetime of WSN that follows Fermat Point based forwarding technique.

Many scientists conducted a survey on battery and solar powered wireless sensor nodes. The vast applicability of sensor nodes is being hindered by problems created through a power supply and source. Therefore, energy conservation should be targeted at first place while implementing battery/solar powered sensor nodes. Previously known batteries served as a power source for nodes [10]. The motive of this paper was to compare solar and cell powered batteries. The vital parameters being studied included capacity volume, energy density, power efficiency, and low self-discharge, shorter recharge time and lower cost in terms of weight or size.

In [11], the researchers conducted a study on mobile ad hoc networks (MANETs) for reducing the power consumption through dynamic power management techniques. These MANETs were able to communicate with other networks as it consisted of free nodes to move randomly. It also enhances the battery life by efficient consumption of power through proper routing techniques/protocols and limited battery supply to each node. The main aim of the paper was to target the energy consumption through optimal path selection. Since a few decades, this field is leading to success. In [12], they had carried out a survey in which various optimization techniques for energy consumption within WSNs were considered. The main motive of the paper was to design a model for reducing battery overhead and enhancing lifetime of WSN that exploits the concept of Epidemic Model [12]. The network monitoring was carried out through a special node which makes use of the same protocol as for communication and tracks the state of

nodes at its propagation. This model can be utilized on the basis of its location sensing, positions, continuous sensing and event detection etc. This goal was achieved through numerical analysis. This literature provides fruitful ways for reduction of energy consumption and enhancement of lifetime of WSNs.

Moreover, in [13], researchers conducted a study for lifetime estimation of Wireless sensor nodes via models of an embedded analytical battery. In this study, the variable behavior of electrochemical batteries in terms of voltage and charge serves as a relevant parameter for implementation of energy policies. Currently, various hardware and software are available in a market that estimates the operational condition of a battery. Hardware approaches are comparatively costly than the software ones. This study focused on software approaches based on the temperature-dependent analytical model for estimation of voltage/charge values of WSNs. Such approaches were found successful without being affecting the overall performance of the WSNs. Still, there is more deficiency in this field of WSNs that needed to be studied.

Section III is describing the mathematical formulation of energy consumption of wireless sensor nodes and our model analysis is discussed in Section IV.

III. ENERGY CONSUMPTION FORMULATION

The Wireless sensor consists of some units which contain sensing, processing, transceiver, and power units as shown in Fig. 1. Each unit has different energy consumption which depends on the working of each unit.

Sensing and processing units collect the data from the environment and process it. Then the transceiver unit transmits and receives the data to the next hop in the wireless network. Power unit provides the power to each unit of a sensor.

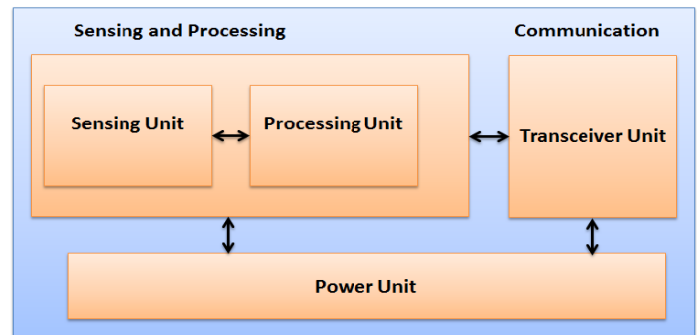


Fig. 1. Wireless sensor units.

Following is the total energy consumption of a wireless sensor node in the interval t :

$$E(t) = \begin{cases} E^{Sens}(t) + E^{Tx}(t) + E^{Rx}(t) \\ + E^{AckTx}(t) + E^{AckRx}(t) + E^{Idle}(t) \end{cases} \quad (1)$$

Equation (1) consists of the whole energy consumption sources during time t due to sensing and processing, data transmitting and receiving, transmitting the acknowledgment (ACK) of successful receiving data frames and during idle time energy consumption.

Sensing and processing energy consumptions are:

$$E^{Sens}(t) = t * f_s * P_s * \Delta t_s \quad \text{where, } t \leq LT \quad (2)$$

According to Eqn. 2, energy consumption of a sensing unit depends on sampling frequency, processing power, sampling duration where LT is a lifetime of node which must be less or equal to the total time. Definitions of symbols are given in Table I.

Transmission energy consumption is:

$$E^{Tx}(t) = NF_{Tx}^{Avg} * P_{Tx} * \Delta t_{Tx} \quad (3)$$

$$NF_{Tx}^{Avg} = NF_{Tx} * \frac{1 - (1 - (1 - \eta)^2)^{R+1}}{1 - (1 - (1 - \eta)^2)}$$

$$\text{where } NF_{Tx} = t * f_{Tx} \text{ \& } t \leq LT \quad (4)$$

Energy consumption due to transmission depends on an average number of the transmitted frame, sensor transmitting power, and transmission time duration as given in (3). Equation (4) defines the average number of frames which also include the retransmission of frames due to frame or ACK loss, where NF_{Tx} is the total number of frames which are transmitted during time t. All the remaining energy consumption parameter equations (i.e. Energy consumption due to reception, transmission of ACK frame, reception of ACK frame and energy consumption during idle time) will follow the average number of frames because of frames or ACK loss issues.

Energy consumption due to reception is:

$$E^{Rx}(t) = NF_{Rx}^{Avg} * P_{Rx} * \Delta t_{Rx} \quad (5)$$

$$NF_{Rx}^{Avg} = NF_{Tx} * (1 - \eta) * \frac{1 - (1 - (1 - \eta)^2)^{R+1}}{1 - (1 - (1 - \eta)^2)} \quad (6)$$

Energy consumption due to receiving the data depends on average number of frames, receiving power and frames receiving duration as given in (5), where (6) defines the average number of receiving frames in which R times reception is included due to frame loss.

Energy consumption due to transmission of ACK frame is:

$$E^{AckTx}(t) = NF_{Rx}^{Avg} * P_{AckTx} * \Delta t_{AckTx} \quad (7)$$

ACK frame is used to give the confirmation message about successfully receiving frames. Due to ACK transmission, energy is consumed which depends on an average number of frame reception, its transmitting power, and ACK transmission duration as given in (7).

Energy consumption due to reception of ACK frame is:

$$E^{AckRx}(t) = NF_{AckRx}^{Avg} * P_{AckRx} * \Delta t_{AckRx} \quad (8)$$

$$NF_{AckRx}^{Avg} = NF_{Tx} * (1 - \eta)^2 * \frac{1 - ((1 - \eta)^2)^{R+1}}{1 - (1 - \eta)^2} \quad (9)$$

If the destination node receives frames successfully then that destination node transmits the ACK frame to give confirmation about successfully receiving frames. Equation (8) defines the energy consumption due to ACK frame reception, which includes the average number of ACK frames, power consumption due to reception of ACK frames and receiving of ACK frames duration. An average number of ACK frames also include R retransmissions which are due to loss of ACK or data frames loss during communication as given in Equation (9).

TABLE I. NOTATION DEFINITIONS

Symbol	Definition
f_s	Sampling frequency
P_s	Power consumption due to samples processing
Δt_s	Sampling duration
LT	Lifetime
NF_{Tx}^{Avg}	Average number of transmitted frames
f_{Tx}	Transmission frequency
P_{Tx}	Power consumption due to transmission
Δt_{Tx}	Duration of transmission
NF_{Rx}^{Avg}	Average number of reception frames
P_{Rx}	Power consumption due to reception
Δt_{Rx}	Duration of reception
NF_{AckRx}^{Avg}	Average number of ACK reception
P_{AckTx}	Power consumption due to ACK transmission
Δt_{AckTx}	Duration of ACK transmission
P_{AckRx}	Power consumption due to ACK reception
Δt_{AckRx}	Duration of ACK reception
P_{Idle}	Power consumption during Idle
η	Probability of error
R	Number of retransmission
V_s	Sensor supply voltage

Energy consumption during the idle situation is:

$$E^{Idle}(t) = \left\{ \begin{aligned} &P_{Idle} * (t - (t * f_s * \Delta t_s) - (NF_{Tx}^{Avg} * \Delta t_{Tx})) - \\ &(NF_{Rx}^{Avg} * \Delta t_{Rx}) - (NF_{AckTx}^{Avg} * \Delta t_{AckTx}) - \\ &(NF_{AckRx}^{Avg} * \Delta t_{AckRx}) \end{aligned} \right. \quad (10)$$

Very low energy is consumed when no process is carried out during this situation that's calculated by (10). Energy consumption during idle situation depends on power consumption rating of a node and idle duration.

However, the lifetime of sensor node is defined by:

$$\text{Life time of sensor node} = \frac{\text{Initial battery energy}}{\text{Total power consumed}} \quad (11)$$

Here we have considered that average battery voltage rating is known. The unit of an initial battery is Joule and power is in Watt. Here in next section, we are going to analyze the performance of the model in term of a lifetime.

IV. PERFORMANCE ANALYSIS OF MODEL AND DISCUSSION

In this section, we will see how different parameters affect the battery lifetime of sensor node. Our results are based on analysis and corroborated by MATLAB Work. We followed the Tmote Sky sensor device rating [14], [15] which is Ultra low power IEEE 802.15.4 complaint wireless sensor module. This module is widely used in sensor networks for monitoring, measuring the temperature and humidity. It has high data rate (250kbps) and an onboard microcontroller with 10k RAM, 48k flash, an antenna with 125m range outdoor and 50m indoor. Due to onboard features, it is cheaper and smaller in size as compared to other motes. The parameter values are given in Table II. Our results are based on the parameters of a real device; it is expected to reflect the actual behavior of a system in terms of lifetime.

TABLE II. PARAMETERS VALUES

Symbol	Value
P_s	24mW [17]
P_{tx}	58.5mW [14], [15]
P_{rx}	65.4mW [14], [15]
P_{ld}	163 μ W [14], [15]
V_s	3V [15]
Δt_s	5ms
Δt_{Tx}	4.2ms [16]
Δt_{Rx}	4.2ms [16]
Δt_{AckTx}	0.35ms [16]
Δt_{AckRx}	0.35ms [16]

In our model parameters, sampling frequency f_s depends on an application because each application required a different number of samples. We are also assuming the sampling time duration.

We compared four different parameters for observation which are transmitting frequency, sampling frequency, transmission, and processing power.

Fig. 2 shows the effect of a sampling frequency (F_s), transmission frequency (F_{tx}), processing power (P_s) and transmission power (P_{tx}) on a lifetime of a sensor node. In Fig. 2(a), the effect on sampling frequency and transmission frequency at the lifetime of a sensor node is shown. The lifetime of sensor node is decreasing with increase in both sampling and transmission frequency. From this graph, we can see that transmission frequency is more effective on lifetime

as compared to the sampling frequency. Lifetime is decreasing exponentially with increase in transmission frequency. However, the lifetime is also decreasing when the sampling frequency increases but not exponentially. With F_{tx} varying, remaining lifetime of sensor node is lower as compared to F_s varying scenario.

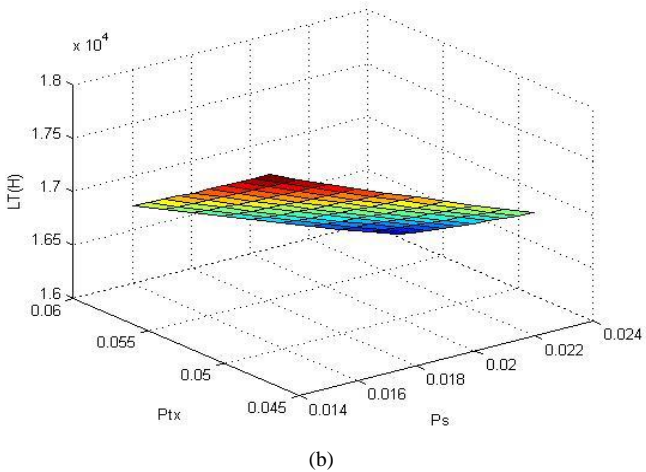
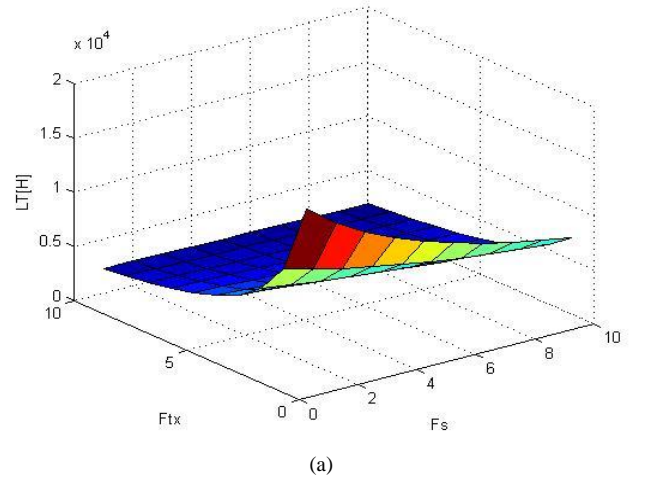


Fig. 2. Effect of frequencies and powers on node lifetime (a) Effect of sampling and transmission frequency on lifetime (b) Effect of processing and transmission power on lifetime.

In Fig. 2(b), the effect on the lifetime of a sensor node due to processing and transmission power is shown. The lifetime of sensor node is decreasing exponentially while transmission power increases. However, the lifetime of a sensor node is also decreasing when the sampling frequency increases but not exponentially. In Fig. 2(b) scenario, with P_{tx} varying, remaining lifetime of sensor node is lower as compared to P_s varying scenario.

From both Fig. 2(a) and 2(b), it can be predicted that more effective parameters on lifetime of the sensor node are sampling and transmission frequency. The lifetime of wireless Sensor node can be increased by decreasing these parameters.

Fig. 3 shows the effect of time and our model parameters (sampling frequency, transmission frequency, and processing power and transmission power) on the lifetime of a sensor

node. In Fig. 3(a) effect of time, sampling frequency and transmission frequency is shown. Sampling frequency has a very low effect on the energy consumption of sensor node as compared to a transmission frequency that is why remaining lifetime of sampling frequency parameter is more than transmission frequency. In Fig. 3(a) we can see that the remaining lifetime of sensor during transmission frequency effect is near 2000 hours. However, during sampling frequency effect, the sensor node remaining lifetime is nearly 5800 hours. In Fig. 3(b), 3(c) effect of transmission power and effect of processing power is shown. Processing power has less effect on energy consumption as compared to transmission power that is why the remaining lifetime of processing power parameter is more than the transmission power parameter. In Fig. 3(b) we can see that the remaining lifetime of the sensor is 10000 during transmission power varying. However, during processing power effect, the sensor node remaining lifetime is nearly 10500 hours as shown in Fig. 3(c). Here the graphical representation of Fig. 3(b) and 3(c) are not very accurate because of scaling issues.

From all parameters, we can see the more effective parameters on wireless node energy consumption are sampling frequency and transmission frequency. So, wireless sensor energy consumption can be minimized by reducing both parameters which are highly affecting the battery of sensor node.

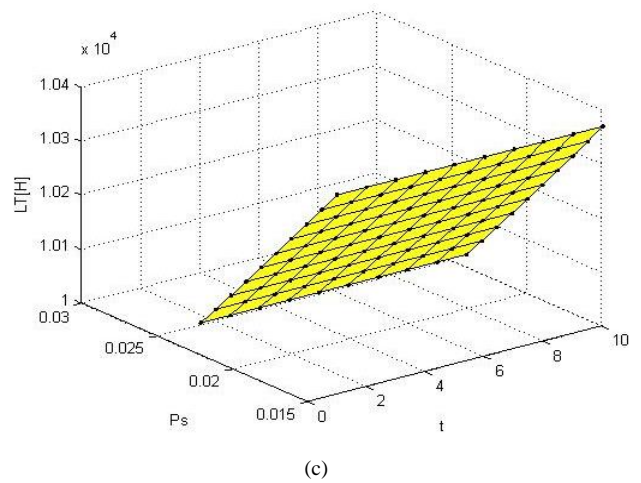
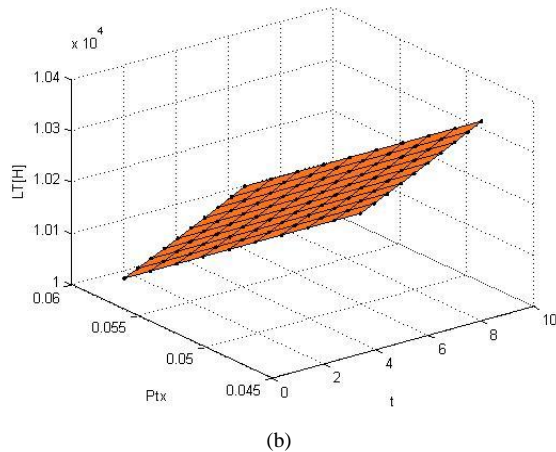
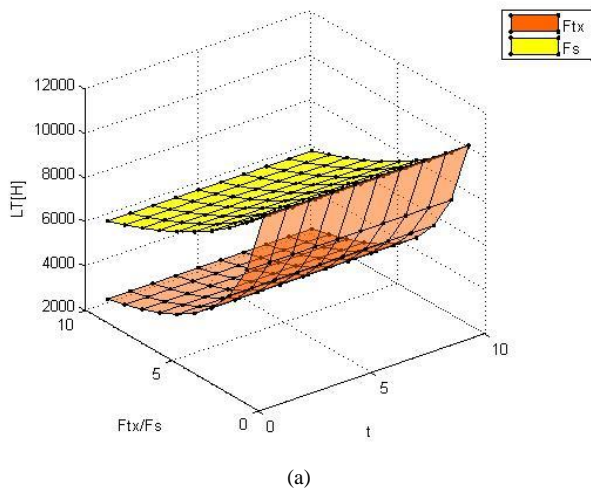


Fig. 3. Effect of time, frequencies and powers on node lifetime (a) Effect of time, sampling and transmission frequency on lifetime (b) Effect of time and transmission power on lifetime (c) Effect of time and processing power on lifetime.

Sensor lifetime totally depends on its energy consumption. The relation of sensor lifetime with energy consumption is given below:

$$\text{Life time of sensor} \propto \frac{1}{\text{Total energy consumption of sensor}} \quad (12)$$

According to the sensor lifetime relation, lifetime graphs are approximately resampled with the relation.

The overall goal is to derive a formulation for total energy consumption of wireless sensor node in order to get the best selection of wireless sensor parameters, which can reduce the energy consumption and enhance the battery life. As explained in graphical detail, we compared the impact of mainly four parameters on wireless sensor node which are the sampling frequency, transmission frequency, processing power and transmission power. According to Fig. 2 and 3, transmission frequency and sampling frequency have a less remaining lifetime as compared to processing power and transmission power. As per our model, WSN lifetime can be enhanced by reducing the transmission and sampling frequency parameters.

V. CONCLUSION

In this paper, we proposed a new and realistic energy model for WSN. Energy consumption of four WSN parameters (sampling frequency, transmission frequency, processing power and transmission power) are investigated. We analyzed the effects of these parameters on a lifetime of wireless sensor nodes. The results show that two parameters, sampling frequency, and transmission frequency are much more effective on energy consumption and lifetime of wireless sensor nodes as compared to processing and transmission power. By reducing sampling and transmission frequency, energy consumption of wireless sensor nodes can be reduced. We expect that our work will help to improve the lifetime performance of wireless sensor networks.

ACKNOWLEDGMENT

This work is supported by the Higher Education Commission of Pakistan.

REFERENCES

- [1] Gannapathy, Vigneswara Rao, MohdRiduan Ahmad, MohdKadimSuaidi, Muhammad Syahrir Johal, and ErykDutkiewicz. "Concurrent MAC with short signaling for multi-hop wireless mesh networks." In *Ultra Modern Telecommunications & Workshops, 2009. ICUMT'09. International Conference on*, pp. 1-7. IEEE, (2009).
- [2] Ibrahim, Tuani, Ahamed Fayeez, Vigneswara Rao Gannapathy, Md Isa, Ida Syafiza, Sarban Singh, Ranjit Singh, and Siva Kumar Subramaniam. "Throughput Analysis of Energy Aware Routing Protocol for Real-Time Load Distribution in Wireless Sensor Network (WSN)." *International Journal of Research Engineering and Technology* 2 (2013): 540-544.
- [3] Wang, Andrew Y., and Charles G. Sodini. "A simple energy model for wireless microsensor transceivers." In *Global Telecommunications Conference, 2004. GLOBECOM'04. IEEE*, vol. 5, pp. 3205-3209. IEEE, (2004).
- [4] Sha, Kewei, and Weisong Shi. "Modeling the lifetime of wireless sensor networks." *Sensor Letters* 3, no. 2 (2005): 126-135.
- [5] Wang, Andrew Y., and Charles G. Sodini. "On the energy efficiency of wireless transceivers." In *Communications, 2006. ICC'06. IEEE International Conference on*, vol. 8, pp. 3783-3788. IEEE, (2006).
- [6] Zheng, Meng, Haibin Yu, Jianying Zheng, and Peng Zeng. "Tradeoff between utility and lifetime in energy-constrained wireless sensor networks." *Journal of Control Theory and Applications* 8, no. 1 (2010): 75-80.
- [7] Liu, Tao, Qingrui Li, and Ping Liang. "An energy-balancing clustering approach for gradient-based routing in wireless sensor networks." *Computer Communications* 35, no. 17 (2012): 2150-2161.
- [8] Kamyabpour, Najmeh, and Doan B. Hoang. "Modeling overall energy consumption in Wireless Sensor Networks." arXiv preprint arXiv:1112.5800 (2011).
- [9] Kaurav, Jyoti, and Kaushik Ghosh. "Effect of Transmitting Radius, Coverage Area and Node Density on the Lifetime of a Wireless Sensor Network." (2012).
- [10] Fayeez, A. T. I., V. R. Gannapathy, Ida S. Md Isa, M. K. Nor, and N. L. Azyze. "Literature review of battery-powered and solar-powered wireless sensor node." *Asian Research Publishing Network-Journal of Engineering and Applied Sciences* 10, no. 2 (2015): 671-677.
- [11] AkanshaTomar and Prof.GauravBardwaj, "A survey on dynamic power management techniques in wireless sensor networks", *INT.J.AREEIE*, (2016), vol.5(6):2320-3765.
- [12] Krishan Kumar Ms. Shruti Goel,"Literature Review to Optimize the Energy Consumption in Wireless Sensor Network" *International Journal of Computer Science and Mobile Computing*, Vol.6 Issue.7, July- (2017), pg. 106-113
- [13] Rodrigues, Leonardo M., Carlos Montez, Gerson Budke, Francisco Vasques, and Paulo Portugal. "Estimating the Lifetime of Wireless Sensor Network Nodes through the Use of Embedded Analytical Battery Models." *Journal of Sensor and Actuator Networks* 6, no. 2 (2017): 8.
- [14] Corporaton, Moteiv. "Tmote Sky: Datasheet." (2006).
- [15] Amiri, Moslem. "Measurements of energy consumption and execution time of different operations on Tmote Sky sensor nodes." PhD diss., Masarykovauniverzita, Fakultainformatiky, (2010).
- [16] DEVADIGA, Ketan. IEEE 802.15. 4 and the Internet of things.
- [17] Sivagami, A., K. Pavai, D. Sridharan, and SAV Satya Murty. "Estimating the energy consumption of wireless sensor node: Iris." *International J. of Recent Trends in Engineering and Technology* 3, no. 4 (2010).

Day-Ahead Load Forecasting using Support Vector Regression Machines

Lemuel Clark P. Velasco, Daisy Lou L. Polestico, Dominique Michelle M. Abella,
Genesis T. Alegata, Gabrielle C. Luna
Mindanao State University-Iligan Institute of Technology
Premier Research Institute of Science and Mathematics
Iligan City, The Philippines

Abstract—Accurate day-ahead load prediction plays a significant role to electric companies because decisions on power system generations depend on future behavior of loads. This paper presents a strategy for short-term load forecasting that utilizes support vector regression machines. Proper data preparation, model implementation and model validation methods were introduced in this study. The SVRM model being implemented is composed of specific features, parameters, data architecture and kernel to achieve accurate pattern discovery. The developed model was implemented into an electric load forecasting system using the java open source library called LibSVM. To confirm the effectiveness of the proposed model, the performance of the developed model is evaluated through the validation set of the study and compared to other published models. The created SVRM model produced the lowest Mean Average Percentage Error (MAPE) of 1.48% and was found to be a viable forecasting technique for a day-ahead electric load forecasting system.

Keywords—Support vector regression machines; day-ahead load forecasting; energy analytics

I. INTRODUCTION

Accurate day-ahead load prediction demand plays a very significant role to electric companies because operation decisions in power systems such as unit commitment, contingency analysis, field scheduling, reducing spinning reserve, reliability analysis, load flow, and scheduling device maintenance depend on future behavior of loads [1]-[3]. It was pointed out that there is no substantial energy storage in the electric transmission and distribution system [1], [4]. Because of this existing limitation, utility companies invest greatly in load prediction to ensure that the basis of their operational decisions are reliable and in keeping the equilibrium between production and consumption since electricity cannot be stored. It should be stressed that inaccurate load predictions are costly to utility companies. When there is an underestimation in energy demand, it may result in limited supply of electricity at the consumer end, which leads to energy quality reduction in system reliability and there is an increase in operating costs when there is an overestimation in forecasting error [2], [3].

A computational intelligence method involving Support Vector Machines (SVM) has gained attention in the field of forecasting. SVM is a machine learning method based on statistical learning theory [1], [2], [5]. It was originally used for pattern recognition and classification but its importance

increased when its algorithm was extended to solve regression problems, thus the nomenclature: Support Vector Regression Machine (SVRM). Only in 2001 on a European Network on Intelligent Technologies for Smart Adaptive Systems (EUNITE) competition in Taiwan was it realized that SVRM can also be used for load forecasting. Since then there have been several studies that explored different techniques to use or optimize SVRM for load forecasting of unique data sets [1], [2], [6], [7].

In the Philippines, a certain power utility is faced with a challenge to predict electric load using the historical data they accumulated. The power utility's current attempt involves using linear regression model and SVRM has not been utilized in their context. The historical load data of the power utility company can be used to develop a day ahead electric load prediction model. This study attempted to develop a day-ahead electric load prediction model using SVRM using electric load data provided by the power utility. Specifically, the study developed a data preparation model for load forecasting and implemented a SVRM model into an electric load forecasting system using LibSVM and Java. Measures were then conducted to quantify the efficiency and validate the accuracy of the developed SVRM prediction model. With this, SVRM was utilized to analyze and predict day-ahead load forecasting using the historical load data that a power utility company has accumulated with the aim to solve the long term problem of managing the supply and demand of the locality's power system.

II. METHODOLOGY

A. Load Data Preparation Methodology

There are many factors that can affect the success of machine learning, one of which is the quality of the data, so pre-processing of the data is essential [8]-[10]. In this study, a series of steps was conducted involving data description, data representation and feature selection. Data description discusses the time range of the data, and the description of its contents. Daily historical delivered load data was acquired from an electric utility which details were thoroughly recorded and examined. A description of the features present in the data was formulated as well as its structure along with other attributes including additional features. In data representation, the load data were represented, scaled and then partitioned. Binary was used represent non-numeric features, e.g. one (1) marks weekday which is a day type feature, while one-one-zero (110)

This work is supported by the Mindanao State University-Iligan Institute of Technology (MSU-IIT) as an internally funded research under the Premier Research Institute of Science and Mathematics (PRISM).

marks January which is a month type feature. The rest of the possible features that require representation used the same method of binary representation [7]. Scaling was also implemented to the load data since a study suggested that scaling is an important stage for training the SVRM in such a way that the higher values should not suppress the lower values in order to retain the activation function [11]. Min - Max scaling method as shown in (1) was then used as suggested by authors [3], [8], [11].

$$x' = \frac{x - \min(x)}{\max(x) - \min(x)} \quad (1)$$

After representation and scaling, the load data was partitioned into two data sets: the training set and validation set where the training set was used for training the model while the validation set was used for testing the design of the model to confirm its predictive accuracy. Features which are data attributes in a specific data set that can affect the performance of machine learning were then filtered by feature selection. Feature selection, also known as variable selection or attribute selection, aims to identify the most relevant input variables within a data set and removing irrelevant, redundant, or noisy data [9], [10], [12]. It is defined as the process of selecting D most discriminatory features of $d > D$ available ones [13]. Proper selection of features can improve the prediction performance and provide a better understanding of the underlying process that generated the data [9], [10], [12], [13].

The expected output of feature selection is a list of relevant features that is used in making the predictive model. Given a subset of the whole data set, various feature selection algorithms were tested for performance. According to a study there are two broad categories in feature selection: the wrappers and the filters [9]. The study proved that filters are more practical than wrappers because they are much faster in large databases while supporting correlation-based approach. A study conducted suggested using the same approach through the Baye's function method while a separate study proposed another feature selection method based on information gain approach [13]. Thus in this study, correlation-based filter feature selection was used implemented in R programming and Weka software open source environments. After identifying the correct features the data in an .xls format were converted into a libsvm format using R programming.

To eliminate human opinion on selecting the appropriate attributes for the electric load prediction, this research used correlation-based feature selection, namely, Pearson's correlation, Spearman correlation matrix, and Kendall's correlation to improve the accuracy of machine learning. The value of a correlation coefficient ranges between -1 and 1. The strongest linear relationship is indicated by a correlation coefficient of -1 or 1 while the weakest linear relationship is indicated by a correlation coefficient equal to 0. A positive correlation means that if one variable gets bigger, the other variable tends to get bigger. A negative correlation means that if one variable gets bigger, the other variable tends to get smaller. This study used R programming language to implement the three correlation based approach. To implement these three correlation based approaches, the function `cor()` of R was used. The `cor()` function calculates the weighted

correlation of the given data set. The format used for this function is shown in (2) where x is the matrix or the data set, use specifies the handling of missing data with options: .obs, complete.obs, pairwise.complete.obs and method to specify the type of correlation: pearson, spearman or kendall.

$$\text{cor}(x, \text{use} = , \text{method} =) \quad (2)$$

B. SVRM Model Implementation Methodology

The researchers used LIBSVM's Java library, an open source integrated software for support vector classification, regression and distribution estimation. It was developed by the National Taiwan University and written in C++ through a C API [14]. It has many bindings for programming languages such as Java, MATLAB and Python. Creating the model, selecting the kernel and the parameters were done through the use of LIBSVM functions such as `svm-train()` and `svm-predict()`. A software was designed and developed to implement a SVRM model as well as carry out the process needed for the load prediction starting from data loading to the generation of the predicted values. The process started with the development of the module for the data loading and scaling so that it can be loaded into the system. Then the researchers proceeded in implementing a SVRM model into the system wherein the already prepared data was loaded and will then output the predicted load values in table form. System reports such as visualization for comparing the actual and forecasted load, exporting the results to a spreadsheet file, and printing the predicted load values were also included in the system adding to its functionality. After all the development has been done, the researchers performed various tests to the software to check for bugs and errors to assess the software's quality and usability and to ensure that it will produce accurate results. Once the testing has been performed and all the quality checks were done, the system was packaged ready for deployment.

The SVRM model was identified to consist of Radial Basis Function (RBF) kernel with parameters of $c=125$, $g=0.001$, $e=0.01$ and $p=0.0045$ to train the SVRM model. The model's architecture has day load consumption attributes in 15-minute resolution from each of the following: 1 day before, 2 days before, 7 days before, and 14 days before. This architecture is denoted as $i-1$, $i-2$, $i-7$, $i-14$ where i represents the day to be predicted and the number after the subtraction sign represents the number of days before the predicted data. After implementing the SVRM model, the predictive accuracy of the model was validated by comparing the resulting forecasted electric load values to the actual delivered load values performed in ten repetitions of day-ahead load forecast. To assess the predictive accuracy of the SVRM model, Mean Absolute Percentage Error (MAPE) as suggested by researchers [6], [7], [11]. Since smaller MAPE values would indicate consistency and accuracy, daily MAPE were computed to test the day-to-day accuracy of the model along with the average MAPE to evaluate the performance of the model in a monthly scale. The resulting values were compared to the tolerance error and standard set by the local power utility. A tabular and graphical representation of the computations was then generated with the purpose of illustrating the comparison between the actual and predicted electric load values.

III. RESULTS AND DISCUSSION

A. Load Data Preparation Results

Electric load data from January 2013 to December 2014 were stored in spreadsheets with .xls file format. Each file represents the electric load data for a single month and contains three sheets corresponding to the three metering substations of the power utility. As shown in Table I, each sheet contains the metering point (SEIL), the billing date (BDATE), time in 15 minute resolution, kilowatt delivered (KW_DEL), kilowatt per hour delivered (KWH_DEL), and kilo volt amps reactive hours delivered (KVARH_DEL). KW_DEL is the load to maintain and the basis for load prediction while KWH_DEL is for billing consumption and kilo volt amps reactive hours delivered (KVARH_DEL) represents the reactive power. The data used as input for the SVRM models is the attribute kilowatt delivered (KW_DEL) for the reason that it is also the column considered by power utilities in determining forecasted load values for the next day. A total of 70,109 rows of data was then fed into the SVRM model.

TABLE I. SAMPLE RAW DATA FORMAT

SEIL	BDATE	TIME	KW_DEL	KWH_DEL	KVARH_DEL
XX	12/26/11	00:15	XXXX	XXXX	XXXX
...
XX	12/26/11	24:00	XXXX	XXXX	XXXXX

This study added attributes such as calendar day, holiday, day type, and day to the original data set since a study strongly suggest that these attributes will affect the electric load [2]. These attributes will then be represented by binary variables as suggested by authors [7], [15]. Table II shows the binary equivalent for the said attributes. The time attribute in 15-minute resolution was converted into numerical values since LIBSVM does not accept variables represented with a semicolon. Starting at 00:15, which is 12:15 AM, time was given a representation value of 1. And for every increment of 15 minutes, the representation value is incremented by 1. This process iterates until 00:15-24:00 is converted from 1 to 96. Part of data representation is data scaling which is expected to aid in a more accurate SVRM model. In this research, the predictive variable which is the KW_DEL has been scaled using Min - Max with a scale from zero to one. After data was scaled, the data was partitioned into training data set and validation data set. January 1, 2013 to November 2014 was set as training dataset while December 2014 was set as validation and testing dataset. The available dataset of December 2014 starts from December 1, 2014 to December 25, 2014. Partitioning the electric load data is necessary to group them according to their use. The training set which should comprise the largest part of the datasets was used to train the models with different parameters and the validation set was used to check the accuracy of the trained models [3], [8], [16].

TABLE II. ATTRIBUTE-BINARY TABLE

Day	Binary Value	Day	Binary Value	Day Type	Binary Value	Date Type	Binary Value
Monday	100000	Friday	111110	Week - Day	1	Holiday	1
Tuesday	110000	Saturday	111110	Week - end	0	Non-holiday	0
Wednesday	111000	Sunday	111111				
Thursday	111100						

To improve the accuracy and effectiveness of the model, this study performed feature selection. The effect of not undergoing feature selection is that researchers will have to do more unnecessary data training with and without certain features to determine whether or not certain attributes have effects on the accuracy of the prediction [2], [5]. To show that feature selection has a significant effect on prediction accuracy, this research ran a sample model with parameters $c=125$ $g=0.001$ $e=0.01$ $p=0.0045$, kernel Radial Basis Function along with the model's architecture with two data sets. The first data set was filtered by feature selection and the second data set was one that did not undergo feature selection. Table III shows that the SVRM model with a data set that underwent feature selection with a MAPE value of 4.09% performs better than the model without feature selection with 6.77% MAPE value. The MAPE value generated in the two datasets is the average of the daily MAPE values of the validation set used in this study. This study confirms that feature selection does increase accuracy.

TABLE III. MODEL WITH FEATURE SELECTION VS. MODEL WITHOUT FEATURE SELECTION

Model	MAPE Values
Model with Feature Selection	4.09%
Model without Feature Selection	6.77%

Table IV summarizes the correlation of KW_DEL to time, month, year, day type, date type and day to systematically choose features for the implemented SVRM model. Time attribute has a 0.52901261, 0.56725912 and 0.39739378 respectively as correlation values to Pearson's, Spearman's and Kendall's tests. It is shown that the time attribute has the highest correlation to KW_DEL while month, year, day type, day, and date type have a relatively low correlation to KW_DEL. Performing the three types of correlation based approach resulted to the selection of time attribute as the only attribute that can affect the predictive variable KW_DEL. All three approaches have shown that time has the highest correlation to KW_DEL and thus a valid candidate as a feature for the SVRM model while the rest of the attributes show a low correlation to KW_DEL.

TABLE IV. SUMMARY OF THE CORRELATION BETWEEN KW_DEL AND OTHER ATTRIBUTES

	Pearson	Spearman	Kendall
Time	0.52901261	0.56725912	0.39739378
Month	-0.270584464	-0.2463835254	-0.1805927803
Year	-0.0675271275	-0.0749241004	-0.0615430231
Day type	-0.028027669	-0.0489527428	-0.0402100228
Date type	-0.021399675	-0.027798819	-0.022834086
Day	-0.0183968342	-0.0434596375	-0.0312288852

B. SVRM Model Implementation Results

The developed software allows the user to set the parameters in training the SVRM model such as the cost value of C, the epsilon function, width of epsilon function and the gamma function for the radial basis function kernel. In addition, the user can also select which kernel to use for training the SVRM. As shown in Fig. 1, these options will add flexibility for the users and will enable the support vector regression machines to be retrained in the future if there will be possible significant changes on the behavior of the daily load consumption.

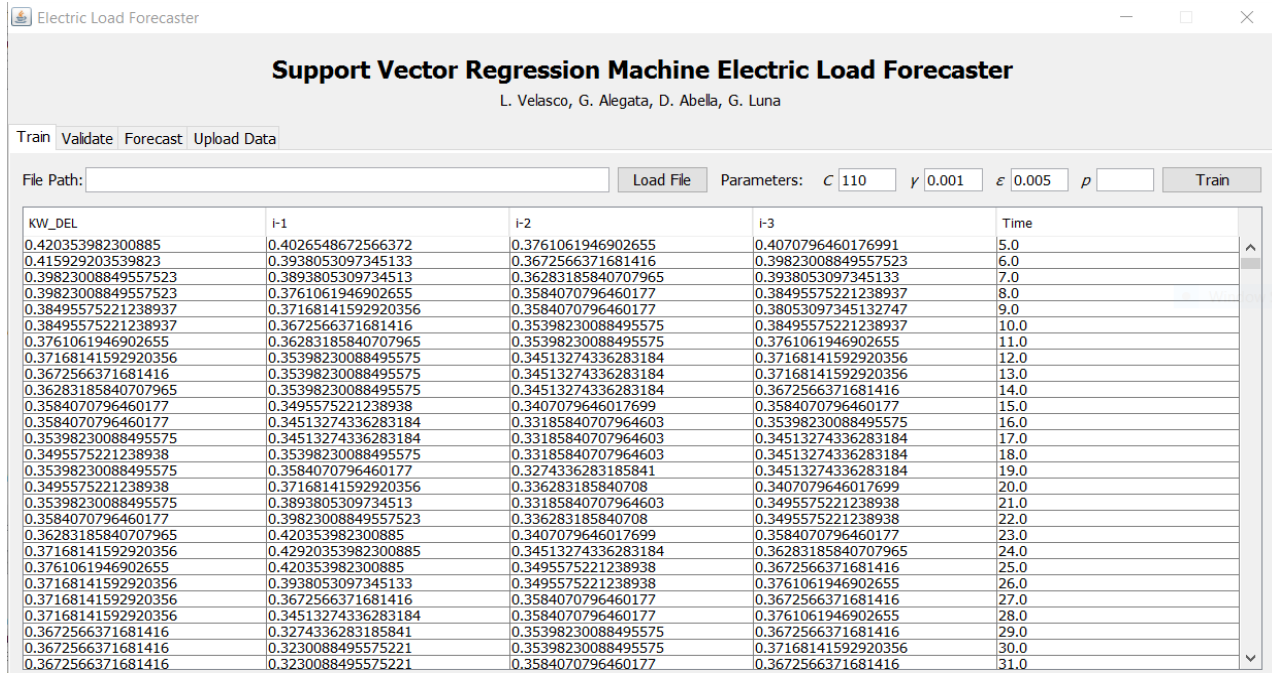


Fig. 1. The input interface of the load prediction software.

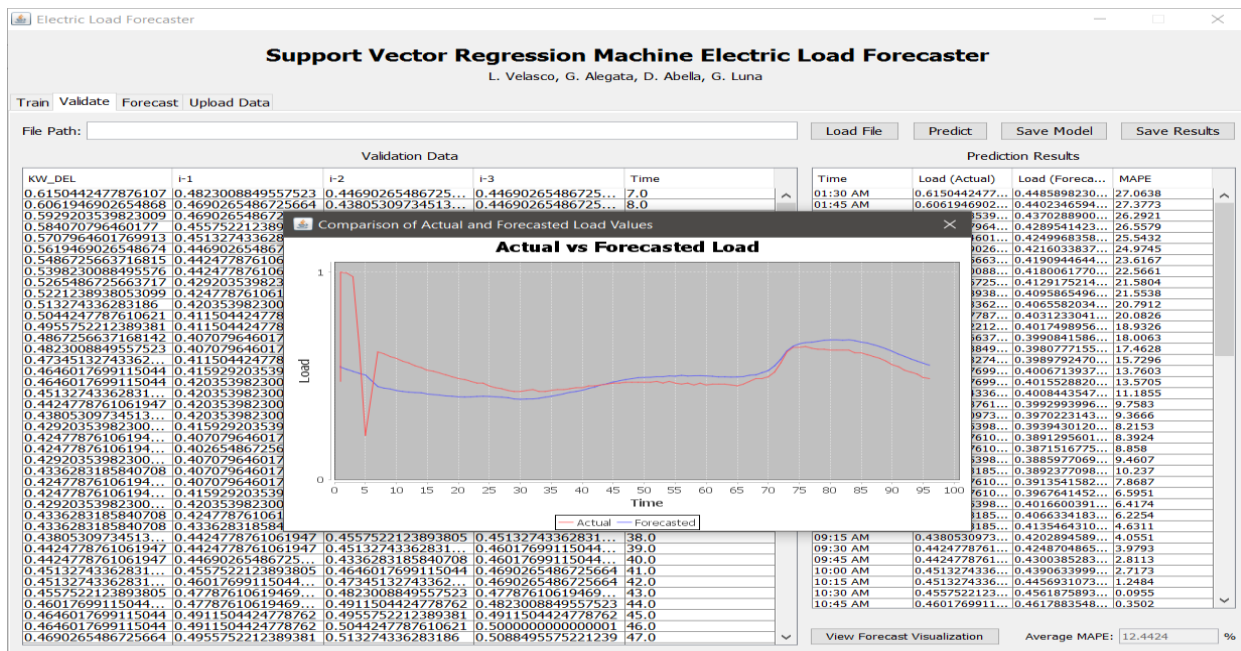


Fig. 2. The output interface of the load prediction software.

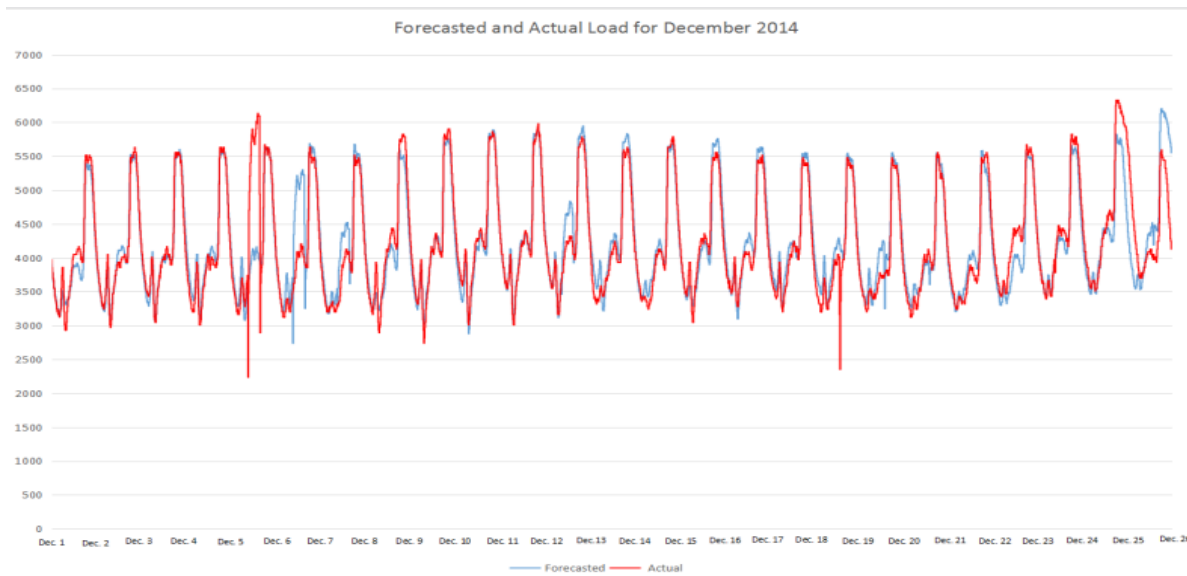


Fig. 3. Actual load vs. predicted load.

The model was trained based on the architecture using the function called `svmTrain()`. After training the data, the developed system automatically validated the trained data and forecasted results. A table and a graph were generated to compare the actual values and the predicted values as shown in Fig. 2.

The model achieved an average of 4.03% for the 25 days of December while the lowest MAPE achieved for a day was 1.59% achieved in the prediction for Dec. 11, 2014 load. As shown in Fig. 3, the highest MAPE was 11.29% taken on December 25, 2014.

The developed SVRM model, taking past electric load data and time as the only attributes, was not optimized enough to adjust for KW_DEL prediction for Christmas day since holiday and special events were not considered in training the model. If Christmas day was excluded in validation set, the average MAPE for the 24 remaining days of December 2014 would be 3.73%, which is significantly lower, instead of 4.03%. Table V shows a portion of MAPE values of the predicted days for one week. While the implemented SVRM model produces a MAPE of 4.03%, a study produced an SVRM model with MAPE of 3.67% [2]. But it is worth noting that the study used attributes day, date type, electricity price, and daily temperature. Another study which also used the same architecture produced a MAPE of 2.86% and used only the attributes day and date while this study only used attributes of past KW_DEL and time [6]. Also, comparing with other load forecasting studies which does not use SVRM showed that the model generated in this study performs at par, if not, better with other models created using different methods. This is a study which used ANN in load forecasting for a Nigerian electrical power system and yielded an average error of 2.54% and lowest error in a day of 1.73% [17]. The study used the load values of the previous hour, day and week, the day of the week and the hour of the day as network inputs. While another study on day-ahead load forecasting which utilized ANN on this study's datasets only yielded 2.40% and 2.80% as the lowest and highest MAPE respectively on a week's forecast [16].

TABLE V. SUMMARY OF THE CORRELATION BETWEEN KW_DEL AND OTHER ATTRIBUTES

DATE	MAPE	DATE	MAPE
Dec-09	2.54%	Dec-13	3.44%
Dec-10	3.68%	Dec-14	2.01%
Dec-11	1.58%	Dec-15	2.57%
Dec-12	3.44%		

Moreover, validation was also done by comparing the performance of the SVRM model with local forecasting standards. Having a lowest error of 1.59% places the prediction accuracy of the model well under the 5% acceptable tolerance rate of the locality's electricity spot market and according to a study, 2%-3% error range for a day-ahead prediction is considered normal and will be considered as reliable [18]. Thus, the forecasting performance of the SVRM model is within the acceptable error and considered as accurate and reliable. Below illustrates the results of the developed model which confirms the ability of the model to forecast a day-ahead load within the acceptable error.

IV. CONCLUSION AND RECOMMENDATIONS

This paper proposed a short term electric load forecasting strategy using SVRM by executing data preparation and by implementing an SVRM model in LIBSVM. An application software with features to scale, train, validate, forecast and visualize results of the data was developed using Java. Data preparation which is composed of data representation and correlation-based feature selection paved the way for the implementation of an SVRM model with Radial Basis Function kernel. Having parameters of $C = 110$, $g = 0.001$, $e = 0.01$ and $p = 0.005$ implemented in an architecture, the implemented model produced the lowest MAPE of 1.48% in day ahead load prediction and an average of 4.44% for the prediction in December 2014.

Based on the findings of the study, the researchers would like to recommend for further studies in utilizing SVRM to

expand the pool of knowledge on electric load forecasting using. It is recommended to explore different methods in selecting kernels as this will help in establishing a reliable SVRM process in electric load forecasting. Studies focused on ensuring that kernels would fit a given electric load data can be conducted as this will increase potential in the accuracy of prediction using SVRM models. The researchers also recommend for the conduct of performing grid-search for parameters and an automated system that performs parameter selection that are suited and optimized for SVRM as this will also help in improving the accuracy of prediction.

This study aims to contribute to the technologies of developing an electric load forecasting model and an electric load forecasting software that could aid power utility companies in their decision-making, electric load planning and load power utilization. The results generated and obtained in this study clearly suggests that with proper data representation, feature selection, and SVRM model implementation, SVRM is a viable forecasting technique for a day - ahead electric load forecasting system.

ACKNOWLEDGMENT

The authors would like to thank the support of the MSU-IIT Office of the Vice Chancellor for Research and Extension and PRISM-Premiere Research Institute in Sciences and Mathematics for their assistance in this study.

REFERENCES

- [1] E. E. Elattar, J. Goulermas, and Q. H. Wu, Electric load forecasting based on locally weighted support vector regression. In Proc. IEEE Transactions on Systems, Man and Cybernetics C, Vol. 40, No. 4, pp. 438–447 (2010).
- [2] B. E. Türkay, and D. Demren, Electrical load forecasting using support vector machines. In Proc. 7th International Conference on Electrical and Electronics Engineering (ELECO), pp. I-49-I-53, (Bursa, 2011).
- [3] L. C. P. Velasco, P. B. Bokingkito, and J. T. Vistal, Week-Ahead Load Forecasting using Multilayer Perceptron Neural Network for a Power Utility. In Proc. 17th Conference of the Science Council of Asia, (Manila, 2017)
- [4] E. Almehaie, and H. Soltan, A methodology for electric power load forecasting, Alexandria Engineering Journal, 50(2), pp. 137-144 (2011)
- [5] B. Schölkopf, and A. J. Smola, A. J. (2002), Support vector machines and kernel algorithms. The Handbook of Brain Theory and Neural Networks, (MIT Press, 2002).
- [6] S. Ostojin, F. Kulić, G. Švenda, and R. Bibić, Short-term electrical load forecasting using support vector machines. Computers and simulation in Modern Science Vol I; Mathematics and Computers in Science Engineering, (WSEAS Press, A Series of Reference Books and Textbooks, 2008)
- [7] E. Ceperic, V. Ceperic, and A. Baric, A strategy for short-term load forecasting by support vector regression machines. In Proc. IEEE Transactions on Power Systems, Vol. 28, No. 4, pp. 4356–4364, (2013).
- [8] L. C. P. Velasco, P. N. C. Palahang, C. R. Villezas, and J. A. A. Dagaang, Performance Analysis of Different Combination of Training Algorithms and Activation Functions in Predicting the Next Day Electric Load. In Proc. of 16th Philippine Computing Science Congress 2016, Computing Society of the Philippines, (Puerto Princesa, 2016)
- [9] M. A. Hall, L. A. Smith, Feature Selection for Machine Learning: Comparing a Correlation-Based Filter Approach to the Wrapper. In Proc. 12th Int'l Florida Artificial Intelligence Research Society Conference, pp. 235-239, (Florida, 1999).
- [10] V. Kumar and S. Minz, Feature Selection: A Literature Review. Smart Computing Review, Korea Academia-Industrial Cooperation Society, Vol. 4, No. 3, pp. 211-229, (2014).
- [11] A. Jain and B. Satish, Clustering based Short Term Load Forecasting using Support Vector Machines. In Proc. 2009 IEEE Bucharest PowerTech, pp. 1-8. (Bucharest, 2009)
- [12] M. Sarhani, A. El Afia, Electric load forecasting using hybrid machine learning approach incorporating feature selection. In Proc. International Conference on Big Data Cloud and Applications pp. 1-7, (2015).
- [13] M. Haindl, P. Somol, D. Verweridis and C. Kotropoulos, Feature Selection Based on Mutual Correlation. Progress in Pattern Recognition, Image Analysis and Applications (Springer, 2006).
- [14] C. Chang and C. Lin, LIBSVM - A Library for Support Vector Machines, Retrieved April 17, 2017, from National Taiwan University: <https://www.csie.ntu.edu.tw/~cjlin/libsvm/>, (2011).
- [15] J. M. Espinoza, J. Suykens, R. Belmans, and B. D. Moor, Electric load forecasting, In Proc. IEEE Control Systems, 27(5), pp. 43–57 (2007).
- [16] L. C. P. Velasco, C. R. Villezas, P. N. C. Palahang, and J. A. A. Dagaang, Next day electric load forecasting using Artificial Neural Networks. In Proc. of the IEEE International Conference on Humanoid, Nanotechnology, Information Technology, Communication and Control, Environment and Management (HNICEM), (Cebu, 2015).
- [17] G. A. Adepoju, S. O. A. Ogunjuyigbe, and K. O. Alawode, Application of Neural Network to Load Forecasting in Nigerian Electrical Power System. The Pacific Journal of Science and Technology, 8(1), pp. 68-72, (2007).
- [18] H. Soliman, K. Sudan, and A. Mishra, A smart forest-fire early detection sensory system: another approach of utilizing wireless sensor and neural networks, IEEE Sensors, pp.1900-1904, (2010).

Online Estimation of Wind Turbine Tip Speed Ratio by Adaptive Neuro-Fuzzy Algorithm

Aamer Bilal Asghar¹, Xiaodong Liu²

School of Control Science & Engineering
Faculty of Electronic Information & Electrical Engineering
Dalian University of Technology
Dalian 116024, P.R. China

Abstract—The efficiency of a wind turbine highly depends on the value of tip speed ratio during its operation. The power coefficient of a wind turbine varies with tip speed ratio. For maximum power extraction, it is very important to hold the tip speed ratio at optimum value and operate the variable-speed wind turbine at its maximum power coefficient. In this paper, an intelligent learning based adaptive neuro-fuzzy inference system (ANFIS) is proposed for online estimation of tip speed ratio (TSR) as a function of wind speed and rotor speed. The system is developed by assigning fuzzy membership functions (MFs) to the input-output variables and artificial neural network (ANN) is applied to train the system using back propagation gradient descent algorithm and least square method. During the training process, the ANN adjusts the shape of MFs by analyzing training data set and automatically generates the decision making fuzzy rules. The simulations are done in MATLAB for standard offshore 5 MW baseline wind turbine developed by national renewable energy laboratory (NREL). The performance of proposed neuro-fuzzy algorithm is compared with conventional multilayer perceptron feed-forward neural network (MLPFFNN). The results show the effectiveness of proposed model. The proposed system is more reliable for accurate estimation of tip speed ratio.

Keywords—Wind speed; rotor speed; power coefficient; tip speed ratio; ANFIS

I. INTRODUCTION AND MOTIVATION

Wind is a sustainable source of energy and is considered as a best alternate of limited fossil fuel resources. Wind power is economical and environment friendly. Wind power generation system mainly consists of a wind turbine and an electric generator. Wind turbine blades convert the kinetic energy of wind into mechanical energy and generator converts the mechanical energy into electrical energy. Wind turbine plays a vital role in power generation. The wind turbine rotor speed must be controlled in varying wind speed conditions [1].

The mechanical power captured by wind turbine depends on the value of power coefficient (C_p). Wind turbine operating at maximum value of power coefficient ($C_{p_{max}}$) captures maximum power from wind. The power coefficient is a nonlinear function of tip speed ratio (λ) and blade pitch angle (β). Wind turbine achieves maximum value of power coefficient ($C_{p_{max}}$) at optimal tip speed ratio (λ_{opt}) [2], [3].

TSR actually compares the rotor speed with the wind speed (v). Higher rotor speed as compared to wind speed means higher TSR. The wind turbine has maximum efficiency at optimal TSR (λ_{opt}) which corresponds to maximum power coefficient ($C_{p_{max}}$). Therefore, it is very important to control the rotor speed according to the available wind speed. The optimal tip speed ratio (λ_{opt}) depends on many factors such as number of blades, size (length) of blade and the shape of airfoil used [4]. The lesser number of blades and longer blade length leads to higher optimal TSR. Small wind turbines have higher rotational speed but as their blade length is small, so their optimal TSR is not as much as large wind turbines. The optimal TSR for single blade and 2 blade wind turbine is around 9 and 6 respectively. The optimal TSR for a 3 blade wind turbine is 5 which can be further improved up to 7 or 8 by using highly efficient and well-designed airfoil rotor blades. Generally, it is taken as 7 for a 3 blade wind turbine. The optimal TSR for a 4 blade wind turbine is around 3. The flow of air around wind turbine blades produces aerodynamic noise which keeps growing with wind speed. The speed of blade tip (end point of the blade) is a critical factor in deciding the aerodynamic noise produced by the wind turbine. Wind turbine with higher TSR produces more aerodynamic noise [5]. Moreover, the aerodynamic noise also depends on the shape of blade. Thin airfoil is used because of its aerodynamic benefits [6], [7]. A 3 blade wind turbine produces less noise as compared to a 2 blade wind turbine of the same size because of its lesser TSR. The higher number of blades produces more torque. The wind turbines having more than three blades are used for water pumping and grinding purposes. But, 4 blade wind turbines are not used for power generation because of their much higher cost, weight and less profit in terms of efficiency gain (0.5%) or power capturing. On the other hand, 2 blade wind turbines are also not preferred for power generation due to their higher aerodynamic noise. Moreover, 2 blade wind turbines with same size have higher TSR and in turn higher rotor speed, which increases the apparent weight (higher structural loading) of the blades. Therefore, brakes can fail in strong wind and a 2 blade wind turbine can collapse. So, a 3 blade design can produce more power at slower rotational speed than a 2 blade design and more cost efficient as compared to a 4 blade option. Therefore, 3 blade wind turbines are mostly used for power generation.

TSR varies with wind speed and tip speed of wind turbine. TSR should be maintained around its optimal value to extract maximum power. It is very important to estimate the TSR of wind turbine to control the power produced during its operation. In [8], [9] ANN based structure was built to predict the tip speed ratio for wind turbine profile types NACA 4415 and LS-1. The system was capable to efficiently estimate the value of TSR. An adaptive perturbation and observation (P&O) method was proposed in [10] for estimation of TSR and maximum power point tracking (MPPT). The proposed system was found more efficient than the classical perturbation and observation method. In [11], [12] tip speed ratio and MPPT was performed by measuring the wind speed and generator voltage and current. The designed system was implemented on a small scale wind turbine to validate its performance. In [13] two ANN models were proposed, one to operate the variable-speed wind turbine at optimum TSR for MPPT and the second ANN model for pitch control. The proposed model was found to have the capability of MPPT for varying wind speed.

The perturbation and observation (P&O) based algorithm is one of the most widely used methods for MPPT of wind turbine. The main disadvantage associated to this technique is that it keeps on oscillating around the maximum power point (MPP). Therefore, it does not exactly track the MPP which results in losing some part of the available power. However, this discrepancy can be covered by using smaller perturbation step. But it makes the algorithm slow in response and also affects the performance of controller to optimize the dynamic response of system. So, we have to compromise between reduced oscillations and fast dynamic response. The adaptive P&O method involves complex computation of derivatives. So, there is need to use some soft computing based techniques. The ANN is the most widely used soft computing technique to estimate the TSR. The ANNs have shown much better performance over conventional methods. The accuracy of ANN depends on the number of hidden layer neurons and the type of activation function used. The learning rate and optimization methods used (back propagation algorithm or Levenberg-Marquardt algorithm) also effect the performance. The training of ANN may be time taking as it involves many tuning parameters.

Hybrid intelligent systems are becoming very popular because of their ability to dealing with nonlinear systems. Hybrid systems are actually the combination of two different techniques. These systems are capable of realizing the nonlinear relationships with much higher accuracy. The ANFIS is also a type of hybrid systems. ANFIS is a combination of Takagi-Sugeno fuzzy inference system (T-S FIS) and ANN. Fuzzy systems make decisions of the basis of human reasoning and ANNs are trained to learn from the previous experiences or data. Researchers have successfully implemented ANFIS to deal fitting, forecasting, regression and classification problems [14]-[16].

The major aim of this study is to propose a hybrid intelligent learning based neuro-fuzzy methodology for accurate estimation of TSR for offshore 5 MW baseline wind turbine. The experimental data of wind turbine is collated to design the ANFIS model. The ANN trains the system using

hybrid learning method. The results of ANFIS are then compared with conventional MLPFFNN. The results show that ANFIS can estimate the TSR with much higher accuracy as compared to MLPFFNN.

II. WIND POWER FUNDAMENTALS AND SPECIFICATIONS OF NREL OFFSHORE 5 MW BASELINE WIND TURBINE

The mechanical power ' P_m ' captured by a wind turbine is expressed as,

$$P_m = \frac{1}{2} \rho A v^3 C_p(\lambda, \beta) \quad (1)$$

Here, ' ρ ' is the density of air in (kg/m^3), ' A ' is the area of the wind turbine rotor in (m^2) and ' v ' is the wind velocity in (m/s). The wind turbine power coefficient ' C_p ' is the measure of the efficiency of wind turbine. The power coefficient varies with the TSR (λ) and blade pitch angle (β).

The NREL virtually designed an offshore 5 MW baseline wind turbine to standardize the advancements is new techniques [17]. Researchers around the world use this model as a reference to investigate the aerodynamics and control of wind turbine. The specifications of offshore 5 MW baseline wind turbine are given in Table I.

As mentioned in Table I, the wind turbine reaches to its maximum power coefficient of 0.4868 at TSR of 7.55. The C_p -TSR curve of 5 MW wind turbine is shown in Fig. 1.

TABLE I. SPECIFICATIONS OF NREL OFFSHORE 5 MW BASELINE WIND TURBINE

Parameter	Value
Rated power	5 MW
Rotor configuration	Upwind,3 blades
Rotor, hub diameter	126 m, 3 m
Hub height	90 m
Cut-in, rated, cut-out wind speed	3 m/s, 11 m/s, 25 m/s
Cut-in, rated rotor speed	6.9 rpm, 12.1 rpm
Rated generator speed	1174 rpm
Peak power coefficient	0.4868
Tip speed ratio at peak power coefficient	7.55
Collective blade pitch angle at peak power coefficient	0°

When ' $\lambda < \lambda_{opt}$ ', the turbine speed is slow and a large fraction of undisturbed wind passes through the blades. Therefore, less energy is harnessed because of poorly designed rotor blades. When ' $\lambda = \lambda_{opt}$ ', the wind turbine operates at maximum value of power coefficient ($C_{P_{max}}$). Therefore, maximum energy is harnessed. When ' $\lambda > \lambda_{opt}$ ',

the turbine speed is so fast that the rotor behaves like a disk (wall). Therefore, less energy is harnessed. The wind turbine rotor is highly stressed and there is a risk of structure failure.

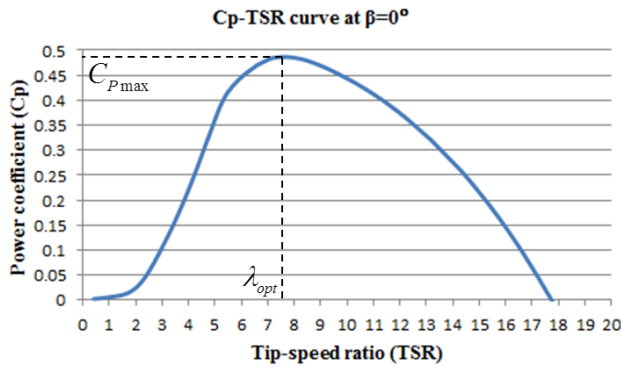


Fig. 1. C_p -TSR curve for NREL offshore 5 MW baseline wind turbine at pitch angle (β) of 0° .

The statistical properties of experimental data collected from offshore 5 MW baseline wind turbine are shown in Table II. The total number of collected data samples is 338. The collected data set is subdivided into training data and testing data. The training data is used to train the ANFIS based TSR estimator and then its performance is checked for testing data.

TABLE II. STATISTICAL PROPERTIES OF DATA USED TO DESIGN ANFIS BASED TSR ESTIMATOR

Wind turbine parameters	Average value	Max. value	Min. value
TSR	5.41	32.96	0.37
Rotor speed (rad/s)	0.8529	1.5707	0.1047
Wind speed (m/s)	13.834	25	3

III. METHODOLOGY

A. Structure of Adaptive Neuro-Fuzzy Inference System (ANFIS)

ANFIS is a soft computing technique to deal with highly nonlinear systems. It combines the features of T-S FIS and ANN in a single frame work to provide accurate decision making results. The ANFIS is a computationally intelligent system which involves parallel computing. The ANN uses the training data to update the parameters of fuzzy MFs [18]. The basic structure of ANFIS is shown in Fig. 2.

The output of first order T-S FIS with two IF-THEN fuzzy rules can be expressed as,

Rule-1: If ' x ' is A_1 and ' y ' is B_1 then

$$f_1 = p_1x + q_1y + r_1$$

Rule-2: If ' x ' is A_2 and ' y ' is B_2 then

$$f_2 = p_2x + q_2y + r_2$$

Here, ' x ' and ' y ' are two inputs and ' f ' is the output.

Where, ' p ', ' q ' and ' r ' are consequent parameters of the first order polynomial.

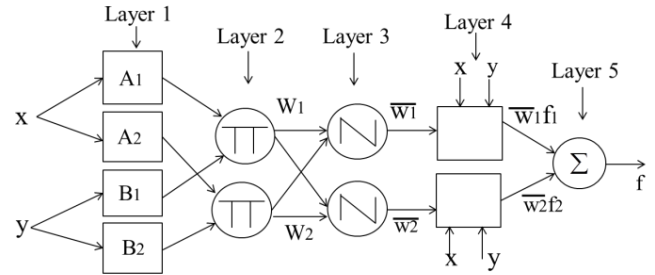


Fig. 2. The basic architecture of ANFIS.

ANFIS architecture consists of five layers of neurons. The first layer is called fuzzification layer and each neuron in this layer is adaptive. In first layer, MFs are assigned to each input variable. The input MFs can be bell-shaped, Gaussian, triangular, trapezoidal and dsigmoid, etc.

Each neuron in second layer computes the firing strength of fuzzy rule by multiplying the incoming signals.

$$W_i = \mu_{A_i}(x) \cdot \mu_{B_i}(y) \quad (2)$$

The neurons in third layer calculate the normalized firing strength of each rule.

$$\bar{W}_i = \frac{W_i}{\sum W_i} \quad (3)$$

Each neuron in the fourth layer is adaptive and this layer is called defuzzification layer. Each neuron multiplies the normalized firing strength of a rule with corresponding output polynomial function to get a crisp output.

$$\bar{W}_i \cdot f_i = \bar{W}_i(p_i x + q_i y + r_i) \quad (4)$$

The fifth layer has a single neuron which sums up all incoming signals from layer 4 and produces a single crisp output.

$$f = \sum \bar{W}_i \cdot f_i = \frac{\sum W_i \cdot f_i}{\sum W_i} \quad (5)$$

IV. DEVELOPING THE TSR ESTIMATORS

A. ANFIS based Estimator

The ANFIS analyzes the input-output training data set and trains the system using hybrid learning algorithm. Experiments are conducted for each type of input MF and ANFIS is designed using grid partitioning. Six MFs are assigned to each input parameters (wind speed and rotor speed) and linear MFs to output (TSR). The system is trained for 200 epochs and error tolerance is set to zero. After the completion of training process, ANFIS automatically generated 36 IF-THEN fuzzy rules for input-output mapping. The training and testing errors produced by ANFIS using different type of input MFs are given in Table III. It has been

noticed that bell-shaped MFs provide least training and testing error followed by Gaussian, dsigmoid, triangular and trapezoidal MFs.

Mathematically, the bell-shaped MF is expressed as,

$$\mu_{A_i}(x) = \frac{1}{1 + \left| \frac{x - c_i}{a_i} \right|^{2b_i}} \quad (6)$$

Where, ‘*a*’, ‘*b*’ and ‘*c*’ are premise parameters and ‘*i*’ is equal to total number of MFs assigned to each input parameter.

During the learning process, the consequent parameters of polynomial functions are updated in the forward pass using least square algorithm and premise parameters of bell-shaped MFs are updated in backward pass using backpropagation gradient descent algorithm. The trained bell-shaped input MFs are shown in Fig. 3 and 4. The decrease in root mean square error (RMSE) during the training of bell-shaped MFs for 200 epochs is shown in Fig. 5.

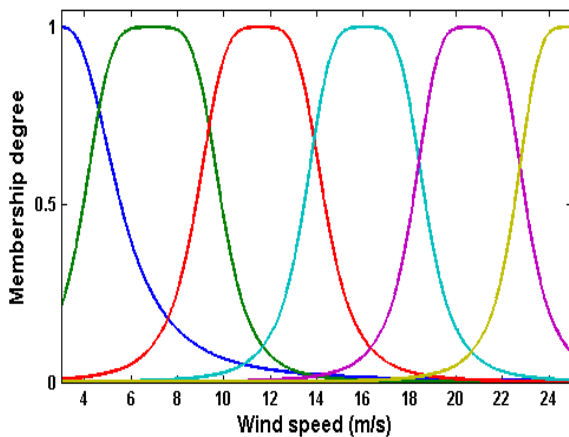


Fig. 3. Trained bell-shaped MFs of wind speed.

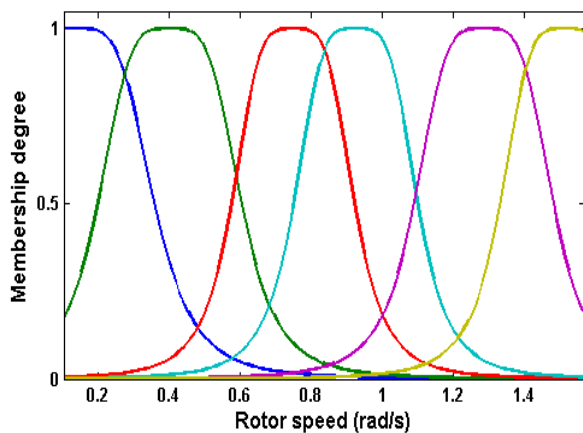


Fig. 4. Trained bell-shaped MFs of rotor speed.

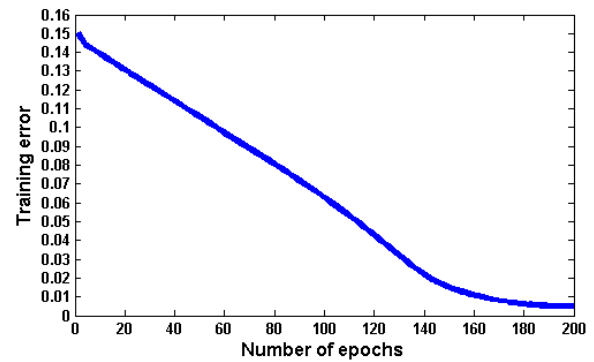


Fig. 5. Training of bell-shaped MFs for 200 epochs.

TABLE III. TRAINING AND TESTING ERRORS PRODUCED BY TSR ESTIMATOR FOR DIFFERENT TYPE OF INPUT MFs

Type of input MFs	No. of input MFs	Type of output MFs	No. of epochs	Training error	Testing error
Bell-shaped	6	Linear	200	0.005299	0.014567
Gaussian	6	Linear	200	0.027864	0.034992
dsigmoid	6	Linear	200	0.061608	0.086566
Triangular	6	Linear	200	0.097743	0.1421
Trapezoidal	6	Linear	200	0.11339	0.12391

B. MLPFFNN based Estimator

MLPFFNN is a biological inspired system which consists of different layers of neurons. Each neuron is a processing unit which processes the information until a threshold is obtained and then passes on the information to the next neuron. MLPFFNN is mainly composed of three layers of neurons. First layer is called input layer, second layer is called hidden layer and third layer is called output layer. The neurons in one layer are directly connected to the neurons of next layers. The basic structure of MLPFFNN is shown in Fig. 6.

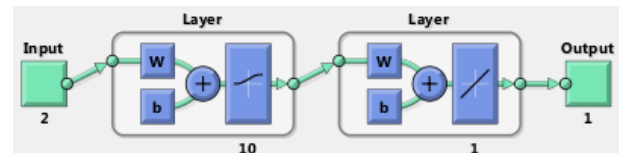


Fig. 6. Structure of designed MLPFFNN.

There are two inputs of the TSR estimator which are wind speed and rotor speed, so there are two neurons in the first layer (input layer). While designing MLPFFNN, ten neurons are assigned to the hidden layer and logistic sigmoid ‘logsig’ transfer function is used as activation function for hidden layer neurons. The logistic sigmoid function can be mathematically expressed as,

$$\text{logsig}(x) = \frac{1}{1 + e^{-x}} \quad (7)$$

The linear transfer function is used as activation function for output layer neuron. In order to train the system, the learning rate is selected as 0.01 and error goal as 0.0001. The Levenberg-Marquardt back propagation algorithm is used to

train the system for 200 epochs. The mean square error (MSE) produced by MLPFFNN after 200 epochs is 0.041279 as shown in Fig. 7.

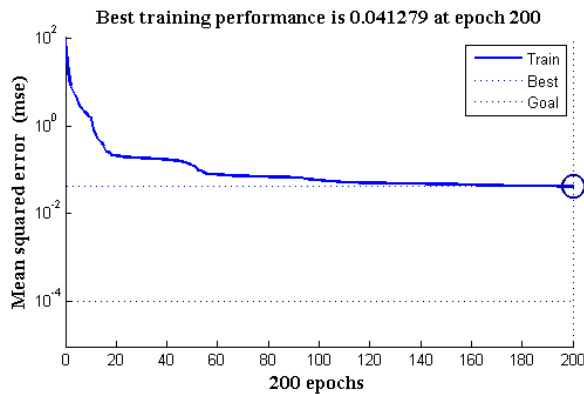


Fig. 7. The MSE produced after 200 epochs.

The MSE and RMSE produced by ANFIS and MLPFFNN are given in Table IV. It is found that ANFIS based estimator provides the best fit of the actual TSR with minimum MSE and RMSE.

TABLE IV. PERFORMANCE INDICES OF BOTH APPROACHES

Model	MSE	RMSE
ANFIS	0.00002808	0.0052991
MLPFFNN	0.041279	0.203172

V. CONCLUSION

The wind turbine efficiency depends on the value of power coefficient, which varies with the TSR. Therefore, it is necessary to accurately estimate the value of TSR to produce optimum power. In this study, a hybrid intelligent methodology based of ANFIS is proposed for accurate estimation of TSR. The experimental data is collected from NREL offshore 5 MW baseline wind turbine. The T-S FIS of ANFIS is designed by assigning bell-shaped, Gaussian, dsigmoid, triangular and trapezoidal MFs to the inputs. Then ANN is used to train the system for 200 epochs using hybrid learning method. It is noticed that ANFIS provides the best results for bell-shaped MFs. Then, conventional MLPFFNN based TSR estimator is designed for the same data. The logistic sigmoid and linear transfer functions are used as activation function for hidden layer and output layer, respectively. The system is trained for 200 epochs using Levenberg-Marquardt back propagation algorithm. The results of ANFIS and MLPFFNN are compared with reference to actual value of TSR. It has been observed that ANFIS has much better performance than conventional MLPFFNN and produces less RMSE even for any type of input MF. Therefore, ANFIS is selected as the best suitable technique for accurate estimation of TSR. The ANFIS involves fewer adjustable (tuning) parameters as compared to ANNs; therefore its training is less time consuming and easy. The ANFIS does not require any detailed and precise mathematical model of the system. It only incorporates the prior knowledge of the system to adapt the system behavior. Moreover, ANFIS does not involve complex computations therefore it is less

computationally complex as compared to other conventional approaches. ANFIS automatically generates the IF-THEN fuzzy rules by analyzing the training data. ANFIS uses the minimum number of fuzzy rules which makes the decision making process fast. ANFIS is robust and adaptive to changing conditions. ANFIS is simple, cheaper to develop and can easily be implemented by using data acquisition cards.

The results presented in this paper are subject to some hardware limitations. The data set used in this study is collected from variable-speed variable-pitch 5 MW offshore wind turbine which is virtually developed by NREL to support the conceptual study of wind turbine aerodynamics and control properties. The actual wind turbine system is not only expensive but also much larger in size. Therefore, it is not usually available in the laboratories, except those which are highly equipped and solely dedicated for wind energy research. The ideal situation is to collect the data samples from an operational wind turbine system and then using the collected data to design estimation and control mechanism.

VI. FUTURE WORK

The optimum TSR is different for every wind turbine type. In future, the proposed approach can be implemented on any wind turbine model in similar fashion to accurately estimate the TSR after collecting the appropriate data. The estimated value of optimum TSR can also be further utilized to design MPPT controller. Future research also includes the implementation of proposed TSR estimator on real wind turbine system to verify the results.

ACKNOWLEDGMENT

This research work is funded by the Natural Science Foundation of China under grant 61673082, 61175041 and 61533005.

REFERENCES

- [1] A. B. Asghar and X. Liu, "Estimation of wind turbine power coefficient by adaptive neuro-fuzzy methodology," *Neurocomputing*, Vol. 238, pp. 227–233, 2017.
- [2] A. B. Asghar and X. Liu, "Adaptive neuro-fuzzy algorithm to estimate effective wind speed and optimal rotor speed for variable-speed wind turbine," *Neurocomputing*, Vol. 272, pp. 495–504, 2018.
- [3] H. Yu, Y. He, Z. Zhao and M. Wu, "Research on fuzzy PID pitch-controlled system based on SVM," *J. Adv. Comput. Intell. Intell. Inform.*, Vol. 20, No.2, 2016.
- [4] J. G. Njiri and D. Söffker, "State-of-the-art in wind turbine control: Trends and challenges," *Renew. Sust. Energy Rev.*, Vol. 60, pp. 377–393, 2016.
- [5] M. H. Mohamed, "Aero-acoustics noise evaluation of H-rotor Darrieus wind turbines," *Energy*, Vol. 65, pp. 596–604, 2014.
- [6] H. R. Kaviani and A. Nejat, "Aerodynamic noise prediction of a MW-class HAWT using shear wind profile," *J. Wind Eng. Ind. Aerodyn.*, Vol. 168, pp. 164–176, 2017.
- [7] M. H. Mohamed, "Reduction of the generated aero-acoustics noise of a vertical axis wind turbine using CFD (Computational Fluid Dynamics) techniques," *Energy*, Vol. 96, pp. 531–544, 2016.
- [8] M. A. Yurdusev, R. Ata and N. S. Cetin, "Assessment of optimum tip speed ratio in wind turbines using artificial neural networks," *Energy*, Vol. 31, pp. 2153–2161, 2006.
- [9] R. Ata and Y. Kocyigit, "An adaptive neuro-fuzzy inference system approach for prediction of tip speed ratio in wind turbines," *Expert Syst. Appl.*, Vol. 37, pp. 5454–5460, 2010.

- [10] A. J. Mahdi, W. H. Tang and Q. H. Wu, "Estimation of tip speed ratio using an adaptive perturbation and observation method for wind turbine generator systems," in: Proceedings of the IET Conference on Renewable Power Generation (RPG), Edinburgh, UK, pp. 1-6, 6-8 Sept. 2011.
- [11] J. D. M. De Kooning, L. Gevaert, J. Van de Vyver, T.L. Vandoornd and L. Vandeveldel, "Online estimation of the power coefficient versus tip-speed ratio curve of wind turbines," in: 39th annual conference of the IEEE Industrial-Electronics-Society (IECON), Vienna, Austria, pp. 1792-1797, 10-14 November 2013.
- [12] L. Gevaert, J. D. M. De Kooning, T.L. Vandoornd, J. Van de Vyver and L. Vandeveldel, "Evaluation of the MPPT performance in small wind turbines by estimating the tip-speed ratio," in: 48th International Universities Power Engineering Conference (UPEC), IEEE, pp. 1-5, 2-5 September 2013.
- [13] H. H. El-Tamaly and A. Y. Nassef, "Tip speed ratio and pitch angle control based on ANN for putting variable speed WTG on MPP," in: 18th International middle-east power systems conference (MEPCON), IEEE Power & Energy Soc, Helwan Univ., Cairo, Egypt, pp. 625-632, 27-29 December 2016.
- [14] M. Negnevitsky, D. Nikolic and M. de Groot, "Adaptive neuro-fuzzy synchronization in isolated power systems with high wind penetration," J. Adv. Comput. Intell. Intell. Inform., Vol. 20, No.3, 2016.
- [15] S. Roy, A. K. Das, V. S. Bhadouria, S. R. Mallik, R. Banerjee and P.K. Bose, "Adaptive-neuro fuzzy inference system (ANFIS) based prediction of performance and emission parameters of a CRDI assisted diesel engine under CNG dual-fuel operation," J. Nat. Gas Sci. Eng., Vol. 27, pp. 274-283, 2015.
- [16] R. Dash and P.K. Dash, "Efficient stock price prediction using a self-evolving recurrent neuro-fuzzy inference system optimized through a modified differential harmony search technique," Expert syst. Appl., Vol. 52, pp. 75-90, 2016.
- [17] J. Jonkman, S. Butterfield, W. Musial and G. Scott, "Definition of a 5-MW reference wind turbine for offshore system development," National renewable energy laboratory, Golden, CO, USA, 2009 Technical report NREL/TP-500-38060.
- [18] A. B. Asghar and X. Liu, "Estimation of wind speed probability distribution and wind energy potential using adaptive neuro-fuzzy methodology," Neurocomputing, Vol. 287, pp. 58-67, 2018. 2018.

AUTHOR'S PROFILE

Aamer Bilal Asghar received the B.S. degree in Electronic Engineering from The Islamia University of Bahawalpur, Pakistan in 2008, the M.S. degree in Electrical Engineering from Government College University Lahore, Pakistan in 2014. Currently, he is a Ph.D. student in School of Control Science and Engineering at Dalian University of Technology, Dalian, P.R. China. He is serving as a Lecturer in Department of Electrical Engineering at COMSATS Institute of Information Technology, Lahore, Pakistan since 2014. His research interest areas include fuzzy control, artificial neural networks, ANFIS, genetic algorithm, granular computing, machine learning and intelligent control.

Xiaodong Liu received the B.S. degree in Mathematics from Northeast Normal University, Jilin, P.R. China in 1986, the M.S. degree in Mathematics from Jilin University, Jilin, P.R. China in 1989, and the Ph.D. degree in Information Science and Engineering from Northeastern University, Shenyang, P.R. China in 2003. Currently, he is a professor in School of Control Science and Engineering at Dalian University of Technology, Dalian, P.R. China. His research areas include fuzzy control, axiomatic fuzzy sets, machine learning, data mining, artificial intelligence, time series analysis and financial mathematics.

Techniques for Improving the Labelling Process of Sentiment Analysis in the Saudi Stock Market

Hamed AL-Rubaiee

Department of Computer Science and Technology
University of Bedfordshire
Bedfordshire, United Kingdom

Khalid Alomar

Department of Information Systems
King Abdulaziz University
Jeddah, Kingdom of Saudi Arabia

Renxi Qiu

Department of Computer Science and Technology
University of Bedfordshire
Bedfordshire, United Kingdom

Dayou Li

Department of Computer Science and Technology
University of Bedfordshire
Bedfordshire, United Kingdom

Abstract—Sentiment analysis is utilised to assess users' feedback and comments. Recently, researchers have shown an increased interest in this topic due to the spread and expansion of social networks. Users' feedback and comments are written in unstructured formats, usually with informal language, which presents challenges for sentiment analysis. For the Arabic language, further challenges exist due to the complexity of the language and no sentiment lexicon is available. Therefore, labelling carried out by hand can lead to mislabelling and misclassification. Consequently, inaccurate classification creates the need to construct a relabelling process for Arabic documents to remove noise in labelling. The aim of this study is to improve the labelling process of the sentiment analysis. Two approaches were utilised. First, a neutral class was added to create a framework of reliable Twitter tweets with positive, negative, or neutral sentiments. The second approach was improving the labelling process by relabelling. In this study, the relabelling process applied to only seven random features (positive or negative): "earnings" (ارباح), "losses" (خسائر), "green colour" (باللون الأخضر), "growing" (زياده), "distribution" (توزيع), "decrease" (انخفاض), "financial penalty" (غرامة), and "delay" (تأجيل). Of the 48 tweets documented and examined, 20 tweets were relabelled and the classification error was reduced by 1.34%.

Keywords—Opinion mining; association rule; Arabic language; sentiment analysis; Twitter

I. INTRODUCTION

Classifying a sentiment polarity as positive or negative is challenging due to the subjectivity factor of the sentiment polarity. Opinionated text can also carry some speech informality—such as sarcasm, subjective language, and emoticons—that makes the opinion detection harder. This required more understanding of the text beyond the facts being expressed [1]. In addition, sentiment polarity might contain positive and negative keywords that can make the labelling process unreliable. This occurred frequently in the neutral class, where one tweet might contain both positive and negative keywords. Labelling carried out by hand can cause human mislabelling sentiments. Therefore, adding the neutral class can help give flexibility for humans to have more options in the labelling process. However, this might cause less

accuracy results. Since, the classifier techniques are used to cover the hall data set vectors, including the neutral data training. The reason behind this is that the data dictionary becomes larger which consist of all vectors that belong to positive, negative, and neutral. But humans will still label the data manually, which may create some mistakes in the labelling process. Consequently, the inaccurate classification creates the need to construct a relabelling process for Arabic tweets to remove noise on labelling. The main goal of the relabelling process is to remove the labelling noise. This will update experts' knowledge about labelling, which may lead to better classification. This is necessary because of the high degree of noise in labelling texts. Especially, for comments are long and consist of multiple sentences such as blogs [2].

This paper presents techniques for improving the labelling process of sentiment analysis. Section 2 shows the need to improve the labelling process for the neutral class. Section 3 demonstrates the Arabic sentiment analysis. Section 4 shows the experiment-classification into positive, negative, and neutral classes. Section 5 shows the need to improve the labelling process by relabelling. Section 6 demonstrates the process of relabelling. Section 7 analyses the experimental findings from Saudi stock market data. The final section contains a conclusion and recommendations for further work in this area.

II. IMPROVING THE LABELLING PROCESS WITH THE NEUTRAL CLASS

Researchers tend to ignore the neutral class under the hypothesis that there is less learning sentiment from neutral texts compared to positive or negative classes. The neutral class is useful, though, in real-life applications since sentiment is sometimes being neutral and excluding it forces instances into other classes (positive or negative) [3]-[5]. In addition, sentiment polarity might have positive and negative keywords that can make the labelling process unreliable. This happened regularly in the neutral class, where one tweet might have both positive and negative keywords. Labelling carried out by hand can cause human mislabelling of sentiments. Therefore, adding the neutral class can give humans more flexibility and options

in the labelling process. However, this might cause less accurate results, since the data dictionary, which consists of all vectors that belong to positive, negative, and neutral, becomes larger.

III. ARABIC SENTIMENT ANALYSIS

Limited research has been conducted on Arabic sentiment analysis, so this is a field that is still in its early stages [6]. However, Boudad et al. [7], [8] reviewed the challenges and open issues that need to be addressed and explored in more depth to improve Arabic sentiment analysis, finding that these include domain, method of sentiment classification, data pre-processing, and level of sentiment analysis. They show that, in contrast to work on the English language, work on Arabic sentiment analysis is still in the early stages, and there are a lot of potential approaches and techniques that have not yet been explored. Another work carried out by Ibrahim et al. [9] have presented a multi-genre tagged corpus of MSA and colloquial language, with a focus on Egyptian dialects. Interestingly, they suggested that NLP supplements, which have been applied to other languages like English, are not valid for processing Arabic directly. Further, Abdulla et al. [10] explored the polarity of 2,000 collected tweets on various topics, such as politics and art. They used SVM, NB, KNN, and D-tree for their documents' sentiment classification. They showed that SVM and NB have better accuracy than other classifiers in a corpus-based approach. Their results reported that the average accuracy of SVM was 87.2%, while the average accuracy of NB was 81.3%. El-Halees's [11] combined approach classified documents using lexicon-based methods, used these as a training set, and then applied k-nearest neighbour to classify the rest of the documents.

IV. EXPERIMENT-CLASSIFICATION INTO POSITIVE, NEGATIVE, AND NEUTRAL CLASSES

In this paper, Twitter has been chosen as a platform for opinion mining in trading strategy with the Saudi stock market to carry out and illustrate the relationship between Saudi tweets (standard and Arabian Gulf dialects) and the Saudi stock market index. The tweets' source data was obtained from the Mubasher company website in Saudi Arabia, which was extracted from the Saudi Stock Exchange (which is known by TASI¹ Index). This experiment will add the neutral class with the N-gram feature. For this study machine learning approach utilised, in which a set of data labelled as positive, negative. The classifiers, which were used to explore the polarity of all the classes' data was Naive-Bayes and SVM. Two different weighting schemes (Term Frequency-Inverse Document Frequency (TF-IDF) and Binary Term Occurrence (BTO)) were used for all classes (Positive, Negative, and Neutral). Table I shows the comparison between the classifiers with the neutral class in term of class accuracy, recall, and precision. Table I shows that SVM with TF-IDF worked better to classify the targeted documents when we add the neutral class.

TABLE I. PRECISION AND RECALL FOR POSITIVE, NEGATIVE, AND NEUTRAL CLASSES USING N-GRAM FEATURE WITH SVM AND NB

Class	Classifier Name	Weighting Schemes	Accuracy	Class Recall	Class Precision	Classification Error
All Classes	Naive-Bayes	BTO	74.16%	74.99%	74.01%	25.84%
		TF-IDF	72.05%	72.05%	71.51%	27.95%
	SVM	BTO	83.02%	81.14%	84.78%	16.98%
		TF-IDF	83.58%	81.67%	84.62%	16.42%

TABLE II. PRECISION AND RECALL FOR POSITIVE, NEGATIVE, AND NEUTRAL CLASSES WITH SVM AND NAIVE-BAYS

Classifier	Accuracy	Recall	Precision
Naive-Bayes with BTO	74.16%	74.99%	74.01%
SVM with TF-IDF	83.58%	81.67%	84.62%

To sum up the classification experiment, the best accuracy achieved by SVM with TF-IDF was 83.58%. Moreover, the best recall and precision was achieved by SVM with less classification error. The analysis shows similar result for SVM with both schemas and only slight differences between recall and precision. Table II shows the comparison between the classifiers in terms of class accuracy, recall, and precision.

A one-to-one model shows the relationships between the positive, negative, and neutral classes and the TASI. The build model illustrates the results in sentiment analysis by showing the positive, negative, and neutral opinions as well as the TASI closing values. Fig. 1 shows the relation between labelling by human operators and the TASI for the Saudi stock market for positive negative and neutral classes between the middle of March 2015 to May 10, 2015. It can clearly be seen that the positive, negative, and neutral classes rise and fall with each other over time; the greatest score for neutral classes occurred on 21/4/2015; the lowest neutral class score occurred on 25/3/2015; and the lowest negative class score occurred on 28/4/2015. Only once did the neutral class get lower than the negative class, over a four-day period between 23/3/2015 and 26/3/2015. At that point, the TASI started to fall sharply. The neutral class frequently went above the positive class, but TASI remained the same. In conclusion, the neutral class mostly rose and fell with TASI. This indicates that the neutral class is an important consideration in the sentiment analysis process.

V. IMPROVING THE LABELLING PROCESS WITH RELABELLING

High dimensionality in texts makes text pre-processing very significant in text classification problems, including sentiment analysis [12], [13]. This problem increases once the dimensionality becomes higher, like when adding neutral class for the classification. For example, in the previous experiment conducted to improve the labelling process of the neutral class, there was approximately 17% misclassification when SVM were used and approximately 28% misclassification when NB

¹ <https://www.tadawul.com.sa>

was used to classify the documents. In addition, labelling the documents conducted manually by humans may have introduced mistakes into the labelling process even when the neutral class was added. Thus, the inaccurate classification

creates the need to construct a relabelling process for Arabic tweets to remove the noise on the original labelling. Below are the suggested steps for a relabelling process for Arabic sentiments analysis.

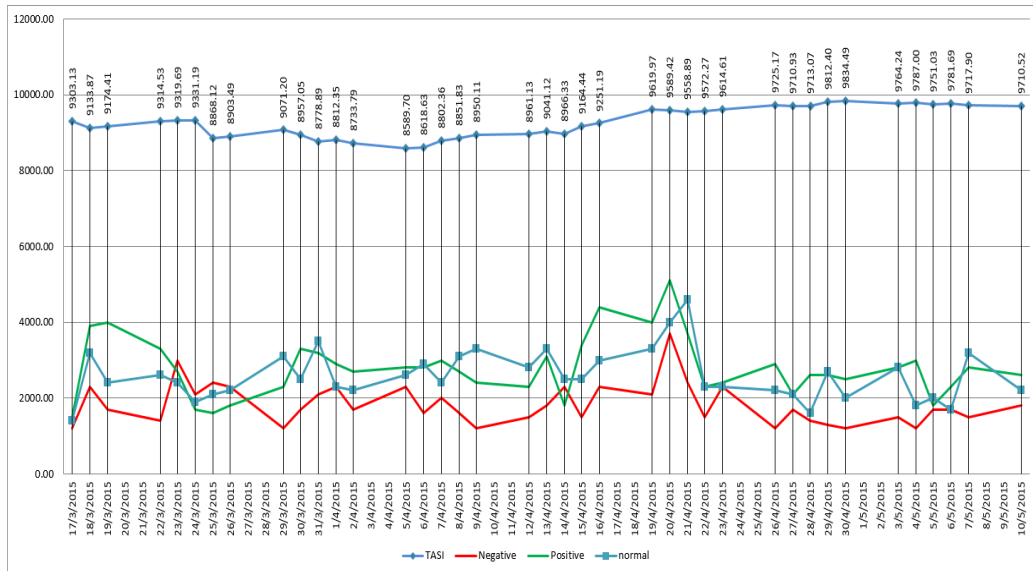


Fig. 1. The relation between labelling by human operators and the TASI for the Saudi stock market for positive, negative, and neutral classes.

The most challenging part of the process is feature selection since any feature can occur in all classes (positive, negative, and neutral). In addition, the main difficulty is to find out how many times the feature occurred in each class. Therefore, a wordlist technique was used to represent the text data as a matrix to show the frequent occurrence of each term within the three classes. Next, filtering the feature helps to select the highest features presented by the wordlist process. Then, in order to understand the sentences' structure and the sentiments behind them, a visualisation technique was used. This visualisation technique was applied to all data to achieve both a high level of understanding of the general structure and of the sentiment within an accumulated corpus. In other words, visualising the text shows the vital importance of the correlation between terms involved in the textual contents in general. However, visualisation shows only the feature with all the related terms in the textual contents without showing the classes they belong to. Using the wordlist technique with the visualisation can produce the important features created by the wordlist technique during the pre-process stage. Overcoming the visualisation limitation for the important features in the targeted text is essential to the relabelling process. After that, association rules extracted from the documents that have features that occurred in a questionable class. Association rules were generated regardless of the minimum support and minimum confidence threshold using the visualisation technique for the features that belong to the questionable class. By following these processes, the documents that have features in the questionable class can be relabelled again and the noise of the original labelling will be reduced.

VI. PROCESS OF RELABELLING

Fig. 2 demonstrates the relabelling process for the Arabic sentiments analysis. The process started by collecting the

corpus of data. The relevant training data were labelled and saved and the irrelevant training data were discarded.

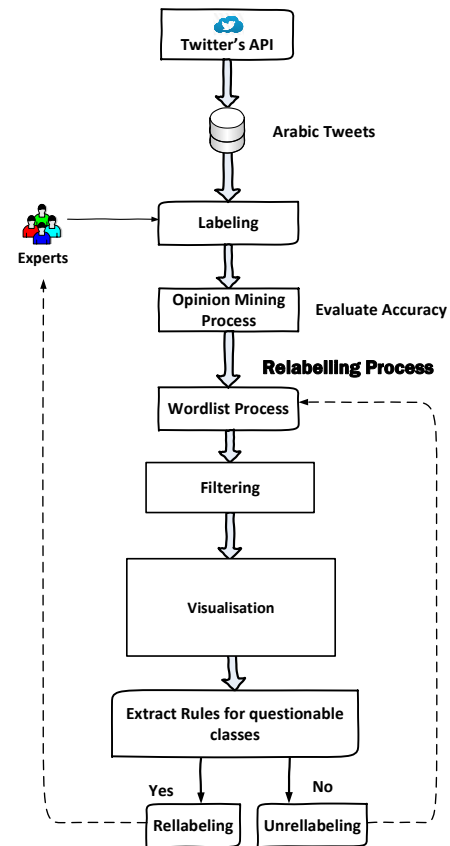


Fig. 2. Relabelling process.

The second step was to pre-processing the data by cleaning up hashtags, duplicate tweets, retweets, URLs, and special characters, and preparing the collected data for the labelling process. The next step is to label the cleaned data as positive, negative, or neutral by the expert in the domain. After that, the relabelling process consists of several steps: the Wordlist process, Filtering, Visualisation, Extract Rule, and Relabelling.

A. Wordlist Process

Fig. 3 shows the wordlist process. This phase uses the same corpus classified—positive, negative, or neutral—and the same data pre-processing procedure used in Opinion mining for the positive, negative, and neutral classes. The goal of visualising association rules as wordlists² is to have data sets that contain a row for each word and attributes for the word itself, and the number of labelled documents in each class for each term or word occurring in the training data. One other word represents the text data as a matrix to show the frequent occurrence of each term within the three classes. The key feature in this process was n-gram, which represents the correlation between the feature selection and other terms with their frequent occurrence for just two nodes within the all-classes data.

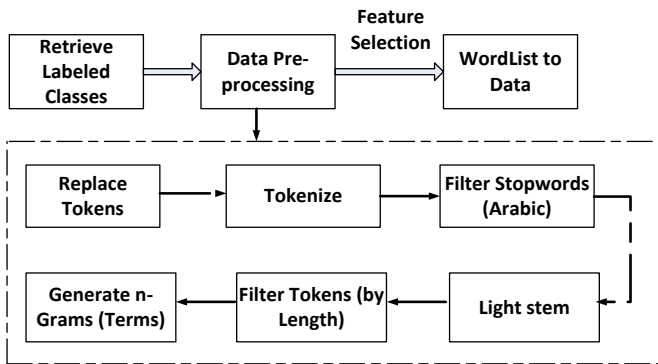


Fig. 3. Wordlist process.

B. Filtering

Features in the context of opinion mining are the words, phrases, or terms that strongly express the opinion as three polarities: positive or negative or neutral. In other words, features are the keywords chosen for the text as positive or negative. That means features have a higher impact on the orientation of a text than other words in the same texts. The impact of feature selection is to help to reduce the dimensionality of a text to increase the classification accuracy. Features in the text are considered explicit or implicit. Features appear in a text as explicit, whereas the feature does not appear is implied [14]. In the proposed process, the explicit features only considered.

C. Visualization

The importance of visualising text is to understand the sentences' structure and the sentiments behind them. Visualising the text shows the vital importance of the correlation between terms in the textual contents. The first step of the visualising technique is to produce the important features created by the wordlist process. Then, it was decided to select

one of the features that appear in the dictionary created by the wordlist. Selection of the feature was done randomly to cover high-, average-, and low-frequency features to prove the concept of investigating the labelling noise. The next step is to visualise the selected feature in all-classes data as a wordlist representation. The wordlist shows how frequently the selected feature occurs in positive, negative, and neutral classes. If the selected feature was positive sentiment and occurred in other classes, such as neutral or negative, then the other classes (neutral, negative) are considered as a questionable class. In other words, if the selected feature is from the positive list, then it should occur only in the positive class—otherwise, this feature occurring in different classes would be considered a questionable class. A strong positive keyword should affect the text to be classified as positive unless there is a negation. Besides, it should not occur in the neutral class unless there are other words in the text affecting the sentiment. However, features that happened in a questionable class need further investigation to confirm the correctness of the labelling.

Fig. 4 illustrates the visualisation association rules process. In this phase, the same corpus classified as positive, negative, or neutral was used in this stage; and the same data pre-processing procedure used in the opinion mining process was carried out. After that, FP-Growth was used to discover frequent items discovery regarding the minimum support and minimum confidence threshold. Then, association rules were generated to expose the relationships between seemingly unrelated data. The output of visualization is the association of the high-frequency terms correlated with the selected feature presented previously from the wordlist process.

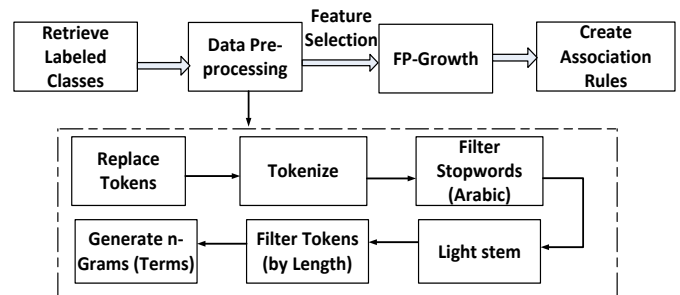


Fig. 4. The visualisation-generated association rules process.

D. Association Rules

The importance of association rule mining is to extract interesting correlations, frequent patterns, associations, or casual structures between sets of items in the transaction databases [15]. Association rule mining is divided into two steps. One, frequent patterns are mined about the threshold minimum support. Second, association rules are built according to the threshold minimum confidence [16]. Some terms or words appear with higher frequency in the dataset, while others rarely occur. In this case, the values of the minimum support will control the rule discovery. For instance, if the minimum support is set at a high value, rules that infrequently occur will not be found. Otherwise, if the minimum support is set at a low value, rules that frequently occur will be found. This cause rules with high confidence have very little support might be ignored [17], [18].

² <https://rapidminer.com/>

Text mining is defined as knowledge revelation from textual databases. Rules are created by analysing data for frequent if/then patterns. The frequent if/then patterns were mined utilizing methods such as the Apriori algorithm and the FP-Growth algorithm [19], [20]. However, for this study, the FP-Growth method was used to discover the frequent item set in the targeted document [21, 22]. Since, the main advantages of the FP-Growth are: passes only two times over data-set, no candidate generation, and compresses data-set [23].

E. Extract Rules

In this phase, the extraction of association rules from collection of documents was based on the features created by the wordlist. Association rules were generated around the minimum support and minimum confidence threshold using the previous visualisation process; the only difference here is the data we are going to use are the data belonging to the questionable class. This step focuses on extracting the rule that occurred less frequently in the questionable class within a specific document.

F. Relabelling

In this step, searching is the training data for the feature occurring less in each questionable classes according to the wordlist matrix. We ensured reliability of the relabelling applied by the expert for a specific document. Then, sentiment with labelling noise was sent as a recommendation to the expert to check its labelling.

VII. EXPERIMENT - RELABELLING

The Arabic text classifications regarding Saudi stock market opinions through the SVM algorithm were designed and implemented. The classification error was 16.42%. Therefore, a framework was created for relabeling.

The relabelling process started by representing the text data as a matrix to show the frequent occurrence of each term within the three classes. The relabelling process focused on representing the correlation between the feature selection and other terms with their high-frequency occurrence for just two nodes within the all-classes data. Table III shows the feature “earnings” (ارباح) as positive sentiment in the Saudi stock market domain. Table III shows the occurrence of the feature “earnings” (ارباح) in the positive, negative, and neutral classes.

TABLE III. OCCURRENCE OF THE FEATURE “EARNINGS” (ارباح)

Feature	Occurrence	Neutral	Positive	Negative
ارباح	304	14	223	67

Fig. 5 shows the association rules that related to the feature “earnings” (ارباح) in all classes with respect to the minimum support and minimum confidence threshold. The feature “earnings” (ارباح) entailed sharing the profits of some company in the Saudi stock market. Fig. 5 shows the most important rules for the feature “earnings” (ارباح) which is “earnings” --> “sharing out” [ارباح] --> [توزيع] (support: 0.031 confidence: 1), “earnings” --> “rise” [ارباح] --> [ارتفاع] (support: 0.071 confidence: 1), and “earnings” --> “decline” [ارباح] --> [تراجع] (support: 0.031 confidence: 1) The term (sharing out) [توزيع] correlated with the feature “earnings” [ارباح] to compose

positive phrases distribute profits in the sentence. Further, the term “raise” [ارتفاع] correlated with the feature “earnings” [ارباح] to compose positive phrases “profits rises” in the sentence. On the other hand, the term “decline” [تراجع] correlated with the feature “earnings” [ارباح] to compose negative phrases profit “decline” in the sentence.

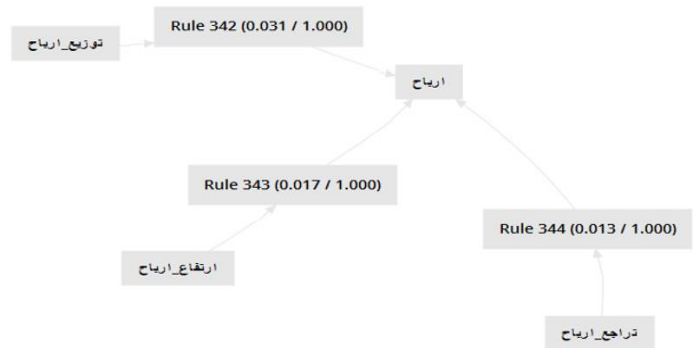


Fig. 5. Visualize the association rules for the feature “Earnings.(ارباح)”

The next step is to find out from the wordlist representation the occurrence of the most frequent phrases that related to feature “earnings” (ارباح). Table IV shows that the phrase “high profits” [توزيع-ارباح] occurred 79 times—three in the neutral class, 66 in the positive class, and 10 in the negative class.

TABLE IV. PHRASES FOR THE FEATURE “EARNINGS” (ارباح) IN ALL DATA

Phrase - Terms	Occurrence	Neutral	Positive	Negative
توزيع-ارباح	79	3	66	10
ارتفاع-ارباح	37	0	37	0
تراجع-ارباح	31	0	0	31

From Table IV, the phrase “high profits” [ارتفاع-ارباح] does not need further investigation since it only occurred in the positive class. In addition, “profits decline” [تراجع-ارباح] does not need further investigation since it only occurred in the negative class. The phrase [توزيع-ارباح] occurred 79 times—three in the neutral class, 66 in the positive class, and 10 in the negative class. Since the phrase “distribute profits” [توزيع-ارباح] occurred in negative and neutral classes then both classes become questionable classes. Therefore, the feature “earnings” (ارباح) needs further investigation in order to find the association rules in both classes. As result, two scenarios will be followed: In the first scenario, the association rules that occurred for the feature “earnings” (ارباح) in the neutral class are extracted. Association rules are generated with regard to the minimum support and minimum confidence threshold using the previous process of the visualisation.

Fig. 6 shows that the feature “earnings” (ارباح) occurred with many rules that appeared in the premises column with the minimum support and minimum confidence values. However, according to the first scenario, the relevant rule here is [ارباح] --> [توزيع-ارباح] (support: 0.005 confidence: 1), which represents the phrase “distribute profits” [توزيع-ارباح] illustrated in the wordlist matrix in the neutral class.

No.	Premises	Conclusion	Support	Confidence
1898	شركات	ارباح	0.003	0.667
3203	توزيع	ارباح	0.005	0.750
3893	بالتربح الآزل	ارباح	0.008	0.833
195	توليدات	ارباح	0.008	1
195	صرف ارباح	ارباح	0.005	1
195	توزيع ارباح	ارباح	0.005	1
195	العائد الفعلي	ارباح	0.005	1
195	وطريقة	ارباح	0.003	1
195	توزيعات بطريقة	ارباح	0.003	1
195	طريقة صرف	ارباح	0.003	1
195	طريقة	ارباح	0.003	1
195	سلك	ارباح	0.003	1
195	توزيع وطريقة	ارباح	0.003	1
195	الصف الثاني	ارباح	0.003	1
195	الصف	ارباح	0.003	1
195	العائد ارباح	ارباح	0.003	1
195	ارباح شركة	ارباح	0.003	1
195	ارباح مساهمين	ارباح	0.003	1
195	ارباح الربع	ارباح	0.003	1
195	العائد ارباح	ارباح	0.003	1
195	ارباح	ارباح	0.003	1

Fig. 6. The correlation rules of the feature “Earnings” (ارباح) in neutral class.

From Fig. 6, the rule [ارباح] --> [توزيع-ارباح] (support: 0.005 confidence: 1) which represent the phrase “distribute profits” occurred in the neutral class. Therefore, the next step is to search for the phrase “distribute profits” [توزيع-ارباح] in the neutral class documents. Table V shows the phrase “distribute profits” [توزيع-ارباح] happened in three documents.

TABLE V. TERM “DISTRIBUTE PROFITS” [توزيع-ارباح] IN THE NEUTRAL CLASS DOCUMENTS

Original Labelling class	Original Arabic tweets with English translations	New Labelling class
Neutral	تعلن شركة اتحاد مصانع الاسلاك اسلاك عن تاريخ وطريقة توزيع ارباح النصف الثاني من عام 2014 م Union Wire Mills Company announces the date and method of distributing dividends for the second half of 2014	Positive
	تعلن شركة مكة للإنشاء والتعمير عن توزيع ارباح على المساهمين عن السنة المالية المنتهية في 30/4/1436 هـ Makkah Construction & Development Company announces the distributing dividends to shareholders for the fiscal year ended 30/4/1436 H.	
Neutral	تعلن شركة فواز عبدالعزيز الحكير وشركاه عن توزيع ارباح على المساهمين عن النصف الثاني من العام 2014 Fawaz Abdulaziz Al Hokair & Co. announces a dividend distribution for the second half of 2014	Positive

From Fig. 6, the rule [ارباح] --> [توزيع-ارباح] (support: 0.021 confidence: 1) which represents the phrase “distribute profits” occurred in the negative class. Therefore, the next step is to search for the phrase “distribute profits” [توزيع-ارباح] in the negative class documents. Table VI shows the phrase

“distribute profits” [توزيع-ارباح] happened in 10 documents. Moreover, only one document has been found to satisfy the rule [ارباح] --> [توزيع-ارباح], so it has been sent again to the expert who labelled the document in the first stage. It can be seen from the structure in the rest of the nine documents that the phrase “distribute profits” توزيع ارباح has occurred with the negation [توزيع ارباح] [عدم] --> [توزيع ارباح] which is the right place for this term in the negative class.

TABLE VI. TERM “DISTRIBUTE PROFITS” [توزيع-ارباح] IN THE NEGATIVE CLASS DOCUMENTS

Original Labelling class	Original Arabic tweets with English translations	New Labelling class
Negative	تأجيل عمومية فيبيكو المتضمنة الموافقة على توزيع ارباح Postpone the Vipco generality agreed on dividend distribution	Positive
	مجلس إدارة العالمية للتأمين يوصي بعدم توزيع ارباح Global Insurance Board recommend on not distribute dividend	
Negative	21 مايو عمومية الدرغ العربي للموافقة على عدم توزيع ارباح May 21 general Arabian Shield for approval on not distribute dividend	Negative
	غدا التصويت عن يُعد على بنود عمومية كيمانول والمتضمنة عدم توزيع ارباح Tomorrow remote voting on the general terms of Kimanol, including on not distribute dividend	
Negative	ايس للتأمين تقر عدم توزيع ارباح وتنتخب أعضاء مجلس إدارتها ACE Insurance recognizes on not distribute dividend and elects its board of directors	Negative
	تعلن شركة اتحاد اتصالات موبيلي عن توصية مجلس الإدارة بعدم توزيع ارباح عن الربع الأول من العام المالي 2015م Etihad Etisalat announces the recommendation of the Board of Directors on not distribute dividend for the first quarter of the fiscal year 2015	
Negative	إدارة موبيلي تقر عدم توزيع ارباح عن الربع الأول من هذا العام Mobily's management confirms Directors on not distribute dividend for the first quarter of this year	Negative
	9 يونيو عمومية موبيلي للموافقة على عدم توزيع ارباح June 9 Mobily's approval for not distribute dividend	
Negative	609 % خسائر المتراكمة حتى 30 أبريل عمومية للموافقة على عدم توزيع ارباح 609% accumulated losses until 30 April general to approve on not distribute dividend	Negative
	شركه صافولا توصي 22 يونيو عمومية للموافقة على عدم توزيع ارباح Savola recommends a June 22 general meeting to approve not distribute dividend	

Fig. 7 shows that the feature “earnings” (ارباح) occurred with many rules that appeared in the premises column with the minimum support and minimum confidence values. According to the second scenario, the interested rule here is [ارباح] --> [توزيع-ارباح] (support: 0.021 confidence: 1), which represents the phrase “distribute profits” [توزيع-ارباح] illustrated in the wordlist matrix in the negative class.

No.	Premises	Conclusion	Support	Confidence
147	ربح	ارتفاع	0.004	0.667
148	مجلس_دارة	ارتفاع	0.004	0.667
149	حافولا	ارتفاع	0.004	0.667
150	التركة_الربح	ارتفاع	0.004	0.667
151	انصاء	ارتفاع	0.004	0.667
152	انصحت_كوكبه	ارتفاع	0.004	0.667
153	انتر_الصناعة	ارتفاع	0.004	0.667
154	انقرا	ارتفاع	0.004	0.667
854	تراجع_نسبه	ارتفاع	0.013	0.750
855	بتراجع	ارتفاع	0.006	0.750
856	دارة	ارتفاع	0.006	0.750
972	مجلس	ارتفاع	0.009	0.800
973	كثيرة	ارتفاع	0.009	0.800
1014	الارز_العالم	ارتفاع	0.011	0.833
2234	تراجع_ارتفاع	ارتفاع	0.054	1
2235	توزيع_ارتفاع	ارتفاع	0.021	1
2236	توزيع	ارتفاع	0.021	1

Fig. 7. The correlation rules of the feature “Earnings” in the negative class.

Fig. 8 shows the correlation rules that can happen with the feature “earnings” (ارباح) in the negative class. This process can identify the negation terms, such as عدم, which means the opposite of positive to help solving the negations problem with Arabic sentiment analysis.

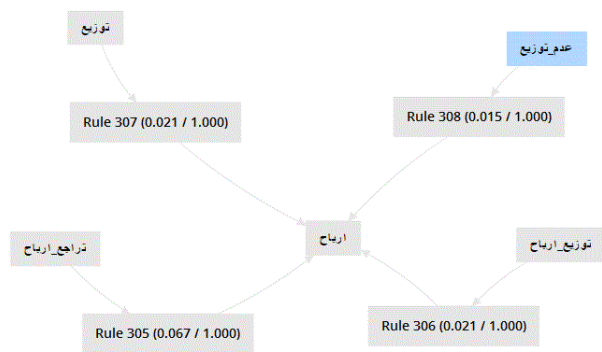


Fig. 8. The correlations of the “negation term” (عدم) and the feature “Earnings” (ارباح) in the negative class.

The second example verifies our experiment with another positive sentiment “Rise” (ارتفاع). Table VII shows the feature “Rise” (ارتفاع) as positive sentiment in the Saudi stock market domain. Table VII also shows the occurrence of the feature “Rise” (ارتفاع) in the positive, negative, and neutral classes.

TABLE VII. FEATURE “RISE” (ارتفاع) OCCURRENCE

Feature	Occurrence	Doc-tot	Neutral	Positive	Negative
ارتفاع	161	158	3	113	47

Fig. 8 shows the association rules related to the feature “Rise” (ارتفاع) in all classes with respect to the minimum support and minimum confidence threshold. The feature “Rise” (ارتفاع) is meant to obtain a financial advantage or benefit from an investment of some company in the Saudi stock market. In addition, Fig. 9 shows the most important rules for the feature

“Rise” (ارتفاع), which is “earnings” --> “rise” [ارباح] --> [ارتفاع] (support: 0.091 confidence: 1), and the feature “percentage” --> “rise” [نسبه] --> [ارتفاع] (support: 0.013 confidence: 1). The term “earnings” [ارباح] correlated with the term “rise” (ارتفاع) to compose positive phrases High profits in the sentence. Further, the term “percentage” [نسبه] correlated with the feature “rise” (ارتفاع) to compose positive phrases high ratio in the sentence.

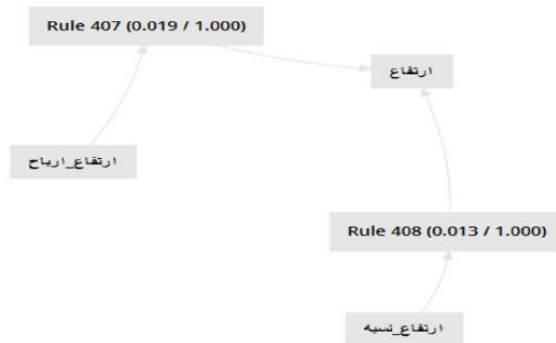


Fig. 9. Visualize the association rules for the feature “Rise” (ارتفاع).

The next step is to from the wordlist the representation of the occurrence of the most frequent phrases related to the feature “Rise” (ارتفاع). Table VIII shows that the phrase “high profits” [ارتفاع-ارباح] occurred 30 times—zero in the neutral class, 23 in the positive class, and seven in the negative class.

TABLE VIII. PHRASES FOR THE FEATURE “RISE” (ارتفاع) IN ALL DATA

Phrase - Terms	Occurrence	Neutral	Positive	Negative
ارتفاع - ارباح	37	0	37	0
ارتفاع - نسبه	30	0	23	7

In Table VIII, the phrase “high profits” [ارتفاع-ارباح] does not need further investigation since it only occurred in the positive class. The phrase “high profits” [ارتفاع - نسبه] occurred 30 times—zero times in the neutral class, 23 in the positive class, and seven in the negative class. Since the phrase “high profits” [ارتفاع - نسبه] occurred in the negative class, the negative class becomes a questionable class. Therefore, the feature “Rise” (ارتفاع) in the negative class needs further investigation to find the association rules in the negative class. As a result, the second scenario will be followed: Extract the association rules that occurred for the feature “Rise” (ارتفاع) in the negative class. Association rules are generated around the minimum support and minimum confidence threshold using the previous process of the visualisation.

The feature “Rise” (ارتفاع) occurred with many rules that appeared in the premises column with the minimum support and minimum confidence values. However, according to the second scenario, the interested rule here is [ارتفاع] --> [ارتفاع - نسبه] (support: 0.015 confidence: 1) which represents the phrase “high profits” [ارتفاع - نسبه] illustrated in the wordlist matrix in the negative class. The rule [ارتفاع] --> [ارتفاع - نسبه] (support: 0.015 confidence: 1) which represents the phrase “high profits” [ارتفاع - نسبه] occurred in the negative class. Therefore, the next step is to search for the phrase “high profits” [ارتفاع - نسبه] in the negative class documents. Table IX shows the phrase “high

profits” [ارتفاع – نسبه] happened in three documents. In addition, three documents have been found to satisfy the rule [ارتفاع] --> [ارتفاع – نسبه], so it has been sent again to the expert who labelled the document in the first stage. It can be seen from the structure of the three documents that the Arabic language is a derivative language in which new words are created from other words. For example, ارتفاع can create مرتفعا, يرتفع, يرتفع, يرتفع — all those words have the same meaning which “rise” in English language, and each term has different shape and this one of the problems that can be solved by the light stemming in the pre-process phase. Moreover, the replace token operator was used to replace “%” by the term “percentage” (نسبه) during the Pre-process phase. For this reason, the term “percentage” (نسبه) cannot be seen in the original documents.

TABLE IX. PHRASE “HIGH PROFITS” [ارتفاع-نسبه] IN THE NEGATIVE CLASS DOCUMENTS

Original Labelling Class	Original Arabic Tweets with English Translation	New Labelling Class
Negative	صافي أرباح قطاع التجزئة ترتفع 12% رغم تراجع ثلث شركاته	Positive
	Net profit for the retail sector increase 12% despite a third of its companies falling	
Negative	السوق السعودي يرتفع 04% بنهاية الأسبوع وصافولا تتراجع بقطاعها	Positive
	The Saudi market is up 04% at the end of the week and Savola is falling in its sector	
Negative	المؤشر العام يغلق مرتفعا وميدغلف يتراجع بأكثر من 8%	Positive
	General index closes higher and Medgulf went down more than 8%	

For the third example for “losses” (خسائر), which is negative sentiment, first we visualize the most important rules for the term “losses” (خسائر). Table X shows the feature “losses” (خسائر) as negative sentiment in the Saudi stock market domain. Table X shows the occurrence of the feature “losses” (خسائر) in the positive, negative, and neutral classes.

TABLE X. PHRASES FOR THE FEATURE “LOSSES” (خسائر) IN ALL DATA

Feature	Occurrence	Neutral	Positive	Negative
خسائر	87	0	25	62

Fig. 10 shows the association rules related to the feature “losses” (خسائر) in all classes with respect to the minimum support and minimum confidence threshold. The feature “losses” (خسائر) means losing an investment in some company in the Saudi stock market. In addition, Fig. 10 shows the most important rules for the feature “losses” (خسائر), which is [خسائر] --> [المتراكمة] (support: 0.013 confidence: 1). The term “losses” [خسائر] correlated with the term “accumulated” (المتراكمة) to compose the positive phrase “accumulated losses” in the sentence.



Fig. 10. Visualize the association rules for the feature “losses” (خسائر).

The next step is to find out from the wordlist representation of the occurrence of the most frequent phrases that related to feature “losses” (خسائر). Table XI shows that the phrase “accumulated losses” [خسائر-المتراكمة] occurred 14 times—zero in the neutral class, four in the positive class, and 10 in the negative class.

TABLE XI. PHRASES FOR THE FEATURE “ACCUMULATED LOSSES” (خسائر-) [خسائر-المتراكمة] IN ALL DATA

Phrase -Terms	Occurrence	Neutral	Positive	Negative
خسائر-المتراكمة	14	0	4	10

Since the phrase “accumulated losses” [خسائر-المتراكمة] occurred in the positive class, the positive class becomes the questionable class. Therefore, the feature “losses” (خسائر) in the positive class needs further investigation in order to find out the association rules in the positive class. As result, the second scenario will be followed to extract association rules that occurred for the feature “losses” (خسائر) in the positive class. Association rules are generated with regard to the minimum support and minimum confidence threshold using the previous process of the visualisation. The rule [خسائر] --> [خسائر-المتراكمة] (support: 0.005 confidence: 1) which represent the phrase “accumulated losses” [خسائر-المتراكمة] occurred in the positive class. Therefore, the next step is to search for the phrase “accumulated losses” [خسائر-المتراكمة] in the positive class documents. Table XII shows the phrase “accumulated losses” [خسائر-المتراكمة] happened in three documents. Three documents have been found to satisfy the rule [خسائر] --> [خسائر-المتراكمة], so it has been sent again to the expert who labelled the document in the first stage. It can be seen from the structure of the three documents that the term “descent” (إنخفاض) as negative sentiment came before the phrase “accumulated losses” [خسائر-المتراكمة], also a negative phrase that puts the three documents in the positive situation.

TABLE XII. PHRASE “ACCUMULATED LOSSES” [خسائر-المتراكمة] IN THE POSITIVE CLASS DOCUMENTS

Original Labelling Class	Original Arabic Tweets with English Translations	New Labelling Class
Positive	تعن الشركة السعودية الهندي للتأمين التعاونيه وفا للتأمين عن انخفاض خسائرها المتراكمة إلى أقل من 50 % من رأسمالها	Positive
	Saudi Indian Cooperative Insurance Company (Wafa) announces its decrease accumulated losses to less than 50% of its capital	
Positive	انخفاض الخسائر المتراكمة لـ وفا للتأمين عن 50% من رأسمالها	Positive
	Wafa Insurance's decrease accumulated loss of 50% of its capital	
Positive	تعن الشركة المتحدة للتأمين التعاوني عن انخفاض خسائرها المتراكمة إلى أقل من 50 % من رأسمالها	Positive
	United Cooperative Insurance Company announces a decrease in its accumulated losses to less than 50% of its capital	
Positive	انخفاض الخسائر المتراكمة لـ وفا للتأمين عن 50% من رأسمالها	Positive
	Decrease loss of Wafa Insurance accumulated 50% of its capital	

Finally, colour is used as for both positive and negative sentiment in this domain. For instance, green colour indicates a positive sentiment in the stock market domain, while red indicates negative sentiment with the HMI field in computing. Table XIII shows the feature “green” (الأخضر) as positive sentiment in the Saudi stock market domain. Table XIII also shows the occurrence of the feature “green” (الأخضر) in the positive, negative, and neutral classes.

TABLE XIII. PHRASES FOR THE FEATURE “GREEN” (الأخضر) IN ALL DATA

Feature	Occurrence	Neutral	Positive	Negative
الأخضر	15	0	10	5

Fig. 11 shows the association rules related to the feature “green” (الأخضر) in all classes with respect to the minimum support and minimum confidence threshold. The feature “green” (الأخضر) indicates that the Saudi stock market values are closing green. Fig. 11 shows the most important rules for the feature “green” (الأخضر), which is [الأخضر] --> [باللون] (support: 0.006 confidence: 1). The feature “green” (الأخضر) correlated with the term “colour” (اللون) to come up with the positive phrase “green colour” in the sentence.



Fig. 11. Visualize the association rules for the feature “Green” (الأخضر).

The next step is to find out from the wordlist representation of the occurrence of the most frequent phrases that related to the feature “green” (الأخضر). Table XIV shows that the phrase “green colour” [باللون_الأخضر] occurred 12 times—zero in the neutral class, eight in the positive class, and seven in the negative class.

TABLE XIV. PHRASES FOR THE FEATURE “GREEN COLOR” (باللون_الأخضر) IN ALL DATA

Phrase -Terms	Occurrence	Neutral	Positive	Negative
باللون_الأخضر	14	0	8	5

Since the phrase “green colour” [باللون_الأخضر] occurred in the negative class, the negative class becomes the questionable class. Therefore, the feature “green” (الأخضر) in the negative class needs further investigation in order to find out the association rules in the positive class. As result, the second scenario will be followed: Extract the association rules that occurred for the feature “green” (الأخضر) in the negative class. Association rules are generated with regard to the minimum support and minimum confidence threshold using the previous process of the visualisation. The rule [الأخضر] --> [باللون_الأخضر] (support: 0.011 confidence: 1) which represents the phrase “green colour” [باللون_الأخضر] occurred in the negative class. Therefore, the next step is to search for the phrase “green colour” [باللون_الأخضر] in the negative class documents. Table XV shows the phrase “green colour” [باللون_الأخضر] happened in seven documents. Seven documents have been found to satisfy the rule [الأخضر] --> [باللون_الأخضر], so it has been sent again to the expert who labelled the

document in the first stage. It can be seen from the structure of the seven documents that the term “decline” (تراجع) as negative sentiment came sometimes before and after the phrase “green colour” [باللون_الأخضر], which is a negative term that puts the seven documents in the unreliable situation during the labelling process.

TABLE XV. PHRASE “GREEN COLOR” [باللون_الأخضر] IN THE NEGATIVE CLASS DOCUMENTS

Original Labelling Class	Original Arabic Tweets with English Translations	New Labelling Class
Negative	المؤشر العام يعلق باللون الأخضر والتطوير العقاري يتراجع 3% Index closes in green and real estate development falls 3%	Positive
Negative	الأسواق الخليجية تتراجع على خلفية عاصفة الحزم وأبوظبي باللون الأخضر Gulf markets retreat against the backdrop of the Al-Hazm Storm and Abu Dhabi in green	Negative
Negative	السوق السعودي يغلق متراجعا بنسبة 17% وقطاع واحد باللون الأخضر The Saudi market closed down 17% and one sector in green	Negative
Negative	عمليات جني ارباح تغلق السوق السعودي دون 9750 نقطة وقطاعا واحدا باللون الأخضر Profits taking closes the Saudi market below 9750 points and one sector in green	Negative
Negative	السوق السعودي يعلق باللون الأحمر وقطاع واحد باللون الأخضر The Saudi market closes in red and one sector in green	Negative

In addition, the same process was carried out for random features (positive or negative), namely, “growing” (زيادة), “distribution” (توزيع), “decrease” (انخفاض), “financial penalty” (غرامة), and “delay” (تأجيل). The result shows that, after completing the process, 23 documents were sent to experts to check the labelling. Of the 48 tweet documents examined, 20 tweets were relabelled.

In the last stage, the original data were updated according to the new labelling. Then, the updated data were loaded to run a new classification process. A comparison was carried out between the original classification and the new classification. Tables XVI and XVII show the performance accuracy for the SVM with TF-IDF schema for both, the original classification and the new classification, respectively. For the neutral class, the precision for the original classification is 92.59%, which rose to 94.09% for the new classification after the relabeling process. On the other hand, the recall for the original classification for the neutral class is 82.74%, which rose to 84.40% for the new classification after the relabeling process.

TABLE XVI. ALL CLASS PERFORMANCE ACCURACY IN ORIGINAL CLASSIFICATION FOR SVM WITH TF-IDF SCHEMA

	True Normal	True Positive	True Negative	Class Precision
Pred. Neutral	537	26	17	92.59%
Pred. Positive	103	757	119	77.32%
Pred. Negative	9	45	330	85.94%
Class Recall	82.74%	91.43%	70.82%	

TABLE XVII. ALL CLASS PERFORMANCE ACCURACY IN NEW CLASSIFICATION FOR SVM WITH TF-IDF SCHEMA

	True Normal	True Positive	True Negative	Class Precision
Pred. Neutral	541	21	13	94.09%
Pred. Positive	91	786	123	78.60%
Pred. Negative	9	36	323	87.77%
Class Recall	84.40%	93.24%	70.37%	

Table XVIII shows the comparison carried out between the result with the original classification and the new classification. The result showed that there was an improvement of 1.34% using SVM with TF-IDF with the new classification.

TABLE XVIII. ALL CLASS PERFORMANCE ACCURACY COMPARISON FOR SVM WITH TF-IDF SCHEMA

Classifier	Accuracy	Recall	Precision	Classification Error
SVM with the Original Classification	83.58%	81.67%	84.62%	16.42%
SVM with New Classification	84.92 %	82.66%	85.40%	15.08%

To sum up, the results show that our process can readily classify Arabic tweets. Furthermore, they can handle many antecedent text association rules for the positive class, the negative class, and the neutral class. The analysis shows the importance of the neutral class in sentiment analysis of Arabic documents; adding the neutral class shows different results of classification accuracy. The reason results are different is that the new vectors dictionary for the text data consists of all the words that belong to positive and negative classes as well. The obtained results help to understand the text structure and the sentiment behind them. Finally, these efforts are meant to add to the breadth of expert knowledge in this field and to be beneficial to the future of machine learning methods.

VIII. CONCLUSION

This study presents a relabeling process to enhance the classification accuracy and update the expert knowledge in the original labelling. Since human error occurs in labelling data, visualisation of the text can show the importance of the correlation between terms involved in the textual structured contents. This is especially apparent in the wordlist and the N-gram steps of the pre-process stage. After the relabeling process applied for random only seven features (positive or negative), namely, “earnings” (ارباح), “losses” (خسائر), “Green color” [باللون الاخضر], “growing” (زياده), “Distribution” (توزيع), “Decrease” انخفاض, “Financial penalty” غرامة, and “delay” تاجيل. Of the 48 tweets documented and examined, 20 tweets were relabelled and the classification error was reduced by 1.34%. The current study should be repeated in other domains such as education.

REFERENCES

- [1] Haddi, E., Sentiment analysis: text, pre-processing, reader views and cross domains. 2015, Brunel University London.
- [2] Yoshida, S., et al. Sentiment analysis for various SNS media using Naïve Bayes classifier and its application to flaming detection. in Computational Intelligence in Big Data (CIBD), 2014 IEEE Symposium on. 2014. IEEE.
- [3] Go, A., R. Bhayani, and L. Huang, Twitter sentiment classification using distant supervision. CS224N Project Report, Stanford, 2009. 1(2009): p. 12.
- [4] Koppel, M. and J. Schler, The importance of neutral examples for learning sentiment. Computational Intelligence, 2006. 22(2): p. 100-109.
- [5] Agarwal, A., et al. Sentiment analysis of twitter data. in Proceedings of the Workshop on Languages in Social Media. 2011. Association for Computational Linguistics.
- [6] Hamed, A.-R., R. Qiu, and D. Li. Analysis of the relationship between Saudi twitter posts and the Saudi stock market. in Intelligent Computing and Information Systems (ICICIS), 2015 IEEE Seventh International Conference on. 2015. IEEE.
- [7] Boudad, N., et al., Sentiment analysis in Arabic: A review of the literature. Ain Shams Engineering Journal, 2017: p. 1-12.
- [8] Kaseb, G.S. and M.F. Ahmed, Arabic Sentiment Analysis approaches: An analytical survey.
- [9] Ibrahim, H.S., S.M. Abdou, and M. Gheith. MIKA: A tagged corpus for modern standard Arabic and colloquial sentiment analysis. in Recent Trends in Information Systems (ReTIS), 2015 IEEE 2nd International Conference on. 2015. IEEE.
- [10] Abdulla, N.A., et al. Arabic sentiment analysis: Lexicon-based and corpus-based. in Applied Electrical Engineering and Computing Technologies (AEECT), 2013 IEEE Jordan Conference on. 2013. IEEE.
- [11] El-Halees, A.M., Arabic text classification using maximum entropy. IUG Journal of Natural Studies, 2015. 15(1).
- [12] Das, S.R. and M.Y. Chen, Yahoo! for Amazon: Sentiment extraction from small talk on the web. Management science, 2007. 53(9): p. 1375-1388.
- [13] Sebastiani, F., Machine learning in automated text categorization. ACM computing surveys (CSUR), 2002. 34(1): p. 1-47.
- [14] Liu, B., Sentiment Analysis and Subjectivity. Handbook of natural language processing, 2010. 2: p. 627-666.
- [15] Agrawal, R., T. Imieliński, and A. Swami. Mining association rules between sets of items in large databases. in AcM sigmod record. 1993. ACM.
- [16] Wu, X., C. Zhang, and S. Zhang, Efficient mining of both positive and negative association rules. ACM Transactions on Information Systems (TOIS), 2004. 22(3): p. 381-405.
- [17] Liu, B., Y. Ma, and C.K. Wong. Improving an association rule based classifier. in European Conference on Principles of Data Mining and Knowledge Discovery. 2000. Springer.
- [18] Karthikeyan, T. and N. Ravikumar, A survey on association rule mining. International Journal of Advanced Research in Computer and Communication Engineering, 2014. 3(1): p. 2278-1021.
- [19] Deng, Z.-H., K.-H. Luo, and H.-L. Yu, A study of supervised term weighting scheme for sentiment analysis. Expert Systems with Applications, 2014. 41(7): p. 3506-3513.
- [20] Nasukawa, T. and J. Yi. Sentiment analysis: Capturing favorability using natural language processing. in Proceedings of the 2nd international conference on Knowledge capture. 2003. ACM.
- [21] Han, J., J. Pei, and Y. Yin. Mining frequent patterns without candidate generation. in ACM sigmod record. 2000. ACM.
- [22] Witten, I.H., et al., Data Mining: Practical machine learning tools and techniques. 2016: Morgan Kaufmann.
- [23] Verhein, F., Frequent Pattern Growth (FP-Growth) Algorithm. School of Information Studies, The University of Sydney, Australia, 2008: p. 1-16.

Designing of Cell Coverage in Light Fidelity

Rabia Riaz¹

Department of CS & IT, University of Azad Jammu and
Kashmir, Muzaffarabad, 13100, Pakistan

Farina Riaz³

Independent Researcher

Sanam Shahla Rizvi²

Department of Computer Sciences, Preston University, 15,
Banglore Town, Shahrah-e-Faisal, Karachi, 75350, Pakistan

Sana Shokat⁴, Naveed Akbar Mughal⁵

Department of CS & IT, University of Azad Jammu and
Kashmir, Muzaffarabad, 13100, Pakistan

Abstract—The trend of communication has changed and the internet user demands to have higher data rate and secure communication link. Wireless-Fidelity (Wi-Fi) that uses radio waves for communication has been used as an internet access methodology for many years. Now a new concept of wireless communication is introduced that uses visible light for communication and is known as the Light-Fidelity (Li-Fi). Li-Fi attracted the researchers for its vast advantages over Wi-Fi. Wi-Fi is now an integral part of everyday life. In near future, due to scarcity of spectrum, it would be quite difficult to accommodate new users in limited spectrum of Wi-Fi. To overcome this, Li-Fi is a good option because of its infinite spectrum range, as it uses the visible range of the spectrum. Many researchers discussed that Li-Fi is secure when compared to Wi-Fi. But is it really secure enough? Can anybody access hotspot of Li-Fi? Or is there a need to develop a technique that is used to block the unauthorized access? In this research work, a cellular concept is introduced for the Li-Fi usage in order to increase the security. This research presents a flexible and adjustable cell structure that enhances the security of Li-Fi. The coverage area is shown by utilizing the geometrical structure of the cone and the area of the cone can be controlled. A mechanical system is also installed on the roof to control the coverage area of a Li-Fi by moving LED bulb slightly up and down. A mathematical expression for the proposed coverage area of the cell is provided, which is formed on the ground level by a beam of light originating from the source of light. The adjustable and controlled structure provides security benefits to the owner. Finally, the research is backed by its simulation in Matlab.

Keywords—Light-Fidelity (Li-Fi); Wireless-Fidelity (Wi-Fi); communication technology; light emitting diode (LED)

I. INTRODUCTION

Light has been utilized as a communication medium for many years and still light has a very vital role in the field of communication. For making signals of smoke on a cloud, fire was used in the past. But in the 19th century the light bulb was invented by Thomas Alva Edison that introduced new options to use light for communication [1]. After the invention of electric bulb another invention for optical communication to visualize signals was signal lamp. It was used along with Morse's code to relay message to the onlooker.

In year 1880 Graham Bell implemented the idea for utilization of light as a communication medium, when he invented the photo phone. Working of photo-phone depends upon a beam of light in which voice signal is super imposed. A

mirror was used to focus sunlight and then apply voice pressure on a mechanism that causes the mirror to vibrate. At receiving end the detector detects the vibrating beam and decodes it reverse to the voice indicator, the same method was implemented inside phone in the occurrence of electric signals. However, Graham Bell did not give any idea for point to point transmission of light and couldn't produce a carrier frequency. Also photo-phone, made by Bell, was affected by the obstacles in nature such as rain, fog, and noise [2].

Light's use as a medium of communication progressed again when light emitting diode (LED) was invented. Visible light communication (VLC) uses white LED for transmission of data and flickering of LED generates a signal in the form of digital pulses. The frequency of LED flickering is very high, thus human eye perceives this light as constant and stable. Due to this flickering of LED, the signal is modulated by using binary codes in order to turn the communication off-on. This encoded signal is used for transmission of data in optical wireless communication (OWC) [3].

Li-Fi got much attention after August, 2011 in technology, entertainment, design (TED) global conference where Professor Harald, commonly known as the father of Li-Fi, introduce Li-Fi to the audience in a very dramatic and magical way. He presented the idea that how an LED bulb can communicate along with its ordinary working of illumination. With the help of LED bulb he stopped the high definition (HD) video on screen and then played it again by obstructing light of the lamp. It made a very astonishing impact on the audience as well as the researchers from the whole world [4].

Li-Fi communication is more secure than Wi-Fi in a sense that a user can access the Li-Fi access point only when he is in the line-of-sight (LoS). In the non-line-of-sight (NLoS) situation, a user cannot receive light from the source and hence cannot use the internet from the Li-Fi access point. Unlike Li-Fi, a user can access the Wi-Fi access point in the communication range whether he is in LoS or NLoS. This is one of the strongest issues that provide motivation for a coverage based Li-Fi communication channel model. The proposed research work provides an adjustable coverage cell size to accommodate the desired number of users in the region of interest.

A lot of work has been done in the field of Li-Fi. The researchers from all over the world are doing research in this

area. Because of the vast advantages of Li-Fi over Wi-Fi, it got much attention, especially for its speed that is undefeatable. But there is no work found on the cellular side of Li-Fi and it is totally a new concept. The Wi-Fi signals cannot be controlled and limited to some specific point; a user cannot restrict the Wi-Fi signal due to its open nature. An unauthorized user or intruder can intervene with the Wi-Fi signals. On the other hand Li-Fi uses light as a signal that can be restricted and a user can control it not to cross some point. So Li-Fi can be secured by designing a cell for it. This novel research area is quite challenging.

The objectives of this research work are to design cell coverage for the users of Li-Fi such that users can access the Li-Fi hotspot more securely and communication could be speedier.

There is no doubt on the importance of the cell in the cellular network. The mobile networks become more efficient and effective through the use of cell. By imagining the cells in the cellular network, the goal is to introduce the cellular concept in the Li-Fi. In this paper, we designed three types of cells on the basis of number of users and we explored the number of users to be accommodated in each cell.

Paper is divided into following sections. Previous work for and Li-Fi is discussed in Section II. Proposed method to model curve shapes, surfaces, two dimensions (2D) and three dimension (3D) structures is presented in Section III. Mathematical derivation for cell coverage of Li-Fi is carried out in Section IV where we also analyzed the achieved data, and retrieved simulation results in Matlab are discussed in detail. Finally, the paper is concluded and future work is highlighted in Section V.

II. LITERATURE REVIEW

As the trends are changing, communication has become vital like oxygen for humans. So it must be accurate, secure, cheaper and faster. Yesterday's light was introduced to visualize the objects, but today's light is effective tool using for communication. Li-Fi is a term used for Light Fidelity.

Khandal et al. described in their paper, cell coverage will be controlled by using VLC. Li-Fi is much effective than Wi-Fi because of its speed and privacy. Visible spectrum is used in VLC so it means that LoS communication will be applicable in VLC [5]. Li-Fi is 100 times faster than Wi-Fi and its speed is more than one GBPS. It can work those places where Wi-Fi cannot be applicable. It can be used in airlines, undersea exploration, theaters in operation, etc. The LED bulb is used as a transmitter and a photo detector diode is used as receiver along with light driver in Li-Fi system. Every light bulb can behave like a Wi-Fi access point in the near future [6].

It seems an idea of Li-Fi is little older than August 2011 where Professor Harald from university of Edinburg introduced Li-Fi. In real, Li-Fi emerged in 2006, and a lot of patents written by researchers in the year followed by 2006 inclusive. Li-Fi captivated the sight of researchers, companies and countries to focus on this new era in technology. Fig. 1 shows the companies and organization focused on activities of patent filing on Li-Fi before 2011.

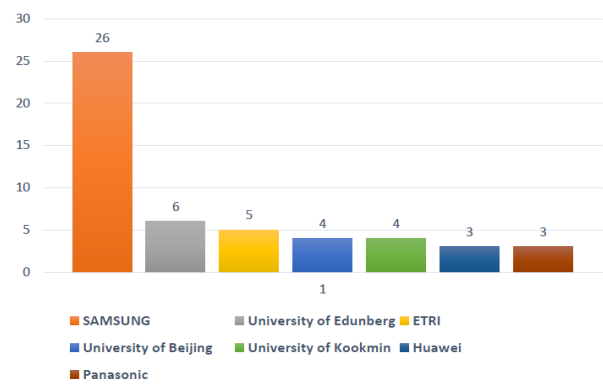


Fig. 1. Li-Fi patents by companies before 2011.

Aside from the research area, some of the world most famous countries that paid attention to convert LED bulb into Li-Fi access point in the past are shown in Fig. 2. The South Korea is the leading country with the most number of patents than any other country. The comparison relating to the number of patents written per year from 2006 to 2015 is shown in Fig. 3. The number of patents are increased gradually from only 3 patents in 2006 to highest 39 patents in 2013 and 34 patents in 2014. Only 8 patents written in 2015 do not mean that Li-Fi does not attract researchers, but it takes time for the patents to release usually 1 to 2 years. These figures were taken in 2016 so many of the patents that were written in 2015, not completely published. The point is that the gradual increase in the number of patents clearly shows the importance of Li-Fi in the sight of researchers [7].

Researchers and inventors of Li-Fi were doing research and writing patents before the publicly announced of Li-Fi in 2011. The first research on Li-Fi is written by Prof. Mr. Harald Haas in the early days of 2006, states of all top five researchers are coincidentally working for Samsung [8], see Fig. 4. Li-Fi is expected to become a world huge industry estimated 113 billion dollars in 2022 due to its unique characteristics and advantages.

According to a CISCO survey about existing spectrum usability that is about 80% of spectrum has been utilized. Currently Wi-Fi is deployed within universities, hotels, offices, buildings, cafes, homes, airports and provides connectivity of ten to hundred meters distant. The very rapid growth in radio frequency spectrum utilization made it very dense and there exists insufficiency of available frequencies. So people start pondering upon VLC communication because it is free from spectrum scarcity.

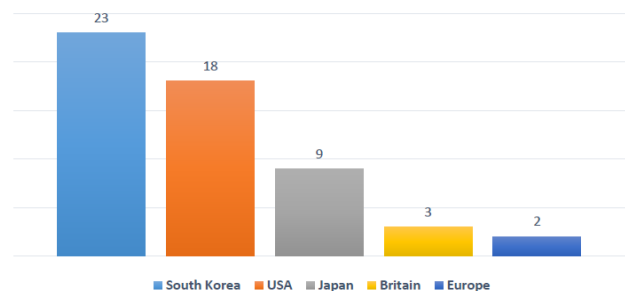


Fig. 2. Li-Fi patents by countries before 2011.

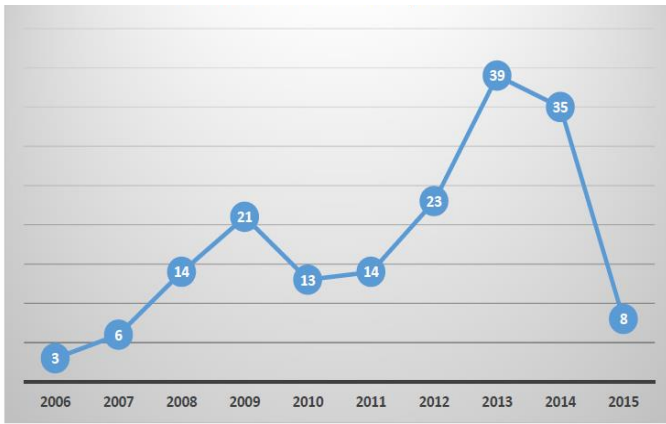


Fig. 3. Number of patents per year.

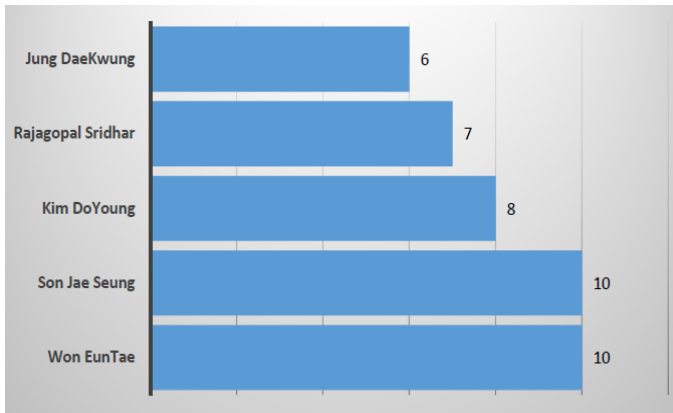


Fig. 4. Top Li-Fi inventors before 2011.

Li-Fi uses optical part of the spectrum instead of the radio part of the spectrum that is used by Wi-Fi. This new spectrum is ten thousand times greater in size than radio spectrum [9]. The operating frequency on which Li-Fi operates is in terahertz while Wi-Fi is operated at 2.4GHz usually except for some standard that uses 5GHz and 60GHz frequency band.

The frequency spectrum consists of many regions on the basis of characteristics of frequency. These regions include infrared rays, X-rays, radio region, microwaves, ultra violet rays, gamma rays and visible light region. Among these regions anyone can be used for upcoming technology but VIBGYOR portion is chosen because it does not encompass harmful effects on the human body. VIBGYOR region that is visible to human eye comprises of seven colors that combine to make a white light, see Fig. 5. The wavelength of these colors ranging from 390nm to 700nm. As frequency is reciprocal of wavelengths, so in frequency terms that are vicinity of 770 terahertz greatest for violet to 430 terahertz smallest for red [10], see Table I.

Security of Li-Fi is much better than Wi-Fi. Light can never penetrate through walls and communication can be easily established within the room without any security flaws because no one can hack or decode the signals of Li-Fi. A person cannot use the Li-Fi hotspot without the permission of owner [11].

There is no method available to restrict the Wi-Fi signal. So the signal of Wi-Fi transmits away from the service providers so any unauthorized user or intruder can interrupt the Wi-Fi signal and hackers can hack important or confidential information by applying some easy decryption methods [12]. The only way to provide security in Wi-Fi is to pursue wireless intrusion prevention system (WIPS) and follow the security measures describe by WIPS.

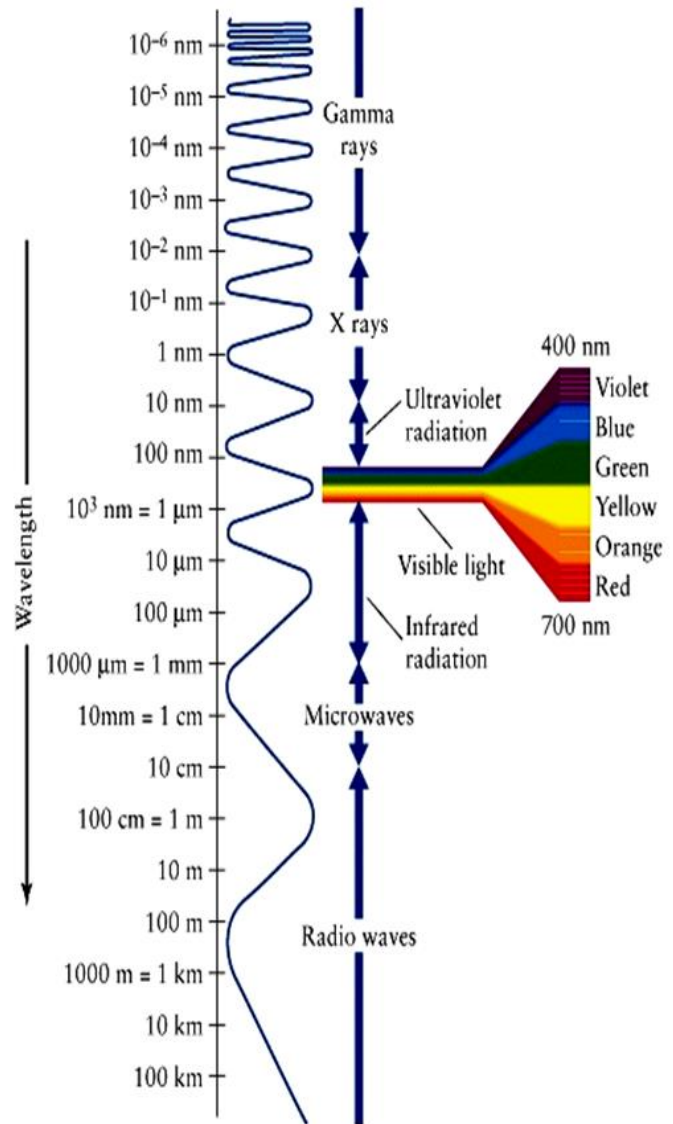


Fig. 5. Full electromagnetic spectrum.

TABLE I. VIBGYOR FREQUENCIES AND WAVELENGTHS

COLOR	WAVELENGTH (nm)	FREQUENCY (THz)
<i>Violet</i>	400.0 – 440.0	680.0–789.0
<i>Indigo</i>	440.0 – 460.0	668.0–680.0
<i>Blue</i>	460.0 – 500.0	606.0–668.0
<i>Green</i>	500.0 – 570.0	526.0–606.0
<i>Yellow</i>	570.0 – 590.0	508.0–526.0
<i>Orange</i>	590.0 – 620.0	484.0–508.0
<i>Red</i>	620.0 – 720.0	400.0–484.0

TABLE II. SPEED COMPARISON OF WIRED, WI-FI AND LI-FI

Technology	Speed
Wired	Speed (Gbps)
Fire Wire	0.80
USB 3.0	5.0
Thunderbolt	2*10.0
Wireless (Current)	Speed (MBPS)
WI-FI-IEEE 802.11n	150.0
Bluetooth	3.0
IrDA	4.0
Wireless(Future)	Speed (GBPS)
WiGig	2.0
Giga-IR	1.0
Li-Fi	>10.0

A. Li-Fi Advantages

There are lots of advantages Li-Fi has over Wi-Fi. Li-Fi is faster than Wi-Fi, speed in the order of 500MBPS. Wi-Fi uses radio waves that have to bear disturbances and others hazardous while Li-Fi uses the light which is robust to disturbances. In February 2015, the researchers at Oxford University acquired a record breaking speed of 224GBPS with Li-Fi. With this pace twenty HD movies can be downloaded in one second. Though these results were experimental and are not achieved practically, but still considering data transfer rate Li-Fi has a potential to thrash Wi-Fi [13]. Table II shows the speed comparison of technologies.

VLC safely could be used in aircrafts without affecting aircrafts signals. Li-Fi can be integrated into medical devices with no side effects to patients and in hospitals as this technology doesn't deal with radio waves, so it can merely be used in all such places where Bluetooth, infrared, Wi-Fi and internet are broadly in use. Wi-Fi does not work under water, but Li-Fi can effortlessly be deployed in water and undersea working can be performed with ease [14].

Millions of bulbs in the world can be replaced with LED, in order to transmit data along with illumination. Li-Fi is much secured than Wi-Fi as it won't penetrate through walls. For controlling traffics on highways, motorways, the vehicles can be integrated with LED and can be used to avoid accidents. Every lamp on the street would be used as an access point. The deficiency in radio spectrum can also be addressed using Li-Fi. LED consumes very less power and high patience to humidity [5].

B. Li-Fi Limitations

Even though, there are many advantages, Li-Fi is not widely deployed yet because it requires the source and destination to be in the LoS. If the photo detector is blocked or the receiver is blocked the signal cannot be destined. If there is an external source of light, that can also disturb Li-Fi signal. Li-Fi is good for indoor communication unless and until there is no other source of light or ambient light. For working Li-Fi needs a direct LoS and distance from the LED bulb is also

needed to be defined because light intensity decreases with distance from the source [9].

C. Li-Fi Application

Li-Fi can prove itself in areas where other technologies along with Wi-Fi either could not be deployed or failed to provide higher data rates. Such applications include underwater, power plant, airplanes, and hospitals, especially in operation theaters where other technologies can be harmful for patients. Other applications include medical science, aircrafts, learning purposes and in avoiding accidents on the roads. Li-Fi can be used in any emergency situation like flood, earthquake, and nuclear plants or where security cannot be compromised, thermal plants and in all sensitive locations [3].

Due to increase in demand the spectrum of electromagnetic is near to fill so solution of this problem is to introduce an alternate to overcome this situation. Spectrum of visible light has a very large bandwidth that enables many users to fulfill their requirements. It is also cost effective as it is licensed free and also has a large number of applications.

White LED is an important part of VLC because it works as a source in OWC. When multiple parallel lights have been installed within the room, then interference between the lights and reflection of lights are considerable. The spectrum of visible light ranging from 380 nm to 780 nm is followed the range of personal area network (PAN). But VLC sends data by using different intensity modulated optical sources, like LED and laser diode which are faster than the persistence of vision of the human eye [15].

Data rate of LED is much higher than any other visible light such as incandescent bulb and fluorescent tube. LED consumes very low power, but provides longer life time, which is easy to control and also has high luminance. LEDs are operated as an optical transceiver which can be used for communication purpose [16].

VLC can work only in those places where light is present so communication can be more secure than radio frequency (RF). VLC can be used under water where RF couldn't throw the signals. Aero plane is operated in RF so that hotspot which is operated in RF become reasons for interference, but if VLC is used for communications there will be no interference.

Yingshu discussed a framework that is based upon algorithms to solve the coverage area problems of wireless sensor network (WSNs). This algorithm has very low time for complexity than all the previous algorithms. Also, it prolongs the network life and saves energy by not covering the area where coverage is not needed [17].

To avoid interference a femtocell has been discussed for indoor wireless environment, a femto cell is a cellular base station consumes low power and is very small in size and it is used for home and office. Femto cells control the convergence plan between service providers and users. It is useful for both user and service provider also because it fills the gaps and eliminates the loss of energy [18].

A research has been published in CISCO Systems Inc. that every person in the world is going to use mobile data that shows that there is a large number of increase in the mobile

web applications and mobile videos. This research is named as the visual network index (VNI), which estimates that in next few years usage of mobile data may increase from 90 thousand terabytes to 3,600 thousand terabytes in each month. After 5 years, this factor may increase to 40 or in case more than hundred percent cumulative annual growth rate (CAGR). This will become a huge growth in mobile data, mobile videos will cover sixty six percent, PCs, tablet, networking equipment, laptops, and mobile devices may be used seventy percent of it. A data is further share between these devices within the buildings, offices and classrooms. So one can guess the amount of data which will be shared or transferred in communication. Because transfer rate for data in VLC is very high, so these challenges can be catered in the future [19].

The reason of using LED instead of Laser diode is that LEDs is not harmful for eye of human and light of LEDs is less penetrating than laser diode. Spectrally, modulated techniques are used to achieve high speed communication that is based upon high rise times of LEDs [20].

Initially, the communication between end terminals took place via a very high tall tower with huge transmitting power. There was no idea of the frequency-reuse and cell splitting. After it became popular in the market, it was necessary to increase the spectrum bandwidth to increase the number of channels in the given coverage area. First of all, the existing bandwidth which was 30 kHz is split into three 10 kHz, narrow bands and increased the capacity in terms of customer by three times. American mobile phone system (AMPS) was fully analog and manual dialing system. To increase the system capacity, a cellular concept was introduced [22]-[24].

In cellular mobile communication system, the allocated spectrum is insufficient to provide services to the large number of subscribers. While the goal of cellular communication is to increase capacity, increase coverage within the same limiting spectrum. The reuse of frequency concept is introduced in a cell after a suitable distance among cell to avoid interference between same cells [21], [25].

Cells with the identical alphabets in Fig. 6 using the same frequencies with frequency reuse pattern 7. That means same frequency is to be allocated to every seventh cell. To increase capacity and coverage some other techniques were introduced such as sectored antennas, umbrella cells, small cell sizes or micro cells, and channel assignment strategies etc. In each cell two types of channel assignment strategy are used. First one is fixed channel assignment and second one is a dynamic channel assignment. In the first one, pre-defined numbers of channels are allocated in the cells while in the latter one; channels are assigned on demand of the active customers [21].

A VLC can be used in homes for monitoring appliances with cameras. Cameras have recent exchange data with other embedded devices at a rate less than one KBPS, which is insignificant. A VLC can give high downstream speed and better performance for communicating indoors in homes, schools, universities, organizations, etc. This process requires very low power and can be initiated in ten milliseconds [26].

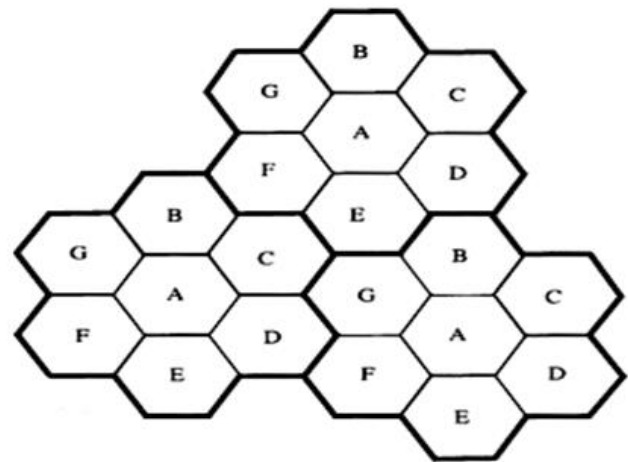


Fig. 6. Frequency reuse.

III. PROPOSED METHOD

In this research work, geometric modeling approach is chosen to address cellular coverage area of Li-Fi. Geometric modeling is applied mathematical concepts and approaches to model curve shapes, surfaces, two dimensions (2D) and three dimension (3D) structures. It clearly states simple mathematical equations and to combine them to make more complex models [27].

A cellular concept for Li-Fi usage along with a flexible and adjustable cell structure enhances its security while utilizing geometry of cone. There are three main units of communication; transmitter, receiver and medium and other subunits are used for driving these main units.

In VLC, LED lamp acts as transmitter which transmits light signals in the form of pulses and pulses on-off is generated due to flickering of the LED lamp. The lamp driver is further connected to these parallel connected LEDs. Power is provided to the transmitter unit after rectification. The data that is transmitted by lamp driver is further gone through medium and form a conical shape at the base of floor. This data signal is received by the photo sensing device called photo detector. Photo detector is acted as receiver along with the processing and amplification units. After the signal is processed and amplified by the amplifier unit, it relays data to the destination devices, see Fig. 7.

When light start to travel, the beam of light become scattered or spread out as light travels on more distance. A cone is formed when the beam of light from the source through a small hole is thrown on a flat surface. This conical form made of light is supposed to be called as cell or coverage area for Li-Fi. The area of a cell is to be controlled by adjusting the distance of light source from the small hole or slit. A mechanical system is to be installed above the slit in the ceiling holding LED bulb, which is used to control the distance by moving LED up and down according to the requirement of number of users to be accommodated in the cell.

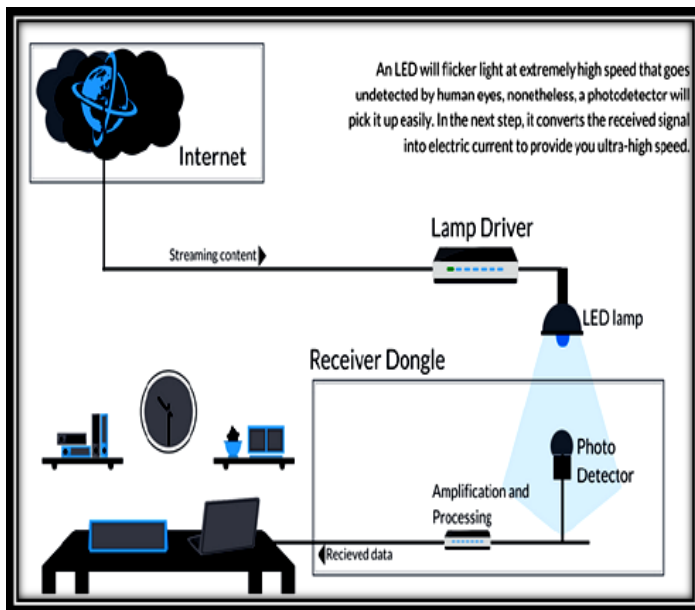


Fig. 7. Working of VLC.

A wide hole with diameter “d” is created in the ceiling through which light can easily pass. By changing the distance between the hole and LED bulb, the area of a cell can be controlled, which in turn can control the number of users who can access or connect with the hotspot of Li-Fi. The cell size dynamically adjusts to accommodate more users by mechanically decreasing the separation between LED and slit. We design three categories for conical cell with respect to coverage. Each category will have different number of users on the basis of mathematical and theoretical calculations.

A. Small Conical Cell

This section describes the formation of small cell size using the proposed conical beam of light from the LED towards the users on the ground. To achieve this, the distance between LED bulb and the hole in the ceiling is kept large enough through the mechanical system. Due to this large gap between the LED bulb and hole in the ceiling resultantly the beam of light went pass through the hole with a narrow beam. This narrow beam forms a cone with a small conical area which will cover a small circular region on the ground that covers lowest number of users and can be labeled as small cell, see Fig. 8.

A small conical area is covered on the ground because the angle of incident light ‘a’ through the slit with diameter ‘d’ on the ceiling is very small.

A cone has two right angle triangles and both triangles are congruent with each other so the single triangle is taken which has three angles (a,b,c) and right angle ‘b’ is 90 degrees and the sum of these angles must be 180 degrees. So if the incident angle ‘a’ has a minimum value, then scattered angle ‘c’ will be maximized and when scattered angle ‘c’ has maximum value then the cell will cover a small area. When the coverage area is smaller than minimum number of users can connect with the hotspot.



Fig. 8. Small cell area.

B. Medium Conical Cell

This section describes the formation of medium sized cell when the distance between the hole in the ceiling and LED bulb is moderate; neither large nor small gap. Due to this moderate gap, a medium sized cone is formed on the ground at the receiver end. The base of the cone covered circular area between the small sized and large sized cell and consequentially provides an accommodation for more number of users as compared to small sized cell.

The moderate conical area of cell can be covered by the light because of the incident angle of light ‘a’ is less scattered than one in the case of the small cell area and distance between LED bulb and slit opens hole ‘h1’ is also kept less than in case of small sized cell. So if the incident angle ‘a’ becomes almost equal to the scattered angle ‘c’ that is nearly 45 degrees, then the cell will cover medium area and when the coverage area will be medium then more numbers of users can connect with hotspots as shown in Fig. 9.

C. Large Conical Cell

When the distance between the hole in the ceiling and the LED bulb is kept almost zero, it covers a large area that is formed on the surface of the floor. Due to no gap between them the beam of light went pass straight toward and scattered more enough to reach the receivers and makes a wider cone shaped form from ceiling to the receiver, see Fig. 10.

Very large conical area of cell can be covered by the light that is ‘h1’ is equal to zero, and the incident angle of light ‘a’ through slit will spread more having large diameter. So if incident angle ‘a’ is maximum then scattered angle ‘c’ is minimized and then the cell will cover a very large area. Ultimately, maximum numbers of user can connect to the hotspot of Li-Fi.

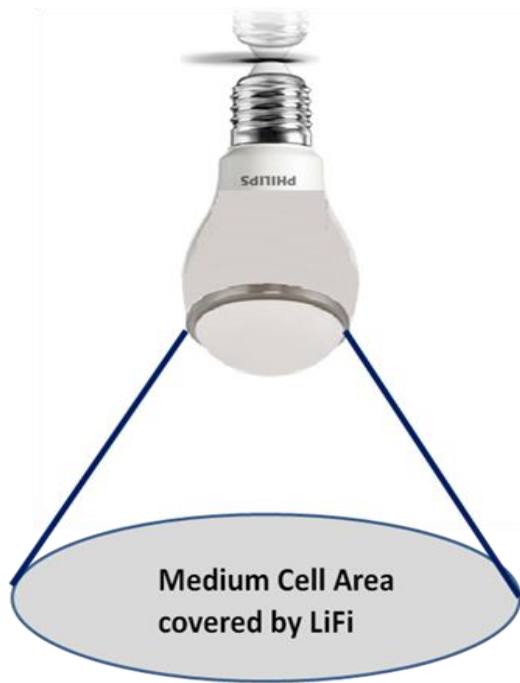


Fig. 9. Medium cell area.

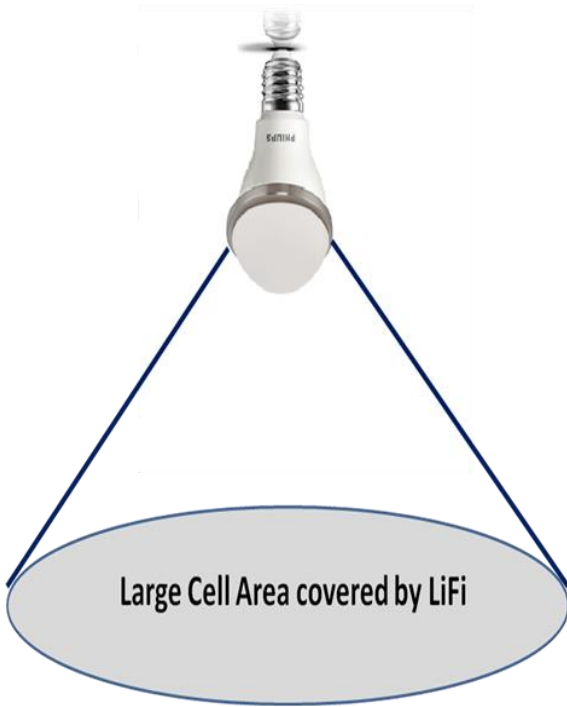


Fig. 10. Large cell area.

IV. RESULTS AND DISCUSSION

In this section, the mathematical derivation for cell coverage of Li-Fi is carried out. The equations from the cone with the help of mathematical theorems, formulas and trigonometric identities are derived. Using these equations area of the cone is calculated for all three cell sizes and estimates the number of users that can exist in a small area, medium area and large area.

A. Layout of Geometry of Cone

By drawing a vertical on the cone the two right angled triangles are formed, see Fig. 11. As these two triangles are congruent to each other so focused on just one and find a solution by applying trigonometric function.

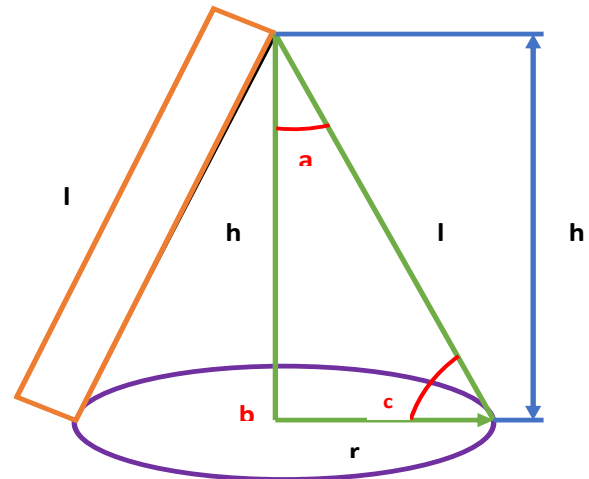


Fig. 11. Geometry of cone.

From the geometry of the cone, the equations can be drawn using basic mathematical concepts. The right angled triangle is shown in the Fig. 12 and for any arbitrary triangle the interior angle sums equals to 180° degrees, see (1). The very familiar trigonometric functions sine (Sin), cosine (Cos) and tangent (Tan), can be used to solve the sides of a cone.

$$a+b+c=180^\circ \tag{1}$$

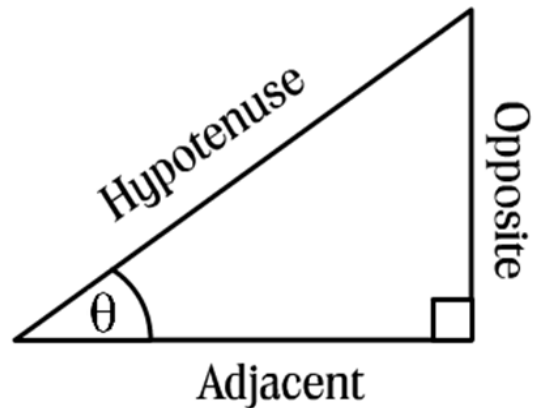


Fig. 12. Right angle triangle.

By applying (1) sine and tangent is calculated by (2) and (3).

$$\sin\theta = H/l \tag{2}$$

$$\tan\theta = H/r \tag{3}$$

Where H is a sum of the heights from the floor to the roof, h_0 (constant) and LED bulb height h_1 from roof slit. The height h_1 can be varied only if the separation between LED bulb and slit is increased or decreased, depending on the requirements of coverage. So H is calculated by (4):

$$H = h_0 + h_1 \quad (4)$$

Now for right circular cone, let say cone area A is the sum of the curved surface area of cone A_l and circular surface area of cone A_c. Lateral surface area of the cone or curved part area of the cone is given by (5).

$$A_l = \pi r l \quad (5)$$

Where r is the radius at the cone bottom and l is the lateral height of the cone.

The circular part area is simply the circle at the bottom with radius r is given by (6).

$$A_c = \pi r^2 \quad (6)$$

Hence the total area of cone A, the (6) can be written as (7).

$$A = A_c + A_l \quad (7)$$

The incident angle 'a' is controlled by the gap h₁ between LED bulb and slit and the diameter 'd' of slit is fixed by (8).

$$\Theta = \arctan (d/2 * h_1) \quad (8)$$

The incident angle 'a', scatter angle 'c' and right angle 'b' relation is given by (9).

$$\Phi = 90 - \theta \quad (9)$$

h₀ is the constant height from floor to roof slit, and h₁ is controlled by mechanism, when both h₀ and h₁ is known then length 'l' and base 'r' can be found easily by arranging (2) and (3) into (10) and (11).

$$l = H / \sin\theta \quad (10)$$

$$r = H / \tan\theta \quad (11)$$

When the values of 'l' and 'r' has been evaluated then by putting these values in (5) and (6), the lateral surface area of cone A_l and area of circular part of cone A_c can be found. After inserting all the values in (7), total area of cone A can be inquired, number of users to be adjusted in the circular part of the cone A_c by rearranging (7) into (12).

$$A_c = A - A_l \quad (12)$$

B. Data Analysis

Few of the terms in these calculations are constant such as height of floor h₀, right angle in all cases, and some of the terms are specifically constant in each case that are height of LED bulb from slit h₁, angle θ and angle φ. Values of heights and angels for all three cases are elaborated in Tables III and IV, respectively.

TABLE III. VALUES OF HEIGHTS FOR THREE CASES

Cases	Height (h ₀)	Height (h ₁)	Height (H)
Small	10	1	11
Medium	10	0.5	10.5
Large	10	0	10

TABLE IV. VALUES OF ANGLES FOR THREE CASES

Cases	Angle (a)	Angle (b)	Angle (c)
Small	30	90	60
Medium	45	90	45
Large	60	90	30

The standard designated area per person in buildings is 0.6 square meters. As feet square unit are used in our calculation so converting 0.6 square meters to square feet, will get 6.45 square feet. If the user is working by having a laptop on the desk or working in an office or laboratory, then this reserved space can be increased from 6.45 square feet. It is better to use 10 square foot area for each user that is almost equal to 1 meter square space for better utilization of cell area and coverage, see (13).

$$\text{No. of users} = A_c / 10 \quad (13)$$

To extend our equation for 'n' number of cells because there can be more LED bulb fitted into the room in order to fill up the gaps. So (13) becomes (14).

$$\begin{aligned} \text{no of users in "n" cells} &= \sum_{i=1}^n \frac{A_{C_i}}{10} \\ \text{no of users in "n" cells} &= \frac{1}{10} \sum_{i=1}^n A_{C_i} \end{aligned} \quad (14)$$

The values utilizing from Tables III and IV are applied to the calculations and final results are presented in Table V.

TABLE V. NUMBER OF USERS FOR THREE CASES

Cases	Radius(r) feet	Cone Area (A) ft ²	Circular Area (A _c) ft ²	No. of Users
Small	6.35	380	126.7	13
Medium	10.5	834.6	346.4	35
Large	17.3	1483.5	940	94

From the Table VI, conclusion can be drawn that if scattered angle 'c' is less than 30 degrees, then the result will be a large sized cell. Similarly, if scattered angle 'c' is greater than 30 degrees and less than or equal to 50 degrees, the results show it will be a medium sized cell. Finally, if the scattered angle is greater than 50 degrees results in small sized cell. The number of users with respect to cell size is clarified in the Fig. 13. The maximum users in small cell are almost 13, covering each user a space of 10 square feet.

TABLE VI. SCATTERED AND INCIDENT ANGLE FOR THREE SIZED CELL

Cell Types	Scattered Angle 'c' (degrees)	Incident Angle 'a' (degrees)
Small Cell	θ > 50	θ ≤ 30
Medium Cell	30 < θ ≤ 50	30 < θ ≤ 50
Large Cell	θ ≤ 30	θ > 50

The conclusion can be drawn on the basis of incident angle 'a' as well. If the incident angle 'a' is greater than the scattered angle 'c' will be smaller, so greater the value of incident angle 'a' results in large sized cell that can cover large areas with

more number of users in large halls. Similarly, if incident angle 'a' is small then the scattered angle 'c' will be large, so smaller the incident angle results in small sized cell for a small portion of the building.

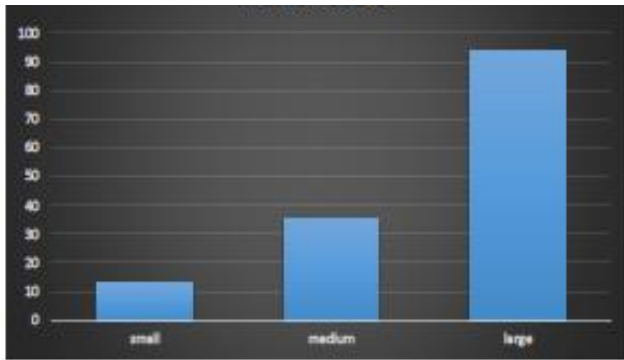


Fig. 13. Number of users for three cells sizes.

C. Simulation Results in Matlab

When the distance between the light source and the slit is zero, then maximum coverage area is achieved, as the distance from the slit increases coverage area at ground decreases. The comparison is shown in Fig. 14.

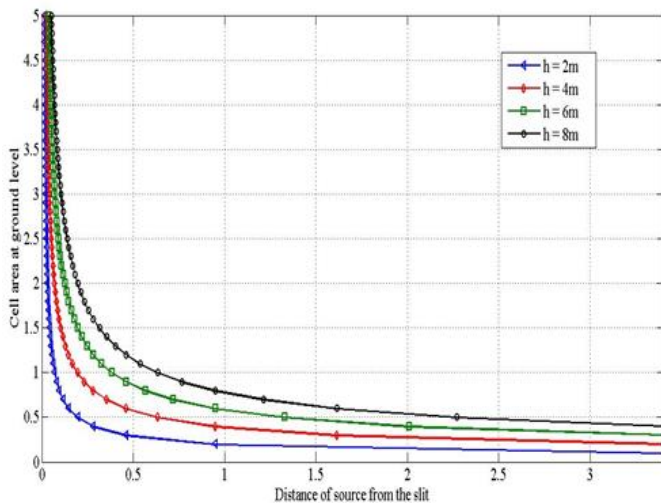


Fig. 14. Distance of source from slit and circular cell area at ground.

By analyzing the results against the height of the building and for different values of h_1 , it is observed that coverage area at ground level has a maximum value of high-rise building and the cell area decreases with the decrease in the building height.

The proposed model is also analyzed for the different building heights with respect to angle of incidence. With the increase in building heights will increase circular cell size at the base of the ground due to increase in distance between source LED and ground, see Fig. 15. The light beam spreads for larger distances results in large circular cell formed at ground level. The cell size increases for increasing heights of the buildings. It means spreading of beam is directly proportional to the height of the roof, increase in the height of roof results in more spreading of the beam and finally achieves a large circular area at the base of the floor.

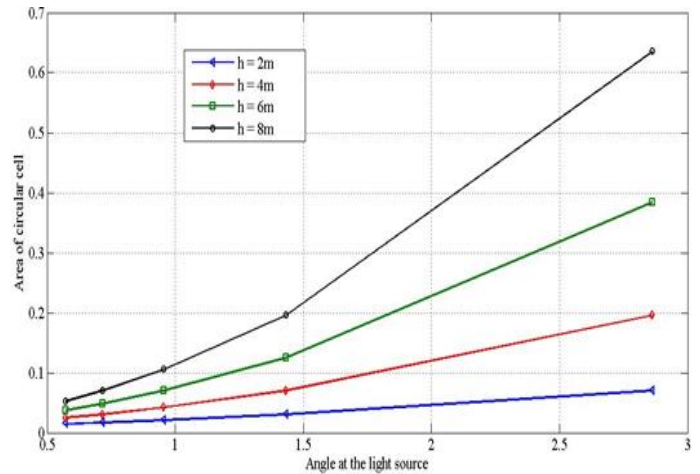


Fig. 15. Circular cell areas for different building heights and incident angles.

V. CONCLUSION

The basic principle and source using VLC is the radiation in the visible spectrum region which has not been for wireless communications till the introduction of VLC. The reason for using visible light for communication is its wider bandwidth and is not in the use of any other communication system as a source. Another main factor using VLC is that spectrum is licensed-free and anyone can use it anywhere without huge investment in spectrum license. In daily life, visible light is used for different purposes like reading, writing, working in homes, playing, street lights, in operation theaters, etc. In all these activities, Li-Fi access points can be used for internet using these light sources. Li-Fi is now used under the communication rules of VLC and implemented using IEEE 802.15.7 Standard.

The Li-Fi is an internet transmission source similar to Wi-Fi that communicates signals, data, picture, video and live streaming data using LED light source instead of radio waves as a transmitter and a photo detector for a purpose of receiver. The data is traveled wirelessly with the speed of light faster optical fiber communications.

Li-Fi will replace Wi-Fi in the near future as it is more economical wireless communication internet access point. Li-Fi is a very secure communication access point because it is used in the LoS situation. Only those users can access the Li-Fi point when light from the Li-Fi point falls on their devices, that's why Li-Fi is more secure than Wi-Fi.

We proposed a model for secure communication which enables to optimize the cell coverage according to the number of users in the area of interest. The proposed scheme made hotspot more secure and can be used to block an unauthorized access. Our idea provides a controlled coverage of cell that is used to enhance the security of Li-Fi. The coverage area is shown by cone shape and area of the cone can be controlled by many factors. A mechanical system is also installed on the roof to control the coverage area of a Li-Fi. Area of the cone is categorized in three forms small, medium and large. Every form has different values for different factors. This provides more security to Li-Fi because the number of users in connection is controllable now.

REFERENCES

- [1] G. Durgesh, "Visible Light Communication," Master of Applied Science thesis, Dalhousie University, 2012.
- [2] M. Ahmad, "Wireless network security vulnerabilities and concerns," In Security Technology, Disaster Recovery and Business Continuity, pp. 207-219, 2010.
- [3] T. M. Navyatha, N. Prathyusha, V. Roja, and M. Mounika, "Li-Fi (Light fidelity)-LED Based Alternative," International Journal of Scientific & Engineering Research, vol. 4, no. 5, pp. 1039-1042, 2013.
- [4] H. Haas, "Wireless data from every light bulb," TED Global, Edinburgh, July 2011.
- [5] D. Khandal, and S. Jain, "Li-fi (light fidelity): The future technology in wire-less communication," International Journal of Information & Computation Technology, vol. 4, no. 16, pp. 1-7, 2014.
- [6] K. V. Gagandeep, "Li-Fi: A New Communication Mechanism," International Journal of Computer Applications, vol. 118, no. 15, 2015.
- [7] M. Shaoyang, P. Charge, and S. Pillement, "A robust and energy efficient cooperative spectrum sensing scheme in cognitive wireless sensor networks," Network Protocols and Algorithms, vol. 7, no. 3, pp. 140-156, 2015.
- [8] D. Kumar, "Li-Fi- from Illumination to Communication," Grey B Services, 2016. Available Online: www.greyb.com.
- [9] S. Rastogi, "Li-Fi: A 5G Visible Data Communication," International Journal of Science and Research (IJSR), vol. 5, no. 9, 2016.
- [10] E. K. L. Ranjeet, "Fidelity (LI-FI)-A Comprehensive Study," International Journal of Computer Science and Mobile Computing, vol. 3, no. 4, pp. 475-481, 2014.
- [11] K. Yash, V. P. Tiwari, A. B. Patil, and K. Bala, "Li-Fi Technology, Implementations and Applications," IRJET, vol. 03, no. 04, 2016.
- [12] R. Jyoti, P. Chauhan, and R. Tripathi, "Li-Fi (Light Fidelity)-The future technology in wireless communication," Int. J. of Applied Engineering Research, vol. 7, no. 11, 2012.
- [13] A. Kumar, A. Raj, L. Sugacini, "IoT enabled by li-fi technology," An international journal of advanced computer technology, 2016.
- [14] D. Pummy, "A Review on Li-Fi (Light Fidelity): The Future Technology," IJARCCCE ISO, vol. 5, no. 10, 2016.
- [15] K. Sindhubala, B. Vijayalakshmi, "Design and performance analysis of visible light communication system through simulation," In Proc. IEEE International Conference on Computing and Communications Technologies, pp. 215-220, 2015.
- [16] A. M. Khalid, G. Cossu, R. Corsini, P. Choudhury, and E. Ciaramella, "1-Gb/s transmission over a phosphorescent white LED by using rate-adaptive discrete multitone modulation," IEEE Photonics Journal, vol. 4, no. 5, pp. 1465-1473, 2012.
- [17] L. Yingshu, C. Vu, C. Ai, G. Chen, and Y. Zhao, "Transforming complete coverage algorithms to partial coverage algorithms for wireless sensor networks," IEEE Transactions on Parallel and Distributed Systems, vol. 22, no. 4, pp. 695-703, 2011.
- [18] H. Li, G. Zhu, and X. Du, "Cognitive femtocell networks: an opportunistic spectrum access for future indoor wireless coverage," IEEE Wireless Communications, vol. 20, no. 2, pp. 44-51, 2013.
- [19] K. Forum, G. Hardik, "Li-Fi Technology—A survey on Current IT Trends," International Journal on Advances in Engineering Technology and Science, vol. 1, no. 2, pp. 29-31, 2015.
- [20] H. Harald, "High-speed wireless networking using visible light," SPIE Newsroom, vol. 19, 2013.
- [21] R. S. Theodore, "Wireless communications: principles and practice," vol. 2, New Jersey: Prentice Hall PTR, 1996.
- [22] B. J. Neil, "The cellular radio handbook: a reference for cellular system operation," Wiley-Interscience, 2001.
- [23] C. C. Donald, "Wireless network access for personal communications," IEEE Communications Magazine, vol. 30, no. 12, pp. 96-115, 1992.
- [24] Y. Yasushi, T. Otsu, A. Fujiwara, H. Murata, and S. Yoshida, "Multi-hop radio access cellular concept for fourth-generation mobile communications system," In Proc. of IEEE International Symposium on Personal, Indoor and Mobile Radio Communications, vol. 1, pp. 59-63, 2002.
- [25] F. Hiromasa, and H. Yoshino, "Theoretical capacity and outage rate of OFDMA cellular system with fractional frequency reuse," In IEEE Vehicular Technology Conference, pp. 1676-1680, 2008.
- [26] N. Rajagopal, P. Lazik, and A. Rowe, "Hybrid Visible Light Communication for Cameras and Low-Power Embedded Devices," In Proc. of ACM/IEEE Conference on Information Processing on Sensor Networks, 2015.
- [27] M. E. Michael, "Geometric modeling," New York: Wiley Computer Publishing, 1997.

A Collective Neurodynamic Approach to Survivable Virtual Network Embedding

Ashraf A. Shahin^{1,2}

¹College of Computer and Information Sciences, Al Imam Mohammad Ibn Saud Islamic University (IMSIU)
Riyadh, Kingdom of Saudi Arabia

²Department of Computer and Information Sciences, Institute of Statistical Studies & Research,
Cairo University, Cairo, Egypt

Abstract—Network virtualization has attracted significant amount of attention in the last few years as one of the key features of cloud computing. Network virtualization allows multiple virtual networks to share physical resources of single substrate network. However, sharing substrate network resources increases impact of single substrate resource failure. One of the commonly applied mechanisms to protect against such failures is provisioning redundant substrate resources for each virtual network to be used to recover affected virtual resources. However, redundant resources decreases cloud revenue by increasing virtual network embedding cost. In this paper, a collective neurodynamic approach has been proposed to reduce amount of provisioned redundant resources and reduce cost of embedding virtual networks. The proposed approach has been evaluated by using simulation and compared against some existing survivable virtual network embedding techniques.

Keywords—Collective neurodynamics; integer linear programming; global optimization; network virtualization; survivable virtual network embedding

I. INTRODUCTION

Virtualization is one of the distinctive features of cloud computing. Virtualization increases utilization of substrate resources and increases revenue of cloud datacenters by allowing embedding multiple virtual networks in a single substrate network. However, mapping virtual resources to substrate resources is known to be NP-hard even without considering other cloud computing features such as scalability and survivability [1]-[3].

Although, sharing substrate resources among multiple virtual networks sustains cloud computing with many valuable benefits, it brings critical survivability issues. Single substrate resource failure can cause long service downtime and waste a lot of date from several virtual networks (VNs) [4]. Substrate resource failure becomes a part of everyday operation in today's Internet Service Provider (ISP) networks [5].

One of the most efficient protection approaches is provisioning redundant resources for each virtual network (VN). Redundant resources enable fast reallocating affected virtual resources after substrate resource failures. Nevertheless, redundant resources increase capacity of required virtual resources, which reduces revenue and reduces acceptance ratio of cloud datacenters.

In this paper, a collective neurodynamic optimization approach has been proposed to reduce amount of required redundant resources and to optimize virtual network embedding. To guarantee virtual network restorability after substrate node failure, the proposed approach enhances virtual network by adding one virtual node and set of virtual links. Virtual networks are enhanced by applying virtual network enhancing design proposed by Guo et al. in [1]. The problem has been formulated as Mixed-Integer Linear Programming and solved by applying neural network proposed by Xia in [6]. To guarantee survivability against substrate link failure, virtual links are embedded by applying multi-path link embedding approach proposed by Khan et al. in [7].

The problem of multi-path link embedding of enhanced virtual network has been formulated as Mixed-Integer Linear Programming and has been solved by using collective neurodynamic optimization approach, which combines the ability of social thinking in Particle Swarm Optimization with the local search capability of Neural Network.

Effectiveness of the proposed approach has been evaluated by comparing its performance with other approaches. Simulation results show that the proposed model reduces required redundant resources and increases revenue.

The rest of this paper is organized as follows. Section 2 describes the related work. Section 3 briefly describes the proposed model. Section 4 experimentally demonstrates the effectiveness of the proposed model. Finally, Section 6 concludes.

II. RELATED WORK

Several survivable virtual network embedding (SVNE) approaches have been proposed in the last few years [1]-[4]. Guo et al. [1] have proposed survivable virtual network embedding approach. The proposed approach enhanced virtual network by adding additional virtual resources and redesigning virtual network with considering failure dependent protection technique, which provides backup substrate node for each substrate node failure scenario. Enhanced virtual network has been formulated using binary quadratic programming, and virtual network embedding has been formulated using mixed integer linear programming. Although, the proposed approach reduces amount of required substrate resources to design survivable virtual network, it increases number of required migrations after failures, which increases service down time.

A topology-aware remapping policy has been proposed by Xiao et al. [2] to deal with single substrate node failures. Based on network topology, a set of candidate backup substrate nodes has been defined for each substrate node and a set of candidate backup substrate links has been defined for each substrate link. In [8], Xiao et al. have extended the proposed policy in [2] to handle multiple nodes failures. However, the proposed policy uses all substrate nodes to accommodate incoming virtual networks. Therefore, when a substrate node failure happens, the proposed policy does not grantee that for each migrated virtual node there is a candidate backup substrate node with enough free resources to accommodate migrated virtual node.

Zhou et al. [3] have studied survivability of virtual networks against multiple physical link failures. They have formulated the problem of remapping virtual network with multiple physical link failures using mixed integer linear programming and have proposed an approach to find exact solution for the formulated problem. However, the proposed approach can deal only with small virtual networks.

Qiang et al. [9] have modeled the survivable virtual network embedding problem as an integer linear programming model and have used bee colony algorithm to find near optimal virtual network embedding solution. After substrate node failure, virtual nodes are migrated to normal node, which is specified by greed rules first, and virtual links are migrated to shortest substrate path. However, finding suitable substrate node for each migrated virtual node is a very complicated task. The reasons behind this complexity are not only connectivity and CPU constraints, but also lack of substrate resources. The proposed approach does not reserve a backup quota to be used after failures, which decreases the probability of finding enough and free substrate resources for recovering affected virtual resources and increases the probability of violating service level agreement.

To enhance virtual network survivability against single substrate link failure, Chen et al. [10] have proposed a linear programming model to formulate problem of allocating bandwidth for primary paths, backup paths, and shared backup paths. Performance of bandwidth allocation scheme has been improved by employing load-balancing strategy. After link failure, instead of migrating affected virtual links from failed substrate link, allocated bandwidths are reconfigured to cover affected virtual links.

Gu et al. [11], [13], [14] have proposed virtual network embedding scheme to guarantee recovery from single regional failure event. Before embedding each virtual network requests, working and recovery embeddings are specified to grantee that it is failure region disjoint. The problem has been formulated as a mixed integer linear programming problem and has been solved by proposing two heuristic solutions. The proposed solutions have improved resource efficiencies by considering mapping cost and load balancing during embedding process.

Mijumbi et al. [12] have proposed a distributed negotiation protocol to support virtual network survivability against physical link failures in multi-domain environments. The proposed protocol contains seven messages, which forms interactions between infrastructure providers and virtual

network providers during backup and restoration for single physical link failures.

Meixner et al. [15] have proposed a probabilistic model to reduce the probability of virtual network disconnections and capacity loss due to single substrate link failure. The problem has been modeled as integer linear program model based on risk assessment to economically select sustainable backup substrate node.

Sun et al. [16] have modeled the problem of survivable virtual network embedding using mixed-integer linear programming (MILP) and proposed two algorithms: Lagrangian Relaxation based algorithm, and Decomposition based algorithm. While experimental shows that the proposed algorithms reduce computational complexity compared to MILP, they sustain the same embedding cost.

Rahman and Boutaba [5] have provided a mathematical formulation of the survivable virtual network embedding (SVNE) problem. To avoid mixed-integer programs complexity, Rahman and Boutaba have proposed hybrid policy heuristic, which proactively solves the problem of single substrate link failure with considering customer service level agreement constraints. Before any virtual network arrives, a set of candidate backup detours is calculated for each substrate link. After receiving new virtual network request, virtual nodes are embedded by applying two node-embedding algorithms: greedy node embedding heuristic that has been proposed by Zhu and Ammar in [17], and D-ViNE Algorithm, which has been proposed by Chowdhury and Rahman in [18]. To recover from substrate link failure, they have proposed hybrid and proactive backup detour algorithms. Performance of different combination of virtual node embedding algorithms and substrate link failure recovery algorithms have been evaluated by using ViNE-Yard simulator with different VN request topologies. Simulation results demonstrate that the proposed solutions outperform BLIND policy heuristic, which re-computes a new link embedding for each VN affected by the substrate link failure.

III. COLLECTIVE NEURODYNAMIC SURVIVABLE VNE

Cloud datacenter receives users' requests as virtual networks (VNs). Each VN contains a set of virtual nodes (virtual machines) and a set of virtual links connect these nodes. Virtual network VN is modeled as a weighted undirected graph $G_v = (N_v, L_v)$, where N_v is the set of virtual nodes and L_v is the set of virtual links. Virtual nodes and virtual links are weighted by the required CPU and bandwidth, respectively.

Enhancing virtual network to improve survivability of virtual network $G_v = (N_v, L_v)$ with $n = |N_v|$ virtual nodes, an enhanced virtual network $G_e = (N_e, L_e)$ is constructed. Enhanced virtual network G_e extends G_v by adding one additional virtual node and set of virtual links. Resources of G_e are specified to guarantee that there are enough resources to reallocate G_v after any substrate link or single node failures.

Each reallocation is represented by using three matrices A , B , and C . A is $(n + 1)$ matrix, where $a_i = j$ means that virtual node i is allocated on node j . B is $(n + 1) \times (n + 1)$

matrix, where b_{ij} refers to the required bandwidth for the virtual link that connects virtual nodes i and j . C is $(n + 1)$ matrix, where $c_i = y$ implies that virtual node i requires CPU with capacity y .

Virtual network enhancing process is initialized by allocating virtual nodes from virtual network (which contains n virtual nodes) to the first n nodes in the enhanced virtual network. The initial allocation matrix A^0 becomes as following

$$A^0 = (1, 2, \dots, n, 0)$$

$a_{n+1}^0 = 0$ refers to that node $n + 1$ in the enhanced virtual network is empty and is not used in this case.

To recovery from k^{th} substrate node failure, re-embedding matrix A^k can be generated by permuting matrix A^0 . Matrix A^k can be represented by permutation matrix X^k , which is an orthogonal matrix of size $(n + 1) \times (n + 1)$ such that

$$x_{ij}^k = \begin{cases} 1 & \text{if } a_i^k = j, \\ 0 & \text{otherwise.} \end{cases}$$

Thus, re-embedding matrices is calculated as

$$A^k = A^0 X^k$$

$$C^k = C^0 X^k$$

$$B^k = (X^k)^T B^0 X^k$$

Therefore, the problem of enhancing virtual network is formulated as following:

$$\text{Min } \left(\sum_{i=1}^{n+1} c_i^e + \alpha \sum_{i=1}^{n+1} \sum_{j=1}^{n+1} b_{ij}^e \right) \quad (1)$$

Subject to

$$c_i^e = \max_k c_i^k, \forall k \in \{1, \dots, n\}, i \in \{1, \dots, n+1\} \quad (2)$$

$$b_{ij}^e = \max_k b_{ij}^k, \forall k \in \{1, \dots, n\}, i, j \in \{1, \dots, n+1\} \quad (3)$$

$$c_i^k = \sum_{j=1}^{n+1} c_j^0 x_{ji}^k, \forall k \in \{1, \dots, n\}, i \in \{1, \dots, n+1\} \quad (4)$$

$$b_{ij}^k = \sum_{m=1}^{n+1} \sum_{l=1}^{n+1} b_{lm}^0 x_{li}^k x_{mj}^k, \forall k \in \{1, \dots, n\}, i, j \in \{1, \dots, n+1\} \quad (5)$$

$$\sum_{j=1}^{n+1} x_{ij}^k = 1, \forall k \in \{1, \dots, n\}, i \in \{1, \dots, n+1\} \quad (6)$$

$$\sum_{i=1}^{n+1} x_{ij}^k = 1, \forall k \in \{1, \dots, n\}, j \in \{1, \dots, n+1\} \quad (7)$$

$$x_{ik}^k = 1, \forall k \in \{1, \dots, n\}, i = n + 1 \quad (8)$$

$$x_{ij}^k \in \{0, 1\}, \forall k \in \{1, \dots, n\}, i, j \in \{1, \dots, n+1\} \quad (9)$$

Where, α is the weight coefficient to represent importance of bandwidth and CPU resources. Constraints (2) - (5) ensure that there are sufficient resources to re-allocate virtual network after different failures. Constraint (6) reveals that each virtual node is allocated to only one substrate node and constraint (7) makes certain that each substrate node contains only one virtual node from the same virtual network. Constraint (8) guarantees that for each k^{th} substrate node failure there is a permutation matrix X^k to generate re-embedding matrix A^k from the initial matrix A^0 .

This problem is nonconvex due to bilinear constraints (5) and it can be linearized by replacing the quadratic terms $x_{li}^k x_{mj}^k$ by five-dimensional array $Y = (y_{limjk})$

$$y_{limjk} = x_{li}^k x_{mj}^k, \forall k \in \{1, \dots, n\}, l, i, m, j \in \{1, \dots, n+1\}$$

After replacing the zero-one integrality constraint (9) with non-negativity constraint, the problem becomes equivalent to the following linear programming problem:

$$\text{Min } P(Z) = \left(\sum_{i=1}^{n+1} c_i^e + \alpha \sum_{i=1}^{n+1} \sum_{j=1}^{n+1} b_{ij}^e \right) \quad (10)$$

Subject to

$$\sum_{i=1}^{n+1} c_i^0 x_{ij}^k - c_j^e \leq 0, \forall k \in \{1, \dots, n\}, j \in \{1, \dots, n+1\}$$

$$-b_{lm}^e \leq 0, \forall k \in \{1, \dots, n\}, l, m \in \{1, \dots, n+1\} \quad (11) \sum_{j=1}^{n+1} \sum_{i=1}^{n+1} b_{ij}^0 y_{limjk}$$

$$-b_{lm}^e \leq 0, \forall k \in \{1, \dots, n\}, l, m \in \{1, \dots, n+1\}$$

$l, m \in \{1, \dots, n+1\}$

$$+ 1\} \quad (12) \sum_{l=1}^{n+1} \sum_{i=1}^{n+1} \sum_{m=1}^{n+1} \sum_{j=1}^{n+1} y_{limjk}$$

$$= (n + 1)^2, \forall k \in \{1, \dots, n\} \quad (13)$$

$$2y_{limjk} - x_{li}^k - x_{mj}^k \leq 0, \forall k \in \{1, \dots, n\}, l, i, m, j \in \{1, \dots, n+1\} \quad (14)$$

$$y_{limjk} \geq 0, \forall k \in \{1, \dots, n\}, i, j, l, m \in \{1, \dots, n+1\} \quad (15)$$

$$\sum_{j=1}^{n+1} x_{ij}^k = 1, \forall k \in \{1, \dots, n\}, i \in \{1, \dots, n+1\} \quad (16)$$

$$\sum_{i=1}^{n+1} x_{ij}^k = 1, \forall k \in \{1, \dots, n\}, j \in \{1, \dots, n+1\} \quad (17)$$

$$x_{ik}^k = 1, \forall k \in \{1, \dots, n\}, i = n + 1 \quad (18)$$

$$x_{ij}^k \geq 0, \forall k \in \{1, \dots, n\}, i, j \in \{1, \dots, n+1\} \quad (19)$$

Z is defined as $Z = (C^e, B^e, Y', X')^T$, where C^e and B^e are vectors represent required CPU and bandwidth for the enhanced virtual network. Y' and X' are vectors represent all variables in the five-dimensional array Y and in the three-dimensional array X , which contains all permutations.

The primal problem (10)-(19) is liner programming and it can be written in the following general matrix form:

$$\text{Minimize } d^T z \quad (20)$$

Subject to

$$M_{11}z_1 + M_{12}z_2 \geq r_1 \quad (21)$$

$$M_{21}z_1 + M_{22}z_2 = r_2 \quad (22)$$

$$z_1 \geq 0 \quad (23)$$

where $z = \begin{pmatrix} z_1 \\ z_2 \end{pmatrix} \in \mathbb{R}^{q_1}$, $d = \begin{pmatrix} d_1 \\ d_2 \end{pmatrix} \in \mathbb{R}^{q_1}$,

$$r = \begin{pmatrix} r_1 \\ r_2 \end{pmatrix} \in \mathbb{R}^{q_2},$$

$$q_1 = n + n^2 + n \cdot (n + 1)^2 + n \cdot (n + 1)^4,$$

$$q_2 = n^5 + 2n^4 + 3n^3 + 8n^2 + 7n$$

From dual theory [6], dual problem for the previous primal problem is:

$$\text{Maximize } r^T \xi \quad (24)$$

Subject to

$$M_{11}\xi_1 + M_{21}\xi_2 \leq d_1 \quad (25)$$

$$M_{12}\xi_1 + M_{22}\xi_2 = d_2 \quad (26)$$

$$\xi_1 \geq 0 \quad (27)$$

Where $\xi = (\lambda, \mu)^T$, and $\xi = \begin{pmatrix} \xi_1 \\ \xi_2 \end{pmatrix} \in \mathbb{R}^{q_2}$

To solve the primal problem (20)-(23) and dual problem (24)-(27), Xia [6] has proposed neural network with the following differential equation to drive its state vector $u = (z, \xi)^T$.

$$\frac{du}{dt} = -\nabla E(u) \quad (28)$$

Where, $\nabla E(u)$ is the gradient of the energy function $E(u)$, which is defined as following:

$$\begin{aligned} E(z, \xi) = & \frac{1}{2} (d^T z - r^T \xi)^2 + \frac{1}{2} z_1^T (z_1 - |z_1|) \\ & + \frac{1}{2} \xi_1^T (\xi_1 - |\xi_1|) \\ & + \frac{1}{2} \|M_2 z - r_2\|_2^2 + \frac{1}{2} \|M_4 \xi - d_2\|_2^2 \\ & + \frac{1}{2} [M_1 z - r_1]^T [(M_1 z - r_1) - |M_1 z - r_1|] \\ & + \frac{1}{2} [d_1 - M_3 \xi]^T [(d_1 - M_3 \xi) - |d_1 - M_3 \xi|], \quad (29) \end{aligned}$$

Where, $M_1 = (M_{11}, M_{12}), M_2 = (M_{21}, M_{22}),$

$$M_3 = (M_{11}^T, M_{21}^T), \text{ and } M_4 = (M_{12}^T, M_{22}^T)$$

To apply the previous neural network to the primal problem (10)-(19), constraints are switched to penalties by using Lagrange and Karush-Kuhn-Tucker multipliers as follows:

$$\begin{aligned} L(z, \lambda, \mu) = & \left(\sum_{i=1}^{n+1} c_i^e + \alpha \sum_{i=1}^{n+1} \sum_{j=1}^{n+1} b_{ij}^e \right) \\ & + \sum_{k=1}^n \lambda_k \cdot \left(\sum_{l=1}^{n+1} \sum_{i=1}^{n+1} \sum_{m=1}^{n+1} \sum_{j=1}^{n+1} y_{limjk} - (n+1)^2 \right) \\ & + \sum_{i=1}^{n+1} \sum_{k=1}^n \lambda_{k+n.i} \cdot \left(\sum_{j=1}^{n+1} x_{ij}^k - 1 \right) \\ & + \sum_{j=1}^{n+1} \sum_{k=1}^n \lambda_{k+n.j+n.(n+1)} \cdot \left(\sum_{i=1}^{n+1} x_{ij}^k - 1 \right) \\ & + \sum_{i=1}^{n+1} \sum_{k=1}^n \lambda_{k+n.i+2.n.(n+1)} \cdot \left(x_{ik}^k - 1 \right) \\ & + \sum_{j=1}^{n+1} \sum_{k=1}^n \mu_{q_{kj}} \cdot \left(\sum_{i=1}^{n+1} c_i^0 x_{ij}^k - c_j^e \right) \end{aligned}$$

$$\begin{aligned} & + \sum_{l=1}^{n+1} \sum_{m=1}^{n+1} \sum_{k=1}^n \mu_{q_{kml}} \cdot \left(\sum_{j=1}^{n+1} \sum_{i=1}^{n+1} b_{ij}^0 y_{limjk} - b_{lm}^e \right) \\ & + \sum_{l=1}^{n+1} \sum_{m=1}^{n+1} \sum_{i=1}^{n+1} \sum_{j=1}^{n+1} \sum_{k=1}^n \mu_{q_{kjiml}} \cdot \left(2y_{limjk} - x_{li}^k - x_{mj}^k \right), \quad (30) \end{aligned}$$

$$\mu_i \geq 0, \forall i \in \{1, \dots, n^5 + 2n^4 + 3n^3 + 5n^2 + 3n\}$$

Where, λ and μ are vectors of Lagrange and Karush-Kuhn-Tucker multipliers, respectively.

$$\lambda = (\lambda_1, \dots, \lambda_i), i \in \{1, \dots, 3n^2 + 4n\}$$

$$\mu = (\mu_1, \dots, \mu_i), i \in \{1, \dots, n^5 + 2n^4 + 3n^3 + 5n^2 + 3n\}$$

q_{kj}, q_{kml} , and q_{kjiml} are defined as following:

$$q_{kj} = k + n \cdot (j - 1), \forall k \in \{1, \dots, n\}, j \in \{1, \dots, n + 1\}$$

$$q_{kml} = k + n \cdot (m + n) + n \cdot (n + 1) \cdot (l - 1),$$

$$\forall k \in \{1, \dots, n\}, m, l \in \{1, \dots, n + 1\}$$

$$q_{kjiml} = k + n \cdot j + n^2 + n \cdot (n + 1) \cdot (i + n \cdot m + n^2 \cdot l - n^2),$$

$$\forall k \in \{1, \dots, n\}, i, j, l, m \in \{1, \dots, n + 1\}$$

To find the dual function, which is infimum value of the lagrangian function $L(z, \lambda, \mu)$, the derivative of the function $L(z, \lambda, \mu)$ with respect to z must be zero. Thus, the dual problem is formulated as follows:

Maximize

$$\begin{aligned} D(\lambda, \mu) = & - \sum_{k=1}^n (n+1)^2 \cdot \lambda_k - \sum_{i=1}^{n+1} \sum_{k=1}^n \lambda_{k+n.i} \\ & - \sum_{j=1}^{n+1} \sum_{k=1}^n \lambda_{k+n.j+n.(n+1)} - \\ & \sum_{i=1}^{n+1} \sum_{k=1}^n \lambda_{k+n.i+2.n.(n+1)} \quad (31) \end{aligned}$$

Subject to

$$1 - \sum_{k=1}^n \mu_{k+n.(j-1)} = 0, \forall j \in \{1, \dots, n + 1\} \quad (32)$$

$$\alpha - \sum_{k=1}^n \mu_{k+n.(j+n)+n.(n+1).(i-1)} = 0, \forall i, j \in \{1, \dots, n + 1\} \quad (33)$$

$$\begin{aligned} \lambda_k + b_{ij}^0 \cdot \mu_{q_{kml}} + 2 \mu_{q_{kjiml}} = 0, \forall i, j, l, m \\ \in \{1, \dots, n + 1\}, k \in \{1, \dots, n\} \quad (34) \end{aligned}$$

$$\begin{aligned} \lambda_{k+n.i} + \lambda_{k+n.k+n.(n+1)} + \lambda_{k+n.i+2.n.(n+1)} + \\ c_i^0 \cdot \mu_{k+n.(k-1)} - \sum_{l=1}^{n+1} \sum_{m=1}^{n+1} \mu_{q'_{kml}} = 0, \quad (35) \end{aligned}$$

$$\begin{aligned} q'_{kml} = & k + n \cdot k + n^2 \\ & + n \cdot (n + 1) \cdot (m + n \cdot i + n^2 \cdot l - n^2), \\ & \forall i, m, l \in \{1, \dots, n + 1\}, k \in \{1, \dots, n\} \end{aligned}$$

$$\begin{aligned} \lambda_{k+n.i} + \lambda_{k+n.j+n.(n+1)} + c_i^0 \cdot \mu_{k+n.(j-1)} - \\ \sum_{l=1}^{n+1} \sum_{m=1}^{n+1} \mu_{q_{kjiml}} = 0, \quad (36) \end{aligned}$$

$$\begin{aligned} q_{kjiml} = & k + n \cdot j + n^2 \\ & + n \cdot (n + 1) \cdot (m + n \cdot i + n^2 \cdot l - n^2), \\ & \forall i, j, m, l \in \{1, \dots, n + 1\}, k \in \{1, \dots, n\}, j \neq k \\ \mu_i \geq 0, \forall i \in \{1, \dots, n^5 + 2n^4 + 3n^3 + 5n^2 + 3n\} \quad (37) \end{aligned}$$

The time derivative of a state variable is calculated as partial derivative of the energy function in (28). Thus, the dynamic equation of the neural network is defined by the following differential equations:

$$\frac{dc_i^e}{dt} = -\beta \left\{ \sum_{m=1}^{n+1} c_m^e + \alpha \sum_{j=1}^{n+1} \sum_{k=1}^{n+1} b_{mj}^e + \sum_{k=1}^n (n+1)^2 \cdot \lambda_k + \sum_{m=1}^{n+1} \sum_{k=1}^n \lambda_{k+n.m} + \sum_{j=1}^{n+1} \sum_{k=1}^n \lambda_{k+n.j+n.(n+1)} + \sum_{m=1}^{n+1} \sum_{k=1}^n \lambda_{k+n.m+2.n.(n+1)} + \sum_{k=1}^n (c_i^e - \sum_{j=1}^{n+1} c_j^e x_{ji}^k - |c_i^e - \sum_{j=1}^{n+1} c_j^e x_{ji}^k|) \right\}, \forall i \in \{1, \dots, n+1\} \quad (38)$$

$$\frac{db_{ij}^e}{dt} = -\beta \left\{ \alpha \cdot (\sum_{l=1}^{n+1} c_l^e + \alpha \sum_{l=1}^{n+1} \sum_{m=1}^{n+1} b_{lm}^e + \sum_{k=1}^n (n+1)^2 \cdot \lambda_k + \sum_{l=1}^{n+1} \sum_{k=1}^n \lambda_{k+n.l} + \sum_{l=1}^{n+1} \sum_{k=1}^n \lambda_{k+n.l+n.(n+1)} + \sum_{l=1}^{n+1} \sum_{k=1}^n \lambda_{k+n.l+2.n.(n+1)}) + \sum_{k=1}^n (b_{ij}^e - \sum_{l=1}^{n+1} \sum_{m=1}^{n+1} b_{ml}^0 y_{imjlk} - |b_{ij}^e - \sum_{l=1}^{n+1} \sum_{m=1}^{n+1} b_{ml}^0 y_{imjlk}|) \right\}, \forall i, j \in \{1, \dots, n+1\} \quad (39)$$

$$\frac{dy_{ijlmk}}{dt} = -\beta \left\{ y_{ijlmk} - |y_{ijlmk}| + \sum_{p=1}^{n+1} \sum_{q=1}^{n+1} \sum_{r=1}^{n+1} \sum_{s=1}^{n+1} y_{pqrsk} - (n+1)^2 - b_{jm}^0 \cdot b_{il}^e + b_{jm}^0 \cdot \sum_{q=1}^{n+1} \sum_{p=1}^{n+1} b_{pq}^0 y_{ipqlk} - b_{jm}^0 \cdot |b_{il}^e - \sum_{q=1}^{n+1} \sum_{p=1}^{n+1} b_{pq}^0 y_{ipqlk}| - 2x_{ij}^k - 2x_{lm}^k + 4y_{ijlmk} + 2|x_{ij}^k + x_{lm}^k - 2y_{ijlmk}| \right\}, \forall i, j, l, m \in \{1, \dots, n+1\}, k \in \{1, \dots, n\} \quad (40)$$

$$\frac{dx_{ij}^k}{dt} = -\beta \left\{ x_{ij}^k - |x_{ij}^k| + \sum_{p=1}^{n+1} (x_{ip}^k + x_{pi}^k) - 2 - c_p^0 \cdot c_j^e + c_p^0 \cdot \sum_{p=1}^{n+1} c_p^0 x_{pj}^k + c_p^0 \cdot |c_j^e - \sum_{p=1}^{n+1} c_p^0 x_{pj}^k| + \sum_{q=1}^{n+1} \sum_{m=1}^{n+1} (x_{ij}^k + x_{mq}^k - 2y_{ijmqk}) - \sum_{q=1}^{n+1} \sum_{m=1}^{n+1} |x_{ij}^k + x_{mq}^k - 2y_{ijmqk}| + \sum_{l=1}^{n+1} \sum_{p=1}^{n+1} (x_{lp}^k + x_{ij}^k - 2y_{lpijk}) - \sum_{l=1}^{n+1} \sum_{p=1}^{n+1} |x_{lp}^k + x_{ij}^k - 2y_{lpijk}| - 2x_{ij}^k + 2y_{ijijk} + |2x_{ij}^k - 2y_{ijijk}| \right\}, \forall i, j \in \{1, \dots, n+1\}, k \in \{1, \dots, n\}, \text{ such that } (i \neq n+1) \text{ or } (j \neq k) \quad (41)$$

$$\frac{dx_{(n+1)k}^k}{dt} = -\beta \left\{ x_{(n+1)k}^k - |x_{(n+1)k}^k| + \sum_{p=1}^{n+1} (x_{(n+1)p}^k + x_{p(n+1)k}^k) - 2 - c_p^0 \cdot c_k^e + c_p^0 \cdot \sum_{p=1}^{n+1} c_p^0 x_{pk}^k + c_p^0 \cdot |c_k^e - \sum_{p=1}^{n+1} c_p^0 x_{pk}^k| + \sum_{q=1}^{n+1} \sum_{m=1}^{n+1} (x_{(n+1)k}^k + x_{mq}^k - 2y_{(n+1)kmqk}) - \sum_{q=1}^{n+1} \sum_{m=1}^{n+1} |x_{(n+1)k}^k + x_{mq}^k - 2y_{(n+1)kmqk}| + \sum_{l=1}^{n+1} \sum_{p=1}^{n+1} (x_{lp}^k + x_{(n+1)k}^k - 2y_{lp(n+1)kk}) - \sum_{l=1}^{n+1} \sum_{p=1}^{n+1} |x_{lp}^k + x_{(n+1)k}^k - 2y_{lp(n+1)kk}| \right\}, \forall k \in \{1, \dots, n\} \quad (42)$$

$$\frac{d\lambda_i}{dt} = -\beta \left\{ \sum_{s=1}^{n+1} \sum_{j=1}^{n+1} \sum_{l=1}^{n+1} \sum_{m=1}^{n+1} (\lambda_i + b_{sj}^0 \cdot \mu_{qiml} + 2\mu_{qijsm}) + (n+1) \cdot (\sum_{s=1}^{n+1} c_s^e + \alpha \sum_{s=1}^{n+1} \sum_{j=1}^{n+1} b_{sj}^e + \sum_{k=1}^n (n+1)^2 \cdot \lambda_k + \sum_{s=1}^{n+1} \sum_{k=1}^n \lambda_{k+n.s} + \sum_{j=1}^{n+1} \sum_{k=1}^n \lambda_{k+n.j+n.(n+1)} + \sum_{s=1}^{n+1} \sum_{k=1}^n \lambda_{k+n.s+2.n.(n+1)}) \right\}, \forall i \in \{1, \dots, n\} \quad (43)$$

$$\frac{d\lambda_{k+n.s}}{dt} = -\beta \left\{ \sum_{j \in \{1, \dots, n+1\} - \{k\}} (\lambda_{k+n.s} + \lambda_{k+n.j+n.(n+1)} + c_s^0 \cdot \mu_{k+n.(j-1)} - \sum_{l=1}^{n+1} \sum_{m=1}^{n+1} \mu_{qkjmsl}) + \lambda_{k+n.s} + \lambda_{k+n.k+n.(n+1)} + \lambda_{k+n.s+2.n.(n+1)} + c_s^0 \cdot \mu_{k+n.(k-1)} - \sum_{l=1}^{n+1} \sum_{m=1}^{n+1} \mu_{qkmsl} + \sum_{i=1}^{n+1} c_i^e + \alpha \sum_{i=1}^{n+1} \sum_{j=1}^{n+1} b_{ij}^e + \sum_{r=1}^n (n+1)^2 \cdot \lambda_r + \sum_{i=1}^{n+1} \sum_{r=1}^n \lambda_{r+n.i} + \sum_{j=1}^{n+1} \sum_{r=1}^n \lambda_{r+n.j+n.(n+1)} + \sum_{i=1}^{n+1} \sum_{r=1}^n \lambda_{r+n.i+2.n.(n+1)} \right\}, \forall k \in \{1, \dots, n\}, s \in \{1, \dots, n+1\} \quad (44)$$

$$\frac{d\lambda_{k+n.j+n.(n+1)}}{dt} = -\beta \left\{ \sum_{s=1}^{n+1} (\lambda_{k+n.s} + \lambda_{k+n.j+n.(n+1)} + c_s^0 \cdot \mu_{k+n.(j-1)} - \sum_{l=1}^{n+1} \sum_{m=1}^{n+1} \mu_{qkjmsl}) + \sum_{i=1}^{n+1} c_i^e + \alpha \sum_{i=1}^{n+1} \sum_{r=1}^{n+1} b_{ir}^e + \sum_{s=1}^n (n+1)^2 \cdot \lambda_s + \sum_{i=1}^{n+1} \sum_{s=1}^n \lambda_{s+n.i} + \sum_{r=1}^{n+1} \sum_{s=1}^n \lambda_{s+n.r+n.(n+1)} + \sum_{i=1}^{n+1} \sum_{s=1}^n \lambda_{s+n.i+2.n.(n+1)} \right\}, \forall k \in \{1, \dots, n\}, j \in \{1, \dots, n+1\}, k \neq j \quad (45)$$

$$\frac{d\lambda_{k+n.k+n.(n+1)}}{dt} = -\beta \left\{ \sum_{s=1}^{n+1} (\lambda_{k+n.s} + \lambda_{k+n.k+n.(n+1)} + c_s^0 \cdot \mu_{k+n.(k-1)} - \sum_{l=1}^{n+1} \sum_{m=1}^{n+1} \mu_{qkkmsl}) + \sum_{s=1}^{n+1} (\lambda_{k+n.s} + \lambda_{k+n.k+n.(n+1)} + \lambda_{k+n.s+2.n.(n+1)} + c_s^0 \cdot \mu_{k+n.(k-1)} - \sum_{l=1}^{n+1} \sum_{m=1}^{n+1} \mu_{qkmsl}) + \sum_{i=1}^{n+1} c_i^e + \alpha \sum_{i=1}^{n+1} \sum_{r=1}^{n+1} b_{ir}^e + \sum_{s=1}^n (n+1)^2 \cdot \lambda_s + \sum_{i=1}^{n+1} \sum_{s=1}^n \lambda_{s+n.i} + \sum_{r=1}^{n+1} \sum_{s=1}^n \lambda_{s+n.r+n.(n+1)} + \sum_{i=1}^{n+1} \sum_{s=1}^n \lambda_{s+n.i+2.n.(n+1)} \right\}, \forall k \in \{1, \dots, n\} \quad (46)$$

$$\frac{d\lambda_{k+n.j+2.n.(n+1)}}{dt} = -\beta \left\{ \sum_{i=1}^{n+1} c_i^e + \alpha \sum_{i=1}^{n+1} \sum_{r=1}^{n+1} b_{ir}^e + \sum_{s=1}^n (n+1)^2 \cdot \lambda_s + \sum_{i=1}^{n+1} \sum_{k=1}^n \lambda_{s+n.i} + \sum_{r=1}^{n+1} \sum_{s=1}^n \lambda_{s+n.r+n.(n+1)} + \sum_{i=1}^{n+1} \sum_{s=1}^n \lambda_{s+n.i+2.n.(n+1)} + \lambda_{k+n.j} + \lambda_{k+n.k+n.(n+1)} + \lambda_{k+n.j+2.n.(n+1)} + c_j^0 \cdot \mu_{k+n.(k-1)} - \sum_{l=1}^{n+1} \sum_{m=1}^{n+1} \mu_{qkmj} \right\}, \forall k \in \{1, \dots, n\}, j \in \{1, \dots, n+1\} \quad (47)$$

$$\frac{d\mu_{k+n.(j-1)}}{dt} = -\beta \left\{ \mu_{k+n.(j-1)} - |\mu_{k+n.(j-1)}| + \sum_{s=1}^n \mu_{s+n.(j-1)} - 1 + \sum_{i=1}^{n+1} \left(\lambda_{k+n.i} + \lambda_{k+n.j+n.(n+1)} + c_i^0 \cdot \mu_{k+n.(j-1)} - \sum_{l=1}^{n+1} \sum_{m=1}^{n+1} \mu_{q_{kjmil}} \right) \right\}, \forall j \in \{1, \dots, n+1\}, k \in \{1, \dots, n\}, j \neq k \quad (48)$$

$$\frac{d\mu_{k+n.(k-1)}}{dt} = -\beta \left\{ \mu_{k+n.(k-1)} - |\mu_{k+n.(k-1)}| + \sum_{s=1}^n \mu_{s+n.(k-1)} - 1 + \sum_{s=1}^{n+1} \left(\lambda_{k+n.s} + \lambda_{k+n.k+n.(n+1)} + \lambda_{k+n.s+2.n.(n+1)} + c_s^0 \cdot \mu_{k+n.(k-1)} - \sum_{l=1}^{n+1} \sum_{m=1}^{n+1} \mu_{q'_{kmsl}} \right) \right\}, q'_{kmsl} = k + n.k + n^2 + n.(n+1).(m+n.s+n^2.l-n^2), \forall k \in \{1, \dots, n\} \quad (49)$$

$$\frac{d\mu_{q_{kji}}}{dt} = -\beta \left\{ \mu_{q_{kji}} - |\mu_{q_{kji}}| + \sum_{s=1}^n \mu_{q_{sji}} - \alpha + \sum_{r=1}^{n+1} \left(\lambda_k + b_{sr}^0 \cdot \mu_{q_{kji}} + 2 \mu_{q_{krsji}} \right) \right\}, q_{kji} = k + n.(j+n) + n.(n+1).(i-1), \forall i, j \in \{1, \dots, n+1\}, k \in \{1, \dots, n\}$$

$$\frac{d\mu_{q_{kjmil}}}{dt} = -\beta \left\{ \mu_{q_{kjmil}} - |\mu_{q_{kjmil}}| + \lambda_{k+n.i} + \lambda_{k+n.j+n.(n+1)} + c_i^0 \cdot \mu_{k+n.(j-1)} - \sum_{s=1}^{n+1} \sum_{r=1}^{n+1} \mu_{q_{kjrjs}} + \lambda_k + b_{mj}^0 \cdot \mu_{q_{kij}} + 2 \mu_{q_{kjmil}} \right\}, q_{kjmil} = k + n.j + n^2 + n.(n+1).(m+n.i+n^2.l-n^2), \forall i, j, m, l \in \{1, \dots, n+1\}, k \in \{1, \dots, n\}, j \neq k \quad (50)$$

$$\frac{d\mu'_{q_{kmil}}}{dt} = -\beta \left\{ \mu'_{q_{kmil}} - |\mu'_{q_{kmil}}| + \lambda_{k+n.i} + \lambda_{k+n.k+n.(n+1)} + \lambda_{k+n.i+2.n.(n+1)} + c_i^0 \cdot \mu_{k+n.(k-1)} - \sum_{s=1}^{n+1} \sum_{r=1}^{n+1} \mu'_{q_{krs}} + \lambda_k + b_{mk}^0 \cdot \mu_{q_{kil}} + 2 \mu'_{q_{kmil}} \right\}, q'_{kmil} = k + n.k + n^2 + n.(n+1).(m+n.i+n^2.l-n^2), q_{kil} = k + n.(i+n) + n.(n+1).(l-1), \forall i, m, l \in \{1, \dots, n+1\}, k \in \{1, \dots, n\} \quad (51)$$

Where, β is a nonnegative parameter that scales the convergence rate of the neural network.

Survivable virtual network embedding after describing neural network that has been used for enhancing virtual network, this subsection explains the collective neurodynamic approach that has been employed for finding optimal multi-path link embedding solution.

Multiple neurodynamic models have been exploited to enhance candidate virtual network embedding solution. First, set of neurodynamic models are initialized and distributed in the substrate network. Second, each model improves its local optimal solution by using its dynamic equation. After all neurodynamic models converge to its local optimal, Particle

Swarm Optimization (PSO) technique is employed to exchange information between neurodynamic models. Third, each model adjusts its state with considering its own best solution as well as the best solution found so far. The previous two steps are repeated until a termination criterion is reached. The position and velocity of each neurodynamic model can be expressed using the following equations [19]:

$$V_i(t+1) = wV_i(t) + c_1r_1(pBest_i(t) - X_i(t)) + c_2r_2(gBest(t) - X_i(t)) \quad (52)$$

$$X_i(t+1) = X_i(t) + V_i(t+1) \quad (53)$$

Where, $pBest_i(t)$ is the local optimal solution of the neurodynamic model i at time t , $gBest(t)$ is the global optimal solution at time t , r_1 and r_2 are two random numbers between 0 and 1. The constants c_1 , and c_2 are specified to control influence of $pBest_i(t)$ and $gBest(t)$ on the search process. The constant w is called inertia weight, which controls effect of the previous velocity on the new one.

In the remaining of this subsection, the problem of multi-path link embedding of enhanced virtual network has been formulated as quadratic integer program and transformed into mixed integer linear program. Finally, dynamic equation of the neurodynamic model has been explained.

In multi-path link embedding [7], each virtual link is divided into $\eta > 1$, $\eta \in \mathbb{Z}$ virtual sub-links, which connect the same virtual nodes as the original virtual link. Bandwidth of each virtual sub-link is equal to $1/(\eta - 1)$ of the original virtual link bandwidth. Consequently, there is only one extra sub-link is added for survivability against substrate link failure. The problem of embedding enhanced virtual network is formulated as quadratic integer program:

$$Min \sum_{i=1}^n \sum_{j=1}^n \sum_{k=1}^m \sum_{l=1}^m Length(p_{kl}) x_{ik} x_{jl} b_{ij} \quad (54)$$

$$(c_i^p - c_i^s) x_{ik} \leq 0, \forall i \in \{1, \dots, n\}, k \in \{1, \dots, m\} \quad (55)$$

$$\left(\frac{1}{\eta - 1} b_{ij} - Band(p_{kl}) \right) x_{ik} x_{jl} \leq 0, \forall i, j \in \{1, \dots, n\}, k, l \in \{1, \dots, m\} \quad (56)$$

$$\sum_{k=1}^m x_{ik} = 1, \forall i \in \{1, \dots, n\} \quad (57)$$

$$\sum_{i=1}^n x_{ik} = 1, \forall k \in \{1, \dots, m\} \quad (58)$$

$$x_{ik} \in \{0, 1\}, \forall i \in \{1, \dots, n\}, k \in \{1, \dots, m\} \quad (59)$$

Where, p_{kl} is a set of η disjoint paths between substrate nodes k and l . $Length(p_{kl})$ is the total length of all substrate paths in the set p_{kl} . $Band(p_{kl})$ is the minimum free bandwidth in all substrate links that participate in substrate paths of p_{kl} .

Main goal of the objective function (54) is minimizing cost of embedding enhanced virtual networks. Cost of embedding virtual nodes depends on total CPU capacity of enhanced virtual network. Each virtual node is allocated to one and only one substrate node. Therefore, cost of embedding virtual nodes is considered unvarying in the previous formulation. In the

other side, each virtual link is divided into η links and embedded in η substrate paths, which contain sequences of substrate links. Thus, cost of embedding virtual link depends on total lengths of all required substrate paths to accommodate this virtual link.

Constraint (55) ensures that there is sufficient substrate CPU to embed virtual node. Constraint (56) reveals that there is enough free bandwidth in all substrate links that are employed to embed virtual link.

To solve the quadratic integer program (54)-(59), the quadratic term $x_{ik} x_{jl}$ is eliminated to transform the problem into mixed integer linear program. The linearization of the problem allows us to solve the problem by applying the neural network that is proposed in [6]. After replacing quadratic term $x_{ik} x_{jl}$ with four-dimensional array y_{ikjl} and replacing zero-one integrality constraints with nonnegativity constraints, the problem becomes equivalent to the following linear programming problem.

$$\text{Min } F(Z) = \sum_{i=1}^n \sum_{j=1}^n \sum_{k=1}^m \sum_{l=1}^m \text{Length}(p_{kl}) y_{ikjl} b_{ij} \quad (60)$$

$$(c_i^v - c_k^s) x_{ik} \leq 0, \forall i \in \{1, \dots, n\}, k \in \{1, \dots, m\} \quad (61)$$

$$\left(\frac{1}{\eta-1} b_{ij} - \text{Band}(p_{kl}) \right) y_{ikjl} \leq 0, \forall i, j \in \{1, \dots, n\}, k, l \in \{1, \dots, m\} \quad (62)$$

$$\sum_{l=1}^m \sum_{k=1}^m \sum_{j=1}^n \sum_{i=1}^n y_{ikjl} = n \cdot m \quad (63)$$

$$2y_{ikjl} - x_{ik} - x_{jl} \leq 0, \forall i, j \in \{1, \dots, n\}, k, l \in \{1, \dots, m\} \quad (64)$$

$$y_{ikjl} \geq 0, \forall i, j \in \{1, \dots, n\}, k, l \in \{1, \dots, m\} \quad (65)$$

$$\sum_{k=1}^m x_{ik} = 1, \forall i \in \{1, \dots, n\} \quad (66)$$

$$\sum_{i=1}^n x_{ik} = 1, \forall k \in \{1, \dots, m\} \quad (67)$$

$$x_{ik} \geq 0, \forall i \in \{1, \dots, n\}, k \in \{1, \dots, m\} \quad (68)$$

Z is defined as (X, Y), where X and Y are vectors represent all variables in the two-dimensional array X and in the four-dimensional array Y.

By using Lagrange and Karush-Kuhn-Tucker multipliers, constraints are switched to penalties in the following Lagrangian function:

$$\begin{aligned} L(Z, \lambda, \mu) = & \sum_{i=1}^n \sum_{j=1}^n \sum_{k=1}^m \sum_{l=1}^m \text{Length}(p_{kl}) \cdot y_{ikjl} \cdot b_{ij} \\ & + \lambda_1 (\sum_{i=1}^n \sum_{k=1}^m \sum_{j=1}^n \sum_{l=1}^m y_{ikjl} - n \cdot m) \\ & + \sum_{i=1}^n \lambda_{i+1} \cdot (\sum_{k=1}^m x_{ik} - 1) \\ & + \sum_{k=1}^m \lambda_{k+(n+1)} \cdot (\sum_{i=1}^n x_{ik} - 1) \\ & + \sum_{i=1}^n \sum_{k=1}^m (\mu_{k+m \cdot (i-1)} \cdot x_{ik} \cdot (c_i^v - c_k^s)) \\ & + \sum_{i=1}^n \sum_{k=1}^m \sum_{j=1}^n \sum_{l=1}^m \left(\mu_{n \cdot m + q_{ikjl}} \cdot y_{ikjl} \cdot \left(\frac{1}{\eta-1} b_{ij} - \text{Band}(p_{kl}) \right) \right) \end{aligned}$$

$$+ \sum_{i=1}^n \sum_{k=1}^m \sum_{j=1}^n \sum_{l=1}^m \left(\mu_{n \cdot m + n^2 \cdot m^2 + q_{ikjl}} \cdot (2y_{ikjl} - x_{ik} - x_{jl}) \right), \quad (69)$$

$$q_{ikjl} = i + n \cdot (k - 1) + n \cdot m \cdot (j - 1) + n^2 \cdot m \cdot (l - 1)$$

Where, $\lambda = (\lambda_1, \dots, \lambda_i), i \in \{1, \dots, n + m + 1\}$ is vector of Lagrange multipliers and $\mu = (\mu_1, \dots, \mu_i), i \in \{1, \dots, n \cdot m + 2n^2 \cdot m^2\}$ is vector of Karush-Kuhn-Tucker multipliers. The dual problem is formulated as follows:

Maximize

$$D(\lambda, \mu) = -n \cdot m \cdot \lambda_1 - \sum_{i=1}^n \lambda_{i+1} - \sum_{k=1}^m \lambda_{k+(n+1)} \quad (70)$$

Subject to

$$\begin{aligned} & \text{Length}(p_{kl}) \cdot b_{ij} + \lambda_1 + \mu_{n \cdot m + q_{ikjl}} \cdot \left(\frac{1}{\eta-1} b_{ij} - \right. \\ & \left. \text{Band}(p_{kl}) \right) + 2\mu_{n \cdot m + n^2 \cdot m^2 + q_{ikjl}} = 0, \forall i, j \in \{1, \dots, n\}, k, l \in \\ & \{1, \dots, m\}, q_{ikjl} = i + n \cdot (k - 1) + n \cdot m \cdot (j - 1) + n^2 \cdot m \cdot (l - 1) \end{aligned} \quad (71)$$

$$\begin{aligned} & \lambda_{i+1} + \lambda_{k+(n+1)} + \mu_{k+m \cdot (i-1)} \cdot (c_i^v - c_k^s) - \\ & \sum_{j=1}^n \sum_{l=1}^m \mu_{n \cdot m + n^2 \cdot m^2 + q_{ikjl}} - \sum_{j=1}^n \sum_{l=1}^m \mu_{n \cdot m + n^2 \cdot m^2 + q_{jlik}} = \\ & 0, \forall i \in \{1, \dots, n\}, k \in \{1, \dots, m\}, q_{ikjl} = i + n \cdot (k - 1) + \\ & n \cdot m \cdot (j - 1) + n^2 \cdot m \cdot (l - 1) \end{aligned} \quad (72)$$

$$\mu_i \geq 0, \forall i \in \{1, \dots, n \cdot m + 2 \cdot n^2 \cdot m^2\} \quad (73)$$

Finally, the dynamic equation of the neural network is defined by the following differential equations:

$$\begin{aligned} & \frac{dy_{ikjl}}{dt} = \\ & -\beta \left\{ \text{Length}(p_{kl}) \cdot b_{ij} \cdot \left(\sum_{s,q=1}^n \sum_{r,v=1}^m \text{Length}(p_{rv}) \cdot y_{srqv} \cdot b_{sq} + \right. \right. \\ & n \cdot m \cdot \lambda_1 + \sum_{i=1}^n \lambda_{i+1} + \sum_{k=1}^m \lambda_{k+(n+1)} \left. \right) + y_{ikjl} - \\ & |y_{ikjl}| + \sum_{s=1}^n \sum_{q=1}^n \sum_{r=1}^m \sum_{v=1}^m y_{srqv} - n \cdot m + \\ & \left(\text{Band}(p_{kl}) - \frac{1}{\eta-1} b_{ij} \right)^2 \cdot y_{ikjl} - \left(\text{Band}(p_{kl}) - \right. \\ & \left. \frac{1}{\eta-1} b_{ij} \right) \left| \left(\text{Band}(p_{kl}) - \frac{1}{\eta-1} b_{ij} \right) \cdot y_{ikjl} \right| - 2x_{ik} - \\ & 2x_{jl} + 4y_{ikjl} + 2|x_{ik} + x_{jl} - 2y_{ikjl}| \left. \right\}, \forall i, j \in \\ & \{1, \dots, n\}, k, l \in \{1, \dots, m\} \end{aligned} \quad (74)$$

$$\begin{aligned} & \frac{dx_{ik}}{dt} = -\beta \left\{ x_{ik} - |x_{ik}| + \sum_{r=1}^m x_{ir} + \sum_{q=1}^n x_{qk} - 2 + \right. \\ & (c_k^s - c_i^v)^2 \cdot x_{ik} - (c_k^s - c_i^v) \cdot |(c_k^s - c_i^v) \cdot x_{ik}| + \\ & \sum_{j=1}^n \sum_{l=1}^m (x_{ik} + x_{jl} - 2y_{ikjl}) + \sum_{j=1}^n \sum_{l=1}^m (x_{ik} + \\ & x_{jl} - 2y_{jlik}) - 2x_{ik} + 2y_{ikik} - \sum_{j=1}^n \sum_{l=1}^m |x_{ik} + x_{jl} - \\ & 2y_{ikjl}| - \sum_{j=1}^n \sum_{l=1}^m |x_{ik} + x_{jl} - 2y_{jlik}| + \\ & \left. |2x_{ik} + 2y_{ikik}| \right\}, \forall i \in \{1, \dots, n\}, k \in \{1, \dots, m\} \end{aligned} \quad (75)$$

$$\begin{aligned} \frac{d\lambda_1}{dt} = & -\beta \left\{ n \cdot m \cdot \left(\sum_{i=1}^n \sum_{j=1}^n \sum_{k=1}^m \sum_{l=1}^m \text{Length}(p_{kl}) y_{ikjl} b_{ij} + \right. \right. \\ & n \cdot m \cdot \lambda_1 + \sum_{i=1}^n \lambda_{i+1} + \sum_{k=1}^m \lambda_{k+(n+1)} \Big) + \\ & \sum_{i=1}^n \sum_{k=1}^m \sum_{j=1}^n \sum_{l=1}^m \left(\text{Length}(p_{kl}) \cdot b_{ij} + \lambda_1 + \right. \\ & \left. \left. \mu_{n,m+q_{ikjl}} \cdot \left(\frac{1}{\eta-1} b_{ij} - \text{Band}(p_{kl}) \right) + \right. \right. \\ & \left. \left. 2\mu_{n,m+n^2,m^2+q_{ikjl}} \right) \right\} \quad (76) \end{aligned}$$

$$\begin{aligned} \frac{d\lambda_{r+1}}{dt} = & -\beta \left\{ \left(\sum_{i=1}^n \sum_{j=1}^n \sum_{k=1}^m \sum_{l=1}^m \text{Length}(p_{kl}) y_{ikjl} b_{ij} + \right. \right. \\ & n \cdot m \cdot \lambda_1 + \sum_{i=1}^n \lambda_{i+1} + \sum_{k=1}^m \lambda_{k+(n+1)} \Big) + \\ & \sum_{k=1}^m \left(\lambda_{r+1} + \lambda_{k+(n+1)} + \mu_{k+m,(r-1)} \cdot (c_r^v - c_k^s) - \right. \\ & \left. \sum_{j=1}^n \sum_{l=1}^m \left(\mu_{n,m+n^2,m^2+q_{rkjl}} + \right. \right. \\ & \left. \left. \mu_{n,m+n^2,m^2+q_{jlrk}} \right) \right) \Big\}, \forall r \in \{1, \dots, n\} \quad (77) \end{aligned}$$

$$\begin{aligned} \frac{d\lambda_{r+(n+1)}}{dt} = & -\beta \left\{ \left(\sum_{i=1}^n \sum_{j=1}^n \sum_{k=1}^m \sum_{l=1}^m \text{Length}(p_{kl}) y_{ikjl} b_{ij} + \right. \right. \\ & n \cdot m \cdot \lambda_1 + \sum_{i=1}^n \lambda_{i+1} + \sum_{k=1}^m \lambda_{k+(n+1)} \Big) + \\ & \sum_{i=1}^n \left(\lambda_{i+1} + \lambda_{r+(n+1)} + \mu_{r+m,(i-1)} \cdot (c_i^v - c_r^s) - \right. \\ & \left. \sum_{j=1}^n \sum_{l=1}^m \left(\mu_{n,m+n^2,m^2+q_{irjl}} + \right. \right. \\ & \left. \left. \mu_{n,m+n^2,m^2+q_{jlr}} \right) \right) \Big\}, \forall r \in \{1, \dots, m\} \quad (78) \end{aligned}$$

$$\begin{aligned} \frac{d\mu_{k+m,(i-1)}}{dt} = & -\beta \left\{ \mu_{k+m,(i-1)} - \left| \mu_{k+m,(i-1)} \right| + \right. \\ & (c_i^v - c_k^s) \cdot \left(\lambda_{i+1} + \lambda_{k+(n+1)} + \mu_{k+m,(i-1)} \cdot (c_i^v - \right. \\ & \left. c_k^s) - \right. \\ & \left. \sum_{j=1}^n \sum_{l=1}^m \left(\mu_{n,m+n^2,m^2+q_{ikjl}} + \right. \right. \\ & \left. \left. \mu_{n,m+n^2,m^2+q_{jlik}} \right) \right\}, \forall i \in \{1, \dots, n\}, k \in \\ & \{1, \dots, m\} \quad (79) \end{aligned}$$

$$\begin{aligned} \frac{d\mu_{n,m+q_{ikjl}}}{dt} = & -\beta \left\{ \mu_{n,m+q_{ikjl}} - \left| \mu_{n,m+q_{ikjl}} \right| + \right. \\ & \left(\frac{1}{\eta-1} b_{ij} - \text{Band}(p_{kl}) \right) \cdot \left(\text{Length}(p_{kl}) \cdot b_{ij} + \lambda_1 + \right. \\ & \left. \mu_{n,m+q_{ikjl}} \cdot \left(\frac{1}{\eta-1} b_{ij} - \text{Band}(p_{kl}) \right) + \right. \\ & \left. \left. 2\mu_{n,m+n^2,m^2+q_{ikjl}} \right) \right\}, \forall i, j \in \{1, \dots, n\}, k, l \in \\ & \{1, \dots, m\} \quad (80) \end{aligned}$$

$$\begin{aligned} \frac{d\mu_{n,m+n^2,m^2+q_{ikjl}}}{dt} = & -\beta \left\{ \mu_{n,m+n^2,m^2+q_{ikjl}} - \left| \mu_{n,m+n^2,m^2+q_{ikjl}} \right| + \right. \\ & 2 \text{Length}(p_{kl}) \cdot b_{ij} + 2\lambda_1 + 2\mu_{n,m+q_{ikjl}} \cdot \left(\frac{1}{\eta-1} b_{ij} - \right. \\ & \left. \text{Band}(p_{kl}) \right) + 4\mu_{n,m+n^2,m^2+q_{ikjl}} - \lambda_{i+1} - \lambda_{k+(n+1)} - \\ & \mu_{k+m,(i-1)} \cdot (c_i^v - c_k^s) + \\ & \sum_{r=1}^n \sum_{u=1}^m \left(\mu_{n,m+n^2,m^2+q_{ikru}} + \mu_{n,m+n^2,m^2+q_{ruik}} \right) - \\ & \lambda_{j+1} - \lambda_{l+(n+1)} - \mu_{l+m,(j-1)} \cdot (c_j^v - c_l^s) + \\ & \sum_{r=1}^n \sum_{u=1}^m \left(\mu_{n,m+n^2,m^2+q_{jlru}} + \right. \\ & \left. \mu_{n,m+n^2,m^2+q_{rujl}} \right) \Big\}, \forall i, j \in \{1, \dots, n\}, k, l \in \\ & \{1, \dots, m\} \quad (81) \end{aligned}$$

IV. EVALUATION

To evaluate the performance of the proposed approach (CND-SVNE), its performance has been compared with Failure Independent Protection (FIP) approach [1]. FIP adds one redundant node and set of links to connect this node with all remaining nodes. Three metrics are used in the evaluation: VNE revenue, VN acceptance ratio, and substrate resources utilization. Where VNE revenue is the sum of all accepted and accommodated virtual resources, VN acceptance ratio is number of accepted virtual networks divided by total number of submitted virtual networks, and substrate resources utilization is used substrate resources divided by total substrate resources.

In the Evaluation environment, substrate network topology has been generated with 100 nodes and 500 links by using Waxman generator. Bandwidth of the substrate links are uniformly distributed between 50 and 150 with average 100. Each substrate node is randomly assigned one of the following server configurations: HP ProLiant ML110 G4 (Intel Xeon 3040, 2 cores X 1860 MHz, 4 GB), or HP ProLiant ML110 G5 (Intel Xeon 3075, 2 cores X 2660 MHz, 4 GB). We generated 1000 Virtual network topologies using Waxman generator with average connectivity 50%. The number of virtual nodes in each VN is variant from 2 to 20. Each virtual node is randomly assigned one of the following CPU: 2500 MIPS, 2000 MIPS, 1000 MIPS, and 500 MIPS, which are correspond to the CPU of Amazon EC2 instance types. Bandwidths of the virtual links are real numbers uniformly distributed between 1 and 50. VN's arrival times are generated randomly with arrival rate 10 VNs per 100 time units. The lifetimes of the VNRs are generated randomly between 300 and 700 time units with average 500 time units. Generated SN and VNs topologies are stored in brite format and used as inputs for all mapping algorithms.

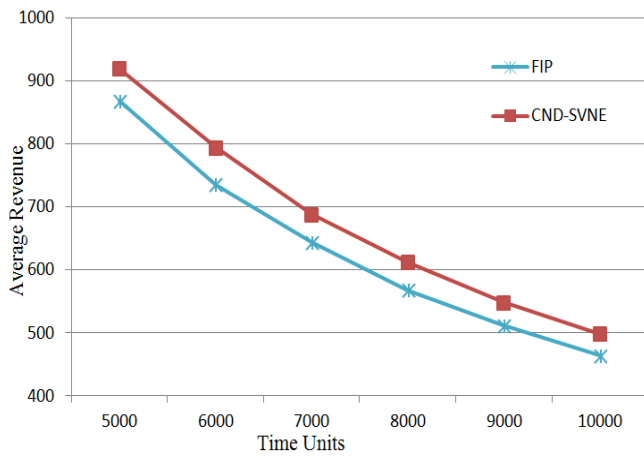


Fig. 1. Revenue comparison.

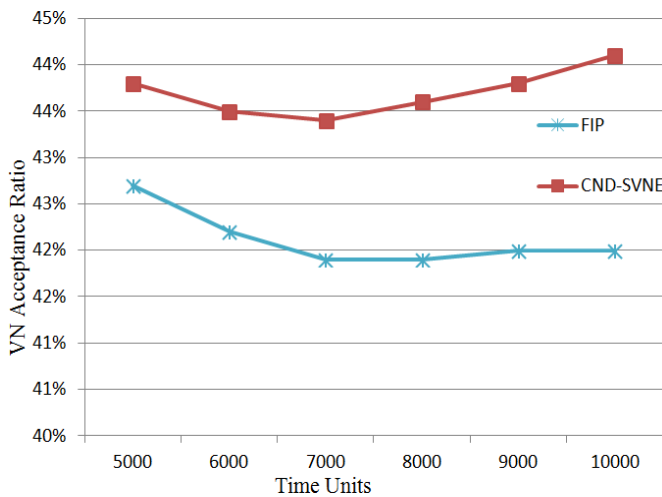


Fig. 2. VN Acceptance ratio comparison.

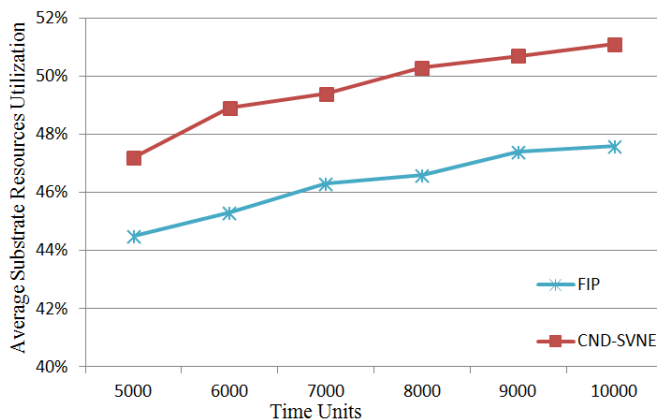


Fig. 3. Substrate resources utilization comparison.

As shown in Fig. 1, 2, and 3, the proposed approach increases VN acceptance ratio compared with FIP. By accepting and accommodating more virtual network requests, the proposed approach increases datacenter's revenue and increases substrate resources utilization. This improvement comes from reducing amount of required redundant virtual links in the proposed approach. Additionally, the proposed

approach does not require any additional computation after failures this is due to existence of recovery plan (mutation matrix) for each failure.

V. CONCLUSION

In this paper, a collective neurodynamic survivable virtual network embedding approach has been proposed. The proposed approach combines substrate node failure survivable virtual network embedding approach proposed by Guo et al. [1] with substrate link failure survivable virtual network embedding approach proposed by Khan et al. [7]. Fast convergence of the neural network optimization that has been proposed by Xia [6] has been exploited to reduce amount of required redundant resources, while co-ordination between neurodynamic models has been done by using particle swarm optimization. Experimental results show that the proposed approach outperforms Failure Independent Protection approach.

For the future work, we plan to extend the proposed approach to consider virtual network size during specifying redundant resources. Instead of adding fixed number of redundant nodes for each virtual network, number of redundant nodes will be proportional to size of virtual network. Furthermore, influence of the proposed approach on fragmentation of substrate resources will be investigated for further improvement.

ACKNOWLEDGMENT

The authors would like to express their cordial thanks to the department of Research and Development (R&D) of IMAM, university for research grant no: 370903.

REFERENCES

- [1] B. Guo, C. Qiao, J. Wang, H. Yu, Y. Zuo, J. Li, Z. Chen, and Y. He, "Survivable virtual network design and embedding to survive a facility node failure," *Journal of Lightwave Technology*, vol. 32, no. 3, pp. 483–493, Feb 2014.
- [2] A. Xiao, Y. Wang, L. Meng, X. Qiu, and W. Li, "Topology-aware remapping to survive virtual networks against substrate node failures," in *2013 15th Asia-Pacific Network Operations and Management Symposium (APNOMS)*, Sept 2013, pp. 1–6.
- [3] Z. Zhou, T. Lin, and K. Thulasiraman, "Survivable cloud network mapping with multiple failures," in *2015 IEEE International Conference on Communications (ICC)*, June 2015, pp. 5491–5496.
- [4] H. Jiang, L. Gong, and Z. W. Zuqing, "Efficient joint approaches for location-constrained survivable virtual network embedding," in *2014 IEEE Global Communications Conference*, Dec 2014, pp. 1810–1815.
- [5] M. R. Rahman and R. Boutaba, "Svne: Survivable virtual network embedding algorithms for network virtualization," *IEEE Transactions on Network and Service Management*, vol. 10, no. 2, pp. 105–118, June 2013.
- [6] Y. Xia, "A new neural network for solving linear programming problems and its application," *IEEE Transactions on Neural Networks*, vol. 7, no. 2, pp. 525–529, Mar 1996.
- [7] M. M. A. Khan, N. Shahriar, R. Ahmed, and R. Boutaba, "Multi-path link embedding for survivability in virtual networks," *IEEE Transactions on Network and Service Management*, vol. 13, no. 2, pp. 253–266, June 2016.
- [8] A. Xiao, Y. Wang, L. Meng, X. Qiu, and W. Li, "Topology-aware virtual network embedding to survive multiple node failures," in *2014 IEEE Global Communications Conference (GLOBECOM)*, Dec 2014, pp. 1823–1828.
- [9] Z. Qiang, W. Qiang, F. Sheng, and L. Wu, "Heuristic survivable virtual network embedding based on node migration and link remapping," in

- 2014 IEEE 7th Joint International Information Technology and Artificial Intelligence Conference (ITAIC), Dec 2014, pp. 181–185.
- [10] Q. Chen, Y. Wan, X. Qiu, W. Li, and A. Xiao, “A survivable virtual network embedding scheme based on load balancing and reconfiguration,” in 2014 IEEE Network Operations and Management Symposium (NOMS), May 2014, pp. 1–7.
- [11] F. Gu, K. Shaban, N. Ghani, S. Khan, M. Naeini, M. Hayat, and C. Assi, “Survivable cloud network mapping for disaster recovery support,” IEEE Transactions on Computers, vol. 64, no. 8, pp. 2353–2366, Aug 2015.
- [12] R. Mijumbi, J.-L. Gorricho, J. Serrat, J. Rubio-Loyola, and R. Aguero, “Survivability-oriented negotiation algorithms for multi-domain virtual networks,” in 2014 10th International Conference on Network and Service Management (CNSM), Nov 2014, pp. 276–279.
- [13] F. Gu, H. Alazemi, A. Rayes, and N. Ghani, “Survivable cloud networking services,” in 2013 International Conference on Computing, Networking and Communications (ICNC), Jan 2013, pp. 1016–1020.
- [14] F. Gu, “Survivable cloud networking services,” Ph.D. dissertation, The University of New Mexico, Albuquerque, New Mexico, July, 2013.
- [15] C. Meixner, F. Dikbiyik, M. Tornatore, C. Chuah, and B. Mukherjee, “Disaster-resilient virtual-network mapping and adaptation in optical networks,” in 2013 17th International Conference on Optical Network Design and Modeling (ONDM), April 2013, pp. 107–112.
- [16] G. Sun, H. Yu, L. Li, V. Anand, H. Di, and X. Gao, “Efficient algorithms for survivable virtual network embedding,” in Asia Communications and Photonics Conference and Exhibition, Dec 2010, pp. 531–532.
- [17] Y. Zhu and M. Ammar, “Algorithms for assigning substrate network resources to virtual network components,” in Proceedings IEEE INFOCOM 2006. 25TH IEEE International Conference on Computer Communications, April 2006, pp. 1–12.
- [18] M. Chowdhury, M. R. Rahman, and R. Boutaba, “Vineyard: Virtual network embedding algorithms with coordinated node and link mapping,” IEEE/ACM Transactions on Networking, vol. 20, no. 1, pp. 206–219, Feb 2012.
- [19] A. Shahin, “Memetic Multi-Objective Particle Swarm Optimization-Based Energy-Aware Virtual Network Embedding” International Journal of Advanced Computer Science and Applications(IJACSA), Vol.6, NO 4, May 2015, pg. 35-46

Breast Cancer Classification in Histopathological Images using Convolutional Neural Network

Mohamad Mahmoud Al Rahhal

Information Science

College of Applied Computer Science, King Saud University
Riyadh, KSA

Abstract—Computer based analysis is one of the suggested means that can assist oncologists in the detection and diagnosis of breast cancer. On the other hand, deep learning has been promoted as one of the hottest research directions very recently in the general imaging literature, thanks to its high capability in detection and recognition tasks. Yet, it has not been adequately suited to the problem of breast cancer so far. In this context, I propose in this paper an approach for breast cancer detection and classification in histopathological images. This approach relies on a deep convolutional neural networks (CNN), which is pretrained on an auxiliary domain with very large labelled images, and coupled with an additional network composed of fully connected layers. The network is trained separately with respect to various image magnifications (40x, 100x, 200x and 400x). The results presented in the patient level achieved promising scores compared to the state of the art methods.

Keywords—Convolutional neural network (CNN); histopathological images; imagenet; classification

I. INTRODUCTION

According to reports of the world health organization (WHO), breast cancer (BC) is the most prevalent type of cancer in women. For instance, incidence rates range from 19.3 per 100,000 women in Eastern Africa to 89.7 per 100,000 women in Western Europe [1]. Current scientific findings indicate that such high variability might be traced back to differences in lifestyle and urbanization. Although early diagnosis is more affordable in developed countries, it is less likely in underdeveloped nations, which implies that undertaking preventive measures only does not offer a cutting-edge solution.

Mammography is a common screening protocol that can help distinguish dubious regions of the breast, followed by a biopsy of potentially cancerous areas in order to determine whether the dubious area is benign or malignant [2], [3]. In order to produce stained histology slides, samples of tissue are taken from the breast during biopsy. In spite of the considerable improvement incurred by such imaging technologies, pathologists tend to visually inspect the histological samples under the microscope for a final diagnosis, including staging and grading [4].

In this context, automatic image analysis is prone to play a pivotal role in facilitating the diagnosis; so far, the relevant processing and machine learning techniques. For instance, the authors in [5] present a comparison of different algorithms of

nuclei segmentation, where the cases are categorized into benign or malignant.

Deep CNNs learn mid-level and high-level representations obtained from raw data (e.g., images) in an automatic manner. Recent results on natural images indicate that CNN representations are highly efficient in object recognition and localization applications. This has instigated the adoption of CNNs in the biomedical field, such as breast cancer diagnosis and masses classification [6]–[11], abdominal adipose tissues extraction [12], detection and classification of brain tumour in MR images [13]–[16], skeletal bone age assessment in X-ray Images [17], EEG classification of motor imagery [18], and arrhythmia detection and analysis of the ECG signals [19]–[21]. In particular, in [9], the authors propose a framework for masses classification, which mainly encompasses a CNN and a decision mechanism for breast cancer diagnosis as either benign or malignant in a DDSM mammographic dataset. In [4], the authors propose an improved hybrid active contour model based segmentation method for nuclei segmentation. They adopt both pixel and object-level features in addition to semantic-level features. The semantic-level features are computed using a CNN architecture which can learn additional feature representations that cannot be represented through neither pixel nor object-level features.

Thus, it is to stress the fact that, relatively to other biomedical applications, breast cancer diagnosis has not benefited enough from deep learning, which inspired us to investigate it thoroughly. In particular, I opt for several deep architectures in the context of breast cancer histological image classification, and demonstrate that the common belief that high level deep features are more capable of capturing the contextual as well as spectral attributes in optical images remains valid also in histological breast cancer images. This, in fact, is confirmed by the very satisfactory results reported hereby, which advance late works often by large margins.

The rest of this paper is organized as follows. Material and methods are exposed in Section II. Results are presented in Section III. Finally, conclusion is provided in Section IV.

II. MATERIAL AND METHODS

A. Dataset Description

In order to realistically assess any BC diagnosis system, the experiments shall be performed on a large-scale dataset accommodating 1) numerous patients, 2) abundant images. The

latter component is essential to any deep learning model as large data is required for the training phase.

The Breast Cancer Histopathological Image Classification (BreakHis), which was established recently in [22], is an optimal dataset as it meets all the above requirements. Precisely, it is composed of 9,109 microscopic images of breast tumour tissue collected from 82 patients using different magnifying factors (40X, 100X, 200X, and 400X). For convenience, Fig. 1 and 2 display a slide of breast benign and malignant tumour for the same patient seen in different magnification factors.

To date, the dataset contains 2,480 benign (taken from 24 patients) and 5,429 malignant samples (taken from 58 patients) of 700X460 pixels, 3-channel RGB, 8-bit depth in each channel, and PNG format. In its current version, samples present in the dataset were collected by SOB method, also named partial mastectomy or excisional biopsy. This type of procedure, compared to any methods of needle biopsy, removes the larger size of tissue sample and is performed in a hospital with general anaesthetic. This dataset is structured as shown in Table I.

TABLE I. BREAST CANCER DATABASE USED IN THE EXPERIMENT

	Magnification				Total	Patient
	40x	100 x	200x	400x		
Benign	652	644	623	588	2480	24
Malignant	1370	1437	1390	1232	5429	58
Total	1995	2081	2013	1820	7909	82

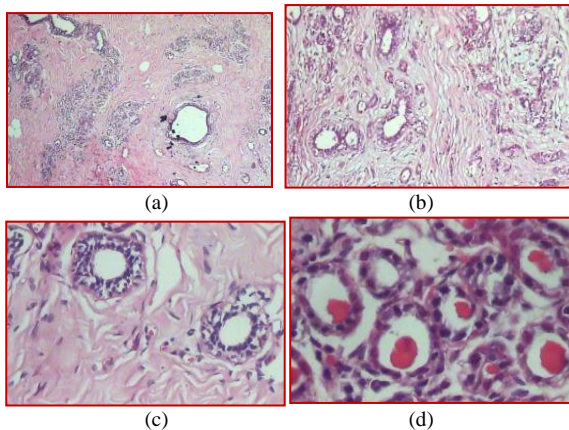


Fig. 1. A slide of breast benign for the same patient seen in different magnification factors: (a) 40X, (b) 100X, (c) 200X, and (d) 400X.

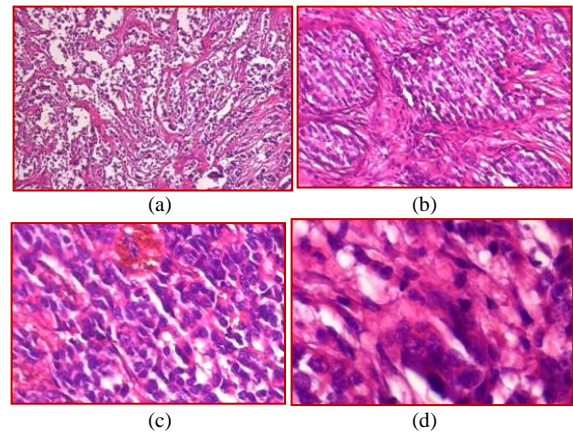


Fig. 2. A slide of breast malignant tumor for the same patient seen in different magnification factors: (a) 40X, (b) 100X, (c) 200X, and (d) 400X.

B. Proposed Methodology

Let us consider $D^{(s)} = \{x_i, y_i\}_{i=1}^{n_s}$ as the labeled source data and $y_i \in \{1,2\}$ is its corresponding class label either to be benign or malignant. Similarly, let us refer to $D^{(t)} = \{x_j\}_{j=1}^{n_t}$ as the unseen target data. This paragraph consists of two steps as shown in Fig. 3.

1) Feature Extraction

Deep CNNs are composed of multiple layers of processing which are learnt jointly, in an end-to-end manner, to address specific issues [23]–[25]. Particularly, Deep CNNs are commonly composed of four types of layers namely convolution; normalization, pooling and fully connected. The convolutional layer is considered the main building block of the CNN and its parameters consist of a set of filters (or sometimes referred to as a neuron or a kernel). Every filter is small spatially (along width and height), but extends through the full depth of the input image. The output of this layer is called activation maps or feature maps which are produced via sliding the filters across the input image. The feature maps are then fed to a non-linear gating function such as the Rectified Linear Unit (ReLU). Then the output of this activation function can further be subjected to normalization layer to help in generalization. Regarding the pooling layers, they are usually used immediately after convolutional layers in order to control overfitting and reduce the amount of parameters in the network.

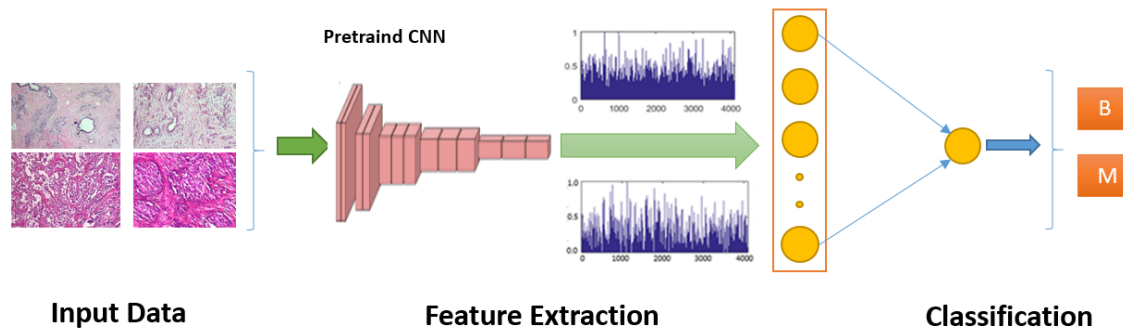


Fig. 3. Flowchart of the proposed approach.

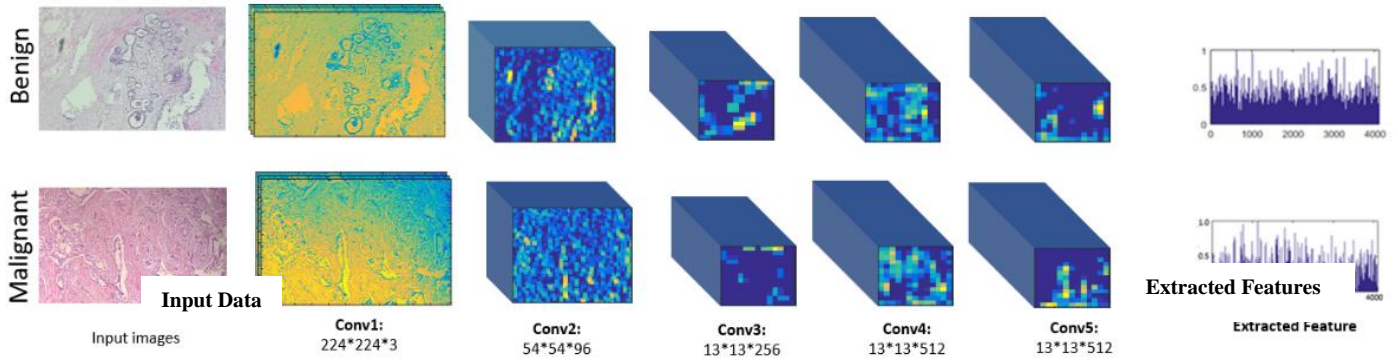


Fig. 4. Convolutional layers feature maps with corresponding extracted feature.

In this work, I follow the recent approaches for exploiting pretrained CNN models by taking the output of the last fully connected layer (before the sigmoid layer) to represent the images. That is I feed each image I_i as input to the network and generate its corresponding CNN feature representation vector $x_i \in \mathbb{R}^d$ of dimension d :

$$x_i = f_{L-1}^{\text{CNN}} \left(\dots f_2^{\text{CNN}} \left(f_1^{\text{CNN}} (I_i) \right) \right), i = 1, \dots, n_s \quad (1)$$

Where $f_j^{\text{CNN}}, j = 1, \dots, L - 1$ represent the functions defining the different layers of CNN, L is the total number of layers, and n_s and n_t represent the number of labeled source images and unlabeled target images, respectively. Fig. 4 shows feature maps with corresponding extracted features.

2) Classification

I feed the CNN feature vectors from the previous stage to an extra network placed on the top of the pretrained CNN as shown in Fig. 3. Specifically, this network is composed of two fully-connected layers, a hidden layer followed by binary classification layer: a sigmoid layer. The hidden layer maps the input x_i to another representation $h_i^{(1)} \in \mathbb{R}^{d^{(1)}}$ of dimension $d^{(1)}$ through the nonlinear activation function f as follows:

$$h_i^{(1)} = f(W^{(1)}x_i) \quad (2)$$

Where mapping weight matrix referred as $W^{(1)} \in \mathbb{R}^{d^{(1)} \times d}$. I adopt the sigmoid function i.e. $f(v) = 1/(1 + \exp(-v))$ as a nonlinear activation function. For simplicity, the bias vector in the expression is ignored as it can be incorporated as an additional column vector in the mapping matrix, whereby the feature vector is appended by the value 1.

I adopt the recently introduced dropout technique [26] to increase the generalization ability of the network and prevent it from overfitting.

III. RESULTS

A. Experimental Results

For the sake of comparison, I followed the protocol proposed in [22], the dataset has been divided into training (70%) and testing (30%) sets taking in consideration that the

patient used in training and testing sets are mutually exclusive for training i used 58 patients (17 Benign and 41 Malignant), for test use used 24 patients (7 Benign and 17 Malignant) for test. The adopted protocol was applied independently to each of the four different available magnifications factor (40X, 100X, 200X, and 400X) in the patient level, the recognition rate is computed as follows:

$$\text{Patient Recognition Rate} = \frac{\sum \text{Patient score}}{\text{Total Number of Patient}} \quad (3)$$

While

$$\text{Patient score} = \frac{C_{rec}}{C_N} \quad (4)$$

Here, C_N be the number of cancer images of patients, and C_{rec} represent the cancer images that are correctly classified.

For the pretrained CNN, I explore VGGm model [27] which composed of 8 layers, and uses five convolutional filters of dimensions (number of filters \times filter height \times filter depth: $96 \times 7 \times 7$, $256 \times 5 \times 5$, $512 \times 3 \times 3$, $512 \times 3 \times 3$, and $512 \times 3 \times 3$) and three fully connected layers with the following number of hidden nodes (fc1: 4096, fc2: 4096, and softmax: 1000). This network was pretrained on the ILSVRC-12 challenge dataset. I recall that the ImageNet dataset used in this challenge is composed of 1.2 million RGB images of size 224×224 pixels belonging to 1000 classes and these classes describe general images such as beaches, dogs, cats, cars, shopping carts, minivans, etc. As can be clearly seen, this auxiliary dataset is completely different from the ECG signals used in the experiments.

For training the extra network placed on the top of the pretrained CNN, I follow the recommendations of [28] for training neural networks. I set the dropout probability p to 0.5. I use a sigmoid activation function for the hidden layer. For the backpropagation algorithm, I use a mini-batch gradient optimization method with the following parameters (i.e., learning rate: 0.01, momentum: 0.5, and mini-batch size: 50). The weights of the network are set initially in the range [-0.005 0.005].

TABLE II. CLASSIFICATION ACCURACIES (%) WITH MAGNIFICATION 40X

Test	Patient no.	40x				
		1	2	3	4	5
Benign	1	100	100	91.9	73.3	96.2
	2	65.7	30.6	100	100	48.6
	3	96.8	53.8	100	37.9	20.0
	4	100	100	93.3	100	100
	5	100	100	51.7	91.3	100
	6	84.6	38.5	100	94.6	92.9
	7	18.2	48.3	0.0	9.1	0.0
Malignant	8	100	96.9	90.0	100	85.7
	9	100	100	100	100	68.0
	10	100	82.8	82.8	78.3	100
	11	96.9	95.2	100	94.7	100
	12	100	100	90.6	100	100
	13	100	100	100	97.3	100
	14	82.6	95.0	100	100	100
	15	92.3	57.1	74.2	91.4	100
	16	33.3	96.2	78.3	100	100
	17	100	100	100	100	100
	18	97.2	90.0	100	100	88.5
	19	98.0	100	100	100	100
	20	93.8	72.0	26.7	100	97.4
	21	23.5	94.4	23.5	100	100
	22	100	100	100	92.3	100
	23	100	100	71.9	90.0	100
	24	100	100	100	100	91.7
Average		86.8	85.4	82.3	89.6	87.0

TABLE IV. CLASSIFICATION ACCURACIES (%) WITH MAGNIFICATION 200X

Test	Patient no.	200x				
		1	2	3	4	5
Benign	1	100	100	100	0.0	84.2
	2	48.4	52.6	100	86.8	25.8
	3	100	73.7	100	100	6.3
	4	100	88.1	91.7	92.9	100
	5	100	94.6	100	60.0	100
	6	57.1	45.7	97.3	88.2	100
	7	12.5	87.5	12.5	97.3	0.0
Malignant	8	93.3	100	100	100	92.9
	9	100	100	100	100	77.8
	10	95.8	100	78.7	90.0	86.7
	11	97.1	94.7	86.7	92.9	100
	12	100	100	100	100	100
	13	100	96.4	94.1	95.5	100
	14	23.8	92.9	93.8	100	100
	15	100	85.7	84.8	100	97.1
	16	85.7	100	100	85.7	100
	17	100	86.7	100	100	100
	18	100	100	100	100	100
	19	94.5	80.0	100	91.2	100
	20	90.6	92.6	100	88.9	100
	21	0.0	96.9	100	76.2	100
	22	100	100	100	82.8	100
	23	100	23.8	94.4	40.9	100
	24	100	89.3	100	100	100
Average		86.8	83.3	86.7	93.1	86.2

TABLE III. CLASSIFICATION ACCURACIES (%) WITH MAGNIFICATION 100X

Test	Patient no.	100x				
		1	1	1	1	1
Benign	1	72.7	72.7	72.7	72.7	72.7
	2	66.7	66.7	66.7	66.7	66.7
	3	100	100	100	100	100
	4	100	100	100	100	100
	5	100	100	100	100	100
	6	70.6	70.6	70.6	70.6	70.6
	7	21.2	21.2	21.2	21.2	21.2
Malignant	8	97.1	97.1	97.1	97.1	97.1
	9	100	100	100	100	100
	10	100	100	100	100	100
	11	92.7	92.7	92.7	92.7	92.7
	12	100	100	100	100	100
	13	100	100	100	100	100
	14	40.9	40.9	40.9	40.9	40.9
	15	100	100	100	100	100
	16	26.7	26.7	26.7	26.7	26.7
	17	95.2	95.2	95.2	95.2	95.2
	18	100	100	100	100	100
	19	90.7	90.7	90.7	90.7	90.7
	20	93.9	93.9	93.9	93.9	93.9
	21	87.5	87.5	87.5	87.5	87.5
	22	100	100	100	100	100
	23	100	100	100	100	100
	24	100	100	100	100	100
Average		86.8	85.7	85.7	85.7	85.7

TABLE V. CLASSIFICATION ACCURACIES (%) WITH MAGNIFICATION 400X

Test	Patient no.	400x				
		1	2	3	4	5
Benign	1	93.8	94.1	40.0	52.9	100
	2	66.7	89.2	88.2	88.5	50.0
	3	100	69.2	91.7	80.0	20.7
	4	94.1	79.5	53.3	84.6	88.9
	5	93.3	96.9	100	50.0	88.2
	6	70.8	45.8	96.9	71.4	100
	7	3.0	60.0	9.1	96.9	11.8
Malignant	8	100	92.3	93.1	100	80.0
	9	100	100	100	100	81.8
	10	100	100	85.7	100	73.3
	11	92.1	100	60.0	100	100
	12	100	100	100	100	100
	13	100	95.1	100	100	100
	14	54.2	92.9	100	100	100
	15	100	53.3	86.1	96.6	100
	16	45.5	100	100	92.9	100
	17	100	80.0	100	100	100
	18	100	100	100	100	93.5
	19	90.2	100	96.4	100	100
	20	96.2	100	95.8	100	100
	21	26.7	100	100	66.7	100
	22	100	100	100	71.4	100
	23	100	75.0	93.8	26.7	100
	24	100	100	100	60.0	100
Average		86.8	84.4	88.5	87.1	84.9

TABLE VI. THE PATIENT-LEVEL CLASSIFICATION ACCURACIES (%),
COMPARING OUR METHOD WITH EXISTING RESULTS ON THE BREAKHIS
DATASET

Retrained CNN	Magnification				Average
	40x	100x	200x	400x	
[22]	83.8±2.0	82.1±4.9	85.1±3.1	82.3±3.8	83.33
CNN [29]	83.1±2.1	83.2±3.5	84.6±2.7	82.1±4.4	83.25
Vgg_m	86.2±2.7	85.9±0.5	87.2±3.6	86.3±1.7	86.80

To present our results, I train the CNN networks depending on their magnifications (40x, 100x, 200x, and 400x) separately. The experiment was repeated five times as shown in Tables II-V, the average accuracy for five cases of the proposed CNN methods has been reported in Table VI which shows the superior accuracy of the proposed methods at patient level against state of the art methods in different magnification factors.

IV. CONCLUSION

This paper proposed a deep learning framework for breast cancer detection and classification. The yielded results confirm that deep learning can incur large margin improvements with respect to handcrafted features. Although the presented method achieves plausible scores, it can benefit from further improvements, potentially by 1) customizing more deep models; and 2) fusing several deep architectures in order to elevate the performance. Another direction to undertake is to adopt active learning in order to raise the classification scores. Ultimately, domain adaptation is another research line that can introduce tangible improvements.

ACKNOWLEDGMENT

The author would like to extend their sincere appreciation to the Deanship of Scientific Research at King Saud University for its funding this Research Group No. (RG -1435-050).

REFERENCES

[1] A. Jemal et al., "Cancer statistics, 2008," *CA. Cancer J. Clin.*, vol. 58, no. 2, pp. 71–96, Apr. 2008.

[2] L. Adepoju, W. Qu, V. Kazan, M. Nazzal, M. Williams, and J. Sferra, "The evaluation of national time trends, quality of care, and factors affecting the use of minimally invasive breast biopsy and open biopsy for diagnosis of breast lesions," *Am. J. Surg.*, vol. 208, no. 3, pp. 382–390, Sep. 2014.

[3] J. M. Eberth et al., "Surgeon Influence on Use of Needle Biopsy in Patients With Breast Cancer: A National Medicare Study," *J. Clin. Oncol.*, vol. 32, no. 21, pp. 2206–2216, Jul. 2014.

[4] T. Wan, J. Cao, J. Chen, and Z. Qin, "Automated grading of breast cancer histopathology using cascaded ensemble with combination of multi-level image features," *Neurocomputing*, vol. 229, pp. 34–44, Mar. 2017.

[5] M. Kowal, P. Filipczuk, A. Obuchowicz, J. Korbicz, and R. Monczak, "Computer-aided diagnosis of breast cancer based on fine needle biopsy microscopic images," *Comput. Biol. Med.*, vol. 43, no. 10, pp. 1563–1572, Oct. 2013.

[6] Z. Jiao, X. Gao, Y. Wang, and J. Li, "A deep feature based framework for breast masses classification," *Neurocomputing*, vol. 197, pp. 221–231, Jul. 2016.

[7] W. Sun, T.-L. (Bill) Tseng, J. Zhang, and W. Qian, "Enhancing deep convolutional neural network scheme for breast cancer diagnosis with unlabeled data," *Comput. Med. Imaging Graph.*

[8] S. Albarqouni, C. Baur, F. Achilles, V. Belagiannis, S. Demirci, and N. Navab, "AggNet: Deep Learning From Crowds for Mitosis Detection in Breast Cancer Histology Images," *IEEE Trans. Med. Imaging*, vol. 35, no. 5, pp. 1313–1321, May 2016.

[9] F. A. Spanhol, L. S. Oliveira, C. Petitjean, and L. Heutte, "Breast cancer histopathological image classification using Convolutional Neural Networks," in *2016 International Joint Conference on Neural Networks (IJCNN)*, 2016, pp. 2560–2567.

[10] K. Sirinukunwattana, S. E. A. Raza, Y. W. Tsang, D. R. J. Snead, I. A. Cree, and N. M. Rajpoot, "Locality Sensitive Deep Learning for Detection and Classification of Nuclei in Routine Colon Cancer Histology Images," *IEEE Trans. Med. Imaging*, vol. 35, no. 5, pp. 1196–1206, May 2016.

[11] J. Xu et al., "Stacked Sparse Autoencoder (SSAE) for Nuclei Detection on Breast Cancer Histopathology Images," *IEEE Trans. Med. Imaging*, vol. 35, no. 1, pp. 119–130, Jan. 2016.

[12] F. Jiang et al., "Abdominal adipose tissues extraction using multi-scale deep neural network," *Neurocomputing*.

[13] M. Havaei et al., "Brain tumor segmentation with Deep Neural Networks," *Med. Image Anal.*, vol. 35, pp. 18–31, Jan. 2017.

[14] X. W. Gao, R. Hui, and Z. Tian, "Classification of CT brain images based on deep learning networks," *Comput. Methods Programs Biomed.*, vol. 138, pp. 49–56, Jan. 2017.

[15] J. Kleesiek et al., "Deep MRI brain extraction: A 3D convolutional neural network for skull stripping," *NeuroImage*, vol. 129, pp. 460–469, Apr. 2016.

[16] K. Kamnitsas et al., "Efficient multi-scale 3D CNN with fully connected CRF for accurate brain lesion segmentation," *Med. Image Anal.*, vol. 36, pp. 61–78, Feb. 2017.

[17] C. Spampinato, S. Palazzo, D. Giordano, M. Aldinucci, and R. Leonardi, "Deep learning for automated skeletal bone age assessment in X-ray images," *Med. Image Anal.*, vol. 36, pp. 41–51, Feb. 2017.

[18] Z. Tang, C. Li, and S. Sun, "Single-trial EEG classification of motor imagery using deep convolutional neural networks," *Opt. - Int. J. Light Electron Opt.*, vol. 130, pp. 11–18, Feb. 2017.

[19] M. M. A. Rahhal, Y. Bazi, H. AlHichri, N. Alajlan, F. Melgani, and R. R. Yager, "Deep learning approach for active classification of electrocardiogram signals," *Inf. Sci.*, vol. 345, pp. 340–354, Jun. 2016.

[20] S. Kiranyaz, T. Ince, and M. Gabbouj, "Real-Time Patient-Specific ECG Classification by 1-D Convolutional Neural Networks," *IEEE Trans. Biomed. Eng.*, vol. 63, no. 3, pp. 664–675, Mar. 2016.

[21] P. Xiong, H. Wang, M. Liu, S. Zhou, Z. Hou, and X. Liu, "ECG signal enhancement based on improved denoising auto-encoder," *Eng. Appl. Artif. Intell.*, vol. 52, pp. 194–202, Jun. 2016.

[22] F. A. Spanhol, L. S. Oliveira, C. Petitjean, and L. Heutte, "A Dataset for Breast Cancer Histopathological Image Classification," *IEEE Trans. Biomed. Eng.*, vol. 63, no. 7, pp. 1455–1462, Jul. 2016.

[23] A. Krizhevsky, I. Sutskever, and G. E. Hinton, "ImageNet Classification with Deep Convolutional Neural Networks," in *Advances in Neural Information Processing Systems 25*, F. Pereira, C. J. C. Burges, L. Bottou, and K. Q. Weinberger, Eds. Curran Associates, Inc., 2012, pp. 1097–1105.

[24] C. Farabet, C. Couprie, L. Najman, and Y. LeCun, "Learning Hierarchical Features for Scene Labeling," *IEEE Trans. Pattern Anal. Mach. Intell.*, vol. 35, no. 8, pp. 1915–1929, Aug. 2013.

[25] P. Sermanet, D. Eigen, X. Zhang, M. Mathieu, R. Fergus, and Y. LeCun, "OverFeat: Integrated Recognition, Localization and Detection using Convolutional Networks," Dec. 2013.

[26] N. Srivastava, G. Hinton, A. Krizhevsky, I. Sutskever, and R. Salakhutdinov, "Dropout: A Simple Way to Prevent Neural Networks from Overfitting," *J. Mach. Learn. Res.*, vol. 15, pp. 1929–1958, 2014.

[27] K. Simonyan and A. Zisserman, "Very Deep Convolutional Networks for Large-Scale Image Recognition," Sep. 2014.

[28] Y. Bengio, A. Courville, and P. Vincent, "Representation Learning: A Review and New Perspectives," *IEEE Trans. Pattern Anal. Mach. Intell.*, vol. 35, no. 8, pp. 1798–1828, 2013.

[29] Neslihan Bayramoglu, Juho Kannala, and Janne Heikkilä, "Deep Learning for Magnification Independent Breast Cancer Histopathology Image Classification," in *23rd International Conference on Pattern Recognition*, 2016.

A Portable Natural Language Interface to Arabic Ontologies

Aimad Hakkoum¹, Hamza Kharrazi², Said Raghay³

Faculty of Science and Techniques, Cadi Ayyad University, Marrakesh, Morocco

Abstract—With the growing expansion of the semantic web and its applications, providing natural language interfaces (NLI) to end-users becomes essential to querying RDF stores and ontologies, using simple questions expressed in natural language. Existing NLIs work mostly with the English language. There are very few attempts to develop systems supporting the Arabic language. In this paper, we propose a portable NLI to Arabic ontologies; it will transform the user's query expressed in Arabic into formal language query. The proposed system starts by a preparation phase that creates a gazetteer from the given ontology. The issued query is then processed using natural language processing (NLP) techniques to extract keywords. These keywords are mapped to the ontology entities, then a valid SPARQL query is generated based on the ontology definition and the reasoning capabilities of the Web Ontology Language (OWL). To evaluate our tool we used two different Arabic ontologies: a Qur'anic ontology and an Arabic sample of Mooney Geography dataset. The proposed system achieved 64% recall and 76% precision.

Keywords—Natural language interface; ontology; Semantic web; Arabic natural language processing (NLP)

I. INTRODUCTION

The semantic web is the natural extension of the current web, it is centered on enabling machines to understand web content so it can be easier for agents to look for information in a more precise and efficient way [1]. To accomplish this task, the semantic web proposed a set of new technologies; the most important one is the use of ontologies. An ontology can be defined as “an explicit specification of a conceptualization” [2]. Ontologies explicitly structure and represent domain knowledge in a machine-readable format so they can be incorporated into computer-based applications to facilitate automatic annotation of web resources, reasoning task and decision support [3].

Traditional search engines rely only on keyword search; they return a set of documents that contain one or more words of the initial query. On the other hand, semantic search engines rely on understanding the meaning of the user query through the use of NLP techniques and ontologies, then returning the exact answer from multiple data sources using semantic web technologies[4].

Many studies have shown the effectiveness of semantic search engines over classic keyword search engines when dealing with natural language queries. Singh [5] compared keyword search engines like Google and Yahoo to semantic search engines like Hakia and DuckDuckGo and concluded that semantic search returns more relevant answers.

In order to develop an ontology-based search engine, we have to create a natural language interfaces (NLI) to hide the complexity of the ontology to the end-user [6]. It will transform the user query expressed in natural language to a formal language query.

The aim of our research is to develop a portable NLI that can be used with any ontology or RDF store. The proposed system starts by a preparation phase that creates a gazetteer from the given ontology. When the user issues a query, it is processed using NLP techniques to extract keywords; these keywords are mapped to the ontology entities, then a valid SPARQL query is generated based on the ontology definition and the reasoning capabilities of the Web Ontology Language (OWL). Finally, the SPARQL query is executed against the ontology and the result is formatted and aggregated if needed before returning the answer to the user.

The rest of this article is organized as follow: Section 2 summarizes the related work. Section 3 presents the ontologies used to evaluate the system. Section 4 describes the proposed system. Section 5 discusses the evaluation of our system. Finally, Section 6 brings conclusions and sheds light on future work.

II. RELATED WORK

There is a noticeable growth in using semantic web technologies for search systems development. This can be justified by the gain of accuracy using semantic search compared to keyword search as explained by Singh [5].

One way to take advantage of semantic web technologies is to utilize ontologies to expand the user query; this will improve the initial query by adding more related terms, and therefore improve the search results. This method has been adopted by many researchers, Alawajy [7] used domain ontologies and the Arabic WordNet (AWN) to provide reliable extended keywords in order to enhance Arabic web content retrieval. Besbes [8] proposed a new question analysis method based on ontologies, it consists of representing generic structures of questions by using typed attributed graphs and integrating domain ontologies and lexico-syntactic patterns for query reformulation.

Hattab [9] proposed the utilization of different levels of Arabic morphological knowledge to improve the search process in a search engine. The least degree of relationship is the strongest between the original word and the alternatives starting from the identical word, then its stem, its inflections and finally the root of the word.

These methods are suitable when fetching data from unformatted sources like text documents. We can benefit further from semantic web technologies by fetching data from RDF stores and knowledge bases. For that, we have to implement a NLI that will hide the complexity of the ontology to the end-user.

Based on different surveys ([10], [11]), most of the NLIs that were developed in the recent years are based on English. They can be classified into close domain NLIs and open domain NLIs. Close domain NLIs are adapted to a specific domain and therefore are more accurate and performant, on the other hand, open domain or portable NLIs are designed to work with any given ontology.

We are going to focus on portable NLIs, as it is the aim of our research. The first example is FREYA [12], it's an interactive NLI for querying ontologies. It uses syntactic parsing in combination with the ontology-based lookup in order to interpret the question, and involves the user if necessary. To help the user formulate his query, GINSENG [13] proposes to control user's input via a fixed vocabulary and predefined sentences structures through menu-based options, this approach gives a very good performance but cannot process all NL queries. Some NLIs like PowerAqua [14] designed a system that can query information from multiple ontologies, it gave promising results by obtaining a success rate of 70% correct answers of the evaluation questions.

Despite the fact that NLIs to ontologies have lately gained a considerable attention, existing approaches do not work with the Arabic language. The first research that worked in implementing a NLI using Arabic language is AlAgha [15] in 2015. This research proposed a system called AR2SPARQL; it translates Arabic questions into triples that are matched against RDF data to retrieve an answer. To overcome the limited support for Arabic NLP, the system does not make intensive use of sophisticated linguistic methods. Instead, it relies more on the knowledge defined in the ontology to capture the structure of Arabic questions and to construct an adequate RDF representation. The system achieved 61% average recall and 88.14% average precision.

In our previous paper [16], we proposed a semantic search system for the Qur'an. It is based on an Arabic NLI and a Qur'anic ontology that represents the Qur'an knowledge. Some of the algorithms used in this system are strongly dependent on the domain of the ontology and therefore cannot be applied to other domains. To overcome this limitation, we modified each algorithm to make it independent. Then we added more functionalities like approximate matching and user interaction in order to improve the performance and the accuracy of the system.

III. USED ONTOLOGIES

Recently, some efforts have been made to support Arabic in the semantic web. There are new Arabic ontologies that are being developed in different domains. The Islamic domain is one of the main topics of ontology development. The semantic Qur'an [17] created a multilingual RDF representation of the Qur'an structure, where the Qur'an ontology [16] extracted a

set of concepts from the Qur'an like locations, living creations and events. Another interesting research is the translation of DBpedia to Arabic [18].

We based our selection of the evaluation ontologies on the following criteria:

- The ontology contains enough data to formulate at least 50 different questions.
- All the entities of the ontology have labels in Arabic.
- The ontology is available in a valid RDF representation format.

We chose two ontologies that meet these criteria. The first one is the Qur'an ontology [16]. The second ontology is Mooney GeoQuery dataset that contains data about the geography of the United States.

A. Qur'an Ontology

The Qur'an ontology¹ aims to represent the knowledge contained in the Qur'an in the form of Ontology. It represents the following concepts: chapters, verses, words, pronouns, verse topics, locations, living Creations and events. Table I presents some statistics of the ontology:

TABLE I. QUR'AN ONTOLOGY STATISTICS

Object type	Count
Classes	49
Object properties	47
Data properties	23
Chapter	114
Verse	6236
Topic	1181
Living Creation	234
Location	69
Events	219

B. Geography Dataset

The Mooney GeoQuery dataset² describes the geography of the United States. Several English NLIs like FREYA and GINSENG used it to evaluate their system. It was translated to Arabic by AlAgha [15] for his system's evaluation. He translated all the classes and properties of the ontology, but not only 81 entities. We translated more labels to obtain 713 entities translated in Arabic. Table II shows some statistics of the ontology:

TABLE II. GEOQUERY ONTOLOGY STATISTICS

Object type	Count
Classes	9
Object properties	17
Data properties	11
State	51
Capital	51
City	351
Mountain	50
Road	40

¹ www.quranontology.com

² <http://www.cs.utexas.edu/users/ml/geo.html>

IV. NLI SYSTEM ARCHITECTURE

The NLI we are proposing is inspired from our semantic search system for the Qur'an [16]. After adapting the different algorithms of the system to be generic, we added a new component that enables the users to import new ontologies. Then we created a prototype and we run a set of tests using two different ontologies to analyze the possible causes of failure; this allowed us to improve the algorithms of matching, mapping and answer generation.

The structure of the proposed system is composed of five main components:

- 1) Knowledge base preparation.
- 2) Query processing.
- 3) Entity mapping.
- 4) Formal query generation
- 5) Answer generation.

A. Ontology Preparation

The ontology preparation component is triggered when the user imports a new ontology. It is composed of three sub-tasks: the extraction of the ontology definition, the generation of the inferred model and the construction of the gazetteer.

1) Extraction of the ontology definition

The extraction of the ontology definition consists of getting the ontology class hierarchy and the properties domain and range. Properties can be either object properties or datatype properties. Object properties have a domain and a range as a class; it is a relation between two entities. Datatype properties have a domain as a class and a range as a literal data like strings and numbers. The ontology definition will be used later in the automatic disambiguation task and the validation of the generated query triples.

2) Inferred model generation

The ontology specifies a set of facts and axioms. They can be used to generate new inferred triples in order to obtain an extended model. To avoid generating this model at each query execution, we will generate it the first time when the ontology is loaded and save it along with the ontology. We will use Jena Framework (<http://jena.apache.org/>) to manipulate the ontology model and generate the inferred model. Jena provides an API that enables to work with ontologies in different formats. It is widely used with semantic web technologies and is well documented and maintained.

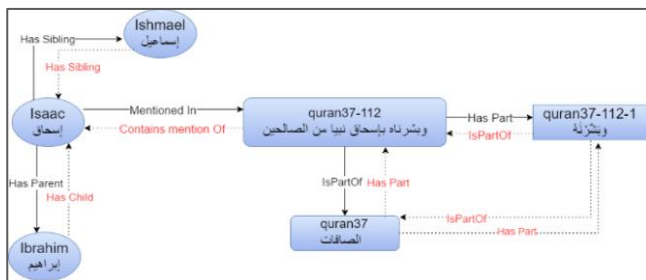


Fig.1. Example of inferred triples.

The inferred model will contain all the ontology triples in addition of the new deducted triples. Fig. 1 shows an example of the triples that we can get by this process. The black links represent the initial model, while the red links are obtained after generating the inferred model.

We will use this model to execute the SPARQL query generated by our system; this will increase the possibility to find an answer in the ontology. Table III shows the number of triples for the original model and the inferred model of the two evaluation ontologies:

TABLE III. INFERRER MODEL STATISTICS

	Quran	Geo
Initial model triples count	182 908	4 981
Inferred model triples count	473 353	14 830

3) Gazetteer construction

The construction of the gazetteer starts by the extraction of all the entities' labels. This includes the classes, the properties and the individuals. The extracted list of labels is then enhanced by generating synonyms from dictionaries and linguistic resources. The final step is to process each term of the gazetteer using NLP techniques.

a) Synonyms generation

Despite the recent efforts to support the Arabic language on the semantic web and NLP, it still lacks proper resources like WordNet and offline dictionaries. The Arabic version of the WordNet (AWN) developed by Abouenour [19] includes in its latest version about 17,785 words, it is still a work in progress and need more work to be comparable to the English WordNet which contains about 117,000 words. Therefore, using only the AWN will not be enough to generate synonyms. The other resource that we are going to use to accomplish this task is the on-line dictionary Almaany (www.almaany.com), it is the best tool we found and besides, no useable offline dictionary could be found.

b) Linguistic processing

The challenges of Arabic NLP are discussed in [20]. The main challenges are as follows:

- Lack of dedicated letters to represent short vowels, they are represented by diacritics.
- Changes in the form of the letter depending on its place in the word.
- Word agglutination: Arabic words often contain affixes representing various parts of speech. For example, a verb may embed within itself its subject and its object as well as the gender, person, number, and voice.

The first solution we are going to use to address these challenges is normalization. It consists of representing the Arabic text in a canonical form and thus avoiding the use of different forms to designate the same letter. The process of normalization is performed with Lucene Arabic analyzer³. An

³ <http://lucene.apache.org/>

example of transformation is to replace all the forms of "alif" ("ا", "آ", "إ" and "أ") by "ا".

The second solution is stemming, which is the process of extracting the stem and the root by removing prefixes and affixes from words. There are several tools available for Arabic stemming. One of the recent and advanced tools is the Arabic Toolkit Service ATKS⁴. It contains multiple components like the Arabic parser, the Arabic speller and the morphological analyzer (SARF). These components are integrated into several Microsoft services such as Office, Bing, SharePoint and Windows. We are going to use SARF for stemming; in addition to the word root, it gives the stem, the morphological pattern and all the inflections of the word.

B. Query Processing

The user is assisted when entering his query with an autocomplete component. We use the terms of the gazetteer to give suggestions to complete each word of the query when the user enters two letters. After a new word is entered, the ATKS spell checker highlights the misspelled words.

Once the user validates his query, the query-processing component will start by tokenizing the query words, then removing stop words. We provide an initial list of stop words that the user can change depending on the domain of the ontology. After removing irrelevant words, we generate synonyms for each word using the AWN and Almaany. The final step is to process these words the same way the gazetteer terms were processed, which includes normalizing and stemming each word along with its synonyms.

C. Entity Mapping

The entity mapper is a critical component of any NLI system. It is responsible of mapping the query words to the ontology entities. To accomplish this task, we will start by comparing the query words to the gazetteer terms, if we find more than one match, we will try to choose one with an automatic disambiguation algorithm using the ontology definition. As a final step, we will ask the user to clarify the ambiguity manually by choosing one of the matching entities.

1) String matching

In order to match the user query with the ontology entities, we are going to combine two approaches of string matching: exact and approximate matching. We will start the comparison process by generating all possible n-grams starting from the highest n-gram that contains all the user query keywords to the unigrams that contain one word at a time. These n-grams are compared to the gazetteer terms according to the following order: 1) complete word; 2) normalized word; 3) word stem, 4) synonym; 5) normalized synonym; 6) synonym stem; 7) word root; 8) synonym root. We loop through all the possible n-grams starting from the highest ones, each time we found a match; we remove the n-gram words from the list of words to match. The matching algorithm is finished when we match all the words or when we arrive to unigrams.

The exact matching may not yield a result because of typographical errors, or phonetic similarity errors. In this case, we will use approximate matching. There are many methods to perform approximate matching [21], the most used one is known as the Levenshtein distance (also called "edit distance"). It consists of computing the minimum number of single characters edits needed to change one word into the other. We compute the Levenshtein distance on normalized words in order to have a result that is more pertinent. The similarity rate is computed as follows:

$$Sim(Word1, Word2) = 1 - \frac{Lev(Word1, Word2)}{Max(Length(Word1), Length(Word2))}$$

Where $Lev(Word1, Word2)$ is the Levenshtein distance

We compute this distance for all the gazetteer terms. We consider as a match the entity with the highest similarity rate. If this rate is over 90%, it is considered automatically as a match. Otherwise, we ask the user to validate the matching entity manually if this rate is between 90% and 70%. The user can then confirm the match or exclude the word from the answer generation process.

The approximate matching is especially useful for comparing proper names that can have multiple forms of writing in Arabic and for which the generation of the root does not return any value. Table IV shows some results obtained using approximate matching:

TABLE IV. EXAMPLES OF APPROXIMATE MATCHING

User word	Ontology word	Similarity rate
زكرياء	زكريا	83%
الذريات	الذاريات	87%
كالفورنيا	كاليفورنيا	88%
سان فرانسيسكو	سان فرانسيسكو	92%

2) Entity disambiguation

This step is optional; however, it is very important when working with large ontologies because the same word can be used to identify different entities. As an example from the Qur'an ontology, we can find that the name of a chapter is the same as the name of a prophet or a topic. In this case, we are going to use the ontology definition and inference to try to find the accurate entity.

We have two ways to achieve the disambiguation: by class or by property. The first type of disambiguation corresponds to the scenario when the query contains a class and an individual from this class. In this case, if we have an ambiguity on the individual, we choose the one that is an instance of the class. The second type of disambiguation is used when the query contains an individual and a property that has as domain or range the type of this individual. In this case, we choose the individual that corresponds to the definition of the property.

To illustrate each type of disambiguation, let us analyze these two questions:

⁴ <http://research.microsoft.com/en-us/projects/sarf>

- 1) من هم أبناء ابراهيم عليه السلام؟ (Who are the children of Abraham?)
- 2) ما على الحدود مع ولاية ميشيغان؟ (What on the border with the state of Michigan?)

The first question is executed against the Qur’anic ontology and the second one against the Geography ontology. Fig. 2 and 3 describe the mapping and the disambiguation process for each question:

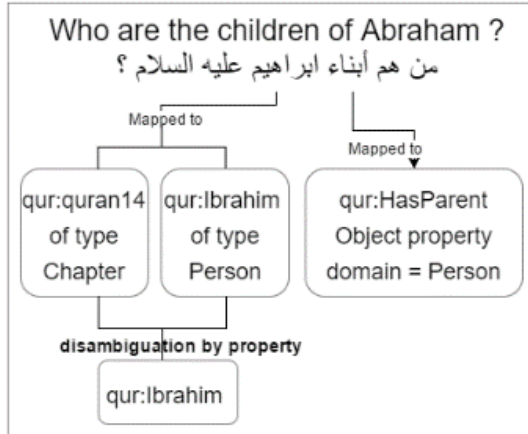


Fig.2. Automatic disambiguation of question 1.

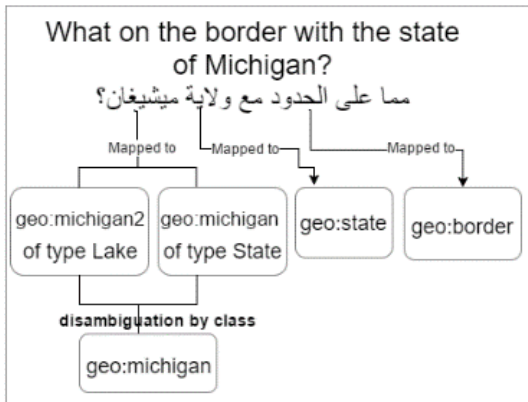


Fig.3. Automatic disambiguation of question 2.

If the automatic disambiguation does not return a match, we ask the user through the interface to clear the ambiguity manually. We computed the number of each applied disambiguation when executing the evaluation questions on the system. Table V represents the list of the computed statistics:

TABLE V. DISAMBIGUATION STATISTICS

Dataset	Quran	Geo
Number of questions	60	90
Number of manual disambiguation	30	20
Number of auto disambiguation	11	10

We can see from these statistics that the contribution of the user is crucial in order to understand the meaning of the query. The Qur’an ontology needed more manual disambiguation; this can be explained by the fact that the same word is used to represent two or more concepts at the same time.

D. Query Generation

This component consists of generating a valid SPARQL query from the mapped entities. It is mainly based on the ontology definition and the reasoning capabilities of OWL.

1) Triple generation

The first step to construct the SPARQL query is to generate an initial set of query triples, these triples are in the following format: (s, p, o) where s, p and o respectively represent the subject, the predicate and the object. Each element can be either a known entity or a variable that the SPARQL query must return.

We loop through the mapped entities following the order of the user query, to each entity we apply a transformation function that will either create a new triple or modify an existing one. Fig. 4 describes the transformation algorithm of an entity (E_i):

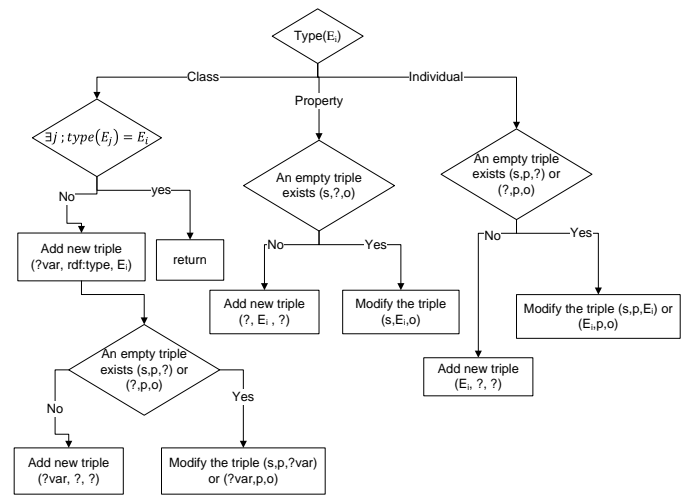


Fig.4. Transformation function algorithm.

The first case of the algorithm is when the type of the entity is a class. If there is already an individual that have the type of this class, the entity will be ignored. Otherwise, we create a new triple (?var, rdf:type, E_i) and we add the variable into an incomplete triple (?var, p, o) or we create a new triple (?var, ?, ?).

Once we perform the transformation function on all entities, we obtain a list of triples: (s₁, p₁, o₁), (s₂, p₂, o₂), ...

These triples may be incoherent and not representing a valid RDF triple, therefore in the next step we will perform more processing to validate and expand these triples in order to obtain the final triples list.

2) Query expansion

A valid query triple (s, p, o) must verify the following integrity conditions:

$$\text{domain}(p) = \text{type}(s) \text{ and } \text{range}(p) = \text{type}(o)$$

In order for each triple to comply with these conditions, we will apply a set of changes by expanding the triple or by simply changing the order between the object and the subject.

When the property is a variable, we check the ontology definition for a property that satisfies the integrity condition, if we do not find any, we expand the initial triple to obtain the two triples: (s, p', o') , (o', p'', o) . This scenario corresponds to two entities on the ontology graph that are not linked directly by a relation so we have to add an intermediate node in order to link them.

When the property of the triple is not a variable and does not satisfy the integrity condition, we add a new individual (i) and a new property (p') to obtain two triples as a result. Table VI lists all the possible transformation of a query triple:

TABLE VI. QUERY TRANSFORMATION SCENARIOS

Condition	Transformation
$\text{domain}(p) = s$ and $\text{range}(p) \neq o$	(s, p, i) , (i, p', o)
$\text{domain}(p) = o$ and $\text{range}(p) = s$	(o, p, s)
$\text{domain}(p) = o$ and $\text{range}(p) \neq s$	(o, p, i) , (i, p', s)
$\text{domain}(p) \neq s$ and $\text{range}(p) = o$	(s, p', i) , (i, p, o)
$\text{domain}(p) \neq o$ and $\text{range}(p) = s$	(o, p', i) , (i, p, s)

3) SPARQL generation

SPARQL is the W3C (World Wide Web Consortium) standard to query RDF data stores. A SPARQL query uses a "SELECT" statement to define which data the query should return, and a "WHERE" statement that defines a graph pattern where some nodes are known and others are not, the query should then find all possible subgraphs that meet the pattern.

The generation of the SPARQL query consists of putting the variables in the SELECT statement and the query triples in the WHERE statement. For each variable, we add an optional variable that corresponds to the Arabic label with an optional filter as follows:

```
SELECT ? var1 ? var1Label ? var2 ? var2Label ...
Where { (s1, p1, o1). (s2, p2, o2), ... }
OPTIONAL { ? var1 rdfs:label ? var1Label.
Filter ( langMatches(lang(? var1Label), ar). ) }
```

E. Answer Generation

The SPARQL query is executed against the inferred model of the ontology using the Jena Framework. After getting the result of the query, we apply two functions to format and remove redundant information. The first function removes duplicate rows and columns that contain the same data. The second function perform an aggregation on the result, it is used when the first column contains a limited number of non-duplicated values while the number of lines is very important. In this case, the rows are aggregated using the values of the first column, which is considered the main object of the question.

F. System Interface

We designed a simple interface that implements the NLI system. It consists of a desktop application. It does not need any installation and can run directly after downloading the binaries from the project webpage.

The application allows the user to perform a set of actions in addition to using the search engine. The application menu enables the user to import new ontologies and remove existing ones. When an ontology is selected, the user can use the menu to edit the gazetteer or the stop words list.

To use the search engine, the user must choose the desired ontology from the list of ontologies and enter his query in Arabic. The autocomplete component will propose suggestions when the user enters two letters for a word. When the user executes the search, he may need to disambiguate some of the query words. Here is an example of the disambiguation process:

Fig. 5 shows an example of the disambiguation process. In this example, we have one word that can be mapped to two entities from the ontology, and one word that was mapped using approximate matching. The user can select one entity for the first word, and validate the approximate matching for the second word. He can also exclude a word and it will be removed from the rest of the process.

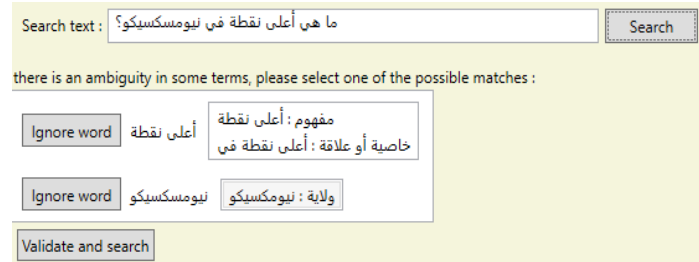


Fig.5. Disambiguation process screen.

The search result is displayed in a group of tabs. The first one is the answer of the query; it may contain a single element, a list with a single column or a table with multiple columns. The other tabs describes the details of each component of the system, they can help the user understand how the answer was generated. The last tab contains the SPARQL query used to retrieve the answer. The user can modify it and click on the "Exec query" button, the result of the query is then displayed in the first tab.

V. SYSTEM EVALUATION

A. Evaluation Questions

We prepared a set of evaluation questions for the two ontologies. We ensured that the questions are in the scope of the ontology and the system has the ability to answer them, this will allow us to analyze the causes of failure for unanswered queries in order to improve the system effectiveness.

For the Qur'an ontology, we used the sample questions available on the project website; we added some more questions to reach 70 questions. For the Mooney GeoQuery dataset we took the 877 questions used by AlAgha [15] to evaluate his system, then we removed the questions that are rather similar. We also removed the improperly formatted ones to obtain 90 questions.

The evaluation questions along with the two ontologies can be accessed in the project webpage.

B. Evaluation Results

To calculate the performance of the proposed NLI system, we executed all the evaluation questions using the user interface after importing the two ontologies. We analyzed the result of each question in order to compute the statistics about the mapping and disambiguation components, we also classified the reasons behind the system's failure.

We are going to compute the following metrics: precision and recall. The precision is the number of correctly answered questions over the number of questions that the system provided an answer for, while the recall is the number of questions correctly answered over the number of all questions in the dataset.

The webpage of the project contains the detail of the evaluation process. For each question, we define if the system provides an answer or not, and if this answer is correct. Table VII shows the general result of the evaluation:

TABLE VII. EVALUATION RESULTS

Ontology	Quran Ontology	Geography	Total
Total number of questions	70	90	160
Questions with an answer	53	80	133
Questions with correct answer	47	56	103
Precision	88%	70%	76%
Recall	67%	62%	64%

The system gave answers to 133 questions, among which 103 are correct, thus achieving 64% average recall and 76% average precision. We can see that the Qur'an ontology gives more precision than the geography dataset. This can be explained by the fact that the Qur'an ontology defines several possible labels to identify its entities; this helps the mapping of the user keywords to the ontology entities.

The NLI (AR2SPARQL) proposed by [15] claims a recall of 61% and a precision of 88.14%. This system is not publically available; therefore, we cannot make a pertinent comparison of the performance of the two systems, because we have to use the same questions to evaluate both systems. On the overall, our system is based on the same approach of AR2SPARQL, which is the use of the knowledge defined in the ontology to process the user query. Both systems do not make intensive use of sophisticated linguistic and semantics techniques. However, some components are different between the two; for instance, we use approximate matching and user interaction for entity mapping. Our system also relies on the involvement of the user to clarify his question and the use of a set of rules to validate and enhance the SPARQL query.

C. System Failure Analysis

We analyzed the reasons of failure for each question that the system could not answer correctly, we classified these reasons into three categories: mapping error, complex questions and uncovered questions. The first category represents 40%; the second 50% while the last one 10%.

The mapping error category represents the questions where we could not map the user terms to the entities of the ontology or that we mapped a term to the wrong entity. This kind of error is due to the challenges of Arabic NLP discussed earlier. Some of the unanswered questions can be fixed by editing the gazetteer of the ontology via adding new alternative labels for the entities. Where some questions need to be reformulated by the user in order to get an answer.

The second category represents complex questions that require adding more rules and algorithms to the system in order to be able to answer them. We can identify different kinds of complex queries:

- Long questions with term dependencies: This kind of questions needs deep linguistic analysis to extract the dependencies between terms. Some of the English NLIs used syntactic parsing and part-of-speech tags to extract the parse tree of the question, this helps understand the question's structure and to generate valid query triples. The use of this method with the Arabic language is still challenging due to the lack of efficient NLP tools and the high productivity of the Arabic language.
- Questions with superlatives and comparatives: The interpretation of comparative and superlative words depend on the domain of the ontology, and even in the same ontology, we can find multiple interpretations for the same term.
- Vague questions: The user may use vague expressions to formulate his question, making the understanding of its meaning very difficult. An example of this type of question is "ما يمكنك ان تقول لي عن سكان ميسوري؟" (What can you tell me about Missouri residents?), we can see that the question is not precise enough because we have two properties that describe the population: the number of inhabitants and the population density.

The third category represents the questions that the ontology does not contain an answer for even if the query processing was successfully performed. This kind of questions needs the enrichment of the ontology by adding more properties and entities.

D. Publishing the Results

We created a webpage for the project at the following address: <https://sites.google.com/site/arabicnliystem>. It contains all the resources necessary to use and evaluate the NLI system.

We also shared the source code of the project for other researchers to leverage on their research. The source code is composed of two layers. The first one is the user interface that contains the definition of the application forms, and the second one is the business layer that contains all the system's logic and algorithms.

VI. CONCLUSION

In this research, we developed a portable NLI to Arabic ontologies. The system can be used with any ontology that defines Arabic labels to its entities. We tested our approach on

two different ontologies that represent two separate domains, the system gave better results when the ontology is well structured and provides alternative labels to describe its entities.

We used existing Arabic NLP tools to process the ontology labels and the user question, this allowed us to map the user terms to the ontology entities, and then we relied on the ontology definition and the reasoning capabilities of OWL to create a SPARQL query that will be used to extract the answer from the ontology.

We believe that our work will be a step toward adopting semantic search engines for the Arabic language. The researchers can integrate our system library in their projects with minimum effort to have a semantic search tool for their ontologies.

The next step of our research is to study the reasons behind the system's failure and try to improve the capabilities of the system to answer unmanaged questions patterns. Another perspective is to improve the search system to answer questions from multiple ontologies. This will require the use of ontology alignment frameworks in order to allow multiple ontologies to interoperate.

REFERENCES

- [1] Y. Badr, R. Chbeir, A. Abraham, and A.-E. Hassanien, "EmergentWeb Intelligence: Advanced Semantic Technologies.," in Springer Science & Business Media, 2010, p. Page: 26-36.
- [2] T. R. Gruber, "Toward principles for the design of ontologies used for knowledge sharing," *Int. J. Hum. Comput. Stud.*, vol. 43, no. 5–6, pp. 907–928, 1995.
- [3] N. Shadbolt, T. Berners-Lee, and W. Hall, "The Semantic Web - The Semantic Web Revisited," *IEEE Intell. Syst.*, vol. 21, no. 3, p. 96, 2006.
- [4] T. Tran, P. Haase, and R. Studer, "Semantic search--using graph-structured semantic models for supporting the search process," in *International Conference on Conceptual Structures*, 2009, pp. 48–65.
- [5] J. Singh, "A Comprative Study Between Keyword and Semantic Based Search Engines," in *International Conference on Cloud, Big Data and Trust*, 2013, pp. 13–15.
- [6] E. Kaufmann and A. Bernstein, "How useful are natural language interfaces to the semantic Web for casual end-users?," in *The Semantic Web*. Springer Berlin Heidelberg, 2007, vol. 4825 LNCS, pp. 281–294.
- [7] A. M. Alawajy and J. Berri, "Combining semantic techniques to enhance arabic Web content retrieval," 2013 9th Int. Conf. Innov. Inf. Technol. IIT 2013, pp. 141–147, 2013.
- [8] G. Besbes, H. Baazaoui-Zghal, and A. Moreno, "Ontology-based question analysis method," in *International Conference on Flexible Query Answering Systems*. Springer Berlin Heidelberg., 2013, pp. 100–111.
- [9] M. Hattab, B. Haddad, M. Yaseen, A. Duraidi, and A. A. Shmais, "Addaall Arabic Search Engine: Improving Search based on Combination of Morphological Analysis and Generation Considering Semantic Patterns," in *The second International Conference on Arabic Language Resources and Tools*, Cairo, Egypt., 2009, pp. 159–162.
- [10] S. Kalaivani and K. Duraiswamy, "Comparison of question answering systems based on ontology and semantic web in different environment," *J. Comput. Sci.*, vol. 8, pp. 1407–1413, 2012.
- [11] A. Bouziane, D. Bouchiha, N. Doumi, and M. Malki, "Question Answering Systems: Survey and Trends," *Procedia Comput. Sci.*, vol. 73, no. Awict, pp. 366–375, 2015.
- [12] D. Damjanovic, M. Agatonovic, and H. Cunningham, "FREyA : an Interactive Way of Querying Linked Data Using Natural Language," in *Extended Semantic Web Conference*. Springer Berlin Heidelberg., 2011, pp. 125–138.
- [13] A. Bernstein, E. Kaufmann, and C. Kaiser, "Querying the Semantic Web with Ginseng : A Guided Input Natural Language Search Engine," in *15th Workshop on Information Technologies and Systems Las Vegas NV*, 2005, no. December, pp. 45–50.
- [14] V. Lopez, V. Uren, M. Sabou, E. Motta, and Acm, "Cross Ontology Query Answering on the Semantic Web: An Initial Evaluation," *K-Cap'09 Proc. Fifth Int. Conf. Knowl. Capture*, pp. 17–24, 2009.
- [15] I. Alagha, "AR2SPARQL : An Arabic Natural Language Interface for the Semantic Web," in *International Journal of Computer Applications (0975–8887)*, 2015, vol. 125, no. 6, pp. 19–27.
- [16] A. Hakkoum and S. Raghay, "Semantic Q&A System on the Qur'an," *Arab. J. Sci. Eng.*, vol. 41, no. 12, 2016.
- [17] M. A. Sherif and A. C. Ngonga Ngomo, "Semantic Quran A multilingual Resource for Natural-Labguage Processing," *Semant. Web J.*, vol. 6, pp. 339–345, 2009.
- [18] H. Al-Feel, "The Roadmap for the Arabic Chapter of DBpedia," *Math. Comput. Methods Electr. Eng.*, pp. 115–125, 2015.
- [19] L. Abouenour, K. Bouzoubaa, and P. Rosso, "On the evaluation and improvement of Arabic WordNet coverage and usability," *Lang. Resour. Eval.*, vol. 47, no. 3, pp. 891–917, 2013.
- [20] A. Farghaly and K. Shaalan, "Arabic natural language processing : Challenges and solutions," in *ACM Transactions on Asian Language Information Processing (TALIP)*, 2009, vol. 8, no. 4, pp. 1–22.
- [21] G. Navarro, "A guided tour to approximate string matching," *ACM Comput. Surv.*, vol. 33, no. 1, pp. 31–88, 2001.

Online Incremental Rough Set Learning in Intelligent Traffic System

Amal Bentaher^{1,2}, Yasser Fouad², Khaled Mahar³

¹Faculty of Science, Hadhramout University., Hadhramout, Yemen

²Computer Science Department, Faculty of Science, Alexandria University, Alexandria, Egypt

³College of Information Technology, Arab Academy for Science and Technology, Alexandria, Egypt

Abstract—In the last few years, vehicle to vehicle communication (V2V) technology has been developed to improve the efficiency of traffic communication and road accident avoidance. In this paper, we have proposed a model for online rough sets learning vehicle to vehicle communication algorithm. This model is an incremental learning method, which can learn data object-by-object or class-by-class. This paper proposed a new rules generation for vehicle data classifying in collaborative environments. ROSETTA tool is applied to verify the reliability of the generated results. The experiments show that the online rough sets based algorithm for vehicle data classifying is suitable to be executed in the communication of traffic environments. The implementation of this model on the objectives' (cars') rules that define parameters for the determination of the value of communication, and for reducing the decision rules that leads to the estimation of their optimal value. The confusion matrix is used to assess the performance of the chosen model and classes (Yes or No). The experimental results show the overall accuracy (predicted and actual) of the proposed model. The results show the strength of the online learning model against offline models and demonstrate the importance of the accuracy and adaptability of the incremental learning in improving the prediction ability.

Keywords—Vehicle to vehicle communication; online learning; rough sets theory; intelligent traffic system

I. INTRODUCTION

Nowadays, road accidents are one of the major problems in modern societies that lead to death. The increase of travel time is a main reason for increasing traffic accidents, fuel consumption and increased pollution [1], [2]. Road safety field is on focus by researchers to detect traffic congestions and, thereby, to offer solutions.

The Intelligent Transport System (ITS) is a technology to achieve safe roads and comfortable driving, by reducing accidents and delay [3]. In recent years, a research area in the road safety called vehicular network offers a possible solution that allows a communication and information exchange between vehicles, which is called vehicle to vehicle (V2V) communication, or between vehicles and road infrastructure, which is called vehicle to infrastructure (V2I) communication, [4] as shown in Fig. 1.

Since its development, Rough sets theory has been able to devise a computationally efficient and mathematically sound techniques handling imprecision in decision making [5]. The optimal solutions without losing any information can be found

by using the rough sets theory which find reduces the rules for training the dataset and classifying the test set [6].

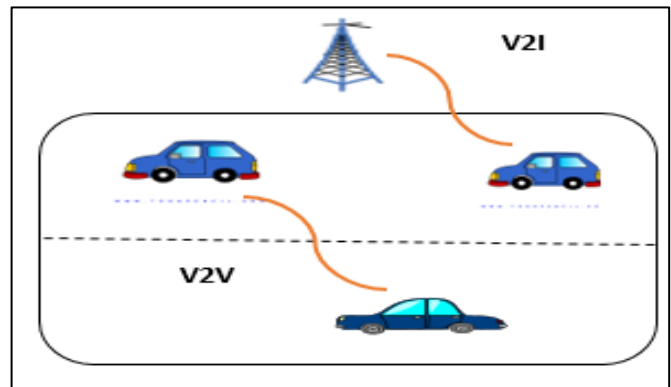


Fig. 1. V2V and V2I communication.

The remainder of this paper is organized as follows. In Section 2, we describe basic concepts of rough sets; in Section 3 we describe architecture and the feasibility decision table of our model. In Section 4, we present the implementation of our proposed model and show the results. Finally, we conclude our paper at Section 5.

II. BASIC CONCEPTS OF ROUGH SETS

Rough sets theory (RST) is a mathematical tool that is developed by Pawlak in 1982 [7]. In this theory, the data is collected in a table, called a decision table. Rows of concepts on rough sets theory are reviewed as follows:

Definition 1 (Information system): Is the 4-tuple [8], [9] (U, A, C, D) where U consists of objects and A consists of attributes, the subsets C and D are called condition attribute set and decision attribute set, respectively. Every $a \in A$ corresponds to the function $a: U \rightarrow V_a$ where V_a is the value set of a .

Definition 2 (Indiscernibility relation): Let $S=(U,A)$ be an information system, and $B \subseteq A$. we define the B -indiscernibility relation as [8], [10]:

$$INDs(B) = \{ (x,y) \in U^2 \mid \forall b \in B (b(x) = b(y)) \} \quad (1)$$

If $(x,y) \in INDs(B)$, then x and y are indiscernible by attributes from B . The equivalence classes of the B -indiscernibility relation of an object x is denoted by $[x]_{ind(B)}$.

Definition 3 (Lower and upper approximation): Two fundamental concepts of rough sets are the lower and upper approximations of sets (which are a classification of the domain of interest into disjoint categories) in Fig. 2 [8], [9]. Given a set $B \subseteq A$, the lower and upper approximations of a set $X \subseteq U$ are defined by, respectively,

$$\underline{B}Y = \{ x \mid [x] B \subseteq X \} \quad (2)$$

$$\overline{B}Y = \{ x \mid [x] B \cap X \neq \varphi \} \quad (3)$$

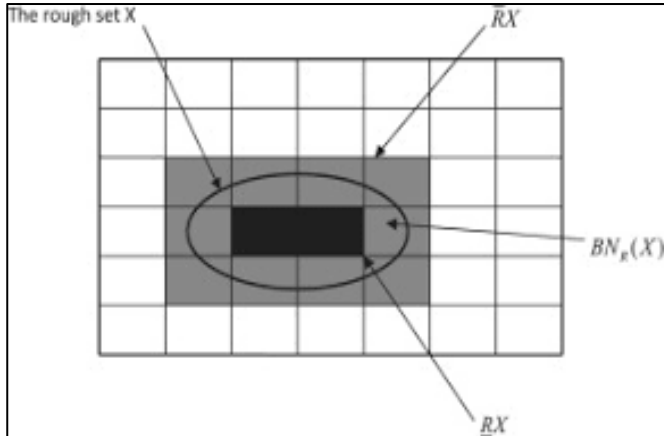


Fig. 2. Depiction of rough set.

Definition 4 (Lower approximation and positive region): [8]-[10]. The positive region $POS_B(X)$ is defined by:

$$POS_B(X) = \underline{B}X \quad (4)$$

If an object $x \in POS_B(X)$, then it belongs to target set X certainly.

Definition 5 (Upper approximation and negative region): The negative region $NEG_B(X)$ is defined by [8]-[10]:

$$NEG_B(X) = U - \overline{B}X \quad (5)$$

If an object $x \in NEG_B(X)$, then it cannot be determined whether the object x belongs to target set X or not.

Definition 6 (Boundary region): The boundary region is the difference between upper and lower approximations of a set X [8]-[10]:

$$BND_B(X) = \overline{B}X - \underline{B}X \quad (6)$$

If an object $x \in BND_B(X)$ it doesn't belong to target set X certainly.

III. PROPOSED MODEL

Continuous data streams reflect continuous environmental changes, raising the need for online learning to adapt to changing conditions [11]. In this section we present the proposed model that is online rough sets learning vehicle to vehicle communication algorithm. The proposed algorithm is a methodology which uses rough sets theory to compute accurate objects for new (rules) data streams from online traffic environments. Vehicles can detect potential issues on the road and alert nearby users about incoming dangers and reduce the risk of accidents as shown in Fig. 3.

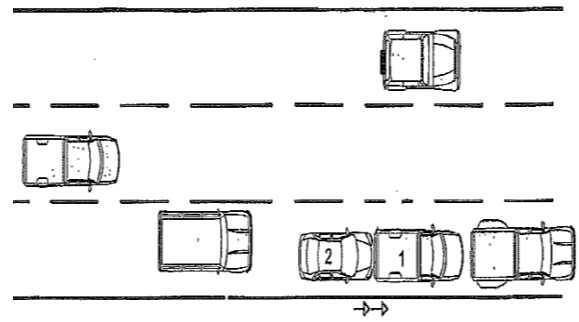


Fig. 3. Vehicles rough set learning communication in online environment.

A. Model Algorithm

In our method online learning rough sets theory in vehicle to vehicle (V2V) communication environment determines objects (cars) one by one and satisfying any object to any rule or addition new rules. Our model use GPS and a wireless LAN module to allow cars to communicate within a range of 100-to-300 meters.

The proposed model is designed to work based on the following algorithm:

Algorithm: Proposed model Algorithm

Input: Incrementally arriving objects in traffic environment.

Output: Optimal decision of communication.

Step 1. Initial data have one object and set of rules R .

Step 2. $F = \phi$ {List all best of objects}

Step 3. $f \leftarrow$ get new object (car)

Step 4: Determine object and rule r

Step 5. If $f \subset F$ then the rule r is satisfying to any existed rules

Step 6. Otherwise compute a decision table, generate reduct and generate rules R .

Step 7. Update online data streaming

Step 8. Repeat steps 3-7 until finish all objects.

B. Decision Table of the Model

The rough sets theory has been developed for knowledge discovery in databases and experimental data sets. An attribute-oriented rough sets technique reduces the computational complexity of learning processes and eliminates the unimportant or irrelevant attributes so that the knowledge discovery in database or in experimental data sets can be efficiently learned [12].

The Rough Sets analysis of data involved calculation of reducts from data, derivation of rules from reducts, rule evaluation and prediction processes. The rosetta rough sets toolkit was employed to carry out reducts and generate decision rules. The reducts were created from our selected data are revealed in Fig. 4. We used the Johnhon's reducer algorithm and the equal binning decretized method.

	Id	Speed	Range	direction	vehicle color	vehicle type	Decision
1	1	2	13	-1	green	Truck	Yes
2	2	5	2	-1	indigo	lorry	No
3	3	3	5	-1	orange	lorry	No
4	4	2	6	1	blue	van	Yes
5	5	10	15	1	indigo	bus	No
6	6	4	15	0	green	bus	No
7	7	9	5	-1	blue	lorry	No
8	8	10	18	1	red	car	No
9	9	5	2	1	blue	lorry	Yes
10	10	3	11	1	violet	Truck	No
11	11	6	7	-1	yellow	van	No
12	12	8	3	-1	red	lorry	Yes
13	13	10	9	0	indigo	lorry	Yes
14	14	3	19	1	green	lorry	Yes
15	15	2	11	-1	red	Truck	Yes
16	16	9	8	0	indigo	bus	Yes
17	17	1	9	-1	green	lorry	Yes
18	18	7	5	-1	blue	lorry	No
19	19	10	12	0	red	car	Yes
20	20	8	4	1	green	Truck	No
21	21	4	5	1	violet	car	No
22	22	6	15	-1	red	lorry	No
23	23	10	7	-1	orange	van	No
24	24	10	14	1	violet	car	No
25	25	2	9	-1	blue	Truck	Yes
26	26	8	6	0	yellow	lorry	Yes
27	27	4	4	-1	violet	van	Yes

Fig. 4. Car dataset after use decision table.

A data set can be represented as a decision table, which is used to specify what conditions lead to decisions. A decision table is defined as $T = (U, C, D)$ where U is the set of objects in the table, C is the set of the condition attributes and D is the set of the decision attributes as shown in Fig. 4. The features are: decision, the speed of cars, the range between cars, the directions of the cars, the color and the type of cars. Fig. 4 can be used to decide whether a car has a Yes or No decision according to its features (e.g., the speed, the range and the directions). For example, the first row of this table specifies that the speed of the car is 2, with 13 range, -1 direction, green color and a truck type. The rows in this table are called the objects, and the columns in this table are called attributes. Condition attributes are the features of a car related to its decision communication; therefore, $C = \{Speed, Range, direction, vehicle\ color, vehicle\ type\}$. Decision communication is the decision attribute; therefore, $D = \{Decision\}$.

To evaluate the ability of our model to learn incrementally, we conducted experiments using 10 objects in different behaviors. Data are divided into two parts: training and testing sets. The very first task is to find reducts and rules. This Data set contains 7 attributes including the decision attribute which may be Yes or No, and there are 100 objects (or) records in this data and with no missing attribute values. The value and meaning of condition and decision attributes is shown in Fig. 4 as true (Yes) class, or false (NO) class.

IV. EXPERIMENT, RESULTS AND DISCUSSION

In the experiment, we have evaluated the data with ROSETTA software. ROSETTA is a toolkit application which allows the analysis of tabular data using the rough sets methodology to implement Johnson’s algorithm rough sets for attribute selection. Rosetta is an open source collection of C++ classes and routines used for data mining and machine learning in general and particularly for rough sets theory [13].

The toolkit follows some important procedures for producing the accurate result.

A. Implementation Process

The steps are: importing data from any valid data source (e.g. Excel format), applying the binary splitting algorithm in the imported data to split the original dataset into training and test data, removing the missing values, and finally applying the reduction and classification algorithms. The reduction algorithm is used to compute the reduct set and the classification algorithm is used to reduct rules and compute the classification result.

The input data set is divided into two parts with the 0.9, 0.8, 0.7, 0.6 and 0.5 split factor. The first part is known as training data set and the other one is known as test data set. The training set was reduced by using Johnson’s reduction algorithm [14], which uses greedy search to find one reduct. In Table I, numbers of reduct sets produced through the application of Johnson’s reduction algorithm are illustrated. The Johnson’s reduction algorithm produced 9 combinations of reduct sets. An example of a rule obtained from reducts is shown in Table I. A full training dataset of each dataset object is used to train the classifiers to build the classification models that were evaluated on the test data of the same objects.

TABLE I. REDUCTS OF THE CAR DATASETS

	Reduct	Support	Length
1	{Speed, Range}	100	2
2	{Speed, vehicle type}	100	2
3	{Speed, direction}	100	2
4	{Range}	100	1
5	{Speed, vehicle color}	100	2
6	{Range, direction}	100	2
7	{direction, vehicle color}	100	2
8	{Speed, vehicle color}	100	2
9	{Range, vehicle color}	100	2

The table shows the average accuracy for the predicted accuracy and the accuracy sensitivity as 50.59% and 65.87%, respectively.

The testing1 is training-testing of 90-10, testing 2 is training-testing of 80-20, testing 3 is training-testing of 70-30, testing 4 is training-testing of 60-40 and testing 5 is training-testing of 50-50. The classification results of original object are shown in Table II.

The reduction rule explains the rule support, stability, length, coverage and accuracy. Each row of the reduction rule is called descriptors (Attribute→ value). The left hand side of the rule is called the antecedent and right hand side of the rule is called consequent. This reduction rule result used in the classification process. This rule is used to make the confusion matrix.

A. Results and Discussion

Table II exhibits the classification accuracy of original object. To find the percentage of accuracy, dataset has been changed as training set and testing set according to the mentioned ratio.

For more evaluation for the model’s capability to learn incrementally, we conducted experiments using different testing types this process was repeated 10 times in different (10 objects) cars. The ten different testing results (classification accuracy) for our model are shown in Table III.

Our model has the capability to learn new objects (cars) from data streams in online environments and can accurately detect the appropriate car to communicate in road traffic. Fig. 5 and 6 show the predicted accuracy and the actual accuracy of our proposed model, respectively. The results suggest that our proposed model can handle the concept of vehicle to vehicle communication in online environments.

TABLE II. CLASSIFICATION RESULTS OF ORIGINAL OBJECT

Data Allocation (%)	The predicted accuracy	The actual accuracy	The overall accuracy
Testing 1	66.67%	40.00%	40.00%
Testing 2	42.86%	50.00%	45.00%
Testing 3	46.15%	66.67%	46.67%
Testing 4	48.48%	85.71%	50.00%
Testing 5	48.78%	86.96%	52.00%
Average	50.59%	65.87%	46.37%

TABLE III. CLASSIFICATION RESULTS OF ORIGINAL TEN OBJECT

	Data Allocation (%)	The predicted accuracy	The actual accuracy	The overall accuracy
Testing Object 1	Testing 1	75.00%	50.00%	60.00%
	Testing 2	50.00%	41.67%	40.00%
	Testing 3	50.00%	58.82%	45.16%
	Testing 4	47.37%	39.13%	41.46%
	Testing 5	33.33%	21.43%	33.33%
	Average	51.14%	42.21%	43.99%

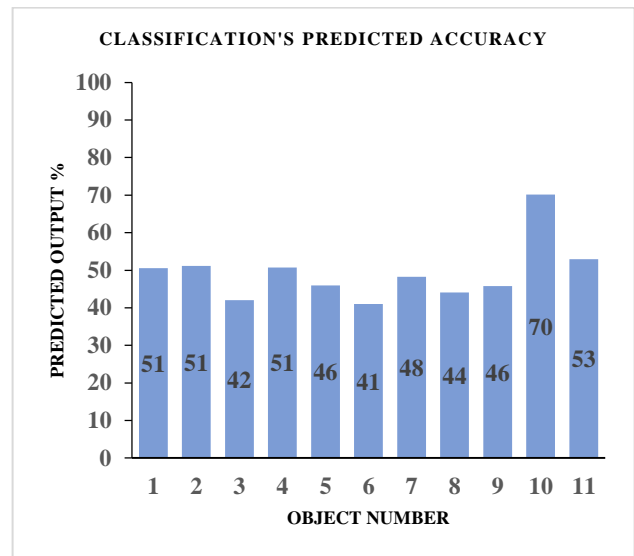


Fig. 5. Classification’s prediction accuracy.

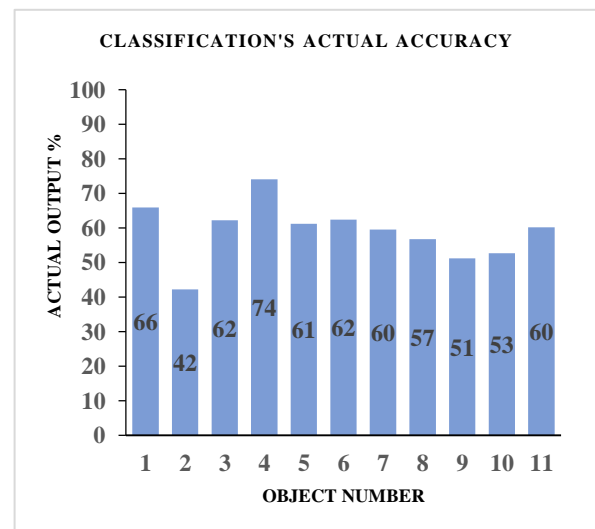


Fig. 6. Classification’s actual accuracy.

Rough sets have been employed here to remove redundant conditional attributes from discrete-valued datasets, while retaining their information content. This approach has been applied to aid classification of online traffic environment, with very promising results.

Using online rough sets in our model allows efficient updates and avoids the process of retaining the whole data, a major disadvantage of offline models, when new data are coming, and it is most helpful when dealing with big data.

Testing Object2	Data Allocation (%)	The predicted accuracy	The actual accuracy	The overall accuracy
	Testing 1	45.95%	70.83%	47.06%
	Testing 2	40.00%	40.00%	40.00%
	Testing 3	42.86%	54.55%	38.10%
	Testing 4	40.91%	69.23%	45.16%
	Testing 5	40.63%	76.47%	43.90%
	Average	42.07%	62.22%	42.84%
Testing Object3	Data Allocation (%)	The predicted accuracy	The actual accuracy	The overall accuracy
	Testing 1	66.67%	80.00%	70.00%
	Testing 2	42.86%	66.67%	47.62%
	Testing 3	47.37%	69.23%	54.84%
	Testing 4	48.15%	76.47%	57.14%
	Testing 5	48.65%	78.26%	53.85%
	Average	50.74%	74.13%	56.69%
Testing Object4	Data Allocation (%)	The predicted accuracy	The actual accuracy	The overall accuracy
	Testing 1	50.00%	66.67%	45.45%
	Testing 2	42.86%	66.67%	47.62%
	Testing 3	40.00%	53.33%	40.63%
	Testing 4	50.00%	61.90%	50.00%
	Testing 5	46.88%	57.69%	46.15%
	Average	45.95%	61.25%	45.97%
Testing Object5	Data Allocation (%)	The predicted accuracy	The actual accuracy	The overall accuracy
	Testing 1	28.57%	40.00%	27.27%
	Testing 2	41.67%	62.50%	52.38%
	Testing 3	47.62%	66.67%	50.00%
	Testing 4	44.83%	72.22%	50.00%
	Testing 5	42.50%	70.83%	43.40%
	Average	41.04%	62.44%	44.61%
Testing Object6	Data Allocation (%)	The predicted accuracy	The actual accuracy	The overall accuracy
	Testing 1	50.00%	33.33%	45.45%
	Testing 2	50.00%	70.00%	52.38%
	Testing 3	50.00%	73.33%	53.13%
	Testing 4	48.00%	57.14%	48.84%
	Testing 5	43.24%	64.00%	43.40%
	Average	48.25%	59.56%	48.64%
Testing Object7	Data Allocation (%)	The predicted accuracy	The actual accuracy	The overall accuracy
	Testing 1	50.00%	50.00%	45.45%
	Testing 2	46.15%	54.55%	45.45%
	Testing 3	45.00%	64.29%	50.00%
	Testing 4	37.50%	50.00%	44.19%
	Testing 5	41.67%	65.22%	46.30%
	Average	44.06%	56.81%	46.28%
Testing Object8	Data Allocation (%)	The predicted accuracy	The actual accuracy	The overall accuracy
	Testing 1	40.00%	28.57%	27.27%
	Testing 2	50.00%	42.86%	36.36%
	Testing 3	45.00%	50.00%	39.39%
	Testing 4	46.43%	61.90%	47.73%
	Testing 5	47.50%	73.08%	48.15%
	Average	45.79%	51.28%	39.78%
Testing Object9	Data Allocation (%)	The predicted accuracy	The actual accuracy	The overall accuracy
	Testing 1	100.00%	55.56%	63.64%
	Testing 2	75.00%	60.00%	59.09%
	Testing 3	66.67%	60.00%	57.58%
	Testing 4	57.14%	48.00%	50.00%
	Testing 5	52.17%	40.00%	47.27%
	Average	70.20%	52.71%	55.52%
Testing Object10	Data Allocation (%)	The predicted accuracy	The actual accuracy	The overall accuracy
	Testing 1	57.14%	66.67%	50.00%
	Testing 2	60.00%	69.23%	50.00%
	Testing 3	50.00%	68.75%	46.67%
	Testing 4	56.00%	60.87%	50.00%
	Testing 5	41.67%	35.71%	36.00%
	Average	52.96%	60.25%	46.53%

V. CONCLUSION AND FUTURE WORKS

Vehicle to vehicle communication has offered several solutions for traffic problems that reduce the danger of collision. This research aimed to design a prototype online rough sets learning in traffic vehicular communication. Optimal communication vehicles were decided by using online learning rough sets to evaluate the percentage of accuracy decision (Yes or No). Generally, online learning data requires an updatable model. That is, the model should in some objects “evolve” in response to the streaming data.

This study presents an incremental learning algorithm which learns new classes in online environments, allowing our model to be updatable and evolve to detect new objects (cars). The model attempts to learn the rules of objects (cars) where the following vehicle notifies the cars.

Our model uses ROSETTA tool in rough sets data analysis to emphasize the classification, in prediction of the learning. Several tests were done by changing the training and the testing dataset ratio. The confusion matrix is used to assess performance of chosen model and classes (Yes or No). The experimental results show that overall accuracy (predicted and actual accuracy) of the object is evolved in our proposed online model.

The limitation of our model is that the run time is not perfect which affects the classification accuracy. More experiments are needed in future.

REFERENCES

- [1] G. Bulumulle and L. Bölöni, “Reducing Side-Sweep Accidents with Vehicle-to-Vehicle Communication,” *J. Sens. Actuator Netw.*, vol. 5, no. 4, p. 19, Dec. 2016.
- [2] M. Kang, P. Bao, and Y. Cai, “Effect of Residential Quarters Opening on Urban Traffic from the View of Mathematical Modeling,” *Open J. Model. Simul.*, vol. 05, no. 01, pp. 59–69, 2017.
- [3] S.-Z. Huang, C.-L. Hu, S. Chen, and L. Guo, “Inter-vehicle Media Distribution for Driving Safety,” in *Advances in Intelligent Information Hiding and Multimedia Signal Processing*, vol. 81, J.-S. Pan, P.-W. Tsai, J. Watada, and L. C. Jain, Eds. Cham: Springer International Publishing, 2018, pp. 121–128.
- [4] A. Bhawiyuga, R. A. Sabriansyah, W. Yahya, and R. E. Putra, “A Wi-Fi based Electronic Road Sign for Enhancing the Awareness of Vehicle Driver,” *J. Phys. Conf. Ser.*, vol. 801, p. 012085, Jan. 2017.
- [5] M. Aggarwal, “Rough Information Set and Its Applications in Decision Making,” *IEEE Trans. Fuzzy Syst.*, vol. 25, no. 2, pp. 265–276, Apr. 2017.
- [6] M. T. Rezvan, A. Z. Hamadani, and S. R. Hejazi, “An exact feature selection algorithm based on rough set theory,” *Complexity*, vol. 20, no. 5, pp. 50–62, May 2015.
- [7] Z. Pawlak, “Rough sets,” *Int. J. Comput. Inf. Sci.*, vol. 11, no. 5, pp. 341–356, Oct. 1982.
- [8] Q. Zhang, Q. Xie, and G. Wang, “A survey on rough set theory and its applications,” *CAAI Trans. Intell. Technol.*, vol. 1, no. 4, pp. 323–333, Oct. 2016.
- [9] S. Eskandari and M. M. Javidi, “Online streaming feature selection using rough sets,” *Int. J. Approx. Reason.*, vol. 69, pp. 35–57, Feb. 2016.
- [10] J. Bai, K. Xia, Y. Lin, and P. Wu, “Attribute Reduction Based on Consistent Covering Rough Set and Its Application,” *Complexity*, vol. 2017, pp. 1–9, 2017.
- [11] H.-S. Chiang and Z.-W. Wu, “Online incremental learning for sleep quality assessment using associative Petri net,” *Appl. Soft Comput.*, Aug. 2017.
- [12] S. Danjuma, T. Herawan, M. A. Ismail, H. Chiroma, A. I. Abubakar, and A. M. Zeki, “A Review on Soft Set-Based Parameter Reduction and Decision Making,” *IEEE Access*, vol. 5, pp. 4671–4689, 2017.
- [13] A. Øhrn, *The ROSETTA C++ Library: Overview of Files and Classes*. 2000.
- [14] X. Li, “Attribute Selection Methods in Rough Set Theory,” San Jose State University, California, 2014.

Permanent Relocation and Self-Route Recovery in Wireless Sensor and Actor Networks

Khalid Mahmood^{1*}, Muhammad Amir Khan¹, Mahmood ul Hassan¹, Ansar Munir Shah¹, Muhammad Kashif Saeed¹

¹Department of Computer Science, IIC University of Technology, Phnom Penh, Kingdom of Cambodia

Abstract—Wireless sensor and actor network's connectivity and coverage plays a significant role in mission-critical applications, whereas sensors and actors respond immediately to the detected events in an organized and coordinated way for an optimum restoration. When one or multiple actors fail, the network becomes disjoint by losing connectivity and coverage; therefore, self-healing algorithm is required to sustain the connectivity and coverage. In this paper two algorithms; *Permanent Relocation Algorithm for Centralized Actor Recovery (PRACAR)* and *Self-Route Recovery Algorithm (SRRA)* for sensors have been proposed for connectivity and coverage. The effectiveness of proposed technique has been proved by realistic simulation results which ensure that our proposed technique better handles the connectivity and coverage.

Keywords—Wireless sensor and actor networks; connectivity restoration; node mobility; route recovery node relocation

I. INTRODUCTION

Wireless sensor and actor networks (WSANs) consist of stationary sensor nodes and some moveable actor nodes [1]. Actor nodes are efficient than the sensor nodes in terms of their resources, including processing capabilities, energy and transmission ranges, etc. These actor nodes collaborate with each other and gather the data from the sensor nodes. For example, sensor nodes can detect the rising temperatures in specific areas in forest and forward this information to actor nodes in the form of packets [2]. The actor nodes correlate sensor nodes information and conclude the explosion of fire, and then actor nodes would stop the unwanted activity by coordinating.

Given the coordinative nature of WSAN activity, the inter-actor nodes connectivity is very important [3]. The failure of the actor nodes may disrupt the network which may block the collaboration among the actor nodes. For example, in environment like battlefield, an actor node may be destroyed by the bomb blast, or in the security applications, an enemy attack may cause some actor nodes out of order instantaneously. Relocation of the survival actor nodes is the best solution to establish the sensor network. The attractive solution depends on the cut-vertex only if, it restores the connectivity of the disjoint network due to the failure of cut-vertex. Additionally, the actor nodes relocation distance must be minimized because more energy consumes during the mobility and this recovery must be self-healing.

In this paper we present two algorithms, namely, Permanent Relocation Algorithm for Centralized Actor Recovery (PRACAR) and Self-Route Recovery Algorithm (SRRA) for the sensor nodes. The Permanent Relocation

Algorithm for Centralized Actor Recovery replaces the failed centralized actor permanently by one of its neighbors and Self-route Recovery Algorithm recovers the optimum route for those sensors whose actor node is permanently relocated to a new position.

The proposed algorithms efficiently overcome the problems faced in existing techniques that are discussed in literature review section. Unlike, existing works that move a large number of nodes to the failed node's position, our proposed technique permanently replaces the failed node's position with its redundant nodes and provides an alternate route to the neighbors of failed node.

The main contribution of our proposed technique summarizes as follows:

- Firstly, Permanent Relocation Algorithm for Centralized Actor Recovery (PRACAR) is proposed to maintain the WSAN connectivity.
- Secondly, Self-Route Recovery Algorithm (SRRA) for the sensor nodes to find an optimal route for the transmission of data.

In the organization of rest of the paper, the next section explains the literature review, Section 3 describes the proposed research methodology, Section 4 explains the realistically simulated results, and Section 5 finally concludes this article.

II. LITERATURE REVIEW

In recent years, many approaches have focused on the restoration of disjoint WSANs network which is caused by the single actor failure. A Distributed Actor Recovery Algorithm (DARA) for WSANs which is based on cascaded movement and two-hop information of neighbors. This algorithm restores the broken WSANs [4]. Unlike DARA, an algorithm is proposed which is based on inward motion, called Recovery through Inward Motion (RIM) [5]. In RIM all the neighbors of the failed node move toward the location of failed node until they all are connected to each other. The individual overhead of the RIM is better than the DARA but the average overhead of the DARA is considered more optimal. A fault-tolerant algorithm is presented in [6], which is based on the multiple sensors to individual actor and multiple actors to individual sensor. This technique is applicable for the event notification in any case of the failure. To minimize latency and increase the lifetime of the sensors, the base-station movement based algorithm is proposed in [7].

In [8], [9], the authors proposed purely reactive algorithms for the restoration of the actor network connectivity. Once the

failure of the actor node is detected, the centralized idea is to replace the failed actor with one of its neighbors or move neighbors inward in the area of failed actor. Normally, this type of recovery processes may causes the breakage/loss of more links, and the process of recovery repeats cascaded movement. Meanwhile, these reactive algorithms require collaboration among the healthy actor nodes. This type of recovery processes normally cause high overhead of messaging. Additionally, these algorithms only consider the single actor node failure considering the efficiency of resources, and do not focus on the recovery time.

The recovery of the WSNs is categorized into two categories; cascaded and block movement recovery. The higher connectivity of the pre-failure for the response coordination is required in the block movement [10]. An algorithm is proposed to maintain the two level connectivity of WSNs even under the node or link failure [11]. A similar idea is proposed by the authors of [12], which also aim to maintain the two level connectivity of the WSNs.

Block movement is often impossible in the absence of the higher connectivity level. Though, a fewer number of researchers focused on the shifted relocation and cascaded movement of the actor nodes [13], [14]. This type of algorithms are based on the shortest path movement. Simply, the cascaded movement idea is similar to RIM and Distributed Connectivity Restoration (DCR). The main objective of these techniques is to reduce the coverage holes which appeared due to the failure of the nodes. Some techniques like Partition Detection and Recovery Algorithm (PADRA) and DARA assume each actor node to maintain the two level connectivity information [10]. Volunteer-instigated Connectivity Restoration (VCR), RIM, and Coverage Conscious Connectivity Restoration (C³R) avoid the two level connectivity information to decrease the overhead and maintain the single level connectivity information [15], [16]. The DARA and the DCR have been proposed to restore the connectivity which occurs due to the failure of the cut-vertex. The PADRA assume dominating set of connection (CDS) for the identification of the cut-vertex while DARA assume to ensure the convergence by considering all multiple network states.

For the critical detection of the node, CDS is not the accurate option; they apply Depth-First Search (DFS) to each node for the detection of the cut-vertex. Simply, a distributed algorithm is used by them, which requires the two level of connectivity information that directly increases the message overhead. Another technique that has been proposed also bases on the two level connectivity information for the detection of cut-vertex. The RCR (Resource Constrained Recovery) algorithm is proposed for the connectivity of restoration for disjoint WSNs which is based on the relay actor nodes [17]. In CBMAR (Connected and Balanced Mobile Actor Relocation) authors proposed to solve the load balance and connectivity problem which is based on the virtual Voronoi architecture of the actors [18]. NSCRA (Node Stability aware Connectivity Restoration Algorithm) technique has been proposed to handle the network partition issue by using efficient energy mechanism in which the selection of the actor for relocation is based on the backup power of the actor nodes [19]. A realistic technique is proposed in [20] to handle the

connectivity restoration in WSNs. This technique is purely based on the path planning algorithm. A novel technique is proposed for the performance improvement in WSNs which is based on the coordination of the actor nodes [21].

The limitations of aforementioned techniques are cascaded and block movement of large number of nodes that result in more power and energy consumption. The proposed technique efficiently overcomes these limitations and provides permanent relocation of nodes to the failed node's position. Moreover, the proposed technique also provides an alternate route for the neighboring nodes of the failed node in order to transmit the important data to the concerned actor node.

III. RESEARCH METHOD

We have the prior information that WSN concludes two types of entities, i.e. sensors and actors. Sensors have relatively low price, extremely restrained in energy consumption and limited computational abilities. On the other hand actors are highly capable of having more onboard energy, good data processing and communication capabilities. Sensor detects the observed phenomena, acquire the information from that phenomena and forwards it to the cluster head actor (which will be referred as CHA here after) for proceedings. Whereas, upon reception of the data from sensors, the actors react to the observed phenomena accordingly as well as at the same time forwards the data to the sink for remote monitoring in mission critical applications.

We take the following set of assumptions in our proposed techniques:

- It has been assumed that sensors and actors have three types of links, i.e. sensor-to-sensor, sensor-to-actor/actor-to-sensor and actor-to-actor. Sensor-to-sensor link can be classified further, i.e. as a routing path, for data transmission from a down-stream node towards the up-stream node by the remote sensors and as a link, used when needed in critical times.
- Sensors are assumed to be stationary and intelligent enough to discover the route for data forwarding in times when needed, whereas actors can move on demand when required.
- The assumed deployment of WSN is shown in the figure A. Generally number of sensors nodes deployed are in abundance as compared to number of actors, where fewer number of actors are deployed. After random deployment of actors and sensors, both of them are assumed to discover each other and form the network as explained in [22].
- Range of communication (r_c) of an actor is the maximum Euclidean distance where its radio coverage can reach.
- Area that an actor can cover and serve is the action range of that actor and is assumed to be same for all actors as addressed in [23].
- It has also been assumed that actors can also find their location comparative to its neighbor utilizing the

onboard GPS by using existing techniques of localizations as explored in [24].

- Each of the actors maintains the list of its neighbors connected to and updates it through the heart beat messages [25].
- Application examples are recon mission in remote deserts and bordering coast areas, surveillance through unattended air-born-vehicles, under water monitoring where unattended water vehicles gather the information from static sensor nodes, which are connected through high speed optical communications to each other.

The problem that we are dealing with in this paper is that of coverage and connectivity in WSAN. We assume the failure of an actor which can cause the network into disjoint segments and can cause two issues that need to be overlooked which are coverage and connectivity.

In this article two algorithms are proposed for WSANs connectivity and coverage. We assume that a scenario as shown in Fig. 1 that there are seven CHA's (A,B,C,D,E,F, and G) and each having its own sensing area. The whole area of interest is covered through these CHA's and their associated sensor nodes. In this scenario the CHA "G" and its surrounding area is considered very important. The failure of "G" can result a huge coverage-hole. To fill this coverage-gap and maintain the inter-actor node connectivity two algorithms are proposed in this section: Virtual-Voronoi based Permanent Relocation Algorithm for Centralized Actor Recovery in WSAN and Self-route Recovery Algorithm to find the optimal path for the sensor node transmission.

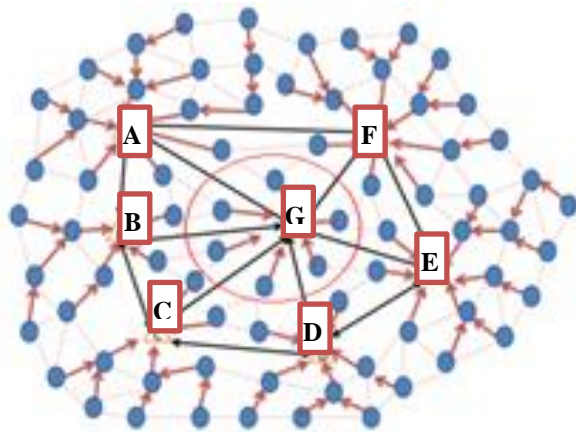


Fig. 1. WSAN Scenario.

A. Permanent Relocation Algorithm for Centralized Actor Recovery (PRACAR) in WSAN

The hybrid technique better suits the time-sensitive applications which are required fast recovery. The proposed model is hybrid because it consists of two algorithms. It is

assumed that CHA "G" failure occurs as shown in Fig. 2. Fast relocation is necessary to maintain the network, therefore, Permanent Relocation Algorithm for Centralized Actor Recovery (PRACAR) starts working and inform all the actor nodes that the failed node is a critical node and fast recovery is needed for the network maintenance. PRACAR then select the best actor node for the recovery process on the basis of shortest-distance, lowest cluster sensors, and lowest coverage area. Every neighbor first calculates the distance from the failed CHA which is based on theorem 1, and then calculates the coverage area which is based on theorem 2, and share these information with neighbor actor along with the number of cluster sensor nodes. Now the WSAN having all the required information for PRACAR and considers that CHA "F" is efficient/optimal for the recovery process, so the "F" relocates failed actor permanently and continue the activity. In this way the WSAN restoration is completed as shown in Fig. 3.

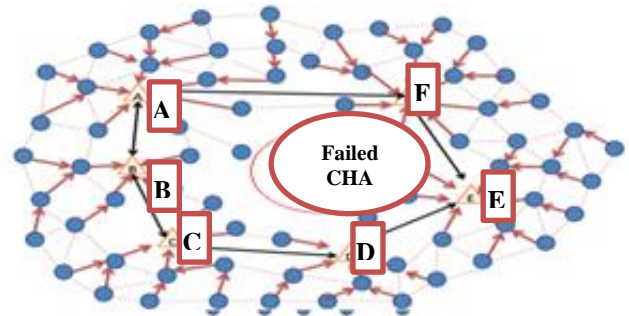


Fig. 2. Shows the Failed CHA "G" Scenario.

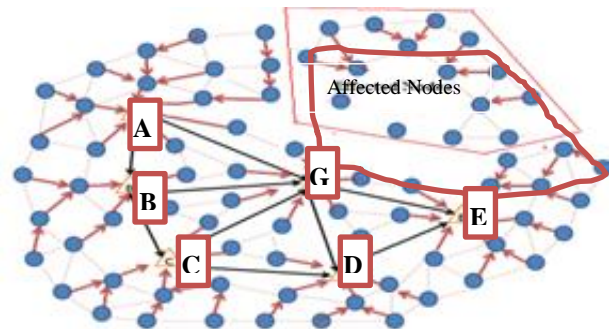


Fig. 3. Shows the Recovered WSAN.

B. Self-Route Recovery Algorithm (SRRA)

After the permanent relocation of CHA "F", its cluster nodes are lack of CHA and these affected nodes need the optimal route. Now SRRA starts working and finds an optimal route for the transmission of data. Firstly, each and every node broadcasts the recovery-packet (RP) and upon receiving of this RP in neighborhood cluster, the nodes acknowledge the message to the effected nodes. So, the affected cluster-nodes now evaluate the relative route distance as explained in theorem 3. Upon the discovery of multiple routes, nodes can select either single optimal route for transmission or multiple routes as shown in Fig. 4.

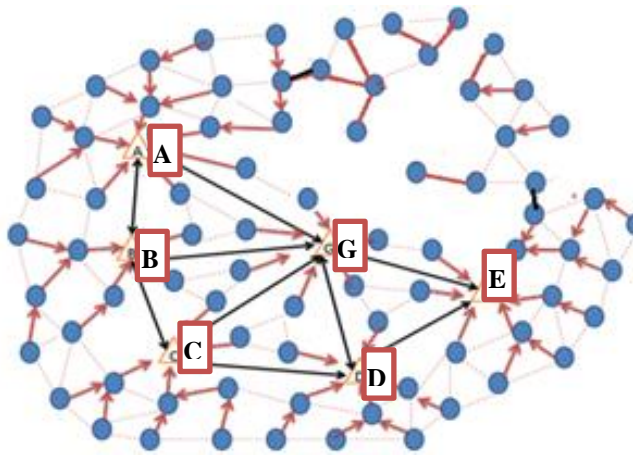


Fig. 4. Self-route established.

C. Theorem 1: Proof/Explanation for Shortest Distance

The recovery CHA synchronizes the concerned CHAs. As the CHA having maximum overlapped area and less number of the cluster-sensors is selected as a recovery CHA. The overlapped area of a CHA is the ratio of area lies within the range of failed CHA and the total area of the survival CHA. Whereas CHAs know their position with respect to its neighbors, estimation the overlapped area based on the communication range of the CHA. Considering the relation between r_c and the proximity of nodes to its neighbors, the intersection between the circles of radii r_c is higher if the distance between the two CHAs is smaller and vice versa. The two CHAs having overlapped area if the distance among CHAs satisfies the following relation:

$$d \leq 2 * r_c \tag{1}$$

As shown in Fig. 5, the overlapped area of two CHAs can be assessed if we calculate the $chord(B)$. If the two CHAs are neighbors, then they can evaluate the “d” between them by using the cosine law.

$$\angle A = 2 \sin^{-1}(d / 2r_c) \tag{2}$$

Then, $chord(B)$ can be found by the sum of angles of the triangle.

$$chord(B) = \frac{B}{\pi} r_c^2 - \frac{d}{2} r_c \sin\left(\frac{B}{2}\right) \tag{3}$$

By using the below formula overlapped ratio can be calculated:

$$Overlapped_{Area} = \frac{2chord(B)}{\pi r_c^2} \tag{4}$$

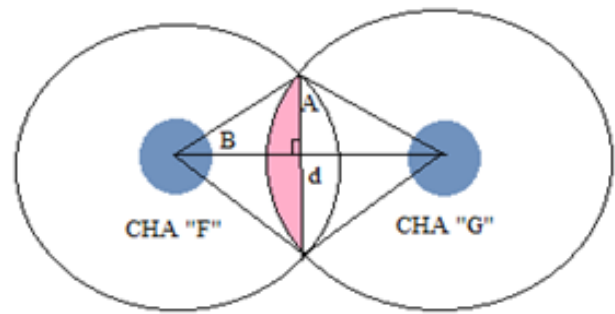


Fig. 5. Calculation of distance between CHAs.

D. Theorem 2: Proof/Explanation for Virtual-Voronoi

Virtual-Voronoi is the major portion which evaluates the optimal CHA in the WSA. After the initial deployment, the critical CHA calculates this information by forming a virtual-Voronoi polygon based on the CHA smaller distance and with smaller coverage area. This calculation is very near to [15].

As every CHA repel each other with a force and the effect of this force is reduced and becomes inverse by the variation of the cluster-sensors. The CHA “F” is considered the optimal according to this theorem because it has smaller distance from critical CHA. So it indicates that “F” having less number of cluster-sensors and smaller area of coverage, that’s why attracted little bit towards critical CHA “G” and considers the optimal CHA.

If $CHA(G) \geq CHA(F)$ then $distance(d_G) \leq distance(d_F)$; where d_G and d_F are the cluster-sensor separation from the CHA.

The CHA is assumed at the center of the cluster, having the CHA “F” with the smaller separation among the cluster-sensor and less number of the cluster-sensors. The smaller number of cluster-sensors is also proved by the smallest distance between the corresponding CHAs. Fig. 6 illustrates the scenario of the Virtual-Voronoi.

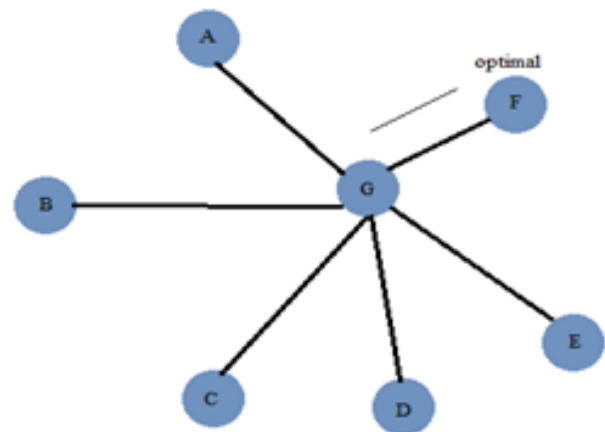


Fig. 6. Virtual-Voronoi polygon.

E. Theorem 3: Self-Route Recovery

Route recovery reduces latency and messaging, and improves the efficiency of energy, connectivity and coverage of the network. For WSANs, recovery of route is normally done using extension of the transmission power or multi-path routing. The estimation of the route process approximates the available path probability and the process of route selection, selects the set of paths that may be used for the routing. Simply, if a sensor detects that there is absence of next hop, then the sensor node increases the power of transmission to extend its range of communication to reach the further nodes. Another technique is recovery of the route by one-hop broadcast. This technique is a normal scheme of recovery that bypasses the faulty sensors or the compromised nodes and uses the information neighbor sensors to develop a new route. Our work assumes that the end cluster-sensor of each CHA lies in the range of the end cluster-sensor of another CHA. But before the relocation of CHA cluster-sensor repels another cluster-sensor as explained in theorem 2.

IV. RESULTS AND ANALYSIS

We have compared our technique with two baseline algorithms DCR and RCR. As without the information of the partition, a centralized technique cannot be the best solution. Hence, we assume that the information of partition with the location of all CHAs is available at critical/centralized CHA. In this section we have discussed the results of our proposed technique PRACAR and the results of baseline techniques (i.e., DCR and RCR). In the experimental simulation, we have generated wireless sensor and actor topologies which consist of varying CHAs. CHAs are randomly deployed in the area of $600\text{ m} \times 600\text{ m}$. We have changed the communication ranges of the CHAs between 50-200 m hence the network becomes very strongly connected. Simulation parameters are shown in Table I.

TABLE I. SIMULATION PARAMETERS

Parameters	Values
Number of nodes	100 – 200
Area	$600 \times 600\text{ m}^2$
Communication range	25 - 200 m

The performance is evaluated by using the following metrics:

- Number of CHAs moved during the process of recovery: this parameter shows the efficiency of the recovery process.
- The number of exchange messages among the CHAs: this parameter tells about the recovery overhead and dissipation of energy.
- Total distance moved by CHAs during the process of recovery: this parameter scales the efficiency of proposed technique in terms of overhead and efficiency of energy.

A. Total Distance Travelled

Fig. 7 and 8 show the total distance moved by CHA until the connectivity restored. The proposed technique PRACAR outperforms significantly because it competes to move only those CHA which having the smaller distance from failed CHA. The performance efficiency of proposed technique remains consistently same even with higher communication ranges and higher densities of CHAs. However, this technique applies self-route only when the CHA permanently relocated. This technique evaluate to minimize the scope by moving the smaller distance CHA because they are even non-critical CHAs having smaller coverage area and less number of cluster-sensors. So, the results show the effectiveness of the proposed technique because by changing communication ranges and number of CHAs, the performance is not affected.

B. Number of CHA Moved

Fig. 9 shows the total number of CHAs that were moved during the process of recovery where proposed and baseline techniques were applied. The graph shows the effectiveness of the proposed technique which moves very less number of CHAs than the baseline approaches. The scope of relocation is limited because the proposed technique avoids the cascaded movements by choosing non-critical CHA that often has smaller coverage area and less number of cluster-sensors.

C. Number of Exchanged Messages

Fig. 10 and 11 show that message overhead is the function of communication range and network size. As the figures show, the proposed technique having very less messaging overhead than the baseline techniques. This is because only optimal CHAs are involved in recovery process, while in baseline algorithms, the messaging overhead is much higher. When the communication range increased then the messaging overhead remains same for proposed technique.

D. Coverage Reduction

Fig. 12 shows the effect of connectivity restoration on the field coverage, and the percentage field coverage reduction measurement. Overall proposed technique having very less coverage loss. In the sparse network coverage overlapped area is very little. The field coverage reduction in case of proposed technique with respect to baseline techniques is very less.

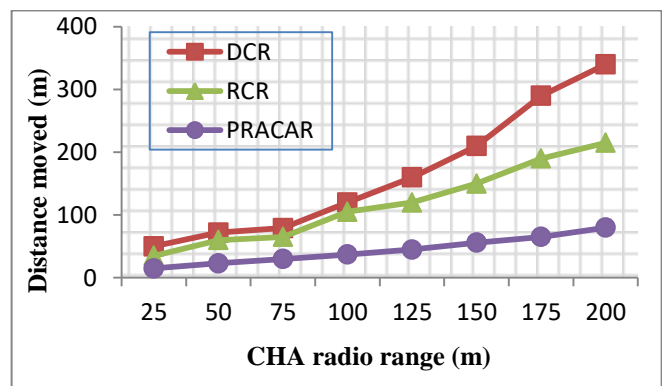


Fig. 7. Total distance moved in recovery against CHA radio range.

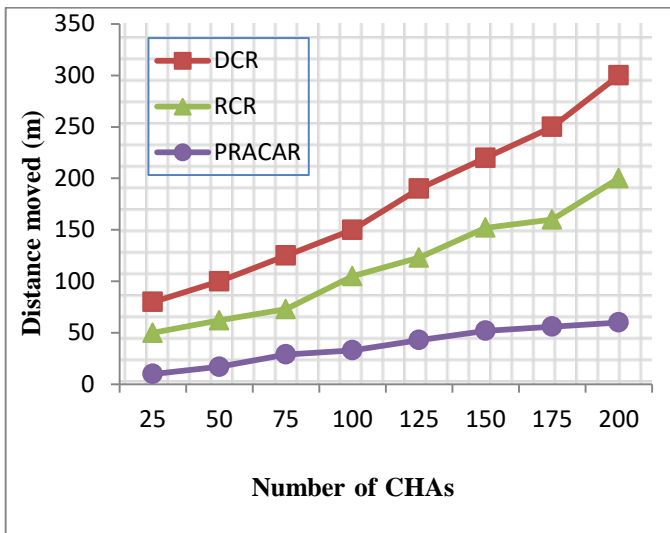


Fig. 8. Total distance moved in recovery against number of CHAs.

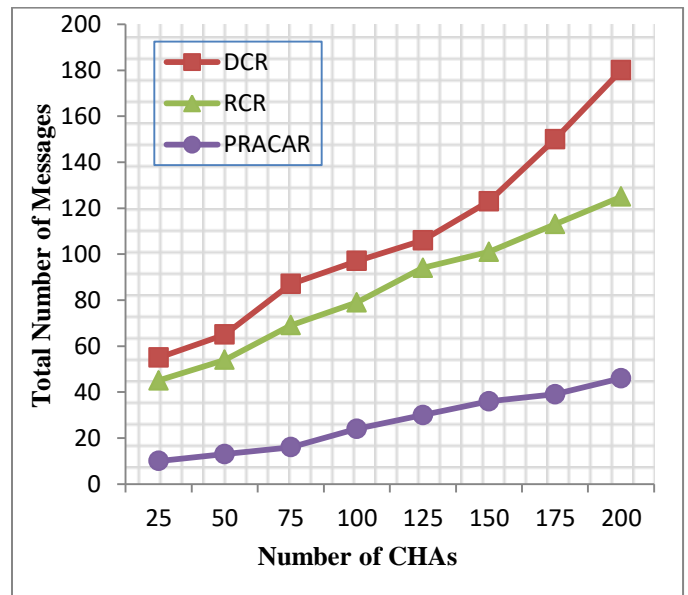


Fig. 11. Messaging overhead against CHAs.

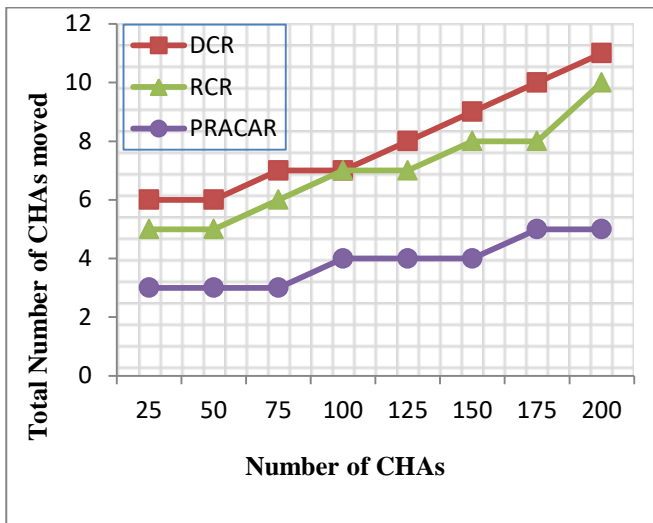


Fig. 9. Total number of CHAs moved.

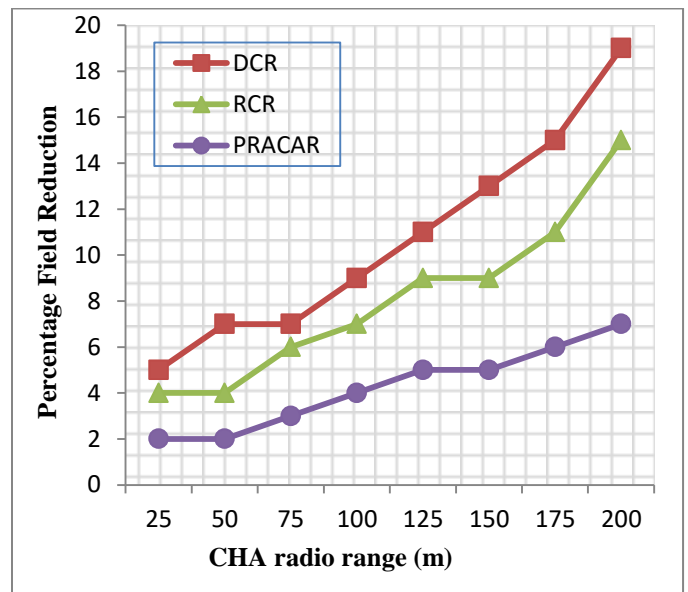


Fig. 12. Percentage reduction in field coverage.

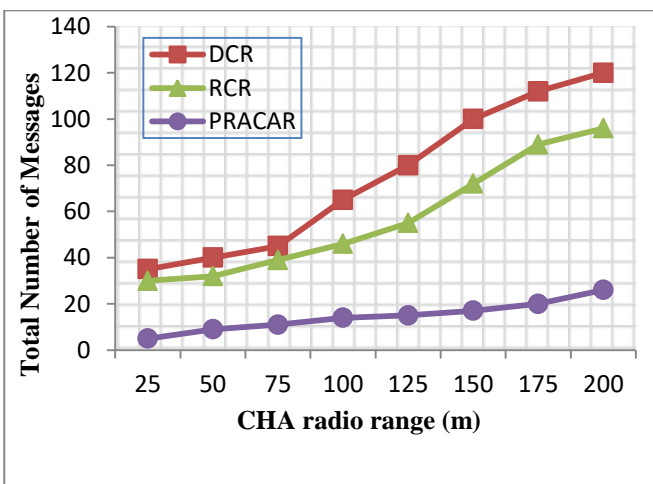


Fig. 10. Message overhead against communication range.

V. CONCLUSION

WSANs started to use mobile sensors (Actors) which improved the flexibility of data collection and maintenance. In this article, we have proposed centralized permanent relocation algorithm for actors and self-route recovery algorithm for sensors. PRACAR attempts permanent relocation in such a way that it reorganizes the WSAN topology and retrieves the strong pre-failure connectivity. In order to recover self-route for sensors after the relocation of actor node, we proposed SRRA. The PRACAR and SRRA have been termed as hybrid-technique that relocates actor for the maintenance of WSANs connectivity and recovers self-route for sensors to maintain the coverage of the WSANs. The experimented simulation results have shown the effectiveness of this proposed technique.

Although, the proposed technique is an efficient technique, but it is designed only for the scenarios where the deployment area contains stationary sensor nodes surrounded by mobile actor nodes. In future, we will consider the scenarios where area of interest will have more mobile sensor and actor nodes. Moreover, we will also provide a routing technique to find an optimal path for routing in wireless sensor network using evolutionary technique i-e genetic algorithm.

ACKNOWLEDGMENT

We would like to express our gratitude to IIC University of Technology, Kingdom of Cambodia for providing us good research environment.

REFERENCES

- [1] Akyildiz et al., "Wireless sensor and actor networks: research challenges." *Ad hoc networks* 2.4 :351-367, 2004.
- [2] Yu et al., "Distributed geographical packet forwarding in wireless sensor and actuator networks-a stochastic optimal control approach." *IET wireless sensor systems* 2.1 : 63-74, 2012.
- [3] Kashi et al. "Connectivity weakness impacts on coordination in wireless sensor and actor networks." *IEEE Communications Surveys & Tutorials* 15.1 : 145-166, 2013.
- [4] Tamboli et al. "Coverage-aware connectivity restoration in mobile sensor networks." *Journal of Network and Computer Applications* 33.4 : 363-374, 2010.
- [5] Abbasi et al. "A survey on clustering algorithms for wireless sensor networks." *Computer communications* 30.14 : 2826-2841, 2007.
- [6] Younis et al., "Strategies and techniques for node placement in wireless sensor networks: A survey." *Ad Hoc Networks* 6.4 : 621-655, 2008.
- [7] Ozaki et al., "A fault-tolerant model of wireless sensor-actor network." *Ninth IEEE International Symposium on Object and Component-Oriented Real-Time Distributed Computing (ISORC'06)*. IEEE, 2006.
- [8] Abbasi et al. "A distributed connectivity restoration algorithm in wireless sensor and actor networks." *32nd IEEE Conference on Local Computer Networks (LCN 2007)*. IEEE, 2007.
- [9] Erupe et al., "Determination of methylamines and trimethylamine-N-oxide in particulate matter by non-suppressed ion chromatography." *Journal of Chromatography A* 1217.13 : 2070-2073, 2010.
- [10] Akkaya, et al. "Distributed recovery of actor failures in wireless sensor and actor networks." *IEEE Wireless Communications and Networking Conference*. IEEE, 2008.
- [11] Akkaya et al., "A survey on routing protocols for wireless sensor networks." *Ad hoc networks* 3.3 : 325-349, 2005.
- [12] Basu et al., "Movement control algorithms for realization of fault-tolerant ad hoc robot networks." *IEEE network* 18.4 : 36-44, 2004.
- [13] Castillo et al., "Implementation of a rule-based routing protocol for wireless sensor networks." *Proceedings of the 2nd ACM workshop on Performance monitoring and measurement of heterogeneous wireless and wired networks*. ACM, 2007.
- [14] Li et al., "SNMS: an intelligent transportation system network architecture based on WSN and P2P network." *The journal of China universities of posts and telecommunications* 14.1 : 65-70, 2007.
- [15] Imran et al., "Partitioning detection and connectivity restoration algorithm for wireless sensor and actor networks." *Embedded and ubiquitous computing (EUC), IEEE/IFIP 8th international conference on*. IEEE, 2010.
- [16] Ahmadi et al., "Channel aware sensor selection in distributed detection systems." *IEEE 10th Workshop on Signal Processing Advances in Wireless Communications*. IEEE, 2009 .
- [17] Joshi et al., "Restoring connectivity in a resource constrained WSN." *Journal of Network and Computer Applications* 66 : 151-165, 2016.
- [18] Wu et al., "Range-Free Mobile Actor Relocation in a Two-Tiered Wireless Sensor and Actor Network." *ACM Transactions on Sensor Networks (TOSN)* 12.2 (2016): 15, 2012.
- [19] Ranga et al., "Node Stability Aware Energy Efficient Single Node Failure Recovery Approach for WSANs." *Malaysian Journal of Computer Science* 29.2, 2016.
- [20] Senturk et al., "Towards realistic connectivity restoration in partitioned mobile sensor networks." *International Journal of Communication Systems* 29.2: 230-250, 2016.
- [21] Khan et al, "Performance Improvement in Wireless Sensor and Actor Networks." *Journal of Applied Environmental and Biological Sciences* 6 : 191-200, 2016.
- [22] Wang et al., "Sensor relocation in mobile sensor networks." *Proceedings IEEE 24th Annual Joint Conference of the IEEE Computer and Communications Societies.. Vol. 4*. IEEE, 2005.
- [23] Liang et al. "A fault tolerant and energy efficient routing protocol for urban sensor networks." *Proceedings of the 2nd international conference on Scalable information systems. ICST (Institute for Computer Sciences, Social-Informatics and Telecommunications Engineering)*, 2007.
- [24] Wang et al., "Movement-assisted sensor deployment." *IEEE Transactions on Mobile Computing* 5.6 : 640-652, 2006.
- [25] Xue et al., "Fault tolerant routing in mobile ad hoc networks." *Wireless Communications and Networking, WCNC , IEEE*. Vol. 2. IEEE, 2003.

Optimization based Approach for Content Distribution in Hybrid Mobile Social Networks

Rizwan Akhtar¹, Imran Memon², Zuhaib Ashfaq Khan³ and Changda Wang^{1,*}

¹School of Computer Science and Communication Engineering
Jiangsu University, Zhenjiang P.R China

²College of Computer Science
Zhejiang University, Hangzhou P.R China

³Department of Electrical Engineering
Comsats Institute of Information Technology, Attock, Pakistan

Abstract—This paper presents the new strategy for smooth content distribution in the mobile social network. We proposed a new method, hybrid mobile social network architecture scheme considered as one node of a social community called social super node with higher capacity provides the services of content distribution. We proposed methods and techniques that are introduced to set the criteria to select a social super node (SSN). The simulation results are carried out to measure the correctness of the network performance of the proposed method. These results indicate that the accessing of those content of nearby social super node instead of the content provider is used to improve overall network performance in terms of content end-to-end delays, delivery ratio, throughput, and cost.

Keywords—Mobile social network; social super node; delays; network performance; end-to-end delays; content delivery

I. INTRODUCTION

The mobile social network (MSN) is a future emerging wireless network that provides the combination of social science with wireless communications for purpose of creating mobile networking. The MSN is kind of network which gives different variety of content delivery services and application while involving the social interest of the mobile users. The technique of social networking has been implemented in the research domain of communication technologies to support efficient data exchange, delivery services and sharing [2]. The mobile social networking can be build on the existing mobile network infrastructure i.e. centralized or distributed. The interdependency of such network devices can be exploited by the use of social network analysis concept to provide a better quality of service (QoS).

Different types of network infrastructures utilize in the MSN for the improvement of the performance of content delivery service in MSN such as cellular and Wi-Fi networks, a delay-tolerant network which include opportunistic networks [4]. Other types are MANETs, disconnected delay-tolerant [6], [8], and wireless sensor networks [11]. Nowadays cellular network is most popular and it can be utilized as a backhaul of the network where MSN can be deployed. The cellular networking is able to provide the network infrastructure that can provide social web-based mobile networking services. In this context Facebook, QQ, Twitter, and MySpace are the commonly available applications. WI-Fi networks are also

supporting the similar services like in cellular networks along with higher content rate but their coverage areas are smaller. In [14] the method of social networking is described to support the teachers to access the desired content through the social network site (SNS) called ‘Facebook’. In this method, the teachers can share their content with their community in six different ways by creating online groups. It gives the evidence from a large, open social teachers online group over the time frame of the 12 week period. The findings indicate that large social online open groups in SNSs are useful for the pragmatic advice for teachers.

Content distribution in the MSN is one of the challenging issues that needs to be addressed due to its sparse connectivity along with resource limitation of the mobile devices. To ensure smooth content distribution among the nodes of the MSN, the new appropriate methods and techniques are required for forwarding the data to nodes and also the links for the purpose of increasing the delivery efficiency and reduces the delay. Furthermore, several important factors those are important for content distribution are mobility, time, bandwidth utilization and along with duration of encounters, a freshness of the content, and message duplication available to the users.

Our major contribution of this work is to improve the network performance in term of increasing the probability of successful content delivery and minimizes the delay. It also includes saving the users cost and lowering the system-wide traffic on the backbone of MSN. We proposed a hybrid infrastructure of MSN for efficient content distribution among the users of a certain social community exploiting the social relationship. We select a social super node (SSN) from the social community users of MSN by setting strategies by considering the fluctuating link quality, closeness centrality, mobility pattern and computing resources. Social super node encounters with the content provider server by accessing the cellular network and broadcast to all the users of a certain social community.

This manuscript is organized as follows. Section II explains some related approaches. In Section III we present the analytical model of our scheme. Section IV details our social super node strategies. Section V describes simulation

results. Section VI concludes the research. Lastly, Section VII Presents the future research direction of the MSN.

II. RELATED WORK

The approaches that mainly based on social network analysis such as degree centralities, tie strength, a distance of the links and the node, and mobility pattern is implemented to distribute the data efficiently among the social nodes of the MSN. The affect of the social patterns not only influence the node's interest but their willingness as well (i.e., selfish behavior) for sharing their content [10]. In [1] Peer-to-peer streaming is proposed to enable end-to-end users to communicate and utilize the available resources in the network to share video content. In [3], the time duration of the contact and the frequency of the social pattern (called tie strength) has been used to recognize the contact pattern of the mobile nodes to create a opportunistic contacts social group. In [4], the concept based on flooding is given to distribute the content in the detected social community. However, in such scheme, the flooding message incurs a high volume of the data traffic on the network, which unnecessarily consumes energy, bandwidth usage, and also memory.

In [5] the method of distributed buffer storage in MSN is implemented. Based on such method, a novel solution for the intermittently connected MSN with distributed aid storage for fast and reliable end-to-end content delivery is presented. They proposed an architecture of MSN that is able to offer fast delivery services with the help of distributing buffer storage at the edge of the MSN. It was the attempt to give the solution for connected MSN in the situation, where an offered content rate is higher than the processing content rate of the mobile devices having limited buffer storage. The contribution of that research work is the suppression of information congestion before it occurs by utilizing an extra buffer storage on the access of MSN.

In [12], an algorithm called SMDRA (simple message duplication reduction algorithm) is proposed. This algorithm uses the property of mobility predictability. The limitation of such algorithm is that it incurs larger memory usage, this because it uses graphs pattern to store the desired information related to nodes and edges. In [7], the performance of hierarchical super-node overlays under different configurations is investigated. The configuration parameters include super-node neighbor number (out degree), super node redundancy and request TTL (time to live). In [1], another aspect of the super-node selection for file sharing and streaming application is discussed. The authors developed theoretical methodologies for a super-node selection schemes.

In the work proposed by Nazir et al. [2] describe that the mobility patterns of the nodes can be predicted if both the record of the time and duration of encounters are maintained. Such information is also beneficial to improve the content delivery ratio. In [8], Costa et al. Present social cast for efficient message routing for publish and subscribe given network by the help of co-location and movement patterns of the nodes mobility pattern together with co-location metric can be utilize to predict the nodes availability so that the appropriate node for forwarding can be selected for content dissemination. In [9], a scheme to direct unconnected social

nodes toward connecting mobile social nodes of the social community is proposed. The connected nodes communicate with the main server via a base station, the unconnected nodes can use these connected users to build a relay to obtain connectivity. In [13], an optimized solution based on the content update is proposed. In order to distribute new arrival content as fresh as possible from the server (content provider) to the mobile users.

All the above work are proposed to solve the problems related to content distribution in the MSN. But none of the approach was given for the in shape of the super social node (SSN) across MSN to distribute the content efficiently. Our proposed network architecture is the attempt to fill research gape by taking advantage of the declaring one node as a social super node from the certain social communities.

III. PROPOSED MSN ARCHITECTURE

Our proposed scheme is based on a hybrid architecture of MSN that utilizes social super node as an intelligent agent for sharing the content by exploiting the social relationship among users. Since our scheme is based on hybrid infrastructure of the MSN that involve both cellular network and ad hoc network. Hybrid MSN guarantee the performance of content delivery and can reduce the network cost.

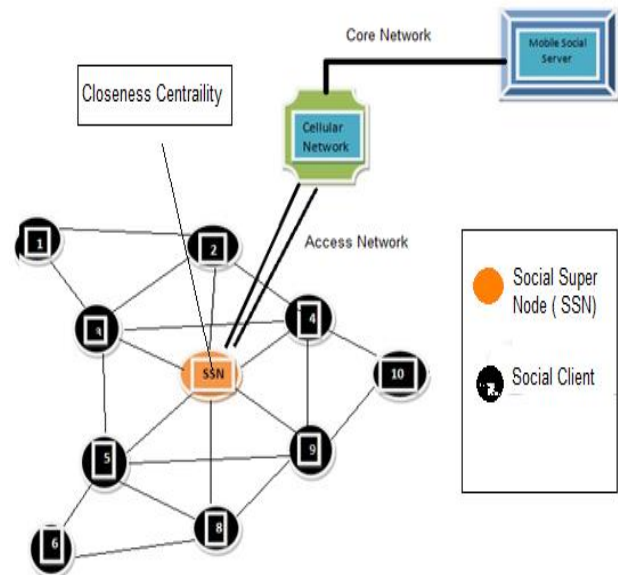


Fig. 1. Social super node of MSN.

In Fig. 1 content provider services declare one node as an SSN on the basis of assumptions in term of a Node, closeness and degree centrality, physical location and storage capacity of the single social community.

In this scheme SSN selection of the P2P applications is designed to work in backbone networks; SSN is selected to active for a certain period of time to get the content and distribute to the MSN users. Fig. 2 shows there can be multiple communities under base stations of the cellular network. Every community has its own social super node (Table I).

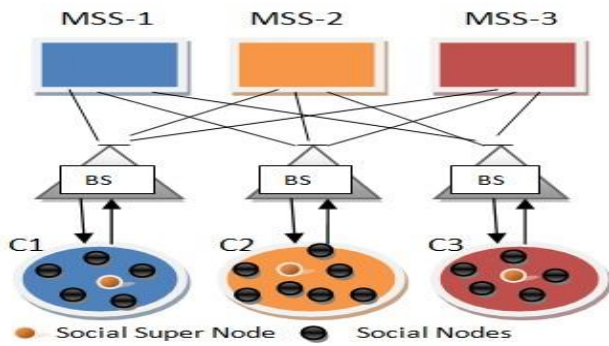


Fig. 2. Multiple social communities.

TABLE I. BINDING TABLE FOR SSN

Social Super Node ID	IP Addresses	Community ID
2	192.168.2.0	C1
6	192.168.5.71	C2
7	192.168.5.111	C3
3	192.168.4.42	C4

MSS is the mobile social server and C is a social community. The main contribution of this paper is to define efficient and simple strategies for social super node admission, adapted to wireless ad-hoc network conditions of mobile social network.

IV. SOCIAL SUPER NODE SELECTION

A social super node can be selected from social community nodes on the assumption of closeness and degree centrality, tie strength, similarity and physical location of the node. The SSN must have higher storage capacity, processing power and energy. The selected SSN of the community can announce it to all associated nodes about its status by broadcasting or MSN server can send a contact message to all the associated node of community and provide information about SSN. Algorithm 1 explains our proposed scheme.

Algorithm 1: Selection / Re-selection of Social Super Node

```

Input N, C // N is number of nodes and C is the social
community
Input  $\mu, \alpha$  //  $\mu$  is processing rate of SSN and  $\alpha$  is arrival
rate
Output SSN // Selecting Social Super Node
Begin
N  $\leftarrow$  C
SSN  $\leftarrow$  N
SSN  $\leftarrow$  C
If (TTL N = 2-hop count && distance L= threshold)
// distance of node N with other nodes
Equation  $L_i = \sum_j q_{ij} L_{ij}$ 
If ( $N\mu \geq N\alpha$ ) // processing rate is greater than arrival rate
of Node N
Equation  $\pi_j = C\alpha^i = \frac{1-\alpha}{1-\alpha^{j+1}} \alpha^i \approx (1-\alpha)\alpha^i$ 
Return N = SSN1 // social node N is set as Social super
node 1
If (TTL N = 2-hop count && distance L= threshold &&  $N\mu \leq N\alpha$ )

```

```

Return N2 = SSN 2 // Set another node N as SSN2
to share the traffic load
End If
End If
End If
End Begin

```

In case of failure of a selected social super node because of overloading, long distance or weak tie strength, MSN server can select another better-positioned node of the community by the assumption of physical location and distance to all the associated nodes and past history of mobility area. MSN services can keep track the social super node and its associated social clients via a cellular system. In case of any social node moves out of the community radio range the MSN server can request them to move back to the community range.

The distance between social super nodes and its node can be calculated as

$$L_i = \sum_j q_{ij} L_{ij} \quad (1)$$

In our system, each super social node of every community C determines its mean distance to its node. Let L_{ij} denote the number of physical hops between SN_i and its j -th node. Then, the mean hop number between the social super node and its node is denoted by L_i , can be calculated based on the distance and the hit rate of each node To calculate L_i , each Social super node estimates q_{ij} for each node j , as follows:

$$q_{ij} = \frac{NQ_{ij}}{NQ_i} \quad (2)$$

NQ_i is Total number of queries received in by SSN and NQ_{ij} is Number of queries with j as the MSN server.

In case if the current SSN is far from its community nodes, the admission strategy should seek to replace Selected SSN with a better positioned social super node as SSN-2.

The selected social super node becomes overloaded in a situation where arrival content rate is much higher than the processing rate of super node. The probability of buffer overloaded with its size J of a SSN can be calculated as

$$\pi_i = C\alpha^i \quad (3)$$

Where c is the constant value, and α is the exponential controlling the stability margin of the buffer content queue

$$\lambda(1-\mu)\pi_j = \mu(1-\lambda)\pi_{j+1} \quad (4)$$

λ is arrival probability with arrival rate, μ is departure probability with departure rate and π is limiting distribution

$$\alpha = \frac{\lambda(1-\mu)}{(\mu(1-\lambda))} \quad \text{and} \quad C = \frac{1-\alpha}{1-\alpha^{j+1}}$$

Using (3) we get

$$\pi_j = C\alpha^i = \frac{1-\alpha}{1-\alpha^{j+1}} \alpha^i \approx (1-\alpha)\alpha^i \quad (5)$$

Equation (5) shows that if the value of alpha (Arrival content) is larger, it can be prone to have more contents in the queue and thus SSN can be in the overloaded state.

We assume that the SSN has 100 KB of the buffer with size J and arrival content rate (AR) at SSN via MSN server is at very high than processing rate. We found out the number of times a buffer overflow occurs for a particular time span of 2000 seconds when the same experiment is conducted 100 times at SSN of MSN. The SSN can be overloaded by considering content rate $\lambda = 0.43\text{KB}$ while processing rate (PR) of contents $\mu = 0.40\text{KB}$ on the fixed buffer J of the mobile node of 100 KB. By the help of the probabilistic model, we found out the number of overflows incur for an experiment that is repeated for 100 times across the super social node of MSN. The results show that buffer J overflow occurred 34, 55 and 73 times out of 100 experiments in the conditions when offered content rate is greater, equal and less than the processing rate of the contents. In Fig. 3 red color curve indicates that SSN is in the overloaded state. Whenever an overloaded state is achieved by SSN the admission strategy should seek for the associated social super node as an Assistant Social Super Node (ASSN) for the purpose of sharing loads of the content and can control the arrival traffic rate from the MSN server.

Closeness centrality measures the shortest distance to the entire nodes, whereas degree centrality measures the most direct connections to all nodes of MSN. These two social metrics are also based on the quality of links between nodes, So a selection of SSN also depends on these two social matrices. The best candidate among nodes for the selection of SSN is one who has the shortest distance and most direct connection with all the associated nodes of social community.

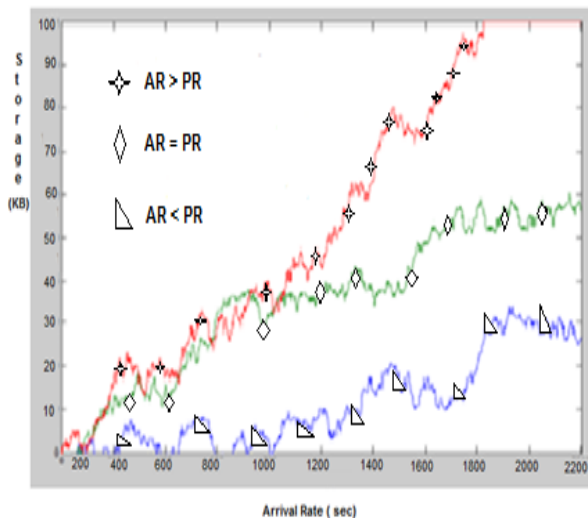


Fig. 3. Curve of overloaded social super node.

V. PERFORMANCE EVALUATION

In this section, the simulation results are conducted by using NS-2 to evaluate our proposed scheme for efficient content distribution. In the simulation scenario, we have taken several mobile social nodes and declare one social node from the social community as social super node (SSN) for

experiments, a SSN encounter with the mobile social server via cellular network and share the content of all connected friends (nodes) by direct link along with multi-hop connectivity.

Simulation results leverage network performance can be significantly improved if the nodes of the social community can have fresh content from the nearby super node to access instead of content provider at the core of networking. Table II summarizes the parameters used in the simulations.

TABLE II. SYSTEM PARAMETERS FOR SIMULATIONS

Parameters	Values
Number of server	1 or 2.... N
Number of nodes	1,30,50,100
Distance	10-50 km/h
Simulation time	36 hours
Bandwidth/good put	3 Mbit/s
3G bandwidth/good put	200 kbit/s
Nodes access network bandwidth	10 Mbit/s
Content sizes	1, 20, 40,60 MB
Content popularity	0.1 to 1.0
Latency (deferred transmission)	0, 10, 50, 80, 150,300, 600, 1800, 2200 s

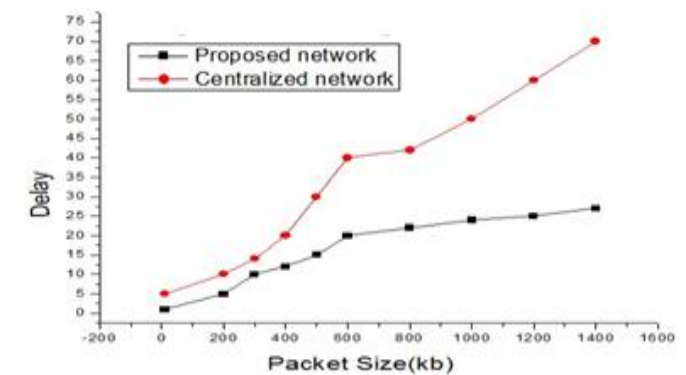
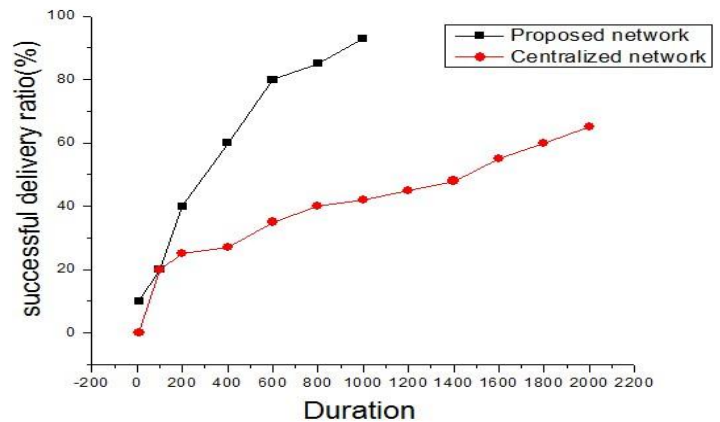


Fig. 4. Successful delivery ratio and delay.

Fig. 4 shows the comparison between the content accessed from source available on access closer to the user with the content access by users from core network by accessing the main social server. Fig. 3 demonstrate that by accessing the content locally from SSN of MSN can increase the successful delivery ratio and reduce the delay.

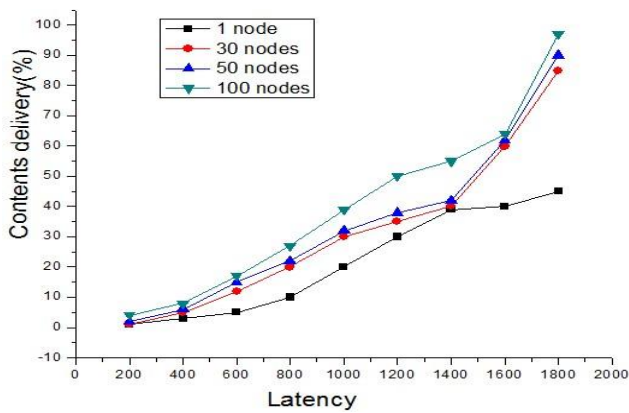


Fig. 5. Latency.

Fig. 5 shows that if nodes access the content of the local SSN would have better latency with a high probability of delivery ratio and lower the delays.

VI. CONCLUSION

We present the new strategy for smooth content distribution in mobile social network. We proposed a new method, hybrid mobile social network architecture scheme considered as one node of social community called social super node with higher capacity provide the services of content distribution. In this method, techniques are introduced to set the criteria to select a social super node. Our major contribution of this work is to improve the network performance in term of increasing the probability of successful content delivery and minimizes the delay. It also includes saving the users cost and lowering the system wide traffic on the backbone of MSN.

VII. FUTURE WORK

Although some challenges in the MSN are identified in this research paper, there are still many problems remaining that need to be addressed. Also, there exist many opportunities to improve the effectiveness and efficiency of the MSN. In this section, some of the future possible research recommendations are presented from the perspective of protocol and architecture design in the MSN.

Interoperability is now an important issue because multiple MSN want to communicate at the same with each other. For routing standard protocol, interfaces for exchanging information and signaling of social-based relationship and content delivery among different MSN may be required that can ensure seamless applications. The standard protocols can be useful for data distribution and context awareness and secrecy in the MSNs. Also, the interoperability among mobile users and desktop platforms is an important factor.

Bandwidth allocation within the MSN can be optimized for achieving the best performances. However, the impact of mobile social network of exporting social relationship within

the radio resources management of several wireless systems has not been yet investigated. In addition, some of the existing optimization formulations ignore the QoS of the MSN applications. Due to the absence of centralized control, radio resources management and also the QoS support are coming more challenging in the distributed architecture of the MSN.

ACKNOWLEDGMENT

This work was supported by the National Science Foundation of China under grant 61672269 and the Jiangsu Provincial Science and Technology Project under grant BA2015161.

REFERENCES

- [1] Adler M, Kumar R, Ross KW, Rubenstein D, Suel T, Yao DD (2005) Optimal peer selection for P2P downloading and streaming. In: Proceeding of 24th annual joint conference of the IEEE computer and communications societies (INFOCOM), vol 3, pp 1538–1549
- [2] F. Nazir, J. Ma, and A. Seneviratne, Time critical content delivery using predictable patterns in mobile social networks, in Proc. Int. Conf. Comput. Sci. Eng., Aug. 2009, vol. 4, pp. 1066–1073
- [3] R. Cabaniss, S. Madria, G. Rush, A. Trotta, and S. S. Vulli, Dynamic social grouping based routing in a mobile ad-hoc network, in Proc. 11th Int. Conf. Mobile Data Manage., May 23–26, 2010, pp. 295–296
- [4] E. Yoneki, P. Hui, S. Chan, and J. Crowcroft, A socio-aware overlay for publish/subscribe communication in delay tolerant networks, in Proc. ACM Symp. Model. Anal. Simul. Wireless Mobile Syst., Oct. 2007, pp. 225–234
- [5] Akhtar R, Leng S, Memon I, et al. Architecture of hybrid mobile social networks for efficient content delivery[J]. Wireless Personal Communications, 2015, 80(1): 85-96.
- [6] E. M. Daly and M. Haahr, Social network analysis for routing in disconnected delay-tolerant manets, in Proc. ACM Int. Symp. Mobile Ad Hoc Netw. Comput., Sep. 2007, pp. 32–40
- [7] Yang B, Garcia-Molina H (2003) Designing a super-peer network. In: Proceeding of 19th International Conference on Data Engineering (ICDE). Bangalore, India, pp 49–60
- [8] P. Costa, C. Mascolo, M. Musolesi, and G. P. Picco, Socially-aware routing for publish-subscribe in delay-tolerant mobile ad hoc networks, IEEE J. Sel. Areas Commun., vol. 26, no. 5, Jun. 2008, pp. 748–760
- [9] B. Chelly and N. Malouch, Movement and connectivity algorithms for location-based mobile social networks, in Proc. IEEE Int. Conf. Wireless Mobile Comput. Netw. Commun., Oct. 2008, pp. 190–195
- [10] K. Kwong, A. Chaintreau, and R. Guerin, Quantifying content consistency improvements through opportunistic contacts, in Proc. 4th ACM Workshop Challenged Netw., Sep. 25, 2009, DOI: 10.1145/1614222.1614230.
- [11] E. Miluzzo, N. D. Lane, K. Fodor, R. Peterson, H. Lu, M. Musolesi, S. B. Eisenman, X. Zheng, and A. T. Campbell, BSensing meets mobile social networks: The design, implementation and evaluation of the CenceMe application, in Proc. ACM Conf. Embedded Netw. Sensor Syst., Apr. 2008, pp. 337–350
- [12] K. Kawarabayashi, F. Nazir, and H. Prendinger, Message duplication reduction in dense mobile social networks, in Proc. 19th Int. Conf. Comput. Commun. Netw., Aug. 2–5, 2010, DOI: 10.1109/ICCCN.2010.5560124
- [13] S. Ioannidis, A. Chaintreau, and L. Massoulie, Optimal and scalable distribution of content updates over a mobile social network, in Proc. IEEE Int. Conf. Comput. Commun., Apr. 2009, pp. 1422–1430
- [14] Kelly, N.; Antonio, A. (2016). "Teacher peer support in social network sites.". *Teaching and Teacher Education*. **56** (1): 2016 138-149. doi:10.1016/j.tate.2016.02.007.

Distributed Energy Efficient Node Relocation Algorithm (DEENR)

Mahmood ul Hassan¹, Muhammad Amir Khan², Shahzad Ali³, Khalid Mahmood¹, Ansar Munir Shah¹

¹Department of Computer Science IIC University of Technology, Cambodia

²Department of Information Systems, King Khalid University, Abha, Kingdom of Saudi Arabia

³Department of Computer Science, Al Jouf University, Tabarjal, Kingdom of Saudi Arabia

Abstract—Wireless Sensor Networks (WSNs) due to their inherent features are vulnerable to single or multiple sensor node failure. Node's failure can result in partitioning of the networks resulting in loss of inter-node connectivity and eventually compromising the operation of the sensor network. The recovery from partitioning of network is crucial for inter-node connectivity. In literature, a number of approaches have been proposed for the restoration of inter-node connectivity. There is a need for a distributed approach that has an energy efficient operation as energy is a scarce resource. By keeping this in mind we propose a novel technique to restore the connectivity that is distributed and energy efficient. The effectiveness of the proposed technique is proven by extensive simulations. The simulation results show that the proposed technique is efficient and capable of restoring network connectivity by using the mechanisms for improving the coverage.

Keywords—Wireless sensor network; node failure; network connectivity

I. INTRODUCTION

In recent years, a number of applications have gained interest in wireless sensor networks for the fact that they are applicable in harsh environments predominantly in the setup of hostile applications, such as reconnaissance of the battlefield, surveillance of coast and border, rescue and search, outer space, and deep ocean exploration [1]. Mainly, wireless sensor nodes are used for monitoring in the areas of health, residential, and military purposes since they are self-healing, self-organized, and fault tolerant. In the application for military, WSNs are widely used and apt to different tasks such as command and control, targeting, communication, and surveillance [2].

Wireless sensor nodes are small, having limited computing and processing power. Each node can be equipped with one or multiple sensors. A variety of magnetic, chemical, thermal, optical, biological and mechanical sensors could be combined to the wireless sensor nodes to measure the properties of the environment [2]. These sensors can measure, sense and collect data from the environment and they can also broadcast the sensed data to the manipulator. These nodes comprise a power supply, an actuator, memory, processing unit, and radio transceivers. Typically, wireless sensor nodes are deployed in hard-to-access areas where human intervention is difficult or not possible. As the sensor nodes are generally cheap therefore they have very limited memory, limited power source and a transceiver for sending and receiving data. The central power source of sensor node is the battery. A secondary power

source that gathers energy from the external environment could be added such as solar cell, depending on the sensor nodes and the type of application [3].

The topology of network, scheme of deployment, and the size of the network is affected by monitoring environment. In an indoor environment, less number of nodes can be deployed and a pre-planned network can be initiated. When the sensor nodes need to be deployed in a large area in open then pre-planned network is not ideal. For a large area in open, a large number of sensor nodes should be deployed for making sure that the whole area is covered [4]-[6]. Increasing the number of nodes in an area can also improve the reliability of collected information. WSNs can be deployed in the areas where it is humanly impossible to go therefore they can reduce the risks associated to human life. Once the nodes in a sensor network are deployed, these nodes establish a network to coordinate their actions and share information while performing the assigned task. Normally in all of these activities, sensor nodes need to collaborate with each other for optimizing the performance and increasing the network lifetime. Over time, the battery of the sensor nodes is depleted due to communication and processing. It is of immense importance that the nodes distribute the tasks of communication and processing among themselves in such a way that the total lifetime of the network extends to the maximum. As the nodes in a network start to die, the connectivity of nodes is affected. Inter-node connectivity is very important in sensor networks because dis-connectivity among nodes may lead to loss of important data to be communicated with the user terminal. In case of dis-connectivity among nodes, a sensor node first need to detect a node that failed/died in its vicinity and typically have to notify its neighboring node to reposition itself in such a way that the nodes become connected again [7]. However, nodes in the network may die at any time due to depleted batteries or physical impairments produced by an unfriendly environment in which WSNs operate in.

The failed node could disturb the connectivity of network and disorder the collected sensed information. In the worst case the network could be separated into numerous segments or partitions as well as the information flow from sensor nodes to the user terminal can be completely cut-off. In order to avoid this scenario, the connectivity of network should be restored. Quick recovery of connectivity is necessary in order to maintain the network to observe activity. Deploying redundant nodes instead of dead nodes is a slow process and is

repeatedly impossible in harsh and environmentally challenging areas. Therefore, the healing process should be self-organized comprising of the existing alive nodes. Provided the unsupervised and autonomous supervision of WSN allows the failure that could be recovered in a categorized way. In addition, overhead of sensor nodes should be minimized in order to meet with the resource constraints. A number of approaches have preferred the repositioning of survivor node for the recovery of the partitioned network [8], [9]. However, these works have focused on recovery of inter-node connectivity except for observing the unfavorable effects of repositioning nodes on the network coverage and energy consumption. Primarily, it depends upon sensing and communication ranges, along with the deployment of redundant nodes. Formerly proposed algorithms for connectivity restoration may exclude several segments of the examined area uncovered by any node. Though coverage is a vital design parameter for sensor networks, connectivity together with coverage can be further utilized to evaluate the quality of service of WSN [10]. Certainly, connectivity and coverage have to be considered in an integrated manner. In this work, we present a distributed energy efficient node relocation algorithm that is capable of recovering the network from node failure.

The rest of the paper is organized as follows. Section II explains the related work and Section III explains the proposed algorithm. In Section IV, simulation results are presented and Section V presents the discussion. Subsequently Section VI concludes this paper.

II. RELATED WORK

The relocation of wireless sensor nodes is thoroughly studied in [11]. Some algorithms allow movement on-demand while others allow post-deployment movement. In hostile environments, designers cannot place the node in most effective areas by hand. Nodes are randomly deployed by aerial deployment. Some areas may receive a dense amount of nodes while some areas may remain vacant. As a result, nodes are deployed inefficiently and nodes relocation or deploying more nodes might be considered.

A number of approaches have only focused on the connectivity aspect. Different techniques are proposed to maximize nodes coverage without affecting connectivity. In [16] the authors proposed a distributed algorithm capable of restoring network connectivity in case of node failure. The mobility of nodes is exploited and for the better coverage of area, the repelling forces idea is proposed among. However, the technique does not restore network disjoint issues originated by failed nodes. In robot networks, a similar technique is studied for the maintenance of connectivity [12]. The 2-connected network concept is used which means that there should be minimum of two pathways among each pair of nodes. The objective of this technique is to achieve a 2-degree of connectivity in case of a node failure. In this technique, a pair of sensor nodes is moved in such a way that 2-connectivity is restored in case of a failure of a node. The techniques that resemble our work are explained below. C^2AP is a technique that considers post-deployment coverage and connectivity and increases coverage by spreading inter-

connected nodes [13]. A hierarchical architecture is proposed in COCOLA [14], where coverage is maximized without forwarding data path to 1-tier node by the incremental relocation of higher-tier nodes. Neither C^2AP nor COCOLA deals with the implications related to failed nodes.

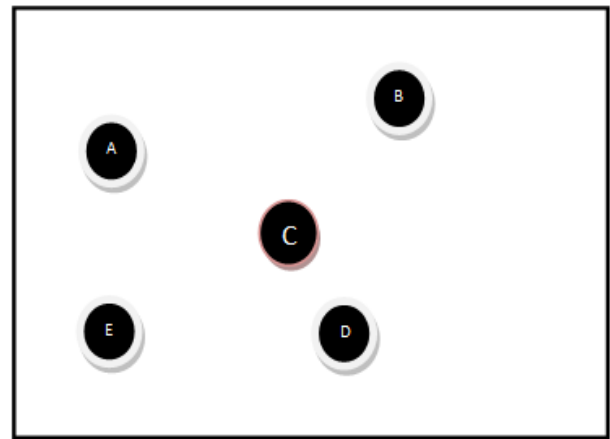
In [15], a cascaded movement technique is proposed for the recovery of node failure. In this technique, a failed node is replaced with the nearby node, which is then replaced by another node and this process continues until reaching to a redundant node. The techniques more related to our work are C^3R [18], RIM [16] and AUR [19]. C^3R assumes single or multiple neighbor nodes failure. The failed node is substituted by each neighbor node temporarily and gets back to its original position after spending limited time at a new location. Another approach named DARA [17] considers a probability scheme for the identification of cut vertices and selects a neighbor node to the failed node for relocation based on the number of communication links. In [16], a multimode repositioning technique called RIM (Recovery by Inward Motion) is considered in which all the neighbor nodes of a failed node temporary relocate it. RIM requires just 1-hop information. It is a scheme based on localized information about the neighbors. The main idea is to move the neighbors of a failed node inward towards the position of the failed node so that they would be able to reach each other. The main idea is that these neighbors are the ones directly impacted by the failure, and when they can reach each other again, the network connectivity would be restored to its pre-failure status. The relocation procedure is recursively applied to handle any node that gets disconnected due to the movement of one of their. RIM is known for its simplicity and effectiveness. However, the main drawback of RIM is that under higher node densities it tends to move many nodes and increases the total travel overhead on the network. Moreover, it is not very effective in case of multi-node failure.

In [19], the authors proposed a new approach called Autonomous Repair (AuR). AuR is based on repositioning of nodes towards the center of the deployment area. The design principle of AuR is based on modeling connectivity between neighboring nodes as a modified electrostatic interaction based on Coulomb's law between charges. In AuR, the recovery is based on the nodes having only localized information about the immediate neighbors. The neighbors of the failed nodes detect the failed nodes and lead the recovery process by spreading out towards the lost nodes, causing the intra-segment topology to be stretched. If connectivity is not restored, the segment is then moved as a block towards the center of the deployment area. Moving all segments towards the center will increase the node density in the vicinity of the center point and ensures that the connectivity gets reestablished. However, none of the above mentioned works considers connectivity, coverage, and energy efficiency collectively. Our work addresses connectivity restoration, better coverage, and efficient use of energy in an integrated manner.

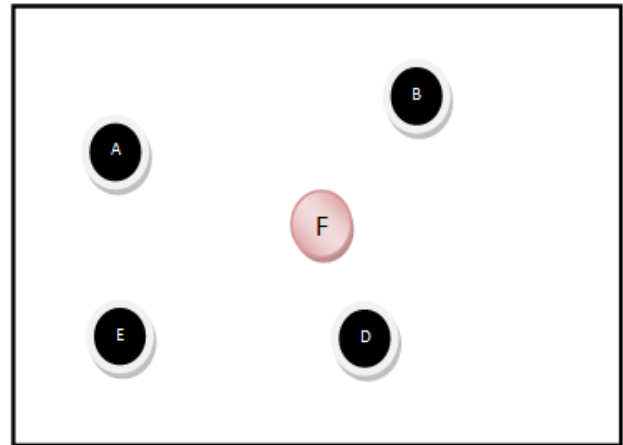
III. DEENR ALGORITHM DESCRIPTION

DEENR is a distributed algorithm with an objective to restore connectivity for sensor networks. For our proposed

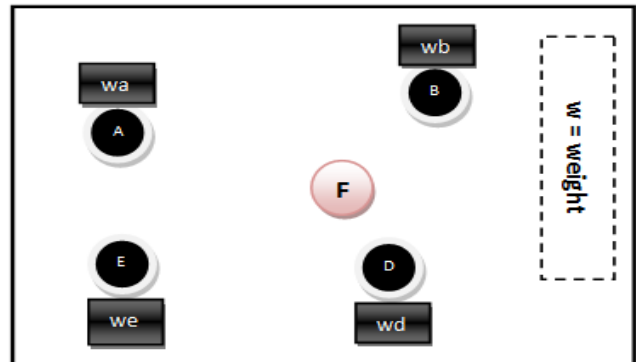
algorithm we assume that all the sensor nodes are densely deployed in an integrated manner and their sensing and communication ranges are equal. The proposed algorithm is presented in Table I. All the nodes are deployed randomly in an area of interest and upon deployment the nodes discover each other. Nodes send periodic hello messages to all their neighbors. In this way each node maintains a neighbor list. When a node dies due to drainage of the battery, it will not send the hello message. In this way the neighboring nodes know about the failure of a certain node. When a node identifies a failed node within its vicinity, it consider itself a potential candidate node to take part in the recovery process and calculates a weight based on the closeness from the failed node and its current residual energy. After calculation of weight, each node sets a timer based on the calculated weight as shown in line 20 of algorithm. The timer is set in a way such that a node having a more weight sends the broadcast message before the nodes having lesser weights. In this way the number of messages transmitted by the nodes can be reduced. Upon receiving a message containing a weight, each node analyzes the weight and compares the received message weight with its current weight. Receiving a weight higher than its own weight means that a more suitable node is available in the vicinity of the failed node. This enables our algorithm to refrain from cascaded relocation which has been proven to be detrimental for the network in terms of network coverage and energy efficiency. After the selection of the appropriate node that will take part in the recovery process, the next step is movement of that node towards the failed node. The node that is selected as the recovery node for the failed node calculates the maximum distance from itself from all of its neighbors. If this distance is greater than $R_c/2$, then this node has the potential to move a maximum of $R_c/2$ towards the failed node without disturbing the network topology or doing a cascaded movement. Else if the distance is less than $R_c/2$, it means that the node can move towards the failed node with a maximum distance of the R_c minus the maximum distance from the neighboring node. Therefore this node moves towards the failed node with this distance. Then it stays at this place until it receives hello messages from the neighbors of the failed node. Upon receiving these messages if the node determines the recovery was successful then it stays at the current position. If not, then it has to rely on cascaded relocation of the neighboring nodes for the recovery. The initial weight calculation for our algorithm is depicted in Fig. 1. Fig. 1(a) shows the initial simple topology having 5 nodes. Now let's suppose that node C fails as shown in Fig. 1(b). The node failure of node C will be found by absence of periodic hello message from node C. Upon detecting the failure of node C, all the nodes that are neighbors of node C will compute a weight on the basis of their current energy level and the closeness to node C. These weights are represented by w_a , w_b , w_d , and w_e respectively as shown in Fig. 1(c). On the basis of these weights, each node calculates a timer for sending a broadcast message containing the computed weight as shown in Fig. 1(d). If the node having the highest weight does not receive any broadcast message having more weight than itself then it means that this node is the suitable candidate node for relocation. Therefore as shown in Fig. 1(e), this node moves towards the failed node according to the proposed algorithm.



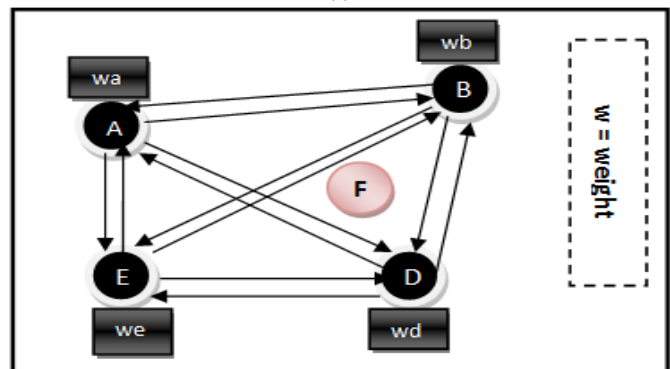
(a)



(b)



(c)



(d)

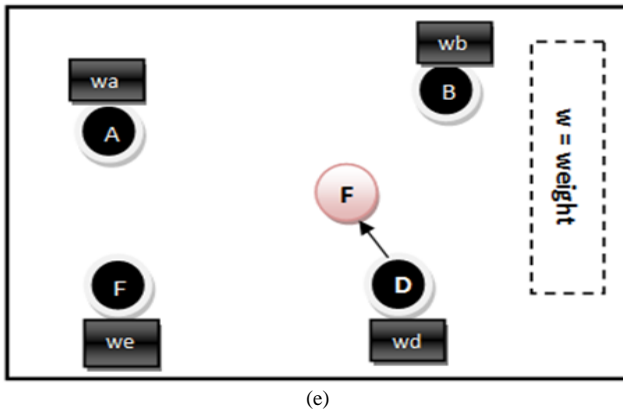


Fig. 1. (a) Initial topology, (b) Node failure, (c) Calculation of weights, (d) Broadcast message, (e) Node relocation.

A. Energy Model

We have assumed the energy model depicted in [20] to transmit and receive a β -bit data packet over distance d . The energy consumption of a sensor node when it transmits a β -bit data packet over distance d is calculated as:

$$E_{Tx}(\beta, d) = \begin{cases} E_{elec} + \epsilon_{fs}d^2\beta & d < d_0 \\ E_{elec} + \epsilon_{mp}d^4\beta & d \geq d_0 \end{cases} \quad (1)$$

where ϵ_{fs} is the energy required by the radio frequency (RF) amplifier in free space and ϵ_{mp} is the energy required by the radio frequency (RF) in multipath. E_{elec} is the energy consumption per bit of the transmitter circuitry.

The energy consumption of a sensor node to receive a β -bit data is given by:

$$E_{Rx}(\beta) = E_{Rx-elec}\beta \quad (2)$$

Where $E_{Rx-elec}$ is the energy consumed per bit by the receiver circuitry.

The remaining residual energy of a sensor node is given by:

$$E_{reng}(n) = E_{max} - E_{Tx}(\beta, d) - E_{Rx}(\beta) \quad (3)$$

TABLE I. DISTRIBUTED ENERGY EFFICIENT NODE RELOCATION ALGORITHM (DEENR)

Input: Area, Rc, n	
1	begin // Randomly deploy all nodes in the network
2	For each node N_i ,
3	Send Hello message()
4	Maintain neighbor list L_i
5	For each end
6	For each node N_i do
7	For each neighbor
8	If $E_{n_j} = 0$ // Means n_j is dead
9	Calculate $weight(N_i, n_j)$
10	SendDeadNodeBroadcastMessage(n_i, N_i)
11	end
12	SendDeadNodeBroadcastMessage(n_j, N_i)
13	begin
14	For each node N_j receiving this message

15	If n_i is present in neighbor list // means that n_i is a common neighbor
16	Add N_i as candidate node for recovery
17	$weight_{i,j} = (\alpha \times energy_i) + (\beta \times distance_from_n_i)$
18	Where $\alpha + \beta = 1$
19	Before Moving \rightarrow send Broadcast msg containing weight.
20	Broadcast Timer = $1/weight \times seconds$
21	end
22	Calculate $weight(N_i, n_j)$
23	begin
24	$W_{i,j} = \alpha * energy_i + \beta * distance_from_n_j$
25	end
26	MoveTowardsFailedNode()
27	begin
28	Set $max=0$;
29	/* Calculate the maximum distance of the current node from all of its neighbors */
30	For each node N_i do
31	For each neighbor
32	If $distance_{i,c} > max$
33	$max = distance_{i,c}$
34	//end if
35	//endforeach
36	//endforeach
37	If $max < Rc/2$
38	Move the node with distance $Rc/2$ towards failed node
39	Else
40	Move a distance max towards the failed node
41	Wait for broadcast hello messages from neighbors
42	If recovery successful
43	Stay at the current position
44	Else
45	Cascaded relocation until recovery

IV. RESULTS AND DISCUSSION

Randomly dense deployed WSN topologies are involved in the experiment with varying communication ranges and number of nodes. The number of nodes has been set to 100, 150, 200 and 250 in the field with dimensions of $900 \times 900 m^2$. However, for our algorithm DEENR, experiments were conducted by varying the sensing and communication ranges. The initial energy of every node has been set to 100 joules avoiding the energy consumption in initial relocation. Table II summarizes the simulation parameters used during simulation.

Consumption of energy occurs due to communication, sensing, and movement. Each experiment is done 20 times and then result is averaged. All the results are subjected to 88% confidence analysis interval and stay within 12% of simple mean. The results are compared with baseline algorithms RIM [6], C^3R [8], and AUR [9]. The major difference between our algorithm and the baseline algorithms is that the former describes nodes permanent relocation with less traveled distance.

TABLE II. SIMULATION PARAMETERS

Simulation parameters	Value
Simulation Area	$900 \times 900 m^2$
Number of nodes	100 - 250
R_c	25 - 150 m
Simulation tool	OMNeT++

A. Total Distance Moved during Relocation

Fig. 2 presents the total distance moved by all nodes until the restoration of connectivity is done. Our algorithm outperforms all the other algorithms because it moves only non-critical nodes in order to avoid cascaded relocation. The improvement in performance by our algorithm remains consistent even by increasing node communication ranges and densities. This is because our algorithm avoids the movement of critical nodes which causes further partitioning of the network. Furthermore, our algorithm implements cascaded relocation only when non-critical neighbor nodes fail.

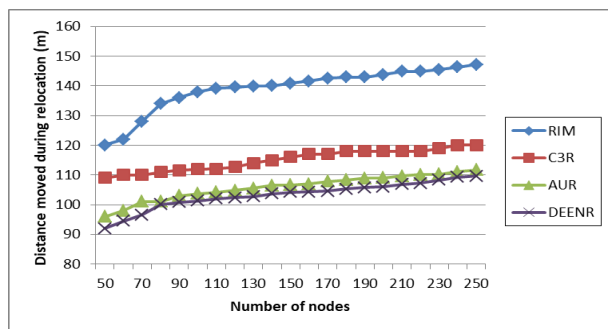


Fig. 2. Node relocation.

B. Number of Nodes Moved

Fig. 3 presents the average number of nodes moved while connectivity restoration. The simulation results confirm the advantage of DEENR which moves fewer nodes as compared to other algorithms. The main reason behind this is that DEENR limits the recovery scope and avoids continuous and cascaded relocation. Moreover, the average number of nodes moved for the case of DEENR increases less significantly as compared to RIM, C3R, and AUR which shows the great scalability that our algorithm can achieve.

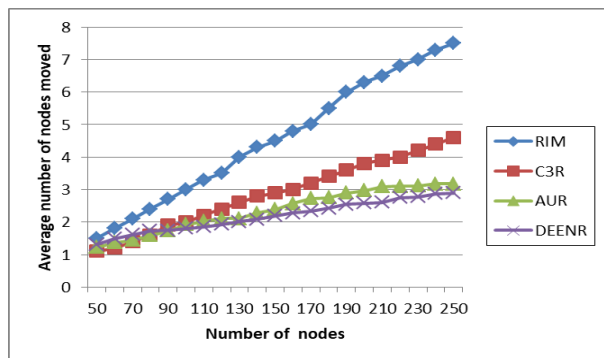


Fig. 3. Average number of nodes moved during recovery.

C. Reduction in Field Coverage

Fig. 4 show how coverage is influenced by analyzing the percentage reduction in field coverage. It can be seen from the figure that increasing communication range decreases the percentage reduction in the field coverage for all the protocols. However, our protocol yields the least percentage reduction in the field coverage as compared to the other protocols. In general, DEENR efficiently limits the coverage loss; the nodes having less coverage overlap area in sparse networks. The field coverage under our algorithm is much better as compared

to the baseline algorithms. Field coverage is highly reduced in the case of RIM. In the case of proposed technique, the overlapped coverage is higher due to which substitute nodes have to move a smaller distance. When a node is relocated, its neighbor nodes mostly cover the home area. In sparse networks, less number of nodes are eligible for substitution of failed node and the larger region remains uncovered during this relocation.

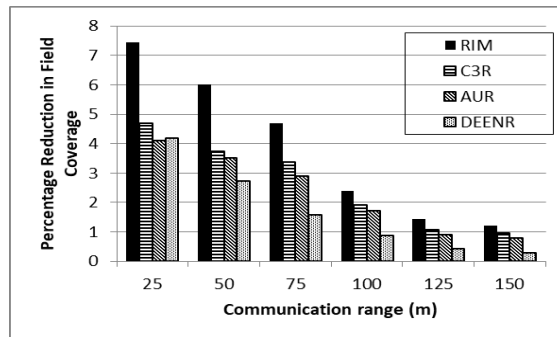


Fig. 4. Percentage reduction in field coverage.

D. Number of Exchanged Packets

Fig. 5 presents the average number of packets exchanged during restoring connectivity both under proposed technique and baseline techniques. Every broadcast is considered as a single message. In case of the proposed technique, the messaging overhead is the minimum, while RIM exchanges maximum number of packets. This is because in proposed algorithm only neighbors are engaged in relocation. As it is proven that reducing the number of messages during the operation of the protocol leads to achieving energy efficiency [5], therefore DEENR algorithm proves to be energy efficient as well as more scalable as compared to the baseline protocols. In comparison with the baseline protocols, there is a substantial difference in terms of total number of packets exchanged.

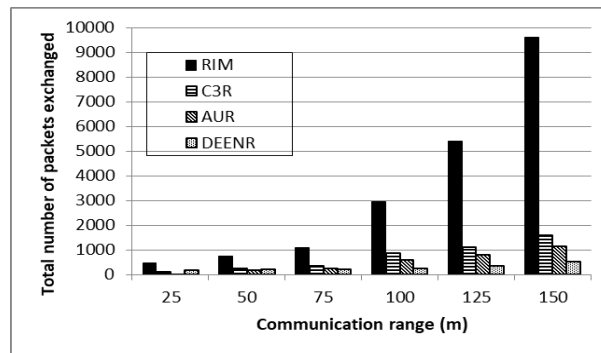


Fig. 5. Total number of exchanged packets.

Connectivity restoration is critical for the operation of sensor networks. A technique is desired that is capable of not only restoring the connectivity but also be coverage-aware and energy efficient. Many techniques proposed in the literature focuses on one of the above features but not all at once. Our goal was to design a technique capable of achieving all the above goals. Achieving connectivity restoration by making the nodes to move the minimum possible distance, making less

number of nodes to move, reducing the decrease in field coverage, and achieving energy efficiency is the primary goal of every connectivity restoration technique. We developed our solution by keeping all these goals in mind. With the help of extensive simulations, we compared the performance of our proposed technique with the baseline techniques and concluded that our technique outperforms the baseline techniques in terms of all the above mentioned performance metrics.

V. DISCUSSION

It can be observed from the presented results that the proposed protocol outperforms some of the well-known protocols proposed in the literature. A realistic simulation evaluation was performed during this work and the comparison with the existing protocols is also presented. However, there are a few aspects that can be studied in future and are out of scope of the current work. First of all, as connectivity restoration is one of the most studied topics in sensor networks therefore recently a lot of new approaches have been presented in literature. There is a need to compare the performance of the proposed protocol with the more recent approaches. Secondly, a more realistic communication model incorporating the effect of propagation and other factors can also be considered for the performance evaluation. Last but not least, a more realistic mobility model can be considered for the performance evaluation. One option can be to use the real world traces for mobility models because they will make the performance evaluation more realistic. All of these questions are open for research and can be considered by the researchers as a possible extension of the current work.

VI. CONCLUSION

In this work, we presented a novel technique capable of providing a solution to the connectivity restoration. The proposed technique is distributed and energy efficient and with the help of extensive simulations, the effectiveness of the proposed technique is proven. Simulation results revealed that the proposed technique requires less number of nodes to be moved for connectivity restoration. The distance that nodes have to move is also less as compared to existing techniques. Moreover, the proposed technique also does not significantly affect the percentage of reduction of the coverage of the field and it is also more energy efficient as compared to other existing techniques. As a future work, a more realistic communication and mobility model can be considered for evaluation of the proposed protocol.

REFERENCES

- [1] Lee, Sookyoung, Mohamed Younis, and Meejeong Lee. "Connectivity restoration in a partitioned wireless sensor network with assured fault tolerance." *Ad Hoc Networks* 24 (2015): 1-19.
- [2] Bhuiyan, MdZakirulAlam, et al. "Deploying wireless sensor networks with fault-tolerance for structural health monitoring." *IEEE Transactions on Computers* 64.2 (2015): 382-395.
- [3] Yick, Jennifer, Biswanath Mukherjee, and DipakGhosal. "Wireless sensor network survey." *Computer networks* 52.12 (2008): 2292-2330.
- [4] Ranga, Virender, Mayank Dave, and Anil Kumar Verma. "Node Stability Aware Energy Efficient Single Node Failure Recovery Approach for WSANs." *Malaysian Journal of Computer Science* 29.2 (2016).
- [5] Sharma, Abhinav, and Sandeep Sharma. "A Comparative Review on Reliability and Fault Tolerance Enhancement Protocols in Wireless Sensor Networks." (2016).
- [6] Senouci, Mustapha Reda, and AbdelhamidMellouk. *Deploying Wireless Sensor Networks: Theory and Practice*. Elsevier, 2016.
- [7] Bao, Lichun, and Jose Juaquin Garcia-Luna-Aceves. "Topology management in ad hoc networks." *Proceedings of the 4th ACM international symposium on Mobile ad hoc networking & computing*. ACM, 2003.
- [8] Abbasi, Ameer Ahmed, and Mohamed Younis. "A survey on clustering algorithms for wireless sensor networks." *Computer communications* 30.14 (2007): 2826-2841.
- [9] Akkaya, Kemal, and Mohamed Younis. "Coverage and latency aware actor placement mechanisms in WSANs." *International Journal of Sensor Networks* 3.3 (2008): 152-164.
- [10] Akkaya, Kemal, and Mohamed Younis. "C2AP: Coverage-aware and connectivity-constrained actor positioning in wireless sensor and actor networks." *2007 IEEE International Performance, Computing, and Communications Conference*. IEEE, 2007.
- [11] Younis, Mohamed, and Kemal Akkaya. "Strategies and techniques for node placement in wireless sensor networks: A survey." *Ad Hoc Networks* 6.4 (2008): pp. 621-655.
- [12] P. Basu and J. Redi, "Movement Control Algorithms for Realization of Fault-Tolerant Ad Hoc Robot Networks." *IEEE Networks*, vol. 18, no. 4, pp. 36-44, Aug. 2004.
- [13] Akkaya K, Younis M, "Coverage-aware and connectivity-constrained actor positioning in wireless sensor and actor networks," In: *Proceedings of the 26th IEEE international performance computing and communications conference (IPCCC 2007)*, New Orleans, pp. 281-288
- [14] Akkaya K, Younis M. "Coverage and latency aware actor placement mechanisms in wireless sensor and actor networks." *International Journal of Sensor Networks special vol.3, Issue.3*, pp. 152-164
- [15] Wang G, Cao G La Porta T, "Movement-assisted sensor deployment," *IEEE Transactions on Mobile Computing*, vol. 5, Issue. 6, pp. 640-652, 2006
- [16] Younis M, S. Lee, S. Gupta and K. Fisher, A localized self-healing algorithm for networks of moveable sensor nodes, In: *Proceedings of the IEEE global telecommunications conference (Globecom'08)*, New Orleans, LA, and November 2008.
- [17] Abbasi A, Akkaya K Younis M, A distributed connectivity restoration algorithm. *Wireless sensor and actor networks*. In: *Proceedings of the 32nd IEEE conference on local computer networks (LCN 2007)*, Dublin, Ireland, pp. 1-5, October 2007.
- [18] Tamboli, Neelofer, and Mohamed Younis. "Coverage-aware connectivity restoration in mobile sensor networks." *Journal of Network and Computer Applications* 33.4 (2010): pp. 363-374.
- [19] Y. K. Joshi and M. Younis, "Autonomous recovery from multi-node failure in Wireless Sensor Network," *2012 IEEE Global Communications Conference (GLOBECOM)*, Anaheim, CA, 2012, pp. 652-657.
- [20] Chanak, Prasenjit, Indrajit Banerjee, and R. Simon Sherratt. "Energy-aware distributed routing algorithm to tolerate network failure in wireless sensor networks." *Ad Hoc Networks* 2017: 158-172.

Secure and Privacy Preserving Mail Servers using Modified Homomorphic Encryption (MHE) Scheme

A Technique for Privacy Preserving Big Data Search

Lija Mohan¹, Sudheep Elayidon M²

Division of Computer Science, School of Engineering,
Cochin University of Science & Technology,
CUSAT, Kochi, Kerala, India

Abstract—Electronic mail (Email) or the paperless mail is becoming the most acceptable, faster and cheapest way of formal and informal information sharing between users. Around 500 billion mails are sent each day and the count is expected to be increasing. Today, even the sensitive and private information are shared through emails, thus making it the primary target for attackers and hackers. Also, the companies having their own mail server, relies on cloud system for storing the mails at a lower cost and maintenance. This affected the privacy of users as the searching pattern is visible to the cloud. To rectify this, we need to have a secure architecture for storing the emails and retrieve them according to the user queries. Data as well as the queries and computations to retrieve the relevant mails should be hidden from the third party. This article proposes a modified homomorphic encryption (MHE) technique to secure the mails. Homomorphic encryption is made practical using MHE and by incorporating Map Reduce parallel programming model, the execution time is exponentially reduced. Well known techniques in information retrieval, like Vector Space model and Term Frequency – Inverse Document Frequency (TF-IDF) concepts are utilized for finding relevant mails to the query. The analysis done on the dataset proves that our method is efficient in terms of execution time and in ensuring the security of the data and the privacy of the users.

Keywords—Big data; encrypted data searching; privacy preserving; homomorphic encryption; hadoop; map reduce

I. INTRODUCTION

Today, the data is evolving at an enormous rate and Cloud Computing paved the way to economic and easy storage of Big Data. World Wide Web (WWW), Social Media, Electronic Health Records, etc. are all sources of Big Data. Since this Big Data cannot be stored and processed using single system, it is stored in multiple systems or preferably outsourced to cloud system. But, this data outsourced to a third party system like cloud raises some security challenges. NIST [23] identifies the ‘Security and Privacy of the stored data’ as one of the major challenge to be addressed while storing sensitive data in the cloud. According to the application requirement, methods adopted to ensure the security and privacy differs. This article explains a novel technique to implement secure Email servers that ensures the privacy of each user.

Emails are becoming the easiest, inexpensive and faster method of personal and formal communications. Many people

utilize the free email service provided by Google, Yahoo, etc. Private organizations maintain their own mail servers to ensure more privacy and security of the users and data transferred. But, as the employees increase and as the size of mails increases, these organizations should maintain a good amount of infrastructure for the efficient storage which will result in a heavy maintenance cost. Cloud computing comes to the rescue here. But, ensuring the privacy and security of the users and emails is a challenging issue. “Hillary Clinton’s Email Leak”, “Effect of Email Leak during French Elections” [24], etc. are the result of inefficient and insecure storage and transfer of emails.

This article proposes a secure and privacy preserving technique to store, retrieve and transfer of sensitive e-mails. To ensure security, traditional encryption techniques can be utilized. Encrypt each email before passing through the network and decrypt it at the receiver side. Also, before storing the mails in cloud system encrypt it.

Thus, storage and transmission of encrypted mail is possible by utilizing existing well known cryptosystems. But, search and retrieval of specific mail is the difficult part. Since, all mails are stored in an encrypted form, the direct solution is to download all the mails to the client machine, decrypt them and find the matching mails. But, this will consume a large bandwidth and hence, not at all an economic solution, considering the pay-as-you-use pricing model of cloud. Also, if there are too much mails, download and decryption of each mail will be a time consuming task and will not be feasible, if the client machine does not have much processing capability.

The scenario given in Fig. 1 illustrates the need for secure email server. Alice is working in ABC Company which processes information dealing with the national security. They maintain their own mail server for transfer of mails between their employees. The mail server is hosted on a Cloud system. Hence, to ensure the security, mails are stored in an encrypted form. Later, to retrieve all mails related to “Mission X”, either Alice need to download all mails to her system, decrypt them and search or decrypt all mails at the Cloud system and search and retrieve only the specific mails. The former method wastes a lot of bandwidth and later results in security violation as decryption is done at a cloud machine.

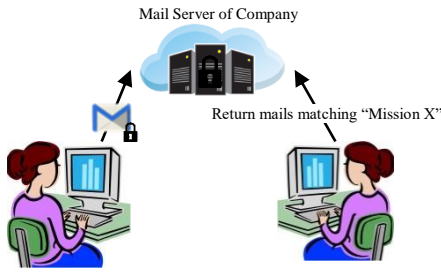


Fig. 1. Scenario illustrating the need for secure Email server.

II. RELATED WORK

Encrypted data searching is partially made possible through different techniques like Property Preserving Encryption [15], Searchable Symmetric Encryption [16], [17], Homomorphic Encryption [10], etc. But none of these methods have been found to be efficient and practical for real word applications. Hence, based on the application context, an algorithm is selected and modified to meet the privacy and security constraints. Statistical and access pattern leakage makes PPE schemes less adoptable to Cloud [1], [2]. SSE schemes are preferred over PPE for more storing more sensitive data but at the cost of complex operations like pairing, elliptic curves, etc. Attribute Based Encryption, Identity Based Encryption, etc. helps to restrict the access to the documents but does not support content searching. Fully Homomorphic Encryption scheme put forward by Gentry in 2012 [11]-[13] is considered as a holy grail for encrypted data operations but no practical methods have been put forth which can be directly applied to any application. Oblivious RAMS [19] are another concept to prevent access leakage but with a higher implementation cost.

III. BACKGROUND

The authors utilise the well-known techniques for information retrieval, like vector space model [3] and TF-IDF [4], for retrieving the relevant documents. The search similarity index thus generated is encrypted using homomorphic encryption [5] scheme and encrypted functions are applied on it to retrieve the similar document indices. This list is then sent to the client side and the ranking is done there by decrypting the obtained indices and sorting them based on their similarity score.

A. TF-IDF Calculation

Term Frequency – Inverse Document Frequency is a statistical measure used to evaluate the importance of a word in a document, or a corpus. Term Frequency implies the cardinality of occurrence of each word in a document and Inverse Document Frequency implies the importance of a word in the entire corpus.

$$TF_{ij} = N_{ij} / \sum N_{kj} \quad (1)$$

Where TF_{ij} implies the term frequency of an i^{th} word in j^{th} document, N_{ij} implies the frequency of occurrence of i^{th} word in j^{th} document and $\sum N_{kj}$ implies the total number of words in the j^{th} document. Since we are dealing with Big Data, we utilise a normalised TF value for further evaluations.

$$TF_{nij} = TF_{ij} / \max(TF) \quad (2)$$

Where TF_{nij} implies the normalised TF value for the i^{th} word in the j^{th} document and $\max(TF)$ implies the maximum value for TF obtained for any word in the document collection.

$$IDF_i = 1 + \log(D/|F_i|) \quad (3)$$

Where, $|D|$ implies a total number of documents in the corpus and $|F_i|$ implies a total number of occurrence of terms in the corpus.

B. Vector Space Model

Vector Space model [6]-[9] represents text documents in rows and columns, where the rows are distinct words, and the columns are documents in the corpus and each cell represents the degree to which each word belongs to a document. TF-IDF is used as the metric to represent the degree of relevance of words in a document. This model represents documents and words as a vector.

Document collection, $D_t = (d_1, d_2, d_3, \dots, d_t)$

Word Collection, $W_k = (w_1, w_2, w_3, \dots, w_k)$

If D_t is arranged in columns and W_k in rows, each cell, C_{tk} represents the similarity score.

When a query comes with x words, $Q_x = (w_1, w_2, \dots, w_x)$, the similarity of the document is identified by (4).

$$\text{Similarity Score, } S_t = \sum_{i=1}^x C_{ti} * B_i \quad (4)$$

Here, B_i has a value 0/1, depending on whether the word is present in the query list or not.

After obtaining the similarity score for ‘t’ documents, they are ranked in order to find the most similar documents.

IV. MODIFIED HOMOMORPHIC ENCRYPTION (MHE) SCHEME

According to Gentry’s Homomorphic Encryption scheme using ideal lattices, the encryption scheme is $c = pq + 2r + m$ and the decryption scheme is $m = (c \pmod{p}) \pmod{2}$. Before encrypting any message, it should be converted to binary and each bit is encrypted by using this formula. This is a generalized method to be adopted if we do not know the value of message to be encrypted. But if we know this message range prior, the complexity of this scheme could be greatly reduced. Binary conversion and bit by bit encryption can be replaced by a single step encryption and decryption vice versa. Also, the number of bits needed to store the encrypted value will be drastically reduced to approximately $1/|n|$ where n is the number of bits in the binary representation of the message.

A. Modified Homomorphic Encryption (MHE) Algorithm

Let m ranges from 1 to n , then set $s = 2^{2|n|}$. The secret key, p should be a large number of the order of $O(s^3)$. The noise parameter, r will be a smaller value compared to s and p ; i.e. $p \gg s \gg r$.

Encryption: Encrypt(SK, m):

Given $m \in Z_n$ and the secret key p , choose a random value for r and q .

Cipher Text, $c = pq + sr + m$

Decryption: Decrypt(SK,c):

Given the secret key, 'p' and the cipher text, 'c' then output is, $m = (c \bmod p) \bmod s$.

B. Proof of Correctness for MHE Algorithm

Proof of correctness for decryption

$$\begin{aligned} m &= (c \bmod p) \bmod s \\ &= ((pq+sr+m) \bmod p) \bmod s \\ &= m \bmod s \text{ (since } p > s.r) \\ &= m \end{aligned}$$

Proof of correctness for homomorphic addition

$$\begin{aligned} m_1 + m_2 &= ((C_1 + C_2) \bmod p) \bmod s \\ &= ((pq_1+sr_1+m_1 + pq_2+ sr_2+m_2) \bmod p) \bmod s \\ &= ((p(q_1+q_2)+s(r_1+r_2)+m_1+m_2) \bmod p) \bmod s \\ &= (s(r_1+r_2)+m_1+m_2) \bmod s \text{ (since } p \gg s(r_1+r_2)) \\ &= m_1 + m_2 \end{aligned}$$

Proof of correctness for homomorphic multiplication

$$\begin{aligned} m_1 * m_2 &= ((c_1 * c_2) \bmod p) \bmod s \\ &= (((pq_1+sr_1+m_1 * pq_2+ sr_2+m_2) \bmod p) \bmod s \\ &= (s^2r_1r_2 + sr_1m_2 + sr_2m_1 + m_1m_2) \bmod s \\ &\quad \text{(since } p \gg s^2.\text{noise)} \\ &= m_1.m_2 \end{aligned}$$

V. SYSTEM DESIGN

Secure Mail Servers encrypt each mail before passing it through the network. Public Key Cryptosystem powered by LDAP is utilized for this. For storage of mails, as well as for the secure transfer of mails, traditional cryptographic techniques are utilized, as it is found to be more efficient and less time complex. For encrypting the mails, AES is utilized. Each mail is encrypted by user's secret key and uploaded to cloud. To fetch a mail, the same key is used for decryption. Also, while sending a mail, it is encrypted by receivers' public key using RSA encryption system. Receiver can use his secret key to decrypt and view the contents of the mail.

Each mail will be stored in the cloud system in an encrypted form. To search and retrieve the matching mails from this encrypted domain, a vector space is generated and encrypted using the Modified Homomorphic Encryption scheme (discussed in Section 3.1). A two round search and retrieval strategy is followed. During the first round, a trapdoor is generated with the query keywords and is used to calculate the encrypted score of each mail. Cloud system will return the Mail-ID along with the encrypted score to the user. User will decrypt the scores, rank them and send the top-K Mail-IDs to the cloud. Cloud will now send the corresponding encrypted mails to the user in the second round of communication. Fig. 2 illustrates the two round search and retrieval scheme. As explained in Section 1, secure mail storage and transmission is achieved using traditional cryptosystems. How to securely retrieve the relevant mails are discussed in the next section.

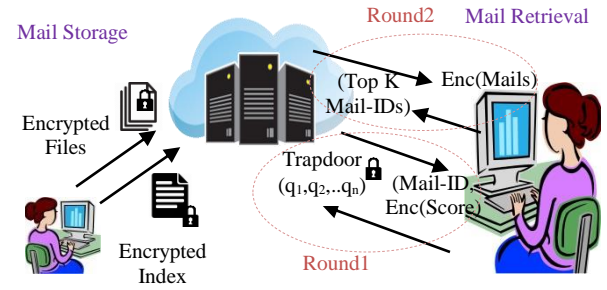


Fig. 2. Two round search and retrieval scheme.

A. Secure Mail Storage for Secure Retrieval

To implement secure ranked mail retrieval, we adopt the indexing technique used in Information Retrieval. Before encrypting a mail for the secure storage, generate the vector space model filled with TF-IDF values. The TF-IDF value is then normalized using min-max normalization to put within the range 1 to n. Each cell value is then encrypted using the MHE scheme described. Words and Mail-IDs are removed from this index and its order is kept as a key for recovering the relevant files. The MHE encrypted index is uploaded to cloud along with the encrypted mails. Each time when a mail is sent or received, only this index has to be updated and the changed order of words and mail IDs will be made available to the owner.

B. Secure and Ranked Mail Retrieval

To search for a particular mail containing some query keywords $Q = (q_1, q_2, \dots, q_n)$, a string, S is generated which is a combination of 0s and 1s. The length of the string will be equal to the size of the Wordlist. Corresponding to each word in the Wordlist, if that word is present in the query, it will be set otherwise it will be unset. Each bit of this string is then encrypted using MHE to form the trapdoor.

for each word_i in the Wordlist

$$\text{If}(\text{word}_i \text{ in } Q) S_i = 1; \text{ else } S_i = 0 \quad (5)$$

On receiving the trapdoor, the cloud will do multiplication and summation on the index to obtain the encrypted scores corresponding to each column using equation 6. Due to the additive and multiplicative homomorphic property of MHE, the operations done on this encrypted data will be homomorphic to the operations done on raw data. The list of encrypted scores thus obtained is returned to the user.

$$\text{Similarity_Score, } SS_m = \sum_{i=1}^w TF-IDF_{id} * Tw_i. \quad (6)$$

User will decrypt the score with his secret key and rank them to identify the top-K matching mails. The corresponding mail IDs are sent to the cloud. The cloud will return the encrypted mails which are then decrypted at the client side. Thus a two round communication is initiated between user and cloud system to retrieve the matching mails. Decryptions take place only at the client side to ensure absolute security. Also, compute intensive operations like score calculation take place at the cloud which ensures efficiency.

Ranking of scores involve finding the greatest 'k' values from the list. To reduce the complexity of ranking procedure using sorting techniques, an efficient swapping strategy is adopted. This method is less time intensive compared to traditional sorting. Ranking is achieved using Algorithm 1. There is no need of sorting the entire list. Suppose we need to identify the top k scores, add k values to a 'topKlist' from the input values arranged in ascending order. For each next value in the input array, if it is less than the first value of 'topKlist', discard it otherwise, remove the first value of the list and add the new value to the correct position in the 'topKlist'. After each value in the input array is scanned, the 'topKlist' will contain the most relevant k mails arranged in ascending order. This algorithm reduces the complexity to $O(mk)$ where m is the total number of mails and k is the number of mails to be retrieved. Complexity can further be reduced by applying a tree structure.

C. Improving the Ranking of Mails

Apart from the content similarity of the mail with the query keywords, there are other factors that affect the ranking of similar documents. For example, if a user has marked one email as 'important', then such mails shall be given some weightage even if their similarity score is a bit less. This is achieved by adding one more row to the vector space for including the weight of the mail. If the mail has been marked as 'important' by the user, the filed will be set 1 else 0. The value can be increased or decreased based on application requirement. The same technique can be applied to emails tagged as spam, promotions, etc.

The entire stages of the Secure Index Generation are summarised below:

- 1) Setup(λ): Based on the security parameter, λ the data owner generates the secret key SK.
- 2) IndexBuild(DocCollection,SK): Documents are arranged in vector space model after applying IR techniques like stemming and stop word elimination. The index is homomorphically encrypted to generate a secure index, I_w with height w and width m, using the secret key, SK. Then, I_w is uploaded to cloud server along with other encrypted mails.
- 3) TrapdoorGenerate(Query,SK): The query keywords obtained from user, Q_n are arranged into a Boolean Query vector form Q_w , where $Q_j = 1$ if w_j is present in Q_n else 0. Q_w is then homomorphically encrypted using SK to form the trap door, T_w . T_w is sent to the cloud server.
- 4) ScoreCalculate(T_q, I_e): Encrypted score, 'es' of each mail is calculated using equation 1. Resulting vector will be $SS_m = (es_1, es_2, \dots, es_m)$
- 5) Rank(SS_m, SK, n): Encrypted Scores are decrypted at client machine using secret key, SK and retrieve the actual scores, $S_m = ((fid_1, s_1), (fid_2, s_2), \dots, (fid_m, s_m))$. Sort the scores to find the top n similar mails matching with the query.
- 6) Retrieve Top Matching Files: The top-K ranked document ids are sent to the cloud server and it returns the encrypted documents to the clients, which can then be decrypted to view the mail contents.

Algorithm 1: Top-K Similar Document Select Algorithm (S_d, K)

Input :
 S_d : list containing scores of each file $S_d = ((fid_1, s_1), (fid_2, s_2), \dots, (fid_d, s_d))$
K : number of files to be retrieved.
Output:
TopList_K = Top K-Relevant Files

1. Initialize: TopList_K = NULL
2. For each item $\in S_d$
3. If length(TopList_n) < K
4. Add item to TopList_n in ascending order of the score
5. Else
6. If(item['score'] > TopList₀['score'])
7. Replace TopList₀ with item
8. Sort first K elements in TopList_n in ascending order.
9. Else
10. Discard the item
11. End IF
12. End For
13. End For
14. Return TopList_n

VI. SECURITY ANALYSIS

The security of the proposed scheme should guarantee that the outsourced data is safe at the third party storage. The cloud server that we consider is always an honest, but curious system. Hence, the data as well as the related information like index, keywords, etc. should be protected against statistical leakage, access pattern identification and term distribution. The overall security of our information retrieval system

depends on the security of the proposed encryption scheme and the distributed implementation of the index creation and retrieval phase.

A. Security of the Homomorphic Encryption Scheme used for Securing the Index

The proposed MHE scheme is secure and can be explained based on the approximate GCD problem. Consider the approximate-GCD instance $\{x_0, x_1, \dots, x_t\}$ where $x_i = pq_i + r_i$.

Known attacks on the approximate-GCD problem for two numbers include brute forcing the reminders, continued fractions, and Howgrave-Graham's approximate-GCD algorithm [14].

A simple brute-force attack is to try to guess r_1 and r_2 and verify the guess with a GCD computation. Specifically, for $r_1', r_2' \in (2^p, 2^p)$, set $x_1' = x_1 - r_1', x_2' = x_2 - r_2', p' = \text{GCD}(x_1', x_2')$.

If p' has n bits, output p' is a possible solution. The solution p will definitely be found by this technique, and for the parameter choices, where p is much smaller than n , the solution is likely to be unique. The running time of the attack is approximately 2^{2p} .

Attacks for arbitrarily large values of t include lattice-based algorithms for simultaneous Diophantine approximate [20], Nguyen and Stern's orthogonal lattice [21], and extensions of Coppersmith's method to multivariate polynomials [22].

Apart from the security of the homomorphic encryption, our scheme utilised word order and document order as the keys for correct retrieval. W words and D documents can be arranged in $W! \times D!$ ways and as W or D increases, the complexity increases.

B. Security of the Index Creation and Information Retrieval Scheme

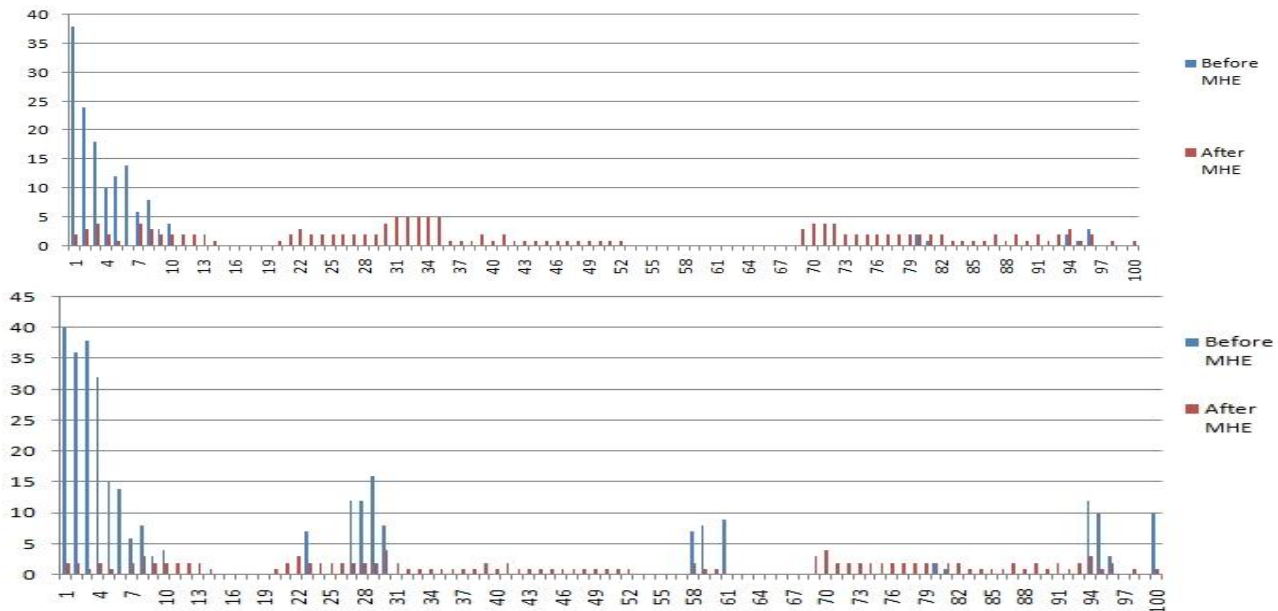


Fig. 3. Distribution of similarity relevance of 142 terms with (a) “data”, and (b) “resources” before and after FHEI in the 20 Newsgroups data set.

Complex operation like encrypted score calculation is done at the cloud server and ranking of the scores is done at the client side thus ensuring the security of the data. Also, the privacy of the user is ensured by encrypting the query before sending it to cloud server.

VII. ACCELERATING MHE IMPLEMENTATION USING MAP REDUCE

Distributed processing using Map Reduce over Hadoop accelerates the speed of execution of the index creation and

The proposed scheme uses homomorphic encryption to secure the index and without decrypting the index at server side, the encrypted similarity score of the documents is identified and returned to the client side. Hence, the method ensures that the data is secured against statistical and access pattern leakage. Suppose, if two queries contain the keyword q , then the word vector v_q in W will be set to 1, and will be homomorphically encrypted with two different keys K_1, K_2 , which will yield two different cypher values, C_1 and C_2 . Hence, seeing the values of the cypher text, we cannot predict the keywords that are searched and the frequency or order of accessing different keywords. Also, to prevent access pattern leakage, apart from k relevant files, k irrelevant files are also retrieved which reduces the chance of probabilistic approaches to find the file content.

The proposed scheme hides the term distribution, as tf-idf values are normalised, encrypted and stored in the cloud. Since, the encryption is not ordered preserving, depending on the absolute value of weights, a relevance of documents cannot be identified. Thus, the term distribution, as well as the inter distribution, is hidden from third party.

Fig. 3 illustrates the term distribution of the terms “data” and “resources” with other terms in the dataset.

retrieval stages. Fig. 2 illustrates the working of MHE using Map Reduce.

Phase 1: Encrypted Index Creation

Stage 1: Inverted Index Creation with the frequency of occurrence.

An inverted index is a data structure which stores the details of mapping from words to files. After forming the inverted index, we need to form a vector space model with each cell containing TF-IDF values. In order to simplify the vector space generation stage, we calculated the frequency of occurrence of each word in each document, simultaneously

with the inverted index creation. This list is kept separately so that it can be re-used when some modifications happen in the input document collection.

Stage 2: Encrypted Vector Index Generation

After obtaining the output from Stage 1, each Mapper for the next stage will be assigned with finding the TF-IDF of each cell. TF can be obtained from the stage1 output and DF, by summing all values. TF-IDF is calculated as per (5). After obtaining the TF-IDF value, MHE is applied as per (6) to form the encrypted value. The entire output from different mappers is then merged to form the final encrypted vector space index. This is then uploaded to cloud. Stage 2 does not require a Reduction stage. Fig. 4 illustrates the details of Map Reduce Stages. Encryption of each document can also be done efficiently by adding one more Mapper stage.

Phase 2: Ranking to retrieve K-Similar Documents.

To retrieve top k similar documents, in an ideal case, assign the task to K mappers with D/K input, where D is the total number of documents. Each mapper evaluates Algorithm 1 to find the most similar document. Collecting the output from K Mappers will give the top K matching documents. There is no Reducer needed in this case. If only N (N<K) mappers are available, assign D/N input to each mapper and evaluate Algorithm 1 to get matching K/N documents. The reducer will select top K from the final result.

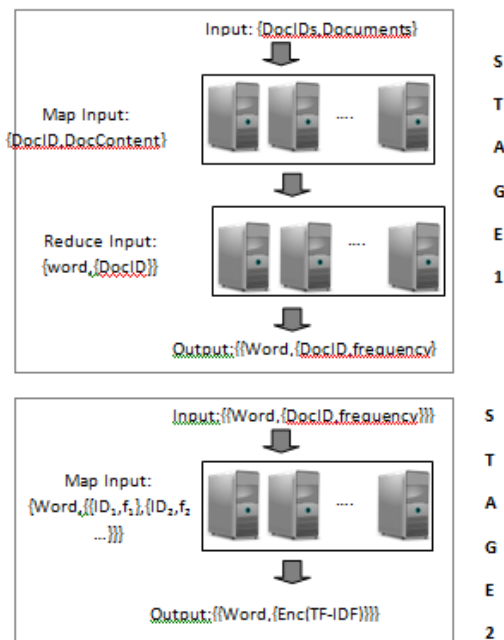


Fig. 4. Map reduce implementation of encrypted vector index creation.

VIII. EXPERIMENTAL SETUP AND EVALUATIONS

The experiment is evaluated on 10 node Hadoop cluster setup on Amazon Web Service (AWS). Namenode is a t2.large instance. Secondary namenode and datanodes are t2.micro instances. All machines are Ubuntu 14.2 installed with OpenJDK 1.7 and Hadoop stable version 1.0.2. HDFS Replication factor is set to 3 and HDFS block size is 8MB.

A. Dataset

The dataset used for testing is Thomson Reuters Text Research Collection (TRC2). The dataset contains 1,800,370 stories which occurred at period 01-01-2008 00:00:03 to 28-02-2009 23:54:14. The size of the dataset is 2,871,075,221 bytes. TRC2 is a single long file with date, headlines and stories stored in comma separated form. To match our testing requirement, we split this large file into multiple files where each file is named with a date in ddmmyyy.txt format and the content of that file is the headlines and stories on that particular day. Thus 419 files have been generated where each file size ranges from 8MB to 16MB. To store and retrieve these small files efficiently from Hadoop Distributed File System, BAMS [18] technique is followed.

B. Performance Analysis

The entire scheme is broadly divided into 2 phases; the Documents Upload phase and the Document retrieval phase. Performance of each phase is separately analyzed and explained.

a) Performance of the Initialization phase

Initially, we need to run the setup (λ) algorithm to derive the public and secret keys needed for encryption and decryption. To reduce the tradeoff between security and efficiency, we fixed the value of λ as 128. Secret key will be a value between $[2^{n-1}, 2^n]$. Thus the complexity of this stage will be $O(\lambda^n)$ which is a constant, as λ is constant.

The index building stage involves tf-idf calculation and homomorphic encryption. To reduce the execution time of index building of large data, we implemented a distributed map reduce parallel programming model that reduces the complexity to linear. Also, tokenization, stemming and stop word elimination is done to reduce the volume of keywords to be indexed. To update the documents, re-iteration of the entire index building stage is needed and to avoid such a scenario, we store idf values separately and hence only the updated part of the file needs to be re-evaluated to find tf-idf of the corresponding words. Encryption can be implemented in $O(dw)$ time, where d is the number of documents and w is the number of words. Index generation and retrieval stage is accelerated by following a MapReduce distributed implementation. Time needed to generate the index is same for all methods whereas time needed to encrypt the index using traditional SSE, proposed MHE and MHE implemented using Map Reduce is illustrated in Fig. 5.

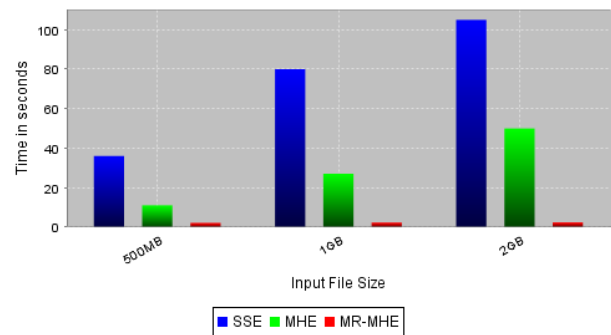


Fig. 5. Comparison of execution time for encrypted index generation.

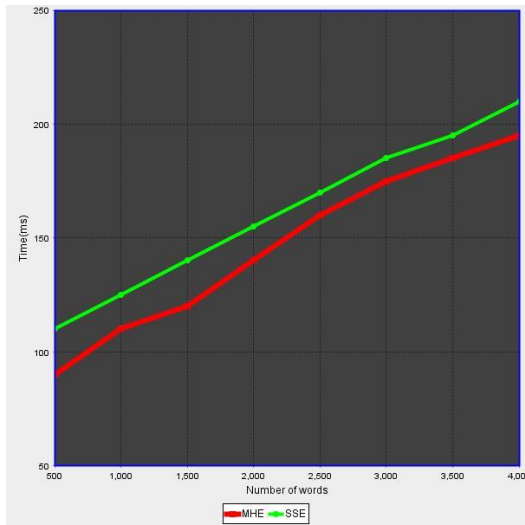
b) Performance of the Similar Document Retrieval Phase

The retrieval phase includes different stages like Trapdoor generation, Score Calculation and Sorting & shuffling to identify the top-k documents. The complexity of our proposed scheme is highly dependent on the retrieval phase, as this has to be repeated each time a user posts a query. Hence, we parallelize the most time-consuming retrieval phase i.e., sorting and shuffling of top-k results.

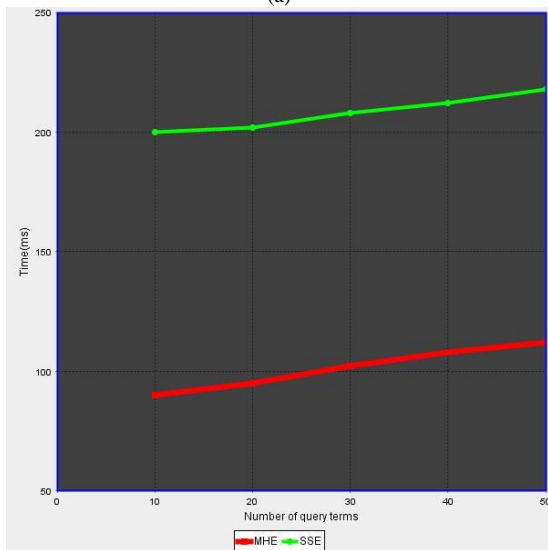
Trapdoor Generation involves the binary conversion of a posted query and the homomorphic encryption of each bit. If the query contains n keywords, then the complexity will be $O(n)$. Fig. 6 illustrates the time needed to compute the Trapdoor by employing homomorphic encryption as well as traditional searchable symmetric encryption (SSE), by varying the number of total distinct words in the document collection and the number of terms in a query. It is well observed that, the execution time is approximately half for our proposed modified homomorphic encryption scheme (MHE).

Fig. 6. (a) Execution Time by varying the total number of words in the document collection; (b) Execution Time by varying the total number of terms in the query.

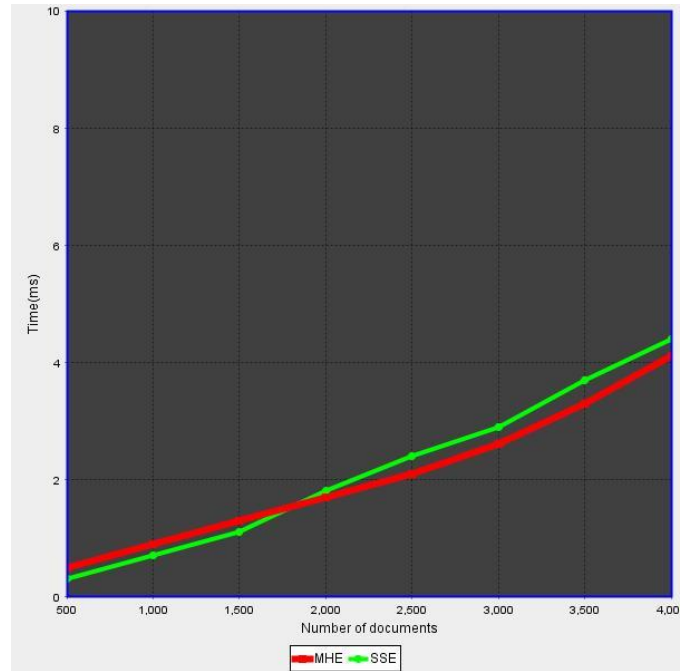
To calculate the encrypted similarity score, the inner product has to be performed. This calls for w multiplications and d additions, where w is the number of words and d is the number of documents which leads to a complexity of $O(wd)$. Here, the execution time varies with a variation in the number of query terms and documents. The comparison is illustrated in Fig. 7. It is well observed that, for the MHE scheme, the execution time is increasing almost linearly, whereas for SSE, it is an exponential increase.



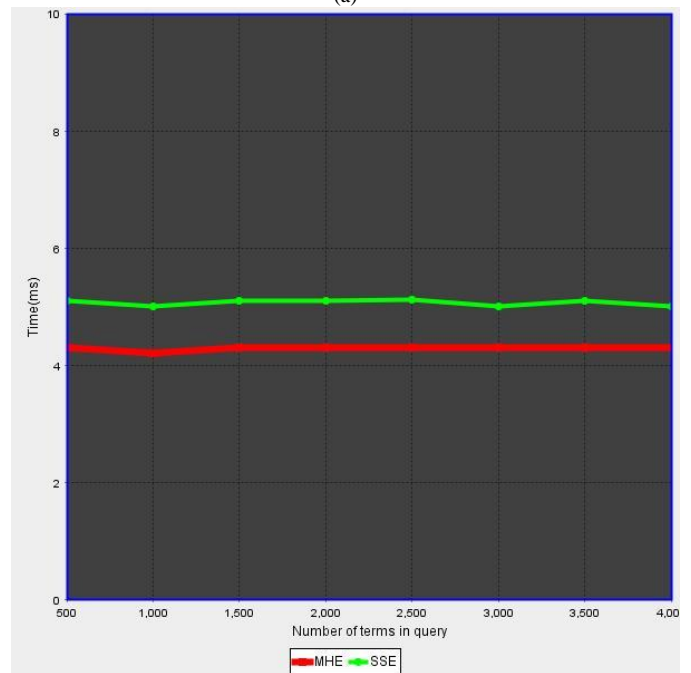
(a)



(b)



(a)



(b)

Fig. 7. (a) Execution Time by varying the total number of words in the document collection; (b) Execution Time by varying the total number of terms in the query.

Decryption of scores to obtain the similarity score is done at client side and the number of terms to be decrypted depends on total number of documents in the collection. Hence, the complexity will be utmost $O(d)$. If there are too many documents, then distributed parallel processing can be employed to decrypt the terms. Fig. 8 illustrates how the decryption time of normal MHE scheme and MHE scheme using Map Reduce Programming Model (MR-MHE) varies with the number of documents and the number of terms in the query. Map Reduce implementation always transforms the execution time to a linear scale. Here, we implemented a cluster with only 10 nodes. The number of nodes is inversely proportional to the execution time. Hence, to decrease the execution time, the nodes can be increased. But, if the collection contains only less number of documents, map reduce processing will result in an overhead.

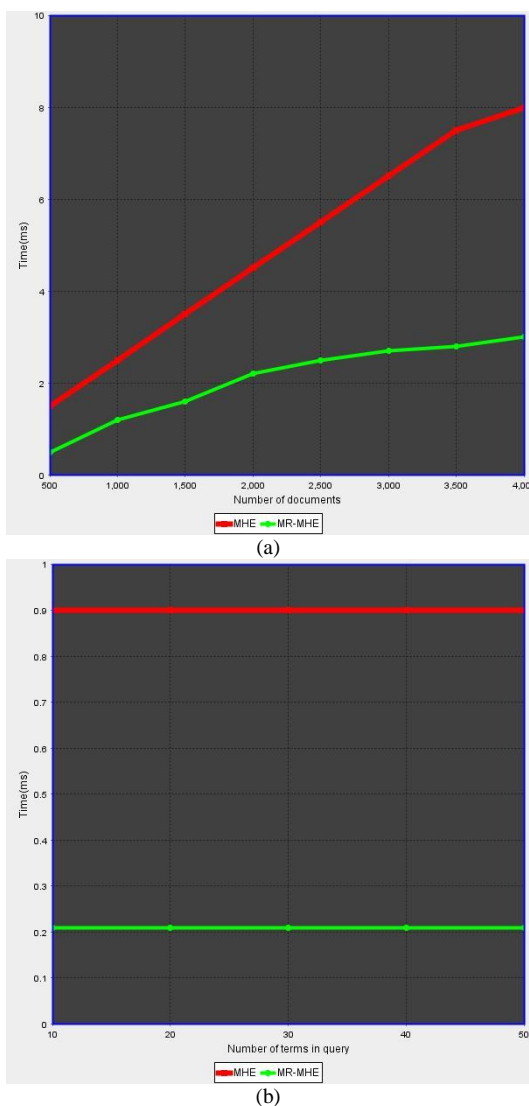


Fig. 8. (a) Execution Time by varying the total number of words in the document collection; (b) Execution Time by varying the total number of terms in the query.

Ranking and shuffling of File identifiers based on similarity score is the last stage to be executed, to identify the most similar documents. Modifying the sorting algorithm as described in Algorithm 1 itself will reduce the execution time to $O(d.n)$ and by introducing MR programming, it can be again reduced to $O(d)$. More reduction is possible by introducing heap tree implementation. Comparison of the execution time is shown in Fig. 8.

Fig. 9(a) shows how distributed processing improves the execution time of ranking, with a variation in k , where k denotes the number of similar files to be retrieved by the user. Here, the number of documents is set to 1000. Then, Fig. 9(b) illustrates how the performance of MR-MHE improves, with an increase in the query terms. As the number of query terms change, there is no much observable difference in execution time, as the query is distributed and evaluated. Hence, the algorithm is more scalable when the Map Reduce programming model is adopted for the implementation of our proposed scheme.

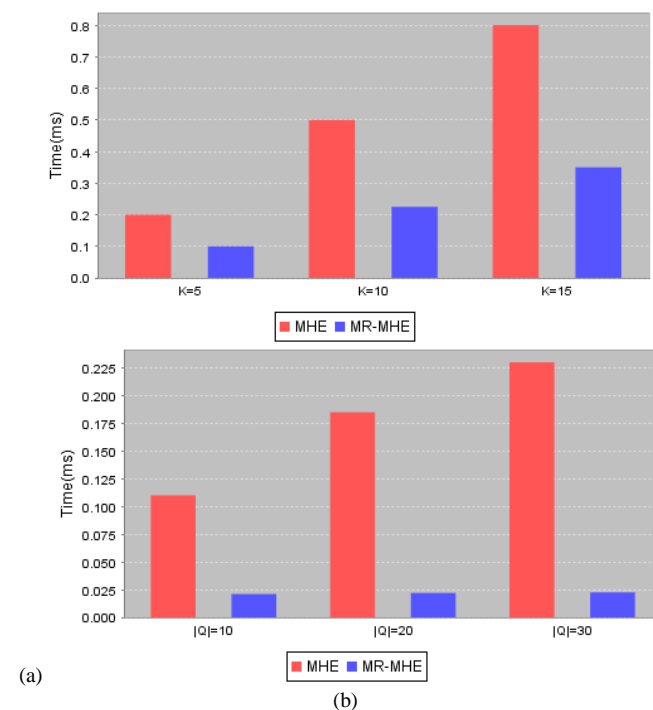


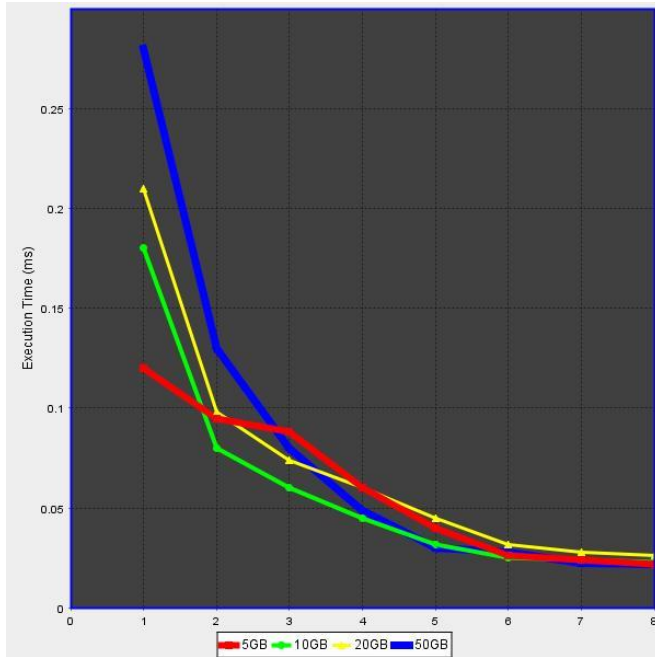
Fig. 9. (a) Execution time by varying K ; (b) Execution time by varying the number of query terms.

Scalability of the proposed MHE scheme is evaluated using SpeedUp metric. The SpeedUp factor defines the ratio of time needed to execute an algorithm in one machine, to the time needed to execute it on N machines. In an ideal case, the method is considered scalable, if the speedup factor remains constant for different values of N .

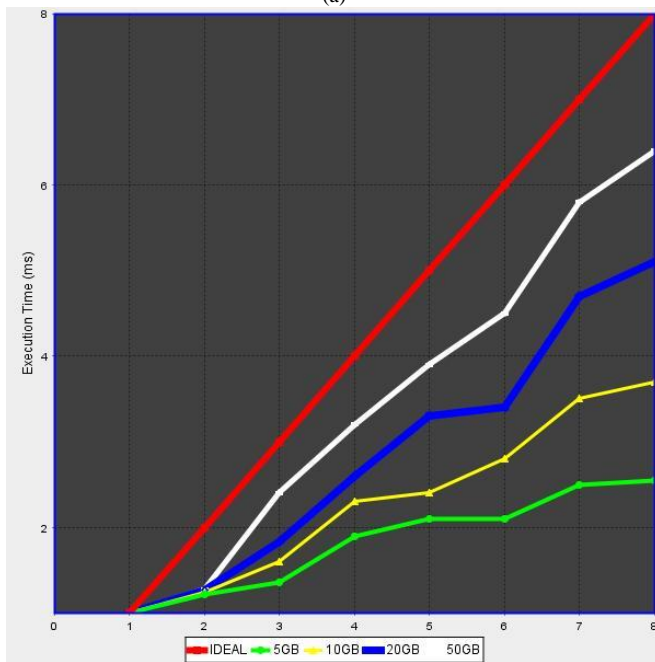
$$SpeedUp, S_u = T_1/T_N \dots (7)$$

Fig. 10(a) illustrates the change in execution time for varying values of data set size. The speedup for the same is illustrated in Fig. 10(b). From the figure, it is clear that, even if the data size increases, there is no much variation in the execution time, as the number of nodes increase. Thus the

algorithm is becoming more scalable, and approaching ideal values with the increase in data size.



(a)



(b)

Fig. 10. (a) Execution time by varying data size; (b) Speedup.

C. Communication Overhead

The core of our approach is the homomorphic encryption of vectored index which eliminates the need of transferring the entire index to the client side for decryption and ranking. The score is calculated at the server side itself and only the encrypted scores are forwarded to the client for ranking. Consider there are 100 files and 1000 distinct keywords. Then the size of index file to be transferred for traditional SSE will

be approximately $100 \times 1000 \times 1024$ bits equals 12MB, if each cell value is set to 1024 bits. But, for the Modified Homomorphic Encryption Scheme, it will only be 100×1024 bits which are equal to .01MB. Hence, there is a large variation in the amount of data to be transferred through the network, when we compare SSE and MHE.

IX. CONCLUSION AND FUTURE WORKS

The authors have proposed a novel scheme for the implementation of encrypted mail storage and retrieval based on similarity relevance. A modified and practical version of Homomorphic encryption scheme has been utilised and the execution is accelerated, by introducing distributed Map Reduce programming model. The scheme supports multiple keyword queries, ranking of mails based on user ranking ('important', 'spam' etc.) and text matching by utilising most of the basic techniques in information retrieval, like vector space model, TF-IDF etc. Analysis done on the MHE scheme proves the correctness and security of the proposed scheme. The entire scheme is evaluated on a live Hadoop cluster, and proven to be efficient, secure, scalable and accurate and hence found suitable for securing a large amount of data. Currently, the updates on uploaded mails need revision for the entire Index creation and encryption stage, except for the TF and IDF calculation. The revised word order and file order are encrypted using the public key for each user, and passed to them whenever an update occurs. This limitation can overcome by experimenting other dynamic indexing techniques which help in storing real time data as well.

ACKNOWLEDGMENT

Authors sincerely thank Department of Science & Technology (DST), India for the financial support offered through INSPIRE Research Fellowship under the grant number IF140608 and Amazon Web Service (AWS) in Education Research Grant (No. 651699140108) for utilising AWS resources for free of cost.

REFERENCES

- [1] C. Wang, N. Cao, J. Li, K. Ren, and W. Lou, "Secure Ranked Keyword Search over Encrypted Cloud Data," Proc. IEEE 30th Int'l Conf. Distributed Computing Systems (ICDCS), 2010.
- [2] Cong Zuo, James Macindoe, Siyin Yang, Ron Steinfeld, Joseph K. Liu, "Trusted Boolean Search on Cloud Using Searchable Symmetric Encryption View Document", IEEE Trustcom/BigDataSE/ISPA, UK, 2016.
- [3] Yun Zhang, David Lo, Xin Xia, Tien-Duy B. Le, Giuseppe Scanniello, Jianling Sun, "Inferring Links between Concerns and Methods with Multi-abstraction Vector Space Model" ,IEEE International Conference on Software Maintenance and Evolution (ICSME), Pages: 110 - 121, DOI: 10.1109/ICSME.2016.51, 2016.
- [4] Nasser Alsaedi, Pete Burnap, Omer Rana, "Temporal TF-IDF: A High Performance Approach for Event Summarization in Twitter", IEEE/WIC/ACM International Conference on Web Intelligence (WI), Pages: 515 - 521, DOI: 10.1109/WI.2016.0087, 2016.
- [5] Yasmina Bensitel, Rahal Romadi, "Secure data storage in the cloud with homomorphic encryption", 2nd International Conference on Cloud Computing Technologies and Applications (CloudTech), Pages: 1 - 6, DOI: 10.1109/CloudTech.2016.7847680, 2016.
- [6] G. Salton, A. Wong, C. S. Yang, "A Vector Space Model for Automatic Indexing", Communications of the ACM, Volume 18 Issue 11, Pages 613-620, November 1975.
- [7] Wong S. K. M., Ziarko Wojciech, Wong Patrick C. N., "Generalized vector spaces model in information retrieval", SIGIR '85 Proceedings of

- the 8th annual international ACM SIGIR conference on Research and development in information retrieval, Pages 18-25, Montreal, Quebec, Canada — June 05 - 07, 1985.
- [8] Waitelonis Jörg; Exeler, Claudia Sack, Harald, "Linked Data enabled Generalized Vector Space Model to improve document retrieval", The 14th International Semantic Web Conference, Pennsylvania, October, 2015.
- [9] George Tsatsaronis and Vicky Panagiotopoulou, "A Generalized Vector Space Model for Text Retrieval Based on Semantic Relatedness", Proceedings of the EACL 2009 Student Research Workshop, pages 70–78, Athens, Greece, April 2009.
- [10] Xun Yi, Russell Paulet, Elisa Bertino, "Homomorphic Encryption and Applications", Chapter 2, Springer Briefs in Computer Science, pages 27-46, Springer 2014.
- [11] C. Gentry, "Fully Homomorphic Encryption Using Ideal Lattices," Proceedings of the 41st Annual ACM Symposium on Theory of computing (STOC), pp. 169-178, 2009.
- [12] M. van Dijk, C. Gentry, S. Halevi, and V. Vaikuntanathan, "Fully Homomorphic Encryption over the Integers," Proc. 29th Ann. International Conference on Theory and Applications of Cryptographic Techniques, H. Gilbert, pp. 24-43, 2010.
- [13] Nathanael David Black , "Homomorphic Encryption and the Approximate GCD Problem", A Dissertation Presented to the Graduate School of Clemson University, August 2014. http://tigerprints.clemson.edu/cgi/viewcontent.cgi?article=2281&context=all_dissertations
- [14] N. Howgrave Graham, "Approximate Integer Common Divisors", Proceedings of the International Conference on Cryptography and Lattices, (CaLC' 01), pp. 51-66, 2001.
- [15] R. Curtmola, "Searchable Symmetric Encryption: Improved Definitions and Efficient Constructions," Proceedings of ACM Conference on Computer and Communications Security (CCS), pp. 79–88, 2006.
- [16] Alexandra Boldyreva, Nathan Chenette, Younho Lee, and Adam O'Neill. Order-preserving symmetric encryption. In Antoine Joux, editor, EUROCRYPT, volume 5479 of Lecture Notes in Computer Science, pages 224–241. Springer, 2009.
- [17] Sanjit Chatterjee and M. Prem Laxman Das, "Property Preserving Symmetric Encryption Revisited", International Conference on the Theory and Application of Cryptology and Information Security, ASIACRYPT, Lecture Notes in Computer Science, vol 9453. Springer, Berlin, Heidelberg, 2014.
- [18] Lija Mohan, Sudheep Elayidom M, "Balanced MultiFileInput Split (BaMS) Technique to solve Small File Problem in Hadoop", IEEE 11th International Conference on Industrial and Information Systems (ICIIS), IIT Roorkee, India, 2016.
- [19] Lija Mohan, Sudheep Elayidom M. (2017) Encrypted Data Searching Techniques and Approaches for Cloud Computing: A Survey. In: Mandal J., Satapathy S., Sanyal M., Bhateja V. (eds) Proceedings of the First International Conference on Intelligent Computing and Communication. Advances in Intelligent Systems and Computing, vol 458. Springer, Singapore, 2016.
- [20] J.C. Lagarias, "The computational complexity of simultaneous diophantine approximation problems", SIAM Journal on Computing (SICOMP), Volume 14(1), pp 196–209, 1985.
- [21] P.Q. Nguyen, J. Stern, "Adapting density attacks to low-weight knapsacks", Proceedings of Advances in Cryptology, ASIACRYPT'05, pp. 41–58, 2005.
- [22] D. Coppersmith, "Small solutions to polynomial equations, and low exponent RSA vulnerabilities", Journal of Cryptology, volume 10(4), pp 233–260, 1997.
- [23] "The NSA Scandal's Impact on the Future of Cloud Security - Data Security and Protection in the Wake of the Spying Scandal", White Paper issued by Porticor, February, 2017. <http://mobility-sp.com/images/gallery/PORTICOR-The-NSA-Scandal%27s-Impact-on-the-Future-of-Cloud-Security.pdf>
- [24] Guidelines on Security and Privacy in Public Cloud Computing, NIST Special Publication 800-144, December 2011.

Strategic Framework and Maturity Index for Measuring Knowledge Management Practices in Government Organizations

Shilpa Vijaivargia

Head (IT), Consultancy Development Centre, Department of Scientific and Industrial Research, Ministry of Science and Technology, New Delhi, India

Dr. Hemant Kumar Garg

Lecturer (Selection Grade),
Govt. Women Polytechnic College,
Jaipur, Rajasthan, India

Abstract—Knowledge is considered as an intellectual asset of any Organization through which performance of the Organization could be enhanced exponentially. Harnessing of the Organization's Tacit and Explicit knowledge and its Management is a crucial task as Knowledge Management Practices adopted by Government Organizations are not standardized yet. They are depending on the structure and processes adopted by the organizations at their own level. This paper presents a Strategic Framework of Knowledge Management and defines Maturity Index at three levels for measuring Knowledge Management Practices adopted by an Organization. This paper defines Value of the Knowledge at all the three defined Maturity levels which is based on number of times the knowledge content is viewed, benefits gained against viewing such contents in terms of tangible asset and Socio-Economic Impact. Knowledge Management Practices adopted by Bharat Electronics Limited (BEL) studied and measured at the Maturity Level is defined in this paper.

Keywords—Knowledge; Explicit knowledge; Tacit knowledge; knowledge management; knowledge architecture; knowledge process framework; knowledge audit; maturity index; knowledge audit

I. INTRODUCTION

Knowledge needs to be managed timely and cost effectively in order to streamline processes. Storage of knowledge in structured manner generates a repository of it which would help in accessing the knowledge contents as per the requirements. Knowledge Management helps organization to perform its tasks with more efficacies in less time. If it is developed through IT platform, provides the overall strategy to manage the e-contents by providing Knowledge Management tools and techniques, monitoring updates on knowledge contents and define mechanism to access the contents as per the defined roles. Such a Knowledge Management System supports the concept of e-governance and becomes part of it.

The benefits of Knowledge Management in government are bringing conduciveness to enhance government's competence, raising government's service quality and

promoting development of e-repositories. It also helps in bringing transparency through execution of processes as per the defined rules and mechanism results in value oriented government. In today's digital era, success of e-governance depends and directly proportionate to knowledge management practices adopted by the Organization [1].

IT based Knowledge Management Practices had initiated in Indian Government Organizations three decades ago, but many of the Government organizations are still facing challenges to transform its knowledge available in manual processes into electronic format due to inappropriate categorization of data, non-structured storage, non-defining of schemas, metadata and ontology for government processes.

Knowledge, its Architecture and connecting elements in brief are described in Section II, Maturity levels for measuring Knowledge Management Practices adopted by the Organizations are given in Section III with a Framework of Knowledge Management Process Workflow. Knowledge Management Systems studied for BEL along with measuring its Knowledge Practices with the defined Maturity levels are given in Section IV. Limitations of the study are given in Section V. Conclusion and Future Work is provided in Section VI.

II. KNOWLEDGE, ITS MANAGEMENT AND ARCHITECTURE

Knowledge has been defined by various researchers. One of the definition is "Knowledge is a fluid mix of experience, values, contextual information and expert insight that provides a framework for evaluating and incorporating new experiences and information. It is often embedded not only in documents or repositories but also in organizational routines, processes, practices, and norms [2]". Similarly, Knowledge Management (KM) could be defined as "The creation and subsequent management of an environment, which encourages knowledge to be created, shared, learnt, enhanced, organized and utilized for the benefit of the organization and its customers" [3].

The architecture of Knowledge Management can be broadly categorized in the following four layers (Fig. 1):

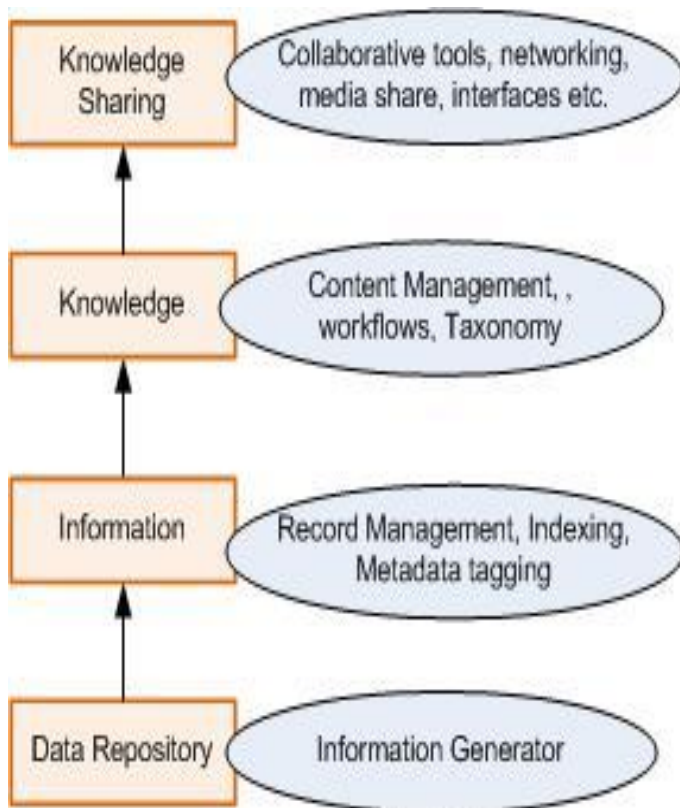


Fig. 1. KM architecture.

Generation of knowledge is based on data capturing techniques from data repository. The data is transformed into information through segregation of it on usability basis. The information gets classified through hashing, indexing and tagging which further converted into knowledge supporting taxonomies, workflows, multilevel navigation and federated search mechanism on the Content Management System (CMS) which can be shared through presentation interfaces and networking tools as per the defined rules.

III. MATURITY INDEX FOR ANALYSING KM IN AN ORGANIZATION

Though, various Knowledge Management Systems are available nowadays in standard and customized form such as Microsoft SharePoint, IBM Lotus Notes, SAP NetWeaver, Sales force, eXo platform, etc., yet there is no standard practice on which maturity level of KM Systems implemented by the organization can be measured [6]. KM practices at three levels are defined here. The characteristics of each level as defined are as follows:

A. Maturity level I- Beginner's Level

A KM activity initiated and carries out in the organization on voluntary basis. There is no well-defined Institutional framework for KM. Work related to KM activities carried by existing official giving him additional charge for it. Ontology, roles and privileges are not defined or strictly follow in binding with knowledge resources. IT enabled technology

does not well merge with the rules and procedures for KM and are not linked through Strategic goals of the organization.

Value of Knowledge (K_b) = (Number of times the uploaded Knowledge resources had accessed in a defined interval in a particular category/ Total Knowledge resources uploaded in that category) *100 (1)

Wherein

Defined interval = the time defined by the organization in which number of tasks were performed

B. Maturity level II- Intermediate Level

A team is placed to work, monitor and review Knowledge Management activities. Various initiatives are taken to promote KM in the organization such as direct talks, seminars, workshops, media promotional tools, etc. Technology leveraged to support Knowledge Management along with IT enabled features for navigation, search, role base authority, etc. Organization realises link of Strategic goals to available knowledge. The Value of Knowledge can be assessed as:

Value of Knowledge (K_i) = [(Number of tasks performed in reduced time in defined interval)/(Total number of tasks performed in defined interval)] *100 + K_b]/2 (2)

Wherein

Reduced time= the time which is less than (<) average time taken for performing a task in the defined interval

C. Maturity level III- Mature Level

A dedicated team takes care of KM related activities. Institutional mechanism supports KM activities which are linked to Organization's Objectives and strategic goals. Tools and technologies are enough mature to access, search and modify knowledge resources as per the assigned role privileges and could be upgraded as per the requirements. Uploading of knowledge resources aligned with process workflows related to role privileges and linked to Annual Performance Appraisal Report (APAR) of the employees. Knowledge Audit gets performed and total value of the knowledge can be assessed through Internal and External both factors.

Value of Knowledge (K_m) = [(Value measured in tangible form through Knowledge Audit on scale of 100) + (Conversion of Socio-Economic Impact of Knowledge through Knowledge Audit on scale of 100) + K_i]/3 (3)

Wherein

Knowledge Audit (Tangible form of Knowledge) = (Increase in performance of employee evident through measurements mentioned in their APAR)

Knowledge Audit (Intangible form of Knowledge which is Socio-Economic Impact) = Benefits in terms of socio-economic status by using the knowledge (based on inputs from knowledge users for a respective knowledge)

A Knowledge Management Process Framework is given below for all the three levels as aforesaid mentioned (Fig. 2).

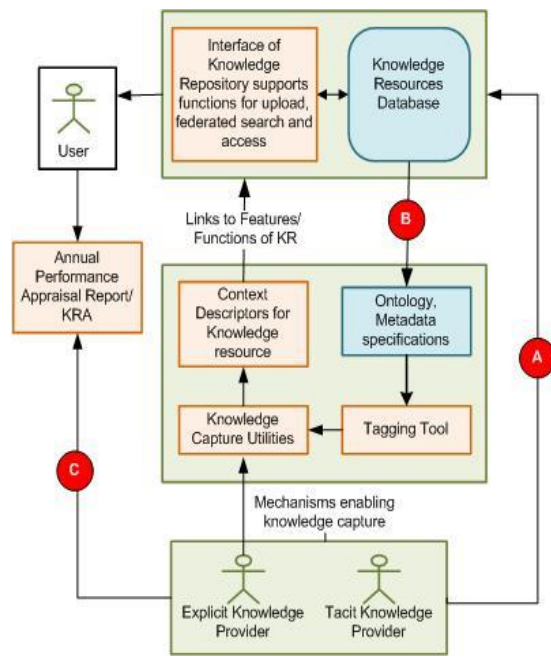


Fig. 2. Strategic framework of KM.

IV. KNOWLEDGE MANAGEMENT AT BHARAT ELECTRONICS LIMITED (BEL)

A. Background

Bharat Electronics Limited (BEL) was established by Government of India in 1954 under Ministry of Defence to cater Electronics need of Defence. It works in professional Electronics for Defence and other organizations. The work associated with BEL requires storage of voluminous and highly diverse documents which could be in the form of standards, manuals, technical specifications, research papers, articles, power point presentations, conference proceedings, e-books, workflow of procedures, contracts and agreements. Knowledge Management of such documents helps in reducing learning time period for a definite process workflow which results in increase of productivity of manpower [4].

B. Knowledge Management Workflow Adopted by BEL

A Knowledge Officer is designated to perform Knowledge Management related activities in BEL, which is supported by cross functional groups work in technology and innovation promotion. BEL encourages their employees to use KM Systems through circulation of Guidelines regarding access and use of KM Practices and workshops conducted time to time. KM system in BEL accepts knowledge pieces in the form of document, image or in other form. Knowledge contributor sends knowledge content(s) to Knowledge Officer along with context descriptor and other requisite details. Subsequent to the review and approval of Competent Authority on the sent content(s), it is accessible to its stakeholders based on their roles and authorized privilege for sharing and viewing [4].

C. Tools and Technology used for KM

BEL uses SAP based technology for its Knowledge Management Systems. The information may be captured from

file server or intranet as per its defined rules. The functional unit can integrate multiple repositories to share its contents due to which contents from various units of BEL could be shared and accesses through a centralized platform [5].

The System supports multilevel navigation and advanced search mechanism to access the information based on their privileged roles. Knowledge contents are classified through taxonomies as defined. This feature also supports online messaging and sharing of information on real time and concept of Virtual rooms [5].

D. Measurement of KM Systems at BEL as Per the Defined Maturity Index

Knowledge Management Systems at BEL supports in speeding of their deliverables through usage of available manuals, standards, workflows etc. Hence, standardization and dissemination of processes helps in achieving deliverables in time. The manpower exchange knowledge pieces through interactive platform as per the requirements and authorized privilege which helps in reducing the learning curve. However, some of the manpower is habitual to work on Windows platform did not find SAP based KM System much user friendly. Therefore, awareness about KM systems required to be further strengthened. KM systems at BEL found at Maturity level II- Intermediate level as defined in this paper with an interval of 10 days.

V. LIMITATIONS OF THE STUDY

Value of Knowledge can be measured at Maturity level I- Beginner's level and Maturity level II- Intermediate level on definite parameters as it is based on data analytics provided by the system supporting digital Knowledge Repository. However, Value of Knowledge at Maturity level III- Mature level cannot be analysed without sharing compiled information on the parameter: Number of Knowledge articles read through digital Knowledge Repository which has to link with Performance improved of the employee. Such information to be extracted from employee's APAR for the category of employees through which Value of Knowledge to be measured and a Review Report which has assessed Socio-Economic Impact of the Knowledge stakeholders in a particular category. Similarly, results extracted from Knowledge Audit which is conducted by third party on individual basis need to be shared for measuring Value of Knowledge at Maturity level III- Mature level.

VI. CONCLUSION AND FUTURE WORK

This paper defines Knowledge, its main elements, tool and technologies used for Knowledge Management in brief. Knowledge Management Architecture, a Framework containing process workflow of Knowledge Management Systems and Knowledge Management Maturity Index at three levels presented in the paper based on study and understanding of structure and processes followed by Government Organizations. Equations from extraction of Value of Knowledge could be extracted for each Maturity level. Learnings gained from study of BEL also helped in defining the framework and Maturity Index of Knowledge Management Systems in Government Organization.

Knowledge Management Practices adopted by BEL is mapped on the defined Maturity level.

Further, BEL or any other Government Organization may be mapped at Maturity Index and Value of Knowledge can be extracted from the relationships presented in this paper. Organizations' knowledge may be got audited and Value of knowledge may be extracted. Socio-Economic Impact and conversion of intangible benefits in tangible asset may be worked upon.

REFERENCES

- [1] Florian Resatsch et.al, Measuring the performance of knowledge management initiatives,2004
- [2] James Sheffield, Pluralism in Knowledge Management: a Review University of Auckland, New Zealand, 1998(URL: file:///C:/Users/shilpa/Downloads/ejkm-volume7-issue3-article190.pdf)
- [3] Angela Abell and Nigel Oxbrow, Competing with Knowledge, The information professional in the knowledge management age, 2006, Paperback 9781856045834
- [4] CDC Study Report by Deloitte, Study and Analysis of Knowledge Management Systems in Indian Government and Public Sector Organization for generating a model framework for Knowledge Management System including compilation of success stories, 2015
- [5] Knowledge Management for the Public Sector; Asian Productivity Organization, 2013,
- [6] Dr.Alea M. Fairchild, Knowledge Management Metrics via a Balanced Scorecard Methodology, 2002

Smart Card ID: An Evolving and Viable Technology

Praveen Kumar Singh¹, Research Scholar,
Department of Computer Application,
Shri Ramswaroop Memorial University,
Lucknow-Deva Road, India

Neeraj Kumar², Assistant Professor,
Department of CS & IT,
Babasaheb Bhimrao Ambedkar University (A Central
University) Satellite Campus, Teekarmafil, Amethi, India

Bineet Kumar Gupta³, Associate Professor
Department of Computer Application,
Shri Ramswaroop Memorial University,
Lucknow-Deva Road, India

Abstract—In today's world carrying a number of plastic smart cards to establish our identity has become an integral segment of our routine lives. Identity establishment necessitates a pre stored readily available data about self and to the administrator to authenticate it with claimer's personal information. There is a distinct requirement of a technological solution for nationwide multipurpose identity for any citizen across the board. Number of options has been exercised by various countries and every option has its own pros and cons. However, it has been observed that in most of the cases Smart Card solution has been preferred by a user and administrator both. The use of Smart cards are so prevalent that be it any profession, without incorporating its application, identity of any individual is hardly considered complete. In this paper, the principle aim is to discuss the viability of Smart Card technology as an identity solution and its ability to perform various functions with strong access control that increases the reliability of Smart Cards over other technologies. It outlines the overview of smart card technology along with its key applications. Security concerns of smart card have been discussed through an algorithm with the help of a division integer proposition. Possibilities of upgrading it with evolving technology offer it as a universal acceptability of identification. Capability of storing desired amount of information by an administrator to compute multiple operations to authenticate a citizen dictates its widening acceptability and an endeavor has been made in this paper to explain it through a proposed system flow chart.

Keywords—ISO; IoT; multipurpose; authentication; security; smart card reader; cryptography; identification technology; smart card application

I. INTRODUCTION

One takes today a burden of carrying a wallet with full of cards to establish his/her identity like official ID card, canteen cards, library cards, driving license, etc. Smart card ID has a potential to replace all these cards by a single smart ID cards to serve the desired purpose. Varieties of smart cards are available as on date with progressive technologies where developers use different data structures and standards for programming. In this paper, we will discuss about viability of smart cards as a solution to requirement of nationwide multipurpose smart ID for each and every citizen with continuous evolving technology. Our aim is to propose a viable technological solution for a single multipurpose smart

ID card to do away with carrying multiple cards by an individual. It will assist governments across the globe in better administration with cost effective solution for multiple application single smart ID cards. It will also need management of a large database with processing and scalable computing to home on desired ID. Data centers handling these big data are contributing in reducing the delay and costs in data processing and improving the quality of service to include certain discrete services using internet based services. A smart card is an electronic device with micro-processor based system containing embedded integrated circuits which can process and store a large chunk of data and applications [4]. A smart card reader is used to access the stored information and it is also called smart called terminal when a card is plugged into this reader. Apart from the card reader, radio frequencies are also used to operate a smart card. Different protocols are being used for different types of card readers to communicate between card and the reader.

The standard of security adopted in the smart cards defines the degree of protection about sensitivity and confidentiality of data against the breaches. The issue with smart cards is its data storage capacity and processing capability. If we choose to associate any new application with smart card then the security mechanism would require consume more space which in turn necessitates use of lightweight security algorithm. In this paper a hypothetical case of a division integer algorithm is taken and then a viable system has been proposed to ensure appropriate security measures and to combat epidemics of cyber-crimes. In this respect, all the states need stringent legislations with effective law enforcement to prevent any frauds [5]. The objective of this paper is to touch upon smart card technology and its viability as single ID alternative with desired identity standards by various states and to study its viability with feasible applications.

II. BACKGROUND

In order to drive any evolution, necessity propels an environment conducive to that particular commodity. The genesis of smart cards during later half of 1980's decade too in Europe was no exception. It was not security rather needs to do away with handling of large amount of cash which become the prime reason behind its evolution. The government of France used it as a technological solution against secure

financial transactions. However, varying nature of issues cropped up including fraudulent production and failure of transactions in establishing identities of those initial smart card holders which were quite primitive in nature. It drove the manufacturers to introduce the cryptographic session between the control terminals and smart cards. Possibility of any skimming of smart cards could be ruled out due to their non-visibility by anyone from outside and no clone of any smart chips could be generated. It had a positive impact on transaction time and it was more cost effective too. In 1990's when magnetic stripes were replaced by microchips, the huge investment with support infrastructure by telecom companies in US brought revolutionary changes in smart cards. In those years, offline authentication continued to happen in Europe and with newer applications, they still dominate the smart card industry [1]. In contrast, US had no trouble with respect to overhead costs due to non-committal of desired level of authentication and having no bandwidth limitations.

During initial years, smart cards were used mainly in telephonic and health sectors. Those cards were utilized as memory cards and their implementation in 1990's as e-purse was no less than a revolution. Subsequently, US and Europe both adopted secure microcontroller smart cards against all financial transactions with debit/credit cards. 9/11 tragedy forced the world to have a relook in identity issues against terrorism and illegal immigration which boosted the required changes and resulted evolution in smartcards. With continuous evolution, smart cards now offer an excellent opportunity to various governments worldwide to implement e-governance applications [2], [3]. Utility of smart cards range from different applications, such as public usages like driving license, e-passports, etc. to private usages as cashless payment system like e-purse, access cards for identity verifications, etc.

III. SMART CARD: AN OVERVIEW

A smart card is known as a portable device which can compute, store and carry the data in an embedded processor chip for verification of personal identity in a secure repository. A smart card can also store a data in relation to any individual in the form of a barcode which are extracted through an optical scanner. Barcode is a representation of data displayed in a stripe of alternate black and white lines which is machine readable optically illustration of an object that carries it. Barcodes are depicted in a smart card by parallel lines with varied spacing's and widths. The initial smart cards were contact based while the contactless smart cards came in the early 90s. Later, smart card with contactless ICs completely revolutionized the smart card applications and its utility.

The contactless smart cards offer a high order of comfort to a user whereas it can be read without any physical contacts with bar code readers. It also extends an advantage over contact smart cards in terms of costs, durability and reliability [6]. An easy carriage of such smart cards in a wallet offers a good convenience to the users. A dedicated and secure transmission protocol is employed in a contactless smart card which offers it an excellent security. A magnetic tape is attached in the form of a stripe in the magnetic stripe smart cards. Memory smart cards are having a peculiar feature of storing and carry information which may be personal,

financial or any other specific information. An embedded circuitry of IC on a card is referred as microprocessor smart cards which can process and store the subject data [7].

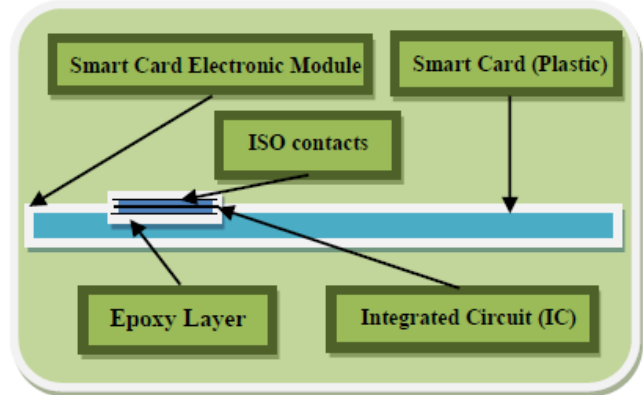


Fig. 1. Sideway structural view of a plastic smart card.

A sideways structural view of a plastic smart card is illustrated in Fig. 1 above. In order to protect the smart card chip from bends, it is generally placed on one of the edges of the smart cards. An Epoxy layer on this magnetic stripe is also visible when we take a view of its internal structure. Various applications, communication protocols and manufacturing specifications are defined by International Standardization Organization (ISO). Currently, there are following ISO standards for smart cards:

- A. *Physical Characteristics:* Initial ISO standard (ISO 7816-1) in 1987 defined the card size of a smart card as 0.76 mm thick, 53.98 mm height and 85.6 mm wide. It has again been revised in 1998.
- B. *Electronic Contacts:* ISO standard (ISO 7816-2) defined the size and location of the electronic contacts in smart cards. This too has been revised in 1998.
- C. *Electrical Signals:* ISO standard (ISO 7816-3) defined transmission protocol along with the nature of electrical signals in smart cards. It has been thrice in 1992, 1994 and 1998.
- D. *Communication Protocols:* ISO standard (ISO 7816-4) defined the communication protocols in different types of applications and file structure to be stored in these applications in smart cards. It has been revised twice in 1995 and 1998.
- E. *Language:* ISO standard (ISO 7816-7) defined the commands of query language used in smart cards. This has been revised again in 1998.

The use of internet technology has changed the whole perception of security systems. Smart card technology too is not an exception. Identification of an individual is to do more with secure authentication rather secure identification. Individual credentials are required to be stored in a secured manner for which a portable smart card provides a good platform. The transactions made through the magnetic stripe of smart cards are processed by an electronic connection

between the smart card and the service provider. Processor and memory chip in a smart card allows storing of required data which are processed by a smart card reader when connected through a centralized database [8]. Unlike the contact smart cards in which they have electrical contacts with a card reader, contactless smart cards operate through a transmission frequency and an internal antenna coil. It can be picked up and read through the external aerial.

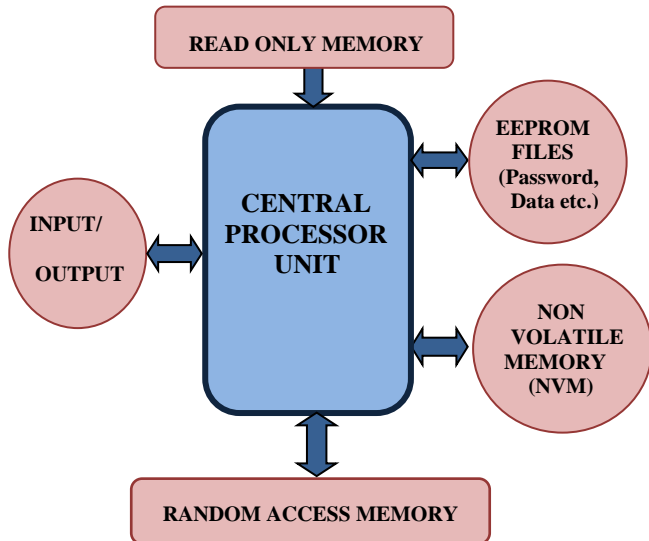


Fig. 2. Basic architecture of an electronic module of smart card.

TABLE I. PROCESS ENABLED VERSES MEMORY SMART CARD

Smart Card Features	Types of Smart Cards	
	Processor Enabled Smart Cards	Memory Smart Cards
Interfaces with Contact/Contactless Cards	Contact/Contactless/Both	Contact/Contactless/Both
Read Only Memory	YES	YES
Random Access Memory	YES	NO
Secure with Certified Data	YES	NO
Microprocessor	YES	NO
Example	Multi-Application Cards	Phone Card

The two most common materials utilized for manufacturing of smart cards are Acrylonitrile Butadiene Styrene (ABS) and Polyvinyl Chloride (PVC). There are two main categorizations of smart cards, namely, as processor enabled and memory smart cards. A relative comparison based on the various features between the two is shown above in Table I. Out of these two, memory smart cards are considered as basic smart cards with limited data storage capability with a nonvolatile memory features. These cards are transmitting data in only one direction and also termed as asynchronous smart cards and they are used offline only. On the other hand, processor enabled cards are using semiconductor technology and being a sophisticated cards they are also called as ‘true smart cards’. These cards have smart chip which operates cryptographic functions and encryption technology to process secure data transmission [9]. In general, biometric technology

is used to establish the identity of the user. These cards have bi-directional data transmission, possess significant memory and they are also termed as ‘synchronous smart cards’ and difficult to be duplicated. Data storage in such smart cards is nonvolatile and stored in EEPROM.

An electronic module of a smart card apart from an input/output component consists of different types of memories which include Read Only Memory (ROM), A (Random Access Memory), an electronically erasable Memory (EEPROM) and a non-volatile memory (NVM) as illustrated in Fig. 2 above. It is placed in the second layer of embedded processor chip of smart card as illustrated in the Fig. 1. These memory chips are incorporated in such electronic modules based on the projected requirement and at the same time presence of all memory chips is not sacrosanct. Bringing all these memories in a single integrated chip together not only reduces the size significantly, combining it with cryptography technology it also increases the security of smart card [10].

IV. SECURITY CONCERNS IN SMART CARD ID

The primary function of a multipurpose smart card ID is to establish the identity of the user. One way of establishing an identity of an individual is to recognize him or her by verbal or visual means. For verification of facts with respect to the individual encryption technologies are being used. With number of transactional applications are being prevalent in smart cards, use of PIN is the most common methodology to establish the identity for any user. However, the constraint is to remember the number of PINs for different applications for any user. Therefore, to overcome this binding, biometric technology for verification of identity of an individual was introduced [11]-[13].

Biometric technology measures individual personal features. Presently, there are various kinds of biometric technologies are being used like signature, Retinal, palm geometry, fingerprints, recognition of facials and voice signatures, etc. Table II below indicates a comparison amongst the different types of biometric technologies. It offers a relatively fair comparison on different parameters like rate of acceptance, rate of rejections and comparative costs, etc.

There are better security provisions in smart cards than the normal printed/magnetic stripe identity cards. The primary motive of this security is to offer an authenticated access control or establishing guaranteed identity before any financial transactions to all the users of Smart cards [14]. As the security infrastructure is handled by human therefore, attacks of malicious users or hackers cannot be ruled out. There are various kinds of provisions which are prevalent to address the security concerns which include like micro-printing, holograms, optically variable printing in the memory technologies of smart cards. While employing security system in a smart card, the basic principles of security remains same as Privacy, Non-repudiation, Authentication, Integrity and Verification [15], [16].

Various types of encryption algorithms are being used in security systems of smart cards. These security mechanisms require a robust key management with a well-defined

procedures and strong policy in place. A widely used public key infrastructure (PKI) security mechanism for data encryption ensures secure data exchange and confidentiality in most of these security systems. In order to establish authentication in security provisions like digital certificates or digital signatures, the encryption algorithms have a key role to play. Smart cards too make use of different encryption algorithms to implement the basic security principles [17]-[19].

TABLE II. A COMPARATIVE TABLE FOR SOME COMMON BIOMETRIC IDENTIFICATION (SOURCE: THE IBM SMART CARD DEVELOPMENT GROUP)

Methodology	Rate of Acceptance	Rate of Rejection	File Size in Bytes	Relative Cost of Device
Static Signature	20-90%	5%	1000-2000	Cheap
Dynamic Signature	20-70%	1-20%	40-1000	Medium
Hand Pattern	0-90%	5%	10-30	Medium to Expensive
Retinal Pattern	0-10%	1%	80-1000	Very Expensive
Fingerprint	0-100%	1-10%	300-800	Medium to Expensive
Voice Pattern	100%	10%	100-1000	Cheap
PIN	50%	1%	1-8	Very cheap

Let us take an example of a mathematical algorithm to be used for encryption of a message to be exchanged. A message is considered encrypted, if the information associated with the message can be veiled with some coding and it cannot be decipher by anyone until it is unveiled through decoding. The encrypted message is called crypto text while the normal message is called plaintext. In order to encrypt a message, one requires a key for coding which can be decrypted only if a receiver has same set of keys for decoding. For different individuals, different keys shall be required. Security of the key is of paramount importance against keeping confidentiality of information. As loosing either an encrypting or decrypting key to an eavesdropper can lead to compromise the entire message.

If the keys used for encrypting or decrypted the message is same then the procedure is called ‘Symmetric’, however if the keys are different then it is called ‘Non symmetric’. Usually, if one of the keys is available in public domain then the procedure is called ‘public-key cryptography’. Symmetric encryption is also referred as ‘cryptosystem’ if it is in the form of a quintet (F, T, R, E, D), where R is a finite key, F is the finite ‘message’ (plaintexts) and T is a finite ‘crypto text’. If for each key $r \in R$ then $e_r \in E$ stands for an ‘encrypting function’ and $d_r \in D$ stands for each ‘decrypting function’ whereas E is an ‘encrypting function’ which incorporates all achievable encrypting function. At the same time, D is referred as ‘decrypting function’ which incorporates all achievable decrypting function.

It signifies, $d_r(e_r(w)) = w$; where, w denotes the block message and r is referred to encrypting key.

A same message can be encrypted into different crypto texts by an encrypting function while encryption can be random and not a mathematical function. Mostly, all

common encryption procedures are used either on number theory or on algebraic functions.

Let us take an example of “long division” Newton’s method with a large base number in which M represents the dividend length whereas $O(M^2)$ indicates the basic operations. This method is quite efficient in which, m and n indicate divisor and dividend respectively. If we, assume $M > N$ where M refers to length of a dividend and N refers to length of divisor, we find the result as $m = qn + r$ in which q denotes quotient whereas r denotes remainder.

$$\text{If DIV } (m, n) = (q, r), \text{ then } q = \lfloor m/n \rfloor.$$

Now, let us commence through the results of the divisor’s inverse to obtain root of a function.

$$f(y) = n - 1/x, \text{ i.e. } 1/n, \tag{1}$$

If, we use the Newton iteration

$$y_{i+1} = y_i - \{F(y_i) / F'(y_i)\} = 2y_i - n y_i^2$$

and compute $1 = 10^N/n$, which indicates $g(y) = n - 10^N/y$ for a root of given function in which we achieve the accurate Newton iteration.

$$y_{i+1} = 2y_i - (m y_i^2 / 10^N) = 2y_i - (y_i^2 / L) \tag{2}$$

In order to stay solely on integers, we may utilize an account of this iteration which becomes proximity to integers:

$$x_{i+1} = 2x_i - \lfloor (n / 10^N) \lfloor (x_i^2 / 10^{M-N}) \rfloor \rfloor$$

In a decimal arrangement, divisions through powers of 10 become insignificant. The aim of doing it is to determine $\lfloor L \rfloor$, with the floor $\lfloor m10^{-M} \rfloor \lfloor L \rfloor$ we find the required result and finally obtain the remainder. The properties which may be validated are expressed as:

$2x - \lfloor n10^{-N} \lfloor x^2 10^{N-M} \rfloor \rfloor \geq 2x - x^2/L$, it also signifies that iterants values are not reduced by rounding the integers.

At the same time, if $y \neq L$ then $2y - y^2/L < L$. Because $m/10^N < 1$,

We, therefore, find following corresponding value for rounded iteration from (2):

$$\begin{aligned} x_{i+1} &= 2x - \lfloor (n / 10^N) \lfloor (x^2 / 10^{M-N}) \rfloor \rfloor \\ &\leq 2x - \lfloor (n / 10^N) \{ (x^2 / 10^{M-N}) - 1 \} \rfloor \\ &\leq 2x - \lfloor (x^2 / L) - 1 \rfloor < 2x - \lfloor (x^2 / L) - 1 \rfloor \\ &\leq 1 + 2 \end{aligned} \tag{3}$$

If $x < 1$ then $2y - y^2/L > y$; therefore the precise iteration grows till iterants become < 1 and the same phenomenon is applicable to a rounded iteration as well.

$$\text{When, we express } L = x_i + \epsilon_i \tag{4}$$

In which ϵ_i represents an error. In Newton’s methods for each correct number as per (3), amount compounds to double with each step and the same is applicable here as if $x_i < L$.

$$|\epsilon_i| = 1 - y_i \leq 1 - 2y_{i-1} + (y_{i-1}^2 / L) = (\epsilon_{i-1}^2 / L)$$

$$\begin{aligned}
 |\epsilon_i| &\leq (\epsilon_{i-1}^2 / L) \leq (1/L) (\epsilon_{i-2}^2 / L)^2 \\
 &\leq \dots \leq L^{-(1+2+2^2+\dots+2^{i-1})} \epsilon_0^{2^i} \\
 &= L^{(1-2^i)} \epsilon_0^{2^i} < 10^{(1-2^i)(N-M)} \epsilon_0^{2^i}
 \end{aligned}$$

In this case, it is deduced that $10^{(1-2^i)(N-M)} \epsilon_0^{2^i} \leq 1$.

Suppose that $|\epsilon_0| < 10^{(N-M)}$ which amounts to

$$i \geq \log_2 \lceil (N-M) / (N-M - \log_{10} |\epsilon_0|) \rceil$$

Therefore, we find,

$$x_0 = 10^{M-N} \lfloor (10^N / n) \rfloor \quad \text{or}$$

$$x_0 = 10^{M-N} \lceil (10^N / n) \rceil$$

It all depends upon that which is closure to $10^N / n$, when $|\epsilon_0| \leq 10^{M-N} / 2$, it then finds

$$\begin{aligned}
 I &= \log_2 \lceil (N-M) / (\log_{10} 2) \rceil \\
 &= \lceil \log_2(N-M) - \log_2(\log_{10} 2) \rceil \quad (5)
 \end{aligned}$$

Akin to the iterations numbers, a set of growing sequence of integers is produced by using rounded integers with iteration till we find a value within $[L, L + 2)$. Thereafter, we may check if it is the preceding correct value $[L]$ or the obtained value only. The entire procedure is as follows (output becomes $\text{DIV}(m,n)$):

Applicability of Newton's method: Division

We return (0, 0) and leave, if $m = 0$, we return (m, 0) and leave if $n = 1$ and with the corresponding value of equation (1), we return $(-p, q)$ and leave, if $n < 0$, we find $\text{DIV}(m, -n) = (p, q)$

We return $(-p - 1, n - q)$, if $q > 0$ or $(-p, 0)$, if $q = 0$ and leave, if $m < 0$, we find $\text{DIV}(-m, n) = (p, q)$

Length of divisor $n \rightarrow$ length of dividend m

and $N \rightarrow$ Set M

We return (0, m) and leave, if $M < N$,

We return $(p, m - np)$ and leave, if $M = N$, since $0 \leq p \leq 9$ (By trial), we easily find the quotient p

We find $\lfloor 10^N / n \rfloor$, if $M > N$, since $1 \leq \lfloor 10^N / n \rfloor \leq 10$ (By trial) And we set $10^{M-N} \lfloor 10^N / n \rfloor \rightarrow y_0$, or else we set $10^{M-N} (\lfloor 10^N / n \rfloor + 1) \rightarrow y_0$, if $10^N / m - \lfloor 10^N / n \rfloor \leq 1/2$ i.e.

$2 \times 10^N - 2n \lfloor 10^N / n \rfloor \leq n$, It is conditional with rider that at least one iteration has to be performed, if $y_0 > 1$

The recursion will be

$$x_{i+1} = 2 x_i \lfloor (n / 10^N) \rfloor \lfloor (x_i / 10^{M-N}) \rfloor$$

It will commence from x_0 till $i \geq 1$ and $x_{i+1} \leq x_i$.

It is checked through multiplications that either of the findings of $x_i, x_i - 1, \dots$ is right $\lfloor \rfloor$ and $\lceil \rceil \rightarrow$ set q

$mp/10^M \rightarrow$ We set t (a multiplication) and verified by multiplications only as to which value t or $t + 1$ is the right

quotient p in division $\text{DIV}(m, n) = (p, q)$. We find $(p, m - np)$ and then we may leave.

$$p = (m - q) / n \leq n / m < (10^M / n) \quad (6)$$

The accurate quotient is produced as #12 because firstly $q < n$ and then further, if $\text{DIV}(10^M, n) = (k, q')$ then $q' < n$ and

$$\begin{aligned}
 mk / 10^M &= (pn + q') (10^M - q) / n 10^M \\
 &= p - (p q' / 10^M) + q \{ (10^M - q') / n 10^M \} \quad (7)
 \end{aligned}$$

On the right side of middle term in a interval is $(-1, 0)$ and the last term becomes $[0, 1)$. Therefore, p is having a value of either $t+1$ or t .

Since the iterations become very small due to the maximum number of 1 for the length M with the algorithm difference of the dividend and for the length N of the divisor whereas there are always at least three multiplications with an iteration step as described in 6 and 7 and for a maximum of length $2N$, there will be at least one subtraction for integers (some will remain constant). That is just an example of a division algorithm that is how it ensures security of information exchanged between two users.

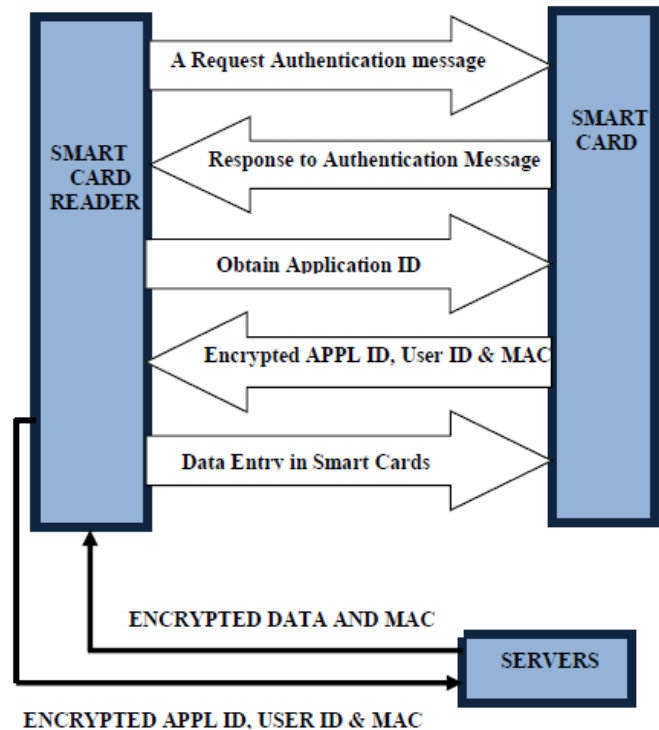


Fig. 3. Authentication process in smart card.

Let us also examine another cryptography technique of an authenticated encryption. This technique is used to ensure integrity and confidentiality of data. A Message Authentication Code (MAC) is combined with this and a symmetric encryption algorithm is used in this technique. In order to see how a smart card uses the symmetric encryption, we need to go through the mutual authentication process between a smart card and a smart card reader [20]. This authentication process requires a source of data which is

provided by a server which holds a data structure for number of users.

The above mentioned flow amongst the server, a smart card and a smart card reader explains the authentication process in Fig. 3. In this process, the moment a smart card comes in contact with a card reader, an initial request of authentication is processed by smart card reader. Once the response from smart card is received by the card reader, an application ID is issued by smart card reader. It is responded by smart card with a user ID and a message authenticated code which is followed by an encrypted data feeding to smart card by the card reader [21], [22]. Meanwhile, the card reader is also attached to a server which responds with the user ID and an application ID along with a message authenticated code which precisely describes the authentication process in a smart card.

User trust is an important factor for success of any security system. Security measures used in a smart card needs to ensure of prevention of loss of data due to any human error or ill intent. Presently, encryption technology with computers is widely used for transmission or exchange of information. Ciphers were the most common methods to ensure security of data. Since, the complex security algorithms like DES, AES and many others are associated with data, probability of any direct attack is very minimal in various data transmission associated technologies including smart card security systems. However, a side channels attack on software and hardware systems of smart card cannot be ruled out. A malware to capture the key mechanism of security system may be employed by an attacker. Likewise, use of spy camera and other hardware technology to breach the security system of smart card to track the human implementation of encryption technology too warrants a high degree of caution while implementing the smart card technology [23].

V. SMART CARD APPLICATIONS

The major advantage of a smart card over a normal ID card is its capacity to store larger amount of information and its programmability for various applications. Its feature of having a possibility through contactless readers gives it an edge over similar technologies in pursuits of finding a nationwide single ID for multiple usages. The term 'smart', relates with a particular type of application like memory/magnetic stripe/optical/microprocessor cards. The larger application of smart cards is its utility in financial transactions with faster processing of revenues or payments [24]-[27]. Its capability to carry the related information of an individual and to deliver it at desired destination distinguishes it from other such applications in identifying the veracity of the individual.

Smart card applications include its use as GSM mobile phone for the identity requirements. It's wider use as a banking card in the form of debit/credit cards or being a tamper-proof/counterfeit device increase its popularity. Electronic coupons and credit programs are other attractive applications of smart cards [28]. The inherent security and flexibility of smart cards increases its utility. With improved data storage and security supplemented with provisioning of encryption and decryption by a user offers high rate of

convenience to users. Some notable applications of smart cards are as:

- A. *ID Validation*: The basic premise of storing the individual information is to verify him/her for any further uses in smart cards. Currently, A large number of organizations and institutions including government and private both are using smart card to extend access control to their members/employees only after due verification of their ID based on their personal information stored in their smart ID cards. It's viability as an option for secure ID credential verification makes it a lucrative tool to be adopted by every potential organization.
- B. *Data Authentication*: Information with respect to the user is authenticated by the data already stored in the smart card or a token system also known as knowledge arrangement based may be exercised for the purpose [29]. Token systems are generally employed in applications like passport verifications; credit cards, driving license, etc. whereas knowledge based authentications are exercised in applications with tokens system like PIN numbers.
- C. *Financial Transactions*: Smart cards are very handy as a tool for financial transactions both in traditional and web based applications. A cash value can be stored in smart cards to use it as credit cards. It's potential to support both consumers and business against lower rate of transactions widens its applicability in marketing targeted programs in financial services.
- D. *Telecom Sector*: Provisioning of secure cellular communication is assisted by smart cards. New apps and functions are providing real time download capabilities by smart cards [30], [31]. A SIM card given by cellular operators to their subscribers and its use of multimedia applications like pay TV cards are making a very productive tool amongst normal public.
- E. *Loyalty Marketing Programs*: A huge number of loyalty programs are being run by smart cards based applications by various business houses in services like retail shopping, telecommunications, air travel, etc. in which customers are being offered very attractive discounts. Such applications not only make business market very competitive, it also helps to normal public to receive benefits at relatively lower rates.
- F. *Secure Computer Networks*: A secure access for networks can be assured through digital signatures of a user. They are utilized in granting only specified people to have the access to a particular computer network [32]. This mechanism is very handy and vital for the security related organizations. Encryption technology is making today computer networks more secure than the erstwhile networks.
- G. *Healthcare*: Professionals from healthcare services are using smart card based applications to gain access for continuous updating of their data and its processing. A colossal amount of information is being shared in the form

of drug prescription, physician details, dosage, etc. by these professionals. Patients use smart cards to provide their pre stored medical history with doctors and in making payments of their medical treatments as well.

H. Other Smart Card Applications: Its flexibility and potential to have repository of information supports it in vast number of applications. With secured online transactions in many commercial activities augurs well for both the service provider and subscribers. A wide range of services which are exploiting the smart card based applications include agricultural products, Life Insurance sector, vending machines, libraries, restaurants, laundry services, set top box facilities, software based games for kids, electronic toll collection, information technology, mass transit, parking facilities, e-passports etc. are just the few names to be counted [33]. Utility services like payment transaction, call counters, memory storage etc. employ smart card based applications.

Earlier, the smart cards were used as a memory card or PC cards. However, latest ones are having a smaller size, lighter weights, better storage capacity with lesser power needs are able to influence a wider chunk of applications. By using the radio frequency with inbuilt antenna embedded in the smart card, it enables data transmission without any physical contact with the card reader from a distant terminals. Pre fielded biometric data about the user like, fingerprints, retina/iris scan; DNA pattern etc. increases its credibility in user's authentication. Smart cards do possess ability to assist in garnering demographic data for exercising the franchise by the voter. Industry association of smart cards has reported about use of billions of smart cards in healthcare, family planning, individual IDs and in many other applications [34]. The factors like privacy, economy, legal and technological issues require a continuous address due to its widespread usage. Worldwide, travelers are using it as an international traveler check which is facilitated by secured transactions.

VI. RESEARCH APPROACH

On one hand, where internet has revolutionized the world, it has also driven the life from being physical interaction to virtual world. The basic challenge in this scenario is to facilitate it with an instrument which can guide people to identify the differences between real and the virtual world. Smart cards have ensured that there is no need for physical presence. It's more of an authentication than the identification now. Individual credentials should be authenticated by a well-defined entity within the structured legal framework of all the user states. Securing all the individual credentials should be the top priority of all the administrators of smart card technology. Use of cryptographic technology is one of the recommended options to be exercised upon [35]. Since, security concerns demand that all the security measures should be progressive with evolving technology as it affects same both for malicious attackers and the users.

The main application approach with respect to smart card technology has now been driven from having a secured ID to multifaceted smart card applications which can offer not only the authentication for a an administrator, it should also assist

the user to access a wide range of applications offered by the smart card technology. Focus gradually has shifted from the contact to contactless application in respect of smart card technology which facilitates the user to avail the various types of applications from a distant location. Radio frequency driven communication for the smart card applications is vital as it allows the transactions exercised by the cardholder and the administrator both. The objective of this technology is to bring upon a solution which can facilitate the provisioning of a single card to a user to use it not only as an authentication tool for him/her, it should also offer a viable option for many other applications [36]. Smart card exactly fits in this framework due to its inherent flexibility and security.

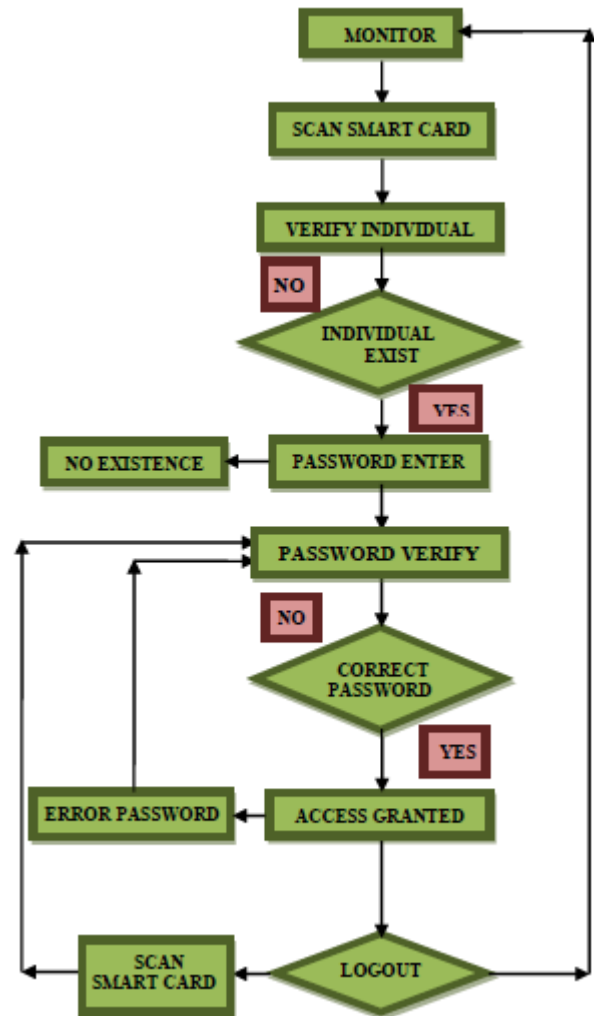


Fig. 4. Flow chart for smart card login.

In order to have the unambiguous understanding of functionality, let us have a look on a flow chart of a small application of a smart card as illustrated in Fig. 4 below. To access the database of any application for establishing the credentials, all individuals will be required to login. It can provide the required interface for all individuals in possession of smart cards to access the desired application. Initially, the user needs to scan his/her smart card through the designated card reader. The system then verifies the personal credentials

of user from the database and if, the login ID exists, it asks the verification code which may be a PIN number or a password. In case the user's login credentials are verified, access is granted by the system. However, if login credentials of user do not match then the password/incorrect PIN whichever is applicable is reflected by the system with request to re-enter the access code [37]. This repetition of access is granted only for finite number of times or with restriction of certain seconds and thereafter the access of that smart card may invite temporary/permanent blockade of card.

This complete cycle of processing of authentication of a user of smart card has been shown below in the algorithm through a flow chart. This module can also be used for uploading of various subjected documents for a particular application provided that administrator of that application has granted that access right to that user. The distinct advantage of this access is that user does not need to carry all the documents all the time and they are available in the database repository of server which can be accessed at any point of time whenever needed by the user through his/her access rights.

The proposed algorithm is a basic system module which can be customized for any application of smart card technology based on the particular requirement of the organization/institution. To design a smart card application demands first to design the smart card with desired specification of the card itself [38]. A well thought out plan to be put on board regarding amount of data required to be stored, suitability of a particular application in the desired operation, kind of customization required in the existing tools, etc. The security concerns of the particular applications demands utmost attention. Adequate resources are required to be earmarked for exact authentication to the specific user so that rightful allocation of designated benefits can be assigned. Prevention of any unauthorized access is needed to be ensured. In all the arrangements where financial transactions are involved, a cap for every single as well as for the overall transactions must be exercised to rule out any kind of fraudulent or abuse against any individual or an institution. Our research approach is to propose a solution through smart card technology which facilitates in achieving the digital and cashless economy.

VII. FUTURE SCOPE OF RESEARCH WORK

In last two decades a large amount of work has been put in development of smart card ID technology. Whether it is establishing an online authentication of a user, implementation of government run services or even execution of digital signatures, all these related issues have been dwelled in quite deliberation. Countries, like Germany, Italy, Mexico, Taiwan and many other countries worldwide are in the process of implementation of National E-Id. There is a need of elaborative plan to be adopted by all the countries whosoever are aspiring to implement it after thoroughly evaluating opportunities and challenges. A comprehensive guideline which is easy to assimilate by the user is required to be issued before implementation of such nationwide multipurpose smart card identity projects. The hardware involved must be cost effective with higher adoption rates in order to absorb the vast

infrastructure during execution of such projects. There is a need to gain a good trust of the citizens for any country with easier use and larger acceptance before implementing such public projects.

To understand the software application dynamics of smart cards or its advantages over a computer based platform, we require a closer look of its evaluation in this respect. One most prominent advantage of smart card is its relatively quiet lesser vulnerability from Trojan horses or viruses/malwares compare to PC based platforms. Protection of data is ensured by stronger security mechanism in smart cards [39]. While any new smart card applications come in force, it is thoroughly evaluated and validated by independent certification agencies with respect to its provisioning or sustenance of degree of security. Since, the attackers too keep applying different methodology to find their way through the vulnerability of the system, there is a continuous requirement for an administrator using smart card technology to keep evolving themselves with latest threats or malpractices used by the attackers. Despite of a continuous evolving technology, there are certain points which can be identified as future scope for the smart card technology and these points are:

- 1) Focus on evolution of transistor technology of smart chip for better integration of new hardware applications. Due to space constraints, area required for inclusion of new circuitry in the chip is always a challenge.
- 2) Rate of power dissipation of smart card batteries too require adequate attention. A continuous endeavor to increase the battery life of smart card demands ample consideration in the design technology of its power circuits.
- 3) Credibility of any technology lies in its scope and reach to draw desired amount of benefit accrued out of this. It dictates to deliberate for a larger amount of applications of smart card technology for maximum gains to people. It must be ensured by a wide range of applications in all the walks of life.
- 4) Interoperability of smart card technology with other evolving technologies must be assured. Various networks operating in the complex internet environment have different communication protocols. Synchronization with these networks is the key for success of smart card technology [40].
- 5) The operating system of software used in this technology is another area which warrants desired amount of consideration. Smart card system requires an uninterrupted connectivity with other information systems in pursuit of matching pace with other evolving technology.
- 6) A concerted effort is needed to meet the challenges posed by an attacker on vulnerabilities of security threats on smart card technology both for hardware and software mechanisms.
- 7) Sensors, special material for design, alarm systems, inclusion of complex cryptographic algorithm, lower dimensional optimization are just the few other suggested areas which do require additional focus.
- 8) A consolidated single multipurpose global smart card ID to do away with all other kinds of identity requirements

should be the ultimate aim of smart card technology [41]. It may necessitate associating various other evolving technologies with this to accomplish the desired outcome.

VIII. CONCLUSION

The emphasis on correct identification of every citizen is the basic proposition of all the sovereign governments across the globe. Perceived security threats to existing identification technologies are compelling factors to pursuit for evolving smart card technology. Security mechanism incorporating the complex encryption technology in place by this technology makes it more attractive compared to similar other available applications. This is a tool which offers to store and use the minimum desired data against a set of people or entity [42]. A suitable authentication scheme and security algorithm for faster and protected processing of data is always a challenge for any such technology. The above proposed study illustrates that user acceptance for constant evolving smart card technology will be the most prominent factor for the expected outcome. Further studies on the smart card system are likely to bring better dividends on issues as discussed in the subjects to be dealt with in above mentioned future scope.

Adaptability of this multifunctional technology in Internet of Things (IoT) with varieties of purposes makes it a lucrative proposition for commercial aspirants. Concerns on accessibility for both physical and logical control of the smart card applications are needed to be addressed adequately. The underlying intent of this research paper is to make the most of the smart card technology to exploit it to the fullest for the benefit of civilization. Endeavor is to combine all the existing traditional identity technologies and propose a workable single multipurpose identity supported by smart card technology [43]. Simplicity in use and robustness of the system must be assured in all the applications of this technology. A fundamental prerequisite for any modern technology including smart card technology increasingly relies on its adjustment with all accessible applications by of online services. The degree of convenience, cost effectiveness, multi-application solution and reasonable execution time for transactions are some of the few factors contributing in successful implementation of the smart card technology [44]. Above all, potential of this technology to replace all existing identity solution shall lead to a much desired instrument for all the government across the world to exercise their authority on their citizens and to ensure that all the warranted privileges to be driven to the deserving entities only. Implementation of a nationwide single multipurpose smart card ID will enable to carry forward the vision of having a worldwide single global ID for every user across the globe.

ACKNOWLEDGMENT

We are humbled to acknowledge the priceless guidance offered by Prof. (Dr.) Mukul Misra, Director (Research & Consultancy) Shri Ramswaroop Memorial University, Lucknow-Deva Road, 225003, U.P., India for this research paper. We are also indebted to Col A.K. Singh, Ph.D., Vice Chancellor, Shri Ramswaroop Memorial University, Lucknow-Deva Road, 225003, U.P., India for his precious

guidance in making this paper in the desired shape. We record our deepest admiration of Col V.K. Tiwari, Ph.D. for his invaluable suggestions.

REFERENCES

- [1] Munizaga, Marcela A and Carolina Palma, "Estimation of a disaggregate multimodal public transport origin-destination matrix from passive smartcard data from Santiago to Chile" in Transportation Research Part C: Emerging Technologies 2012, vol. 24 pp. 11-17.
- [2] Sven Vowe, Ulrich Waldmann, Andreas Poller and Sven Türpe, "Electronic Identity Cards for User Authentication Promise and Practice", IEEE Security & Privacy January/February 2012, vol.10, No. 1, pp. 48-53.
- [3] Y. Wang and X. Ma, "Development of a data-driven platform for transit performance measures using smart card and GPS data" J. Transp. Eng 2014, vol. 140 no. 12 pp. 4026-4053.
- [4] M. Batty, C. Zhong, J. Wang, E. Manley, F. Chen, Z. Wang and G. Schmitt, "Variability in regularity: Mining temporal mobility patterns in London Singapore and Beijing using smart-card data" PLoS ONE 2016, vol. 11 no. 2 pp. 1-15.
- [5] M. Mesbah, A.A. Alsger and L. Ferreira, "Use of smart card fare data to estimate public transport origin-destination matrix" Transp. Res. Rec. J. Transp. Res. Board 2015, vol. 2535, pp.89-94.
- [6] Y. Asakura, T. Kusakabe and T. Iryo, "Estimation method for railway passengers train choice behavior with smart card transaction data" Transportation 2010, vol. 37 no. 5, pp.732-747.
- [7] C. Morency, M. P. Pelletier and M. Trépanier, "Smart card data use in public transit: A literature review" Transp. Res. C Emerging Technol 2011, vol. 19, no. 4, pp.558-567.
- [8] Al Khouri A. M, "Targeting Results: Lessons Learned from UAE National ID Program", Global Journal of Computer Application & Technology 2012, vol. 2, no. 1, pp.832-835.
- [9] Albert Levi and Omer Mert Candan, "Robust Two-factor smart card authentication", IEEE International Black Sea Conference on Communications and Networking (Black Sea Com) Year: 2017, pp.1-4.
- [10] Jisung Kim, Hyongmin Lee, Taehoon Kim, Dongwoo Ha and Suhwan Kim, "Differentiating ASK Demodulator for Contactless Smart Cards Supporting VHBR", IEEE Transactions on Circuits and Systems II: Express Briefs 2015, Vol 62, Issue: 7, pp.642-644.
- [11] A. M. Ali and H. K. Lu, "Making Smart Cards Truly Portable," in IEEE Security & Privacy 2010, vol. 8, no. 8, pp.29-33.
- [12] Latifa Oukhellou, Michel Verleysen, Mohamed K, El Mahrsi and Etienne Come, "Clustering Smart Card Data for Urban Mobility Analysis", IEEE Transactions on Intelligent Transportation Systems Year: 2017, Vol 18, Issue: 3, pp.714-725.
- [13] Goswami A, Odolu V and Das AK, "A secure biometrics-based multi-server authentication protocol using smart cards", IEEE Trans In Forensics Secure 2015, vol 10, pp.1962-1964.
- [14] Moradi A, Schneider T, In Güneysu G and Handschuh H, "Leakage Assessment Methodology - A Clear Roadmap for Side-Channel Evaluations", Cryptographic Hardware and Embedded Systems, Springer-Verlag, CHES 2015, volume 9293 of Lecture Notes in Computer Science; 496-511.
- [15] Ashok Kumar Das, Kee-Young Yoo, Alavalapati Goutham Reddy and Eun-Jun Yoon, "Lightweight authentication with key-agreement protocol for mobile network environment using smart cards", IET Information Security 2016, vol 10, Issue 5, pp.274-280.
- [16] C. Kumar, W. Sharon Inbarani, Charlie Paul, G and Shenbaga Moorthi "An Approach for Storage Security in Cloud Computing- A Survey", International Journal of Advanced Research in Computer Engineering & Technology (IJARCET) January 2013, vol 2, Issue 1.
- [17] Zhang QM, Ma CG and Wang D, "Cryptanalysis and improvement of dynamic ID-based authentication scheme", in ICDCIT Springer: Berlin/Heidelberg 2012, vol. 7154, pp.143-151.
- [18] Wu S and He D, "Security flaws in a smart card based authentication scheme for multi-server environment", Wireless Personal Communications 2012; DOI: 10.1007/s11277-012-0696-1.

- [19] A. K. Das, "Analysis and improvement on an efficient biometric-based remote user authentication scheme using smart cards", *Information Security IET* 2013, vol. 5, no. 3, pp.147-150.
- [20] N.W. Lo, J. L. Tsai and T. C. Wu "Novel anonymous authentication scheme using smart cards", *IEEE Trans. Ind. Informant* Nov 2013, vol. 9, no. 4, pp.2006-2011.
- [21] Wang C, X. Li, J W. Niu, J. Ma, W D. and L. Liu "Cryptanalysis and improvement of a biometrics-based remote user authentication scheme using smart cards", *Journal of Network and Computer Applications* 2011, vol. 34, no. 1, pp.74-78.
- [22] K. B. Bey and F. Benhammedi, "EMBEDDED FINGERPRINT MATCHING ON SMART CARD", *International Journal of Pattern Recognition and Artificial Intelligence* 2013, vol. 27.
- [23] Won D, Choi Y and Lee, Y, "Security improvement on biometric based authentication scheme for wireless sensor networks using fuzzy extraction", *Int. J. Distrib; Sens Netw* 2016, pp.1-14.
- [24] S.V.K. Llingeswaran and Arul Das, "GPS Based Automated Public Transport Fare Collection Systems Based On Distance Travelled By Passenger Using Smart Card", *International Journal of Scientific Engineering and Research (IJSER)* March 2014, vol. 2, issue 3.
- [25] Ferreira L, Alsger AA, Safi H and Mesbah M, "Use of smart card fare data to estimate public transport origin-destination matrix Transportation research record", *J Transp Res Board* 2015, pp.89-94.
- [26] Dobraunig C, Joye M, Mangard S, Eichlseder M and Moradand Mendel F, "On the Security of Fresh Re-keying to Counteract Side-Channel and Fault Attacks". In *Smart Card Research and Advanced Applications - 13th International Conference*, Springer - Verlag, *CARDIS 2014*, volume 8968 of *Lecture Notes in Computer Science*, pages 235–242.
- [27] Chengzhong Xu, Fan Zhang, Lei Rao, Juanjuan Zhao, Chen Tian and Xue Liu, "Spatiotemporal Segmentation of Metro Trips Using Smart Card Data", *IEEE Transactions on Vehicular Technology* 2016; vol: 65, Issue: 3, pp.1139-1146.
- [28] P. Venkatesh, R. Padmavathi, K. M Mohammed, Azeezulla, Mahato G, Kanchan Kumar and Nitin, "Digitalized Aadhar enabled ration distribution using smart card", *2nd IEEE International Conference on Recent Trends in Electronics, Information & Communication Technology (RTEICT)* 2017, pp.616-617.
- [29] K. Kyoungtae L. Inmook and M. Jaehong "Analyzing passenger's tagging behavior using smart-card data", *Proc. of the 2014 Conf. of the Korean Society for Railway* October 2014, pp.636-637.
- [30] J. Y. Kuo and C. C. Chang, "An efficient multi-server password authenticated key agreement scheme using smart cards with access control" *Proceedings of International Conference on Advanced Information Networking and Applications* Mar 2005, vol. 2, no. 28-30, pp.258-259.
- [31] P. R. White and M. Bagchi, "The potential of public transport smart card data", *Transport Policy* 2005, vol. 12, no. 5, pp.467-473.
- [32] C. Seaborn J. Attanucci N. Wilson, "Analyzing multimodal public transport journeys in London with smart card fare payment data", *Transp. Res. Rec. J. Transp. Res. Board* Dec 2009, vol. 2121, no. 1, pp. 57-61.
- [33] K. Markantonakis and K. Mayes, "Smart Cards, Tokens, Security and Applications", Springer, January 2008.
- [34] S. Feng, J. Zhao C, Tian F and Zhang C. Xu, "Understanding temporal and spatial travel patterns of individual passengers by mining smart card data" *Proc. IEEE 17th ITSC* 2014, pp.2992-2996.
- [35] Liu L, F. Zhang, C. Tian, J. Zhao, C. Xu and X. Rao, "Spatio-temporal segmentation of metro trips using smart card data", *IEEE Trans Veh Technol* Mar. 2015, vol. 65, no. 3, pp.1139-1147.
- [36] M. Mesbah, A. Alsger, L. Ferreira and H. Safi, "Use of smart card fare data to estimate public transport origin-destination matrix", *Transp. Res. Rec. J. Transp. Res. Board* 2015, vol. 2535, pp.89-95.
- [37] Premila Bai, T Daisy Rabara M, S Albert and Vimal Jerald, "An Adaptable Secure Smart Card Architecture for Internet of Things and Cloud Computing", *IJRET* 2016, vol. 5, pp.163-169.
- [38] Etienne Come, Mohamed K, El Mahrsi, Michel Verleysen and Latifa Oukhellou, "Clustering Smart Card Data for Urban Mobility Analysis", *IEEE Transactions on Intelligent Transportation Systems* 2017, vol. 18, Issue: 3, pp.718-727.
- [39] K. Michael Raj, T. Daisy, Premila Bai and S. Albert Rabara, "Elliptic Curve Cryptography Based Security Framework for Internet of Things (IoT) Enabled Smart Card", *World Congress on Computing and Communication Technologies (WCCCT)* 2017, pp.44-45.
- [40] S. A. Suandi and V. T. De Zhi "Fingercode for identity verification using fingerprint and smart card", *10th Asian Control Conference (ASCC)* 2015, pp.1-5.
- [41] R. Chakra, R. Lamrani, J. L. Lanet, G. Bouffard, A. Mestiri, M. Monsif and A. Fandi, "Memory forensics of a java card dump", in *Smart Card Research and Advanced Applications*, Paris; France, Springer 2014, pp.4-15.
- [42] A. Bhaskar, L. M. Kieu and E. Chung, "Passenger segmentation using smart card data", *IEEE Trans. Intell Transp Sys* Jun 2015, vol.16, no.3, pp.1539-1546.
- [43] Lai Tu, Juanjuan Zhao, Fan Zhang, Dayong Shen, Chengzhong Xu, Xiang-Yang Li, Chen Tian and Zhengxi Li, "Estimation of Passenger Route Choice Pattern Using Smart Card Data for Complex Metro Systems", *IEEE Transactions on Intelligent Transportation Systems* 2017, vol. 18, Issue 4, pp.792-800.
- [44] Himanshu Thapliyal, Azhar Mohammad and S. Dinesh Kumar, "EE-SPFAL: A Novel Energy-Efficient Secure Positive Feedback Adiabatic Logic for DPA Resistant RFID and Smart Card", *IEEE Transactions on Emerging Topics in Computing* 2016, vol. PP, Issue: 99, p.1.

A Smart Under-Frequency Load Shedding Scheme based on Takagi-Sugeno Fuzzy Inference System and Flexible Load Priority

J. A. Laghari¹, Suhail Ahmed Almani²,

Department of Electrical Engineering, Quaid-e-Awam
University of Engineering Science & Technology, (QUEST)
Nawabshah, 67480, Sindh, Pakistan

Hazlie Mokhlis⁴

Department of Electrical Engineering, Faculty of
Engineering, University of Malaya, 50603 Kuala Lumpur,
Malaysia

Jagdish Kumar³

School of Technology and Innovations, University of Vaasa,
Finland,

Department of Electrical Engineering, Quaid-e-Awam
University of Engineering Science & Technology, (QUEST)
Nawabshah, 67480, Sindh, Pakistan

Ab Halim Abu Bakar⁵

University of Malaya Power Energy Dedicated Advanced
Centre (UMPEDAC), Level 4, Wisma R&D UM, Jalan
Pantai Baharu, University of Malaya, 59990 Kuala Lumpur,
Malaysia

Abstract—This paper proposes a new smart under frequency load shedding (UFLS) scheme, based on Takagi-Sugeno (TS) fuzzy inference system and flexible load priority. The proposed scheme consists of two parts. First part consists of fuzzy load shed amount estimation module (FLSAEM) which uses TS-fuzzy to estimate the amount of load shed and sends its value to accurate load shedding module (ALSM) to perform accurate load shedding using flexible load priority. The performance of the proposed scheme is tested for intentional islanding case and increment of sudden load in the system. Moreover, the response of the proposed scheme is compared with adaptive UFLS scheme to highlight its advantages. The simulation results show that the proposed UFLS scheme provides the accurate load shedding due to advantage of flexible priority whereas adaptive UFLS scheme due to fixed load priority does not succeed to achieve accurate load shedding.

Keywords—Distributed generation (DG); flexible load priority; fuzzy load shed amount estimation module (FLSAEM), islanded distribution network; under-frequency load shedding (UFLS)

I. INTRODUCTION

The global apprehension on environmental security and deregulation in the power industry has make it inevitable to utilize the DG resources for the production of electrical energy [1]. Currently, most of DGs are operating in parallel with the utility grid to fulfil the enhanced demand of load. However, in case of islanding event, these DGs are disconnected from the grid to avoid any severe consequences. Islanding condition is a phenomenon in which distribution system is isolated from grid due to severe fault; yet continue to be supplied from the distributed generation unit connected to distribution system [2]-[4].

Islanding may cause several safety hazards issues, power quality issues, voltage and frequency stability issues during islanding. Due to the aforementioned severe consequences of

islanding, it is recommended by the IEEE Std 1547 [5], and IEEE Std 929 [6] to disconnect the DG within 2 seconds from the distribution network. However, if DG is isolated from the distribution network then its full capacity will not be utilized.

Furthermore, an intentional islanding operation of distribution network may have the advantage that it can utilize the maximum capacity of DG, improve reliability of distribution system, reduce the congestion of transmission and distribution network [7]. Thus, an intentional islanding operation of a distribution system may be advantageous if various issues concerned to it are addressed satisfactorily.

When a distribution system operating at peak capacity is islanded, the frequency will go down very fast and requires an efficient load shedding technique to shed some load in order to stabilize the frequency [8]. However, despite of the development in computer and communication technologies, power system around the globe still using conventional load shedding approaches and has not changed for decades. The conventional UFLS scheme has the limitation that they shed surplus or insufficient amount of load shed. Due to this, conventional under frequency load shedding (UFLS) schemes has resulted in huge number of power blackouts around the globe. This has put question mark on the reliability of these conventional UFLS schemes [9], [10]. The use of latest advancement in computer and communication may be a good option in terms of the technical perspectives to enhance the reliability of existing huge and complicated power systems [11].

Accurate load shedding depends upon two main factors; estimation of load shed amount and accurately disconnecting that amount of load. However, most of the research trend remains in the direction of accurate estimation of load shed amount only. For accurate estimation of load shed amount, mostly power swing equation is employed. However, power

swing equation also suffers from inaccurate estimation due to variations in rate of change of frequency (ROCOF) behavior. It has been found that ROCOF value greatly affects due to operating capacities of a power system (base load and peak load capacity), system voltage profile and load voltage characteristics [12]. The values of ROCOF are different for similar amounts of load variation at base and peak capacity. This variation in ROCOF behavior causes the inaccurate estimation of the power imbalance which leads to inaccurate load shedding [13]. In order to overcome this difficulty, a novel UFLS scheme is presented in reference [14], using the frequency second derivative as a source of information to predict the trajectory of frequency. The scheme used Newton method based approximation and the interpolation of the frequency second derivative to predict the minimum frequency value that can provide the actual load shedding. The scheme has the advantage that it sheds lesser amount of load shed and supplied most of the load to the system [14].

Further efforts to accurately estimate the load shed amount/power imbalance were the application of computational intelligence based techniques such as artificial neural network, fuzzy logic control, adaptive neuro fuzzy inference system, and genetic algorithm. However, as the accurate load shedding not only depends upon the accurate estimation of load shed amount but accurate amount of load to be disconnected is also another important factor to be considered. This resulted inaccurate load shedding in many adaptive techniques proposed in [15]-[18] and computational intelligence techniques proposed in [19]-[23] despite of accurate estimation. Though, it was proved by above researchers that adaptive and computational intelligence based UFLS schemes shed lesser amount of loads compared to traditional UFLS schemes. Nevertheless, the frequency overshoot in all of these techniques clearly indicates that these techniques have disconnected some extra loads.

The justification for accurate load shedding may be obtained if the DG frequency restores to reference value without any overshoot. This may be obtained if the loads of distribution system which are taking part in load shedding are given some flexible priority instead of fixed priority. This flexibility can be achieved if vital loads are given fixed priority and non-vital loads are given flexible priority. With this flexible load priority arrangement, the accurate amount of load can be shed by disconnecting those loads whose total value is almost equal or near to the load shed amount. This may also lead to frequency recovery without overshooting. The proposed UFLS scheme employs both factors. For accurate estimation of load shed amount, it employs Takagi–Sugeno fuzzy inference system and for accurate amount of load to shed, it employs flexible load priority.

II. METHODOLOGY

The proposed UFLS scheme is considered to operate and monitor distribution network after the occurrence of islanding event. It consists of two main modules:

- 1) Fuzzy Load Shed Amount Estimation Module (FLSAEM)
- 2) Accurate Load Shedding Module (ALSM)

The explanation of these modules is presented in the following sections:

A. Fuzzy Load Shed Amount Estimation Module (FLSAEM) Description

The first module of the proposed UFLS scheme consists of fuzzy load shed amount estimation module. This module is used to estimate the accurately load shed amount during islanding, or load increment events. It uses Takagi–Sugeno fuzzy inference system. The FLSAEM has two inputs namely centre of inertial frequency and rate of change of centre of inertial frequency and one output load shed amount [24]:

FLSAEM will estimates the accurate amount of load shed between the generation and load demand using these input values. The modeling of Takagi–Sugeno fuzzy inference system comprises fuzzification, rule base inference mechanism, and defuzzification steps. Fuzzification is the process of converting crisp statements into fuzzy statements by using membership functions. The membership function of input and output are shown in Fig. 1 to 3.

The linguistic variables membership functions of input centre of inertial frequency are COF (Cut-off frequency), VELF (Very extremely low frequency), ELF (Extremely low frequency), VLF (Very low frequency), LF (Low frequency), and NF (Normal frequency).

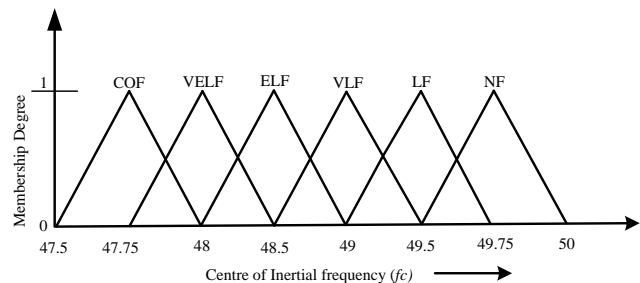


Fig. 1. Centre of inertial frequency membership functions.

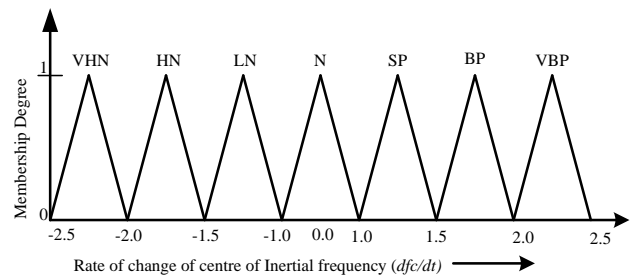


Fig. 2. Rate of change of centre of inertial frequency membership functions.

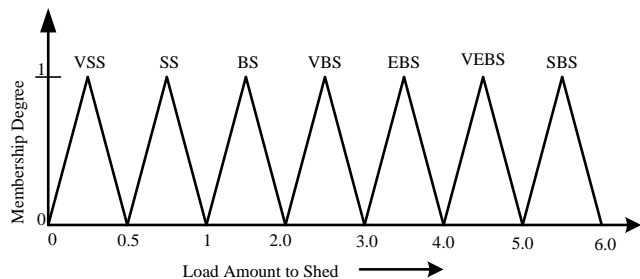


Fig. 3. Load shed amount membership functions.

The input rate of change of centre of inertial frequency membership functions are VHN (very high negative), HN (High negative), LN (Low negative), N (normal), SP (small positive), BP (big positive), VBP (very big positive). The linguistic variables of output power imbalance are VSS (very small shed), SS (small shed), BS (big shed), VBS (Very big shed), EBS (Extremely big shed), VEBS (Very extremely big shed), SBS (Super big shed).

These fuzzified inputs are evaluated by rules through fuzzy inference mechanism and are applied in IF-THEN rule form followed by defuzzification step through weighted average method to get final real output. FLSAEM sends this value to Accurate Load Shedding Module (ALSM) via a communication link to disconnect the loads.

B. Accurate Load Shedding Module

ALSM module after receiving the load shed amount (LSA) from FLSAEM module, it will check frequency limit of 49.5 Hz in order to prevent the activation of load shedding schemes for smaller load variations [25]. From this step, amount of load can be shed by two ways. One way to perform load shedding is to disconnect the loads with fixed load priority. This may result in inaccurate load shedding despite of accurate estimation of power imbalance. Another way to get accurate load shedding is to disconnect the loads with random load priority. This random load priority may be able to accurately disconnect the required load and frequency may restore to its nominal value without overshoot. The proposed UFLS scheme applies the later approach to obtain the accurate load shedding. Hence, ALSM after receiving the load shed amount from FLSAEM determines the magnitudes of random priority loads. By using this information, the proposed algorithm calculates the number of possible combinations, as given by:

$$\text{Max. No. of Combinations} = 2^N - 1 \quad (1)$$

where N shows the quantity of random loads. After this, ALSM determines the load summation and absolute error in each combination as below:

$$\text{Error}_i = \text{LSA} - \sum P_{i_combination} \quad (2)$$

where,

(Error)_i = absolute error of the ith combination,

LSA = load shed amount,

$\sum P_{i_combination}$ = sum of active power of ith combination.

The combination with minimum error is selected for disconnecting the loads in order to obtain the accurate load shedding. To perform this, the proposed ALSM module sends the signals directly to the breakers of these loads in order to trip them. In case, the load shed amount is higher than the total magnitude of random priority loads, ALSM will perform load shedding in two steps. At the first step, ALSM will disconnects all random priority loads whereas in the second step, it will start disconnecting the fixed priority loads until the condition $\Delta P \leq 0$ is achieved. The delay time consisting of computation, communication, and breaker operation is

considered as 120 milliseconds. The flow chart of proposed UFLS scheme is shown in Fig. 4.

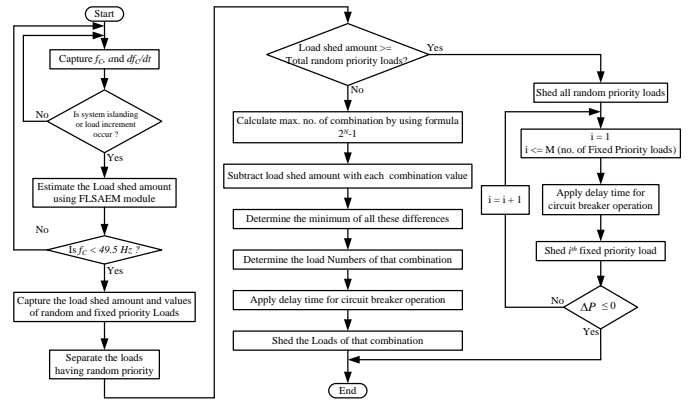


Fig. 4. Flow chart of proposed UFLS scheme.

III. MODELING OF TEST SYSTEM AND PROPOSED UFLS SCHEME

In this research, a 102-bus distribution network is considered to validate the proposed under-frequency load shedding scheme. The network is part of an existing Malaysia distribution network. The test system consists of 102 buses, 79 lumped loads and 9 mini-hydro generators as shown in Fig. 5.

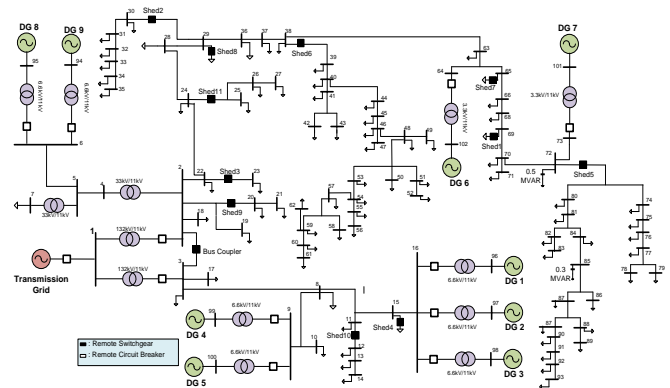


Fig. 5. 102-Buses test system.

As indicated in Fig. 5, a bus coupler's breaker for an 11kV network is located at the intersection of bus 2 and bus 3. To improve the voltage profile, capacitor banks with ratings 0.3MVAR and 0.5MVAR are used at buses 85 and 72, respectively. The modeling of the various components of test system is done by using the standard models for exciter, governor, and hydraulic turbine in PSCAD/EMTDC library.

A. Modeling of Proposed UFLS Scheme in Matlab and Interfacing with PSCAD

PSCAD/EMTDC and MATLAB interface technologies are used for FLSAEM and ALSM modeling. More specifically, the Takagi-Sugeno fuzzy inference system and ALSM module are built in MATLAB and distribution system is modelled in PSCAD. This FLSAEM modeling and its interfacing with MATLAB requires three main components to perform interfacing successfully.

- 1) Sub routine to call for MATLAB and PSCAD interface.

- 2) M-File for calling the Takagi-Sugeno fuzzy inference system.
- 3) MATLAB fis file which consists of Takagi-Sugeno fuzzy inference system.

To call sub routine, MATLAB block in PSCAD/EMTDC is built by creating a new component. This new MATLAB block can be developed by using a program written by the authors. The program asks for the name of the new component and number of input, output and their names. A graphical icon of the block is then automatically generated along with an empty m-file, which is opened for user input in a text editor shell. The user should then enter the appropriate MATLAB statements into this m-file. Fig. 6 shows the sub routine written in FORTRAN command for interfacing with PSCAD.

```

1  storf(nstorf) = $fc
2  storf(nstorf + 1) = $dfc_dt
3  call MLAB_INT("D:\FPIEM Module", "Fuzzy_Power", "R R", "R")
4  $power_imbalance = storf(nstorf + 2)
5  NSTORF = NSTORF + 3

```

Fig. 6. Sub routine for calling MATLAB & PSCAD interfacing.

The second step required is to write MATLAB code in M-File for calling fuzzy inference system (fis) file. Fig. 7 shows the m-file structure in which TS-fuzzy is called to estimate the power imbalance whereas Fig. 8 shows the PSCAD and Matlab interface arrangement.

```

File Edit Text Go Cell Tools Debug Desktop Window Help
[Icons]
- 1.0 + ÷ 1.1 x % % % % %
1  function [power_imbalance]=fuzzy_power(fc,dfc/dt)
2  a = readfis('FPIEM');
3  power_imbalance = evalfis([fc,dfc/dt],a);
4

```

Fig. 7. M-File for calling Takagi-Sugeno inference system.

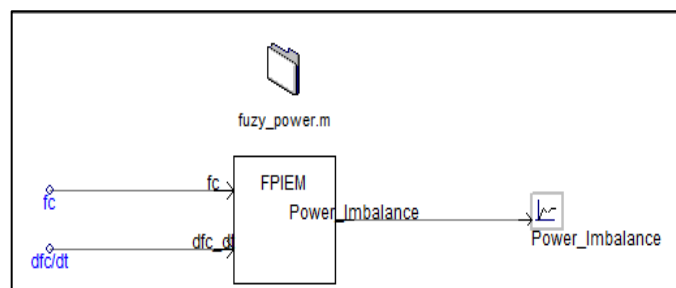


Fig. 8. New component with M-File.

In total, 11 loads in distribution system are chosen to take part in load shedding. Among these loads, load ranked 1 to 6 are given random priority and load ranked 7-11 are given fixed priority. Table I shows loads with their priority rankings.

The loads with random priority can be disconnected without following any sequence.

TABLE I. LOAD DATA WITH THEIR PRIORITY

Load Rank	Bus No.	Active Power (MW)	Adaptive scheme Priority	Proposed scheme priority
1	69	0.1	Fixed	Random
2	30-35	0.196	Fixed	Random
3	23	0.413	Fixed	Random
4	15	0.71	Fixed	Random
5	74-93	0.75	Fixed	Random
6	39-62	1.35	Fixed	Random
7	65	0.14	Fixed	Fixed
8	29	0.153	Fixed	Fixed
9	20-21	0.21	Fixed	Fixed
10	12-14	0.37	Fixed	Fixed
11	25-27	0.55	Fixed	Fixed

B. Modeling of Adaptive UFLS Scheme

To highlight the robustness of the proposed UFLS scheme, its response will be compared with adaptive UFLS scheme which employs swing equation to perform load shedding. This UFLS scheme will also initiates when the system frequency falls below the 49.5 Hz threshold. The overall 11 stage load shedding plan considered for proposed UFLS scheme; and adaptive scheme are shown in Table I.

IV. SIMULATION RESULTS

To demonstrate the effectiveness of proposed UFLS scheme, its response is tested for several intentional islanding, and load increment cases. Furthermore, its response is also compared with adaptive UFLS scheme to show its effectiveness. The following sections provide the detailed comparison of both schemes for different cases.

A. Intentional Islanding Operation Case

In this case, islanding operation of distribution system is simulated. For this purpose, grid breaker is disconnected at $t=5$ s. The total load demand of the test system in this case is 18.7 MW from which 15.2 MW is supplied by the DG units and 3.5 MW is supplied by the utility grid. This results in power mismatch of 3.5 MW. The test system possesses a 0.9 MW of total spinning reserve. Upon occurrence of islanding event, FLSAEM checks first frequency limit of 49.5 Hz. After checking this, FLSAEM using frequency and rate of change of frequency measurements, estimates the load shed amount for this case and sends this amount to ALSM module. For a 3.5 MW power imbalance, the FLSAEM module determines 2.6 MW as the load shed amount. The ALSM module after receiving load shed amount, determines that among 11 loads, six loads have random priority. The maximum number of combinations for 6 random priority loads is 63 and is shown in Table II. After this, the ALSM module determines the sum and absolute error of each combination. The ALSM will select the combination with minimum error for load shedding.

Table II shows that the combination no. 50 has the minimum error (0.013). The combination number 50 consists of load ranked 1st, 3rd, 5th and 6th respectively. The proposed UFLS scheme directly sends signals to shed these loads in order to make islanding operation successful. The frequency response of all three UFLS schemes is shown in Fig. 9,

whereas power imbalance, total amount of load shed, and other parameters of both these techniques are shown in Table III.

TABLE II. PROCEDURE FOR FINDING LOADS OF BEST COMBINATION

No.	Variables Combination	Σ combination	ΔP	Absolute ($\Delta P - \Sigma$ combination)	No.	Variables Combination	Σ combination	ΔP	Absolute ($\Delta P - \Sigma$ combination)
1	1	0.1	2.6	2.5	33	2,3,5	1.359	2.6	1.241
2	2	0.196	2.6	2.404	34	2,3,6	1.959	2.6	0.641
3	3	0.413	2.6	2.187	35	2,4,5	1.656	2.6	0.944
4	4	0.71	2.6	1.89	36	2,4,6	2.256	2.6	0.344
5	5	0.75	2.6	1.85	37	2,5,6	2.296	2.6	0.304
6	6	1.35	2.6	1.25	38	3,4,5	1.873	2.6	0.727
7	1, 2	0.296	2.6	2.304	39	3,4,6	2.473	2.6	0.127
8	1,3	0.513	2.6	2.087	40	3,5,6	2.513	2.6	0.087
9	1,4	0.81	2.6	1.79	41	4,5,6	2.81	2.6	0.21
10	1,5	0.85	2.6	1.75	42	1, 2,3,4	1.419	2.6	1.181
11	1,6	1.45	2.6	1.15	43	1,2,3,5	1.459	2.6	1.141
12	2,3	0.609	2.6	1.991	44	1,2,3,6	2.059	2.6	0.541
13	2,4	0.906	2.6	1.694	45	1,2,4,5	1.756	2.6	0.844
14	2,5	0.946	2.6	1.654	46	1,2,4,6	2.356	2.6	0.244
15	2,6	1.546	2.6	1.054	47	1,2,5,6	2.396	2.6	0.204
16	3,4	1.123	2.6	1.477	48	1,3,4,5	1.973	2.6	0.627
17	3,5	1.163	2.6	1.437	49	1,3,4,6	2.573	2.6	0.027
18	3,6	1.763	2.6	0.837	50	1,3,5,6	2.613	2.6	0.013
19	4,5	1.46	2.6	1.14	51	1,4,5,6	2.91	2.6	0.3
20	4,6	2.06	2.6	0.54	52	2,3,4,5	2.069	2.6	0.531
21	5,6	2.1	2.6	0.5	53	2,3,4,6	2.669	2.6	0.069
22	1,2,3	0.709	2.6	1.891	54	2,3,5,6	2.709	2.6	0.109
23	1,2,4	1.006	2.6	1.594	55	2,4,5,6	3.006	2.6	0.406
24	1,2,5	1.046	2.6	1.554	56	3,4,5,6	3.223	2.6	0.623
25	1,2,6	1.646	2.6	0.954	57	1,2,3,4,5	2.169	2.6	0.431
26	1,3,4	1.223	2.6	1.377	58	1,2,3,4,6	2.769	2.6	0.169
27	1,3,5	1.263	2.6	1.337	59	1,2,3,5,6	2.809	2.6	0.209
28	1,3,6	1.863	2.6	0.737	60	1,2,4,5,6	3.106	2.6	0.506
29	1,4,5	1.56	2.6	1.04	61	1,3,4,5,6	3.323	2.6	0.723
30	1,4,6	2.16	2.6	0.44	62	2,3,4,5,6	3.419	2.6	0.819
31	1,5,6	2.2	2.6	0.4	63	1,2,3,4,5,6	3.519	2.6	0.919
32	2,3,4	1.319	2.6	1.281	-	-	-	-	-

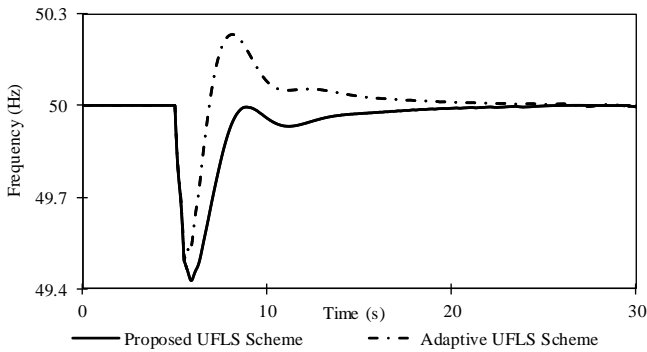


Fig. 9. Frequency response of UFLS schemes for islanding event.

It can be observed from Fig. 9 that adaptive scheme possess very high overshoot compared to proposed UFLS scheme. On the other hand, absence of overshoot in the frequency response of proposed UFLS scheme justifies that it has achieved the accurate load shedding.

The adaptive UFLS scheme has resulted in an overshoot of 50.23 Hz. The reason for this overshoot is that an adaptive UFLS scheme has not included the spinning reserve in estimating the load shed amount. Due to this, it has resulted in

shedding of extra loads. Hence, for 3.5 MW power imbalance, adaptive UFLS scheme has shed 3.519 MW load whereas, the proposed UFLS scheme has shed the 2.613 MW due to the advantage of random priority. This accurate load shedding has caused the restoring of system frequency to its original value without overshoot. The adaptive based UFLS scheme has disconnected the first 6 loads whereas the proposed UFLS scheme has disconnected 1st, 3rd, 5th and 6th loads only. Thus, addition of random priority to few loads can provide flexibility to achieve accurate load shedding.

TABLE III. UFLS PARAMETERS FOR ISLANDING EVENT

Parameter	Adaptive UFLS scheme	Proposed UFLS scheme
Power Imbalance	3.5 MW	3.5 MW
Total load shed	3.519 MW	2.613 MW
Loads Disconnected	Load1–Load6	Load1, Load3, Load5–Load6
Frequency Undershoot	49.494 Hz	49.43 Hz
Frequency Overshoot	50.23 Hz	-

B. For Load Increment

This case is simulated for load increment scenario when the system is operating in islanded mode. For this case, an addition of 1.5 MW load at Bus 10 is simulated at $t=5$ s. Upon addition of this load, FLSAEM checks first frequency limit of 49.5 Hz. After checking this, FLSAEM using frequency and rate of change of frequency measurements, estimates the load shed amount for this case and sends this amount to ALSM module. For a 1.5 MW load increment, the FLSAEM module determines 0.6 MW as the load shed amount. The frequency response of both UFLS schemes is shown in Fig. 10, whereas power imbalance, total amount of load shed, and other parameters of all these schemes are shown in Table IV.

TABLE IV. UFLS PARAMETERS FOR LOAD INCREMENT CASE

Parameter	Adaptive UFLS scheme	Proposed UFLS scheme
Power Imbalance	1.5 MW	1.5 MW
Total load shed	2.142 MW	0.609 MW
Loads Disconnected	Load1-Load5	Load2, Load3
Frequency Undershoot	49.499 Hz	49.482 Hz
Frequency Overshoot	50.24 Hz	-

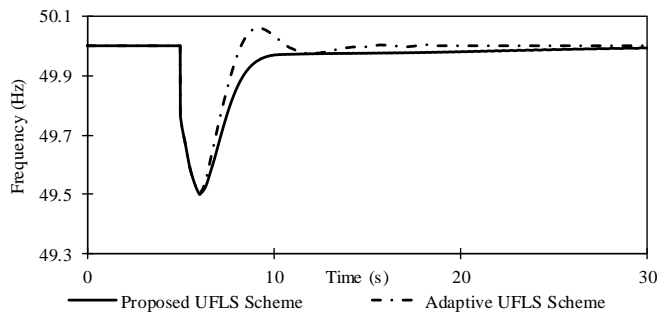


Fig. 10. Frequency response of UFLS schemes for load increment case.

It can be noticed from the Fig. 7 and Table IV that the adaptive UFLS scheme has very high overshoot compared to proposed UFLS scheme. The adaptive UFLS scheme has resulted in an overshoot of 50.24 Hz. The reason for this overshoot is that an adaptive UFLS scheme has not included the spinning reserve in estimating the load shed amount that has resulted in shedding of extra loads. However, the proposed UFLS scheme because of random load priority has disconnected 0.609 MW load.

The frequency response of the proposed UFLS scheme restores to its original value without overshoot. The adaptive UFLS scheme has disconnected the loads up to 5th ranked whereas the proposed UFLS scheme has disconnected 2nd and 3rd ranked loads only. This accurate load shedding has caused the restoring of system frequency to its original value without overshoot.

V. DISCUSSIONS

From the simulation results, it can be observed that proposed UFLS scheme based on combination of random and fixed load priority provides flexibility that leads to accurate load shedding. The response of the proposed UFLS scheme

has been compared with adaptive based UFLS scheme in terms of load amount shed, frequency undershoot and overshoot for different scenarios of islanding event, and load increment case. The simulation results of adaptive UFLS scheme have shown that despite of the accurate estimation of power imbalance, adaptive UFLS scheme is not succeeded to achieve accurate load shedding. This happened due to fixed load priority, and inability to consider the spinning reserve in estimation of load shed amount. Furthermore, the adaptive UFLS scheme possessed very high overshoot, disconnected higher amount of load compared to proposed UFLS scheme. On the other hand, the performance of proposed UFLS scheme in all cases has shown that it has smaller undershoot, shed lesser loads compared to adaptive UFLS scheme. In proposed UFLS scheme performance, the restoring of system frequency to its original value without overshoot has justified that the proposed scheme has achieved the accurate load shedding. Hence, it can be concluded that providing random load priority in few loads of the distribution system can assist the UFLS scheme to obtain accurate amount of load shedding. The proposed technique considers only six random loads. However, in future, some optimization techniques may be used to overcome this limitation of random load priority. It is necessary because power system may contain large number of loads and the performance of the proposed technique can be improved by overcoming this limitation.

VI. CONCLUSION AND FUTURE WORK

This research has proposed a new smart under frequency load shedding (UFLS) scheme to enable successfully the intentional islanding operation of distribution system connected with distributed generation. The proposed UFLS scheme was mainly consisted of fuzzy load shed amount estimation module (FLSAEM) and accurate load shedding module (ALSM). The FLSAEM used Takagi-Sugeno fuzzy inference system to estimate the accurate load shed amount and ALSM perform the accurate load shedding based on flexible load priority. The performance of the proposed UFLS scheme is validated for islanding event, and load increment case. To further highlight the advantages of proposed UFLS schemes, its response has been compared with adaptive UFLS scheme. The simulation results have shown that the proposed UFLS scheme has achieved the accurate load shedding due to advantage of flexible priority whereas adaptive UFLS scheme due to inaccurate estimation and fixed load priority have not succeeded to achieve accurate load shedding. Thus, it has been proved that load priority plays an important role in accurate amount of load shedding. In future, for smart grid, this factor should also be considered in order to achieve enhanced accuracy of the under frequency load shedding schemes. In the future work, an optimization technique will be used to consider large number of random priority loads in order to enhance the capability of the proposed technique for large power system.

REFERENCES

- [1] M. Silva, H. Morais, and Z. Vale, "An integrated approach for distributed energy resource short-term scheduling in smart grids considering realistic power system simulation," *Energy Conversion and Management*, vol. 64, pp. 273-288, 2012.
- [2] V. L. Merlin, R. C. Santos, A. P. Grilo, J. C. M. Vieira, D. V. Coury, and M. Oleskovicz, "A new artificial neural network based method for

- islanding detection of distributed generators," *International Journal of Electrical Power & Energy Systems*, vol. 75, pp. 139-151, 2// 2016.
- [3] P. A. Gooding, E. Makram, and R. Hadidi, "Probability analysis of distributed generation for island scenarios utilizing Carolinas data," *Electric Power Systems Research*, vol. 107, pp. 125-132, 2014.
- [4] J. A. Laghari, H. Mokhlis, A. H. Abu Bakar, and H. Mohamad, "A fuzzy based load frequency control for distribution network connected with mini hydro power plant," *Journal of Intelligent & Fuzzy Systems*, vol. 26, pp. 1301-1310, 2014.
- [5] IEEE Std 1547, "IEEE Standard for Interconnecting Distributed Resources With Electric Power Systems," IEEE Std 1547-2003, pp. 0_1-16, 2003.
- [6] IEEE Std 929, "IEEE Recommended Practice for Utility Interface of Photovoltaic (PV) Systems," IEEE Std 929-2000, p. i, 2000.
- [7] J. A. Laghari, H. Mokhlis, M. Karimi, A. H. A. Bakar, and H. Mohamad, "Computational Intelligence based techniques for islanding detection of distributed generation in distribution network: A review," *Energy Conversion and Management*, vol. 88, pp. 139-152, 2014.
- [8] H. Samet and M. Rashidi, "Coordinated under frequency load and capacitor shedding for bulk power systems," *Generation, Transmission & Distribution, IET*, vol. 7, pp. 799-812, 2013.
- [9] M. D. Maram and N. Amjady, "Event-based remedial action scheme against super-component contingencies to avert frequency and voltage instabilities," *Generation, Transmission & Distribution, IET*, vol. 8, pp. 1591-1603, 2014.
- [10] Y. Dai, Y. Xu, Z. Y. Dong, K. P. Wong, and L. Zhuang, "Real-time prediction of event-driven load shedding for frequency stability enhancement of power systems," *Generation, Transmission & Distribution, IET*, vol. 6, pp. 914-921, 2012.
- [11] U. Rudez and R. Mihalic, "Predictive underfrequency load shedding scheme for islanded power systems with renewable generation," *Electric Power Systems Research*, vol. 126, pp. 21-28, 2015.
- [12] U. Rudez and R. Mihalic, "Analysis of Underfrequency Load Shedding Using a Frequency Gradient," *Power Delivery, IEEE Transactions on*, vol. 26, pp. 565-575, 2011.
- [13] J. A. Laghari, H. Mokhlis, A. H. A. Bakar, and H. Mohamad, "Application of computational intelligence techniques for load shedding in power systems: A review," *Energy Conversion and Management*, vol. 75, pp. 130-140, 2013.
- [14] U. Rudez and R. Mihalic, "A novel approach to underfrequency load shedding," *Electric Power Systems Research*, vol. 81, pp. 636-643, 2011.
- [15] W. Gu, W. Liu, C. Shen, and Z. Wu, "Multi-stage underfrequency load shedding for islanded microgrid with equivalent inertia constant analysis," *International Journal of Electrical Power & Energy Systems*, vol. 46, pp. 36-39, 2013.
- [16] P. Mahat, C. Zhe, and B. Bak-Jensen, "Underfrequency Load Shedding for an Islanded Distribution System With Distributed Generators," *IEEE Transactions on Power Delivery*, vol. 25, pp. 911-918, 2010.
- [17] A. A. M. Zin, H. M. Hafiz, and W. K. Wong, "Static and dynamic under-frequency load shedding: a comparison," in *Power System Technology, 2004. PowerCon 2004. 2004 International Conference on*, 2004, pp. 941-945 Vol.1.
- [18] F. Ceja-Gomez, S. S. Qadri, and F. D. Galiana, "Under-Frequency Load Shedding Via Integer Programming," *Power Systems, IEEE Transactions on*, vol. 27, pp. 1387-1394, 2012.
- [19] H. Ying-Yi and W. Shih-Fan, "Multiobjective Underfrequency Load Shedding in an Autonomous System Using Hierarchical Genetic Algorithms," *IEEE Transactions on Power Delivery*, vol. 25, pp. 1355-1362, 2010.
- [20] E. J. Thalassinakis, E. N. Dialynas, and D. Agoris, "Method Combining ANNs and Monte Carlo Simulation for the Selection of the Load Shedding Protection Strategies in Autonomous Power Systems," *IEEE Transactions on Power Systems*, vol. 21, pp. 1574-1582, 2006.
- [21] C.-T. Hsu, H.-J. Chuang, and C.-S. Chen, "Adaptive load shedding for an industrial petroleum cogeneration system," *Expert Systems with Applications*, vol. 38, pp. 13967-13974, 2011.
- [22] M. A. Mitchell, J. A. P. Lopes, J. N. Fidalgo, and J. D. McCalley, "Using a neural network to predict the dynamic frequency response of a power system to an under-frequency load shedding scenario," in *IEEE Power Engineering Society Summer Meeting, 2000*, pp. 346-351 vol. 1.
- [23] H. Mokhlis, J. A. Laghari, A. H. A. Bakar, and M. Karimi, "A Fuzzy Based Under-Frequency Load Shedding Scheme for Islanded Distribution Network Connected With DG," *International Review of Electrical Engineering (I.R.E.E)*, vol. 7, 2012.
- [24] V. V. Terzija, "Adaptive underfrequency load shedding based on the magnitude of the disturbance estimation," *IEEE Transactions on Power Systems*, vol. 21, pp. 1260-1266, 2006.
- [25] A. A. Mohd Zin, H. Mohd Hafiz, and M. S. Aziz, "A review of under-frequency load shedding scheme on TNB system," in *Power and Energy Conference, PECon 2004. Proceedings. National*, pp. 170-174.

Fuzzy Gains-Scheduling of an Integral Sliding Mode Controller for a Quadrotor Unmanned Aerial Vehicle

Nour Ben Ammar, Soufiene Bouallègue, Joseph Haggège

Research Laboratory in Automatic Control (L.A.R.A.),
National Engineering School of Tunis (ENIT),
University of Tunis El Manar,
BP 37, Le Belvédère,
1002 Tunis, Tunisia

Abstract—This paper investigates an Adaptive Fuzzy Gains-Scheduling Integral Sliding Mode Controller (AFGS-ISMC) design approach to deal with the attitude and altitude stabilization problem of an Unmanned Aerial Vehicles (UAV) precisely of a quadrotor. The Integral Sliding Mode Control (ISMC) seems to be an adequate control tool to remedy this problem. The selection of the controller parameters is done most of the time using repetitive trials-errors based methods. This method is not completely reliable and becomes a time-consuming and difficult task. Here we propose the tuning and selection of all ISMC gains adaptively according to a fuzzy supervisor. The sliding surface and its differential are declared as Fuzzy Logic Supervisor (FLS) inputs and the integral sliding mode control gains as the FLS outputs. The proposed fuzzy-based supervision mechanisms modify all ISMC gains to be time-varying and further enhance the performance and robustness of the obtained adaptive nonlinear controllers against uncertainties and external disturbances. The proposed adaptive fuzzy technique increases the effectiveness of the ISMC structure compared to the classical SMC strategy and excludes the dull and repetitive trials-errors process for its design and tuning. Various simulations have been carried out and followed by comparison and discussion of the results in order to prove the superiority of the suggested fuzzy gains-scheduled ISMC approach for the quadrotor attitude and altitude flight stabilization.

Keywords—Quadrotor UAV; modeling; flight dynamics stabilization; integral sliding mode control; fuzzy gains-scheduling, adaptive control

I. INTRODUCTION

Unmanned Aerial Vehicles (UAVs) are volant robots with no aviator that are capable of carrying out various missions in inimical and unsettled environments [1]. The quadrotor, a type of these UAVs, is a very promising concept with a Vertical Take-Off and Landing (VTOL) motion thanks to four rotors which are independently controlled [2]-[7]. These rotorcrafts have been developed to perform various tasks in different fields whether in the military or even civilian. As a class of unmanned rotorcraft, quadrotors are arising as an incomparable and promising stand for various tasks such as recognition, surveillance, environmental monitoring, life-saving operations and aerial photography through their VTOL capacity yet its structure is simple. In some aspects, the quadrotors have better maneuverability than other VTOL vehicles due to the four rotors which can increase the mobility and load ability.

Unfortunately, the difficulty of control design of such a type of rotorcrafts increases under the dynamics nonlinearity, parametric uncertainties and external disturbances. Moreover, the dynamical model of a quadrotor UAV has six Degree-Of-Freedom (DOF) with only four independent thrust forces generated by four rotors. It is difficult to control all these six outputs with only four control inputs. For this problem, it is necessary to use adequate control methods such as the nonlinear ones to design robust and effective flight controllers. Nonlinear control is one of the significant challenges in the modern control theory [8], [9]. Facing this defiance, it is obvious that there is not a particular procedure that must be applied to all nonlinear systems. So, we must resort to employing the best adapted tools to the current problem. In this context, the Sliding Mode Control (SMC) strategy presents a promising solution [10]-[15].

The SMC approach is a control technique known for its robustness for the complex and nonlinear systems. The best constructive characteristic of this controller is in the total adjustment of the perturbation wherever the system is in the sliding phase and a sliding mode is imposed. This last one takes place when the state is on an appropriate subspace of the state-space. The compensated dynamics become insensible to perturbation and uncertainties below the SMC design [16]-[18]. Sliding mode control has been successfully applied to robot manipulators, high-performance electric motors, underwater vehicles and UAV [19]. Regrettably, a perfect sliding mode controller has a discontinuous switching function which causes a fast switching of the signal from one value to another. Due to the limitation of physics and the finite time delay of the control computation, it is intolerable to attain boundedly fast switching control in the practical implementation [20], [21].

In the literature, the Integral Sliding Mode Control (ISMC) variant appears at first as an answer to the achieving phase question for systems with matched disturbances only [23]. Recently, the ISMC technique has been used in order to analyze the problem of minimizing the disturbance of systems taken into account a nonlinear drift term and a constant input matrix [3], [19]. This outcome has been applied evenly in connection with different control strategies like the Model Predictive Control (MPC) in [25]. In [26] an integral sliding mode altitude control for a small model helicopter with ground effect compensation is proposed. The authors then present the

implementation of an integral action on the controller based on sliding modes for a conventional helicopter. In [27], an adaptive integral sliding mode control for a small scale quadrotor is designed to online estimate the attitude controllers' parameters. Authors in [28] applied the L1 adaptive control theory to design the attitude stabilization against the model uncertainties and environmental disturbances.

Based on the aforementioned studies, the main challenging stage in the ISMC design for quadrotors UAV is the choice of appropriate controllers' gains that define, as the effective control parameters, the dynamics of such feedback controllers. Such gains tuning provides a desired balance between the state variable responses and control efforts. In the ISMC framework, these decision variables are selected by repetitive trials-errors based methods that become time consuming and difficult task [4], [5]. Indeed, the methods described above in [22]-[25] are interesting but may not lead to satisfactory results because they are usually time-consuming and very restrictive. Looking for new ways to handle these complex problems, a systematic approach to tune these design parameters is then an interesting task in the sliding mode control of VTOL rotorcrafts.

Inced by its noticeable draw in diverse control appliance as well as its straightforwardness in real-world implementation, the fuzzy control theory has been applied to attain advanced performances and robustness for complex and nonlinear systems [26]-[28]. The tuning and selection of all ISMC gains, systematically and without any trials-errors based stage, thanks to a proposed fuzzy supervision mechanism, is a promising idea and efficient solution given the complexity and the hardness design of the conventional ISMC approach. Such a proposed fuzzy gains-scheduling technique allows having variable gains over time based integral sliding mode controllers that are more appropriate and efficient to uncertainties, disturbances and faults of UAV rotorcrafts. So, the principal contribution of this paper is to propound a novel strategy to conceit and adjust adaptive integral sliding mode controllers for the attitude and altitude stabilization problem of a quadrotor. Both gains of the sliding surfaces and sign functions selection problem is formulated and is efficiently solved thanks to proposed fuzzy supervision mechanisms.

The remained of this paper is organized as follows. In Section II, a mathematical nonlinear model of the quadrotor is presented thanks to the Euler-Newton formalism. In Section III, the adaptive fuzzy gains-scheduling integral sliding mode controller problem is formulated for the altitude and attitude quadrotors dynamics' stabilization. All sliding mode controllers' gains, as effective design parameters, are scheduled based on proposed fuzzy supervision mechanisms leading to reduce the chattering phenomenon. In Section IV, various simulations are done to point the efficacy the proposed fuzzy-based sliding mode controllers for the flight stabilization of the UAV drone. Finally, conclusions are drawn in Section V.

II. MODELING OF THE QUADROTOR UAV

A quadrotor is an UAV with four rotors that are controlled independently as shown in Fig. 1. The movement of the

quadrotor results from changes in the speed of the rotors. The quadrotor structure is assumed to be rigid and symmetrical. The propellers are rigid and the thrust and drag forces are proportional to the square of propeller's speed [1], [2], [6], [7].

To develop a mathematical model of such device, both coordinate systems such as the earth-frame $\mathbf{F}_E = \{O_e, \mathbf{x}_e, \mathbf{y}_e, \mathbf{z}_e\}$ and the body-frame $\mathbf{F}_B = \{O_b, \mathbf{x}_b, \mathbf{y}_b, \mathbf{z}_b\}$ are considered [29]. Let denote by m the total mass of the quadrotor, g the acceleration of the gravity and l the distance from the center of each rotor to the Center (COG) [].

The orientation of the quadrotor is given by the rotation matrix $\mathbf{R} : \mathbf{F}_E \rightarrow \mathbf{F}_B$ which depends on the Euler angles (ϕ, θ, ψ) and defined by the following equation:

$$\mathbf{R}(\phi, \theta, \psi) = \begin{bmatrix} c\psi c\theta & s\phi s\theta c\psi - s\psi c\theta & c\phi s\theta c\psi + s\psi s\phi \\ s\psi c\theta & s\phi s\theta s\psi + c\psi c\theta & c\phi s\theta s\psi - s\phi c\psi \\ -s\theta & s\phi c\theta & c\phi c\theta \end{bmatrix} \quad (1)$$

where $c(\cdot) = \cos(\cdot)$ and $s(\cdot) = \sin(\cdot)$.

The position and the attitude angles of the quadrotor in the earth-frame are defined as $\boldsymbol{\xi} = [x, y, z]^T$ and $\boldsymbol{\eta} = [\phi, \theta, \psi]^T$, respectively. We denote by $-\pi/2 \leq \phi \leq \pi/2$, $-\pi/2 \leq \theta \leq \pi/2$ and $-\pi \leq \psi \leq \pi$ the roll, pitch and yaw angles, respectively. The complete dynamical model of the studied quadrotor is established applying the Newton-Euler formalism. The Newton's laws convey to the pursuant motion equations [1]-[3]:

$$\begin{cases} m\ddot{\boldsymbol{\xi}} = \mathbf{F}_{th} + \mathbf{F}_d + \mathbf{F}_g \\ \mathbf{J}\dot{\boldsymbol{\Omega}} = \mathbf{M} - \mathbf{M}_{gp} - \mathbf{M}_{gb} - \mathbf{M}_a \end{cases} \quad (2)$$

where $\mathbf{F}_{th} = \mathbf{R}(\phi, \theta, \psi) \left[0, 0, \sum_{i=1}^4 F_i \right]^T$ denotes the total thrust force of the four rotors, $\mathbf{F}_d = \text{diag}(\kappa_1, \kappa_2, \kappa_3) \dot{\boldsymbol{\xi}}^T$ is the air drag force which resists to the quadrotor motion, $\mathbf{F}_g = [0, 0, mg]^T$ is the gravity force, $\mathbf{M} = [\tau_\phi, \tau_\theta, \tau_\psi]^T$ represents the total rolling, pitching and yawing moments, \mathbf{M}_{gp} and \mathbf{M}_{gb} are the propellers and quadrotor body gyroscopic torques, respectively, and $\mathbf{M}_a = \text{diag}(\kappa_4, \kappa_5, \kappa_6) [\dot{\phi}^2, \dot{\theta}^2, \dot{\psi}^2]^T$ is the moment resulting from the aerodynamic frictions [29].

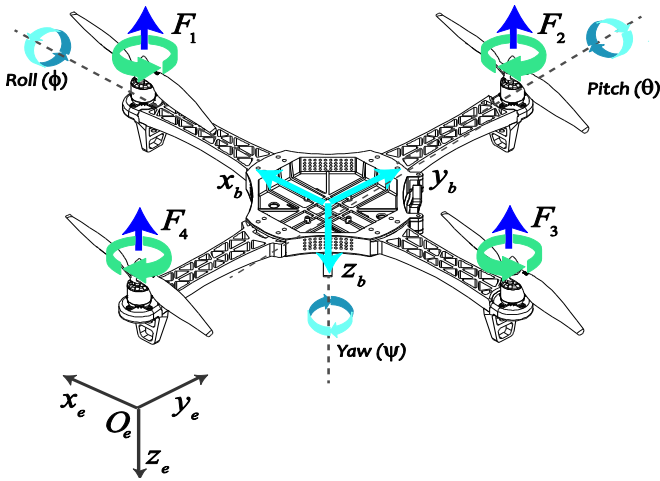


Fig. 1. Mechanical structure of the quadrotor and related frames.

By replacing the position vector and the forces expressions in (2), we acquire the next translational dynamics of the quadrotor:

$$\begin{cases} \ddot{x} = \frac{1}{m}(c\phi c\psi s\theta + s\phi s\psi)u_1 - \frac{\kappa_1}{m}\dot{x} \\ \ddot{y} = \frac{1}{m}(c\phi s\psi s\theta - s\phi c\psi)u_1 - \frac{\kappa_2}{m}\dot{y} \\ \ddot{z} = \frac{1}{m}c\phi c\theta u_1 - g - \frac{\kappa_3}{m}\dot{z} \end{cases} \quad (3)$$

From the second part of (2), we deduce the rotational dynamics of the quadrotors:

$$\begin{cases} \ddot{\phi} = \frac{(I_y - I_z)}{I_x}\dot{\theta}\dot{\psi} - \frac{J_r}{I_x}\bar{\Omega}_r\dot{\theta} - \frac{\kappa_4}{I_x}\dot{\phi}^2 + \frac{1}{I_x}u_2 \\ \ddot{\theta} = \frac{(I_z - I_x)}{I_y}\dot{\phi}\dot{\psi} - \frac{J_r}{I_y}\bar{\Omega}_r\dot{\phi} - \frac{\kappa_5}{I_y}\dot{\theta}^2 + \frac{1}{I_y}u_3 \\ \ddot{\psi} = \frac{(I_x - I_y)}{I_z}\dot{\theta}\dot{\phi} - \frac{\kappa_6}{I_z}\dot{\psi}^2 + \frac{1}{I_z}u_4 \end{cases} \quad (4)$$

where $\bar{\Omega}_r = \omega_1 - \omega_2 + \omega_3 - \omega_4$ denotes the overall residual rotor angular speed, I_x , I_y and I_z are the body inertia, J_r is the rotor inertia and $\kappa_i, i=1,2,\dots,6$ are the aerodynamic friction and translational drag coefficients.

The system's inputs are defined as u_1 , u_2 , u_3 and u_4 that represent the total thrust force in the z-axis, the roll, pitch and yawing torques, respectively:

$$\mathbf{u} = \begin{bmatrix} u_1 \\ u_2 \\ u_3 \\ u_4 \end{bmatrix} = \begin{bmatrix} b & b & b & b \\ 0 & -lb & 0 & lb \\ -lb & 0 & lb & 0 \\ d & -d & d & -d \end{bmatrix} \begin{bmatrix} \omega_1^2 \\ \omega_2^2 \\ \omega_3^2 \\ \omega_4^2 \end{bmatrix} \quad (5)$$

where b is the thrust coefficient, d is the drag coefficient, and ω_i is the angular speed of the i^{th} rotor.

Taking

$\mathbf{x} = (\phi, \dot{\phi}, \theta, \dot{\theta}, \psi, \dot{\psi}, x, \dot{x}, y, \dot{y}, z, \dot{z})^T \in \mathbf{R}^{12}$ as the state vector, the dynamical nonlinear model of the studied quadrotor is obtained as follows:

$$\dot{\mathbf{x}} = f(\mathbf{x}, \mathbf{u}) = \begin{cases} \dot{x}_1 = x_2 \\ \dot{x}_2 = a_1 x_4 x_6 + a_3 \bar{\Omega}_r x_4 + a_2 x_2^2 + b_1 u_2 \\ \dot{x}_3 = x_4 \\ \dot{x}_4 = a_4 x_2 x_6 + a_6 \bar{\Omega}_r x_2 + a_5 x_4^2 + b_2 u_3 \\ \dot{x}_5 = x_6 \\ \dot{x}_6 = a_7 x_2 x_4 + a_8 x_6^2 + b_3 u_4 \\ \dot{x}_7 = x_8 \\ \dot{x}_8 = a_9 x_8 + \frac{1}{m}(c\phi c\psi s\theta + s\phi s\psi)u_1 \\ \dot{x}_9 = x_{10} \\ \dot{x}_{10} = a_{10} x_{10} + \frac{1}{m}(c\phi s\theta s\psi - s\phi c\psi)u_1 \\ \dot{x}_{11} = x_{12} \\ \dot{x}_{12} = a_{11} x_{12} + \frac{c\phi c\theta}{m}u_1 - g \end{cases} \quad (6)$$

Where,

$$a_1 = \frac{I_y - I_z}{I_x}, \quad a_2 = -\frac{\kappa_4}{I_x}, \quad a_3 = -\frac{J_r}{I_x}, \quad a_4 = \frac{(I_z - I_x)}{I_y},$$

$$a_5 = -\frac{\kappa_5}{I_y}, \quad a_6 = -\frac{J_r}{I_y}, \quad a_7 = \frac{(I_x - I_y)}{I_z}, \quad a_8 = -\frac{\kappa_6}{I_z},$$

$$a_9 = -\frac{\kappa_1}{m}, \quad a_{10} = -\frac{\kappa_2}{m}, \quad a_{11} = -\frac{\kappa_3}{m}, \quad b_1 = \frac{l}{I_x}, \quad b_2 = \frac{l}{I_y}$$

$$\text{and } b_3 = \frac{1}{I_z}.$$

III. ADAPTIVE FUZZY GAINS-SCHEDULING OF INTEGRAL SLIDING MODE CONTROLLERS

A. Control Problem Statement

The control aims to establish an adaptive controller that eliminates the attitude and altitude error dynamics of the quadrotor to assure high performances and robustness. The desired trajectories of the controlled states are defined as $\mathbf{x}_d = [\phi_d, \theta_d, \psi_d, z_d]^T$ and the actual ones are set as $\mathbf{x} = [\phi, \theta, \psi, z]^T$.

As shown in Fig. 2, the altitude controller takes an error signal e as an input that introduce the gap between the desired altitude z_d and the actual state z and produces a control signal u_1 . In a similar way, the attitude and heading controllers take as inputs the error signals between the desired roll ϕ_d , pitch θ_d and yaw ψ_d and their actual values ϕ , θ and ψ to produce the output control signals u_2 , u_3 and u_4 , respectively.

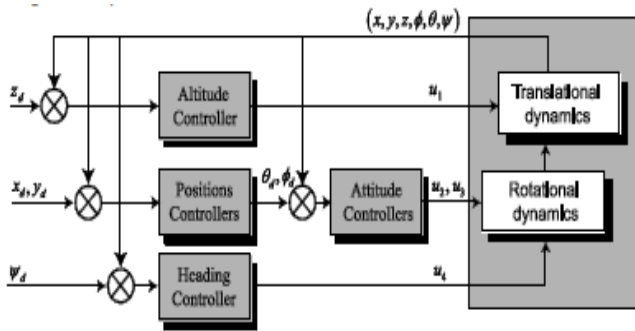


Fig. 2. Block diagram for altitude, attitude and heading controllers of the quadrotor.

The ISMC is a type of conventional SMC where an integral action is added to the general form of the sliding surface shape as proposed by [16]. The main aim is to lead the system states to the surface appropriately selected and conceive a stabilizing control law that maintains it. The sliding surface indicated by $s(\cdot)$ is specified as follows:

$$s_i(\mathbf{x}, t) = \left(\frac{d}{dt} + \lambda_i \right) e_i(\mathbf{x}, t) + \beta_i \int_0^\infty e_i(\mathbf{x}, t) dt \quad (7)$$

where \mathbf{x} denotes the accessible variables (states), $e_i(\mathbf{x}, t)$ is the tracking errors defined as $e_i(\mathbf{x}, t) = \mathbf{x}_d(t) - \mathbf{x}(t)$, λ_i is a positive constant that interprets the dynamics of the surface and β_i is the integral gain, $i \in \{\phi, \theta, \psi, z\}$.

The first time derivative of the sliding surface of (7) is given by:

$$\dot{s}(\mathbf{x}, t) = \ddot{\mathbf{x}}(t) + \lambda_i \dot{\mathbf{x}}(t) + \beta_i e(\mathbf{x}, t) \quad (8)$$

As shown in [14], [19], [20], the sliding control law includes two terms as given by the following equation:

$$u(t) = u_{eq}(t) + u_D(t) \quad (9)$$

with $u_{eq}(t)$ indicate the equivalent control which defines the behavior of the system when the perfect sliding regime is settled, and $u_D(t)$ is a discontinuous function, called switching control, obtained by verifying of the condition of the attractiveness [1]. It is helpful to make up the uncertainties of the model and frequently is introduced as:

$$u_D(t) = -K_i \text{sgn}(s_i(\mathbf{x}, t)) \quad (10)$$

Where, K_i presents a positive control parameter and $\text{sgn}(\cdot)$ denotes the mathematical signum function defined as:

$$\text{sgn}(s) = \begin{cases} 1, & s > 0 \\ 0, & s = 0 \\ -1, & s < 0 \end{cases} \quad (11)$$

Lyapunov stability analysis is the most common approach to demonstrate and to assess the stable convergence property of nonlinear controllers. Here, direct Lyapunov stability approach is used to consider the stability property of the suggested integral sliding mode controller. It consists to make a positive scalar function, given by (12), for the system state variables and then chooses the control law that will decrease this function:

$$\dot{V}(\mathbf{x}, t) < 0 \text{ with } V(\mathbf{x}, t) > 0 \quad (12)$$

This Lyapunov function can be chosen, to prove the closed-loop stability, as follows:

$$V(t) = \frac{1}{2} s^2(t) \quad (13)$$

Where, $V(0) = 0$ and $V(t) > 0$ for $s(t) \neq 0$.

The derivative of this above function is negative when the following expression, called the reaching condition [1], is checked:

$$s(\mathbf{x}, t) \dot{s}(\mathbf{x}, t) < 0 \quad (14)$$

For the quadrotor's altitude stabilization, we consider the following reduced model of such a flight dynamics:

$$\ddot{z} = a_{11} \dot{z} + \frac{c\phi c\theta}{m} u_1 - g \quad (15)$$

The design issue is to force the performance of the system states to the desired trajectories which are known. While

considering the reference trajectories \dot{z}_d and z_d which are the desired velocity and altitude, respectively, we define the relative tracking error by:

$$e_z = z - z_d \quad (16)$$

Referring to (8), the corresponding sliding surface is defined as follows:

$$s_z(t) = \dot{e}_z(t) + \lambda_z e_z(t) + \beta_z \int_0^\infty e_z(t) dt \quad (17)$$

Where, $\lambda_z > 0$ and $\beta_z > 0$ are the effective design parameters for the ISMC law.

According to (8) and (17), the integral sliding mode control law for the quadrotor's altitude dynamics is expressed as follows:

$$u_1 = \frac{m}{c\phi c\theta} [-a_{11}x_{12} - \lambda_z \dot{z} - \beta_z(z - z_d) - g] - K_z \operatorname{sgn}(s_z) \quad (18)$$

Where, $K_z > 0$ is a design ISMC parameter and $\phi, \theta \in]-\pi/2, \pi/2[$ to avoid singular positions.

So, while following the same steps as for the altitude dynamics, the integral sliding mode control laws u_2, u_3 and u_4 responsible of the roll, pitch and yaw dynamics stabilization, respectively, are calculated as follows:

$$u_2 = \frac{1}{b_1} [-a_1 x_4 x_6 - a_3 \bar{\Omega}_r x_4 - a_2 x_2^2 - \lambda_\phi x_2 - \beta_\phi e_\phi] - K_\phi \operatorname{sgn}(s_\phi) \quad (19)$$

$$u_3 = \frac{1}{b_2} [-a_4 x_2 x_6 - a_6 \bar{\Omega}_r x_2 - a_5 x_4^2 - \lambda_\theta x_4 - \beta_\theta e_\theta] - K_\theta \operatorname{sgn}(s_\theta) \quad (20)$$

$$u_4 = \frac{1}{b_3} [a_7 x_2 x_4 + a_8 x_6^2 - \lambda_\psi x_4 - \beta_\psi e_\psi] - K_\psi \operatorname{sgn}(s_\psi) \quad (21)$$

Where, $\lambda_i > 0$, $\beta_i > 0$ and $K_i > 0$ are the effective design parameters for the ISMC-based stabilization of the roll, pitch and yaw motions, $i \in \{\phi, \theta, \psi\}$.

B. Fuzzy Gains-Scheduling of Integral Sliding Mode Controllers

The fuzzy gains scheduling scheme of Fig. 3 is proposed for the ISMC parameters selection and tuning. Such fuzzy inference mechanisms adjust with an adaptive manner all ISMC gains leading to a systematic selection approach for ISMC design. As depicted in Fig. 3, both gains of the sliding surfaces and sign functions shown in (19) to (21), will be generated using fuzzy supervisors FLS1 and FLS2 based on fuzzy rules and reasoning.

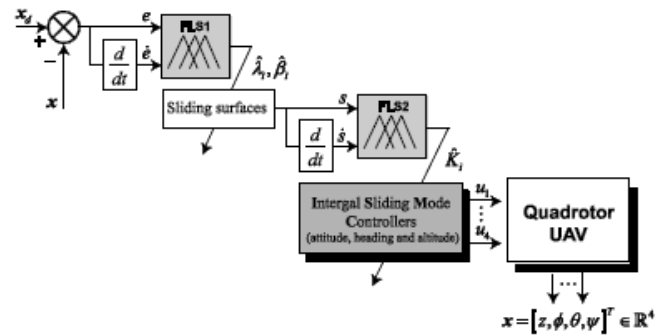


Fig. 3. Proposed fuzzy gains-scheduled integral sliding mode controllers.

The proposed fuzzy inference system FLS1 has two inputs $e(t)$ and its derivative $\dot{e}(t)$ and two outputs λ_i and β_i gains. The sliding surface gains are no longer fixed values. In fact, the gains are calculated at each sample period according to the evolution of the error. The decision-making outputs are obtained using a Max-Min fuzzy inference method where the crisp output is calculated by the center of gravity defuzzification technique. Tables I and II give the defined linguistic rules with the following assigned levels of the fuzzy inputs/outputs: N (Negative), NB (Negative Big), Z (Zero), P (Positive), PS (Positive Small), PM (Positive Medium), NB (Negative Big) and PB (Positive Big). All membership functions are defined with triangular and uniformly distributed shape.

TABLE. I. FUZZY RULES FOR λ_i VARIABLES.

		e				
		NB	N	Z	P	PB
\dot{e}	NB	Z	Z	Z	PS	PM
	N	Z	PS	PS	PS	PM
	Z	Z	PS	PM	P	PB
	P	PM	P	P	P	PB
	PB	PM	P	PB	PB	PB

TABLE. II. FUZZY RULES FOR β_i VARIABLES.

		e				
		NB	N	Z	P	PB
\dot{e}	NB	PB	Z	PB	PS	Z
	N	PB	P	P	PM	Z
	Z	P	P	PM	PS	Z
	P	PM	P	PS	PS	Z
	PB	PM	PS	Z	Z	Z

In this proposed supervision strategy, a set of linguistic rules in the form of Eq. (22) is used in the fuzzy inference block FLS1:

$$\text{If } e_i(x) \text{ is } A_i \text{ and } \dot{e}_i(x) \text{ is } B_i \text{ then } \lambda_i \text{ is } C_i \text{ and } \beta_i \text{ is } D_i \quad (22)$$

where A_i , B_i , C_i and D_i are the fuzzy sets corresponding to $e_i(\mathbf{x})$, $\dot{e}_i(\mathbf{x})$, λ_i and β_i linguistic variables, respectively.

The switching gains K_i are the main parameters to rise above perturbation and external interaction. Usually, the chattering amplitude of the controller is proportional to K_i , so the chattering could be diminished by setting this gain adaptively. The gains K_i should be smaller when it is near to the sliding surface and larger when it is farther [16].

As illustrated in Fig. 3, K_i gains will be generated using a second fuzzy supervisor, denoted as FLS2, where the sliding surface $s_i(\mathbf{x})$ and its differential $\dot{s}_i(\mathbf{x})$ are selected as inputs and K_i $i \in \{\phi, \theta, \psi, z\}$ are selected as outputs. The fuzzy rules for the proposed FLS2 are given in Table III.

TABLE III. FUZZY RULES FOR K_i VARIABLES

		s				
		Z	PS	PM	P	PB
\dot{s}	Z	PB	PB	P	P	PM
	PS	PB	P	P	PM	PS
	PM	PB	P	PM	PS	Z
	P	P	PM	PS	PS	Z
	PB	PM	PS	PS	Z	Z

The decision-making outputs are obtained using a Max-Min fuzzy inference and the crisp output is calculated by the center of gravity defuzzification method. A set of linguistic rules in the form of (23) is used in such a fuzzy supervisor to determine the gains K_i :

$$\text{If } s_i(\mathbf{x}) \text{ is } E_i \text{ and } \dot{s}_i(\mathbf{x}) \text{ is } F_i \text{ then } K_i \text{ is } G_i \quad (23)$$

where E_i , F_i and G_i are the fuzzy sets corresponding to $s_i(\mathbf{x})$, $\dot{s}_i(\mathbf{x})$ and K_i linguistic variables, respectively.

IV. NUMERICAL RESULTS AND DISCUSSIONS

The simulations have been established to validate the proposed adaptive fuzzy gains-scheduled ISMC approach. The physical parameters of the quadrotor UAV are given in Table IV.

The initial states of the quadrotor are set as $[x, y, z] = [0, 0, 0]$ and $[\phi, \theta, \psi] = [0, 0, 0]$ which means that the quadrotor is initially on the ground. The purpose of the designed adaptive fuzzy sliding mode controllers is to drive the rotorcraft to rise to 4 meters high and then keep hovering. At the same time, the quadrotor is controlled to bring the system states to be stabilized around the desired references [0.9; 0.5; 0.5] rad.

TABLE IV. QUADROTOR'S MODEL PARAMETERS

Symbol	Description	Value
b	Lift coefficient	$2.984 \times 10^{-5} N \cdot s^2 / rad^2$
d	Drag coefficient	$3.30 \times 10^{-7} N \cdot s^2 / rad^2$
m	Mass	1.1 Kg
l	Arm length	0.50 m
J_r	Motor inertia	$2.8385 \times 10^{-5} N \cdot m \cdot s^2 / rad$
I	Quadrotor inertia	$diag(0.005, 0.005, 0.010)$
g	Acceleration of the gravity	$9.81 m \cdot s^{-2}$

Unlike the conventional ISMC approach, the control gains λ_i , β_i and K_i of the proposed AFGS-ISMC are time-varying thanks to the supervisors FLS1 and FLS2 using the fuzzy rules of Tables I, II and III. The obtained fuzzy surfaces for all λ_i , β_i and K_i decision parameters are given in Fig. 4, 5 and 6, respectively.

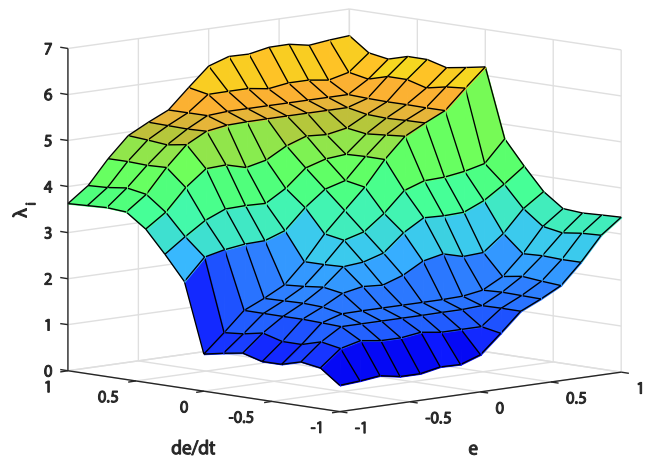


Fig. 4. Fuzzy surface for the λ_i gains.

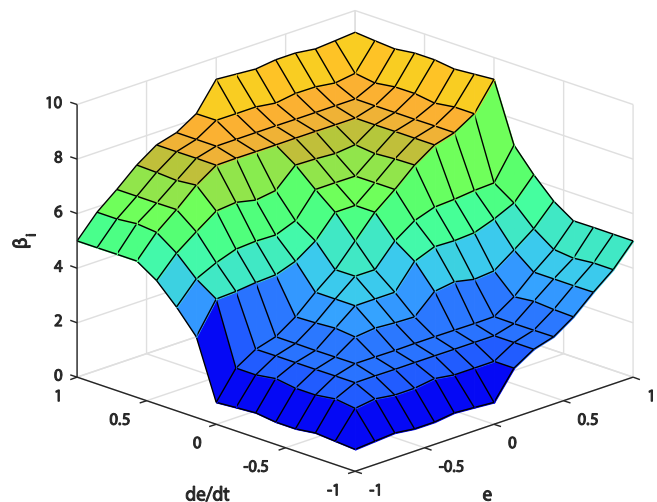


Fig. 5. Fuzzy surface for the β_i gains.

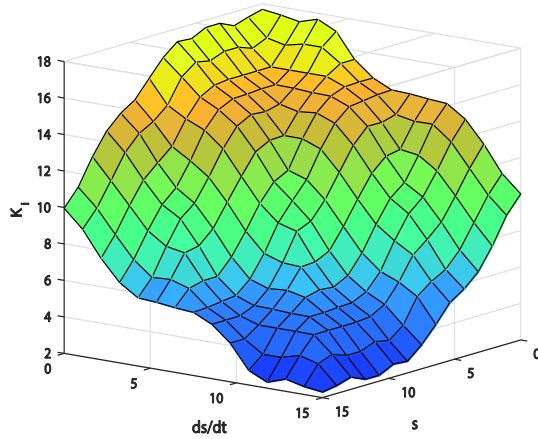


Fig. 6. Fuzzy surface for the K_i gains.

In this simulation scenario, external disturbances are applied on the quadrotor's outputs at the simulation time $t = 10\text{sec}$. The generated AFGS-based ISMC gains for the closed-loop altitude and attitude dynamics are shown in Fig. 7 to Fig. 10. All these controller's gains become time-varying which are more adapted and efficient to uncertainties and disturbances rejection as well as for the unwanted chattering phenomenon's attenuation.

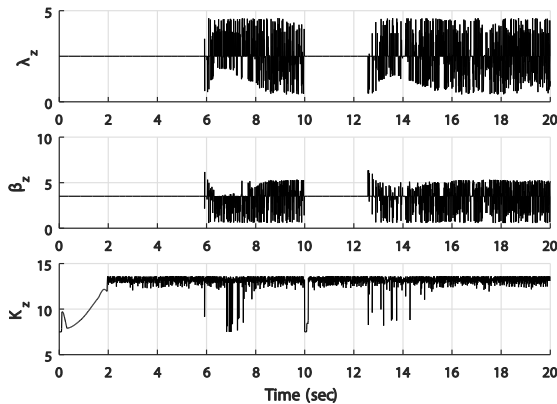


Fig. 7. Time evolution of the fuzzy gains-scheduled integral sliding mode gains: altitude dynamics.

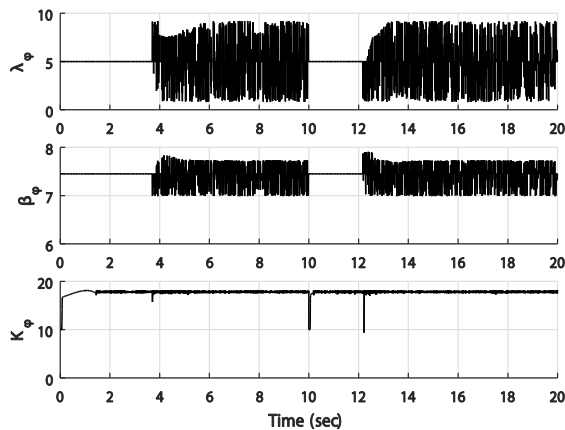


Fig. 8. Time evolution of the fuzzy gains-scheduled integral sliding mode gains: roll dynamics.

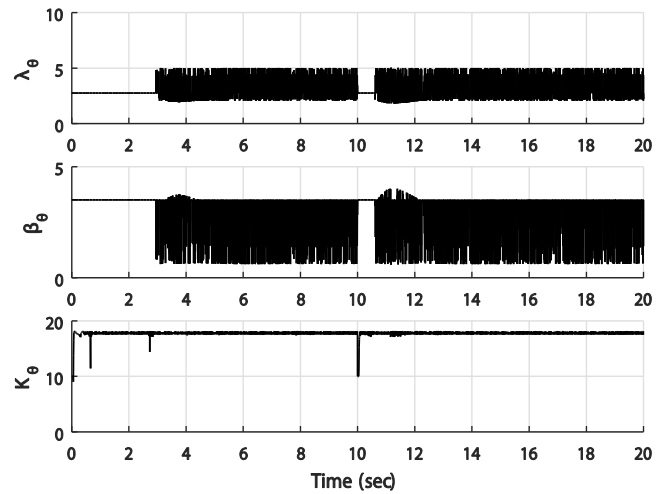


Fig. 9. Time evolution of the fuzzy gains-scheduled integral sliding mode gains: pitch dynamics.

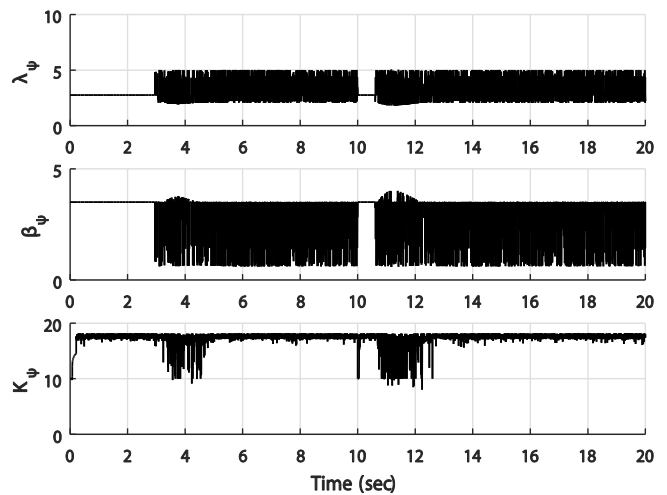


Fig. 10. Time evolution of the fuzzy gains-scheduled integral sliding mode gains: yaw dynamics.

So as to show the time-domain performances of the proposed AFGS-based sliding mode controllers, a comparison to the conventional ISMC case, using both $\text{sgn}(\cdot)$ and $\text{sat}(\cdot)$ based sliding functions, has been carried out and relative results are pictured in Fig. 11 to 14 for the altitude, roll, pitch and yaw motions, respectively. From these closed-loop step responses, it is verified that both ISMC and AFGS-ISMC strategies are effective for the attitude and altitude control. The AFGS-based controllers provide better results in terms of disturbances rejection and transient response damping. A slight overshoot is observed in the AFGS-based controllers' responses but with the advantage of high performance tracking responses. The steady-state precision and fastness of the AFGS-based controlled UAV dynamics are more improved related to the standard ISMC approach. Indeed, the dynamic response of the ISMC is delayed and the steady-state regime is reached within 3 seconds when applying an external disturbances.

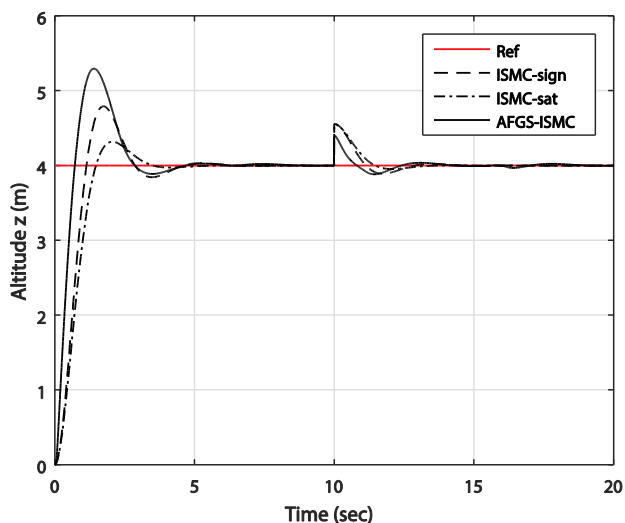


Fig. 11. Closed-loop step responses of the altitude dynamics.

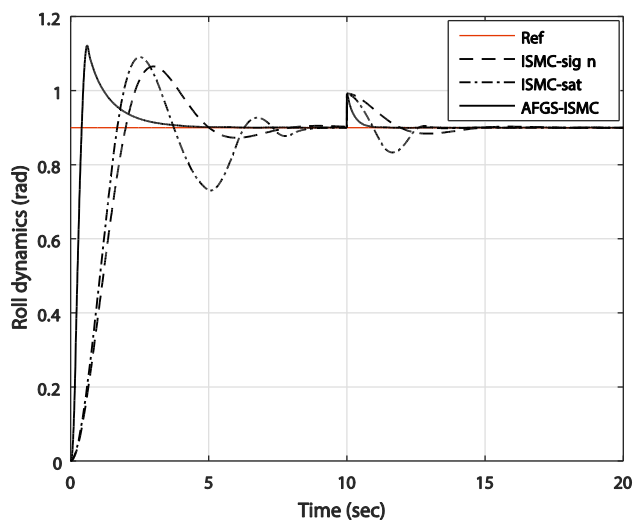


Fig. 12. Closed-loop step responses of the roll dynamics.

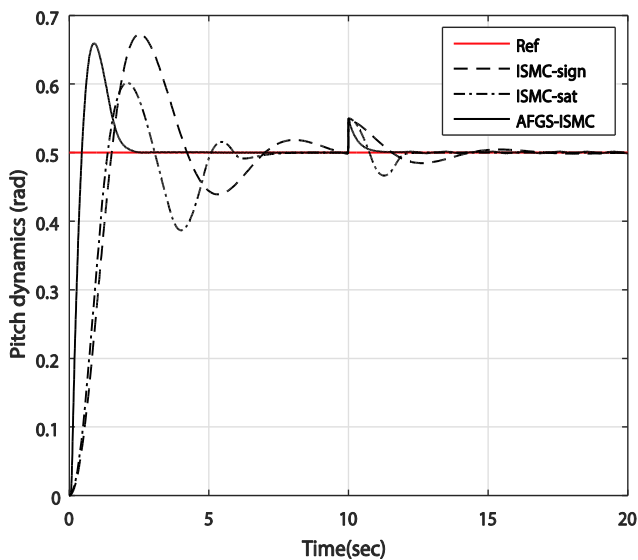


Fig. 13. Closed-loop step responses of the pitch dynamics.

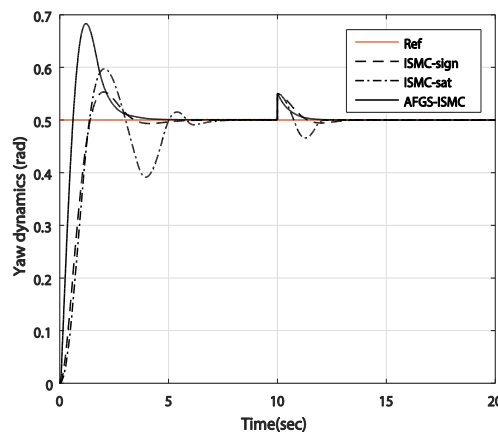


Fig. 14. Time-domain performances of the controlled yaw dynamics.

On the other hand, Fig. 15, 16, 17 and 18 display all control laws for the quadrotor's dynamics stabilization. The chattering phenomena are further reduced and the control laws are smoother due to the use of adaptive fuzzy gains-scheduling supervisors in the contrast to the classical ISMC without gains supervision mechanisms. Based on these results, the proposed free-chattering AFGS-based ISMC approach is promising in the definitive real-world implementation and hardware prototyping of the designed flight controllers for such a type of VTOL vehicles.

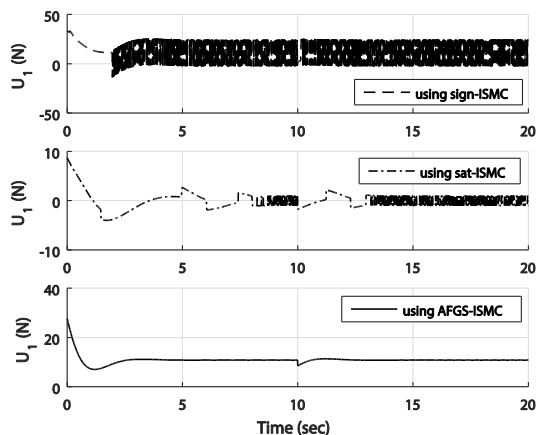


Fig. 15. Control laws for the altitude dynamics stabilization.

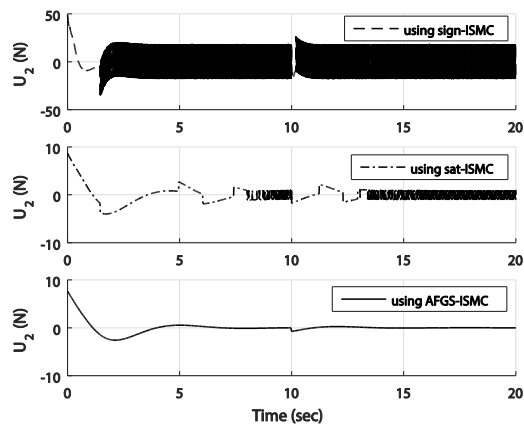


Fig. 16. Control laws for the roll dynamics stabilization.

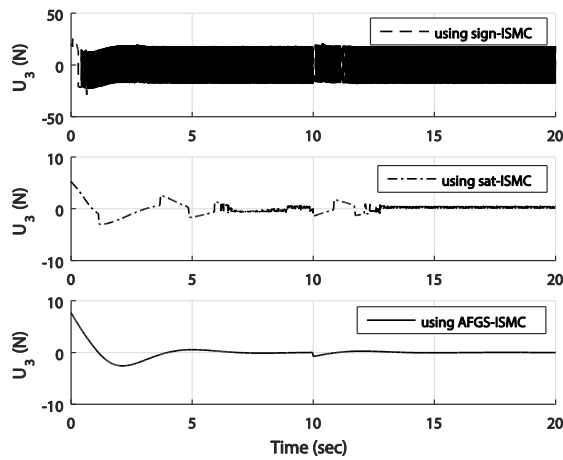


Fig. 17. Control laws for the pitch dynamics stabilization.

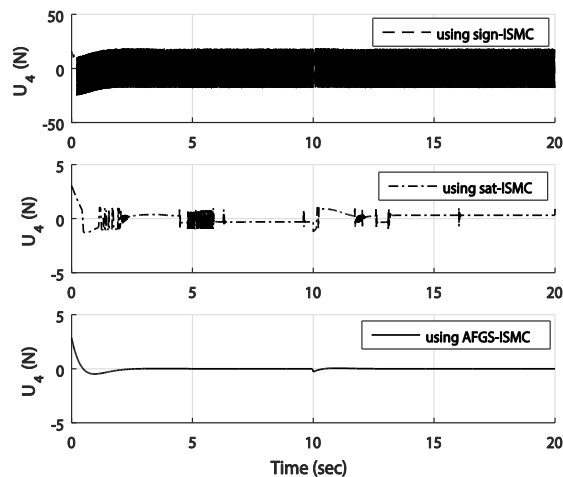


Fig. 18. Control laws for the yaw dynamics stabilization.

V. CONCLUSION

In this work, an adaptive fuzzy gains-scheduled integral sliding mode control approach is suggested and successfully applied for a quadrotor UAV. With a remarkable decreasing of the chattering phenomenon, this strategy is proposed to address the stabilization problem of the attitude and altitude dynamics of the studied vehicle. The dynamical model of the quadrotor was firstly settled using the Newton-Euler formalism. Then, the design of adaptive fuzzy gains-scheduled integral sliding mode controllers is detailed for each flight dynamics. In order to select and tune the gains of sliding controllers, as effective decision parameters, two fuzzy logic supervisors are proposed and implemented to make the controllers' gains varying adaptively. A comparison with the conventional ISMC strategy was made in terms of time-domain performances and chattering phenomenon attenuation. Through the simulation results, the proposed fuzzy gains-scheduling approach outperforms all other classical ISMC techniques with sign and saturation-based sliding functions. The design of integral sliding mode controllers with time-varying gains further enhances high closed-loop performances of the rotorcraft UAV in terms of stability and robustness. Forthcoming works deal with the Hardware-In-the-Loop (HIL) co-simulation of the designed ISMC approach.

REFERENCES

- [1] S.Vaidyanathan and C-H.LIEN,(Ed.),“*Applications of Sliding Mode Control in Science and Engineering*”,Springer-Verlag, Germany ,2017.
- [2] R. Lozano, (Ed.), “Unmanned Aerial Vehicles: Embedded Control”, ISTE and John Wiley & Sons, London UK and Hoboken USA,2013.
- [3] K. Nonami, F. Kendoul, S. Suzuki, W. Wang, and D. Nakazawa, “Autonomous Flying Robots: Unmanned Aerial Vehicles and Micro Aerial Vehicles”, Springer, New York,2010.
- [4] N. Ben Ammar, S. Bouallègue, J. Haggège, and S. Vaidyanathan “Chattering Free Sliding Mode Controller Design for a Quadrotor Unmanned Aerial Vehicle”, In S. Vaidyanathan and C-H. Lien (Eds.), *Applications of Sliding Mode Control in Science and Engineering*, Springer-Verlag, pp. 61-79, Germany,2017.
- [5] N. Ben Ammar, S. Bouallègue and J. Haggège. “Modeling and Sliding Mode Control of a Quadrotor Unmanned Aerial Vehicle”, In *Proceedings of the 3th International Conference on Automation, Control Engineering and Computer Science*, pp. 834-840, Hammamet, Tunisia,2016.
- [6] I. Fantoni, and R. Lozano, “Nonlinear Control for Underactuated Mechanical Systems”, Springer-Verlag, London, 2012.
- [7] J. Guerrero, and R. Lozano, “Flight Formation Control”, Wiley-ISTE, UK , 2012.
- [8] M.O. Efe, “Robust Low Altitude Behavior Control of a Quadrotor Rotorcraft through Sliding Modes”, In *Proceedings of the Mediterranean Conference on Control and Automation*, pp.1-6, Athens, Greece ,2007.
- [9] H.K . Khalil, “Nonlinear Systems”, Prentice Hall, New Jersey, 2002.
- [10] B.M . Meghni, D. Dib, A.T. Azar, “A Second-order sliding mode and fuzzy logic control to Optimal Energy Management in PMSG Wind Turbine with Battery Storage”, *Neural Computing and Applications*, Springer. DOI 10.1007/s00521-015-2161-z , 2016.
- [11] H. Mekki, D. Boukhetala, and A.T. Azar, “Sliding Modes for Fault Tolerant Control”, In: A.T Azar, Q. Zhu, (eds.), *Advances and Applications in Sliding Mode Control systems, Studies in Computational Intelligence book Series*, vol. 576, pp. 407-433, Springer-Verlag GmbH Berlin/Heidelberg. DOI 10.1007/978-3-319-11173-5_15 , 2015.
- [12] X. Li and J. Zhou, “A sliding mode control design for mismatched uncertain systems based on states transformation scheme and chattering alleviating scheme”, *Transactions of the Institute of Measurement and Control*, DOI:0142331216680351 , 2017.
- [13] Y. Liu and Y. Niu “Sliding mode control for uncertain switched systems subject to state and input delays”, *Transactions of the Institute of Measurement and Control*, DOI: 0142331217724195 , 2017.
- [14] B.B. Musmade and B.M. Patre, “Sliding mode control design for robust regulation of time-delay processes”, *Transactions of the Institute of Measurement and Control*, vol. 37, no. 6, pp. 699-707, 2015.
- [15] I. González-Hernández, S. Salazar, A. E. Rodríguez-Mata, F. Muñoz-Palacios, R. López, and R. Lozano, “Enhanced Robust Altitude Controller via Integral Sliding Modes Approach for a Quad-Rotor Aircraft: Simulations and Real-Time Results,” *J. Intell. Robot. Syst. Theory Appl.*, vol. 88, no. 2–4, pp. 313–327, 2017.
- [16] J-J.E. Slotine and W. Li, “Applied Nonlinear Control”, Prentice-Hall, Englewood Cliffs, New Jersey, 1991.
- [17] J-Z. Zhang and H-T. Zhang,“Vehicle Stability Sliding Mode Control Based on Fuzzy Switching Gain Scheduling”, In *International Conference on Measuring Technology and Mechatronics Automation* ,pp. 1067-1070, Changsha City, China,2010.
- [18] H. Sira-Ramirez, “On the dynamical sliding mode control of nonlinear systems”, *International Journal of Control*, vol. 5, no. 57, pp.1039-1061, 1993.
- [19] Y. Shtessel, C. Edwards, L. Fridman and A. Levant, “Sliding mode control and observation”, Springer, New York , 2014.
- [20] V. Utkin, J. Guldner and J. Shi, “Sliding mode control in electro-mechanical systems”, CRC Press, 2009.
- [21] S. Bouabdallah, A. Noth and R. Siegwart, “PID vs. LQ Control Techniques Applied to an Indoor Micro Quadrotor”, In *Proceedings of the IEEE/RSJ International Conference on Intelligent Robots and Systems*, pp. 2451-2456, Sendai, Japan , 2004.

- [22] F. Castañós and L. Fridman, "Analysis and design of integral sliding manifolds for systems with unmatched perturbations", *IEEE Transactions on Automatic Control*, vol. 51, no. 5, pp.853-858, 2006.
- [23] V. Utkin and J. Shi, "Integral sliding mode in systems operating under uncertainty conditions", *In Proceedings of the 35th IEEE Conference on Decision Control*, pp. 4591-4596, Dec, Kobe, 1996.
- [24] K. P. Ramesh, S. Kamal, A. Chalanga, and B. Bandyopadhyay, "Multivariable continuous integral sliding mode control," in *International Workshop on Recent Advances in Sliding Modes, RASM 2015*.
- [25] M. Rubagotti, D.M. Raimondo, A. Ferrara and L. Magni, "Robust model predictive control with integral sliding mode in continuous time ampled-data nonlinear systems", *IEEE Transactions on Automatic Control*, vol. 56, no. 3, pp. 556-570, 2011.
- [26] K. Nonaka and H. Sugizaki, "Integral Sliding Mode Altitude Control for a Small Model Helicopter with Ground Effect Compensation", *In Proceedings of the 2011 American Control Conference*, pp. 202-207, San Francisco, USA , 2011.
- [27] R.N.T. Dief and G.M. Abdelhady, "Attitude and altitude stabilization of quad rotor using parameter estimation and self-tuning controller", *In Proceedings of the AIAA Atmospheric Flight Mechanics Conference*, Dallas , 2015.
- [28] S.M. Mallikarjunan, B. Nesbitt and E. Kharisov, "L1 adaptive controller for attitude control of multi-rotors", *In Proceedings of the AIAA Guidance, Navigation, and Control Conference*, Minneapolis, Minnesota , 2012.
- [29] S.Bouallègue and R.Fessi, "Rapid control prototyping and PIL co-simulation of a quadrotor UAV based on NI myRIO-1900 board" *International Journal of Advanced Computer Science and Applications*, vol.7, no.6, pp.26-35, 2016.
- [30] W. Siler, and J.J. Buckley, "Fuzzy expert systems and fuzzy reasoning", John Wiley & Sons, New Jersey, 2005.
- [31] E. Mohammadi and M. Montazeri-Gh, "A fuzzy-based gas turbine fault detection and identification system for full and part-load performance deterioration", *Aerospace Science and Technology*, vol. 46, pp. 82-93, 2015.
- [32] S., Yin, P. Shi, and H.Y. Yang, "Adaptive fuzzy control of strict-feedback nonlinear time-delay systems with unmodeled dynamics", *IEEE Transactions on Cybernetics*, vol. 46, no. 8, pp. 1-12,2015.
- [33] I. Eker, and S.A. Akinal, "Sliding mode control with integral augmented sliding surface: design and experimental application to an electromechanical system", *Journal of Electrical Engineering*, vol. 97, no. 3, pp. 90-189,2008.

Interactive Hypermedia Programs and its Impact on the Achievement of University Students Academically Defaulting in Computer Sciences

Mohamed Desoky Rabeh

Department of Computer Science, Faculty of Community College, Northern Border University, Saudi Arabia
Department of Computer Teacher Preparation, Faculty of Specific Education,
Mansoura University, Egypt

Abstract—Traditional teaching practices through lecture series in a classroom have shown to have less universal efficacy in imparting knowledge to every student. Some students encounter problems in this traditional setting, especially in subjects that require applied instruction rather than verbal teaching. University students who have problems in understanding computer science have been hypothesized in this study to achieve better results on the application of interactive hypermedia programs in their curricula. The study has, thus, conducted a teaching survey through pretest-posttest control group design where computer science students of the Community College of Northern Border University were selected through non-probability sampling methodology and were made to undergo traditional teaching followed by interactive hypermedia sessions on the same subject. The evaluations of the change in performance provided results that showed that there existed a statistically significant difference in the mean scores of students after attending the interactive hypermedia program, providing evidence that hypermedia induced educational sessions were better to induce performance of students than those sessions that did not have any hypermedia exposure. However, the study also provided an understanding of limitations such as generalized quantitative experiments on computer science students of the Northern Border University, but the researcher believes that more widespread experimentation of the same kind can help establish the unbiased performance supremacy of hypermedia instruction in improving the academic performance of university students in different subjects.

Keywords—Interactive hypermedia program; traditional teaching; university students; computer sciences; achievement; impact

I. INTRODUCTION

Though technology is rapidly transforming how individuals live and work, the majority of the students are seen to have very less exposure to computers, as well as the subject of computer science [1]. The school administrators and principals of the schools are of the view that other subjects, such as science and mathematics are of more importance than computer science. It has also been noted that even though the aforementioned subjects are compulsory in higher education in many regions of the world, computer science is provided to the curriculum as an optional subject, and the students opting for these subjects are very less [1], [2]. The less exposure to the subject increases the chances of defaulting in the same in

higher education, such as when the student reaches college and university level. Many low-income countries also prioritize their curricula in accordance to the budgets, where many students are not made accustomed to a computer due to low budgets of procuring enough that all students can become familiar with the processes and technology [3]. Also, the existing curricula for computer science lack core elements such as programming and coding, instead of teaching how to use applications such as Office, without any chance of providing any advanced courses in computer science [4]. These challenges show the need of creating a different curriculum for computer science for students at the school, college and university level so that there is increased familiarity with the computer science as a subject and also in programming languages and coding as advanced courses for decreasing the level of defaulters in the academics.

There are various processes that can be implemented to change the present situation of computer science, such as allocating budget for specific subject groups, conducting workshops and seminars on the importance of computer science in the professional world due to increased use of technology in day-to-day life, but the most impactful change that can bring about a considerable change is the implementation of a modified and better curricula for computer sciences in various levels of academic learning [5]. Teaching strategies that can help the students to increase their interest and also their skills are through increased interaction, but the most important strategy that can work is an interactive program that uses computer to show graphics, media such as images and videos to aid towards the progression of understanding among students that have had problems with computer science and are academically defaulting on the subject [4].

Student learning is a process that involves many factors apart from the cognitive skills of the student in question, but also on the process or mode of teaching, mood and motivation, teacher's skills in teaching and the process of uptake of the lesson by the student [6]. The process of student-teacher interaction has been a tradition for many decades, but with the advent of technology in every sphere of an individual's life, there has been a rise of new processes that can help students and teachers in conducting the curricula of a particular course. The advancements seen in the media industry have seen a rise in the hypermedia processes, where the programs that use images and videos to put, a point across, has become a new

interface for teaching and has also led to an opening for teachers who want to increase the level of performance in their specific subjects [7]. Hypermedia programs are learning process programs that use web-based application and adaptive learning environments to provide a personalized learning experience for the students and help increase the level of teaching methods [8]. It has also been noted that the programs that come under the hypermedia can be tailored as per the needs of the students of that particular subject, and the teachers have the support of the interactive multimedia through coursework design so that students' performance increases in the subject of computer science. The hypermedia programs are developed in a way that they stimulate different aspects of a student's mind as they have different types of content as per the age range of the students [9]. The coursework which is supported by hypermedia programs is able to improve the performance of students on a specific topic. The most important need for this program, however, is that the teachers need to be updated with the learning, academic content so that the theoretical content of the program is aligned with the programs, and the teacher is able to use the support of multimedia in their individual teaching and support learning of their respective students. It has also been noted that there are certain types of students with different learning styles that are able to perform better in the hypermedia course, ones that were not able to grasp concepts in a traditional learning environment [6]. The academic ability is generally observed to be the deciding factor for success in academic pursuit, by recent researchers also suggests that learning on an individual level through different strategies might help in increasing the level of learning outcomes. Being able to match the individual preferences in a traditional lecture setting is difficult for the teachers, however, the programs offered by hypermedia and its assisted teaching processes are able to enhance the quality of interaction between a student and a teacher, leading the vulnerable and defaulting category of students to thrive away from a traditional setting [10]. Here, it is also important for teachers to be innovative and creative to understand which alternative method will help a defaulting student create more interest in learning computer science. The use of various ICT tools and courseware in multimedia can help in the learning process that aims to stimulate the interest of these students in computer science [11]. Thus, hypermedia can become a good tool in the teaching arena that involves creating interest and participation of students in stimulating faster uptake of lessons and more precise learning. By promoting interest and creating a sense of academic adventure through graphics, animation, audio, and text, the program can act as a catalyst in delivering better performance outputs and effectively help the students become performers in the said subject of computer science [12].

II. NEED FOR THE STUDY

Through the literature review, it can be assessed that there has been little to no research on the effectiveness of hypermedia programs in decreasing the chances of students' defaulting in computer science at the university level, specifically by creating processes that can lead them to achieve high in the subject instead. Thus, this research has been conducted to understand the impact of hypermedia in increasing chances of academic achievement in students that

otherwise default in computer science, and to assess the significant difference that the hypermedia programs brings into the performance of these different groups of students, through a pre and post-test analysis. Additionally, the study also seeks to analyze whether the hypermedia programs are significant enough in improving academic score to be included in the curriculum of the Northern Border University.

III. AIMS OF THE STUDY

The aims of the study are to analyze the effect of a proposed hypermedia program based on Interactive processes have on the achievement of university students, who are otherwise academically defaulting in computer sciences and provide a significant assessment of the choice to include it in the curriculum of the university. The research questions that needed to be answered through this were:

- a) What is the impact of a proposed program based on interactive multimedia to teach the computer skills on the achievement of students who failed to study at the Faculty of Community at Northern Border University?
- b) Are there statistically significant differences between the average scores of the students (the research sample) in the pre-application and the post-application test in favor of the post-application, after exposure to the use of the interactive hypermedia program in the computer, and the average grades through teaching in the usual way?
- c) Is the program optimal for application of the same for every student of the course, regardless of their learning abilities?

IV. METHODOLOGY

For assessing the significant change of students defaulting in computer science program in Community College of Northern Border University, the researchers employed a pretest-posttest control group design. The process of the test included two stages- first; the students underwent performance tests based on their knowledge on computers gained through traditional teaching methods, followed by a period of exposure of hypermedia programs for these students. To achieve the purpose of implementing hypermedia program, the largest interactive program devised by [13]. The program was based on 3 nodes, namely, movie, visualization and ready or commercial nodes. A system used to comprise of hypermedia capabilities such as photo-realistic images, sound generation, real-time animation, with additional peripherals including CD-ROM, a fixed-disk drive, and a mass storage of at least 500Mbytes. Students were integrated through simulation, wherein each of the questions resembled as below in Fig. 1.

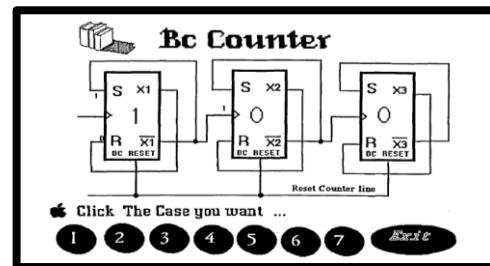


Fig. 1. Simulation of the binary counter (Source: [13]).

Upon completion of the hypermedia program, Stage 2 commences where students' knowledge of computers was evaluated through post-test. A particular set of students (N=30) enrolled in the Northern Border University was evaluated for both the tests to measure the degree of change in their acquired knowledge. The students have been chosen through purposive non-probability sampling methodology, as the objective of the study is only to measure the difference in performance of 30 students reading in a class before and after implementation of the hypermedia program. An experimental survey strategy was applied to data collection where an achievement test designed by the researcher was used to measure the performance. Upon obtaining prior permission from the University authority and in-charge of a particular class, and fixing a date to conduct the survey, data collection was carried by the distribution of achievement test questionnaires. The aim of the study was explained to the students followed by asking them to answer options, which they perceive as proximally correct. Upon collecting the data of pre-test, the hypermedia program for learning computer science was introduced to the students for a month. Observations on their degree of involvement and learning were noted, followed by the post-test applying the same achievement test. Answers in both pre- and post-test were measured on a dichotomous scale of 0 and 1, where 0 signified incorrect and 1 signified correct answer. Analysis of the scores collected has been conducted using paired samples T-test and ANOVA. While T-test measured the mean difference of pre- and post-test, ANOVA enabled to measure the mean difference in scores of between and within the group for individual tests.

V. RESULTS

As the study included only quantitative analysis (through an experimental survey), the researcher used only inferential statistics to deduce the results. In inferential statistical technique paired sample t-test was conducted on the data in both terms individually. The paired-samples t-test is considered to be applied to compare two means for those situations where every participant is involved in both samples [14].

Here, the aim of the study is to study the effect of a proposed program based on Interactive hypermedia on the achievement of university students academically defaulting in computer sciences. The analysis is based on the repeated measures on the same respondents before and after implementing the interactive hypermedia computer program. Therefore, the level of significant differences in the performance before and after implementing the program has been checked using paired sample t-test.

In order to move with the analysis, the assumption of normality has been performed. Shapiro-Wilk normality test has been performed to check the normality due to the small sample size.

In Table I, it can be seen that the average sample score data of 30 students are normally distributed as the significance value is higher than 0.05. Shapiro-Wilk value of the data collected by variable pre-computer training average performance of the students was $0.75 > 0.05$, and for the variable post-computer training average performance of the students, it was observed to be $0.057 > 0.057$.

TABLE I. NORMALITY TEST FOR PRE AND POST-TESTS CONDUCTED TO MEASURE STUDENTS' PERFORMANCE

Tests of Normality						
	Kolmogorov-Smirnov ^a			Shapiro-Wilk		
	Statistic	Df	Sig.	Statistic	df	Sig.
Pre-computer training average performance of the students	.134	30	.175	.937	30	.075
Post-computer training average performance of the students	.168	30	.030	.932	30	.057

a. Lilliefors Significance Correction

After proving that the data is normally distributed the next step is to look for the statistical difference in the performance of the University students before and after implementing the interactive hypermedia computer program.

TABLE II. DESCRIPTIVE FOR PRE AND POST-TEST CONDUCTED ON MEAN SCORES OF STUDENTS

Paired Samples Statistics					
		Mean	N	Std. Deviation	Std. Error Mean
Pair 1	Pre-computer training average performance of the students	.26909	30	.085200	.015555
	Post-computer training average performance of the students	.70485	30	.130561	.023837

Looking at the above Table II, a notable difference can be seen between the mean and standard deviation for both variables- pre-computer training average performance of the students and post-computer training average performance of the students. The average of average scores of all the students before implementing the hypermedia, interactive program is observed only to be 0.269; whereas the average of average scores of students after implementation of hypermedia program is 0.70485.

Table III shows that there is no significant association between the average performance of the students before and after training as the significant value is much higher than the standard acceptable level of significant value 0.05. However, no correlation between both the tests leaves any effect on the significance of t-test.

TABLE III. CORRELATION BETWEEN THE PRE AND POST-TEST CONDUCTED ON MEAN SCORES OF STUDENTS

Paired Samples Correlations				
		N	Correlation	Sig.
Pair 1	Pre-computer training average performance of the students & Post-computer training average performance of the students	30	-.067	.725

TABLE IV. PAIRED SAMPLE T-TEST FOR MEASURING THE SIGNIFICANCE DIFFERENCE BEFORE AND AFTER IMPLEMENTING THE HYPERMEDIA PROGRAM FOR COMPUTER SCIENCE STUDENTS

Paired Samples Test									
		Paired Differences					t	df	Sig. (2-tailed)
		Mean	Std. Deviation	Std. Error Mean	95% Confidence Interval of the Difference				
					Lower	Upper			
Pair 1	Pre- minus Post-computer training average performance of the students	-.435758	.160612	.029324	-.495731	-.375784	-14.860	29	.000

The above Table IV shows that the average scores obtained by the students in the test conducted after implementing the hypermedia interactive computer program in the University are .43 units higher than before after implementing the hypermedia, interactive computer program. Here, the significance value is less than <0.05 which shows that there is a significant difference in the performance of the students before and after implementing the computer program for University students. The higher mean value of average scores obtained post implementation of the computer program also supports the same.

Based on the t-test results it can be seen that the implementation of hypermedia computer program in University affects the difference on the performance as the mean score of the student increase post-program implementation.

VI. EFFECT SIZE OF STUDY PROGRAM

The value of Cohen's d and the effect-size correlation, r_{YX} was determined by calculating the mean difference between Result of the achievement test, before and after implementing the hypermedia program for computer science students and then dividing the result using the means and the pooled standard deviation.

$$\text{Cohen's } d = M_1 - M_2 / \sigma_{\text{pooled}}$$

$$\text{where } \sigma_{\text{pooled}} = \sqrt{[(\sigma_1^2 + \sigma_2^2) / 2]}$$

$$r_{YX} = d / \sqrt{(d^2 + 4)}$$

$$\text{Cohen's } d = -3.9528$$

$$\text{Effect-size} = 0.8922$$

The calculation of the Cohen's d value and the correlation size effect showed that there was a large effect size equal to 0.8922 after attending the interactive multimedia program. Thus, the proposed program based on interactive media to achieve academically backward university students in computer science affect the performance of students.

The results from this study suggest that the effects of using hypermedia in instruction are positive over the non - hypermedia instruction as a whole, however, the effects may be varied depending on what type of instruction that hypermedia compares to.

TABLE V. ANOVA TABLE FOR MEASURING THE SIGNIFICANCE OF MEAN DIFFERENCE BETWEEN THE SCORES OF ALL 30 STUDENTS BEFORE IMPLEMENTING THE HYPERMEDIA PROGRAM

ANOVA					
Effect of interactive hypermedia program on computer science students					
	Sum of Squares	df	Mean Square	F	Sig.
Between Groups	1.367	14	.098	1.098	.428
Within Groups	1.333	15	.089		
Total	2.700	29			

While looking at the above ANOVA Table V, it has been observed that before imposing the interactive hypermedia program for enhancing the computer skills of students there was not a statistically significant difference in the average scores of all students. The same has been deduced based on the significant level less than the standard acceptable level of significance $p\text{-value} > .05$.

In Table VI, it can be seen that there is a statistically significant difference between the mean score of students after proposing an interactive hypermedia program for increasing computer skills.

TABLE VI. ANOVA TABLE FOR MEASURING THE SIGNIFICANCE OF MEAN DIFFERENCE BETWEEN THE SCORES OF ALL 30 STUDENTS AFTER IMPLEMENTING THE HYPERMEDIA PROGRAM

ANOVA					
Effect of interactive hypermedia program on computer science students					
	Sum of Squares	df	Mean Square	F	Sig.
Between Groups	2.200	17	.129	3.106	.026
Within	.500	12	.042		

Groups					
Total	2.700	29			

VII. DISCUSSION

In this section of the study, the discussion of the findings has been done using the research question developed in the study.

1) What is the impact of a proposed program based on interactive multimedia to teach the computer skills on the achievement of students who failed to study at the Faculty of Community at Northern Border University?

Performing the analysis, it has been observed that the proposed program based on the interactive hypermedia program to teach the computer skills to the students result in improving the performance of the students who failed at the faculty of the community at the Northern Border University. Before imposing the program, the performance of the students was counted to be highly poor, but with the improved quality teaching through implementing the multimedia program at the campus the students' performance improved significantly. Based on which it can be said that the continuous adoption of new innovative technology and innovations for the purpose of improving student's IT and other skills help in developing the skills in students and improving their knowledge base.

A study conducted by Aloraini in [15] on testing the significant difference in the understanding of 20 females before and after using a multimedia computer-based presentation program showed that after implementing the computer-based interactive program there was a statistically significant difference in average scores of female students. On the other hand, the lecture delivered using traditional approach of dialogue and discussion did not show any statistically significant difference in the mean score of the female students. Osman Ilhan & Oruç in [16] aiming towards examining the effectiveness of the multimedia program on the academic success of 4th-grade students in Kayseri, Turkey also showed the consistency with the results obtained in the current study. This study was performed on 67 students of 4th class who were studying social studies section where I was treated as a control group and section II was referred to the experimental group. Further, it was concluded that multimedia program has a positive effect on student's academic success. Another study carried out by Nusir et al in [10] has also shown consistency with the results of the current study. This study was also performed using two specific groups and the difference in the performance of their scores in mathematics. It was found that the multimedia attracts the students and improve their level of learning math, which helps the students in performing well in their studies.

Thus, the implementation of the multimedia program would not only help the students in sharpening their future but also help the tutors and University management in understanding how they can improve the interest of students towards learning the computer. At the end, it can be said that the rapidly changing technology has a positive significant effect on the education of students. The multimedia program has increased the success of students in a more enjoyable and positive way.

2) Are there statistically significant differences between the average scores of the students (the research sample) in the pre-application and the post-application test in favor of the post-application, after exposure to the use of the interactive hypermedia program in the computer, and the average grades through teaching in the usual way?

While running the t-test on the mean of a student's score obtained before imposing the proposal of interactive hypermedia and the after imposing it has been obtained, there was the statistically significant difference between the average scores obtained. After exposure received by the students due to using the interactive hypermedia program a significant improvement in the score of students was observed. While looking at the value of mean scores in case of the traditional teaching way the mean scores of the students were highly poor. Implementing the hypermedia program can help in raising the performance. Examining the effect of multimedia material-based learning on two groups who received traditional and multimedia both types of materials (Yamauchi, 2008) in [5] showed that in pretest and posttest there was no statistically significant difference in the average scores of the students. (Shah & Khan, 2015) in [17] showed that there is a statistically significant difference between the average scores of the students' post providing multimedia-based teaching. On the other hand, there was no statistical difference in the mean scores of the students while providing traditional teaching. The current study has also shown the similarity with the results achieved in this study.

3) Is the program optimal for application of the same for every student of the course, regardless of their learning abilities?

Based on the results obtained from ANOVA, it can be seen that there is a statistically significant difference between the mean score of students after proposing an interactive hypermedia program for increasing computer skills. All the students in a course have a different level of learning abilities. However, combining the average scores of all students together, there is a statistically significant difference in the performance of the students between pre and post implementation of interactive hypermedia program. Therefore, it can be said that proposing the interactive hypermedia program is beneficial for the students, regardless of their abilities.

VIII. STUDY IMPLICATIONS

This entire study has focused on understanding the difference in the student's performance before and after implementing the hypermedia program in the University. The study may further help the students in understanding the effectiveness of the hypermedia digital program on their performance and thereby adapting themselves as per the new coursework for their future growth. The study has also helped in understanding the difference between the teaching way through traditional and advance digital media programs and their performance on the student's performance. Based on the findings obtained in the study the management can improve the performance of the students emphasizing more on hypermedia programs as part of their curriculum and pedagogy over

traditional approaches, thereby improving the teaching standards of the University in turn.

IX. LIMITATIONS

This entire study has focused on understanding the process of hypermedia in increasing chances of academic achievement in students that otherwise default in computer science, and to assess the significant difference that the hypermedia programs brings into the performance of these different groups of students, through a pre and post-test analysis. Though the research has met the objective of the study, the study is entirely based on only quantitative experiments done on the same sample set and its extent is limited to the students of the Northern Border University only. The generalization of the study may also have lesser scope due to the limited research conducted on the computer science students of the Northern Border University. Moreover, the study is quantitative study, if done qualitative study through interviews of teachers at the University the scope would have been clearer.

X. CONCLUSIONS

This study suggest that the effects of using hypermedia program in education are positive over the non-hypermedia education where the correlation size effect showed that there was a significant impact size of 0.8922 after students were exposed to the interactive hypermedia program. Though the researcher has tried to uncover the difference between the performances of computer science students before and after implementing the hypermedia program for enhancing computer skills, still there remain the facts uncovered which can be covered up in future studies. The future may explore the effectiveness of digital media program on the student's performance riding in the different domain also. In addition, the qualitative study may be performed to know the perception of teachers on students' performance through implementing the hypermedia digital program for students' learning skills. In addition, there have been only two pre and posted; there must be repeated tests so that the reliability of the implementation of digital media program can be ensured. Similar studies can be performed on a large sample size including the computer science students of another university as well. This will ensure the consistency in findings of this current study.

ACKNOWLEDGMENT

The author wish to acknowledge the approval and the support of this research study by the grant N° (6934-COM-2017-1-7-F) from the Deanship of the Scientific Research in Northern Border University (N.B.U.), Arar, KSA and all the collaborators in this study.

REFERENCES

- [1] Delen, E., & Bulut, O. (2011). The relationship between students' exposure to technology and their achievement in science and math. *TOJET: The Turkish Online Journal of Educational Technology*, 10(3), 1.
- [2] Fetler, M. (1985). Sex differences on the California statewide assessment of computer literacy. *Sex Roles*, 13 (3), 181–191.
- [3] Meerbaum-Salant, O., Armoni, M., & Ben-Ari, M. (Moti). (2013). Learning computer science concepts with Scratch. *Computer Science Education*, 23(3), 239–264.
- [4] Hazzan, O., Lapidot, T., & Ragonis, N. (2015). *Guide to teaching computer science: An activity-based approach*. Springer.
- [5] Yamauchi, L. G. (2008). Effects of multimedia instructional material on students' learning and their perceptions of the instruction. Iowa State University.
- [6] Zarei, A., Yusof, K., & Daud, M. (2016). A NOVEL APPROACH OF MULTIMEDIA INSTRUCTION APPLICATIONS IN ENGINEERING EDUCATION. *Journal of Theoretical and Applied Information Technology*, 93(2), 472.
- [7] Mora, J. (2012). The Analysis of Interactive Media and Digital Culture-Hypermedia Literacy in Peru and Bolivia/Medios interactivos y cultura digital: Alfa betización hipermedia en Perú. *Comunicar*, 20(39), 139.
- [8] Sun, P., & Cheng, H. (2007). The design of instructional multimedia in e-Learning: A Media Richness Theory-based approach. *Computers & Education*, 49(3), 662–676.
- [9] Pun, M. (2014). The use of multimedia technology in English language teaching: A global perspective. *Crossing the Border: International Journal of Interdisciplinary Studies*, 1 (1), 29–38.
- [10] Nusir, S., Alsmadi, I., Al-Kabi, M., & Sharadgah, F. (2013). Studying the Impact of Using Multimedia Interactive Programs on Children's Ability to Learn Basic Math Skills. *E-Learning and Digital Media*, 10(3), 305–319. <https://doi.org/10.2304/elea.2013.10.3.305>
- [11] Alhajri, R., & Alhunaibyan, A. A. (2017). Understanding the Impact of Individual Differences in Learner Performance Using Hypermedia Systems. *International Journal of Web-Based Learning and Teaching Technologies (IJWLTT)*, 12(1), 1–18.
- [12] Chandler, P. (2009). Dynamic visualisations and hypermedia: Beyond the "Wow" factor. *Computers in Human Behavior*, 25(2), 389–392.
- [13] Nasri, A. H. (2006). Developing a Hypermedia System for Computer Systems Education. *Computer Science Education*, 6(1), 33–47. Retrieved from <http://dx.doi.org/10.1080/0899340950060103>
- [14] Prophet. (1997). Do your data violate paired t test assumptions?
- [15] Aloraini, S. (2012). The impact of using multimedia on students' academic achievement in the College of Education at King Saud University. *Journal of King Saud University - Languages and Translation*, 24 (2), 75–82. <https://doi.org/10.1016/J.JKSULT.2012.05.002>
- [16] Osman Ilhan, G., & Oruç, Ş. (2016). Effect of the use of multimedia on students' performance: A case study of social studies class, 11 (8), 877–882. <https://doi.org/10.5897/ERR2016.2741>
- [17] Shah, I., & Khan, M. (2015). Impact of Multimedia-aided Teaching on Students' Academic Achievement and Attitude at Elementary Level. *US-China Education Review A*, 5(5), 349–360. <https://doi.org/10.17265/2161-623X/2015.05.006>

Mobile Phone Operations using Human Eyes Only and its Applications

Kohei Arai

Information Science Department
Graduate School of Science and Engineering, Saga University
Saga City, Japan

Abstract—Mobile phone operations using human eyes only is proposed together with its applications for cooking with referring to recipes and manufacturing with referring to manuals, production procedure, so on. It is found that most of mobile phone operations can be done without touching the screen of the mobile phone. Also, mobile phone operation success rate based on the proposed method is evaluated for the environmental illumination conditions, visible or near infrared (NIR) cameras, the distance between user and mobile phone, as well as pupil size detection accuracy against the environmental illumination changes. Meanwhile, the functionality of two typical applications of the proposed method is confirmed successfully.

Keywords—Mobile phone operations; line of sight estimation; gaze estimation; wearable computing; pupil detection

I. INTRODUCTION

Evaluation of users' impact for using the proposed Eye Based Human-Computer Interaction: EBHCI with moving and fixed keyboard by using EEG signals is investigated [1]. Electric wheel chair controlled by human eyes only with obstacle avoidance is proposed [2]. Robot arm control with human eyes only and its application to help having meal for patients is proposed [3]. These methods and systems are overviewed (Human-Computer Interaction with human eyes only and its applications) [4].

A new keyboard for improving accuracy and minimizing fatigue effect is invented [5] followed by moving keyboard for EBHCI [6]. Service robot which is controlled by human eyes only with voice communication capability is developed as an example of EBHCI [7] followed by eye-based domestic robot allowing patient to be self-services and communications remotely [8].

Method for psychological status estimation by gaze location monitoring using EBHCI is proposed [9] followed by method for psychological status monitoring with line of sight vector changes (Human eyes movements) detected with wearing glass [10]. It becomes wearable computing system with input output devices based on EBHCI allowing location based web services [11].

Speed and vibration performance as well as obstacle avoidance performance of electric wheel chair controlled by human eyes only is evaluated [12]. Service robot with communication aid together with routing controlled by human eyes is overviewed [13]. On the other hand, information collection service system by human eyes for disable persons is

developed [14]. Meanwhile, the relation between psychological status and eye movement is clarified [15].

Method for 3D image representation with reducing the number of frames based on characteristics of human eyes is proposed [16]. On the other hand, error analysis of line of sight estimation using Purkinje images for EBHCI is made [17]. Then, new service robot controlled by human eye which allows patients in hospitals self-services remotely is overviewed [18].

In the paper, mobile phone operations using human eyes only is proposed together with its applications for cooking with referring to recipes and manufacturing with referring to manuals, production procedure, so on. Although EBHCI is computer based method and systems, the proposed system EBHCI can be realized with mobile phone. Without touching the screen of the mobile phone, some of the operations can be done with human eyes only.

The following section describes the proposed system. Then, experiments are described with some experimental results of the mobile operation success rate followed by some applications of the proposed system. Finally, conclusion is described with some discussions.

II. PROPOSED SYSTEM

A. Proposed Methods

Fig. 1 shows the proposed gaze estimation procedure. With Near Infrared: NIR camera, face image is acquired followed by face detection by using OpenCV. Then, eye detection is made with OpenCV followed by pupil detection with ellipsoidal shape approximation. Also, Purkinje image which is acquired with six NIR Light Emission Diodes: LEDs are used for estimation of cornea curvature and curvature center.

Example of the acquired Purkinje image (Red ellipsoid) and pupil (Blue ellipsoid) of which the shape is approximated with ellipsoid is shown in Fig. 2(a). The Purkinje images are aligned with ellipsoidal shape because the reflected light of six LEDs at the surface of the eye is aligned with the hexagonal shape as is shown in Fig. 2(b). The line of sight is defined as the line on the curvature center and pupil center. Using the estimated line of sight, gaze location is estimated. It, however, is not stable enough during the period of the gaze estimation, every 0.5 sec. It is shorter than 0.3 sec. for typical accidental blink time. Therefore, it is intentional blink if user close their

eye for much longer than 0.3 sec. Thus, the line of sight can be estimated every 0.5 sec.

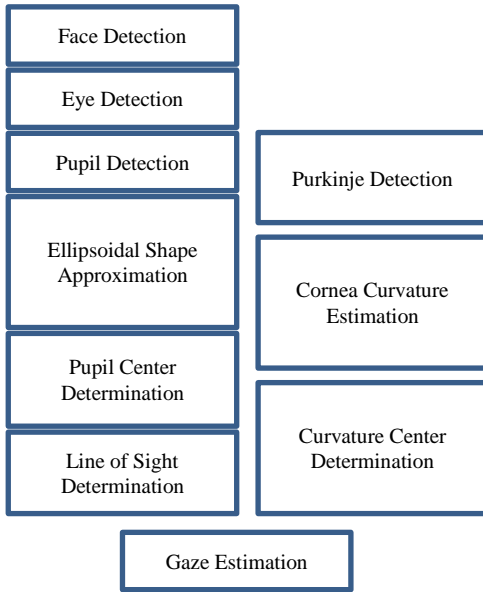


Fig. 1. Procedure of the proposed gaze estimation.

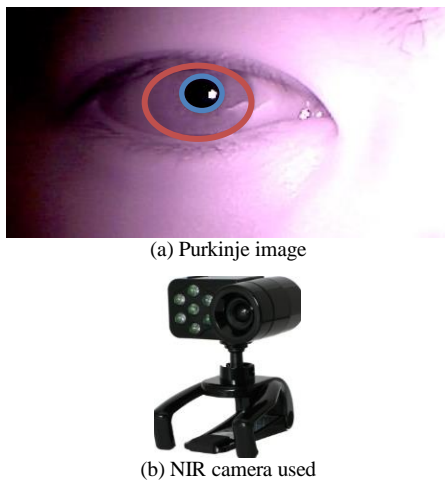


Fig. 2. Example of Purkinje image (red ellipsoid) and pupil of which the shape is approximated with ellipsoid (blue ellipsoid) and NIR camera used.

Pupil detection procedure is illustrated in Fig. 3. The acquired eye image is binarized first, then edge is detected with Canny filter. After that, ellipsoidal shapes are selected from the edge images as candidates of the pupil. Then, the shorter and the longer radius is estimated followed by pupil center determination of which the two radius are crossing at the pupil center.

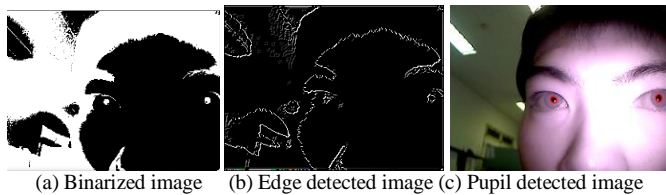


Fig. 3. Pupil detection method.

B. Mobile Phone Operation Selection

Fig. 4 shows the designed four mobile phone operations with the estimated gaze location and blinks. Due to the fact that line of sight estimation cannot be made accurately and stable, just four operations can be detected with the estimated line of sights. These four operations would be enough for choosing the required operations of the applications of the proposed method.

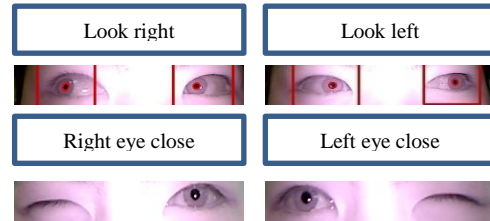
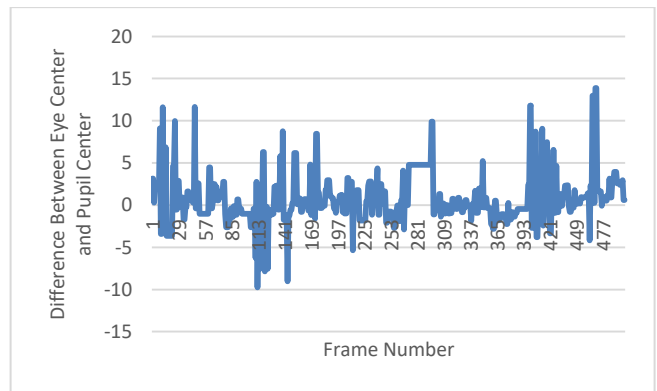


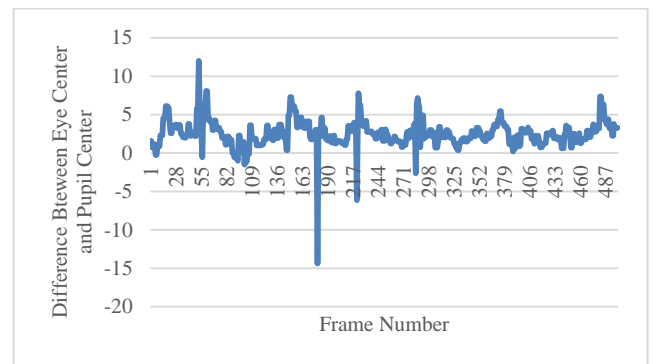
Fig. 4. Four mobile phone operations with the estimated gaze location and blinks.

It, however, is still difficult to identify the direction of which user is looking to. Therefore, the proposed method defines the direction by using the difference between the estimated eye center and pupil center. It is relatively easy to find the eye center because the two ends of eye can be identified using acquired eye images.

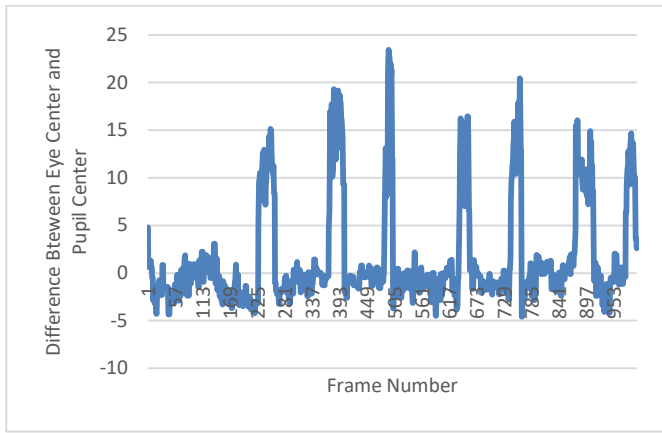
Fig. 5 shows the estimated gaze location when user is looking to up and down directions as well as right and left directions. It is relatively easy to discriminate for to right and left directions while it is not so easy to discriminate for up and down directions. Therefore, just the discrimination of right and left directions is used.



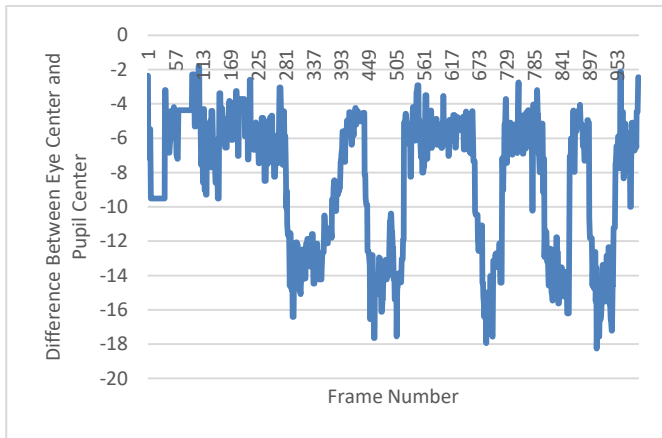
(a) Upward



(b) Downward



(c) Rightward



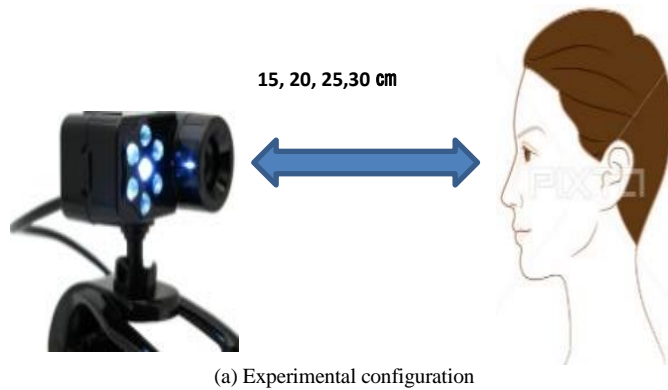
(d) Leftward

Fig. 5. Estimated gaze location when user is looking to up and down directions as well as right and left directions.

III. EXPERIMENT

A. Experimental Configuration

Fig. 6(a) shows the experimental configuration. The distance between user and NIR camera and LED is set at 15, 20, 25, and 30 cm. Illuminations are set at three conditions, 40 to 50 Lux, 140 to 150 Lux. On the other hand, Fig. 6(b) shows the outlook of the experimental configuration.



(a) Experimental configuration



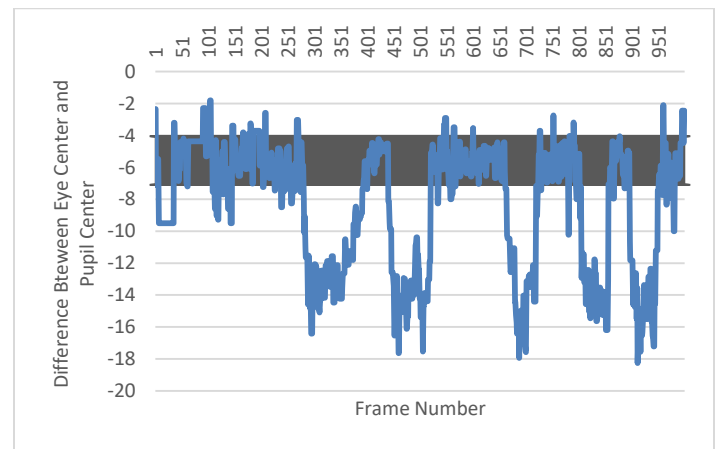
(b) Outlook

Fig. 6. Experimental configuration.

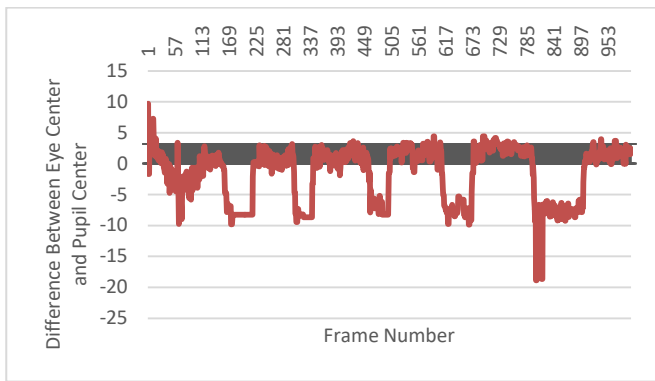
B. Threshold Determination using Standard Deviation of the Difference between Eye Center and Pupil Center

Meanwhile, Fig. 7 shows the difference between eye center and pupil center of right and left eyes when user is looking to right and left directions. In the figure, average and standard deviation of the difference between eye center and pupil center are also shown with the black bars. It is relatively easy to discriminate the direction of which user is looking to. Thus, the direction of which user is looking to can be detected.

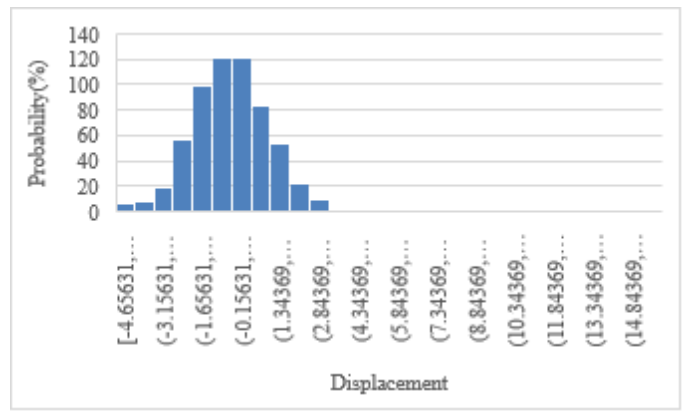
As shown in Fig. 7(a) and (b), it can be decided that the user is now looking to the left direction because the difference between eye center and pupil center is lower than the standard deviation for a while. Meanwhile, it also can be recognized the user is now looking to the right direction because the difference is larger than the standard deviation for a while as shown in Fig. 7(c) and (d).



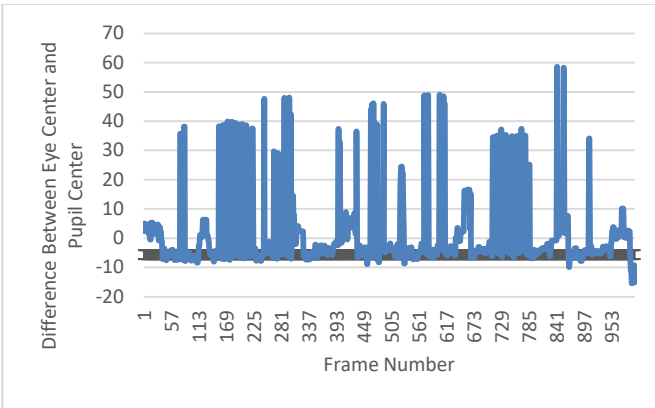
(a) Looking to left, Right eye



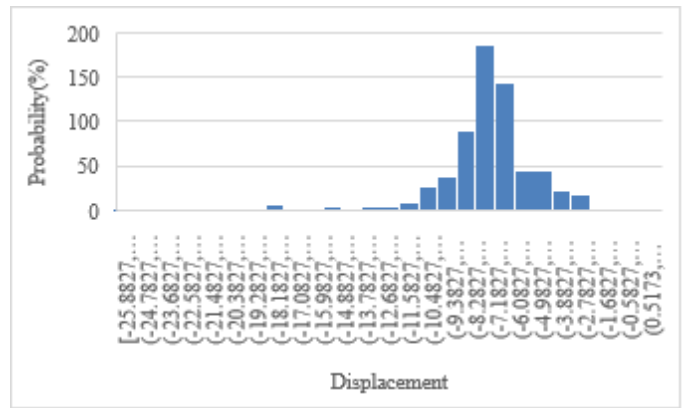
(b) Looking to left, Left eye



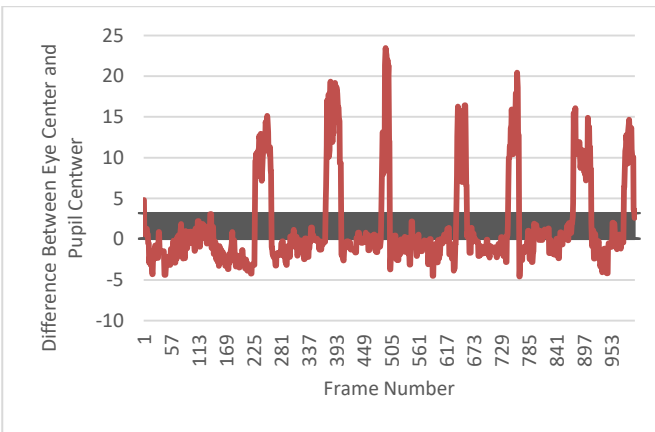
(a) Right eye, 15cm



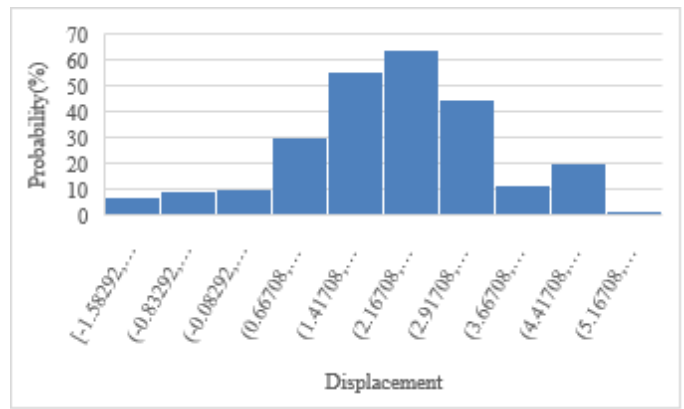
(c) Looking to right, Right eye



(b) Left eye, 15cm



(d) Looking to right, Left eye

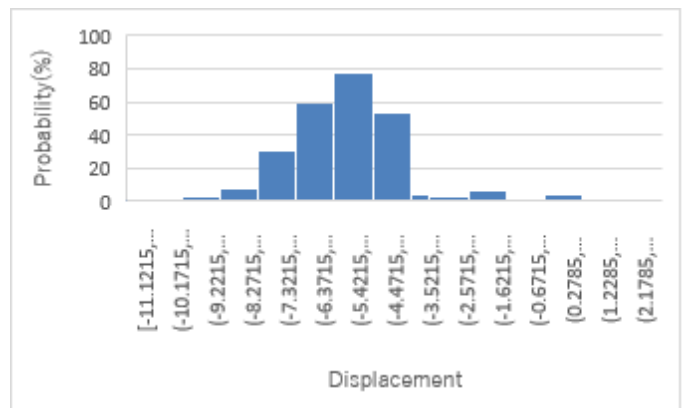


(c) Right eye, 20cm

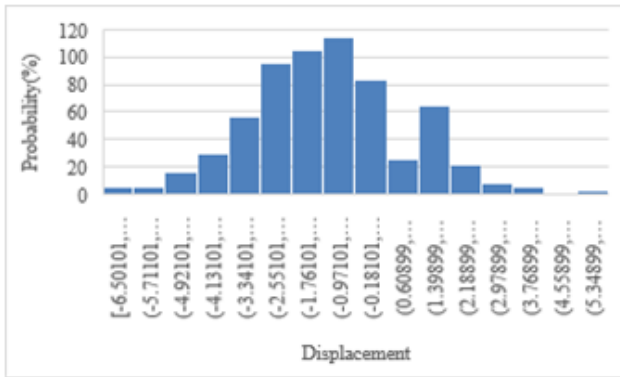
Fig. 7. Estimated gaze locations when user is looking to right and left directions.

C. Evaluation of Probability Density Function of the Difference between Eye Center and Pupil Center

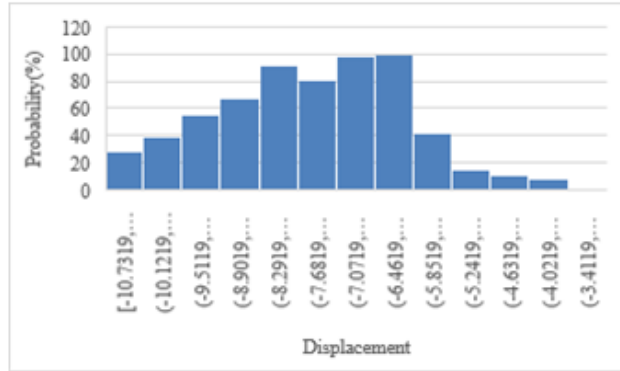
Probability Density Function: PDF of the difference between eye center and pupil center is evaluated as a function of the distance between user and mobile phone NIR camera. As the result of the experiment, shown in Fig. 8, it is found that shortest distance of 15 cm shows the best performance in terms of identification if the direction of which the user is looking to.



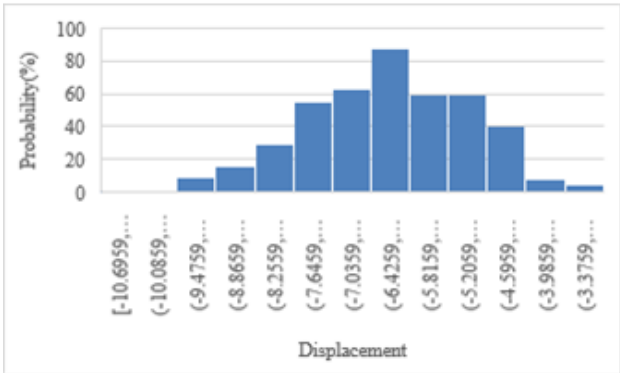
(d) Left eye, 20cm



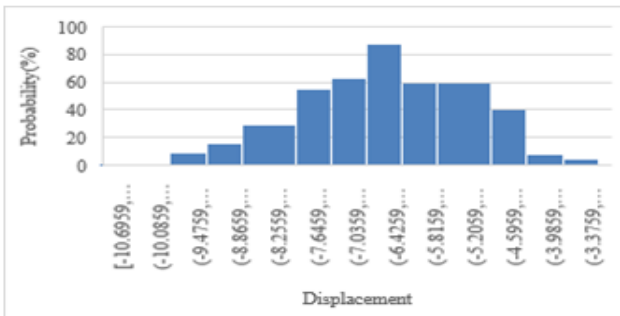
(e) Right eye, 25cm



(f) Left eye, 25cm



(g) Right eye, 30cm



(h) Left eye, 30cm

Fig. 8. Probability density function of the difference between eye center and pupil center as a function of the distance between user and the NIR camera attached to the mobile phone.

D. Illumination Condition

On the other hand, the area and the short radius as well as the long radius of the ellipsoid of which pupil shape is approximated depend on the illumination conditions. Fig. 9(a) shows the area which is determined with the short radius over 2 multiplied by the long radius over 2 of the ellipsoid of which pupil shape multiplied by π is approximated for the right eye while those of the left eye is shown in Fig. 9(b), respectively. The grey colored line shows the right eye area for the illumination condition of 1 to 10 Lux, while red colored line shows that of 40 to 50 Lux. On the other hand, the blue colored line shows that of 140 to 150 Lux, respectively. Those are same thing for the left eye of the illumination condition. It is obvious that the area and the short radius as well as the long radius of the ellipsoid of which pupil shape is approximated is getting smaller when the brighter illumination condition.

Fig. 10 also shows the estimated short radius and the long radius of the ellipsoid of which the acquired pupil shape is approximated.

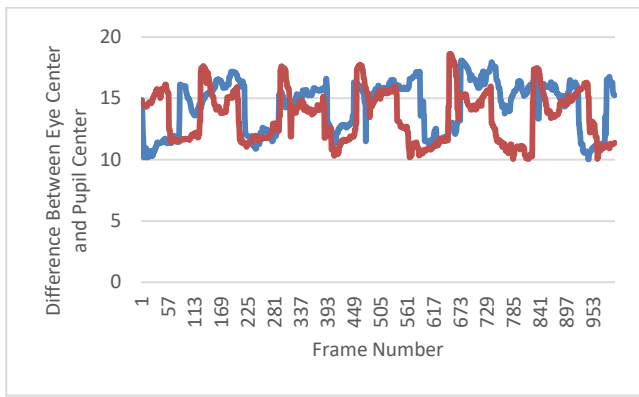


(a) Right eye

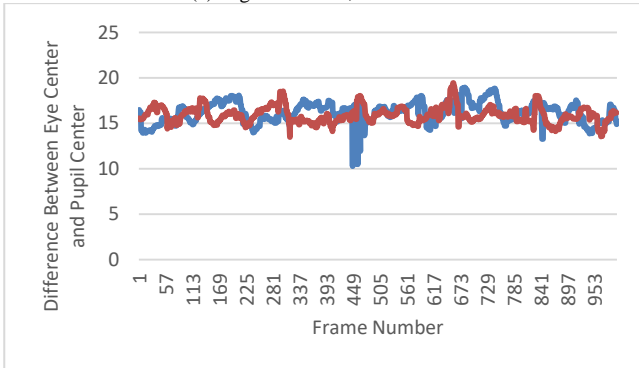


(b) Left eye

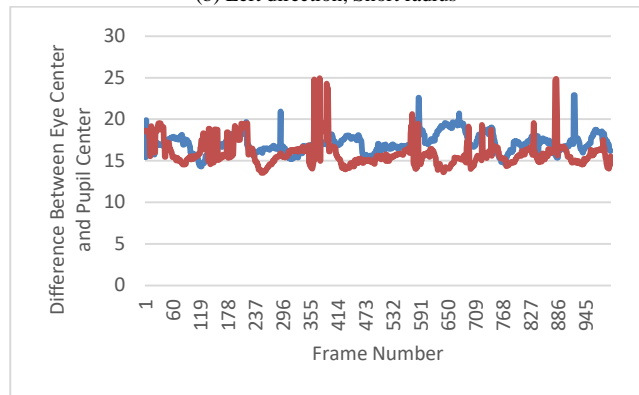
Fig. 9. The calculated area of the detected pupil under the different illumination conditions, 0-10 (grey), 40-50 (orange) and 140-150 (blue) Lux.



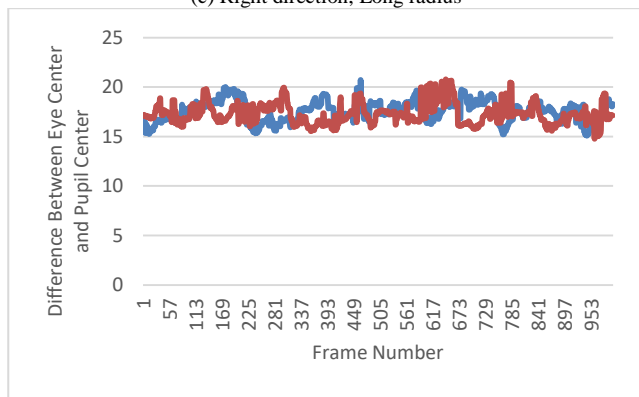
(a) Right direction, Short radius



(b) Left direction, Short radius



(c) Right direction, Long radius



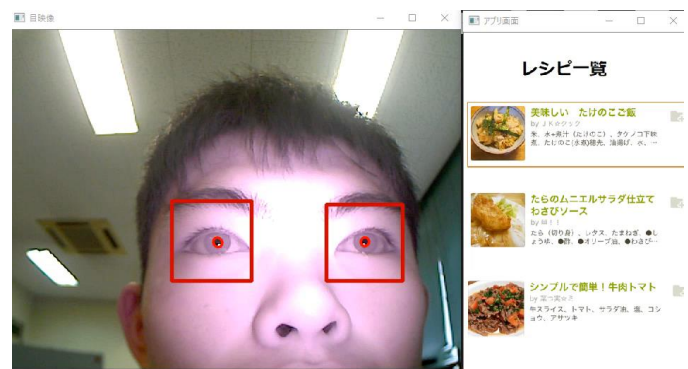
(d) Left direction, Long radius

Fig. 10. Difference between eye center and pupil center of long and short radius when the user is looking to the right and left directions.

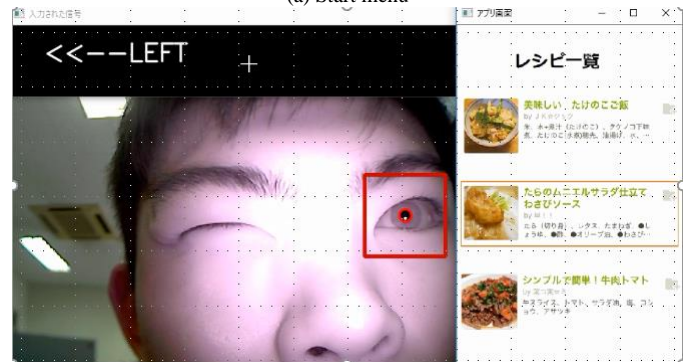
IV. EXAMPLES OF APPLICATION

One of the applications of the proposed system is cooking with referring to a recipe. Fig. 11 shows an example of mobile phone operation with look direction and blink detections for the cooking with referring to the recipe. Without touching to mobile phone, user can use mobile phone operation, page forward, backward, showing the content, as well as the menu for cooking. Users' response is positive for all. Fig. 11(a) shows the start menu (main menu) while Fig. 11(b) shows the sub-menu when the user selected the second recipe from the main menu by using the right eye close (user select the desired downward direction of sub menu).

Another example is construction of houses and buildings with referring to design drawings as well as construction procedures without touching screen of the display of their mobile phone. Constructing workers can refer the documents and drawings when they working at construction sites in a safe manner.



(a) Start menu



(b) Selection of the second sub menu

Fig. 11. Example of mobile phone operation with look direction and blink detections.

V. CONCLUSION

Mobile phone operations using human eyes only are proposed together with its applications for cooking with referring to recipes and manufacturing with referring to manuals, production procedure, and so on. It is found that most of mobile phone operations can be done without touching the screen of the mobile phone. Also, mobile phone operation success rate based on the proposed method is evaluated for the environmental illumination conditions, visible or Near Infrared: NIR cameras, the distance between user and mobile phone, as well as pupil size detection

accuracy against the environmental illumination changes. Meanwhile, the functionality of two typical applications of the proposed method is confirmed successfully.

Further investigation is required for application of the proposed method and system.

ACKNOWLEDGMENT

Author would like to thank Mr. Ryuichi Ohmori of Saga University for his cooperation through this research work.

REFERENCES

- [1] Kohei Arai, R.Mardiyanto, Evaluation of users' impact for using the proposed eye based HCI with moving and fixed keyboard by using eeg signals, International Journal of Research and review on Computer Science, 2, 6, 1228-1234, 2012.
- [2] Kohei Arai, R.Mardiyanto, Electric wheel chair controlled by human eyes only with obstacle avoidance, International Journal of Research and Review on Computer Science, 2, 6, 1235-1242, 2012.
- [3] Kohei Arai, R.Mardiyanto, Robot arm control with human eyes only and its application to help having meal for patients, Journal of Electrical Engineering Society of Japan, Transaction C, C132, 3, 416-423, 2012.
- [4] Kohei Arai, Human-Computer Interaction with human eyes only and its applications, Journal of Image Electronics Society of Japan, 41, 3, 296-301, 2012.
- [5] R.Mardiyanto, Kohei Arai, Eye-based Human Computer Interaction (HCI) A new keyboard for improving accuracy and minimizing fatigue effect, Scientific Journal Kursor, (ISSN 0216-0544), 6, 3, 1-4, 2012.
- [6] Kohei Arai, R.Mardiyanto, Moving keyboard for eye-based Human Computer Interaction: HCI, Journal of Image and Electronics Society of Japan, 41, 4, 398-405, 2012.
- [7] Kohei Arai, R.Mardiyanto, Service robot which is controlled by human eyes only with voice communication capability, Journal of Image Electronics Society of Japan, 41, 5, 535-542, 2012.
- [8] Kohei Arai, Ronny Mardiyanto, Eye-based domestic robot allowing patient to be self-services and communications remotely, International Journal of Advanced Research in Artificial Intelligence, 2, 2, 29-33, 2013.
- [9] Kohei Arai, Ronny Mardiyanto, Method for psychological status estimation by gaze location monitoring using eye-based Human-Computer Interaction, International Journal of Advanced Computer Science and Applications, 4, 3, 199-206, 2013.
- [10] Kohei Arai, Kiyoshi Hasegawa, Method for psychological status monitoring with line of sight vector changes (Human eyes movements) detected with wearing glass, International Journal of Advanced Research in Artificial Intelligence, 2, 6, 65-70, 2013.
- [11] Kohei Arai, Wearable computing system with input output devices based on eye-based Human Computer Interaction: HCI allowing location based web services, International Journal of Advanced Research in Artificial Intelligence, 2, 8, 34-39, 2013.
- [12] Kohei Arai Ronny Mardiyanto, Speed and vibration performance as well as obstacle avoidance performance of electric wheel chair controlled by human eyes only, International Journal of Advanced Research in Artificial Intelligence, 3, 1, 8-15, 2014.
- [13] Kohei Arai, Service robot with communication aid together with routing controlled by human eyes, Journal of Image Laboratory, 25, 6, 24-29, 2014
- [14] Kohei Arai, Information collection service system by human eyes for disable persons, Journal of Image Laboratory, 25, 11, 1-7, 2014
- [15] Kohei Arai, Relations between psychological status and eye movements, International Journal of Advanced Research on Artificial Intelligence, 4, 6, 16-22, 2015.
- [16] Kohei Arai, Method for 3D Image Representation with Reducing the Number of Frames Based on Characteristics of Human Eyes, International Journal of Advanced Research on Artificial Intelligence, 5, 8, 7-12, 2016.
- [17] Kohei Arai, Error Analysis of Line of Sight Estimation Using Purkinje Images for Eye-Based Human Computer Interaction: EBHCI, International Journal of Advanced Research on Artificial Intelligence, 5, 10, 14-23, 2016.
- [18] Kohei Arai, New service robot controlled by human eye which allows patients in hospitals self-services remotely, Austin Journal of Robotics & Automation, 3, 1, 1-7, ISSN 2471-0407, 2017.

AUTHOR'S PROFILE

Kohei Arai, He received BS, MS and PhD degrees in 1972, 1974 and 1982, respectively. He was with The Institute for Industrial Science and Technology of the University of Tokyo from April 1974 to December 1978 and also was with National Space Development Agency of Japan from January, 1979 to March, 1990. During from 1985 to 1987, he was with Canada Centre for Remote Sensing as a Post Doctoral Fellow of National Science and Engineering Research Council of Canada. He moved to Saga University as a Professor in Department of Information Science on April 1990. He was a councilor for the Aeronautics and Space related to the Technology Committee of the Ministry of Science and Technology during from 1998 to 2000. He was a councilor of Saga University for 2002 and 2003. He also was an executive councilor for the Remote Sensing Society of Japan for 2003 to 2005. He is an Adjunct Professor of University of Arizona, USA since 1998. He also is Vice Chairman of the Commission-A of ICSU/COSPAR since 2008. He received Science and Engineering Award of the year 2014 from the minister of the ministry of Science Education of Japan and also received the Best Paper Award of the year 2012 of IJACSA from Science and Information Organization: SAI. In 2016, he also received Vikram Sarabhai Medal of ICSU/COSPAR and also received 37 awards. He wrote 37 books and published 570 journal papers as well as 370 conference papers. He is Editor-in-Chief of International Journal of Advanced Computer Science and Applications as well as International Journal of Intelligent Systems and Applications. <http://teagis.ip.is.saga-u.ac.jp/>

Computerized Steganographic Technique using Fuzzy Logic

Dr. Abdulrahman Abdullah Alghamdi

College of Computing and IT,
Shaqra University, Kingdom of Saudi Arabia

Abstract—Steganography is the method of providing Computer security in which hiding the required information is done by inserting messages within other messages, which is a string of characters containing the useful information, in a carrier image. Using this technique, the required information from the secret image is embedded into individual rows as well as columns present in the pixels of carrier image. In this paper, a novel fuzzy logic based technique is proposed to hide the secret message in individual rows and in individual columns of pixels of the carrier image and to extract the hidden message in the same carrier image. The fuzzification process transforms the image in to various bitplanes. Pixel number and Correlation Value is computed in the original image for hiding the secret information in to the original image. The pixel number and Correlation value is also used as the key for retrieving the embedded image from the receiver side. Pixel merging is done in the sender side by assigning a steganographic value of white and black pixels in original image based on the fuzzy rules by comparing the pixels present in the original and secret images. The information which is hidden can be retrieved by using the same fuzzy rules. Experimental results show that the proposed method can hide and retrieve the secret and important messages in an image more effectively and accurately.

Keywords—Computer security; fuzzy logic; carrier image; secret image; steganography; fuzzification; peak signal to noise ratio

I. INTRODUCTION

The method of hiding an information on a medium as image as is called as Steganography. Steganographic technique is done for the past decades with various enhancements in medium and in the secret images for providing the Computer Security. Information hidden in photographs or an image is more common recently [2], [3], [4]. In this case, the medium of information hiding is an image. An image can be defined as a function of two dimension coordinates $f(x, y)$, where x and y represents the spatial co-ordinates, and f is called as its intensity [1]. In this method an image is considered to be a matrix of two dimension where each point represents its pixel which is the rows and columns. It also has a medium level of brightness. The increased use of multimedia data tends to do fast and convenient exchange of digital information throughout the Internet. With the simplicity of editing and reproduction of the content, the protection of possession for materials of digital audio, video and image video become an important topic of research. In this proposed method, a text which is present in an image is embedded into a gray image. This process can be

done by using the fuzzy rule-based region merging. The embedded text can be retrieved easily only by the receiver who knows the defuzzification process. The main importance of this proposed methodology is that it can be used easily by any end user. This methodology solely concentrates on steganography based on an image which is most widely used because of its capacity of carrying hidden data is higher and hence it is very difficult to find a steganographic data from a normal digital image.

The salient features of the proposed Steganographic technique are:

- 1) It is a completely automatic and an unsupervised method.
- 2) No assumption is made prior about the type and contents of images which is given as input.
- 3) This method has a novel information hiding process which is based on fuzzy logic for merging pixels of the carrier image and the secret information present in another image.
- 4) This method is robust in information hiding since this method incorporates of Fuzzy Logic with region merging.

II. LITERATURE SURVEY

Many techniques of steganography were proposed by recent researchers [5]-[6], [8]-[10], [11]-[15], [18]. In this paper, various steganography techniques which are based on fuzzy based techniques have only been discussed. Khursheed and Mir in [16], [17] applied the methodologies based on fuzzy logic for hiding information in another data. In their method, they tried to embed the information in a domain based on fuzzy logic. The advantages are lower computationally expense when it is compared to existing domain transformation methods. Their method provides embedding versatility and safety from common cover attacks, as well as appropriate imperceptibility and payload capacity. However, the secret data is sensitive in nature and it is easy to be destroyed by making a small change in the overall cover and by changing without any particular visibility.

Toony et al. [19] proposed a new image hiding method. In their method, a secret information as image is hidden by using a fuzzy based coding and decoding technique. A fuzzy coder compresses each and every block which is there in the form of secret information into a smaller block and utilizes model-based steganography for hiding the entire message towards a carrier image. This creates minimum distortion in the entire image which results in a quality stego image. Main advantage of their proposed methodology is it yields a higher rate in

embedding data and enhancement in the overall security. Hussain et al. [20] designed a methodology based on the combination of a hybrid fuzzy c-means algorithm and support vector machines model for implementing steganography in images. Their proposed model creates the capability of hiding the secret messages which is convertible to visual system of human. This approach has an advantage of clustering feature using Fuzzy C Means Clustering and a classification technique based on support vector machines.

Goodarzi et al. [21] developed a new scheme for steganography based on the Least Significant Bit method for utilizing the hybrid-based edge detector method. Their method uses the edge detection methodology such as canny and edge detection algorithms based on fuzzy logic. This proposed methodology overcomes the Fridrich's based methods, and steganalysis based systems based on the methodology of statistical based analysis. It also generates high quality stego images. Each and every steganography-based method has its own disadvantages. Petitcolas et al. [6] concludes the various disadvantages of various often used steganography systems. Finding and deletion or modification of secret data in a medium is called as steago attacks. These attacks can be described in many forms which are based on various techniques of information hiding. Craver et al. in [7] elaborates three types of steago attacks namely attacks in robustness, attacks in presentation, and attacks in interpretation.

From the works found in the literature, it has been observed that most of the existing works used. Thresholding

based algorithm, Fuzzy C means algorithm, neural networks based algorithms and operators for Background removal. However, in case of medical applications, the accuracy provided by various phases of segmentation is not sufficient to make effective decisions. Therefore, it is necessary to propose a new and efficient technique to enhance the accuracy of segmentation.

This paper is organised as follows: Section 3 presents the methodology of the proposed steganographic technique, explaining in detail the use of techniques, such as Fuzzification, Pixel number and Correlation value calculation, Pixel merging based on Fuzzy rules, Retrieving message from stego-image. In Section 4, the complete results obtained for the proposed methodology is presented. Finally, Section 5 presents the conclusions and future enhancements about this work.

III. PROPOSED METHODOLOGY

In this paper, a fuzzy logic based pixel merging method has been proposed for hiding the secret information which is present in an image in to an original image more clearly. This combination of helps to make effective steganographic process regardless of the type of information even the secret information is more or less since it is based on black and white pixels. The proposed methodology is a collection of processing bitplanes of an image and fuzzy logic applied to each pixel present in the original and secret image. Overall architecture of the proposed methodology is shown in Fig. 1.

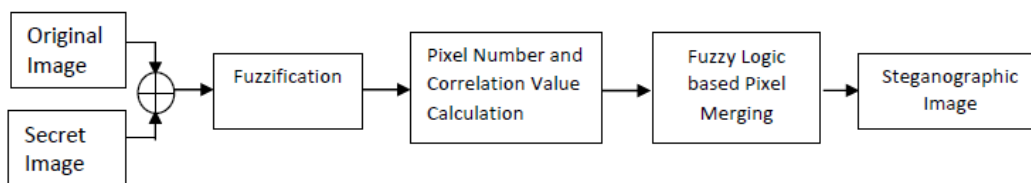


Fig. 1. Proposed steganography method.

A. Generating the Steganographic Image

This proposed method consists of the following steps:

- 1) The grey scale original and the secret images are considered to be the Input images.
- 2) The algorithm counts the number of black and white pixels present in both the original and secret images.
- 3) Since the input images are grey, it is separated into 4 monochrome images in order to obtain the bit values from each bitplanes.
- 4) The 2 bits which represents the background picture are called as “lower nibble” and the remaining 2 bits which represents the foreground picture called as “upper nibble”.
- 5) Pixel merging is done in the sender side by assigning a steganographic value of white and black pixels to the original image which is based on the rules of fuzzy logic by comparing the pixels present in the original and secret images. It also calculates the pixel number in original image at which the pixel from secret image is merged.
- 6) A textural property called as Correlation is also

calculated for the original pixel. This value is used as the key for receiving the image which is encrypted from the receiver side.

- 7) Obtained pixels are the steganographic image.
- 8) Defuzzification is performed by reversing the pixel merging process in the receiver side in order to get the secret information from the carrier image.

B. Fuzzification

The process of changing the values from one crisp sets in to another fuzzy set member for the process of qualitative representation is called as fuzzification. In many Fuzzy segmentation methods such as Fuzzy based clustering, Fuzzy C-means and Fuzzy based inference, intensity transformation of values towards a range of different numerals is done in the initial stage. In this work, the transformation (fuzzification) process as shown in Fig. 2 is equivalent to the formation of 4 bitplanes which is shown in Fig. 3(a)-(h). The input is a monochrome in nature, the entire image contains various pixels of black and white. By observing each bitplane, the gradient of the original image is calculated, and a decision is made whether information hiding is required at such gradients.

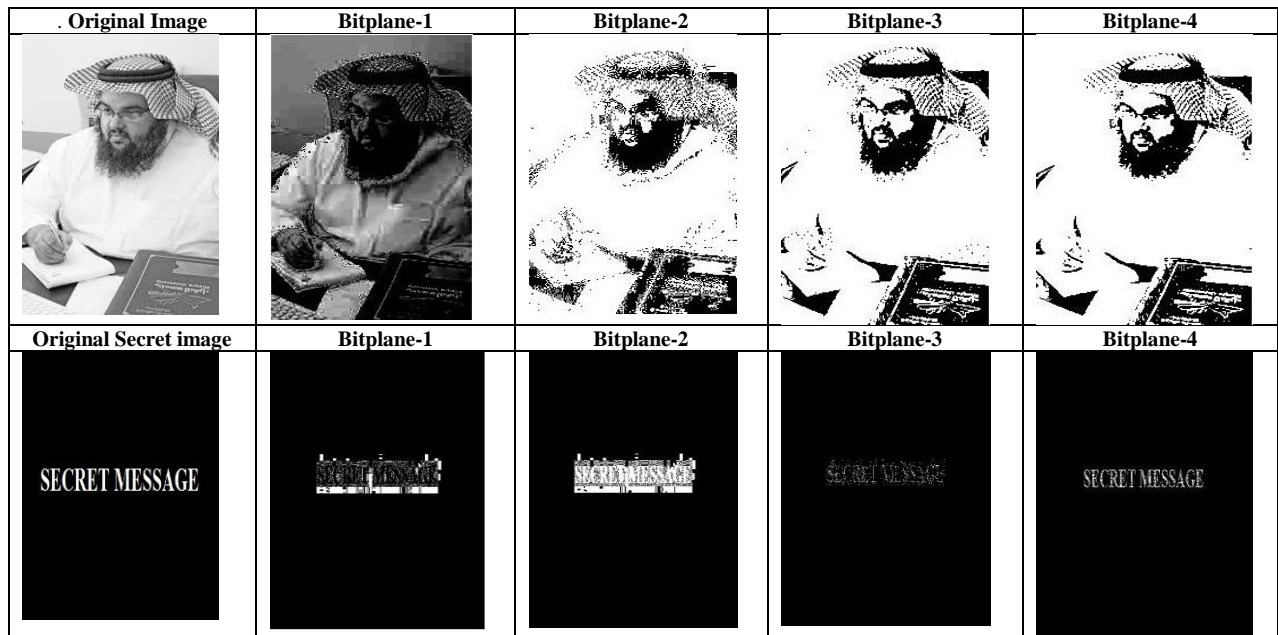


Fig. 2. Results of fuzzification: a) Original image and Secret image, b) Bitplane-1, c) Bitplane-2, d) Bitplane-2, e) Bitplane-4.

C. Pixel Number and Correlation Value Calculation

Pixel number is calculated to identify the place in original image at which the pixel from secret image is merged. It can be used at the point of Retrieving message from stego-image at the receiver side. Calculation of Correlation value is performed as an additional security measure. Correlation value is calculated for the pixels present in the original image and it is merged along with the pixel contains the information from secret image. The formula for calculating the correlation of a pixel is as follows:

$$Correlation = \sum_{ij} \frac{(i-\mu_j)(j-\mu_j)P(i,j)}{\sigma_i\sigma_j} \quad (1)$$

An intruder who is wishing to detect or modify the hidden data can't predict or calculate the correlation value of the pixel where the data maybe hidden. This ensures that the data cannot be deciphered without the knowledge of both sender or receiver.

D. Pixel Merging Based on Fuzzy Rules

Pixel merging is the process of merging two or more pixels with each other. In this work, the pixel merging is done based on the defined fuzzy rules shown in Table I. Four rules are written for this process. This process compares the pixels of original and secret images and hides the secret image in the original image based on the below rules. Rule 1 compares the first pixel of original image with the first pixel of secret image.

Fuzzy Rule 1: If the pixel in Original image (O) is Black (b) and the pixel in Secret image (S) is White (w) then, go to the next pixel in original image.

Fuzzy Rule 2: If the pixel in Original image is white and the pixel in Secret image is black then, Calculate the pixel number and Correlation value of the entire pixel of the original image. Then, merge the pixel of secret image with original image. After merging, go to next pixel in both images.

Fuzzy Rule 3: If the pixel in Original image is white and the pixel in Secret image is black, then go to the next pixel in secret image.

Fuzzy Rule 4: If the pixel in Original image is Black and the pixel in Secret image is black, then go to the next pixel in both original and secret image.

TABLE I. FUZZY RULES

Fuzzy Rule 1	IF $p_b(O) = p_w(S)$ then Go to the next pixel in original image ENDIF
Fuzzy Rule 2	IF $p_w(O) = p_b(O)$ Then Calculate pixel number and Correlation value. Merge the secret image pixel in original image pixel. Go to next pixel in both images. ENDIF
Fuzzy Rule 3	IF $p_w(O) = p_b(O)$ then Go to the next pixel in secret image ENDIF
Fuzzy Rule 4	IF $p_b(O) = p_b(O)$ then Go to the next pixel in both original and secret image ENDIF

E. Retrieving Message from Stego-image

Pixel number of original along with its correlation value is given as key towards the receiver. The receiver can extract the hidden information from original image by identifying the correct pixel and by subtracting the correlation value from it in order to obtain the original pixel from it. Since the pixel number along with correlation value is considered as a key for extracting the hidden information, the proposed methodology can be taken as more secured when compared to other existing steganographic methods.

IV. RESULTS AND DISCUSSION

The proposed methodology is implemented using MATLAB and the resulting image was obtained by giving the input image along with the carrier image. From the result obtained, it can be observed that both the carrier and the output stego-image were indistinguishable visually. The carrier and the secret images are shown in Fig. 3. The efficiency of the proposed method is determined from the Peak Signal to Noise Ratio (PSNR) and the Mean Square

Error (MSE) value. The MSE and the PSNR are the two error metrics used for comparing quality of an image. These ratios are often used as a quality measurement between the original and processed image. In general, the higher is the PSNR, the better is the quality of the processed image. MSE is the cumulative squared error which lies between the processed and the original image, moreover PSNR is the measure of peak error. When the MSE value is low, then the error is also Low. These parameters are defined as follows:

$$PSNR = 10 \log_{10}(R^2/MSE) \tag{2}$$

Where, M and N are the number of rows and columns in the input images, respectively. Then the algorithm calculates the PSNR value using the below equation:

$$MSE = \frac{\sum_{M,N}[I_1(m,n) - I_2(m,n)]^2}{M*N} \tag{3}$$

Where, R is the maximum fluctuation in the input image data type.

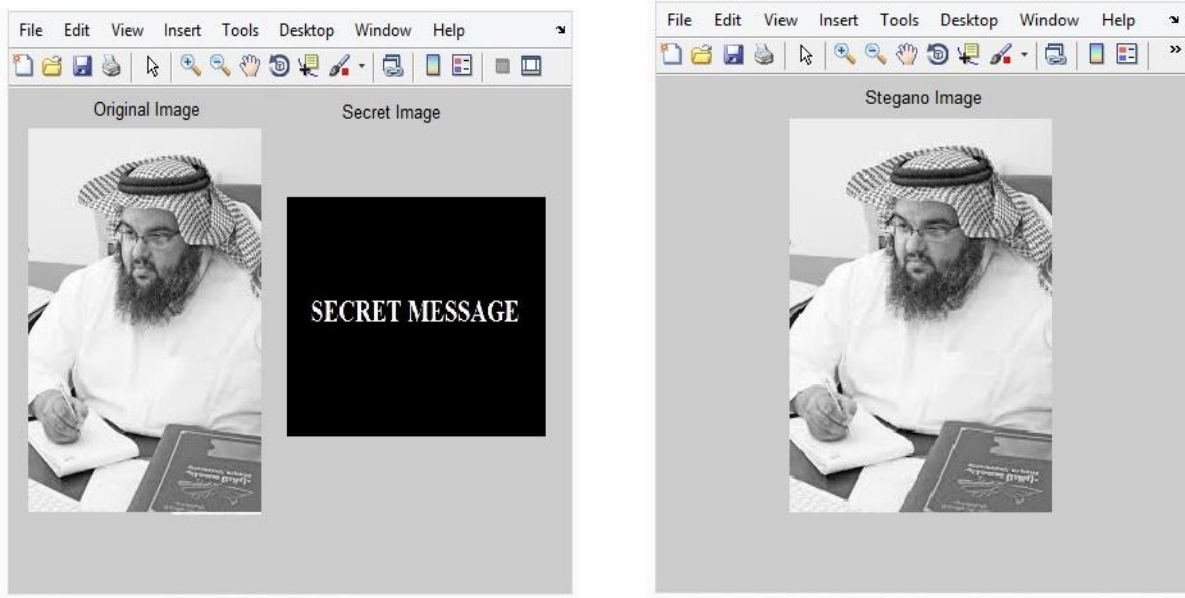


Fig. 3. Results of the original and Steago image.

Table II presents the accuracy estimation based on PSNR and MSE values for some of the sample information as secret image and one original image on which the proposed methodology was implemented. The proposed methodology is compared with LSB based steganography technique.⁴ From the results, it can be observed that the proposed technique gives better performance than the LSB technique in terms of the PSNR and MSE values.

In general, it is more suitable to obtain a low in MSE values and a high of PSNR values. These values indicate the better quality of the output image. The LSB technique gives high values of MSE irrespective of the inputs. In all the types of images, the proposed methodology produces a better result. Hence, the calculation based on PSNR is also suitable for the proposed methodology.

TABLE II. ACCURACY ESTIMATION BASED ON PSNR AND MSC

Image	PSNR	MSE	PSNR(LSB)	MSE (LSB)
Image 1	58.0288	0.1076	57.1268	0.1184
Image 2	62.0198	0.1184	60.0918	0.1390
Image 3	61.1187	0.2317	60.0435	0.2106
Image 4	59.0198	0.1296	58.0211	0.1093
Image 5	60.0139	0.2264	58.9131	0.2142

The significances of the proposed methodology over the existing are as follows:

- 1) The number of messages that can be hidden is greater than the existing methods.

2) The efficiency is Greater since the proposed methodology process with each and every pixel of the total image.

3) Better quality and security is obtained when compared with the LSB technique.

4) The proposed methodology obtains a high PSNR and less MSE values when compared to the existing methodologies.

V. CONCLUSION AND FUTURE ENHANCEMENTS

A novel steganographic technique is proposed using the fuzzy logic to embed the secret message in the carrier image is performed in this paper. The proposed technique can produce better results when compared to the existing LSB based steganographic techniques with respect to the number and size of messages that can be hidden. This method also performs well in terms of the time taken to retrieve the hidden information from the carrier image as well as in the quality of the retrieved image. Based on the results obtained, it can be observed that the proposed methodology gives better results for hiding the secret information in an image when compared to the existing LSB based steganographic techniques. It also gives additional security for hiding the secret message in an image by calculating the Correlation value in the pixel present in the original as well as in the secret information. The performance is shown by the increased PSNR and decreased MSE values which are obtained for the tested images. Future enhancement in this work is to propose a feature extraction process in order to enhance the security and also to reduce the time taken to process the complete scenario.

REFERENCES

- [1] Image definition, Gonzalez, Woods – Digital Image Processing.
- [2] Z Neil F. Johnson and Sushhil Jajodia. "Steganalysis: The Investigation of Hidden Information" - Proceedings of the IEEE Information Technology Conference, Syracuse, New York, USA, 1998.
- [3] I.Aveibas, N.Memon, B.Sankur. "Steganalysis based on image quality metrics" - Multimedia Signal Processing, 2001 IEEE Fourth Workshop on, 2001.
- [4] A.S.Abdullah, "Text Hiding Based On Hue Content In HSV Color Space", International Journal of Emerging Trends & Technology in Computer Science, vol. 4, Issue 2, pp. 170-173, March 2015.
- [5] AL-Ani, Z.K., Zaidan, A.A., Zaidan, B.B., and Alanazi, H.O., "Overview: Main Fundamentals for Steganography," Computer Engineering, vol.2, pp.158-165, 2010.
- [6] Petitcolas, F.A.P., Anderson, R.J., and Kuhn, M.G., "Information hiding-a survey," In Proceedings of the IEEE , vol.87, no.7, pp.1062- 1078, 1999.
- [7] Craver S., Yeo B.-L., and Yeung M., "Technical trials and legal tribulations." Communications of the A.C.M., vol.41, no. 7, pp. 44-54, 1998.
- [8] Anderson, R.J. and Petitcolas, F.A.P., "On the limits of steganography," IEEE Journal on Selected Areas in Communications, vol.16, pp.474-481, 1998.
- [9] Cheddad A., Condell J., Curran K., and Mc Kevitt P., "Digital image steganography: Survey and analysis of current methods," Signal Processing, vol.90, pp.727-752, 2010.
- [10] Johnson N.F. and Jajodia S., "Exploring steganography: seeing the unseen," IEEE Computer, vol. 31, no. 2, pp. 26–34, 1998.
- [11] Bender W., Butera W., Gruhl D., Hwang R., Paiz F.J., and Pogreb S., "Applications for data hiding," IBM Systems Journal, vol.39, no.3 & 4, pp.547–568, 2000.
- [12] Petitcolas F.A.P., "Introduction to information hiding," In: Katzenbeisser S., Petitcolas F.A.P. (Eds.), Information Hiding Techniques for Steganography and Digital Watermarking, Artech House, Inc., Norwood, 2000.
- [13] Miaoou S., Hsu C., Tsai Y., and Chao H., "A secure data hiding technique with heterogeneous data-combining capability for electronic patient records," in: Proceedings of the IEEE 22nd Annual EMBS International Conference, pp. 280–283., 2000.
- [14] Fujitsu Ltd., "Steganography technology for printed materials (encoding data into images)," Tackling new challenges, Annual Report 2007, Fujitsu Ltd., pp.33, 2007, Access at: <http://www.fujitsu.com/downloads/IR/annual/2007/all.pdf>.
- [15] Provos N. and Honeyman P., "Hide and seek: an introduction to steganography," IEEE Security and Privacy, vol.1, no.3, pp.32–44, 2003.
- [16] Khursheed F. and Mir A.H., "Fuzzy logic-based data hiding," In Proceeding of Cyber Security, Cyber Crime, and Cyber Forensics, Department of Electronics and Communication, National Institute of Technology, Srinagar, India, 2009.
- [17] Mir A.H., "Fuzzy entropy based interactive enhancement of radiographic images," In Journal of Medical Engineering and Technology, vol.31, no.3, pp.220–231, 2007.
- [18] Munirajan V.K., Cole E., and Ring S., "Transform domain steganography detection using fuzzy inference systems," In Proceeding of IEEE Sixth International Symposium on Multimedia Software Engineering, pp.286- 291, 2004.
- [19] Toony Z., Sajedi H., and Jamzad M., "A high capacity image hiding method based on fuzzy image coding/decoding," In 14th International 'Computer Society of Iran' Computer Conference (CSICC'09), pp.518-523, pp.20-21, 2009.
- [20] Hussain H.S., Aljunid S.A., Yahya S., and Ali F.H.M., "A novel hybrid fuzzy-SVM image steganographic model," In Proceeding of International Symposium in Information Technology, vol.1, pp.1-6, 2010.
- [21] Goodarzi M.H., Zaeim A., and Shahabi A.S., "Convergence between fuzzy logic and steganography for high payload data embedding and more security," In Proceedings of 6th International Conference on Telecommunication Systems, Services, and Applications, pp.130-138, 201.

An Efficient Algorithm for Load Balancing in Multiprocessor Systems

Saleh A. Khawatreh

Dept. of Computer Engineering, Faculty of Engineering, Al-Ahliyya Amman University
Amman-Jordan

Abstract—A multiprocessor system is a computer with two or more central processing units (CPUs) with each one sharing the common main memory as well as the peripherals. Multiprocessor system is either homogeneous or heterogeneous system. A homogeneous system is a cluster of processors joined to a high speed network for accomplishing the required task; also it is defined as parallel computing system. Homogeneous is a technique of parallel computing system. A heterogeneous system can be defined as the interconnection of a number of processors, having dissimilar computational speed. Load balance is a method of distributing work between the processors fairly in order to get optimal response time, resource utilization, and throughput. Load balancing is either static or dynamic. In static load balancing, work is distributed among all processors before the execution of the algorithm. In dynamic load balancing, work is distributed among all processors during execution of the algorithm. So problems arise when it cannot statistically divide the tasks among the processors. To use multiprocessor systems efficiently, several load balancing algorithms have been adopted widely. This paper proposes an efficient load balance algorithm which addresses common overheads that may decrease the efficiency of a multiprocessor system. Such overheads are synchronization, data communication, response time, and throughput.

Keywords—Multiprocessor system; homogeneous system; heterogeneous system; load balance; static load balancing; dynamic load balancing; response time; throughput

I. INTRODUCTION

Parallel processing has emerged as a key enabling technology in modern computers, driven by the ever increasing demand for higher performance, lower costs and sustained productivity in real life applications. Concurrent events are taking place in today's high-performance computers due to the common practice of multiprogramming and multiprocessing [1].

Parallel processing is an efficient form of information processing. Parallel events may occur in multiple resources during the same interval. Parallel processing demands concurrent execution of many programs in the computer [2].

Multiprocessor management and scheduling has been a fertile source of interesting problems for researchers in the field of computer engineering. In its most general form, the problem involves the scheduling of a set of processes on a set of processors with arbitrary characteristics in order to optimize some objective function.

Basically, there are two resource allocation decisions that are made in multiprocessing systems. One is where to locate code and data in physical memory, a *placement decision*. The other is on which processor to execute each process, an *assignment decision*. Assignment decision is often called processor management. It describes the managing of the processor as a shared resource among external users and internal processes. As a result, processor management consists of two basic kinds of scheduling: long-term external load scheduling and short-term internal process scheduling [1], [2].

A scheduler performs the selection a process from the set of ready to run processes, and assigns it to run on a processor in the *short-term process scheduling* operation. The *medium* and *long-term load-scheduling operation* is used to select and activate a new process to enter the processing environment [2].

The general objectives of many theoretical scheduling algorithms are to develop processor assignments and scheduling techniques that use minimum numbers of processors to execute parallel programs in the least time. In addition, some algorithms are developed for processor assignment to minimize the execution time of the parallel program when processors are available. There are two types of models of scheduling *deterministic* and *nondeterministic*. In deterministic models, all the information required to express the characteristics of the problem is known before a solution to the problem, a schedule, is attempted. Such characteristics are the execution time of each task and the relationship between the tasks in the system. The objective of the resultant is to optimize one or more of the evaluation criteria. Nondeterministic models, or *stochastic models*, are often formulated to study the dynamic-scheduling techniques that Adaptive Scheduling Algorithm for Load Balance in Multiprocessor System take place in a multiprocessor system [2].

The simplest dynamic algorithm is called *self-scheduling*. Self-scheduling [6] achieves almost perfect load balancing. Unfortunately, this algorithm incurs significant synchronization overhead. This synchronization overhead can quickly become a bottleneck in large-scale systems or even in small-scale systems if the execution time of one process is small. *Guided self-scheduling* [6], [7] is a dynamic algorithm that minimizes the number of synchronization operations needed to achieve perfect load balancing.

Guided self-scheduling algorithm can suffer from excessive contention for the work queue in the system.

Adaptive guided self-scheduling [6], [7] address this problem by using a backoff method to reduce the number of processors competing for tasks during periods of contention. This algorithm also reduces the risk of load imbalance.

Adaptive guided self-scheduling algorithm performs better than guided self-scheduling in many cases.

All these scheduling algorithms attempt to balance the workload among the processors without incurring substantial synchronization overhead.

An affinity scheduling algorithm [5], [6] attempts to balance the workload, minimize the number of synchronization operations, and exploit processors affinity. Affinity scheduling Employs a per-processor work queues which minimizes the need for synchronization across processors.

Adaptive affinity scheduling algorithm [5], [6] maintains excellent load balance and reduces synchronization overhead. The main idea behind this algorithm is to minimize local scheduling overhead so that the phase of dynamically balancing the workload can be speeded up, which results in reduction of execution time.

There are many other different algorithms for scheduling the workload on multiprocessor systems. Such algorithms are the factoring algorithm, the tapering algorithm, and the trapezoid self-scheduling algorithm.

These algorithms basically depend on the described algorithms in them structure with some alterations made for improving the algorithm in some characteristic or another [8].

A task for transfer is chosen using Selection Strategy. It is required that the improvement in response time for the task and/or the system compensates the overhead involved in the transfer. Some prediction that the task is long-lived or not is necessary in order to prevent any needless migration which can be achieved using past history [8], [10], [11].

The dynamic load balance algorithm applies on Folded Crossed Cube (FCC) network. Basically, FCC is a multiprocessor interconnection network [9].

This paper is divided into the following sections: The proposed method is described in Section 2. Results of the study are analyzed in Section 3. Finally, Section 4 presents the conclusions.

II. PROPOSED SCHEDULING ALGORITHM

A. Assumptions and Considerations

In this section, some considerations are stated concerning the multiprocessor system for which the algorithm is designed. Following are the main assumptions characterizing this multiprocessor system:

1) System Topology

The multiprocessor system is assumed to be configured using homogeneous processors. These processors are connected using the crossbar switches organization of interconnection networks. Crossbar switches have a good potential for high bandwidth and system efficiency.

2) Operating System Characteristics

During the course of design of the scheduling algorithm, it became apparent that the most suitable operating system to govern the multiprocessor system is the floating supervisor control. This operating system provides the flexibility needed to implement the scheduling algorithm since it treats all the processors as well as other resources symmetrically, or as an anonymous pool of resources.

3) Design Characteristics

Similar to the affinity and adaptive affinity scheduling algorithms [5], [6], the proposed scheduling algorithm is also constructed to have three phases as follows:

B. Process Scheduling Phase

Processes arriving at a process queue are organized using Nonpreemptive Priority scheduling algorithm, where the process with the highest priority is always found at the top of the process queue. When two processes have the same priority First-In-First-Out scheduling algorithm is applied.

C. Processor Scheduling Phase

In this phase, processes are distributed among processor queues. Each processor in the system has a local queue scheduled using Round-Robin scheduling algorithm with a dynamically adjustable quantum. Processor work states are defined in this phase, and are used to achieve a balanced load distribution in the multiprocessor system.

D. Remote Scheduling Phase

This phase is concerned with load redistribution in case a faulty processor or a heavily loaded processor is detected. A feedback approach is utilized to transfer the processes in a faulty or heavily loaded processor back to the process queue for redistribution. This phase ensures that the reliability of the system is maintained and thrashing is avoided. Fig. 1 illustrates the basic idea behind the design.

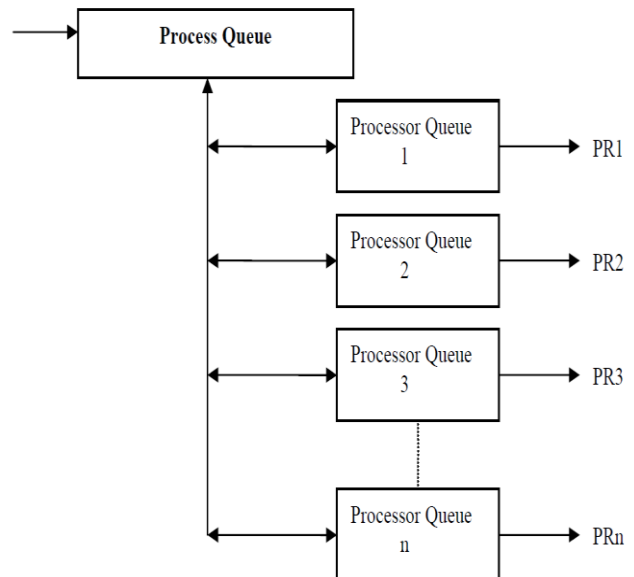


Fig. 1. Process and processor queues.

E. Scheduling Algorithm Design

This section contains the detailed design of the proposed scheduling algorithm. The algorithm consists of three phases, as described above, and it proceeds as follows:

1) Process Scheduling Phase

- a) Construct a process queue Q.
- b) Each process P_i arrives to the process queue carrying a priority variable PP_i .

The process with the highest priority is assigned an *HP* variable; the **highest priority variable**.

- c) To place a process P_i in the right priority order, its PP_i is compared with *HP*. Then after iteratively with the rest of the *PP*'s until the correct position is found.

2) Processor Scheduling Phase

- a) Construct processor queues PQ_i for each processor PR_i
- b) The work states of a processor are partitioned as follows:

- Faulty Processor *FP*: $NF = NT$.
- Heavily-Loaded Processor *HL*: $NF > NT/2$.
- Normally-Loaded Processor
- *NL*: $NF = NT/2$.
- Lightly-Loaded Processor *LL*: $NF < NT/2$.

Where;

NT is the total number of processes in a *PQ*.

NF is the number of processes left in a *PQ*.

- 3) Define a **processor-state checking variable** SC_i for each PR_i . This variable indicates the state of a PR_i as follows:

- a) For a *FP*: $SC = 3$.
- b) For a *HL* processor: $SC = 2$.
- c) For a *NL* processor: $SC = 1$.
- d) For a *LL* processor: $SC = 0$.

- 4) Distribute processes to *PQ*'s from *Q* by checking the SC variable for each PQ .

A process is assigned to the *LL* processors first, then to the *NL* processors. In case of high load, processes are also assigned to the *HL* processors when needed.

5) Remote Scheduling Phase

- a) A procedure for checking the workload in each PR is as follows:
 - When $SC = 3$, a *FP* is detected:
 $NR = NF$.
 - When $SC = 2$, a *HL* is detected:
 $NR = NT - NF$.

Where;

NR is the number of processes to be remotely scheduled.

- b) NR processes are returned to *Q* for redistribution to *LL* processors and *NL* processors.

- c) This procedure is repeated until the SC variable for all PR 's indicates a *NL* or *LL* work states.

TABLE I. WITH LOAD BALANCE

Pr..	Resp. Time	Exec. Time	Start Time	End Time	Av. Res. Time	Orig. Job	Mig. Job	Ack. Job	Run Jobs
1	0	37	1	64	3.64	14	5	2	11
2	1	21	4	66	1.91	6	0	5	11
3	2	22	1	64	2.00	13	2	0	11
4	3	21	2	47	2.30	9	1	2	10
5	3	13	14	66	1.86	7	0	0	7
6	0	10	3	68	1.43	7	0	0	7
7	1	11	3	68	1.38	8	0	0	8
8	3	26	3	39	2.36	14	0	0	14
9	0	10	3	47	1.25	8	0	0	8
10	1	30	4	48	2.38	14	1	0	13
	14	201	1	68	2.14	100	9	9	100

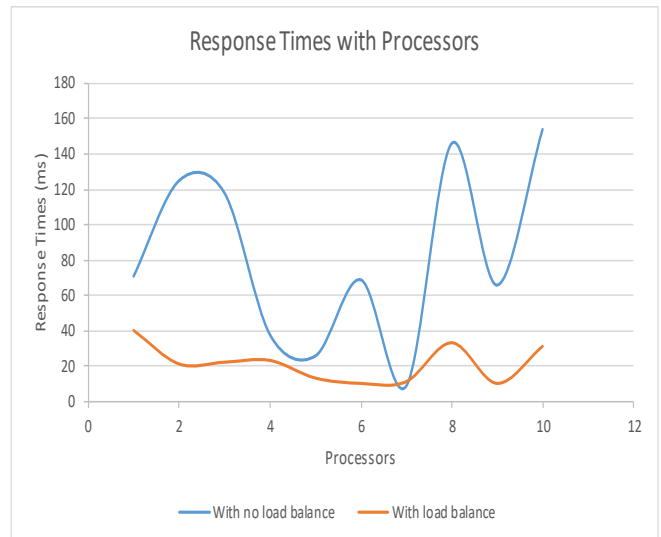


Fig. 2. Response times variations.

III. RESULTS

This algorithm is applied on a simulated system consists of 10 processors and 100 jobs.

The response time is taken as a performance measure. Table I contains the results where the load balance algorithm is applied.

Table II contains the results where load balance algorithm is not applied.

By comparing the results of Table II with the results of Table I, the difference in the response time is clear where the total response times is 214 ms compared with 822 ms.

Fig. 2 shows the difference in the response time between the systems with load balance and without load balance.

The terms which are used in the tables are defined as follows:

Response time = finish time – arrival time

Average response time = response time/ number of jobs executed

Orig. jobs = jobs which originated at this processor.

Mig. Jobs = jobs which were migrated to other processors.

Acq. Jobs = jobs which were acquired from other processors.

TABLE II. WITH NO LOAD BALANCE

Pr.	Resp. Time	Exec. Time	Start Time	End Time	Average Res. Time	Orig. Job	Mig. Job	Ack. Job
1	71	48	1	64	5.46	13	0	0
2	125	37	2	39	12.5	10	0	0
3	118	46	1	52	11.8	10	0	0
4	38	35	5	44	5.43	7	0	0
5	26	24	2	64	3.71	7	0	0
6	69	39	3	58	6.9	10	0	0
7	9	9	3	22	1.8	5	0	0
8	146	43	3	64	12.17	12	0	0
9	66	52	3	65	5.5	12	0	0
10	154	51	4	55	11.0	14	0	0
	822	384	1	65	8.22	100	0	0

IV. CONCLUSION

The main objective of this paper is to design an algorithm that achieves a balanced load state on a multiprocessor system. The proposed scheduling algorithm is a deterministic dynamic algorithm, which outlines an excellent load balancing strategy. It also addresses some major overheads that may prove problematic in the multiprocessing operation. Multiprocessor systems have many advantages, which make them economical compared to multiple single systems. One advantage is *increased throughput*. By increasing the number of processors, more work would get done in a shorter period of time.

Another reason for multiprocessor systems is that they increase *reliability*. When functions are distributed properly among several processors, failure of one processor will not halt the system, but would only slow it down. This ability to continue providing service proportional to the level of non-failed hardware is called *graceful degradation*. *Resource sharing*, *computation speedup*, and *communication* are other advantages for building multiprocessor systems [2]-[4].

In the algorithm presented in this paper, we tried to maximize the advantages of multiprocessor systems. By achieving a balanced load distribution state on the multiprocessor system, it was possible to observe the properties of this system. Throughput is increased. Graceful degradation is another apparent characteristic. In addition to these advantages, this algorithm overcomes many overheads that may occur in a multiprocessor system when it applies other algorithms. One overhead is synchronization. In the presence of the process queue and processor queues,

synchronization does not have to be addressed as a complication. Synchronization is automatically achieved in the design of the adaptive scheduling algorithm. Data communication overheads are minimum, since the queue length at all times is kept relatively short for all the system queues. The only state which may suffer this overhead is when the system is in a high load state.

The proposed scheduling algorithm adopts an organization with a process queue, where each arriving process to the system is entered, and processor queues for each existing processor in the system. The processes are distributed from the process queue to processor queues, where they await execution. The process queue is scheduled with a *nonpreemptive priority algorithm*. This has many advantages but may present some limitations. One advantage is prevention of deadlocks [4]. The main problem of priority scheduling is starvation [4]. This can be solved by aging low priority processes [4]. Processor queues are scheduled using *Round-Robin scheduling algorithm*. The quantum is utilized here as a control factor. Response time and the throughput depend on the quantum, which may be dynamically adjusted to give the desired characteristics [4]. A major limitation of RR scheduling is the switching between processes present in the processor queues. This presents an overhead to this algorithm, which may be overcome by practical testing to achieve an optimal quantum value. On comparing it with other scheduling algorithms, the proposed scheduling algorithm proved superior to them in many aspects. In its unique design of having both a process queue supported by processor queues, the proposed scheduling algorithm utilized the advantages of the various other designs while overcoming many of them limitations. The presence of a central work queue unsupported in a multiprocessor tends to be a performance bottleneck, resulting in a longer synchronization delay. Heavy traffic is generated because only one processor can access the central work queue during allocation. The third limitation is that a central work queue does not facilitate the exploitation of processor affinity. On the other hand, including a process queue in the presented design, provides the possibility of evenly balancing the workload. To eliminate the central bottleneck, the proposed scheduling algorithm supported the process queue with local processor queues. This approach reduces contention and so, prevents thrashing. Thrashing occurs when the degree of multiprocessing increases beyond the maximum level and this causes the system utilization to drop sharply [4]. A central work queue may cause thrashing during heavy traffic.

For future work, the process queue is to be scheduled with a *preemptive priority algorithm* and the results will be compared with non-preemptive queue scheduling.

REFERENCES

- [1] K. Hwang, 'Advanced Computer Architecture: Parallelism, Scalability, Programmability,' McGraw-Hill, Inc., 1993.
- [2] K.Hwang and F.A.Briggs` Computer Architecture and Parallel Processing,' McGraw-Hill, Inc., 2002.
- [3] A. S. Tanenbaum, `Computer Networks,' Prentice Hall, FourthEdition,2003.
- [4] Silberschatz and Galvin, `Operating System Concepts,' Addison-Wesley Publishing Company, sixth Edition,2003.

- [5] Y.Yan, C.Jin, and X.Zhang, 'A datively Scheduling Parallel Loops in Distributed Shared-Memory System,' *IEEE Trans. Parallel and Distributed. Systems*, Vol.8, No. 1, pp. 70-81, January 1997.
- [6] E.P.Markatos and T.J.LeBlanc, 'Using Processor Affinity in Loop Scheduling On Shared-Memory Multiprocessors ,' *IEEE Trans. Parallel and Distributed Systems*, Vol.5, No. 4, pp. 370-400, April 1994.
- [7] C.D. Polychronopoulous and D.J.Kuck, 'Guided Self-Scheduling: A Practical Scheduling Scheme for Parallel Super Computers,' *IEEE trans. Computer*, Vol. C-36, No. 12, pp.1425-1439, December 19987.
- [8] Samad, A., Siddiqui, J., & Ahmad, Z,' Task Allocation on Linearly Extensible Multiprocessor System. *International Journal of Applied Information Systems*, 10(5), 1–5, 2016.
- [9] Samad, A., Siddiqui, J., & Khan, Z. A.,' Properties and Performance of Cube-Based Multiprocessor Architectures,' *International Journal of Applied Evolutionary Computation*, 7(1), 63–78, 2016.
- [10] Singh, J., & Singh, G., 'Improved Task Scheduling on Parallel System using Genetic Algorithm,' *International Journal of Computers and Applications*, 39(17), 2012.
- [11] K., Alam, M., & Sharma, S. K. (2015). A Survey of Static Scheduling Algorithm for Distributed Computing System. *Interconnection Network. International Journal of Computers and Applications*, 129(2),25–30, 2015.

Performance Evaluation of a Deployed 4G LTE Network

E.T. Tchao¹

Dept. of Computer Engineering, KNUST
Kwame Nkrumah Univ. Science and Tech.,
Kumasi, Ghana

J.D. Gadze², Jonathan Obeng Agyapong³

Dept. of Electrical/Electronic Engineering
Kwame Nkrumah University of Science and Tech.,
Kumasi, Ghana

Abstract—In Ghana and many countries within Sub-Sahara Africa, Long Term Evolution (LTE) is being considered for use within the sectors of Governance, Energy distribution and transmission, Transport, Education and Health. Subscribers and Governments within the region have high expectations for these new networks and want to leverage the promised enhanced coverage and high data rates for development. Recent performance evaluations of deployed WiMAX networks in Ghana showed promising performance of a wireless broadband technology in supporting the capacity demands needed in the peculiar Sub-Saharan African terrain. The deployed WiMAX networks, however could not achieve the optimal quality of service required for providing a seamless wireless connectivity demands needed for emerging mobile applications. This paper evaluates the performance of some selected key network parameters of a newly deployed LTE network in the 2600 MHz band operating in the peculiar Sub-Saharan African terrain under varied MIMO Antenna Configurations. We adopted simulation and field measurement to aid us in our evaluation. Genex Unet has been used to simulate network coverage and throughput performance of 2X2, 4X4 and 8X8 MIMO configurations of the deployed networks. The average simulated throughput per sector of 4X4 MIMO configuration was seen to be better than the 2X2 configuration. However, the percentage coverage for users under the 2x2 MIMO simulation scenario was better than that of the adaptive 4x4 MIMO configuration with 2x2 MIMO achieving 60.41% of coverage area having throughput values between 1 - 40Mbps as against 55.87% achieved by the 4x4 MIMO configuration in the peculiar deployment terrain.

Keywords—Long term evolution; MIMO; performance evaluation; sub-Saharan African; propagation environment

I. INTRODUCTION

Fourth Generation Long Term Evolution (4G-LTE) being a technology for data communication designed by 3rd Generation Partnership Project is meant to provide high speed and low latency mobile wireless connectivity over long distances. LTE has a flexible spectrum supporting the bands ranging from 450 MHz to 4.5 GHz. LTE also support bandwidth ranging from 1.25 MHz to 20MHz [1].

LTE has a flat Internet Protocol (IP) Based architecture. To able to achieve this, it is deployed with Orthogonal Frequency Division Multiple Access (OFDMA) in the downlink. The uplink is implemented using Single Carrier Division Multiple Access. This helps to enhances high data rate. Another feature in 4G LTE which enhances high

throughput over long distances is Multiple Input Multiple Output (MIMO) systems. MIMO is a multi-antenna technology which uses M multiple antennas at the transmitting and N multiple antennas at the receiving ends. This configuration can be denoted by a $M \times N$ MIMO system. Increasing the number of transmitting antennas increases the average signal to noise ratio per receiver which enhances cell range and throughput capacity in MIMO systems [2].

A simplified 4G LTE architecture is generally made up of the evolved Packet Core, the eNodeB and the User equipment. The user connects to the network via the wireless air interface to the eNodeB. This wireless medium is enhanced by MIMO which allows multiple data streams to be transmitted and received concurrently through multiple antennas [3].

The competitive advantage that LTE therefore has is its ability to provide a very high throughput and longer coverage for the end users [4]. When a user is connected to a 4G LTE network, then he is connected to a network with a flat IP-based architecture which uses OFDMA and SC-DMA multiple access in the downlink and uplink respectively and employs MIMO in the wireless medium. This enables the technology to provide wireless broadband internet access to its end users even in remote areas.

II. 4G LTE DRIVES DEMAND

There has been a significant increase in mobile subscription over the past five years. According to Ericsson's mobility report for June 2016 which provides statistics for mobile data subscription for the past five years and a forecast into the next five years, the total number of mobile subscription as at the first quarter of 2016 was up to 7.4 billion [5]. Their analysis showed that, mobile broadband subscription increases continuously every year while fixed broadband subscriptions remains nearly constant over the years. Gee Rittenhouse [6] also predicts a 1000X of data by the year 2020. His estimation showed an increasing demand for data services for the past five years and a greater demand is predicted for the next five years ahead.

4G LTE promises high wireless mobile data rate of up to 300Mbps depending on the MIMO type which far exceeds the throughput of the preceding Third Generation (3G) mobile wireless access technology [7]. 4G LTE subscriptions reached 1.2 billion in 2016 with about 150 million new subscriptions and an estimated subscription of up to 4.3 billion by the end of 2021.

In developed markets there has been a large migration to this new technology resulting in decline in the use of EDGE/GSM [8]. However, in developing market, such as that of Ghana and many countries within the Sub-Saharan Africa sub-region, migrating to LTE is an option due to high cost of devices and network deployment. However, because of the high capacity network LTE assures, some countries within Sub-Saharan African have started deploying LTE solutions to provide mobile wireless connectivity to serve eager customers who have ever increasing broadband internet demands. Ghanaians have only just begun to connect to these newly deployed 4G LTE networks to enjoy the quality of experience that the technology promises.

III. RELATED WORKS

The network performance of LTE networks have been studied extensively in Literature. The authors in [9] presented a computation of path loss using different propagation models for LTE Advance networks in different terrains; rural, dense urban and suburban. The paper analyzed path loss for broadband channels at 2300MHz, 2600MHz and 3500 MHz using MATLAB. The paper performed this study using the following prediction models; Stanford University Interim model, COST 231 Walfisch-Ikegami model, ECC-33/Hata Okumura extended model and COST 231 Hata model. The comparison of the various propagation models showed that the least path loss was obtained by using COST-231 Hata prediction method. It was concluded that the prediction errors for SUI and ECC models are significantly more than COST 231 Hata and COST Walfisch-Ikegami models.

The research work published in [10] investigates three empirical propagation models for 4G LTE networks in the 2-3 GHz band. This was undertaken in urban and rural areas in Erbil city in Iraq. The results were compared with field measurements and tuning methods were suggested to fit the measured path loss results of the Standford University Interim (SUI) model and Okumura Hata, extended COST 231 Hata model. It was seen that the optimum model which was closer to the measured path loss data was the extended COST 231 Hata model. COST 231 Hata model had the mean error value lowered to a zero value, the mean standard deviation value lowered to 7.8dB and root mean square error being 7.85dB. Thus the COST 231 Hata model was the propagation prediction model predicted for the city.

The research work published in [11] makes a comparison for the diverse suggested propagation models to be implemented for 4G wireless at various antenna heights. The path loss for the various models; Stanford University Interim model, COST 231 Hata model and COST Walfisch-Ikegami model were computed in different environmental scenarios; Urban, suburban and rural areas. MATLAB simulation was used for the computation for frequencies in the 2300 MHz, 2600 MHz and 3500MHz band. It was concluded that path loss was least using COST 231 Hata model for all environmental scenarios and the different frequencies than the other models. The advantages of this approach were in its adaptability to dissimilar environments by infusing the appropriate correction factors for diverse environments. It was concluded that path loss was least in urban areas for 1900

MHz and 2100 MHz frequencies using SUI model. COST231 gave the highest path loss for 1900 MHz and Ericsson 9999 predicted the highest path loss for 2100 MHz band.

The research work published in [12] presents a computation of path loss using different propagation models for WiMAX in urban environments. The paper analyzed path loss and took field measurement at 3500 MHz using MATLAB. The paper performed this study using the following prediction models; COST 231 Hata model, Stanford University Interim model, Ericsson model, ECC-33/Hata Okumura extended model and free space path loss model. Simulations were performed at different receiver height at 3m, 6m and 10m. It was inferred that the best results were obtained from ECC-33 and SUI models with respect to least path loss in urban environments.

The effect of MIMO configurations on network deployments have also been widely studied in Literature. Authors in [13] presented a deterministic approach for simulating bit error rate (BER) of MIMO antenna configuration but this time in the presence of multiple interferers in the Sub-Saharan African terrain. The pattern of radiation was simulated for the WiMAX Antenna by the authors using Genex-Unet and NEC. To model BER performance, a Monte Carlo strategy was employed in the presence of 2x2 and 4x4 in the sight of ten intruding Base Stations (BS). In the presence of a number of interferers, poor estimates for average BER were observed for 2x2 MIMO deployments. 4x4 MIMO antenna configurations with efficiently suppressed side lobes were proposed for future WiMAX deployment for a better BER performance.

In [14], the network capacity performance of 2x2, 4x4, 8x8 and 12x12 systems was analyzed by the authors using MATLAB for real-time simulations. The authors simulated the channel capacity of the different MIMO schemes against probability error at different signal to noise ratio; 0dB, 10dB, 20dB, 40dB and 60dB. It was concluded that the maximum channel capacity is achieved at 60dB and 0dB for 12x12 and 2x2 MIMO configurations respectively.

There is little information on the performance of 4G networks in the sub-region. Authors in [15] measured 9.62Mbps downlink throughput for a deployed WiMAX network under realistic network conditions in the Sub-Saharan African terrain. This throughput performance was poor when compared with reported network performance of deployed LTE networks in Europe and Asia. Documented results of the performance of LTE under various deployment scenarios in Europe and Asia were also presented in [16] and [17] respectively. In [16], the maximum reported measured downlink throughput was 52Mbps while a maximum throughput of 32Mbps was measured in [17] as compared to the simulated throughput of 60Mbps and 35Mbps respectively. Despite the variations between the measured and simulated results, an impressive performance of the deployed networks was realized confirming the assurance LTE gives.

Deployment of Long Term Evolution networks have just begun in Ghana and operators are very optimistic LTE could help address the limitations of the WiMAX networks. There is therefore the need to evaluate the performance of recently

deployed networks to determine if they can deliver on their promised performance. It can also be seen from the related work however that, there are variations between promised results and actual performance of deployed network. Some of the related research works have studied the maximum theoretical values in terms of throughput which cannot best represent the realistic capacity that end users enjoy. The related work on coverage estimation studied the Path loss models but failed to apply the models to a typical deployment scenario to provide achievable cell range for the various antenna configurations. There is therefore the need to provide a realistic data on throughput and coverage which can fairly represent consumer experience an LTE subscriber will enjoy.

IV. NETWORKING DIMENSIONING PROCESS

There have been several attempts aimed at deploying 4G networks in Ghana. Earlier pilot deployment of LTE and WiMAX networks in Ghana suffered from high levels of co-channel and adjacent channel interference from co-located Third generation antenna systems [18]. This high level of interference led to low capacity networks with limited connectivity in earlier deployed networks. This section retraces the steps followed by network and radio planning engineers in planning the first successful LTE network in Ghana.

Radio network planning is a significant process in all wireless propagation. It enables a planner to estimate expected network performance by the use of planning tools to validate theoretical models, technological requirements and business models. During the radio network planning stage of the network in the pilot area, the main goal was to simulate the throughput and the coverage that will best serve end users using theoretical models with the help of a radio planning tool. The dimensioning process which was used in successfully deploying the LTE under study involved a sequence of steps which served different requirements such as antenna radiation pattern simulation, coverage and capacity estimations to derive the final radio network plan for the 2X2 MIMO system. The dimensioning process is shown in Fig. 1. The dimensioning processes included:

- Selection of site. This should be closer to our target consumers and also have easy access to road and power source. Also, the type of area should be noted, whether urban, sub-urban or rural.
- Consideration of environmental factors: This involved analyzing the peculiar terrain which included vegetation, climate, height of buildings around the site, the topology of the land. This helps in considering how to tilt our antenna electrically and mechanically and the height of the transmitting antenna to be used.
- Frequency and interference planning: PUSC 1x3x3 is used for the deployment. There is therefore some probability of interference at high transmit powers so we simulated the added sidelobe suppression factor needed.
- Coverage Prediction analysis: This analysis is carried out in an outdoor environment to determine signal

strength within the coverage area and the network accessibility.

- Capacity Analysis: This enables prediction of the average throughput within the cell. It will also consider throughput distribution within the cells.

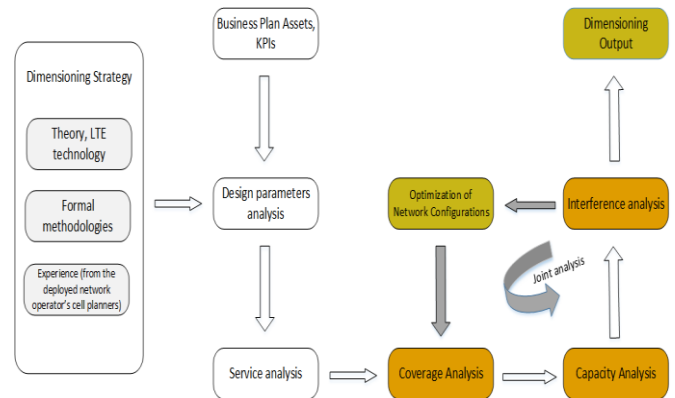


Fig. 1. Radio planning methodology.

The input parameters used for planning the network consisted of the business plan, the assets and the key performance indicators (KPIs). The first step of the dimensioning process obtained all the necessary information on the configurations which were be used in the process. During the input analysis stage, theoretical and technological expertise was drawn from the network planning engineers who worked on deploying the initial WiMAX networks. This expert advice was adapted, taking into consideration of LTE technological standards, to implement the radio network plan for the LTE network.

The radio network planning was split into three main analysis namely; coverage, capacity and interference analysis. As part of the coverage analysis, the provided service areas were identified and the required number of LTE sites estimated. Further to the coverage analysis, the service areas had to be dimensioned to offer sufficient capacity as dictated by the number of users and services profiles. Therefore the next step was to estimate the required number of sectors to achieve this capacity. The estimates of LTE sites and sectors were then used to determine the configuration of the BS in the final joint analysis step. After the capacity and coverage analysis, the results of the initial configurations were evaluated followed by customizations to further improve the solution.

V. SYSTEMS MODEL

This section presents and discusses the coverage and capacity models adopted to successfully dimension the network.

A. Coverage Model

In this analysis, an N element MIMO antenna system in a one tier multicarrier system using a Partial Usage Sub-Channelization (PUSC), will be discussed. The frequency reuse scheme will be denoted by $N_c \times N_s \times N_f$, where:

- N_c is number of individual frequency channels in the LTE network.
- N_s is the number of sectors per cell.
- N_f is the number of segments in exploited frequency channel.

The deployed network uses a reuse scheme of PUSC 1x3x3. The layout of this frequency reuse scheme is shown in Fig. 2. The scheme uses three sector antennas and requires only one radio frequency (RF) channel for all sectors. The scheme uses three different sets of tones. Each of these tones is for a sector of a Base Station. This reduces significantly inter-cell interference and the outage area of the cell. Radio frequency (RF) planning is greatly made simple because the segments just have to be assigned to sectors while using the same RF channel among all Base Stations (BS).

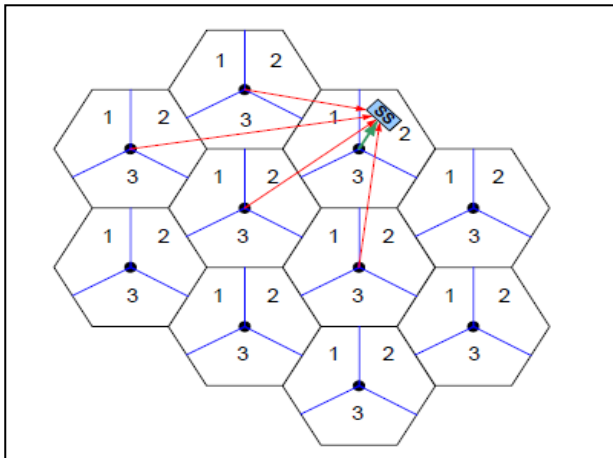


Fig. 2. PUSC 1x3x3 frequency reuse scheme.

Co-channel interference typically affects system configuration performance in the cell border areas for PUSC schemes. Authors in [19] evaluated the capacity of WiMAX MIMO systems in the cell borders for PUSC schemes and realized that, the degradation in network performance at cell borders were due to the presence of recorded high co-channel interference values. Results discussed in [20] showed that in a multicarrier system, each BS antenna can receive unsuppressed sidelobe emission from the antenna of adjacent cell BS. There was therefore the need to model the maximum range of the LTE network under evaluation by considering the effect of the unsuppressed sidelobe power emission that could come from neighboring cell sites during the radio planning stage.

In determining the maximum cell range, Friis transmission model played an essential role in the analysis and design of the network because when transmitting and receiving antennas are sufficiently separated by a considerable distance, Friis model would seek to make a relation between the power that is supplied to a transmitting antenna and the power that is received on the other end by a receiving antenna. The adopted transmission model is shown in Fig. 3. This model assumes that a transmitting antenna produces power density $W_t(\theta_t, \varphi_t)$ in the direction (θ_t, φ_t) .

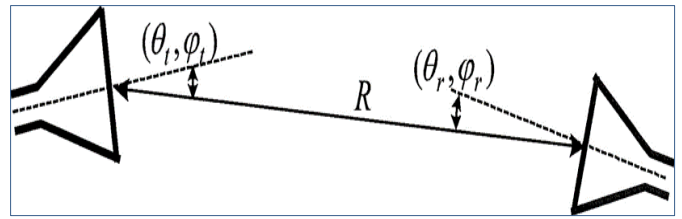


Fig. 3. Adopted wireless propagation model.

The transmitting antenna gain determines the power density in the given direction $G(\theta_t, \varphi_t)$, on the distance R between the point of observation and the antenna and the on the power that is supplied to the transmitter P_t . The power density can be modelled as [21]:

$$W_t = \frac{P_t}{4\pi R^2} G_t(\theta_t, \varphi_t) = \frac{P_t}{4\pi R^2} e_t D_t(\theta_t, \varphi_t) \quad (1)$$

Here, e_t denotes the radiation efficiency of the transmitting antenna and D_t is its directivity. The receiving antenna has the power P_r at its terminals expressed by its effective area A_r and W_t :

$$P_r = A_r W_t \quad (2)$$

To include polarization and heat losses in the receiving antenna, we add the radiation efficiency of the receiving antenna e_r and the polarization loss factor (PLF) to the receive power equation as:

$$P_r = e_r \cdot PLF \cdot A_r W_t = A_r W_t e_r |\hat{\rho}_t \cdot \hat{\rho}_r|^2 \quad (3)$$

$$\Rightarrow P_r = \underbrace{D_r(\theta_r, \varphi_r)}_{A_r} \cdot \frac{\lambda^2}{4\pi} \cdot e_r W_t |\hat{\rho}_t \cdot \hat{\rho}_r|^2 \quad (4)$$

Here, D_r represents the directivity of the receiving antenna. When calculating PLF, the polarization vectors of the receiving and transmitting antennas, $\hat{\rho}_r$ and $\hat{\rho}_t$, are evaluated based on their respective coordinate systems and so one of them has to be conjugated.

The signal is incident upon the receiving antenna from a direction (θ_r, φ_r) , which is defined in the coordinate system of the receiving antenna. The received power can hence be modelled as:

$$P_r = D_r(\theta_r, \varphi_r) \cdot \frac{\lambda^2}{4\pi} \cdot \frac{P_t}{4\pi R^2} e_t D_t(\theta_t, \varphi_t) \cdot e_r |\hat{\rho}_t \cdot \hat{\rho}_r|^2 \quad (5)$$

The ratio of the received to the transmitted power is given by:

$$\frac{P_r}{P_t} = e_t e_r |\hat{\rho}_t \cdot \hat{\rho}_r|^2 \left(\frac{\lambda}{4\pi R}\right)^2 D_t(\theta_t, \varphi_t) D_r(\theta_r, \varphi_r) \quad (6)$$

Once the impedance-mismatch loss factor is included in the transmitting and the receiving antenna systems, then the ratio above becomes:

$$\frac{P_r}{P_t} = (1 - |\Gamma_t|^2)(1 - |\Gamma_r|^2) e_t e_r |\hat{\rho}_t \cdot \hat{\rho}_r|^2 \left(\frac{\lambda}{4\pi R}\right)^2 D_t(\theta_t, \varphi_t) D_r(\theta_r, \varphi_r) \quad (7)$$

Where,

Γ_t and Γ_r are the reflection coefficients of the transmitting and receiving antenna,s respectively.

The efficient design of wireless systems and the approximation of antenna radiation efficiency when the antenna gain is established can be done using (6.7) which is a variation of Friis' transmission model.

In order to estimate the maximum cell detectable range, it is important to know all the specifications of the receiving and transmitting antenna like the gain, impedance-mismatch, polarization, losses and the minimum power at that the receiver would need to accurately operate $P_{r\ min}$ as well as the nominal power of the transmitter P_t . The maximum range can then be calculated as:

$$R^2_{max} = (1 - |\Gamma_t|^2)(1 - |\Gamma_r|^2)e_t e_r |\hat{p}_t \cdot \hat{p}_r|^2 \left(\frac{\lambda}{4\pi}\right)^2 \left(\frac{P_t}{P_{r\ min}}\right) D_t(\theta_t, \varphi_t) D_r(\theta_r, \varphi_r) \quad (8)$$

The receiver can reliably and effectively operate with a minimum power which is dependent on numerous factors, of which has Signal-to-noise-ratio (SNR) being the core one.

B. Antenna Beamwidth and Sidelobe Power Modelling

The emergence of technology has greatly helped in antenna design because of the application of analytical and numerical optimization techniques. A number works related to the area of antenna array analysis and design have been presented in [22] and [23] where the optimization of the relative position of the antenna elements has been made possible by particle swarm optimization (PSO) as well as other well-known algorithms to get the minimum Sidelobe Levels (SLL) suppression factors. This part of the research summarizes the interference analysis stage which seeks to investigate the effect of antenna sidelobe emissions on multicarrier MIMO systems when the antenna beamwidth and side lobe level are considered with respect to other system parameters.

There are several techniques discussed in the open literature that avoid both the mutual coupling effects and the different implementation mismatches introduced by antenna sidelobe emission [24]-[28]. This is because it is more difficult to model the effects that the radio channel has on the real radiation pattern due to its volatility. This research focuses on these issues and adopts a solution using a simple concept of the effective radiation pattern (ERP) using Friis equation.

Friis equation shows that, the product of the transmitting antenna gain G_t and the transmitter power P_t is the most important result as far as the received power, P_r , is concerned. Any introduction of losses by the transmission line has to be added to that of the antenna system and the total losses accounted for. This is the reason why a transmission system is often represented by its effective isotropic radiated power (EIRP):

$$EIRP = P_t G_t e_{TL}, \quad (9)$$

Where, e_{TL} is the loss efficiency of the transmission line connecting the transmitter to the antenna. Usually, the EIRP is given in dB, in which case (9) becomes:

$$EIRP_{dB} = P_{tdB} + G_{tdBi} + e_{TL,dB} \quad (10)$$

Bearing in mind that $P_{in,t} = e_{TL} P_t$ and $G_t = 4\pi U_{max,t} / P_{in,t}$, the EIRP can also be written as

$$EIRP = 4\pi U_{max,t}, W \quad (11)$$

It is obvious from (11) that the EIRP is an imaginary amount of power that is emitted by the isotropic radiator to produce the peak power density that is seen in the direction of the maximum antenna gain. It is also clear from (9) that, the EIRP is greater than the power that is actually needed by the antenna to achieve a speculated amount of radiation intensity in its direction of maximum radiation. Hence we will model the antenna radiation power using the concept of effective radiated power (ERP).

The analytical ERP solution is developed with an assumption that the radiation pattern ($G_{real}(\varphi)$) is produced after the effect of the radio channel. Effective beamwidth (BW_{effect}) and effective Sidelobe suppression level (SLL_{effect}) are used to reflect the modified beamwidth and average sidelobe level of an ideal radiation pattern, if multipath is taken into consideration, both could be calculated via a cost function minimization that best fits the ERP with the real radiation pattern. The ERP concept assumes some factors such as the necessary number of antenna array elements, appropriate array geometry and adaptive algorithms which make up the beamforming capability that would produce radiation patterns with the desired peculiarity in relation to beamwidth and average sidelobe level. In measuring the gain of an antenna, authors in [29] started by modeling the azimuth (φ) radiation pattern ($G_{real}(\varphi)$) by spreading the ideal antenna pattern ($G_{ideal}(\varphi)$) over the environment power azimuth pattern ($A(\varphi)$).

The real radiation pattern on the antenna can also be modeled by determining the convolution of the ideal radiation pattern with the environment power azimuth pattern. Using this approach, the radiation pattern can be expressed as:

$$G_{real}(\varphi) = \oint_{\varphi} G_{ideal}(\varphi) \cdot A(\varphi - \varphi_0) d\varphi \quad (12)$$

Following the approach in [30], the best way to model the power azimuth spectrum (PAS) around the BS for urban environments is to find the Laplacian distribution (LD). The LD of the environment power azimuth $A(\varphi)$ can be solved as:

$$\text{Let } f(\varphi) = A(\varphi - \varphi_0)$$

$$\text{Then LD of } f(\varphi) \text{ denoted as } F(s) = \int_0^{\infty} f(\varphi) e^{-(\varphi - \varphi_0)\sigma} d\varphi$$

$$\text{which implies } F(s) = \int_0^{\infty} A(\varphi - \varphi_0) \cdot e^{-(\varphi - \varphi_0)\sigma} d\varphi$$

$$F(s) = \frac{1}{\sqrt{2}\sigma} e^{-\sqrt{2}|\varphi - \varphi_0|/\sigma} \quad (13)$$

Substituting $A(\varphi)$ in (12) with its LD in (13), the antenna radiation pattern can be rewritten as:

$$G_{real}(\varphi) = \frac{1}{\sqrt{2}\sigma} \oint_{\varphi} G_{ideal}(\varphi) \cdot e^{-\sqrt{2}|\varphi-\varphi_0|/\sigma} d\varphi \quad (14)$$

Where, σ is the angular spread (AS). Let us assume an ideal N element linear antenna array with an element distance of $\lambda/2$ and bore-sight radiation. The ideal antenna radiation pattern ($G_{ideal}(\varphi)$) for the N array antenna can be found by solving for the area of mainlobe. The ideal radiation pattern is calculated as:

$$G_{ideal}(\varphi) = \left| \frac{\sin((N/2)\pi \cos \varphi)}{(N/2)\pi \cos \varphi} \right| \quad (15)$$

The impact of the environment azimuth power profile on $G_{ideal}(\varphi)$ can be calculated using (12)-(15) as:

$$G_{real}(\varphi) = \frac{1}{\sqrt{2}\sigma} \int_0^{\pi} \left| \frac{\sin((N/2)\pi \cos \varphi)}{(N/2)\pi \cos \varphi} \right| \cdot e^{-\sqrt{2}|\varphi-\varphi_0|/\sigma} d\varphi \quad (16)$$

Where, $\varphi \in (-\pi, \pi)$

The antenna analysis in this research consider only the upper part of the antenna array pattern; that is, $\varphi \in (0, \pi)$. The aim is to use a simple step function with the sidelobe level (SLL) and the effective beamwidth (BW) to help model the antenna radiation pattern diagram with its effective radiated power(ERP) given by that step function. The ERP can only have two values, that is:

- The ERP=1, if the emission from the sidelobe of the antenna of the adjacent cell falls within the main lobe of the victim MIMO antenna.
- The ERP= $10^{-SLL/10}$, if the emission from the sidelobe of the BS of the adjacent cell falls outside the main lobe of the victim antenna.

The total amount of interference on the MIMO antenna from the sidelobe emissions depends on the number of interfering Base Station antennas having the N element MIMO antenna in their side lobe emission path. Since the antennas is uniformly distributed in the multicarrier system in Fig. 2, the probability of ERP=1 depends only on the antenna array's main lobe beamwidth, $b=BW/2$. Hence, the ERP values are given as:

$$G_{ERP}(\varphi) = f(x)$$

$$f(x) = \begin{cases} 1, & \varphi \in \left[\varphi_m - \frac{BW}{2}, \varphi_m + \frac{BW}{2} \right] \\ 10^{-\frac{SLL}{10}}, & \varphi \in \left[0, \left(\varphi_m - \frac{BW}{2} \right) \cup \left(\varphi_m + \frac{BW}{2} \right), \pi \right] \end{cases} \quad (17)$$

Where, φ_m is the pointing angle of the main lobe. In order to provide the best fit between G_{real} and G_{ERP} the BW and SLL parameters must be defined in a way that the cosine function given in (16) is minimized. As such:

$$\{BW_{effect}, SLL_{effect}\}_{argmin} = \int_0^{\pi} |G_{ERP}(\varphi) - G_{real}(\varphi)| d\varphi \quad (18)$$

$BW \in (0, \pi), SLL \in (a, 0)$

Where a is the minimum sidelobe level value that is utilized to outline the search area for the effective SLL. The model in (18) will enable us determine the amount of added suppression required to reduce interference within the deployment area. The results of this solution will be used to determine appropriate sidelobe emission suppression factors during the deployment stage. This suppression value will be used in the antenna simulation parameters to simplify the coverage analysis and yet produce realistic performance estimations during the radio planning phase later in this work.

C. Received Power and Network Capacity Simulation Methodology

As part of the coverage analysis, an estimation of the Reference Signal Received Power (RSRP) was made. The information provided by RSRP is about the signal strength but rather not the quality of the signal. RSRP is the linear average of the reference signals of the downlink across the bandwidth of the channel. Some practical uses of the RSRP in LTE networks is that it is used for handover, cell selection and cell re-selection. RSRP for usable reference signals typically varies [31]. Table I gives a description of the different ranges of RSRP which is used for our coverage analysis.

TABLE I. RSRP REFERENCE RANGE

RSRP Power (dBm)	Description
< -90	Excellent/Near cell
-90 to -105	Good/Mid-cell
-106 to -110	Fair/Cell edge
-110 to -120	Poor

TABLE II. ANTENNA RADIATION PATTERN SIMULATION PARAMETERS

Frequency Range	2300 MHz - 2700MHz
Angular Spread	0, 10, 20 and 30
Number of elements	320
VSWR	≤ 1.5
Input Impedance	50Ω
Gain	18 dBi \pm 0.5dBi
Polarization	$\pm 45^\circ$
Horizontal Beamwidth (3dB)	60 \pm 5 $^\circ$
Vertical Beamwidth (3dB)	7 $^\circ \pm 0.5^\circ$
Electrical Downtilt	2 $^\circ$
Isolation Between Ports	≥ 30 dB
Front to Back Ratio	≥ 30 dB ± 2 dB
Cross Polarization Ratio	≥ 18 dB
Null-Fill	≤ 18 dB
Max, power	250W

Generally, RSRP is given in terms of Received Power (RSSI). RSSI refers to the wideband power of the user equipment (UE) that is received in total. It is made up of power from serving cells as well adjacent cell interference, thermal noise. This helps us to determine the interference from other cells. RSRP is modelled as [32]:

$$RSRP (dBm) = Received\ power - 10 * \log (12 * N) \quad (19)$$

Where N denotes the number of resource blocks which is dependent on the bandwidth. From the allocated 10 MHz bandwidth for the network deployment in Table II, the number of resource blocks will be 50. It implies that (19) can be rewritten as:

$$RSRP (dBm) = Received\ Power (dBm) - 27.78 \quad (20)$$

This implies that RSRP will be about 27dBm lower than RSSI value. Therefore RSRP coverage simulation results will be calculated as:

$$RSRP = D_r(\theta_r, \varphi_r) \cdot \frac{\lambda^2}{4\pi} \cdot \frac{P_t}{4\pi R^2} e_t D_t(\theta_t, \varphi_t) \cdot e_r |\hat{p}_t \cdot \hat{p}_r|^2 - 27.78 \quad (21)$$

In this work Genex Unet will be used to predict RSRP distribution using (21) and urban parameters.

In evaluating the capacity of LTE network, the fluid model proposed by authors in [33] was used. The signal interference plus noise ratio for PUSC scheme is calculated as [33]:

$$YPUSC(r) = \frac{K\sqrt{3}}{\pi} (\eta - 2)(2\sqrt{K} - r)^{-2} \left(\frac{2\sqrt{K}}{r-1} - 1\right)^\eta \quad (22)$$

Where

$K = Reuse\ factor$

$\eta = interference\ to\ noise\ ratio$

$r = cell\ radius$

Hence the capacity for the PUSC 1x3x3 scheme can be evaluated as [33]:

$$C_{PUSC}(k) = \log_2[1 + YPUSC(r)] \quad (23)$$

The capacity estimation will be done with (23) under varying reuse schemes and discussed in subsequent sections.

VI. SIMULATION PARAMETERS AND FIELD MEASUREMENT SETUP

The radiation pattern of the MIMO antenna is simulated using the parameters in Table III. Unsuppressed sidelobe emissions distort the performance of MIMO antenna systems used in deploying multicarrier networks. In order to accurately evaluate the performance of any MIMO antenna configurations used in a realistic network deployment scenario, this effect must be modeled and simulated.

The received power and throughput of three MIMO configurations used in a practical network deployment scenario are also simulated using the adopted step function, coverage and capacity estimation models with the parameters in Table II.

TABLE III. RADIO NETWORK PLAN SIMULATION PARAMETERS

Parameter	Description
Carrier Frequency	2620-2630 MHz
System Bandwidth	10MHz
OFDM Symbol time	102.8 ms
Transmit Power	43dBm
Receiver Sensitivity	-110 dBm
Mobile Receiver Height	0.5m
Base Station antenna height	35 m
Transmitter antenna gain	18.5 dBi
Area	Urban
LTE Duplex mode	TDD
MIMO Scheme	2X2, 4X4, 8X8 MIMO
Downlink multiple access	OFDMA
Azimuth (degree)	0/120/240

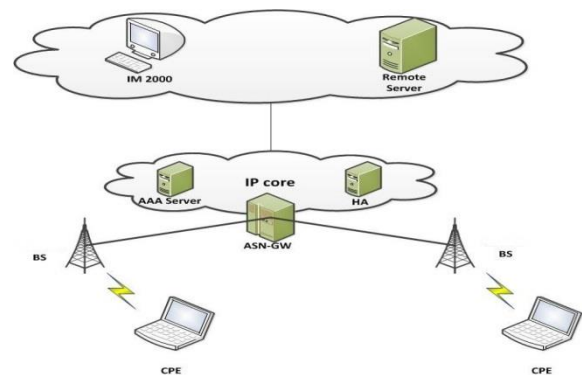


Fig. 4. Field experimental setup.

The field experimental trial results will be presented after the simulation results have been discussed. The objective of the field experimental test was to compare simulated and actual deployment results. The field measurement setup is shown in Fig. 4. The measurement set up is comprised of a GPS connected to an LTE customer premise equipment (CPE) with Genex-probe software installed on it, and a Kathrein omnidirectional with 2x2 MIMO configuration.

The data was collected by undertaking a drive test and querying a remote server using IM2000, a live network monitoring tool. The data was collected at hourly intervals in the month of December when traffic on networks in Ghana are generally high. The field measurements were done for only 2x2 MIMO because the deployed LTE network under study uses adaptive 2x2 MIMO configuration.

VII. SIMULATION RESULTS AND ANALYSIS

This section presents the simulation results obtained for network coverage and throughput when the theoretical coverage, sidelobe power and coverage models are implemented in NEC and Genex Unet.

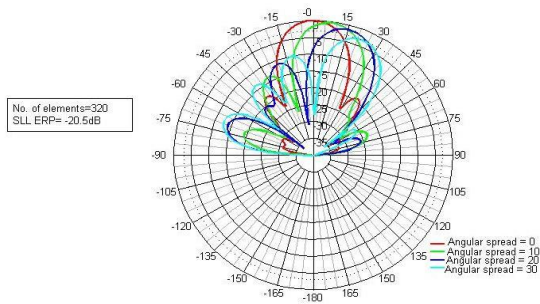


Fig. 5. Antenna radiation pattern simulation result.

A. Antenna Radiation Pattern

In this section, the step function in (18) is used for evaluating the effective beamwidth and the suppression factors of the antenna radiation using NEC simulation tool. Following the conclusions derived in [34], the Angular Spread (AS) for a bad urban microcell radio node was chosen as 330. Therefore, we employed in the Laplacian distribution different AS values of the MIMO antenna and perform the analysis to model the real radiation patterns shown in Fig. 5 using the simulation parameters in Table III.

Results of the vertical radiation patterns shown in Fig. 5 indicates that the limiting case for the minimum value of side lobe level is when the angular spread is under the selected antenna element of 320. From results, when the angular spread is almost 0 and the number of linear array elements is 320, the corresponding effective radiated sidelobe power level is -20.5 dB. From this result, a value of optimal sidelobe level suppression of $a \geq -20.5\text{dB}$ is recommended for an antenna with $n \geq 320$ for network deployment under bad urban conditions. As a result, a value of $a = -20\text{dB}$ and $n=320$ was used to model practical deployment scenarios presented in this research.

B. RSRP Simulation Results

To find out the maximum cell range under the deployment scenario, a single site simulation was conducted for 2X2 MIMO, 4X4 MIMO and 8X8 MIMO. Simulation was performed for users in urban areas within the Accra metropolis operating at 2600MHz.

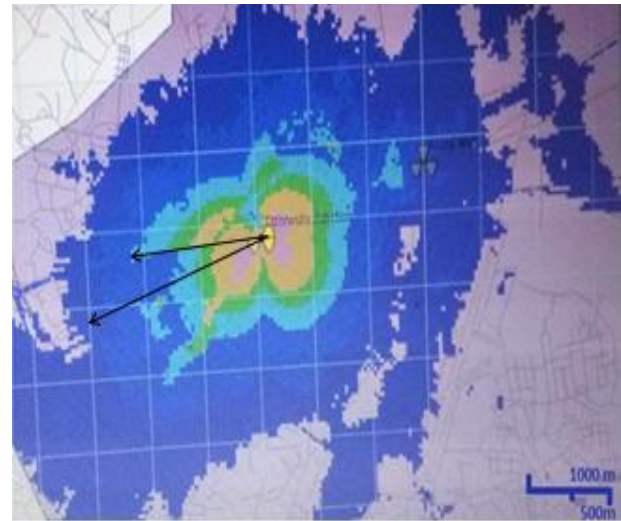
The RSRP levels were randomly distributed ranging between -50 to -140dBm for the three MIMO configurations. The receiver sensitivity required for minimum performance was obtained at -110 dBm which implies that a cell usable range of 2km was achievable using 2X2 MIMO as indicated in Fig. 6. The minimum threshold sensitivity however was -133 dBm which implies that the network can be sensed at about 3 km using 2X2 MIMO but a user will not enjoy expected throughput after 2km away from the cell site.

For the coverage simulation of a single 4x4 MIMO configuration shown in Fig. 7, RSRP levels were also randomly distributed ranging between -140 to -50 dBm similar to that of the 2x2 MIMO configuration. The receiver sensitivity required for minimum throughput was obtained at -110 dBm which implies that a cell usable range of 2.5km is achievable using 4X4 MIMO under the deployment scenario.

The detectable cell range for the adaptive 4x4 MIMO configuration was obtained at 3.5km.

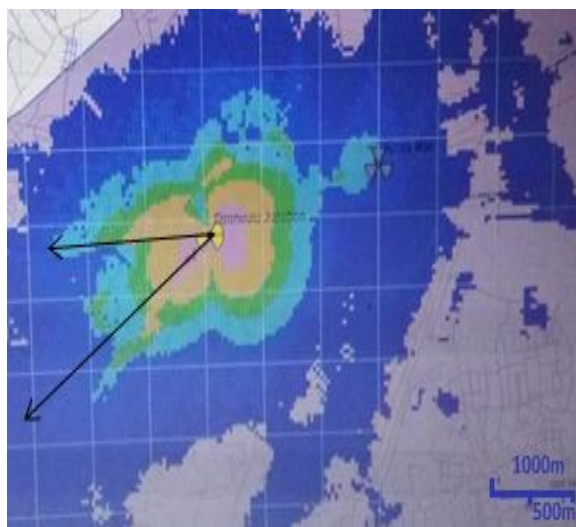
The receiver sensitivity required for maximum throughput is -110 dBm which implies that the cell's usable and detectable ranges of 2.8km and 4km respectively were achievable using 8X8 MIMO as summarized in Fig. 8. Cell usable ranges of 2km, 2.5km and 2.8km were obtained for 2X2, 4X4 and 8X8 MIMO respectively. It can be observed that as the number of transmitting antennas increases, the coverage of cell is enhanced as shown in the comparison results in Fig. 9.

The main purpose of the initial planning process was to investigate and develop efficient and low cost radio access systems to provide users in an urban environment a full range of broadband services. The final radio plan in Fig. 6 for the deployed 2X2 MIMO configuration helps achieve this objective through efficient utilization of radio frequency bands and optimization of transmission capacities for the different variety of users within the pilot network. To predict the radio wave propagation in the network, the planning tool took into account the antenna radiation patterns results. Since the information used to determine the simulation parameters were obtained from the network planning engineers, the result in Fig. 6 produces similarly structured cell plans as the one being used by the network operator.



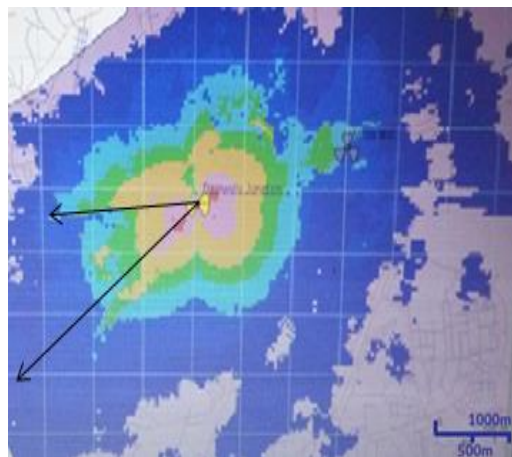
Color	Legend	Percentage
Red	[-50,0]	0.00
Dark Red	[-70,-50]	0.01
Light Red	[-80,-70]	0.75
Yellow	[-90,-80]	3.38
Green	[-105,-90]	4.12
Light Blue	[-110,-105]	6.91
Blue	[-120,-110]	21.39
Dark Blue	[-140,-120]	63.43

Fig. 6. RSRP coverage performance of a single site that uses 2X2 MIMO (dBm).



Color	Legend	Percentage
Red	[-50,0]	0.00
Dark Red	[-70,-50]	0.06
Light Red	[-80,-70]	1.24
Yellow	[-90,-80]	4.43
Green	[-105,-90]	4.96
Light Blue	[-110,-105]	8.58
Blue	[-120,-110]	20.56
Dark Blue	[-140,-120]	60.07

Fig. 7. RSRP coverage performance of a single site using 4X4 MIMO (dBm).



Color	Legend	Percentage
Red	[-50,0]	0.00
Dark Red	[-70,-50]	0.14
Light Red	[-80,-70]	1.66
Yellow	[-90,-80]	5.77
Green	[-105,-90]	6.15
Light Blue	[-110,-105]	8.72
Blue	[-120,-110]	20.23
Dark Blue	[-140,-120]	57.33

Fig. 8. RSRP coverage performance of a single site using 8X8 MIMO (dBm).

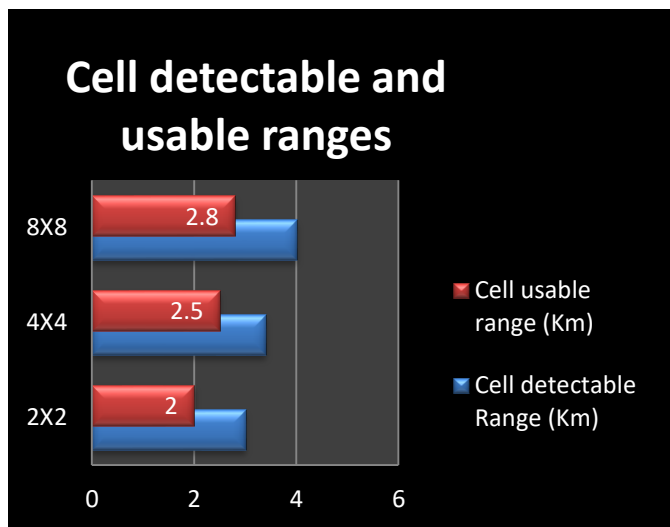


Fig. 9. Graph showing the cell ranges for single site for 2X2, 4X4 and 8X8 MIMO.

The simulated radio plans in this research however achieves a coverage level above 97% as compared to the 90-92% which was obtained by the network engineers during the planning stage. The increase in the coverage level could be attributed to the usage of sidelobe suppression in the final radio network plan. This in turn implies that the modeling of antenna sidelobe suppression factors in any multicarrier network system will maximize the overall network service level of its MIMO configuration.

C. Throughput Simulation

From the network simulation parameters in Table II, at 10MHz, the OFDMA symbol time is 102.8microseconds and so there are 48.6 symbols in a 5 millisecond frame. Of these, 1.6 symbols are used for TTG (Transmit to Transmit Gap) and RTG (Receive to Transmit Gap) leaving 47 symbols. If n of these symbols are used for DL, then 47 - n are available for uplink. Since DL slots occupy 2 symbols and UL slots occupy 3 symbols, it is best to divide these 47 symbols into a Time Division Duplexing (TDD) Downlink/Uplink (DL/UL) split ratio such that 47 - n is a multiple of 3 and n is of the form 2k + 1. Based on the propagation mode, the required frequency reuse scheme and the DL/UL channel ratio are used. For a capacity limited network, a 35:12 TDD split ratio is used to serve the users in the network. When the sole purpose of the network is to cover a larger area, a DL/UL ratio of 26:21 is used. Under the adaptive 2x2 MIMO deployment scenario, the maximum average DL and UL throughput per sector are 28.51 Mbps and 11.98 Mbps respectively for a coverage limited network using a 26:21 DL/UL ratio and a PUSC 1x3x3 reuse scheme. The results of the LTE capacity simulation results in this work is compared with the results presented in [15] for the first successfully deployed WiMAX network in Ghana in Fig. 10. It can be seen that, the results of the LTE throughput simulation indicates an impressive performance of a Wireless network never seen before in the sub-region.

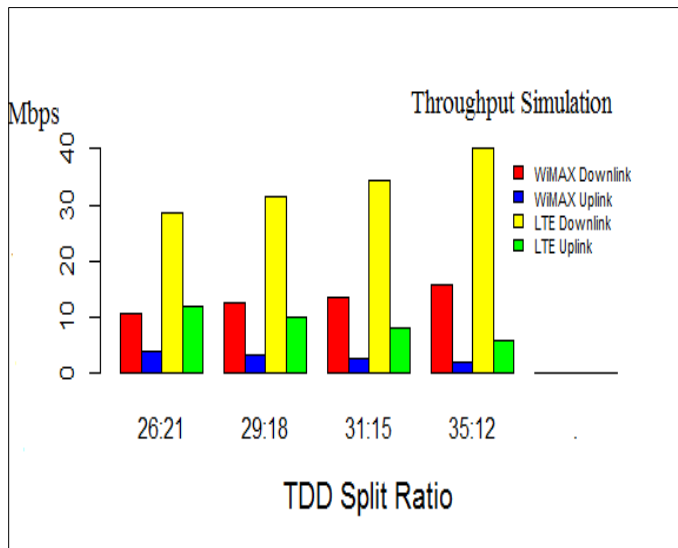


Fig. 10. Throughput simulation under varied TDD Split ratios.

Due to this impressive performance of the LTE network, the DL/UL ratio can also be chosen to be flexible to adapt to the differing demands of wireless services, whether to support high bandwidth, low latency, bursty traffic, ultra-reliable services based on the type of application being deployed in the network. For example, in deploying a mobile Telemedicine network which requires a higher UL throughput, a DL/UL split ratio of 26:21 is best suited for such network deployments while a DL/UL ratio of 36:12 can be used to deploy a network that provides online streaming services. The simulation performance of the deployed LTE network gives the Ghanaian mobile data subscriber hope of optimizing and leveraging the use of communication resources to support diverse business models, interactive applications and solve the limited wireless connectivity problems widely experienced in Ghana.

This research further performed average throughput per sector simulation for the pilot area under varied MIMO configurations. This enabled comparison of the results of the deployed 2X2 MIMO configuration with alternative 4X4 and 8X8 MIMO configuration. This simulation was carried out using 1000 users for each cell site. 20 cell sites were put together in this simulation with each cell site having three sectors to be able to fairly represent the number of cell sites serving end users within the pilot network. Fig. 11 presents 2x2 MIMO throughput distribution simulation. The area as indicated by the red ink has between 0-1 Mbps throughput coverage using 2X2 MIMO. Very poor power levels of -120 to -110 dBm were observed in this area. Throughput distribution however varied between 0 and 40 Mbps in the simulation. Average downlink throughput of 8.324 Mbps was obtained using 2X2 MIMO.

The throughput simulation results for adaptive 4x4 MIMO antenna configuration is summarized in Fig. 12. Using 4X4 MIMO, the areas indicated by the highlighted regions on Fig. 12 show very similar throughput results to 2X2 MIMO within those areas with coverage gaps. However, throughput values of 0-1 Mbps that were observed in 2X2 MIMO was

considerably reduced in 4X4 MIMO. On close observation 4X4 MIMO gave better average throughput results over 2X2 MIMO. Using 4X4 MIMO an average downlink throughput of 9.1782 Mbps was obtained.

Fig. 13 also presents 8X8 MIMO throughput distribution simulation for the study area. From the results, it was realized that an average downlink throughput of 9.517 Mbps was obtained using 8X8 MIMO. 8X8 MIMO produced the best throughput coverage for high throughput values of 10 - 30 Mbps. Throughput values obtained from all simulation gives a correlation to RSRP coverage results. Areas with low RSRP -120 to -110dBm had low throughput 1-5Mbps values. Areas with high RSRP coverage levels -100 to -50dBm had high throughput 5-40 Mbps. Generally the throughput behavior varied randomly. The average values however gave us an idea about the throughput performance using different MIMO schemes and this comparison as has been shown in Fig. 14. The downlink throughput prediction for the cluster analysis generally gave a higher average throughput for 8X8 MIMO. 2X2 MIMO gave the least average average throughput per sector. 8X8 MIMO with the highest number of transmitting antennas gave the highest average throughput compared to 2X2 and 4X4 MIMO. The percentage coverage for users under the 2x2 MIMO simulation scenario was better than that of the adaptive 4x4 MIMO configuration with 2x2 MIMO achieving 60.41% of area having throughput values between 1 - 40Mbps as against 55.87% achieved by the 4x4 MIMO configuration. This result seems to support the conclusions by authors in [13] that 2x2 MIMO seems to perform better in the peculiar Sub-Saharan terrain profile than adaptive 4x4 MIMO configuration.

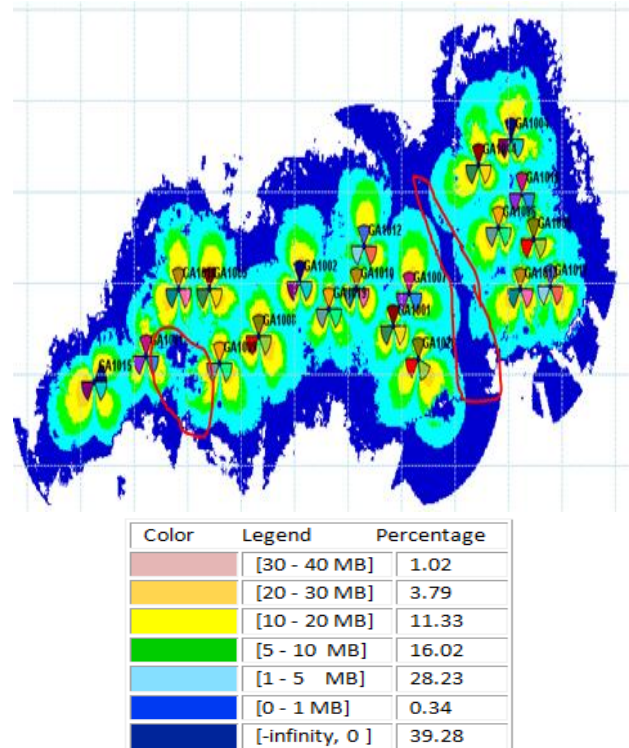
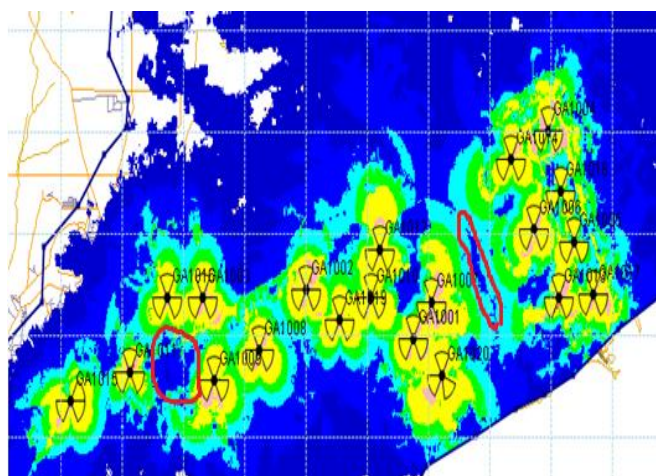
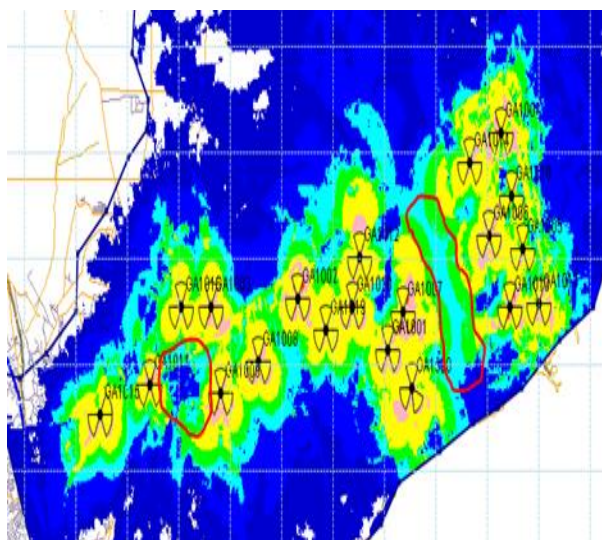


Fig. 11. Throughput distributions simulation for 2X2 MIMO.



Color	Legend	Percentage
[Red]	[30 - 40 MB]	0.87
[Orange]	[20 - 30 MB]	3.98
[Yellow]	[10 - 20 MB]	12.36
[Green]	[5 - 10 MB]	18.25
[Light Blue]	[1 - 5 MB]	20.41
[Dark Blue]	[0 - 1 MB]	0.07
[Darkest Blue]	[-infinity, 0]	44.07

Fig. 12. Throughput distributions simulation for 4X4 MIMO.



Color	Legend	Percentage
[Red]	[30 - 40 MB]	0.87
[Orange]	[20 - 30 MB]	4.11
[Yellow]	[10 - 20 MB]	12.60
[Green]	[5 - 10 MB]	18.24
[Light Blue]	[1 - 5 MB]	24.80
[Dark Blue]	[0 - 1 MB]	0.1
[Darkest Blue]	[-infinity, 0]	39.28

Fig. 13. Throughput distributions simulation for 8X8 MIMO.

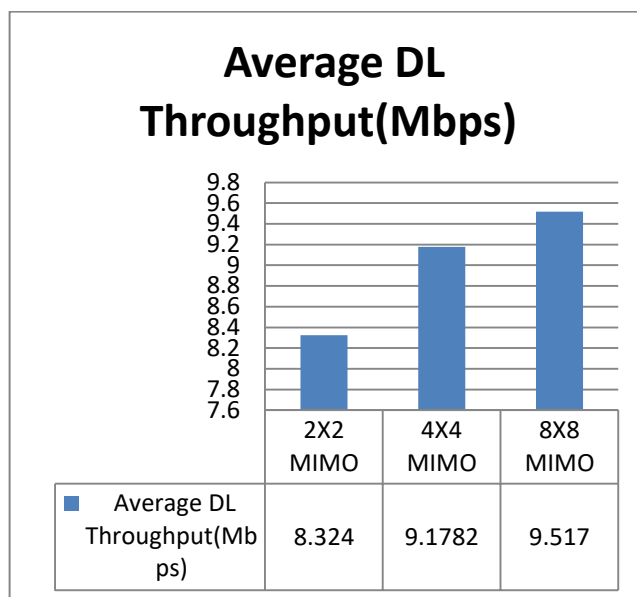


Fig. 14. Average throughput comparison for 2X2, 4X4 and 8X8 MIMO.

VIII. FIELD MEASUREMENT TRIALS RESULTS

This section presents the results collected during the field experimental trials. A comparison analysis has subsequently been done.

A. RSRP Measurements Results

Field results was collected for 2X2 MIMO 4G LTE. Fig. 15 presented below is a graphical representation of the drive test results on the reference signal received power conducted at the test route.

RSRP distribution differs at different points within the coverage area. Very good signal levels up to -110 dBm were measured up to about 2.5 km on route 2. Poor power levels below -110 dBm were not experienced on route 2.

However along route 1, poor levels lower than -110 dBm were experienced at about 1.5 - 2 km. Drive test was conducted on Route 2 which is on the N1 motorway. Here signals traversed free space along the motorway and could go as far as 2.5 km as shown by Fig. 9 on the ash route. Route 1 however finds itself on streets surrounded by cluster of buildings as shown by Fig. 16 and good signal level up to -110 dBm was received as far as 1.4 km. High rise buildings along the street obstructed the signals and increased the path loss reducing the signal received power.

From the drive test conducted in this sector, network coverage can reach a range of about 2.5 km with no obstructions but limited coverage of 1.4km in the presence of obstructions.

Simulation and field collected results for Route 1 showed correlation as shown in Fig. 10. In both cases signals deteriorated after 1.4 km. Simulation results were better in terms of RSRP level than field collected results. The buildings served as obstruction for the signal on this route and impeded the cell range.

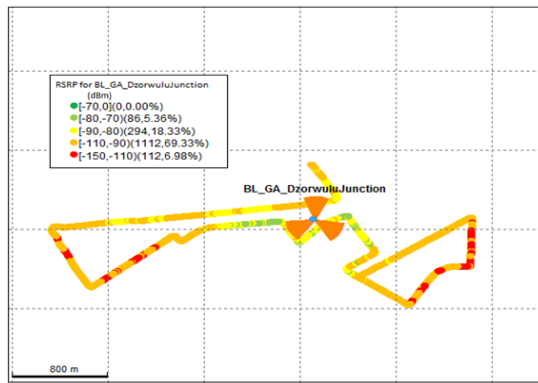


Fig. 15. RSRP distribution at test route (dBm).



Fig. 16. Overview of selected drive test routes.

Simulation results on Route 2 proved that RSRP received power decreases with increasing distance as shown in Fig. 17. Field collected data gave similar results until after 1.5 km when the received level remained nearly constant at (-100 dBm) from this point to about 2.5 km. This shows that RF signals traverse farther distance in a free space.

From the system level simulation results, a peak downlink and uplink throughput values of up to 75Mbps and 35Mbps were obtained respectively. Field measurement using IM2000 Monitor however showed 62.318 Mbps and 10.23 Mbps for downlink and uplink respectively. The deviation of the measured peak throughput values from the expected theoretical throughput could mainly be attributed to losses at the antenna front end and the use of pathloss models which have not been corrected to suite the peculiar Sub-Saharan African terrain among other factors.

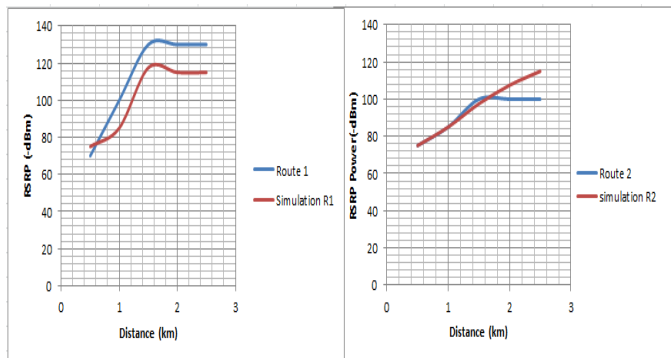


Fig. 17. Simulation against field measured coverage.

B. Throughput Field Collected Results

The results of the peak downlink and uplink measurements are summarized in Fig. 18 and 19.

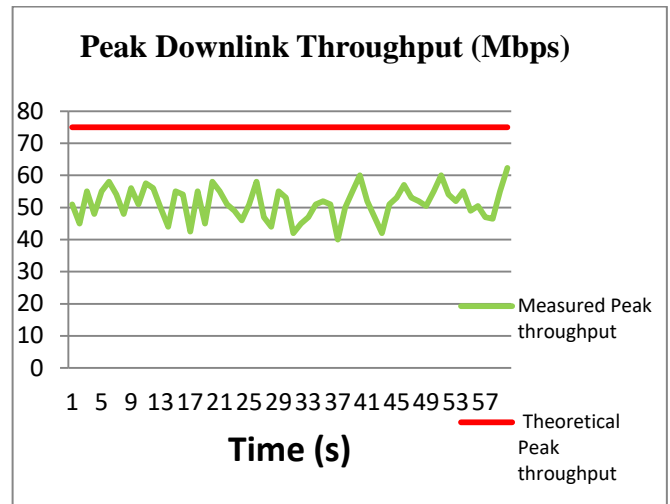


Fig. 18. Graph showing peak downlink throughput from drive test.

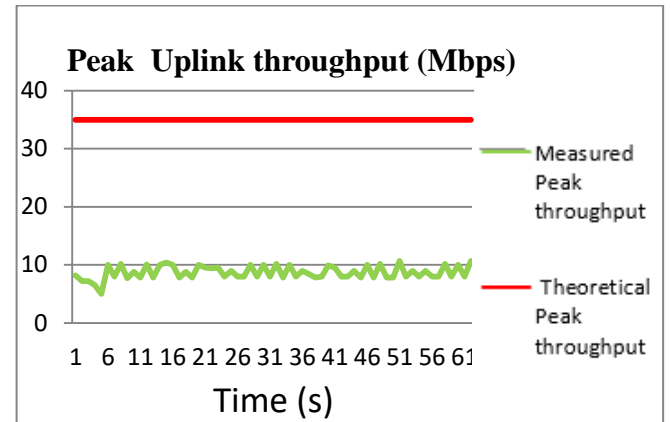


Fig. 19. Graph showing peak uplink throughputs from drive test.

Average throughput per sector measurements was also carried. The summarized results of the average throughput per sector recorded in this study period are presented in Fig. 20. Simulation results gave maximum per sector throughput values up to 40Mbps under a 35:12 TDD split ratio. Results obtained from both field data collection and simulation showed variation in throughput. The maximum simulated was 40 Mbps while field experimental results showed 29.9 Mbps. During the field measurement, it was observed that the throughput values varied depending on the traffic load, number of concurrent users and the distance of the user away from the cell site.

The maximum measured average downlink throughput per sector of 29.9 Mbps showed better performance of the deployed 4G technology when compared to the 9.52 Mbps obtained in the performance evaluation of WiMAX networks in the same study area which was reported in [15]. The comparison of LTE results and the results obtained in the same area for WiMAX is presented in Fig. 21.

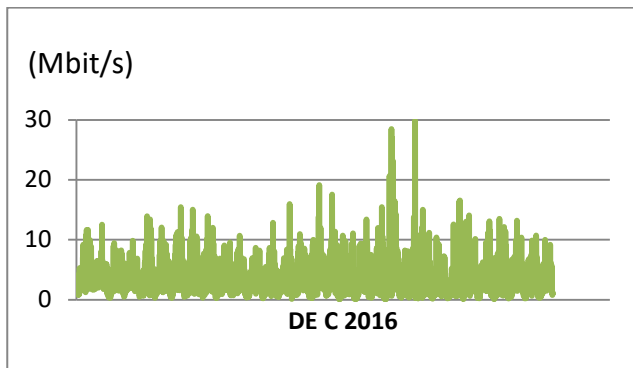


Fig. 20. Downlink average throughput per sector for the measurement period.

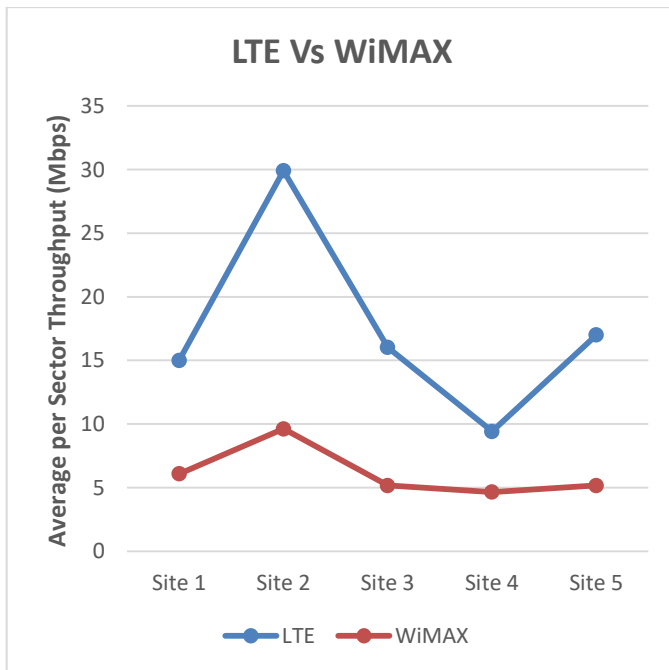


Fig. 21. Measured LTE throughput performance against documented performance of WiMAX in the survey area.

The performance of the two 4G technologies in the pilot area was observed to be directly related to the user densities in the survey area. Site 4 had the highest recorded number of subscription at 15,000 users during the measurement period with Site 2 having the least number of users at 5,113. Even though there is limited documented results on the performance evaluation of wireless networks in the sub-region, the results obtained from the experimental measurement in this work confirm LTE as superior wireless broadband technology which is capable of supporting last mile broadband solutions in the sub-region.

IX. CONCLUSION

This paper has presented throughput and coverage analysis using various MIMO antenna configuration schemes. Simulations showed 8X8 MIMO to perform better over 2X2MIMO and 4X4 MIMO in terms of throughput and coverage. However, it was seen that, the general performance

of adaptive 2x2 MIMO was better than 4x4 MIMO configuration. Field data collected on deployed 2X2 MIMO 4G LTE operating in the 2600 MHz band showed a measured maximum average throughput per sector of 29.9 Mbps and peak downlink throughput of 62.318 Mbps for users within a cell range of 2.5km away from the Base Station. Based on the results in this work, it can be concluded that, 4G LTE therefore is capable of providing the ever increasing broadband demand of Ghanaians when comparison is made with the throughput requirement needed to support data-centric broadband applications.

Future works on antenna configuration could concentrate on studying the effect of the use of propagation pathloss models which don't have offset parameters specified for the peculiar Sub-Saharan African terrain on the coverage gaps found in the detectable cell range.

REFERENCES

- [1] Zhang J., Arunaba G., Jeffery G. A., Rias M.: "Fundamentals of LTE," Prentice Hall, 2011
- [2] Technical Specification: "LTE; Evolved Universal Terrestrial Radio Access (E-UTRA); User Equipment (UE) radio transmission and reception", 3GPP TS 36.101 version 10.3.0 Release 10
- [3] Ghassan A. A., Mahamod I. and Kasmiran J.: "Modeling and Performance Evaluation of LTE Networks with Different TCP Variants". International Scholarly and Scientific Research & Innovation 5(3), pp 443-448. (2011).
- [4] Signals Research Group: "The LTE standard: Developed by a global community to support paired and unpaired spectrum deployments". White paper, available accessed on 23rd July, 2017 at www.signalsresearch.com. R. Nicole, "Title of paper with only first word capitalized," J. Name Stand. Abbrev., in press.
- [5] Ericsson mobility Report June 2016: Available: www.ericsson.com/res/docs/2016/ericsson-mobility-report-2016.pdf. [Accessed: August 17, 2017]
- [6] Rittenhouse G.: "A 1000X of data", in proceedings of IEEE Wireless Telecommunications Symposium 2013, Arizona
- [7] Khan F., "LTE for 4G Mobile Broadband: Air Interface Technologies and Performance," Cambridge University Press, New York, 2009
- [8] Ericsson Mobility Report: Available: <https://www.ericsson.com/assets/local/mobility-report/documents/2017/ericsson-mobility-report-june-2017.pdf> [Accessed: 8th September, 2017]
- [9] Sachin S. K. and Jadhav A.N., "An empirically based path loss model for LTE advanced network and modeling for 4G wireless systems at 2.4, 3.6 and 3.5 GHz," International journal of application or Innovation in engineering and management, September 2013, Vol. 2, Iss 9, pp 252-257.
- [10] Sami A. M.: "Comparison of propagation model accuracy for Long Term Evolution (LTE) Cellular Network," International Journal of Computer Applications (0975-8887), October 2013, volume 79 – No 1, pp 120- 127.
- [11] Rizwan U., Shabbir N, Sadiq M. T. and Kashif H.: "Comparison of radio propagation models for LTE networks," International Journal of Next-Generation networks, Vol.3, No.3, pp 27-41, September 2011.
- [12] Sachin S. K. and Jadhav A. N., "Performance Analysis of Empirical Propagation models for WiMAX in Urban Environment," IOSR journal of Electronics and Communication Engineering, Vol 3. pp 24-28,
- [13] E.T. Tchao, W.K. Ofosu, K. Diawuo, E. Affum, "Analysis of MIMO systems used in planning a 4G WiMAX Network in Ghana," 2013, International journal of Advanced computer science and applications, Vol. 4, No. 7
- [14] Turani S. and Ikpreet K., "Analysis of Multiple – Input – Multiple – Output (MIMO) system with transmit and receive diversity," International Journal of Computer Applications, volume 79, No. 12 pp 71-82, October 2013.

- [15] E. T. Tchao, W. K. Ofori and K. Diawuo.: "Radio Planning and Field Trial Measurement of a Deployed 4G WiMAX Network in an Urban Sub-Saharan African Environment"; International Journal of Interdisciplinary Telecommunications and Networking. September, 2013; 5(5): pp 1-10.
- [16] Curwen P., Whalley J. "Europe. In: Fourth Generation Mobile Communication". Management for Professionals. Springer, Cham. (2013):
- [17] Gabriel C.: "Softbank and China Mobile tout TD-LTE progress". Accessed on 10th August, 2017, from <http://www.rethink-wireless.com>
- [18] E. T. Tchao, W. K. Ofori, K. Diawuo, E. Affum and Kwame Agyekum "Interference Simulation and Measurements for a Deployed 4G-WiMAX Network in an Urban Sub-Saharan African Environment": International Journal of Computer Applications (0975 - 8887) Volume 71 - No. 14, pp 6-10, June 2013
- [19] H. Jia, Z. Zhang, G. Yu, P. Cheng, and S. Li. "On the Performance of IEEE 802.16 OFDMA System under Different Frequency Reuse and Subcarrier Permutation Patterns". In Proc. of IEEE ICC, June 2007.
- [20] G. Kulkarni, S. Adlakha, and M. Srivastava; "Subcarrier Allocation and Bit Loading Algorithms for OFDMA-Based Wireless Networks". IEEE Trans. On Mobile Computing, 4(6), Dec. 2005.
- [21] Nikolova: "Polarization and Related Antenna Parameters", accessed online at www.ece.mcmaster.ca/faculty/nikolova/antenna_dload/current.../L05_Polar.pdf [20-08-2017]
- [22] C. Khodier, M. and Christodoulou, "Linear array geometry synthesis with minimum sidelobe level and null control using particle swarm optimization," *IEEE Transactions on Antennas and Propagation*, vol. 8, no. 53, pp. 2674–2679, August 2005.
- [23] J. Kennedy and W. M. Spears, "Matching algorithms to problems: an experimental test of the particle swarm and some genetic algorithms on multi modal problem generator," in *Proc. IEEE Int. Conf. Evolutionary Computation*, 1998.
- [24] J. Zimmermann, R. Höns, and H. Mühlenbein. Encon: "an evolutionary algorithm for the antenna placement problem". *Computers & industrial engineering*, 44(2):209–226, 2003.
- [25] C.-H. Hsu, W.-J. Shyr, and C.-H. Chen, "Adaptive pattern nulling design of linear array antenna by phase-only perturbations using memetic algorithms," *Innovative Computing, Information and Control*, 2006. *ICICIC*, vol. 3, pp. 308–311, Aug 2006.
- [26] V. Gunasekaran and FC Harmantzis. Affordable infrastructure for deploying wimax systems: Mesh v. non mesh. In *Vehicular Technology Conference*, 2005. VTC 2005-Spring. 2005 IEEE 61st, volume 5, pages 2979–2983. IEEE, 2005.
- [27] J.K. Han, B.S. Park, Y.S. Choi, and H.K. Park. Genetic approach with a new representation for base station placement in mobile communications. In *Vehicular Technology Conference*, 2001. VTC 2001 Fall. IEEE VTS 54th, volume 4, pages 2703–2707. IEEE, 2001.
- [28] P. C. F. Eggers, "Angular dispersive mobile radio environments sensed by highly directive base station antennas," in *Proceedings of the 6th IEEE International Symposium on Personal, Indoor and Mobile Radio Communications (PIMRC '95)*, vol. 2, pp. 522–526, September 1995.
- [29] S. M. Qaseem and Adel A. Ali, "Effect of antenna correlation and Rician fading on capacity and diversity gains of wireless MIMO systems", *International Symposium on Wireless Systems and Networks ISWSN'05*, Apr. 25-27 2005, Kingdom of Bahrain.
- [30] C. M. Simmonds and M. A. Beach, "Downlink calibration requirements for the TSUNAMI (II) adaptive antenna testbed," in *Proceedings of the 9th IEEE International Symposium on Personal, Indoor and Mobile Radio Communications (PIMRC '98)*, pp. 1260–1264, Boston, Mass, USA, September 1998.
- [31] Yuan Y., "LTE-Advanced Relay Technology and Standardization", *Signals and Communication Technology*, DOI: 10.1007/978-3-642-29676-5_2.
- [32] Migliore M. D.: "An intuitive electromagnetic approach to MIMO communication systems", *IEEE Antennas and Propagation Magazine*, Vol. 48, No.3 pp 128-138, June 2006.
- [33] Philippe Godlewski, Masood Maqbool, Marceau Coupechoux and Jean-Marc Kélif, "Analytical Evaluation of Various Frequency Reuse Schemes in Cellular OFDMA Networks", *Telecom ParisTech technical White Paper*, pp 5-11, (2011)
- [34] Y. Zheng and S. Blostein, "Downlink distributed beamforming through relay networks," in *Proceedings of the IEEE Global Telecommunications Conference (GLOBECOM '09)*, Honolulu, Hawaii, USA, December 2009

Automatic Detection Technique for Speech Recognition based on Neural Networks Inter-Disciplinary

Mohamad A. A. Al-Rababah, Abdusamad Al-Marghilani, Akram Aref Hamarshi
Northern Border University, KSA

Abstract—Automatic speech recognition allows the machine to understand and process information provided orally by a human user. It consists of using matching techniques to compare a sound wave to a set of samples, usually composed of words but also of phonemes. This field uses the knowledge of several sciences: anatomy, phonetics, signal processing, linguistics, computer science, artificial intelligence and statistics. The latest acoustic modeling methods provide deep neural networks for speech recognition. In particular, recurrent neural networks (RNNs) have several characteristics that make them a model of choice for automatic speech processing. They can keep and take into account in their decisions past and future contextual information. This paper specifically studies the behavior of Long Short-Term Memory (LSTM)-based neural networks on a specific task of automatic speech processing: speech detection. LSTM model were compared to two neural models: Multi-Layer Perceptron (MLP) and Elman's Recurrent Neural Network (RNN). Tests on five speech detection tasks show the efficiency of the Long Short-Term Memory (LSTM) model.

Keywords—Speech recognition; automatic detection; recurrent neural network (RNN); LSTM

I. INTRODUCTION

Machine learning is a form of Artificial Intelligence (AI) that gives a machine the ability to evolve by acquiring new knowledge. Understanding speech is not an easy task for a machine. A machine, just like the human brain, must first recognize speech before understanding it. The formalism of generative grammars introduced by Noham Chomsky [1] is part of a process of theorizing language and allows a formalization that was possible to teach a machine. In the 1980s, statistical approaches very different from the initial linguistic formalism were born and quickly gained popularity because of their ease of implementation: rather than calling upon experts to formalize a given language, was trying to create a probabilistic model from a representative sample of the language to be modeled automatically. From there, and thanks to the increase of the computing power and the storage capacity of the machines, it became possible to perform many tasks of Automatic Natural Language Processing (ANLP) such as machine translation, automatic summarization, data mining, speech recognition and comprehension [2].

The scope of the ANLP on which this paper is based is the understanding of speech. It is usually done through a number

of stages. The first, optional, can be to transform the initial expression of the language into a format that maximizes the performance of machine learning. For an oral message, for example, a decoder will be used in an Automatic Speech Recognition (ASR) step in order to obtain the message in textual form or in the form of a lattice of textual hypotheses. Indeed the modeling of semantic content is considered easier by working on the text than on the acoustic signal, because the latter has a very high variability.

The second step towards understanding is the learning phase: building a model that will serve as a support for understanding. This model is produced using prior knowledge. This knowledge can come from experts in the field or, for statistical models, from a certain number of data representatives of the phenomenon to be modeled, and it is often necessary to call upon humans to annotate or even transcribe these data.

The third step is the use of this model to offer an understanding to a given statement. It can use several models and cross their results to refine understanding.

In deployed systems based on automatic processing of the natural language, and more specifically with regard to speech recognition systems, another step comes into play: the adaptation of the models. Indeed, such systems must necessarily adapt to follow the evolution of habits and language of users, as well as that of the services offered. Here again, the system needs experts who regularly update the models, classically providing a new body of learning adapted to the observed evolution of users or services.

These four major phases or stages (transformation, learning, understanding and adaptation) are not necessarily sequential and can be combined to maximize their effectiveness. Generally, a model resulting from learning is used many times in an understanding stage, and the adaptation phase often only occurs when the model gives signs of weakness.

The speech recognition consists in giving meaning to an oral utterance. In this it approaches a problem of classification if one considers that one chooses a sense among N possible senses, the sense being the class allotted to the statement. The block scheme of speech recognition system is presented in Fig. 1.

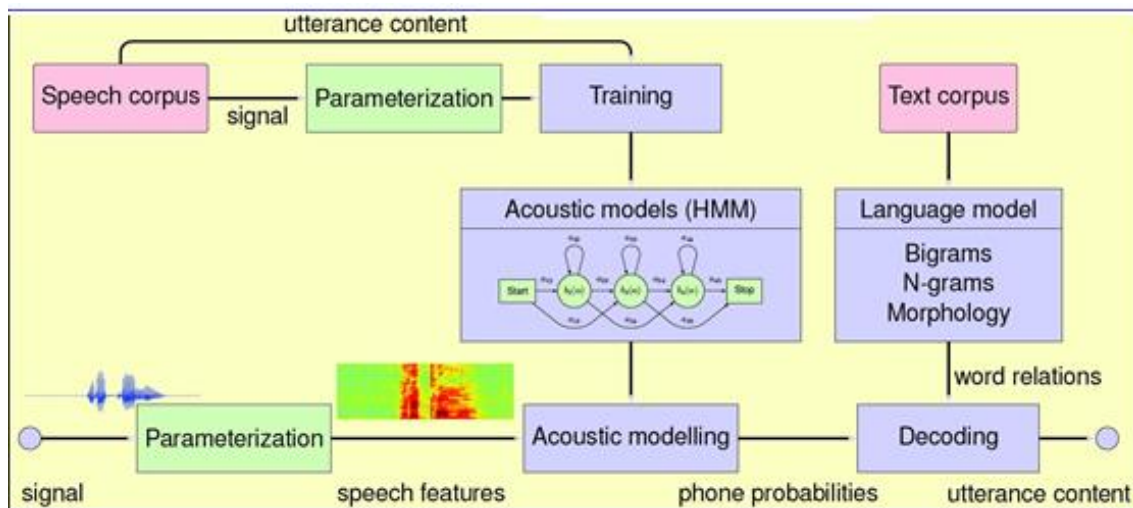


Fig. 1. Block scheme of speech recognition system.

The use of artificial neural networks for automatic speech processing is not recent. As early as the 1980s, systems using neural networks appeared to recognize vowels and then to recognize phonemes. But the results obtained at that time do not make it possible to improve the state of the art. During the next two decades some progress is made [30] but it is necessary to wait until the beginning of 2010 and the emergence of deep neural networks (DNN) with new methods of learning and specific computing resources (GPU), for that they become the state-of-the-art solution for wide vocabulary speech recognition systems [27], [28].

In recent years, a type of recurrent neural network has become the norm thanks to its excellent performance on many and varied tasks: Long Short-Term Memory (LSTM) -based neural networks.

The remainder of this paper is divided into five sections. After introducing, related works on speech recognition systems are presented in Section 2. Section 3 presents the Long Short-Term Memory (LSTM) -based neural networks. Section 4, experiments and results are detailed. Finally, this paper is concluded in Section 5.

II. RELATED WORKS

During the 1950s, speech recognition research focused on the acoustic component of speech. With the help of a tool called a spectrograph, which displays the image of speech spectra, they were able to define the main articulatory characteristics in order to be able to distinguish the different sounds of speech. Based on this visual recognition of sounds, the electrical device created in the Bell lab in 1952 could recognize the ten numbers spoken by a single speaker, comparing the acoustic parameters of the audio signal with reference models [3].

However, the success of the experiments is based on very strict conditions: reduced vocabulary, phonemes/isolated words, few speakers, recordings in laboratory conditions, etc. Acoustic methods alone are therefore insufficient for continuous speech and multi-speaker. As a result, the linguistic information begins to be taken into account in the

recognition systems, to add context to the phonemes/words to be recognized and thus to improve the recognition performance [4].

In 1971, the United States Defense Advanced Research Projects Agency (DARPA) launched a five-year project to test the feasibility of automatically understanding continuous speech, which favors the creation of three new systems [5]. The "Hearsay-II" systems of CMU (Carnegie Mellon University) and "HWIM" (Hear What I Mean) of BBN (Bolt Beranek and Newman Inc.) are based on artificial intelligence: the recognition of speech is formulated as a heuristic research problem among multiple sources of knowledge.

From the 1980s researchers focused on the recognition of connected words. The biggest change of the time is defined by the transition from rule-based systems to systems based on statistical models [6]. The speech signal starts to be represented in terms of probabilities thanks to the HMM (Hidden Markov Models), which makes it possible to combine linguistic information with acoustic temporal realizations of speech sounds. This also motivates the emergence of statistical models of language, called n-grams. The innovation in acoustic signal analysis consists in the combination of the cepstral coefficients and their first and second-order temporal derivatives. These methods have been predominant in subsequent research and continue to be used even nowadays, with constant additional improvements.

From the 1990s researchers focused on minimizing recognition errors. The DARPA program continues with a keen interest in natural language. His biggest challenge is associated with the "Switchboard" corpus which focuses on spontaneous and conversational speech. The University of Cambridge has created and released a set of tools called the Hidden Markov Model Tool Kit (HTK) [7] which is one of the most widely adopted software programs for automatic speech recognition.

In the 2000s, the DARPA program focuses on the detection of sentence boundaries, noises or disfluences, obtaining abstracts or translations in a context of spontaneous speech and multi-languages. Methods to evaluate the

confidence (reliability) of the recognition hypotheses were also studied during this period [8].

Neural networks first appeared in the 1950s, but could not be used because of practical problems. They were reintroduced in the late 1980s [9], but could not provide sufficient improvement over HMM systems. It is only since 2010 that context-dependent neural networks have surpassed HMM-GMM systems [10]. This improvement is due to the use of the many hidden layers (Deep Neural Network), made possible by an efficient unsupervised pre-training algorithm [11]. In addition, the calculation architecture using graphics processors (GPU) can efficiently parallel the learning and decoding of speech [26].

Neural networks are also increasingly used in lexical modeling [12], [13]; recurring models provide significant improvements over traditional n-gram back-off models [14]. A new set of tools called Kaldi [15] makes it possible to use state-of-the-art techniques for speech recognition.

Nowadays, researchers are increasingly interested in making systems capable of meeting all types of needs: machine translation, foreign language learning, assistance for the disabled or elderly, etc. Some examples of common research concern the detection of sentence boundaries [16], speech recognition in noisy environments [17], detection of distress phrases [18], commands [19] or keywords [20], etc. Multimodal communication, which takes into account additional information on the face, the movement of the lips and/or the articulation, also begins to be taken into account [21]-[23].

III. LONG SHORT-TERM MEMORY (LSTM)-BASED NEURAL NETWORKS

The interest of RNNs lies in their ability to exploit contextual information to move from an input sequence to an output sequence that is as close as possible to the target sequence. Unfortunately, for standard RNNs learning can be difficult and the context really exploited very local [29]. The problem lies in the fact that an input vector can only influence future decisions through recursive links (and thus via the repeated multiplication by the matrix V_j and the repeated application of the activation function) and therefore this influence decreases or increases exponentially as one moves forward in the sequence (Fig. 2). This phenomenon is often called a vanishing gradient problem in the literature because it impacts the retro-propagation of the gradient.

In the 1990s, many neural architectures and learning methods were tested to try to counter this phenomenon. Among these methods are heuristic optimization methods that do not use the gradient such as simulated annealing or discrete error propagation methods, the introduction of explicit delays in the recurrent architecture or the hierarchical compression of sequences. But the approach that has proven most effective and has now become the standard for dealing with sequences is the LSTM model. In fact, this model introduces multiplicative logic gates that make it possible to preserve and access relevant information over long intervals, thus reducing the impact of the evanescent gradient problem (Fig. 3). It is to

this type of neural model that this paper is mainly interested and the LSTM model is described in this section.

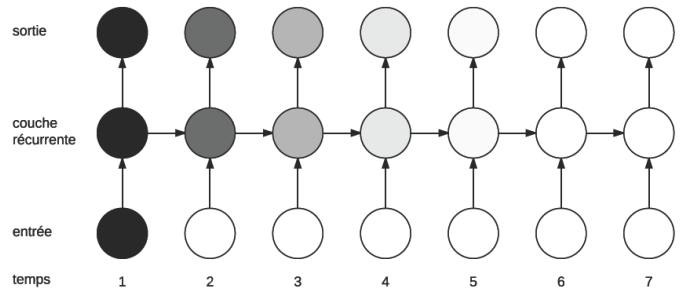


Fig. 2. Evanescent gradient problem in a standard RNN.

A layer of LSTM L_j^n is composed of four RNN layers and which interact with each other. Three of these RNN layers have the function of transfer of the logistic function (and therefore of the outputs between 0 and 1) and act as logical gates controlling:

- The amount of information that enters the LSTM cells of the layer j ,
- The amount of information that is retained by the internal state of the cells from one step to the other,
- The amount of information coming out of the LSTM cells of the layer j .

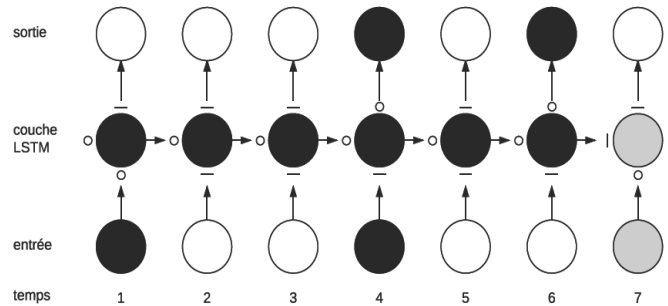


Fig. 3. Preservation of information (and gradient) in an LSTM layer.

The last of the four layers operates as a standard RNN layer and feeds the internal state of the LSTM cells via the gateways. Fig. 4 shows a synthetic description of information flows. Finally, to model the returns between the internal state of the cells and the 3 logic gates introduced by F. Three parameter vectors $u_i, u_f, u_o \in R^{n_j}$ called “peepholes” were added. Fig. 5 shows the detailed operation of an LSTM layer.

As in the case of the standard RNN, the BPTT technique is used to compute the partial derivatives of the cost function $C(z, c)$ that is minimized with respect to the different parameters of the LSTM layers. To do this, we go through the sequence by going back in time: $t: t_f \rightarrow 1$ and for each time step the gradients were determined with respect to the parameters. Then, global gradients are obtained by summing the contributions of each of the time steps. Fig. 6 describes the retro-propagation of the gradient in the layer L_j^n at the time step t in the form of a computational graph.

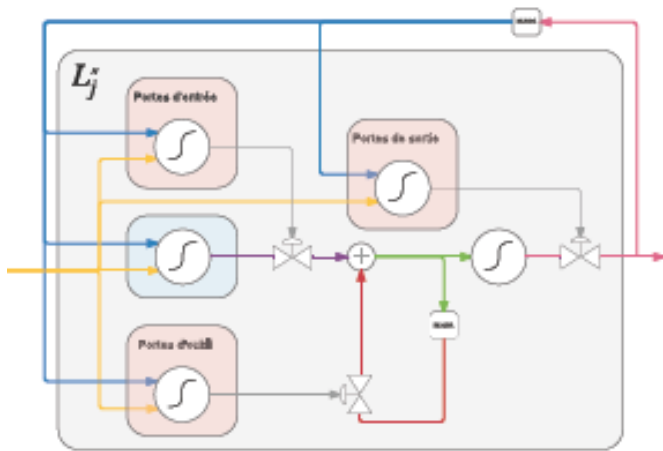


Fig. 4. Synthetic visualization of the propagation of information during the forward pass in an LSTM layer.

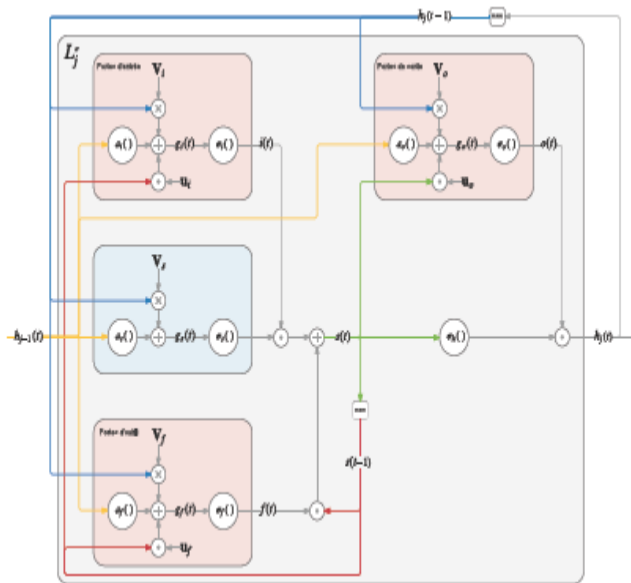


Fig. 5. Visualization of the propagation of the information during the forward pass in a layer of an LSTM.

In order to calculate the partial derivatives of C at the time step t with respect to the parameters of the layer L_j^s , the first step is to retro-propagate the gradient in the whole of the layer L_j^s , starting at the exit gates.

IV. EXPERIMENTS AND RESULTS

During this paper, speech detection tasks are varied in terms of difficulties, languages and acoustic environments. We have worked on pure detection tasks (that is, the goal of minimizing the number of badly signal windows classified speech/not speech) and speech detection tasks for speech recognition, that is to say, so as to minimize the Word Error Rate (WER) of an automatic speech recognition system used downstream of the speech detection system. Very different types of data were used, such as telephone conversations, working meeting recordings, and television series audio tapes.

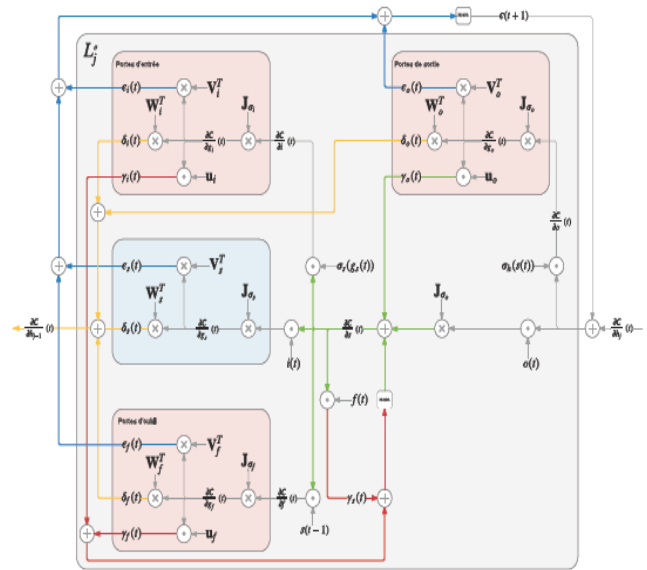


Fig. 6. Visualization of the propagation of the information during the back-pass in a layer of an LSTM.

In 2012, IARPA launched the Babel program with the aim of developing automatic speech recognition technologies that can be quickly applied to any spoken language. For all experiments, state-of-the-art automatic speech recognition systems were used. These systems are similar to those described in [24]. They use Multi-Layer Perceptron (MLP) as acoustic models and language models based on 4-gram models. They also respect the NIST constraint for system evaluation in the Babel program which states that no data other than that provided for the target language of the Babel program may be used. The official metric for the assessments performed is the Word Error Rate (WER) but the Frame Error Rate (FER) is also used in preliminary experiments.

The NIST regularly organizes open and international assessments of the different tasks of automatic speech processing. In 2015, The NIST organized the OpenSAD'15 evaluation to provide a framework for developers of speech detection systems to independently measure the performance of their systems on particular difficult audio data. Indeed, the audio signals collected for this evaluation come from the RATS program of DARPA which was mainly interested in highly distorted and/or noisy channels. These different channels are of type HF, VHF and UHF and are 7 in number (called A, B, C, E, F, G and H) with the particularity that two of these channels (A and C) are voluntarily absent from the learning and validation stages but present in the test stage to evaluate the generalization capacity of speech detection systems.

The official metric of the evaluation was the DCF defined as follows:

$$DCF = 0.75 \times P_{miss} + 0.25 \times P_{fa}$$

Where:

$$P_{miss} = \frac{\text{speech duration labeled as non - speech}}{\text{total speech time}}$$

And

$$P_{fa} = \frac{\text{non - speech duration labeled as speech}}{\text{total duration of non - speech}}$$

Three experiments were conducted on data collected in acoustic environments very different from the telephone conversations of the OpenSAD'15 evaluation and the Babel program. For these three experiments the ultimate goal was to segment into speakers. Segmentation into speakers consists of segmenting an audio signal into homogeneous speech turns, that is to say containing only one speaker. The metric of choice for this task is the Diarization Error Rate (DER) which is broken down into two parts: the FER, to which is added an error term corresponding to the confusions between speakers. Therefore, to optimize a speaker segmentation system it is preferable to minimize the FER of the speech detection system.

We worked on a task of segmentation in speakers in the audio streams of television programs collected for the LNE Audiovisual Emissions Recognition evaluation campaign (REPERE).

We also worked on the data of the AMI project which was a multidisciplinary consortium of 15 members whose mission was the research and development of technologies to improve interactions within a working group.

Finally, we worked on audio data from television series. The TVD corpus were used [25] and focused on the first season of the Game of Thrones (GoT) television series, which offers a variety of acoustic environments (indoor, outdoor, and battle scenes). This corpus is thus composed of ten episodes of 55 minutes approximately with the annotations of turns of speech by speaker.

Here, an overview of the performance gain brought by the LSTM model is presented and compared to other neural models on the speech detection task. The three neuronal models tested are: Multi-Layer Perceptron (MLP), Elman's Recurrent Neural Network (RNN) and LSTM. In order to obtain a fair comparison of the modeling capacity of each of the artificial neural networks (ANN) tested, all the ANNs used are sized to have the same number of parameters: 6000. The different ANNs are compared on five speech detection tasks: minimization of the FER on the data REPERE, AMI, Game of Thrones and the Vietnamese corpus of the Babel program; and minimizing the DCF on the OpenSAD'15 evaluation data. The three ANNs were optimized for these tasks and the results obtained on the different corpus are detailed in Table I. It is important to note that for these tests the decision smoothing module is disabled in order to get a better insight into the raw capabilities of the different neural models.

The RNNs are particularly adapted to speech detection tasks because, by allowing to exploit the temporal context freely, these models are able to improve very significantly the decisions taken locally at each time step. Thus, there is a decrease in error rates of up to 42% relative between the MLP and the simplest of the recurrent models on the data of the AMI corpus.

The most successful recurring model is the LSTM model. In fact, this model, when compared to the standard RNN model, makes it possible to improve the error rates by 17% relative on the OpenSAD'15 and REPERE corpus, by 14% relative on the Game of Thrones corpus and allows obtaining an equivalent performance on the AMI and Babel corpus.

TABLE I. PERFORMANCE OF DIFFERENT SPEECH DETECTION SYSTEMS ON BABEL, REPERE, AMI, GAME OF THRONES AND OPENSAD'15 CORPUS DATA

Type of ANN	FER				DCF
	Babel	REPERE	AMI	Game of Thrones	OpenSAD'15
MLP	9.2	17.1	11.4	17.9	5.3
RNN Standard	6.4	16.4	6.6	12.7	4.1
LSTM RNN	5.9	13.5	6.2	11	3.4

V. CONCLUSIONS

In this paper a particular type of RNN called LSTM were studied and their use for an automatic speech processing task: speech detection. Comparisons with other neural models were presented on five speech detection tasks.

All tests show that the LSTM model is more efficient than Elman MLP and RNN neuron networks. With this model, the proposed method were ranked third in the NIST OpenSAD'15 evaluation campaign with a level of performance very close to the second ranked system while having ten to one hundred times fewer parameters. Future works include the use of LSTM for another task of automatic speech processing such as spoken language identification: separate one language from all others.

REFERENCES

- [1] Chomsky, Noham. Syntactic Structures. Mouton & Co, 1957
- [2] Mekyska J., Beitia B., Barroso N., Estanga A., Tainta M., Ecay-Torres M. Advances on automatic speech analysis for early detection of Alzheimer Disease: a non-literal multi-task approach. *Curr. Alzheimer Res*;15(2):139-148, 2018.
- [3] DAVIS, K. H., R. BIDDULPH et S. BALASHEK. "Automatic Recognition of Spoken Digits". *The Journal of the Acoustical Society of America* 24.6, p. 637-642, 1952.
- [4] REDDY, D. R. "Approach to computer speech recognition by direct analysis of the speech wave". *The Journal of the Acoustical Society of America* 40.5, 1966.
- [5] MEDRESS, M. "Speech Understanding Systems: Report of a Steering Committee". In : *SIGART Newsletter* 62, p. 4-8, 1976.
- [6] ARORA, S. J. and R. P. SINGH. "Automatic Speech Recognition: A Review". *International Journal of Computer Applications* 60.9, p. 34-44, 2012.
- [7] YOUNG, S. J., D. KERSHAW, J. ODELL, D. OLLASON, V. VALTCHEV and P. WOODLAND. *The HTK Book Version 3.4*. Cambridge University Press, 2006.
- [8] JIANG, H. "Confidence measures for speech recognition: A survey". *Speech Communication* 45.4, p. 455-470, 2005.
- [9] KATAGIRI, S. *Pattern Recognition in Speech and Language Processing*. CRC Press 2003.
- [10] DAHL, G. E., D. YU, L. DENG and A. ACERO. "Context-Dependent Pre-trained Deep Neural Networks for Large Vocabulary Speech Recognition". *IEEE Transactions on Audio, Speech and Language Processing*, 2012.

- [11] HINTON, G. E. and S. OSINDERO. "A fast learning algorithm for deep belief nets". In : Neural Computation 18.7, p. 1527–1554, 2006.
- [12] SCHWENK, H. "Continuous space language models". Computer Speech & Language 21.3, p. 492–518, 2007.
- [13] MIKOLOV, T., M. KARAFIÁT, L. BURGET, J. CERNOCKÝ and S. KHUDANPUR. "Recurrent neural network based language model." In Proc of Interspeech, p. 1045–1048, 2010.
- [14] MIKOLOV, T., S. KOMBRINK, L. BURGET, J. CERNOCKÝ and S. KHUDANPUR. "Extensions of recurrent neural network language model". In Proc of the IEEE International Conference on Acoustics, Speech and Signal Processing (ICASSP), p. 5528–5531, 2011.
- [15] POVEY, D. et al. "The Kaldi Speech Recognition Toolkit". IEEE 2011 Workshop on Automatic Speech Recognition and Understanding, 2011.
- [16] READ, J., R. DRIDAN, S. OEPEN and J. L. SOLBERG. "Sentence Boundary Detection: A Long Solved Problem?". In Proc of COLING, p. 985–994, 2012.
- [17] TU, C. and C. JUANG. "Recurrent type-2 fuzzy neural network using Haar wavelet energy and entropy features for speech detection in noisy environments". Expert systems with applications 39.3, p. 2479–2488, 2012.
- [18] AMAN, F., M. VACHER, S. ROSSATO and F. PORTET. "Speech Recognition of Aged Voices in the AAL Context: Detection of Distress Sentences". In Proc of The 7th International Conference on Speech Technology and Human-Computer Dialogue , p. 177–184, 2013.
- [19] VACHER, M., B. LECOUTEUX and F. PORTET. "Multichannel Automatic Recognition of Voice Command in a Multi-Room Smart Home : an Experiment involving Seniors and Users with Visual Impairment". In Proc of Interspeech, p. 1008–1012, 2014.
- [20] JOTHILAKSHMI, S. "Spoken keyword detection using autoassociative neural networks". International Journal of Speech Technology 17.1, p. 83–89, 2014.
- [21] NGIAM, J., A. KHOSLA, M. KIM, J. NAM, H. LEE and A. Y. NG. "Multimodal deep learning". In Proc of the 28th International Conference on Machine Learning (ICML), p. 689–696, 2011.
- [22] GALATAS, G., G. POTAMIANOS and F. MAKEDON. "Audio-visual speech recognition incorporating facial depth information captured by the Kinect". In Proc of the 20th European Signal Processing Conference (EUSIPCO), p. 2714–2717, 2012.
- [23] REGENBOGEN, C., D. A. SCHNEIDER, R. E. GUR, F. SCHNEIDER, U. HABEL et T. KELLERMANN. "Multimodal human communication - Targeting facial expressions, speech content and prosody". In : NeuroImage 60.4, p. 2346–2356, 2012.
- [24] V.-B. Le, L. Lamel, A. Messaoudi, W. Hartmann, J.-L. Gauvain, C. Woehrling, J. Despres, and A. Roy, "Developing STT and KWS systems using limited language resources", Interspeech, 2014, 27
- [25] A. Roy, C. Guinaudeau, H. Bredin, and C. Barras, "Tvd : A reproducible and multiply aligned tv series dataset." , LREC, 30, pp. 418–425, 2014.
- [26] A.L. Maas, P. Qi, Z. Xie, A. Y. Hannun, C.T. Lengerich, D. Jurafsky, A.Y. Ng. "Building DNN Acoustic Models for Large Vocabulary Speech Recognition." arXiv preprint arXiv:1406.7806, 2014 Jun 30.
- [27] Jun Ren, Mingzhe Liu. An Automatic Dysarthric Speech Recognition Approach using Deep Neural Networks. International Journal of Advanced Computer Science and Applications (IJACSA) Vol. 8, No. 12, 2017 .
- [28] Choudhary, A. and Kshirsagar, R. Process Speech Recognition System Using Artificial Intelligence Technique. International Journal of Soft Computing and Engineering (IJSCE), 2, 2012.
- [29] Zhiyan, Han, and Wang Jian. "Research on speech endpoint detection under low signal-to-noise ratios." Control and Decision Conference (CCDC), 2015 27th Chinese. IEEE, 2015.
- [30] A. Graves, S. Fernández, F. Gomez, and J. Schmidhuber, "Connectionist temporal classification : labelling unsegmented sequence data with recurrent neural networks," in Proc of the 23rd international conference on Machine learning, pp: 369-376, ACM, 2006.

Image based Arabic Sign Language Recognition System

Reema Alzohairi, Raghad Alghonaim, Waad Alshehri, Shahad Aloqeely,
Munera Alzaidan, Ouiem Bchir
Computer Science Department, College of Computer and Information Sciences,
King Saud University

Abstract—Through history, humans have used many ways of communication such as gesturing, sounds, drawing, writing, and speaking. However, deaf and speaking impaired people cannot use speaking to communicate with others, which may give them a sense of isolation within their societies. For those individuals, sign language is their principal way to communicate. However, most people (who can hear) do not know the sign language. In this paper, we aim to automatically recognize Arabic Sign Language (ArSL) alphabets using an image-based methodology. More specifically, various visual descriptors are investigated to build an accurate ArSL alphabet recognizer. The extracted visual descriptors are conveyed to One-Versus-All Support Vector Machine (SVM). The analysis of the results shows that Histograms of Oriented Gradients (HOG) descriptor outperforms the other considered descriptors. Thus, the ArSL gesture models that are learned by One-Versus-All SVM using HOG descriptors are deployed in the proposed system.

Keywords—Component; Arabic sign language; image; visual descriptor; recognition

I. INTRODUCTION

Human communication has been evolving over time. Overages, humans have used petroglyphs, pictograms, ideograms, alphabet, sounds, signals, gestures as ways of communication. Nowadays, the dominant communication way relies on alphabet expression either orally, in writing, or as sign language. People suffering from hearing and/or speaking disorders cannot communicate orally with others. Moreover, they usually prove difficulties to learn how to write and read a text. Thus, sign language has emerged as an effective alternative to express their thoughts. According to World Health Organization over 5% of the world's population (360 million people) suffer from hearing impairment. Moreover, the World Federation of the Deaf stated that the number of deaf and hearing-impaired people among the Arab region exceeded 700,000 persons in 2008 [1].

Although many hearing-impaired people master sign language, few “normal” individuals understand and/or can use sign language. This affects the communication with deaf people and results in a kind of isolation between them and “normal” people world. This gap can be reduced using a system that allows the translation of sign language automatically to text and vice versa. Nowadays, many paradigm shifts in many technology fields have helped researchers to propose and implement systems targeting sign languages recognition [2]–[7]. Thus, several works on sign

language recognition have been proposed for various sign languages, including American Sign Language, Korean Sign Language, Chinese Sign Language, etc. [8]. The proposed sign recognition systems rely on either image-based or sensor-based solutions.

Most of the sensor-based systems recognize gestures utilizing glove-based gadgets which provide information about the position and the shape of the hand [9]. However, these gadgets are cumbersome and generally have several links connected to a computer. This yields the need of utilizing non-intrusive, image-based methodologies for perceiving gestures [10]. Image-based systems have been proposed as an alternative solution that allows availability and naturalness. These image-based systems utilize image processing algorithms to recognize and track hand signs. This makes the process easier to the signer, since these systems do not require the impaired person to use any sensor. Moreover, they can be deployed to smart devices. Thus, due to the availability of cameras on the portable devices, image-based sign language recognition system can be used anytime and anywhere.

The key stone of any image-based system is feature (visual descriptor) extraction [11]. The role of these features is to translate the information perceived in the image to a numerical vector that can convey the appropriate information to the recognition system. Many features have been used and reported in the literature [11]–[13]. Some of them are general, describing either colors, textures, edges, or shapes of the content of the image [13]. Others, are application-dedicated and are designed for a specific application [14].



Fig. 1. The 30 gestures of the ArSL letters [14].

Recently, research on image-based recognition for ArSL have been reported [14]–[23]. ArSL include 30 gestures. As shown in Fig. 1, each gesture represents a specific hand orientation and finger positioning. In order to recognize these gestures, features have to be extracted. However, it is not straightforward to choose a feature that allows recognizing and segregating ArSL alphabet. This is due to the fact that ArSL has the characteristic of having several gestures that are very similar to each other like “Dal” and “Thal”, “Ra”, and “Zay”, etc. In the literature [14]–[23], different types of features have been used. However, there is no empirical comparison that investigated which feature is suitable for Arabic letter recognition.

In this paper, we aim to design an ArSL recognition system that captures the ArSL alphabet gestures from an image in order to recognize automatically the 30 gestures displayed in Fig. 1. More specifically, we intend to investigate various features to build an ArSL alphabet recognizer.

This paper is organized as follows: Section I includes an introduction to the problem, Section II briefly explains Arabic sign language and compares it to other sign languages, Section III discusses the existence of related works, Section IV shows the proposed design of Arabic sign language recognizer, Section V discusses the result of running the experiments and how the system has been implemented, and Section VI concludes the paper.

II. ARABIC SIGN LANGUAGE

Sign language is the language that is used by hearing and speech impaired people to communicate using visual gestures and signs [24]. There are three kinds of image-based sign language recognition systems: alphabet, isolated word, and continuous sequences [23]. Usually, hearing and speech impaired communicate with others using words and continuous sequences, since it is faster than spelling each single word. However, if the desired word does not have a standard sign that represent it, signers use finger spelling. They spell out the word using gestures which have corresponding letters in the language alphabet. In this case, each letter is performed independently by a static posture [23]. Finger spelling gestures use a single-hand in some languages and two-hand gestures on others. For example, languages such as Australian, New Zealand and Scotland use two hands to represent the different alphabet [25].

Same as sign languages, finger spelling alphabet are not universal. Each language is characterized by a specific alphabet gestures. However, some languages share similar alphabet gestures. For instance, regardless of the unlikeness between Japanese and English orthography, Japanese Sign Language and American Sign Language (ASL) share a set of similar hand gestures. Also, the German and the Irish manual alphabet hand gestures are similar to the ASL ones. Similarly, French and Spanish alphabets share similar characteristics. Although the Russian language includes more alphabet to represent the Cyrillic ones, it has high similarities with the French and Spanish languages for the other gestures [25].

For Arab countries, Arabic Sign Language (ArSL) is the official sign language for hearing and speech impaired [26]. It

was officially launched in 2001 by the Arab Federation of the Deaf [26]. Although the Arabic Language is one of the most spoken languages in the world, ArSL is still in its evolutionary phases [27]. One of the largest issues that face ArSL is “Diglossia”. In fact, in each country, the regional dialect is spoken rather than the written language [28]. Therefore, variant spoken dialects made variant ArSLs. They are as many as Arab countries but with many words in common and the same alphabet. The 30 Arabic alphabet gestures are represented in Fig. 1. There are also extra letters that have the same original gestures but with different rotation or additional motion. These are the different ways for writing “Alef”. Fig. 2 displays these variants.



Fig. 2. ArSL variants.

ArSL is based on the letters shapes. Thus, it includes letters that are not similar to other languages letter representation. For example, Fig. 3 shows the American Sign Language (ASL) alphabet.

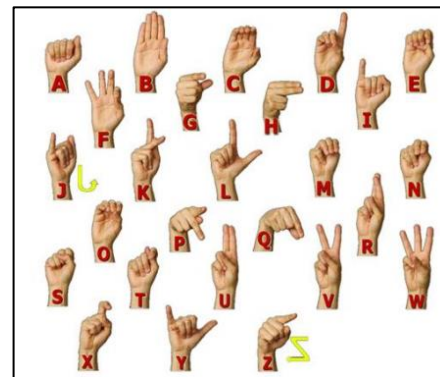


Fig. 3. ASL alphabet [29].

We notice from Fig. 3 that both ArSL and ASL letters are one-handed gestures. In addition to that, ArSL and ASL have some similar gestures (see Fig. 4). Some of them represent the same letter sound such as “Lam” and L (Fig. 4(a)), “Sad” and S (Fig. 4(b)), and “Ya” and Y (Fig. 4(c)). On the other hand, there are other similar gestures for different letters sounds such as “Kaf” and B (Fig. 4(d)), “Ta” and u (Fig. 4(e)), and “Meem” and I (Fig. 4(f)).

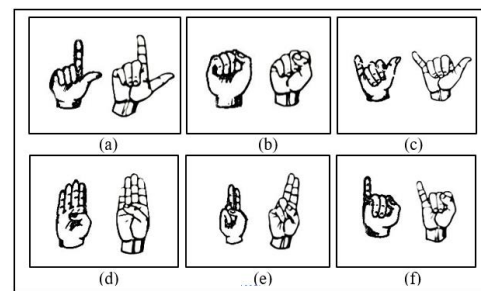


Fig. 4. Similar gestures between ASL and ArSL, (a) “Lam” and L, (b) “Sad” and S, (c) “Ya” and Y, (d) “Kaf” and B, (e) “Ta” and H, (f) “Meem” and I.

On the other hand, several ArSL letters are similarly gestured. This is a characteristic of ArSL since several Arabic letters are similarly shaped. For example, "Tah" and "Thah" are similar in the way that the index finger is raised and the rest of the fingers are facing the right side (Fig. 5(a)). Furthermore, "Ra" is similar to "Zay" but "Zay" has two curved fingers while "Ra" has only one curved finger (Fig. 5(b)). Similarly, the thumb and the index finger are curved in like a C shape in "Dal" and "Thal", yet the middle finger in "Thal" is curved too (Fig. 5(c)).

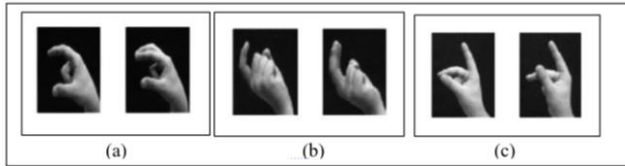


Fig. 5. Similar gestures in ArSL, (a)"Tah" and "Thah". (b)"Ra" and "Zay". (c)"Dal" and "Thal".

III. RELATED WORKS

Recently, sign language recognition has become an active field of research [18]. Sign language recognition systems translate sign language gestures to the corresponding text or speech [30] in order to help in communicating with hearing and speech impaired people. These systems can be considered as HCI applications, where the computer would be able to identify those hand gestures and convert them to text or speech [14], [18]. They have been applied to different sign languages [18], [31], [32]. Sign language recognition systems are based on one of two ways to detect sign languages' gestures. They are sensor-based recognition systems and image-based recognition systems [14].

In sensor-based systems, sign language recognition is based on sensors that detect the hand's appearance. For this kind of system, two types are considered, which are the glove-based systems [33] and the Kinect-based systems [29]. Glove-based systems [33] use electromechanical devices to recognize hand gestures. Hearing and speech impaired signers are required to wear a glove that is linked to some sensors that gather information [34]. Although this technique can offer good results, it can be inconvenient to the signers [34]. For the second category, Kinect sensors are used to detect sign language gestures. Originally, these sensor devices were developed by Microsoft for their Xbox game as an input device to interact with video games without using any remote controllers [35]. Nowadays, the use of this device is expanding to include recognition systems like sign language recognition.

On the other hand, image-based systems use images or videos [32], [36], [37] along with image processing and machine learning techniques to recognize sign language gestures [34]. These systems fall into two categories. The first depends on using gloves containing visual markers to detect hand gestures, such as colored gloves [14]. However, this method prevents sign language recognition systems from being natural, where naturalness is expected from similar HCI systems [14]. The second category depends on images capturing hand gestures of the sign language [34]. When using these image-based recognition systems, hearing and speech

impaired do not need to use any sensors or gloves with visual markers, which eliminates any inconvenience and makes the system more convenient [14]. The mentioned types of sign language recognition systems are shown in Fig. 6.

Image-Based Sign Language Recognition systems categorize the hand gesture from a 2D digital image by using image processing and machine learning techniques [34]. Such systems either recognize static or dynamic continuous gestures [38]. The images of ArSL shown in Fig. 1 are static gestures.

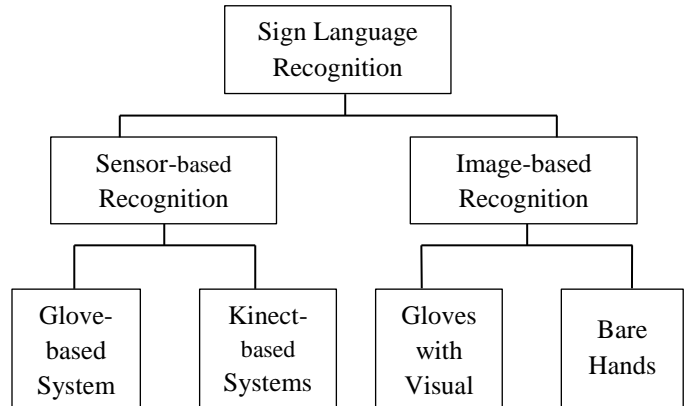


Fig. 6. Sign language recognition systems.

In the literature, various sign language recognition systems have been proposed. The authors in [32] have implemented a video-based continuous sign language recognition system. The system is based on continuous density hidden Markov models (HMM) [39]. It recognizes sign language sentences, based on a lexicon of 97 signs of German sign language (GSL). The system achieves an accuracy of 91.7%. Similarly, HMM [39] has been used by authors in [40]. The system recognizes Japanese sign language (JSL) words. This approach is video-based continuous recognition. Six visual descriptors were defined to recognize JSL, which are the flatness, the gravity center position, the area of the hand region, the direction of hand motion, the direction of the hand, and the number of protrusions. The system recognized 64 out of 65 words successfully. In [41] the authors have used a method to find the centroid for mapping the hand gesture of Sinhala Sign Language (SSL). The system recognizes image-based gestures of SSL words. A dataset of 15 Red-Green-Blue (RGB) image of gestures from 5 signers captured by a web camera has been used in this experiment. The system identified ten gestures with 100% accuracy, four gestures with 80% accuracy and one gesture with 60% accuracy. It recognized 92% of the 15 gestures.

The authors in [42] used HMM [39] classifier. The system recognizes the vocabulary of GSL. The used dataset consists of a vocabulary of 152 signs of GSL performed by a single signer ten times each. The system achieved a recognition rate of 97.6%. The authors in [43] have proposed a novel recognition method based on Spatio-temporal visual modeling of sign language. It uses Support Vector Machines (SVMs) [44] to recognize Chinese Sign Language. Experimentation was conducted with 30 groups of the Chinese manual alphabet images. In [45] the authors have investigated the problem of recognizing words from a video. The words are finger spelled

using British Sign Language (BSL). A dataset of 1,000 low-quality web-cam videos of 100 words has been used in the experiment. The system achieved a word recognition accuracy of 98.9%.

A hand gesture recognition of Indian sign language (ISL) has been suggested in [46]. The system applies Histogram of Gradient Orientation (HOG) visual descriptors extraction approach. It is then converted to a neural network classification recognition purpose. The dataset consists of alphanumeric characters. They are collected using a simple web camera.

Recently, ArSL systems that recognizes static alphabet gestures have been proposed [14], [15], [18], [19], [21], [47]. These are image-based systems that do not rely on the use of sensors or colored gloves. In the following, we describe these approaches.

A. Neuro-Fuzzy based Approach

The authors in [14] proposed an image-based recognition system for ArSL gestures. The system includes 6 phases. After the acquisition, images are filtered using 3×3 median filter to remove the noise and enhance the image quality. Next, the resulting images are segmented into two regions. One region is the gesture, and the other is the background. Segmentation is performed using iterative thresholding algorithm [48]. Then, the hand's direction and the center area are calculated. Border tracing algorithm was applied in order to detect the borders of the hand. Next, borders were smoothed by Gaussian filter [8] [9], to obtain continuous edges. Based on this information, a visual descriptor vector is extracted. It is scale, translation, and rotation invariant. The length of the vector is set to 30. Each entry is the distance between the center area and a point from the hand border. Not all border points are considered. In fact, 30 equidistant points lying from 90° before the orientation axis to 113° after it are selected.

To assure that the chosen visual descriptor is scale-invariant, normalization was applied by dividing each entry by the maximum vector length and then multiplying them by 100 to make the range from 0 to 100. The Adaptive Neuro-Fuzzy inference systems (ANFIS) which is a kind of artificial neural network [49] was used to recognize the different hand gestures. A fuzzy model is built for each of the 30 gestures. The process of fuzzy model identification is done using subtractive clustering algorithm [50] for determining the number of fuzzy rules, and the membership functions. Also, the least square estimate (LSE) method [49] is used for estimating the parameters. Moreover, the hybrid learning algorithm [51] which combines both Gradient descent [49] and LSE [49] was used in training the fuzzy model.

The dataset is acquired using a Computer-connected camera. It includes grayscale images of the 30 ArSL alphabet. The images were taken from 60 different people with different image sizes and orientations. Around 66% of the samples were used for the training set while the rest were used for the testing set. The experimental results were directly affected by the parameter of the cluster radius (r_a). Overfitting occurred when r_a values were small. On the other hand, when r_a values were huge, the training and testing results are not satisfactory. The

best results are obtained with $r_a = 0.8$. In this case, the system recognition rate reached 93.55%. However, some letters that are similar in their gestures were misclassified. These are "Ra" and "Zay", "Tah" and "Thah", and "Dal" and "Thal". Besides, "Ha" and "Sad" were misclassified too, although they are not similar visually.

B. Adaptive Network Fuzzy Inference System based Approach

The authors in [21] developed a recognition system for ArSL alphabet gestures. It is an image-based system that does not rely on the use of sensors or colored gloves. After the acquisition, the images are pre-processed using a 3×3 median filter to reduce the noise. Then an iterative thresholding algorithm is applied in order to generate a binary image with black color as a background and white color for the hand region. The visual descriptors are extracted as in [14]. As described in Section III.A, in order to extract these visual descriptors, the hand direction, the coordinates of the hand area's centroid, and gesture boundary contour are computed. Since global boundary visual descriptors may not allow distinguishing alphabet with similar shapes, a hybrid approach based on both boundary and region information is used. The authors in [21] used k-means clustering technique to cluster the image into five regions. Then, the coordinates of hand centroid of each region are computed, and the distance between the global hand centroid and each region centroid is calculated. The length of the resulting visual descriptor vector is 35.

For the recognition stage, the authors build a fuzzy model for each class. Then an equivalent Adaptive Network-Based Fuzzy Inference System (ANFIS) [49] model is constructed and trained using a hybrid learning algorithm [51] which incorporates gradient descent method [49] and least-squares estimate [49] to estimate parameters values. The dataset used to experiment the system was collected using a camera connected to a computer.

A set of 1800 grayscale images for the 30 gestures was captured from different distances from the camera and different orientations. 1200 of the collected images were used as a training set while the other 600 were used as a testing set without cross-validation. The overall recognition rate of the system depends on the number of rules used in the ANFIS model. A 100% recognition rate was achieved when approximately 19 rules are used, and a 97.5% when approximately ten rules used. However, the authors in [21] are not using cross-validation. This may lead to the overfitting problem. In fact, while 100% accuracy is obtained for the data set when using 19 rules, the result can be different when using another dataset with a different number of rules.

C. "ArSLAT: Arabic Sign Language Alphabets Translator"

The authors in [18] introduced an ArSL Alphabet Translator (ArSLAT) system. The proposed image-based system translates automatically hand gestures representing ArSL alphabet to text without using gloves or visual markers. ArSLAT system undergoes five phases, which are the pre-processing phase, followed by the best-frame detection phase, then the category detection phase, where the ArSL letters are categorized into three categories based on wrist direction to reduce processing time and increase accuracy of the system.

These three categories are wrist appearance from bottom-right, from bottom-left or the down-half. After the category detection phase comes the visual descriptor extraction phase and finally the classification phase.

In the visual descriptor extraction phase, the authors proposed to use visual descriptor vectors that are invariant with translation, scale, and rotation. Similarly as in [14] and in [21], in order to extract the visual descriptor vector. First, edge-detection is performed on all the images in the dataset. Then an orientation point is specified depending on the wrist's location. The visual descriptor vector is computed in such a way that each visual descriptor vector entry represents the distance between the orientation point and a point from the detected edge of the hand. Finally, the visual descriptor vectors are made scaling-invariant by dividing each visual descriptor element of the visual descriptor vector by the maximum value in that vector.

To recognize the alphabet, the system used two different classifiers, which are the minimum distance classifier and multilayer perceptron classifier. The minimum distance classifier (MDC) [52] classifies the visual descriptor vector of an unknown gesture image as the same class of the visual descriptor vector most similar to it from the training set. This similarity is computed based on the Euclidean distance between the two visual descriptor vectors. On the other hand, multilayer perceptron (MLP) classifier [53] is a Neural Network classifier. It learns and produces a model that determines the class of an unknown visual descriptor vector. It consists of a single input layer, a hidden layer, and a single output layer. The input layer is the input data, the hidden layer controls the classifier function, and the output layer returns the output. A dataset of 30 ArSL alphabets is collected. However, the authors limited the dataset to only 15 alphabets. As a result of experimenting only a subset of 15 letters, the accuracy of the system using MDC was 91.3%, while the accuracy of the system when using MLP classifier was 83.7%.

D. Fourier-based Approach

The authors in [19] proposed an image-based system that recognizes ArSL alphabet. The proposed method doesn't require the signers to wear gloves or any other marker devices to ease the hand segmentation. The system performs image preprocessing which consists in size normalization and skin detection. The size of the images is normalized to 150×150 . Then, to detect the skin, images are converted from RGB to HSV, and the pixels values within a specific range are considered as skin.

After skin segmentation, the Fourier transform [54] is applied to the hand region. Then, based on the frequency information provided by the Fourier transformation, the Fourier descriptor (FD) [55] is extracted. The classifier that has been used in [19] is k-Nearest Neighbors algorithm (KNN) [52]. A total number of 180 images have been collected from 30 persons. Only six letters are considered. These are "Sad", "Zay", "Kaf", "Ba", "Lam", "Ya". In order to train the model, the authors in [19], used all the 180 images. As a result, the proposed system achieved a recognition accuracy of 90.55%. However, the number of letters is very limited. Also, since all the data is used for training, this will

yield an over fitting problem. Another limitation of this approach is the range of the colors that have been used in skin detection. In fact, this range which is not specified in the paper [19], is not straightforward to set. In fact, skin color differs from one person to another and from one region to another. The choice of the range of skin color can yield another over fitting problem. Moreover, the parameter k of the KNN classifier [52] have not been specified.

E. Scale-Invariant Visual Descriptors Transform based Approach

The authors in [34] propose an ArSL recognition system. The stages of the proposed recognition system are visual descriptor extraction using SIFT technique [56], visual descriptor vector's dimension reduction using LDA [57], and finally classification. The system uses the Scale-Invariant Features Transform (SIFT) [56] as visual descriptors. The SIFT algorithm [56] is used for visual descriptors extraction for its robustness against rotation, scaling, shifting, and transformation of the image. The SIFT algorithm [56] takes an input image and transforms it into a collection of local visual descriptor vectors. It extracts the most informative points of a given image, called key points. Since, visual descriptor vectors produced by SIFT [56] have high dimensions, Linear Discriminant Analysis (LDA) [57] is used to reduce their dimensions. Three classifiers are used in [34]. They are Support Vector Machine (SVM) [58], k-Nearest Neighbor (k-NN) [52], and minimum distance classifier [52].

The dataset used in the experiments is collected in Suez Canal University [34]. It is an ArSL database which includes 210 gray level ArSL images. Each image is centered and cropped to the size of 200×200 . Thirty Arabic characters (seven images for each character) are represented in the database. The results of this experiment show that applying SVM classifier [58] achieved a better accuracy than the minimum distance [52] and k-NN classifiers [52]. The system has achieved an accuracy around 98.9%. We should mention here that the SIFT parameters have been investigated empirically. Moreover, different portions of training and testing samples have been tried in order to determine the optimal portion. These two facts may lead to an over-fitting problem. Besides, the system needs to be tested on a large dataset to check its scalability.

F. Pulse-Coupled Neural Network based Approach

The authors in [47] introduced a new approach for image signature using a Pulse-Coupled Neural Network (PCNN) [59], [60] for ArSL alphabet recognition.

The recognition system used in [47] includes four main steps. First, the gesture image is put through first layer PCNN [59], [60], where image smoothing is applied to reduce noise. Second, the smoothed image is put through second layer PCNN for a certain number of times to output the image signature, also known as the global activity, which represents the time series that differentiates between the contents of the image. Third, visual descriptor extraction and selection is performed on the image signature using Discrete Fourier Transform (DFT). DFT maximum coefficients represent the visual descriptor vector since they represent the most informative signal. Finally, the visual descriptor vectors are

classified using Multi-Layer Perceptron (MLP) network [53]. The pulse-coupled neural network (PCNN) [59], [60] is a single layer network of neurons, where each neuron is associated with a pixel in the input image [17]. The dataset includes images of 28 ArSL gestures. Eight images are collected for each gesture. The system reaches a recognition rate of 90% when the size of the visual descriptor is equal to 3. However, this system considered only 28 of the 30 letters within a really small dataset. Therefore, this approach needs to be tested over a large data to check scalability and over-fitting.

In summary, different visual descriptors had been used in literature for Sign language recognition. The approaches in [14], [21] and [18] used application-dedicated visual descriptors. In fact, visual descriptor is based on the hand orientation, the hand center, and edges have been designed. Other approaches like in [19], [34], and [47] used general visual descriptors like Fourier descriptor [19], [47] and SIFT descriptor [34]. We also noticed that these approaches need pre-processing steps such as image segmentation and edge detection. We should also mention that some approaches like in [19], [47], [18], and [14] used a subset of the ArSL alphabet. Others, like in [34], [21] used a small data. This is due to the difficulty to recognize and segregate ArSL alphabet. In fact, ArSL has the characteristic of having several gestures that are very similar to each other like "Dal" and "Thal", "Ra", and "Zay", etc. In the literature, no study investigated or compared visual descriptors for ArSL recognition. In this project, we aim to empirically investigate existing visual descriptors in order to determine an appropriate one that will allow us to build an effective ArSL recognition system.

IV. IMAGE BASED ARABIC SIGN LANGUAGE RECOGNIZER

Visual descriptors play a significant role in any image-based recognition system and drastically affect its performance. They are intended to encode the image's visual characteristics into one or more numerical vectors in order to convey the image semantic contents to the machine learning component. Nevertheless, determining the most appropriate descriptor for a recognition system remains an open research challenge.

As reported in Section II, some ArSL alphabet gestures exhibit high similarity. For instance, as shown in Fig. 7, the gestures corresponding to the pairs "Tah" and "Thah", and "Dal" and "Thal" look almost the same. This makes determining the visual descriptor that is able to discriminate between similar gestures even more challenging. The aim of this project is to find a visual descriptor that allows differentiating between different ArSL gestures.

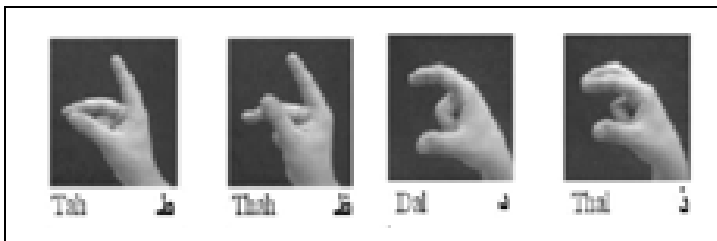


Fig. 7. Similar alphabet gesture example.

Various visual descriptors were proposed in the literature [61]-[63]. Namely, color, shape, and edge-based descriptors have been introduced. The color descriptors fail to extract relevant information for gesture recognition. In fact, the color of the hand, along with the background color, is irrelevant to the gesture characteristics. Moreover, the visual descriptors should not be sensitive to the color of the skin. Also, shape descriptors require prior processing before the extraction phase. Usually, the image needs to be segmented first in order to separate the region including the hand from the surrounding background. Moreover, for pairs of letters such as "Tah" and "Thah", and "Dal" and "Thal" shown in Fig. 7, the shape descriptor is not able to segregate between "Tah" and "Thah", or "Dal" and "Thal". This is because it does not yield information on the spatial position of the fingers. Thus, we do not intend to consider shape descriptors for our system.

On the other hand, texture descriptors [64] provide information on region homogeneity and the edges present in the image. In this paper, we investigate texture descriptors because they can capture ArSL gestures. More specifically, we intend to compare empirically five texture descriptors for the purpose of ArSL alphabet recognition. Namely, they are Histograms of Oriented Gradients (HOG) [66], Edge Histogram Descriptor (EHD) [65], Gray-Level Co-occurrence Matrix (GLCM) [61], Discrete Wavelet Texture Descriptor (DWT) [62], and Local Binary Pattern (LBP) [63].

The methodology of the proposed approach starts with extracting the visual descriptor i from the training images. Then, for each gesture, we build a model using one versus all SVM classifier [67]. In our case, we consider one class per ArSL alphabet gesture. This yields 30 classes. A model is learned for each gesture by training the classifier using one particular class against all the others.

The same i th descriptor is then extracted from the testing set of images. Using the 30 models built during the training phase, the testing alphabet is recognized. Finally, the performance of the recognition using the visual descriptor i is assessed using precision, recall, and accuracy.

This process is repeated for the five considered visual descriptors. Then, the results are compared to determine the most appropriate visual descriptor for ArSL alphabet recognition.

V. EXPERIMENT



Fig. 8. A sample of ArSL alphabet.

The experiment was conducted using MATLAB. We captured the real images collection using different Smartphones and collected them with the help of 30 volunteers. Each volunteer gestured the 30 ArSL alphabets. Each alphabet is represented using a subset of 30 images from the original 900 photos. Fig. 8 shows a sample of ArSL images representing alphabet gestures. As it can be seen, all images have a uniform colored background. We proceeded with this choice in order to bypass the skin detection step, where we have to extract the hand region from the background before starting the gesture recognition phase.

First, we transform the 900 color images into gray level images. Then, we extract the five visual descriptors from the obtained images. These visual descriptors are used sequentially to represent the images and fed into the classifier individually. The recognition process will be conducted once for each visual descriptor. In order to avoid over-fitting, we set K to 10 for the K-fold cross validation training. We validate the discrimination power of each visual descriptor using the ground truth labels and the predicted categories obtained by the cross-validation.

When the HOG descriptor is provided as the input to the soft-margin SVM [44], the proposed ArSL system accuracy is 63.56 %. In order to further investigate this result, we display in Fig. 9 the per class performance. We notice that the performance varies from one letter to another. As can be seen, the letters Shien "ش" and Kha "خ" have an accuracy of 100%. However, Tha "ث" has an accuracy of 23.33 %. On the other hand, when using EHD descriptor [65], the proposed ArSL system accuracy is 42%. We display in Fig. 10 the per class performance. Similarly, we notice that the performance varies from one letter to another. As it can be seen, the letter Kha "خ" has an accuracy of 80%. However, Th "ث" has an accuracy of 6.67 %. Fig. 11 displays the per class performance when using LBP descriptor [63]. The proposed ArSL system accuracy is 9.78%. As can be seen, the letter Alef "ا" has an accuracy of 63.33%. However, many letters like Th "ث" and Ayn "ع" have an accuracy of 0 %. On the other hand, the proposed ArSL system accuracy is 8% when using DWT descriptor [62] as input to the one versus-all SVM [44]. In Fig. 12, we display the per class performance. As can be seen, the letter Dal "د" has an accuracy of 46.67%. However, many letters like Th "ث", Miem "م", and Ayn "ع" have an accuracy of 0 %.

worst accuracy result is obtained when using GLCM descriptor [61]. In fact, the proposed ArSL system accuracy is 2.89%. Fig. 13 displays the per class performance. We notice that the letter He "ه" has an accuracy of 26.67%. However, many letters like Ta "ت", Miem "م", and Ayn "ع" have an accuracy of 0%.

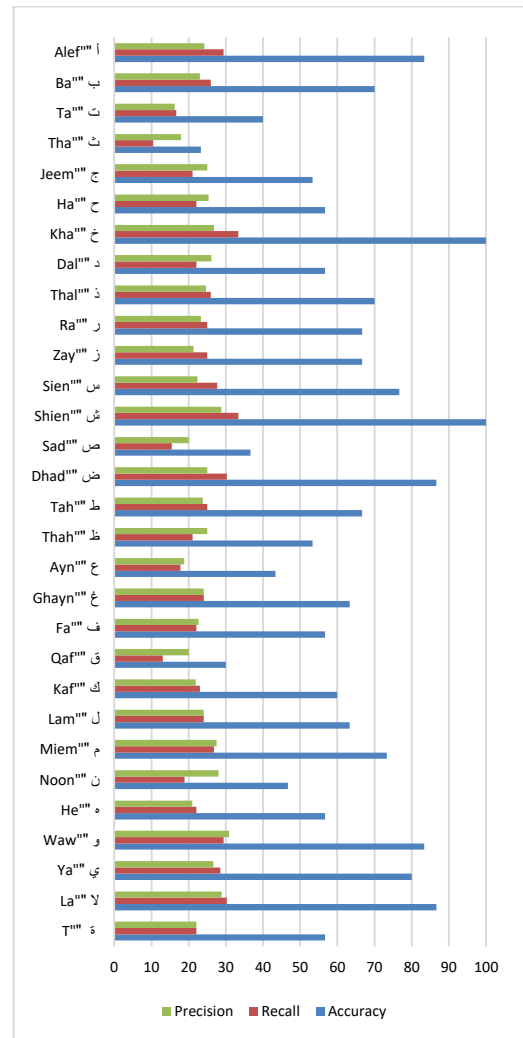


Fig. 9. The proposed ArSL system per class performance when using HOG descriptor.

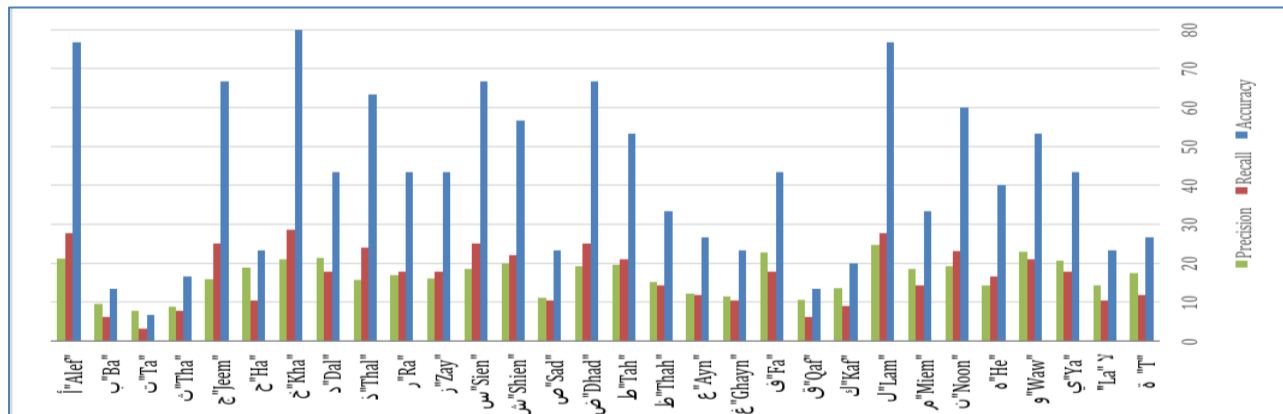


Fig. 10. The proposed ArSL system per class performance when using EHD descriptor.

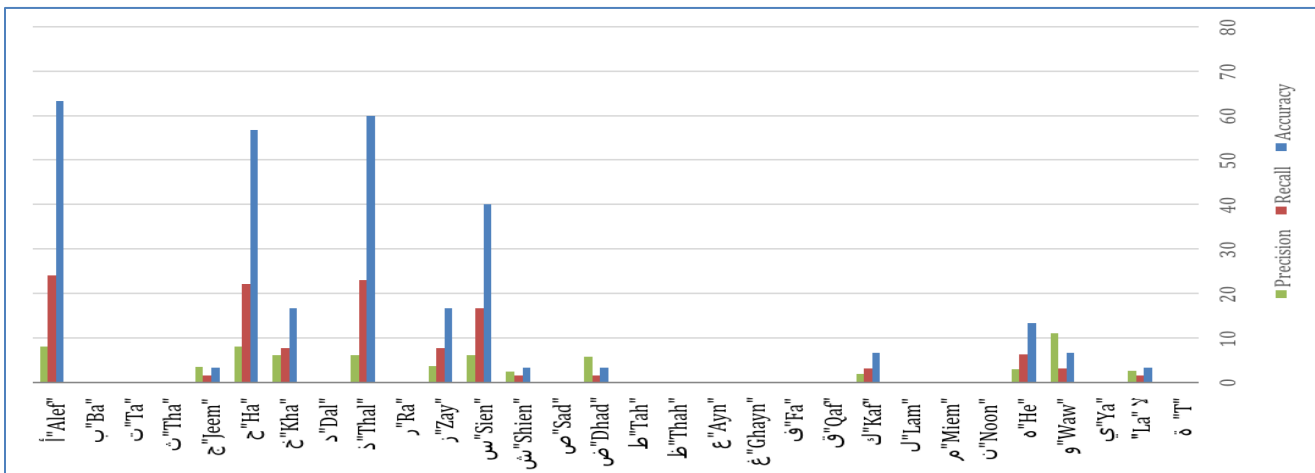


Fig. 11. The proposed ArSL system per class performance when using LBP descriptor.

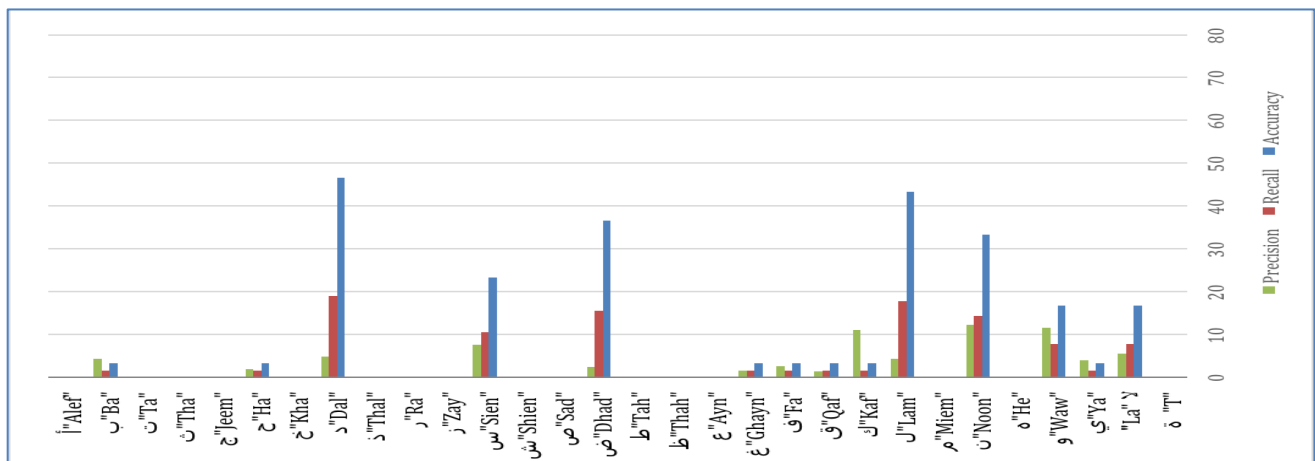


Fig. 12. The proposed ArSL system per class performance when using DWT descriptor.

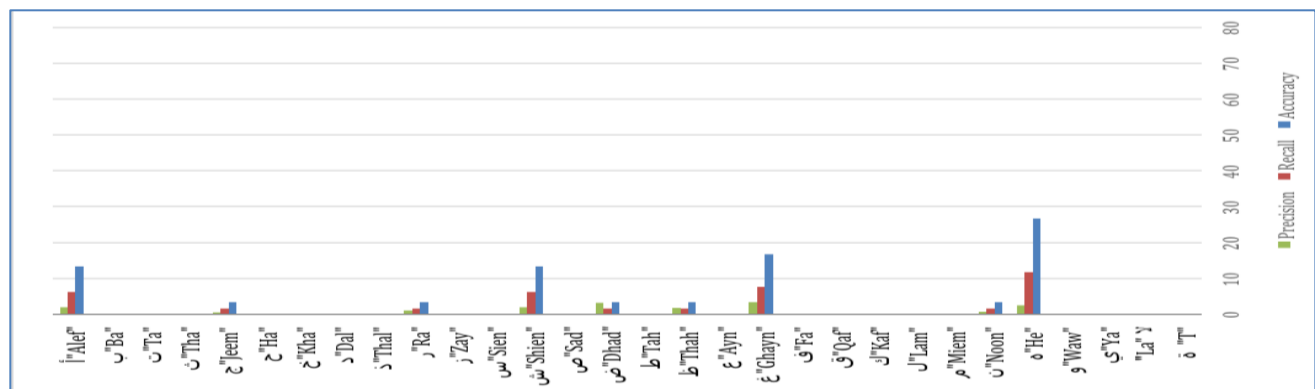


Fig. 13. The proposed ArSL system per class performance when using GLCM descriptor.

The results show that the HOG descriptor [66] achieved the highest performance followed by the EHD descriptor [65]. In fact, based on the achieved accuracy per letter (refer to Fig. 9 to 13), the HOG descriptor gives the highest accuracy for 27 letters. The three remaining letters which are "Noon", "Lam", and "Jeem" are best recognized when using EHD descriptor.

VI. CONCLUSION AND FUTURE WORKS

A Sign language recognition system allows hearing and speech impaired people to communicate and facilitates their societal integration. ArSL is the official sign language for the Arab world. Despite its similarity to other international sign languages, ArSL includes alphabet representations that are exclusive to Arabic language. This makes non-ArSL sign

language recognition systems inapplicable to ArSL. ArSL recognition gets even more challenging due to the highly similar gestures representing Arabic letters. State-of-the-art ArSL recognition systems rely either on a sensor-based or an image-based approach to identify ArSL alphabet. However, image-based systems proved to be more effective because of their flexibility, portability, and friendly use. In fact, they can be deployed using smart devices incorporating digital camera(s), and could be used everywhere. After investigating existing visual descriptors for ArSL alphabet recognition systems, we proposed a new ArSL recognition system. The proposed system consists of extracting the HOG descriptor that is conveyed to a one versus all soft-margin SVM [58]. The resultant system succeeds in recognizing 63.5% of Arabic Alphabet gestures.

As future work, we intend to investigate kernel SVM [68] in order to further enhance the performance of the proposed system. In fact, Kernel SVM [68] allows mapping the features to a new space where it exhibits linear patterns. Thus, the ArSL gestures will be linearly separable in the new space. Besides, since some features achieve a better accuracy in recognizing certain letters than others, we intend to assign a relevance feature weight with respect to each gesture.

REFERENCES

- [1] C. Allen, "Global survey report WFD interim regional Secretariat for the Arab region (WFD RSAR) global education Pre-Planning project on the human rights of deaf people," 2008.
- [2] M. F. Tolba and A. S. Elons, "Recent developments in sign language recognition systems," 2013 8th Int. Conf. Comput. Eng. Syst. ICCES, pp. 26–28, Nov. 2013.
- [3] V. I. Pavlovic, R. Sharma, and T. S. Huang, "Visual interpretation of hand gestures for human-computer interaction: A review," *IEEE Trans. Pattern Anal. Mach. Intell.*, vol. 19, no. 7, pp. 677–695, Jul. 1997.
- [4] S. S. Fels and G. E. Hinton, "Glove-talk: A neural network interface between a data-glove and a speech synthesizer," *IEEE Trans. Neural Netw.*, vol. 4, no. 1, pp. 2–8, 1993.
- [5] D. J. Sturman and D. Zeltzer, "A survey of glove-based input," *IEEE Comput. Graph. Appl.*, vol. 14, no. 1, pp. 30–39, Jan. 1994.
- [6] D. L. Quam, "Gesture Recognition with a Dataglove," *Proc. IEEE Natl. Aerosp. Electron. Conf. NAECON 90*, vol. 2, pp. 755–760, May 1990.
- [7] J. Eisenstein, S. Ghandeharizadeh, L. Huang, C. Shahabi, G. Shanbhag, and R. Zimmermann, "Analysis of clustering techniques to detect hand signs," *Proc. 2001 Int. Symp. Intell. Multimed. Video Speech Process. ISIMP 2001 IEEE Cat No01EX489*, pp. 259–262, May 2001.
- [8] H. Brashear, V. Henderson, K. Park, H. Hamilton, S. Lee, and T. Starner, "American Sign Language Recognition in Game Development for Deaf Children," Oct. 2006.
- [9] K. Mahesh, S. Mahishi, S. R. N. S., and V. Pujari, "Finger Detection for Sign Language Recognition," Mar. 2009.
- [10] S.-K. Kang, K.-Y. Chung, K.-W. Rim, and J.-H. Lee, "Development of Real-Time Gesture Recognition System Using Visual Interaction" 2011.
- [11] S. Ding, H. Zhu, W. Jia, and C. Su, "A survey on feature extraction for pattern recognition," *Artif Intell Rev*, vol. 37, pp. 169–180, 2012.
- [12] B. Manjunath, P. Salembier, and T. Sikora, "Introduction to MPEG 7: Multi-media content description language," 2002.
- [13] M. Nixon and A. Aguado, "Feature Extraction and Image Processing for Computer Vision," 2012.
- [14] O. Al-Jarrah and A. Halawani, "Recognition of gestures in arabic sign language using neuro-fuzzy systems," *Artif. Intell.*, vol. 133, no. 1–2, pp. 117–138, Dec. 2001.
- [15] K. Assaleh and M. Al-Rousan, "Recognition of Arabic sign language alphabet using polynomial classifiers," vol. 2005, pp. 2136–2145, 2005.
- [16] "Error detection and correction approach for arabic sign language recognition," 2012 Seventh Int. Conf. Comput. Eng. Syst. ICCES, pp. 117–123, Nov. 2012.
- [17] M. F. Tolba, A. Samir, and M. Aboul-Ela, "Arabic sign language continuous sentences recognition using PCNN and graph matching," *Neural Comput. Appl.*, vol. 23, no. 3–4, pp. 999–1010, Aug. 2012.
- [18] N. El-Bendary, H. M. Zawbaa, M. S. Daoud, A. E. Hassanien, and K. Nakamatsu, "ArSLAT: Arabic sign language Alphabets translator," 2010 Int. Conf. Comput. Inf. Syst. Ind. Manag. Appl. CISIM, 2010.
- [19] N. R. Albelwi and Y. M. Alginahi, "Real-time arabic sign language (arsl) recognition," 2012, pp. 497–501.
- [20] M. F. Tolba, A. Samir, and M. Abul-Ela, "A proposed graph matching technique for Arabic sign language continuous sentences recognition," 8th IEEE Int. Conf. Inform. Syst. INFOS, pp. 14–20, 2012.
- [21] O. Al-Jarrah and F. A. Al-Omari, "IMPROVING GESTURE RECOGNITION IN THE ARABIC SIGN LANGUAGE USING TEXTURE ANALYSIS," *Appl. Artif. Intell.*, vol. 21, no. 1, pp. 11–33, Jan. 2007.
- [22] A. A.A. A. Elsayed, and H. Hamdy, "Arabic sign language (ArSL) recognition system using HMM," *Int. J. Adv. Comput. Sci. Appl.*, vol. 2, no. 11, 2011.
- [23] M. Mohandes, M. Deriche, and J. Liu, "Image-based and sensor-based approaches to Arabic sign language recognition," vol. 44, no. 4, pp. 551–557, 2014.
- [24] "Sign language - definition," *Oxford Dictionaries*. [Online]. Available: en.oxforddictionaries.com/definition/sign_language. [Accessed: 04-Oct-2016].
- [25] J. D. Schein and D. A. Stewart, *Language in motion: Exploring the nature of sign*. Gallaudet University Press, 1995.
- [26] N. Cleaver, "WASLI country reports issue 1-November 2005," presented at the WASLI 2007, Spain, 2007, p. 2.
- [27] M. A. Abdel-Fattah, "Arabic sign language: A perspective," *J. Deaf Stud. Deaf Educ.*, vol. 10, no. 2, pp. 212–221, 2005.
- [28] Cambridge University, *Sign Languages*. Cambridge University Press, 2010.
- [29] A. Agarwal and M. K. Thakur, "Sign language recognition using Microsoft Kinect," presented at the 2013 Sixth International Conference on Contemporary Computing (IC3), 2013.
- [30] A. K. Sahoo, S. Gouri, K. Mishra, and R. Kumar, "SIGN LANGUAGE RECOGNITION: STATE OF THE ART," vol. 9, no. 2, 2014.
- [31] T. Starner, J. Weaver, and A. Pentland, "Real-time American sign language recognition using desk and wearable computer based video" *IEEE Trans. Pattern Anal. Mach. Intell.*, vol. 20, no. 12, pp. 1371–1375, 1998.
- [32] B. Bauer and H. Hienz, "Relevant Features for Video-Based Continuous Sign Language Recognition," presented at the Proceedings of the Fourth IEEE International Conference on Automatic Face and Gesture Recognition, 2000, pp. 64–75.
- [33] N. Tubaiz, T. Shanableh, and K. Assaleh, "Glove-based continuous arabic sign language recognition in user-dependent mode," *IEEE Trans. Hum.-Mach. Syst.*, vol. 45, no. 4, pp. 526–533, Aug. 2015.
- [34] A. Tharwat, T. Gaber, A. E. Hassenian, M. K. Shahin, and B. Refaat, "SIFT-Based Arabic Sign Language Recognition System," vol. 334, Nov. 2014.
- [35] J. Han, L. Shao, D. Xu, and J. Shotton, "Enhanced computer vision with Microsoft Kinect sensor: A review," *IEEE Trans. Cybern.*, vol. 43, no. 5, pp. 1318–1334, Oct. 2013.
- [36] M. AL-Rousan, K. Assaleh, and A. Tala'a, "Video-based signer-independent arabic sign language recognition using hidden Markov models," *Appl. Soft Comput.*, vol. 9, no. 3, pp. 990–999, Jun. 2009.
- [37] T. Shanableh, K. Assaleh, and M. Al-Rousan, "Spatio-Temporal feature-extraction techniques for isolated gesture recognition in arabic sign language," *IEEE Trans. Syst. Man Cybern. Part B Cybern.*, vol. 37, no. 3, pp. 641–650, Jun. 2007.
- [38] S. Kausar and Y. Javed, "A Survey on Sign Language Recognition," 2011.

- [39] P. Dymarski, "Hidden Markov models, theory and applications," 19-Apr-2011. [Online]. Available: <http://www.intechopen.com/books/hidden-markov-models-theory-and-applications>. [Accessed: 18-Nov-2016].
- [40] T. Nobuhiko, S. Nobutaka, and S. Yoshiaki, "Extraction of Hand Features for Recognition of Sign Language Words."
- [41] H. C. M. Herath, W. A. L. V. Kumari, W. A. P. . Senevirathne, and M. . Dissanayake, "IMAGE BASED SIGN LANGUAGE RECOGNITION SYSTEM FOR SINHALA SIGN LANGUAGE," SAITM Res. Symp. Eng. Adv., pp. 107–110, 2013.
- [42] J. Zieren and K.-F. Kraiss, "NON-INTRUSIVE SIGN LANGUAGE RECOGNITION FOR HUMAN-COMPUTER INTERACTION," 2000.
- [43] Q. Yang, "Chinese sign language recognition based on video sequence appearance modeling," 2010, pp. 1537–1542.
- [44] C. Cortes and V. Vapnik, "Support-vector networks," vol. 20, no. 3, pp. 273–297, 1995.
- [45] S. Liwicki and M. Everingham, "Automatic recognition of fingerspelled words in British sign language," 2009, pp. 50–57.
- [46] N. V. Tavari and A. Deorankar, "Indian Sign Language Recognition based on Histograms of Oriented Gradient," vol. 5, 2014.
- [47] M. Fahmy Tolba, M. Saied Abdel-Wahab, M. Aboul-Ela, and A. Samir, "Image signature improving by PCNN for arabic sign language recognition," vol. Volume 1, no. 1, pp. 1–6, Jan. 2010.
- [48] R. C. Jain, R. Kasturi, and B. G. Schunck, Machine vision. New York: McGraw Hill Higher Education, 1995.
- [49] J.-S. R. Jang, "ANFIS: Adaptive-network-based fuzzy inference system," IEEE Trans. Syst. Man Cybern., vol. 23, no. 3, pp. 665–685, 1993.
- [50] A. Priyono, M. Ridwan, A. J. Alias, R. A. O. K. Rahmat, A. Hassan, and M. A. Mohd. Ali, "Generation of fuzzy rules with Subtractive clustering," J. Teknol., vol. 43, no. 1, 2005.
- [51] D. . Loganathan and K. . Girija, "Hybrid Learning For Adaptive Neuro Fuzzy Inference System," Res. Inven. Int. J. Eng. Sci., vol. 2, no. 11, 2013.
- [52] B. Thuraisingham, M. Awad, L. Wang, M. Awad, and L. Khan, Design and implementation of data mining tools. Boca Raton, FL: Auerbach Publishers, 2009.
- [53] M. Kantardzic, Data mining: Concepts, Models, Methods, and Algorithms, 2nd ed. Oxford: Wiley-Blackwell (an imprint of John Wiley & Sons Ltd), 2011.
- [54] S. Bochner and K. Chandrasekharan, Fourier Transforms.(AM-19), vol. 19. Princeton University Press, 2016.
- [55] R. L. Cosgriff, Identification of shape. 1960.
- [56] D. G. Lowe, "Distinctive image features from scale-invariant Keypoints," Int. J. Comput. Vis., vol. 60, no. 2, pp. 91–110, Jan. 2004.
- [57] J. Lepš, P. Šmilauer, J. Leps, and P. Smilauer, Multivariate analysis of ecological data using CANOCO. Cambridge: Cambridge University Press, 2003.
- [58] S. Abe and A. Shigeo, Support vector machines for pattern classification, 2nd ed. London: Springer-Verlag New York, 2010.
- [59] R. Eckhorn, H. J. Reitboeck, M. Arndt, and P. Dicke, "Feature linking via Synchronization among distributed assemblies: Simulations of results from cat visual cortex," Neural Comput., vol. 2, no. 3, pp. 293–307, Sep. 1990.
- [60] R. C. Mureşan, "Pattern recognition using pulse-coupled neural networks and discrete Fourier transforms," Neurocomputing, vol. 51, pp. 487–493, Apr. 2003.
- [61] M. Partio, B. Cramariuc, M. Gabbouj, and A. Visa, "ROCK TEXTURE RETRIEVAL USING GRAY LEVEL CO-OCCURRENCE MATRIX," Proceeding 5th Nord. Signal Process. Symp., 2002.
- [62] D. F. Long, D. H. Zhang, and P. D. Dagan Feng, "Fundamentals of Content-Based Image Retrieval," in Multimedia Information Retrieval and Management, D. Dagan Feng, W.-C. Siu, and H.-J. Zhang, Eds. pp. 1–26.
- [63] M. Pietikäinen, A. Hadid, G. Zhao, and T. Ahonen, "Local Binary Patterns for Still Images," in Computer Vision Using Local Binary Patterns, pp. 13–47.
- [64] T. Sikora, "The MPEG-7 Visual Standard for Content Description--An overview," IEEE Trans. CIRCUIITS Syst. VIDEO Technol., vol. 11, no. 6, pp. 696–702, Jun. 2001.
- [65] Y. M. R. Ro, M. K. Kim, H. K. K. Kang, B. S. M. Manjunath, and J. K. Kim, "MPEG-7 homogeneous texture Descriptor," ETRI J., vol. 23, no. 2, pp. 41–51, Jun. 2001.
- [66] F. Suard, A. Rakotomamonjy, A. Bensrhair, and A. Broggi, "Pedestrian Detection using Infrared images and Histograms of Oriented Gradients," presented at the Intelligent Vehicles Symposium, 2006.
- [67] A. Statnikov, C. F. Aliferis, D. P. Hardin, and er Statnikov, A gentle introduction to support vector machines in Biomedicine: Volume 1: Theory and methods. Singapore, Singapore: World Scientific Publishing Co Pte, 2011.
- [68] B. Schölkopf, C. J. C. Burges, and A. J. Smola, Advances in Kernel Methods: Support Vector Learning. Cambridge, MA: MIT Press, 1999.

The Adoption of Software Process Improvement in Saudi Arabian Small and Medium Size Software Organizations: An Exploratory Study

Mohammed Ateeq Alanezi
College of Computing and IT
Shaqra University, Kingdom of Saudi Arabia

Abstract—Quite a lot of attention has been paid in the literature on “how to adopt” software process improvement (SPI) in Small and Medium Size (SME) software organization in several countries. This has resulted in limited improvements to the software industry and impacted the Saudi’s economy. However, the SPI adoption is one of the major issues in the domain of small and medium size software organization, especially in developing countries. The objective of this study is to investigate the current state of SPI adoption in Saudi Arabia in comparison to those of the standard models used internationally which could help in improving the software quality and have an impact on Saudi Arabian economy. After examining a number of studies in the literature, we have designed a questionnaire to survey SME software organizations in Saudi Arabia. First, we conducted a pilot study with 24 senior managers to access the intended survey and further improve the process. Then, we sent out 480 questionnaires to the participants and received 291 responses. The most interesting part of this result is that the respondents highlighted the benefits of using SPI standard; whereby, when asked about the reason for not using SPI, 64% of the respondents agree that the usage of SPI standard is time consuming and 55% agree that there is a difficulty in understanding the SPI standard.

Keywords—Software process improvement; software organization; software adoption; small and medium enterprises (SME)

I. INTRODUCTION

Saudi Arabia is developing rapidly in the field of information technology. The number of software organizations in Saudi Arabia is growing daily. Within these organizations, many activities, tasks, scheduling and resources need to be managed and monitored properly by the respective development team. However, according to [1], in the past 5 years, clients have faced difficulties in getting high quality products which are reliable and cheap. This is somewhat considered reasonable since the software industry is relatively young in Saudi Arabia. Accordingly, the challenge for Saudi Arabia software organizations is to find a path to apply Software Process Improvement (SPI) techniques to achieve high quality process. The motivation behind SPI, usually, come as a result of business needs such as strong competition, reduced schedule cycle times, increased product quality and hence more productivity and profit [1], [2]. Several SPI standards and models have been proposed to control software development processes, such as the Capability Maturity Model

Integration (CMMI) [3], International Organization for Standardization ISO 9000 [4], the Software Process Improvement and Capability determination (SPICE) [5], [6], Bootstrap [7], [8], Six Sigma [9]-[11]. However, despite the importance of SPI, it is not clear how these practices are implemented and whether the required skills and knowledge are owned by practitioners. In addition, many studies have proved that all of these models are very difficult to apply in small and medium size software organizations [12]-[16]. Nevertheless, most of the software organizations in the world are considered as small-to-medium size; for example, small-to-medium size organizations represent 97.3 of the total business established in Malaysia [17], whereas they represents 92% in Mexico [18] and more than 85% in India, Canada, China, US, Ireland and Finland [19]. A number of studies have investigated the adoption of SPI models in several countries, for example, in India [19], Malaysia [17], [20]-[23], US and Japan [24], New Zealand [25], Finland [26], Pakistan [27], Australia [23], [24] Ireland [30] and Mexico [18]. However, to the best of our knowledge, no prior work exists which aims at specifically investigating the adoption of SPI in Saudi Arabia. Hence, it is significant to investigate the current state of the SPI adoption to help improve the software industry and its impact on the Saudi Arabian economy. We are not going to measure the extent to which the improved processes have been fully adopted, or if the processes have really changed the hearts and the minds of the practitioners. However, this research attempts to explore, analyze, and evaluate the adoption of SPI in Saudi Arabian software organizations, and then understand the current perspective of software process in comparison to those of the standard models used internationally. More specifically, we aim to answer the following questions:

- What is the state of SPI adoption in Saudi Arabia?
- What are the factors that influence the usage of SPI Standard and the reasons behind not using the SPI standards? SPI is significant because in primary it means a new and enhanced software development process is created.
- Have the employees had a clear explicit understating of the SPI theory? This is because it is difficult to apply the SPI model without fully understanding the model theory behind it.

- To what extent can the process activity be supported by Computer Aided Software Engineering tool.

This paper is organized as follows: Section II discusses related works, Section III describes the methodology used in the study, Section IV presents the results of the study as well as our interpretation of these findings, Section V presents discussion of the results and finally, the paper is concluded in Section VI.

II. RELATED WORK

Several published researches were conducted to investigate the adoption of SPI in different parts of the world. A survey of six small-to-medium size software organizations investigated the adoption of SPI in Malaysia [16]. The results of the study showed that the level of adoption of SPI in Malaysia is still very much at the low level. Nizam et al. [31] also surveyed 39 organizations which operate in Malaysia to analyze factors that negatively influence the adoption of SPI. They concluded that the adoption of SPI is still at its early stage in small and medium size organizations. This shows that Malaysian software organizations are mostly not aware of the importance of SPI and its impact on product quality. Another survey on SPI implementation with 50 small-to-medium Indian companies is conducted in [19]. The findings showed that developers were responding relatively positively to SPI. Similarly, 15 companies showed their eagerness for achieving a CMMI level as the primary goal. In recent study, Mahmood Niazi [28] investigated the risks that can undermine SPI implementation from the perspective of software development practitioners. He interviewed 34 Australian's SPI practitioners, and the results clearly identified the differences and the similarities of the risks by organizational size (i.e. small-medium and large) and practitioner's positions (i.e. developers, managers and senior managers). However, the small sample data and the weak methodology are not sufficient to draw statistically significant conclusions. The reasons why organizations do not adopt CMMI in Australian companies were investigated in [29]. The outcomes showed the most frequent reasons given by organizations were: 1) the organization was small; 2) the adoption was too costly, and 3) the organization had no time. In [16] a survey was conducted over 400 volunteers from 32 countries to question small organizations about their utilization of SPI models. The results showed that many difficulties must be overcome to consider the process effectiveness. As we have seen in the above literature, there were numerous publications which study the adoption and implantation of SPI models in Malaysia, India, Pakistan, Australia, New Zealand, Mexico and United States. Notably, there is still a huge gap of research and published studies on the adoption of SPI in Saudi Arabian.

III. RESEARCH DESIGN AND METHOD

Since this is an exploratory research, the author wanted to get both a broad view of the software organization in Saudi Arabia as a whole, and a more detailed picture of SPI practices. Initially, a detailed literature review on the adoption of SPI model was performed, looking at the implementation of SPI in context of SME organizations, the key success factors and the

difficulties of the adoption of SPI. After that, a questionnaire was created to investigate the adoption of SPI in the country's SMEs. Questionnaire approach have been used in a number of similar studies and are presented as a proven technique of data gathering and analysis [17], [19], [25], [27]. In this section, the details of the survey are given as shown in the following sub-sections:

A. Survey Design

A number of experienced studies were analyzed in order to identify questions that can play a positive role in the adoption of SPI model. The questionnaire consisted of 21 questions that were selected mainly from [17], [19], [20], [31], [32]. A pilot study with 24 senior managers was conducted to validate the questionnaire. After considering their comments, the questionnaire was modified and improved. All questions were close ended in order to get better number of respondents. The questionnaire consists of four major parts to capture the required data as follows:

- The first part is background information of the companies (size, status, market access, and culture).
- The second part aims to get information about the respondents (education, experience, and job nature).
- The third part contains SPI practices and knowledge, and the last part concerns about software development practice and related project issues.

To conduct this survey, Google forms which is a web-survey tool was adopted.

B. Survey Approach

The empirical method used in this study is survey approach. This approach is properly common used method to collect data from targeted respondents who have the required knowledge to address the objective of the study. 480 SMEs organizations were identified to be suitable candidates for the survey through the small and medium enterprises general authority's web site¹. Then, a short letter that explains the research objectives along with the questionnaire was sent to them and 291 responses were received. The response rate was acceptable due to the privacy policies of the organizations. The duration of questionnaire was four weeks along with follow up emails to resolve raised confusions.

C. Analysis

Two basic statistical methods were used to analyze the collected quantitative data; the methods are descriptive statistics and frequent analysis. Additionally, the results were revised by two experts separately to guarantee the accuracy of the outcome.

IV. RESULTS

This section presents the analysis performed on the information gathered from the survey. It shows that a well-designed development process has positive consequences on the productivity and cost. On the negative side, poor software

¹ <https://smea.gov.sa/en>

development has negative impact on the quality and poor customer satisfaction [33].

Respondents were asked about their opinion on the factors which influence their usage of SPI Standard and the reasons for not using the SPI standards. To simplify these two questions, a list of some factors affecting the usage of SPI standard were

selected carefully from the literature [17], [19], [20], [31], [32]. First, an overview of the respondents' impression of the benefits of using the SPI standards is presented and it is shown in Fig. 1. In this 3D graph, the x-axis (horizontal line) present the benefits of using SPI standard, the y-axis (left side of the graph) presents the number of respondents and on the z-axis (right side of the graph), the rating scales are shown.

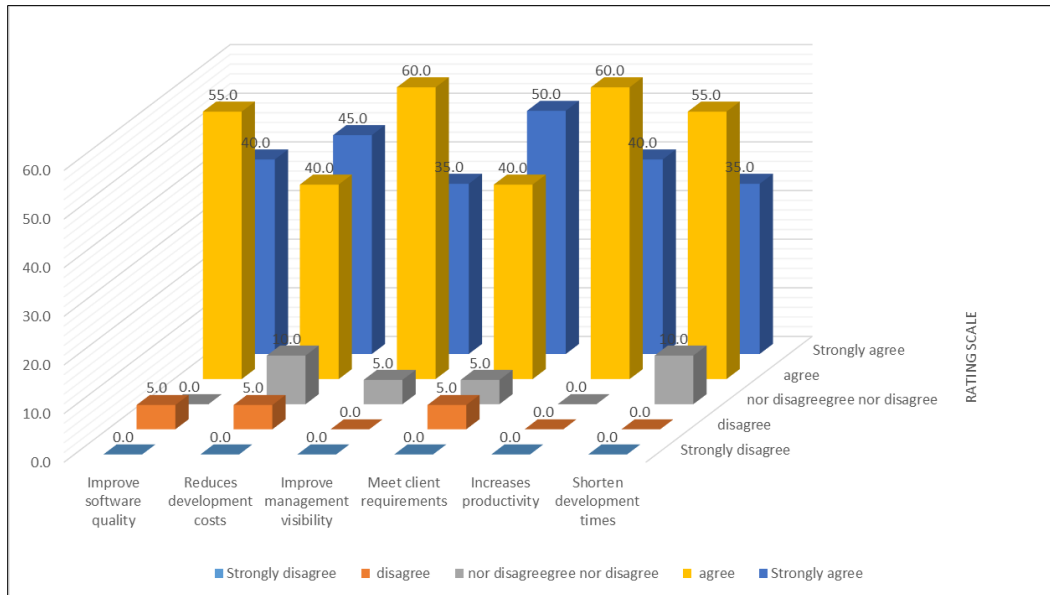


Fig. 1. Rating the benefits of using the SPI.

The results show that 60% of the respondents agree that the usage of SPI standard will increase productivity and improve management visibility; whereas, 55% agree that the SPI standard will shorten development time and improve software quality. Moreover, the respondents strongly agree that the usage of SPI standard has a significant impact on meeting client requirements 50% and reducing development cost 45%. These presented results are consistent with [34], in which they stated that, most software houses are not able to quantify the benefits of implementing SPI standard clearly.

Secondly, the reasons of not using the SPI standards were shown in Fig. 2. In this graph, the rating process shows that most of the respondents strongly agree that inexperienced staff 59.1% and staff turnover 54.4% are also reasons for not using of SPI. The most disappointing aspect about the reasons of not using of SPI standard throughout the ratings scales is that (64%) of the respondents agree that the usage of SPI standard is time consuming, and 55% agree that there is a difficulty in understanding the SPI standard. However, this result occurred because 73% of the respondents are suffering from the lack of resources to adopt the SPI standard.

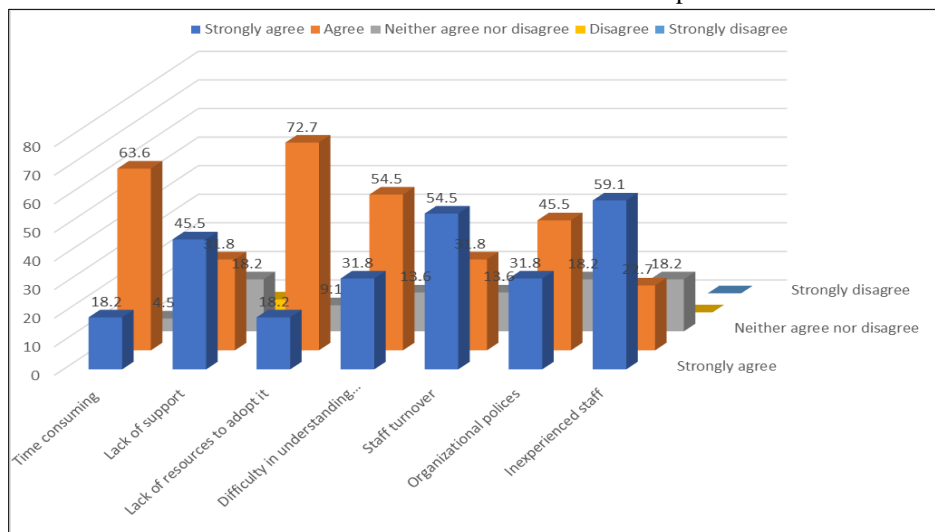


Fig. 2. Rating reasons of not using SPI.

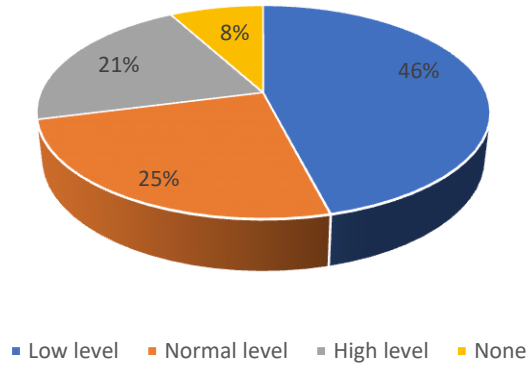


Fig. 3. Knowledge of SPI implementation.

The result of the level of knowledge in SPI practices is depicted in Fig. 3. Despite the importance of the SPI standard, majority of the employees 46% have low knowledge level of SPI practice and a 25% have normal level of practices. It is also shown that 8% of the respondents have zero knowledge while only 21% have high level of knowledge in SPI standard.

On the other hand, Fig. 4 shows the level of employees' experience in small and medium size Saudi Arabian companies. Slightly over two third 69% of the respondents have between 5 to 10-years of experience and only a quarter of them 23% have more than 10 years of experience. However, this was an expected result since the SPI standards were not written for developed organizations with fewer than 25 employees and are consequently difficult to apply in such small settings.

In addition, it is shown in Fig. 5 that 46% of the respondents have used the standard ISO 9000 in software development and a very small percentage only 17% of the respondents used CMMI. Although, the ISO 9001 standard has been implemented by many organizations in 187 countries [35], yet, this standard is criticized in journals, textbooks and at conferences as it is written for industry (i.e large size), and its application to the development in the small size organizations may pose some problem [36]–[38].

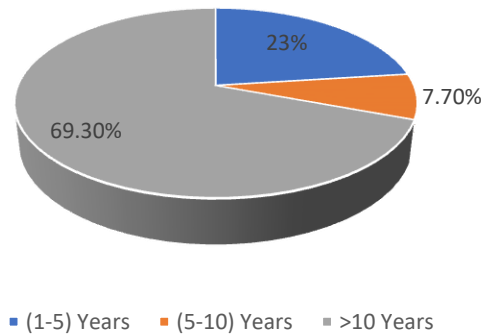


Fig. 4. The level of employee's experiences.

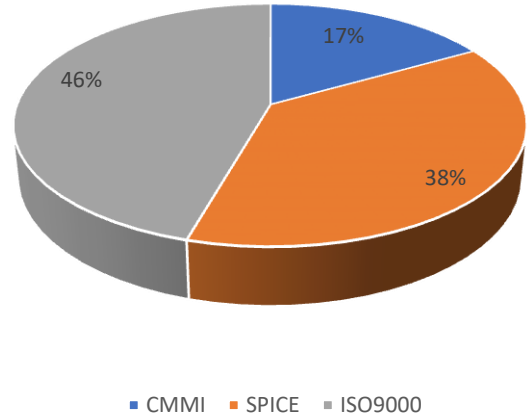


Fig. 5. SPI standard used in Saudi Arabia.

Regarding the duration of SPI adoption in the organization, the result of the survey shows that 62% of the respondents stated that they adopted process improvement program for more than 5 years. Meanwhile, 13% of the respondents are yet to start adopting the SPI standard as shown in Fig. 6.

More often, problems arise in every project. Therefore, the project managers have to strictly comply with software development process and with management tools such as budget management, resource allocation, time control, priority of tasks, testing technology and decision-making tools. Consequently, whether the projects are completed on time and (or) on budget is investigated. The participants were asked if they are receiving technical training courses or not and whether the communication method is formal or informal. As shown in Fig. 7, 62% of the projects are completed on budget while 38% are completed over budget. Comparatively, the results stated that 46% of projects completed on time while 54% are completed over time.

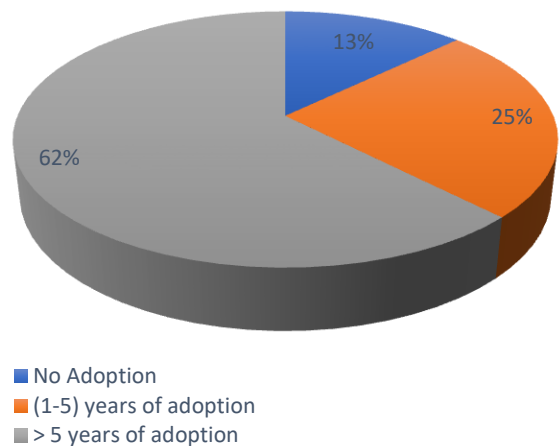


Fig. 6. Duration of SPI standard adoption.

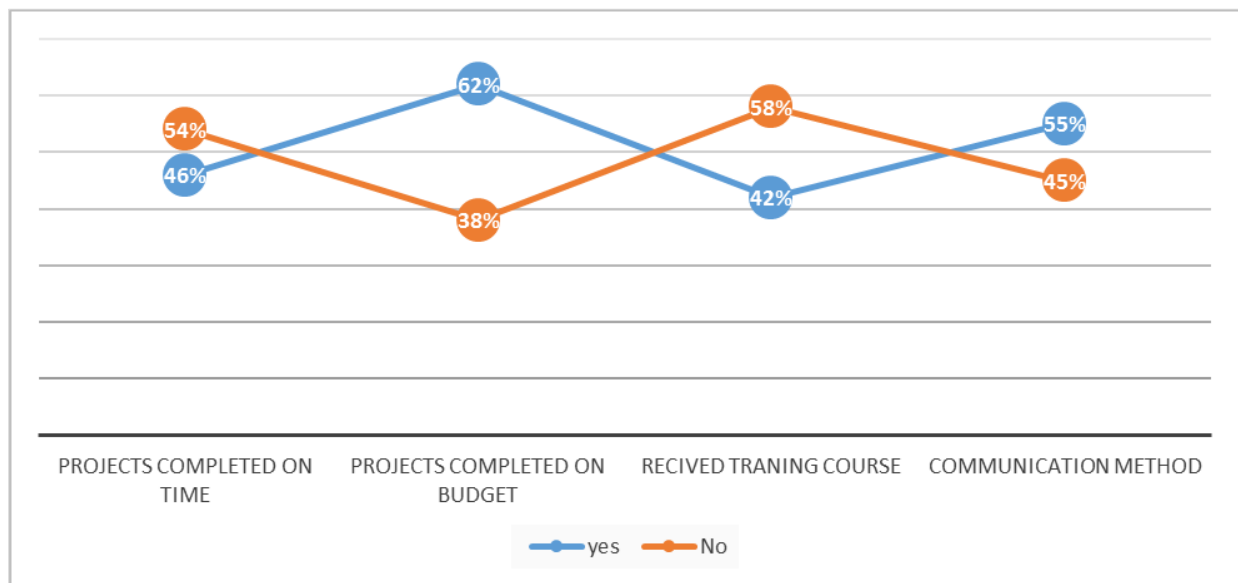


Fig. 7. Project management method.

The training courses provided to employees working in the Saudi SMEs are also surveyed. In this survey, 58% of the respondents stated that they did not receive training courses to improve their development skills while 42% of them indicated that they received course training to improve their managerial and technical skills. Given these point, self-training method represented 46%, while 54% used formal training to improve their knowledge. Moreover, with reference to communication within the organizations, 55% of the respondents stated that they use the formal communication channels of the organization such as official letters and Emails. This means that the flow of information between sender and receiver is controlled. Often, Information is collected and flows up to the top levels of management for review and decision making, while orders flow down from the top to the place where it will be implemented. On the other hand, 45% of the respondents

stated that the communication between employees is informal or through the ad-hoc method; in which the interchange of information does not follow any channels. Often, they use social media tools such WhatsApp, Tweeter and Telegram with any documentary evidence.

The final question outlined project management (Tools and Techniques) adopted to execute and monitor the engineering process to ensure conformance of quality as per organization's standards. Better use of project management tool help planning, organizing, and managing project resources and tasks. After analyzing the results, it was found that the most dominant software tool used by project managers in Saudi Arabia is scheduling tools. The result shows that 37.5% of the respondents use scheduling tools, while 25% use quality management tools, 20.8% use project management tools and 16.7% use CASE tools shown in Fig. 8.

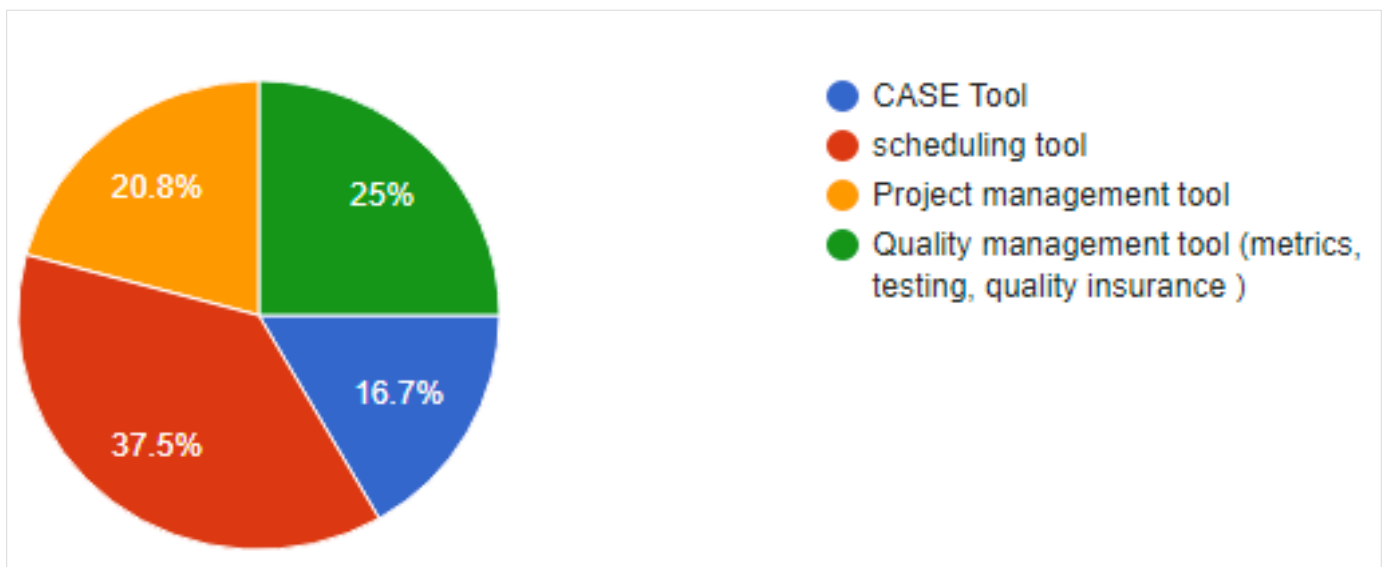


Fig. 8. Project management (tools and techniques).

V. DISCUSSION

The results presented in Fig. 1 are interesting where respondents identified multiple benefits of using of SPI standard such as increased productivity and management visibility as well as shortening development time and improve quality. This was confirmed by [40] who claimed that SPI models and standards can improve the quality of software by reducing cost and increasing productivity. In addition, the respondents highlighted the significant impact of SPI on meeting clients' requirements and reducing development cost. This shows a good level of awareness among the respondents on the significance of SPI adoption. However, as shown in Fig. 2, most of the respondents indicated lack of resources as well as time consuming as the top reasons for not using SPI standard in Saudi Arabia. The same reasons were highlighted in other studies in different countries such as Canada [40] and English-Speaking Caribbean [41]. In addition, and with reference to the lack of resources, it is worth mentioning that SMEs have limited financial resources which negatively impact resources needed to adopt SPI.

As for the level of knowledge, the majority of respondents have low level of knowledge as shown in the results in Fig. 3. This result is considered normal as per Colomo-Palacios [2] claim that the long goal in SPI is to accelerate the implementation and institutionalization of improved software development practices. The knowledge will be obtained individually by the participants in the process, and then expand the level of the organization to be applied in new projects.

Furthermore, it can be argued from the results presented in Fig. 7 about project management methods that Saudi's SMEs are majorly concerned with the delivery of software products to client on budget within the stipulated time and this is consistent with findings in [23]. It also means that, they do not pay any critical attention to best practice standards in software development but find it easier to employ ad-hoc and/or agile approach, enabling quicker delivery of a working software product. However, without properly defined software process and practices, it would be difficult to deliver software product on time and right on budget. On the other hand, and with reference to project management techniques, several tools are used by companies to conduct projects. This result is consistent with the view of Almobarak et al. [39], who have reported that more than 90% of respondents use at least one project management tool to help in planning, organizing, and managing project resources and tasks.

All in all, the current SPI adoption level in Saudi Arabian SMEs is very much in the low level. This has been shown in the result in the previous section as well as from the discussion presented here.

VI. CONCLUSION AND FUTURE WORK

This study was conducted to investigate small and medium size organizations in Saudi Arabia on their utilization of SPI standards and to collect data to identify problems and potential solutions to help them apply these standards. Our research found that although there is positive favor towards SPI adoption among Saudi organizations, it seems that the practical understanding of SPI adoption is extremely yet to be mature

amongst small and medium size software companies. A primary reason is that many staff do not have the appropriate knowledge to deal with the process of SPI and many managers are reluctant to implement SPI because of the associated costs. Most of staff in these organizations are aware that the adoption of SPI will increase productivity, improve management, shorten development time and improve software quality. However, inexperienced staff and staff turnover are the main reasons for not using of SPI.

Some recommendations can be drawn here to improve the adoption of software engineering practice and techniques:

- Training: One important factor that influences the adoption of SPI is proper and regular education and training of technical staff.
- Finding organization weakness: The key issue in accelerating the adoption of SPI practices is to identify the areas that need most improvement and then find the best way to support organizations in improving these areas.

Common weaknesses are in need to be solved in workplaces in the majority of organizations. These working obstacles can be minimized by strengthening the skills and enriching the knowledge of the employees. Providing the necessary training will bridge the gap and reduce the weaknesses between the levels of the knowledge of the employees and provide them with a common base.

Since the study is performed in Saudi Arabia, it is not clear whether the result can be generalized in the countries that have similar characteristics especially other Arabic countries. Using this data in various environments and contexts to provide cross-cultural comparisons may enrich the literature and result in understanding and applying SPI techniques to achieve high quality process. Assuming that software is developing rapidly and significantly and SPI is becoming very importantly day by day, a future work can use this study as first step towards producing software process improvement standard for Saudi Arabian industry. Also future research can investigate the relationship between organizational size and the SPI success by identifying factors and barriers influencing the SPI implementation activities for large organizations.

ACKNOWLEDGMENT

The author would like to Thank Shaqra University, Saudi Arabia for providing a great research environment with excellent infrastructure. The author would also like to thank all participants who have completed the questionnaire.

REFERENCES

- [1] Fauzi, S. S. M. (2011). Software Process Improvement and Management: Approaches and Tools for Practical Development: Approaches and Tools for Practical Development, IGI Global.
- [2] Colomo-Palacios, R. (2014). Agile Estimation Techniques and Innovative Approaches to Software Process Improvement, IGI Global.
- [3] SCAMPI Upgrade Team, "Standard CMMI Appraisal Method for Process Improvement (SCAMPI) A, Version 1.3: Method Definition Document," Softw. Eng. Inst., Mar. 2011.
- [4] C. N. Murphy and J. Yates, The International Organization for Standardization (ISO): global governance through voluntary consensus. Routledge, 2009.

- [5] W. Melo, K. El Emam, and J. Drouin, "SPICE: The theory and practice of software process improvement and capability determination," IEEE Comput. Soc. Wiley Los Alamitos CA, 1998.
- [6] K. E. Emam, W. Melo, and J.-N. Drouin, SPICE: The theory and practice of software process improvement and capability determination. IEEE Computer Society Press, 1997.
- [7] B. Efron and R. J. Tibshirani, An introduction to the bootstrap. CRC press, 1994.
- [8] B. Efron, "Bootstrap methods: another look at the jackknife," in Breakthroughs in Statistics, Springer, 1992, pp. 569–593.
- [9] P. Pande, R. Neuman, and R. Cavanagh, The Six Sigma way team fieldbook: An implementation guide for process improvement teams. McGraw Hill Professional, 2001.
- [10] R. G. Schroeder, K. Linderman, C. Liedtke, and A. S. Choo, "Six Sigma: Definition and underlying theory," J. Oper. Manag., vol. 26, no. 4, pp. 536–554, 2008.
- [11] R. B. Coronado and J. Antony, "Critical success factors for the successful implementation of six sigma projects in organisations," TQM Mag., vol. 14, no. 2, pp. 92–99, 2002.
- [12] I. Garcia, C. Pacheco, and J. Calvo-Manzano, "Using a web-based tool to define and implement software process improvement initiatives in a small industrial setting," IET Softw., vol. 4, no. 4, pp. 237–251, 2010.
- [13] C. Y. Laporte, S. Alexandre, and A. Renault, "The application of international software engineering standards in very small enterprises," Softw. Qual. Prof. Mag., vol. 10, no. 3, 2008.
- [14] M. Staples, M. Niazi, R. Jeffery, A. Abrahams, P. Byatt, and R. Murphy, "An exploratory study of why organizations do not adopt CMMI," J. Syst. Softw., vol. 80, no. 6, pp. 883–895, 2007.
- [15] I. Richardson and C. G. Von Wangenheim, "Guest editors' introduction: Why are small software organizations different?," IEEE Softw., vol. 24, no. 1, pp. 18–22, 2007.
- [16] C. Y. Laporte, S. Alexandre, and A. Renault, "The application of international software engineering standards in very small enterprises," Softw. Qual. Prof. Mag., vol. 10, no. 3, 2008.
- [17] M. A. T. Almomani, S. Basri, A. K. B. Mahmood, and A. O. Bajeh, "Software Development Practices and Problems in Malaysian Small and Medium Software Enterprises: A Pilot Study," in IT Convergence and Security (ICITCS), 2015 5th International Conference on, 2015, pp. 1–5.
- [18] H. Oktaba and A. Vázquez, "MoProSoft®: A Software Process Model," Softw. Process Improv. Small Medium Enterp. Tech. Case Stud. Tech. Case Stud., 2008.
- [19] M. P. Thapliyal and P. Dwivedi, "Software process improvement in small and medium software organisations of India," Int. J. Comput. Appl., vol. 7, no. 12, pp. 37–39, 2010.
- [20] S. Ibrahim and R. Z. R. M. Ali, "Study on acceptance of customised Software Process Improvement (SPI) model for Malaysia's SME," in Software Engineering (MySEC), 2011 5th Malaysian Conference in, 2011, pp. 25–30.
- [21] A. R. Khan, R. Akbar, and D. W. H. Tan, "A Study on Global Software Development (GSD) and Software Development Process in Malaysian Software Companies," J. Telecommun. Electron. Comput. Eng. JTEC, vol. 8, no. 2, pp. 147–151, 2016.
- [22] S. S. M. Fauzi and M. H. N. M. Nasir, "Software Process Improvement Models Implementation in Malaysia," Innov. Adv. Comput. Sci. Eng., pp. 85–90, 2010.
- [23] R. Z. R. M. Ali and S. Ibrahim, "An application tool to support the implementation of integrated software process improvement for Malaysia's SME," in Software Engineering (MySEC), 2011 5th Malaysian Conference in, 2011, pp. 177–182.
- [24] M. A. Cusumano and C. F. Kemerer, "A quantitative analysis of US and Japanese practice and performance in software development," Manag. Sci., vol. 36, no. 11, pp. 1384–1406, 1990.
- [25] L. Groves, R. Nickson, G. Reeve, S. Reeves, and M. Utting, "A survey of software development practices in the New Zealand software industry," in Software Engineering Conference, 2000. Proceedings. 2000 Australian, 2000, pp. 189–201.
- [26] I. Saastamoinen and M. Tukiainen, "Software process improvement in small and medium sized software enterprises in eastern Finland: A state-of-the-practice study," in European Conference on Software Process Improvement, 2004, pp. 69–78.
- [27] S. N. M. Shah, M. Khalid, A. K. B. Mahmood, N. Haron, and M. Y. Javed, "Implementation of software process improvement in pakistan: An empirical study," in Computer & Information Science (ICIS), 2012 International Conference on, 2012, vol. 2, pp. 1006–1013.
- [28] M. Niazi, "An exploratory study of software process improvement implementation risks," J. Softw. Evol. Process, vol. 24, no. 8, pp. 877–894, 2012.
- [29] M. Staples, M. Niazi, R. Jeffery, A. Abrahams, P. Byatt, and R. Murphy, "An exploratory study of why organizations do not adopt CMMI," J. Syst. Softw., vol. 80, no. 6, pp. 883–895, 2007.
- [30] G. Coleman and R. O'Connor, "Using grounded theory to understand software process improvement: A study of Irish software product companies," Inf. Softw. Technol., vol. 49, no. 6, pp. 654–667, 2007.
- [31] M. H. N. Nasir, R. Ahmad, and N. H. Hassan, "Issues in the implementation of software process improvement project in Malaysia," WSEAS Trans. Inf. Sci. Appl., vol. 5, no. 6, pp. 1031–1043, 2008.
- [32] R. Asato, M. de M. Spinola, I. Costa, and W. H. de F. Silva, "Alignment between the business strategy and the software processes improvement: A roadmap for the implementation," in PICMET '09 - 2009 Portland International Conference on Management of Engineering Technology, 2009, pp. 1066–1071.
- [33] M. A. Resources Information, Software Design and Development: Concepts, Methodologies, Tools, and Applications: Concepts, Methodologies, Tools, and Applications. IGI Global, 2013.
- [34] "Software process improvement via ISO 9000: Results of two surveys among European software houses - IEEE Conference Publication." [Online]. Available: <http://ieeexplore.ieee.org/document/495524/>. [Accessed: 24-Oct-2017].
- [35] B. Manders, H. J. de Vries, and K. Blind, "ISO 9001 and product innovation: A literature review and research framework," Technovation, vol. 48–49, no. Supplement C, pp. 41–55, Feb. 2016.
- [36] D. Stelzer, W. Mellis, and G. Herzwurm, "A critical look at ISO 9000 for software quality management," Softw. Qual. J., vol. 6, no. 2, pp. 65–79, Jun. 1997.
- [37] T. Stålhane and G. K. Hanssen, "The Application of ISO 9001 to Agile Software Development," in Product-Focused Software Process Improvement, 2008, pp. 371–385.
- [38] G. Coleman and R. O'Connor, "Investigating software process in practice: A grounded theory perspective," J. Syst. Softw., vol. 81, no. 5, pp. 772–784, May 2008.
- [39] N. AlMobarak, R. AlAbdulrahman, S. AlHarbi, and W. AlRashed, "The Use of Software Project Management Tools in Saudi Arabia: An Exploratory Survey," Int. J. Adv. Comput. Sci. Appl. IJACSA, vol. 4, no. 7, 2013.
- [40] D. Chevers, "Software Process Improvement: Awareness, use, and Benefits in Canadian Software Development Firms" Revista de Administração de Empresas, 57(2), 2017, 170-177
- [41] D. Chevers, "The Adoption of Software Process Improvement Programs in the English-Speaking Caribbean" in International Conference on Information Resources Management (CONF-IRM), 2014.

Ant Colony Optimization for a Plan Guide Course Registration Sequence

Wael Waheed Al-Qassas¹,

Mohammad Said El-Bashir², Rabah Al-Shboul³

Faculty of Information Technology
Al Al-Bayt University, Mafraq, Jordan

Anwar Ali Yahya⁴

Science and Information Systems
Najran University
Najran – 61441, Saudi Arabia

Abstract—Students in universities do not follow the prescribed course plan guide, which affects the registration process. In this research, we present an approach to tackle the problem of guide for plan of course sequence (GPCS) since that sequence may not be suitable for all students due to various conditions. The Ant Colony Optimization (ACO) algorithm is anticipated to be a suitable approach to solving such problems. Data on sequence of the courses registered by students of the Computer Science Department at Al Al-Bayt University over four years were collected for this study. The fundamental task was to find the suitable pheromone evaporation rate in ACO that generates the optimal GPCS by conducting an Adaptive Ant Colony Optimization (AACO) on the model that used the collected data. We found that 17 courses out of 31 were placed in semesters differing from the semesters preset in the course plan.

Keywords—Ant colony; optimization; guide plan; university course registration

I. INTRODUCTION

The aim of this paper is to propose an algorithm that extracts a guide plan for course sequence from the registration behaviors of university students in order to solve the problem of disobedience of the students of the sequence of courses set in the course plan guide.

The course plan guide is a sequence of courses ordered by semester that the students should follow, semester by semester, during their study. Problems in following the sequence of courses to register according to the guide plan periodically arise in universities. This sort of problem is known to be NP-hard.

In this paper, we focus on students of the computer science (CS) department in an effort to find the optimal plan guide for course sequence as a case study. The proposed algorithm was evaluated using real data taken from the registration department of Al Al-Bayt University related to the courses registered for by students who graduated from the CS department. These courses were studied by students during their four-year study period. In each study year, the student registers for two or three semesters; the first, second, and summer semesters. Quite often, the students register for four to six courses in the first and second semesters and up to three courses in the summer semester. This means that actually the students need to register for up to 11 semesters to be able to graduate within four years, based on that the last study year consists of only two semesters with no summer semester.

There exists a plan guide, but the students do not follow it. They usually prefer to register courses in a sequence that differs from that set in the course plan following the behavior of previous students and based on the difficulties they sometimes face in registering the due courses. The prerequisite courses also affect the decision taken by the student on the courses to register. In consequence, this research was intended to find the best sequence of courses (plan guide) to register based on the courses which the previous students actually registered. The best sequence (optimal path) will be found by implementing ACO model on data taken from the registration records of previous CS students who already graduated.

To conduct ant colony optimization, a software module specially-tailored for the data and need of the present study was built. This module generates paths (plan guide) depending on the course sequence patterns of the courses registered actually by students. Using the Ant Colony methodology, an optimal path for course sequence will be found. This path represents the actual guide for course registration that depends on student student's actual course registration behavior [1], [2].

II. LITERATURE REVIEW

Ant Colony Optimization (ACO) is used to solve combinational problems such as vehicle routing [3], [4], salesman's travel problem [5], [6], graph coloring [7], the quadratic assignment problem [8], and process planning and scheduling [9].

Zuo et al. [10] investigated task-scheduling problems in cloud computing and proposed a resource cost model that defines the demand of tasks on resources that depend on a multi-objective optimization method. Simulation experiments were designed to evaluate performance of their proposed method [10].

In 2003, Dr. Dorigo won the Marie Curie excellence award for inventing the Ant Colony algorithm. This algorithm is considered as a population-based algorithm and classified within the field of swarm intelligence. The course time tabling problem was researched by Socha et al. [11]. In [12], the Ant Colony algorithm was applied on 11 courses to produce optimal timetable sets. Behavior of the real ant corresponds to communication via sharing and distributing information according to a biological method known as the pheromone trails. Many combinatorial optimization problems have been solved successfully by implementing ACO [13]-[15]. Real

ants search for food. When the first ant finds food it returns back to the nest (colony), leaving a pheromone trail. Other ants will follow this pheromone trail to reach the food source. However, the pheromone evaporates with time. Therefore, the long paths that are used by few ants will have less pheromone concentration due to evaporation of the pheromone. On the other hand, more ants use the short paths, thus resulting in increment of the pheromone levels of these paths [16]. Normally, most of the ants follow the path that has the higher pheromone concentration. Only few ants do not usually follow that path. These ants are the ones which often find other possible good paths. In the case of appearance of any obstacle or interruption in the main path that is followed by most ants, the other paths that were detected by the fewer ants become a useful solution. This frequently happens if the path is interrupted by an obstacle or if the food runs out.

Use of the pheromone by ants represents a way of indirect coordination and communication between the colony members. This method of communication is separated in time. Hence, one member of the community modifies the same parameters in the environment and the others see this modification later and use this information to take suitable decision, which is a form of self-organization in a large community that produces intelligent complex structure without need for direct communication or centralized decision and control.

In 2009, Jardat proposed a hybrid algorithm using an Ant Colony system with simulated annealing to solve the problem of university course timetable, which is regarded as a complex organization problem for which it is hard to find an optimal solution [17].

Socha et al. (2002) developed a min-max ant system algorithm for the university course time tabling problem. They used data sets for 11 course time tabling tests and compared their results with those of a random restart local search algorithm. The comparison results uncovered that the proposed algorithm was able to give better results than the random restart local search algorithm and to produce viable solutions [12].

III. METHODOLOGY

In this study, data were collected and cleaned. Then, an ACO algorithm was applied to the cleaned data in order to extract an optimal path for a course plan guide.

A. Data Collection

Data were collected from the Registration and Admission Department in Al Al-Bayt University. The collected registration data pertain to 200 students formerly admitted to the CS department in the academic years 2009/2010 and 2010/2011 and who already graduated from the university. These data represent the sequence of the courses registered for each student. This sequence consists of the registered courses and the semester and year in which each course was registered. A sample of the collected data is show in Table I.

TABLE I. SAMPLE OF THE RAW DATA

Student number	Academic Year	Semester	Course Code	Course Name
1000901074	2009	2	901210	Object Oriented Programming
1000901074	2009	2	901131	Computer Skills
1000901074	2009	3	901200	Discrete Math
1050901044	2010	1	901220	Logic Design
1050901044	2010	1	901099	Computer 1
1050901044	2010	1	901200	Discrete math
1050901044	2010	1	902230	Info. Systems
1050901044	2010	1	901131	Computer Skills
1050901031	2012	2	901325	Networks
1050901031	2012	2	901240	Data Structures
1050901031	2012	2	901211	Java Lab
1050901031	2012	2	901300	Computation
1050901031	2012	2	901320	Architecture

B. Data Cleaning

In order to prepare the data for processing, there was a need for these data to be cleaned by removing the compulsory courses and grouping the different elective courses under a unique course code (i.e., 'elective') so as to treat the various elective courses in the same way how the compulsory courses are treated [18]. Furthermore, if a student re-registered a course due to inability to pass it from the first time, then we only considered the first registration for the course and removed the repetitive registrations, if any.

C. Ant Colony Algorithm

A software module was designed for performing the ACO in order to generate the optimal path (sequence plan guide). This module has n nodes, each representing a course in the guide plan. Theoretically, this module should be able to find a path that goes through all nodes, which is due to be generated based on information taken from the students' course registration sequences. However, since there are 200 students, then the maximum number of possible paths is only 200, but practically this will not be the case since there will be some impossible paths for certain sequences due to the constraint of the prerequisite course requirement. According to the ACO algorithm, the particular path generated will depend on different paths.

The ACO uses the concept of pheromone evaporation with time. Thus, the less visited nodes or edges will contain lower amount of pheromone than the nodes and edges which are more visited. On this account, the student represents the ant agent and the sequence of courses taken by a student will draw the path from beginning to end and, in consequence, increment the amount of pheromone in that path.

The path consists of a set of edges that connect the nodes (courses). Each edge has a parameter representing the amount of pheromone at that edge. The pheromone evaporates at a constant rate. Thus, if an edge is not visited for a long time, then the pheromone level at it will be zero. If the evaporation rate is set too high, then the pheromone rate at all edges will rapidly reach to zero, which will not help in finding a path. On the other hand, if the evaporation rate is too low, then the pheromone will be saturated at the edges, which too will not help in finding a path. Experimentally, we will find the suitable pheromone evaporation rate in order to identify an optimal path. The ant system algorithm that was designed in the present study to optimize the course plan guide problem is presented next.

Owing to that the number of possible routes is large because of the large number of courses (31 course), which will lead to 31x31 possible edges, and as an improvement over the algorithm, this study did not use a connection matrix to represent this model. Instead, an ad-hoc connection was constructed so as to reduce the time complexity. This was achieved by preparing a dynamic list that contains the visited edges. By so doing, the model only modifies the visited edges.

Algorithm: An Ant System for Optimizing the Course Plan Guide Problem

initialization:

initialize : Q : amount of pheromone increased when an edge is visited

initialize : p : evaporation rate.

initialize : m = 100 students.

initialize : c = 27 number of courses.

initialize : S = 11 number of semesters.

initialize : MSC matrix, that consists the pheromone value for every course in each semesters.

for k=1 to m

for g=1 to c

 get course from the input data for each student

 update pheromone trails on the specified semester-course in the MCS

for i=1 to S

 for j=1 to c

 apply evaporation on all edges

 find the path with the highest pheromone rate

D. Results and Discussion

The raw data were drawn from the Admission and Registration Department of Al Al-Bayt University. They pertain to students who already graduated. Those students were admitted to the university in the academic years 2009/2010 and 2010/2011. The data consist of records that include the student number, course number, course name, and the semester and year in which the student registered each course (Table I).

The collected data first passed through a preprocessing stage comprising several steps of data cleaning. These steps included elimination of some courses that were unrelated, and were, therefore, out of the study scope such as the university required courses. Moreover, cleaning included elimination of the courses that were re-registered by the students who failed to pass them from the first time.

Afterwards, the ACO model was applied by running a module that was specially tailored and customized to fit the research data. Structurally, this module consists of a set of nodes, each representing one course. Overall, the number of nodes in this study was 31, corresponding to 31 courses. Every student must register for the 31 courses during her/his study period, which is normally four academic years, each consisting of a maximum of three semesters. This means that each student can register a maximum of 11 semesters until graduation, assuming that only two semesters are registered for in the last year. The 11 semesters represent stages in our model. Hence, the final results will correspond to the 31 courses distributed among 11 stages (semesters) and the optimal extracted path shown in Fig. 1. In this figure, S_i ($i = 1, 2, 3, \dots, 11$) represents the semester number.

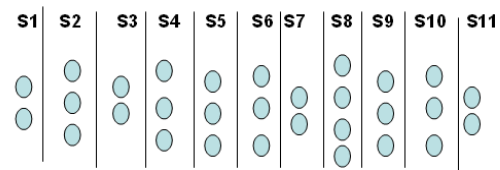


Fig. 1. Sample plan guide.

The experiment was run 10 times for different pheromone evaporation rates, ranging from 0.1 to 1 at a step of 0.1. A table of distribution of the courses among semesters was constructed for each run. Then, the information in those tables was normalized in order to compare the results between the tables and validate them. The paths were then extracted from these tables on the basis of the pheromone rate as shown in Table II.

It was found that some courses were located in the same semesters regardless of the pheromone evaporation rate. On the other hand, allocation of some other courses to semesters varied from semester to another, depending on the pheromone evaporation rate (Table II).

As Table II reveals, fourteen courses were not affected by change in the pheromone rate. These courses are the courses listed in Table II with the numbers 1, 2, 5, 6, 11, 12, 13, 17, 19, 23, 25, 27, 28, and 29.

On the other hand, sixteen courses moved between semesters with the change in the pheromone evaporation rate. These courses are the courses appearing in Table II with the numbers 3, 4, 7, 8, 9, 10, 14, 15, 16, 18, 21, 22, 24, 26, 30, and 31.

TABLE II. DISTRIBUTION OF COURSES AMONG SEMESTERS FOR DIFFERENT PHEROMONE EVAPORATION RATES

		Pheromone Evaporation Rate									
		0.1	0.2	0.3	0.4	0.5	0.6	0.7	0.8	0.9	1
Course Number	1	2	2	2	2	2	2	2	2	2	2
	2	4	4	4	4	4	4	4	4	4	4
	3	5	5	5	7	7	7	7	7	7	7
	4	5	5	5	7	7	7	7	7	7	7
	5	4	4	4	4	4	4	4	4	4	4
	6	1	1	1	1	1	1	1	1	1	1
	7	7	7	7	8	8	8	8	8	8	8
	8	7	7	7	8	8	8	8	8	8	8
	9	8	8	8	3	3	3	3	3	3	3
	10	5	7	7	7	7	7	7	7	7	7
	11	4	4	4	4	4	4	4	4	4	4
	12	7	7	7	7	7	7	7	7	7	7
	13	4	4	4	4	4	4	4	4	4	4
	14	8	8	8	8	10	10	10	10	10	10
	15	5	5	5	8	8	8	8	8	8	8
	16	7	5	5	5	5	5	5	5	5	5
	17	7	7	7	7	7	7	7	7	7	7
	18	6	8	8	8	8	8	8	8	8	8
	19	10	10	10	10	10	10	10	10	10	10
	20	9	10	10	9	9	9	9	9	9	9
	21	8	8	8	8	11	11	11	11	11	11
	22	8	8	8	8	8	9	9	9	9	9
	23	9	9	9	9	9	9	9	9	9	9
	24	7	10	10	10	10	10	10	10	10	10
	25	10	10	10	10	10	10	10	10	10	10
	26	10	10	10	10	8	8	8	8	8	8
	27	10	10	10	10	10	10	10	10	10	10
	28	11	11	11	11	11	11	11	11	11	11
	29	3	3	3	3	3	3	3	3	3	3
	30	11	11	11	8	8	8	8	8	8	8
	31	10	10	10	10	11	11	11	11	11	11

Course number 20 moved twice from semester 9 to semester 10 at the pheromone evaporation rate of 0.2. It then returned back to semester 9 at the pheromone evaporation rate of 0.4. The numbers and names of all courses are shown in Table III.

After analyzing the data generated by the built model, it was found that there is a stable guide plan for the pheromone evaporation rates ≤ 0.3 (Table IV). On the other hand, when increasing the pheromone evaporation rate above 0.3 the results become unstable and unaccepted logically based on the researchers' knowledge of the sequence of registration of courses.

TABLE III. NUMBERS AND NAMES OF COURSES

Index	Course Number	Course Name	Index	Course Number	Course Name
1	901131	Computer Skills IT	17	901327	Wireless Networks
2	901210	OOP	18	901331	DBMS
3	901211	Java	19	901332	Operating Systems
4	901213	Java Lab	20	901340	Algorithm
5	901214	Object Oriented Lab	21	901341	Software Engineering
6	902230	Information Systems	22	902410	Fourth Generation Languages
7	902350	Web Design	23	901430	Distributed Systems
8	902354	Web Design Lab	24	902444	System Analysis
9	902450	E-Commerce	25	901470	Artificial Inelegance
10	902201	Numerical Analysis	26	901480	Data Security
11	901220	Digital Logic Design	27	901499	Graduation Project
12	901240	Data Structures	28	901500	Training
13	901300	Computation Theory	29	901200	Discrete Math
14	901310	Visual Programming	30	901351	Human Computer Interaction
15	901320	Computer Architecture	31	902481	Special Topics
16	901325	Computer Networks			

TABLE IV. DISTRIBUTION OF COURSES AMONG SEMESTERS FOR PHEROMONE RATES ≤ 0.3 AND > 0.3

Course number	Semester Number with pheromone evaporation ≤ 0.3	Semester Number with pheromone evaporation > 0.3	Course number	Semester Number with pheromone evaporation ≤ 0.3	Semester Number with pheromone evaporation > 0.3
1	2	2	17	7	7
2	4	4	18	8	8
3	5	7	19	10	10
4	5	7	20	10	9
5	4	4	21	8	11
6	1	1	22	8	8
7	7	8	23	9	9
8	7	8	24	10	10
9	8	3	25	10	10
10	7	7	26	10	8
11	4	4	27	10	10
12	7	7	28	11	11
13	4	4	29	3	3
14	8	10	30	11	8
15	5	8	31	11	11
16	5	5			

As can be seen in Table IV, for 11 courses the registration semester differed by increasing the evaporation rate beyond 0.3. Meantime, for the remaining 20 courses the registration semester was not affected by increasing the evaporation rate. In view of these findings, the pheromone evaporation rate of 0.3 was selected as the optimum pheromone evaporation rate for generation of the course plan guide.

TABLE V. DISTRIBUTION OF COURSES AMONG SEMESTERS AS GENERATED BY THE PROPOSED ALGORITHM

S1	S2	S3	S4	S5	S6	S7	S8	S9	S10	S11
6	1	29	2	3		7	9	23	19	28
			5	4		8	14		20	30
			11	15		10	18		24	31
			13	16		12	21		25	
						17	22		26	
									27	

TABLE VI. ACTUAL DISTRIBUTION OF COURSES IN SEMESTERS

S1	S2	S3	S4	S5	S6	S7	S8	S9	S10	S11
1	2		6	3		7	9		22	23
	5		10	4		8	17		25	26
	29		11	13		14	19		27	28
			12	15		16	20		31	30
						18	21			
						24				

A comparison of the results generated by this study (Table V) and the existing plan guide (Table VI) indicates that for 14 courses the registration semesters matched while 17 courses were registered in different semesters.

By Taking the ‘Computer Skills for IT Students’ course as an example to explain the observed differences between the plan guides in Tables V and VI, it can be said that this course is a programming course that is usually registered in the second semester since most of the students prefer to register fundamental courses (e.g., Information Systems) in the first semester in addition to university requirement courses, even though the ‘Computer Skills for IT Students’ course is supposed to be registered in the first semester as shown in Table VI.

E. Conclusion

This study developed a course plan guide based on real data on courses registered by CS students in Al Al-Bayt University over their four-year study period. An Ant Colony algorithm was used to monitor the actual sequence of the courses registered by the students. The developed plan guide explains why some course sections were cancelled; the numbers of students registering in them were not high enough. Comparison in the course registration sequence between the present and the proposed plan guides uncovered match between the two plans in the order of registration for 14 courses and differences for 17 courses. In future work, the size of data can be increased and the proposed algorithm can be applied to the course schedule so as to monitor its performance.

ACKNOWLEDGMENTS

The authors express their sincere thanks to Al Al-Bayt University – Jordan for cooperation in providing them with the necessary data and facilities.

REFERENCES

- [1] Clemens Nothegger, Alfred Mayer, Andreas Chwatal and Günther R. Raidl, “Solving the post enrolment course timetabling problem by ant colony optimization.” *Annals of Operations Research* April 2012, Volume 194, Issue 1, pp 325-339.
- [2] C.W. Leung, T.N. Wong, K.L. Mak and R.Y.K. Fung. “Integrated process planning and scheduling by an agent-based ant colony optimization”. *Computers & Industrial Engineering* 59 (2010) 166–180.
- [3] John E. Bella and Patrick R. McMullenb. Ant colony optimization techniques for the vehicle routing problem.” *Advanced Engineering Informatics* 18 (2004) pp.41–48.
- [4] Dongming Zhao, Liang Luo and Kai Zhang. “An improved ant colony optimization for the communication network routing problem.” *Mathematical and Computer Modelling* 52 (2010) pp. 1976–1981.
- [5] Marco Dorigo and Luca Maria Gambardella. “Ant colony system: a cooperative learning approach to the traveling salesman problem.” *IEEE Transactions on Evolutionary Computation*, VOL. 1, NO. 1, APRIL 1997, pp 53 – 66.
- [6] Marco Dorigo, Luca Maria Gambardella. Ant colonies for the travelling salesman problem. *Biosystems* Volume 43, Issue 2, July 1997, Pages 73–81.
- [7] Thang N. Bui, ThanhVu H. Nguyen, Chirag M. Patel and Kim-Anh T. Phan. An ant-based algorithm for coloring graphs. *Discrete Applied Mathematics*, Volume 156, Issue 2, 15 January 2008, Pages 190–200.
- [8] L. M. Gambardella; E. D. Taillard and M. Dorigo. Ant Colonies for the Quadratic Assignment Problem. *The Journal of the Operational Research Society*, Vol. 50, No. 2 (Feb., 1999), pp. 167-176.
- [9] S. Zhang, and T. N. Wong, Integrated process planning and scheduling: an enhanced ant colony optimization heuristic with parameter tuning. *Journal of Intelligent Manufacturing* December 2014.
- [10] L. Zuo, L. Shu, S. Dong, C. Zhu, T. Hara, “A Multi-Objective Optimization Scheduling Method Based on the Ant Colony Algorithm in Cloud Computing,” *IEEE Access*, vol. 3, pp. 2687-2699, 2015.
- [11] Krzysztof Socha, Michael Sampels and Max Manfrin. Ant Algorithms for the University Course Timetabling Problem with Regard to the State-of-the-Art. *Proceedings of the 2003 international conference on Applications of evolutionary computing*, Pages 334-345 Springer-Verlag Berlin, Heidelberg.
- [12] Krzysztof Socha, Joshua Knowles and Michael Sampels. A MAX-MIN Ant System for the University Course Timetabling Problem, *Third International Workshop, ANTS 2002 Brussels, Belgium, September 12–14, 2002 Proceedings*, Pages pp 1-13.
- [13] E. Bonabeau, M. Dorigo, and G. Theraulaz, “From Natural to Artificial Swarm Intelligence,” Oxford University Press, Oxford, 1999.
- [14] M. Dorigo, V. Maniezzo, and A. Coloni, “The Ant system: optimization by a colony of cooperating Agents.” *IEEE Transactions on Systems, Man, and Cybernetics-Part B*, 26(1):29-41, 1996.
- [15] M. Dorigo and B. Christian. *Ant Colony Optimization: A Survey*. Elsevier B.V., *Theoretical Computer Science* 344 (2005) 243 – 278. 2005.
- [16] Anuj K. Gupta. Computation of Pheromone Values in AntNet Algorithm. *International Journal of Computer Network and Information Security*, 2012, 9, pp. 47-54.
- [17] Masri Ayob, Ghaith Jaradat. Hybrid Ant Colony Systems for Course Timetabling Problems. *2nd Conference on Data Mining and Optimization*, Selangor, Malaysia, IEEE, pp. 120-126 ,2009.
- [18] Ajith Abraham and Vitorino Ramos. Web Usage Mining Using Artificial Ant Colony Clustering and Genetic Programming. *The 2003 Congress on Evolutionary Computation*, 2003.

Continuous Path Planning of Kinematically Redundant Manipulator using Particle Swarm Optimization

Affiani Machmudah, Setyamartana Parman, M.B. Baharom
Mechanical Engineering
Universiti Teknologi PETRONAS
Bandar Seri Iskandar, Tronoh, Perak, Malaysia

Abstract—This paper addresses a problem of a continuous path planning of a redundant manipulator where an end-effector needs to follow a desired path. Based on a geometrical analysis, feasible postures of a self-motion are mapped into an interval so that there will be an angle domain boundary and a redundancy resolution to track the desired path lies within this boundary. To choose a best solution among many possible solutions, meta-heuristic optimizations, namely, a Genetic Algorithm (GA), a Particle Swarm Optimization (PSO), and a Grey Wolf Optimizer (GWO) will be employed with an optimization objective to minimize a joint angle travelling distance. To achieve n -connectivity of sampling points, the angle domain trajectories are modelled using a sinusoidal function generated inside the angle domain boundary. A complex geometrical path obtained from Bezier and algebraic curves are used as the traced path that should be followed by a 3-Degree of Freedom (DOF) arm robot manipulator and a hyper-redundant manipulator. The path from the PSO yields better results than that of the GA and GWO.

Keywords—Path planning; redundant manipulator; genetic algorithm; particle swarm optimization; grey wolf optimizer insert

I. INTRODUCTION

Nowadays, researches in the robotic field are focusing on the use of robot to substitute human operator jobs in dangerous environment because it involves the high risk for human safety. Human operator is usually still used due to the task is conducted in a difficult environment involving a very complex geometrical path. The time to finish the job by manually programming, for example in the arc welding robotic system for manufacturing the large vehicle hull, is very long time [1] so that in this application, using the robotic system is still very challenging and high cost. Thus, the path planning to track the prescribed path is very important research to be conducted toward the automation in the manufacturing industry involving complex geometrical path.

Using the manipulator to track a complex geometry in the manufacturing industry, the goal is to achieve the high precision as well as satisfy the optimality criteria so that the production efficiency can be improved. For very challenging environmental conditions, an off-line tracking algorithm is considered as an efficient approach because an online path planning is only available for very simple tasks such as a pick and place [1]. Different with a point-to-point path planning where the end-effector path is free to be chosen, in the

continuous path planning, the arm robot manipulator needs to move along the prescribed end-effector path. Thus, the continuous path planning needs to solve an Inverse Kinematic (IK) problem for the entire traced path.

Solving the IK of the arm robot manipulator is a long-term research where it has been conducted since the past five decades. The Jacobian pseudoinverse technique was firstly employed to solve the IK problem of the robotic arm manipulator by Whitney in 1969 [2]. Baillieul [3] developed an extended Jacobian to achieve the cyclic properties. This approach imposed some additional constraints to be achieved along with the end-effector task to identify an appropriate solution. IK function approach by constructing a mathematical function to model the joint angle trajectories was presented by Wampler [4].

Burdick [5] presented a concept of self-motion manifold which considered global solution of the IK rather than instantaneous solution. Khatib [6] presented a generalized inverse which was consistent with the system dynamics namely, a dynamically consistent Jacobian. Tcho'n et al. [7] studied the design of the extended Jacobian algorithm which approximate the Jacobian pseudoinverse. Variational calculus and differential geometric were employed. 3-DOF manipulator and mobile robot were used in numerical examples.

In the case of the hyper-redundant robot, the computation of the Jacobian based approach becomes computationally expensive because of increasing the degrees of freedom. Furthermore, the Jacobian based methods are only suitable for serial link morphologies, and impractical for applications of locomotion and tentacle-like grasping [8]. Because of this drawback, the geometrical approach which does not require the computation of the Jacobian inverse becomes an alternative solution to the hyper-redundant manipulator IK [9].

Studies of the path planning to track the prescribed path have been conducted using both serial and parallel manipulators. Ebrahimi et al. [10] applied heuristic optimizations, such as genetic algorithm and particle swarm optimization to achieve an optimal path using the four-bar mechanism. Yue et al. [11] presented a computer-aided linkage design for tracking open and closed planar curves. Merlet [12] studied trajectory verification for Gough-Stewart parallel manipulator. The algorithm was proposed considering a real-

time method so that it may deal with any path trajectory and validity criterion. Yao and Gupta [13] studied the collision-free path planning of the arm robot manipulator whose end-effector traveled along a prescribed path. Yahya et al. [9] proposed the geometrical approach to the hyper-redundant robot to track the prescribed path. The angles between the neighboring links were arranged to be the same to avoid the singularities. Ananthanarayanan and Ordonez [14] proposed a novel approach to solve an IK problem for $2n+1$ degree of freedom manipulator. The IK was modeled as a constrained optimization considering collision-free and joint limits.

The complexity of the arm robot motion presents because the task is naturally delivered in the Cartesian coordinate while the motion is conducted in the joint space. This paper uses an interval analysis of the self-motion in generating joint space trajectories and applying the meta-heuristic optimization technique to choose the optimal solution among infinite possible solutions. The self-motion will be mapped into the interval of the angle domain variable, θ_g . The redundancy resolution exists within the angle domain boundary. To choose the best solution among infinite possible solutions, the meta-heuristic optimizations, which are the GA, the PSO and the GWO will be employed with the optimization objective is to minimize the total joint angle travelling distance. The 3-DOF planar series redundant manipulator and 6-DOF planar series hyper-redundant manipulator will be used to track the complex geometrical curve.

The present paper is organized as follows: Section 2 presents the self-motion of the arm robot manipulator. Section 3 describes the path planning optimization problem. Section 4 presents the methodology to solve the path planning optimization of the planar redundant and hyper-redundant manipulators. Section 5 presents the GA, PSO, and GWO algorithms to solve the path planning. The proposed method is applied to the planar redundant and hyper-redundant manipulators in the Section 6. The conclusion is presented in Section 7.

II. SELF-MOTION OF KINEMATICALLY REDUNDANT MANIPULATOR

The self-motion can be used to repair infeasible trajectories due to collision, singularity, and connectivity issues. The self-motion is the case where the end-effector does not move while the positions of the joints are moved. To generate the smooth trajectories, there is the requirement of the connectivity among sampling points of the generated trajectories from the initial configuration to the final configuration. The concept of connectivity is one of the important performances of the manipulator motion [15], [16].

Fig. 1(a) illustrates an example of inappropriate configurations because of disconnection of postures. Kinematically redundant manipulator has the self-motion capability which has an advantage in finding the proper posture. However, because there are many possible configurations to achieve single end-effector position for the redundant manipulator, finding the feasible trajectories is a challenging computational problem. The posture in Fig. 1(a) is possible to be repaired using the self-motion. Fig. 2 is the example of the feasible motion where the joint angle

trajectories, as shown in Fig. 2(b), are smooth and the postures of the robot, as shown in Fig. 2(a), have satisfied n -connectivity.

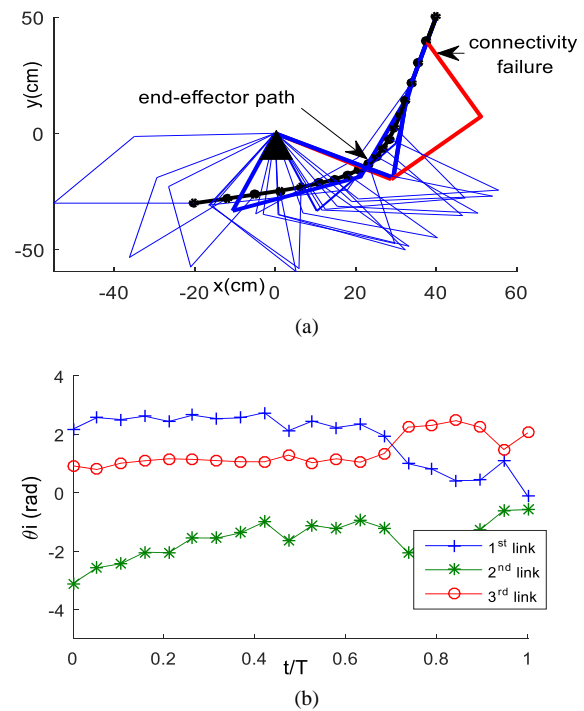


Fig. 1. Connectivity failure (a) improper posture (b) Joint angle trajectories of (a).

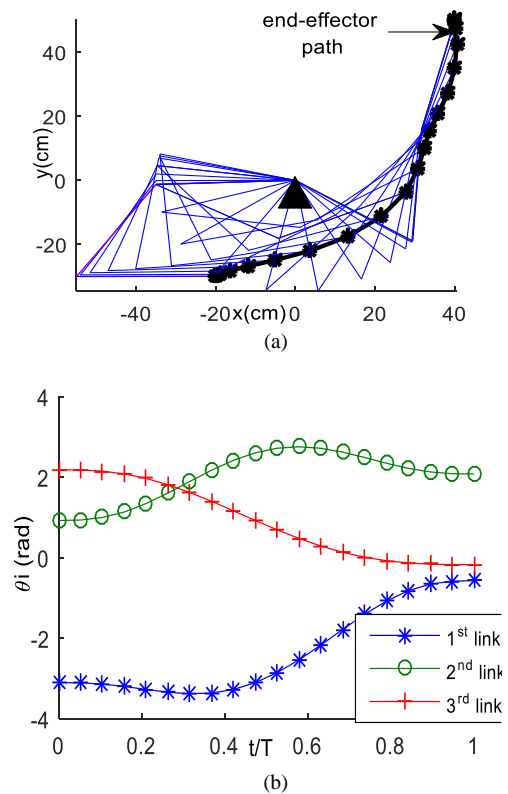


Fig. 2. Repair trajectories by self-motion (a) proper posture (b). Joint angle trajectories of (a).

III. PROBLEM FORMULATIONS

The continuous path planning is the problem to find the joint angle θ_i when the end-effector moves along the specified path. Since for kinematically redundant manipulator, there are infinite possible solutions to achieve the desired end-effector movement, the path planning can be modelled as the optimization problem to find the optimal solution based on the optimization objective.

This paper considers planar redundant and planar hyper-redundant manipulators where the path planning can be formulated as the optimization problem as follows:

Objective:

$$\text{Min } F_{path} = \sum_{i=1}^n \int_0^1 \sqrt{1 + \left(\frac{d\theta_i(r)}{dr}\right)^2} dr \quad (1a)$$

Constraints:

$$\theta_{imin} \leq \theta_i \leq \theta_{imax} \quad (1b)$$

$$(x_e, y_e) = (x, y) \quad (1c)$$

$$x = l_1 \cos \theta_1 + l_2 \cos(\theta_1 + \theta_2) + \dots + l_n \cos(\theta_1 + \theta_2 + \dots + \theta_n) \quad (1d)$$

$$y = l_1 \sin \theta_1 + l_2 \sin(\theta_1 + \theta_2) + \dots + l_n \sin(\theta_1 + \theta_2 + \dots + \theta_n)$$

$$x_e = f(t) ; y_e = f(t) \quad (1e)$$

where F_{path} , r , n , l_i , θ_i , θ_{imin} , θ_{imax} , (x, y) , and (x_e, y_e) are the objective function, a linear time-scale, number of links, i th manipulator length, i th joint angle, minimum of θ_i , maximum of θ_i , actual end-effector path, desired end-effector path, respectively.

Equation (1a) is the joint angle traveling distance which is the objective of optimization. Equations (1b) and (1e) are the joint angle constraint and the forward kinematics of the manipulator, respectively.

IV. METHODS

Since the end-effector path is constrained, all possible trajectories are due to the contribution of the self-motion. This section will investigate the available solution of the IK for tracking the path in the area of nearest maximum reachable workspace by mapping the angle domain interval.

For the IK problem of 3-DOF planar robot, it has the analytic solution using the geometrical method in the following [17]:

$$w_x = x_p - l_1 \cos(\theta_g) ; w_y = y_p - l_1 \sin(\theta_g) \quad (2)$$

$$c_2 = \frac{(w_x^2 + w_y^2 - l_1^2 - l_2^2)}{2l_1 l_2} ; s_2 = \pm \sqrt{1 - c_2^2} \quad (3)$$

$$\theta_2 = a \tan 2(s_2, c_2) \quad (4)$$

where (x_p, y_p) , l_i , θ_g , θ_2 , c_2 , s_2 , are the position of end-effector in Cartesian coordinate, the length of i th link, the angle domain, the second joint angle, the cosines of θ_2 , and the sine of θ_2 , respectively.

First and third joint angles can be obtained by following equations:

$$\Delta = w_x^2 + w_y^2 ; s_1 = \frac{(l_1 + l_2 c_2)w_y - (l_2 s_2 w_x)}{\Delta} \quad (5)$$

$$c_1 = \frac{(l_1 + l_2 c_{21})w_x + (l_2 s_{21} w_y)}{\Delta} ; \theta_1 = a \tan 2(s_1, c_1) \quad (6)$$

$$\theta_3 = \theta_g - \theta_2 - \theta_1 \quad (7)$$

where θ_i , c_i , s_i and θ_3 are the first joint angles, the cosine of θ_i , the sine of θ_i , and the third joint angle, respectively.

Using (7), the self-motion of 3-DOF planar robot can be modelled as interval-valued function in the following:

For $P(x_p, y_p)$:

$$\theta_g = \theta_1 - \theta_2 - \theta_3 ; \theta_1 = (\theta_{1min}, \theta_{1max}) \quad (8)$$

$$\theta_2 = (\theta_{2min}, \theta_{2max}) ; \theta_3 = (\theta_{3min}, \theta_{3max})$$

By this approach, θ_g is a function of variables, θ_1 , θ_2 , and θ_3 where they are real numbers in radian with specific intervals. The problem becomes how to find these intervals for specific value of $P(x_p, y_p)$. Posture analysis will be employed to investigate these intervals in this section.

A. Interval Analysis

This paper considers tracking the end-effector path in the case of nearest maximum reachable workspace, which is defined as the end-effector trajectories in the range of radius in the following:

$$R^*_{min} \leq R < R_{max} = (l_1 + l_2 + l_3) \quad (9)$$

$$R^*_{min} = \sqrt{(l_1 + l_2)^2 - l_3^2} \quad (10)$$

where R and R_{max} are radius or distance of the end-effector trajectories from the base and the maximum reachable radius, respectively.

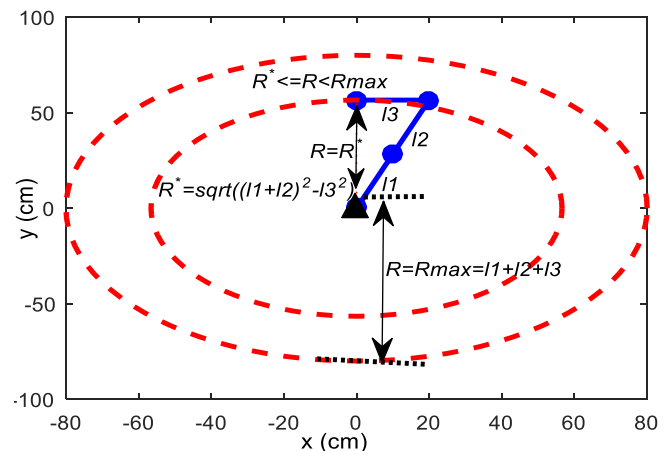


Fig. 3. Nearest maximum reachable workspace area.

Fig. 3 illustrates the nearest maximum reachable workspace defined in this paper. In this nearest maximum reachable workspace, the self-motion capability is reduced due to the limitation of the arm robot geometry. Analysis the feasible range of the trajectories is very important step in the path planning, since to track the entire path, the joint space trajectories should have connectivity without any error in position. Any joint space trajectories that are outside this feasible interval will contribute to the tracking position errors.

For the nearest maximum reachable workspace, regarding the range of reachable point by the arm robot manipulator, there are the maximum and minimum configurations contributing the maximum and minimum angle domain as illustrated in Fig. 4. Posture A is the maximum configuration while posture B is the minimum configuration. These are the maximum and minimum configurations that can be reached by the arm robot at the curve point (x_p, y_p) . These maximum/minimum postures can be mapped into interval of the angle domain. For the near maximum reachable workspace at curve point (x_p, y_p) , the angle domain solution lies within this interval. Outside this interval, the arm robot cannot reach due to geometrical limitation so that it will contribute to the position error.

Since the value of joint angle is periodic with period 2π , the minimum value should be chosen in constructing the proper interval of the angle domain. The angle domain for maximum and minimum configurations can be expressed in the following:

$$\theta_{g \min/\max} = \theta_{1\max/\min} + \theta_{3\max/\min} \quad (11)$$

where $\theta_{g\min/\max}$, $\theta_{1\max/\min}$, and $\theta_{3\max/\min}$ are the maximum or minimum of theta global, the first joint angle at maximum or minimum posture, and the third joint angle of maximum/minimum posture, respectively.

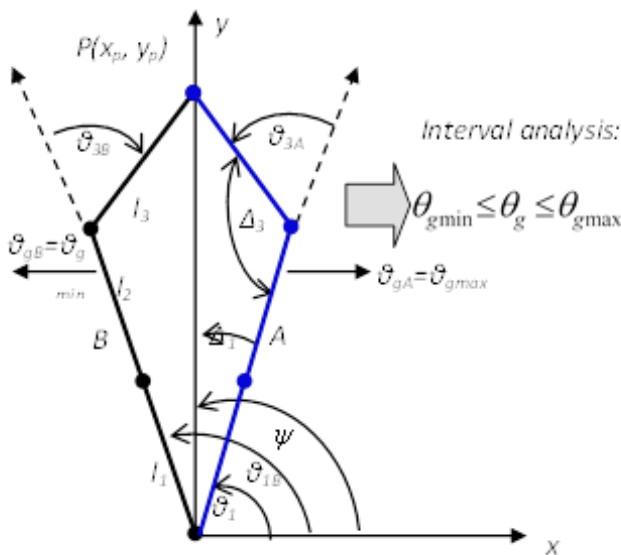


Fig. 4. Mapping the feasible postures into interval analysis.

Refer to Fig. 4, the value of $\theta_{1\max/\min}$ and $\theta_{3\max/\min}$ can be obtained using trigonometric rule as follows:

$$\theta_{1\max} = \psi - \Delta_1; \theta_{1\min} = \psi + \Delta_1 \quad (12)$$

$$\theta_{3\max} = 2\pi - \Delta_3; \theta_{3\min} = -(2\pi - \Delta_3) \quad (13)$$

$$\theta_{g\min} = \theta_{1\min} + \theta_{3\min} \quad (14)$$

$$\theta_{g\max} = \theta_{1\max} + \theta_{3\max} \quad (15)$$

where ψ , $\theta_{1\max}$, $\theta_{1\min}$, $\theta_{3\max}$, and $\theta_{3\min}$ are the angle of radius of curve point (x_p, y_p) from x-axis, the first joint angle of maximum configuration, the first joint angle of minimum configuration, the third joint angle of maximum configuration, and the third joint angle of minimum configuration, respectively.

The value of Δ_1 and Δ_3 can be obtained from geometrical analysis of triangular of maximum-minimum configurations using cosine rule.

The posture of the point in the near maximum reachable workspace area then can be mapped into interval of the angle domain in the following:

$$(\theta_{g \min} \pm p.2\pi) \leq \theta_g \leq (\theta_{g \max} \pm p.2\pi) \quad (16)$$

where p is an integer value, respectively.

The inverse trigonometric function is not injective function. The value is periodic with period 2π so that the angle domain interval is expressed in (16). Making constraint in interval of first and second joint angles range within $[-\pi, \pi]$ is necessary to avoid the disconnection problem of the sampling points. By making this interval constraint, the value of p in (16) will be zero, and (16) can be expressed in the following

$$\theta_{g \min} \leq \theta_g \leq \theta_{g \max} \quad (17)$$

$$-\pi \leq \theta_1, \theta_2, \theta_3 \leq \pi \quad (18)$$

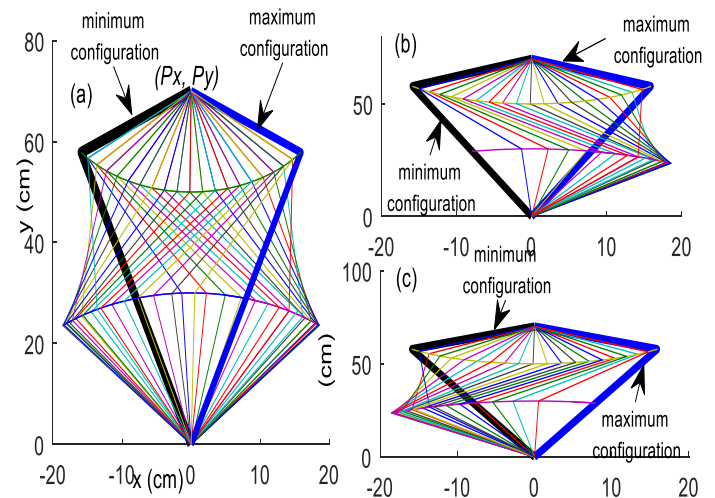


Fig. 5. (a) Posture interval for curve point (P_x, P_y) for both positive and negative sign of (3) (b) Posture plots for positive value of (3) (c) posture plots for negative value of (3).

The maximum and minimum of the angle domain represent the maximum and minimum configurations that can be reached by arm robot manipulator at such corresponding point. Illustration of all postures that can be reached by the arm robot from minimum configuration to maximum configuration is shown in Fig. 5.

Using this posture analysis, interval-valued function in (8) can be expressed in the following:

$$\theta_g = \theta_1 - \theta_2 - \theta_3 ; (\theta_{g \min}, \theta_{g \max}) \quad (19)$$

In the case there is joint angle constraint, it needs to check the feasible interval according to the corresponding joint angle constraint. The angle domain interval may decrease as compared to the case when the manipulator does not have the joint angle limit.

For the hyper-redundant manipulator, using the concept of a moving base of the previous 3-link component, the geometrical approach (2-7) can be employed. The local angle domain boundary is computed with respect to the moving base by employing the interval analysis of the self-motion of the tracked path and the trajectories of the local angle domain are generated inside the boundary.

B. Sinusoidal Function as the Joint Angle Trajectories

This paper uses the continuous function of the angle domain to achieve the n -connectivity among the sampling points of the generated trajectories.

The angle domain as function of time can be expressed as composition function of the angle domain profile and linear time-scale as follows:

$$\theta_g(t) = \theta_g(r) \circ r(t) \quad (20)$$

$$r(t) = \frac{t}{T} \quad (21)$$

where $\theta_g(t)$, $\theta_g(r)$, $r(t)$, t , and T are the theta global, the joint angle profile, linear time-scale, the time, and the total travelling time, respectively.

The angle domain trajectories will be generated in the form of the sinusoidal function as follows:

$$\theta_g(r) = \theta_{gi} + A \sin 2\pi fr \quad (22)$$

where $\theta_g(t)$, $\theta_g(r)$, $r(t)$, t , and T are the angle domain, the angle domain profile, linear time-scale, the time, and the total travelling time, respectively.

The path planning problem then can be reduced as the problem to find the feasible angle domain from parameter 0 to 1. Using the sinusoidal function, f is the parameter to be searched in the optimization step.

C. Boundary of the Angle Domain Representing the Feasible Zone Trajectories

Computing the angle domain for the entire traced path will construct the boundary as illustrated in Fig. 6. The angle domain trajectories during the motion should be maintained inside this boundary to avoid the position error. Using interval analysis of the self-motion, the angle domain boundary for the

path in Fig. 6(a) can be illustrated as Fig. 6(b). The boundary lines are composed from the minimum angle domain trajectories and the maximum angle domain trajectories.

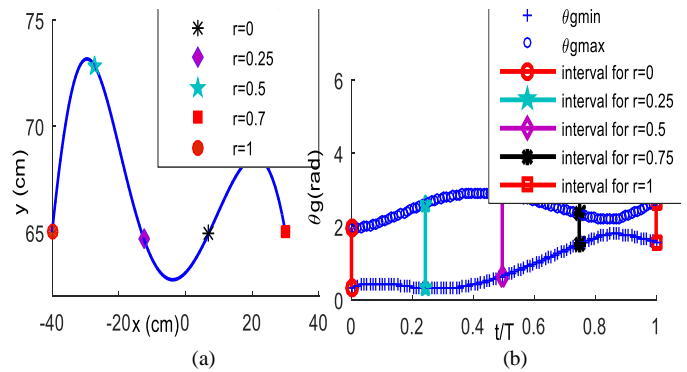


Fig. 6. (a) Traced path (b) the angle domain boundary of traced path in (a).

D. Algorithm

Based on previously presented analyses, the IK algorithm for manipulator continuous path planning can be computed using the following procedure:

- 1) Compute the angle domain boundary using the interval analysis to obtain minimum and maximum angle domains trajectories.
- 2) In the case of hyper-redundant manipulator, defined the additional path in such a way so that such path is used as the moving base of 3-link component and compute the angle domain boundary using interval analysis with respect to the fixed base and the moving base.
- 3) Consider the interval-limited as the interval of interest so that the analysis can be focused on this interval to avoid an ambiguity of values of the angle domain trajectories.
- 4) Completely map the trajectories of minimum/maximum angle domains from the initial configuration to the final configuration to construct the angle domain boundary.
- 5) Choose the initial configuration inside the angle domain boundary.
- 6) Optimize the joint angle path by generating the angle domain trajectories, (22), inside the angle domain boundary using the meta-heuristic optimization with the optimization objective is to minimize the joint angle traveling distance.
- 7) The joint angle trajectories can be obtained using (2-7). For the hyper-redundant manipulator, compute the joint angle trajectories with respect to fixed base and the moving.

V. PATH PLANNING OPTIMIZATION

For kinematically redundant manipulator, there will be many possible solutions to achieve the desired motion. Using the proposed approach, the redundancy resolution of the continuous path planning lies within the angle domain boundary. There will be one searching parameter, f , as (22). To choose the best solution, the meta-heuristic optimizations, which are the GA, the PSO and the GWO will be employed in this paper to search the optimal solution with the optimization objective is to minimize joint angle traveling distance as (1a).

A. Genetic Algorithm

There are three main operators in the GA: reproduction, crossover, and mutation. The searching parameter is represented into the chromosome to be coded to find the best individual with the best fitness value. Fig. 7 gives the illustration of the GA procedure to solve the continuous path planning of the arm robot manipulator.

B. Particle Swarm Optimization

The PSO is firstly proposed by Kennedy and Eberhart [18]. The searching parameters are denoted as particles in the PSO. The particle moves with a certain velocity value. Fig. 8 illustrates the PSO procedure to solve the continuous path planning of the arm robot manipulator.

Velocities and positions are evaluated according to the local and global best solutions. The velocity for each particle is updated and added to the particle position. If the best local solution has better fitness than that of the current global solution, then the best global solution is replaced by the best local solution.

Eberhart and Shi [19] proposed the velocity by utilizing constriction factor, χ , in the following:

$$v_{t+1} = \chi \{ \omega v_t + \varphi_1 \beta_1 (p_i - x_i) + \varphi_2 \beta_2 (p_g - x_i) \} \quad (23)$$

$$\chi = \frac{2}{2 - \varphi - \sqrt{\varphi^2 - 4\varphi}}; \varphi = \varphi_1 + \varphi_2 \quad ; \quad \varphi > 4$$

where v_t , v_{t+1} , φ_1 , and φ_2 are the velocity, the update velocity, cognitive parameter, social parameter, respectively. β_1 and β_2 are independent uniform random number, p_i and p_g are best local solution, and best global solution, while x_i is the current position in the dimension considered.

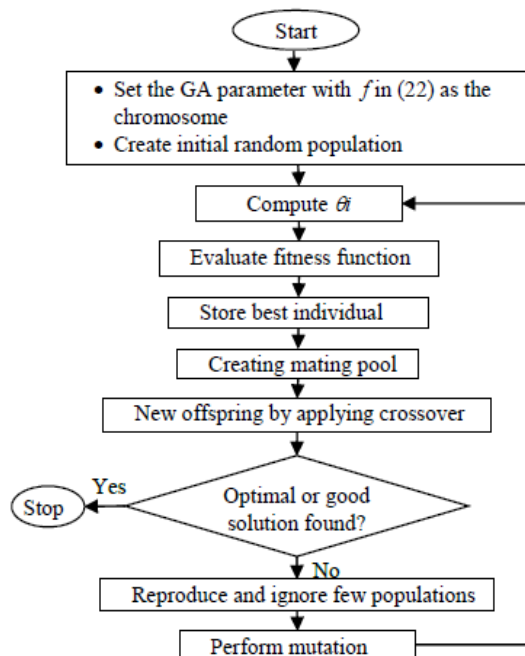


Fig. 7. GA algorithm to solve the continuous path planning.

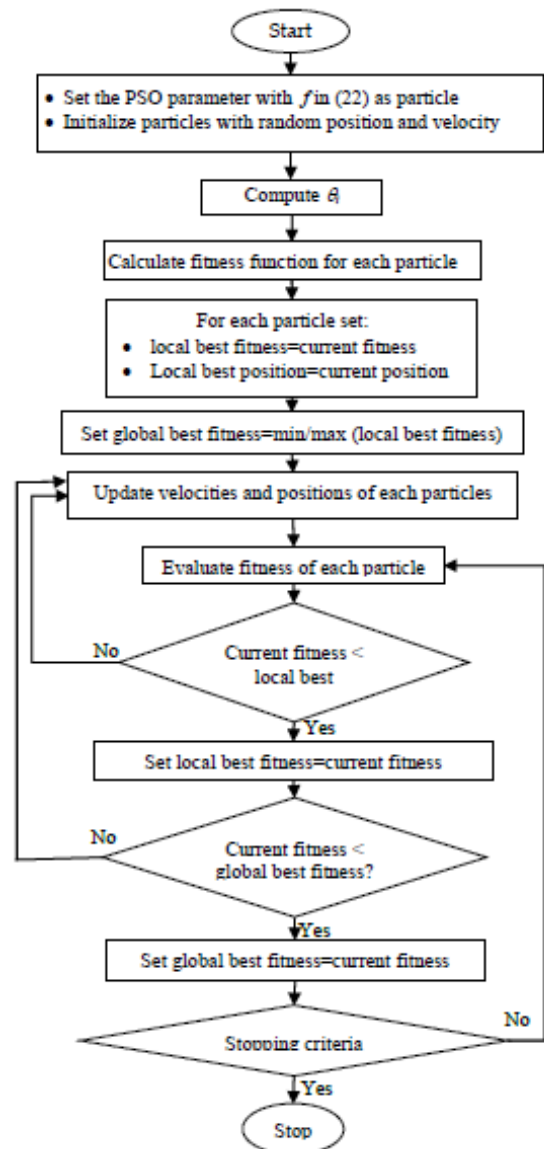


Fig. 8. PSO algorithm to solve the continuous path planning.

C. Grey Wolf Optimizer

The GWO is the meta-heuristic technique developed by Mirjalili et al in 2014 [20]. It is inspired from the leadership hierarchy and hunting mechanism of grey wolves in nature. There are four types of grey wolves which are alpha, beta, delta, and omega. It involves three steps, namely hunting, searching for prey, encircling prey, and attacking prey. Fig. 9 illustrates the path planning algorithm using the GWO.

The encircling prey by the grey wolves is modelled as follows:

$$D = |\vec{C} \cdot \vec{X}_p(t) - \vec{X}(t)| \quad (24)$$

$$\vec{X}_p(t+1) = |\vec{X}_p(t) - \vec{A} \cdot \vec{D}|$$

where t , \vec{A} , \vec{C} , \vec{X}_p , \vec{X} are the current iteration, coefficient vector, coefficient vectors the position vector of the prey, and the position vector of a grey wolf, respectively.

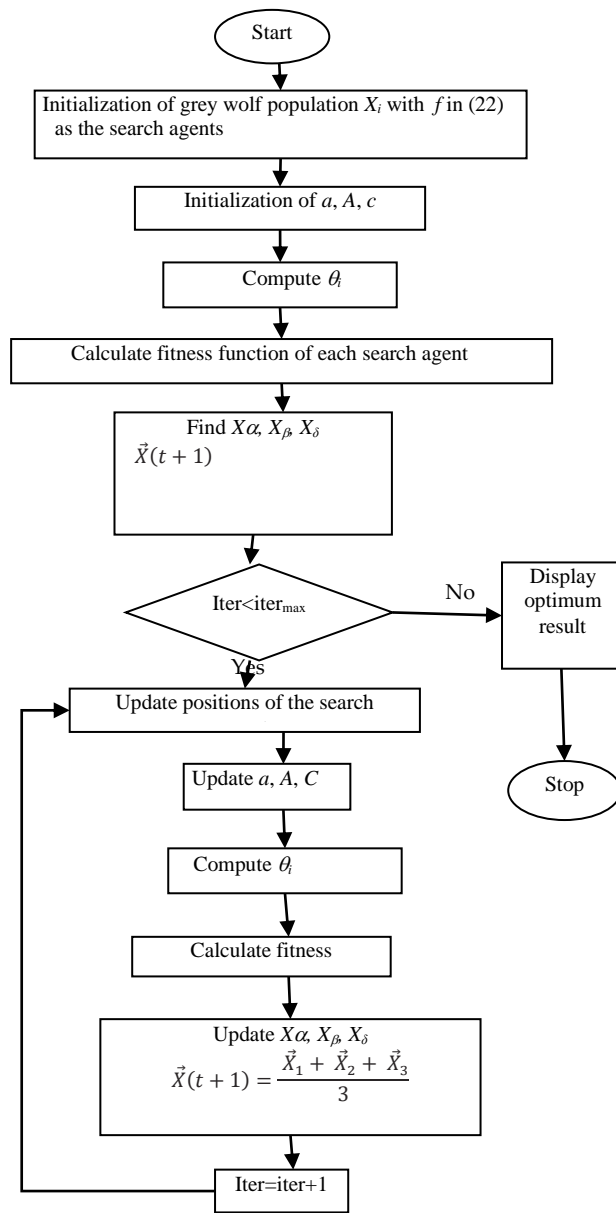


Fig. 9. GWO algorithm to solve the continuous path planning.

The vectors \vec{A} , and \vec{C} are calculated as follows:

$$\begin{aligned} \vec{A} &= 2\vec{A} \cdot \vec{r}_1 - \vec{a} \\ \vec{C} &= 2\vec{r}_2 \end{aligned} \quad (25)$$

\vec{a} are linearly decreased from 2 to 0 over the course of iterations and r_1, r_2 are random vectors in [0, 1].

To simulate the hunting behavior of grey wolves, the first three best solutions obtained are saved and the other search

agents (including the omegas) need to update their positions according to the position of the best search agents. The following formulas are proposed:

$$\begin{aligned} \vec{D}_\alpha &= \vec{C}_1 \cdot \vec{X}_\alpha - \vec{X}; \quad \vec{D}_\beta = \vec{C}_2 \cdot \vec{X}_\beta - \vec{X}; \quad \vec{D}_\delta = \vec{C}_3 \cdot \vec{X}_\delta - \vec{X}; \\ \vec{X}_1 &= \vec{X}_\alpha - \vec{A}_1 \cdot (\vec{D}_\alpha); \quad \vec{X}_2 = \vec{X}_\beta - \vec{A}_2 \cdot (\vec{D}_\beta); \end{aligned} \quad (26)$$

$$\vec{X}_3 = \vec{X}_\delta - \vec{A}_3 \cdot (\vec{D}_\delta);$$

$$\vec{X}(t+1) = \frac{\vec{X}_1 + \vec{X}_2 + \vec{X}_3}{3}$$

The grey wolves finish the hunting by attacking the prey when it stops moving. Approaching the prey is modeled by decreasing the value of \vec{a} . \vec{A} is a random value in $[-2a, 2a]$ where a is decreased from 2 to 0. When random values of \vec{A} are in $[-1, 1]$, the next position of the search agent lays between its current position and the position of the prey. Grey wolves search for prey based on the position of the alpha, beta, and delta to model divergence. \vec{A} values are chosen as random values greater than 1 or less than -1. \vec{C} vector contains random values in interval [0, 2].

VI. RESULTS AND DISCUSSIONS

A numerical experiment has been conducted in MATLAB environment by writing a computer program. The PSO used cognitive and social parameters 1.5 and constriction factor 1. For the GA, the real value coded is used with the selection and mutation rates are 0.5 and 0.1, respectively. The GA, PSO, and GWO are evaluated using 100 iterations and 20 individuals in the population. The computation of the path planning algorithm used 1000 sampling points to conduct the motion from the initial point to the final point.

A. 3-DOF Manipulator

Bezier curve, which is frequently used in the manufacturing, will be employed as the end-effector path to be tracked by the 3-DOF planar series manipulator which has the lengths $l=[30 \ 30 \ 20]$. A fifth-degree Bezier curve is utilized as the tracked curve as illustrated in Fig. 10(a). Detail of these tracked curves can be seen in Table I. Using the interval analysis of the self-motion, Fig. 10(b) shows the result of the angle domain boundary of the Bezier curve.

This paper considers the first and third joint angle does not have joint limits and only the second joint angle, θ_2 , has constraint as follows:

$$0 \leq \theta_2 \leq \pi \quad (27)$$

Considering the above joint angle constraint, the second joint angle trajectories from the negative root of (3) is not feasible, so that only the positive root of (3) is considered in the optimization.

TABLE I. BEZIER CURVE TRACKED PATH CONTROL POINTS

B_0	B_1	B_2	B_3	B_4	B_5
(50,-10)	(85,30)	(50,50)	(60,-10)	(58,30)	(70,-10)

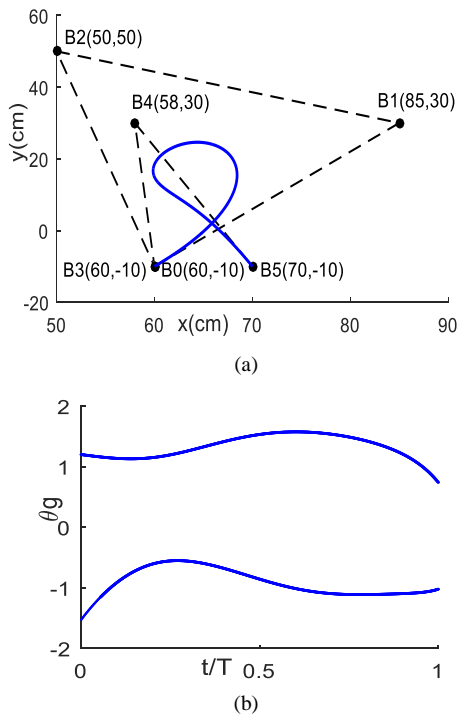


Fig. 10. (a) Fifth Bezier tracked path (b) Boundary of angle domain of path (a).

The angle domain trajectories should be kept inside the angle domain boundary. This requirement can be achieved by choosing the proper value of amplitude A and initial angle domain, θ_{gi} , in (22) in such way so that the generated angle domain trajectories lie within such boundary. This paper uses the value of $A=0.4$ and $\theta_{gi}=0.3$. Fig. 11 shows the result of the fitness value evolution during 100 iterations for the GA, the PSO, and the GWO. The searching area for f is $[0, 15]$. Detail of the path planning results is tabulated in Table II. According to the fitness value, the PSO yields better result than that of the GA and the GWO. The GWO result is near to the value of the PSO result while the result from the GA is quite far from the PSO value. Fig. 12(a) illustrates the joint angle results of the optimal solution obtained by the optimal result obtained from PSO. The posture during the motion to track the Bezier curve using this optimal value is shown in Fig. 12(b).

TABLE II. PATH PLANNING RESULTS

	Fitness	f
GA	4.8486	0.5562
PSO	4.84829399	0.5329
GWO	4.84829414	0.5330

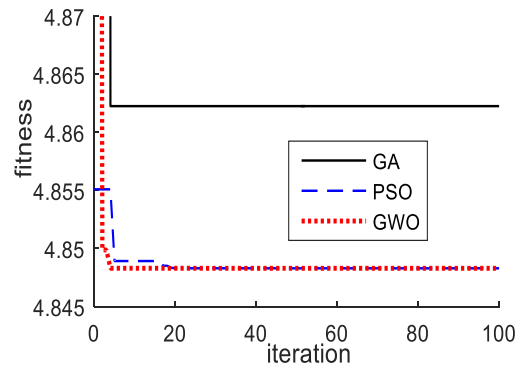


Fig. 11. Fitness value evolution (a) GA (b) PSO (c) GWO.

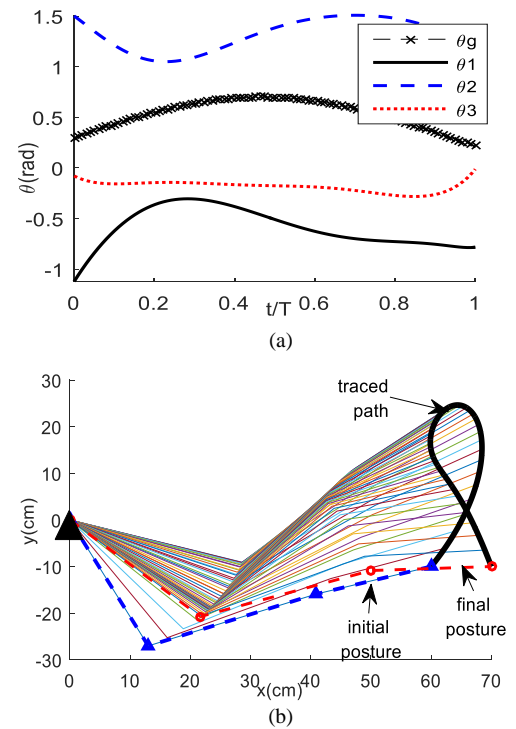


Fig. 12. Optimal result by PSO (a) joint angle, $f=0.5329$ (b) configuration.

B. Hyper-Redundant Manipulator

This section applies the proposed approach to the 6-link planar series manipulator. The manipulator has the same length for each link, $l=[30\ 30\ 30\ 30\ 30\ 30]$ cm.

Fig. 13 shows the illustration of the developed approach applied to the 6-link serial manipulator. Tracking point A' can be carried out using the same procedure as in a 3-DOF planar series manipulator with respect to point A. There will be a moving coordinate system: (x_o', y_o') . In the case of the first 3-DOF planar series robot, the coordinate is fixed because the base does not move. The moving coordinate or moving frame should be kept inside the first three-link manipulator workspace. 6-DOF planar series robot will consist of 3-DOF planar series robot with fix base and virtual 3-DOF planar series robot with moving base.

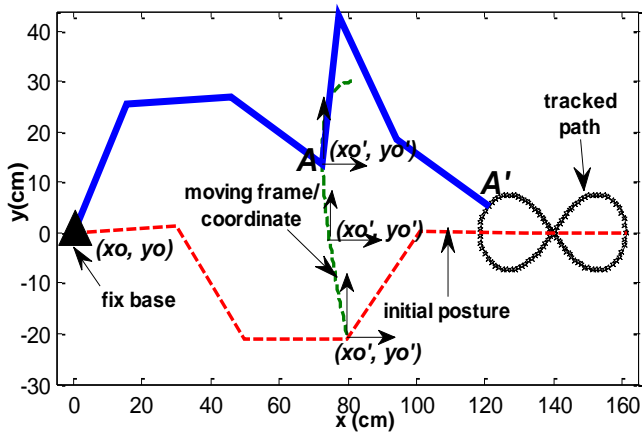


Fig. 13. Moving frame/coordinates of 6-DOF manipulator.

A complex geometrical curve, namely, generalized clothoid [12], is used as the traced curve. The clothoid is generalized using the polynomial function as follows:

$$x(t) = x_c + k \int_0^t \sin(p(u)) du \quad (28)$$

$$y(t) = y_c + k \int_0^t \cos(p(u)) du$$

where (x_c, y_c) , k , and $p(u)$ are the center of the curve, the scale factor, and the polynomial function, respectively.

This paper uses $(x_c, y_c) = (110, 20)$, $k = 25$, $t = [-4.712, 0]$ and the polynomial function in the following:

$$p(u) = (0.33u^3 - 4u) \quad (29)$$

The manipulator has constraints of the second and fifth joint angle as follows:

$$0 \leq \theta_2 \leq \pi ; 0 \leq \theta_5 \leq \pi \quad (30)$$

Considering the above constraints, only the positive root of (3) is feasible. The moving base for the virtual 3-DOF planar robot needs to be determined. This paper models the moving base using a cubic Bezier curve with the control points: $B_0(80, 30)$, $B_1(70, 30)$, $B_2(70, 10)$, and $B_3(80, -21)$. This moving base should be kept inside the workspace of the first 3-DOF planar series manipulator.

Computing the angle domain boundary for the first 3-link manipulator to track the cubic Bezier curve of the moving base, the angle domain boundary is illustrated in Fig. 14(a). Fig. 14(b) shows the angle domain boundary to track the clothoid curve with respect to the moving base. The value of amplitude used is 0.4 for both the fixed base and the moving base. For the value of θ_{gi} , this paper uses 0.35 and 0 for the fixed base and the moving base, respectively. The searching area for f is $[0, 15]$. Detail of the path planning results is presented in Table III. As in the 3-DOF planar series manipulator, for the fixed base, the PSO has outperformed the GA and the GWO where the PSO yields the lowest fitness

value. For the moving base, the PSO and the GWO converge to the same optimal value. They have lowest fitness value as compare with the GA result.

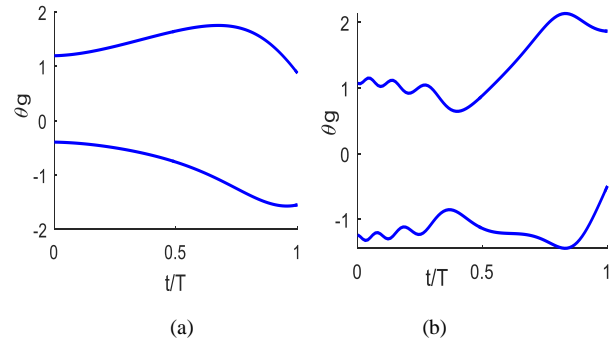


Fig. 14. Angle domain boundary (a) fixed base (b) moving base.

TABLE III. PATH PLANNING OF CLOTHOID PATH BY 6-LINK MANIPULATOR

	Fix base		Moving base	
	Fitness	f	Fitness	f
GA	5.1635	0.5304	9.6343	0.1748
PSO	5.147048672	0.5524	9.6279	0.1551
GWO	5.147048758	0.5523	9.6279	0.1551

Fig. 15 shows the fitness value evolution during 100 iterations to track the Bezier curve with respect to the fixed base for the GA, the PSO, and the GWO. Fig. 16 shows the fitness value evolution during 100 iterations to track the clothoid curve with respect to the moving base for the GA, the PSO, and the GWO.

Fig. 17(a) and 17(b) show the joint angle domain trajectories for the first 3-link and the second 3-link using the optimal value of f , respectively. Here, the fourth joint angle is in the form of the absolute angle where the positive direction is calculated counter clockwise from the x -axis. The configuration of the optimal path to track the clothoid using the 6-DOF hyper-redundant manipulator is illustrated in Fig. 17(c).

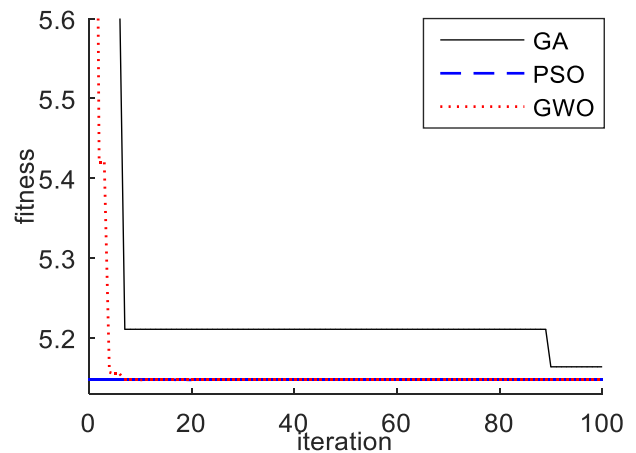


Fig. 15. GA, PSO, GWO fitness value evolution for fix based.

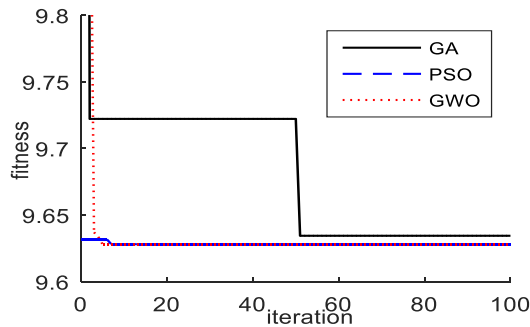


Fig. 16. GA, PSO, GWO fitness value evolution for moving base.

The results in this section have shown that the developed approach have succeeded to solve the continuous path planning of the redundant manipulator. The approach has also succeeded to be applied to the hyper-redundant manipulator. The proposed approach is based on the interval analysis of the self-motion of the 3-link serial manipulator. The connectivity of the generated path is achieved by modeling the angle domain trajectories inside the angle domain boundary. The proposed approach is very promising for solving the redundant/hyper-redundant manipulator since it does not require the matrix inversion. To select the best solution among many possible solutions, the meta-heuristic optimization is employed with the objective is to minimize the joint angle traveling distance. The optimization can be focused in keeping the angle domain trajectories within the angle domain boundary of the traced path while satisfying the optimization criterion. In general, the PSO has better performance than that of the GA and the GWO, except for the case of hyper-redundant manipulator in tracking the clothoid curve where the PSO and the GWO converge to the same fitness value for the moving base.

For future works, developing the computational strategy to generate the angle domain trajectories inside the boundary which give better results than that of the sinusoidal function is an open research to be conducted.

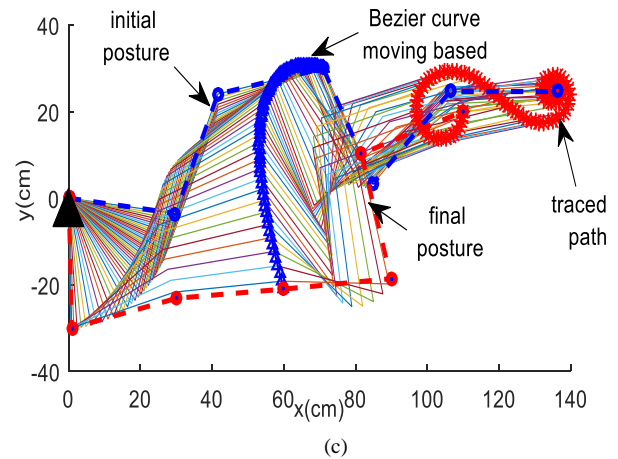
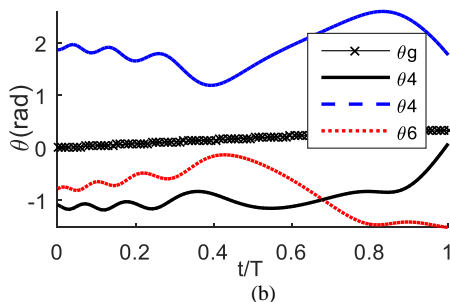
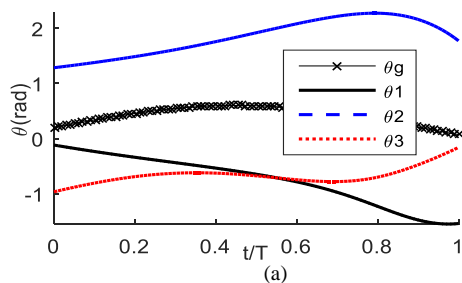


Fig. 17. Optimal result (a) joint angle of fix base, $f=0.5524$ (b) joint angle of moving base, $f=0.1551$ (c) configuration of 6-DOF manipulator to track the clothoid curve.

VII. CONCLUSIONS

The path planning algorithm of the redundant and hyper-redundant manipulators to track the complex geometrical path has been developed. The self-motion of the traced path was mapped into the interval of the angle domain and the redundancy resolution existed within the angle domain boundary. Generating the angle domain trajectories using the continuous function, namely the sinusoidal function, the connectivity among the sampling points can be achieved where the generated joint angle trajectories and posture were smooth. To solve kinematic redundancy problem, the meta-heuristic optimization, namely the GA, the PSO, and the GWO was employed to achieve the optimal solution with the objective optimization is to minimize the joint angle travelling distance. Results showed that the PSO had better performance than that of the GA and GWO where during 100 iterations the PSO yielded the lowest fitness value.

REFERENCES

- [1] X. Pan, J. Polden, N. Larkin, S. V. Duijn, J. Norrish, "Recent progress on programming methods for industrial robots," *Robot. Comput.-Integr. Manuf.*, Vol. 28, pp. 87-94, 2012.
- [2] D.E. Whitney, "Resolved motion rate control of manipulators and human prostheses," *IEEE Trans. Man-Mach. Syst.*, Vol. 10, pp.47-53, 1969
- [3] J. Baillieul, "Kinematic programming alternatives for redundant manipulators," *Proceedings IEEE International Conference on Robotics and Automation*, pp. 722-728, 25-28 March 1985.
- [4] C. W. Wampler, "Inverse kinematic function for redundant manipulators," *Proceedings IEEE International Conference on Robotics and Automation*, pp. 610-617, March 1987
- [5] J. W. Burdick, "On the inverse kinematics of redundant manipulators: characterization of the self-motion manifolds," *proceedings IEEE International Conference on Robotics and Automation*, pp. 264-270, May 1989.
- [6] O. Khatib, "Inertial properties in robotic manipulation: An object-level framework," *Int. J. Robot. Res.* Vol. 14, pp.19-36, 1995.
- [7] K. Tcho'n, J. Karpi'nska, M. Janiak, "Approximation of Jacobian inverse kinematics algorithms", *Int. J. Appl. Math. Comput. Sci.* Vol. 19, pp. 519-531, 2009

- [8] G. S. Chirikjian, J. W. Burdick, "A modal approach to hyper-redundant manipulator kinematics Robot," IEEE Trans. Robot. Autom. Vol. 10, p. 343-354, 1994.
- [9] S. Yahya, M. Moghavvemi, H. A. F. Mohamed, " Geometrical approach of planar hyper-redundant manipulators: Inverse kinematics, path planning and workspace," Simul. Model. Pract. Theory, Vol. 19, pp. 406-422, 2011.
- [10] S. Ebrahimi, P. Payvandy, "Efficient constrained synthesis of path generating four-bar mechanisms based on the heuristic optimization algorithms," Mech. Mach. Theory Vol. 85, pp.189-204, 2015
- [11] C. Yue, H-J. Su, Q. J. Ge, "A hybrid computer-aided linkage design system for tracing open and closed planar curves," Comput.-Aided Des. Vol. 44, pp. 1141-1150, 2012.
- [12] J. P. Merlet, "A generic trajectory verifier for the motion planning of parallel robot," J. Mech. Des., Vol. 123, pp. 510-515, 2001.
- [13] Z. Yao, K. Gupta, "Path planning with general end-effector constraints," Robot. Auton. Syst. Vol. 55, pp. 316-327, 2007.
- [14] H. Ananthanarayanan, R. Ordonez, "Real-time inverse kinematics of (2n+1) DOF hyper-redundant manipulator arm via a combined numerical and analytical approach," Mech. Mach. Theory, Vol. 91, pp. 209-226, 2015
- [15] P. Wenger, P. Chedmail, "Ability of a robot to travel through its free workspace," Int. J. Robot. Res. Vol. 10, pp. 214-227, 1991.
- [16] P. Wenger, "Performance Analysis of Robots." in Robot manipulators: modeling, performance, analysis, and control, E. Dombre, W. Khalil, Eds. ISTE Ltd, London, UK, 2007, pp. 141-183
- [17] J. Angeles, "Fundamental of Robotic : Mechanical Systems: Theory, Methods, and Algorithms," Springer, New York, NY, 2002
- [18] J. Kennedy, R. C. Eberhart, "Particle Swarm Optimization," Proceedings IEEE International Conference on Neural Networks, pp. 1942-1948, Nov 1995.
- [19] R. C. Eberhart, Y. Shi, "Comparing inertia weights and constriction factors in particle swarm optimization," Proceedings IEEE Congress Evolutionary Computation, pp. 84-88, July 2000.
- [20] S. Mirjalili, S. M Mirjalili, A. Lewis, "Grey wolf optimizer," Adv. Eng. Softw., Vol. 69, pp. 46-61, 2014.

On the Sampling and the Performance Comparison of Controlled LTI Systems

Sirine FEKIH, Boutheina SFAIHI, Mohamed BENREJEB

Université de Tunis El Manar,
Laboratoire de Recherche en Automatique (LARA),
BP37, 1002 Tunis, Le Belvédère, Tunisia

Abstract—In this paper, the impact of the discretization techniques and the sampling time, on the finite-time stabilization of sampled-data controlled Linear Time Invariant (LTI) systems, is investigated. To stabilize the process in finite time, a discrete-time feedback dead-beat controller is designed for the sampled-data system. Checkable conditions on the approximate discrete-time plant model and the associated controller that guarantee the finite-time stabilization of the exact model are developed. The trade-off between the discretization technique, the sampling time and the desired performances is illustrated and discussed. Results are presented through a case study.

Keywords—Sampled-data systems; discretization; finite time stabilization; dead-beat control

I. INTRODUCTION

Most real systems evolve naturally in continuous time, but, nowadays, modern control strategies are typically implemented through digital devices to meet high-demanding control performance specifications. For these purposes, different discretization schemes and numerical approximation techniques are developed [1]-[4]. The most cited methods include the Zero Order Hold (ZOH) technique, which is an exact sampling-data representation of the original continuous system, and numerical approximations techniques [4], [5]. The ZOH is placed at the input of the considered process to hold the input signal constant until the next sample becomes available. However, very often exact solutions of the differential equations process are not available. In consequence, numerical approximation approaches turn out to be essential to yield accurate approximations of the real solutions [5], Euler approximation methods (forward and backward) are basic approaches of numerical integration [4], [5]. The Euler rule for discrete approximation of integral functions between two sampling instant gives an approximate area of a rectangle whose base is the sampling interval and whose height is the value of the function at the lower limit (forward) or final limit (backward Euler). This simple and easy to implement technique became a popular digital implementation method. The stability conditions and convergence of the Euler techniques have been developed for linear systems [3] and for some classes of nonlinear systems [6]. The main disadvantage of the Euler's techniques is that either they overestimate or underestimate the integral. Tustin (bilinear, trapezoidal) approximation [7], [8] overcomes these disadvantages by taking the average of the limiting values of the integrand. As such, it treats the area between the two integration limits as trapezium.

The problems of control design and performances analysis for linear and nonlinear dynamical systems [9]-[18] are still important nowadays. Three techniques are known in the literature for the digital controllers construction of continuous-time systems: 1) Design of a continuous-time controller and, then, its discretization; 2) Discretization of the plant and construction of a discrete-time controller on the basis of the associated sampled-data model [19]; and 3) Direct digital controller design based on a continuous-time plant model without approximations [19]. Cited techniques show acceptable performances when the sampling is fast. But, the discrete construction controller method (b) does not need a fast sampling to maintain stability as it utilizes an approximation of the process ignoring the inter-sample system behavior.

In practical engineering processes, the increase need of time performance criteria and exact time specifications of the dynamics behaviors has led to the development concept of finite-time convergence stability and stabilization [20]. Considered in the literature of dead-beat control and optimality, the capacity to force a dynamic control system to reach a specified target in a finite time called settling time, represents the main merit of the finite-time control. Finite-time stabilization techniques have attracted a great deal of attention and have become a heated research issue in control systems theory [21]-[24]. Early works on the topic developed relevant finite-time stabilization approaches for different classes of linear and nonlinear discrete-time systems. Researchers have investigated the finite-time stabilization of discrete time linear time-varying systems in [25], subject to disturbances in [26], with time-varying delay in [27] and uncertain and subject to exogenous disturbances in [28]. Finite-time stabilization issues of nonlinear plants have been investigated. Systems which can be represented by affine fuzzy systems were considered in [24], the class Lur'e type systems in [5] and uncertain systems in [29], [30]. Although the encouraging works in the field, investigations about the effect of the sampling technique on the system performance in term of stability and finite-time stabilization were not included.

In this note we discuss important issues when selecting the sampled-data description in the context of a dead-beat control applied to LTI systems. The discussion is based on an example of a third order system that, from our point of view, can be understood in a common framework to select discrete-time models and synthesize dead-beat controllers. The treatment is limited for simplicity to the linear case but the extension to the

nonlinear case is possible, at least for some class of Lure-type systems, by considering sector bounded nonlinearities [23].

The remainder of this work is organized as follows. In Section II, the problem setup to be considered is introduced and previous results concerning the stability and the finite-time stabilization are recalled. In Section III, a discussion of the influence of the discretization techniques and the sampling times on the system performances is developed through a third order case study. Concluding remarks are drawn in Section IV.

II. PROBLEM STATEMENT AND PRELIMINARIES

In this section, the sampled-data system under consideration is introduced and the problem formally stated.

A. System Description and Discretization

Let's consider the controlled sampled-data system S of Fig. 1, in which S_c denotes a continuous Linear Time Invariant (LTI) plant. Blocs (A-D), (DTC), and (D-A) designate the zero-order hold, the discrete-time controller and the ideal sampler, respectively, synchronized by the same sampling time T . We suppose that S_c can be described by the n^{th} following differential equation:

$$S_c : y^{(n)} + \sum_{i=1}^n a_i^c y^{(n-i)} = \sum_{j=0}^{n-1} b_j^c u^{(n-1-j)} \quad (1)$$

and in the state space description by

$$S_c : \begin{cases} \dot{x}(t) = Ax(t) + Bu(t) \\ y(t) = Cx(t) \end{cases} \quad (2)$$

$u(t) \in \mathbb{R}$ denotes the control signal delivered to the plant, $y(t) \in \mathbb{R}$ the plant's measured output, $x(t) = (y, y^{(1)}, \dots, y^{(n-1)})^T \in \mathbb{R}^n$ the state vector and t the time. a_i^c and b_j^c are constant parameters for $i=1,2,\dots,n$ and $j=0,1,\dots,n-1$. A , B and C are known matrices of appropriate dimensions.

It is desired to develop a state feedback control to the introduced continuous-time system in a discrete-time approach by sampling the continuous plant and applying a discrete-time controller. Using the sampler and ZOH, the continuous plant (2) is discretized to the following exact sampled-data representation

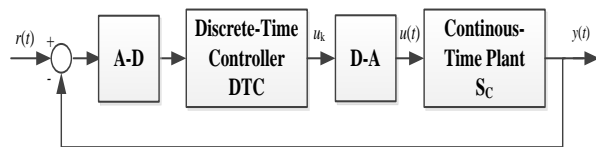


Fig. 1. Sampled-data controlled system.

$$(S_{SD}) : \begin{cases} x_{k+1} = Fx_k + Gu_k \\ y_k = Cx_k \end{cases} \quad (3)$$

Applying, now, the discrete-time state feedback control

$$u_k = -\Lambda x_k + Lr_k \quad (4)$$

the closed-loop controlled system becomes

$$(S) : \begin{cases} x_{k+1} = Mx_k + GLr_k \\ y_k = Cx_k \end{cases} \quad (5)$$

With

$$M = F - G\Lambda \quad (6)$$

x_k , y_k , u_k and r_k define, respectively, $x(kT)$, $y(kT)$, $u(kT)$ and $r(kT)$; $k \in \mathbb{Z}$. We assume that the state measurements x_k are available at sampling instants kT and the pair (F, G) is controllable. $F \in \mathbb{R}^{n \times n}$ and $G \in \mathbb{R}^n$ are the discrete system matrices defined, respectively, by [4]

$$F = e^{AT}, \quad G = \int_0^T e^{At} B dt \quad (7)$$

$\Lambda = [\lambda_j] \in \mathbb{R}^n$, $j=0,1,\dots,n-1$ and $L = [\gamma] \in \mathbb{R}$ are the static gains controller.

Finally, we suppose that the controlled sampled-data system (5)-(6) can be described by the recursive input/output scalar equation, as

$$(S) : y_{k+n} + \sum_{i=1}^n a_i y_{k+n-i} = \sum_{j=0}^{n-1} b_j r_{k+n-1-j} \quad (8)$$

ZOH discretization approach leads to an exact sampled-data model S_{SD} ; the continuous-time output of (2) is exactly recovered at the sampling instants, i.e., $y_k = y(kT)$. But, in many cases, analytical integration may be impossible or infeasible, in particular for nonlinear systems. Numerical integration techniques become essential to yield accurate approximations of the actual solutions. In that respect, forward Euler and Tustin are basic and well used approximations approaches. An approximate discrete-time state space model of (2) can be given by

$$(\hat{S}_{SD}) : \begin{cases} x_{k+1} = \hat{F}x_k + \hat{G}u_k \\ y_k = Cx_k \end{cases} \quad (9)$$

where, for forward Euler approximation, matrices \hat{F} and \hat{G} are defined, respectively, by [3], [4]

$$\hat{F} = I + TA, \quad \hat{G} = TB \quad (10)$$

and for Tustin approximation, respectively, by [19], [31]

$$\hat{F} = \left(\frac{I}{T} - \frac{A}{2} \right)^{-1} \left(\frac{I}{T} + \frac{A}{2} \right), \quad \hat{G} = \left(\frac{I}{T} - \frac{A}{2} \right)^{-1} B \quad (11)$$

The evaluation of the exponential and integral matrices (7) for the exact discretization technique, and the matrix inversion (11) for the Tustin approximation, are generally time-consuming and may necessitate a high speed processor for real-time implementations, especially for large scale systems.

Besides, the forward Euler approximation technique is a simpler and less costly representation.

B. Finite-Time Stabilization and Problem Statement

Stability property of the discretized LTI closed loop system (5)-(6) depends on the state matrix M and the sampling time choice. Let us denote by $\sigma(M)$ the spectral radius, i.e., $\sigma(M) = \text{Max}\{|\lambda| : \lambda \text{ is an eigenvalue of } M (n \times n) \text{ matrix}\}$.

Lemma 1. [32] If $\sigma(M) < 1$, the eigenvalues of the matrix M are located within the unit circle, then the system (5)-(6) is asymptotically stable.

Considered as an advanced control design technique, dead-beat control [33], [34] is developed in the context of finite time stabilization and finite settling time, which aims to perfectly tracking a step reference in a finite number of sampling periods.

Definition 1. [35] A stabilizing controller of systems are said to be a dead-beat controller if the tracking output $y(kT)$ settles down to zero in a finite number of steps $k = N_d$ and $y(kT) = 0, \forall k \geq N_d; N_d$ is the settling step.

Definition 2. [36] Consider a continuously working system. Then, the finite number of control steps is such a finite number of values n of the sequence $U = \{u(k_0), u(k_0+1), \dots, u(k_0+n-1)\}$ by which the system is transferred from an arbitrary initial state $x(k_0) \neq 0$ to the final state $x(k_0+n) = 0, \forall k_0 \in \mathbb{Z}$.

Now, let consider the discretized system described by (8) such that for $\forall i = 1, 2, \dots, n$, a_i are expressed in terms of λ_j , $j = 0, 1, \dots, n-1$, and T .

Lemma 2. [37] The n^{th} linear discrete-time system (8) is said to be stabilizable in n sampling time, if the gains λ_j , $j = 0, \dots, n-1$, and T , are synthesized, such that y_{k+n} settles down to zero in n steps, that's equivalent to setting $(F - G\Lambda)^n = 0$ ($(F - G\Lambda)$ is nilpotent with the index n), or equivalently, the $a_i = 0$ for $i = 1, 2, \dots, n$.

This note investigates the influence of the discretization method in the controlled system properties. The work is a continuation of the previous paper [23] in which the effects of a ZOH discretization on the stability and stabilization properties of linear and nonlinear Lure-type systems are considered. The aim of this paper is to investigate more discretization techniques, mainly, the forward Euler and the Tustin approximations, and study the impact of a numerical approximation on the control system (5) on the system properties in term of stability and finite-time stability.

III. CASE STUDY

In this section, we develop sufficient finite-time stability conditions of a controlled sampled-data third-order system via 1) the exact solution; and 2) the discrete-time model

approximations. Based on the continuous-time plant model, our main results specify checkable conditions ensuring that a finite-time control stabilizing the approximate model would also stabilizes the exact model in finite-time. These conditions can be used as guidelines for controller design based on approximate nonlinear models.

The main results described in this case study focus on the at sample response.

A. Studied Third Order System Description and Discretization

Consider the third order continuous LTI system configured as in Fig. 1, with the following plant transfer function:

$$S_c : F(s) = \frac{k_s}{s(1 + \tau_1 s)(1 + \tau_2 s)} \quad (12)$$

leading to the following state space controllable form:

$$A = \begin{pmatrix} 0 & 1 & 0 \\ 0 & 0 & 1 \\ 0 & -\frac{1}{\tau_1 \tau_2} & -\frac{\tau_1 + \tau_2}{\tau_1 \tau_2} \end{pmatrix}, B = \begin{pmatrix} 0 \\ 0 \\ \frac{k_s}{\tau_1 \tau_2} \end{pmatrix}, C = \begin{pmatrix} 1 \\ 0 \\ 0 \end{pmatrix}^T \quad (13)$$

k_s is the static gain and τ_1 and τ_2 the constant times of the continuous-time process. The developed sampled-data models of (13) based on the ZOH technique, forward Euler and the Tustin approximations, are $S_{SD} : (F, G, C)$, $\hat{S}_{SD}^e : (\hat{F}^e, \hat{G}^e, C)$ and $\hat{S}_{SD}^t : (\hat{F}^t, \hat{G}^t, C)$, respectively, such that

$$F = \begin{pmatrix} 1 & \frac{\tau_1^2(1-d_1) - \tau_2^2(1-d_2)}{\tau_1 - \tau_2} & \frac{\tau_1 \tau_2 (\tau_1(1-d_1) - \tau_2(1-d_2))}{\tau_1 - \tau_2} \\ 0 & \frac{\tau_1 d_1 - \tau_2 d_2}{\tau_1 - \tau_2} & \frac{\tau_1 \tau_2 (d_1 - d_2)}{\tau_1 - \tau_2} \\ 0 & \frac{d_2 - d_1}{\tau_1 - \tau_2} & \frac{\tau_1 D_2 - \tau_2 d_1}{\tau_1 - \tau_2} \end{pmatrix}$$

$$G = k_s \begin{pmatrix} T - (\tau_1 + \tau_2) + \frac{\tau_1^2 d_1 - \tau_2^2 d_2}{\tau_1 - \tau_2} \\ 1 - \frac{\tau_1 d_1 - \tau_2 d_2}{\tau_1 - \tau_2} \\ \frac{d_1 - d_2}{\tau_1 - \tau_2} \end{pmatrix} \quad (14)$$

$$d_1^{-1} = e^{\frac{T}{\tau_1}} \text{ and } d_2^{-1} = e^{\frac{T}{\tau_2}},$$

$$\hat{F}^e = \begin{pmatrix} 1 & T & 0 \\ 0 & 1 & T \\ 0 & -\frac{T}{\tau_1 \tau_2} & 1 - \frac{(\tau_1 + \tau_2)T}{\tau_1 \tau_2} \end{pmatrix}, \hat{G}^e = \begin{pmatrix} 0 \\ 0 \\ \frac{T k_s}{\tau_1 \tau_2} \end{pmatrix} \quad (15)$$

and

$$\hat{F}^i = \begin{pmatrix} 1 & \frac{2T(\tau_1 + \tau_2) + 2\tau_1\tau_2}{(T + 2\tau_1)(T + 2\tau_2)} & \frac{2T^2\tau_1\tau_2}{(T + 2\tau_1)(T + 2\tau_2)} \\ 0 & \frac{2T(\tau_1 + \tau_2) + 4\tau_1\tau_2 - T^2}{(T + 2\tau_1)(T + 2\tau_2)} & \frac{4T\tau_1\tau_2}{(T + 2\tau_1)(T + 2\tau_2)} \\ 0 & \frac{4T}{(T + 2\tau_1)(T + 2\tau_2)} & \frac{2T(\tau_1 + \tau_2) - 4\tau_1\tau_2 + T^2}{(T + 2\tau_1)(T + 2\tau_2)} \end{pmatrix} \quad (16)$$

$$\hat{G}^i = \begin{pmatrix} \frac{k_s T^3}{(T + 2\tau_1)(T + 2\tau_2)} \\ \frac{2k_s T^2}{(T + 2\tau_1)(T + 2\tau_2)} \\ \frac{4k_s T}{(T + 2\tau_1)(T + 2\tau_2)} \end{pmatrix}$$

Applying a state feedback controller (4), with $\Lambda = (\lambda_0 \quad \lambda_1 \quad \lambda_2)$, the resulting free closed-loop system based on the zero order hold (exact) discretization can be expressed by the recursive input/output (8) where the coefficients a_i ($i=1,2,3$) (A.1)-(A.3) are developed in the Appendix. Now, based on the model approximation, the free controlled system based on the forward Euler technique is such that

$$\hat{S}^e : y_{k+3} + \sum_{i=1}^3 \hat{a}_i^e y_{k+3-i} = 0 \quad (17)$$

with

$$\begin{cases} \hat{a}_1^e = \frac{T}{\tau_1\tau_2} \times (\tau_1 + \tau_2 + k_s\lambda_2) - 3 \\ \hat{a}_2^e = \frac{T}{\tau_1\tau_2} \times ((1 + k_s\lambda_1)T - 2k_s\lambda_2 - 2(\tau_1 + \tau_2)) + 3 \\ \hat{a}_3^e = \frac{T}{\tau_1\tau_2} \times (\lambda_0 k_s T^2 - (1 + k_s\lambda_1)T + \lambda_2 k_s + \tau_1 + \tau_2) - 1 \end{cases} \quad (18)$$

and on the Tustin technique

$$\hat{S}^t : y_{k+3} + \sum_{i=1}^3 \hat{a}_i^t y_{k+3-i} = 0 \quad (19)$$

with

$$\begin{cases} \hat{a}_1^t = \frac{\lambda_0 k_s T^3 + (2\lambda_1 k_s + 1)T^2 + 2(2\lambda_2 k_s - \tau_1 - \tau_2)T - 12\tau_1\tau_2}{(T + 2\tau_1)(T + 2\tau_2)} \\ \hat{a}_2^t = \frac{2\lambda_0 k_s T^3 - T^2 - 2(\tau_1 + \tau_2 + 4\lambda_2 k_s)T + 12\tau_1\tau_2}{(T + 2\tau_1)(T + 2\tau_2)} \\ \hat{a}_3^t = \frac{\lambda_0 k_s T^3 - (2\lambda_1 k_s + 1)T^2 + 2(2\lambda_2 k_s + \tau_1 + \tau_2)T - 4\tau_1\tau_2}{(T + 2\tau_1)(T + 2\tau_2)} \end{cases} \quad (20)$$

Next, we study the finite-time stability based on the exact discretization technique and on the approximations methods.

B. Finite-Time Stability

To illustrate the finite-time stability behavior of the controlled sampled data developed models (8) with (A.1)-(A.3), (17)-(18) and (19)-(20), we consider the process (12) parameters such that $\tau_1 = 0,05s$, $\tau_2 = 0,1s$ and $k_s = 5,89$. The dead-beat controller's output is calculated according to Lemma 2.

1) Control Synthesis based on the Exact Discretion

Based on the ZOH discretization, synthesized controller u_k gains are:

$$\lambda_0 = 1; \quad \lambda_1 = 1,45 \times 10^{-1}; \quad \lambda_2 = 4,8 \times 10^{-3} \quad (21)$$

for a sampling time $T_{db} = 0,2s$ [23]. In order to illustrate the developed controller performances applied to (a) the sampled-data system using a sampler and zero order hold (8) with (A.1)-(A.3), (b) the forward Euler based approximation system (17)-(18) and (c) the Tustin based approximation system (19)-(20), conditions relating stability domains and sampling periods (formulation based on the Jury criteria) are presented in Table I. Maximum values of sampling times T^* , T_e^* and T_t^* (corresponding to ZOH, forward Euler and Tustin discretizations, respectively) that can be simulated maintaining the stability of the sampled data closed-loop system, are calculated. While T_t^* is close to T^* , we note that $T_e^* \ll T^*$; the closed loop-system (17)-(18) is stabilizable for very small time steps with $\Omega^e \subset \Omega^t$ and $\Omega \subset \Omega^t$. Stability conditions introduced in Table I. are tested numerically. The ZOH and Tustin discretization-based techniques are applied with five (05) values of discretization steps (0,1; 0,12; 0,15; 0,17 and 0,2). Forward Euler discretization-based technique is applied with three (03) sampling periods (0,04; 0,06; 0,07). Simulations are carried on for the same initial conditions $x(0) = 10^{-1} \times [1 \quad 0,11 \quad -0,73]^T$. The discrete dynamics of the controlled system based, ZOH, forward Euler and Tustin schemes, are shown in Fig. 2, 3 and 4, respectively. From Fig. 2, it is easy to check that (a) the controlled system based ZOH discretization is asymptotically stable for selected numerical sampling times verifying $T \in \Omega$ and (b) the developed dead-beat control with (21) ensures a transient behaviour elimination in three (03) sampling periods for $T_{db} = 0,2$ with a settling time $t_s = 0,6s$. When the sampling period decreases, the models exhibit a finite-time stability convergence to $t_s = 0,6s$ with a number of steps $m > 3$. Based on simulation results shown in Fig. 3 and 4, forward Euler and Tustin approximations demonstrate, respectively, a stability convergence to the origin $x = 0$, for the developed control (21) for $T \in \Omega^e$ and $T \in \Omega^t$, respectively. Now, comparing the finite time stability performance of the exact discretization ZOH, and approximate based Euler and Tustin techniques, we notice that for the different sampling times (a) the control (21) stabilizes controlled systems based Euler and Tustin approximations, (b) no settling time t_1 ; $t_1 < t_s = 0,6s$ is

obtained, (c) Tustin approximation fails to exhibit a three-sampling time convergence to the origin with T_{db} but, displays a finite time convergence with a settling time $t'_s = t_s$ for $T = 0,12s < T^{db}$ and $T = 0,15s < T^{db}$. The performance deteriorates if we increase the sampling time, as shown in Fig. 4(d) Forward Euler approximation is finite-time stable in $t'_s = 0,77s > t_s$, as shown in Fig. 3. The system shows bad finite-time performances, for small sampling periods. The highest sampling periods that guarantee a minimum settling time are summarized in Table II. It is observed that, with a ZOH discretization, the states of the proposed dead-beat controlled system settle down to the steady-state in three sample periods where $T_{db} = 0,2s$. For a relatively shorter sampling period $T = 0,15s$ and based on a Tustin approximation, the states of the sampled-data controlled system settles down in four sampling periods for $t'_s = t_s = 0,6s$, whereas the states of the conventional forward Euler digitally redesigned sampled-data controlled system has the largest settling time with $t'_s = 0,77s$ and exhibits a Finite-Time Stability (FTS) convergence in eleven sampling periods with $T = 0,07s$. The approximation introduced by the forward Euler model affects the desired dead-beat response and creates an unexpected behaviour for relatively small T .

TABLE I. STABILITY DOMAINS

Stability domains	Zero Order Hold Technique	Forward Euler Approximation	Tustin Approximation
	$\Omega : 0,005s < T < 0,336s$	$\Omega' : 0s < T < 0,099s$	$\Omega' : 0s < T < 0,354s$

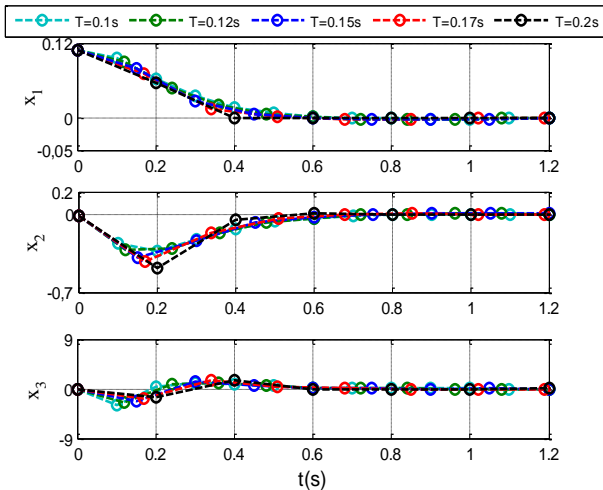


Fig. 2. Sampled-Data Controlled Model Dynamics - ZOH Technique

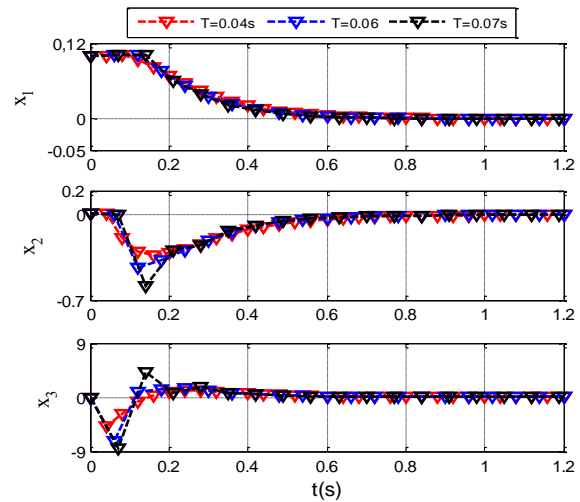


Fig. 3. Sampled-Data Controlled Model Dynamics - Forward Euler Approximation

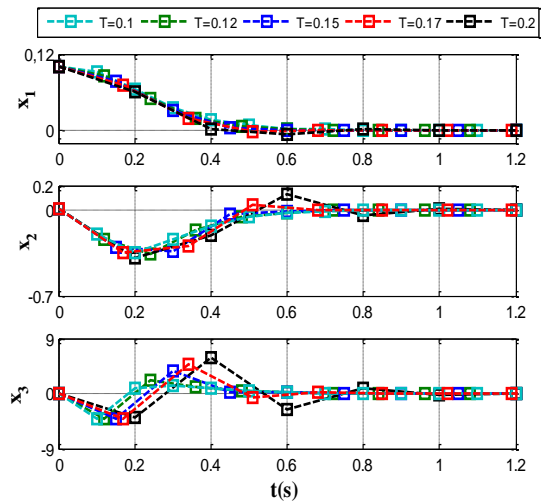


Fig. 4. Sampled-Data Controlled Model Dynamics - Tustin Approximation

TABLE II. FTS COMPARISON OF THE ZOH, FORWARD EULER AND TUSTIN DISCRETIZATIONS

	Sampling Time [s]	Settling Time [s]	Number of Steps
ZOH Technique	$T = 0,2$	$t_s = 0,6$	3
Forward Euler Approximation	$T = 0,07$	$t'_s = 0,77$	11
Tustin Approximation	$T = 0,15$	$t'_s = 0,6$	4

2) *Controller Synthesis based Tustin Approximate Discretization*

Now, the aim is to test if a dead-beat controller which stabilizes a Tustin based approximate discrete-time model also stabilizes in three sampling times the exact discrete model (based on the ZOH) of the plant. For convenience, we use $(u_{k,T_2}^{i,db})$ to refer to the dead-beat controller based Tustin approximation for a sampling time T_2 and $S_i : (F_{T_1}, u_{k,T_2}^{i,db})$ to the sampled-data model F , based ZOH discretization with a sampling time T_1 , for which a stabilizing control $u_{k,T_2}^{i,db}$ is applied. The dead-beat controllers $u_{k,T_2}^{i,db}$ parameters λ_0 , λ_1 and λ_2 , relevant to the sampling periods $T_2 = 0,1, 0,12, 0,15, 0,17$ and $0,2$ are shown in Table III. These parameters values are computed referring to Lemma 2. We note, in regard to the obtained gain parameters, that the λ_0 , λ_1 and λ_2 values become quite large as the sampling period becomes smaller. Developed state feedback dead-beat control $u_{k,T_2}^{i,db}$ is, then, applied to the associated exact sampled-data model with $T_1 = T_2$. The essential characteristics of the system $S_i : (F_{T_1}, u_{k,T_2}^{i,db})$ response, obtained with the proposed control are illustrated in the in Fig. 5. As depicted, the controlled sampled-data systems $S_i : (F_{T_1}, u_{k,T_2}^{i,db})$, for $T_1 = T_2 = 0,1, 0,12, 0,15, 0,17$ and $0,2$, are finite-time convergent in 5, 5, 5, 5 and 4 steps, respectively. The synthesized dead-beat control $u_{k,T_2}^{i,db}$, cannot stabilize the associated exactly discretized system in 3– sampling periods. In order to optimize the system’s performance in accordance to the specified objective, we propose to (i) calculate the dead-beat control u_{k,T_1}^{db} based on the ZOH discretization for the sampling period T_1 , then, (ii) for obtained value parameters, solve $\hat{a}_i^i = 0, i = 1,2,3$ (20), for T_2 . The correspondence between the sampling periods T_1 and T_2 is developed in Table IV. The main point noted from this data is that, considering the set of sampling periods $\Delta = \{0,1; 0,12, 0,15, 0,17; 0,2\}$, T_2 is smaller than T_1 . More tests, for T_1 in $[0,01 .. 0,3]$, have been carried on. The results are depicted in Fig. 6. Clearly, while, for small sampling periods $T_1 \leq 0,05$, we obtain $T_2 = T_1$; for larger sampling periods, $T_2 < T_1$. Fig. 7 shows the simulations results. The controlled system performance gets better for new developed $u_{k,T_2}^{i,db}$. The system states are brought to the origin in three steps. By consequence, for large sampling periods, the dead-beat controller based on the Tustin approximation can lead to an n -finite-time stabilization of the exact sampled-data n -order system by choosing $T_2 < T_1$.

TABLE III. DEAD-BEAT CONTROLLER SYNTHESIS BASED ON THE TUSTIN APPROXIMATION

Sampling Period	$u_{k,T_2}^{i,db}$ Dead-Beat Controller Parameters
$T_2 = 0,1$	$\lambda_0 = 2,54, \lambda_1 = 3,39 \times 10^{-1}$ and $\lambda_2 = 1,06 \times 10^{-2}$
$T_2 = 0,12$	$\lambda_0 = 1,72, \lambda_1 = 2,45 \times 10^{-1}$ and $\lambda_2 = 7,9 \times 10^{-3}$
$T_2 = 0,15$	$\lambda_0 = 1,10, \lambda_1 = 1,60 \times 10^{-1}$ and $\lambda_2 = 5,1 \times 10^{-3}$
$T_2 = 0,17$	$\lambda_0 = 0,86, \lambda_1 = 1,23 \times 10^{-1}$ and $\lambda_2 = 3,8 \times 10^{-3}$
$T_2 = 0,2$	$\lambda_0 = 0,63, \lambda_1 = 0,84 \times 10^{-1}$ and $\lambda_2 = 2,1 \times 10^{-3}$

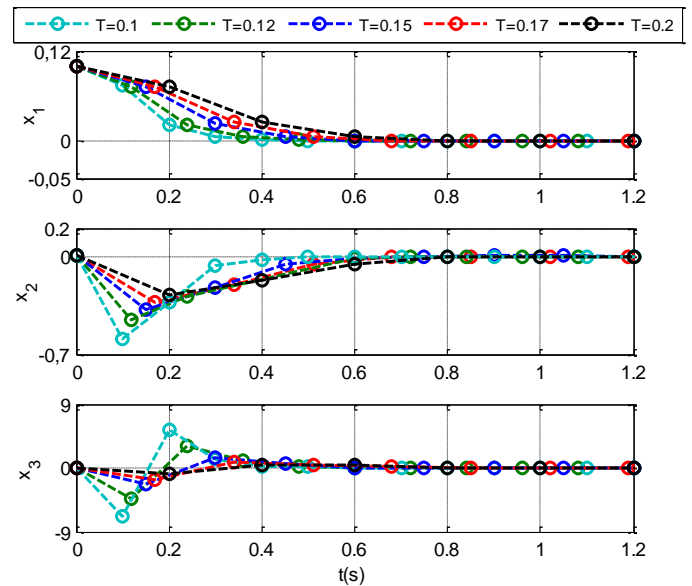


Fig. 5. Controlled Exact sampled-Data Model dynamics – Case 1: Dead-Beat Control based on the Tustin approximation with $T_1 = T_2$

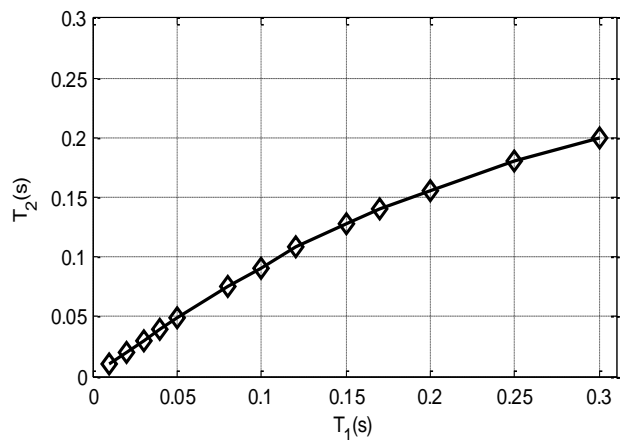


Fig. 6. $T_1 - T_2$ Matching

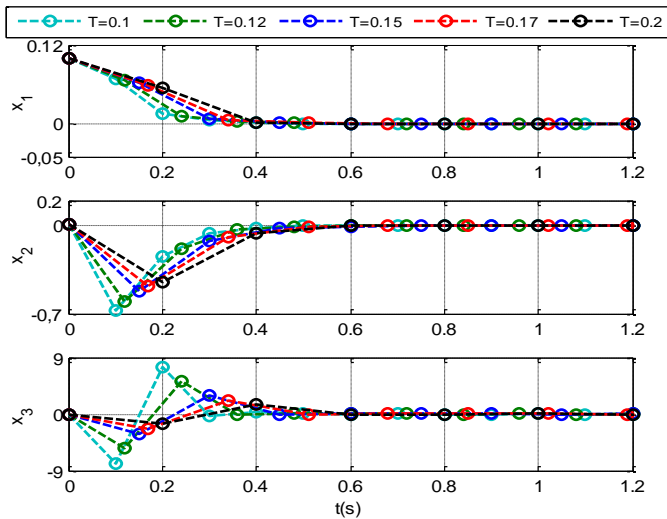


Fig. 7. Controlled Exact sampled-Data Model dynamics – Case 2: Dead-Beat Control based on the Tustin approximation with $T_2 < T_1$

IV. CONCLUSION

The finite-time stabilization issues of sampled-data linear time invariant systems are discussed. Based on a third-order case study, sufficient conditions ensuring the finite-time stabilization for the exact and the approximate Forward Euler and Tustin approximation models, are derived. Models performances have been compared for some stabilizing sample periods. It has been shown that, while Forward Euler technique outlines a constraining stability domain, Tustin approximation shows better performances. Moreover, it was observed that under some matching conditions, the dead-beat controller based on the Tustin approximation leads to an n -finite-time stabilization of the exact sampled-data n order system. Developed results can be extended to finite-time stabilization of nonlinear systems as shown in [23].

TABLE IV. DEAD-BEAT CONTROLLER SYNTHESIS BASED ON THE TUSTIN APPROXIMATION WITH $T_2 < T_1$

T_1	T_2	u'_{k,T_2} Dead-Beat Controller Parameters
$T_1 = 0,1$	$T_2 = 0,09$	$\lambda_0 = 3,10, \lambda_1 = 0,37$ and $\lambda_2 = 1,12 \times 10^{-2}$
$T_1 = 0,12$	$T_2 = 0,108$	$\lambda_0 = 2,22, \lambda_1 = 0,29$ and $\lambda_2 = 0,89 \times 10^{-2}$
$T_1 = 0,15$	$T_2 = 0,128$	$\lambda_0 = 1,53, \lambda_1 = 0,21$ and $\lambda_2 = 0,68 \times 10^{-2}$
$T_1 = 0,17$	$T_2 = 0,14$	$\lambda_0 = 1,26, \lambda_1 = 0,18$ and $\lambda_2 = 0,58 \times 10^{-2}$
$T_1 = 0,2$	$T_2 = 0,155$	$\lambda_0 = 1, \lambda_1 = 0,14$ and $\lambda_2 = 0,48 \times 10^{-2}$

APPENDIX

The free controlled sampled-data model based on a zero order hold discretization of (12) can be given by

$$S: y_{k+3} + \sum_{i=1}^3 a_i y_{k+3-i} = 0$$

where the coefficients a_i , $i = (1,2,3)$, are defined, respectively, by

$$a_1 = (d_1^{-1}d_2^{-1}(\tau_2 - \tau_1))^{-1} \times \begin{pmatrix} k_s \lambda_0 d_2^{-1} (d_1^{-1} - d_2^{-1}) \tau_1^2 + k_s \lambda_0 d_1^{-1} (1 - d_2^{-1}) \tau_2^2 \\ + (d_1^{-1} + d_2^{-1} + d_1^{-1}d_2^{-1} + k_s \lambda_1 d_2^{-1} (1 - d_1^{-1}) - Tk_s \lambda_0 d_1^{-1} d_2^{-1}) \tau_1 \\ - (d_2^{-1} + d_1^{-1} + d_1^{-1}d_2^{-1} + k_s \lambda_1 d_1^{-1} (1 - d_2^{-1}) - Tk_s \lambda_0 d_1^{-1} d_2^{-1}) \tau_2 \\ + k_s \lambda_2 (d_1^{-1} - d_2^{-1}) \end{pmatrix} \quad (A.1)$$

$$a_2 = k_s ((d_1^{-1}d_2^{-1})(\tau_2 - \tau_1))^{-1} \times \begin{pmatrix} \lambda_0 \tau_1^2 (1 - d_1^{-1} + d_2^{-1} - d_1^{-1}d_2^{-1}) \\ - \lambda_0 \tau_2^2 (1 + d_1^{-1} - d_2^{-1} - d_1^{-1}d_2^{-1}) \\ + \tau_1 \left(\lambda_1 (d_1^{-1} - d_2^{-1} + d_1^{-1}d_2^{-1} - 1) + T \lambda_0 (d_1^{-1} + d_2^{-1}) - d_1^{-1} - d_2^{-1} - 1 \right) \\ + \tau_2 \left(\lambda_1 (d_1^{-1} - d_2^{-1} - d_1^{-1}d_2^{-1} + 1) - T \lambda_0 (d_1^{-1} + d_2^{-1}) + d_1^{-1} + d_2^{-1} + 1 \right) - 2\lambda_2 (d_1^{-1} - d_2^{-1}) \end{pmatrix} \quad (A.2)$$

$$a_3 = d_2 d_1^{-1} (\tau_2 - \tau_1)^{-1} \times \begin{pmatrix} \tau_1 - \tau_2 \\ -k_s \lambda_0 (\tau_1^2 - \tau_2^2 - \tau_1^2 d_1^{-1} + \tau_2^2 d_2^{-1}) \\ + k_s \lambda_1 (\tau_1 - \tau_2 - \tau_1 d_1^{-1} + \tau_2 d_2^{-1}) \\ + k_s \lambda_2 (d_1^{-1} - d_2^{-1}) - Tk_s \lambda_0 (\tau_1 - \tau_2) \end{pmatrix} \quad (A.3)$$

$$\text{with } d_1^{-1} = e^{\frac{T}{\tau_1}} \text{ and } d_2^{-1} = e^{\frac{T}{\tau_2}}$$

REFERENCES

- [1] H. Bemri and D. Soudani, "Discrete-Time Approximation for Nonlinear Continuous Systems with Time Delays," (IJACSA) International Journal of Advanced Computer Science and Applications, vol. 7, no. 5, pp. 431-437, 2016.
- [2] M. Allen and E. Isaacson, Numerical Analysis for Applied Science.: Wiley, 1998.
- [3] J. C. Butcher, Numerical Methods for Ordinary Differential Equations.: John Wiley & Sons, 2008.
- [4] G. C. Goodwin, J. C. Aguero, M. E. Cea Garridos, M. E. Salgado, and J. I. Yuz, "Sampling and Sampled-Data Models," IEEE Control Systems Magazine, vol. 33, no. 5, pp. 34-53, 2013.
- [5] D. Nesić, A. R. Teel, and P. V. Kokotović, "Sufficient conditions for stabilization of sampled-data nonlinear systems via discrete-time approximations," Systems & Control Letters, vol. 38, no. 4-5, pp. 259-270, 1999.
- [6] D. Efimov, A. Polyakov, A. Levant, and W. Perruque, "Realization and Discretization of Asymptotically Stable Homogeneous Systems," IEEE Transactions on Automatic Control, vol. 62, no. 11, pp. 5962-5969, 2017.
- [7] H. Bemri and D. Soudani, "Discretization of linear continuous systems with input output time delay," in 7th International Conference on Modelling, Identification and Control (ICMIC), Sousse, 2015, pp. 1-6.
- [8] M. A. Al-Alaoui, "Novel Stable Higher Order s-to-z Transforms," IEEE Transactions on Circuits and Systems, vol. 48, no. 11, pp. 1326-1329, November 2001.
- [9] I. Amri, D. Soudani, and M. Benrejeb, "Exponential stability and stabilization of linear systems with time varying delays," in Int Multi-Conference on Systems, Signals and Devices, 2009, pp. 1-6.
- [10] Y. Manai and M. Benrejeb, "New Condition of Stabilisation for Continuous Takagi-Sugeno Fuzzy System based on Fuzzy Lyapunov Function," International Journal of Control and Automation, vol. 4, no. 3, pp. 51-63, 2011.

- [11] M. Ksouri-Lahmari, A. El Kamel, P. Borne, and M. Benrejeb, "Multimodel multicontrol decision making in system automation," in *International Conference on Systems, Man, and Cybernetics. Computational Cybernetics and Simulation*, vol. 4, 1997, pp. 3490-3494.
- [12] M. Benrejeb and P. Borne, "On an algebraic stability criterion for nonlinear processes. Interpretation in the frequency domain," *Proceedings of the Measurement and Control International Symposium MECO'78*, vol. 78, pp. 678-682, Athens, 1978.
- [13] M. Benrejeb, "Stability study of two level hierarchical nonlinear systems," *International Federation of Automatic Control Large Scale System Symposium: Theory and Applications IFAC LSS*, vol. 9, no. 1, pp. 30-41, 2010.
- [14] M. Benrejeb and M. Gasmi, "On the use of an arrow form matrix for modelling and stability analysis of singularly perturbed nonlinear systems," *Systems Analysis Modelling Simulation*, vol. 40, no. 4, pp. 509-525, 2001.
- [15] M. Benrejeb, M. Gasmi, and P. Borne, "New stability conditions for TS fuzzy continuous nonlinear models," *Nonlinear Dynamics and Systems Theory*, vol. 5, no. 4, pp. 369-379, 2005.
- [16] M. Benrejeb and M. N. Abdelkrim, "On order reduction and stabilization of TSK nonlinear fuzzy models by using arrow form matrix," *Systems Analysis Modelling Simulation*, vol. 43, no. 7, pp. 977-991, 2003.
- [17] H. Degachi, W. Chagra, and M. Ksouri, "Nonlinear Model Predictive Control for pH Neutralization Process based on SOMA Algorithm," (IJACSA) *International Journal of Advanced Computer Science and Applications*, vol. 9, no. 1, pp. 391-398, 2018.
- [18] W. R. Abdul-Adheem and I. K. Ibraheem, "From PID to Nonlinear State Error Feedback Controller," (IJACSA) *International Journal of Advanced Computer Science and Applications*, vol. 8, no. 1, pp. 312-322, 2017.
- [19] T. Chen and B. A. Francis, *Optimal Sampled-Data Control Systems*.: Springer-Verlag, 1995.
- [20] G. Chen and Y. Yang, "New necessary and sufficient conditions for finite-time stability of impulsive switched linear time-varying systems," *IET Control Theory & Applications*, vol. 12, no. 1, pp. 140-148, 2018.
- [21] W. M. Haddad and A. L'Afflitto, "Finite-Time Stabilization and Optimal Feedback Control," *IEEE Transactions on Automatic Control*, vol. 61, no. 4, pp. 1069-1074, 2016.
- [22] A. Polyakov, D. Efimov, and W. Perruquetti, "Finite-time stabilization using implicit Lyapunov function technique," in *IFAC Symposium on Nonlinear Control Systems*, Toulouse, September, 2013.
- [23] B. Sfaihi, S. Fékih, and M Benrejeb, "Finite-Time Convergence Stability of Lur'e Discrete-Time Systems," *Studies in Informatics and Control*, vol. 25, no. 4, pp. 401-410, Décembre 2016.
- [24] H. Liu, X. Zhao, and H. Zhang, "New approaches to finite-time stability and stabilization for nonlinear systems," *Neurocomputing*, vol. 138, no. 22, pp. 218-228, 2014.
- [25] F. Amato, M. Ariola, and C. Cosentino, "Finite-time control of discrete-time linear systems, Analysis and design conditions," *Automatica*, vol. 46, no. 5, pp. 919-924, 2010.
- [26] F. Amato and M. Ariola, "Finite-time control of discrete-time linear systems," *IEEE Transactions on Automatic Control*, vol. 50, no. 5, pp. 724-729, 2005.
- [27] Zh. Zhang, Ze. Zhang, H. Zhang, B. Zheng, and H. R. Karim, "Finite-time stability analysis and stabilization for linear discrete-time system with time-varying delay," *Journal of the Franklin Institute*, vol. 351, no. 6, pp. 3457-3476, 2014.
- [28] L. Zhu, Y. Shen, and C. Li, "Finite-time control of discrete-time systems with time-varying exogenous disturbance," *Communications in Nonlinear Science and Numerical Simulation*, vol. 14, no. 2, pp. 371-370, 2009.
- [29] P. Siricharuanun and C. Pukdeboon, "Robust Finite-Time Controllers for Magnetic Levitation System Via Second Order Sliding Modes," *International Review of Automatic Control*, vol. 10, no. 2, pp. 143-151, 2017.
- [30] H. Du, C. Qian, M. T. Frye, and S. Li, "Global finite-time stabilisation using bounded feedback for a class of non-linear systems," *IET Control Theory & Applications*, vol. 6, no. 14, pp. 2326-2336, 2012.
- [31] Z. Kowalczyk, "Discrete approximation of continuous-time systems: a survey," *IEE Proceedings G (Circuits, Devices and Systems)*, vol. 40, no. 4, pp. 264-278, 1993.
- [32] A. N. Michel, L. Hou, and D. Liu, *Stability of Dynamical Systems: Continuous, Discontinuous, and Discrete Systems*. Birkhäuser Basel, 2008.
- [33] H. Wang, Y. Tian, and C. Vasseur, "Non-Affine Nonlinear Systems Adaptive Optimal Trajectory Tracking Controller Design and Application," *Studies in Informatics and Control*, vol. 24, no. 1, pp. 05-12, 2015.
- [34] A. Emami and G. F. Franklin, "Dead-beat control and tracking of discrete-time systems," *IEEE Transactions on Automatic Control*, vol. 27, no. 1, pp. 176-181, 1982.
- [35] A. Casavola, P. Mosca, and P. Lampariello, "Robust Ripple-free Deadbeat Control Design," *Intl. Journal of Control*, vol. 72, no. 6, pp. 564-573, 1999.
- [36] V. Strejč, "State Space Approach to linear Computer Control," in *Proceedings of the 7 th IFAC/IFIP/IMACS Conf. on Digital Computer Applications to Process Control*, Vienna, 1985.
- [37] P. Dorato, "Theoretical Developments in Discrete-time Control," *Automatica*, vol. 33, no. 4, pp. 395-400, 1983.

Arabic Text Categorization using Machine Learning Approaches

Riyad Alshammari

College of Public Health and Health Informatics King Saud Bin Abdulaziz University for Health Sciences
P.O. Box 22490, Riyadh 11426 Kingdom of Saudi Arabia

Abstract—Arabic Text categorization is considered one of the severe problems in classification using machine learning algorithms. Achieving high accuracy in Arabic text categorization depends on the preprocessing techniques used to prepare the data set. Thus, in this paper, an investigation of the impact of the preprocessing methods concerning the performance of three machine learning algorithms, namely, Naïve Bayesian, DMNBtext and C4.5 is conducted. Results show that the DMNBtext learning algorithm achieved higher performance compared to other machine learning algorithms in categorizing Arabic text.

Keywords—Arabic text; categorization; machine learning

I. INTRODUCTION

Constructing an automated text categorization system for Arabic articles/documents is a difficult work as a result of the unique nature of the Arabic language. Arabic language consists of 28 letters and is written from right to left. It has a distinctive morphology and orthography principles.

The number of text information accessible on the Internet has increased rapidly on the last few years since many private and public organizations are publishing their text information such as documents, news, books, etc. on the World Wide Web (WWW). This creates a vast amount of text information that makes the manual categorization of text information a very impractical task. Thus, the development of automated text categorization/classification system is important work.

Text categorization is the automatic mapping of texts to predefine labels (classes). Text categorization methods are deployed in many systems such as searching e-mails, spam filtering, and classification of news. Most of the text categorization methods are developed to deal with texts written in the English language. Hence, there are not suitable to documents written in the Arabic language.

Several works had been conducted on this topic using machine learning algorithms such as decision trees [1]–[3], k-nearest neighbour [4]–[8], Support Vector Machines (SVMs) [5], [9] regression model [10], [11], and other techniques and algorithms [12]–[14]. The previous study compared the performance of the classifiers based on the English articles utilizing the Reuters Newswire Corpus.

Several papers had focused on the use of machine learning algorithms to categorize Arabic Text. El-Kourdi et al. [15] used Naïve Bayes machine learning Algorithm to classify Arabic website data. They achieved an accuracy of ≈

69%. Mesleh [16] utilized three machine learning algorithms (SVM, KNN and Naïve Bayes) to classify Arabic data that were collected from Arabic newspaper. They divided the texts into nine labels that were Economics, Education, Computer, Engineering, Medicine, Law, Politics Sports and Religion. He used Chi-square statistics as the feature sets. He achieved high performance with F-measure equal to 88.11%. Furthermore, Syiam et al. [17] applied many stemming techniques and different features selection for Arabic text categorization. They discovered that combination of light stemmer and statistical method achieved the best performance.

On the other hand, few studies focus their study on the performance of automatically classifying Arabic language using Arabic corpora [18], [19]. This is due to the fact that the Arabic language is highly abundant in grammars and needs special handlings for morphological analysis. Furthermore, constructing an automated text categorization system for Arabic articles/documents is a challenging work as a result of the unique nature of the Arabic language. The Arabic language has complicated morphological principles comparing to English. The root of the words can have either tri-letter (most of the words), Quad-letter, Penta-letter or even Hexa-letter [20]. As a result, the Arabic Language demands enormous processing to construct an accurate categorization system [21]. Thus, Arabic text categorization is considered as a very challenging task for researchers because of the language complexity.

In this paper, an automated categorization system has been introduced based on machine learning algorithms for Arabic text documents. The impact of the preprocessing techniques related to the term weighing schemes for Arabic Text has not been studied in the literature. In this research paper, we focus on exploring this impact on Arabic corpora to improve the categorization accuracy by investigating different machine learning approaches, mainly Naïve Bayesian, DMNBtext and C4.5 algorithms.

The rest of this paper is organized as follows. Section II presents the methods that includes the machine learning algorithms employed, details description of the data sets, features and evaluation criteria. The experimental results and analysis are discussed in Section III. Finally, conclusions are drawn and future work is discussed in Section IV.

II. METHODS

This section describes the methods employed in this

research paper.

A. Corpora

This section contains a brief description of the corpora used to evaluate the ML algorithms. Two corpora have been used to perform the experiments that were collected and formed from online text documents by [22]. These were BBC Arabic and CNN Arabic corpora. The BBC Arabic corpus collected from the BBC Arabic website (bbc.com) that contains 4763 text documents, 1.8 M words and 106K distinct keywords (when removing stop words). The corpus consisting of seven categories that are Middle East News, World News, Business & Economy, Sports, International Press, Science & Technology, and Art & Culture where each category contains the following document numbers: 2356, 1489, 296, 219, 49, 232, and 122, respectively.

On the other hand, the CNN Arabic corpus collected from the CNN Arabic website (cnn.com) contains 5070 text documents, 2.2 M words and 144K distinct keywords (when removing stop words). The corpus consisting of six categories that are Business, Entertainments, Middle East News, Science & Technology, Sports, and World where each category contains the following documents numbers: 836, 474, 1462, 526, 762, and 1010, respectively.

B. Text Preprocessing Techniques

The text documents must go through a preprocessing phase. The preprocessing phase usually consists of the tasks of document conversion, tokenization, stop-word removal and stemming. The task of stemming is to remove all the affixes and suffixes from a word to extract its root. Since the Arabic language has different variations in representing text, three stemming techniques have been applied which are: Khoja stemming [23], light stemming [24] techniques and compared with Raw text (no stemming).

The next task is the feature extracting/selection. This phase, the influence of text preprocessing functions on text categorization is measured, especially the impact of using stemming from Arabic text categorization. In this task, a term weigh is representing each document as a weight vector; this regularly mentioned as the bag of words method. The goal of this work is to measure the influence of text preprocessing tasks on text categorization, especially the impact of using stemming with term weighing on Arabic text. Therefore, three stemming techniques with twelve-term weighing schemes have been applied (Table I). For instance, Term frequency (tf) measures the occurrence of term t in document d while document frequency (df) counts the number of documents that the term t presented at least once. On the other hand, the inverse document frequency (idf) measures how common the term in all the documents. The idf is going to be low if the term appears in many documents and high if the term appears in few documents.

TABLE. I. TERMS WEIGHING SCHEMES

Schema	Description
bool	boolean model (0 means absent while 1 means)
idf	Inverse Document Frequency
tf	Term Frequency
tfidf	Term Frequency-Inverse Document
tfidf-norm-minFreq3	Apply normalization with minimum frequency
tfidf-norm-minFreq5	Apply normalization with minimum frequency
wc	output word counts
wc-minFreq3	Minimum frequency <3 for wc
wc-minFreq5	Minimum frequency <5 for wc
wc-norm	Apply normalization for wc
wc-norm-minFreq3	Apply normalization with minimum frequency
wc-norm-minFreq5	Apply normalization with minimum frequency

C. Machine Learning Algorithms

For this work, three Data Mining algorithms have been used that are C4.5, Naive Bayesian and DMNBtext.

1) *C4.5*: C4.5 is an improvement of the ID3 decision tree based algorithm where the tree is built in a top-down approach. It applies the divide-and-conquer strategy to construct a decision tree by dividing the input space into local regions based on a distance metric. It uses information theory of choosing attributes to be selected in the root and internal nodes. The process of constructing a decision tree by C4.5 algorithm starts at the root node and is repeated until a leaf node is encountered. Additional detailed information on the C4.5 algorithm can be obtained in [25].

D. Naive Bayesian

Naive Bayesian is a statistical classification system based on the application of Bayes theorem. This classification technique examines the relationship between an instance of each class and each feature assuming that all feature values are conditionally independent in a data set. It separately considers each feature and obtains a conditional probability for the associations linking the feature values and the class. The class with the highest probability value is selected as the predicted class. Additional detailed information on the Naive Bayesian algorithm can be obtained in [26].

E. DMNBtext

The learning process for the Bayesian network from data consists of two fundamental elements that are structure learning and parameter learning. When the Bayesian network has fixed structure, parameters learning can have two kinds of approaches that are discriminative and generative learning. The generative learning parameter appears to be more efficient while the discriminative parameter learning considers being more efficient. Hence, Discriminative parameter learning for Bayesian networks for text (DMNBtext)

consists of the benefits of discriminative learning and Bayesian network. Accordingly, it provides efficient, practical and straightforward discriminative parameter learning approach that discriminatively calculates frequencies from a dataset and after that uses the appropriate frequencies to estimate parameters. Additional detailed information on the DMNBtext algorithm can be obtained in [27].

F. Metrics for Evaluation

Accuracy is used as an evaluation criterion for text classification to measure the performance of the learning algorithms. The Accuracy, (1), reflects the total number of flows that are correctly classified from All- classes (the ones which the algorithm aims to classify):

$$Accuracy = \frac{TP + TN}{All} \tag{1}$$

The desired outcomes are to obtain a high percentage value for the Accuracy. In this paper, stratified 10 fold-cross validation is used to evaluate each of the learning algorithms on each datasets. To this end, Weka [28] is used with the default parameters for running the learning algorithms.

III. EXPERIMENTAL RESULTS AND ANALYSIS

In this section to evaluate the different preprocessing methods and to show the effectiveness of data mining algorithms in finding sound signatures, we use two different datasets (BBC and CNN) to provide some measure of choosing

proper preprocessing methods with classifier generalization (robustness).

Results presented in Tables II and III illustrate that the DMNBtext-based classification approach is observed to provide outstanding performances on both datasets. C4.5 delivers better performance on the BBC datasets while achieved lower performance on the CNN dataset compared with the other two data mining algorithms. Naïve Bayesian algorithms performance is the second best classifier comparing with the different two learning algorithms on both datasets.

On term of the both the stemming and preprocessing methods, the DMNBtext learning algorithms are achieving higher performance when Khoja and Light stems with boolean, idf, tfidf, wc and wc-norm preprocessing methods on the BBC data set. The DMNBtext attained an accuracy of 99% on the BBC data set. On the other hand, evaluating the DMNBtext on the CNN data sets, it produced higher performance using Light stem and Raw Text with boolean, idf, tf, tfidf and wc-norm preprocessing methods. The DMNBtext achieved an accuracy higher than 93% on the CNN data set. Moreover, C4.5 produced higher performance using the Light stem and Raw Text.

One of the significant concerns with Arabic Text categorization is the lack of standardized public Arabic corpora. Furthermore, most of the text data is obtained from online websites or newspapers. Hence, the performance of the machine learning models is biased to such corpora and would be difficult to generalize the models to all Arabic text.

TABLE. II. ACCURACY PERFORMANCE FOR EACH CLASSIFIER ON THE BBC DATA USING STRATIFIED 10-FOLD CROSS-VALIDATION

Preprocessing Methods	DMNBtext			C4.5			Naïve Bayes		
	Khoja stem	Light stem	Raw Text	Khoja stem	Light stem	Raw Text	Khoja stem	Light stem	Raw Text
bool	99.0	98.9	98.7	99.3	99.5	99.5	92.3	91.0	91.0
idf	99.0	99.0	98.8	99.4	99.5	99.5	75.0	77.2	78.6
tf	99.0	98.9	98.7	99.4	99.5	99.5	78.0	80.3	81.5
tfidf	99.0	99.0	98.8	99.4	99.5	99.5	78.0	80.2	81.5
tfidf-norm-minFreq3	98.5	98.4	98.3	99.4	99.5	99.3	83.5	77.6	71.8
tfidf-norm-minFreq5	98.5	98.2	98.3	99.3	99.5	99.4	85.8	80.3	76.0
wc	99.0	98.9	98.7	99.4	99.5	99.5	75.0	77.1	78.4
wc-minFreq3	98.4	98.1	98.2	99.5	99.4	99.5	74.8	77.4	78.9
wc-minFreq5	98.5	98.2	98.3	99.3	99.4	99.5	75.7	78.8	79.9
wc-norm	99.0	98.9	98.7	99.4	99.5	99.5	83.1	78.0	72.3
wc-norm-minFreq3	98.4	98.1	98.2	99.4	99.5	99.5	84.9	79.9	74.6
wc-norm-minFreq5	98.5	98.2	98.3	99.3	99.5	99.5	86.8	82.1	79.1

TABLE III. ACCURACY PERFORMANCE FOR EACH CLASSIFIER ON THE CNN DATA USING STRATIFIED 10-FOLD CROSS-VALIDATION

Preprocessing Methods	DMNBtext			C4.5			Naïve Bayes		
	Khoja stem	Light stem	Raw Text	Khoja stem	Light stem	Raw Text	Khoja stem	Light stem	Raw Text
bool	93.0	93.5	93.6	75.6	77.2	78.5	86.3	87.5	89.1
idf	93.0	93.5	93.6	76.3	78.5	78.5	88.4	89.4	89.9
tf	93.0	93.5	93.6	76.3	78.3	78.5	88.1	87.8	88.1
tfidf	93.0	93.5	93.6	76.3	78.3	78.5	88.2	88.0	88.3
tfidf-norm-minFreq3	92.9	93.4	93.5	76.5	78.5	78.3	89.3	88.7	88.4
tfidf-norm-minFreq5	92.4	93.1	93.5	77.2	79.4	79.0	89.3	89.7	89.6
wc	93.0	93.5	93.5	76.4	78.5	78.5	88.5	89.5	90.0
wc-minFreq3	92.9	93.4	93.5	76.0	79.1	78.3	88.2	89.5	90.1
wc-minFreq5	92.4	93.1	93.5	75.8	80.7	79.0	87.4	89.5	89.5
wc-norm	93.0	93.5	93.5	76.7	79.6	79.2	88.6	86.5	85.7
wc-norm-minFreq3	92.9	93.4	93.5	76.5	79.1	78.9	89.0	89.0	89.0
wc-norm-minFreq5	92.4	93.1	93.5	77.1	78.9	79.3	89.0	89.5	90.0

IV. CONCLUSION

Arabic Text categorization is considered one of the difficult problems in classification using machine learning algorithms. Achieving high accuracy in Arabic text categorization depends on the preprocessing techniques used to prepare the data set. Thus, in this paper, an investigation of the impact of the preprocessing techniques in relation to the performance of three machine learning algorithms, namely Naïve Bayesian, DMNBtext and C4.5 is conducted.

The preprocessing step is an essential element in text categorization. Many preprocessing techniques that can be applied but it is very complicated to find the most suitable one. In this research paper, several preprocessing techniques were evaluated on Arabic text corpora using Machine learning algorithms. The DMNBtext learning algorithm is showing superior performance compared to other machine learning algorithms in categorizing Arabic text with different preprocessing techniques.

In the future, the plan is to apply genetic programming and deep learning techniques to improve the performance of the models and to use more extensive datasets.

REFERENCES

[1] D. D. Lewis and M. Ringuette, "A comparison of two learning algorithms for text categorization," in *Third annual symposium on document analysis and information retrieval*, vol. 33, 1994, pp. 81–93.

[2] C. Apte, F. Damerau, S. Weiss et al., *Text mining with decision rules and decision trees*. IBM Thomas J. Watson Research Division, 1998.

[3] F. Harrag, E. El-Qawasmeh, and P. Pichappan, "Improving arabic text categorization using decision trees," in *Networked Digital Technologies, 2009. NDT'09. First International Conference on*. IEEE, 2009, pp. 110–115.

[4] R. Al-Shalabi and R. Obeidat, "Improving knn arabic text classification with n-grams based document indexing," in *Proceedings of the Sixth International Conference on Informatics and Systems, Cairo, Egypt, 2008*, pp. 108–112.

[5] I. Hmeidi, B. Hawashin, and E. El-Qawasmeh, "Performance of knn and svm classifiers on full word arabic articles," *Advanced Engineering Informatics*, vol. 22, no. 1, pp. 106–111, 2008.

[6] B. Masand, G. Linoff, and D. Waltz, "Classifying news stories using

memory based reasoning," in *Proceedings of the 15th annual international ACM SIGIR conference on Research and development in information retrieval*. ACM, 1992, pp. 59–65.

[7] W. Lam and C. Y. Ho, "Using a generalized instance set for automatic text categorization," in *Proceedings of the 21st annual international ACM SIGIR conference on Research and development in information retrieval*. ACM, 1998, pp. 81–89.

[8] Y. Yang, "Feature selection in statistical learning for text categorization," in *14th International Conference on Machine Learning, 1997*, 1997.

[9] T. Joachims, "Text categorization with support vector machines: Learning with many relevant features," *Machine learning: ECML-98*, pp. 137–142, 1998.

[10] N. Fuhr, S. Hartmann, G. Lustig, M. Schwantner, K. Tzeras, and G. Knorz, "Air/x-a rule based multistage indexing system for large subject fields," in *RIAO*, vol. 91, 1991, pp. 606–623.

[11] Y. Yang and C. G. Chute, "An example-based mapping method for text categorization and retrieval," *ACM Transactions on Information Systems (TOIS)*, vol. 12, no. 3, pp. 252–277, 1994.

[12] S. Al-Harbi, A. Almuhareb, A. Al-Thubaity, M. Khorsheed, and A. Al-Rajeh, "Automatic arabic text classification," 2008.

[13] S. Dumais, J. Platt, D. Heckerman, and M. Sahami, "Inductive learning algorithms and representations for text categorization," in *Proceedings of the seventh international conference on Information and knowledge management*. ACM, 1998, pp. 148–155.

[14] R. M. Duwairi, "Arabic text categorization," *Int. Arab J. Inf. Technol.*, vol. 4, no. 2, pp. 125–132, 2007.

[15] M. El Kourdi, A. Bensaid, and T.-e. Rachidi, "Automatic arabic document categorization based on the naïve bayes algorithm," in *Proceedings of the Workshop on Computational Approaches to Arabic Script-based Languages*. Association for Computational Linguistics, 2004, pp. 51–58.

[16] A. Moh'd A Mesleh, "Chi square feature extraction based svms arabic language text categorization system," *Journal of Computer Science*, vol. 3, no. 6, pp. 430–435, 2007.

[17] M. M. Syiam, Z. T. Fayed, and M. B. Habib, "An intelligent system for arabic text categorization," *International Journal of Intelligent Computing and Information Sciences*, vol. 6, no. 1, pp. 1–19, 2006.

[18] A. M. El-Halees, "Arabic text classification using maximum entropy," *IUG Journal of Natural Studies*, vol. 15, no. 1, 2015.

[19] L. Khreisat, "Arabic text classification using n-gram frequency statistics a comparative study," *DMIN*, vol. 2006, pp. 78–82, 2006.

[20] S. Al-Fedaghi and F. Al-Anzi, "A new algorithm to generate arabic root-pattern forms," in *proceedings of the 11th national Computer*

- Conference and Exhibition, 1989, pp. 391–400.
- [21] F. Harrag and E. El-Qawasmah, “Neural network for arabic text classification,” in *Applications of Digital Information and Web Technologies, 2009. ICADIWT'09. Second International Conference on the*. IEEE, 2009, pp. 778–783.
- [22] M. K. Saad and W. Ashour, “Arabic text classification using decision trees,” in *Proceedings of the 12th international workshop on computer science and information technologies CSIT*, vol. 2, 2010, pp. 75–79.
- [23] S. Khoja and R. Garside, “Stemming arabic text,” *Lancaster, UK, Computing Department, Lancaster University*, 1999.
- [24] L. Larkey, L. Ballesteros, and M. Connell, “Light stemming for arabic information retrieval,” *Arabic computational morphology*, pp. 221–243, 2007.
- [25] E. Alpaydin, *Introduction to machine learning*. MIT press, 2014.
- [26] G. H. John and P. Langley, “Estimating continuous distributions in bayesian classifiers,” in *Proceedings of the Eleventh conference on Uncertainty in artificial intelligence*. Morgan Kaufmann Publishers Inc., 1995, pp. 338–345.
- [27] J. Su, H. Zhang, C. X. Ling, and S. Matwin, “Discriminative parameter learning for bayesian networks,” in *Proceedings of the 25th international conference on Machine learning*. ACM, 2008, pp. 1016–1023.
- [28] M. Hall, E. Frank, G. Holmes, B. Pfahringer, P. Reutemann, and I. H. Witten, “The weka data mining software: an update,” *ACM SIGKDD explorations newsletter*, vol. 11, no. 1, pp. 10–18, 2009.

2-D Object Recognition Approach using Wavelet Transform

Kamelsh Kumar¹

Department of Computer Science
Sindh Madressatul Islam University
Karachi, Sindh, Pakistan

Riaz Ahmed Shaikh², Rifaqat Hussain Arain³,

Safdar Ali Shah⁴, Hidayatullah Shaikh⁵
Department of Computer Science
Shah Abdul Latif University, Khairpur, Sindh, Pakistan

Abstract—Humans have supernatural ability to observe, analyze, and tell about the layout of the 3D world with the help of their natural visual system. But contrary to machine vision system, it remains a most difficult task to recognize various objects from images being captured by cameras. This paper presents 2-D image object recognition approach using Daubechies (Db10) wavelet transform. Firstly, an edge detection is carried out to delineate objects from the images. Secondly, shape moments have been used for object recognition. For testing purpose, different geometrical shapes such as rectangle, circle, triangle and pattern have been selected for image analysis. Simulation has been performed using MATLAB, and obtained results showed that it accurately identifies the objects. The research goal was to test 2-D images for object recognition.

Keywords—Wavelet transforms; db10; edge detection; object recognition; shape moments

I. INTRODUCTION

Since last few years, object recognition has remained one of the challenging tasks in different applications of domain, namely, computer vision, pattern recognition, data mining, object tracking and remote sensing. It can be defined as a process for highlighting, identifying, and extracting the targeted objects from the image and video based repositories. Object recognition is being extensively used in various applications for different purposes, such as in medical technology, researchers are interested in finding the specific regions that can assist doctors to recognize abnormalities in human body, in surveillance and monitoring systems, inspection is necessary security measure to point out a particular person for fraudulent activities. Similarly, in bio related trait systems, individual object verification is required for authentication [1]-[4]. Object recognition is core area of pattern recognition, which uses supervised as well as unsupervised machine learning techniques for mining hidden structures in the data. However, building an efficient object recognition system heavily relies over proper image segmentation method. In this paper, research has been solely carried out for 2-D images for the shape recognition. There are various techniques that have been used for shape representation; however, they are roughly categorized into contour and region methods. First one retrieve the shape from the boundary and second one extracts the shape from the whole region. The comprehensive study on shape features have been given in [5]. The contents of this paper are arranged in the following order. Section one describes the literature review,

which is related to 2-D objects for shape recognition and retrieval. Section 2 explains wavelets transform and its methodology for edge detection and object recognition. Section 3 describes the experimental calculation and simulation results for object retrieval and finally Section 4 provides the conclusion.

II. LITERATURE REVIEW

Over the past, various approaches have been put forwarded by authors for 2-D images for shape recognition. In [6] Jiann-Der Lee and Jau-Yien Lee suggested a recognition technique for partial 2-D perspective shapes. This method was able to recognize the unknown shape from arbitrary perspective. However, efficiency of the system was limited for those objects missing only 20% of data. Similarly, K.C. Wong and Y.Cheng presented a recognition method for polyhedral objects with the aid of triangular pair feature. The rate of identification for objects was relatively high but their method does not considered spatial and temporal information [7]. In other paper [8], P.K Sinha and F-Y Chen, implemented Hough parameter space in which shapes were recognized along with their location. The drawback of this method is that Hough transform is good for line detection but it is not feasible for circle object recognition. The wavelets transform for the 2-D occluded object recognition was given by Tiehua Du and Kah Bin Lim, where boundary of the object was extracted for shape detection. But this method is only suitable for partially overlapped objects [9]. Object corner detection using wavelet transform was proposed by Lu Sun and Y.Y Tang, this method uses local extrema as well as modulus of the transform results for the detection of corner and its arcs. However, the system suffers from few missed corner detections [10]. A linear discriminant analysis LDA technique for box structure objects detection was described by Chia-Chih Chen and J.K Aggarwal [11]. This method outperforms in different angle view of objects but provided some false positive and negative detection results due to over segmentation. Random transform for object matching was suggested by Yi Wan and Ning Wei [12]. This method recognizes the objects from rotated, reflected and scaled projection, while it is only useful for non-occluded objects. Similarly, 2-D objects retrieval and shape matching using B-spline representation was given by Nacera Laiche and Slimane Larabi [13]. A contemporary method of content analysis using shape and spatial layout with MRF has been proposed by Shaikh et al. [14]. Experimental results

demonstrate the effectiveness of the proposed method to efficient content analysis.

III. WAVELET TRANSFORM

Wavelet is a type of frequency transform technique which is being used for signal analysis. Also, it has been an important tool for researchers for image analysis since more than a decade. Wavelet transform is characterized by its orthogonal function, which can be used on limited group of data. It provides multi scale signal analysis using low pass and high pass filter. In this paper, wavelet has been implemented on 2-D images for edge detection and object retrieval. This technique is efficient in the sense that discrete image is decomposed through these filters and change in grey level intensity can easily be detected for object recognition. There are number of wavelets families which are known by their particular name. However, each of them is characterized by its basic scaling function and wavelet shape function; these values are used for particular signal analysis.

A. Proposed Methodology

Our proposed methodology is based on our previous research work which was carried out for 2-D edge detection [15]. In this paper, it has been extended for 2-D object recognition.

Initially, an original image in Fig. 1 is given as an input to db10 wavelet transform for edge detection [16]. After that it decomposes image up to three levels for separation of approximation and details co-efficient. The details contain higher frequencies which correspond to the actual edges, so we have suppressed the approximation effect.

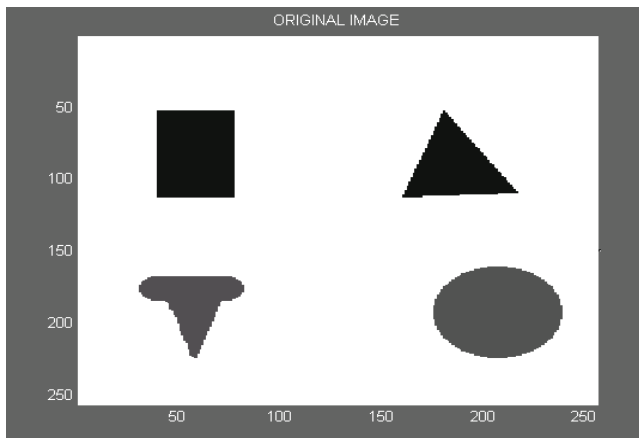


Fig. 1. Original image.

Secondly, an original image has been reconstructed for the detection of image edges as shown in Fig. 2. For this purpose, an algorithm is devised below:

Algorithm for Reconstruction of Image

1. Take approximations as well as detailed coefficients for three level decomposition.
2. Perform up sampling.
3. Use low and high pass filter (Reconstructed filter).

4. Save them in an array.
5. Combine them to get approximations and details.
6. Save them into workspace.
7. Now, this is first level reconstruction.
8. Do it again from step 2 through 6 by taking first level reconstructed approximations and details.
9. This process is carried out until we get original image.
10. The edges of original image will be retrieved at CA3=0
11. Meanwhile, Use thresholding to nullify ghost edges.
12. Finally, an original image will be displayed with edges.

B. Object Recognition

Once the edges are found, the next step is to recognize objects. For this purpose, database has been created as shown in Fig. 3, which consists of different object patterns, such as rectangle, triangle, circle and pattern. Later, these objects have been taken as query image for object recognition.

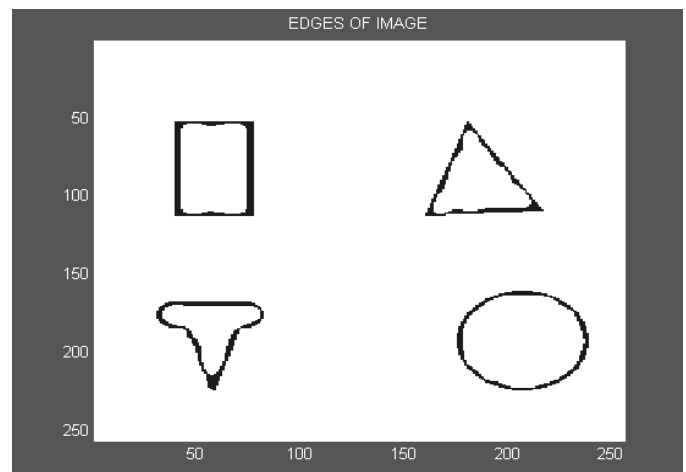


Fig. 2. Edges of the image.

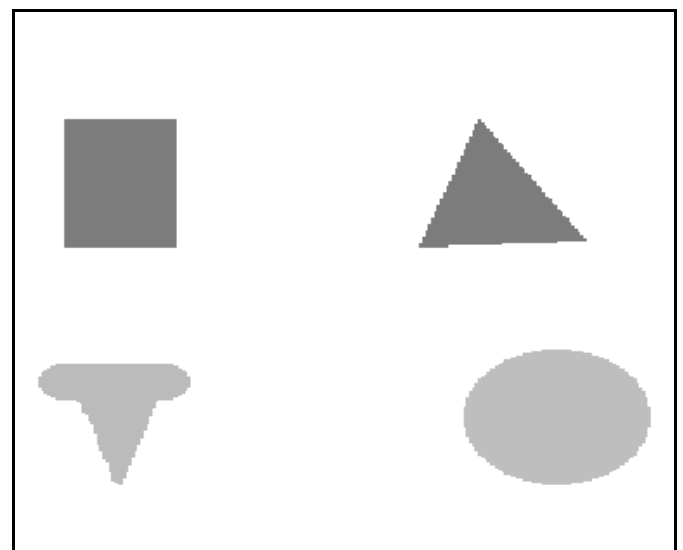


Fig. 3. Database for object recognition.

The algorithm for object recognition has been described as below.

Algorithm for Object Recognition

1. Find first pixel
2. Store its location in arrays individually containing rows and columns
3. Zero the pixel from an input image
4. Check its 8 neighbour-hood connectivity
5. Save its neighbour-hood pixel locations in the same array containing first pixel location
6. Simultaneously, zeroing those pixels from input image
7. Taking pixels immediately next to the first pixel from arrays containing locations of detected pixels
8. Check its 8 neighbour-hood connectivity
9. Store the location of the detected pixel in the same array declared previously
10. This process is repeated until the time 8 neighbour-hood connectivity pixels of preceding pixels exit
11. Declare it the first object
12. Again first pixel is detected
13. Repeat steps from 2 to 11
14. Declare it the second object

C. Shape Moments

Shape moments are good at exploiting global features of an image which is useful for object recognition. These moments are defined over Cartesian moments that contain basic set function {xp, yq}. However, (p + q) th 2-D geometric moments for an image I (x,y) are denoted by a matrix mpq and can be narrated as:

$$m_{pq} = \int_{-\infty}^{\infty} \int_{-\infty}^{\infty} x^p y^q I(x, y) dx dy \tag{1}$$

In (1) I(x, y) depicts the continuous image function, which is stored as two- dimensional array I (i,j) in the computer memory. The i = 0,1,....,Nx - 1 and j = 0,1,....,Ny -1 represents an array Nx × Ny. However, moments are calculated by omitting integrals with summation as shown in (2).

$$m_{pq} = \sum_i \sum_j I(i, j) \cdot i^p j^q \tag{2}$$

And, also normalized moments for x-y axis can be approximated by:

$$m_{pq} = \sum_i I(x_i, y_i) \cdot x_i^p y_i^q \tag{3}$$

Similarly, in (3) summation is performed for all image pixels where xi, yi are central coordinates of ith pixel. Shape moments are efficient in finding intensity distribution of an image. These are invariant to translation, rotation and scale. Therefore, central moments, normalized moments and

invariant moments have been calculated for each object and then stored in an array. Later, individual query object is recognized through comparing its actual moments in the database.

D. Mathematical Calculation

In this section, central moments, normalized moments and invariant moments of Rectangle, Triangle, Pattern and Circle have been calculated for shape recognition, respectively as shown below in Table I.

In addition to aforementioned tabular calculation, central, normalized and invariant moments have been computed using following formulae:

1) Central moments

$$\begin{aligned} r\text{-bar} &= \text{mean}(r); \\ c\text{-bar} &= \text{mean}(c); \\ \text{Momlist}(i) &= (r(i) - r\text{bar})^p * (c(i) - c\text{bar})^q; \\ \text{Momlist}(i) &= \frac{1}{(r_i - \bar{r})^p} * (c_i - \bar{c})^q; \\ \text{Central moments (CM)} &= \text{sum}(\text{momlist}); \end{aligned}$$

Where, p and q are showing the order of CM, are saved in an array.

2) Normalized moments

$$\begin{aligned} \text{NCM} &= \text{CM}_{pq} / \text{CM}_{00}^J \\ \text{Whereas } J &= (p+q)/2+1; \\ \text{Normalized moments} &\text{ are saved in an array.} \end{aligned}$$

3) Invariant moments

$$\begin{aligned} \text{Inva_moment1} &= h20^2 + h02^2; \\ \text{Inva_moment2} &= (h20-h02)^2 + 4*h11^2; \\ \text{Inva_moment3} &= (h30-3*h12)^2 + (h03-3*h21)^2; \\ \text{Inva_moment4} &= (h30+h12)^2 + (h03+h21)^2; \\ \text{Inva_moment5} &= (h30^3*h12)*(h30+h12)*((h30+h12)^2-3*(h03+h21)^2+(3*h21+h03)*(h03+h21)* \\ &\quad *(3*(h30+h21)^2 - (h03+h21)^2)); \\ \text{Inva_moment6} &= (h20-h02)*((h30+h21)^2-(h03+h21)^2) + 4*h11*(h30+h12)*(h03+h21); \\ \text{Inva_moment7} &= (3*h21-h03)*(h30+h12)*((h30+h12)^2-3*(h03+h21)^2-(h03-3*h21)*(h03+h21)*(3*(h30+h12)^2 - (h03+h21)^2)); \\ \text{Invariant moments} &\text{ are saved.} \end{aligned}$$

TABLE I. SHAPE MOMENTS CALCULATION

Moment Triangle	0.0197	0.0014	0.0047	0.0000	0.0000	0.0000
Moment Circle	0.0127	0	0	0	0	0
Moment Rectangle	0.0201	0.0062	0	0	0	0
Moment Pattern	0.0254	0.0017	0.0094	0.0004	0.0000	0.0001

IV. RESULTS AND DISCUSSIONS

In this section, we have shown results which are being generated using MATLAB programming. For this purpose, discussion has been made for object detection. In order to detect object, an input query image is feed to a system, after that it computes its features using shape moments. Then matching of features is achieved from the database. And finally system recognizes shape of an object. It can be observed from Fig. 4 to 7 that detected object are rectangle, triangle, pattern, and circle respectively. From these results, it can be concluded that wavelet transform for edge detection and shape moments for object recognition performed well over grey level intensity images.

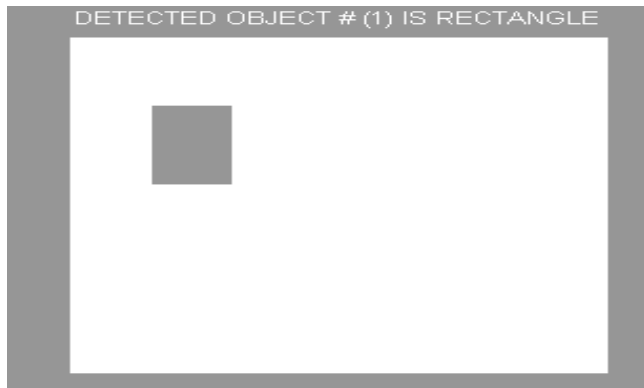


Fig. 4. Rectangle object detection.

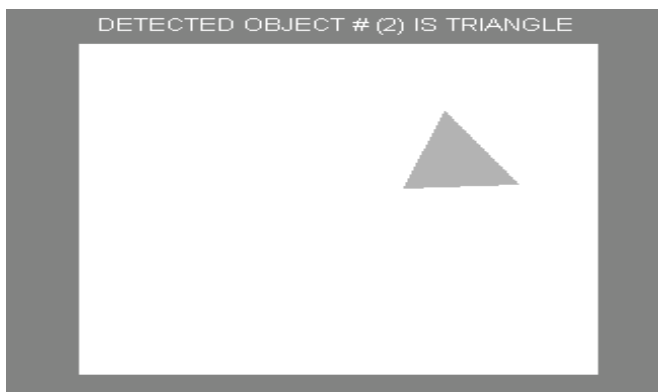


Fig. 5. Triangle object detection.

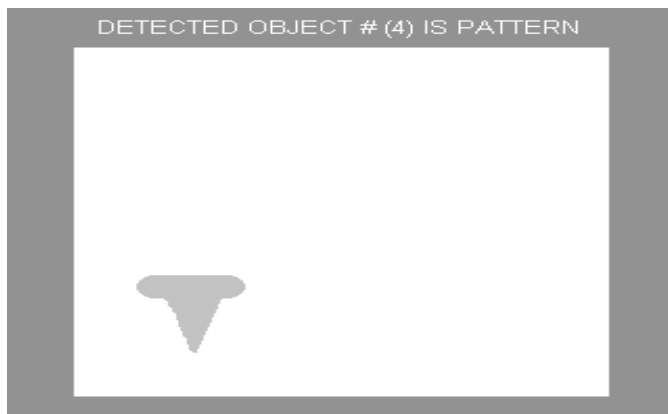


Fig. 6. Pattern object detection.

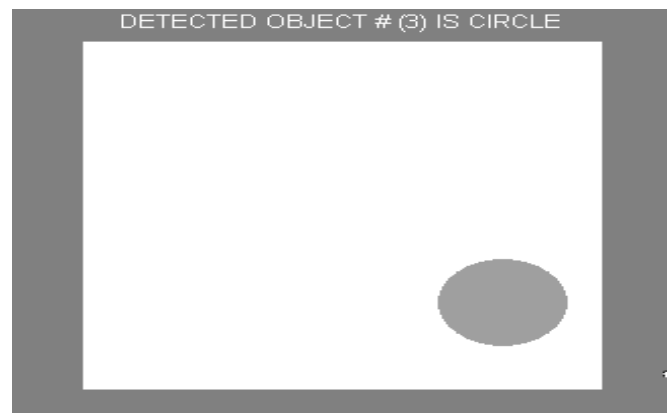


Fig. 7. Circle object detection.

V. CONCLUSIONS

In this paper, 2-D image edge detection and object recognition approach was achieved using Db10 wavelet transform and with shape moments. Simulation results showed that wavelet transforms for edge detection and shape moments for object recognition generate efficient results for 2-D type images. And it is suitable for grey scale images for object recognition. However, proposed system has some limitation, as it does not work well with colour images. Therefore, in future one can improve these algorithms for the sake of high level pattern recognition.

REFERENCES

- [1] Patrick Connor, Arun Ross, "Biometric Recognition By Gait: A Survey of Modalities and Features", *Journal Of Computer Vision and Image Understanding*, vol. 167, pp. 1-27, 2018.
- [2] K. Nguyen, C. Fookes, R. Jillela, S. Sridharan, A. Ross, "Long Iris Recognition: A Survey", *Journal of Pattern Recognition*, vol. 72, pp. 123-143, 2017.
- [3] Swaroop Guntupalli, M. Ida Gobbini, "Reading Faces: From Features to Recognition", *Journal of Trends in Cognitive Sciences*, vol. 21, no. 12, pp. 915-916, 2017.
- [4] J. Liang, J. Zhou, L. Tong, X. Bai, B. Wang, "Material Based Silent Object Detection from Hyper spectral Images", *Journal of Pattern Recognition*, vol. 76, pp. 476-490, 2018.
- [5] Dengsheng Zhang, Guojun Lu, "Review of Shape Representation and Description Techniques", *The Journal of Pattern Recognition Society*, vol. 34, pp. 1-19, 2004.
- [6] Jiann-Der Lee, Jau-Yien Lee and Chin-Hsing Chen, "A New Recognition Method for Partial 2-D perspective", *IEEE Region 10 Conference on Computer and Communication System*, pp. 601-605, September 1990.
- [7] K.C. Wong, Y. Cheng and J. Kittler, "Recognition of Polyhedral Objects Using Triangle Pair Features", *IEEE Proceedings-1*, vol. 140, pp. 72-85, February, 1993.
- [8] P. K. Sinha, F-Y Chen and R E N Horne, "Recognition and Location of Shapes in the Hough Parameter Space", *IEE, Savoy Place, London WC2R 0BL, UK*, 1993.
- [9] Tiehua Du, Kah Bin Lim, and Geok Soon Hong, "2D Occluded Object Recognition Using Wavelets", *International Conference on Computer and Information Technology*, vol. 4, 2004.
- [10] Lu Sun, Y. Y Tang and Xinge You, "Corner Detection for Object Recognition by Using Wavelet Transform", *International Conference on Machine Learning and Cybernetics*, pp. 4347-4351, August. 2004.
- [11] Chia-Chih Chen and J.K Aggarwal, "Recognition of Box-Like Objects by Fusing Cues of Shapes and Edges", *IEEE*, 2008.

- [12] Yi Wan, and Ning Wei, "A fast Algorithm for Recognizing Translated, Rotated, Reflected, and Scaled Objects from only their projections", *IEEE Signal Processing Letters*, vol. 17, pp. 71-74, January. 2010.
- [13] NaceraLaiche, SlimaneLarabi, "Retrieval of 2-D Objects and Shape Matching Using B-splines Representation", *International Conference on Signal and Image Processing Applications*, pp. 495-500, 2011.
- [14] Riaz Ahmed Shaikh, Jian-Ping Li, Asif Khan, Kamlesh Kumar, "Content Analysis Using Shape and Spatial Layout with Markov Random Field", *Indian Journal of Science and Technology*, Vol 9(7), pp. 1-6, February 2016.
- [15] Kamlesh Kumar, Jian-Ping Li, Saeed Ahmed Khan, "Image Edge Detection Scheme Using Wavelet Transform", *International Conference on Wavelets Active Media and Information Processing*, vol. 11, pp. 261-256, December. 2014.
- [16] DAUBECHIES, Ingrid. *Ten Lectures on Wavelets*. Philadelphia, Pennsylvania: Society for Industrial and Applied Mathematics, 1992. CBMS-NSF regional conference series in applied mathematics; vol. 61. ISBN 0898712742.

Evaluation for Feature Driven Development Paradigm in Context of Architecture Design Augmentation and Perspective Implications

Shahbaz Ahmed Khan Gahyyur¹, Abdul Razzaq²

Department of Computer Science and Software
Engineering
International Islamic University Islamabad
Islamabad, Pakistan

Syed Zeeshan Hasan³

Department of Computer Science & Software
Engineering
Faculty of Basic and Applied Sciences
International Islamic University
Islamabad, PAKISTAN

Salman Ahmed⁴

Department of Computer Science and Software
Engineering
International Islamic University Islamabad
Islamabad, Pakistan

Rafi Ullah⁵

Department of Computer Science & Software
Engineering
Faculty of Basic and Applied Sciences
International Islamic University
Islamabad, PAKISTAN

Abstract—Agile is a light weight software development methodology that is useful for rapid application development which is the need of current software industry. Since the focus of agile software development is the customer but it does not provide the detailed information about the application's architecture and documentation, so software architecture has its own benefits and use of it has many positive effects. The focus of this paper is to provide a systematic mapping of emerging issues in feature driven development that arises due to lack of architecture support in agile methodology and proposed solution's model. Results of this mapping provides a guideline for researcher to improve the agile methodology by achieving the benefits employed by having an architecture in place that is aligned with agile values and principles. Following research addresses to implement the SEI architecture centric methods in FDD methodology in an adapted form, such that the burden of architecture doesn't affect the agility of FDD. And the researcher found the de-motivators of agile which helps to understand the internal cycle and reduces the issues to implement the architecture. This study helps to understand the difference between architecture and FDD. This researcher mapping creates awareness about the process improvement with the combination of architecture and FDD.

Keywords—Software architecture; agile; architecture and agile; integration of architecture and agile; agile architecting practices

I. INTRODUCTION

Agile practices have gained popularity among various organizations due to its feature of reducing cost and

encouraging change during the development cycle. In modern software development environment, changes to any software product are inevitable [39]. Agile methodology provides answer for this issue. Feature driven development lies under the umbrella of Agile. FDD is a process for assisting teams in producing features incrementally that are useful for the end user. It is extremely iterative and collaborative in nature [5]. The FDD process has extensive guidelines for identifying issues in the system. It also supports in providing builds to the end user on daily or weekly to add more features to the existing software. FDD process requires configuration management for its proper execution because features are being developed in parallel. In this way, integration of the features is made easy while executing the process. Feature Driven Development provides activity tracking support. Activities can include coding, design or testing. Details of this process are reflected in Fig. 1. Feature tracking is implemented by assigning the value ranging from 0 to 1 to the feature. 0 shows that this feature has not yet been developed and 1 depicts the completed feature [1].

Literature defines the software architecture as “The architecture of a software-intensive system is the structure or structures of the system, which comprises software elements, the externally visible properties of those elements, and the relationships among them” [3]. Software architecture defined by IEEE 1471 standard is “The fundamental organization of a system embodied in its components, their relationships to each other and to the environment, and the principles guiding its design and evolution” [7].

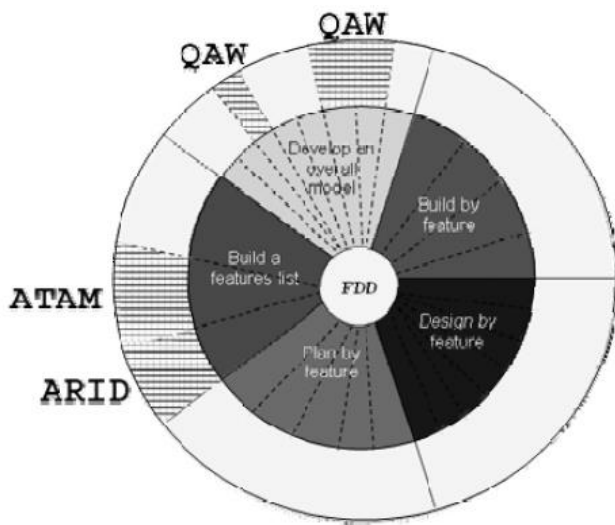


Fig. 1. Hybrid FDD with architecture evaluation methods [16].

A. FDD (Feature Driven Development)

Feature driven Development is a procedure for helping groups deliver visit, substantial working outcomes. It utilizes little squares of customer esteemed usefulness called highlights. It sorts out those little pieces into business-related capabilities. Fig. 1 demonstrates the half and half FDD with an engineering assessment. FDD centers engineers around creating working outcomes at regular intervals. FDD is better arranged to work with group where engineers' experience shifts. It offers advance following and announcing abilities. This solaces supervisors and makes it more alluring for enormous organizations [3].

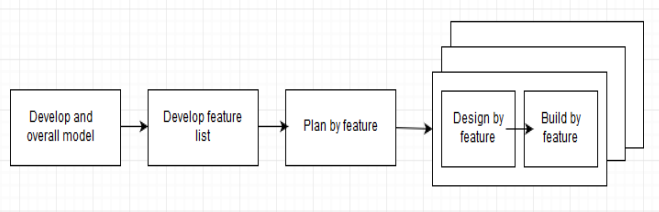


Fig. 2. Feature driven development [8].

- Process # 1: Develop an overall model

The first step of the FDD procedure is to make a detailed model of the system. The clue is for both field and progress members of the team to increase a worthy, shared understanding of the tricky domain. Fig. 2 shows all the phases flow of FDD.

- Process # 2: Build a feature list

The initial step of the FDD procedure is to manufacture an itemized model of the framework to be produced, which catches the partners' suspicions and necessities. The sign is for both field and advance individuals from the group to build a commendable, shared comprehension of the precarious space. Fig. 2 demonstrates every one of the stages stream of FDD [3].

- Process # 3: Plan by feature

Manager of project, Development Manager, and Chief Programmers design the request that the highlights are to be executed, in light of highlight conditions, stack over the improvement group, and the intricacy of the highlights to be actualized [3].

- Process # 4: Design by feature

Highlights different features are planned for improvement by doling out them to a Chief Programmer. Boss Programmer plans little gathering of high spot at once for enhancement. Such a gathering of highlights shapes a Chief Programmer's work Package. The Chief Programmer at that topic an element group by distinguishing the proprietors of the classes (designers) liable to be associated with the improvement of the chose feature(s). The central Programmer at that point refines the protest demonstrate in view of the substance of the succession diagram(s). The engineers compose class and technique prefaces [3].

- Process # 5: Build by feature

Working of the design plan bundle delivered amid the Design by Feature process, the class proprietors execute the things fundamental for their class to help the outline for the feature(s) in the work bundle. The code created is then unit tried and code examined, the request of which is controlled by the Chief Programmer. After an effective code assessment, the code is allowed to build [3].

B. Architecture – centric methods

IEEE 1471 standard [6] explains software architecture as “The fundamental organization of a system exemplified in its components [40], their relationships to each other and to the environment, and the principles managing its design and evolution”.

The software architecture serves as the outline or skeleton of a software system to be built [8], [9]. The benefits of software architecture include a tool for stakeholder communication [7], designing decision documents, identifying design decision risks, reusing [10] scalability [2], allows to program, saving time, the cost of correction or reprocessing is recorded and above all, it helps to avoid software catastrophes [4].

C. Need of Systematic Mapping

In this paper, systematic mapping was explored to find problems that are faced during measurement of individual's performance. PSP quality principles were explored during systematic mapping which can be used for individual's performance measurement in agile team. Main purpose of study is to calculate architecture support provided in feature driven development that resides under the umbrella of agile [12], and how researcher can achieve benefits of architecture using agile methodologies without compromising the agile values [32]. This paper also describes how to cumulate the knowledge by performing systematic mapping study, there are few steps such as “planning”, “conduct the research” and “selection of primary study”.

II. LITERATURE AND BACKGROUND STUDY

Architecture-centric approaches feature early suspicion, arranging and documentation of programming engineering. This infers a specific accentuation on quality traits and outline choices, exercises depend on across the board correspondence and joint effort among partners [13].

In Agile procedures clients or individuals are focal point of focus [35]. Touching delivery of working programming is need over weighted documentation and reports. Testing obliges the conveyance of each little working programming units and successive customer criticism on these product units enables keeping the product to extend on right track and lined up with objectives of the client. XP, Scrum, Feature Driven development are few examples of agile methodologies.

Since agile approaches have important influence on software development practices from industry perspective. However, there is also a prominent impact regarding issues that arises due to lack of SA, which is considered most important artifacts in traditional software development. Many industry professionals who are involved in using agile approaches view software architecture from the perspective of the plan- driven development paradigm [38]. According to them, software architecture design and evaluations requires too much effort which has very little impact to customer's needs from the system [37]. Hence, they view architectural activity as a part of highly formal processes. On the other hand, practitioners of software architecture believe that solid architectural practices cannot be followed using agile methods [36]. However, recently there is an increased appreciation related to the importance of incorporating architectural practices in agile methods. Hence, there is a growing interest and research in this perspective of integrating these two different cultures [11]. Researcher trust that a decent comprehension of current industry practices and issues identified with software architecture is a most important for building strategies to incorporate architecture in agile methodologies [31]. Literature has additionally highlighted a Hybrid Software Architecture Evaluation Method for FDD [33], [34]. Utility trees, affectability focuses and tradeoffs are the characteristic highlights of ATAM [18], [19].

III. RESEARCH METHOD

A. Rational

Researcher undertake the study to improve/evaluate the tailored feature driven development methodology by integrating software architecture support that was originally part of traditional software development so that organizations using FDD can also achieve benefits that are provided by Software architecture. Since software architecture is a very heavy activity which is against the agile core principles so a light weight version of software architecture has been proposed and evaluation will be made on this tailored FDD process as against with traditional FDD process. There is limited published research that validates and measures the impact of integrating architecture in FDD without compromising agile values, and this case study sought to contribute to the body of research in this area.

B. Objective of the Study

The objective of this study is to evaluate the impact of integrating architecture in FDD methodology with respect to reusability, cost, effort, requirement traceability and project failure risks due to unknown domain and untried solutions. Researcher proposed the solution model in proposed solution section.

C. Factors Analysis Method

Researcher used the Minitab static tool [49] for finding and analyzing the results of factors of Agile. Minitab tool helps to create the different types of graphs which help to understand the scenario of factors. Researcher provided the complete results of all factors in Appendix 'A' part and factor analysis result table. Moreover, Appendix 'B' section show result in different graphs [49].

D. Planing of Mapping

In this mapping, issues have been gathered that arises due to lack of architecture in agile methodology with reference to feature driven development (FDD). This mapping will help us to evaluate the benefits [49] that can be achieved if architecture support is provided in agile development.

E. Research Questions

RQ1. What are the problems that can be effectively resolved by integrating architecture in agile methodologies?

RQ2. What are the mapping drawbacks of agile with architecture?

Drawbacks of agile have been discussed in Table IV.

RQ3. What are the mapping limitations and benefits of agile with architecture?

Limitations and benefits of agile is discussed in Table V.

RQ4. What are the emerging challenges have been reported in literature about FDD?

Emerging challenges have been discussed in Table VI.

RQ5. What are the demotivators factors in agile have been reported in literature?

De-motivators have been discussed in Table VII.

F. Search Strategy

Computing databases become the basis for searching primary studies. Following search strings and keywords are used in these databases.

G. Keywaords

The following keywords are used for searching the studies: {architecture}, {architecture centric method}, {agile}, {Feature Driven development}, {FDD}, {integration}, {incorporation}, {combination}, {effect}, {influence}, {Values}, {principles}.

H. Search String(s)

1) {Architecture centric method} AND {agile} OR {Feature Driven development}.

- 2) {Integration} OR {incorporation} OR {combination} of {architecture} AND {agile} OR {Feature Driven development}.
- 3) {Agile issues} OR {software architecture benefits} OR {agile drawbacks} OR {agile problems}.

IV. SELECTION OF PRIMARY STUDY

A. Search Engine

Search strings are put in advanced search of following software engineering databases: IEEE, ACM, Science direct, Springer and Google Scholar. Fig. 3 shows all the digital libraries.



Fig. 3. Databases for paper selection.

B. Inclusion Criteria

Research papers are selected based on their titles and abstracts. Following criteria will be used to select the papers.

- Research papers discussing the integration of agile and architecture at any level.
- Research papers that highlights project failure using agile methodology.
- Research papers relevant to agile values will be included.

- Research papers that discusses the architecture impact on reusability, cost, effort and requirement traceability.

C. Exclusion Criteria

These papers were excluded.

- Books and slides, etc. were excluded.
- Papers other than primary and irrelevant studies.

V. CONDUCTING MAPPING

Search results from different digital libraries are mentioned in Table I. These digital libraries were selected because they were highly known for having empirical studies and literature surveys and are most relevant to software engineering field [27]. Digital libraries search was made to include all the papers that identify agile issues, architecture benefits, or any other paper that discusses integration of both of them. After this initial search, papers were selected from the digital libraries based on the inclusion and exclusion criteria mentioned in Section IV. With further investigation of selected papers, researcher has filtered studies that are most appropriate to the problem in hand. Table I shows all the found publications. These filtered papers are shown in Table II. Relevant studies are shown below in Table III.

TABLE I. PUBLICATION COUNT

Database	Publications count
IEEE	80
ACM	105
Springer	65
Science Direct	110
Scopus	149
Google Scholar	290

TABLE II. PRIMARY STUDIES

No	Reference	Primary study
1	[5]	FDRD: Feature Driven Reuse Development Process Model
2	[38]	A Applied Example of Attribute-Driven Design (ADD)
3	[14]	FORM: A Feature-Oriented Reprocess Method with Domain-Specific Reference Architectures
4	[15]	Foremost Functional Development Session Agile Techniques for Project Management Engineering Software
5	[3]	Software Architecture as a Set of Architectural Design Decisions
6	[11]	An experimental study of architectural practices and challenges in term of used of agile software development approaches
7	[16]	Agile techniques, organizational culture and agility: few insights
8	[17]	Reuse in large-scale agile software development and different factors of Communication for speed
9	[18]	Software architecture and ASD: clash of two cultures?
10	[19]	Flexible Working Architectures: Agile Architecting Using PPCs
11	[20]	A systematic mapping study on the combination of software architecture and agile development

TABLE III. RELEVANT STUDIES

No	Reference	Relevant study
1	[21]	ASD with CBSE
2	[22]	Effort approximation in Agile software development: A survey on practices
3	[23]	On the Responsibilities of Software Architects and Software Engineers in an Agile Environment: Who Should Do What?

4	[24]	Perceived Productivity Threats in Large Agile Development Projects
5	[25]	The combined OPN and UML method for developing an agile manufacturing control system
6	[26]	Building Software Solutions in an Industrial Information System: The 5+1 Software Architecture Model
7	[27]	The necessary nature of product traceability and its relation to Agile approaches
8	[1]	Agile software development methods review and analysis
9	[7]	IEEE Std 1471-2000, Recommended Practice for the Architectural Description of High Intensity Systems
10	[2]	Get ready for agile methods, with care
11	[21]	Agile software development for component based software engineering
12	[23]	On the Responsibilities of Software Architects and Software Engineers in an Agile Environment: Who Should Do What?

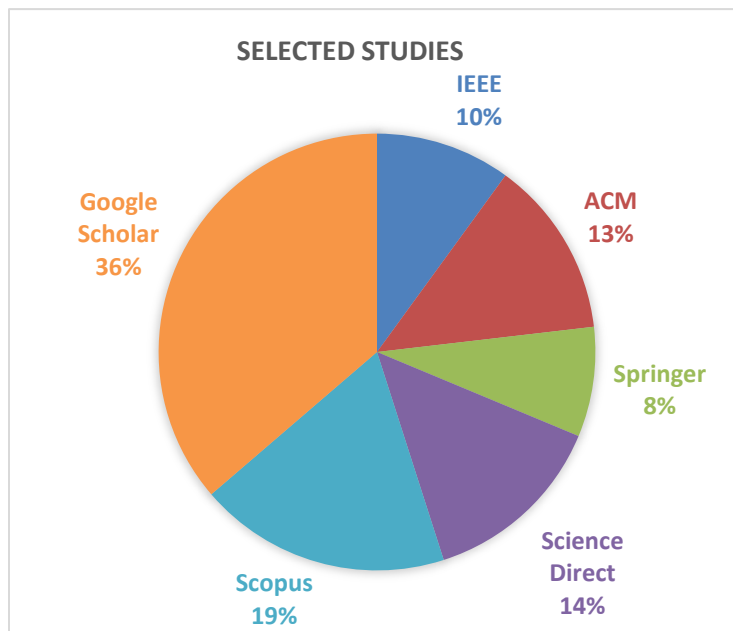


Fig. 4. Selected studies.

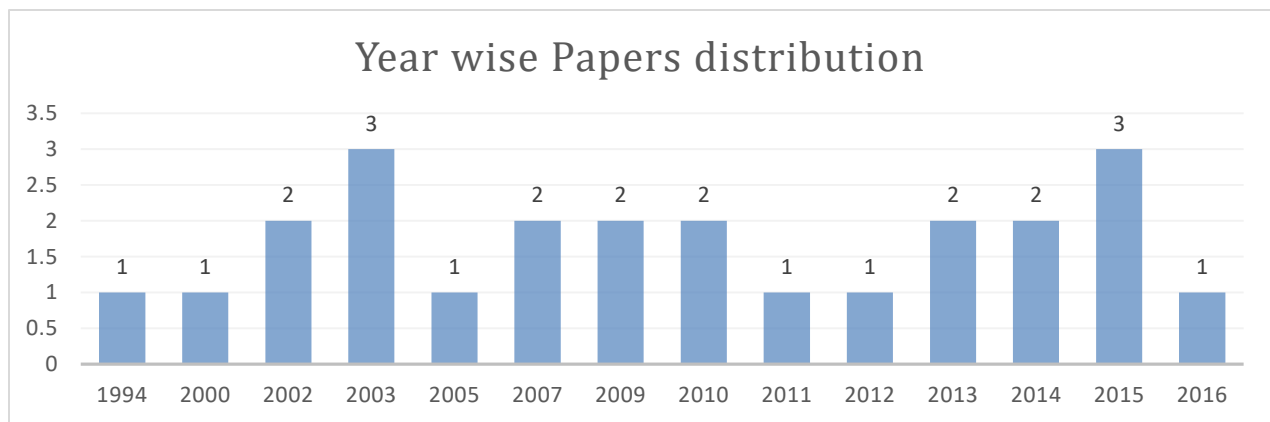


Fig. 5. Year wise paper distribution.

The total of primary and relevant study count that was included in this mapping is 23. These are the strong evidence that shows conflicting as in Fig. 4. Study source distribution on IEEE, Google Scholar, ACM, Springer, Science Direct and Scopus is displayed in the graph on the right side Fig. 3.

A. Data Collection

Data obtained from each study was:

- Source and full reference.
- Grouping of the study type (Agile architecture integration, Agile issues, Architecture benefits, Architecture agile conflict)
- Summary of each study that includes main research questions.

B. Data Analysis

The data was collected to show:

- Whether the study presents high level architecture support with evidence in feature driven development.
- Whether the study presents explained low level design support with evidence in feature driven development.
- Whether the study highlights any risks due to lack of architecture.

- Factors that are inherited by architecture but are against the agile values and vice versa.

VI. MAPPING OF AGILE DRAWBACKS RELATED TO ARCHITECTURE

The issues are described in the below table (Table IV). By adding an architecture support in agile process, researcher can remove these drawbacks.

TABLE IV. MAPPING OF AGILE DRAWBACKS RELATED TO ARCHITECTURE

Years in which issues are highlighted	Incapability to reuse components	Design erosion, knowledge and rationale vaporization	Risk of failure (or delayed feature distribution) in case of unknown domain	Highly experienced domain developers required for successful projects	Primary study references
2015	x				[5]
2013	x				[17]
2007		x			[15]
2014		x			[16]
2009			x	x	[11]

TABLE V. MAPPING OF AGILE LIMITATIONS AND ARCHITECTURE BENEFITS

Sr. #	Agile limitations	Architecture benefits
1	Incapability to reuse components due to architecture discontinuities[5][17]	Documentation of Architecture is explicitly defined architecture discontinuities are limited and reusing component is made possible due to availability of documentation and design rationale[13] [14]
2	knowledge and foundation disappearance in Design destruction, as a result of ad-hoc design decisions documentations[15][16]	Design decisions' documentations addresses knowledge and design erosion, and rationale vaporization. [13][3]
3	In case of unidentified domain and novel solutions the Risk of failure [11]	[14] and [13] provides an unambiguous study of architectural decisions and a clear classification of user stories as quality scenarios and should decrease these risks.
4	Extremely skilled domain developers mandatory for successful projects[11]	[14] and [13] provides a step-by-step approach to architecture, which is also referred to as a plan-based approach, known for a person's exploration of the new domain.
5	Lack of requirements traceability[11]	[13] The step-by-step approach to architecture classifies the requirements according to their importance and documents them in the development of software

TABLE VI. EMERGING CHALLENGES OF FDD

No.	Challenges	Ref.
1	Secure Development	[29]
2	Requirements gathering and managing	[29] [30]

MAPPING OF AGILE DRAWBACKS RELATED TO ARCHITECTURE

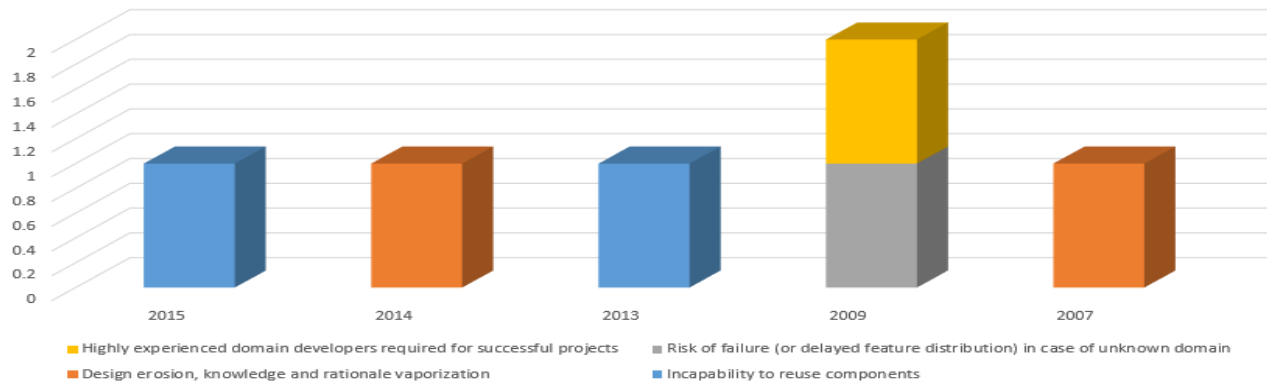


Fig. 6. Mapping of agile drawbacks.

TABLE VII. DE-MOTIVATORS OF AGILE FROM LITERATURE [50]

No	De-motivators factors	Ref.
1	Communication barrier	[22] [41][47] [48] [46]
2	Lack of relationship opportunities	[42] [43] [47] [45]
3	Unrealistic goals	[47] [45] [48]
4	Injustice in promotions	[47]
5	Poor quality software	[13] [47] [48]
6	Political environment	[44]
7	Uncompetitive pay	[47] [45] [48]
8	Unsupportive management	[45]
9	Lack of influence	[47] [45] [48]
10	Unfair reward system	[47] [45] [48]
11	Non-interesting work	[45]
12	personal preferences	[45] [48]
13	Risk	[11] [41] [47] [45] [48]
14	Stress	[45]

De-Motivator Factors Frequency of Agile

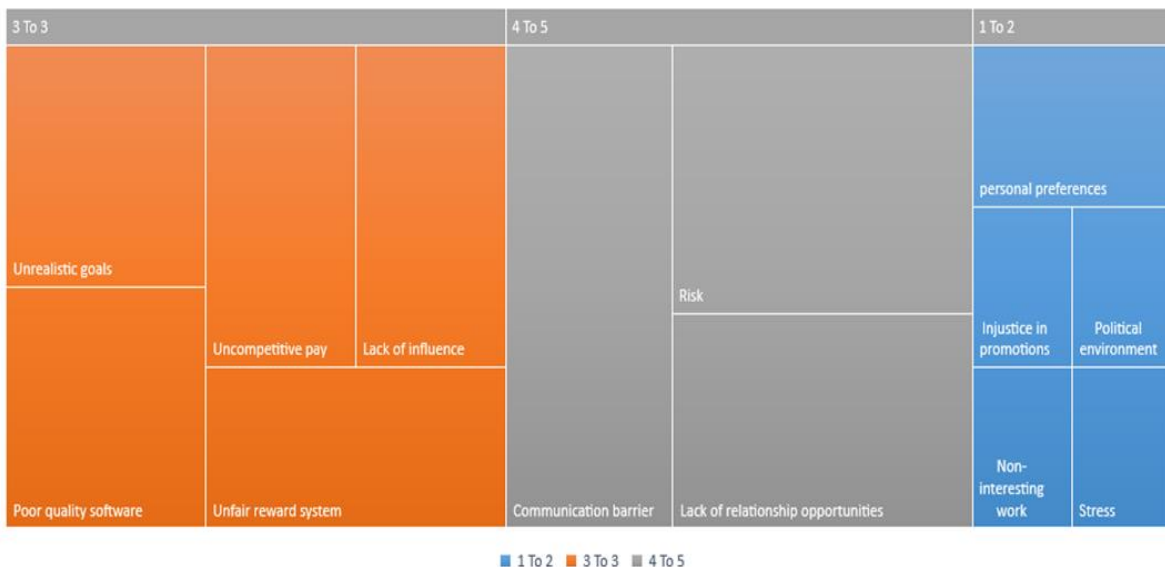


Fig. 7. Demotivator factors of agile.

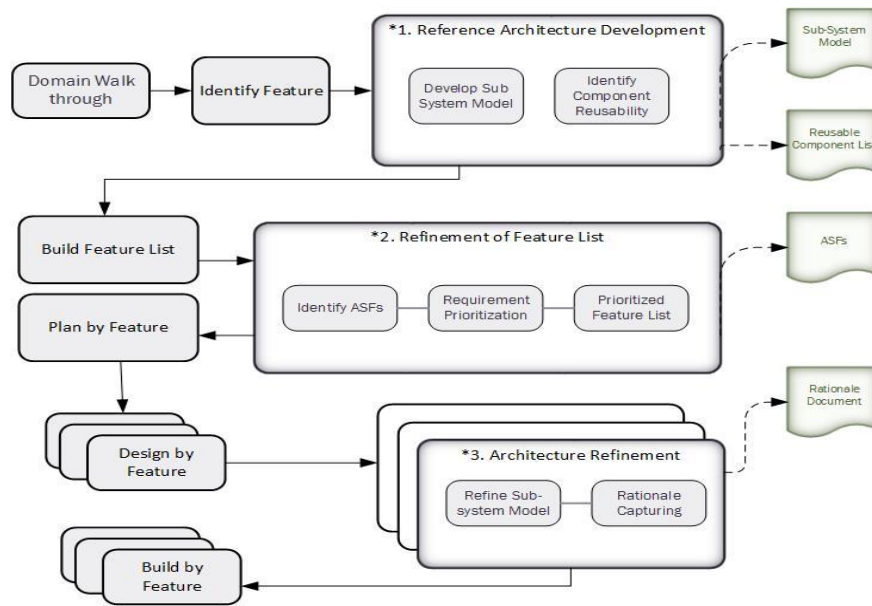


Fig. 8. Proposed solution.

VII. PROPOSED SOLUTION MODEL

With the problem in hand, Researcher proposed the following model that suits the agility and embeds architecture support in FDD so that Researcher can achieve benefits of architecture without losing agility of Feature Driven development.

Following new artifacts have added in proposed process model:

- Reference architecture development
- 1) Refinement of Feature List
- 2) Architecture refinement

Following new documents have produced in proposed model:

- 1) Sub-system model
- 2) Reusable component list
- 3) Architecturally significant Features (ASFs)
- 4) Rationale Document

Each sub process in the newly added artifacts is explained below.

A. Reference Architecture Development

1) Develop Sub-System Model

To develop sub-system model, engineering principles are used as an input to these models [28]. The engineering principles include design principles and general guidelines for subsystem design. Overall system structure is defined by grouping functions into subsystems, which are, then allocated to different hardware the model created for them is called subsystem model.

2) Identify component reusability

Reusability of the components and their fitness for large architecture is determined from subsystem model.

B. Refinement of Feature List

1) Identify ASFs

Indicators for architectural significance include:

- Extraordinary business value and/or technical risk.
- Important (influential, that is) stakeholder.
- budget overruns or client dissatisfaction

At the end of this activity, Researcher has a list of ASFs in hand to perform further processing based on this list.

2) Requirement Prioritization

Prioritization is done by ranking. Researcher gave each one a different numerical value based on its importance. For example, the number 1 can mean that the requirement is the most important and the number n can be assigned to the least important requirement, n being the total number of requirements based on the combined importance relevant to architecture and stakeholders. Researcher choose this method as it can be difficult to align different stakeholders' perspectives on what the priority of a requirement should be; taking an average can however, address the problem in this prioritization method.

3) Prioritized feature list

Prioritization done in the previous activity will listed down to form a Prioritized Feature list along the rationale of prioritization and get it approved from the concerned stakeholders.

C. Architecture Refinement

1) Refine sub-system model

Sub system model is refined in each iteration as the knowledge of stakeholder increases and issues they faced with the delivered iteration.

2) Rationale capturing

In refinement of sub-system model, every decision and change is documented in the specified template, so that back tracking is possible whenever needed.

VIII. CONCLUSION

In this paper, a systematic mapping of agile issues, the proposed model provides the detail to reduce these issues and architecture benefits have been presented so that researcher can address by integrating architecture in agile methodologies with reference to feature driven development. There are different types of architectural challenges reported in literature Table VI. Researcher has discussed in details about SA with FDD. Researcher discussed very clearly about drawbacks of agile related to architecture in Table IV. Researcher found the agile drawbacks and benefits of architecture in Table V. Fig. 5 shows the distribution of papers years wise. Fig. 6 shows the drawbacks in agile. Fig. 7 discusses the most important demotivators of agile. Fig. 8 is the main thing that is proposed solution model. Minitab static tool is used to analyze the factors of agile which are mentioned in Fig. 7 and produce the result in the form of quantitative values and different views that graphs are Scree plot which is the major graph (Fig. 6) of this analysis. Other graphs and results are shown in Appendix section which are: Fig. 9, 10, 11, and 12. Research questions have been discussed through table for data. This mapping acts as a foundation for further research to incorporate architecture in agile methodologies in a way that is aligned with agile principles. In this systematic mapping, researcher described the concepts of Software Architecture with FDD.

IX. FUTURE WORK

Researcher will experiment based on the proposed model an adapted architecture that will be light weighted and can be integrated with feature driven development without harming the agility of this process. Researcher evaluated the proposed method and it proved to be useful in increasing reusability, traceability and also cost effective for middle sized projects. Moreover, this proposed process also puts positive effect on agile values and principles.

REFERENCES

- [1] S. Thakur and H. Singh, "FDRD: Feature driven reuse development process model," Proc. 2014 IEEE Int. Conf. Adv. Commun. Control Comput. Technol. ICACCCT 2014, no. 978, pp. 1593–1598, 2015.
- [2] P. Abrahamsson, O. Salo, J. Ronkainen, and J. Warsta, "Agile software development methods review and analysis," VTT Publ., no. 478, pp. 3–107, 2002.
- [3] D. Ph, "Major Seminar On Feature Driven Development Agile Techniques for Project Management Software Engineering By Sadhna Goyal Guide : Jennifer Schiller Chair of Applied Software Engineering," p. 4, 2007.
- [4] S. R. Palmer and J. M. Felsing, A Practical Guide to Feature-Driven Development. 2002.
- [5] A. . Fallis, "No Title No Title," J. Chem. Inf. Model., vol. 53, no. 9, pp. 1689–1699, 2013.
- [6] I. A. W. Group, "IEEE Std 1471-2000, Recommended practice for architectural description of software-intensive systems," p. i–23, 2000.
- [7] J. Bosch, "Software Architecture : The Next Step," Lect. Notes Comput. Sci., vol. 3047, pp. 194–199, 2004.
- [8] "Len Bass, Paul Clements, Rick Kazman-Software Architecture in Practice-Addison-Wesley Professional (2003)." .
- [9] B. Boehm, "Get ready for agile methods, with care," Computer (Long Beach, Calif.), vol. 35, no. 1, pp. 64–69, 2002.
- [10] D. Garlan and M. Shaw, "An Introduction to Software Architecture," Knowl. Creat. Diffus. Util., vol. 1, no. January, pp. 1–40, 1994.
- [11] J. Melorose, R. Perroy, and S. Careas, "FORM: A Feature-Oriented Reuse Method with Domain-Specific Reference Architectures," Statew. Agric. L. Use Baseline 2015, vol. 1, pp. 1–28, 2015.
- [12] P. O. Bengtsson and J. Bosch, "Scenario-Based Architecture Reengineering," Proc. Fifth Int'l Conf. Softw. Reuse (ICSR 5), pp. 1–10, 1998.
- [13] M. R. Barbacci, R. Ellison, A. J. Lattanze, J. a. Stafford, C. B. Weinstock, and W. G. Wood, "Quality Attribute Workshops, Third Edition," Quality, no. August, p. 38, 2003.
- [14] R. Kazman, L. Bass, and M. Klein, "The essential components of software architecture design and analysis," J. Syst. Softw., vol. 79, no. 8, pp. 1207–1216, 2006.
- [15] C. Hofmeister, P. Kruchten, R. L. Nord, H. Obbink, A. Ran, and P. America, "A general model of software architecture design derived from five industrial approaches," J. Syst. Softw., vol. 80, no. 1, pp. 106–126, 2007.
- [16] A. Tang, Y. Jin, and J. Han, "A rationale-based architecture model for design traceability and reasoning," J. Syst. Softw., vol. 80, no. 6, pp. 918–934, 2007.
- [17] X. Cui, Y. Sun, S. Xiao, and H. Mei, "Architecture design for the large-scale software-intensive systems: A decision-oriented approach and the experience," Proc. IEEE Int. Conf. Eng. Complex Comput. Syst. ICECCS, pp. 30–39, 2009.
- [18] M. a Babar, "An exploratory study of architectural practices and challenges in using agile software development approaches," 2009 Jt. Work. IEEE/IFIP Conf. Softw. Archit. Eur. Conf. Softw. Archit., pp. 81–90, 2009.
- [19] W. G. Wood, "A Practical Example of Applying Attribute-Driven Design (ADD), Version 2 . 0," Technology, vol. Version 2, no. February, p. 59, 2007.
- [20] A. Jansen and J. Bosch, "Software Architecture as a Set of Architectural Design Decisions," 5th Work. IEEE/IFIP Conf. Softw. Archit., pp. 109–120, 2005.
- [21] L. Kompella, "Agile methods, organizational culture and agility: some insights," Proc. 7th Int. Work. Coop. Hum. Asp. Softw. Eng. - CHASE 2014, pp. 40–47, 2014.
- [22] A. Martini, L. Pareto, and J. Bosch, "Communication factors for speed and reuse in large-scale agile software development," Proc. 17th Int. Softw. Prod. Line Conf. - SPLC '13, p. 42, 2013.
- [23] P. Kruchten, "Software architecture and agile software development: a clash of two cultures?," 2010 ACM/IEEE 32nd Int. Conf. Softw. Eng., vol. 2, pp. 497–498, 2010.
- [24] and P. P. A. Jennifer Pérez, Jessica Diaz, Juan Garbajosa, "Flexible Working Architectures: Agile Architecting Using PPCs," October, vol. 2, pp. 1–20, 2003.
- [25] C. Yang, P. Liang, and P. Avgeriou, "A systematic mapping study on the combination of software architecture and agile development," J. Syst. Softw., vol. 111, pp. 157–184, 2016.
- [26] W. Radinger and K. M. Goeschka, "Agile software development for component based software engineering," Companion 18th Annu. ACM SIGPLAN Conf. Object-oriented Program. Syst. Lang. Appl., pp. 300–301, 2003.
- [27] M. Usman, E. Mendes, and J. Börstler, "Effort estimation in Agile software development: A survey on the state of the practice," ACM Int. Conf. Proceeding Ser., vol. 27–29–Apr, 2015.
- [28] A. Tang, T. Gerrits, P. Nacken, and H. van Vliet, "On the Responsibilities of Software Architects and Software Engineers in an Agile Environment: Who Should Do What?," SSE '11 Proc. 4th Int. Work. Soc. Softw. Eng., pp. 11–18, 2011.
- [29] J. E. Hannay and H. C. Benestad, "Perceived Productivity Threats in Large Agile Development Projects," Proc. 2010 ACM-IEEE Int. Symp. Empir. Softw. Eng. Meas., no. 1325, pp. 1–10, 2010.
- [30] M.-S. Lu and L.-K. Tseng, "The integrated OPN and UML approach for developing an agile manufacturing control system," 2009 Int. Conf. Autom. Robot. Control Syst. ARCS 2009, pp. 24–31, 2009.

[31] S. B. A. Guetat and S. B. D. Dakhli, "Building Software Solutions in an Urbanized Information System: The 5+1 Software Architecture Model," *Procedia Technol.*, vol. 5, no. 33, pp. 481–490, 2012.

[32] K. D. Palmer, "The essential nature of product traceability and its relation to Agile approaches," *Procedia Comput. Sci.*, vol. 28, no. Cser, pp. 44–53, 2014.

[33] F. Kanwal, K. Junaid, and M. A. Fahiem, "A hybrid software architecture evaluation method for fdd-an agile process model," *Comput. Intell. Softw. Eng. (CiSE), 2010 Int. Conf.*, pp. 1–5, 2010.

[34] R. L. Nord and J. E. Tomayko, "Software architecture-centric methods and agile development," *IEEE Softw.*, vol. 23, no. 2, pp. 47–53, 2006.

[35] F. Breu, S. Guggenbichler, and J. Wollmann, *The Agile Samurai*. 2008.

[36] M. Fowler and J. Highsmith, "The agile manifesto," *Softw. Dev.*, vol. 9, no. August, pp. 28–35, 2001.

[37] H. P. Breivold, D. Sundmark, P. Wallin, and S. Larsson, "What does research say about agile and architecture?," *Proc. - 5th Int. Conf. Softw. Eng. Adv. ICSEA 2010*, pp. 32–37, 2010.

[38] R. Wojcik and P. Clements, "Attribute-Driven Design (ADD), Version 2 . 0," *Design*, no. November, p. 55, 2006.

[39] A. en Claes Wohlin, Per Runeson, Martin Host, Magnus C.Ohlsson, Bjorn Regnell, *Experimentation is Software Engineering*.

[40] D. Hristov, O. Hummel, M. Huq, and W. Janjic, "Structuring Software Reusability Metrics for Component-Based Software Development," no. c, pp. 421–429, 2012.

[41] Akhtar, M.J., Ahsan, A. and Sadiq, W.Z., 2010, October. Scrum adoption, acceptance and implementation (a case study of barriers in Pakistan's IT industry and mandatory improvements). In *Industrial Engineering and Engineering Management (IE&EM), 2010 IEEE 17th International Conference on* (pp. 458-461). IEEE.

[42] Wagener, R.P., 2012. Investigating critical success factors in agile systems development projects (Doctoral dissertation, North-West University)..

[43] Chow, T. and Cao, D.B., 2008. A survey study of critical success factors in agile software projects. *Journal of systems and software*, 81(6), pp.961-971.

[44] Baddoo, N. and Hall, T., 2002. Motivators of Software Process Improvement: an analysis of practitioners' views. *Journal of Systems and Software*, 62(2), pp.85-96.

[45] Asghar, I. and Usman, M., 2013, December. Motivational and de-Motivational factors for software engineers: an empirical investigation. In *Frontiers of Information Technology (FIT), 2013 11th International Conference on* (pp. 66-71). IEEE.

[46] Beecham, S., Sharp, H., Baddoo, N., Hall, T. and Robinson, H., 2007, August. Does the XP environment meet the motivational needs of the software developer? An empirical study. In *Agile Conference (AGILE), 2007* (pp. 37-49). IEEE.

[47] Beecham, S., Baddoo, N., Hall, T., Robinson, H. and Sharp, H., 2006. Protocol for a systematic literature review of motivation in software engineering. University of Hertfordshire.

[48] França, A.C.C., Gouveia, T.B., Santos, P.C., Santana, C.A. and da Silva, F.Q., 2011, April. Motivation in software engineering: A systematic review update. In *Evaluation & Assessment in Software Engineering (EASE 2011), 15th Annual Conference on* (pp. 154-163). IET.

[49] Shahbaz Ahmed, Abdul Razzaq, S. Ullah, S. Ahmed, *Matrix Clustering Based Migration of System Application to Microservices Architecture*, ijacsa, Jan, 2018.

[50] Ahmed, Shahbaz & Ahmed, Salman & Naseem, Adnan & Razzaq, Abdul. (2017). Motivators and Demotivators of Agile Software Development: Elicitation and Analysis. *International Journal of Advanced Computer Science and Applications*. 8. 10.14569/IJACSA.2017.081239.

FACTOR ANALYSIS RESULT REPORT

APPENDIX A

Factor: Communication barrier, personal preferences, Unrealistic goals, Poor quality software, Uncompetitive, Lack of influence, Unfair reward

system, Uncompetitive pay, Lack of relationship opportunities, Risk, Political environment, Non-interesting work, Stress, Injustice in promotions

A. Principal Component Factor Analysis of the Correlation Matrix

I) Unrotated Factor Loadings and Communalities:

Variable	Factor1	Factor2	Factor3	Factor4	Factor5	Factor6
personal preferences	0.851	0.355	-0.007	0.068	-0.153	-0.028
Unrealistic goals	-0.102	0.279	0.579	0.496	0.273	-0.049
Poor quality software	-0.089	0.304	-0.517	-0.309	0.301	0.032
Uncompetitive pay	-0.140	0.552	-0.254	-0.408	0.335	-0.049
Lack of influence	-0.296	0.266	0.140	-0.214	-0.545	0.360
Unfair reward system	0.688	0.480	0.090	-0.308	-0.002	-0.072
Lack of relationship opportunit	-0.108	0.051	0.023	0.030	-0.665	-0.194
Communication barrier	0.152	-0.425	0.497	-0.495	0.170	-0.029
Risk	-0.235	0.430	0.471	0.192	0.332	0.262
Injustice in promotions	0.789	0.135	0.017	0.151	-0.009	0.002
Political environment	0.238	-0.412	0.408	-0.579	0.057	0.145
Unsupportive management	0.001	-0.296	-0.315	0.126	0.121	0.729
Non-interesting work	0.672	-0.135	-0.062	0.196	-0.034	0.418
Stress	-0.294	0.565	0.230	-0.226	-0.235	0.347
Variance	2.6294	1.8820	1.4870	1.3985	1.2537	1.0958
% Var	0.188	0.134	0.106	0.100	0.090	0.078

Variable	Factor7	Factor8	Factor9	Factor10	Factor11
Factor12					
personal preferences	-0.011	0.063	-0.152	0.001	0.233
Unrealistic goals	-0.045	0.117	-0.126	0.334	-0.275
Poor quality software	-0.200	0.471	0.352	0.196	0.036
Uncompetitive pay	-0.050	-0.427	-0.112	0.076	-0.305
Lack of influence	0.285	0.428	-0.068	0.037	-0.216
Unfair reward system	-0.125	0.125	-0.354	-0.041	0.060
Lack of relationship opportunit	-0.659	-0.136	0.106	0.192	-0.047
Communication barrier	0.071	-0.033	0.092	0.418	0.239
Risk	-0.348	0.109	0.173	-0.282	0.186
Injustice in promotions	0.126	0.018	0.271	0.116	-0.181
Political environment	-0.244	0.060	0.006	-0.264	-0.274
Unsupportive management	-0.248	-0.035	-0.351	0.204	0.059
Non-interesting work	0.006	-0.207	0.344	-0.028	-0.152
Stress	0.198	-0.365	0.176	0.064	0.199
Variance	0.8782	0.8332	0.7019	0.5790	0.5417
% Var	0.063	0.060	0.050	0.041	0.039

Variable	Factor13	Factor14	Communality
personal preferences	0.013	-0.172	1.000
Unrealistic goals	0.152	-0.014	1.000
Poor quality software	0.126	-0.008	1.000
Uncompetitive pay	-0.176	-0.051	1.000
Lack of influence	-0.175	-0.017	1.000
Unfair reward system	0.027	0.156	1.000
Lack of relationship opportunit	-0.037	0.004	1.000
Communication barrier	-0.167	0.002	1.000
Risk	-0.199	-0.003	1.000
Injustice in promotions	-0.046	0.013	1.000
Political environment	0.187	-0.057	1.000
Unsupportive management	0.014	-0.005	1.000
Non-interesting work	-0.057	0.046	1.000
Stress	0.251	0.012	1.000

Variance	0.2744	0.0630	14.0000
% Var	0.020	0.004	1.000

Factor Score Coefficients

Variable	Factor1	Factor2	Factor3	Factor4	Factor5	Factor6
personal preferences	0.324	0.189	-0.005	0.049	-0.122	-0.025
Unrealistic goals	-0.039	0.148	0.389	0.355	0.218	-0.045
Poor quality software	-0.034	0.161	-0.348	-0.221	0.240	0.029
Uncompetitive pay	-0.053	0.293	-0.171	-0.292	0.267	-0.045
Lack of influence	-0.112	0.142	0.094	-0.153	-0.435	0.329
Unfair reward system	0.261	0.255	0.060	-0.220	-0.002	-0.066
Lack of relationship opportunit	-0.041	0.027	0.016	0.021	-0.530	-0.177
Communication barrier	0.058	-0.226	0.334	-0.354	0.135	-0.027
Risk	-0.089	0.228	0.317	0.137	0.265	0.239
Injustice in promotions	0.300	0.072	0.011	0.108	-0.007	0.002
Political environment	0.091	-0.219	0.275	-0.414	0.045	0.132
Unsupportive management	0.001	-0.157	-0.212	0.090	0.097	0.665
Non-interesting work	0.256	-0.072	-0.041	0.140	-0.027	0.381
Stress	-0.112	0.300	0.155	-0.162	-0.188	0.317

Variable	Factor7	Factor8	Factor9	Factor10	Factor11
Factor12					
personal preferences	-0.013	0.076	-0.217	0.001	0.429
Unrealistic goals	-0.052	0.140	-0.179	0.578	-0.509
Poor quality software	-0.228	0.565	0.502	0.338	0.066
Uncompetitive pay	-0.056	-0.512	-0.160	0.131	-0.562

Lack of influence	0.324	0.514	-0.097	0.063	-0.399	-0.095
Unfair reward system	-0.142	0.149	-0.505	-0.071	0.111	-0.125
Lack of relationship opportunit	-0.751	-0.164	0.152	0.331	-0.086	0.036
Communication barrier	0.081	-0.040	0.131	0.721	0.440	-0.097
Risk	-0.396	0.131	0.247	-0.488	0.343	0.183
Injustice in promotions	0.143	0.022	0.387	0.200	-0.333	1.167
Political environment	-0.278	0.072	0.008	-0.455	-0.506	0.116
Unsupportive management	-0.282	-0.043	-0.501	0.352	0.108	0.370
Non-interesting work	0.007	-0.248	0.490	-0.048	-0.281	-0.912
Stress	0.226	-0.438	0.250	0.111	0.367	0.162

Variable	Factor13	Factor14
personal preferences	0.046	-2.736
Unrealistic goals	0.554	-0.219
Poor quality software	0.460	-0.126
Uncompetitive pay	-0.640	-0.816
Lack of influence	-0.639	-0.271
Unfair reward system	0.097	2.479
Lack of relationship opportunit	-0.136	0.071
Communication barrier	-0.608	0.025
Risk	-0.727	-0.045
Injustice in promotions	-0.167	0.207
Political environment	0.682	-0.904
Unsupportive management	0.050	-0.085
Non-interesting work	-0.209	0.738
Stress	0.916	0.185

APPENDIX B

Fig. 9 shows the variation among all factors.

Fig. 10 provides the analysis of relationships amongst all the factors in the form of groups. This graph provides different relations in the context of positive and negative.

Fig. 11 tells the co-relationships in two ways amongst factors vertically and horizontally. These relationships are between two factors.

Fig. 12 biplot shows by using the both points.

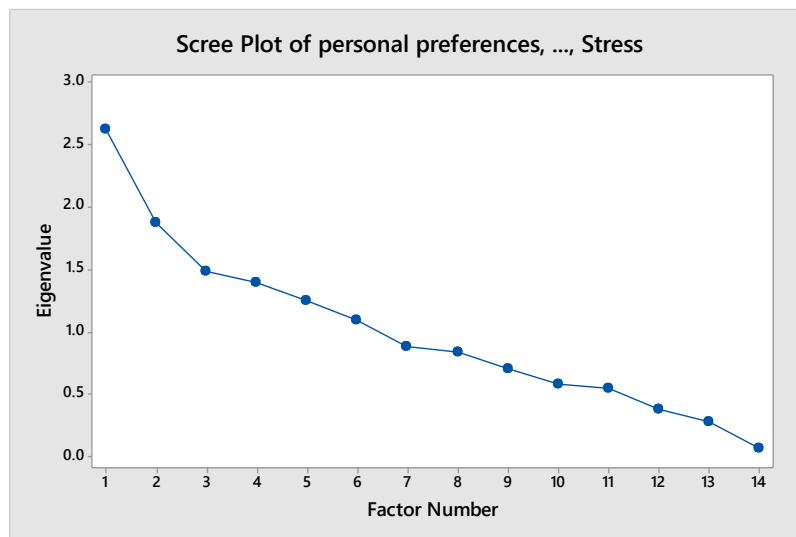


Fig. 9. Factors list analysis variation graph.

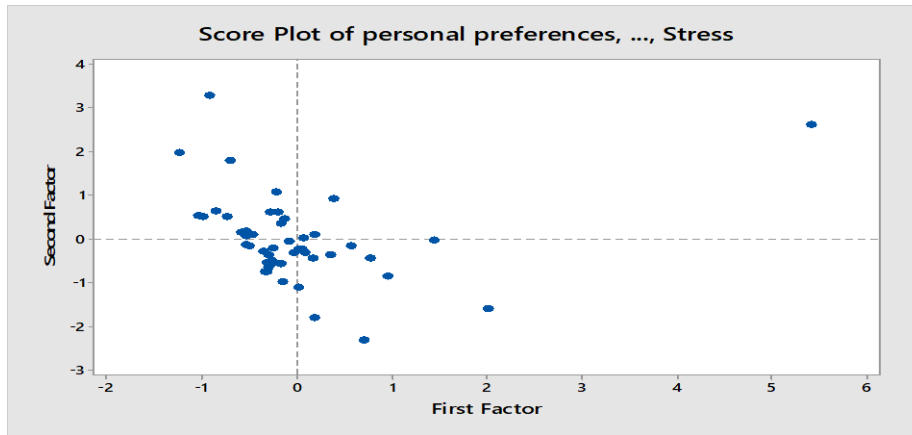


Fig. 10. Score plot.

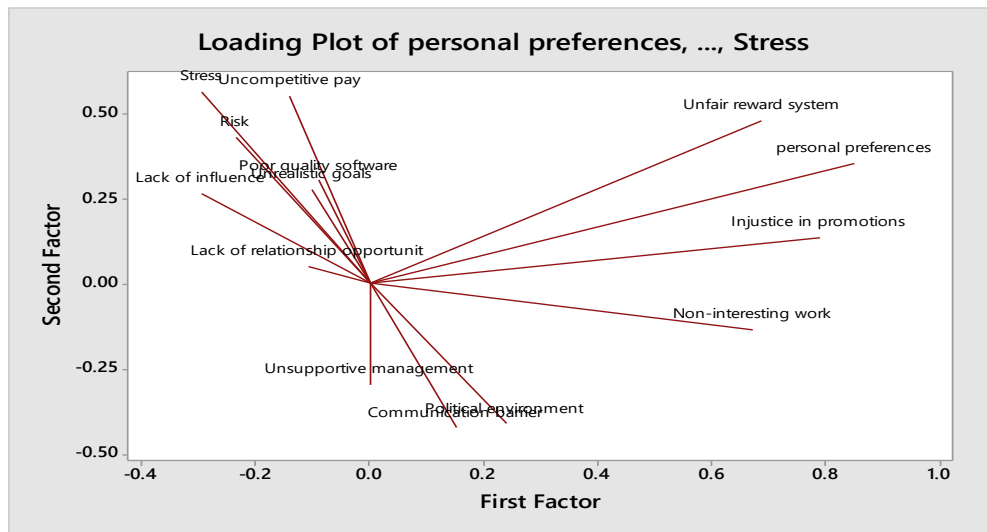


Fig. 11. Loading plot.

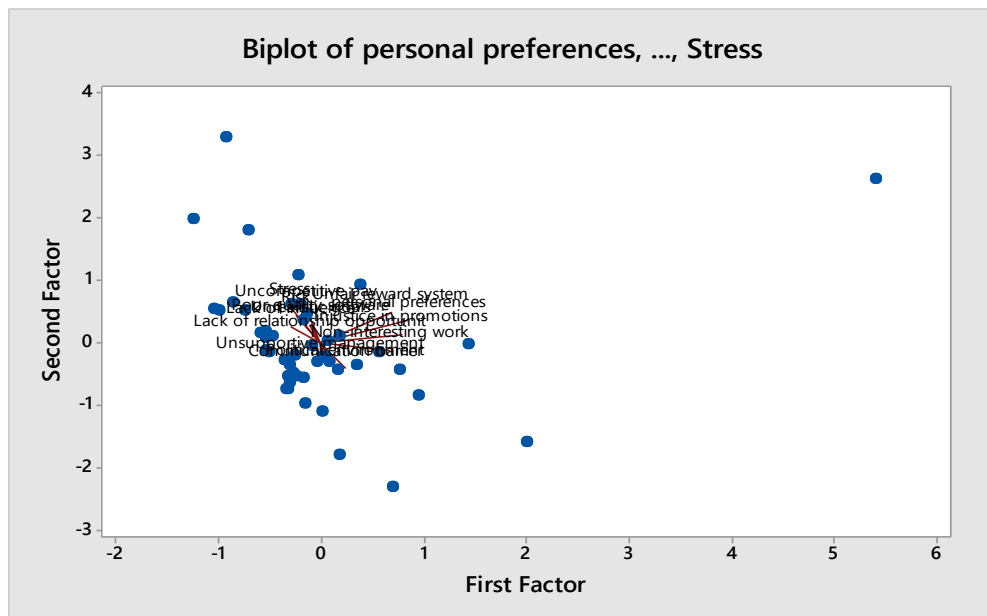


Fig. 12. Biplot.

A High Gain MIMO Antenna for Fixed Satellite and Radar Applications

Ahsan Altaf

Electrical-Electronics Engineering
Department,
Istanbul Medipol University,
Istanbul, Turkey

Khalid Mahmood

Electrical Engineering Department
University of Technology
Nowshehra,
Pakistan

Mehre Munir, Saad Hassan Kiani

Electrical Engineering Department
Iqra National University
Peshawar,
Pakistan

Abstract—Patch antennas have emerged rapidly with advancement of communication technology. For antenna design purposes, Finite difference time domain (FDTD) method is a commonly used. This paper focuses on the interaction among elements of MIMO antenna also known as mutual coupling using FDTD method. An M shape is introduced and with placement of isolating structure, round about 12dB of isolation is increased without degradation of performance parameters. The proposed antenna design can be used for radar and satellite services applications.

Keywords—Mutual coupling; isolating structure; multiple input multiple output; radar application; finite difference time domain

I. INTRODUCTION

Patch antennas have several advantages over non planar Antennas [1]. Due to their light weight, cost effectiveness and multiband properties [2], patch structures have been of central attention among antenna designers and researchers. Computational electro magnetics (CEM) methods have become mostly important with the rapid developments in technologies in fields such as electromagnetic compatibility, antenna analysis, target recognition and lightning strike simulation [3]. Electromagnetic phenomena are ruled by the Maxwell equations, which can be calculated in either the frequency or the time domain. The finite difference time domain (FDTD) technique is possibly the simplest, both conceptually and in terms of implementation, of the full-wave techniques used to solve complications in electromagnetics [4], [5]. It can exactly tackle a wide range of complications. The FDTD algorithm as first suggested by Kane Yee in 1966 employs second-order central differences. Basic FDTD unit cell is shown in Fig. 1.

Mutual coupling is very common unwanted phenomena degrading antenna performance by degrading its parameters. Different approaches have been made in order to improve isolation including electro-magnetic band gap (EBG), Defected ground structure (DGS), line resonators of different shapes, ground patterning [6]-[8]. In this paper, a high gain MIMO antenna has been designed and in order to enhance isolation among patch elements an M shape on ground plane is patterned. The antenna has been analyzed with the in-house prepared FDTD package. This paper is organized as follows:

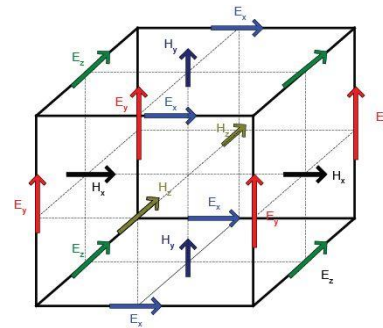


Fig. 1. Basic FDTD unit cell.

Section I covers Introduction, Section II covers antenna design. Section III focuses on Results and Discussions and in the last Section IV, Conclusion is covered.

II. ANTENNA DESIGN

Before designing a patch antenna, a single patch element is designed. In substrate selection, Rogers 5880 with permittivity of 2.2 and thickness comprising of 0.796mm is selected. The cell dimension used in the FDTD simulation program is $x = 0.4mm$, $y = 0.389mm$, $z = 0.265mm$ and $\Delta t = 0.6407ps$. An 8-cell thick PML layer is used resulting in an overall computation domain of $69 \times 80 \times 18$ cells.

The antenna is fed by a z -directed electric field Gaussian pulse, E_s , of $50ps$ waist and maximum amplitude of 1 in the manner described in [2] with a source resistance, R_s of 50Ω to reduce the number of time steps needed for convergence. The length and width of the patch are calculated using equations given below:

$$W = \frac{C}{2f_0 \sqrt{\frac{\epsilon_r + 1}{2}}} \quad (1)$$

Here ϵ_r is the relative constant with f_0 functioning frequency and C is the rapidity of light in vacuum.

$$L = L(eff) - 2\Delta L \quad (2)$$

Where

$$L(eff) = \frac{C}{2f_0 \sqrt{\epsilon_{(reff)}}} \quad (3)$$

And

$$\epsilon_{(reff)} = \frac{\epsilon r + 1}{2} + \frac{\epsilon r - 1}{4} \left(1 + \frac{12h}{W}\right)^{-1/2} \quad (4)$$

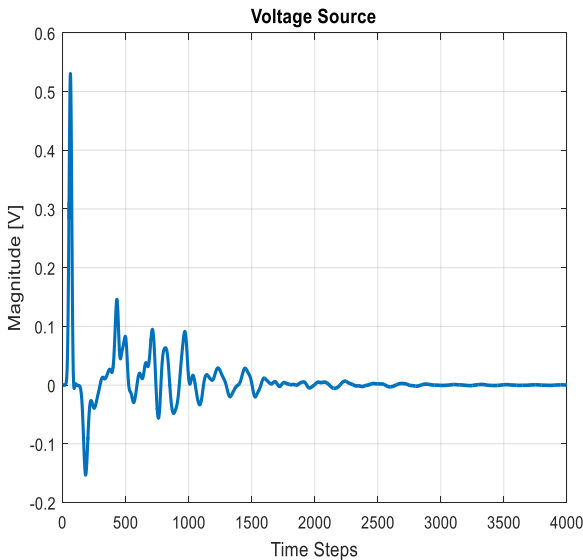


Fig. 2. Patch antenna simulated waveform of voltage with 50Ω Resistance.

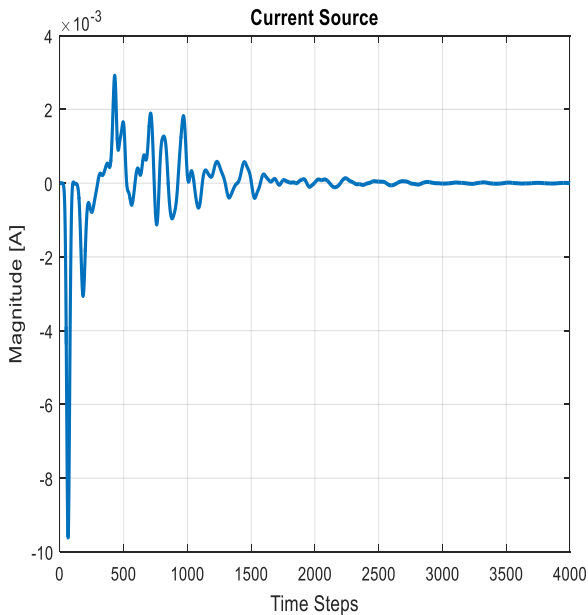


Fig. 3. Patch antenna simulated waveform of current with 50Ω Resistance.

Fig. 2 and 3 shows patch antenna simulated wave form of voltage and current source respectively with 50ohms of resistance. The design parameters are given in Table I. The antenna is as stated above designed at fundamental frequency of 7.45GHz. The isolating structure is then imposed between patch antenna elements as shown in Fig. 4, in order to improve isolation as high level of isolation can degrade antenna performance making it un-useful for applications.

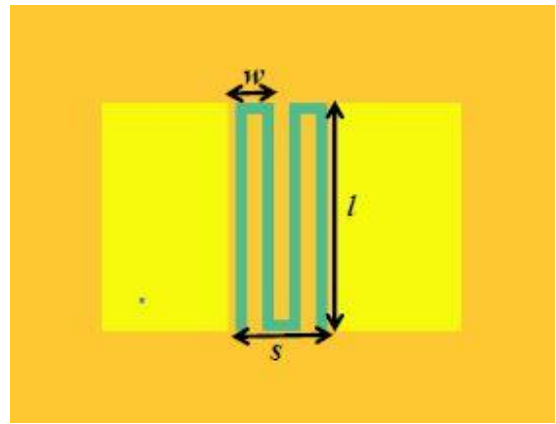


Fig. 4. MIMO antenna design with isolation element.

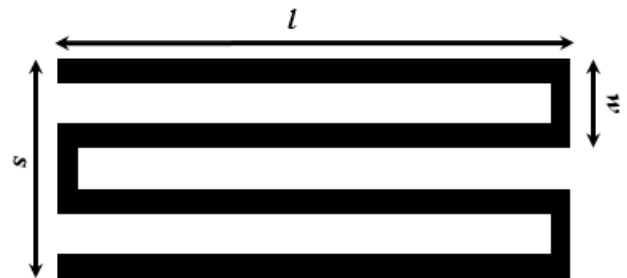


Fig. 5. M Shape structure for surface currents suppressions.

Among isolation techniques, EBG and DGS structures have been found very efficient by antenna designers. In our proposed M shape shown in Fig. 5, l is the overall width of the structure, while s is the overall length. w is the distance between the 2 arms. Input resistance is set to be 50 ohms. The decoupling section. The decoupling unit act as a LC circuit and the resonance frequency of such decoupling unit is dependent on the value of inductance and capacitance.

TABLE I. PATCH ANTENNA DIMENSIONS

Parameters	Length of patch	Width of Patch	Height of Patch	Substrate Height
Values in mm	16	12	0.8	0.796

TABLE II. DIMENSIONS OF M SHAPED STRUCTURES

Parameters	l	s	w
Value (mm)	40	10	0.8

Table II shows the dimensions of M shape isolating structure. The proposed structure is resonated at our desired frequencies and blacks the surface wave's interference between resonating elements.

III. RESULTS AND DISCUSSIONS

The S parameters show the performance of an antenna, as S_{11} is reflection co efficient and mutual coupling is taken in terms of S_{12} . From Fig. 6, showing the S parameters, it is cleared that our isolating structure has increased 18dB of isolation.

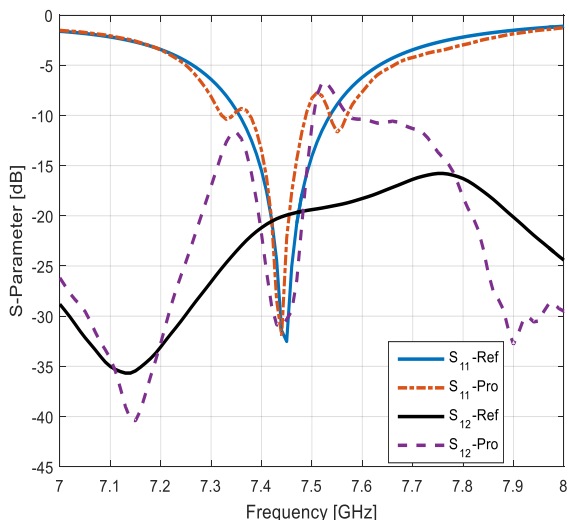


Fig. 6. S-Parameters plot of reference and proposed antenna.

The results between reference and proposed antenna have been summarized in Table III.

TABLE III. PERFORMANCE PARAMETERS OF ANTENNA ARRAY

Parameters	Conventional	Proposed
S11	-32dB	-31.85dB
S12	-18.00dB	-31.0dB
Gain	7.45dB	7.34dB
VSWR	1.03	1.04
Bandwidth	290MHZ	270MHZ

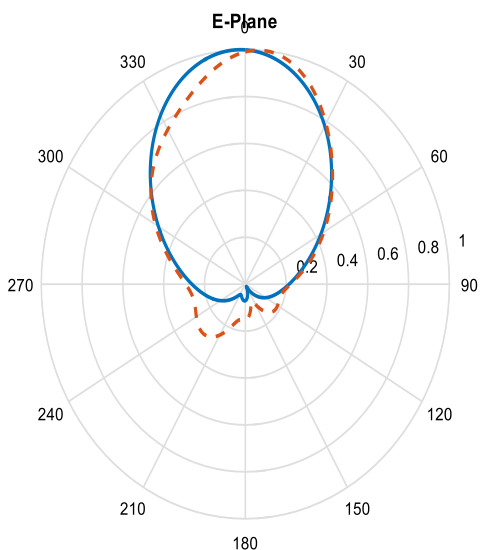


Fig. 7. E field pattern of reference and proposed antenna.

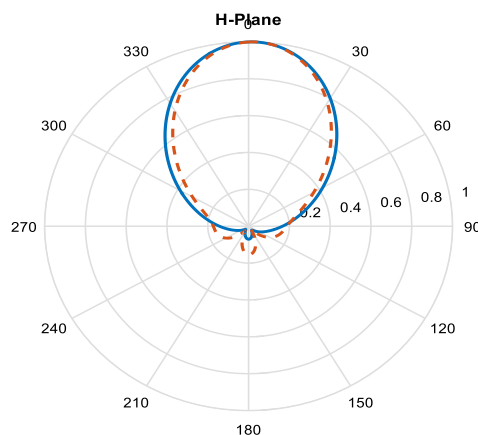


Fig. 8. H field pattern of reference and proposed antenna.

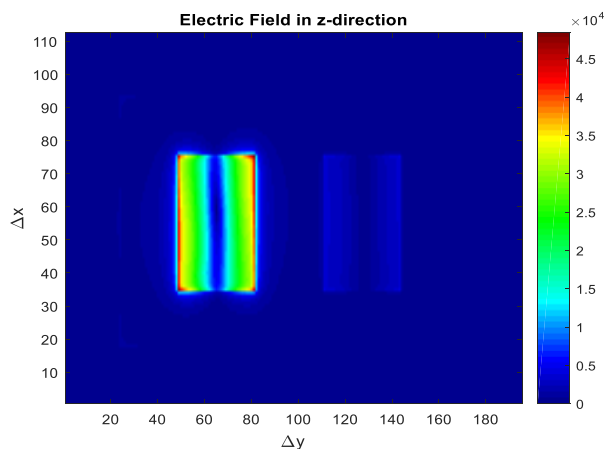


Fig. 9. Current distribution path of reference antenna.

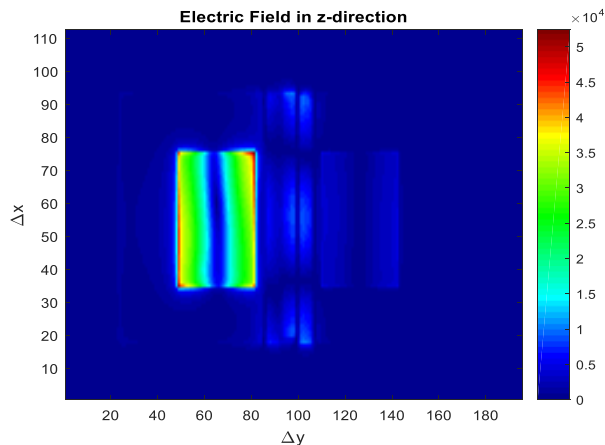


Fig. 10. Current distribution path of proposed antenna.

As seen from Fig. 7 and 8, the E and H plane of proposed and conventional antennas are nearly same showing our structure has not degrade antenna radiation patterns. Surface waves are undesirable in antenna arrays as the increase the back lobe radiation and antenna efficiency is decreased. Also with the increasing level of back lobe radiation SNR ration gets worse.

By looking at Fig. 9 and 10, we can clearly indicate that with insertion of proposed structure, the radiating patch surface current is being blocked by isolating structure and is being prevented as compared to Fig. 9 in conventional MIMO antenna where surface current is directly interfering to passive patch and giving rise to coupling. From the above results, it is clear that our proposed isolating structure has resonated on our desired band frequency and has act as an LC circuit to stop unwanted coupling.

IV. CONCLUSION

This paper presents a simple approach of isolation enhancement using FDTD analysis. With insertion of proposed M shape structure, an enhancement of 12dB was increased and the performance parameters were not affected at all. With high gain of above 6.5dB, proposed antenna can be used for satellite services and radar applications.

REFERENCES

- [1] Balanis, Constantine A. Antenna theory: analysis and design. John Wiley & Sons, 2016.
- [2] Saad Hassan Kiani, Shahryar Shafique Qureshi, Khalid Mahmood, Mehr-e- Munir and Sajid Nawaz Khan, "Tri-Band Fractal Patch Antenna for GSM and Satellite Communication Systems" International Journal of Advanced Computer Science and Applications(IJACSA), 7(10), 2016.
- [3] Ergul, Ozgur, et al. "Open problems in CEM: Error-controllable and well-conditioned MoM solutions in computational electromagnetics: Ultimate surface integral-equation formulation." IEEE Antennas and Propagation Magazine 6.55 (2013): 310-331.
- [4] Sullivan, Dennis M. Electromagnetic simulation using the FDTD method. John Wiley & Sons, 2013.
- [5] Li, Hanyu, et al. "Massively parallel FDTD program JEMS-FDTD and its applications in platform coupling simulation." 2014 International Symposium on Electromagnetic Compatibility. IEEE, 2014.
- [6] Sharawi, Mohammad S., Ahmed B. Numan, and Daniel N. Aloï. "Isolation improvement in a dual-band dual-element MIMO antenna system using capacitively loaded loops." Progress In Electromagnetics Research 134 (2013): 247-266.
- [7] Ghosh, Jeet, et al. "Mutual Coupling Reduction Between Closely Placed Microstrip Patch Antenna Using Meander Line Resonator." Progress In Electromagnetics Research Letters 59 (2016): 115-122.
- [8] Zhang, Y., Yu, T., Kong, L.Y., Lang, R.L. and Qin, H.L., 2016, May. Design of Fermat-Archimedes spiral dual-via EBG structure for low mutual coupling antenna array. In Electromagnetic Compatibility (AP EMC), 2016 Asia-Pacific International Symposium on (Vol. 1, pp. 515-517).IEEE.

Circular Calibration of Depth Extraction in Stereo Configuration

Zulfiqar Ibrahim, Zulfiqar Ali Bangash
Department of Computing and Technology
Iqra University, Islamabad Campus
Islamabad, Pakistan

Muhammad Zeeshan
School of Electrical Engineering and Computer Science
National Institute of Science and Technology (NUST)
Islamabad, Pakistan

Abstract—Lens distortion is defined as departure from rectilinear projection of an imaging system which affects the accuracy of almost all vision applications. This work addresses the problem of distortion with investigating the effects of camera's view angle and spherical nature of lens on image, and then derives a closed-form solution for the correction of distorted pixel's angle in image according to geometric shape of lens. We first propose technique that explores the linear relation between lens and charge-coupled device in intrinsic environment of camera, through analysis of pixel's angle in field of view. Second technique for depth extraction through linear transformation in rectangular configuration is achieved by considering the camera's background in field of view which provides optimal results in closed environment. As the object moves away from the center of image in image plane, depth accuracy starts to deteriorate due to radial distortion. To rectify this problem, we finally propose circular calibration methodology which addresses this inaccuracy and accommodate radial distortion to achieve optimal results up to 98%, in great depth with very large baseline. Results show the improvement over established stereo imaging techniques in depth extraction where the presented considerations are not observed. This methodology ensures high accuracy of triangulated depth with very large base line.

Keywords—Stereo imaging; depth extraction; triangulation; radial distortion; lenses; rectilinear projection component

I. INTRODUCTION

Camera calibration is the process of finding the internal and external parameters of camera so that correspondence between object point in object space and its respective image point in image plane can be computed accurately. Due to distortion factor, the relationship between image point and its object point can be difficult to establish. These distortions result in inaccurate measurements of depth estimation in images. Generally, a camera comprised of lens and image plane, light ray from world enters the image plane through lens which describes the transformation exist between world space and image space. This transformation cannot be described perfectly by using perspective transformation due to the distortion. Distortion develops between the points of the world space and location of the images of those points. The camera calibration techniques allow us to model those points on image plane. These techniques will always be approximation to the real relationship of image points to world point. There is always a room for improvement in these approximations. Many techniques have been presented to eradicate this distortion in images with different levels of accuracy and robustness.

Earlier some techniques [1] require proper lab equipment to find the parameters of distortion but most recent techniques [2]-[5] utilized nonlinear iterative mathematical model to estimate the coefficient of distortion model. These techniques suffer from high computation, complexity and inaccuracy which lead to suboptimal solutions. In [2], [3] managed external and internal parameters of camera in his calibration process by using pin hole camera model and special complex techniques for one-pixel width calibration such as 1-D FFT [3]. When this model [2] is introduce to high distortion lenses, significant error occurs in the calibration process which results in inaccuracy of data and loss of robustness [6].

Zhang et al. [4] proposes famous versatile calibration algorithm in which planner surface with known measurements is utilized to find the correspondence between object space and image space. Homography is also being applied between the target plan and its image plane for the calibration process. Lens distortion coefficients are filtered by minimizing algebraic distance defined by associated camera model. To minimize the algebraic distance, nonlinear refinement by Levenberg-Maruardt algorithm [7] is used. Heikkila et al. [5] introduced a very distinctive calibration process in which approximation of forward lens distortion model is being applied that associate with distorted image coordinates with equivalent undistorted image points. The distortion is minimized through nonlinear iterative refinement in distorted image space. For lens Distortion model, authors incorporated two tangential and two radial distortion terms.

F. Devernay et al. [8] presented field of view (FOV) distortion correction model for fish eye lens. The pixel of image from wide fish eye lens, has measured distance from principle point. This distance is approx. proportional to angle between 3D point, optical center and optical axis. The field of view is proportional to image resolution along image radius. Field of view (FOV) [9] is the ability of the lens to absorb the angular extent of the world scene and it is both dependent on lens and image sensor. This angular extent of scene generates the radial distortion due to low quality circular nature of lenses. A.W. Fitzgibbon [10] presented a division model for the distortion correction. The tangential distortion is not consideration in this model. The nature of this model is polynomial. The advantage of division model over polynomial model is its ability to address higher distortion in lower order. Polynomial model is linear model which address the radial distortion due to the hemispherical shape of lens. The paper by Hartley and Zisserrman [11] holds very important status in the

subject of epipolar geometry. Our research is based on multi view geometry which is heavily influenced by this research work from R. Hartly and A. Zisserman [11].

In this work, a homography relates to two views of the world scene when transformations between two cameras are strictly rotational about an axis through its principle point. Epipolar geometry is intrinsic projective geometry between two views which is independent of structure of the scene. It solely depends on internal parameters of camera and relative pose. Disparity is used to extract the depth of point in image plane which is comparable to our research. This paper extensively borrows work from D.C. Brown et al. [1] and F. Devernay et al. [8] for radial distortion correction by using straight line method which is also known as “Plumb Line” method. The reason for the selection of this paper to be compared with our method is the feasibility of widespread deployment of the cameras in local market. The depth extraction algorithm presented by R. Hartley and Zisserman [11] doesn't do not require high end hardware and can easily be developed using OpenCv tool. The availability of the low cost cameras in local market allows this algorithm to be deployed extensively where depth is required for the certain operations and also keep the cost of development low.

Distortion correction is the most important procedure in a camera calibration process where true correspondence between pixel and its respective world point is approximately established. Radial distortion is the deviation of lens from rectilinear projection where straight lines in world appear as curved lines in image. This form of distortion occurs in wide angle and fish eye lenses due to substandard use of materials. Radial distortion can be removed in post processing software by using different methodologies. First we purpose linear transformation technique in stereo configuration where the division model is used to find the angle of object's pixel. This angle is then considered in triangulation with the help of second camera with known baseline, for the depth extraction of the observed pixel. Linear transformation technique produces very optimal results in object's depth for close-range and when object lies in the center of image. In second technique, Linear transformation in rectangular configuration is applied where two camera are placed perpendicularly towards the object for depth extraction. This technique is suitable for indoor environment where background of object in world plane is known. In third technique, circular calibration in stereo configuration, we derive closed form mathematical treatment to eradicate radial distortion by considering non-linear nature of relationship between lens and CCD where the pixel's depth on both sides of image starts distorting in first and second technique. This later technique helps to maintain 98% accuracy when great depth is under consideration.

Followings are the contributions of this work:

- Linear transformation in stereo configuration is the first technique that we purpose to extract the depth information of object in close range without considering radial distortion correction.
- In second technique, we present linear transformation in rectangular configuration where two cameras are

perpendicularly placed around object for depth extraction in indoor environment.

- We also propose Circular Calibration in Stereo Configuration technique where radial distortion correction method is applied for the great depth extraction with very large baseline.

Rest of the paper is organized as: Section II discusses the prominent works in the field of epipolar geometry and camera calibration. In Section III, we provide brief discussion about the mathematical modeling of three proposed techniques. In Section IV, we analyze the data acquired through proposed techniques in previous section and compare the results with one of the established techniques and in Section V, we did model validation and Section VI concludes the overall discussion and also discusses future work.

II. RELATED WORK

In recent years, many distortion models have been proposed to address the needs various applications of image analysis. Daniel Herrera et al. [12] propose a unique technique to calibrate the Kinect Sensor with the help of in build depth camera. In this paper, authors presented a new technique to calibrate both color and depth camera simultaneously and estimate the pose between them. An image of planer surface is required from different poses of color camera as depth camera is not used during the calibration process which provides robustness and flexible to noise. A new depth distortion model is also proposed when this technique is applied to Kinect sensor. Radial and tangential distortion is usually used to correct the position of pixel in color cameras; depth cameras require more complex techniques to address the distortion model due to the 3D nature of pixel.

Significant distortion is developed in rolling shutter cameras when they capture images during the course of movement. Intrinsic parameters such as focal length and distortion coefficient, modeling of shutter timing must be accurately calibrated. In this paper [13], authors purpose a software solution which required video of known calibration pattern. A continuous time trajectory model is proposed combined with rolling shutter model which provides solution of batch estimate problem to estimate the camera pose and time delay of shutter. In [14], researchers use pinhole camera model with lens distortion model in order to remove inaccuracy in distortion correction model by computing the Jacobean matrix analytically for the representation of 3D world points. Another self-calibration technique [15] is proposed by authors, using single image combined with vanishing points and ellipse/circle. The orthogonal vanishing points are then utilized to compute principal distance and principal points. Then this principle points are considered as distortion center which then are corrected to acquire the distortion free image.

Antonin Mikis et al. [16] described theoretical analysis of radial distortion in wide angle camera lenses and its effects on change of object location on image plane with respect of optical system. Authors present approximation formulas to model such change from object space to image space. The derivation of approximation formulas to model radial distortion are within the validity of third order aberration theory. The

quality of image is being measured by taking center of image as object point and its measure of radial distortion in image plane around center.

In [17], researchers purpose a combined radial and tangential distortion correction algorithm for lens distortion. They propose straight lines quick remedy algorithm to correct lens bending to an expected normal mistake under 1 pixel. Trial comes about demonstrate that the algorithm can advance the accuracy and reinforce the heartiness, in the meantime, significantly lessen the computation time. In this work [18], a new radial distortion correction method is introduced which require single image with radial distortion and noise. The classical pinhole camera model is applied for the distortion correction model. The first step in this algorithm is to find the position of corners in distorted image by using procedure defined by Geiger et al. [19]. A division model to reduce the radial distortion lower order is used. When there is slight change in position of center of distortion, a triangle is formed between undistorted and distorted point against feature corner point. Different values of radial distortion parameters and different set of noises being used in these experiments to check the validity of work.

Hamza Alzaroket et al. [20] propose the idea of utilizing extrinsic parameters of camera using the calibration process. The 3D extrinsic information is obtained through set of 2D frames then this information is used to find the proper location of the camera mounted on robot using new mathematic formula. Zhang et al. [4] calibration method is used to acquire the external and internal parameters due to its flexibility in distortion correction model. Extrinsic parameters obtained through camera calibration are then utilized to compute the location of camera where the best detection can be achieved. In another work [21], authors discuss an idea to use the camera calibration process to estimate the speed of incoming vehicle in camera frame. An equilateral triangle is drawn on image to extract camera parameters. Optical flow vector is used with camera parameters to determine the speed of vehicle in image frames.

In another technique [22], authors purpose a unique method to address problems related to object-triangulation and 3d object tracking within the limits of unified Bayesian framework for joint multi tracking and camera calibration. When an image is observed from cameras located at known distance from each other, binocular disparity starts to affect the data. Due to this effect, depth perception is achieved. In another application of camera calibration [23], a new approach is proposed by the authors to classify the road lanes using on board mounted camera. First they detect the road lanes using linear parabolic lane model then automatic on board camera calibration is deployed. First step is to detect the near field road lines by linear function and parabolic function to detect far field lanes so the curved lines can easily be tracked. Another application of camera calibration is presented by researchers in [24] to extract the human height by acquiring information of line from background, pedestrians and estimation of vanishing points of extracted lines. Vanishing points are extracted from background and pedestrians are then used to calibrate the cameras to estimate the human height.

3D reconstruction of the scene from multiple images of two or more cameras is being under consideration for very long time. R. Hartley et al. [11] presented techniques to resolve this issue which are derived from Projective geometry and photogrammetry. The authors described extensively the geometric principles with respect to their algebraic representation in terms of camera projection matrices, the fundamental matrix and trifocals tensor. Authors presented the epi-polar geometry of two cameras and projective reconstruction from resulting image map correspondence which helps to identify the depth of image point. This work is extensively used in speed estimation of incoming vehicles on the road due to its ease in deployment, development and maintainability. Our work is derived from work presented by the R. Hartley et al. [11] because of its close bonded relationship of projective geometry.

III. LINEAR TRANSFORMATION MODEL

View angle of camera describes the angular area of the scene imaged by a given camera which can be measured vertically, horizontally and diagonally. It is dependent on focal length of lens and size of the image sensor. Lenses produce rectilinear images of distant object, from which the view angle (VA) can be completely determined by the effective focal length and image sensor dimensions. But due to distortion factor presents in lenses, the calculations required for VA become very complex and produce very inconvenient results for applications. In the first technique of linear transformation in stereo configuration, we use division model to calculate the angle of observed pixel which helps in triangulation for depth extraction.

This methodology provides optimal results for close range environment. In second technique, we present the linear calibration in rectangular configuration where cameras are placed perpendicularly from object. This technique only suitable for closed environment where the object's background in world plane is known. When the distance between object and two cameras increases and object shifts from the center of image, the depth calculated through above techniques starts deteriorating due the radially distorted image. To resolve this problem, we provide another methodology where close form equation is derived to sustain circular nature of lens on CCD in pixel's angle. The angle of pixel on the sides of image will be according to the rounded nature of lens which will produce accurate depth for the observed pixel, in triangulation.

A. Linear Transformation in Stereo Configuration

Horizontal view angle of given camera is computed by using the topology presented by E. McCollough [25]. A division model is proposed that will calculate the angle of each pixel distributed horizontally in image:

$$A.P.P = \frac{\text{View angle}}{\text{Resolution on x - axis}}$$

A.P.P is defined as angle per pixel where view angle of a camera is divided with the image's resolution on x-axis where each pixel has equal portion of the total view angle in image. Fig. 1 is basic triangulation, Object lies in the view angles of Right and Left Cameras where A'B' are internal angles of

object's pixel and A, B are external angles with baseline. a, b are total angles from object's line to the baseline.

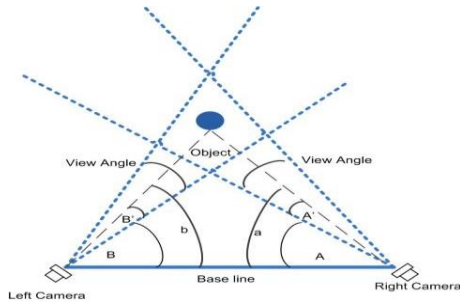


Fig. 1. Linear calibration in stereo configuration, two cameras are looking at object with known distance between them.

Internal angles A'B' of object's pixels within the view angles of left and right cameras are computed as

$$A' = x_axis's \text{ pixel of object} \times A. P. P$$

$$B' = x_axis's \text{ pixel of object} \times A. P. P$$

The total angle (a, b) between object line and baseline is the addition of internal angles A'B' and external angles with baseline A, B which is $b = B + B'$ and $a = A + A'$. The external angles (A, B) are measured manually with the help of protractor. The total angle of triangle is 180° so the angle of the object in world space with respect to two cameras is $c = 180^\circ - a - b$. In Fig. 2, we have the triangle with all the sides $\bar{A}, \bar{B}, \bar{C}$ and angle (a, b, c), the distance between two cameras is known which helps to calculate other parameters. By using the Law of sines, the sides of above triangle are determined as follows:

$$\frac{\bar{A}}{\sin b} = \frac{\bar{B}}{\sin a} = \frac{\bar{C}}{\sin c} \quad (1)$$

By using 1, the side B can be computed as

$$\bar{B} = \sin a \times \frac{\bar{C}}{\sin c}$$

Side B and angle "a" is calculated from above equations. Now to calculate the perpendicular distance, trigonometric functions of right angle triangle is utilized which will extract the depth of object from two cameras. We have

$$\sin \theta = \frac{\text{Perpendicular}}{\text{hypotenuse}} \quad (2)$$

After applying (2) in our scenario, we have

$$\sin b = \frac{\text{Perpendicular}}{\bar{B}}$$

We know the side B and angle "b" so the perpendicular distance of object from two cameras will be

$$\sin b \times \bar{B} = \text{perpendicular}$$

This is called the linear transformation in stereo configuration where view angle is utilized to find the angle of object's pixel which is further used to extract the depth of object. This technique produces optimal results of depth of

object in stereo images where the distance is not very large and object's pixel remains in central area of image where distortion can be neglected.

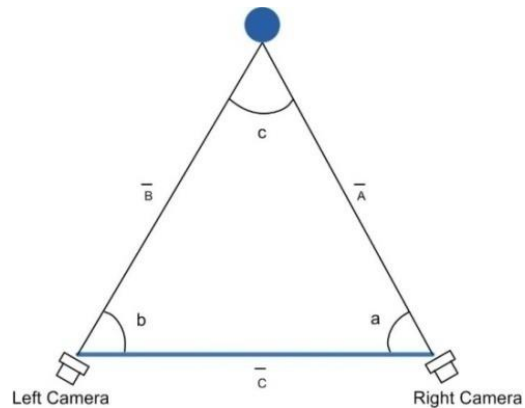


Fig. 2. Stereo configuration of two cameras. Triangle of stereo configuration with all the sides A, B, C and angles (a, b, c).

B. Linear Transformation in Rectangular Configuration

Now we introduce another technique to extract the depth of object in indoor environment where the measurement of background of each camera is known. These cameras are placed perpendicular to the object which makes Rectangle in this basic configuration. This is the rectangular configuration of cameras where object lies in the center of both cameras in Fig. 3, the measurements of both camera's background (x, y) is known. Now we need to find the length of principal axis of each camera to object placed in the middle of rectangular configuration. In this derivation, I.P.P stands for inches per pixel. Initially, we assume that each camera's view angle covers entire background. For first camera, we have:

$$I. P. P = \frac{y}{\text{width of first camera's image}}$$

$$\text{Distance}_{\text{from first camer}} = I. P. P \times X_{\text{Object}}$$

For second camera, we have

$$I. P. P = \frac{x}{\text{width of second camera's image}}$$

$$\text{Distance}_{\text{from second camera}} = I. P. P \times X_{\text{Object}}$$

When the view angle does not cover entire background then we have to make certain adjustment in above equations. In a real scenario, when the view angle of given camera does not cover the entire background i.e. Fig. 4, then I.P.P equations are changed slightly to accommodate this problem. This change is given as:

$$I. PP = \frac{x}{\text{width of second camera's image}}$$

$$\text{Distance}_{\text{from second camera}} = I. P. P \times X_{\text{Object}} + \alpha$$

" α " is considered when the second camera is on the left side of the wall covering object. We present another situation when the view angle is larger than the background in Fig. 5. In this situation, the change in I.P.P is given as:

$$I.P.P = \frac{y}{\text{width of first camera's image}}$$

$$\text{Distance}_{\text{from first camer}} = I.P.P \times X_{\text{Object}} - \alpha$$

“ α ” is considered when the second camera is on the left side of the wall. This technique is best suited for indoor environment where the backgrounds of cameras can be measured. This process can be used to analyze the speed of coming car where the background of camera can be measured.

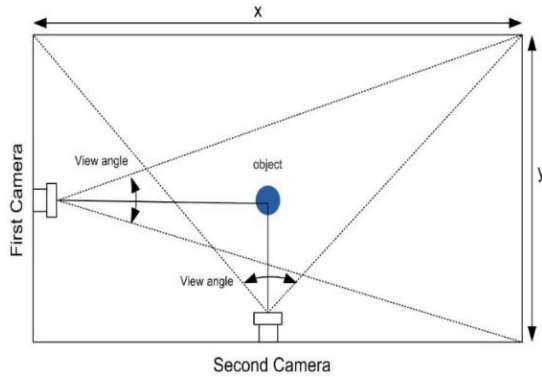


Fig. 3. Linear calibration in rectangular configuration where two cameras are perpendicularly placed from each other and object lies in the center of view angles of both cameras.

Algorithm 1: Linear Transformation in Stereo Configuration

- Result:** Find depth from stereo camera configuration
- 1 Get Horizontal view angle of cameras;
 - 2 READ images;
 - 3 Get distance between cameras;
 - For Left Camera;
 - 4 Divide view angle with x-resolution of image(A.P.P);
 - 5 Get internal angle within view angle of left camera(B’);
 - 6 Calculate angle between Right hand of view angle and base line (B);
 - 7 Add the internal angles(B’) with external(B) to get total angle (b);
 - 8 Get side of left camera by using the Law of sines;
 - For Right camera;
 - 9 Divide view angle with x-resolution of image(A.P.P);
 - 10 Get internal angle within view angle of right camera(A’);
 - 11 Calculate angle between left hand of view angle and base line (A);
 - 12 Add the internal angles(A’) with external(A) to get total angle (a);
 - 13 $c = 180^\circ - a - b$;
 - 14 Get side of Right camera by using the Law of sines;
 - 15 Use right angled trigonometric function for perpendicular distance from left camera according to the position of object’s image point(x,y);

C. Circular Calibration in Stereo Configuration

In previous two proposed techniques, view angle of the given camera is divided with the width of image to acquire angle of certain pixel which is then utilized in the triangulation technique for the extraction of the object’s distance from two cameras. But as the distance of object increases and object shifts away from center of image, these linear techniques start to give less accurate results of depth. The lens is circular body and the sensor is linear so there is no one-to-one relationship between object point on lens and its respective image point on sensor plane. This is the reason when object is in the center of image and closer to camera then depth extraction from linear techniques improves but as the object moves to the sides of image and distance between camera and object increases, the results of depth deteriorate. To improve this situation, we have to come up with closed form equation for the rectification of radially distorted images.

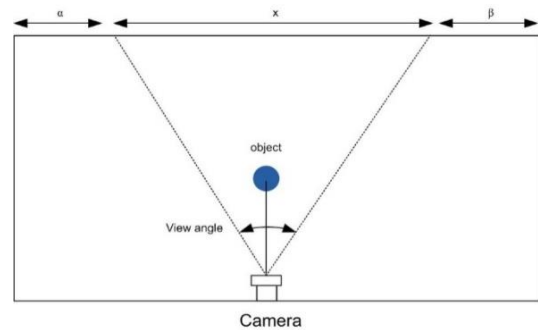


Fig. 4. Rectangular Configuration with small view angle, when the view angle is small compared to its background then we update the equations of linear calibration in rectangular configuration.

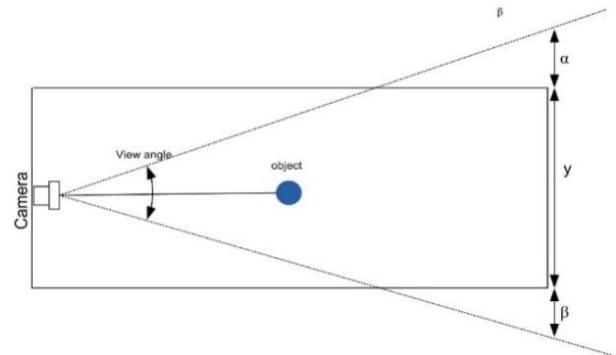


Fig. 5. Rectangular Configuration with large view angle. When the view angle is large compared to its background then we update the equations of linear calibration in rectangular configuration.

In Fig. 6 image and its field of view angle is divided among a/b and α/β , respectively, according to object location (x, y) on image plane. View angle of the given camera is the area cover by a sensor. Anything outside the image is also outside from view angle. A point in 3D world object (x, y, z) is represented by point $p(x, y)$ in an image plane by projective transformation. The view angle and image plane is related to each other mathematically. The view angle of the given camera is already known .which is divided in α and β horizontally according to the position of object in world plane. Its respective image is divided in "a" and "b" similarly according to the position of object in image plane. By using law of sines,

relation between α/β and a/b is established in 3, 4. After multiplying $\frac{1}{a}$ on both sides (5), $\frac{1}{b}$ on both sides of (6) and inverting these equations we acquire (7), (8).

$$\beta = \text{view angle} - \alpha$$

$$b = \text{image}_{\text{width}} - a$$

$$a: R = \sin \alpha : \sin \gamma \quad (3)$$

$$b: R = \sin \beta : \sin \gamma \quad (4)$$

$$\frac{a}{R} = \frac{\sin \alpha}{\sin \gamma} \quad (5)$$

$$\frac{b}{R} = \frac{\sin \beta}{\sin \gamma} \quad (6)$$

$$\frac{1}{R} = \frac{\sin \alpha}{a \sin \gamma}, \quad \frac{1}{R} = \frac{\sin \alpha}{b \sin \gamma} \quad (7)$$

$$R = \frac{a \sin \gamma}{\sin \alpha} \quad (8)$$

$$R = \frac{b \sin \gamma}{\sin \beta} \quad (9)$$

Equations (7) and (8) are equal, therefore we get:

$$\frac{a \sin \gamma}{\sin \alpha} = \frac{b \sin \gamma}{\sin \beta}$$

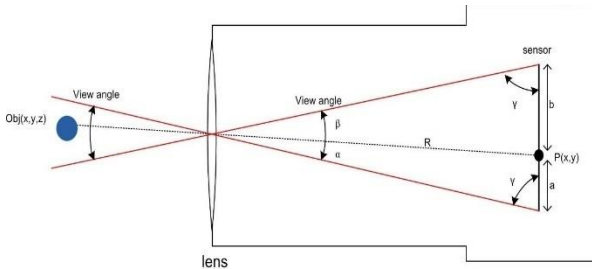


Fig. 6. Circular Calibration between lens and CCD. Ratio between the view angle and its image plane is utilized for the derivation of circular equation.

Multiply both sides with $\frac{1}{\sin \gamma}$ and shift "b" to left and $\sin \alpha$ to right, we have:

$$\frac{a}{\sin \alpha} = \frac{b}{\sin \beta}, \quad \frac{a}{b} = \frac{\sin \alpha}{\sin \beta}$$

For the ease of derivation of the final formula, we denote $\text{Cir} = \frac{a}{b}$ and use the difference of angles in sin formula. Let's also assume that view angle of our camera is equal to 40° then equation 9 becomes as follows, we have already discussed that $\beta = \text{view angle} - \alpha$ so above equation becomes:

$$\frac{a}{b} = \frac{\sin \alpha}{\text{view angle} - \alpha} \quad (10)$$

$$\text{Cir} = \frac{\sin \alpha}{(\sin 40^\circ \cos \alpha - \cos 40^\circ \sin \alpha)}$$

Now multiply the above equation with $\frac{1}{\sin \alpha}$ on both sides for further simplification, shift "Circular" to Right hand side and Invert the both sides of above equation, we get:

$$\frac{1}{\sin \alpha} \times \text{Cir} = \frac{\sin \alpha}{(\sin 40^\circ \cos \alpha - \cos 40^\circ \sin \alpha)} \times \frac{1}{\sin \alpha}$$

$$\frac{1}{\sin \alpha} = \frac{1}{(\sin 40^\circ \cos \alpha - \cos 40^\circ \sin \alpha) \times \text{Cir}}$$

$$\sin \alpha = (\sin 40^\circ \cos \alpha - \cos 40^\circ \sin \alpha) \quad (11)$$

Algorithm 2: Linear Transformation in Rectangular Configuration

Result: Find depth from Rectangular camera configuration

- 1 Get Horizontal view angle of cameras;
- 2 READ images;
- 3 Background=100;
- 4 view-angle;
- if view-angle-camera==Background then
For First camera;
- 5 Divide "y" background of first camera of with width of image(I.P.P);
- 6 $\text{Depth} = I.P.P \times X_{\text{Object}}$;
- For Second camera;
- 7 Divide "x" background of second camera with width of image(I.P.P);
- 8 $\text{Depth} = I.P.P \times X_{\text{Object}}$;
- else if view-angle-camera < Background then
For First camera;
- 9 Divide "y" background of first camera with width of image(I.P.P);
- 10 $\text{Depth} = I.P.P \times X_{\text{Object}} + \alpha$;
- For Second camera;
- 11 Divide "x" background of first camera with width of image(I.P.P);
- 12 $\text{Depth} = I.P.P \times X_{\text{Object}} + \alpha$;
- else if view-angle-camera > Background then
For First camera;
- 13 Divide "y" background of first camera with width of image(I.P.P);
- 14 $\text{Depth} = I.P.P \times X_{\text{Object}} - \alpha$;
- For Second camera;
- 15 Divide "x" background of second with width of image(I.P.P);
- 16 $\text{Depth} = I.P.P \times X_{\text{Object}} - \alpha$;

Now for ease of representation, we have:

$$A = \text{Cir} \sin 40^\circ$$

$$B = \text{Cir} \cos 40^\circ$$

Now we will use above equations in equation 10 for further simplification:

$$\sin \alpha = A \cos \alpha - B \sin \alpha$$

Multiply both sides of above equation with $\frac{1}{\sin \alpha}$ we get

$$1 = \frac{A \cos \alpha - B \sin \alpha}{\sin \alpha}$$

$$1 = \frac{A \cos \alpha}{\sin \alpha} - B$$

According to the Trigonometric identities, $\cot^{-1} a = \frac{\sin \alpha}{\cos \alpha}$,
so after applying that we have

$$1 = A \cot^{-1} \alpha - B$$

After re arrangements of the above equation, we get:

$$\alpha = \cot^{-1} \frac{(B + 1)}{A}$$

Algorithm 3. Circular transformation in Stereo Configuration

Result: Find depth from stereo configuration using circular transformation

- 1 Get Horizontal view angle of cameras(view angle=40°);
- 2 READ images;
- 3 Get x,y coordinates of object in image from both cameras;
- 4 According to object position(x,y), calculate "a" in both cameras;
- 5 Calculate the distance between two cameras;
For Left camera;
- 6 $\beta = \text{view angle} - \alpha$;
- 7 $b = \text{image width} - a$;
- 8 $\text{Circular} = a/b$;
- 9 $A = \text{Circular} \sin 40^\circ$;
- 10 $B = \text{Circular} \cos 40^\circ$;
- 11 $\alpha = \cot^{-1} \left(\frac{B+1}{A} \right)$;
- 12 Calculate angle between right hand of view angle and base line (B);
- 13 $b = \alpha + B$;
- 14 $C = 180^\circ - a - b$;
- 15 Get side of left camera by using the Law of sines;
For Right camera;
REPEAT step 6,7,8,9,10,11,12,13,15;
- 16 Use right angled trigonometric function for perpendicular distance of object from baseline;

This is the circular angle "α", calculated according to the geometric shape of the lens. Now depth extraction from the method of triangulation, discussed earlier, is improved significantly when the object lies on the sides of image or lens. This angle is added with external angles (A, B), discussed in Fig. 1. For the triangulation to extract the depth of object, object present at great distance will also be accurately triangulated according to this proposed technique.

In the initial two proposed techniques, due to the linear transformation, the produced data has some significant radial distortion which affects the accuracy of the overall system. To address this problem, we derive the third technique which reduces the radial distortion in an angle to exhibits accuracy of the depth of the object. If we have to acquire the depth of the object which is for example 400 Km away from the cameras then we need very high resolution cameras to capture the object. Limitation in our third technique, the acquired depth exhibits radial distortion when object moves away from the center of the image.

IV. RESULTS AND DISCUSSIONS

We used industrial grad cameras for the experiments to validate three proposed techniques. These cameras have 640×480 resolution with 1/3" optical format and produce 259 frames per second. To measure the success of the results produce by these techniques, we use measuring instruments to acquire the distance of the object from cameras. This data is then compared to the data produced by the three techniques to visualize the efficiency of the results. Calculation of intrinsic parameter of the camera required deployment of the precision engineering techniques to produce accurate results. Each technique required more than 100 experiments to acquire stable results. In initial phase of the testing we have used 5000 frames to check the authenticity of the depth data. The results can be produced from continuous video feed of the cameras which benefits many applications related to the surveillance or inspection. For first and third technique, we performed in indoor and outdoor environments to check the validity of the results. Whereas second technique requires the measurement of the object's background which allows us to place the camera setup only in indoor environment. We label the right image which is produced by the right camera and left image which produced by the left camera to differentiate between the objects images.

For analysis of the proposed technique, we compared depth extraction of our work with S. Sengupta's [26] method. Sengupta's [26] defined:

$$Z = \lambda + \frac{\lambda \Delta x}{x_L - (x_R + \Delta x)}$$

Where λ is focal length of camera and (x_L, x_R) are x-coordinates of detected object of left and right cameras with known distance (Δx) between them. By using this equation, in our experiment, we get around 740 mm while the actual distance of object from cameras is 440 mm.

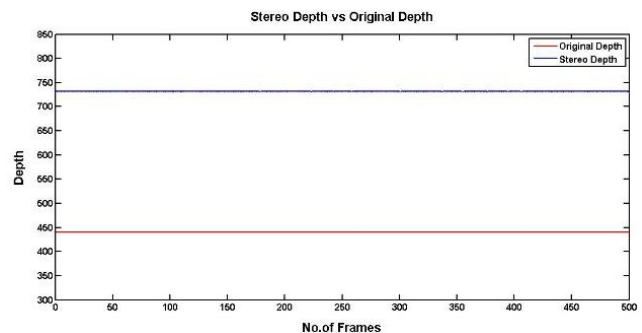


Fig. 7. Comparison between Original depth versus stereo calibrated depth. The data between original depth and stereo calibrated one is compared.

Blue line represents the stereo vision's depth through above mentioned technique, comparable to original depth. Red line represents original depth (440 mm). As we can see in Fig. 7, the computed depth from the above mention technique has 25% error margin compared to the original depth (440mm). Total number of frames is 500 to examine the accuracy of depth, acquired by the given technique.

We use bar graph representation of comparison between original depth of object and calibrated depth using

conventional stereo vision technique in Fig. 8. Original depth measured using measuring scale is 440 millimeter illustrated as red color while Blue color is calibrated through above mentioned technique. Bar graphs are also used to better visualize the depth acquired by the given technique.

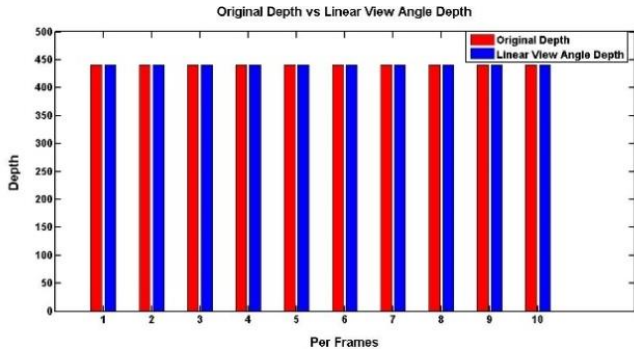


Fig. 8. This is the bar graph representation of comparison between Original depth and Stereo calibrated depth.

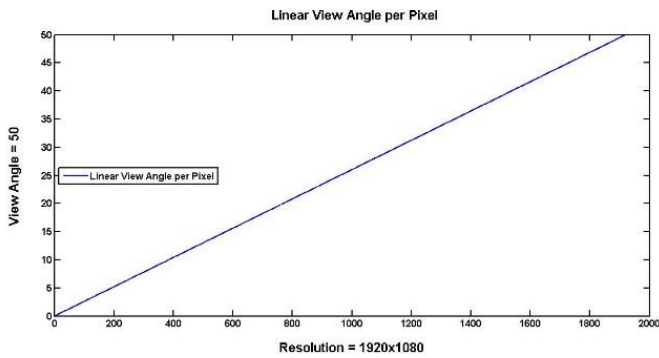


Fig. 9. Linear distribution of the angle per pixel. This is distribution of the angle per pixel through linear calibration technique among the pixels of image.

Fig. 9 shows the linear division of a view angle among the pixels of image. Initial and final pixels shows the sides of an image and it can be seen that this where the graph is straight line which results in less accurate depth calculation when the object lies on the sides of image. We place the object in center of image, in Fig. 10 where there is perfect one-to-one mapping between lens and image resolution. This is where the results are very accurate but due to linear division of the view angle on image resolution, the depth starts to deviate from its result on the sides of image.

In Fig. 11, Depth calculated using linear transformation technique in stereo configuration has staggering accuracy against original depth. It can be seen in the bar graphs about the accuracy of depth. Fig. 12 illustrates the data acquired by linear transformation in rectangular calibration in which left Camera is represented by light blue color and yellow color represents right camera. Red and light blue color shows Original depth for Left and Right cameras respectively. This technique is suitable in indoor environment where the background of each camera is known. The above bar graphs show very prominent results.

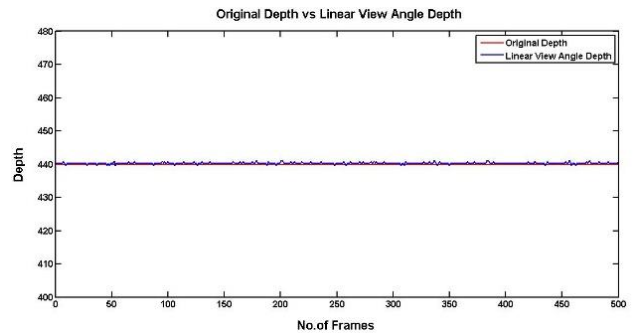


Fig. 10. Comparison of depths acquired through linear transformation (Linear view angle) in stereo configuration and original depth.

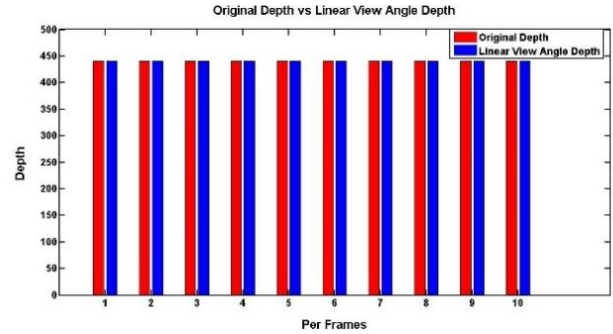


Fig. 11. This is the bar graph representation of linear transformation.

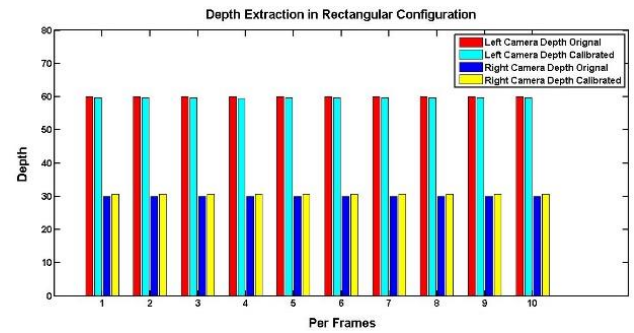


Fig. 12. Depth extraction in Rectangular Configuration. This figure illustrates comparison of rectangular calibration technique between two cameras versus original depths from cameras.

In Fig. 13 Circular Calibration technique is used to extract the depth of object from frames in stereo configuration. We can observe the accuracy of depth acquired using circular calibration against original depth. Red bar shows the Original depth and Blue bar shows calibrated depth. An image is divided among A and B where "A" is right side of detected object's pixel and B is the left side of image resolution. We move image center of the detected object from right to left as A increases and B decreases. Then we calculate the angle of each pixel calculated by the Circular angle per pixel formula which is already being derived.

Hartley and Zizzerman et al. [11] method is closest to our method and also very famous for their results. Comparatively, our method shows better stability in Depth extraction in

Fig. 14. The actual distance is 440 mm from cameras and our method produced less noisy results as compare to Zizzerman et al. [11] method. This method relays on the disparity map of the stereo image of pixel where motion or difference of color is considered for depth extraction. This consideration allows the depth extraction with noisy results. This technique is ideal when there are low cost cameras available and required low maintenance. Our technique is heavily influenced by this technique but produce less noisy results in depth extraction which further improve the functionality of imaging system with low cost development, deployment and maintainability. The purpose of choosing this state of the art technique is its ease of development and deployment from the local market perspective. Keeping these parameters in mind, we have produced better results as compared to Zizzerman's [11] technique.

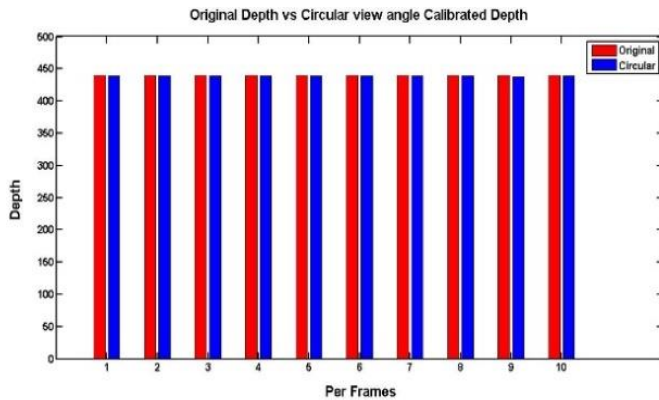


Fig. 13. Bar representation of comparison between depths acquired through Circular calibration technique and original depth.

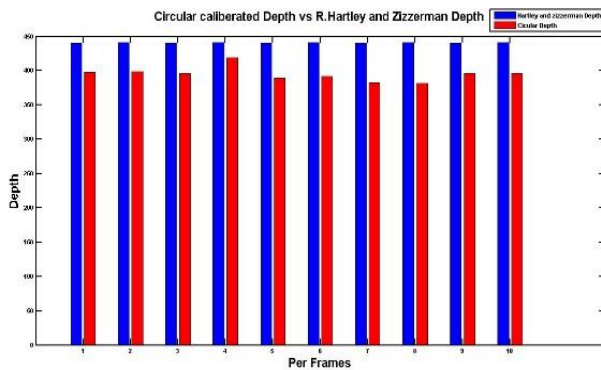


Fig. 14. Bar graph representation of comparison between Circularly Calibrated depth and R. Hartley, Zizzerman's [11] method.

There is a curve in Fig. 15 which is undetectable through naked eye but if we combined both graphs of linear and circular transformation of stereo configuration then we can see the circular angle per pixel depicts the $\cot^{-1} \alpha$ graph around 25° angle as shown in figure below. When the distance is great and object lies away from center of image then Circular calibration tends to hold the accuracy of depth close to 98% due to radial distortion correction of observed pixel.

In Fig. 16, the change in circular angle per pixel increases as it reaches towards the center of image and decreases when it leaves the center. This change in linear angle per pixel remains

the same which contributes to the inaccuracy in depth extraction when the distance between object and camera increases and object lies to the sides of image. The comparison shows difference between linear and circular angle per pixel.

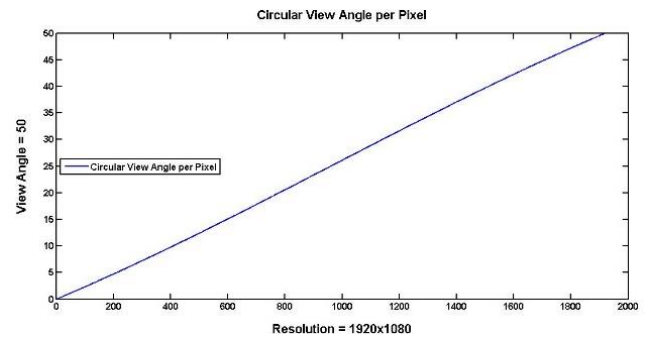


Fig. 15. Plot for circular angle A plot of circular angle per pixel for each pixel of 1920 resolution image.

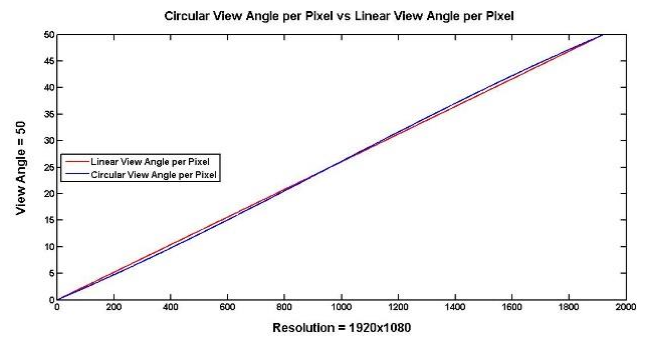


Fig. 16. Linear view angle per pixel versus Circular view angle per pixel Comparison between two graphs: linear view angle per pixel and Circular angle per pixel.

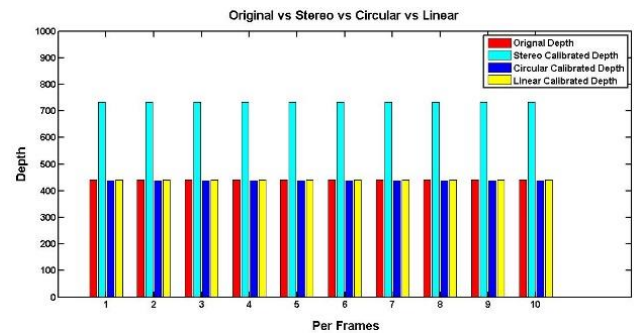


Fig. 17. Original vs. Circular View Angle vs. Linear View angle

In Fig. 17 linear calibration shows the one-to-one mapping between camera lens and image plane which gives us wrong approximation of an angle. This unrealistic result does not produce significant marginal error when the object is placed very near to cameras and lies in the center of image but when we extend the distance between object and cameras, also object shifts away from center of image then radial distortion starts playing its role in accuracy of depth which cannot be ignored.

Now question arises how much distance should exist between two cameras? There is no direct answer for this question as depth calculation or the perpendicular distance relies on angle made by two incident rays from object. The bigger the angle (distance between cameras increases) the more

accurate result we extract but if we increase the distance between cameras, we must increase their resolution so that incident rays coming from object must be properly absorbed by CCD through lens therefore inter-pixel accuracy will not be affected by less resolution camera.

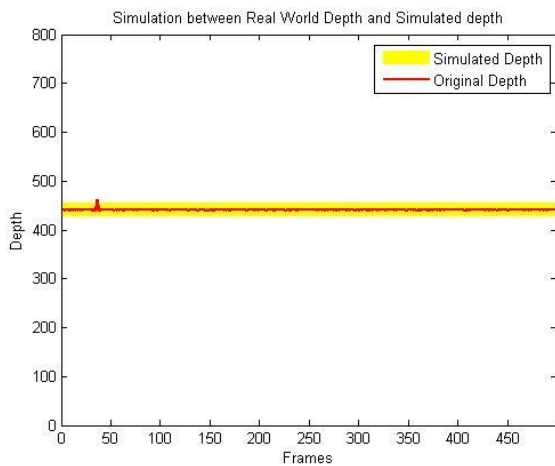


Fig. 18. Original depth acquired through cameras is projected as red color line and the depth acquired through simulation is presented as thick yellow line.

V. MODEL VALIDATION

We have derived the final mathematical formula for the radial distortion in stereo depth extraction. In this section, we have performed a simulation of our technique with comparison of the real world data. The view angle in the given equations is set to 40° which is same as in cameras which are being tested. In the real world scenario, we have placed the cameras apart with known distance and then applied circular calibration in triangulation for depth extraction. The same depth is also acquired through simulation of the equations by giving the same values of distance and view angle. This is done to see the amount of difference these equations produced when tested in real world scenario and in simulation.

In Fig. 18, we have acquired the data from 500 frames for the purpose of comparison to analyze with simulated data. We set the original depth line to thick yellow line because the difference between simulated and original data is very small. This simulation shows the accuracy of the data produced by circular calibration in depth extraction and insures the application of this technique in real world scenarios.

VI. CONCLUSION AND FUTURE WORK

In this work, we propose three techniques to extract the depth of object from image. In first technique, a linear transformation in stereo configuration is applied where view angle of the given camera is divided on image resolution to extract the distribution of view angle in pixels. Due the spherical shape of the lens, triangulation results are accurate in the central area of the image in close range but less accurate on the sides in long range. In the quest for improvement in depth extraction, we derive another technique, linear transformation in Rectangular Configuration where two cameras are placed perpendicularly from object. The backgrounds of both cameras are measured for the depth extraction. This procedure is most

suitable for indoor environment where the length of camera's background is known. In both techniques, when the objects shift away from center of image and distance between object and cameras increases, the distortion starts to hamper the accuracy of depth. To improve this situation, we derive circular equation to extract the angle of observed pixel according to geometric shape of the lens, which is used in triangulation for the depth extraction. Results show the accuracy of proposed solution where the depth of object is approximately 98% accurate, compared to the earlier techniques. We have also insured the cost of deployment and maintainability of the system is less than previous techniques.

We are currently working to further improve the accuracy because with the increase in resolution of the image, division of pixel's angle starts behaving linearly. In future work, we plan to acquire the height of the object from the surface using single camera by deploying circular calibration technique which will have significance scope in the surveillance and inspection applications.

REFERENCES

- [1] Brown, D.C.,1966.Decentering distortion of lenses,photogrammetric Engineering and Remote Sensing, , vol. 32, no. 3, pp.440-462.
- [2] Tsai, R.,1987.A versatile camera calibration technique for high-accuracy 3D machine vision metrology using off-the-shelf TV cameras and lenses. IEEE Journal on Robotics and Automation, Vol. 3,no. 4, pp. 323-344.
- [3] Lenz, R.K. and R.Y. Tsai, 1988. Techniques for calibration of the scale factor and image center for high accuracy 3-D machine vision metrology. IEEE Transactions on pattern analysis and machine intelligence, Vol. 10,no. 5, pp. 713-720.
- [4] Zhang, Z., 2000. A flexible new technique for camera calibration. IEEE Transactions on pattern analysis and machine intelligence, Vol. 22,no. 11, pp. 1330-1334.
- [5] Heikkila, J.,2000.Geometric camera calibration using circular control points. IEEE Transactions on pattern analysis and machine intelligence, Vol. 22,no. 10,pp. 1066-1077.
- [6] Nomura, Y., et al.,1992Simple calibration algorithm for high-distortion lens camera. IEEE Transactions on Pattern Analysis and Machine Intelligence, Vol. 14,no. 11,pp. 1095-1099.
- [7] Levenberg, K.,1944.A method for the solution of certain non-linear problems in least squares. Quarterly of applied mathematics, Vol.2,no. 2,pp. 164-168.
- [8] Devernay, F. and O. Faugeras,2001.Straight lines have to be straight. Machine vision and applications, 13(1): p. 14-24.
- [9] Dobbert, T.,2006.Matchmoving: the invisible art of camera tracking.: John Wiley & Sons.
- [10] Fitzgibbon, A.W.2001.Simultaneous linear estimation of multiple view geometry and lens distortion. in Computer Vision and Pattern Recognition, 2001. CVPR 2001. Proceedings of the 2001 IEEE Computer Society Conference on. IEEE.
- [11] Hartley, R. and A. Zisserman,2005.Multiple view geometry in computer vision. Robotica, Vol. 23,no. 2,pp. 271-271.
- [12] Herrera, D., J. Kannala, and J. Heikkilä,2012.Joint depth and color camera calibration with distortion correction. IEEE Transactions on Pattern Analysis and Machine Intelligence,Vol. 34, no. 10,pp. 2058-2064.
- [13] Oth, L., et al.2013.Rolling shutter camera calibration. in Proceedings of the IEEE Conference on Computer Vision and Pattern Recognition.
- [14] Rahman, T. and N. Krouglicof,2012.An efficient camera calibration technique offering robustness and accuracy over a wide range of lens distortion. IEEE Transactions on Image Processing,Vol. 21,no. 2,pp. 626-637.
- [15] Sun, Q., et al.,2016.Camera self-calibration with lens distortion. Optik-International Journal for Light and Electron Optics, Vol. 127,no.10,pp. 4506-4513.

- [16] Miks, A. and J. Novak,2012.Dependence of camera lens induced radial distortion and circle of confusion on object position. Optics & Laser Technology, Vol. 44,no. 4, pp. 1043-1049.
- [17] Zhou, L., G.-h. Gu, and N. Shao.2016.Straight lines fast correction algorithm for lens array distortion. in SPIE Optical Engineering+ Applications. International Society for Optics and Photonics.
- [18] Andrade, J. and L.J. Karam.2016.Robust radial distortion correction based on alternate optimization. in Image Processing (ICIP), IEEE International Conference on. 2016. IEEE.
- [19] Geiger, A., et al.2012.Automatic camera and range sensor calibration using a single shot. in Robotics and Automation (ICRA), IEEE International Conference on. 2012. IEEE.
- [20] Alzarok, H., S. Fletcher, and A.P. Longstaff.2016.A new strategy for improving vision based tracking accuracy based on utilization of camera calibration information. in Automation and Computing (ICAC), 2016 22nd International Conference on. IEEE.
- [21] Do, V.-H., et al.2015.A simple camera calibration method for vehicle velocity estimation. in Electrical Engineering/Electronics, Computer, Telecommunications and Information Technology (ECTI-CON), 12th International Conference on. 2015. IEEE.
- [22] Houssineau, J., et al.,2016.A unified approach for multi-object triangulation, tracking and camera calibration. IEEE Transactions on Signal Processing, Vol. 64,no. 11,pp. 2934-2948.
- [23] de Paula, M.B. and C.R. Jung,2015.Automatic detection and classification of road lane markings using onboard vehicular cameras. IEEE Transactions on Intelligent Transportation Systems, Vol. 16,no. 6,pp. 3160-3169.
- [24] Jung, J., et al.2016.Human height analysis using multiple uncalibrated cameras. in Consumer Electronics (ICCE), IEEE International Conference on. 2016. IEEE.
- [25] McCollough, E.,1893.Photographic topography. Industry: A Monthly Magazine Devoted to Science, Engineering and Mechanic Arts, ,Vol. 54,pp. 65.
- [26] Sengupta, S.,1997.Effects of unequal focal lengths in stereo imaging. Pattern recognition letters, Vol. 18,no. 4,pp. 395-400.

An Automatic Arabic Essay Grading System based on Text Similarity Algorithms

Abdulaziz Shehab, Mahmoud Faroun, Magdi Rashad

Information Systems Dept.

Faculty of Computers and Information, Mansoura University, Egypt

Abstract—Manual grading process has many problems such as time consuming, costly, enormous resources, lot of efforts and huge pressure on instructors. These problems place the educational community in a dire need to have auto-grading systems so as to address these problems associated with manual grading. Auto-grading systems are wide spread over the world because they play a critical role in educational technology. Additionally, the auto-grading system is introducing many advantages as it saves cost, effort and time in comparison to manual grading. This research compares the different algorithms used in automatic grading systems in Arabic languages using string and corpus algorithms separately. This process is a challenging task following the necessity of inclusive assessment to authenticate the answers precisely. Moreover, the challenge is heightened when working with the Arabic language characterized by complexities in morphology, semantics and syntax. The research applied multiple similarity measures and introduces Arabic data set that contains 210 students' answers. The results obtained prove that an automatic grading system could provide the teacher with an effective solution for article grading systems.

Keywords—Auto-grading systems; string-based similarity; corpus-based similarity; N-Gram

I. INTRODUCTION

Nowadays, auto-grading systems are a very important scientific topic within the educational community. The huge amounts of tests and students have brought about the necessity for automatic grading systems. Therefore, researchers pay more attention to such systems which have become a vital component in the educational community because it is capable of reducing the load of the teaching staff due to graded students' exams. These systems have witnessed a continuous development in the last few years [1]-[5]. In fact, most of the teachers' time is wasted due to manual grading. Teaching staff all over the world suffer from wasted time spent on students' essay marking.

There is an increase in the number of student enrolment that makes the marking operation more difficult. Essay Questions are more difficult than other objective questions because it takes much time to mark these questions. But, the essay questions are preferable than objective questions because it makes the cheating process more difficult and raises the student's skills in writing.

In addition, the essay marking can differ from human grader and others in marks, which is unfair. Therefore, the auto-grading systems could automatically grade the student

answers and teachers could utilize the time wasted for marking the essays. In this way, teachers get an opportunity to concentrate on other critical assignments, for example, develop more viable instructional materials and other correspondence capacities.

Essay-typed questions are classified into two main types: short and long answers. For the first, student solutions are written in short sentences. For the latter, it gives the students the freedom to write as long as he or she wants. Hence, teachers look for special characteristics to be graded, for example, style of writing, mechanics, and content [6]. The short answers assessment depends on the content of answers and the style is not significant [7].

Auto-grading system has one of the most convoluted tasks as it depends on the overall semantic meaning, since short answers have many common words [8]. Moreover, the similarity on long essay is complicated to discover as every word could have other synonyms, meanings [9], [10]. The marks could be given to the students based on similar sentences that are prepared in the marking scheme. The majority of automated short answer grading systems are done in English ignoring Arabic because there are many challenges in Arabic those needs to be tackled in different ways. Arabic context has unique characteristics and features so it is challenging task.

In the last few years, many researchers have proposed a number of automated Arabic short answer grading systems [11]-[14]. They proposed many algorithms like Latent Semantic Analysis (LSA) [15], Damera-levenshtein (DL) [16], [17], N-Gram [18], Extracting Distributionally similar words using Co-occurrences (DISCO) [19], [20]. The main idea of automatic grading systems is using n-grams in different applications [21]-[23]. More recently, there are approaches that used LSA model to evaluate written answers automatically [21], [22], [24]-[26]. However, their proposals lack a comparative study that deeply shows the advantages and disadvantages of such algorithms.

Dependently, in this paper, a comparative study between different approaches that are oriented for automatic grading is presented. The main goal of this paper is to find the best suitable technique suitable for Arabic language essay questions. So, we applied four algorithms on the same dataset of questions to compare them and find the optimal algorithm which gives the best correlation between manual grading and automatic grading. The remainder of this paper is as follows: Section II discusses related works; Section III presents the

used dataset. Section IV presents a comprehensive view on string-based and corpus-based while Section V presents the proposed architecture. The experimental results are shown in Sections VI and VII is our conclusion and future work.

II. RELATED WORKS

There are several automatic grading systems conducted in English such as E-rater [27], Automark [28], C-rater [29], and LVQ [30]. On the other hand, a few studies have been done in Arabic [4], [11], [12].

Gomaa and Fahmy [11], one of the most recently published works, present a system that scores Arabic short answers. They prepared a dataset which contains 610 student answers written in the Arabic language. Their proposal evaluates the student answers after they have been translated into English. Their objective was to overcome the challenges that were faced in Arabic text processing. However, the proposed system has many problems namely the missing of utilization of good stemming techniques, the translation from Arabic into English causes the loss of context structure where many words in Arabic are not semantically translated, and the results obtained have to be passed to a machine learning that demands a high processing time.

Mezher and Omar [12] proposed a hybrid method based on a modified LSA and syntactic feature in a trial for automatic Arabic essay scoring. They relied on the dataset proposed in [11]. Their proposal focused on part of speech (POS) tagging in a way to identify the syntactic feature of words within the similarity matrix. Their study sought to resolve the drawbacks of standard LSA which laid emphasis on the limited syntactic analysis. However, utilizing only LSA technique in their study did not guarantee a high correlation ratio.

Emad [13] presents a system based on stemming techniques and Levenshtein edit operations for evaluating student's online exams. The proposed system was mainly based on the capabilities of light and heavy stemming. The dependence only on the string-based algorithm (Levenshtein) is counted as one of the main defects in his study as it ignores corpus-based algorithms that support semantic similarity.

Rashad et al. [31] proposed an Arabic online examination environment that provides an easy interaction between students and instructors. In fact, their proposal is only developed for grading objective (non-essay) questions. For essay grading, the proposed is nothing more than a storage system where the instructor has to manually assess the student's writings.

Alghamdi et al. [14] present a hybrid automatic system that combines LSA and three linguistic features: 1) word stemming, 2) word frequency, and 3) number of spelling mistakes. Their proposal determine the optimal reduced dimensionality used in LSA to evaluate the performance of

their proposed system. Khalid and Izzat [4] present a method depending on synonym and stemming of words. They assign weights the instructor's answer words to benefit the assessing process. Their study was impracticable and had neither a dataset nor an experimental result.

III. DATASET

In this research, general methodology will be used to advance a grading system of Arabic short answers based on text similarity matching methods. To evaluate the methods for short answer grading, we used the dataset prepared in a general sociology course taken by secondary level 3 students where the total short answers in this dataset are 210 short answers (21 questions/assignment x 10 student answers/question). It was evaluated by judges where the scores ranged between 0 (completely wrong) and 5 (completely right). Each judge was unaware of the other's correction and grade. We considered the average score of two annotators as the gold standard to test the automatic grading task. Table I displays a sample question, model answer, student answers, and the average score.

TABLE I. EXPERIMENT'S DATASET SAMPLE

Question	عرف الصراع الاجتماعي؟	Score
Model Answer	هو عملية اجتماعية سلبية هدامة لأنه يعبر عن القوى الاجتماعية و مدى تصادمها و ينشأ نتيجة للظروف الاجتماعية و الاقتصادية و السياسية غير المستقرة و قد يصل الصراع الى حد التناحر من اجل البقاء	
1	هو عملية اجتماعية سلبية هدامة لأنه يعبر عن القوى الاجتماعية و مدى تصادمها و ينشأ نتيجة للظروف الاجتماعية و الاقتصادية و السياسية غير المستقرة و قد يصل الصراع الى حد التناحر من اجل البقاء.	5
2	عملية هدامة تعبر عن القوى الاجتماعية و الصدام بينهما.	2
3	عملية اجتماعية سلبية تنشأ عن الصراع بين القوى الاجتماعية و الاوضاع غير المستقرة.	3
4	عملية اجتماعية تحدث نتيجة الاوضاع السياسية و الاقتصادية و الاجتماعية غير المستقرة.	2.5
5	عملية هدامة تحدث نتيجة الاوضاع غير المستقرة في المجتمع.	1.5
6	عملية اجتماعية سلبية تؤدي لهدم المجتمع.	1
7	هو عملية اجتماعية سلبية هدامة لأنه يعبر عن القوى الاجتماعية و مدى تصادمها و ينشأ نتيجة للظروف الاجتماعية و الاقتصادية و السياسية غير المستقرة و قد يصل الصراع الى حد التناحر من اجل البقاء.	5
8	هو عملية اجتماعية سلبية هدامة لأنه يعبر عن القوى الاجتماعية و مدى تصادمها و ينشأ نتيجة للظروف الاجتماعية و الاقتصادية و السياسية غير المستقرة و قد يصل الصراع الى حد التناحر من اجل البقاء.	5
9	عملية اجتماعية سلبية هدامة.	0.5
10	صراع القوى الاجتماعية التي تؤدي الى التصادم و التناحر.	2

IV. STRING-BASED AND CORPUS-BASED APPROACH

A. String-Based Text Similarity

Damerau-Levenshtein (DL) algorithm works on counting the quorum of processes that are required to map one string into another string. These operations could insert, or a character obliterate from the string. Moreover, it could be a replacement of a single character, or a reversal of two adjacent

characters [16]. In fact, DL is not only limited to these four operations but also it could treat 80% of all human misspellings [16], [17] (Hall & Dowling, 1980; Peterson, 1980). To compute the DL similarity value (DLSim), the DL distance is normalized through the following equation:

$$DL = \frac{MaxLength - DDis}{MaxLength}$$

where MaxLength is the extreme length of the 2 strings and DDis is the obtained DL space between these two strings.

N-gram algorithm [32] works on sliding a window of length *n* over string in order to generate a number of 'n' length grams that are utilized in the matching process. Dependently, a match is then compared to N-gram matches within the other string. Hence, when 2 strings s1 and s2 are within a small edit space of each other, they will share a large number of N-grams in common. For example, the positional q-grams of length q=3 for string "مصر الكنانة" are f(1,##), (2,##م), (3,مصر), (4,صر), (5,ر), (6,ال), (7,الك), (8,لكن), (9,كنا), (10,نان), (11,انة), (12,نة%), (13,%%), where '#' and '%' indicate the beginning and the end of the string.

Consequently getting the q-grams for 2 query strings allows counting of the identical q-grams over the total available N-grams.

B. Corpus-Based Text Similarity

Corpus-based measurements of word semantic resemblance try to recognize the degree of resemblance between words using exclusive information resulting from large corpora.

LSA is the most famous algorithm of Corpus-based similarity. It is the automatic algorithm planned by [15] to construct a vector space. The algorithm works on a big corpus of texts where it is progressively mapped into semantic vector space. It is based on 2 types of spaces between words; paragraphs boundaries and separators.

LSA has three main steps: The first one responsible for representing the body as a matrix of co-occurrences. The second is to apply Singular Value Decomposition (SVD) to the matrix obtained in step 1 in order to get a space. The last step is to eliminate a number of dimensions that are obtained from step 2 counted as irrelevant.

DISCO [20] works on measuring distribution similarity which upholds that usually synonyms fall in similar context. Distributional similarity is calculated through statistical analysis for large text collections. In a pre-processing step, the corpus is tokenized and stop words are deleted. In the main step, a simple context window of size ± 3 words generates co-incidences between words. DISCO comes in two flavors: DISCO1, that matches words using their sets of co-occurring words, and DISCO2, that matches words using their sets of distributional similarity.

V. PROPOSED SYSTEM

The proposed system is based on measuring the similarity of student answer by comparing each word in the model answer with each word in student's answer using a bag of words (BOW) model to produce the final automatic score. Several string and corpus algorithms run individual answers to obtain similarity values. Fig. 1 shows the steps of the systems.

A. Raw

The similarity in Raw method is computed without applying any Natural Language Processing (NLP) task. Stemming techniques are applied to Arabic words to extract the trilateral roots of words.

B. Tokenization

The first step in the pre-processing is Tokenization, where it divides the text sequence into sentences and the sentences into tokens. In alphabetic language, words are usually surrounded by whitespace. Besides the whitespace and the commas, the tokenization also removes $\{([\ \backslash\{ \}():; \])\}$ from the text and presents the words in the model answer. Tokenizing is the process of separating each word in the document which becomes the basis of the word, removing prefix, insertion, suffix and duplication.

C. Stopwords

As a pre-processing step for all of the fourteen string similarity measures, removes ineffective common words. Stop-words filters out common words that do not have significant meaning to measuring the similarity. In our system, the stop words are removed according to a predefined list that has 378 words in Arabic. This process is aimed to get the word to represent the content of the document.

These are typically what linguists would call function words, consisting mostly of a relatively small class of articles ('ال', 'الا', etc.), prepositions ('في', 'على', 'الى', 'من', etc.), pronouns ('هو', 'هي', 'نحن', 'هم', 'هما', etc.). These stop words does not convey a meaning.

D. Stemming

Arabic word stemming is a technique that finds the lexical root or stem for words in natural language, by removing affixes attached to its root, because an Arabic word can have a more complicated form with those affixes. An Arabic word ذهاب فسيديون can be represented after stemming process as ذهب.

Several types of affixes are agglutinated at the beginning and the end of the words: antefixes, prefixes, suffixes and postfixes. One can categorize them according to their syntactic role. Antefixes are generally prepositions agglutinated to words at the beginning.

Prefixes, usually represented by only one letter, indicate the conjugation person of verbs in the present tense.

Suffixes are the conjugation ending of verbs and the dual/plural/female markers for the nouns.

Finally, postfixes represent pronouns attached at the end of the words. All these affixes should be treated correctly during word stemming [33].

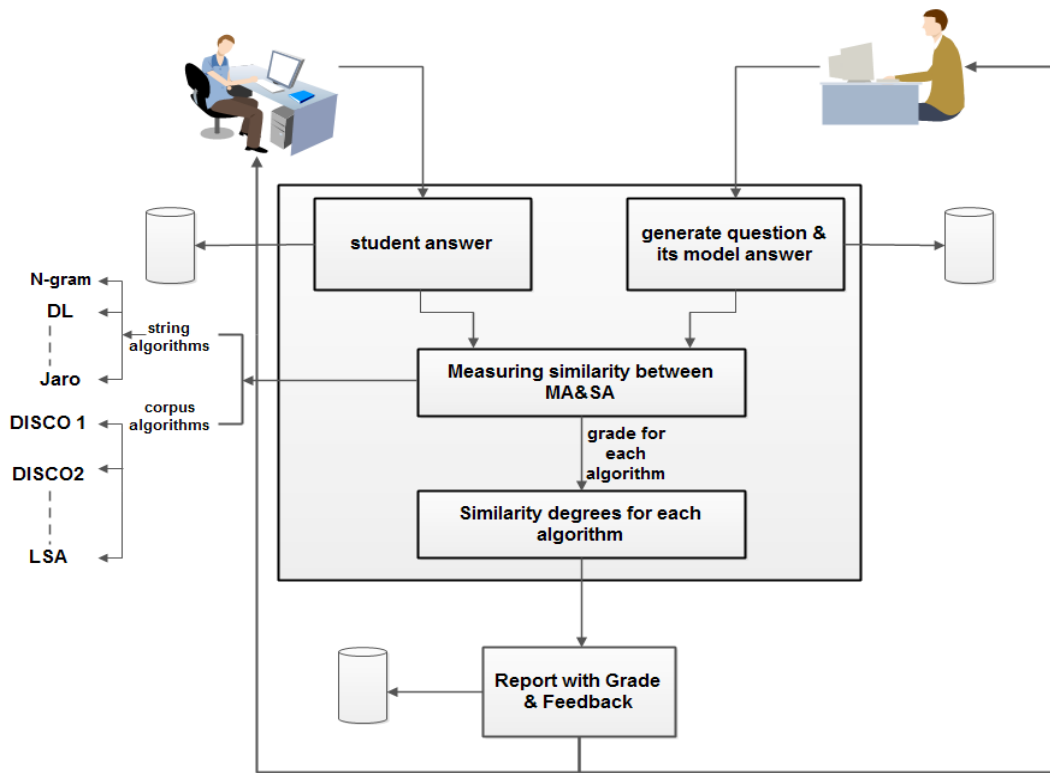


Fig. 1. Proposed system.

The objective of stemming is to find the representative indexing form of a word by truncating these affixes.

Antefixes (وبال, وال, بال, فال, كال, ول, ال, وب, ول, لل, فس, فب, فل, وس, ك, ف, و, ب, ل)

Prepositions meaning respectively: and with the, and the, with the, then the, as the, and to (for) the, the, and with, and to (for), then will, then with, then to (for), and will, as, then, and, with, to (for).

Prefixes (ن, ي, ت)

Letters inflecting morphologically for person.

Suffixes (تما, يون, تين, تان, ات, ان, ون, ين, وا, تا, تم, تن, نات, ن, ا, ي, و)

Word endings inflecting for verb ending, and dual/plural/female markers

Postfixes (كما, هما, كن, هن, تي, ها, نا, هم, كم, ك, ه, ي)

Pronouns meaning respectively: your, their, your, their, my, her, our, their, your, your, his, me.

E. Stopstem

A combination of stop-words and stemming tasks are applied.

VI. EXPERIMENTAL RESULTS

Our experiments were performed using two string-based algorithms and two corpus-based algorithms. Four different methods Stop, Raw, Stop-Stem and Stem are used in testing for string-based algorithms. However, only the Stop method is

used in corpus-based algorithms where Raw, Stem, and Stop-Stem methods cannot be utilized because there is no need to measure the semantic similarity between the Stop words.

The correlation constant was calculated between automatic system and the human grading. The correlation coefficient is used to determine to what extent the system and the human are correlated in assigning the grades.

Equation (1) is correlation constant where X, Y are two sets and \bar{x}, \bar{y} are the averages of each set in series.

$$Cor(X, Y) = \frac{\sum (x - \bar{x})(y - \bar{y})}{\sqrt{\sum (x - \bar{x})^2 \sum (y - \bar{y})^2}} \tag{1}$$

As shown in Fig. 2 and 3 the correlation between the applied algorithms and the manual grading are presented for the same question. The main target of any algorithm is to be very near to the manual grading to prove the efficiency of this technique. The degrees are from 0 to 5 and the number of students is ten. The figures show that the N-gram can be used as the nearest algorithm to the manual grading.

As noticed from Table II, in string -based distance measures; DL resemblance got the best association value 0.803 practical to the Stop-Stem text. The reason behind this could be Stop stem works on the origin of the words comparing the characters against the model answer and neglects the stop-words. This enables the algorithm provide very high results.

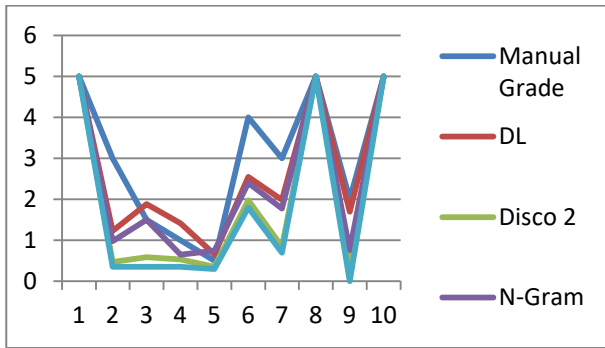


Fig. 2. The grades assigned by teacher, DL, for 10 students' response to the question 'عرف الظاهرة الاجتماعية؟'.

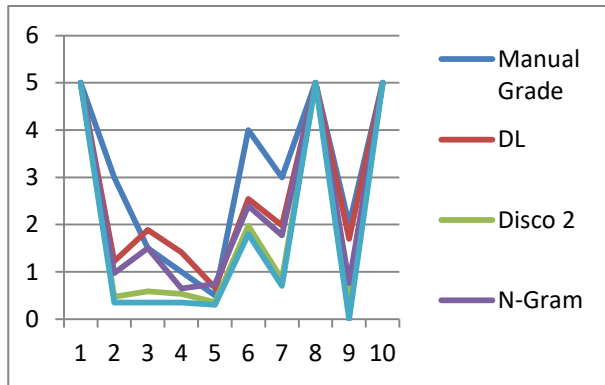


Fig. 3. The grades assigned by teacher, DL, for 10 students' response to the question 'عرف علم الاجتماع؟'.

Moreover, for N-gram algorithm, the best correlation achieved while using Stop method is 0.820. The character-based N-gram algorithm achieved better results than the other three types. In general, the character-based N-gram approach has many advantages, such as: simplicity; it is more reliable for noisy data such as misspellings and grammatical errors; it outputs more N-grams in given strings than N-grams resulting from a word-based approach, which leads to collecting a sufficient number of N-grams that are significant for measuring similarity, and easy to conceptually understand, fast to calculate, language-neutral (i.e., it allows neglected characteristics of language features), error-tolerant.

For corpus-based similarity, LSA achieved 0.781 correlation value while DISCO2 achieved 0.796. Dependently, DISCO2 achieved a higher correlation compared to LSA because DISCO2 depends on groups of distributionally similar words.

TABLE II. THE CORRELATION RESULTS BETWEEN MODEL ANSWER AND STUDENT ANSWERS USING DL, N-GRAM, LSA, AND DISCO2.

Algorithm	Correlation			
	Raw	Stop	Stem	Stop-Stem
DL	0.799	0.800	0.798	0.803
N-Gram	0.800	0.820	0.796	0.795
LSA	N/A	0.781	N/A	N/A
Disco2	N/A	0.796	N/A	N/A

VII. CONCLUSION AND FUTURE WORK

The automatic grading system is an efficient way for grading even if it is used for article questions. The automatic grading system provides many advantages, it is very quick in implementation of results, provides an easier and flexible platform for subjective questions, workload of invigilators is reduced, manual performance is reduced by performing everything online and it is Low cost. The character-based N-gram algorithm achieved better results than the other three types. The N-gram approach has many advantages, such as: simplicity; it is more reliable for noisy data such as misspellings and grammatical errors; and it outputs more N-grams in given strings than N-grams resulting from a Word-based approach, which leads to collecting a sufficient number of N-grams that are significant for measuring the similarity. The paper proved that using string algorithms gives the teacher an effective solution to help them to undertake student grading with high precision. The paper presented the comparison between four effective algorithms to prove the possibility of automatic grading over manual grading systems.

In future work, we are aiming to combine the string algorithm and corpus algorithm together to achieve the highest possible results depending on the synonymous method and content method to decrease automation grading errors. We are aiming to use different datasets in different subjects to find out the reliability of those algorithms in applications.

REFERENCES

- [1] S. Valenti, F. Neri, and A. Cucchiarelli, "An overview of current research on automated essay grading," *Journal of Information Technology Education*, vol. 2, pp. 319-330, 2003.
- [2] T. Miller, "Essay assessment with latent semantic analysis," Department of Computer Science, University of Toronto, Toronto, ON M5S 3G4, Canada, 2002.
- [3] L. M. Rudner and T. Liang, "Automated essay scoring using Bayes' theorem," *The Journal of Technology, Learning, and Assessment*, vol. 1, no. 2, 2002.
- [4] K. M. Nahar and I. M. Alsmadi, "The automatic grading for online exams in Arabic with essay questions using statistical and computational linguistics techniques," *MASAUM Journal of Computing*, vol. 1, no. 2, 2009.
- [5] S. Ghosh and S. S. Fatima, "Design of an Automated Essay Grading (AEG) system in Indian context," in *Proceedings of TENCON 2008-2008 IEEE Region 10 Conference*, 2008, pp. 1-6. "doi:10.1109/TENCON.2008.4766677"
- [6] Callear D., Jennifer Jerrams-Smith and Victor Soh. CAA of Short Non-MCQ Answers. *Proceedings of the 5th CAA Conference*, Loughborough, UK, 2001.
- [7] Pulman S. G. and Sukkarieh J. Z. Automatic Short Answer Marking. *Proceedings of Second Workshop on Building Education Application Using NLP*, Ann Arbor, Michigan, 2005.
- [8] Aziz, M. and F. Ahmad, 2009. Automated Marking System for Short Answer Examination (AMS-SAE). *Proceedings of the IEEE Symposium on Industrial Electronics and Applications*, Oct. 4-6, IEEE Xplore Press, Kuala Lumpur, pp: 47- 51. DOI: 10.1109/ISIEA.2009.5356500.
- [9] F. Mozgovoy, T. Kakkonen and E. Sutinen, "Using natural language parsers in plagiarism detection," in *Proceedings of the SLATE Workshop on Speech and Language Technology in Education*, Farmington, Pennsylvania, USA, 2007.
- [10] S. Alzahrani, N. Salim and A. Abraham, "Understanding plagiarism linguistic patterns, textual features, and detection methods," *IEEE Transactions on Systems, Man, and Cybernetics—Part C: Applications and Reviews*, vol. 42, no. 2, pp. 133-149, 2012.

- [11] Goma, Wael Hassan, and Aly Aly Fahmy. "Automatic scoring for answers to Arabic test questions." *Computer Speech & Language* 28.4 (2014): 833-857.
- [12] R. Mezher and N. Omar." A Hybrid Method of Syntactic Feature and Latent Semantic Analysis for Automatic Arabic Essay Scoring." *Journal of Applied Sciences* ,16(5): 209-215(2016).
- [13] Al-Shalabi, Emad Fawzi." An Automated System for Essay Scoring of Online Exams in Arabic based on Stemming Techniques and Levenshtein Edit Operations." *International Journal of Computer Science Issues(IJCSI)* 13.5(2016).
- [14] Alghamdi, M.,M. Alkanhal,M. Al-Badrashiny, A.Al-Qabbany,A. Areshey,A. Alharbi. A hybrid automatic scoring system for Arabic essays.*J.AI Commun.*,27:103-111.
- [15] Landauer, T.K., Dumais, S.T., 1997. A solution to Platos problem: the latent semantic analysis theory of acquisition, induction and representation of knowledge. *Psychological Review* 104 (2), 211–240.
- [16] Hall, P.A., Dowling, G.R., 1980. Approximate string matching. *ACM Computing Surveys (CSUR)* 12 (4), 381–402.
- [17] Peterson, J.L., 1980. Computer programs for detecting and correcting spelling errors. *Communications of the ACM* 23 (12), 676–687.
- [18] Barrón-Cedeno, A., Rosso, P., Agirre, E., Labaka, G., 2010. Plagiarism detection across distant language pairs. In: *Proceedings of the 23rd International Conference on Computational Linguistics*, August. Association for Computational Linguistics, pp. 37–45.
- [19] Kolb, P., 2008. Disco: A multilingual database of distributionally similar words. In: *Proceedings of KONVENS-2008*, Berlin.
- [20] Kolb, P., 2009. Experiments on the difference between semantic similarity and relatedness. In: *Proceedings of the 17th Nordic Conference on Computational Linguistics-NODALIDA'09*, May.
- [21] Noorbehbahani F, Kardan AA (2011) The automatic assessment of free text answers using a modified bleu algorithm. *Comput Educ* 56:337–45.
- [22] He Y, Hui SC, Quan TT (2009) Automatic summary assessment for intelligent tutoring systems. *Comput Educ* 53:890–9.
- [23] Chu-Carroll J, Carpenteru B (1999) Vector-based natural language call routing. *J Comput Linguist* 25:361–88.
- [24] Landauer TK, Foltz PW, Laham D (1999) An introduction to latent semantic analysis. *Discourse Process* 25:259–84.
- [25] Bestgen Y (2006) Improving text segmentation using latent semantic analysis: a reanalysis of Choi, Wiemer-hastings, and Moore. *Comput Ling* 32:5–12.
- [26] Magliano JP, Graesser AC (2012) Computer-based assessment of student-constructed responses. *Behav Res Methods* 44:608–21.
- [27] Burstein, J., "The e-rater scoring engine: Automated Essay Scoring with natural language processing", In M. D. Shermis and J. C. Burstein (Eds.), *Automated Essay Scoring: A cross disciplinary approach* (pp. 113–121). Mahwah, NJ: Lawrence Erlbaum Associates, 2003.
- [28] Mitchell, T., Russel, T., Broomhead, P., & Aldridge N., "Towards robust computerized marking of free-text responses", In M. Danson (Ed.), *Proceedings of the Sixth International Computer Assisted Assessment Conference*, Loughboroug University, Loughborouh, UK., 2002.
- [29] Leacock C., Chodorow M. C-rater: Automated Scoring of Short-Answer Questions. *Computers and Humanities* 37, 2003.
- [30] A. Shehab, M. Elhoseny, and A. E. Hassanien, "A hybrid scheme for Automated Essay Grading based on LVQ and NLP techniques," in *2016 12th International Computer Engineering Conference (ICENCO)*, 2016, pp. 65-70.
- [31] Rashad, Magdi Z., et al. "An Arabic web-based exam management system." *International Journal of Electrical & Computer Sciences IJECS-IJENS* 10.01 (2010): 48-55.
- [32] Dunning, T. (1994). *Statistical identification of language* (pp. 10-03). Computing Research Laboratory, New Mexico State University.
- [33] Karen R and and Ramsayb J. Now what was that password again? A more flexible way of identifying and authenticating our seniors. *Behaviour and Information Technology* 2007; 26(4): 309–322.

An Effective Automatic Image Annotation Model Via Attention Model and Data Equilibrium

Amir Vatani*

Department of Computer Engineering, Islamic Azad
University, Science & Research Branch of Tehran, P.O. Box
14515/775, Iran

Milad Taleby Ahvanooeey

School of Computer Science and Engineering, Nanjing
University of Science and Technology, Nanjing, P.O. Box
210094 P.R. China

Mostafa Rahimi

Department of Electrical and Computer Engineering,
Shahid Beheshti University G.C, Tehran, Iran

Abstract—Nowadays, a huge number of images are available. However, retrieving a required image for an ordinary user is a challenging task in computer vision systems. During the past two decades, many types of research have been introduced to improve the performance of the automatic annotation of images, which are traditionally focused on content-based image retrieval. Although, recent research demonstrates that there is a semantic gap between content-based image retrieval and image semantics understandable by humans. As a result, existing research in this area has caused to bridge the semantic gap between low-level image features and high-level semantics. The conventional method of bridging the semantic gap is through the automatic image annotation (AIA) that extracts semantic features using machine learning techniques. In this paper, we propose a novel AIA model based on the deep learning feature extraction method. The proposed model has three phases, including a feature extractor, a tag generator, and an image annotator. First, the proposed model extracts automatically the high and low-level features based on dual tree continuous wavelet transform (DT-CWT), singular value decomposition, distribution of color ton, and the deep neural network. Moreover, the tag generator balances the dictionary of the annotated keywords by a new log-entropy auto-encoder (LEAE) and then describes these keywords by word embedding. Finally, the annotator works based on the long-short-term memory (LSTM) network in order to obtain the importance degree of specific features of the image. The experiments conducted on two benchmark datasets confirm that the superiority of proposed model compared to the previous models in terms of performance criteria.

Keywords—Automatic image annotation; attention model; skewed learning; deep learning, word embedding; log-entropy auto-encoder

I. INTRODUCTION

Automatic image annotation (AIA) is one of the image retrieval techniques in that the images can be retrieved in the same way as text documents. In the AIA, the main idea is to automatically learn the semantic concept models from a huge number of image samples and utilize the conceptual models to label new images with proper tags [1]. The AIA has a lot of applications in various fields including access, search, and navigate the huge amount of visual data which stored in online

or offline data sources, image manipulation and annotation application that used on a mobile device, [2]-[4]. The typical image annotation approaches rely on human viewpoints and the performance of them is highly dependent on the inefficient manual operations. Recently, many types of research [5], [6], [12], [31] have been conducted on the AIA that can be grouped into two different models [13]; generative models, such as [1], [7], and discrimination or conditional models such as [3], [12]. The generative models try to learn the joint probability distribution between keywords and image features [8], [13]. Simultaneously, conditional models are a class of models used in machine learning for modeling the dependence of semantic keywords on visual features [8]. During the last decade, deep learning techniques have reached excellent performance in the field of image processing. Furthermore, visual attention with deep neural networks has been utilized successfully in many natural languages processing and computer vision systems. It also has been used for image annotation issue in some existing literature [17], [19], [24], [34]. Although the existing deep learning based techniques have improved the performance of AIA models, still there are two major limitations including management of imbalanced distribution keywords and selection of correct features. To address these problems, we propose a technique for extracting the high-level and low-level features that are able to extract them automatically based on dual tree continuous wavelet transform (DT-CWT), singular value decomposition, distribution of color ton and the deep neural network. Next, we utilized an attention model for weighting the important feature by considering suitable coefficient. Moreover, we suggested a tag generator that works based on the log-entropy auto-encoder, and LSTM networks and then treat each keyword equally, in imbalanced distribution dictionary in order to find the better similar tags (e.g., keywords are described by word embedding approach).

The rest of this paper is organized as follows. Section II presents a brief description of existing literature on image annotation. Section III presents the proposed AIA model. Section IV discusses the experimental results and compares the proposed AIA model with the state of art techniques. Section V draws some conclusions.

II. RELATED WORK

In this section, we introduce some existing literature on AIA. During the last two decades, the AIA has been an active research area in the field of pattern recognition and computer vision. Several AIA techniques have been proposed to improve the performance of AIA models, which some of them try to learn the joint probability distribution between keywords and image features called generative models [1], [3]. In addition, some other techniques treat based on supervised learning problem in order to overcome the issue of image annotation, which is named discrimination models [1], [3]. Furthermore, some existing techniques have utilized a combination of these two methods; for example, in visual object classification, the combination of generative and discrimination model has been used. However, the difference between the AIA and the classification task is that each sample always has multiple correlated annotations, which makes it difficult to apply the combination of generative and discrimination techniques for the AIA [13].

Ping et al. [1] combined the generative and discriminative models by local discriminant topics in the neighborhood of the unannotated image by applying the singular value decomposition grouped the images of the neighborhood into different topics according to their semantic tags.

Mei Wang et al. [3] suggested an AIA model via integrated discriminative and generative models. This model first identifies a visual neighborhood in the training set based on generative technique, and then, the neighborhood is defined by an optimal discriminative hyperplane tree classifier based on the feature concept. The tree classifier is generated according to a local topic hierarchy, which is adaptively created by extracting the semantic contextual correlations of the corresponding visual neighborhood.

Duygulu et al. [33] expressed an object recognition model as machine translation. In that model, the recognition is a process of annotating image regions by words. In addition, it utilizes a translation model to form the relations between the image visual words and words in order to label new images. This model provides a possibility to extract features by some approaches, which tries to select proper features for improving the performance of recognition.

Dongping et al. [5] proposed a new AIA model based on Gaussian mixture model (GMM) by considering cross-modal correlations. In this model, first, the GMM is fitted by the rival penalized competitive learning (RPCL) or expectation-maximization algorithm in order to predict the posterior probabilities of each annotation keyword. Moreover, an annotation similarity graph is generated with a weighted linear combination of visual similarity and label similarity by integrating the information from both high-level semantic concepts and image low-level features together. The most important merit of this model is that it is able to effectively avoid the phenomena of synonym and polysemy appeared during the annotating process.

Song et al. [12] introduced a Sparse Multi-Modal Coding for image annotation using an efficient mapping method, which functions based on stacked auto-encoders. In this work,

they utilized a new learning objective function, which obtains both intra-modal and semantic relationships of data from heterogeneous sources effectively. Their experimental results conducted on some benchmark datasets demonstrate that it outperforms the baseline models for the task of image annotation and retrieval.

Wang et al. [27] provided a new image annotation method by focusing on deep convolutional neural network for large-scale image annotation. They contacted the proposed method on the MIRFlickr25K and NUS-WIDE datasets in order to analyze its performance. In practice, this method analyzes a pre-specify dual-model learning scheme which consists of learning to fine-tune the parameters of the deep neural network with respect to each individual modality and learning to find the optimal combination of diverse modalities simultaneously in a coherent process.

Karpathy and Fei-Fei [35] presented a novel AIA model that produces natural language descriptions of images and their regions based on the weak labels by performing on a dataset of images and sentences (e.g., with respect to very few hardcoded assumptions). This model employs the leverages images and their sentence descriptions in order to learn about the inter-modal correspondences between language and visual features. In the results, they evaluated its performance on both full-frame and region-level experiments, and, moreover, they claimed that the Multimodal RNN outperforms the retrieval baselines in both of them.

Feng et al. [36] proposed a robust kernel metric learning (RKML) algorithm based on the regression technique which can be directly utilized in image annotations. The RKML algorithm is also computationally more efficient due to the PSD feature is automatically ensured by regression algorithm.

Liu et al. [19] proposed a novel CNN-RNN image annotation model which utilizes a semantically regularized embedding layer as the interface between the CNN and RNN. However, they proposed semantic regularization that enables reliable fine-tuning of the CNN image encoder as well as the fast convergence of end-to-end CNN-RNN training. In practice, the semantic regularization generates the CNN-RNN interface semantically meaningful, and distributes the label prediction and correlation tasks between the CNN and RNN models, and importantly the deep supervision, i.e., it makes training the full model more stable and efficient.

Li et al. [24] introduced a global-local attention (GLA) method by combining local representation at object-level with global representation at image-level through attention mechanism. This method focuses on how to predict the salient objects more accurately with high recall while keeping context information at image-level. In the experimental results, they claimed that it achieved better performance on the Microsoft COCO benchmark compared with the previous approaches.

III. PROPOSED ANNOTATION MODEL

As depicted in Fig. 1, the overall structure of proposed model has three major sub-subsystems: the feature extractor, the tag generator, and the image-annotator. In the following, we will explain the basics, individual components, and their relationships in details.

A. RNN and LSTM

Since the Recurrent Neural Network (RNN) [19], [22] and the Long Short Term Memory (LSTM) [23], [25], [32] are the basic components of the proposed annotation model, we

describe briefly the RNN and the LSTM. A RNN networks at time t reads a unit of the input sequence, which is a sequence of vectors such as $K = (k_1, k_2, \dots, k_T)$ and gets the previous state, h_{t-1} .

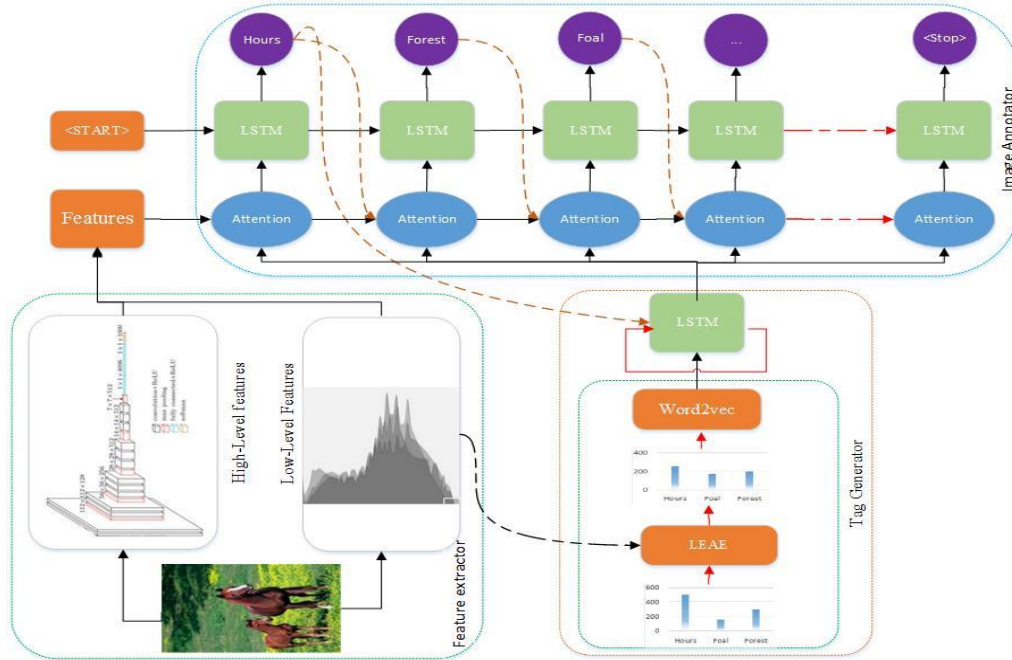


Fig. 1. The overall structure of proposed automatic image annotation model.

In addition, it generates the output and hidden layer at time t . The most common RNN approach can be calculated as follows:

$$h_t = f(k_t, h_{t-1}) \tag{1}$$

Where f is a nonlinear function and h_t is a hidden state at time t .

The LSTM is an advanced version of RNN with distinctive unit, which is able to manipulate the long-term dependencies. A LSTM unit consists of a cell state, and three gates (e.g., input, output, and forget gates). The input gate decides which values should be updated, while a sigmoid function does this operation. The forget gate decides what information should be removed from the cell state. Finally, the LSTM unit employs output gate by taking the same value with input and forget gates in order to obtain result based on the cell state. Fig. 2 shows the basic LSTM unit of the proposed model.

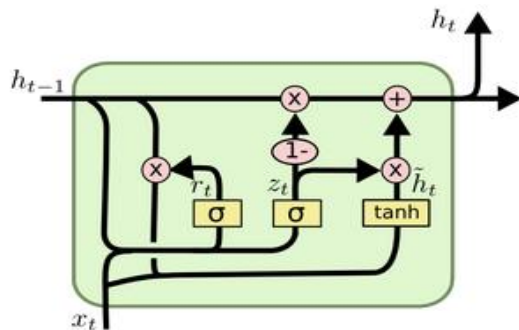


Fig. 2. Basic LSTM unit [48].

$$\begin{aligned} z_t &= \sigma(w_z \times [h_{t-1}, x_t]) \\ r_t &= \sigma(w_r \times [h_{t-1}, x_t]) \\ \tilde{h}_t &= \tanh(w \times [r_t \times h_{t-1}, x_t]) \\ h_t &= (1 - z_t) \times h_{t-1} + z_t \times \tilde{h}_t \end{aligned} \tag{2}$$

B. Problem Formulation

Let $X = \{I_1, I_2, \dots, I_N\}$, $I_i \in R^d$ denote N training images that each. $\nabla = \{K_1, K_2, \dots, K_M\}$ defines the dictionary of M possible annotation keywords. if the I_i annotated by the K_j , $\varphi(i, j) = 1$ Otherwise $\varphi(i, j) = 0$, and the i th image is annotated by $\varphi_i = \{\varphi(i, 1), \varphi(i, 2), \dots, \varphi(i, M)\}$. The goal of image annotation is to select the appropriate set of tags for a given image. Image is represented by a d -dimensional features vector.

The upper LSTM of the proposed model used to train the images and predict the next appropriate annotation tag using a given attention vector. That A_t is an attention output that can be calculated as follows:

$$\begin{aligned} A_t &= g(A_{t-1}, TG, k'_{t-1}) \\ A_1 &= g(\text{Attention weight}, TG) \end{aligned} \tag{3}$$

The g is a nonlinear function and attention weight which obtains the high and low level features.

$$TG_t = \sigma(\hat{k}_1, TG_t, k_{t-1}) \tag{4}$$

TG is the set of words that is generated by the tag generator sub-system. The k_1 is the first annotation tag, which is generated by supervised training. In other words, it inputs to the tag generator and lead to production of words, which is closed to k_1 and thus other sections of the proposed model select the appropriate tag.

C. Feature Extractor

In this section, we describe the feature extractor (low and high-level features) for image annotation in details. Low-level features and high-level features are essential for pattern recognition and associative learning (i.e., a proper combination of these features give a very important information from the details of the image, where the high-level features usually contain the context information about objects, and low-level features always contain context and background information) [26]. Therefore, we utilize both features for appropriate representation of the images. The detail structures of both features are described as follows.

1) Low-level features

Low-level image's features refer to a set of combination of elements or independent objects in an image [9]. These features are attributes that describes more specific individual components (e.g., color, shape, texture and background) of an image by focusing on the details of rudimentary micro information of images [15]. In this paper, we inspired the low-level features from the previous works in order to express the color and texture information of the image [37], [38].

The low-level features extraction method based on Distribution of Color Ton called "DCTon" works based on the structures of Texton methods [37], [39], [40]. Regular textures are the scanning result of images by the Texton component [39]. While the DCTon can be considered as the extended version of the Texton [38]. In the approach, the color connectivity regions of an image are considered as the proper properties for extract features that contain the color and texture information simultaneously. If $R, G, \text{ and } B$ are the color components, and the DCTon components are utilized to describe a pixel with components (R_1, G_1, B_1) (i.e., it appears a specified spatial relationship by considering distances and orientations of the corresponding pixel with components (R_2, G_2, B_2) for each pixel of the image) [38]. After extracting the DCTon components, the values of pixels are set to their average in order to make the DCTon image. After creating the DCTon image, the Co-occurrence matrixes are extracted from this image. The Co-occurrence matrix of this quantized component is established and its contrast, correlation, energy, and homogeneity features are extracted by a vector which can be defined as follows:

$$LL_{DCTon} = [Contrast, Correlation, Energy, Homogeneity] \quad (5)$$

Another low-level features extraction method operates based on the Dual Tree-CWT and SVD (Support Vector Machine), and conceptual segmentation, which was introduced in [38]. These features extracted from n-levels decomposition of 2-D, DT CWT of a $W \times H$ input image. Each scale has a set of sub bands with size $\frac{W}{2^n} \cdot \frac{H}{2^n}$ of complex

coefficients, which can be denoted by (6):

$$M_{c, lowpass}^i = \begin{bmatrix} ll_{1,1}^i & \dots & ll_{1, \frac{H}{2^n}}^i \\ \vdots & \ddots & \vdots \\ ll_{\frac{W}{2^n}, 1}^i & \dots & ll_{\frac{W}{2^n}, \frac{H}{2^n}}^i \end{bmatrix} \cdot c \quad (6)$$

$= \{real, imaginary\}, i$
 $= 1, 2.$

$$M_{c, highpass}^j = \begin{bmatrix} hh_{1,1}^j & \dots & hh_{1, \frac{H}{2^n}}^j \\ \vdots & \ddots & \vdots \\ hh_{\frac{W}{2^n}, 1}^j & \dots & hh_{\frac{W}{2^n}, \frac{H}{2^n}}^j \end{bmatrix} \cdot c$$

$= \{real, imaginary\}, j = 1, 2, \dots, 6.$

For the conceptual segmentation of images, we divided the images into 5 regions (A_1 to A_5) same as the [38]. Moreover, we extracted the Real and the imaginary sub-band coefficients of four levels DT-CWT [14] decomposition from each image segment and calculated the SVD [18] of each of the derived matrixes using the vectors of eigenvalues such that the features of an image can be defined as (7).

$$LL_{tf} = \begin{bmatrix} A_1 = [\sigma_1, \dots, \sigma_{Rank(M_1)}, \sigma_1, \dots, \sigma_{Rank(M_2)}, \dots, \sigma_1, \dots, \sigma_{Rank(M_{16})}] \\ \vdots \\ A_5 = [\sigma_1, \dots, \sigma_{Rank(M_1)}, \sigma_1, \dots, \sigma_{Rank(M_2)}, \dots, \sigma_1, \dots, \sigma_{Rank(M_{16})}] \end{bmatrix} \quad (7)$$

Where the $\sigma_1, \dots, \sigma_i$ are the diagonal eigenvalues.

Therefore, the final low-level features of the image in the proposed model are a fusion of the DCTon based features and DT-CWT features, which can be denoted as follows:

$$LL = [LL_{DCTon}, LL_{tf}^T] \quad (8)$$

2) High-level Features

High-level features or thematic features are important attributes for image representation. These properties represent the image with a global perspective and refer to the definition of the image or concept of the image [20], [24]. Details of these features can imitate the human perceptual system very well. During the last decade, several approaches have been proposed to improve the high-level feature extraction in pattern recognition area. Convolutional Neural Network (CNN, or ConvNet) has recently utilized as a powerful class of models for feature extraction purpose such as VGG16, VGG19 and ResNet50 [16], [21]. In this study. We employ the VGG16, and the ResNet50 in order to extract the high-level features. If the ResNet models are at properly tuned. The feature extractor provides better results than other architectures. For example, the deeper ResNet with '34' layers has a smaller training error compared with the 18 layer. The ResNet model should utilize a direct path for propagating information through the residual block in the network as a result. It allows the information to propagate from one block to any other ones during both forward and backward passes. Due to this reason, it causes to reduce the complexity of the training process.

D. Attention Mechanism

During the process of image annotation, some important features of attention are very essential (e.g., some features are important and some others are not). In practice, each feature has a special weight for generating the image representation. Herein, the way of fusing the low-level features and high-level features are important for images annotation. Due to this reason, we proposed an attention mechanism to integrate the high and low-level features so that it can selectively focus on some important objects of the image at different time. Moreover, it brings up the appropriate keywords at the same time using (9).

$$\text{Attention weight} = \sum_i^{\#(LL)} \gamma_i^{(t)} LL_i + \sum_j^{\#(HL)} \xi_j^{(t)} HL_j \quad (9)$$

Where $\gamma_i^{(t)}$ and $\xi_j^{(t)}$ denotes the attention weights of low and high-level features at time (t), that

$$\sum_i^{\#(LL)} \gamma_i^{(t)} + \sum_j^{\#(HL)} \xi_j^{(t)} = 1 \quad (10)$$

$\gamma_i^{(t)}$ and $\xi_j^{(t)}$ can be calculated by the Softmax function [28],

$$\begin{aligned} \gamma_i^{(t)} &= \tau \times \frac{\exp(\zeta_i^t)}{\sum_i^{\#(LL)} \exp(\zeta_i^t)} \\ \xi_j^{(t)} &= \left(\frac{1}{2} - \tau\right) \times \frac{\exp(\varrho_j^t)}{\sum_j^{\#(HL)} \exp(\varrho_j^t)} \\ 0 &\leq \tau \leq 1 \end{aligned} \quad (11)$$

The attention weight at time (t) has a direct relation to the previous information and the other features. Therefore, these relations can be modeled in a nonlinearity function. ζ_i^t and ϱ_j^t can be defined as follows:

$$\begin{aligned} \zeta_i^t &= \Gamma^T \sigma(W_h h^{t-1} + W_l \times LL_i + b) \\ \varrho_j^t &= \Gamma^T \sigma(W_h h^{t-1} + W_l \times HL_j + b) \end{aligned} \quad (12)$$

That h^{t-1} is the previous hidden state.

Since ζ_i^t and ϱ_j^t are not normalized, for normalizing these weights, we used the Softmax function and calculated the final weights. In addition, due to the numbers and dimensions of the low and high level features are different, there are various effects during annotation process. Therefore, we considered the τ coefficient for learning the proportional in order to define importance degree of the high and low features. Others parameters Γ , W_l and W_h are coefficients that can be learned by our attention model.

E. Tags Generator

During the process of automatic image annotation, a sub-system that produces the cluster of same family words for image annotation is very important. For this purpose, as shown in Fig. 1, we proposed a tag generator which consists of two phases including, word embedding, and data equilibrium. The word embedding describes the keywords (as a text modal) by appropriate vectors and data equilibrium in order to apply to the imbalanced keywords and generates different weights for different frequency keywords. In addition, it balances the keyword dictionary. In the following, these two phases are described.

1) Balanced/skewed distribution keywords

In the image-annotation datasets, the keywords are extremely diverse with the skewed distribution, and the number of different keywords used for annotation of images is imbalanced. For example, the ESP game dataset [41], has over 20,000 images and 268 keywords. A high-frequency tag generator has been used for over 500 images, while a low-frequency tag is used for less than 50 images [13]. This problem extremely affects the performance of image annotation, and the low-frequency keywords have less effect during the annotation. As a result, the existing techniques have low percent accuracies, and conversely. Due to this, we utilize the imbalanced learning for generating tags with respect to variance distribution. In practice, it can increase the training intensity of low-frequency keywords for image samples in order to enhance the generalization performance of the whole model. For addressing this problem, we introduce an ANN based Auto-encoder method, which is used for unsupervised learning [2], [3]. The aim of an auto-encoder is to learn a representation for a set of data, typically for the purpose of dimensionality reduction. An auto-encoder always consists of two phases: the encoder e_θ and the decoder $d_{\theta'}$. The encoder transforms an input vector k in to the hidden layer h . In addition, the decoder maps the h back in order to reconstruct the input vector k' (e.g., reconstructed vector is optimized by the cost function).

$$e_\theta(k) = \sigma(w \times k + b) . \theta = \{w, b\} \quad (13)$$

Where W is weighted the matrix, b is a bias vector, and σ is a nonlinear activation function. Moreover, the decoder has the following relation.

$$\begin{aligned} d_{\theta'}(h) &= \begin{cases} \sigma(w' \times h + b') & \text{when input vector} \in [0 \ 1] \\ w' \times h + b' & \text{when input vector} \in \mathbb{R} \end{cases} . \theta' \\ &= \{w', b'\} \end{aligned} \quad (14)$$

Where $w' = w^T$ and $b' = b^T$

If the input vector is k and the approximation of input vector is k' , the auto-encoder minimizes the loss function by the $|k - k'| < \mathcal{E}$. With respect to the mentioned relation, $k' = d_{\theta'}(e_\theta(k))$; and the auto-encoder model can be learned by the following optimization:

$$\theta^* . \theta'^* = \arg \min \frac{1}{M} \sum_{i=1}^M |k_i - d_{\theta'}(e_\theta(k_i))| \quad (15)$$

Herein, the M is the number of samples.

For the proposed balanced model, we consider L as hidden layer. Let h_l be the output vector of layer l , the feed-forward operation for L layer of auto encoder can be described as follows:

$$h_{l+1} = \sigma(W^{l+1} h^l + b^{l+1}) . l \in \{0, \dots, L-1\} \quad (16)$$

The h_0 and h_L are the input and output vectors using the following backpropagation algorithm.

$$\theta^* = \arg \min \sum_{i=1}^M |F_{\theta}(I_i). K_i| \quad (17)$$

Where $F_{\theta}(I)$ is a composition of activation function σ from θ_1 to θ_L and $\theta_i = \{W_i, b_i\}$ are the model parameters.

The low-level image features are the input to the model and the image tags are the supervision information. The backpropagation algorithm is used to create the relation between the features and tags. But the imbalanced distribution of the image keywords generates a model such that provides a skew degree of accuracies. To enhance the annotation performance, we propose a balanced Log-Entropy-Auto-Encoder (LEAE) that can enhance the training process for low frequency tags. We utilized the [8], [13], [42] for giving the appropriate coefficients to the tags using the concept of log-entropy. Assuming that there are N images and M different tags in the training dataset. If we increase the coefficients of low-frequency keywords, then it provides a balance training. For this purpose, we construct a coefficient matrix $W_{N \times M}$ for training all the images as follows:

$$W = \begin{bmatrix} W_{11} & \dots & W_{1M} \\ \vdots & \ddots & \vdots \\ W_{N1} & \dots & W_{NM} \end{bmatrix}_{N \times M} \quad (18)$$

Each w_{ij} can be calculated as follows:

$$w_{ij} = \varphi(i, j) \times \left(1 + \frac{1}{T_j \log N} \sum_{i=1}^N \varphi(i, j) [\log \varphi(i, j) - \log T_j] \right) \quad (19)$$

Where the T_j is total number of occurrence of j th tag in training images. The $(i, j) \in \{0, 1\}$, the i th image is annotated by keyword j , $\varphi(i, j) = 1$ otherwise $\varphi(i, j) = 0$.

For example, assuming that, there are three images including:

I_1, I_2 and I_3 and three keywords in the training dataset, K_1, K_2 and K_3 are the annotation tags are assigned as depicted in Table I.

TABLE I. EXAMPLE OF IMAGE AND ANNOTATION TAGS

Images	I_1	I_2	I_3
Annotation tags	K_1, K_2 and K_3	K_2 and K_3	K_3

Note that the K_1 is the low-frequency tag.

The $w_{12} = 0.36$ and $w_{11} = 1$.

Therefore, we train the proposed model by the following optimization in order to balanced learning.

$$\theta^* = \arg \min \sum_{i=1}^M |F_{\theta}(I_i). W_i \times K_i| \quad (20)$$

Where W_i denotes the i th row of coefficient matrix W .

2) Word-embedding descriptor

In the task of AIA based on modals data such as image and text, there are many kinds of relations that are included of image-to-image, image-to-word, and word-to-word relations [5]. We address these mutual modal relations between image and word due to it is very important during the annotating

process. In this sub section, we will describe the relation of word-to-word.

If we employ a proper description of the words, then the quality of the tag generator, the consequently, and the quality of the AIA system will be increased. In the both situations, if the words semantically are similar, and described with similar vectors; or the words semantically are not similar described by vectors with proper semantic distance; the tag generator can suggest the best words to other sub-system of model.

In general, the word embedding approaches are used in the natural language processing in order to transform the bag-of-words representation to a continuous space representation [28]. There are some advantages to this continuous space since the dimensionality is largely reduced and the words closer in meaning are close in this new continuous space. There have been introduced some applications of the word embedding based on neural networks including the word2vec [26], Dictionary of Affect in Language (DAL) [44], SentiWordNet [43], Glove [26] and Wikitionary [45].

We have used the word2vec [26], which offer two possible ways to generate the word embedding continuous bag-of-words- and skip-gram (CBOW). After training the word embedding, an n-dimensional vector is available for each word in the dictionary. In order to training the Word2Vec, we utilized a Large Textual Corpora such as all Wikipedia articles in a certain language. Moreover, we applied the thematic textual collections related to semantic concept collections, and annotation keywords during the Word2vec training.

IV. EXPERIMENTAL RESULTS AND ANALYSIS

In this section, we implemented the proposed model on two different datasets in order to evaluate the performance of the proposed model. First, we introduce a detailed description of the datasets and evaluation metrics. Then, we compare the experimental results with the state-of-the-art techniques.

A. Datasets

The Corel-5k dataset is one of the famous benchmarks that have been used for evaluating the AIA models so far. Herein, we used this benchmark in order to analyze and compare the proposed model with other models. The Corel dataset consists of 5000 images from 50 Corel Stock Photo CDs, and each CD includes 100 images on the same topic, an image is manually labeled at least one-annotation word and maximum of five-annotation words [3]. All of distinct tags in dictionary are 260 keywords. The training set consists of 3500 images, validation set includes 750 images and test set contains 750 images.

The IAPRTC-12 dataset consists of 19,627 images of sports, actions, people, animals, cities, landscapes and many other aspects of contemporary life. All of distinct tags in dictionary are 291 keywords. The training set consists 13739 images, the validation set contains 2944 images and the test set consists of 2944 images.

B. Evaluation Metrics

We have implemented the experiments in the Python 3 programming using the *TensorFlow*, *NumPy*, and *Keras* frameworks and run on the same PC with *Intel Centrino Core*

i7 2670QM Duo 2.20 GHz Processor, 8GB of RAM, and Linux Ubuntu 14.1 operating system.

Since the common evaluation metrics can be easily found in recently proposed models [10]-[20], we utilized them in order to evaluate the performance of the proposed model. Moreover, we computed the evaluation metrics including the precision, and recall for each keyword separately (i.e., first, five relevant tags are extracted for each image and all images are annotated with these tags; Second, for each keyword k_j , average recall and precision rate are computed by the following equations). It is assumed that $K_j \in \nabla$ and ∇ is the dictionary of M possible annotation keywords.

$$\overline{Recall} = \frac{\sum_{j=1}^M Precision(k_j)}{M \sum_{j=1}^M R(k_j)} \quad (21)$$

$$\overline{Precision} = \frac{\sum_{j=1}^M precision^j}{M \sum_{j=1}^M Prediction(k_j)} \quad (22)$$

That $Precision(k_i)$ is total number of the correctly predicted keyword k_i , $R(k_i)$ is the relevant annotated counts of the keyword k_j and $Prediction(k_j)$ is the predicted counts of the keyword k_j . The “ $F - measure$ ” is a measure of the test accuracy, which considers both the $\overline{precision}$ and the \overline{recall} of the test in order to compute the score. This measure can be calculated as follows:

$$F - measure = \frac{2 \times \overline{precision} \times \overline{recall}}{\overline{recall} + \overline{precision}} \quad (23)$$

C. Comparison Results

In order to show the superiority of the proposed image annotation model, we compare it with several state-of-the-art models, including L-RBSAE [8], Multi-AE [13], G-LSTM [17], 2PKNN [46], JEC [47] and Soft/Hard Attention [20] by implementing on Corel-5 K and IAPRTC-12 datasets. In practice, there are some differences between the mentioned models. The first difference is the feature extraction subsystem (i.e., the G-LSTM uses GoogLeNet, to extract the features; Multi-AE employs multi-view including the GIST [8], Hue [29] and SIFT [30] in order to extract the features; The JEC exploits the AlexNet to extract image features; The 2PKNN and Soft/Hard Attention employs the VGG16 as the same like our model to extract image features). The second difference is that the structure of image annotation (i.e., the Multi-AE utilizes the basic RNN as the decoder for the annotating process; the G-LSTM and Soft/Hard Attention utilizes the LSTM network for the annotating process).

The evaluated results of proposed model and other mentioned models are listed in the Table II. As we already pointed out, the performance analysis of the proposed model and each of the state-of-the-art models are evaluated based on the accuracy measure $\overline{precision}$, \overline{recall} and $F - measure$. As depicted in Table II, the bold numbers indicate the performance of the proposed model and it is obvious that the proposed model noticeably outperforms most of the evaluated models, especially the Multi-AE, the JEC and the L-RBSAE.

Meanwhile, it is a little better than Soft/Hard Attention and G-LSTM.

TABLE II. PERFORMANCE COMPARISON OF PROPOSED MODEL VS THE EVALUATED MODELS

Datasets	Model	$\overline{precision}$	\overline{recall}	$F - measure$
Corel5k	Multi-AE[13]	0.15	0.2	0.17
	2PKNN[46]	0.22	0.66	0.33
	JEC[47]	0.18	0.47	0.26
	L-RBSAE[8]	0.23	0.24	0.23
	G-LSTM [17]	0.22	0.72	0.33
	Soft/Hard attention[20]	0.22	0.75	0.34
	Proposed Model	0.28	0.96	0.43
IAPRTC-12	Multi-AE[13]	0.43	0.38	0.40
	2PKNN[46]	0.30	0.38	0.34
	JEC[47]	0.29	0.19	0.23
	L-RBSAE [8]	0.28	0.63	0.38
	G-LSTM [17]	0.35	0.57	0.43
	Soft/Hard Attention[20]	0.40	0.48	0.43
	Proposed Model	0.54	0.37	0.44

Obviously, the evaluated results confirm that the proposed model provides almost the same performance results like the G-LSTM and Soft/Hard Attention. In addition, we can observe that the significant performance improvement compared to the Multi-AE or the L-RBSAE. The precision and the recall metrics of proposed model are also comparable with those of the recently proposed models, for the Corel-5 K and IAPRTC-12 datasets. Fig. 3 shows some sample images and annotations examples from the Corel dataset after implementing the proposed model. Even though, some of the predicted tags for these annotations do not match with the image, still they are very meaningful.



Fig. 3. Qualitative image annotation results obtained with our model.

V. CONCLUSIONS AND FUTURE WORK

In this paper, we have presented a novel AIA model based on the deep learning feature extraction method. In addition, we proposed a loge entropy solution in order to solve the problem of imbalanced data in image annotation. First of all, we implemented the proposed model on two popular datasets and, second, we evaluated the obtained results with respect to evaluation metrics. Finally, we compared the proposed model with several state-of-the-art models. The evaluated results confirm that the proposed model provides efficient performance and outperforms the evaluation metrics compared to the evaluated state-of-the-art models.

As for future work, we plan to design an efficient AIA model in order to improve the relevance score of features and utilize the combining generative and discriminant methods to improve the performance of the new AIA model.

REFERENCES

- [1] D. Zhang, Md. M. Islam, G. Lu, A review on automatic image annotation techniques, *Pattern Recognition*, 2012, 45, pp.346-362
- [2] Tiberio Uricchio, L.B., Lorenzo Seidenari, Alberto Del Bimbo., P.R. Automatic Image Annotation via Label Transfer in the Semantic Space, and d. 10.1016/j.patcog.2017.05.019.
- [3] Wang, M., et al., Effective automatic image annotation via integrated discriminative and generative models. *Information Sciences*, 2014. 262: p. 159-171.
- [4] Shih, C.-W., et al., The effectiveness of image features based on fractal image coding for image annotation. *Expert Systems with Applications*, 2012. 39(17): p. 12897-12904.
- [5] Tian, D. and Z. Shi, Automatic image annotation based on Gaussian mixture model considering cross-modal correlations. *Journal of Visual Communication and Image Representation*, 2017. 44: p. 50-60.
- [6] Uricchio, T., et al., Automatic image annotation via label transfer in the semantic space. *Pattern Recognition*, 2017. 71: p. 144-157.
- [7] Bahrololoum, A. and H. Nezamabadi-pour, A multi-expert based framework for automatic image annotation. *Pattern Recognition*, 2017. 61: p. 169-184.
- [8] Ke, X., et al., Data equilibrium based automatic image annotation by fusing deep model and semantic propagation. *Pattern Recognition*, 2017. 71: p. 60-77.
- [9] Tsochatzidis, L., et al., Computer-aided diagnosis of mammographic masses based on a supervised content-based image retrieval approach. *Pattern Recognition*, 2017. 71: p. 106-117.
- [10] Nanni, L., S. Ghidoni, and S. Brahmam, Handcrafted vs. non-handcrafted features for computer vision classification. *Pattern Recognition*, 2017. 71: p. 158-172.
- [11] Sun, T., L. Sun, and D.-Y. Yeung, Fine-grained categorization via CNN-based automatic extraction and integration of object-level and part-level features. *Image and Vision Computing*, 2017. 64: p. 47-66.
- [12] Songhao, L., et al., Sparse Multi-Modal Topical Coding for Image Annotation. *Neurocomputing*, 2016. 214: p. 162-174.
- [13] Yang, Y., W. Zhang, and Y. Xie, Image automatic annotation via multi-view deep representation. *Journal of Visual Communication and Image Representation*, 2015. 33: p. 368-377.
- [14] Jin, C. and S.-W. Jin, Automatic image annotation using feature selection based on improving quantum particle swarm optimization. *Signal Processing*, 2015. 109: p. 172-181.
- [15] Rad, R. and M. Jamzad, Image annotation using multi-view non-negative matrix factorization with different number of basis vectors. *Journal of Visual Communication and Image Representation*, 2017. 46: p. 1-12.
- [16] Zhu, S., X. Sun, and D. Jin, Multi-view semi-supervised learning for image classification. *Neurocomputing*, 2016. 208: p. 136-142.
- [17] Jia, X.; Gavves, E.; Fernando, B.; and Tuytelaars, T. 2015.Guiding long-short term memory for image caption generation. arXiv preprint arXiv:1509.04942.
- [18] and, Y.G., et al., Deep Convolutional Ranking for Multilabel Image Annotation. *CoRR*, 2013. abs/1312.4894.
- [19] Liu, F.X., Tao; Hospedales, Timothy M.; Yang, Wankou; Sun, Changyin, Semantic Regularisation for Recurrent Image Annotation, *IEEE Conference on Computer Vision and Pattern Recognition (CVPR)*, 2017. Doi: 10.1109/CVPR.2017.443
- [20] Vinyals, O.; Toshev, A.; Bengio, S.; and Erhan, D. 2015. Show and tell: A neural image caption generator. In *Proceedings of the IEEE Conference on Computer Vision and Pattern Recognition*, 3156-3164.
- [21] Donahue, J.; Anne Hendricks, L.; Guadarrama, S.; Rohrbach, M.; Venugopalan, S.; Saenko, K.; and Darrell, T. 2015. Long-term recurrent convolutional networks for visual recognition and description. In *Proceedings of the IEEE Conference on Computer Vision and Pattern Recognition*, 2625-2634.
- [22] Mao, J.; Xu, W.; Yang, Y.; Wang, J.; Huang, Z.; and Yuille, A. 2015. Deep captioning with multimodal recurrent neural networks (m-rnn). *ICLR*.
- [23] Jia, X.; Gavves, E.; Fernando, B.; and Tuytelaars, T. 2015. Guiding long-short term memory for image caption generation. *IEEE International Conference on Computer Vision (ICCV)*, 2015.
- [24] Linghui Li, Sheng Tang, Lixi Deng, Yongdong Zhang, Qi Tian; "Image Caption with Global-Local Attention" the Thirty-First AAAI Conference on Artificial Intelligence (AAAI-17) 2017.
- [25] Song, J., Tang, S., Xiao, J. et al. "LSTM-in-LSTM for generating long descriptions of images" *Comp. Visual Media* (2016) 2: 379. <https://doi.org/10.1007/s41095-016-0059-z>.
- [26] Maria Giatsoglou, Manolis G. Vozalis, Konstantinos Diamantaras, Athena Vakali, George Sarigiannidis, Konstantinos Ch. Chatzivasvas, Sentiment Analysis Leveraging Emotions and Word Embeddings, *Expert Systems With Applications* (2016), doi: 10.1016/j.eswa.2016.10.043
- [27] R. Wang, Y. Xie, J. Yang, L. Xue, M. Hu, Q. Zhang, Large scale automatic image annotation based on convolutional neural network, *J. Vis. Commun. Image R.*(2017), doi: <http://dx.doi.org/10.1016/j.jvcir.2017.07.004>
- [28] S. J. Pan and Q. Yang, "A Survey on Transfer Learning," in *IEEE Transactions on Knowledge and Data Engineering*, vol. 22, no. 10, pp. 1345-1359, Oct. 2010. doi: 10.1109/TKDE.2009.191.
- [29] F. Yan and K. Mikolajczyk, "Deep correlation for matching images and text," 2015 IEEE Conference on Computer Vision and Pattern Recognition (CVPR), Boston, MA, 2015, pp. 3441-3450. doi: 10.1109/CVPR.2015.7298966
- [30] S. J. Pan and Q. Yang, "A Survey on Transfer Learning," in *IEEE Transactions on Knowledge and Data Engineering*, vol. 22, no. 10, pp. 1345-1359, Oct. 2010. doi: 10.1109/TKDE.2009.191
- [31] Dhanesh Ramachandram, Graham W. Taylor, "Deep Multimodal Learning: A Survey on Recent Advances and Trends", *Signal Processing Magazine IEEE*, vol. 34, pp. 96-108, 2017, ISSN 1053-5888.
- [32] S. Zhu, X. Li and S. Shen, "Multimodal deep network learning-based image annotation," in *Electronics Letters*, vol. 51, no. 12, pp. 905-906, 6 11 2015. doi: 10.1049/el.2015.0258.
- [33] P. Duygulu, K. Barnard, J. de Freitas, D. Forsyth, Object recognition as machine translation: learning a lexicon for a fixed image vocabulary, *ECCV* (2002).
- [34] Bahdanau, D.C., Kyunghyun; Bengio, Yoshua, Neural Machine Translation by Jointly Learning to Align and Translate. *ARXIV*, 2014.
- [35] Karpathy, A.F.-F., Li, Deep Visual-Semantic Alignments for Generating Image Descriptions. 2014.
- [36] Z. Feng, R. Jin and A. Jain, "Large-Scale Image Annotation by Efficient and Robust Kernel Metric Learning," 2013 IEEE International Conference on Computer Vision, Sydney, NSW, 2013, pp. 1609-1616. doi: 10.1109/ICCV.2013.203.
- [37] Rahimi, M. and M. Ebrahimi Moghaddam, A content-based image retrieval system based on Color Ton Distribution descriptors. *Signal, Image and Video Processing*, 2015. 9(3): p. 691-704.

- [38] Mostafa, R. and E.M. Mohsen. A texture based image retrieval approach using Self-Organizing Map pre-classification. in 2011 IEEE International Symposium on Signal Processing and Information Technology (ISSPIT), 2011.
- [39] Wang, X.-y., Z.-f. Chen, and J.-j. Yun, An effective method for color image retrieval based on texture. *Computer Standards & Interfaces*, 2012. 34(1): p. 31-35.
- [40] Y.J. Zhang, *Visual Information Retrieval Based on Content*, TsingHua University Press, Beijing, 2003 102–126.
- [41] M. Guillaumin, T. Mensink, J. Verbeek J, C. Schmid, Tagprop: Discriminative metric learning in nearest neighbor models for image auto-annotation, in: IEEE 12th International Conference on Computer Vision (ICCV), 2009 pp. 309-316.
- [42] Z. Feng, R. Jin, A. Jain, Large-scale Image Annotation by Efficient and Robust Kernel Metric Learning, in: 2013 IEEE International Conference on Computer Vision (ICCV), 2013, pp. 1609-1616.
- [43] Esuli, A., & Sebastiani, F. (2006). Sentiwordnet: A publicly available lexi resource for opinion mining. In *Proceedings of LREC* (pp. 417–422).
- [44] Li, J., et al., Learning distributed word representation with multi-contextual mixed embedding. *Knowledge-Based Systems*, 2016. 106: p. 220-230.
- [45] De Boom, C., et al., Representation learning for very short texts using weighted word embedding aggregation. *Pattern Recognition Letters*, 2016. 80: p. 150-156.
- [46] Y. Verma, C.V. Jawahar, Image annotation using metric learning in semantic neighbourhoods, in: *Proceeding of the 12th European Conference on Computer (ECCV)*, 2012, pp. 836-849.
- [47] A. Makadia, V. Pavlovic, S. Kumar, A new baseline for image annotation, in: *Proceeding of the 10th European Conference on Computer (ECCV)*, 2008, pp.316-329.
- [48] Cho, K.v.M., Bart; Gulcehre, Caglar; Bahdanau, Dzmitry; Bougares, Fethi; Schwenk, Holger; Bengio, Yoshua, Learning Phrase Representations using RNN Encoder-Decoder for Statistical Machine Translation. ARXIV, 06/2014.

A Systematic Literature Review of Success Factors and Barriers of Agile Software Development

Shahbaz Ahmed Khan Ghayyur¹, Salman Ahmed²,
Mukhtar Ali³, Abdul Razzaq⁵, Naveed Ahmed⁶
Department of Computer Sciences and Software
Engineering, International Islamic University,
Islamabad, Pakistan

Adnan Naseem⁴
Department of Computer Sciences,
COMSATS Institute of Information Technology,
Islamabad, Pakistan

Abstract—Motivator and demotivator plays an important role in software industry. It encompasses software performance and productivity which are necessary for projects of Agile software development (ASD). Existing studies comprise of motivators and demotivators of ASD, which exist in dispersed form. That is why there is a need of a detailed systematic literature review to review the factors and sub-factors effecting motivators and demotivators in ASD. A comprehensive review is executed to gather the critical success factors of motivator and demotivator of Agile software development. Thus, the ongoing study classifies motivator and demotivator factors into four classes, i.e., people, organization, technical and process. However, sub-classification is also executed to clarify more of the motivators of agile. Along with this, motivator and demotivator of scrum process is also categorized to overview a clear vision.

Keywords—Agile methods; systematic literature review; motivator; demotivator; success factors; barriers; scrum; ASD

I. INTRODUCTION

A. Motivation

Agile Software development (ASD) provides an iterative way to make effective and efficient software development. It contains set of rules and principle with self-organizing teams. In Software development, motivator plays an important role to enhance the personal and technical skills. Motivator is a critical factor in achieving project scope by clarifying the business goals. McHugh et al. [1] has analysed the effect of motivator and demotivator on core three agile practices. Qualitative analysis has been performed to fulfil this purpose. This systemic literature review will gather the existing knowledge of motivator and demotivator.

In ASD, due to its iterative nature ratio of failure projects are less than SDLC but when it comes to individual personal and technical skills, there is need of motivator and demotivator factors effecting ASD. These motivators and demotivators works as an umbrella activities throughout the project that's why there is need to control the demotivator factors to increase the motivator factors afterward. The literature depicts that effective management is the backbone of project success and can reduce the failure ratio up to 70% of their total cost. ASD has multiple methods which follow the one agile manifesto for continuous development throughout the life cycle.

B. Need of Systematic Literature Review

From the previous 10 to 15 years, ASD showed great boom in software industry and it bypass the existing SDLC technique due to its more success stories that's why there is a revival of agile industry all over the world and sooner or later it will become the best adopted technique to its flexible environment. Existing literature depicts, that is, it lacks a detailed systematic literature of ASD and there is a need of systematic literature review to cover this gap. This study encounters the existing studies on motivator and demotivator factor to make the detailed list. The data is present in dispersed format and needs to gather for systematic literature review.

This SLR will help in managing the self-organizing teams by providing them confidence and support for help in work done. Cockburn and Highsmith [2] proposed rewards and incentives as most common motivating factor. The literature encompasses the people factor in which stress is a demotivating factor. ASD works on software development that yields success as well as stakeholder satisfaction.

Motivator and demotivator factors are challenging work that they need to be identified and must be noted. Secondly, our main contribution is to categorize the motivator and demotivator factor into people, technical and organization background. For this purpose, we have done a detail study of relevant papers of motivators and demotivators and classified, respectively.

The structure of remaining paper is: Section 2 describes the Literature Review. Section 3 explains methodology of the research. Sections 4 to 7 illustrate the output and findings, classification and quality Assessment. Section 8 encompasses discussion, then finally conclusion in Section 9.

II. LITERATURE REVIEW

The current section emphasises on the studies which are very close to the research of this study.

Several factors of motivators in ASD are focused in [3]. They propose model of motivation of software Engineering (MOCC) in which different factors of software engineering is been identified. To proof his domain study they have done factors with respect to technical aspects. The primary fellow of agile give brief view of how agile can be implemented against

traditional software development [2]. Akhtar et al. [4] find the scrum critical factors in native software industry. As a result, the authors provide different recommendations to increase the productivity of software. Author in [5] has provided scrum adoption and implementation challenges in Pakistan due to its novice adoption in this area. In another study, [6] has focused on success factors of ASD. For this purpose they do a detail study of agile methods. The important contribution of Wagener is the division of the extracted elements in four classes, i.e., process, organizational, technical and people classes. An empirical study along with SLR has been conducted by [7] have on different agile projects. Regression analysis is used to evaluate result of 109 agile teams. Baddoo and Hall [8] describe the rewarding as most motivating factor. Another study on motivators and demotivators were conducted on software industry of Pakistan by [9]. To evaluate the literature regarding motivator and demotivator a systematic literature review is done. They propose an extension in hosted 5D's model by adding culture in it.

III. RESEARCH METHOD

A. Systematic Literature Review

It comprises of snowballing process for the assessment of relevant literature [10]. An evaluation process is used to accomplish the review. After that the output will describe the detailed list of motivators and demotivators, and classification and sub-classification of motivators and demotivators has been done.

B. Planning of Mapping

Current systematic literature review is done for the evaluation of the relevant data comprising motivator and demotivator of agile software development. The data exist in dispersed form and there is a need of complete literature review to collect all such distributed data.

C. Research Questions

There are three research questions of current research as shown in Table I.

D. Search Strings

The search strings used for the extraction of relevant studies are:

((({MOTIVATOR} OR {MOTIVATORS}) OR
{DEMOTIVATOR} OR {DEMOTIVATORS}) OR
{DEMOTIVATOR} OR {DEMOTIVATORS}) OR
{SUCCESS}) OR {BARRIER} OR {AGILE} OR {AGILE
SOFTWARE DEVELOPMENT} OR {ASD}

TABLE I. QUESTIONS OF THE RESEARCH

S. No.	RQs	Motivation
RQ.1	What are the motivator and demotivator factors in ASD?	It intended to provide a detailed list of motivators and demotivators of agile.
RQ.2	How could motivators and demotivators be mapped with common factors?	RQ2 aims to deliver the mapping of motivator factor into procedural, stakeholders, and firm's factors.
RQ.3	How could motivators and demotivators be sub-factorization?	RQ3 emphasizes on the sub-factorization.

E. Databases

We have targeted every search engine and find out maximum no research papers. Mostly papers are extracted by IEEE, ACM and Springer. Paper must publish in between 2000 to 2018.

F. Factor Mining

In order to elaborate the maximum number of motivators and demotivators factors, a selection procedure described in Table II is followed to find relevant papers according to string.

G. Selection of Primary Study

To select any paper title, abstract and conclusion has been explored. Those papers that have ambiguity and unclear objectives have been discarded.

1) Inclusion Criteria

Following points are examined to inclusion criteria:

- Must be published in Conference or Journal.
- Medium of language is English.
- Studies can solid accessible link.
- Paper must publish after 2000.

2) Exclusion Criteria

The exclusion criterion comprises of following points:

- "Tutorials", "slides", "editorials", "posters", keynotes and other non-peer reviews are excluded.
- Peer reviewed, but blog and books are not acceptable.
- Non-English language publications.
- All the studies which are unable to E-access.

H. Performing SLR

All the studies which have a solid background related to agile is been selected as shown in Table III. Conference and Journal papers are selected to give solid background. Selected primary studies are 39. However, the following papers are extracted which are most suitable against our research string.

I. Quality Assessment

Research papers having score in between 1 and 3 are been selected and those who have less than 1 are neglected (Table IV).

J. Selected Paper Description

All the research papers selected after applying the quality assessment criteria are summarized critically in Table V.

TABLE II. DOCUMENT SELECTION PROCEDURE

Step 1.1	Read all the title and abstract and extract relevant paper.
Step 1.2	Intro and conclusion based selection.
Step 1.3	Thoroughly read all the papers to remove any duplication in studies
Step 1.4	Quality Assessment form is made according to compile better result.

TABLE III. FILTRATION OF PAPERS

Databases	Papers	Title Filtration	Abstract Filtration	Selected	Ref.
IEEE Xplore	915	54	24	11	[11][12][13][14][15][16][17][18][19][20][21]
ACM Digital Library	37	17	10	03	[22][23][24]
Science Direct	36	15	07	03	[25][26][27]
Research Gate	32	25	10	06	[28][29][30][31][32][33]
Scopus	07	05	02	03	[7][34][35]
Springer	97	51	11	04	[36][37][38][39]
Google Scholar	300	90	35	05	[40][41][42][1][43]
Others	223	60	30	03	[44][45] [46]
Total	2422	381	226	38	

TABLE IV. QUALITY ASSESSMENT OF PAPERS

Sr. No	Paper	RQ # 1	RQ # 2	RQ #3	Total
1	[47]	0.5	1	0	1.5
2	[48]	0.5	0.5	0	1
3	[49]	0.5	0	0	0.5
4	[15]	1	0.5	0	1.5
5	[46]	0.5	0.5	0.5	1.5
6	[50]	0.5	1	0.5	2
7	[51]	0	0.5	0	0.5
8	[52]	0.5	0	0	0.5
9	[16]	1	0.5	0	1.5
10	[53]	0	0.5	0.5	1
11	[54]	1	1	0.5	2.5
12	[17]	1	1	0.5	2.5
13	[55]	1	0.5	1	2.5
14	[22]	1	0.5	0.5	2.5
15	[23]	1	1	0	2
16	[56]	1	0	0	1
17	[57]	1	1	0.5	2.5
18	[58]	1	1	0.5	2.5
19	[29]	1	0.5	1	2.5
20	[59]	0.5	0.5	0	1
21	[60]	1	1	1	3
22	[61]	0.5	0.5	0	1
23	[40]	1	1	0.5	2.5
24	[62]	1	1	0.5	2.5
25	[63]	1	0.5	0	1.5
26	[14]	0.5	0.5	0.5	1.5
27	[1]	1	0.5	0	1.5
28	[64]	1	0.5	1	2.5
29	[37]	1	1	0.5	2.5
30	[65]	1	0.5	0	1.5
31	[33]	1	1	1	3
32	[66]	0.5	0	0	0.5
33	[67]	1	0	0	1
34	[68]	0.5	0.5	0	1
35	[69]	1	0	0	1
36	[7]	1	1	0.5	2.5
37	[6]	1	0.5	0	1.5
38	[2]	0.5	0.5	0	1
39	[36]	1	0.5	0.5	2
40	[70]	0.5	0	0	0.5
41	[71]	1	1	0.5	2.5
42	[72]	0.5	0	0	0.5
43	[17]	1	0.5	0.5	2
44	[39]	1	1	0.5	2.5

45	[73]	0.5	0	0	0.5
46	[74]	0.5	0.5	0	1
47	[75]	0.5	0	0	0.5
48	[45]	1	1	0.5	2.5
49	[20]	1	1	0.5	2.5
50	[57]	1	0.5	0.5	2
51	[76]	1	0.5	0	1.5
52	[77]	1	1	0	2
53	[78]	1	0.5	0	1.5
54	[38]	1	1	0.5	2.5
55	[26]	1	1	0.5	2.5
56	[43]	1	1	1	3

TABLE V. DETAIL DESCRIPTION OF SELECTED PAPERS

Sr. No	Type: Conference/ Journal	Technique/ Empirical / Survey	Objectives	Results	Contribution	Limitation	Ref.
1	(CHASE) 2013 6th International Workshop	Empirical Analysis	To made a model to minimize software engineer workload	Proposed motivation factors of organization.	Complex interplay among motivational factor.	Systematic cross case analyses of the result is less reported	[47]
2	(CHASE), 2017 10th International Workshop	Statistical and thematic analysis	To identified three groups of factors motivating the self-assignment: task-based, developer-based, and opinion-based factors	Majority of the participants preferred self-assignment	Precedence to task-based and developer-based factors	Developers may deviate from their usual practice	[15]
3	(APSEC) 2012 19 th International conference	Regression model	To check the relationship between the software Project team features and team performance	Administration should pay more consideration within the project teams so that an improved strategy Presentation can be accomplished	The results demonstrated the association among project team features and presentation could be affected with players' inspiration.	The association among software project team features and its presentation is still to gauge.	[46]
4	(ESEM) 2011	Qualitative research	To Update Motivators factors of software Engineers	About the information It's good to work and going 'Man' is important, but this 'obstacle' is really soft The power of software engineers	'Work' (personal interest) You need a fix Screw out.	Focus on working to work Research on Psychological and Social Studies	[50]
5	(CESI) 2017 5 th IEEE/ ACM	An industry experiment with experienced programmers at the Universidad de las Fuerzas Armadas ESPE of Ecuador was performed	To Identify the circumstances that explain why some experimental subjects exhibit poor or null participation during experimental sessions.	Several experienced professionals were found to live a two, mixed-factors reality: old age and technological lapse.	A high percentage of older experienced programmers did not perform meaningful work in their task	Further research is required to better understand this phenomenon, which has several interesting ramifications.	[16]
6	Proceedings of EASE (2011)	This is based on the principles of specific guidance We copied the initial research program.	This work has been updated 2006 encouraged an encouraging result Software Engineering	Manual search and automatic search 6,534 collection 53 papers were selected for extracting figures And studying many solutions to solving excitement Despite quantities scenes and methods	In order to increase future research, research should be more focused on further deep research	Analyse the relationship between the motivation and the results, To provide more reliable results.	[54]
7	SBES 26th conference (2012)	Qualitative and Quantitative analysis	This article discusses how to practice XP Software	Ask for the advice of five adult X teams Consider whether this feature is the indicator	Got the XP team There is a proper process in our research to support	The XP situation is at odds with other motivational needs	[79]

			developers' excitement requirements.	The XP environment exists	many operations One developer needs to be encouraged Traditional Heavyweight Software Development The environment		
8	JSA (2016)	Semi-structured interview was held four times Use monthly rules to analyse data Program	To examine contextualized and the interpretation principle needs to be explained Different	We provide connection statement, Understanding Associate and Related Articles The main story of the company's motivation.	The need for learning and development is the most powerful driver Movement, which increases the turnout of turn Conditions for generating better performance for engineers.	Features of personality as personalities and personality Style, but elements can appear in future reports.	[80]
9	CHASE 2014 7th International Workshop	Statistical and thematic analysis	To compare the team's business-related results (productivity and quality) to two published sources of industry averages.	We identify four factors that potentially impact the outcome of industrial case studies: availability of data, tool support, cooperative personnel and project status. Recognizing and planning for these factors is essential to conducting industrial case studies	We discuss our experience in conducting this case study, including specifics of how data was collected, the rationale behind our process of data collection, and what obstacles were encountered during the case study.	The presence of CASE tools, including automated build tools, integration environments, and defect tracking systems, may alleviate much of the overhead associated with collecting these metrics.	[22]
10	ACM SIGSOFT (SEN) 2005	Quantitative method	Investigate the organization to investigate the impact of the customer developer's discussion	The nature of XP provides itself strong psychology Participants and their pressure have a positive effect Interaction and thus motivated	Creating a specific attitude of personal follow-up control, So in our case, motivate, and investigate Evaluating the main reasons for these behaviour Follow current social psychological ideas.	Their effect Customer and manufacturer interactions are not properly monitored And lower it	[23]
11	IST 2008	Qualitative analysis	To find Low requirements for low quality software Compressed timeline is born and the number is low.	This article will show two Successful industrial software projects are completely different Aspect; However, both of them still use abundant methods to solve social issues Factors	The thesis It will also provide lessons and tips Retro view reviews and observations.	Organization factors are also need to be address.	[81]
12	IST 2008	Systematic Literature review	Review a systematic movement of motion movement in software engineering. The purpose of this review How encourages developers and encourages developers and how to find current reporting knowledge The model encourages.	Our key It has come to know that the concern model released in software engineering is completely different and does not reflect the complex needs of the software. Engineers are in their professional stage, cultural and environmental settings.	Literature on the promotion of software engineering suggests controversial and local explanation in this field. Very clear Depending on the encouraging context and the engineer is different from the engineer.	Our survey results show that there is no clear understanding of the work of software engineers, how software engineers encourage them, and how they encourage them. Promote, or encourage the results and advantages of software engineer.	[82]
13	KMIS	Regression	To implement the	MPS	We will discuss the	The	[29]

	2009	analysis	filter method, possible scores of motivation	Affects positive work like work performance and development of system quality The project does not affect the duration of the project,	actual importance Based on this experience.	Reduction of job performance measurements The purpose and stability is because it is completely According to the theme's opinion	
14	5th Internationa (IRWITPM 2010)	Qualitative analysis	This research is a stimulus study to study using three investigative methods - daily daily, Enhanced and radical planning and initial reviews	The results show the practices of these two countries The team can contribute and motivate the excitement of the team One another	Research in areas of encouragement and development of angel's software development by identifying the auxiliary factors And on the promotion of angels'	Development teams of the Angels, the ban is related to the formation of the team. Even trouble The procedure in a team is only implemented recently. Both teams are well-established and familiar	[60]
15	KAU (2013), Karlstad Business School.	Systematic Literature Review	Determine the importance and encouragement of the report Participants use partial methods in project participants	A list of research paper on project management has been reported.	There exist a detail list of motivator and demotivator from Systematic literature review with respect to project management.	The ability to study is limited to harmony journal arts. Initial examination search Some databases, including conference papers, made a large number of results.	[83]
16	Management Prudence Journal (2010)	Statistical analysis	The impact of job conversions is even more pronounced. This area is relatively new Lack of value and encouragement for her caravan.	Compared with the low Protestant Ec Group, the High Group encourages high interviews, which means that there is a high interest in high technology, more interest/enjoyment, qualifications, choice of choice, but pressure/stress is lower than the low outlook job.	Having chosen it will receive the highest level of encouragement, which will have an effective impact on their profession.	Work value training should be part of the plan, which will help improve the performance of new jobs.	[41]
17	PROFES 2014	Qualitative analysis	Investigates our research factors that lead to software testing professionals Work, choice and stay in the duties and customs practices	This career path can help the results During the recruitment process the company runs on a traditionally transit Encouraged entrepreneurs encourage internal and their examinations, which will improve Job satisfaction and productivity.	We provide a series of factors that have negative and positive effects on daily life. Software tester activities and other types have been included Software published in the field of engineering and published.	Our research plan presents this study into further content Besides checking the company and exam properties and more Relationship with colleagues	[84]
18	38th Euromicro Conference (SEAA) 2012	Systematic literature review	Our research What is motivated is designed to better understand Software developers in imagination environments.	Our research results show that in spite of trouble The background and motivation overall approach is slightly different In general software development.	We have done three cases The fireplace company to confirm our results and to collect new information	To increase confidence factors, we use it very well Created in established investigative methods and early dates By orientation with organizational culture Early visit	[3]
19	SJIS 2011	Qualitative analysis	It is an investigation study of the Swedish and Irish IT Project Team Investigate the three duties, will stand daily	The results of both cases show that in germinating methods can occur The team encourages	Encourages the team to encourage and contribute significantly to the field of floor project management. Identifying the factors that help in	Project team study is limited Because only two APM teams have been examined. There are two teams Get acquainted and familiar with each other.	[85]

			Planning and revised reviews can motivate or encourage harm in an active team.		encouraging IT and prevent IT		
20	SPI 2006	Qualitative Analysis	Especially how to encourage the development to influence growth Work in software engineering.	Our main result is that good software developers Active, flexible and applicable to share and follow knowledge with the team Exercises, such as recording work.	We found According to technical capabilities, mutual expertise and good practices, compliance with all positive effects are related About the success of software projects..	Looking at the current trend Software development, which will be helpful Compare the results of this study with the same study In a delicate environment	[64]
21	APSEEP 2007	Qualitative analysis	This study finds different aspects of team planning Attached, positively related to psychological events Traditional management, out of the era of organization And software engineering research.	Results include profound understanding Relationships between responsibilities and active team results, such as Motivation and harmony.	Looks very strong Add operations and effects	A deeper knowledge of socio knowledge is still need to explore.	[86]
22	In Proceedings of 15th international conference, XP(2014)	Qualitative analysis	Several case design issues have been introduced In three different instant software organizations.	We lie The organization created a culture that supports communication and discussion There is less agility than alternative two organizations to design decisions.	Our theory is that Gulf Environment generates more open communication among developers, which can lead developers to challenge each other's design solutions and to enhance their likeness accordingly.	Review the effect of long-term experimental study design decisions.	[87]
23	Agile Times 2004	Qualitative analysis	This research is contribution towards motivator factor of agile software development to increase the productivity and morale.	Their role in the use of processes and equipment that influence	The most important elements of processing and encouragement is still very important because they are accustomed to it. Focus on all repetitive tasks and focus on what developers are really focused on: the need for things Customers through the production of valuable software	Motivators should also be find against the Non-functional requirements.	[33]
24	Journal of Systems and Software 2008	Statistical analysis	Afterwards, an analysis of reliability and elemental analysis was performed in the initial list to reinforce the 12 potential key endpoint sets. The type of success for each of the four projects - quality factors, scope, time, and success	The results showed that only 10 of the 48 governors were supported and identified the three major success factors of the fire. Software development projects: (a) delivery strategy, (b) Elevail software engineering technology, and (c) team capabilities.	The main part of this study is to obtain the key success factors of the three factors in this incident. According to survey data analysis.	To ensure the success of their project, managers To focus on high-quality team teams, follow the ferrous metal process technology and the above delivery strategies.	[7]

			factors for each cost.				
25	PHD Thesis 2012	Qualitative and Quantitative analysis	This study has investigated the factors of major success involved in the pilot system Development plans of different system development methods and projects Tracking their basic principles and benefits to management practices	And the weaknesses show their results that actually are 16 Key-success factors that have directly impacted the financial system success Development project	Institutions should encourage these important successes The effect of implementing ASDM when this project has a positive impact	Findings of major success factors in the responsibilities system Extensive development projects, including the largest number Project	[6]
26	(XP 2007)	Qualitative analysis	Autonomy, multiple factors, The importance of completing the importance, opinion, and completion of work is very important Ensure factors of satisfaction and encouragement among workers.	Maintain software agility With the development of software and developer team development, it is slowly increasing Like biology, both of them are constantly considering management Business value and encouragement questions about motivation and decision-making Change our independence, variety	The importance of completing the entire mission, opinions and abilities are essential In this project.	A Quantitative analysis is needed to find in-depth results.	[36]
27	IEEE Software (Volume: 28, Issue: 4, July-Aug. 2011)	Qualitative analysis	They apply the angels' implementation in an advanced form In cross organizations or at least business entities.	It is difficult to measure all the methods According to respondents, steps taken in at least one organization have been taken: In every case.	They found out different challenges from literature and give recommendation accordingly.	Some concerns were considered by institutes, people, technical and process is need to explore.	[18]
28	Proceedings - IEEE AGILE 2007	Qualitative analysis	Five adult team consultations Consider whether this feature is the indicator The XP environment exists.	We found that the XP Team has entered There is a proper process in our research to support many operations One developer needs to be encouraged Traditional Heavyweight Software Development The environment	In our research, five XT teams are already under process Supports many encouraging needs Traditional, Heavy Weight software development environment.	The XP environment is contrary to it Other motivation is needed	[17]
29	(XP 2006) 7 th international Conference	Statistical analysis	How and how to increase employee satisfaction with the development process Identify widely used teams and employee satisfaction Area and staff.	This one The three most powerful relationships have the ability to influence decisions Affect people and add interesting items	How much trouble does the team member have with the user/customer twice? His job satisfaction (compared to non-dynamic teams).	Analyse perceived desirability of movement and work stress.	[39]
30	Crosstalk Technology 2004	Qualitative analysis	Identify potential risks, problems and strategies Help your project	Learn More efficient through service methods Development and	Emotionally emotional emotions often appear Cause of basic	Agent does not violate effective project management, but what happens in practice	[45]

			and organization succeed.	communication measurement technology.	damage Communication.	Not all project management provides Need to be successful.	
31	IEEE Software 2005	Qualitative analysis	Identify screenshots instead of technology and some of the obstacles to dynamic the traditional approach.	Learning lessons can help more Enhances high speed integration Disadvantaged methods and methods and experiences across the organization	And the entire community's data is important for the return on investment verification and integration activities.	Research There are many areas where new methods and uniforms need to be provided.	[20]
32	Computer 2001	Qualitative analysis	Exploratory problem areas are extremely, complex, highly variable	The project's ability to work, cooperates and works best on people Culture.	Detailed discussion of factor that influence agile with people, organization and technical.	Systematic literature review is needed to gauge more factors influencing Agile	[21]
33	International Journal of Quality & Reliability Management 2012	Systematic literature review	Researchers need to investigate trust, confidentiality, and security issues associated with them ASD.	Concepts and principles ASD, history and evolution, and criticism of different users Software development community	Generic view of ASD is briefly described.	Researchers also want to deal with success factors and make necessary changes Challenges in adjusting ASD in Outsourcing / Outside Sensing	[76]
34	DOI 2015	Qualitative analysis	What separates successful agility?	Software Project and Minimum Team Successful and busy team and team leader Follow different strategies. They - obviously or (rarely) are obviously intentional Software development is a multi-domain Take questions and related tasks.	When different people or groups People are involved and we are generally dealing with complex (adaptive) systems.	There is no "perfect size" According to procedures and actions, the problem lies in this issue.	[28]
35	CROSSTALK The Journal of Defence Software Engineering 2004	Qualitative analysis	To provide awareness about risk management and to provide a vision for developing the appropriate risk management strategy	, we identified six risks. The potential factors according to our experience There is also a significant impact on success Software programs and projects failed.	By following these points, you can reduce the possibility of a program or project failure.	This article does not intend to provide a complete list of risk factors for a specific program / project - it requires more Space.	[44]
36	XP 2002	Qualitative analysis	To support the selection of the procedure Experience based on submitting and analysing the applicable methods And get background experience.	This experience is once again Ability to support and guide future projects to select the most appropriate assets Hand job	Carefully check and challenge future plans and when they maintain the environment When they should not be caught	A detail cross talk is needed to explore more challenges that effect Agile.	[38]
37	IJPOM 2012	Statistical analysis	We have an integrated development idea The model affects the project manager's encouragement, "Movement Factor Inventory" (MFI).	A clear, interesting task is working with a supportive and objective based team to get the necessary information The possibility of influencing financial and human resources and important decisions	The Governments can positively influence the encouragement of project managers.	Future These important issues related to research need to be solved Personal, situations and active variables Project Manager encourages	[26]

				has been identified as the most important concern Project Manager working in Switzerland			
38	(IJACSA) 2017	Qualitative analysis	To find the detailed list of motivator and demotivator factors	Detailed list of motivators and demotivators is elaborated and classified into people technical and organization factors.	Providing an categorization of motivators with respect to people, organization and technical and sub-categorization accordingly.	There is need of model of motivators for ASD.	[43]

IV. MOTIVATORS AND DEMOTIVATORS IN RQ1

In order to answer the RQ 1, SLR was done by which detailed list of motivator and demotivator has been extracted and list in Table VI.

A. Common DeMotivators Mined from SLR

Specific collective demotivators mined from SLR are presented in Table VII.

TABLE VI. COMMON MOTIVATORS EXTRACTED FROM SELECTED PAPERS

Sr. No	Motivator Factors	No. of Existing Studies
1	High quality Performance	[9][79]
2	Adherence to budget	[79] [57] [72] [4] [6] [88] [82] [9] [19]
3	Identify work balance	[6]
4	Personal interest	[82] [9] [19]
5	Quality work	[7]
6	Follow process life cycle	[32] [82] [9] [19]
7	Feasibility studies	[82] [9]
8	Recognition of good work	[82] [19]
9	Teamwork	[32] [82] [9] [19]
10	Task Identification	[82]
11	Clear domain knowledge	[82] [9] [19]
12	Reduced work repetition	[82]
13	Rapid Feedback	[32] [2] [8] [82] [9] [19]
14	Change interaction	[32] [82] [19] [33]
15	Autonomy	[4] [8] [82] [9] [19]
16	Follow rules and regulations	[33][89]
17	Tolerance to work	[6] [88] [82] [9]
18	Intime and accurate	[82] [19]
19	Rapid communication	[32] [82] [19] [79]
20	Training	[82] [9]
21	Minimize risk	[82] [9] [19]
22	Simple code/ Simplicity	[90]
23	Cooperative organization culture	[8]
24	Face to face communication	[4] [8]
25	Expertise of team members	[6] [8]

TABLE VII. COMMON DEMOTIVATORS EXTRACTED FROM SELECTED PAPERS

Sr. No	Demotivators factors	No. Of existing studies
1	Work location	[4][82] [19] [79] [91]
2	Low Incentives	[6] [7] [82] [9]
3	Large documentation	[82] [9] [19]
4	Uncertain working environment	[82]
5	Change in prioritization	[82] [19]
6	Poor commitment	[8] [92]
7	Low sense of ownership	[82] [9] [19]
8	Less resources	[9]
9	Lack of executive sponsorship	[82] [9] [19]
10	Lack of agile logistic	[82] [9] [19]
11	Lack of necessary skills set	[9]
12	Poorly defined scope	[9] [19]
13	Lack of project tracking mechanism	[4] [82] [9] [19]
14	Partially following Agile practices	[9]

V. CATEGORIZATION OF MOTIVATORS AND DEMOTIVATORS (RQ2)

We have classified motivators and demotivators factors into procedural, stakeholders and firm’s factors as shown in Fig. 1. Following figure shows the general motivators and their classification in which organization of general factors include customer oriented, judgment based, team dissemination and scope, overall culture and organization and mechanism. Stakeholders technical features includes ability, individual features, announcement and conciliation, civilization culture and keeping fit and knowledge while procedural features include individual features, inherent, extrinsic and some overall aspects.

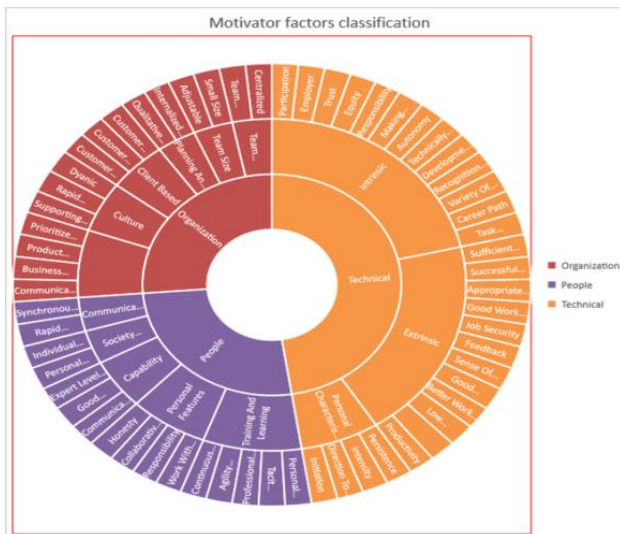


Fig. 1. Classification of motivators.

Classification of demotivators has also been performed to find more precise results (Fig. 2). In organization, the most common factors are: unclear requirement, scope and kind of modification, deadlines, early decision making, current political situation, low productivity, lack of face to face communication, large team size, informal communication,

trusting people, tool process, nature of organization. In people factor, less domain experience, critical communication, time zone, native culture, geographical condition and linguistic difficulty are evaluated.

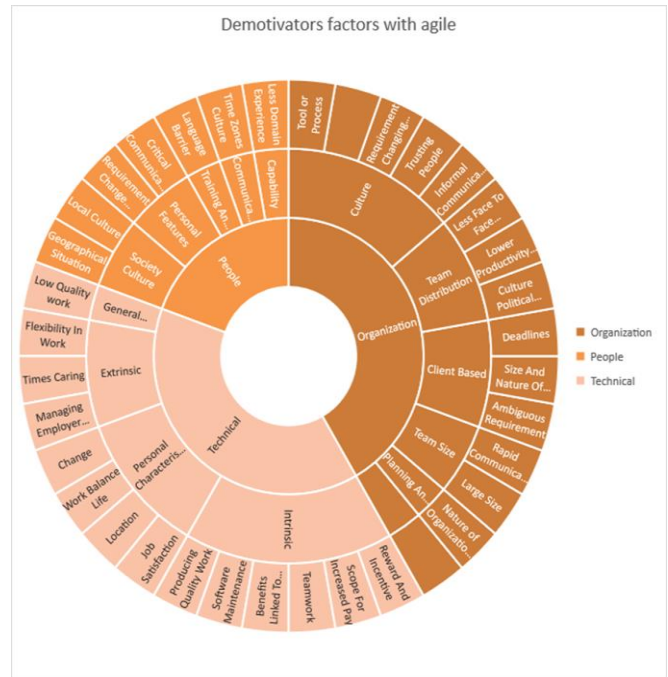


Fig. 2. Classification of demotivator factors.

VI. FACTORIZATION OF MOTIVATORS (RQ3)

This section addresses the answer of RQ3. Subcategorization was done on motivators (Fig. 3). We have done categorization of motivating factors such as diversity of effort which was categorized as individual and marketplace desires. Considering the sense of belonging aspects are categorised as intrinsic and extrinsic. Recognition of work can be classified as reward and incentive. In employee participation individual and team participation are core motivating factors while clear identification with task has motivating factors such as clear goals and stick with plans.

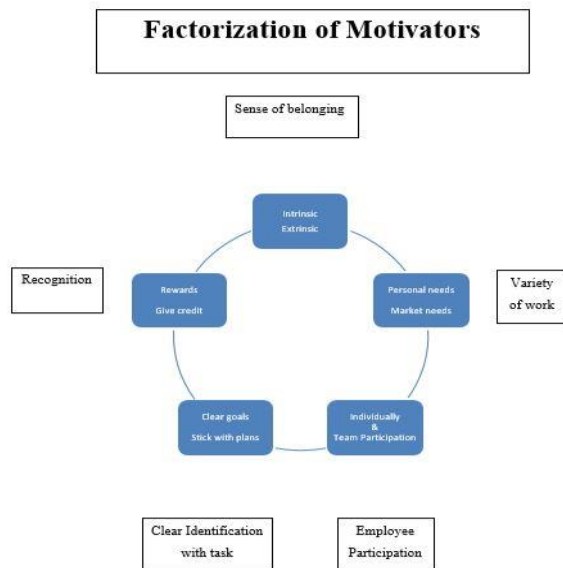


Fig. 3. Factorization of motivator factors.

VII. THREAT TO VALIDITY

There are three systematic steps for threat to validity perspectives.

A. Primary Studies Risk Identification

The motivation is the core domain to motivate someone to enhance their capability that is why it is a tuff task to separate concept of motivation accordingly. For this purpose we have selected the word software to differentiate the concept of motivator from other domains.

B. Threats to Selection and Consistency

Due to selection of research question from the domain of agile their might be possibility of containing magazine contributions and thesis because the data exist in dispersed form.

C. Threats to Data Fusion and Results

This result is evaluated against given string. If a keyword is added or remove against string it might be better filtering result. This snowballing process is to explore what has been done in the field of motivator in ASD.

VIII. DISCUSSION

Current research focused a systematic literature review of motivator and demotivator factor of ASD. For this purpose we have explore against the string and evaluate the result accordingly. The detailed list of motivator and demotivator has been evaluated and classification of motivator and demotivator has done on organization, people and technical level. Then these levels are explored more against general factors, such as client based, decision time, team distribution, team size, general culture, planning and controlling, capability to do work, personal feature, training and learning and intrinsic and extrinsic.

IX. CONCLUSION

This systematic literature describes the synthesis of data available on success and barrier of Agile software development. These success and barrier are also referred as motivator and demotivator factors. For this purpose we have provided a detailed list of motivators and demotivators. Classification is also been performed on the basis of people, technical and organization perspective to give comprehensive detail accordingly. A Quality Assessment has been performed to find the best possible paper according to string. Brief introduction of selected papers has also been described. Along with this, the sub categorization has also been performed to find more brief detail of motivator and demotivator factors. The plan behind this research is described and keywords that support are also been discussed. Literature lacks the open question on challenge and motivator factor of agile software development.

X. FUTURE WORK

In future we will do empirical analysis on motivator and demotivator of Agile Software Development to find more accurate results. Further plans are to provide a demotivation effect model for Agile practitioners which will be helpful in increasing productivity.

REFERENCES

- [1] O. McHugh, K. Conboy, and M. Lang, "Using Agile Practices to Influence Motivation within IT Project Teams," *Scand. J. Inf. Syst. (Special Issue IT Proj. Manag., vol. 23, p. pp 85-110, 2011.*
- [2] J. Highsmith and A. Cockburn, "Agile Software Development: The Business of Innovation," *Science (80-.), vol. 34, no. 9, pp. 120-123, 2001.*
- [3] C. De O. Melo, C. Santana, and F. Kon, "Developers motivation in agile teams," *Proc. - 38th EUROMICRO Conf. Softw. Eng. Adv. Appl. SEAA 2012, no. March 2015, pp. 376-383, 2012.*
- [4] M. J. Akhtar, A. Ahsan, and W. Z. Sadiq, "Scrum adoption, acceptance and implementation (A case study of Barriers in Pakistan's IT Industry and Mandatory Improvements)," *Proc. - 2010 IEEE 17th Int. Conf. Ind. Eng. Eng. Manag. IE EM2010, pp. 458-461, 2010.*
- [5] Colleen Frye, "Agile by the numbers: Survey finds more adoption, but age-old problems." [Online]. Available: <http://searchsoftwarequality.techtarget.com/news/1372395/Agile-by-the-numbers-Survey-finds-more-adoption-but-age-old-problems>. [Accessed: 24-Jul-2017].
- [6] R. P. Wagener, "Investigating critical success factors in agile systems development projects/Ruhan Wagener," no. November, 2012.
- [7] T. Chow and D.-B. Cao, "A survey study of critical success factors in agile software projects," *J. Syst. Softw., vol. 81, no. 6, pp. 961-971, 2008.*
- [8] N. Baddoo and T. Hall, "Motivators of Software Process Improvement: An analysis of practitioners' views," *J. Syst. Softw., vol. 62, no. 2, pp. 85-96, 2002.*
- [9] Maryam, R., Naseem, A., Haseeb, J., Hameed, K., Tayyab, M., & Shahzaad, B. (2017). Introducing Time based Competitive Advantage in IT Sector with Simulation. *International Journal Of Advanced Computer Science And Applications, 8(7), 401-406.*
- [10] K. Petersen, R. Feldt, S. Mujtaba, and M. Mattsson, "Systematic Mapping Studies in Software Engineering," *12Th Int. Conf. Eval. Assess. Softw. Eng., vol. 17, p. 10, 2008.*
- [11] R. Sach, H. Sharp, and M. Petre, "Software Engineers' Perceptions of Factors in Motivation: The Work, People, Obstacles," *2011 Int. Symp. Empir. Softw. Eng. Meas., pp. 368-371, 2011.*

- [12] A. C. C. Franca, D. E. S. Carneiro, and F. Q. B. da Silva, "Towards an Explanatory Theory of Motivation in Software Engineering: A Qualitative Case Study of a Small Software Company," 2012 26th Brazilian Symp. Softw. Eng., pp. 61–70, 2012.
- [13] P. C. Chen, C. C. Chern, and C. Y. Chen, "Software project team characteristics and team performance: Team motivation as a moderator," in Proceedings - Asia-Pacific Software Engineering Conference, APSEC, 2012, vol. 1, pp. 565–570.
- [14] C. de O. Melo, C. Santana, and F. Kon, "Developers Motivation in Agile Teams," in 2012 38th Euromicro Conference on Software Engineering and Advanced Applications, 2012, pp. 376–383.
- [15] Z. Masood, R. Hoda, and K. Blincoe, "Motivation for Self-Assignment: Factors Agile Software Developers Consider," in 2017 IEEE/ACM 10th International Workshop on Cooperative and Human Aspects of Software Engineering (CHASE), 2017, pp. 92–93.
- [16] O. Dieste, E. R. Fonseca C., G. Raura, and P. Rodriguez, "Professionals Are Not Superman: Failures beyond Motivation in Software Experiments," in 2017 IEEE/ACM 5th International Workshop on Conducting Empirical Studies in Industry (CESI), 2017, pp. 27–32.
- [17] S. Beecham, H. Sharp, N. Baddoo, T. Hall, and H. Robinson, "Does the XP environment meet the motivational needs of the software developer? An empirical study," in AGILE 2007 (AGILE 2007), 2007, pp. 37–49.
- [18] K. Conboy and S. Coyle, "People over Process : Key Challenges in Agile Development," IEEE Softw., vol. 28, no. 4, pp. 48–57, 2011.
- [19] A. C. C. Franca, T. B. Gouveia, P. C. F. Santos, C. A. Santana, and F. Q. B. da Silva, "Motivation in software engineering: A systematic review update," 15th Annu. Conf. Eval. Assess. Softw. Eng. (EASE 2011), pp. 154–163, 2011.
- [20] B. Boehm and R. Turner, "Management challenges to implementing agile processes in traditional development organizations," IEEE Softw., vol. 22, no. 5, pp. 30–39, 2005.
- [21] A. Cockburn and J. Highsmith, "Agile software development: The people factor," Computer (Long Beach, Calif.), vol. 34, no. 11, pp. 131–133, 2001.
- [22] L. Layman, L. Williams, and L. Cunningham, "Motivations and measurements in an agile case study," J. Syst. Archit., vol. 52, no. 11, pp. 654–667, 2006.
- [23] D. Woit and K. Bell, "Do XP customer-developer interactions impact motivation? findings from an industrial case study," Proc. 7th Int. Work. Coop. Hum. Asp. Softw. Eng. - CHASE 2014, pp. 79–86, 2014.
- [24] A. Law and R. Charron, "Effects of agile practices on social factors," ACM SIGSOFT Softw. Eng. Notes, vol. 30, no. 4, p. 1, 2005.
- [25] A. Deak, A Comparative Study of Testers' Motivation in Traditional and Agile Software Development. 2014.
- [26] S. Seiler, B. Lent, M. Pinkowska, and M. Pinazza, "An integrated model of factors influencing project managers' motivation - Findings from a Swiss Survey," Int. J. Proj. Manag., vol. 30, no. 1, pp. 60–72, 2012.
- [27] S. Beecham, N. Baddoo, T. Hall, H. Robinson, and H. Sharp, "Motivation in Software Engineering: A systematic literature review," Information and Software Technology, vol. 50, no. 9–10, pp. 860–878, 2008.
- [28] M. Kropp and A. Meier, "Agile Success Factors A qualitative study about what makes agile projects successful," no. May 2015, 2015.
- [29] S. Kim, S. Hwang, and S. Song, "An Empirical Analysis on the Effects of Agile practices on Motivation and Work Performance of Software Developers," pp. 1–16, 2009.
- [30] S. Misra, V. Kumar, U. Kumar, K. Fantasy, and M. Akhter, "Agile software development practices: evolution, principles, and criticisms," Int. J. Qual. Reliab. Manag., vol. 29, no. 9, pp. 972–980, 2012.
- [31] A. Baird and F. J. Riggins, "Planning and Sprinting: Use of a Hybrid Project Management Methodology within a CIS Capstone Course," J. Inf. Syst. Educ., vol. 23, no. 3, pp. 243–257, 2012.
- [32] O. Mchugh, K. Conoby, and M. Lang, "Motivating agile teams: A case study of teams in ireland and sweden," in 5th International Research Workshop on Information Technology Project Management (IRWITPM 2010), 2010, pp. 71–83.
- [33] G. Asproni, "Motivation, Teamwork, and Agile Development," Agil. Times, vol. 4, no. 1, pp. 8–15, 2004.
- [34] A. C. Nelson and C. LeRouge, "Self-esteem: Moderator between role stress fit and satisfaction and commitment?," Proc. ACM SIGCPR Conf., pp. 74–77, 2001.
- [35] M. Ilyas and S. U. Khan, "Software integration in global software development: Success factors for GSD vendors," 2015 IEEE/ACIS 16th Int. Conf. Softw. Eng. Artif. Intell. Netw. Parallel/Distributed Comput. SNPD 2015 - Proc., 2015.
- [36] B. Tessem and F. Maurer, "Job Satisfaction and Motivation in a Large Agile Team," Lncs, vol. 4536, no. 5020, pp. 54–61, 2007.
- [37] E. Whitworth and R. Biddle, "Motivation and Cohesion in Agile Teams," Agil. Process. Softw. Eng. Extrem. Program., pp. 62–69, 2007.
- [38] M. Lindvall et al., "Empirical Findings in Agile Methods," Proc. Extrem. Program. Agil. Methods, XP/Agile Universe 2002, pp. 197–207, 2002.
- [39] G. Melnik and F. Maurer, "Comparative analysis of job satisfaction in agile and non-agile software development teams," in XP'06 Proceedings of the 7th international conference on Extreme Programming and Agile Processes in Software Engineering, 2006, pp. 32–42.
- [40] T. Jansson, "Motivation theory in research on agile project management : A systematic literature review," 2013.
- [41] D. V. Nithyanandan, "Work value as motivation among software professionals," Manag. Prudence J., vol. 1, no. 1, pp. 23–27, 2010.
- [42] D. Hutchison and J. C. Mitchell, Agile Processes in Software Engineering and Extreme Programming. 1973.
- [43] S. Ahmed, K. Ghayyur, S. Ahmed, and A. Razzaq, "Motivators and Demotivators of Agile Software Development : Elicitation and Analysis," vol. 8, no. 12, pp. 304–314, 2017.
- [44] A. Cockburn et al., "Advanced Software Technologies for Protecting America."
- [45] P. E. McMahon, "Bridging agile and traditional development methods: A project management perspective," CrossTalk, no. 5, pp. 16–20, 2004.
- [46] P.-C. Chen, C.-C. Chern, and C.-Y. Chen, "Software Project Team Characteristics and Team Performance: Team Motivation as a Moderator," in 2012 19th Asia-Pacific Software Engineering Conference, 2012, pp. 565–570.
- [47] A. C. C. Franca, A. C. M. L. de Araujo, and F. Q. B. da Silva, "Motivation of software engineers: A qualitative case study of a research and development organisation," in 2013 6th International Workshop on Cooperative and Human Aspects of Software Engineering (CHASE), 2013, pp. 9–16.
- [48] I. de Farias, N. G. de Sa Leitao, and H. P. de Moura, "An empirical study of motivational factors for distributed software development teams," in 2017 12th Iberian Conference on Information Systems and Technologies (CISTI), 2017, pp. 1–6.
- [49] A. César, C. Franca, A. de L C Felix, and F. Q. B. da Silva, "Towards an explanatory theory of motivation in software engineering: a qualitative case study of a government organization," in 16th International Conference on Evaluation & Assessment in Software Engineering (EASE 2012), 2012, pp. 72–81.
- [50] R. Sach, H. Sharp, and M. Petre, "Software Engineers' Perceptions of Factors in Motivation: The Work, People, Obstacles," in 2011 International Symposium on Empirical Software Engineering and Measurement, 2011, pp. 368–371.
- [51] S. U. Gardazi, H. Khan, S. F. Gardazi, and A. A. Shahid, "Motivation in software architecture and software project management," in 2009 International Conference on Emerging Technologies, 2009, pp. 403–409.
- [52] A. Alali and J. Sillito, "Motivations for collaboration in software design decision making," in 2013 6th International Workshop on Cooperative and Human Aspects of Software Engineering (CHASE), 2013, pp. 129–132.
- [53] T. Chintakovid, "Factors Affecting End Users' Intrinsic Motivation to Use Software," in IEEE Symposium on Visual Languages and Human-Centric Computing (VL/HCC 2007), 2007, pp. 252–253.
- [54] A. C. C. Franca, T. B. Gouveia, P. C. F. Santos, C. A. Santana, and F. Q. B. da Silva, "Motivation in software engineering: a systematic review update," in 15th Annual Conference on Evaluation & Assessment in Software Engineering (EASE 2011), 2011, pp. 154–163.
- [55] A. C. C. Franca, D. E. S. Carneiro, and F. Q. B. da Silva, "Towards an Explanatory Theory of Motivation in Software Engineering: A

- Qualitative Case Study of a Small Software Company,” in 2012 26th Brazilian Symposium on Software Engineering, 2012, pp. 61–70.
- [56] J. Noll, M. A. Razzak, and S. Beecham, “Motivation and Autonomy in Global Software Development,” in Proceedings of the 21st International Conference on Evaluation and Assessment in Software Engineering - EASE'17, 2017, pp. 394–399.
- [57] A. Law and R. Charron, “Effects of agile practices on social factors,” ACM SIGSOFT Softw. Eng. Notes, vol. 30, p. 1, 2005.
- [58] A. César, C. França, and F. Q. B. Da Silva, “Towards Understanding Motivation in Software Engineering.”
- [59] E. Asan and S. Bilgen, “Agile Collaborative Systems Engineering - Motivation for a Novel Approach to Systems Engineering,” INCOSE Int. Symp., vol. 22, no. 1, pp. 1746–1760, Jul. 2012.
- [60] O. Mchugh, K. Conoby, and M. Lang, “Motivating agile teams: A case study of teams in ireland and sweden,” in 5th International Research Workshop on Information Technology Project Management (IRWITPM 2010), 2010, vol. 8, pp. 71–83.
- [61] a Fernando, “The Impact of Job Design and Motivation on Employee Productivity as Applicable in the Context of Sri Lankan Software Engineers : A HR Perspective,” A HR Perspect., vol. 6, no. 2, pp. 67–78, 2008.
- [62] D. V Nithyanandan, “WORK VALUE AS MOTIVATION AMONG SOFTWARE PROFESSIONALS.”
- [63] A. Deak, “A Comparative Study of Testers’ Motivation in Traditional and Agile Software Development,” Springer, Cham, 2014, pp. 1–16.
- [64] N. Baddoo, T. Hall, and D. Jagielska, “Software developer motivation in a high maturity company: a case study,” Softw. Process Improv. Pract., vol. 11, no. 3, pp. 219–228, May 2006.
- [65] G. Concas, E. Damiani, M. Scotto, and G. Succi, Eds., Agile Processes in Software Engineering and Extreme Programming, vol. 4536. Berlin, Heidelberg: Springer Berlin Heidelberg, 2007.
- [66] A. Elssamadisy and D. West, “Adopting agile practices: an incipient pattern language,” p. 1:1–1:9, 2006.
- [67] K. Schwaber, Agile Software Development with Scrum. Prentice Hall, 2004.
- [68] C. Hansson, Y. Dittrich, B. Gustafsson, and S. Zarnak, “How agile are industrial software development practices?,” J. Syst. Softw., vol. 79, no. 9, pp. 1295–1311, Sep. 2006.
- [69] D. J. Anderson, Agile Management for Software Engineering: Applying the Theory of Constraints for Business Results. Prentice Hall Professional Technical Reference, 2004.
- [70] C. H. Becker, “Using eXtreme Programming in a Student Environment,” no. December, p. 135, 2010.
- [71] K. Conboy, S. Coyle, X. Wang, and M. Pikkarainen, “People over process: Key challenges in agile development,” IEEE Softw., vol. 28, no. 4, pp. 48–57, 2011.
- [72] E. Programming, “Assessing XP at a European Internet Company,” pp. 37–43, 2003.
- [73] “Towards Understanding of Software Engineer Motivation in Globally Distributed Projects Research proposal,” pp. 9–11.
- [74] Everette R Keith -, “Agile Software Development Processes A Different Approach to Software Design.”
- [75] J. Drobka, D. Nofzt, and Rekha Raghu, “Piloting XP on four mission-critical projects,” IEEE Softw., vol. 21, no. 6, pp. 70–75, Nov. 2004.
- [76] S. Misra, V. Kumar, U. Kumar, K. Fantasy, and M. Akhter, “Agile software development practices: evolution, principles, and criticisms,” Int. J. Qual. Reliab. Manag., vol. 29, no. 9, pp. 972–980, Oct. 2012.
- [77] M. Kropp and A. Meier, “Agile Success Factors - A qualitative study about what makes agile projects successful,” Jan. 2015.
- [78] T. D. LaToza and A. van der Hoek, “Crowdsourcing in Software Engineering: Models, Motivations, and Challenges,” IEEE Softw., vol. 33, no. 1, pp. 74–80, Jan. 2016.
- [79] S. Beecham, H. Sharp, N. Baddoo, T. Hall, and H. Robinson, “Does the XP environment meet the motivational needs of the software developer? An empirical study,” in Proceedings - AGILE 2007, 2007, pp. 37–48.
- [80] A. C. C. Franca, D. E. S. Carneiro, and F. Q. B. da Silva, “Towards an Explanatory Theory of Motivation in Software Engineering: A Qualitative Case Study of a Small Software Company,” in 2012 26th Brazilian Symposium on Software Engineering, 2012, pp. 61–70.
- [81] A. Law, R. Charron, A. Law, and R. Charron, “Effects of agile practices on social factors,” in Proceedings of the 2005 workshop on Human and social factors of software engineering - HSSE '05, 2005, vol. 30, no. 4, pp. 1–5.
- [82] S. Beecham, N. Baddoo, T. Hall, and H. Robinson, “Protocol for a Systematic Literature Review of Motivation in Software Engineering Systematic Review – Cover Sheet,” Computer (Long. Beach. Calif.), no. September, p. 87, 2006.
- [83] T. Jansson, “Motivation theory in research on agile project management : A systematic literature review,” 2013.
- [84] A. Deak, “A Comparative Study of Testers’ Motivation in Traditional and Agile Software Development,” Springer, Cham, 2014, pp. 1–16.
- [85] O. Mchugh, K. Conboy, and M. Lang, “Using Agile Practices to Influence Motivation within IT Project Teams Using Agile Practices to Influence Motivation,” Scand. J. Inf. Syst., vol. 23, no. 2, pp. 1–26, 2011.
- [86] E. Whitworth and R. Biddle, “Motivation and Cohesion in Agile Teams,” in Agile Processes in Software Engineering and Extreme Programming, Berlin, Heidelberg: Springer Berlin Heidelberg, 2007, pp. 62–69.
- [87] M. Dall’Agnol, A. Sillitti, and G. Succi, “Empirical Analysis on the Satisfaction of IT Employees Comparing XP Practices with Other Software Development Methodologies,” Extrem. Program. Agil. Process. Softw. Eng. Proc., vol. 3092, no. June 2014, pp. 223–226, 2004.
- [88] H. M. Huisman and J. Iivari, “Systems development methodology use in South Africa,” Proc. 9th Am. Conf. Inf. Syst., pp. 1040–1052, 2003.
- [89] C. H. Becker, “Using Extreme Programming in a Maintenance Environment,” no. December, p. 135, 2010.
- [90] Martin Fowler, “Writing The Agile Manifesto.” [Online]. Available: <https://martinfowler.com/articles/agileStory.html>. [Accessed: 30-May-2017].
- [91] Ghayyur, S. A. K., Ahmed, S., Naseem, A., & Razaq, A. (2017). Motivators and Demotivators of Agile Software Development: Elicitation and Analysis. International Journal Of Advanced Computer Science And Applications, 8(12), 304-314.
- [92] I. Asghar and M. Usman, “Motivational and de-motivational factors for software engineers: An empirical investigation,” Proc. - 11th Int. Conf. Front. Inf. Technol. FIT 2013, pp. 66–71, 2013.

Standardization of Cloud Security using Mamdani Fuzzifier

Shan e Zahra

Department of Computer Science
Faculty of Information Technology
Lahore Garrison University, Lahore, Pakistan

Muhammad Nadeem Ali

Department of Computer Science
Faculty of Information Technology
Lahore Garrison University, Lahore, Pakistan

Muhammad Adnan Khan

School of Computer Science
National College of Business Administration & Economics
Lahore, Pakistan

Sabir Abbas

Department of Computer Science
Faculty of Information Technology
Lahore Garrison University, Lahore, Pakistan

Abstract—Cloud health has consistently been a major issue in information technology. In the CC environment, it becomes particularly serious because the data is located in different places even in the entire globe. Associations are moving their information on to cloud as they feel their information is more secure and effectively evaluated. However, as a few associations are moving to the cloud, they feel shaky. As the present day world pushes ahead with innovation, one must know about the dangers that come along with cloud health. Cloud benefit institutionalization is important for cloud security administrations. There are a few confinements seeing cloud security as it is never a 100% secure. Instabilities will dependably exist in a cloud with regards to security. Cloud security administrations institutionalization will assume a noteworthy part in securing the cloud benefits and to assemble a trust to precede onward cloud. In the event that security is tight and the specialist organizations can guarantee that any interruption endeavor to their information can be observed, followed and confirmed. In this paper, we proposed ranking system using Mamdani fuzzifier. After performing different ranking conditions, like, if compliance is 14.3, Data Protection 28.2, Availability 19.7 and recovery is 14.7 then cloud health is 85% and system will respond in result of best cloud health services.

Keywords—CC; CS, FIS; FRBS; MIE, standards; compliance; data protection; availability and recovery

I. INTRODUCTION

Cloud Computing (CC) [1] has been envisioned as the next generation paradigm in computation. In the CC environment, both applications and resources are delivered on demand over the Internet as services. Cloud is an environment of the hardware and software resources in the data centers that provide diverse services over the network or the Internet to satisfy user's requirements [1], [2].

In CC, applications are given and overseen by the cloud server and information is likewise put away remotely in the cloud setup [1], [2]. Clients don't download and introduce applications all alone gadget or PC; all handling and capacity is kept up by the cloud server.

CC is a web based exercise of utilizing a framework of far off servers facilitated on the web to store, oversee, and handle information, instead of a neighborhood server or a PC [1], [3].

CC is the after effect of the development and appropriation of existing advances and models. The objective of distributed computing is to enable clients to take benefit from these advancements, without the requirement for profound learning about them or mastery with every one of them. The cloud reason for existing is to diminishing expenses, and help the clients concentrate on their center business as opposed to being hampered by IT hindrances [1], [3], [4].

For CC security [1], one must comprehend your security and administration prerequisites for a particular framework or potentially information store. Individuals who put security around cloud or customary frameworks don't comprehend what issues they are offering to fathom. Individuals need to outline them before all else [4].

One should likewise understand that the area of the information is a great deal more vital than representing access. By taking a gander at chances to break and how the information is gotten to. Once more, a large portion of the information breaks happen around discovering powerlessness, regardless of if it's cloud construct or in light of destinations [4]. At long last, weakness testing is an articulate necessity, regardless of in case you're trying the security of cloud-based or customary frameworks. Unsubstantiated frameworks are dangerous and unsecured frameworks.

Clients will soon think distinctively around the cloud and security as more public cloud-based frameworks and information stores are deployed. In any case, without the appropriate measure of arranging and great innovation, cloud-based stages can turn out to be more secure. There are such a large number of parameters on which the cloud security relies on upon; some being, consistence necessities, misfortune in administration, accessibility and unwavering quality, confirmation and approval, feasibility, information insurance,

get to controls, issue and data security administration, and so forth. As per our exploration we trust that by institutionalization of a couple of parameters the cloud security issue [4], [11] can be diminished. The main parameters that we are going to standardize are compliance, availability, data protection and recovery. By finding out the probability of these four parameters, the cloud could either be protected or perilous. In this paper, we proposed ranking system using Mamdani fuzzifier. After performing different ranking conditions, like, if compliance is 14.3, Data Protection 28.2, Availability 19.7 and recovery is 14.7 then cloud health is 85% and system will respond in result of best cloud health services.

II. LITERATURE REVIEW

In a related research paper, it was expressed there are many cloud benchmarks and numerous in trial or draft organize. A few gauges are gone for particular points; a few measures are gone for the whole cloud biological community [1]. Particularly in the territory of data security administration framework gauges there is a surge of endeavors, frequently matched with affirmation programs, with a comparative objective (“to build confide in cloud suppliers”) [11], [12], [15].

It is intriguing to see that a large portion of these ventures concentrate on rather nonexclusive prerequisites. What is more often than not out of extension are particular criteria, for example, a base level of accessibility, least reaction times to occurrences, a base arrangement of capacities for the authoritative interfaces, or at least obligation or duty regarding security breaks [1], [13], [14]. It was expressed that institutionalization here could make it simpler for clients to assess, look at and embrace cloud benefits by giving institutionalized interfaces.

III. PARAMETERS FOR SECURITY

A. Compliance

Consistence issues in cloud security emerge when one uses the cloud storage or administration. One is concerned how their data will be kept with reference to the rules, regulation and laws. To conquer consistence issues one ought to be very much aware of which sort of cloud administration he is utilizing [3], [14], [15]. Other than that, they must be extremely watchful about which information they are moving to the cloud. Consistence is one of the key parameters with regards to cloud security [1] notwithstanding; it can be traded off in a few circumstances. As in it can extend from very high to very low and still be viewed as secure now and again. This is however safety measures from the client’s end.

In an association, they now and again choose to keep profoundly private data off of a cloud or want to keep it on an inside system with the goal that it is not under any hazard. They once in a while move it to a private cloud where they can without much of a stretch get to both physical and logical infrastructures.

The following thing to investigate once you know which information you will put on the cloud is to investigate the

concurrences with your cloud supplier [1]. All in all, on the off chance that it is an inside cloud, would you say you will have inner consistence agendas? On the off chance that it’s outer, you need to clearly relate to the supplier what kind of information exists on their cloud administrations, how will ensure it, how will back it up and how may you maintain whatever authority is needed to review the security and consistence structure that they work around your information?

B. Data Protection

In cloud security [3], information assurance is the most basic component. Protecting information on the cloud is a noteworthy need. Associations are uncertain by the prospect of presentation or the break of information and additionally the inaccessibility of information [4], [12].

In institutionalization, it is profoundly essential to keep this parameter secure, as without the security, many will quit utilizing the cloud. The real concern is the abuse of the vital information. It might be troublesome for the cloud benefit client to adequately check the information taking care of practices of the cloud supplier [3], [13]. Consequently, cloud specialist organizations are quick to keep their clients upbeat by keeping a standard in cloud security and keeping information ensured constantly [4].

C. Availability

Accessibility is the nearness of the cloud administrations. It is a standout amongst the most fundamental parameters in cloud security. Cloud security [2] depends intensely on accessibility and its standard ought to dependably be high or kept up as it without it cloud can’t work legitimately. It is profoundly versatile and equipped for meeting wide variations [3].

D. Recovery

Recovery is additionally a critical parameter, as associations need to know how they can recoup from aggregate debacle. A specialist organization that does not copy the information over various locales is presented to an aggregate disappointment [4]. Cloud specialist co-ops need to disclose to one where precisely are they putting away the information, and what might happen to your information and administration in the event that one of its destinations respects a disaster. Does it have the inclination to do an entire repair, and to what extent will it take?

IV. METHODOLOGY

We proposed fuzzy rule [5] - [7] based scheme (FRBS) that is capable of choosing cloud health using Mamdani fuzzifier [6] system. The four input and one output fuzzy inference system (FIS) is proposed to calculate cloud health on the basis of fuzzy logic principle [1].

In this method, we have picked Four parameters with respect to cloud security; compliance, data Protection, availability and recovery. We flipped around these parameters considering that they are the more vital than other and sorted them in principles. The brief description of fuzzy rule based scheme is given below. We used Mat-lab 7.12.0 fuzzy system [7] toolbox in designing of FRBS [1].

A. Fuzzy Sets

We used a number of fuzzy sets [6], [8], [9] to cover input-output spaces. The four input variables compliance, data Protection, availability and recovery with one output variable Cloud health are already shown in Fig. 1, 2, 3, 4 and 5. There are 5, 5 fuzzy sets [5], [8] used for the variables: Compliance and data Protection and 3, 3 fuzzy sets [10], [11], [15] used for variable Availability and Recovery.

B. Fuzzifier

We used triangular fuzzifier [5], [6] with “AND” respectively.

C. Rule Base

The rule base [6], [7] contains total 264 output rules. The rules are shown in Fig. 1.

D. Inference Engine

We used Mamdani Inference Engine (MIE) [6] in order to map the four inputs to one output shown in Fig. 6.

E. De-Fuzzifier

We used center average De-fuzzifier [6], [7]. Fig. 8, 9 and 10 represents rule surface of above FRBS.

F. Compliance

Cloud specialist co-ops might be novel, yet it is realized that most directions hold the client of the administration, at last, in charge of the security and veracity of corporate and client information, notwithstanding when it is held by the specialist organization [14], [15]. Customary specialist organizations capitulate to outside reviews and security guarantees, giving their clients data on the exact controls that were assessed. A distributed computing supplier that is unwilling or not able to do this is signaling that clients can just utilize them for the most minor capacities. (Surveying the Security Risks of CC) [14], [15]. We have taken five membership functions: very high, high, medium, low and very low using Mamdani fuzzy logics [5], [8] as shown in Fig. 1.

G. Data Protection

The administration of methodological, basic and lawful measures is so as to accomplish the objectives of information security (protection, trustworthiness and accessibility), straightforwardness, intervene ability and transportability, and in addition consistence with the applicable legitimate system. To measure data protection effect in cloud health we have taken five membership functions: very high, high, medium, low and very low using Mamdani fuzzifier [5], [8], [11], [14] as shown in Fig. 2.

H. Availability

In different papers, it is demonstrated regardless of whether the standard is public and open, with reference to get to. They have recognized three levels:

1) Fully open

Open counsel for drafts (like W3C, IETF, OASIS, and so forth.), and open access to conclusive renditions for a little expense.

2) Partially open

Consultation is shut/enrolment, yet there is open access to the standard.

3) Closed

Consultations are not open to the general population, and the standard is not public either. There is a significant expense [2].

Accessibility is typically secured by authorization at a general level. Accessibility is a key administration level goal, as it characterizes whether the cloud administration can really be utilized, and it is commonly important to determine numeric esteems for accessibility to make significant revelations that are valuable for cloud benefit clients. The topic of what “usable” means is a mind boggling matter, which relies on upon the cloud benefit concerned. An administration can be up and accessible, however it can perform so ineffectively that it will be considered adequately unusable. So also, the administration can be up, however it might react with blunders for legitimate necessities. To measure availability effect in cloud health we have taken three membership functions [6] fully open, partially open and closed using Mamdani fuzzifier [6], [8] as shown in Fig. 3.

I. Recovery

Most cloud suppliers have the money related assets to reproduce content in numerous areas as a matter of course. Along these lines repetition and freedom is expanded from disappointment and gives a level of disaster recovery. Clients of the cloud supplier ensure those measures are conformed to [13], [14]. At times, when delicate information and money related information are prepared, the client need to ensure significantly firmer information safety efforts with regards to the capacity of information, correspondence or transmission of information, information disaster recuperation and ahead transmission [13], [14]. To measure recovery effect in cloud health we have taken three membership functions [5], [8], [11], [15] low, medium and high using Mamdani fuzzifier as shown in Fig. 4.

V. SIMULATION AND RESULTS

In this paper, Mat-lab 7.12.0 fuzzy system [6] toolbox and triangular fuzzifier with “AND” operation has been used. There are four parameters: Compliance, Data Protection, Availability and Recovery that are being utilized to rank any cloud security given by various specialist co-ops. These are the following Ranges and Membership functions:

In Table I, all the ranges and membership functions of the parameters are shown.

TABLE I. RANGES AND MEMBER FUNCTIONS OF CLOUD HEALTH

Parameters	Member Functions	Ranges
Compliance	Very low	0-5.5
	Low	5.2-10
	Medium	8-13
	High	12-20
	Very High	20>
Data Protection	Very low	0-5.5
	Low	5-8
	Medium	8-15
	High	12-20
	Very High	19-30
Availability	Fully Open	0-5.8
	Partially open	5-14
	Closed	12-20
Recovery	Low	0-5
	Medium	4-10
	High	8-15

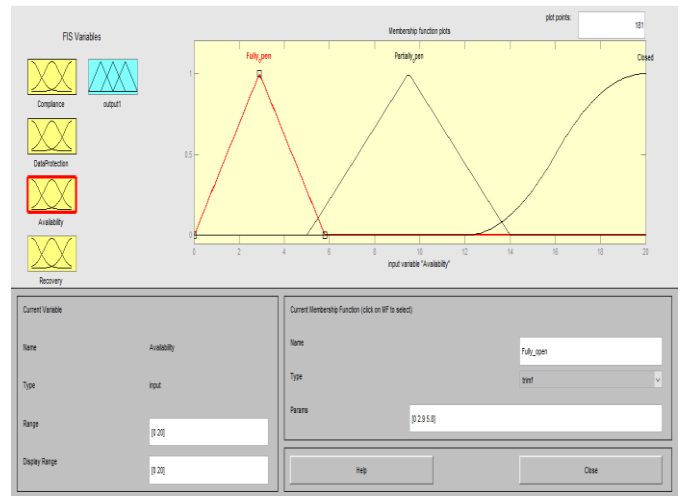


Fig. 3. Fuzzy sets for input variable availability.

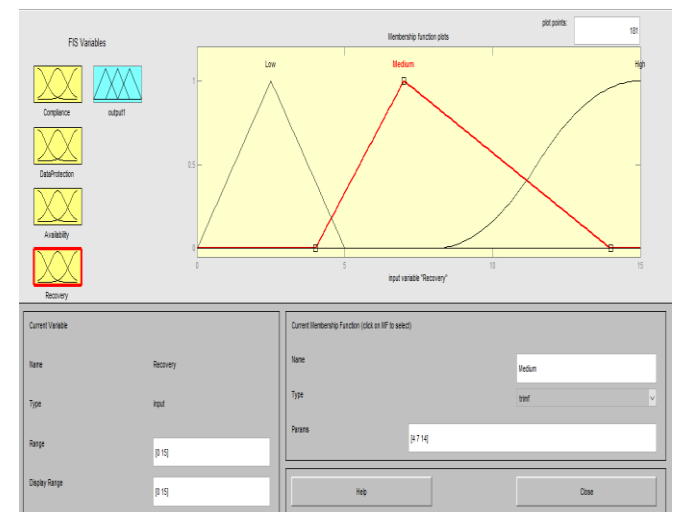


Fig. 4. Fuzzy sets for input variable recovery.

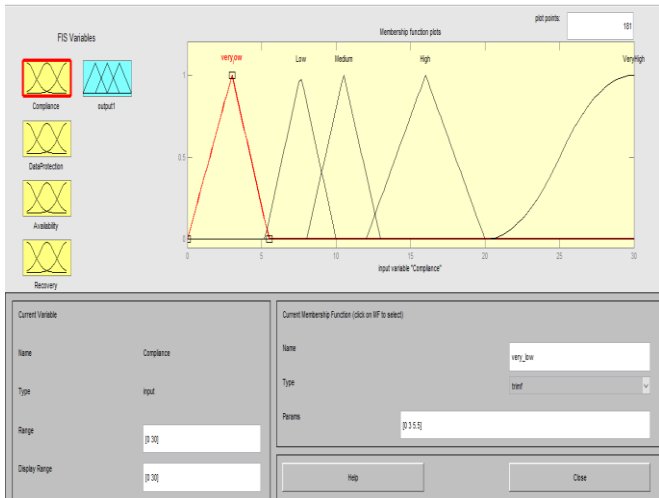


Fig. 1. Fuzzy sets for input variable compliance.

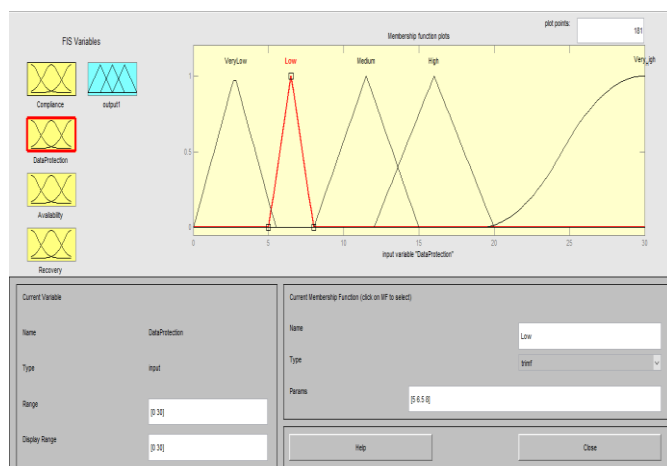


Fig. 2. Fuzzy sets for input variable data protection.

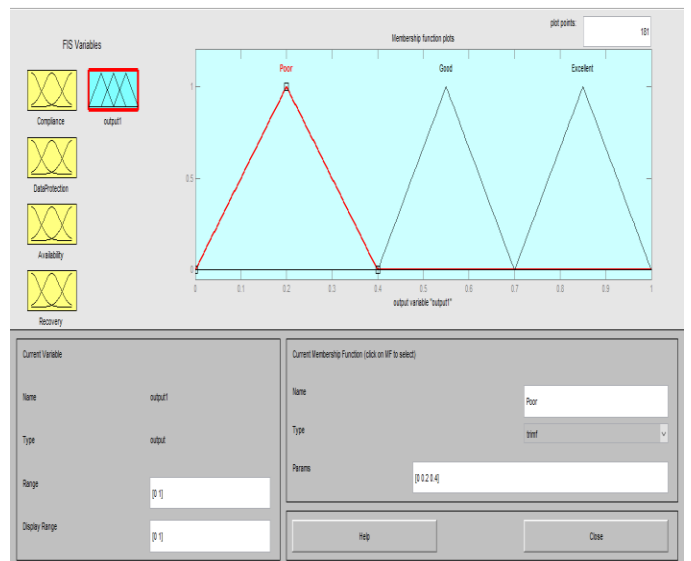


Fig. 5. Fuzzy sets for output variable cloud security.

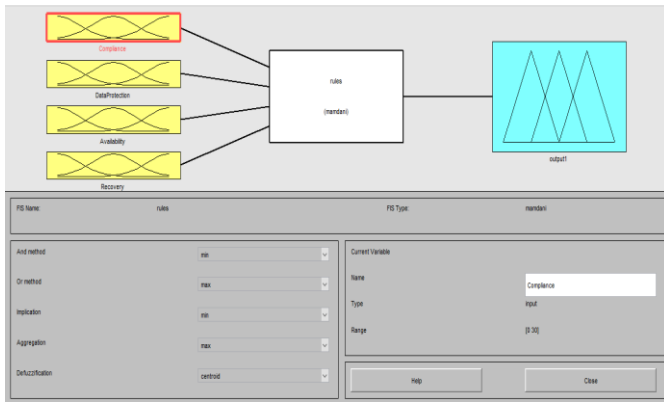


Fig. 6. Mamdani fuzzy rule base system.

1. If (Compliance is very_low) and (Data_Protection is Low) then (output1 is Poor) (1)
2. If (Compliance is very_low) and (Data_Protection is High) then (output1 is Good) (1)
3. If (Compliance is very_low) and (Data_Protection is VeryLow) then (output1 is Poor) (1)
4. If (Compliance is very_low) and (Data_Protection is Medium) then (output1 is Good) (1)
5. If (Compliance is very_low) and (Data_Protection is Very_High) then (output1 is Good) (1)
6. If (Compliance is High) and (Data_Protection is Low) then (output1 is Poor) (1)
7. If (Compliance is High) and (Data_Protection is High) then (output1 is Good) (1)
8. If (Compliance is High) and (Data_Protection is VeryLow) then (output1 is Poor) (1)
9. If (Compliance is High) and (Data_Protection is Medium) then (output1 is Good) (1)
10. If (Compliance is High) and (Data_Protection is Very_High) then (output1 is Excellent) (1)
11. If (Compliance is Medium) and (Data_Protection is Low) then (output1 is Poor) (1)
12. If (Compliance is Medium) and (Data_Protection is High) then (output1 is Good) (1)
13. If (Compliance is Medium) and (Data_Protection is VeryLow) then (output1 is Good) (1)
14. If (Compliance is Medium) and (Data_Protection is Medium) then (output1 is Good) (1)
15. If (Compliance is Medium) and (Data_Protection is Very_High) then (output1 is Good) (1)
16. If (Compliance is Low) and (Data_Protection is Low) then (output1 is Poor) (1)

Fig. 7. Rule base for deciding cloud health

Fig. 7 shows that the rules of the system are shown where all the possibilities were made using the four parameters; compliance, data protection, availability and recovery.

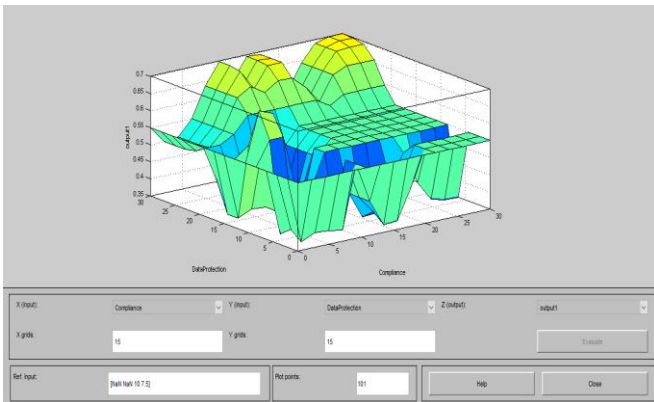


Fig. 8. Rule surface of data protection and compliance.

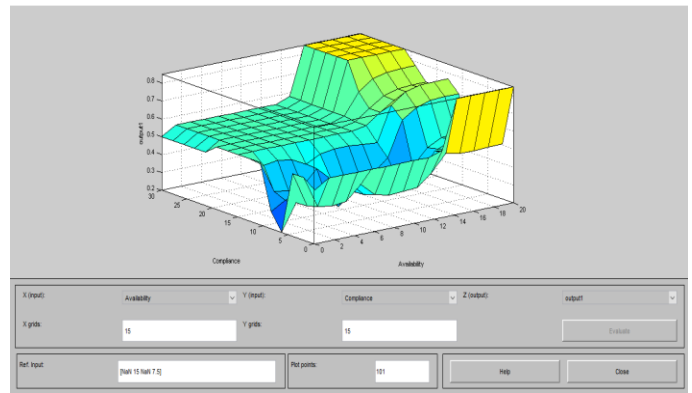


Fig. 9. Rule surface of compliance and availability.

A. Rule Viewer

In this proposed system, all the possibilities were made using the four parameters; compliance, data protection, availability and recovery. Their security statuses were toggled from very high, high, medium, low to very low and in result, cloud security be shown when it was very high, high, medium low or very low depending on the importance of the parameters in the experiment. The ranges given above were all tested one by one and as a result data protection and availability proved to be the most important as security depends on them massively. Recovery and compliance are important parameters too however not as important as the other two. Fig. 8, 9 and 10 depicts the surface view or the data under observation according to the standards of the four parameters.

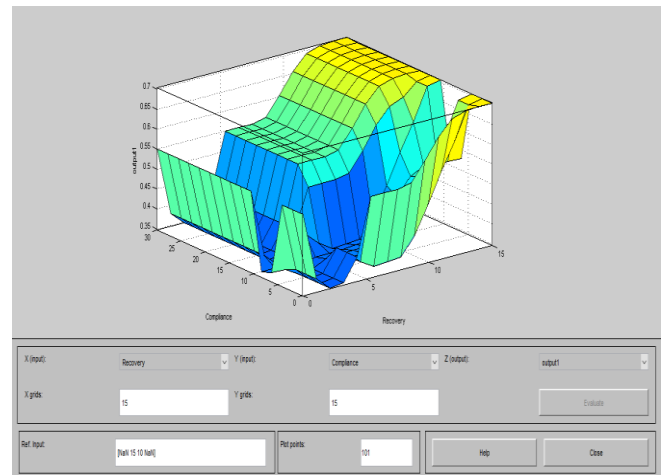


Fig. 10. Rule surface of compliance and recovery.

Fig. 11 shows that if compliance is 0, Data Protection 1.62, Availability 3.79 and recovery is 0.808 then cloud health is 0.2.

Fig. 12 shows that if compliance is 29.7, Data Protection 18.7, Availability 9.24.79 and recovery is 7.96 then cloud health is 0.55.

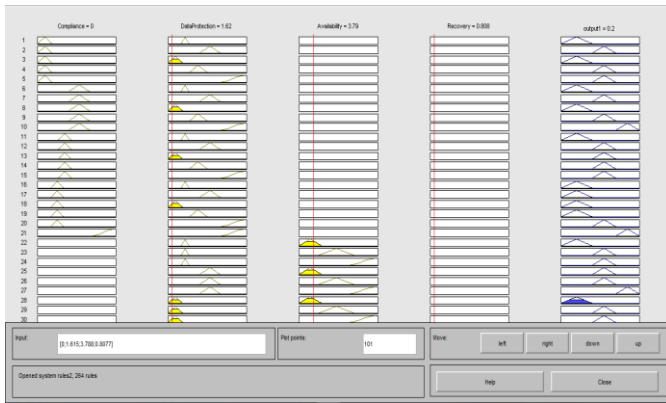


Fig. 11. Rule viewer when cloud health is poor.

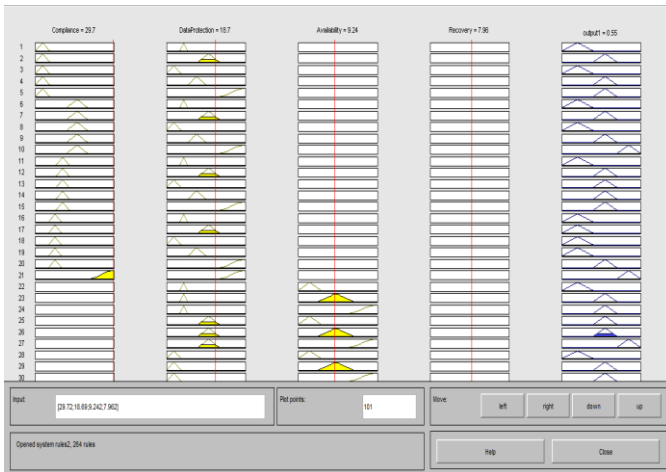


Fig. 12. Rule viewer when cloud health is good.



Fig. 13. Rule viewer when cloud health is excellent.

Fig. 13 shows that if compliance is 14.3, Data Protection 28.2, Availability 19.7 and recovery is 14.7 then cloud health is 0.85.

VI. CONCLUSION

CC is a promising and rising innovation for the up and coming age of IT applications. The obstruction and obstacles toward the quick development of CC are information security

and protection issues. Diminishing information stockpiling and preparing cost is an obligatory prerequisite of any association, while examination of information and data is dependably the most essential assignments in every one of the associations for basic leadership. So no associations will exchange their information or data to the cloud until the point when the trust is worked between the cloud specialist co-ops and buyers. In this research paper, four parameters are listed and their standards relevant for CC security, and we explained how the standards can be set to achieve optimum security in cloud services. They have been classified by standards according to their characteristics, and the reason to standardize these parameters is also explained. We conclude with some general remarks. Ranking based services for selecting the most appropriate methods from given numbers of providers. We proposed ranking system using Mamdani Fuzzifier. After performing different ranking conditions, like, if compliance is 14.3, Data Protection 28.2, Availability 19.7 and recovery is 14.7 then cloud health is 85% and system will respond in result of best cloud health services.

REFERENCES

- [1] "Cloud Security Alliance," a non Profit Cloud Evangelists Group, [Online]. Available: <http://cloudsecurityalliance.org/>.
- [2] M. X. L. R. L. a. X. S. Barua, "ESPA: Enabling Security and Patient-centric Access Control for eHealth in cloud computing," International Journal of Security and Networks 6, pp. 67-76, 2011.
- [3] D.-G. M. Z. Y. Z. a. Z. X. Feng, "Study on cloud computing security," Journal of software 22, vol. 1, pp. 71-83, 2011.
- [4] B. R. a. A. R. Kandukuri, "Cloud security issues In Services Computing," in IEEE International Conference on, pp. 517-520, 2009.
- [5] G. a. B. Y. Klir, "Fuzzy sets and fuzzy logic. Vol. 4. New Jersey: Prentice hall, 1995", New Jersey: Prentice hall, vol. 4, 1995.
- [6] Shahzad, "Fuzzy Approach Based Two Layered Block Coded Adaptive MC-CDMA system with FT/ST," Recent Sci, E-ISSN, vol. 5, no. 3, pp. 50-57, 2016.
- [7] S. M. a. C. Y. C. CHEN, "A new weighted fuzzy rule interpolation method based on GA-based weights-learning techniques," in International Conference on Machine Learning, Qingdao, Shandong, China, 2010.
- [8] S. M. a. K. Y. K. CHEN, "Fuzzy interpolative reasoning for sparse fuzzy rule-based systems based on α -cuts and transformation techniques," IEEE Transaction on Fuzzy System, vol. 16, no. 6, 2008.
- [9] P. P. B. V. C. K. H. a. S. M. J. BONISSONE, "Industrial application of fuzzy logic at general electric," IEEE Transaction on Industrial Application, vol. 38, no. 3, pp. 450-456, 1995.
- [10] Y. C. C. S. M. a. L. C. J. CHANG, "A new fuzzy interpolative reasoning method based on the areas of fuzzy sets," in IEEE International Conference on System, Manufacturing and Cybern, 2007.
- [11] T. S. K. a. S. L. Mather, Cloud security and privacy: an enterprise perspective on risks and compliance., " O'Reilly Media, Inc.", 2009.
- [12] R. E. a. Z. L. A. BELLMAN, "Decision making in a fuzzy environment," Management Science, vol. 17, pp. 141-164, 1970.
- [13] J. C. K. J. M. K. R. a. P. N. R. BEZDEK, "Fuzzy models and algorithms for pattern recognition and image processing," Boston, MA: Kluwer, 1999.
- [14] S. M. a. C. Y. C. CHEN, "A new method for weighted fuzzy interpolative reasoning based on weights-learning techniques," in IEEE International Conference on Fuzzy Systems, Barcelona, Spain, 2010.
- [15] S. M. K. Y. K. C. Y. C. a. J. S. P. CHEN, "Weighted fuzzy interpolative reasoning based on weighted incremental transformation and weighted ratio transformation techniques," IEEE Transaction on Fuzzy System, vol. 17, no. 6, pp. 1412-1427, 2009.

Evolutionary Design of a Carbon Dioxide Emission Prediction Model using Genetic Programming

Abdel Karim Baareh
Information Technology
Computer Science Department
Ajloun College, Al-Balqa Applied University
Ajloun, Jordan

Abstract—Weather pollution is considered as one of the most important, dangerous problem that affects our life and the society security from the different sides. The global warming problem affecting the atmosphere is related to the carbon dioxide emission (CO₂) from the different fossil fuels along with temperature. In this paper, this phenomenon is studied to find a solution for preventing and reducing the poison CO₂ gas emerged from affecting the society and reducing the smoke pollution. The developed model consists of four input attributes: the global oil, natural gas, coal, and primary energy consumption and one output the CO₂ gas. The stochastic search algorithm Genetic Programming (GP) was used as an effective and robust tool in building the forecasting model. The model data for both training and testing cases were taken from the years of 1982 to 2000 and 2003 to 2010, respectively. According to the results obtained from the different evaluation criteria, it is nearly obvious that the performance of the GP in carbon gas emission estimation was very good and efficient in solving and dealing with the climate pollution problems.

Keywords—Fossil fuels; carbon emission; forecasting; genetic programming

I. INTRODUCTION

Weather state and condition is a very important and dangerous issue related to some views health, climate, agriculture, economics, and tourism. Estimating the future events at the proper time is a very important task used to reduce and prevents the risks and the natural disasters. Many researchers were attracted towards this type of problems due to its difficulty and challenges in considering different input variables that should be cautiously considered, studied and measured to build the accurate forecasting models. The events and processes in the world always change due to the circumstances, so these events should be defined and declared to be processed. Climate pollution related to the carbon emission is a general serious world problem. Many international environmental agencies indicated the increase in CO₂ and greenhouse gas emission worldwide [1]. So protecting the civilization from the gas pollution requires a clear and a strict policy [2]. Different protocols and agreements were held between numerous countries to minimize the greenhouse gas emanation, such as the Kyoto protocol and the United Nations

(UN) agreement that confirmed on the continuous percentage checking and monitoring of the CO₂ emission in the atmosphere to reduce it to the desired levels [3].

Many countries stated and started a new policy to decrease and limit the CO₂ emission. Pollution from CO₂ emission is a serious, critical and real society enemy, for example, the UK Government's declared clear plans and aims to minimize the CO₂ emissions to 10% from the 1990 base by 2010 and in equivalent to generate 10% of the UK's electricity from renewable sources by 2010. Renewable electricity has become related and equivalent to CO₂ reduction [4]. Different studies were initiated and proposed to find out the relationship between the different energy consumption and CO₂ emission [5]-[9].

In this paper, the stochastic search algorithm Genetic Programming (GP) was used as an effective and powerful tool in building and estimating the forecasted model. GP as a soft computing technique was widely used in different fields to solve some complicated problems such as forecasting in all its type weather, rain, rivers, carbon, etc. [10]-[13]. GP also as a powerful tool was efficiently used in many applications [14], [15] such as economics and sales estimations [16], shift failures [17], estimating prices [18] and stock returns [19]. In this study, the GP technique was applied to deal with important and dangerous phenomena that are the CO₂ gas emitted based on four related inputs the global oil, natural gas (NG), coal, and primary energy (PE) consumption. This paper is organized as follows. Section II describes the collected data. Section III introduces the genetic programming concepts. Section IV presents the different implemented evaluation criteria. Section V describes the genetic programming model. Section VI describes the experimental results. Finally, Section VII presents the conclusion and the future work.

II. COLLECTED DATA

The carbon dioxide data set was collected from [20] as shown in Table I. The data set was collected for 31 years from 1980 to 2010. The data were trained for 23 years from 1980 to 2002 and tested for eight years from 2003 to 2010. This work is an extension of the previous work published in [12] using Neural network algorithm.

TABLE I. CARBON DIOXIDE DATA SET

Year	Oil Consumption (Mote) X1	NG Consumption (Mote) X2	Coal Consumption (Mote) X3	PE Consumption (Mote) X4	CO2 Emission (Mt) y
1980	2972.2	1296.9	1806.4	6624	19322.4
1981	2863	1309.5	1820.6	6577.5	19073.2
1982	2770.7	1312.5	1846.9	6548.4	18900.7
1983	2748.3	1329	1897.7	6638.2	19072.1
1984	2810.1	1440	1983.2	6960.2	19861
1985	2804.7	1488.3	2056	7137.5	20246.7
1986	2894.1	1503.6	2089.2	7307.5	20688.3
1987	2946.8	1579.6	2169	7555.7	21344.5
1988	3038.8	1654.9	2231.7	7833.5	22052.2
1989	3093	1729.2	2251.2	8001.7	22470.2
1990	3148.6	1769.5	2220.3	8108.7	22613.2
1991	3148.2	1807.5	2196.4	8156	22606.5
1992	3184.8	1817.9	2174.6	8187.6	22656.7
1993	3158	1853.9	2187.6	8257.5	22710.6
1994	3218.7	1865.4	2201.9	8357.6	22980.3
1995	3271.3	1927	2256.2	8577.9	23501.7
1996	3344.9	2020.5	2292.2	8809.5	24089.8
1997	3432.2	2016.8	2301.8	8911.6	24387.1
1998	3455.4	2050.3	2300.2	8986.6	24530.5
1999	3526	2098.4	2316	9151.4	24922.7
2000	3571.6	2176.2	2399.7	9382.4	25576.9
2001	3597.2	2216.6	2412.4	9465.6	25800.8
2002	3632.3	2275.6	2476.7	9651.8	26301.3
2003	3707.4	2353.1	2677.3	9997.8	27508.7
2004	3858.7	2431.8	2858.4	10482	28875.2
2005	3908.5	2511.2	3012.9	10800.9	29826.1
2006	3945.3	2565.6	3164.5	11087.8	30667.6
2007	4007.3	2661.3	3305.6	11398.4	31641.2
2008	3996.5	2731.4	3341.7	11535.8	31915.9
2009	3908.7	2661.4	3305.6	11363.2	31338.8
2010	4028.1	2858.1	3555.8	12002.4	33158.4

III. GENETIC PROGRAMMING CONCEPT

GP is a stochastic search algorithm works on the concept of evolutionary algorithm. This algorithm is driven by the principles of Darwinian evolution theory and natural selection [21], [22]. GP generates a mathematical model for nonlinear systems in the form of a tree consisting of roots and nodes, where the roots constitute the mathematical operations and the nodes constitute the variables. The formulated tree depth depends on the model functional complexity. An example of GP tree structure is shown in Fig. 1.

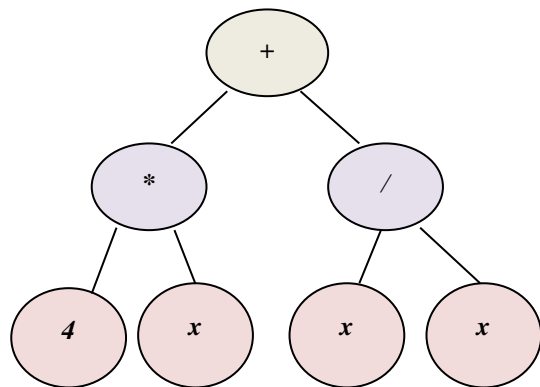


Fig. 1. Example of GP basic tree.

GP was used to encode a computer program in form of a tree structure and evaluate its fitness with respect to the predefined task. In 1991, John Koza suggested LISP programs that deal with various data and structures for a model manipulation due to its flexibility. The GP consists of a population of size n , which is chosen randomly based on the problem. Fig. 2 shows the evolutionary process of GP.

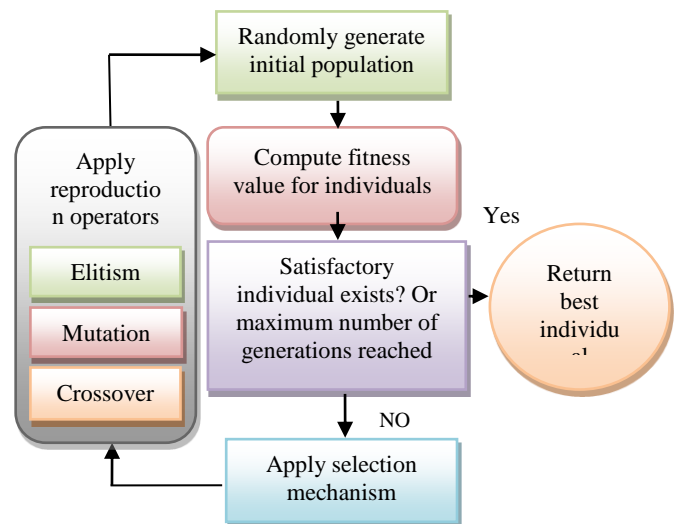


Fig. 2. GP evolutionary process [20].

IV. EVALUATION CRITERIA

In this paper, to solve the modeling problem for the carbon gas (CO₂) estimation, we considered building a model structure that takes into the account the historical measurements of the carbon data during the previous years.

The GP Model was developed using a MATLAB software toolbox called GPTIPS which works as an open source GP Toolbox for MG-GP [23]. GPTIPS defin number of appropriatefunctions for seeking the population of the proper model, such as examining the model behavior, post-run a model simplification function and export the model to some formats, like graphics file, LaTeX expression, symbolic math object or standalone MATLAB file [20]. GP-TIPS can be distinguished by its ability to configure to evolve the multi-gene individuals.

A number of evaluation criteria were used to validate the developed model. These evaluation criteria are the Variance-Accounted-For (VAF), Mean Square Error (MSE), Euclidean distance (ED), Manhattan distance (MD) and Mean magnitude of relative error (MMRE) as shown in equations next.

- Variance-Accounted-For (VAF):

$$VAF = \left(1 - \frac{\text{var}(y-\hat{y})}{\text{var}(y)}\right) \tag{1}$$

- Mean Square Error (MSE):

$$MSE = \frac{\sum_i (y_i - \hat{y}_i)^2}{n} \tag{2}$$

- Euclidean distance (ED):

$$ED = \sqrt{\sum_{i=1}^n (y_i - \hat{y}_i)^2} \tag{3}$$

- Manhattan distance (MD):

$$MD = \sum_{i=1}^n |y_i - \hat{y}_i| \tag{4}$$

- Mean magnitude of relative error (MMRE)

$$MMRE = \frac{1}{N} \sum_{i=1}^N \frac{|y_i - \hat{y}_i|}{y_i} \tag{5}$$

V. GENETIC PROGRAMMING (GP) MODEL

The Developed GP model requires the defining and initialization of some important parameters at the beginning of the evolutionary process. These parameters involve the population size, selection mechanism, crossover and mutation probabilities, the maximum number of genes allowed to constitute the multi-gene and many others. The developed GP model tuning parameters are given in Table II.

The complexity of the evolved models will change according to the maximum tree depth. Restricting the tree depth helps to evolve simple model, but it may also reduce the performance of the evolved model. Thus, we need to keep a balance between the depth, the complexity, and required performance.

TABLE II. GP TUNING PARAMETERS

Population size	50
Number of generations	250
Selection mechanism	Tournament
Max. tree depth	10
Probability of crossover	0.85
Probability of mutation	0.001
Max. genes	7
Function set	*, +, -

The GP model can be shown in Fig. 3 where four inputs were applied to the model, the global oil, natural gas, coal, and primary energy consumption to estimate the output CO₂ gas.

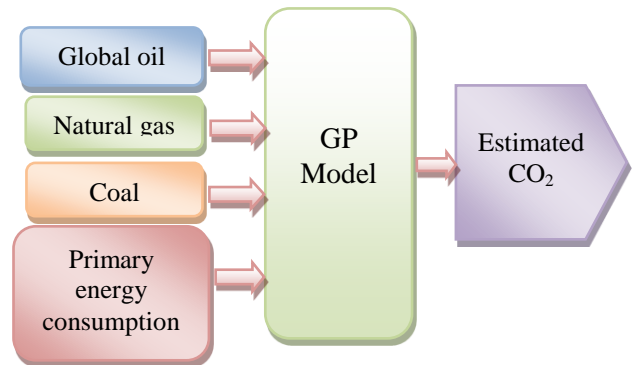


Fig. 3. GP model structure.

Multigene symbolic regression can be defined as a distinctive modification of GP algorithms, where each symbolic model demonstrated by a number of GP trees weighted by a linear combination [24]. In Multigene GP every tree is considered as a “gene” by itself. The predicted output \hat{y} is constituted by adding and combining the weighted outputs that are trees/genes in the Multigene individual with the bias term. Each tree is a function of zero or more of the N input variables z_1, \dots, z_N . Mathematically, a Multigene regression model can be written as:

$$\hat{y} = \gamma_0 + \gamma_1 \times \text{Tree1} + \dots + \gamma_M \times \text{TreeM} \tag{6}$$

Where, γ_0 represents the bias or offset term while $\gamma_1, \dots, \gamma_M$ are the gene weights and M is the number of genes (i.e. trees) which constitute the available individual. An example of a multigene model is shown in Fig. 4 and the mathematical model can be shown in (7).

$$y_0 + y_1 (\cos(x) * (3 + y)) + y_2 (z/2) \tag{7}$$

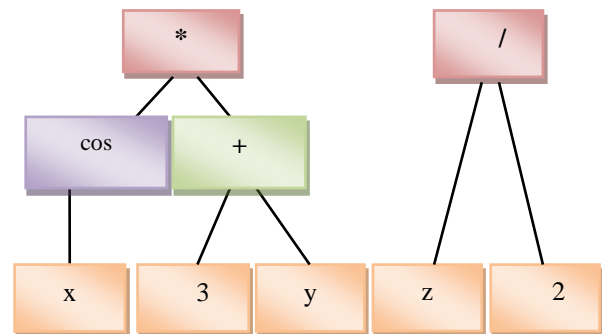


Fig. 4. Example of multi-gene GP model.

VI. EXPERIMENTAL RESULTS

In this paper, the GP model was used to estimate the carbon dioxide gas emission. In our case, four inputs data were used. The inputs are: the oil consumption (X_1), NG consumption (X_2), coal consumption (X_3), PE consumption (X_4) and the output is the CO_2 (y), where the inputs were measured in (Mote) and the output was measured in (Mt). The proposed GP model structure performance was excellent. The estimated CO_2 results for training and testing cases were very close as shown in Tables III and IV. The data were trained for 23 years from 1980 to 2002 and tested for 8 years from 2003 to 2010. Fig. 5 shows the correlation coefficient of the proposed model. In Fig. 6, we show the GP convergence model. In Fig. 7 and Fig. 8, we show the actual and the estimated CO_2 gas emission for training and testing cases.

The mathematical equation promoted for prediction using multi-gene GP can be also shown in (8). The model structure shows a strong linear relationship between the three main attributes Global Oil, Natural Gas and the Coal while the energy consumption was not a significant feature in the modeling process.

$$y = 3.084x_1 + 2.338x_2 + 3.974x_3 - (3.65 \cdot 10^{-6})x_1x_2 - (3.65 \cdot 10^{-6})x_1x_3 - (1.825 \cdot 10^{-6})x_1^2 - 29.47 \quad (8)$$

In Table V, we calculated the error values through a number of validation criteria for both training and testing cases.

TABLE III. ACTUAL AND ESTIMATED CO_2 - TRAINING CASE

Years	Training Case	
	Actual CO_2 (y)	Estimated CO_2 (\hat{y})
1980	19322.4	19322.45
1981	19073.2	19073.02
1982	18900.7	18900.86
1983	19072.1	19072.09
1984	19861	19861.17
1985	20246.7	20246.40
1986	20688.3	20688.30
1987	21344.5	21344.64
1988	22052.2	22052.19
1989	22470.2	22470.25
1990	22613.2	22613.11
1991	22606.5	22606.43
1992	22656.7	22656.84
1993	22710.6	22710.59
1994	22980.3	22980.54
1995	23501.7	23501.70
1996	24089.8	24089.77
1997	24387.1	24386.99
1998	24530.5	24530.54
1999	24922.7	24922.74
2000	25576.9	25576.87
2001	25800.8	25800.64
2002	26301.3	26301.54

TABLE IV. ACTUAL AND ESTIMATED CO_2 - TESTING CASE

years	Testing Case	
	Actual CO_2 (y)	Estimated CO_2 (\hat{y})
2003	27508.7	27508.24
2004	28875.2	28874.02
2005	29826.1	29824.85
2006	30667.6	30665.52
2007	31641.2	31638.96
2008	31915.9	31913.53
2009	31338.8	31336.95
2010	33158.4	33155.47

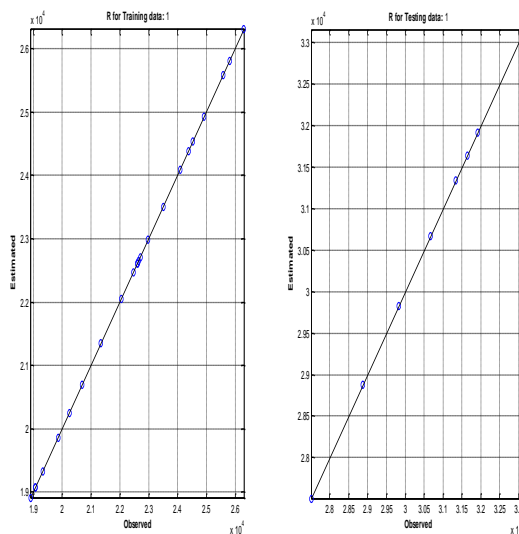


Fig. 5. Correlation coefficient of the proposed GP.

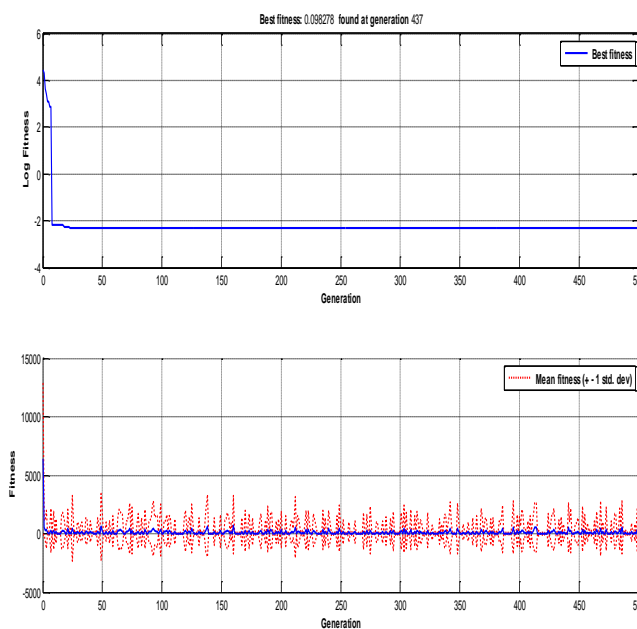


Fig. 6. GP convergence.

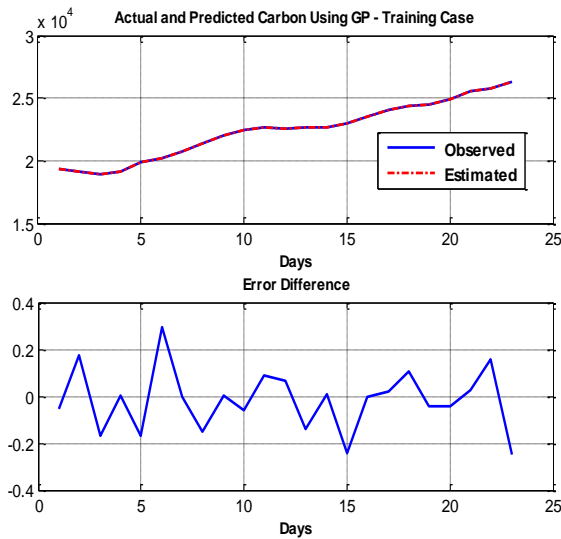


Fig. 7. Actual and predicted CO₂ – training case.

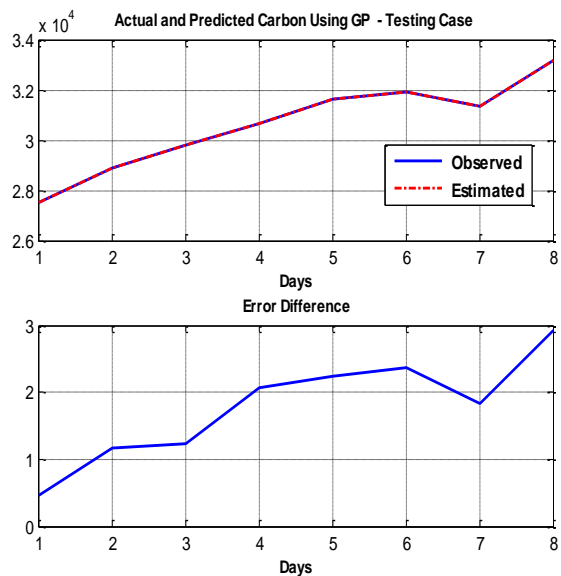


Fig. 8. Actual and predicted CO₂ – testing case.

TABLE V. VALIDATION CRITERIA FOR CO₂

Model	Evaluation Criteria				
	VAF	MSE	ED	MD	MMRE
Training	100	0.017	0.629	0.098	4.46e-06
Testing	100	3.744	5.473	1.788	5.72e-05

VII. CONCLUSIONS AND FUTURE WORK

In this paper, we provided an evolutionary model based multigene GP to predict the carbon dioxide emission and we compared the obtained result with actual one to measure the efficiency and strength of GP algorithm in forecasting, for both training and testing cases. From the obtained results, it was shown that the developed model is quite accurate. We can clearly see the solidity and the efficiency of GP in handling and estimating the CO₂ gas. We plan to extend our research to

include other paradigms of evolutionary modeling to solve various related environmental problems.

REFERENCES

- [1] H. Davoudpourand M. S. Ahadi, “The Potential for Greenhouse Gases Mitigation in Household Sector of Iran: Cases of Price Reform/Efficiency Improvement and Sce- nario for 2000-2010,” Energy Policy, Vol. 34, No. 1, pp. 40-49, 2006.
- [2] M. R. Lotfalipour, M. A. Falahi and M. Ashena, “Economic Growth, CO₂ Emissions, and Fossil Fuels Consumption in Iran,” Energy Policy, Vol. 2010, No. 35, pp. 5115-5120, 2010.
- [3] I. A. Samoilov, A. I. Nakhutin, “Esimation and Meddium-Term Forecasting of Anthropogenic Carbon Diox- ide and Methods Emission in Russia with Statistical Methods,” Vol. 34, No. 6, pp. 348-353, 2009.
- [4] W. David, “Reduction in Carbon Dioxide Emissions: Estimating the Potential Contribution from Wind Power,” Renewable Energy Foundation, December 2004.
- [5] M. A. Behrang., E. Assareh, M. R. Assari and A. Ghan- barzadeh, “Using Bees Algorithm and Artificial Neural Network to Forecast World Carbon Dioxide Emission,” Energy Sources, Part A: Recovery, Utilization, and Envi- ronmental Effects, Vol. 33, No. 19, pp. 1747-1759, 2011.
- [6] H. T. Pao and C. M. Tsai, “Modeling and Forecasting the CO₂ Emissions, Energy Consumption, and Economic Growth in Brazil,” Energy, Vol. 36, No. 5, 2011, pp. 2450-2458.
- [7] C. Saleh, N. R. Dzakiyullah , J. B. Nugroho, “Carbon dioxide emission prediction using support vector machine”, IOP Conf. Series: Materials Science and Engineering 114 (2016).
- [8] J. Wang, H. Chang, “Forecasting Carbon Dioxide Emissions in China Using Optimization Grey Model”, JOURNAL OF COMPUTERS, VOL. 8, NO. 1, January 2013.
- [9] H. Chiroma, S. Abdul-kareem, A. Khan, N. M. Nawi, A. Ya’u Gital, L. Shuib, A. I. Abubakar, M. Z. Rahman, T. Herawan, “Global Warming: Predicting OPEC Carbon Dioxide Emissions from Petroleum Consumption Using Neural Network and Hybrid Cuckoo Search Algorithm”, VOL.10, NO. 8, 2015.
- [10] A. K. Baareh, A. Sheta, K. AL Khnaifes, “Forecasting River Flow in the USA: A Comparison between Auto Regression and Neural Network Non-Parametric Models,” Proceedings of the 6th WSEAS International Conference on Simulation, Modeling and Optimization, Lisbon, 22-24, pp. 7-12, September 2006.
- [11] A. K. Baareh, A. Sheta, K. AL Khnaifes, Forecasting River Flow in the USA: A Comparison between Auto-Regression and Neural Network Non-Parametric Models, Journal of Computer Science Vol. 2, No.10, pp. 775-780, 2006.
- [12] A. K. Baareh, “Solving the Carbon DioxideEmission Estimation Problem: An Artificial Neural Network Model”, Journal of Software Engineering and Applications, Vol. 6 No. 7, PP. 338-342, 2013.
- [13] A. Sheta, H. Faris, A. k. Baareh, “Predicting Stock Market Exchange Prices for the Reserve Bankof Australia Using Auto-Regressive Feed forward Neural Network Model”, International Review on Computers and Software (I.RE.CO.S.), Vol. 10, N. 7, July 2015.
- [14] N. Karunanithi, W. Grenney, D. Whitley and K. Bovee, “Neural Networks for River Flow Prediction,” Journal of Computing in Civil Engg, Vol. 8, No. 2, pp. 371- 379,, 1993.
- [15] P. R. Bulando and J. Salas, “Forecasting of Short-Term Rainfall Using ARMA Models,” Journal of Hydrology, Vol. 144, No. 1-4, pp. 193-211, 1993.
- [16] H. Hruschka, “Determining Market Response Functions by Neural Networks Modeling: A Comparison to Econo- metric Techniques,” European Journal of Operational Research, Vol. 66, pp. 867-888, 1993.
- [17] E. Y. Li, “Artificial Neural Networks and Their Business Applications,” Information and Managements, Vol. 27, No. 5, pp. 303-313, 1994.
- [18] K. Chakraborty, “Forecasting the Behavior of Multivari- able Time Series Using Neural Networks,” Neural Net- works, Vol. 5, pp. 962-970, 1992.

- [19] G. Swales and Y. Yoon, "Applying Artificial Neural Networks to Investment Analysis," *Financial Analyst Journal*, Vol. 48, No. 5, pp. 78-82, 1992.
- [20] H. Kavooosi, M. H. Saidi, M. Kavooosi and M. Bohrng, "Forecast Global Carbon Dioxide Emission by Use of Genetic Algorithm (GA)," *IJCSI International Journal of Computer Science Issues*, Vol. 9, No. 5, pp. 418-427, 2012.
- [21] J. Koza, "Evolving a computer program to generate random numbers using the genetic programming paradigm," in *Proceedings of the Fourth International Conference on Genetic Algorithms*. Morgan Kaufmann, La Jolla, CA, 1991.
- [22] J. R. Koza, *Genetic Programming: On the Programming of Computers by Means of Natural Selection*. Cambridge, MA, USA: MIT Press, 1992.
- [23] D. P. Searson, D. E. Leahy, and M. J. Willis, "GPTIPS: an open source genetic programming toolbox for multigene symbolic regression," in *Proceedings of the International Multiconference of Engineers and Computer Scientists*, Hong Kong, 17-19 March, pp. 77-80.
- [24] A. Sheta and H. Faris. Improving production quality of a hot rolling industrial process via genetic programming model. *International Journal of Computer Applications in Technology*, 49(3/4), 2014. Special Issue on: "Computational Optimisation and Engineering Applications"

Understanding the Factors Affecting the Adoption of Green Computing in the Gulf Universities

ARWA IBRAHIM AHMED

Department of Information System
Princess Nourah Bint Abdulrahman University (PNU)
Riyadh, KSA

Abstract—Many universities worldwide have adopted, or are intend to adopt green computing in their campuses to improve environmental sustainability and efficient-energy consumption. However, the factors affect the adoption of green computing are still not understood. The aim of this study is to investigate the key success factors affecting the adoption of green computing in developing countries' universities, specifically in Gulf States universities. This study draws mainly on the TOE model suggested by Tornatzky and Fleischer [1] to understand the key areas for the success factors of green computing adoption. Data was collected based on survey research design to 118 Gulf universities. The findings revealed that the top five success factors affect the adoption of green computing in gulf universities are: awareness, relative advantage, top management support, adequate resources and government policy. Moreover, among the proposed three contexts the most important one is organizational, followed by environmental, and finally technology factors. This study contributes to the theory by providing taxonomy of the factors affecting the adoption of green computing. For practitioners, this study will assist the decision makers in gulf countries to benefit from the findings of this study to make well informed decisions by focusing on the key factor that have a greater impact on adopting green computing.

Keywords—Success factors; green computing; TOE model and universities

I. INTRODUCTION

Green computing has recently become an imperative aspect in the information technology industry. The rising level of energy consumption, global warming and e-waste have led to pay much attention in green computing by governments and businesses worldwide as kind of moral and environmental commitment for sustainable improvement [2]. Green computing is the process of implementing policies and procedures that support both individual and business computing needs in ecofriendly and sustainable way that enhance the efficiency of computing resources and minimize the energy consumption impact on the environment [3]. Some of the benefits of adopting green computing include ensuring an environmental and economic sustainability, utilizing the recourses in an environmental friendly manner, maintaining the computing performance while minimizing enormous and wasteful consumption of energy and carbon footprint, cutting down costs and improving business and social image [2], [4].

Over the past years, energy consumption concerns have been considered as one of key challenges for IT industry globally. Statistics indicated that the IT industry's CO₂

emission represents approximately 2% of global CO₂ emissions [5], [6]. The concerns rise over huge amounts of dollars spent annually on wasteful and unnecessary computing, where experts mentioned that the cost of wasted energy in computing industry is estimated about \$ 212.5 billion per year [7]. As a result of these concerns, many leading companies attempted to adopt green computing in their operations depending on renewable energy in order to improve computing performance, reduce energy consumption and develop IT operations in a sustainable manner. For example, Yahoo, Microsoft and Google sought to build their data centers in the cities that have renewable energy resources such as hydroelectric, solar and wind power to take advantage of these power, reduce cost and maintain environmental sustainability [8].

Issues related to the green computing have been widely discussed in existing literature. However, much of the green computing research to date have limited to prescriptive and rhetorical studies only. For example, Bisoyi and Das [9] highlight the factors that motivate businesses to implement e-waste management as a kind of green computing practice. They recommended that the lack of awareness, legislative and regulatory aspects, complexity of the materials used, appearance of hazardous substances, availability of appropriate technologies, and the risk in supply chain are among the key issues related to implementation of e-waste management. Similarly, Singh [10] discussed the main issues facing green computing implementation which include infrastructure for environmental sustainability, power management techniques, virtualization, energy efficient coding and recycling. In another study, Borah, et al. [11] investigates the enormous wastage of energy in IT industry and how green computing implementation reduces wasteful consumption of energy in small, medium and large enterprises. A number of studies [11]-[14] addressed the requirements and strategies needed for green computing in a cloud computing environment. They found that the virtualization, terminal servers, power management, power aware hybrid deployment, task consolidation and improve awareness are among the important techniques required to reduce power consumption, minimize toxic gas emissions, and make cloud computing more environmental friendly and more efficient energy usage. Ahmad, et al. [15] emphasized that the successful adoption and implementation of green computing is mainly rely on understanding the success factors of green computing. However, these factors are still poorly understood in the existing literature [5]. Therefore, this study aims to understand

the factors affecting the adoption of green computing in universities, specifically in the context of gulf universities.

Recently, gulf countries have identified renewable energy as a top priority in their agenda and have adopted, or are in the process of adopting green initiatives in all sectors, and the green computing in education sector is certainly no exception. Gulf governments are heavily investing in green projects in order to ensure an environmental and economic sustainability. For example, in 2017 Saudi Arabia spent on renewable energy projects more than \$50 billion with the purpose of cutting down oil use, as well as transforming towards green power in meeting growing energy demand [16]. However, the adoption of green computing is new trend in gulf countries which used to domestic oil use as a main source of energy. Moreover, green computing adoption involves many obstacles and complex processes [10], [17]. Yet, there is lack to empirical evidence to understand the success factors required to manage the adoption green computing successfully [5]. Therefore, this paper is important particularly in the context of gulf countries as developing countries, where most of the recent research of green computing in developing nations indicated that they are suffering from difficulty of managing the adoption of green computing, and struggling with a lack of resources and experiences to handle this new trend of technology. Moreover, the significance of this study lies in providing guidelines for decision makers in gulf universities to optimize their resources and efforts, how they can improve their investments in this new approach, and avoid the potential risks and challenges facing the adoption of green computing.

II. GREEN COMPUTING

Many organizations and individuals around the world have taken advantage of the digital revolution and are already utilizing the IT systems and its features in their daily work. While the use of IT systems are growing rapidly and the computing makes life easier and work faster, it increases significantly power consumption, which in turn amplifies the amount of carbon and hazardous gas emissions [10]. As a result, Green computing is gaining great importance in practical and academic fields. It became utmost priority of the modern world today to save energy consumption, reduce carbon emissions, cut down operational expenses and sustain a green environment [2], [15].

Green computing can be defined as the use of computers the efficient use of computers and its related technology in an ecofriendly manner with the purpose of reducing energy consumption, hazardous gas emissions and sustaining an environment [10]. Murugesan [18] has even broader concept of green computing, who elucidated that the green computing is “the study and practice of designing, manufacturing, using and disposing of computers, servers, and associated subsystems, such as monitors, printers, storage devices, and networking and communication systems, efficiently and effectively with minimal or no impact on the environment” [18 pp. 25-26]. The origin of green computing traced back to 1992 when the U.S. Environmental Protection Agency (EPA) launched Energy Star program with the aim of minimizing energy consumption of computing products [2], [10], [15]. Simultaneously, the Swedish organization TCO Development for sustainable IT

introduced the TCO Certification initiative in order to reduce hazardous emissions from computer materials and support environmentally sustainable computing implementation [17]. These initiatives resulted in wide adoption of the sleep mode for computer monitors as a first step towards green computing. Since then, green computing concept has widely extended to cover all aspects of IT products including CPUs, networks, servers, processors, networks and monitors [2], [15]. During the past two decades, green computing has been developing to include e-waste by designing ecofriendly or green-oriented software, and manufacturing hardware from disposable materials in order to reduce the harmful impacts of computing.

Murugesan [18] identified four key domains of green computing to address the environmental impacts of IT, namely: green use, green disposal, green design and green manufacturing of IT systems (as shown in Fig. 1). According to Murugesan [18], these domains are not only involve efficient energy and carbon free computing, rather they also include hazardous materials used in manufacturing of IT products that have harmful impacts on the environment. There are several methods to implement green computing which can be classified into three main categories, are [10], [14]: 1) improve the efficiency of energy consumption by minimizing the carbon emissions; 2) decrease e-waste as much as possible; and 3) transform the lifestyle towards more environmental friendly and sustainability. With the tremendous development of technology, day to day the adoption and implementation of green computing is gaining a considerable attention globally. The implementation areas of green computing are extending to involve everything that is green. This includes, for example but not limited to, data centers, infrastructure, technology used, virtualization, cloud computing, Internet of Things (IoT), intelligent computing, big data, renewable energy, green buildings, green IT policies, and any green initiative or ideas contribute to reduce energy consumption and carbon emissions and sustain environment [9], [14], [15], [19].

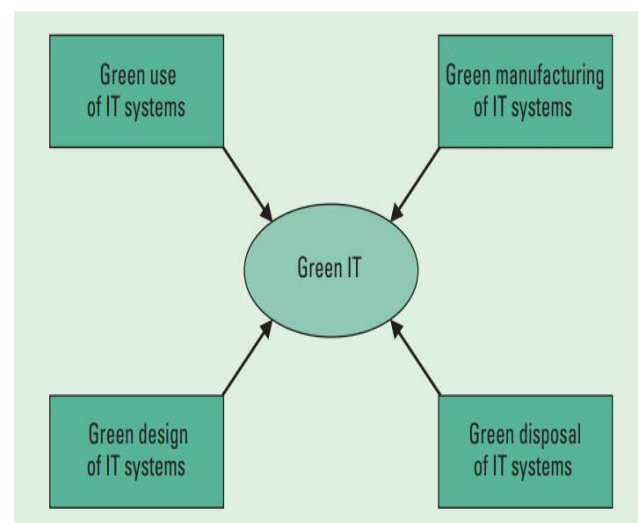


Fig. 1. Green computing domains suggested by Murugesan [18].

Although numerous studies have addressed green computing and its influence on efficient energy consumption and reduce the harmful impact of technology on environment,

the computing worldwide remain has a huge negative impact on environment [19]. Yet, most of green computing projects in developing countries have not been fully exploited to achieve the desired environmental sustainability, and the goals of its adoption are still unrealized [10]. This is due to the fact that the successful adoption and implementation of green computing does not only requires using, designing and manufacturing IT system, but also it requires mainly considering many critical factors such as environmental and organizational elements which are imperative for successful adoption of green computing [5], [17]. However, these factors for green computing adoption have been ignored in the existing literature and still unexplored research area [5]. Therefore, this study fills the gap in the literature by investigating the factors affecting the adoption of green computing using the case of gulf universities.

The use of IT systems is very common in almost all universities worldwide. It became an imperative part of daily practices of administrators, academics and students to utilize of computers, e-learning platforms, monitors, software, printers, projectors and social media networks for edutainment. Therefore, green computing initiatives and their adoption are gaining a particular importance in universities, and they are already shaping the actual practices in all aspects of learning processes. The universities contribute significantly to enhance green computing practices through raising awareness among academics, students and society as a whole on how to efficient use of computing resources in an ecofriendly manner and reduce energy consumption and carbon emissions [15]. Moreover, universities consider as a lead by example of green computing applications, as they practice the green applications to support their computing activities and for scientific research purposes [20].

A number of universities around the world have adopted green computing projects to sustaining a green environment. For example, the University of Utah in the United States, launched e-waste management initiative to reduce e-waste and maintain a sustainability by adopting green policy and implementing a set of measures in its campus such as identifying the dates on which e-waste will be collected. In addition, the University of Copenhagen in Denmark built an efficient energy services center for students in 2009. This building is supported by a renewable energy such as solar panels and it is totally carbon free. The University of Copenhagen also institutionalized the green computing concept by adopting well-planned strategy to improve green habits and practices among staff and students. This strategy resulted in minimizing the energy consumption and the amount of carbon emissions by 2.5% yearly [15]. The Australian National University has sought to adopt cloud computing as kind of green computing applications to support environmentally sustainable computing in its campus. From this approach, the university transformed completely towards e-learning as green way of reducing energy consumption and toxic gas emissions [21]. However, many universities globally, particularly in developing countries, are suffering on how manage green computing projects, and they lack to the experience in handling the issues facing this new trend in their environment and the factors required to avoid the failure [15], [22].

Having reviewed green computing literature, only few researches provided some insight about the green computing state in higher education institutions. For example, Ahmad, et al. [15] examined the awareness of green computing among students in Malaysian universities. While, Paul and Ghose [20] addressed the issues related to green computing practices in Indian universities. Nevertheless, the investigation of the factors affecting the adoption of green computing in universities is still extremely unexplored research area.

III. RESEARCH MODEL

The proposed model of this study is theoretically draws on the Technology-Organization-Environment (TOE) framework suggested by Tornatzky and Fleischer [1]. The TOE comprises three contexts that affect the adoption of any IT innovation which are: technology, organizational and environmental elements. The technology context involves the available IT systems and its related technologies such as software, hardware and networks. Organizational context refers to the characteristics of organizations such as organizational culture, organizational structures, strategies and size. The environmental context is the field in which an organization operates and conducts its business. This includes competitors, partners, legislations and government policies [1].

The TOE model offers a solid theoretical base to gain in-depth insight about the adoption of IT innovations and initiatives, and it has been widely used in different IT areas by many scholars to understand the success factors that affect the adoption of new IT initiatives, such as e-commerce [23], cloud computing [24], [25], e-Learning [26], Enterprise Resource Planning (ERP) systems [27], and E-Medical Record (EMR) systems [28]. However, there is lack of studies that employed the TOE to examine the success factors affecting the adoption of green computing in context of universities.

The TOE model is useful to help in achieving the objective of this research, as it contains an essential context for green computing adoption such as organizational, and environmental contexts. Numerous studies indicated that the adoption of green computing is not merely about the technology aspects, rather it is contingent upon understand other organizational and environmental factors which are imperative and should be considered for the success of green computing initiatives [5], [17], [22]. Moreover, this model helps to investigate the green computing adoption at organization level instead of individual level, and thus it provides further insight on how organization influences and is influenced by the contexts of new IT innovations adoption [29]. Therefore, the TOE assists in exploring the key areas for the success factors of green computing adoption.

Based on TOE framework and the results of green computing and related IT literature, this study suggests three dimensional model (as shown in Fig. 2), which includes the factors of technology, organizational and environmental to understand the adoption of green computing in universities. This study posits that these three contexts will positively affect the universities' decisions to adopt green computing.

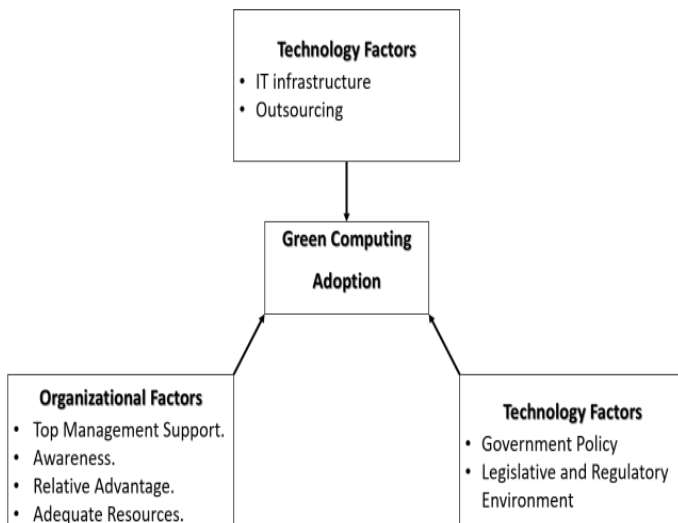


Fig. 2. Research model.

A. Technology Factors

The technology factors involve the internal and external technologies that influence on the adoption of new IT initiatives in particular organization. It also embraces the actual software, hardware, networks and how they are adapted in effective manner to achieve the best practices of green computing [3]. In this study, technology factors comprise IT infrastructure and outsourcing. The fact of green computing adoption requires mainly having an adequate and flexible hardware and software features that are designed and manufactured to reduce energy consumption and carbon emissions, decrease e-waste, and enable to conduct an adaptive maintenance to maintain environmental sustainability [8], [18]. This in turn ensures the green usage of IT systems. Therefore, the IT infrastructure is considered as one of an imperative factor in green computing adoption.

Many studies have also indicated that outsourcing will significantly motivate green computing adoption decision [29], [30]. The outsourcing strategy assists to assure greenness environment in the organizations and increase energy efficiency improvements at low cost. Numerous scholars have emphasized the outsourcing such as fog computing, grid computing and cloud computing are the most effective approaches towards adoption of green computing as they create an ecofriendly infrastructure with e-waste free organization [12], [13], [17]. It contributes greatly to obtain green environmental benefits of virtualization and thus enhance the performance of computing while minimizing energy consumption of data-centers (3#, 4#, 10#, 11#). Consequently, the outsourcing is another key technological factor for green computing adoption.

B. Organizational Factors

Organizational factors are an internal mechanisms, processes and strategies that affect the organization's intention to adopt new IT innovations. In this study, the organizational context embraces different factors, are: top management support, awareness, relative advantage and adequate resources. Top management support has been considered by several

scholars as an imperative factor for adoption any new IT initiative [28], [29]. Top management support is perceived as the commitment and support of executives and they understand and realized the benefits and functions of green computing [31]. As a matter of fact, the adoption of green computing involves many challenges, risks, costs, and it requires allocate resources and reengineer some process and infrastructure. Consequently, it is essential to have a powerful and supportive management to overcome obstacles and address issues facing the adoption of green computing. From this viewpoint, top management support plays a critical role before and after the adoption decision of green computing in universities.

Awareness refers to the knowledge or perceptions of students and staff about green computing practices and its capabilities in promoting environmental sustainability. Many studies indicated that the awareness is an important foundation to ensure the success of green computing projects [2], [13], [14]. According to Ahmad, et al. [15], raising awareness among students and other end users is the first step toward green computing adoption in universities. Relative advantage can be defined as "the degree to which an innovation is perceived as being better than the idea it supersedes" [32]. It also refers to verifying whether green computing project can cut down operating costs and rise the relative benefits for universities and environment. A number of studies affirmed that relative advantage greatly affect organizations and motivate them to adopt new IT initiatives [31], [33]. In addition, the adoption of green computing is often a large project, particularly in universities, which in turn requires having an adequate budget and human resource, sufficient schedule, and effective involvement by top management. Therefore, availability of adequate resources is among essential aspects to the success of IT initiatives adoption [31], [34].

C. Environmental Factors

Environmental factors represent an external pressure in the current operating environment of universities that affect the decision adoption of green computing. In this study, environmental factors consist of two factors, are legislative and regulatory environment, and government policy. (2#) affirmed that the legislative and regulatory environment is an important factor to adopt green computing. In Gulf countries, with the transformation of the energy sector towards renewable energy, many legislations have been enacted to promote environmental sustainability and efficient-energy consumption [16]. In addition, the universities seek to adopt education accreditation standards with the purpose of improving the quality of education, providing better educational services and gaining strategic advantages. These accreditation standards include some criterion of commitment to address energy consumption in ecofriendly manner and engagement in social and environmental responsibility issues. For example, the international criteria and standards for business accreditation (AACSB) involve environmental sustainability criteria that should be implemented in the higher education institutions [35]. Consequently, this legislative and regulatory environment will significantly force universities to adopt green computing projects in their daily practices.

One of the main objectives of the current Gulf governments green policy is determining the best practices to reduce energy

consumption and carbon emissions, and to avoid e-waste. Therefore, Gulf governments launched several initiatives to encourage all sectors including universities to adopt green projects. For example, currently Gulf governments support and fund the green projects, and award the scientific research ideas that promote an environmental and economic sustainability. Thus, the government policies have a significant impact on universities encouraging to encourage them adopt green computing.

Based on above discussions, the key success factors that affect the adoption of green computing in gulf universities are 8 variables and classified based on the TOE model into three contexts are technology, organizational, and environmental dimensions. The technology context includes IT infrastructure and outsourcing. The organizational context consists of top management support, awareness, relative advantage and adequate resources. Meanwhile, the environmental context comprises the legislative and regulatory environment, and government policy.

IV. METHODOLOGY

A. Participants and Data Collection

A survey approach was undertaken to verify the proposed model. The research population of this study is composed of both private and government higher education institutions that already adopted or intend to adopt green computing initiatives in gulf countries. This includes universities and colleges in Saudi, Bahrain, Kuwait, UAE and Oman which amounted around 182 institutions. The research participants of this study are green projects managers and vice presidents for administrative and strategic affairs who are involved in the strategic and operational decisions on the adoption of green computing projects. After e-mail contact, as a result of confidentiality issues or having no attention in adopting green computing initiatives, 19 universities refused to participate in this research. Consequently, only 163 universities and colleges expressed their willingness to participate in this study. Data collection process was begun on 2 July 2017 and was lasting for two months. A 163 questionnaire instruments sent to respondents by e-mail, and after three weeks, an email reminder was sent to participants in order to improve the response rate. A total of 124 responses were obtained, of which 6 were incomplete, and thus rejected. Therefore, the total of valid responses were 118 instruments which represent 72% of response rate that are deemed suitable for data analysis.

B. Measurements

The measurements have been identified and adapted based on the current green computing and related IT studies. This study addresses 9 constructs with a total of 32 items. Table I lists these constructs and the associated references, along with the numbers of items for each construct. A 5-point Likert scale was employed for measuring the items, with values ranking between 1 (strongly disagree) and 5 (strongly agree). A higher value reflects a greater level of respondent's agreement with items of questionnaire instrument.

In order to improve the questionnaire instrument validity and minimize the uncertainty and bias in the questions, a pilot study was conducted. The questionnaire was sent to two green computing experts; the first one is academic staff (Associate professor at Princess Nourah bint Abdulrahman University) who has research contribution in green computing topic. The second one is green computing manager project and has more than six years of experience in green computing projects at gulf universities. Some minor corrections were modified based on the comments of experts before distributing the actual survey.

TABLE I. RESEARCH MEASUREMENTS

Context	Constructs	Item No.	References
Technology	IT infrastructure	4	[36, 37]
	Outsourcing	6	[38, 39]
Organizational	Top management support	4	[38, 39]
	Awareness	4	[15]
	Relative advantage	4	[33]
	Adequate resources	5	[34]
Environmental	Legislative and regulatory environment	3	[1, 40]
	Government policy	2	[41]

V. DATA ANALYSIS

This section addresses the detail descriptive statistics and reliability of items. In this study, the significance of variables is based on frequencies and mean of respondents' view over each point of questionnaire variable using the Statistical Package for the Social Sciences (SPSS) software to validate the success factors affecting the adoption of green computing in gulf universities.

A. Descriptive Statistics

The data collected from 118 respondents indicate that the higher education institutions in gulf countries comprise four types of institutions are: government universities (29%), private universities (25%), government colleges (20%), and private colleges (26%). This distribution is too similar to the real distribution of entire population of higher education institutions in gulf countries. Table II presents the percentage of respondents based on higher education sector in gulf countries. Moreover, data collected shows that 52 university and college (44%) have already adopted green computing initiatives, while the rest (56%) are intend to adopt green IT projects in their campuses.

B. Reliability Analysis

As measurements items of constructs adapted and modified from previous related literature, reliability of measurements had to be tested. Therefore, Cronbach's alpha coefficient was used to test reliability and internal consistency of variables items. Statistically, if Cronbach's alpha coefficient scores is more than 0.70 ($\alpha > 0.70$), the reliability of variable's items is acceptable [42]. In this study, the Cronbach's alpha test indicates that the values for all variables are in the acceptance level ($\alpha > 0.70$). The overall value of Cronbach's alpha is 94.6% of 32 items from 118 respondents. Table III outlines the Cronbach's alpha score for each variable.

TABLE II. PERCENTAGE OF RESPONDENTS

Type	Res.	%	Adopt GC	Intend to adopt GC
Government university	34	29%	23	11
Private university	29	25%	14	15
Government college	24	20%	5	19
Private college	31	26%	10	21
Total	118	100%	52	66

TABLE III. RELIABILITY CRONBACH'S ALPHA TEST

Variables	N of Items	Cronbach's Alpha
IN	4.00	0.798
OS	6.00	0.817
MS	4.00	0.805
AW	4.00	0.874
RA	4.00	0.928
AR	5.00	0.891
LR	3.00	0.784
GP	2.00	0.721
Item-Total	32.00	0.946

VI. FINDINGS AND DISCUSSION

The findings reveal that the top five factors affect the adoption of green computing in gulf universities are: awareness, relative advantage, top management support, adequate resources and government policy. Table IV shows that the organizational factors is the most important dimension affect the universities' decision to adopt green computing initiatives, followed by environmental dimension, and finally technology dimension. This indicates that the universities must concentrate on the organizational and environmental contexts to support green computing adoption in their campuses. The following subsections present in detail the analysis along with discussions of the empirical findings in respect to the success factors affect the adoption of green computing in gulf universities. The classification of these factors draws on the dimensions of TOE model which are technological, organizational, and environmental contexts.

TABLE IV. FINDINGS ANALYSIS

Variables	Mean	Std. Deviation	%	Rank
IN	3.71	0.60	74.2%	8
OS	3.82	0.44	76.4%	7
MS	4.20	0.30	84.0%	3
AW	4.34	0.25	86.8%	1
RA	4.27	0.24	85.5%	2
AR	4.18	0.27	83.6%	4
LR	4.05	0.42	80.9%	6
GP	4.10	0.50	82.1%	5
Overall				
T	3.76	0.40	75.2%	3
O	4.25	0.12	85.0%	1
E	4.08	0.36	81.5%	2
Valid N	118			

A. Technology Factors

The technology factors refer to the internal and external technical aspects involved in green computing adoption. The findings show that 76% of respondents believed that outsourcing is an important technology factor to adopt green computing. While 74% of respondents are stated that the IT

infrastructure is another success technology factor for green computing adoption in gulf universities (as shown in Table IV). This finding is in line with [8], [18] who stated that the IT infrastructure is one of success factors for green computing projects.

Table IV also illustrates that the technology dimension is the least important factors compared to other organizational and environmental dimensions. This justifies that the respondents think that the adoption of green computing in the context of gulf universities primarily needs to consider organizational and environmental aspects. This result is consistent with [5], [17], [22] who affirmed that the organizational and environmental contexts are most important factors than technology aspects for the adoption of green computing.

B. Organizational Factors

The findings indicated that the organizational factors are the most important for green computing adoption in gulf universities. Table IV lists these factors which ranked based on the perceptions of respondents, this includes four factors: awareness (Mean 4.34), relative advantage (Mean 4.27), and top management support (Mean 4.20), adequate resources (Mean 4.18). This is due to the vast majority of respondents perceived the adoption of green computing as a huge project involve many benefits for their universities and environment and need a period of time to implement effectively which in turn require improving the awareness among students and staff, resource allocation, support and commitment by top management. Therefore, the organizational factors are truly crucial for adoption of green computing in gulf universities. Numerous studies [13], [14], [28], [31] confirmed that the organizational dimension is among the essential aspects for adopting any new IT initiative including green computing.

C. Environmental Factors

Analysis shows that the government policy (Mean 4.10), and legislative and regulatory environment (Mean 4.05) are significant environmental factors affect the universities' decision to adopt green computing in gulf countries. This is because the gulf governments have already implemented legislations and launched green initiatives to promote environmental sustainability and efficient-energy consumption. This serves as outside pressures to encourage universities adopt green computing projects in their work as kind of compliance with environmental commitment. This finding is supported by Du Buisson and Naidoo [5] who stated that the environmental pressures play a vital role to adopt green computing projects.

D. Comparison Analysis

The findings revealed that 52 of gulf universities and colleges (44%) have already adopted green IT projects in their campuses, while 66 university and college (56%) are intend to adopt green computing projects in the near future. The findings revealed that 52 of gulf universities and colleges (44%) have already adopted green IT projects in their campuses, while 66 university and college (56%) are intend to adopt green computing projects in the near future. Table V provides comparison between the mean scores of respondents' answers from the universities that already adopted the green computing

and the universities that intend to adopt green computing projects in the near future.

The mean scores of organizational factors for the universities that adopted (4.38) and the universities intend to adopt green computing (4.11). This indicates that the respondents from both categories are strongly agreed that the organizational factors are an imperative aspect for green computing adoption in gulf universities. This means that internal requirements of green computing adoption are deemed to be the most important drivers than other external pressures or technical aspects. Moreover, the analysis showed that the environmental factors are perceived as more important by universities that intend to adopt green computing (Mean 4.45) than early adopters' universities (Mean 3.70). The reason is that, in past two years, the gulf governments have increasingly implemented legislations and launched several green initiatives to promote environmental sustainability. This indicates the government policy, legislative and regulatory environment are play a significant role to increase the adoption level of green computing projects in gulf universities.

TABLE V. COMPARISON ANALYSIS BETWEEN EARLY ADOPTERS UNIVERSITIES AND INTEND TO ADOPT GREEN COMPUTING

Variables	Early adopters GC		Intend to adopt GC	
	Mean	Std. Deviation	Mean	Std. Deviation
IN	3.84	0.60	3.58	0.60
OS	3.62	0.46	4.02	0.42
MS	4.39	0.30	4.01	0.30
AW	4.41	0.23	4.26	0.25
RA	4.59	0.23	3.95	0.25
AR	4.14	0.27	4.21	0.27
LR	3.68	0.42	4.42	0.42
GP	3.72	0.54	4.48	0.45
Overall				
T	3.73	0.41	3.80	0.38
O	4.38	0.14	4.11	0.11
E	3.70	0.37	4.45	0.35

VII. CONCLUSION

This study proposes to understand the factors affect the adoption of green computing in gulf universities. This empirical study draws on the TOE model to investigate three contexts affecting universities' decisions regarding the adoption of green computing projects, namely technological, organizational and environmental aspects. The findings revealed that the organizational factors are the most important dimension affecting the adoption of green computing in gulf universities, followed by environmental context, and finally technology dimension. The organizational factors include awareness, relative advantage, management support and having an adequate resource. The environmental context involves government policy, legislative and regulatory environment while the technology dimension comprises outsourcing and IT infrastructure.

The main contribution of this paper is its implications for academia and practitioners. For academia, this study

contributes to the theory by employing of TOE model to understand the key areas for the success factors of green computing adoption. The use of TEO model assists in providing taxonomy of the factors affect the adoption of green computing. Yet, there is a lack of studies that classified these factors in current literature. This taxonomy offers further insight on contextual understanding of the key success factors for green computing adoption. Moreover, the findings of this study confirm to the previous studies [5], [17], [22] that the organizational factors are most important aspect than other environmental and technology contexts the adoption of green computing. However, this study contributes to the expansion of the boundaries of knowledge by revealing further insight on the critical role of environmental factors such as government policy in increasing the level of adoption for the universities that intend to adopt green computing. For practitioners, this study highlights the key success factors affecting gulf universities' decision to adopt green computing in their campuses. This will assist the decision makers in gulf countries to benefit from the findings of this study to make well informed decisions by focusing on the key factor that have a greater impact on adopting green computing.

The evidence from this study indicates that the development of government policy towards launching and supporting green initiatives will positively affect the adoption of green computing. Therefore, this study suggests for governments to develop well-defined strategies to encourage universities to adopt green computing. For example, governments may launch green awards or prizes to improve competitive advantage between universities in adopting green computing. Moreover, governments should set the green computing practices in the national academic accreditation criteria to force the universities adopt and implement green computing in their learning processes.

The major limitation of this study is limited to examine the key factors affect the universities' decision to adopt green computing in context of gulf area as developing countries. Understanding the green computing adoption is need different requirements which based on the context of investigation. The situation of Gulf States are somewhat different from other developing countries, as they are relying on oil as a main energy source, and have a huge budgets. Therefore, future studies should use the findings of this study to make comparison with other non-oil developing countries to promote the completeness of this study. Moreover, it would be useful for future research to extend the findings this study by investigating new factors affect the adoption of green computing, particularly in environmental context; for example, the influence of donors and international organization on green computing adoption in developing countries.

REFERENCES

- [1] L. G. Tornatzky and M. Fleischer, Processes of technological innovation. Lexington Books, 1990.
- [2] M. A. Mohammed, D. A. Muhammed, and J. M. Abdullahi, "Green Computing Beyond the traditional ways," Int. J. of Multidisciplinary and Current research, vol. 3, 2015.
- [3] N. J. Kansal and I. Chana, "Cloud load balancing techniques: A step towards green computing," IJCSI International Journal of Computer Science Issues, vol. 9, no. 1, pp. 238-246, 2012.

- [4] D. Wang, "Meeting green computing challenges," in Electronics Packaging Technology Conference, 2008. EPTC 2008. 10th, 2008, pp. 121-126: IEEE.
- [5] W. Du Buisson and R. Naidoo, "Exploring Factors Influencing IT Workers' Green Computing Intention at a South African Firm," in Proceedings of the Southern African Institute for Computer Scientist and Information Technologists Annual Conference 2014 on SAICSIT 2014 Empowered by Technology, 2014, p. 148: ACM.
- [6] A. Molla and V. Cooper, "Green IT readiness: A framework and preliminary proof of concept," Australasian journal of information systems, vol. 16, no. 2, 2010.
- [7] S. Aggarwal, M. Garg, and P. Kumar, "Green computing is Smart Computing—A Survey," International Journal of Emerging Technology and Advanced Engineering, vol. 2, no. 2, pp. 297-303, 2012.
- [8] A. Hooper, "Green computing," Communication of the ACM, vol. 51, no. 10, pp. 11-13, 2008.
- [9] B. Bisoyi and B. Das, "An Approach to En Route Environmentally Sustainable Future Through Green Computing," in Smart Computing and Informatics: Springer, 2018, pp. 621-629.
- [10] S. Singh, "Green computing strategies & challenges," in Green Computing and Internet of Things (ICGCIoT), 2015 International Conference on, 2015, pp. 758-760: IEEE.
- [11] A. D. Borah, D. Muchahary, S. K. Singh, and J. Borah, "Power Saving Strategies in Green Cloud Computing Systems," International Journal of Grid Distribution Computing, vol. 8, no. 1, pp. 299-306, 2015.
- [12] P. Malviya and S. Singh, "A Study about Green Computing," International Journal of Advanced Research in Computer Science and Software Engineering, vol. 3, no. 6, 2013.
- [13] R. Sharma, "Approaches for Green Computing," International Journal of Innovative Computer Science & Engineering, vol. 2, no. 3, pp. 52-55, 2015.
- [14] K. Usvub, A. M. Farooqi, and M. A. Alam, "Edge Up Green Computing in Cloud Data Centers," International Journal of Advanced Research in Computer Science, vol. 8, no. 2, 2017.
- [15] T. B. T. Ahmad, A. Bello, and M. S. Nordin, "Exploring Malaysian university students' awareness of green computing," GSTF Journal on Education (JEd), vol. 1, no. 2, 2014.
- [16] Bloomberg, "Saudis Kick Off \$50 Billion Renewable Energy Plan to Cut Oil Use," ed: Bloomberg, 2017.
- [17] N. Xiong, W. Han, and A. Vandenberg, "Green cloud computing schemes based on networks: a survey," Iet Communications, vol. 6, no. 18, pp. 3294-3300, 2012.
- [18] S. Murugesan, "Harnessing green IT: Principles and practices," IT professional, vol. 10, no. 1, 2008.
- [19] S. Saxena, "Green computing: Need of the hour," Small, vol. 8, no. 2.5, p. 20W, 2015.
- [20] P. K. Paul and M. K. Ghose, "Why Green Computing and Green Information Sciences Have Potentialities in Academics and iSchools: Practice and Educational Perspectives," in Advances in Smart Grid and Renewable Energy: Springer, 2018, pp. 103-112.
- [21] D. Akaslan and E. L.-C. Law, "E-learning in the Science of Electricity in Higher Education in Turkey in terms of Environment and Energy," in Proceedings of Postgraduate Research Student Conference, 2010.
- [22] R. R. McWhorter and J. A. Delello, "Green Computing through Virtual Learning Environments," in Handbook of Research on Innovative Technology Integration in Higher Education: IGI Global, 2015, pp. 1-28.
- [23] E. Sultanow, A. Chircu, and F. Chircu, "E-commerce Adoption: A Revelatory Case Study in the German Oncology Pharmaceutical Supply Chain," in Proceedings of the Conference on Information Systems Applied Research ISSN, 2016, vol. 2167, p. 1508.
- [24] H. Gangwar, H. Date, and R. Ramaswamy, "Understanding determinants of cloud computing adoption using an integrated TAM-TOE model," Journal of Enterprise Information Management, vol. 28, no. 1, pp. 107-130, 2015.
- [25] P.-F. Hsu, S. Ray, and Y.-Y. Li-Hsieh, "Examining cloud computing adoption intention, pricing mechanism, and deployment model," International Journal of Information Management, vol. 34, no. 4, pp. 474-488, 2014.
- [26] E. Ansong, S. L. Boateng, R. Boateng, and J. Effah, "Determinants of E-Learning Adoption in Universities: Evidence from a Developing Country," in System Sciences (HICSS), 2016 49th Hawaii International Conference on, 2016, pp. 21-30: IEEE.
- [27] W. Xu, P. Ou, and W. Fan, "Antecedents of ERP assimilation and its impact on ERP value: A TOE-based model and empirical test," Information Systems Frontiers, vol. 19, no. 1, pp. 13-30, 2017.
- [28] H. Sulaiman and A. I. Magaireah, "Factors affecting the adoption of integrated cloudbased e-health record in healthcare organizations: A case study of Jordan," in Information Technology and Multimedia (ICIMU), 2014 International Conference on, 2014, pp. 102-107: IEEE.
- [29] Q. Cao, J. Baker, J. C. Wetherbe, and V. C. Gu, "Organizational Adoption of Innovation: Identifying Factors that Influence RFID Adoption in the Healthcare Industry," in ECIS, 2012, vol. 94.
- [30] R. U. Khan and S. U. Khan, "Green IT-outsourcing assurance model," in Global Software Engineering Workshops (ICGSEW), 2013 IEEE 8th International Conference on, 2013, pp. 84-87: IEEE.
- [31] J.-W. Lian, D. C. Yen, and Y.-T. Wang, "An exploratory study to understand the critical factors affecting the decision to adopt cloud computing in Taiwan hospital," International Journal of Information Management, vol. 34, no. 1, pp. 28-36, 2014.
- [32] L. G. Tornatzky and K. J. Klein, "Innovation characteristics and innovation adoption-implementation: A meta-analysis of findings," IEEE Transactions on engineering management, no. 1, pp. 28-45, 1982.
- [33] G. Premkumar and M. Roberts, "Adoption of new information technologies in rural small businesses," Omega, vol. 27, no. 4, pp. 467-484, 1999.
- [34] I.-C. Chang, H.-G. Hwang, M.-C. Hung, M.-H. Lin, and D. C. Yen, "Factors affecting the adoption of electronic signature: Executives' perspective of hospital information department," Decision Support Systems, vol. 44, no. 1, pp. 350-359, 2007.
- [35] AACSB, "Eligibility Procedures and Accreditation Standards for Business Accreditation," 2013.
- [36] G. Premkumar and K. Ramamurthy, "The role of interorganizational and organizational factors on the decision mode for adoption of interorganizational systems," Decision sciences, vol. 26, no. 3, pp. 303-336, 1995.
- [37] D. E. T. Terry Anthony Byrd, "Measuring the flexibility of information technology infrastructure: Exploratory analysis of a construct," Journal of Management Information Systems, vol. 17, no. 1, pp. 167-208, 2000.
- [38] V. Grover, M. J. Cheon, and J. T. Teng, "The effect of service quality and partnership on the outsourcing of information systems functions," Journal of Management Information Systems, vol. 12, no. 4, pp. 89-116, 1996.
- [39] J. Rhodes, P. Lok, W. Loh, and V. Cheng, "Critical success factors in relationship management for services outsourcing," Service Business, vol. 10, no. 1, pp. 59-86, 2016.
- [40] A. P. Chan, P. T. Lam, D. W. Chan, E. Cheung, and Y. Ke, "Critical success factors for PPPs in infrastructure developments: Chinese perspective," Journal of Construction Engineering and Management, vol. 136, no. 5, pp. 484-494, 2010.
- [41] K. K. Kuan and P. Y. Chau, "A perception-based model for EDI adoption in small businesses using a technology-organization-environment framework," Information & management, vol. 38, no. 8, pp. 507-521, 2001.
- [42] J. F. Hair, W. C. Black, B. J. Babin, R. E. Anderson, and R. L. Tatham, Multivariate data analysis. . Pearson, 2010.

The use of Harmonic Balance in Wave Concept Iterative Method for Nonlinear Radio Frequency Circuit Simulation

Hicham MEGNAFI, Nouredine BOUKLI-HACENE
Telecommunication Laboratory of Tlemcen
University of Abou Bakr Belkaid
Tlemcen, Algeria

Nathalie RAVUE, Henri BAUDRAND
Laboratory of Laplace
LAPLACE, University of Toulouse, CNRS
Toulouse, France

Abstract—This paper presents the birth of the new hybrid method for the non-linear Radio frequency circuits' simulation. This method is based on the combination of the wave concept iterative procedure (WCIP) and the harmonic balance (HB) for their advantages. It consists also the development of an application based on this method for the simulation of nonlinear planar radio frequency circuits. The simulation of the Radio frequency diode implemented in micro-strip line is done. The validations are obtained by the comparison of the results obtained by our new hybrid method and Harmonic Balance under Advanced Design System (ADS) software.

Keywords—WCIP; harmonic balance; nonlinear circuits; planar radio frequency circuits; radio frequency diode

I. INTRODUCTION

The Technological advances have enabled to establish an efficient microwave circuit. To analyze and simulate them in nonlinear regime, several methods of analysis have been implemented to achieve the required performances [1], [2], the basic differences between these methods that exist in the domain of analysis are temporal or frequency.

The nonlinear system response is periodic that can be determined by integrating the differential equations that govern the circuit to steady state.

The Time-domain analysis, if it allows to take in consideration a high number of non linearities, then it is not suitable for circuits having relatively large time constant elements in front of the period of the applied signal. In the other hand, if this approach allows the distortions study, it only applies to circuits with low nonlinearities [3].

To remove the main problems caused by the two previous methods, an alternative approach has been proposed and become the most commonly used method in the analysis of nonlinear circuits. This method is called the harmonic balance (HB) [4].

The basic principle of the harmonic balance is to split the circuit into two sub-circuits; a linear and nonlinear sub-circuits. The linear sub-circuit is necessary to be studied in the frequency-domain and the non-linear sub-circuit is well described in the time-domain. The results of the time-domain

analysis are then converted into the frequency-domain by the Fourier Transform method [4]. The convergence is obtained, only if the interconnection currents between the linear and non-linear sub-circuits, for each harmonic, are the same. The different currents must be balanced for each harmonic [5].

In the other hand, another method that has already shown its effectiveness in the simulation of RF circuits is called the wave concept iterative process (WCIP); this method is based on the concept of waves. It's applied in the planar structures of resolution [6], the micro-strip antennas [7] and the planar filters [8]. This method has the advantage of simplicity because it does not involve the use of basic functions and matrix inversion as in other calculation methods. Therefore, it is possible to analyze a large complex planar microwave structures [9], [10]. Moreover, a high computational speed can be achieved by using the two dimensional the fast Fourier transformation algorithm known as fast modal of transformation (FMT) [11].

The classical wave concept iterative process was not applied in the simulation of nonlinear circuits because this method is based on frequency domain analysis, for which we proposed a combination of HB and WCIP to solve the problem of limited simulation; HB and WCIP are based on the use of the Fourier transform and its inverse. The balance between the two domains related to the Fourier transform is fundamental to develop a model of nonlinear electromagnetic problems and to qualify circuits in microwaves.

The rest of the paper is organized as follows: The next one (Section II) contains a definition of the wave concept, then we describe the iterative process and its algorithm. We are going to show the interest and the principle of the harmonic balance and its algorithm. In Section III, we propose a new approach of WCIP (hybrid method of HB and WCIP) to get the advantages of the two methods for the simulation of nonlinear circuits, we propose also a nonlinear RF diode modeling in small signal regime to validate this new hybrid approach. Where in Section IV, we present the obtained results validated by the comparison with the results obtained by ADS software. And in the last Section V, we present the perspective of this new hybrid method as an improvement of the convergence and the simulation of new non-linear circuit (such as transistor, non-linear capacitor) and a conclusion.

II. METHODS

A. Wave Concept Iterative Method

The main goal of this part is to propose a global electromagnetic analysis for characterizing microwave planar linear circuits based on the use of the iterative method. This method is based on the wave concept. It has the advantage of simplicity because it does not involve the use of basic functions and matrix inversion as in other calculation methods. Therefore, it is capable of analyzing large complex planar microwave structures [12].

1) Waves Definition

The wave concept is introduced by writing the transverse electric field \vec{E}_i and transverse current density \vec{J}_i in terms of incident \vec{A}_i and reflected \vec{B}_i waves in each medium i . It leads to the following set of equations [10], [11]:

$$\begin{cases} \vec{A}_i = \frac{1}{2\sqrt{Z_0}} \cdot (\vec{E}_i + Z_{0i} \cdot \vec{J}_i) \\ \vec{B}_i = \frac{1}{2\sqrt{Z_0}} \cdot (\vec{E}_i - Z_{0i} \cdot \vec{J}_i) \end{cases} \quad (1)$$

Where, Z_0 is an intrinsic impedance of the medium.

B. Principle of Wave Concept Iterative Method

According to the criterion defining the wave concept, we can define the electric field and the current density values in each point of the surface Ω by the determination of the incidental and the reflective waves values. So, the iterative process is based on the creation of a recurrence relation between the incidental and the reflective waves, and the repetition of this relation until convergence [9].

The iterative method can be summarized by the following equations system [3], [4]:

$$\begin{cases} \vec{A} = \hat{S} \cdot \vec{B} + \vec{A}_{0i} \\ \vec{B} = \hat{\Gamma} \cdot \vec{A} \end{cases} \quad (2)$$

Where,

\hat{S} : The transmission operator at the interface Ω ,

$\hat{\Gamma}$: The reflection operator representing the half medium around the interface

\vec{A}_{0i} : The source wave that can be defined by:

$$\vec{A}_{0i} = \frac{\vec{E}_0}{\sqrt{Z_{0i}}} \quad (3)$$

\vec{E}_0 : The total electric field produced by the excitation source.

The first system equation (2) describes the electromagnetic behavior at the circuit interface in spatial domain, while the second system equation (2) describes the waves' reflection in modal-domain.

The iterative process use successively these two equations through a Fast Modal Transform (FMT: from spatial domain to modal domain) and its inverse (conversion from the modal domain to the spatial one) [13].

Wave propagation described by incident and reflected waves, is presented in the planar structure. We can see that the waves will be reflected continuously, as shown in Fig. 1 [14].

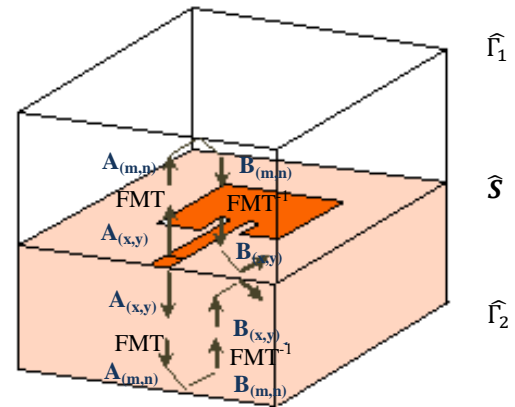


Fig. 1. Wave propagation in planar circuit [5].

1) Wave Concept Iterative Procedure

The procedure of the wave concept iterative method is summarized by the following steps which are shown in Table I:

TABLE I. STEPS OF WAVE CONCEPT ITERATIVE PROCESS PROCEDURE

Steps	Development
First step	Define the excited wave of planar source in spatial-domain \vec{A}_0^i .
second step	transform the incident waves in the spatial-domain to the model-domain by the FMT (Fast Modal Transform) : $\vec{A}_{(m,n)}^i = FMT(\vec{A}_{(x,y)}^i)$
Third step	get the incident waves in model-domain by the application of the reflection coefficient: $\vec{B}_{(m,n)}^i = [\Gamma] \cdot \vec{A}_{(m,n)}^i$
Fourth step	convert the waves in the model-domain to the spatial-domain by the FMT inverse: $\vec{B}_{(x,y)}^i = FMT^{-1}(\vec{B}_{(m,n)}^i)$
Fifth step	Calculate the reflected waves using the scattering parameters of planar circuit: $\vec{A}_{(x,y)}^i = [S] \cdot \vec{B}_{(x,y)}^i + \vec{A}_0^i$
Sixth step	Repeat the second step to the fifth step until the convergence of the S parameters are obtained.
Seventh step	After testing the convergence, we can calculate the tangential electric field and current density

C. Harmonic Balance Method

The Harmonic balance is a hybrid time and frequency domains analysis technique for simulating nonlinear circuits and systems. This hybrid analysis allows all the advantages of nonlinear temporal domain modeling, combined with the strength (efficiency) of the steady-state frequency technique [5].

1) The Standard Harmonic Balance Technique

The basic principle of HB approach is to split the circuit into two sub-circuits of N common ports between the linear and non-linear sub-circuits. Each branch of the circuit circulates a current harmonic component [15], [16]. In this work, the nonlinear sub-circuit consists in a nonlinear diode represented by an algebraic equation $i(t)=F(v(t))$, so the circuit is decomposed as is shown in Fig. 2.

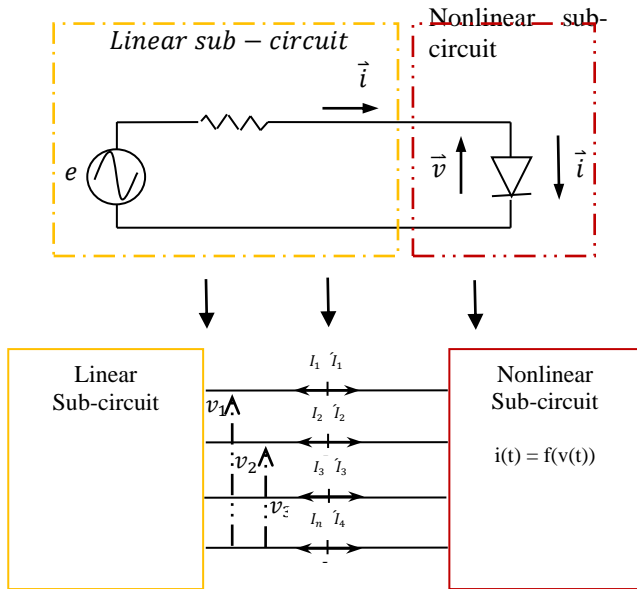


Fig. 2. The Harmonic Balance method split the circuit into linear and nonlinear subcircuits.

The currents flowing from nodes into linear sub-circuit \widehat{I}_k , including all distributed elements, are calculated by means of a frequency-domain linear analysis. And the Currents from nodes into nonlinear sub-circuit \widehat{I}_k are calculated in the time-domain. The balance between the time domain and frequency domains is obtained by Fourier transform; it is necessary to use a sinusoidal excitation to apply this technique. According to Kirchoff's Current Law (K.C.L), the currents sum should be zero at all nodes (4) [17].

$$\widehat{I}_k(k.\omega_0) + \widehat{I}_k = 0 \quad \forall k \in [0, \dots, K] \quad (4)$$

Where, K is the number of harmonic, ω_0 is the pulsation of the source.

The currents' sum computation gives the error of the method, called F_{error} (5). If the method converges (i.e. if the error function is driven to a given small value) then the resulting voltage amplitudes and phases approximate the steady-state solution [17], [18].

$$F_{error} = \widehat{I}_k(\omega) + \widehat{I}_k(\omega) \quad \forall k \in [0, \dots, K] \quad (5)$$

Where; N is the number of harmonic, ω is the pulsation of harmonic for each node.

2) Algorithm of Harmonic balance

The procedure of harmonic balance is summarized by the following steps which are shown in Table II:

TABLE II. STEPS OF HARMONIC BALANCE PROCEDURE

Steps	Development
First step	Initial the estimation of $V_0(t)$ (can be also in the frequency domain), we can estimate the initialization of the excitation by pulses with a broad spectral content or by a value equals to zero.
Second step	Apply nonlinearity in the time-domain, $i(t) = F(v(t))$
Third step	Convert the current in the time-domain to the frequency domain by the FFT.
Fourth step	In the frequency-domain, Check if the harmonics are balanced using the cost, (the use of Kirchoff's Current Law equation).
Fifth step	Still in the frequency-domain, If the convergence criteria were not satisfied, updated the voltages using the cost function and its Jacobian. $v(f)^{k+1} = v(f)^k - J^{-1}(v(f)^k)$
Sixth step	Convert the voltage in the frequency-domain to the time-domain by the FFT-1.
Seventh step	Repeat the second step to the sixth step until the convergence is done.

The Harmonic Balance algorithm works as it is illustrated in Fig. 3 [19].

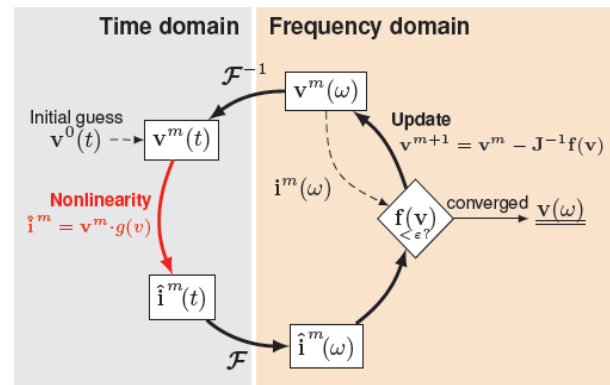


Fig. 3. Algorithm working principle.

III. NEW HYBRID APPROACH FOR NONLINEAR RADIO FREQUENCY CIRCUIT SIMULATION

In this part, we present the new approach of WCIP (hybrid HB-WCIP); it is a combination between WCIP classical and HB that we have proposed as well as their algorithm (hybrid HB-WCIP algorithm).

A. Principle

In the WCIP, a single frequency is used for the linear circuit excitation, so we can say that the wave is defined in space (pixel) and in the frequency at the circuit interface, hence the study is spatial-frequency at the circuit interface. To simulate the non linear circuit, the principle of HB is used to split the circuit into two sub-circuits at its interface; the linear sub-circuit is simulated by the classical iterative method, while the non-linear sub-circuit is solved by a temporal resolution. In this way, we took advantage of the WCIP in the simulation of the linear part of the circuit, and the principle of the harmonic balance in the simulation of the non-linear part.

B. Algorithm

The use of harmonic balance in the wave concept iterative method can be summarized by the diagram illustrated in Fig. 4.

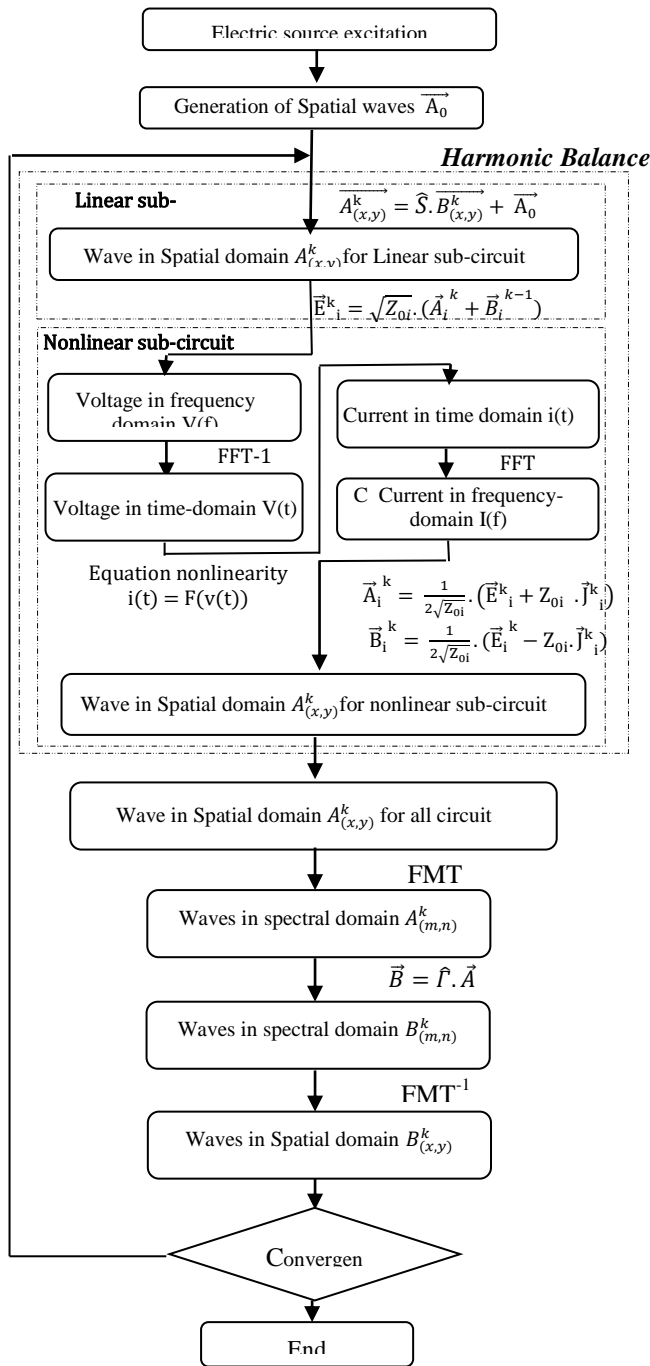


Fig. 4. Harmonic balance – Wave concept iterative process algorithm.

C. Nonlinear Radio Frequency Diode Modeling for Small Signal Regime

As it is noted previously, the modeling of nonlinear sub-circuit that we want to simulate is essential. In this part, we take a diode as an example of a nonlinear sub-circuit, and we propose a diode model that functions in the small signal regime.

The characteristic equation of a diode is given by the following formula [20]:

$$I(V) = I_s(e^{\alpha V} - 1) \quad (6)$$

With: V is the Voltage across the diode junction (volts)

I_s Saturation Current (amperes)

$$\alpha = \frac{q}{\eta \cdot \kappa \cdot T} \quad (7)$$

q is the electron charge = $1.6 \cdot 10^{-19}$ (coulomb),

η is diode Ideality Factor (generally between 1.1 and 1.2)

κ is Boltzmann's constant = $1.38 \cdot 10^{-23}$ (joule/°K),

T is temperature in degrees Kelvin (°K),

Current flowing through the diode obtained by (6) contains two components, alternative $i(t)$ and continuous I_0 , for this the total current $I = I_0 + i(t)$, the same for the voltage, $V = V_0 + v(t)$. Where $v(t)$ is the alternating voltage that consists of n harmonics, hence the formula of the total voltage is as follows:

$$V(t) = V_0 + V_1 \cdot \cos(\omega_0 \cdot t) + \dots + V_n \cdot \cos(n \cdot \omega_0 \cdot t) \quad (8)$$

Where, V_n is the nth harmonic component of the voltage.

In the approximation small signal (i.e.: $i(t) \ll I_0$), the diode current can be developed in Taylor's series:

$$I(V) = I_0 + \frac{V}{1!} \cdot \left. \frac{dI}{dV} \right|_{V_0} + \frac{V^2}{2!} \cdot \left. \frac{d^2I}{d^2V} \right|_{V_0} + \dots + \frac{d^n I}{d^n V} \Big|_{V_0} \quad (9)$$

with

$$\left. \frac{dI}{dV} \right|_{V_0} = G_d, \quad \left. \frac{d^2I}{dV^2} \right|_{V_0} = \alpha \cdot G_d, \quad \left. \frac{d^3I}{dV^3} \right|_{V_0} = \alpha^2 \cdot G_d \quad (10)$$

Where, G_d is the dynamic conductance of the diode junction when the two different frequency voltages are applied across the diode.

The formula of current (9) will be:

$$I(V) = I_0 + G_d \cdot \left(\frac{V}{1!} + \alpha \cdot \frac{V^2}{2!} + \alpha^2 \cdot \frac{V^3}{3!} + \dots + \alpha^{n-1} \cdot \frac{V^n}{n!} \right) \quad (11)$$

To simplify the current (9) we use the Pascal triangle formula (11) to solve the current equation.

$$(a + b)^n = \sum_{k=0}^n C_n^k \cdot a^{n-k} \cdot b^k \quad (12)$$

After calculating, the current formula is described as follows:

$$I(V) = I_0 + G_d \cdot \sum_{k=1}^n \frac{\alpha^{k-1}}{k!} \cdot \left[\dots \left[\sum_{k_{m-1}=0}^{k_{m-2}} C_{k_{m-1}}^{k_{m-2}} \cdot V_{m-1}^{k_2 - k_{m-1}} \cdot V_m^{k_{m-1}} \right] \right] \quad (13)$$

With C_n^m is the coefficient obtained by the Pascal triangle, n is the harmonic number, V_n^m is the nth harmonic component of the voltage for m iterations.

So we can implement this formula in the HB-WCIP algorithm, so that the RF diode can be simulated in the nonlinear regime.

IV. NUMERICAL RESULTS

The validation of the new approach algorithm of WCIP (hybrid HB-WCIP) can be confirmed by the simulation of a diode RF implemented in micro-strip line.

The RF diode model already proposed in Section C of Section III, works in the regime of small signals because we have used Taylor's development. Hence the input power of the source must be low enough to keep this regime.

The micro-strip line is deposited on a relative electric substrate permittivity $\epsilon_2 = 9.6$, thickness 0.635mm, and width $W = 0.375$ mm. The ambient environment is air, therefore the relative electric substrate permittivity $\epsilon_1 = 1$.

The structure shown in (Fig. 5) is enclosed in a box with electrical walls. The box dimensions and heights of the two medium are described as follows:

$$h1 = 4\text{mm}, h2 = 0.635\text{mm}, a = 6\text{mm et } b = 6\text{mm}.$$

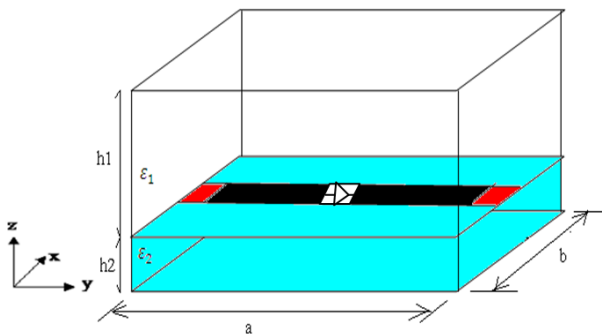


Fig. 5. Radio frequency diode implemented in micro-strip line.

The supply source type of this structure is bilateral and polarized along the axis Ox, and characterized by internal impedance Z0 considered as the paralleling of the characteristic impedances of the two medium in which is delivered, i.e.:

$$Z_0 = Z_{01} // Z_{02} = \frac{Z_{01} \cdot Z_{02}}{Z_{01} + Z_{02}} = 90.57 \text{ Ohm}$$

To stay in small signal regime, we set the power of the source at -20 dbm. The frequency of the source is 2 GHz.

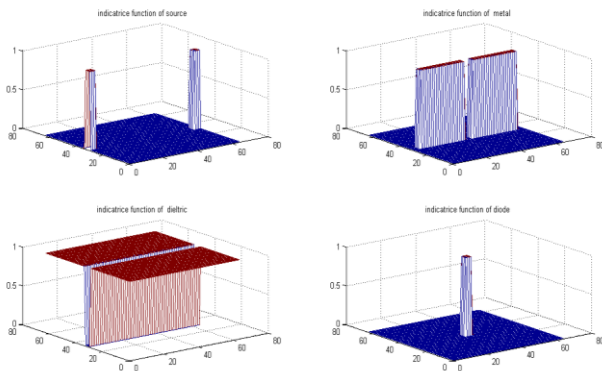


Fig. 6. The indicator functions of all mediums.

A mesh of 64x64 pixels has been chosen to approach the real dimensions (for a good description of the electromagnetic field in the micro-strip line, a mesh of 4 to 5 pixels in the width of the line must be established, one or two pixels for each end describe the boundary conditions, and 1 and more pixels in the middle to express its value inside the line).

The indicator functions of each medium (source, metal, dielectric and diode) are shown in the above (Fig. 6):

The characteristics of the RF diode implemented in the line are described as follows:

Saturation Current $I_s : 5.10 \cdot 10^{-8} \text{ A}$

Diode Ideality Factor $\eta : 1.05$

Temperature T: 300 °K

To validate the results obtained by the new algorithm implementation of WCIP (hybrid HB-WCIP) in Matlab, we compared these results with ADS software. The following figure shows the RF diode simulation implemented in the micro-strip line with these features under ADS software (Fig. 7).

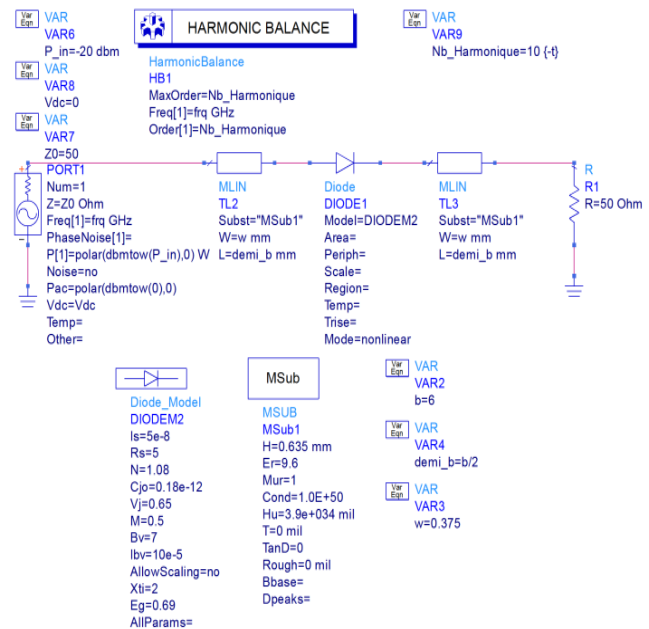


Fig. 7. Simulation by ADS software.

With a maximum harmonic number equals to 5, the implementation results of the new algorithm (hybrid HB-WCIP) as obtained by ADS is described in the following figure (Fig. 8):

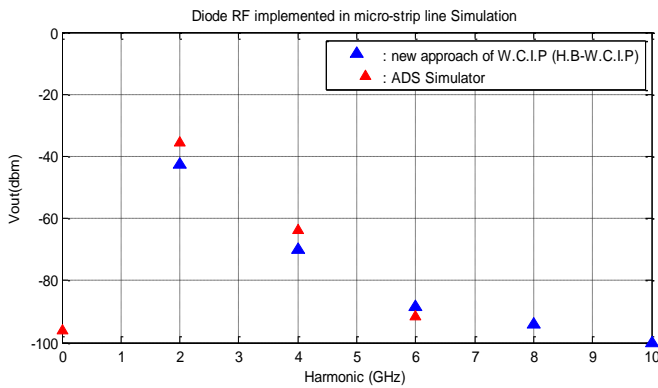


Fig. 8. Radio Frequency diode simulation results implemented in the micro-strip line by the change of the harmonic number used equals to 5.

The figure shows clearly the simulation with the new approach of WCIP (HB-WCIP) and the results obtained by ADS software are comparable, except in the last harmonics (harmonic 4 and 5). This difference comes back to the techniques of analysis used in each method.

A second comparison is needed between the new method (HB-WCIP) and HB implemented under ADS Software to study the convergence of results; the necessary harmonics number to reach a best presentation of the output voltage at the diode. For this, we simulate the RF diode implanted in the micro-strip line by HB.WCIP under Matlab and by ADS software for different number of harmonic.

The following table (Table III) shows the values in dbm of the output voltage harmonics (Fig. 7) obtained by the two methods; HB-WCIP and HB under ADS Software, for the number of harmonic used from 1 to 7.

TABLE III. RF DIODE SIMULATION RESULTS IMPLEMENTED IN THE MICRO-STRIP LINE BY THE CHANGE OF THE HARMONIC NUMBER USED

Number of harmonic used in each simulation		Number of harmonic (dbm)						
		1st	2rd	3rd	4th	5th	6th	7th
1	ADS	-	X	X	X	X	X	X
	HB-WCIP	-	X	X	X	X	X	X
2	ADS	-	-	X	X	X	X	X
	HB-WCIP	-	-	X	X	X	X	X
3	ADS	-	-	-	X	X	X	X
	HB-WCIP	-	-	-87.6	X	X	X	X
4	ADS	-	-	-	-	X	X	X
	HB-WCIP	-	-	-	-96.5	X	X	X
5	ADS	-	-	-	-	-	X	X
	HB-WCIP	-	-	-	-	-	X	X
6	ADS	-	-	-	-	-	-	X
	HB-WCIP	-	-	-	-94.3	-96.5	-	X
7	ADS	-	-	-	-	-	-	-
	HB-WCIP	-	-	-	-94.3	-96.5	-	-

We can consider that the harmonic values of the output voltage less than -100 dbm are negligible noise.

In Table III, we can see clearly that the harmonic values of the output voltage obtained by ADS software are stable at a maximum harmonic number of three, hence three harmonic is necessary to present the output voltage of the diode. While in the HB-WCIP requires a number of harmonic equals to five. On the other hand, the values of the harmonics of the output voltage obtained by the two methods are really comparable between them.

According to the results obtained by the previous simulations, we can conclude that the simulation results are really comparable with those obtained by HB under ADS software. The small difference between the harmonic number is necessary to reach the convergence returns to the techniques of analysis used in each method, as well as WCIP, taking in consideration the box effect, on the other hand ADS neglects this effect.

V. CONCLUSION AND FUTURE SCOPE

In this study, we have started with the presentation of the non-linear circuits' simulation interest, then the advantages and disadvantages of analysis methods of these circuits. After that we have presented the iterative method concept as well as the harmonic balance method. After that, we have proposed a new WICP approach (a hybrid HB-WICP) for the circuit non-linear simulation joined with R.F model diode to validate this approach. The validations are obtained by the comparison of the results obtained by our new hybrid method and HB under ADS software.

Therefore, the future scope of the proposed approach can be developed in the minimization of the time convergence. We can also propose other model of non-linear circuit for small signal regime and also for large signal regime such as transistor, non-linear capacitor.

REFERENCES

- [1] M.B. Stree, "Simulation of nonlinear microwave circuit- an historical perspective and comparisons," 1991 IEEE MTT-S Microwave Symp Dig., vol. 2, pp. 599-602, 1991.
- [2] J. Kunisch, A. Bahr, M. Rittweger, I. Wolff, "Analysis of nonlinear circuits using the compression approach," Proc. IEEE MTT-S Int. Microwave Symp. Digest, pp. 637-640, 1993.
- [3] M. I. Sobhy, E. A. Hosny, M. W. R. Ng, E. A. Bakkar, "Nonlinear system and subsystem modeling in time domain," IEEE Trans. Microw. Theory Tech, vol. 44, no. 12, pp. 2571-2579, Dec. 1998.
- [4] A. Mehrotra, A. Somani, "A Robust and Efficient Harmonic Balance (HB) using Direct Solution of HB Jacobian," In Proc. IEEE/ACM DAC, pp. 370-375, 2009.
- [5] D.Tannir, R. Khazaka, "Efficient Nonlinear Distortion Analysis of RF Circuits," Proc. Design Autom. Test Europe Conf., pp. 1-6, 2007.
- [6] S. Akatimagool, "Fast Iterative Method Package for High Frequency Circuits Analysis," IEEE International Symposium on Circuits and Systems -ISCAS.,pp. 5970-5973, November 2005.
- [7] E. Richalot, M.F. Wong, H. Baudrand, V. Fouad-Hanna, "an iterative method for modelling of antennas," IEEE APS., pp. 194-200, Jan. 2001.
- [8] M. Tellach, Y. Lamhene, B. Haraoubia, H. Baudrand, "An numerical method based iterative process to characterize microwave planar circuits," International Journal of Computing, vol.7, pp. 86-94, August 2014.
- [9] H. Megnafi, N. Boukli hacene, "An Efficient Analysis of Microstrip Trisection Filters Using an Iterative Method Combined by Approach

- Multi-Scale,” International Journal of Electromagnetics and Applications, Vol. 3, No. 2, pp. 9–14, 2013.
- [10] H. Megnafi, N. Boukli hacene, “Analysis of Microstrip Cascaded Quadruplet Filters by a Multi-Scale Wave Concept Iterative Procedure (M.WCIP),” Software Engineering, Vol. 2, No. 4, pp.101–105, 2012.
- [11] H. Megnafi, N. Boukli hacene, N. Raveu, H. Baudrand, “A Monolayer Passive Structure Analysis by WCIP method,”6th International Conference on Sciences of Electronics, pp.212–216, 2012.
- [12] D. Bajon, H. Baudrand, “Application of wave concept iterative procedure (WCIP) to planar circuits,”Microtec’2000, pp. 864–868, 2000.
- [13] H. Trabelsi, A. Gharsallah,H. Baudrand,”Analysis of Microwave Circuits Including Lumped Elements Based on the Iterative Method,” Inc. Int J RF and Microwave CAE, Vol 13., pp 269–275, 2003.
- [14] Nuangpirom, P., Inchan, S. Akatimagool, “Wave Iterative Method for Patch Antenna Analysis,” Applied Mathematics, vol 6., pp. 403–413,2015.
- [15] S. El rabaie, vincent, f.fusco, c. Stewart, “Harmonic balance evaluation of nolinear microwave circuit-A tutorial approach,”I.E.E.E. Transactions on Education, vol. 31, pp. 181–192, 1988.
- [16] M. S. Nakhla, J. Vlach, “A Piecewise Harmonic Balance Technique for Determination of Periodic Response of Nonlinear Systems, ” IEEE Trans. Circuits and Systems, Vol. 23, No.2, pp. 85–91, Feb. 1976.
- [17] R. J. Gilmore, M. B. Steer, “Nonlinear Circuit Analysis Using the Method of Harmonic Balance—A Review of the Art. Part I. Introductory Concepts,” International journal of Microwave and Millimeter-Wave Computer-Aided Engineering, Vol. 1, No. 1, pp. 22–37, 1991.
- [18] J. E. Rayas-Sanchez, F. Lara-Rojo, E. MArtinez-Guerrero, “A linear inverse space mapping (lism) algorithm to design linear and nonlinear RF and microwave circuit, ”IEEE Trans. Microw. Theory Tech., vol. 53, no. 3, pp. 960-968, Mar. 2005.
- [19] L.Hans-Dieter, Z.Xingqi,”The Harmonic Balance Method”, ECE 1254 project report, Spring 2013.
- [20] S. M. Winter, H. J. Ehm, A. Koelpin, and R. Weigel , “Diode Power Detector DC Operating Point in Six-Port Communications,” Proc. European Microwave Conf, pp. 795–798, 2007.

A Solution for the Uniform Integration of Field Devices in an Industrial Supervisory Control and Data Acquisition System

Simona-Anda TCACIUC (GHERASIM)^{1,2}

¹Faculty of Electrical Engineering and Computer Science, Department of Computers

²Integrated Center for Research, Development and Innovation in Advanced Materials, Nanotechnologies and Distributed Systems for Fabrication and Control (MANSiD) Stefan cel Mare University of Suceava, Romania

Abstract—Supervisory Control and Data Acquisition (SCADA) systems are increasingly used solutions for monitoring and controlling various industrial processes. The existence of a large number of communication protocols helps to deploy complex systems that enable users to access data from one or more processes at a certain distance, and even control those processes. This article presents a solution for the uniform integration of field devices in an industrial SCADA system. This uniform integration is based on the CANopen communication protocol and the EDS files containing detailed descriptions of devices in a CANopen network. Based on the information and structure of the EDS files, we have designed and developed a database aimed at storing these data in an organization that enables them to be safely and efficiently processed. This database is the basis of a website application that enables the user to learn the characteristics of the field devices connected to the local industrial networks in a SCADA system.

Keywords—SCADA system; uniform device integration; EDS files; communication protocols; distributed database

I. INTRODUCTION

Once with the development of information technology, more and more automation tools are provided with the help of network functions and intelligent digital processing. These automation tools are used on a large scale in industrial systems. Without the support for device integration technology, many of them are used as traditional tools. Therefore, the International Electrotechnical Commission (IEC) has introduced Electronic Device Description Language (EDDL) [1] and the Field Device Tool (FDT) [2], as two international standards for device integration [3].

This article presents a solution for the uniform integration of field devices in an industrial SCADA system [4]. This uniform integration is based on the CANopen communication protocol [5] and the EDS files which contain detailed descriptions of devices in a CANopen network.

Based on the information and structure of the EDS files, a database has been designed and developed with the purpose to store these data in such a way as to enable their efficient and safe processing. This database is the base for a web-based application that enables the user to discover the characteristics

of the field devices connected to the local industrial networks in a SCADA system.

This article is organized as follows: Section II presents the most important communication protocols and existing technologies for integrating field devices; Section III details the structure of EDS files; Section IV focuses on the design and development of a database for the integration of field devices into a SCADA application; Section V highlights the EDS file management system from a SCADA application, and Section VI concludes the paper.

II. RELATED WORK

SCADA systems are increasingly used solutions for monitoring and controlling various industrial processes. Implementing a SCADA solution involves intensive research regarding the existing models and solutions for integrating various systems in a fieldbus.

The most important technologies for integrating devices into SCADA systems are the following:

- EDDL [6] - is a standard technology launched by IEC for describing the device parameters in a network.
- FDT - is another standard technology [7] launched by IEC, which addresses a different way for the unitary description of field devices in a network.
- FDI (Field Device Integration) - represents the attempt of five well-known foundations to unite EDDL and FDT technologies, with the aim of finding a unified solution for integrating field devices. The five foundations are: FDT Group, Fieldbus Foundation, HART Communication Foundation, PROFIBUS & PROFINET International and OPC Foundation [6].
- EDS (Electronic Data Sheet) - is an alternative to the aforementioned technologies that contains detailed descriptions of devices in a CANopen network. This standard technology has been proposed by CiA (CAN in Automation) [8]. The EDS files are easy to use for integrating the device in a network and have an important role in configuring the CANopen networks [9].

The existence of a large number of communication protocols helps to deploy complex systems that allow users to access data from one or more processes at a certain distance and even control those processes.

Some of the existing and widely used protocols in industry are the following: CAN, CANopen, Modbus, M-bus and ASCII.

CAN - is a standard designed to allow microprocessors and devices in a vehicle to communicate with each other without the need for a host computer. The CANbus protocol is based on messages, being especially designed for applications in the automotive industry. CANbus is one of the five protocols used in OBD-II for standard vehicle diagnosis. It is also used mainly in other areas, such as industrial automation and medical equipment [10].

CANopen - is a communication protocol for embedded systems used in automation. CANopen implements the OSI model, including the network layer. The CANopen standard consists of an addressing scheme, several small communication protocols and an application level defined by the device profile. The communication protocols support the management of the network, the monitoring of devices and node communications, including a simple transport layer for message segmentation and de-segmentation. At lower layers, the physical layer and the data connection, CAN protocol [11] is usually used; even if other devices use other communication methods (Ethernet, Powerlink and EtherCAT for example), these ones can implement the profile of the CANopen devices [12].

Modbus - is a communication protocol based on master-slave or client-server architecture designed by Modicon to be used on its own programmable machines. It became the standard communication protocol used to interconnect electronic industrial devices. Modbus [13], [14] is also often used in data acquisition and control systems (SCADA) to connect a surveillance computer with a remote terminal unit (RTU).

M-bus - is a European standard for remotely reading data from metering devices, sensors or actuators. With the standardization of M-bus [15] as a galvanic interface for monitoring heat meters, this bus becomes quite important in the energy industry.

ASCII (ASCII-based DCON protocol) - is the acronym for American Standard Code for Information Interchange. ASCII is a character encoding system based on the English alphabet. ASCII codes are text characters for computers, communication devices and text-based equipments. Most modern character encoding systems, which represent more than one character, are based on the ASCII code [16].

We can conclude that from all communication protocols presented above, the CANopen protocol represents a complete standard.

Further on, the EDS files will be described in detail.

III. EDS FILES DESCRIPTION

EDS is a device description file structured in six sections, specific to various field devices in a SCADA system [17]. The

format of these files is specified by CiA and contains detailed descriptions of the devices in a CANopen network. All objects and member data of a device are managed in a directory object.

The EDS files are easy to use for integrating the device in a network and have an important role in configuring the CANopen networks.

The six sections of the EDS files are:

- FileInfo
- DeviceInfo
- PdoObject
- SdoObject
- History
- Communication

The **FileInfo** section contains data referring to the EDS file, such as the name, the path where it is saved (FileName), its version (FileVersion), its revision (FileRevision), the time and date when the file was created, as well as the name of the user who modified it. The name of the section is framed in square brackets, making everything more visible and facilitates the identification of each section.

The **DeviceInfo** section describes shortly the vendor, mentioning its name (VendorName) and number (VendorNumber), but also of the supplied product, by name (ProductName), number (ProductNumber); it also contains the revision of the product (RevisionNumber).

The EDS file can contain one or both types of objects in the Object Dictionary, namely PDO (Process Data Object) or SDO (Service Data Object). Therefore, the EDS file can contain both types of sections, **PdoObject** and **SdoObject** or only one of them.

Both sections contain information regarding objects and their member data, the only difference being the type of these objects (SDO or PDO); the name of the section shows this difference.

The two types of specific objects (PDO and SDO) may also contain one or more members. In an EDS file, the member data of an object can easily be identified, by taking into consideration the fact that the suffix "sub" is added to the object name, followed by the number of the data member.

The structure of these sections contains the following fields:

- ObjectName – the name of the object.
- AccessType – type of access (ro - read only, wo - write only, sau rw - read write).
- DefaultValue – the default value of the member data.
- Description – a short description of the member data.
- Type – the data type of the member data.
- LowLimit – the minimum limit taken by a member data.

- HighLimit – the maximum limit taken by a member data.

The **History** and **Communication** sections are optional. Therefore, they may or may not be present in the EDS file.

The **History** section contains only download command templates and response templates, specifying the object to be saved in history.

The **Communication** section also contains the object name, transmission command templates, and response templates.

Further on, the paper presents the design and development of a database for integrating field devices into SCADA applications, based on the EDS files discussed in this section.

IV. DESIGN AND DEVELOPMENT OF A DATABASE FOR INTEGRATING FIELD DEVICES IN SCADA APPLICATIONS

Based on the information and structure of EDS files, a database was designed and developed in Microsoft SQL Server for storing these data in a way that enables them to be managed efficiently and securely. The main objective was to create a web-based software application that would complete the poorly defined protocols, especially to ease the integration of field devices in industrial SCADA applications.

A. Proposed Architecture

Fig. 1 shows the architecture on which the solution proposed in this article is based, namely, the solution for integrating field devices in industrial SCADA applications.

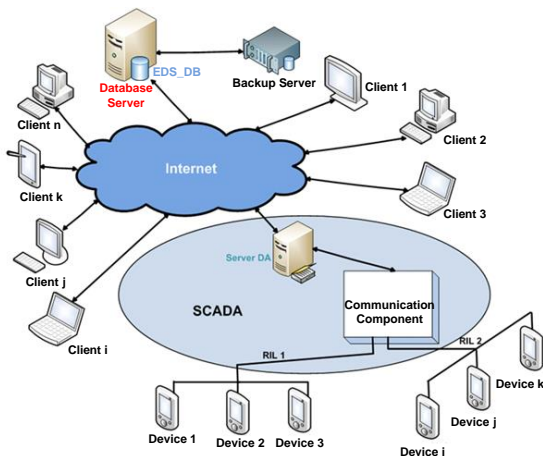


Fig. 1. The architecture of a SCADA system with a distributed database.

B. Structure of the Data Base

The name of the proposed database is EDS_DB (EDS DataBase) and it contains 8 tables, as follows: ObjectMembers, ObjectType, Pdo/SdoObjects, DeviceInfo, FileInfo, Communication, History and Protocol. Fig. 2 shows the EDS_DB Entity-Relationship diagram.

The database size is average. It contains records about devices connected to a local industrial network, data which is structured in the corresponding EDS files. These include: communication protocols used in the local industrial network,

network devices, their objects and member data and the mode of updating objects according to the device protocol.

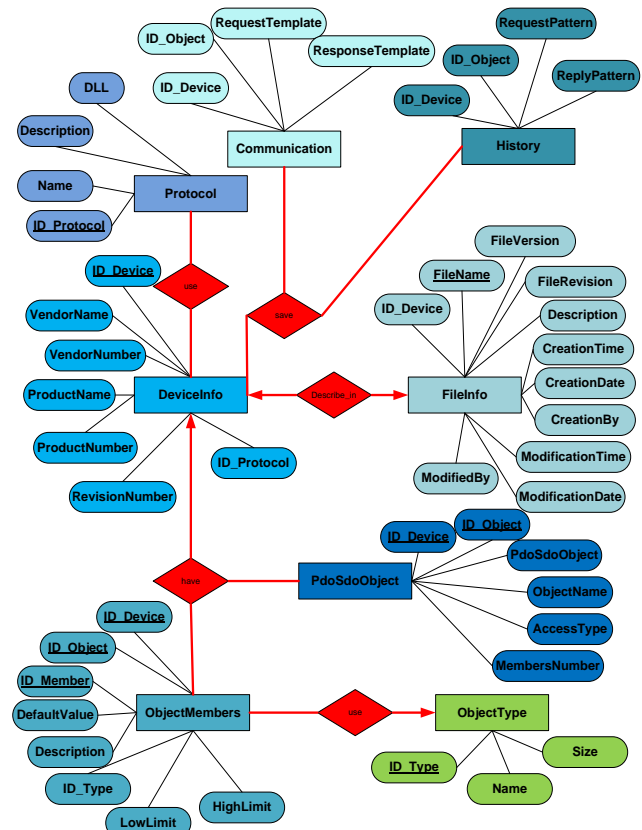


Fig. 2. The EDS_DB Entity-Relationship Diagram

The following section introduces the application regarding “the EDS file management system in a SCADA application”, which brings an improvement to poorly defined protocols, especially for facilitating the integration of field devices in SCADA applications.

V. EDS FILES MANAGEMENT SYSTEM IN A SCADA APPLICATION

This web-based application allows the user to query a centralized database used by the SCADA system to learn the characteristics of field devices connected to local industrial networks.

A. Application Objectives

The application has been developed to meet the following requirements:

- Simplicity.
- High speed and the ability to store a large amount of data.
- Ensuring integrity and confidentiality of data.
- Easy access to data.
- Convenient data entry and editing, as well as easy storage and retrieval.

- Easy data deletion; views updating.
- Local storage of desired data in various formats.
- Dynamic generation of an address space based on all data.

B. Application Structure

The application is built based on the following scenario:

1) Initially, the user must authenticate. *Authentication* is done by entering a user name and a password. By checking the “Keep me logged in” checkbox, the credentials of the user who wants to access the application are saved.

2) Once the user is logged in, he can view the architecture of the SCADA application and read a short description of the management system.

3) The user, can not only view the database scheme, but can also access all entries in the database, classified by protocols, devices, objects, member data and type of objects. For each classification level mentioned above, the user can export data in the following formats: MS-WORD (Microsoft Word), text, MS-EXCEL (Microsoft Excel), PDF (Portable Document Format), XML (Extensible Markup Language), CSV or EDS.

4) At a given moment, the user has the possibility to view the following:

- all data in a single table,
- only certain data of interest in a table, according to various criteria, or
- data from more tables.

5) Depending on the user’s rights in the application, he has the possibility to insert new data in the database.

The insertion of new data can be done in two ways:

- by directly adding data in the “EDS file management system in a SCADA application”,
- by importing EDS files, Excel files or each other.

6) Depending on the user’s rights in an application, he can delete or modify certain data in the database. Fig. 3 shows this process.

	ID_Device	PdoSdoObject	ID_Object	ObjectName
Edit Delete	0000003F00000451	Sdo	1000	1000-Device Type
Edit Delete	0000003F00000451	Sdo	1001	1001-Error Register
Edit Delete	0000003F00000451	Sdo	1003	1003-Pre-defined Error Field
Edit Delete	0000003F00000451	Sdo	1005	1005-COB-ID SYNC
Edit Delete	0000003F00000451	Sdo	1007	1007-Synchronous Window Length
Edit Delete	0000003F00000451	Sdo	1008	1008-Manufacturer Device Name
Edit Delete	0000003F00000451	Sdo	1009	1009-Manufacturer Hardware Version
Edit Delete	0000003F00000451	Sdo	100A	100A-Manufacturer Software Version
Update Cancel	0000003F00000451	Sdo	100C	100C-Guard Time
Edit Delete	0000003F00000451	Sdo	100D	100D-Life Time Factor

Fig. 3. The capture with data modification.

7) The “Save Data” menu allows the user to easily navigate to certain data of interest, and select them to be saved. There is a possibility to select all data (by checking the All check box) or only a part of them.

8) The “Address space” menu enables the user to easily navigate through the address space dynamically generated based on all data in the database.

9) The user can save his address space at a certain time. Data will be stored in a file with the “*.xml” extension, as shown in the following figure. Based on this XML file, the user will upload a new hierarchical tree and will be able to track changes over time regarding the hierarchy of the address space. Thus, the user will be able to decide whether new communication protocols or network devices, or even new objects or member data have been added. This is highlighted in Fig. 4.

Fig. 4. The capture with Address Space.

VI. CONCLUSIONS

The SCADA systems are increasingly used solutions for monitoring and controlling various industrial processes. The existence of a fairly large number of communication protocols helps to deploy complex systems that enable users to access data from one or more processes at a certain distance, and even control those processes.

This article proposes a database model that unitarily describes field devices, with the purpose of integrating them into SCADA applications, based on EDS files for protocols such as: Modbus, CANopen, ASCII, M-bus and Simulator. The database has been developed and populated with EDS files defined by the server’s communication component, and will be integrated into a SCADA system that uses OPC Unified Architecture as middleware. The modifying or addition of a single device can be viewed in the developed database, this

being done without redundancy, as the database is centralized on the server.

The presented web application allows efficient and secure handling of the data stored in the database. With a friendly interface, the application allows not only easy data access, but also easy data entry and editing, as well as easy storage and retrieval. The user can easily delete or update certain data in the database (provided that he has these rights), but also locally save the desired data in different formats.

The most important feature of this application is the dynamic generation of an address space based on all centralized data in the database. Presented as an hierarchical tree, the dynamically generated address space can be saved in XML files. Thus, it is possible to keep track of the changes over time regarding the hierarchical model of the address space.

As future research directions, we want to extend this solution for uniform integration of field devices with the communication protocols used by the new smart devices in the industrial environment.

REFERENCES

- [1] Kofi Atta Nsiah, M. Schappacher and A. Sikora, "Dynamic mapping of EDDL device descriptions to OPC UA," *Journal of Physics: Conference Series*, DOI: 10.1088/1742-6596/870/1/012006, vol. 870 no. 012006, 2017.
- [2] S. Smith, A. Acharya and G. Matzko, "Incorporating FDT/DTM technology into a native control system monitoring application," US Grant, no. US9628341B2, April 2017.
- [3] Bang-teng Li, Yi-ding Yuang, Ze Dong and Ping Ma, "The Design and Development of Interpretation and Execution Program for EDDL," *Proceedings of The 2th International Conference on Computer Science and Technology*, ISBN: 978-1-60595-461-5, DOI: 10.12783/dtcese/cst2017/12494, pp 114-120, 2017.
- [4] P. Church, H. Mueller, C. Ryan, S. V. Gogouvitis, A. Goscinski and Z. Tari, "Migration of a SCADA system to IaaS clouds - a case study," *Journal of Cloud Computing: Advances, Systems and Applications* (2017)6:11, DOI: 10.1186/s13677-017-0080-5, 2017.
- [5] S. C. Joseph, S. Ashok and P. R. Dhanesh, "An effective method of power management in DC nanogrid for building application," 2017 IEEE International Conference on Signal Processing, Informatics, Communication and Energy Systems (SPICES), India, DOI: 10.1109/SPICES.2017.8091303, ISBN: 978-1-5386-3865-1, 2017.
- [6] J. Hodges, K. Garcia and S. Ray, "Semantic Development and Integration of Standards for Adoption and Interoperability," *Computer*, Volume 50, Issue 11, ISSN: 0018-9162, pp. 26-36, November 2017.
- [7] A. J.C. Trappey, C. V. Trappey, U. H. Govindarajan, A. C. Chuang and J. J. Sun, "A review of essential standards and patent landscapes for the Internet of Things: A key enabler for Industry 4.0," Elsevier, *Advanced Engineering Informatics*, ISSN 1474-0346, volume 33, pp. 208-229, 2017.
- [8] R.van Mil, "Interoperability and Intuitive Controls for Smart Homes," Springer International Publishing Switzerland, J. van Hoof et al. (eds.), "Handbook of Smart Homes, Health Care and Well-Being", DOI 10.1007/978-3-319-01583-5_23, ISBN: 978-3-319-01584-2, pp. 325-333, 2017.
- [9] A. Graf-Brill, A. Hartmanns, H. Hermanns and S. Rose, "Modelling and certification for electric mobility," 2017 IEEE 15th International Conference on Industrial Informatics (INDIN), DOI: 10.1109/INDIN.2017.8104755, ISBN: 978-1-5386-0838-8, 2017.
- [10] A. Scholz, T.-H. Hsiao, J.-N. Juang and Claudiu Cherciu, "Open source implementation of ECSS CAN bus protocol for CubeSats," Elsevier, *Advances in Space Research*, ISSN 0273-1177, 2017.
- [11] J.Brindha and V. Vijayakumar, "Proximity Sensors Based Marine Engine Fault Detection Using CAN Protocol," *Indonesian Journal of Electrical Engineering and Computer Science*, volume 9, no. 3, ISSN: 2502-4752, DOI: 10.11591/ijeecs.v9.i3.pp619-623, 2018.
- [12] M. Nicola, D. Sacerdotianu and A. Hurezeanu, "Sensorless control in multi-motors electric drives with high dynamic and flexible coupling," 2017 International Conference on Modern Power Systems (MPS), ISBN: 978-1-5090-6566-0, DOI: 10.1109/MPS.2017.7974386, 2017.
- [13] Sh. Sh. Khuzyatov and R. A. Valiev, "Organization of data exchange through the modbus network between the SIMATIC S7 PLC and field devices," 2017 International Conference on Industrial Engineering, Applications and Manufacturing (ICIEAM), DOI: 10.1109/ICIEAM.2017.8076369, ISBN: 978-1-5090-5649-1, 2017.
- [14] Bo Li, Geng Chen, Le Wang and Zhe Hao, "Tower Crane Remote Wireless Monitoring System Based on Modbus/Tcp Protocol," 2017 IEEE International Conference on Computational Science and Engineering (CSE) and Embedded and Ubiquitous Computing (EUC), DOI: 10.1109/CSE-EUC.2017.217, ISBN: 978-1-5386-3222-2, 2017.
- [15] K. Zeman, P. Masek, J. Krejci, A. Ometov, J. Hosek, S. Andreev and F. Kroepfl, "Wireless M-BUS in Industrial IoT: Technology Overview and Prototype Implementation," *European Wireless 2017, Proceedings of 23th European Wireless Conference*, ISBN: 978-3-8007-4426-8, 2017.
- [16] D. C. Cohen, J. S. Spitaels and D. J. Smith, "Communication protocol and method for authenticating a system," US Grant no. US9660808B2, May 2017.
- [17] V. G. Gaitan, I. Ungurean, N. C. Gaitan and V. Popa, "Keeping industrial systems and communicators up-to-date using interoperable communicating components and electronic data sheets," *IEEE EUROCON 2009*, St.-Petersburg, Russia, pp. 371-378, doi: 10.1109/EURCON.2009.5167658, 2009.

An Efficient Mechanism Protocol for Wireless Sensor Networks by using Grids

Emad Ibbini, Student Member, Kweh Yeah Lun, Mohamed Othman, Zurina Mohd Hanapi, Nonmembers
University Putra Malaysia (UPM), Malaysia

Abstract—Multilevel short-distance clustering communication is an important scheme to reduce lost data packets over the path to the sink, particularly when nodes are deployed in a dense WSN (wireless sensor network). Our proposed protocol solves the problems of single hop paths in the TDTCGE (two-dimensional technique based on center of gravity and energy) method, which addresses only single-hop problems and does not minimize distances between nodes by using multi-hop nodes with multilevel clustering grids to avoid dropped packets and to guarantee reliable paths without failures. In multilevel clustering grids, transmitted data are aggregated from lower-level grids to upper-level grids. In this paper, the proposed protocol obtains the optimal path for data transmission between cluster heads and the sink for heterogeneous WSNs. The cluster head nodes play an important role in forwarding data originating from other normal nodes that aggregate data to upper clusterheads. This routing approach is more efficient than other routing approaches, and it provides a reliable protocol for avoidance of data loss. In addition, the proposed protocol produces sleep and wakeup signals to the nodes and cluster heads via an MD (mediation device), thereby reducing energy consumption. Simulation results demonstrate the efficiency of the proposed method in terms of fewer dropped packets and high energy efficiency. The network environment overcomes the drawbacks of failure paths and provides reliable transmission to the sink.

Keywords—Multilevel; WSN; reliable; heterogeneous; routing

I. INTRODUCTION

Wireless sensor networks (WSNs) have many applications in fields such as agriculture, medical care and health care depending on the type of sensors installed. WSNs are crucial for gathering information necessary for smart devices that are part of pervasive computing, which is utilized in buildings, transportation and industrial systems. A pervasive sensor network consists of individual nodes (sensors) that can interact with the environment by sensing certain physical parameters. All sensor nodes generally have the same task. To complete their tasks, collaboration among nodes is required. Given that sink nodes can occasionally be outside the network, the data collected by sensors are transmitted to sink nodes that are part of the network. Sensors and sinks exchange packets through wireless communication.

Nodes cannot be connected easily to a wired power supply in many WSN applications; the nodes instead depend on onboard batteries [2]. In such cases, the energy efficiency of communication protocols is a crucial concern (i.e., figure of merit) because extended operation time is necessary. In other applications, power supply may not be a problem;

consequently, other metrics (e.g., the accuracy of the delivered results) may be more relevant than energy efficiency.

A sensor is equipped with a radio transceiver or another wireless communication device that transmits and receives data over a wireless channel. A sensor also has a controller for manipulating data and memory for storing software and temporary data. A sensor commonly uses a battery as its energy source.

The concept of a WSN is based on a simple equation [3]: Sensing + CPU + Radio = many applications. However, to create an effective WSN, the combination of sensors, radios, and CPUs requires in-depth understanding of the capabilities and limitations of hardware components and networks. WSNs face several problems that may not occur in other types of networks. Power constraints are a major concern. Communication is the most energy-intensive task a node performs. Nodes must compete for a share of the limited bandwidth available. Networking protocols attempt to reduce energy consumption by two means: neglecting certain communication tasks or turning off the radio transceiver when communications are unnecessary [1].

WSNs combine the latest advances in low-power micro-sensors and short-range wireless radios to yield an attractive new technology. WSNs enable a number of sensing and monitoring services in vital areas such as industrial production, home security and in traffic and environmental monitoring. In addition, some of nodes be in sleep mode most of time to save energy as B-Mac [19].

The proposed protocol is an efficient Clustering Protocol for Heterogeneous energy nodes which divided into levels. There are many examples of Heterogeneous Oblivious Protocols, some of these examples Sep Protocol, ECHERP Protocol, Evolutionary Algorithms (EAs) and EECB (Energy-Efficient Chain-Based routing protocol) [13]-[18].

The rest of the manuscript provides some of the related works and describes the methodology of the proposed protocol then discusses the results with conclusions.

II. LITERATURE REVIEW

The proposed protocol is compared with the TDTCGE [7] protocol.

- Two-Dimensional Technique based on Center of Gravity and Energy (TDTCGE) [7].

This protocol uses two-dimensional techniques. The centers of gravity and energy for each grid are computed. The

optimal node is selected to be the cluster head (CH) because this node is the nearest to one of the centers. The TDTCGE protocol addresses the distance problem, particularly the distance of the CH from the BS. However, the problem of idle listening is overlooked. The results of this protocol indicate that both the lifetime and energy consumption are enhanced.

- In CRCWSN [8] this protocol uses two different techniques for selecting cluster head (CH) that has been initially used by genetic algorithm and re-clustering technique.

A. Network Model

For this study, we randomly deploy N sensor nodes in a monitored area and assume that the sensor network has the following characteristics:

- 1) The position of the BS in the sensor network is fixed.
- 2) All nodes are heterogeneous and stationary and have different initial supplies of energy.
- 3) All the nodes are randomly deployed in the target area, and each can establish a connection with the sink.

B. Energy Consumption

LEACH [4], [5] includes a first-order radio model that can be utilized for calculating hardware energy dissipation. For comparative purposes, this paper uses the same model. In this model, the energy consumptions of radios for sending and receiving data are both expressed as E_{elect} ; the free space and the multi-path fading channel models with respective amplifying indexes ϵ_{fs} and ϵ_{mp} are used; the energy consumption of data fusion is denoted by EDA [9]-[11]. The energy spent by a node that transmits an l-bit packet over distance d is calculated using the Heinzelman model. This model states that for each node to transmit L bits of data a distance d from itself, E_t energy is consumed:

$$E_t = L * E_{elect} + L * \epsilon_{mp} * d^4 \quad d \geq d_0. \quad (1)$$

$$E_t = L * E_{elect} + L * \epsilon_{fs} * d^2 \quad d < d_0. \quad (2)$$

The energy required to receive L bits of data equals.

$$E_r = L * E_{elec}. \quad (3)$$

The parameters are defined as follows:

d_0 : crossover distance

E_{elect} : energy necessary for activating electronic circuits

ϵ_{mp} , ϵ_{fs} : sensitivity and noise in the receiver, respectively.

III. PROPOSED PROTOCOL

In the proposed protocol, the target area is divided into grids, with each grid consisting of a cluster. Using grids reduce distance between nodes within cluster. Each cluster has a CH and connected member nodes. A mediation device (MD) node also exists which is intelligent device [6]; this node schedules and manages the nodes and CH. After performing its task, the MD node synchronizes the nodes and the CH. This node mostly keeps the CH and other nodes in sleep mode. The CH is awakened only for a short time to receive packets. The CH aggregates the data from the nodes and

transmits them to the BS (see Fig. 5). Nine grids are established to ensure a high transmission data rate and to minimize the overall overhead.

The WSN environment is separated into 9 grids in the proposed protocol. Each grid consists of two dimensional centers (centers of gravity and energy). These two points are computed in each grid using the following two formulas (center of gravity and energy center) (see (1), (2), (3), (4)):

$$X_{gc} = (x_1m_1 + x_2m_2) / (m_1 + m_2) \quad (1)$$

$$Y_{gc} = (y_1m_1 + y_2m_2) / (m_1 + m_2). \quad (2)$$

If there are more than two object masses, then the formulas are represented as follows:

$$X_{gc} = \frac{\sum (X - \text{coordinate}(\text{node}) * \text{node} - \text{mass})}{\text{all Mass}}. \quad (3)$$

$$Y_{gc} = \frac{\sum (Y - \text{coordinate}(\text{node}) * \text{node} - \text{mass})}{\text{all Mass}}. \quad (4)$$

The center of energy for each grid is obtained by calculating the center of energy for the two (or more) points.

a) $\sum (X - \text{coordinate}(\text{node}) * \text{node} - \text{mass}) / \text{node} - \text{count}$

b) $\sum (Y - \text{coordinate}(\text{node}) * \text{node} - \text{mass}) / \text{node} - \text{count}$

The proposed protocol has the following rules:

CH: a super node that organizes all the nodes and aggregates data.

Centers of gravity and energy: center points used for reducing the distances between the nodes and CH to choose the optimal CH.

MD node: inelegant node that synchronizes the nodes and CH.

By calculating the formulas for each center, the dimensional centers are included in each grid.

The center of gravity pertains to the average point of the object weight [17] (see Fig. 1).

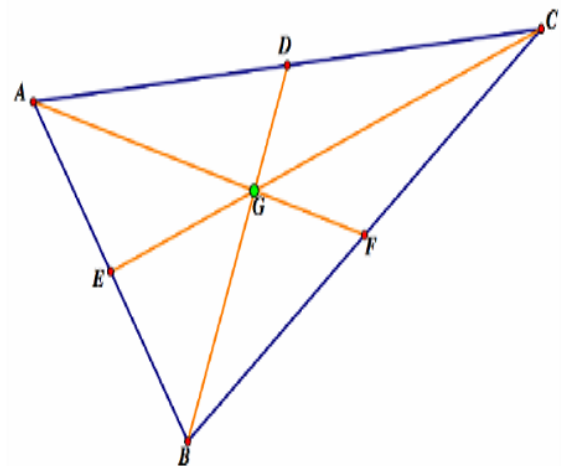


Fig. 1. Center of gravity.

The proposed GMD protocol has two phases: setup and steady state. In the former, the network is divided into nine grids that result in four clusters. Each cluster has two centers (gravity and energy), one CH, and undetermined nodes with different energies. An MD node is also present in each grid (see Fig. 2).

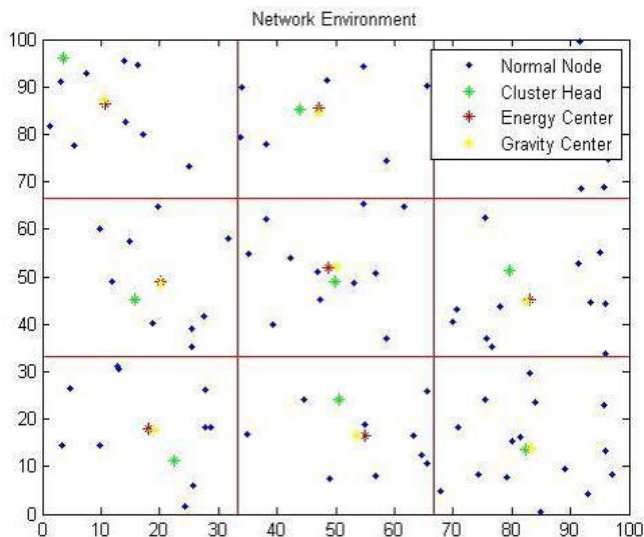


Fig. 2. Network environment.

A. Setup Phase

In the setup phase, the nodes are distributed randomly in the grids. After setup, the sink and centers are identified along with the CH. The node closest to the sink and the energy center is selected as the CH. The center of gravity should also be the closest to the BS for the node to be the CH. If the node is far from the center of gravity but is the closest to the center of energy, it can be the CH. If this center is also the nearest to the BS, then the node that has the most energy is the CH. The proposed Protocol has three types of CHs in each level: normal, advanced, and super CH's. The ranking of CHs is according to the distance of the nodes from the BS and how close the heterogeneous nodes are to the energy center; the node that has the most energy is the CH. The weights of normal CHs are accordingly less than the weights of advanced CHs and super CHs.

B. Steady-State Phase

In the steady-state phase, the BS broadcasts the address and ID number of each node. An MD node that works as a node mediator is present in each grid. This node is responsible for scheduling, managing the suggested routing protocol, and treating the synchronization operations between the nodes and the CH. The MD node performs its operations in the grids in two cases: when the nodes have no data and when they have data.

Case 1: If nodes in each grid have no data to send to the CH, then the MD node keeps the nodes and the CH in sleep mode most of the time by transmitting a sleep signal (see Fig. 3).

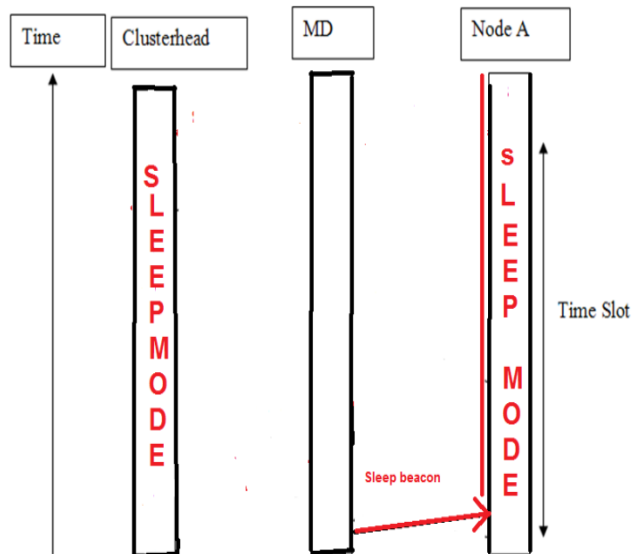


Fig. 3. Case 1: No Data.

Case 2: If new data must be received, the MD node sends a wake-up signal to the nearest node. The wake-up signal is also sent to the CH. The CH and the nodes are in sleep mode most of the time. To receive data, they wake up for a short time. The MD node produces a binary digit "0" for sleep to nodes which doesn't have data and "1" for wake up to nodes have data notify that MD node is intelligent device. The nodes then wait for their time slots to transmit data on their time-division multiple accesses (TDMA) [12] schedule. In this schedule, the nodes that have data when the binary digit is "1" are prioritized. Accordingly, the MD node transmits a wake-up signal to the nearest node up to the farthest one to minimize the delay in sending data and simultaneously save energy (see Fig. 4).

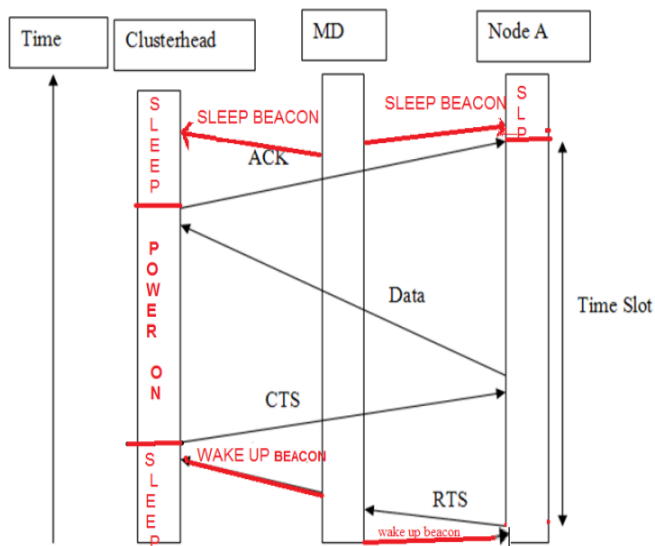


Fig. 4. Case 2: With Data.

The MD node creates a wake-up signal containing the address of the node that must transmit a packet. The signal is passed to the CH, which in turn responds by transmitting a

clear-to-send (CTS) signal to the source node. The source node then transmits the data directly to the CH. After receiving the data, the CH sends an acknowledgment back to the source node A, thus signaling that the transmission is completed. According to Fig. 3, in this proposed study there is multilevel clusterheads and Multilevel MD (see Fig. 5).

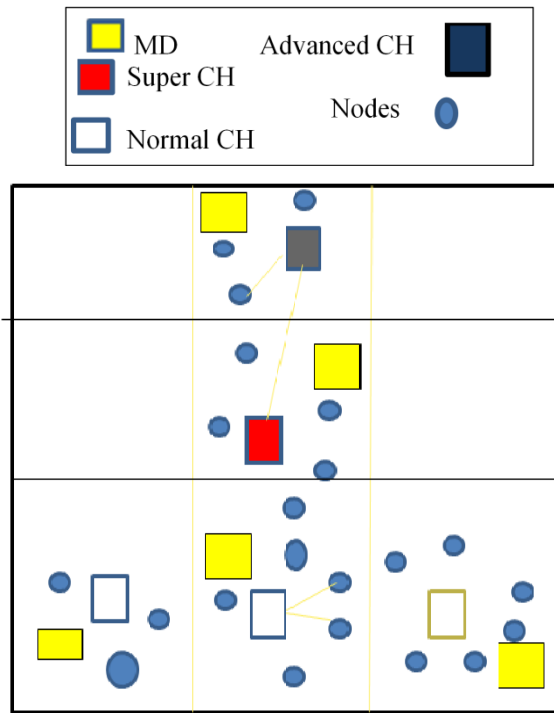


Fig. 5. Multilevel clusterhead grids.

In the first level, the normal CH aggregates the transmission data from normal nodes; this occurs after the MD node lets the nodes sleep most of time unless they have data. When the nodes have data, the MD will wake them up and refer them to the normal CH. All normal CHs will forward the data to the advanced CH; this also aggregates data from its cluster nodes. The MD node then lets normal CHs return to sleep mode. The advanced CH will then forward the aggregated data to the super CH, which will transmit them to the BS. To overcome the above problem, an efficient multi-hop heterogeneity protocol is proposed to obtain an optimal path with no failures or dropped packets between the CHs and the BS during data transmission. This will reduce the transmission path instead of transmitting directly from a normal CHs to the BS, as in the TDTCGE protocol. The second level advances cluster head nodes, which are allowed to communicate with the third level super cluster head node in its TDMA time slot; the same is followed for level 1 nodes to level 2 CHs. In level 2, the advanced CH node performs data aggregation to remove replicate data. In level 2 node sends, the aggregated data advance to the level 3 CH in its TDMA time slot. In level 3 super CH nodes, the data use network coding; they are forwarded to the sink. Owing to a multi-hop link [20] between level 3 CHs, data forwarded to the sink increase the network traffic. The network environment overcomes the disadvantages and provides reliable transmission to the sink.

SETUP PHASE

Algorithm:

```

Divide the network into two grids.
Find the center of gravity for each grid.
1. If node-count = 1
a. The node that is nearer to BS participates in the grid computation.
2. If node-count > 1
a. allMass = calculate sum of the masses of all nodes in grid
b.
b. sum (X-coordinate(node) * node-mass) / allMass
c. sum (Y-coordinate(node) * node-mass) / allMass
3. Find the center of energy for each grid.
1. If node-count = 1
a. The node that is nearer to BS participates in grid computation.
2. If node-count > 1
a. sum (X-coordinate(node) * node-mass) / node-count
b. sum (Y-coordinate(node) * node-mass) / node-count
4. If Distance (normal nodes) <= distance(center of energy, BS),
A. select most energetic node as Normal CH
5. else If (Advanced nodes< Advanced CH)
A. Select Advanced node as Advanced CH.
Else
B. Select Advanced node as Super CH
    
```

STEADY PHASE:

Algorithm:

Steady State Phase: Algorithm

```

Repeat 1. If the node is normal
MD broadcasts IP address and ID number to all nodes
If node = data
MD produces wake-up signal
If Distance(node<=CH)
Node sends RTS to CH
CH sends CTS to node
Node sends data to CH
CH sends acknowledgment to nodes
Flag=1
a. node-energy = node-energy – consumed energy when sending a message
2. Otherwise
a. node-energy = node-energy – aggregated energy – consumed energy )when sending a message until no node has energy(
B. (Advanced-CH) = Node-energy+ Normal CH-energy
C. (Super-CH)=(Advanced-CH)+(Advanced-Nodes-energy)
    
```

IV. PERFORMANCE MEASUREMENT

The performance of the proposed protocol can be evaluated with a number of metrics.

A. Performance Evaluation

- **Energy Consumption:** The total numbers of energy consumed for packets transmitted and packet received during the rounds.
- **Throughput:** It measures the total data rate sent over the network, including the data rate sent from CHs to the sink node and that sent from the nodes to their CHs.
- **Packet loss:** Many causes of data loss would be bit errors in an erroneous wireless network or collisions due to network congestion when the channel becomes overloaded or large distance path to base station.

B. Results and Discussion

TABLE I. SIMULATION PARAMETER

Parameter	Value
Network size	100*100 m
Ee	50nJ/bit
Tevent_all	(randi(9,1,m)+1)*1*10 ⁻³ m
T	10
Pactive	6*10 ⁻³ mw
Tdown	1*10 ⁻³ m
Psleep	1*10 ⁻³ mw
L	1000 bit
Do	87m
Grids Number	4
Mp	0.0013 *10 ⁻⁹
Fs	10*10 ⁻⁹
Position of BS	(75,125)
Number of nodes	100

We use these parameters from Table I in matlab simulation to evaluate the MD Multilevel Proposed Protocol with MD one level and TDTCGE Protocol.

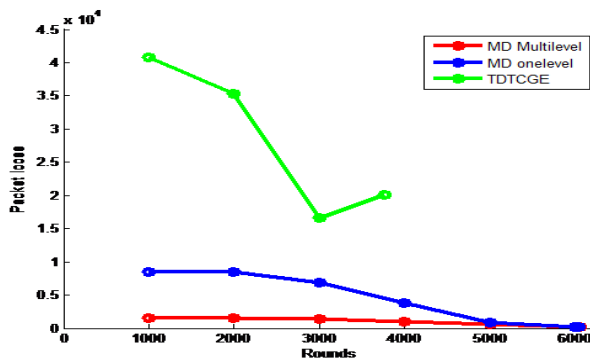


Fig. 6. Drop packets during rounds.

From Fig. 6, we can observe that the Proposed MD multilevel protocol is more reliable than MD onelevel protocol and TDTCGE which is the least of dropping packets between these two existing protocols. The percentage of errors with

dropping packets during rounds for each protocol is 35% to MD Multilevel, 45% to MD one level and 65% to TDTCGE. The MD multilevel obtain the optimal path for data transmission to reach the base station to avoid loose date and guarantee reliable paths without failures.

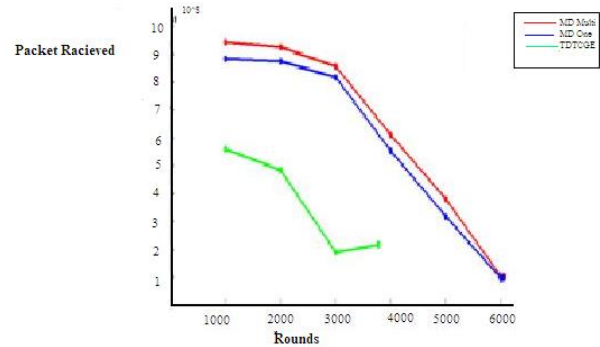


Fig. 7. Number of messages received during rounds.

From Fig. 7, we can observe that the Proposed MD multilevel protocol is more efficient than MD onelevel protocol and TDTCGE. The large volume of successfully messages received to BS by MD multilevel protocol more than these two existing protocols. The received successfully messages by MD-multilevel is 9.5*10⁴, MD-onelevel is 8.7*10⁴. The MD multilevel obtains the optimal path for data transmission to reach the base station.

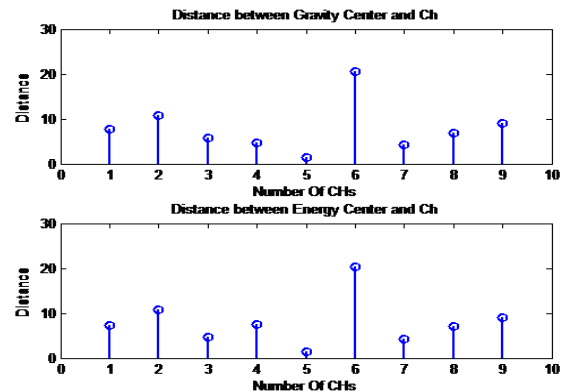


Fig. 8. Distance for MD (multi).

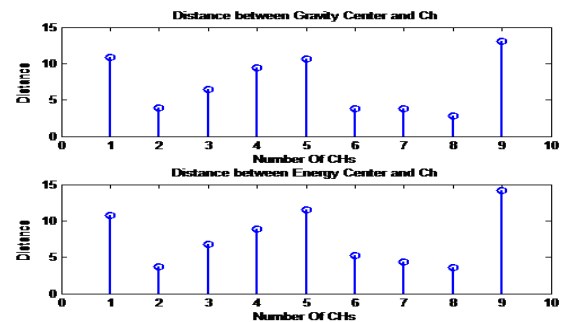


Fig. 9. Distance for MD (one level).

We observe from Fig. 8 and 9 above that for the MD multilevel protocol, all the clusterhead candidates were near

the energy center points except for one candidate, CH6. However, in the MD-one level protocol, all clusterhead candidates were near except three: CH1, CH5 and CH9. Thus, the MD-multilevel protocol was more precise in choosing an efficient clusterhead.

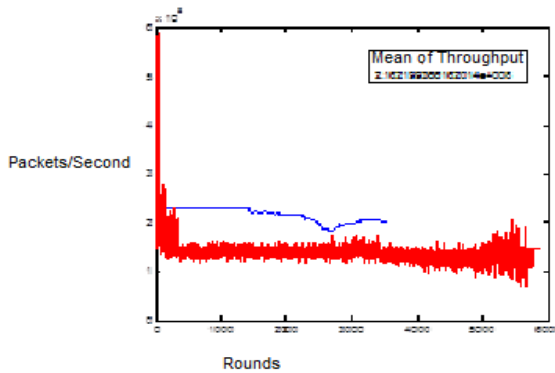


Fig. 10. Mean of throughput.

Fig. 10 compares the throughput values of the MD-one level protocol and the proposed MD multilevel protocol using nine grids for both. A long transmission time implies a low throughput. A large throughput represents a large number of messages delivered per unit time, regardless of whether the delivery was successful, i.e., $\text{Throughput} = (\text{Size of the packet} / \text{Transmission time})$. The TDTTCGE protocol requires a long time to send data to the BS, and it uses nine grids that result in a small throughput. This is due to the small number of nodes in each grid. The time required to reach the BS is thus reduced. The number of data packets received by the BS per unit time in the proposed MD protocol is greater than that received by the BS per unit time in the MD-one level protocol. The proposed protocol exhibits a higher mean throughput than the TDTTCGE protocol. The mean throughput of the latter is 2.1621×10^8 , whereas that of the former is 2.5×10^8 (see Fig. 11).

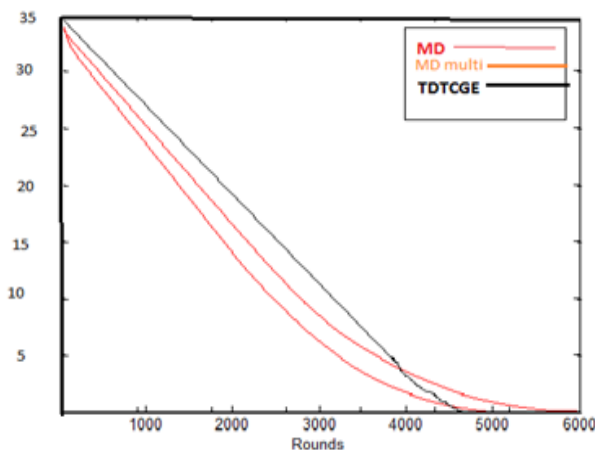


Fig. 11. Energy consumption.

Fig. 11 reveals that the proposed MD-multilevel protocol conserves more energy than the TDTTCGE protocol. The former consumes 34 Joules in 5900 rounds, whereas the latter

consumes 35 Joules in 4880 rounds. However, the MD-one level protocol saves more energy than the MD-multilevel and TDTTCGE protocols; it consumes 33 Joules in 6050 rounds.

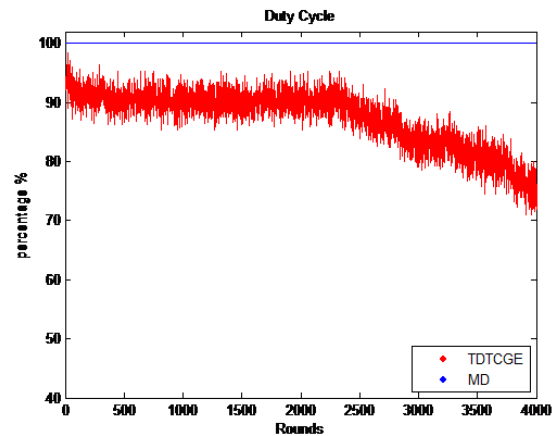


Fig. 12. Duty cycle.

The duty cycle in Fig. 12 pertains to the ratio of time, a node is in the active mode to the entire operational time. WSNs are typically engineered with low duty cycles to guarantee long node and network lifetimes. Therefore, most of the time, the nodes are in extended sleep modes with their radios turned off. Duty cycling limits the number of nodes that synchronously overhear a packet. Thus, the spatial reuse in the forwarding process is restricted. For the proposed and TDTTCGE protocols, the resulting duty cycle for the given nodes was 80%–90% during all rounds (see Fig. 12). The average duty cycle for all nodes was 85%. The average duty cycle was 100% and 95% for the first 400 rounds and for rounds 401–2300, respectively. This percentage then decreased from 95% to 75% at 4000 rounds.

V. CONCLUSIONS

The proposed protocol is more reliable than existing protocols for multilevel heterogeneous WSNs. Comparing TDTTCGE, MD-one level and MD-multilevel protocols, the proposed protocol was evaluated in terms of the messages received by the sink and the network lifetime. The proposed MD-multilevel protocol is well organized in establishing multi-hop communication within grids using link path correlation along with the TDMA time slot. Moreover, multi-hop communication between cluster heads is well controlled by the MD node. Because heterogeneous nodes are usually chosen as clusterhead candidates, incorporating energy-consuming tasks on those nodes increases the number of messages received by the network sink. The simulation results illustrate the efficiency of the multilevel MD protocol compared with the existing protocols in terms of reducing both the energy consumption and the number of dropped packets and hence guarantee the reliability of the proposed multilevel protocol to deliver data without failure.

VI. FUTURE WORK

In the future Research Plans that how to mix fuzzy logic system with MD node and adding grids and Centres. We highlight some interesting on the future research directions:

- Currently, the proposed protocols designed mainly to solve this problem as idle listening and delay with throughput by adding MD node alone also adding Mathematical model will improve the lifetime of the network 90% than TDTCGE.
- In addition, in the Proposed Schemas we will add fuzzy logic with three criteria's to the grids and Centers that the proposed schema minimize the distance and saving more energy which give us a better energy efficiency than TDTCGE Protocol.
- Furthermore, when we plan to mix Fuzzy logic with MD node and adding mathematical model to the grids and Centres which that solve all the problems in this research .in addition, solving the problems of reliability and collisions.

REFERENCES

- [1] David Culler, Deborah Estrin, "Overview Of Sensor Network", Published By IEEE International Conference On Robotics And Automation, 5, 201-290,2004.
- [2] Holger Karl, Andreas Willing, "Protocols And Architecture For Wireless Sensor Network", John Wiley & Sons, 2005.
- [3] Jason Lester Hill, "System Architecture For Wireless Sensor Networks", University Of California, Berkeley, 2003.
- [4] Wei Ye, John Heidmann, Deborah Estrin, "An Energy-Efficient MAC Protocol For Wireless Sensor Network", Information Science Institute (ISI), University Of Southern California. In Proceedings Of The IEEE Infocom, 1567-1576, 2002.
- [5] Wendi Heinzelman, AnanthaChandrkasan, Hari Balakrishnan, "Energy-Efficient Communication Protocol For Wireless Microsensor Network", Proceedings Of The 33rd Annual Hawaii International Conference On System Sciences , 2000.
- [6] Emad Mohammed Ibbini, "An Efficient Mechanism For Saving Energy Of LEACH Protocol In WSN", Masters Thesis, Computer Science, Jordan University Of Science & Technology, Jordan, 2010.
- [7] AtefehHeydariyan, Amir Abbas Baradaran, ElhamRezaei, 2013, "TDTCGE: Two Dimensional Technique Based On Center Of Gravity And Energy Center In Wireless Sensor Network", Journal Of Basic And Applied Scientific Research (ISSN: 2090-4304) Pages:194-201,2013.
- [8] Delavar, A.G. And A.A. Baradaran, "CRCWSN: Presenting A Routing Algorithm By Using Re-Clustering To Reduce Energy Consumption" , In WSN. International Journal Of Computers Communications & Control, 2013.(ISI)(ISSN 1841-9836) 8(1): P. 61-69. , 102– 114\
- [9] I. F. Akyildiz,W. Su, Y. Sankarasubramaniam, and E. Cayirci, "A Survey on Sensor Netowrks," IEEE Communications Magazine, 40, 8, 2002.
- [10] M. BaniYassein And H. Mistareehi, "Improvement On The Lifetime Of The WSN Using Energy Efficiency Saving Of Leach Protocol (New Improved LEACH)", Sensors & Transducers Journal, 130(7): 142-154. , 2011.
- [11] Emad Mohammed Ibbini , Kweh Yeah Lun, Mohamed Othman, Zurinah Mohd Hanapi, Mohammed S Ibbini "A Survey Of Routing MAC Techniques For Wireless Sensor Networks Routing Protocol" Journal Of Theoretical And Applied Information Technology (JATIT) ,2015.
- [12] A 2 RATHNA. R 1 AND SIVASUBRAMANIAN. "IMPROVING ENERGY EFFICIENCY IN WIRELESS SENSOR NETWORKS THROUGH SCHEDULING AND ROUTING", International Journal Of Advanced Smart Sensor Network Systems (IJASSN) , vol 2, No.1, January 2012.
- [13] G. Smaragdakis, I. Matta, A. Bestavros, "SEP,a stable election protocol for clustered heterogeneous wireless sensor networks", in: Second International Workshop on Sensor and Actor Network Protocols and Applications (SANPA 2004), Boston, MA, 2004.
- [14] Enan A. Khalil, Bara'a A. Attea, "Energy-aware evolutionary routing protocol for dynamic clustering of wireless sensor networks. Swarm and Evolutionary Computation", 1(4): p. 195-203 ,2011.
- [15] Stefanos A. Nikolidakis , DionisisKandris, Dimitrios Vergados and Christos Douligeris, "Energy Efficient Routing in Wireless Sensor Networks Through Balanced Clustering". Algorithms, 6, 29-42; doi:10.3390/a6010029, 2013.
- [16] Aimin Wang, Daijiang Yang , Dayang Sun : "A clustering algorithm based on energy information and cluster heads expectation for wireless sensor networks" . Computers and Electrical Engineering 38, 662–671, 2012.
- [17] Bara'a, A. Attea, and Enan A. Khalil. "A new evolutionary based routing protocol for clustered heterogeneous wireless sensor networks." Applied Soft Computing 12.7, 1950-1957, ,2012:
- [18] Sheikhpour, Raziieh, and Sam Jabbehdari. "An energy efficient chain-based routing protocol for wireless sensor networks." KSII Transactions on Internet and Information Systems (TIIS) 7.6.): 1357-1378, 2013.
- [19] Cano, Cristina, et al. "A low power listening MAC with scheduled wake up after transmissions for WSNs." Communications Letters, IEEE 13.4, 221-223, 2009.
- [20] Zhang, Xu, et al. "An efficient hop count routing protocol for wireless ad hoc networks." International Journal of automation and computing 11.1,93-99,2015.

AUTHOR'S PROFILE



EMAD Mohammed Ibbini is a Ph.D Student in Computer Network (UPM), M.Sc in Computer Science (JUST) Bachelor in Computer of Information Systems in (JUST), Specialized in WSN and ad-hoc Networks.



Dr. Kweh Yeah Lun, Dr. B.Sc. in Comp. Sc. (UPM), M.Sc. (UPM), Ph.D (UPM) (in Distributed Computing, Parallel and Distributed Algorithm), Tel: 03-89471797



Prof. Mohamed Othman is an Associate Professor of Computer Science in the Dept. of Communication Technology and Network, Universiti Putra Malaysia (UPM), since 2001. In April 2008, he was appointed as a deputy director of InfoComm Development Centre (iDEC) at the same university. He received his Ph.D in Computer Science from the Department of Industrial Computing, Universiti Kebangsaan Malaysia with distinction (Best PhD Thesis in 2000 awarded by Sime Darby Malaysia and Malaysian Mathematical Science Society) in 1999. During his PhD study, he has contributed and published twelve journal papers in which five were in impact factor journals and the others were in cited and indexed journals. Since 1989, in total, he had published 110 journal papers and more than 300 conference papers, both at national and international levels. He has expertise in several areas of computer science such as parallel and distributed algorithms, grid computing, high-speed computer network and scientific computing.



Associate Prof. Dr. Zurina Mohd Hanapi, B.Comp. Sc. (Strathclyde), M.Sc. (UPM), Ph.D (UKM, Specialized, Computer System Engineering, Network Security, Distributed Computing).

Double Authentication Model using Smartphones to Enhance Student on-Campus Network Access

Zakaria Saleh¹, Ahmed Mashhour²

Information Systems Department
University of Bahrain
Al-Sakhir, Bahrain

Abstract—Computers are widely used by all universities to provide network access to students. Therefore, the securities of these computers play a major role in protecting the network. In light of that, a strong access control is required to ensure that sensitive information will only be accessed through firm authentication mechanism. Smartphones are widely used by students, and can be employed to further enhance student authentication by storing partial access information on the Smartphone. And while students should not leave their computer systems unattended, some do. Therefore, daily network access requires that computer unit to be configured in a way that includes password authentication and an access code stored on a device (the smartphone) which needs to be presented by the user during the authentication process. It is a fact that software and hardware may fail to fully secure and protect systems, but user's negligence to safeguard their systems by logging out of the computer unit before moving away is far more serious security issue. The system being developed in this research will lock the computer unit once the student moves away from that computer unit and losing communication with the smartphone.

Keywords—Bluetooth; double authentication; campus network; computer unit security; model design; smartphone; system design

I. INTRODUCTION

During the last few years, there has been a range of cyber security threats on university campuses worldwide such as phishing, ransomware, malware, and hacking. According to Urrico [1], Higher education institutions continued to see a high proportion of breaches and these threats are expected to rise significantly in the next decade. These threats are alarming for major information security risks in higher education according to Poremba [2], where many universities in the U.S reported data breaches that are caused by hackers infiltrating the college networks, and professors misplacing laptops that stored years of worth of student records. And according to the same report healthcare organizations, an industry that shares copious personal information, the breaches account for 42% of all industry incidents in the first 6 months of 2016, where breaches are caused by unintended disclosure.

In general, universities are being accessed on daily basis by thousands of students, how would brows the institutional data every single minute. All campus network systems, are vulnerable to different kind of security risks, and one of the major vulnerabilities comes directly or indirectly from the student. Implementing a robust access control is a great way to protect campus network and preserve the confidentiality of data it maintains. In this research we believe that the access

control should be “something the user has” and capable of continuance interaction with computer unit being accessed, and continue to maintain control even after the network access is authorized. This means that when a student wants to leave the computer unit without logging off, even if he/she plans to comeback, a firm security system calls for ceasing access the computer unit during the student's absence. This paper will focus on student authentication and control to allow authorized students access to campus network and deny a walking-by student the opportunity of finding a logged on but unattended computer unit. Typically, logging on to campus networks require a student to provide an ID and password and then go through the identification and authentication process to confirm the identity of a student. This study presents an enhancement to that method through the use of double authentication model capable of reliably identifying students before and after accessing the campus network.

II. SIGNIFICANCE OF THE STUDY

Securing desktop computer units is a significant part of the network and information-security strategy in any organization including universities because of the sensitive nature of the information often stored in an organization or university databases. These databases are visible into the Internet and exposed to attacks because they are heavily accessed by staff and students, and as well as the temptations for an unhorsed student of the account to misuse a logged on but left unattended by the authorized student.

Different surveys on security breaches identified several challenges. The SANS Institute [3] conducted a computer security survey on universities and colleges (junior and community colleges), where data was collect from around 300 Information Technology professionals, where (87%) are placed at United States institutions, and 13% from other part of the world. The results show that about 70% of participant expressed worries about the university systems that stores data about students and financial records, and 64% of respondents were concerned about the networks computer units as well as laptops used to access the network [3]. Moreover, Brumfield [4] in Verizon Data Breach Investigations Report, which analyzed security breaches and reiterates the need of organizations for basic security checks in order to protect their data need to know what attack patterns are most common for their business, apply two-factor authentication for their systems and applications, review their logs to help identify malicious activity, encrypt their data and train their staff to developing

security awareness within the organization. The report recorded more than 100,000 security incidents, indicating a 23% increase compared to security breaches in year 2015. Fig. 1 summarized the identified breaches and their relative incidents.

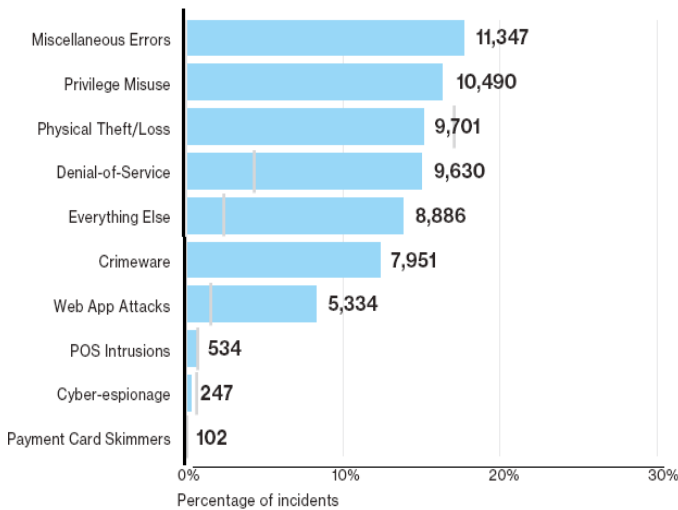


Fig. 1. Incidents and breach breakouts for 2015 (Source: Brumfield [4]).

A report by VMware [5] explored the extent of cyberattacks and the IT security standards used within UK higher education institutions. It also investigates the steps universities can take to protect their intellectual property against today's increasingly sophisticated threat landscape. The report concluded that attacks on student data are common. Over a third (36%) of UK universities are blighted by a successful cyberattack each hour. 43% have had student data attacked, including dissertation materials and exam results. 25% have experienced critical intellectual property theft. 28% have had grant holder research data attacked

Two-factor authentication delivers authentication through devices the users have and the information (such as Pin Code) they already know. Financial institution have applied double (i.e. two-factor) authentication successfully with credit cards and mitigate the rate of breaches of their customers' transactions. Credit card has helped the banking sector to offer security and privacy to their customers because it is reliable, available, and efficient [6].

Smartphones have become an integral part of everyday student's life [7]. In this research we propose using Smartphones and Bluetooth technologies as a second authentication device to minimize students and school records unauthorized access. In light of that, two-factor authentication (2FA) becomes a necessity in higher education transacting to protect against security breaches of higher education sensitive data such as student records, research records, intellectual property records, and so forth. Two factor authentications were recommended by Cristofaro [8] which aims to enhance resilience of password authentication factor. Their research identified popular 2-factor solutions including one time code generated by security token, and one time PINs received by email or SMS and dedicated to smartphone Apps. The two-factor technologies are perceived as applicable regardless of

motivation and/or context of use and no gender differences in terms of adoption rate for token and email/SMS. Digital signatures are usually used by trusted authorities to make unique bindings between a subject and a digital object. Poettering and Stebila [9] proposed a type of signatures called double-authentication-preventing signatures, where a subject/message pair is signed. This is in order to provide self-enforcement for correct signer behavior and provide greater assurance to verifiers that signers behave honestly.

III. LITERATURE REVIEW

According to Kecia [10], in Spring 2017 issue of Converge journal protecting student data are never-ending cybersecurity concerns. It should focus on highlight the role played by technology in modern education by examining networks cybersecurity and data privacy. The study explores two U. S. states where laws have been passed to protect student data including Colorado and Connecticut. It identifies the challenges and possibilities of ensuring student data are protected within the requirements of the law while at the same time enabling school officials to utilize student data for decision-making. In Colorado for example, one main problem to solve is how schools balance student privacy while encouraging teachers to find Apps and Web tools that support their classrooms. In Connecticut State, some of the measures used is Information Technology team provides iPads for students and controls which apps they can access. Principals and curriculum directors have protocols to follow to make sure that educators go through the Technology Department for approval Data and Privacy Council, which developed a student data privacy toolkit that helps them effectively implement the new data privacy legislation Indiana.

University provides students at campus access to two separate secure wireless networks one for academic work, and another for gaming and other extracurricular activities. A recent study by BitSight Technologies [11] report, malware infections increased by a high percent close to 48 percent on the U.S colleges' campuses last year and BitSight Technologies [11] report reveals that as a sector, top schools are at even greater risk for security breaches than retail stores and healthcare. Educause [12], in a nonprofit association whose mission is to advance higher education through the use of information technology, listed information security as the number one issue facing higher education in 2016 and 2017.

In today's schools environment, the need exists to ensure that only authorized individuals gain access to critical devices or services offered. Two-factor authentication (i.e. double authentication) solution equips students with a cost effective means of providing flexible and strong authentication to very large scale, diverse audiences both inside and outside school campus.

Examining networks cybersecurity and data privacy Rasmussen [13] believes that the majority of universities' records of research, financial administrative, and clinical are being access via the university's network. In addition, almost all records on student information, medical information, library use, research, as well as intellectual property-related information are being stored on university servers, which make the network vulnerable to security major breaches by

unauthorized users that could gain access to sensitive and or confidential information and expose the university to financial and reputation losses and other risks posing a threat to future admission, and financial strength. Although universities have lower financial loss rates than the industrial sector their risk managers face the intimidating challenge of identifying and managing the complex and growing risks across their campuses [14]. In the United States alone, security risks have effected more than 200 colleges and universities according to Rasmussen [13], indicating that educational institutes lost control of files in the amount 22 million, which contained detailed information about important research projects, as well as students' personal information such as social security numbers and financial information.

IV. BLUETOOTH OVERVIEW

Bluetooth is a wireless communication technology that was designed and implemented at Ericsson (in Sweden) during 1994. The technology was originally introduced as a method to connect devices to computers and laptops without the need for overcrossing cables. Because of the unlimited potential of Bluetooth wireless communication, Ericsson and other companies (IBM, Intel, Nokia, and Toshiba), established the Bluetooth Special Interest Group (SIG) in February 1998. SIG objectives were to develop an open specification for short-range wireless signals that can be used for connectivity [15]. Bluetooth Specification IEEE 802.15 was then developed so that so that BWT-enabled devices from different manufacturers can work together.

Bluetooth is a packet-based protocol, based on the master-slave structure, and operates within the Industrial, Scientific and Medical (ISM) communication band of 2400 to 2483.5 MHz. A Bluetooth Adapter is capable of performing several tasks. The Adapter can initiate device discovery, it can query a list of paired devices, and create an instance of Bluetooth communication with devices using a known MAC address, and create a listening BluetoothServerSocket that's ready for incoming connections requests from other devices. In addition, the Bluetooth Adapter is also capable of scanning for Bluetooth devices. The master-slave concept within the Bluetooth technology makes the unit that starts a communication link as master and the units that respond to the request as slaves [16]. Such functionalities can be a perfect feature for the proposed Smartphone authentication Logon system.

V. AN OVERVIEW OF COMPUTER UNIT SECURITY

The main objective of network security is to deny unauthorized users to access the network or a network computer unit. Colleges and universities are safeguarding their networks to ensure that students access only the information and network resource they are approved to access. Furthermore, access control methods are utilized to ensure that authorized students are not denied access to resources that they are permitted to access. Procedure for securing unattended computer requires students to turn off computers or logout at the end of the session or set to hibernate when a student will walk away for an extended amount of time with the intention to come back to the same computer. While Computer units are safeguarded from unauthorized access, and shall never be left unattended. However, it has been noticed that many unattended

computer are accessible after the end of session, because none of the security measures were taken by the students to either logout or hibernate the computer. Security was primarily achieved by controlling physical access to system components which were unique and used proprietary communication protocols [17].

Modern methodologies and approaches in the formal education sector used to improve students learning experience are all based on the use of information technology, therefore, institutions in higher education are paying more attention to information technology to deliver and enhance students' knowledge and skills. However, producing and maintaining a convenient and secure campus network system is a challenging task. Universities tend to have a weak centralize policies, which means that they have the tendency toward decentralization where in some universities different departments have their own network equipment, staff and budget [18].

Universities and colleges are being views as good potential targets by data hackers, resulting on and increased security attacks on these institutions [3]. There are three main security issues related to securing a computer unit: Confidentiality, Integrity, and Availability. Information stored on the university servers may be disclosed inappropriately. This can happen for example, when unauthorized students gain access to the unattended computer, and therefore, authorized students gain access to information that they are not supposed to see, or authorized students inappropriately transmit information via the network. The integrity of personal information stored on the server may be changed maliciously (e.g. withdraw from a class). Authorized students may be unable to use the network when the information has been damaged, deleted, or otherwise rendered inaccessible (e.g. having its access privileges changed).

According to Al Maskari [18] identified several vulnerabilities of the unauthorized access to, which includes:

- Ability to executable commands without prior authentication.
- Unauthorized access to data by authorized users.
- Impersonating another use or service within a system.
- Accidentally or intentionally causing a denial of service attack.
- Modifying or removing contents without permission.
- The effort to exploit encrypted data and information.

VI. PROPOSED SYSTEM DESIGN

The present education system, with the advancement of information technology, the objective is to provide students the abilities to access information. As it is evident, the Internet can offer students the gateway to access information and educational materials in different formats, ranging from electronic textbooks, to other interactive models of learning environments. Colleges and universities are increasingly providing students access to information sources through their campus networks. The campus network is typically recognized

as that part of the computing structure that supports access communication services to resources for users including students. In many cases the network covers a group of buildings located throughout the campus geographic area. In some cases, the network could include a distinct campus that would act as the central/backbone of the network that is designated to support interconnectivity between the different segments of the entire network. To access the campus network, the current methods are based on identity registration along with a passcode recognition, where the system assume that the users' identity is a subject to ethical actions. However, statistics accumulated for many years indicate that the major security breaches are caused by trusted, identified, and legitimate users [19]. An access control mechanism imposes selective restriction of access for the users or any process being executed for the users, consuming, entering, or using network resources, like application programs, files, and databases.

The proposed access control system, is intended for controlling access during an access session by a user, and mediates between the students and the network components and services that students are permitted to access, as specified in the standard access control policy and the availability (i.e. presences) of a smartphone running access approval application. Campus Access Control systems (see Fig. 2) will provide the necessary steps needed for identification, authentication, and authorization (access approval), as well as students' accountability by specifying what a student can do. Moreover, while identification and authentication are the standard means to ensure that only legitimate students will be able log on to the network, the proposed system besides the network access control (NAC) system can be a useful technology in providing an enhanced access control. When used together, a combination of NAC and proposed system will provide stronger security and operational safeguard.

For testing the proposed system, we have developed a code to implement the smartphone authentication Logon plug-in to be used on the server to configuring the server and enable it to use the smartphone authentication Logon concept. As for the computer units, for using the extended Smartphone authentication method, there is a need to install the extended application. Conveniently, interacting with Bluetooth communicators available on smartphones is not complicated, and Windows operating systems come with tools for Bluetooth Technology support.

Fig. 3 illustrates the general process of the suggested authentication system. A Bluetooth Adapters is needed for the computer unit to enable students to logon, providing that the smartphone (own by a student) is within the transmission distance of the Bluetooth. Once the student enters the ID and password, and a match is found in the database, the system will attempt to associate the user with a pre-registered smartphone by sending request for the smartphone's MAC address so that the returned value can be compared with the data stored in the database. The logon is based on Single Sign On (SSO), and the student is only asked once to enter the ID and password, a periodic request is set for smartphone's MAC address. The student will be logged off if the smartphone fails to reply, assuming that the student has left the computer unit without

logging off (the detailed process is explained in Section VII, Proposed System Design.

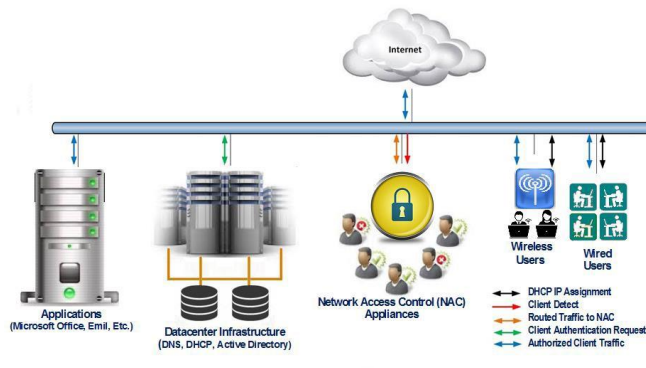


Fig. 2. Campus access control systems.

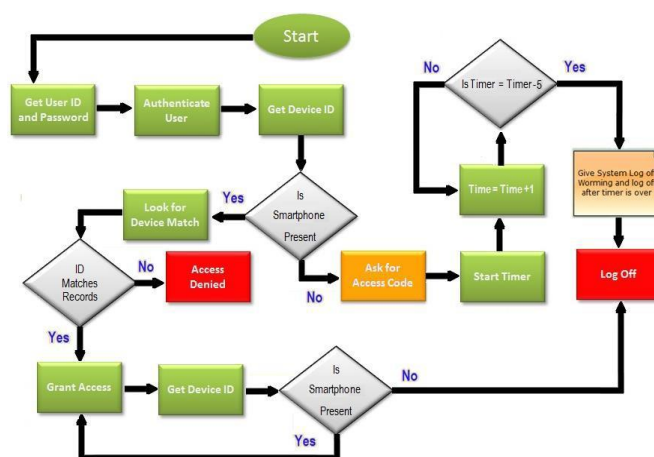


Fig. 3. A simplified process for the proposed authentication Logon.

Sometimes users in general, and students included, avoid locking computers when walking away from the computer unit, because it is more convenient for them than having to type passwords again and again. In light of that, the solution is to have an interactive program running in the background that automatically detects the presence of the user's smartphone. The communication between the smartphone and the computer unit is recommended to be encrypted to ensure that the communication signals are not going to be read if intercepted by someone who maybe intentionally listening for such communications that carries critical piece of sensitive data. However, during our testing of the system, we did not apply any encryption because we were testing in a lab setting, were such information is out of reach for anyone outside the testing environment.

VII. PROPOSED SYSTEM DESIGN

A. Configuring the Server

In order to enable the use of the extended Smartphone authentication method, we have developed an extended Smartphone authentication Logon plug-in. The plug-in will provide three main functions: 1) Bluetooth device name and

user ID matching; 2) Smartphone removal responses; 3) update the windows Logon to include a smartphone based Logon. Therefore, there is a need to install the extended Smartphone authentication Logon plug-in. When installed, the System Administrators use this plug-in to configure settings for global (general), or individual users. The global settings can be used to specify access policies for the entire network. One the installation is completed and the system is up and running, the sever can be configured to apply the Double Authentication, by registering one smartphone for each student. When a smartphone is registered, each smartphone will be assigned a Bluetooth device name, and the name will be bonded with the student ID (of the smartphone owner). Precaution are being made in the extended Smartphone authentication Logon plug-in, to allow for a temporary none existence of smartphone-student ID bonding (the period is flexible for ease of use of the system).

B. Bluetooth Device Name and user ID Matching

When a student attempt to logon, the smartphone needs to be present, and during the Logon, there will be Bluetooth device name matching process to verify if the Bluetooth enabled smartphone presented during Logon is matched to the targeted student account. There are three options: Student Name matching, which will check the device name presented during the Logon against the device name stored for the student smartphone. Matching device name is required to approve access. No Matching means no device name during the Logon process is needed on the target student account. Typically, this option should not be used as the default student accounts. However, when required, access will be allowed for a specific period of time. This will be explained in more details under "Setting up Smartphone Based Windows Logon".

C. Smartphone Removal Responses

Smartphone removal response defines the action taken when a student removes the smartphone away from the Bluetooth reader (Smartphone removal assumes that the student is walking away from the computer unit). In this case, extended Smartphone authentication Logon plug-in application locks the computer unit. If the student smartphone does not become available after a period of time, a "Forced Log Off" will be administrated by the Logon plug-in application. This setting should be used with caution because it can result in the student losing work when the forced logout occurs, so the time for "lock the computer", should not be very short, since no one else can access the account during that period.

D. Setting up Smartphone based Windows Logon

The Smartphone Authentication for Windows Logon support will allow the smartphone to be used for a computer unit login. To enable the Smartphone authentication for Windows Logon feature, the student user will need to check the box that indicates the Use Smartphone for Computer unit Login. This requires the presence of the students' preregistered Computer unit Login Smartphone as per the security requirement of Windows Logon (see Fig. 4). If the student does not have the preregistered Computer unit Login Smartphone, or the phone is not functional (for any reason), then the student does not need to check "use Smartphone for Computer unit Login" box. In that case, per administrator's

imposed access control policy, may grant a temporary access, and before the time is up, a warning message may be displayed asking student to save all data, due to a system administrated log off.



Fig. 4. Windows logon with smartphone authentication support.

VIII. EXPERIMENTATION AND SYSTEM ASSESSMENT

A prototype was developed to determine the systems usability; we implemented the system and developed simple experimental software for the smartphone authentication using a Bluetooth adapter and an Android smartphone. The prototype implementation exhibited the major functional capabilities including 1) establishing communication; 2) requesting smartphone MAC address; 3) continually pinging the smartphone to determine its existence; 4) a function to automatically lock and turn off the screen of the computer unit, and then start the timer; 5) a function for automatic log off when the timer is over.

In the prototype software runs at windows startup as a service that is continuously in a listening status. As soon as users checks the box that indicates the Use of smartphone for Computer unit Logon, the smartphone information are retrieved from the phone and sent to the Access Control in Database Management Systems, which provides access rights to the network. Once the students' identity is verified, the students' relevant access authorization is granted to the student.

IX. UNIVERSITY CAMPUS LAB SIMULATION

A small network (which contained seven nodes), was implemented so that the suggested design of the smartphone authentication system can be tested. On system was assigned the server role, and the database contained 10 user accounts, where only six accounts were bonded with smartphone manually in the database. All test computers were seated in one room of an area of 6 by 8 meter. The computers were about two meters apart. Number of users assumed of no consequence of the tests finding. Besides the number of test computer elements, speed of transmission, the distance of device connectivity, and data quantity were the main qualities selected in the simulation. Those three elements were being adjusted during the system simulation test, because they have a direct

REFERENCES

effect on each other and the overall findings of the tests. Communication distance for the USB Bluetooth devices was assumed to be with 7-8 meters due to assumed added interference and obstructions, but during the test experiment going as far away from the device as possible, we found that none of the systems stayed logged on after about 10 meter range. For the testing simplicity and due to the fact that data quantity is not a major issue in the access confirmation scenario (i.e. one user account was tested at a time), however is different from real life implementations such as several lab rooms where larger volume of data would be transmitted during the authentication of multiple students. In the other hand, speed is significant, so the response time during the test simulation was set in seconds to ensure speedy logging on, due to the fact that the real system would be receiving a much more logon request, and a slow response could affect the overall network access. Three different types of test were conducted: the first one was to test the functionality of the extended Smartphone authentication Logon system by trying to logon during the presence of the smartphone, and then moving the smartphone away from the computer; the second testing was by logging on using the accounts that were not bonded with smartphone to insure that this function works as intended, and the third test was conducted using the accounts that were bonded with smartphone, but the smartphone was not present during the logon. Some modification was made to extended Smartphone authentication Logon plug-in, to resolve some minor issues that were experienced during the system testing. At the final stages of the testing, all tests conducted on the system were fully successful and the functional.

X. CONCLUSION AND FUTURE WORK

College campus is a heaven to thousands of smartphones and computing devices with open, easily hackable Wi-Fi coupled with Students careless or unawareness of digital privacy and security. Using two-factor authentication scheme probably is a partial solution to intractable security problem in a college campus. In this paper, we proposed a second layer authentication system using smartphone to enhance campus network access, which in turn will add a second security layer which combines logical software security (something the user knows) with a smartphone Bluetooth identification (something the user has). Combining what the user knows with what the user has, while the objective of this research is to ensure a log off when a student walks away from the computer unit, the indirect benefit would be an improved security structure of the campus network access systems while at the same time, there were no indications that it would impact the system performance in a negative way.

Smartphone Authentication Logon access control system, as it has been illustrated during our implementations and testing, can be easily installed in the current system with no need for considerable added components in terms of hardware or software. A simple prototype and simulation were developed to establish the feasibility and usability of the proposed system, by evaluating the major functionalities as well as the characteristics that determine selecting the Bluetooth reader in terms of response and communication distance, and all tests conducted on the system were fully successful and the functional.

- [1] R. Urrico, (2016). Malware Attacks Targeting Smaller Financial Institutions, Credit Union Times, July 20, Retrieved from <http://www.cutimes.com>, (in June 30, 2017)
- [2] S. Poremba, (2014). 5 Higher Education Information Security Threats You Should Know Before Your Child Leaves for College. Retrieved from, <https://www.forbes.com/sites/sungardas/2014/11/05/5-higher-education-information-security-threats-you-should-know-before-your-child-leaves-for-college/#7c7788dd1239>, (in April 15, 2017).
- [3] R. Marchany, (2014). Higher Education: Open and Secure?, SANS Institute, A SANS Analyst Survey. Retrieved from <https://www.sans.org/reading-room/whitepapers/analyst/higher-education-open-secure-35240>. (in May 10, 2017).
- [4] J. Brumfield, (2016). Data Breach Investigations Report finds cybercriminals are exploiting human nature. Retrieved from <http://www.verizon.com/about/news/cyberespionage-and-ransomware-attacks-are-increase-warns-verizon-2017-data-breach> (in June 30, 2017).
- [5] VMware (2016). University Challenge: Cyber Attacks in Higher Education. Retrieved from <https://1f289b3qza8o3dim3uta9yl5-wpengine.netdna-ssl.com/wp-content/uploads/2016/06/36300-VMware-Cyber-Security-Report.pdf> (in June 15, 2017), pp 1-12.
- [6] O.S. Adeoye, (2012). Evaluating the performance of two-factor authentication solution in the banking sector, IJCSI International Journal of Computer Science Issues, July, Vol. 9, No. 4, pp.457-462.
- [7] J.n. Alson, and L.V. Misagal, (2016) Smart Phones Usage Among College Students, International Journal of Research in Engineering & Technology, Vol. 4, Issue 3, pp 63-70.
- [8] E. Cristofaro, P.J.F. Parc,h, and G. Norcie (2014). A comparative Usability Study of Two-Factor Authentication, The 18th Network and Distributed System Security Symposium (NDSS), Feb. 23-26, 2014.
- [9] B. Poettering, and D. Stebila (2017). Double-authentication-preventing signatures, International Journal of Information Security, Volume 16, Issue 1, pp. 1-22, doi:10.1007/s10207-015- 0307-8.
- [10] R. Kecia (2017). Are students data laws a blessing or burden? ,Executive Director, Center for Digital Education The Center for Digital Education, Convergence 2017.
- [11] BitSight Technologies (2014). Powerhouses and Benchwarmers: Assessing Cyber Security Performance of Collegiate Athletic Conferences, BitSight Insights Report . Retrieved from <http://bitsig.ht/1oXOLm8> (in May 20, 2017).
- [12] Educase (2017), Educause leadership strategies computers and network security in higher education. Retrieved from <https://www.sans.org/reading-room/whitepapers/analyst/higher-education-open-secure-3524>, (in August 3, 2017).
- [13] R. Rasmussen, (2011). The College Cyber Security Tightrope: Higher Education Institutions Face Greater Risks. Security Week, April, 28, 2011.
- [14] M.A. Bubka, (2010). Best Practices in Risk Management for Higher Education. Retrieved from https://www.pmacompanies.com/pdf/MarketingMaterial/PMA_Education_BestPractices_WhitePaper.pdf (in July 22, 2017).
- [15] K. Sairam, N. Gunasekaran, R. Redd (2002). Bluetooth in Wireless Communication, IEEE Communications Magazine, Volume 40 Issue 6, pp. 90-96.
- [16] S. S. Chadha, M. Singh, and S. K. Pardeshi (2013) Bluetooth Technology: Principle, Applications and Current Status, International Journal of Computer Science & Communication, Volume 4, No. 2 September, pp.16-30 ISSN-0973-7391
- [17] Y. Cherdantseva, P. Burnap, A. Blyth, P. Eden, K. Jones, H. Soulsby, and K. Stoddart (2016) A review of cyber security risk assessment methods for SCADA systems, Computers and Security 56, pp. 1-27.
- [18] S. Al Maskari, D. Saini, S. Raut, and L. Hadimani (2011). Security and vulnerability issues in university networks, Proceedings of the World Congress on Engineering (WCE), Vol 1, July 6-8, 2011, London, U.K.
- [19] Almeahadi, and K. El-Khatib (2015). On the Possibility of Insider Threat Prevention Using Intent-Based Access Control (IBAC), Systems Journal, IEEE , vol. PP, no. 99, pp. 1-12.

A User-Based Trust Model for Cloud Computing Environment

Othman Saeed¹, Riaz Ahmed Shaikh²

Computer Science Department
King Abdulaziz University
Jeddah, KSA

Abstract—There are many trust management models for the cloud environment. Selecting an appropriate trust model is not an easy job for a user. This work presents a new trust model called ARICA model which help a user to reduce the reliance on the trust value of provider and third-party feedback. Simultaneously, the ARICA model increases the dependence on the user trust value. Furthermore, the proposed model measured the trust based on five attributes: Availability, Reliability, Integrity, Confidentiality, and Authentication. This paper presents the comparison of the proposed ARICA trust model with two existing schemes. Results show that the proposed model provides better accurate results.

Keywords—Trust management model; trust value of provider feedback; trust value of third-party feedback; user trust value; availability; reliability; integrity; confidential; authentication

I. INTRODUCTION

Cloud computing is a service that is provided according to the request of the users. In addition, it can be accessed through network anytime. Furthermore, it provides computer resources that are independent of the user location, rapid flexibility, new usage patterns and new business features of IT technology. As a result of that, cloud computing has taken the attention of stakeholders and the researchers as an attractive model.

However, there are several disadvantages that make customers worried from using cloud computing technologies [1]. One of those improper characteristics is less control and less reliability. The biggest fear in any organization is to abandon the administrative responsibility to the external client such as cloud service provider. Moreover, security and privacy are one of the major cloud computing worries. These changes led researchers to find a trust management model which help consumers to control their data.

Lately, many trust management models in cloud computing have presented in the literature. In general, the system of the trust management model works as follows: first, consumers look for a service with good feedback. Next, the users will use this service and give their feedback. After that, cloud providers or third parties take the users' feedback and assess their services using some models. In the end, they save these feedback into the cloud provider database or/and into the third-party database that will be available for other users.

In this paper, the ARICA (Availability, Reliability, Integrity, Confidentiality, and Authentication) is presented.

As compared to the existing models, the proposed model helps users to rely on two or three sources of databases (Provider feedback database - Third-party feedback database - User feedback database). Besides, the model will give the user feedback database more weight than the provider and/or third-party feedback database. Finally, the user will have all three sources of databases. However, the user can rely more on the source of their feedback because users trust their feedback more. There is a scenario in the fourth section to describe this situation in more detail.

The purpose of ARICA model is to help users relying on their feedback more than feedback from any other companies. Moreover, in the evaluation section, the proposed model gave remarkable results. In addition, this paper presents a comparison between the proposed model and two existing schemes (QoS-based Trust Model and FIFO-based trust model [32]). The comparison results (see Section 6) show that the ARICA model provided more accurate results to a user than those two schemes.

Rest of the paper is organized as follow. Section 2 presents literature work of three trust management models for cloud computing. A full description of the proposed model is described in Section 3. In Section 4, a scenario is presented to show the behavior of the ARICA model. Next, an experimental and discussion are given in Section 5. Section 6 shows a comparison and discussion between the proposed model and two other models. Section 7 concludes the paper and highlights some future work.

II. BACKGROUND

Bharathi *et al.* [2] have proposed an extended trust management scheme for cloud computing environment. It composed of four functions: 1) multi-attribute hashing function; 2) real-time service composition; 3) location based service selection; and 4) extended trust management scheme. Details of these functions are defined in very trivial manner. Their proposal is primarily used to verify the user's identity and authenticity. However, it cannot be used to verify the trust level of the cloud service providers.

Zhu *et al.* [3] claim that for different application scenarios, it is useful to integrate the wireless sensor networks with cloud computing environment. Due to resource constraints nature of sensor nodes, it is more feasible to store huge amount of sensory data in the cloud. Moreover, high-performance data

processing capability can also be utilized efficiently in the cloud. The authors have proposed a new authenticated trust and reputation calculation and management (ATRCM) system for cloud computing and wireless sensor network integration. The ATRCM system offers three functions. Firstly, it provides authentication service for cloud service providers and sensor network providers. This service is useful in mitigating malicious impersonation attacks. Secondly, it provides trust and reputation calculation mechanism for cloud and sensor network providers. Finally, cloud service users can select a suitable cloud service provider and it assists them to select an appropriate sensor network provider. The ATRCM system provides protection against good mouthing, bad-mouthing, collusion and white-washing attacks.

Xiao *et al.* [4] proposed a new methodology called attribute-driven. Furthermore, they applied a cloud ecosystem privacy and security within five attributes: 1) confidentiality; 2) integrity; 3) availability; 4) accountability; and 5) privacy-preservability. Furthermore, they focused on the weak relationships between these attributes that the attackers exploit. Moreover, they discussed the threat models and the weaknesses that can be exploited by opponents to proceed various attacks. Also, they talked about the defense strategies. Although several researchers considered privacy as a part of security, the authors extracted privacy from security because it's importance in cloud environments. However, some attack strategies are still not solved. In the end, this review will help researchers to guide their research in cloud security and privacy.

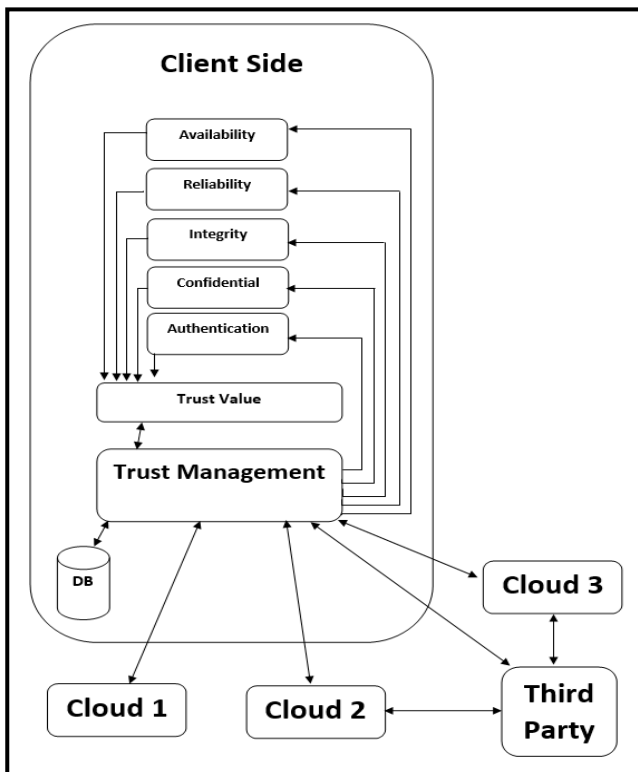


Fig. 1. ARICA model.

III. ARICA MODEL

Instead of depending on the provider feedback or the third-party feedback, the users can be based on their own evaluation or feedback of a particular cloud service. The proposed model helped the user to reduce the reliance on the trust value of provider and third-party feedback. At the same time, the model increases the dependence on the user trust value. As shown in Fig. 1, the proposed model measures the trust based on five attributes: Availability, Reliability, Integrity, Confidentiality, and Authentication.

A. Why these Five Attributes?

There are several attributes existing in the cloud that has been utilized by researchers. Those attributes promote clients to assess and manage the trust of the provider services. In this work, the five attributes (availability, reliability, confidentiality, integrity and authentication) are selected. The reason for selecting these attributes is that they are most commonly used in many recent research papers as shown in Table I.

TABLE I. PAPERS THAT USED SOME OF FIVE ATTRIBUTES

Paper Reference	Paper Year	Authentication	Availability	Reliability	Data Integrity	Confidential
[2]	2015		✓	✓	✓	
[3]	2015	✓				
[5]	2016	✓		✓		✓
[6]	2015	✓			✓	
[7]	2015		✓	✓	✓	✓
[8]	2015		✓	✓		
[9]	2016	✓				
[10]	2015	✓			✓	✓
[11]	2015	✓	✓			
[12]	2016	✓				
[13]	2015	✓	✓			✓
[14]	2015	✓				
[15]	2016		✓			✓
[16]	2016		✓			
[17]	2015	✓	✓		✓	✓
[18]	2016		✓	✓	✓	✓
[19]	2017			✓		
[20]	2016			✓		
[21]	2016				✓	
[22]	2016		✓	✓	✓	
[23]	2016				✓	
[24]	2015		✓	✓	✓	
[25]	2016		✓	✓		✓
[26]	2015		✓	✓		
[27]	2015		✓	✓	✓	
[28]	2015		✓	✓		
[29]	2015		✓			✓

There are many reasons which makes these attributes important, for example, without confidentiality, customer's information will have unlimited access from any user, and they will lose their privacy. Also, integrity gives consumers an insurance that their data is accurate and trustworthy. Furthermore, availability help users to access from anywhere to their data. Reliability describes the possibility of services to fulfill their required functions in a given time. However, without this quality, an environment will not have the desired confidence. In the end, if the authentication was abandoned, it is possible for any users to reach the information without restriction.

To summarize, the five attributes (availability, reliability, confidential, integrity and authentication) are desired for any cloud to acquire the users' trust. As shown in Table I, existing trust management schemes do not incorporate these five attributes all together.

B. Availability (Tv_1)

Availability is the possibility that a service will operate as ordered during a period of time. Equation (3) of Tv_1 is a division of two factors: 1) number of attempts that is accepted by a service (Av_c); and 2) the number of attempts submitted to the service (Se).

$$Av_c = \sum_{i=1}^n (Av_i) \quad (1)$$

$$Se = \sum_{i=1}^n (Se_i) \quad (2)$$

$$Tv_1 = \frac{Av_c}{Se} \quad (3)$$

Where n is the number of attempts on a service.

C. Reliability (Tv_2)

Reliability is the probability that a service will generate accurate results in a given time. Equation (5) of the reliability (Tv_2) is a division of two factors: 1) number of attempts accepted successfully by a service (Re_c); and 2) the number of attempts that is accepted by a service (Av_c).

$$Re_c = \sum_{i=1}^n (Re_i) \quad (4)$$

$$Tv_2 = \frac{Re_c}{Av_c} \quad (5)$$

Where n is the number of attempts on a service.

D. Integrity (Tv_3)

Integrity is to keep data safe from intentional or unintentional data modification from unauthorized users. Moreover, it will emphasize the consistency and the accuracy of data across its lifecycle. The integrity (7) is calculated by dividing the number of attempts that data integrity is preserved by a service (6) with the number of attempts accepted successfully by a service (4).

$$In_c = \sum_{i=1}^n (In_i) \quad (6)$$

$$Tv_3 = \frac{In_c}{Re_c} \quad (7)$$

Where Re_c is the number of attempts accepted successfully by a service, In_c is the number of attempts that data integrity is preserved by a service, and n is the number of attempts on a service.

E. Confidentiality (Tv_4)

Confidentiality will keep the data of the consumer secret in the cloud system. In the proposed model, two parameters will be focused on: 1) the encrypting data that is traveling through the Internet between the cloud and the browser or the application added to 2) the encrypting data in the cloud as shown in (8).

$$Tv_4 = (EnApp * w_1) + (EnCl * w_2) \quad (8)$$

Where $EnApp$ is the encrypting data that is traveling through the Internet between the cloud and the browser or the application, $EnCl$ is the encrypting data in the cloud, and w_1 and w_2 are positive weights such that $w_1 + w_2 = 1$.

F. Authentication (Tv_5)

Authentication confirms the consumer's right to access the information, and preserve the user's account from stealing identity and fraud. In the proposed model, the equation of authentication (9) uses four parameters [30], [31]: password-based, smart card based, one-time password-based and biometrics-based.

$$Tv_5 = \sum_{i=1}^4 (A_i * w_i) \quad (9)$$

Where, A_1 is the password-based, A_2 is the smart card based, A_3 is the one-time password-based, A_4 is the biometrics-based, and $w_1, w_2, w_3,$ and w_4 are positive weights such that $w_1 + w_2 + w_3 + w_4 = 1$.

G. Trust Value Component (Tv)

This component is used to calculate the trust value between 0 and 1. Where, one means the service is fully trusted, and zero means the service is fully untrusted. The component will add these attributes: Availability, Reliability, Integrity, Confidentiality, and Authentication. At the same time, each attribute will multiply by its weight. At the end, the component will take the average by dividing the result by five as shown in (10).

$$Tv = \frac{1}{5} \sum_{i=1}^5 (Tv_i * w_i) \quad (10)$$

Where Tv_1 is the Availability, Tv_2 is the Reliability, Tv_3 is the Integrity, Tv_4 is the Confidentiality, Tv_5 is the Authentication, and $w_1, w_2, w_3, w_4,$ and w_5 are positive weights such that sum of all weight values equals to 1.

H. Database (DB)

The proposed model will create a separate record for each user in the DB. Furthermore, each record contains a trust value for each service that has been used by the user. Every time the customer uses a service, the ARICA model will produce a service evaluation value and store it in the user's DB. By this database, the model can rely on the trust value in the DB more than provider trust value or/and the third-party trust value.

I. Trust Management (TM)

In this section, trust management controls three trust values of the same service as shown in (11) (The Proposed Trust Value (Tv), Provider Trust Value (Tv_p) and Third-Party Trust Value (Tv_{tp})).

$$Tm = Tv * w_1 + Tv_p * w_2 + (\frac{1}{n} \sum_{i=1}^n (Tv_{tp i})) * w_3 \quad (11)$$

Where w_1 , w_2 , and w_3 are positive weights such that $w_1 + w_2 + w_3 = 1$.

These weights are based on the attempts of using the service. In addition, (n) in the equation is based on the number of third parties that voted for the same provider service. That means, if there are more than one third-party assess the provider service then Tv_{tp} will be the mean of the trust values of the third parties.

IV. SCENARIO

There are three main phases when a consumer uses the proposed model. The first one is when the trust management component deals with a provider and a third-party trust value more than the model trust value as shown in Fig. 2. The second phase is when the trust management component has a reliable trusted value in the database; it will deal the trust value in the database on the same level as the provider and the third-party trust value as shown in Fig. 3. Finally, the trust management component deals with the model trust value more than the provider, and a third-party trust value as shown in Fig. 4.

A. First Phase

1) When the customer starts using the service A of the cloud provider P, the model will rely on the P feedback or/and with the third-party of P feedback.

2) Then, the model will calculate the trust value of A by using the five attributes (Availability, Reliability, Integrity, Confidential and Authentication).

3) After that, in the trust value component, the model will take the trust values and calculate the trust value and send it to the trust management component.

4) Next, the trust management component will save the trust value of A in the database.

5) At the end, the trust management component will calculate the total trust value by using the trust value from the model and from P and third party of P.

6) The model in this phase will rely more on the cloud provider and third-party feedback as shown in Fig. 2.



Fig. 2. Less priority on the model trust value.

B. Second Phase

1) After repeating the first phase, the service A will have numbers of trust values saved into the database. These trust values will build good experience of A.

2) By the time, the background of the database will be increased.

3) As a result, the trust management component will reduce the priority of the P trust value and the third party of P trust value.

4) At the same time, the priority of trust value of will be increased as shown in Fig. 3.



Fig. 3. Same level of priority on both trust values.

C. Third Phase

1) By the time, the model will repeat the second phase till the database gets the adequate experience of A.

2) The model in this phase will rely more on model trust value as shown in Fig. 4.



Fig. 4. More priority on the model trust value.

V. EXPERIMENT AND DISCUSSION

The experiments in this study have not been applied to a particular cloud.

Instead of all that, random datasets were used on the proposed model. The reason for that is the unavailability of real world dataset(s). The ten datasets of random 1000 feedbacks are used in the system. These 10 datasets are available online¹. In each experiment, the mean of 10 datasets was taken. So, each experiment had a dataset of 1000

¹https://drive.google.com/file/d/0B_mWyE7-E0r8b0xGc2ISOHUXRWk5Y04IMmJOS0h0Vjc4UHhR/view?usp=drivesdk

feedbacks. Each feedback value was between 1 (trusted value) and 0 (untrusted value).

As mentioned in the introduction that there are three sources of databases (Provider feedback database – Third-party feedback database – User feedback database). This section presents the use case scenarios of these three databases.

There are four trust values in this experiment:

- Trust management value T_m (user feedback database): this value is the outcome feedback from ARICA model. Moreover, this value will send back to the provider or/and to third-party as the user feedback. In addition, it will be saved into the user feedback database.
- Trust value of provider TVP (Provider feedback database): this value will be taken from the provider.
- Trust value of third-party TVTP (Third-party feedback database): this value will be taken from the third-party.
- Trust value of the model TVM (Trust Value Component (T_v)): this value is the outcome from Trust Value Component (T_v).

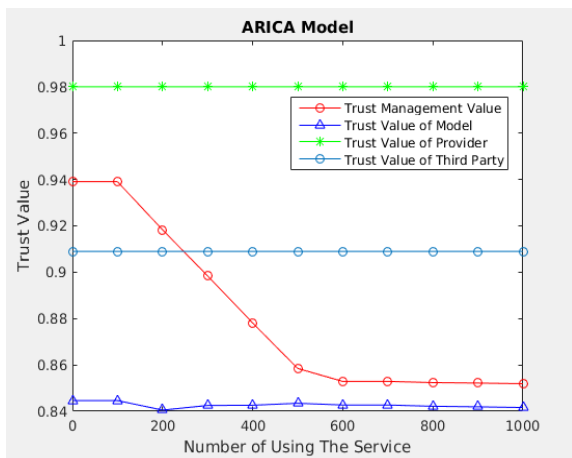


Fig. 5. The results of the first experiment.

The first test made on a service in cloud¹. The results are shown in Fig. 5. There were two evaluation values for this service. One value was taken from a provider feedback database. This value was 0.98 in the first test. The other value was taken from a third-party feedback database. This value was 0.91 in the first test. After using the service 1000 times the user found that the outcome of Trust Value Component (T_v) was between 0.843 and 0.840. Trust Management (T_m) component gave the mean of TVP and TVTP high weight (0.8). On the other hand, the weight of TVM was (0.2). After 100 times of using the service, the T_m started to increase the weight of TVM to 0.4. At the same time, T_m decreased the weight of mean value to 0.6 and so on. After 500 times of using the service, the weight of TVM becomes steady on 0.8 while the weight of the mean value was 0.2. In Fig. 6 there are:

- 1) Trust Value of Provider (TVP) (The weight = 0.8)
- 2) Trust Management Value (T_m) (The manager)

- 3) Trust Value of the Model (TVM) (The weight = 0.2)

The steps of changing the weights are given below:

- 1) Slightly, T_m decreased the weight of TVP.
- 2) In the same time, T_m increased the weight of TVM.
- 3) This process stopped if the weight of TVP = 0.2 and the weight of TVM = 0.8

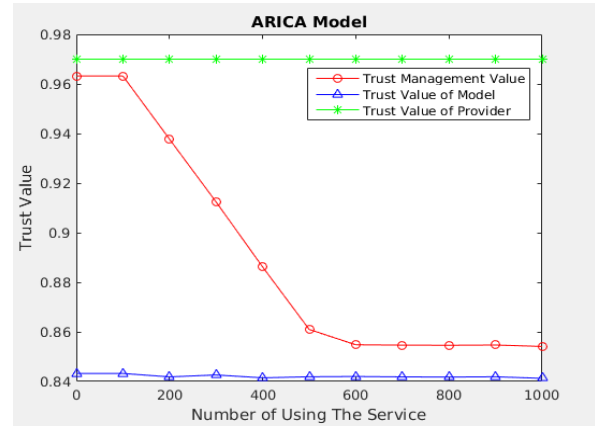


Fig. 6. The results of the second experiment.

In Fig. 7 there are:

- 1) Trust Value of Provider (TVP)
- 2) Four Trust Value of Third-parties (TVTP)
- 3) Trust Management Value (T_m) (The manager)
- 4) Trust Value of the Model (TVM) (The weight = 0.2)

The steps of changing the weights are given below:

- 1) Before the T_m started, it took the mean of the four TVTPs.
- 2) After that, T_m took the total mean of TVP and the mean of the four TVTPs.
- 3) Next, T_m set the weight of the total mean to 0.8
- 4) Slightly, T_m decreased the weight of the total mean.
- 5) In the same time, T_m increased the weight of TVM.
- 6) This process stopped if the weight of the total mean = 0.2 and the weight of TVM = 0.8

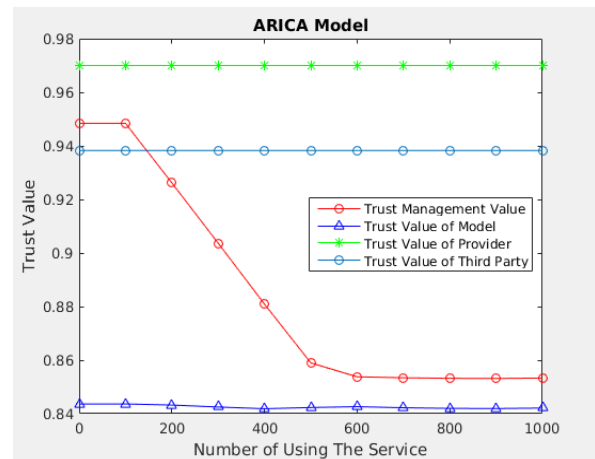


Fig. 7. The results of the third experiment.

These result shows that provider and the third-party feedback database are not reliable because they gave untrusted feedback as compared to user feedback database. Perhaps the reason for these unreliable feedbacks from the providers was that companies wanted to get a large number of customers to distribute their services. These results help users to decide whether to use this service or to choose another cloud provider.

VI. COMPARISON AND DISCUSSION

In this section, the comparison of the proposed model with existing two schemes is presented in two different scenarios. The process of using dataset in this section is the same as the experimental section. That's mean, 10 datasets of random 1000 feedbacks were used in each comparison.

The proposed model is compared with the following two models:

1) Quality of service-based model (QoS based model): Paul Manuel [32] has proposed a new trust model for a cloud resource called QoS Trust model. It is based on four qualities of service parameters, which are: reliability (RE), availability (AV), turnaround efficiency (TE), and data integrity (DI). In order to compute trust, the author has first assigned different weight values ($w_1, w_2, w_3,$ and w_4) for each parameter and then sums them all together in the following manner: $w_1*AV + w_2*RE + w_3*DI + w_4*TE$. Author has compared the proposed QoS trust model with the FIFO model and combined trust model. The experimental results indicate that the QoS trust model performs better than the FIFO model and combined trust model. Author has also provided an architecture for the trust management system that can be used to measure the trust value of the different cloud resources. It also contains details about trust repository, catalog service, and cloud coordinator etc. More QoS parameters like utilization, accountability, auditability any much more can be included in this model.

2) First-in-first-out model (FIFO model): this model is not fully trusted. When a user asks for a service, he/she will get this service whether it is trusted or not trusted. This kind of process is risky.

The dataset of availability, reliability, and data integrity are the same for each comparison. These three attributes have different weight in ARICA model and in QoS based model. The three attributes were equalized to get a fair comparison. The confidential, authentication (in ARICA model) and turnaround efficiency (in QoS based model) were not the same for each comparison. The difference on these three attributes was based on the service level agreement (SLA) between a consumer and a provider. The FIFO model had the same results in all comparison. The three comparisons are below:

A. First Comparison

The first comparison made on a service A, which provides the following features: encrypting data through the Internet, encrypting data in the cloud, password-based, smart card based, one-time password-based and biometrics-based authentication. The turnaround efficiency of service A was

always same as stated in the SLA. That means the turnaround efficiency was one (trusted) in every test.

This SLA was assumed to give the ARICA model and QoS based model the best possible performance. The value of each model's attribute is given below. Furthermore, the results of this comparison are in Fig. 8.

For the first comparison, the ARICA model was configured in the following manner:

- The weight of the **availability** is 0.2
- The weight of the **reliability** is 0.2
- The weight of the **data integrity** is 0.2
- The weight of the **confidential** is 0.2
 - The weight of encrypting data through the Internet is 0.8 (Exist)
 - The weight of **encrypting data in the cloud** is 0.2 (Exist)
- The weight of the **authentication** is 0.2
 - The weight of **password-based** is 0.7 (Exist)
 - The weight of **smart card based** is 0.2(Exist)
 - The weight of **one-time password-based** is 0.05 (Exist)
 - The weight of **biometrics-based** is 0.05 (Exist)

The service-based model was configured in the following manner:

- The weight of the **availability** is 0.3
- The weight of the **reliability** is 0.23
- The weight of the **data integrity** is 0.17
- The weight of the **turnaround efficiency** is 0.3 (Always One)

For the FIFO model, all that a provider gives to the user, the user will take it either it is trusted or not.

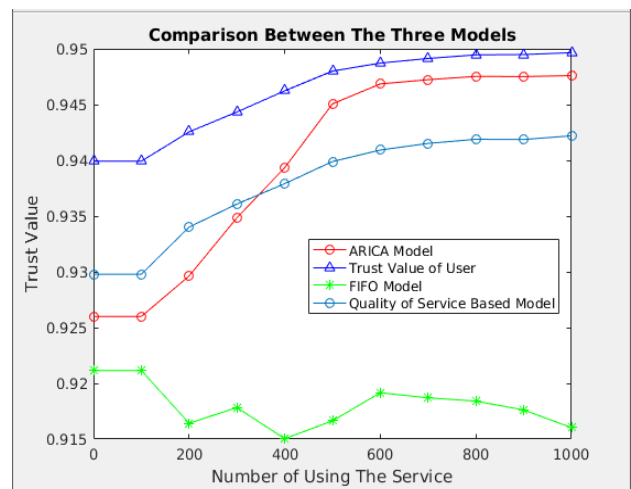


Fig. 8. The results of the first comparison.

As shown in Fig. 8 the ARICA model gave results between QoS based model and FIFO model. After testing service A 500 times², the ARICA model increased and get near to the results of the trust value of the user. The trust value of the user was calculated by ARICA model.

At the end of this comparison, ARICA model generates better results than the QoS based model. This was because ARICA model had more attributes than the QoS based model.

B. Second Comparison

The second comparison made on a service B. SLA of service B provided encrypting data through the Internet, password-based and smart card based. As in the first comparison, the turnaround efficiency of service B was one (trusted) in every test.

This SLA was assumed to make the results of QoS based model much better than the trust value results of the user to see the behavior of ARICA model. The value of each model's attribute is given below. Furthermore, the results of this comparison are shown in Fig. 9.³

For the second comparison scenario, the ARICA model was configured in the following manner:

- The weight of the **availability** is 0.2
- The weight of the **reliability** is 0.2
- The weight of the **data integrity** is 0.2
- The weight of the **confidential** is 0.2
 - The weight of encrypting data through the Internet is 0.8 (Exist)
 - The weight of **encrypting data in the cloud** is 0.2 (Not Exist)
- The weight of the **authentication** is 0.2
 - The weight of **password-based** is 0.7 (Exist)
 - The weight of **smart card based** is 0.2 (Exist)
 - The weight of **one-time password-based** is 0.05 (Not Exist)
 - The weight of **biometrics-based** is 0.05 (Not Exist)

The following values were assumed for quality of service-based model:

- The weight of the **availability** is 0.3
- The weight of the **reliability** is 0.23
- The weight of the **data integrity** is 0.17

² The dataset is available online:
https://drive.google.com/file/d/0B_mWyE7-E0r8dEtQZmpBeHpJLTAWyZdRQUJRUI80eTk2MINj/view?usp=drivesdk

³ The dataset is available online:
https://drive.google.com/file/d/0B_mWyE7-E0r8QWxyYnZJTGpvV2k3QIdHN3ZPeEY1N2RSN0J/view?usp=drivesdk

- The weight of the **turnaround efficiency** is 0.3 (Always One)

For the FIFO model, we used the same assumption which was taken in the first scenario,

The reason for the decline of ARICA model's results in Fig. 9 was that the SLA of service B didn't meet the user requirements. Furthermore, The ARICA model was between QoS based model and FIFO model. After 500 times of testing service B, the ARICA model got adequate experience to decrease and become near to the results of the trust value of the user.

In the end of this comparison, ARICA model was better than QoS based model and FIFO model. The result of that was ARICA model met the user trust results.

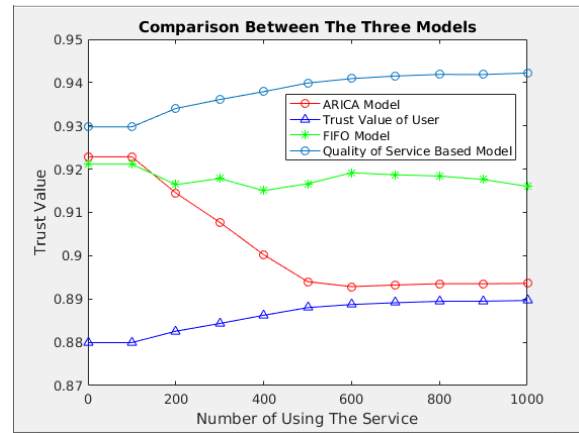


Fig. 9. The results of the second comparison.

C. Third Comparison

This comparison made on a service C and on different SLA. This agreement included encrypting data through the Internet, encrypting data in the cloud, password-based and smart card based. The turnaround efficiency of service C was fluctuated from time to time. That means the turnaround efficiency wasn't always the same as the time in SLA of service C.

This SLA was assumed to make the results of the turnaround efficiency in QoS based model inconsistent. Furthermore, the results of this comparison are in Fig. 10.⁴

The values of ARICA model used for this scenario were:

- The weight of the **availability** is 0.2
- The weight of the **reliability** is 0.2
- The weight of the **data integrity** is 0.2
- The weight of the **confidential** is 0.2
 - The weight of encrypting data through the Internet is 0.8 (Exist)

⁴ The dataset is available online:
https://drive.google.com/file/d/0B_mWyE7-E0r8Q1ZyMGtWa2hBYi1SSloxWVA0UHBHcUF0ZWN/view?usp=drivesdk

- The weight of **encrypting data in the cloud** is 0.2 (Exist)
- The weight of the **authentication** is 0.2
 - The weight of **password-based** is 0.7 (Exist)
 - The weight of **smart card based** is 0.2(Exist)
 - The weight of **one-time password-based** is 0.05 (Not Exist)
 - The weight of **biometrics-based** is 0.05 (Not Exist)

The values of quality of service-based model:

- The weight of the **availability** is 0.3
- The weight of the **reliability** is 0.23
- The weight of the **data integrity** is 0.17
- The weight of the **turnaround efficiency** is 0.3 (Randomly)

The values of FIFO model: All that a provider gives to the user, the user will take it either it is trusted or not.

From the SLA of service C, the trust values of the user were better than QoS based model values and FIFO model values. As a result, ARICA model values increase. In this comparison, ARICA model was the better model that represented the trust results of the user.

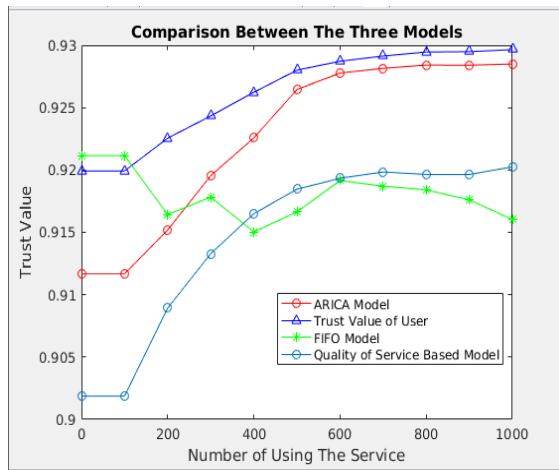


Fig. 10. The results of the third comparison.

D. Fourth Comparison

This comparison made on a service D and on various SLA. This service did not offer any confidentiality and authentication support. The turnaround efficiency of service D was the same as the turnaround efficiency of service C in the previous comparison. This assumption was presented to test the ARICA model in almost the worst scenario to see the reaction of this model.

The values of ARICA model:

- The weight of the **availability** is 0.2
- The weight of the **reliability** is 0.2

- The weight of the **data integrity** is 0.2
- The weight of the **confidential** is 0.2
 - The weight of encrypting data through the Internet is 0.8 (Not Exist)
 - The weight of **encrypting data in the cloud** is 0.2 (Not Exist)
- The weight of the **authentication** is 0.2
 - The weight of **password-based** is 0.7 (Not Exist)
 - The weight of **smart card based** is 0.2(Not Exist)
 - The weight of **one-time password-based** is 0.05 (Not Exist)
 - The weight of **biometrics-based** is 0.05 (Not Exist)

The values of quality of service-based model:

- The weight of the **availability** is 0.3
- The weight of the **reliability** is 0.23
- The weight of the **data integrity** is 0.17
- The weight of the **turnaround efficiency** is 0.3 (Randomly)

The values of FIFO model:

All that a provider gives to the user, the user will take it either it is trusted or not.

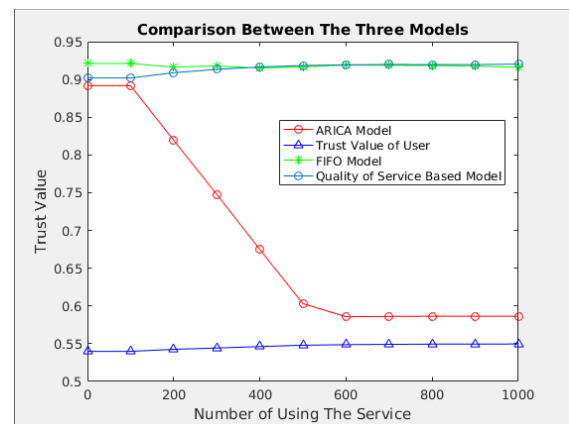


Fig. 11. The results of the fourth comparison.

In Fig. 11,⁵ the trust values of ARICA model were sharply decreased because of the trust values of the user. The result of these low values was the SLA of service D did not meet the user requirements. Moreover, The ARICA model was in the middle of QoS based model and FIFO model. Next, the ARICA model got enough experience to decline and become close to the results of the trust value of the user after 500 times of testing service D.

⁵ The dataset is available online:
https://drive.google.com/file/d/0B_mWyE7-E0r8OUVReDFSNuJQNVVMaXlocTlclVEQTREUKJV/view?usp=drivesdk

At the end of this comparison, ARICA model was better than QoS based model and FIFO model. The results of ARICA model were meeting the user trust results. After that, the user can decide whether to continue using this service or no.

VII. CONCLUSION AND FUTURE WORK

From the comparison, the ARICA model always relied on the trust results of a user. Therefore, ARICA model produced more reliable results than QoS based model and FIFO based model. The proposed ARICA model designed to promote users to rely on different database sources (Provider feedback database – Third-party feedback database – User feedback database). Initially, the model gave the user feedback database more weight than the other two databases. This process continued until the user database feedback get adequate experience. In the end, the user relied on his/her database rather than the provider or/and the third-party database.

With the help of five attributes (Availability, Reliability, Integrity, Confidential and Authentication), the ARICA model gives users the ability to control their data. As a result, the model reduces the fear of customers from using cloud computing technology.

In the future work, to make the model more flexible, the weights will be distributed on the three feedback databases according to the benefit of the business. Also, the model will be tested on a real cloud environment to get more accurate results.

REFERENCES

- [1] Noor, Talal H., Quan Z. Sheng, Sherali Zeadally, and Jian Yu, "Trust management of services in cloud environments: Obstacles and solutions." *ACM Computing Surveys (CSUR)* 46.1 (2013): 12.
- [2] Bharathi, C., V. Vijayakumar, and K. V. Pradeep. "An Extended Trust Management Scheme for Location Based Real-time Service Composition in Secure Cloud Computing." *Procedia Computer Science* 50 (2015): 103-108.
- [3] Zhu, C., Nicanfar, H., Leung, V. C., & Yang, L. T. "An authenticated trust and reputation calculation and management system for cloud and sensor networks integration." *Information Forensics and Security, IEEE Transactions on* 10.1 (2015): 118-131.
- [4] Xiao, Zhifeng, and Yang Xiao. "Security and privacy in cloud computing." *Communications Surveys & Tutorials, IEEE* 15.2 (2013): 843-859.
- [5] Shapiro, D., Socher, M., Lei, R., Muralidhar, S., Loo, B. T., & Heninger, N. "Daruma: Regaining Trust in Cloud Storage." (2016).
- [6] Shaikh, Rizwana, and M. Sasikumar. "Trust model for measuring security strength of cloud computing service." *Procedia Computer Science* 45 (2015): 380-389.
- [7] Monir, M. B., AbdelAziz, M. H., AbdelHamid, A. A., & El-Horbaty, E. S. M. "Trust management in cloud computing: A survey." *Intelligent Computing and Information Systems (ICICIS), 2015 IEEE Seventh International Conference on.* IEEE, 2015.
- [8] Namal, S., Gamaarachchi, H., MyoungLee, G., & Um, T. W. "Autonomic trust management in cloud-based and highly dynamic IoT applications." *ITU Kaleidoscope: Trust in the Information Society (K-2015), 2015. IEEE, 2015.*
- [9] Bhardwaj, Akhilesh Kumar, and Rajiv Mahajan. "TTP based vivid protocol design for authentication and security for cloud." *Computing for Sustainable Global Development (INDIACom), 2016 3rd International Conference on.* IEEE, 2016.
- [10] Yan, Zheng, Peng Zhang, and Athanasios V. Vasilakos. "A security and trust framework for virtualized networks and software-defined networking." *Security and communication networks* 9.16 (2016): 3059-3069.
- [11] Choudhary, Sapna, Amarjeet Kurmi, and Abhishek Dubey. "Monitoring Cloud Resources Based on SAAS Community using Cloud Bee Live Cloud Service." (2015).
- [12] Nagaraju, Sabout, and Latha Parthiban. "SecAuthn: Provably secure multi-factor authentication for the cloud computing systems." *Indian Journal of Science and Technology* 9.9 (2016).
- [13] Tang, Bo, Ravi Sandhu, and Qi Li. "Multi-tenancy authorization models for collaborative cloud services." *Concurrency and Computation: Practice and Experience* 27.11 (2015): 2851-2868.
- [14] Wu, L., Zhou, S., Zhou, Z., Hong, Z., & Huang, K. "A Reputation-based identity management model for cloud computing." *Mathematical Problems in Engineering* 2015 (2015).
- [15] Noor, T. H., Sheng, Q. Z., Yao, L., Dustdar, S., & Ngu, A. H. "CloudArmor: Supporting reputation-based trust management for cloud services." *IEEE transactions on parallel and distributed systems* 27.2 (2016): 367-380.
- [16] Jabbar, S., Naseer, K., Gohar, M., Rho, S., & Chang, H. "Trust model at service layer of cloud computing for educational institutes." *The Journal of Supercomputing* 72.1 (2016): 58-83.
- [17] Bernabe, Jorge Bernal, Gregorio Martinez Perez, and Antonio F. Skarmeta Gomez. "Intercloud trust and security decision support system: an ontology-based approach." *Journal of Grid Computing* 13.3 (2015): 425-456.
- [18] Alabool, Hamzeh Mohammad, and Ahmad Kamil Bin Mahmood. "A novel evaluation framework for improving trust level of Infrastructure as a Service." *Cluster Computing* 19.1 (2016): 389-410.
- [19] Selvaraj, Alagumani, and Subashini Sundararajan. "Evidence-Based Trust Evaluation System for Cloud Services Using Fuzzy Logic." *International Journal of Fuzzy Systems* 19.2 (2017): 329-337.
- [20] Raja, Sivakami, and Saravanan Ramaiah. "2S-FAT-Based DLS Model for Cloud Environment." *Arabian Journal for Science and Engineering* 41.8 (2016): 3099-3112.
- [21] Pinheiro, Alexandre, Edna Dias Canedo, Rafael Timóteo de Sousa Jr, and Robson de Oliveira Albuquerque. "A Proposed Protocol for Periodic Monitoring of Cloud Storage Services Using Trust and Encryption." In *International Conference on Computational Science and Its Applications*, pp. 45-59. Springer International Publishing, 2016.
- [22] Huang, Qiang, Dehua Zhang, Le Chang, and Jinhua Zhao. "Building Root of Trust for Report with Virtual AIK and Virtual PCR Usage for Cloud." *Security, Privacy, and Anonymity in Computation, Communication, and Storage: 9th International Conference, SpaCCS 2016, Zhangjiajie, China, November 16-18, 2016, Proceedings 9.* Springer International Publishing, 2016.
- [23] Boopathy, D., and M. Sundaresan. "Secured Cloud Data Storage—Prototype Trust Model for Public Cloud Storage." *Proceedings of International Conference on ICT for Sustainable Development.* Springer Singapore, 2016.
- [24] Filali, Fatima Zohra, and Belabbas Yagoubi. "Global trust: a trust model for cloud service selection." *International Journal of Computer Network and Information Security* 7.5 (2015): 41.
- [25] Ma, Zifei, Rong Jiang, Ming Yang, Tong Li, and Qiuji Zhang. "Research on the measurement and evaluation of trusted cloud service." *Soft Computing* (2016): 1-16.
- [26] Namal, Suneth, Hasindu Gamaarachchi, Gyu MyoungLee, and Tai-Won Um. "Autonomic trust management in cloud-based and highly dynamic IoT applications." *ITU Kaleidoscope: Trust in the Information Society (K-2015), 2015. IEEE, 2015.*
- [27] Filali, Fatima Zohra, and Belabbas Yagoubi. "A General Trust Management Framework for Provider Selection in Cloud Environment." *East European Conference on Advances in Databases and Information Systems.* Springer International Publishing, 2015.

- [28] Rajendran, V. Viji, and S. Swamynathan. "Hybrid model for dynamic evaluation of trust in cloud services." *Wireless Networks* 22.6 (2016): 1807-1818.
- [29] Fan, Wen-Juan, Shan-Lin Yang, Harry Perros, and Jun Pei. "A multi-dimensional trust-aware cloud service selection mechanism based on evidential reasoning approach." *International Journal of Automation and Computing* 12.2 (2015): 208-219.
- [30] Reshmi, G., and C. S. Rakshmy. "A survey of authentication methods in mobile cloud computing." 2015 10th International Conference for Internet Technology and Secured Transactions (ICITST). IEEE, 2015
- [31] Bhatia, Tarunpreet, and A. K. Verma. "Data security in mobile cloud computing paradigm: a survey, taxonomy and open research issues." *The Journal of Supercomputing* (2017): 1-74.
- [32] Manuel, Paul. "A trust model of cloud computing based on Quality of Service." *Annals of Operations Research* 233.1 (2015): 281-292.

Synthetic Loads Analysis of Directed Acyclic Graphs for Scheduling Tasks

Apolinar Velarde Martinez
Instituto Tecnológico el Llano Aguascalientes
Aguascalientes, México

Abstract—Graphs are structures used in different areas of scientific research, for the ease they have to represent different models of real life. There is a great variety of algorithms that build graphs with very dissimilar characteristics and types that model the relationships between the objects of the problem to solve. To model the relationships, characteristics such as depth, width and density of the graph are used in the directed acyclic graphs (DAGs) to find the solution to the objective problem. These characteristics are rarely analyzed and taken into account before being used in the approach of a solution. In this work, we present a set of methods for the random generation of DAGs. DAGs are produced with three of these methods representing three synthetic loads. Each of the three above characteristics is evaluated and analyzed in each of DAGs. The generation and evaluation of synthetic loads is with the objective of predicting the behavior of each DAG, based on its characteristics, in a scheduling algorithm and assignment of parallel tasks in a distributed heterogeneous computing system (DHCS).

Keywords—*Directed acyclic graph; distributed heterogeneous computing system (DHCS); Algorithm for scheduling and allocation tasks in a DHCS; parallel tasks*

I. INTRODUCTION

In recent years there has been growing interest in scientific applications of workflow, which are often modelled by Directed Acyclic Graphs (DAGs) [1]. This type of graphs, which do not have cycles in parallel connections, allow to represent the relations, the interdependencies and the characteristics between the objects, such as kinship relations between people, the structures of web page designs, basic data structures of applications for information visualisation [2], as well as modelling tool in various fields (social sciences, computer science and biology) [1], and in the representation of parallel programs, which are modelled in the scheduling of tasks in Distributed Heterogeneous Computing System (DHCS) [1], [3]-[6].

In the parallel and distributed computing systems, the DAGs, also allow to show the dependencies among the tasks, the precedence restrictions, the communication links, the calculation costs and the communication costs of the tasks that constitute the application to be executed within the system [1], [7], [8]. In addition to the above, the DAGs are used to distribute and represent the different tasks that make up the solution of a problem, and the way in which these tasks are distributed among the processors, by means of the algorithms of the scheduling and allocation of tasks [7].

The algorithms of the scheduling and the allocation of tasks, seek to optimize one or more performance parameters such as the Makespan [9], the maximization of the resources

of the system [10], [20], the waiting time [21], etc. by means of techniques derived from operations research, evolutionary algorithms, heuristic techniques and other methods of optimization using operations research techniques, heuristics and meta-heuristics.

To carry out the tests of the scheduling algorithms in the parallel and distributed computing systems, the DAGs are generated in two ways: by generating graphs of real applications, and by the random generation of synthetic loads [4].

For the generation of graphs of real applications, the designs of DAGs of real problems are considered, such as the molecular dynamic code [6], [11], the Gaussian elimination, and the Fast Fourier Transform [11], and so on. These applications are processed with the scheduling algorithm to obtain the results in the performance metrics to be evaluated.

For the generation of synthetic loads constituted by DAGs, different algorithms of random generation of graphs can be used, such as: the Erdős-Rényi method [12], the level-by-level method [13], the fan-in fan-out method [14], the Random Orders method [15], the Márkov chain method [7], [16], the parallel approach method for the random generation of graphs on GPUs [17], and so on. These algorithms use a set of parameters in their execution, to generate the DAGs with specific characteristics or properties.

The different research works specify the characteristics and properties of the DAGs in different ways. In [18], the following properties of the DAGs are mentioned and defined: the depth of the graph, the width, the regularity, the density and the number of jumps. In [4], three characteristics of the DAGs are analyzed: the longest route, the distribution of the out-degree (degree of exit) and the number of edges. In [19] author refers to the following parameters of the DAGs: the critical path and the size of the DAG.

These characteristics of the DAGs are decisive in the results of the performance metrics measured by the task scheduling algorithm that uses synthetic loads, so generating synthetic loads to perform the tests of the scheduling algorithms in distributed heterogeneous systems produce two important problems: first, there is no standard algorithm that produces the graphs with specific properties that you wish to evaluate, in the scheduling algorithms; the generated synthetic loads produce evaluations in the scheduling algorithms that are generally adapted to the performance parameters that the algorithm evaluates, producing excellent results with synthetic loads, but with poor results with loads of real users. Second, the graphs do not adapt to the underlying computation system in which the scheduling

algorithms are tested, so it is necessary to execute different graph generation algorithms to produce synthetic loads, that are evaluated with the scheduling algorithm and, with the distributed heterogeneous system.

As explained in the previous paragraph, this paper describes five methods for the generation of random DAGs. Of these five methods, three of them are chosen: the Erdős-Rényi method, the Márkov chain method and the parallel approach method, with the aim of generating synthetic loads that will be analyzed in the characteristics of depth, width and the density of the graph to predict the behavior of a scheduling algorithm and allocation of tasks in a distributed heterogeneous computing system.

The selection of the three methods of generation of random graphs aims to:

- 1) Determine and analyze the values that each method generates in the characteristics of the depth, width and density of the graph.
- 2) Evaluate the convergence speed of each algorithm, considering that two of them run sequentially and the last one in parallel.
- 3) Obtain synthetic loads, which allow the validation of an algorithm for scheduling and allocation tasks in a distributed heterogeneous computing system.

The manuscript is constituted in following ways: In Section 2 related works, the most common algorithms for the generation of DAGs reported in the literature are described, Section 3 justifies the random generation of DAGs for the construction of synthetic loads to be used in the scheduling and allocation of tasks in SCHD. A set of basic definitions of the DAGs is shown in Section 4. Section 5 describes the way in which parallel tasks are modeled with DAGs. The application of the DAGs in the problem of scheduling and allocation tasks in the DHCS is described in Section 6. Section 7 describes the importance of the characteristics of the generated DAGs. Section 8 describes the results obtained from the evaluation of the two methods of generation of DAGs. Section 9 shows the conclusions obtained in this work, and finally Section 10, shows the works that will be developed in the future in this research area.

II. RELATED WORKS

In the problem of task scheduling in heterogeneous distributed systems, different methods have been used for the generation of random graphs. In this section, we describe five of the most common methods that generate random graphs.

The algorithms described here generate the graphs based on a set of parameters that are put into the algorithm. The characteristics of each generated graph are similar to those of the graphs of parallel applications of the real world.

The Erdős-Rényi [12], are two simple, elegant and general mathematical models [17], considered the most popular methods for the random generation of graphs [4]. The first model denoted as $\Gamma_{v,e}$ choosing a uniformly random graph of the set of graphs with v vertices and e edges. The main characteristic of this method is the generation of random graphs, with a fixed number of edges [4].

The second method denoted as $\Gamma_{v,p}$ choose a uniformly random graph of the set of graphs with v vertices, where each

edge has the same p probability of existing [12]. From this method, the following properties can be highlighted [4]:

- When the value of v is sufficiently large, the number of edges in the graphs generated tends to $p\binom{n}{2}$.
- There is a high probability of generating a subgraph weakly connected to most vertices, if np tends to a constant greater than 1 and there is no other component connected with more than $O(\log(n))$ nodes.
- If $p > \frac{(1+\epsilon)\ln n}{n}$ then it is highly probable that the generated graph will not have isolated vertices.

To date this model has been widely used in many fields of research, among which are: communication engineering, social networks, the spread of viruses and worms in networks, data search and replication in point to point networks, evaluate the similarity of the topologies between biological regulation networks and monotonous systems, and used to study genetic variation in human social networks, among other areas [17].

The level by level method designed specifically for the validation of heuristics that are applied in task scheduling [13]. This method is based on the concept of levels. This concept states that if there is an edge from level a to level b , then there is no path from a vertex in b to a vertex in a the edges are created with probability p exactly as in the Erdős-Rényi $\Gamma_{v,p}$ method. The practical utility of this method is due to the possibility of limiting the size of the critical path of the graph, when the value of the variable k in the algorithm is limited.

The Fan-in/Fan-out method, proposed in [14] uses properties of the branch of mathematics called order theory to analyse and generate random graphs. The operation is based on the generation of randomly ordered sets, which are used to generate task graphs. The fundamental concept of the method is to create a partial order by the intersection of several total orders.

The Random Orders method, proposed in [15], uses properties of the branch of mathematics called theory of order to analyze and generate random graphs. Its operation is based on the generation of partially ordered random sets, which are used to generate task graphs. The fundamental concept of the method is based on creating a partial order by the intersection of several total orders.

The Márkov Chain Method is based on a Márkov chain to generate even random acyclic digraphs of a given size [16]. This method, initially proposed for information visualisation applications, seeks to produce random acyclic digraphs with:

- A prescribed number of vertices uniformly random starting from the empty graph.
- Dimensioned total degree or dimensioned vertex degree.
- A way to control the density of the edges of the resulting graphs.

This algorithm uses the following development: let $V = \{1, \dots, n\}$ denote the set of underlying vertices of the considered graph. We define a Márkov chain M with state space of all acyclic digraphs on the set of vertices V A Márkov chain

is completely determined by its transition function, prescribing the probability that the chain goes from a given state to any other possible state. For this case the transition function is as follows:

One position consists of an ordered pair (i, j) of different vertices of V . If X_t denotes the state of the Márkov chain over time t , then T_{t+1} is selected in accordance with rules 1) and 2) described below.

Suppose a position (i, j) which is selected uniformly at random:

- 1) If the position (i, j) corresponds to an arc e in X_t , then $X_t \setminus e$. The edge e is deleted from the graph associated with X_t .
- 2) If the position (i, j) does not correspond to an arc e in X_t , then X_{t+1} is obtained from X_t when adding this arc, as long as the underlying graph remains acyclic; otherwise $X_{t+1} = X_t$.

The algorithm obtains the main characteristics of the Márkov chain: aperiodic and irreducible with a symmetric transition matrix, containing a uniform, limiting stationary distribution in the set of all acyclic digraphs on the set of vertices of V .

A proposal to improve the Márkov chain algorithm has been proposed in [7]. In this research work the algorithm is slightly modified and used to generate acyclic digraphs simply connected evenly at random. This type of digraph is widely used in task scheduling, due to the ease of representing parallel programs that are modelled. For this ease, this improved algorithm of the Márkov chain is selected in this research work.

This algorithm consists of two rules T1 and T2, which appear in the following paragraphs:

Let $N \geq 2$ is a fixed integer, and $V = \{1, \dots, n\}$ denotes a finite set of vertices. Consider the set A of all acyclic directed graphs on V that is, graphs that do not contain circuits. Next, we define the Márkov chain M on the set A . Because the V set of vertices is fixed, there is no distinction between a digraph in A and the set of its arcs. The transition in any two states in M is given as follows:

X_t is the state of the Márkov chain in time t . Assume a pair of integers (i, j) that have been uniformly drawn at random from the set $V \times V$.

- Rule (T1). If (i, j) is an arc in X_t this is deleted from X_t . This is $X_{t+1} = X_t \setminus (i, j)$.
- Rule (T2). If (i, j) is not an arc in X_t then:
 - This is added to X_t if the resulting graph is acyclic. This is, $X_{t+1} = X_t \cup (i, j)$.
 - In another case nothing is done, this is, $X_{t+1} = X_t$.

When starting the algorithm from a graph with an empty array of arcs, it is possible to apply the rules (T1) and (T2) iteratively to construct an acyclic digraph with a nearly uniform distribution.

The characteristics of the algorithm demonstrated by the authors are:

- The probability of a transition going from a state X to a state $Y \neq X$ is $\frac{1}{n^2}$.
- The generation of the transition matrix as symmetric.
- The convergence of the Márkov chain to uniform distribution.
- The irreducibility of the state of space M .

A parallel approach to the random generation of graphs on GPUs is a method proposed in [17], which seeks to solve the problem of the exponential growth of the number of edges in the process of classical generation of graphs with the Erdős-Rényi method.

The general scheme of this research is based on a collection of three sequential algorithms as follows: the first algorithm called ER is the implementation of the random process of the Gilbert model [12]; the second ZER algorithm exploits the availability of an analytical formula for the expected number of edges in the generated graphs, which can be omitted in a geometric approach; A third algorithm, PreLogZER, is implemented to avoid the calculation of logarithms required by the proposed method. The three sequential algorithms are scaled to a parallel format, which is programmed in a GPU environment.

This algorithm was proposed by the authors to be evaluated in a GPU hardware architecture. In our work, the algorithm is evaluated in an architecture of four processing cores using the MPI libraries of the C language.

III. JUSTIFICATION OF THE RANDOM GENERATION OF GRAPHS

In the absence of a procedure for generation of standard random graphs, it is necessary to carry out experiments with different scheduling algorithms, to generate the synthetic loads that will be evaluated with the new scheduling algorithm to be executed in the DHCS.

The random generation of DAGs allows the use of different types of graphs that resemble the designs of the real parallel programs, which causes the values obtained in the performance metrics evaluated to be most attached to the workloads generated by the real users in the DHCS.

Then, the generation of random workloads, to validate a new scheduling algorithm is justifiable because:

- It can help to find a counterexample for the algorithm [4]. Although the algorithm is theoretically correct, the random input data can help find errors in the implementation, or help identify bottlenecks in performance.
- It helps to evaluate the performance of the algorithm in contexts not analyzed theoretically [4]. It allows to predict how the algorithm will be executed in real conditions.
- They allow predicting some of the properties of acyclic graphs [16].
- It is possible to obtain DAG's evenly distributed with bounded total grade or bounded vertex degree [16].

- It is likely to obtain, in a large set of examples, all possible or interesting cases that should be tested or studied [7].
- They allow to synthesize data sets with the objective of evaluating the efficiency and effectiveness of the algorithms [17].

IV. BASIC DEFINITIONS

A graph is a structure that represents relationships and interdependencies between objects, and the characteristics that relate them. Examples of graph applications can be kinship relationships between people, the structure of web page design, basic data structures of applications for information visualization [16], as well as modeling tool in various fields (social sciences, computer science and biology) [7], and in the representation of parallel programs that are modeled in task scheduling in high performance computing systems (HPCS, High Performance Computing System) [18].

Given the variety of graphs in the existing literature [2], in this section we define a special type of graph called acyclic weighted directed graph (which we refer to in the following sections as DAG), using the following definitions.

Definition 1. A graph G is a pair $G = (V, E)$ consisting of a finite set $V \neq \emptyset$ and a set E of two subset elements of V . The elements of V are called vertices. An element $e = \{a, b\}$ of E is called an edge with final vertices a and b . It is said that a and b are incidents with e and that a and b are adjacent or neighbours of each other, and is defined as $e = ab$ or aeb

Definition 2. To determine the relationship between vertex information (which the connections do not model), a digraph is defined. A digraph exists when the set of connections $A = A(G)$ is directed, they distinguish between the connections $e_{i,j} = (v_i, v_j)$ and $e_{j,i} = (v_j, v_i)$, then the graph $D = (V, A)$ is called directed graph or graph.

Definition 3. Now, if between the existing connections, the digraph has related a number $T(v_i, v_j)$ which represents the cost of communication between the vertex v_i and vertex v_j we have a weighted graph. A weighted graph is a pair (G, W) , where G is a graph and W represents a function $W : E \rightarrow \mathbb{R}$ in this way, the weight of a connection e is $W(e)$ The weight of the graph is $W(G) = \sum_{e \in E} W(e)$.

Definition 4. Finally, a graph that has no cycles in parallel connections ie it has no connections of the form: e_{v_i, v_i} is called an acyclic graph.

V. MODELLING OF PARALLEL TASKS WITH GRAPHS

As heterogeneous distributed computing systems (e.g. clusters, grids, clouds, etc.) become commonplace to meet the massive computational demands of executing complex, multi-tasking scientific applications, the process of assigning these tasks to multiple resources, known as scheduling, is important for application performance.

In recent years, DAGs have received much attention as a result of the growing interest in modelling scientific workflow applications [1].

This modelling, in the DHCS allows to show:

- the dependencies between tasks [8],
- the transmission of data between tasks [1],
- the precedence constraints between task [4,8],
- the communication links between tasks,
- the costs of calculating each of the tasks [8], and
- the costs of communication between tasks [8].

VI. APPLICATION OF DAGS IN THE TASK SCHEDULING PROBLEM IN DHCS

Without loss of generality and considering the definitions existing in the literature [1], [3]-[6] in this section, it is defined how the DAGs are applied to the problem of the scheduling and the allocation of tasks in a DHCS.

A DAG consists of v nodes n_1, n_2, \dots, n_v which can be executed on any of the processors available from an DHCS. A node in the DAG represents a task, which is a set of instructions that must be executed sequentially without preferential right on the same processor. A node has one or more entries. When all the entries are available, the node is activated for execution. After its execution, it generates its outputs. A parentless node is called an input node, and a childless node is called an output node. The weight at a node is called the computing cost of a node n_i and is denoted by $w(n_i)$.

The graph also has e directed edges representing a partial order between tasks. The partial order introduces a DAG precedence constraint, and implies that if $n_i \rightarrow n_j$, then n_j is a child who can not start until his father n_i complete and send your data to n_i . The weight at one edge is called the communication cost of the edge and is denoted by $c(n_i, n_j)$. This cost is incurred if, n_i and n_j are scheduled in different processors and is considered zero, if n_i and n_j are scheduled on the same processor. For standardisation we specify that a DAG has only a single input node and a single output node.

VII. CHARACTERISTICS OF THE GENERATED DAGS

When experimenting with a new algorithm for scheduling and allocation tasks, it is necessary to carefully observe each of the parameters that constitute the DAGs. The parameters that are observed allow us to avoid biases in the results obtained in the new algorithms, when testing: convergence, speed, the capacity of resource allocation and transfer speeds.

Some of the works that highlight the importance of the parameters of the DAGs are [3], [4], [18], [19]. In this section, three characteristics of the DAGs that are analyzed in synthetic loads are defined.

The depth of the graph, also known as the critical path or the longest path, is the path from the input node to the output node of the DAG, and has the highest values in the total calculation of execution costs of each task, and the total communication costs of the edges [11], [19]. When parallel tasks are scheduled using the DAGs, the algorithms require an appropriate scheduling of tasks located in the critical path.

The width of the DAG, which determines the maximum parallelism in the DAG, that is, the number of tasks in the longest level.

The density of the graph, denotes the number of edges between two levels of the DAG; with a low value in this property, there are few edges and with large values there are many edges in the DAG.

VIII. SIMULATION AND RESULTS

This section explains the procedure carried out to perform the simulation of the experiments and the results obtained.

The first subsection explains the parallel algorithm for the generation of the synthetic loads; in second section, the specifications of the way, in which the DAGs are used in this work are described; finally the results are depicted in three subsections: number of nodes generated (on average) in the critical path, the maximum parallelism in the DAG and the density of the graph.

We describe an additional feature of the methods: the convergence time of the algorithms. This measurement allows us to know, the times that each method consumes in the generation of synthetic loads. The results obtained are shown in a graph for better understanding.

A. Algorithm for the Generation of Synthetic Loads

For the realization of the simulation, an algorithm that runs on a platform of four cores was used. The division of work between the cores is done in the following way:

Core 0

- 1) Build the symmetric matrix with the number of vertices specified and the probability of inclusion, for the Erdős-Rényi method. Send all parameters to the core 1, to build the DAG with this method.
- 2) Specifies the maximum number of edges and the probability of inclusion. Send all parameters to the core 2, to build the DAG with this method.
- 3) Set v representing the set of vertices. Send all parameters to the core 3, to build the DAG with this method.
- 4) Receives the results of the cores and shows them to the user.

Core 1

- 1) Process the Erdős-Rényi algorithm. Receives the symmetric matrix.
- 2) Build the DAG based on the symmetric matrix.
- 3) Go through all the possible routes in the DAG to get: the depth of the graph that represents the critical route, the width of the DAG and the density of the graph.
- 4) Measures the time consumed by the algorithm.

Core 2

- 1) Process the Parallel approach algorithm. Receives both parameters: maximum number of edges and the probability of inclusion.
- 2) Build the DAG based on this parameters.
- 3) Go through all the possible routes in the DAG to get: the depth of the graph that represents the critical route, the width of the DAG and the density of the graph.

- 4) Measures the time consumed by the algorithm.

Core 3

- 1) Process the Markov algorithm. Receive the set of vertices and build the DAG.
- 2) Go through all the possible routes in the DAG to get: the depth of the graph that represents the critical route, the width of the DAG and the density of the graph.
- 3) Measures the time consumed by the algorithm.

The details of each step, within the processing cores are omitted in this research work for reasons of space; and instead, the results obtained in each experiment are highlighted.

B. Specifications

For a better understanding in the treatment of the DAGs, it is necessary to dictate the following specifications:

- There must be a dummy vertice of entry into the DAG, that indicates the input of the parallel program.
- There must be an exit node that indicates the end of the parallel program to be put into the system.
- There must be at least one route that leads from the input node to the exit node.
- There may be vertices without a link to the main node in the DAG, which represent processes that start after the main program has started.

In this work, the parameters of the algorithm are not compared, such as the probability of inclusion; in any case, these parameters remain fixed for the three methods and, once the DAGs are produced the three proposed parameters are observed, measured and analyzed.

C. Number of Nodes Generated (on Average) in the Critical Path

The objective of this experimentation is to verify the number of vertices generated by each method, in the critical route of the DAG. Obtaining a large number of vertices in the critical path, indicates that the costs of executing each task will be high: the task will remain in the system for a long time and will require a high number of system resources.

The parameters used in this experiment are: N and M . The parameter N stands for the finite set of vertices and takes the values of 5 to 20, and M stands for the number of nodes generated (on average) in the critical path.

What results does each method give? Fig. 1 shows the results for this experiment. For the case of the Erdős-Rényi method, there is a direct relationship between the number of vertices of the critical route and, the parameter of the number of vertices to be generated with the algorithm; this relationship allows generating DAGs with short critical routes, which represent a low consumption of processing resources in the HDCS.

The Markov chain method produces longer critical routes, due to the increase in the number of DAG levels. By producing more levels in the DAG, the Markov method also produces an

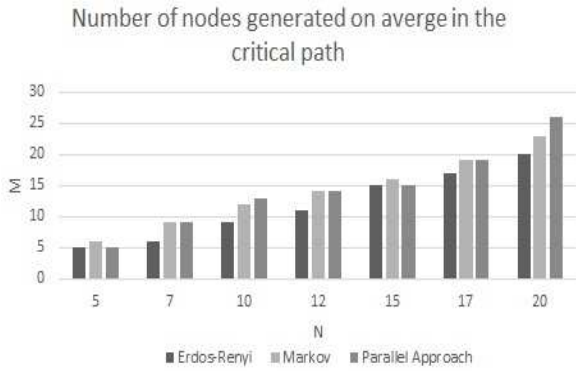


Fig. 1. Number of nodes generated (on average) in the critical path.

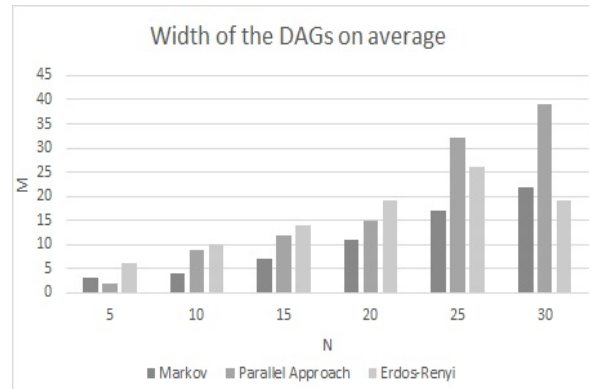


Fig. 2. The maximum parallelism in the DAG: width.

increase in the number of edges. These results allow to test the DAG with heavier loads in the HDCS.

The third method, the parallel approach, can produce critical routes that oscillate between the number of vertices generated and a greater number of vertices. Namely, it is a method that can be used to generate light synthetic loads and heavy synthetic loads, in the same set of tests of the scheduling algorithm.

D. The Maximum Parallelism in the DAG: Width

In general terms, the width determines the maximum parallelism in the DAG, this is the number of tasks in the longest level.

To generate a comparison between the 3 proposed methods, the parameter N was varied with the same values: from 10 to 30 with increments of 5 units.

For the the Markov chain algorithm, the parameters m and p , remain constant during the tests performed. The parameter E is considered a maximum number of edges as N^2 ; m representing the break points of the intervals, E the maximum number of edges and p the probability of inclusion.

The parameter N (the finite set of vertices) takes the values of 10, 20, 30. Thus the probability of a transition going from a state X to a state $Y \neq X$ is given by the formula $\frac{1}{N-1}$.

The width generated in the DAG with this algorithm occurs at the highest levels, i.e. if the graph is produced with 5 levels the maximum width is reached at level 1 or 2, which implies that the assignment and release of the resources in the distributed heterogeneous system are made at an early stage of the execution of the algorithm. The results obtained with this method and, according to the generated variations are shown in Fig. 2.

Given the random nature of the DAG generation, it is very difficult to determine the behaviour of the algorithm under different conditions, but it allows us to determine the resource usage times.

The parallel approach uses the following parameters: m representing the break points of the intervals, E the maximum number of edges and p the probability of inclusion.

The results obtained according to the generated variations are shown in Fig. 2.

The results obtained with this method show a thinning in the width of the DAG, what can be interpreted as the generation of parallel applications with less load of resources for the algorithm that realises the scheduling.

A very important point in this algorithm is the number of edges produced in the DAG. While the previous method generates few edges, in this method it is observable that at each level a substantial number of these are produced, which indicates the parallel applications that are represented contain high indexes of communication between them, allowing to evaluate the means of distributed system communication.

In this set of experimentations, the last method Erdős-Rényi, shows consistent results as shown in Fig. 2. The levels that occur in the DAG, maintain a strict attachment to the number of vertices that are generated, i.e., if 5 or 10 vertices are generated, at least one level in the DAG is produced with this same number of vertices. The consistency of this method makes it suitable for experimenting with light loads in the planning algorithm.

E. The Density of the Graph

We account for each level the number of edges, to determine the communication levels produced by the generated DAG.

According to the number of localized edges, we have classified connectivity levels as low, dense and very dense. A low level refers to the existence of a connectivity of 50% or less of the nodes between one level and another, that is, if level 1 has 6 vertices and level 2 has 2 vertices, a low connectivity refers to that 3 or less vertices of level 1 are connected with the 2 vertices of level 2. High connectivity refers to 80% or less of the vertices of level 1 are connected to the vertices of level 2. A dense communication level refers to there is a total connectivity between the vertices of a level and the vertices of its immediate lower level.

The parameters used in this experiment are: N and M . The parameter N stands for the finite set of vertices and takes the values of 5 to 20, and M stands for the percentage of edges, generated between DAG levels.

Fig. 3 shows the results obtained in the density of graphs. This experiment show that the Markov chain method stand out above the other two methods, by generating high connectivity;

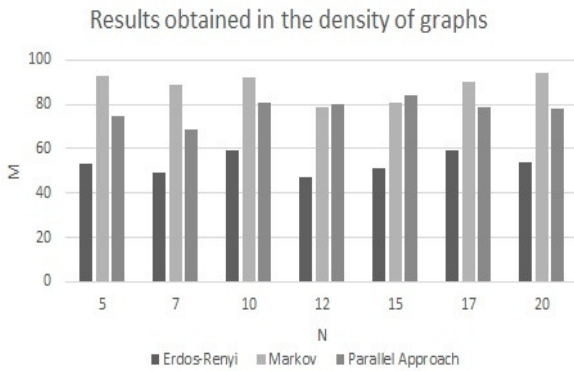


Fig. 3. Results obtained in the density of graphs.

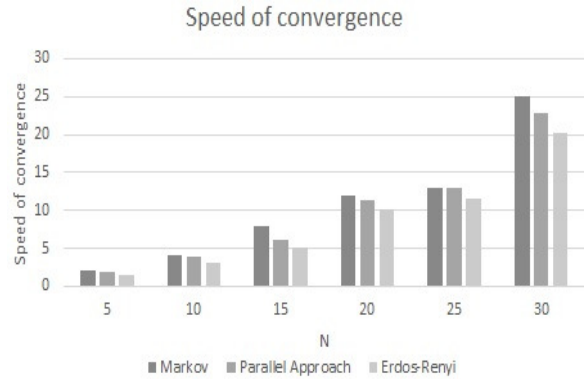


Fig. 4. Convergence time of methods.

with this method the number of connections between all levels of the DAG is very high.

The parallel approach, has an oscillation in the results and exhibits good scalability as the experiment progresses; it can produce dense connectivities and very dense connectivities. is considered in this work as a dual method, which facilitates experimenting with high and low levels of coefficient in the system.

The Erdős-Rényi method holds a stability in the connectivities produced in the DAG. During all the experimentation, the levels remain dense. These results are favorable for experimenting with stable loads in the planning algorithm.

The levels of connectivity of the graph, have been characterized to allow the allocation algorithm to have an “idea” of the location of the tasks in the HDCS. That is, a low connectivity allows the DAG’s tasks to be located in geographically remote computing resources. Whereas a dense connectivity, forces the algorithm to assign tasks as closely as possible.

F. Convergence Time of the Algorithms

Another characteristic observed in the experiments has been the convergence time of the algorithms proposed, i.e. the time that the algorithm needs to generate all the graphs.

The Markov chain method, due to its condition of being a sequential algorithm, its total time for the completion of the generation of total graphs is slightly higher, than the time needed for the parallel approach for random graph method, which was born with a condition of being a parallel algorithm. In summary form in Fig. 4 shows the times of convergence consumed, by each one of the methods.

The Markov chain method is used to represent parallel applications that require a large number of computational system resources, which will be used in the early stages of the algorithm; whereas, the second method facilitates the generation of DAGs with high communication requirements in the system.

The Erdős-Rényi method, accelerates convergence due to the simplicity of the method. In the results obtained, it produces the synthetic loads more quickly.

IX. CONCLUSIONS

The synthetic loads used for the evaluation of scheduling algorithms and assignment of tasks in HDCS, are generated by sophisticated methods that do not consider the characteristics of the DAGs in the scheduling process.

Evaluating an algorithm that discriminates or does not consider the properties of the DAGs, can produce amazing results in the evaluations of the scheduling algorithms with synthetic loads, but can generate devastating results when it is evaluated with loads of real users.

Therefore, in this work we evaluated three methods of generation of random graphs, to produce synthetic loads that were analyzed and evaluated to allow:

- Find the weaknesses and strengths of each method, generating synthetic loads constituted by a large number of DAGs.
- The ability of each method to represent parallel programs of real applications that users submit for execution in an HDCS.
- Evaluate the methods in each of the characteristics of the DAGs, and obtain a comparison of the obtained values.

Finally, with the algorithm proposed in this work, synthetic loads are produced. These loads are evaluated and analyzed before being used in an algorithm for planning and assigning tasks. The evaluations and analyzes generated allow us to design an algorithm, with the ability to predict the planning and allocation of computational resources in the target system.

X. FUTURE WORKS

Currently, we are experimenting with graphs that contain more vertices. The following experiments will have graphs with 20 to 50 vertices, with the same methods of generation.

We are also working with the design of the algorithm of scheduling and allocation of tasks. This algorithm is planned to be designed with a meta-heuristic strategy; the objective computer system to test the algorithm will have a heterogeneous hardware and a heterogeneous operating system. The synthetic loads generated with the methods proposed in this research work, and characterised with 5 parameters, are the

test DAGs that are received in the target system to measure different performance metrics.

ACKNOWLEDGMENT

The authors would like to thank: Tecnológico Nacional de Mexico and Instituto Tecnológico el Llano Aguascalientes, for the support received to carry out this research work.

REFERENCES

- [1] W. Zheng and R. Sakellariou, Stochastic DAG scheduling using a Monte Carlo approach. *Journal of Parallel Distributed Computing*. Vol 73 Num. 12 December 2013. Pp. 1673–1689. Elsevier Science Publishers B. V
- [2] D. Jungnickel, *Graphs, Networks and Algorithms. Algorithms and Computation in Mathematics*. Springer May 2008. Third edition. Vol 1.
- [3] L. Briceño, J. Smith, H. Siegel, A. Maciejewski, P. Maxwell, R. Wakefield, A. Al-Qawasmeh, R. Chiang and J. Li. Robust static resource allocation of DAGs in a heterogeneous multicore system. *Journal of Parallel and Distributed Computing*. Vol 73 Number 12. December 2013. Pp. 1705-1717. Elsevier Science Publishers B. V
- [4] D. Cordeiro, G. Mounie, S. Perarnau, D. Trystram, J. Vincent and F. Wagner. Random graph generation for scheduling simulations. *Proceedings of the 3rd International ICST Conference on Simulation Tools and Techniques*. March 15 - 19, 2010. ACM Digital Library. Torremolinos, Malaga, Spain. Pages 10.
- [5] Y. Xu, K. Li, L. He and T. Truong. A DAG scheduling scheme on heterogeneous computing systems using double molecular structure-based chemical reaction optimization. *Journal of Parallel Distributed Computing*. Vol. 73 Number 9. September 2013. Pp. 1306-1322 Elsevier Science Publishers B. V.
- [6] S. Yu, K. Li and Y. Xu. A DAG task scheduling scheme on heterogeneous cluster systems using discrete IWO algorithm. *Journal of Computational Science*. Vol 24. October 2016. Elsevier Science Publishers B. V.
- [7] G. Melançon and F. Philippe. Generating connected acyclic digraphs uniformly at random. *Information Processing Letters*. Vol 90. Number 4. May 2004. Pp. 209-213. Elsevier Science Publishers B. V. Elsevier Science Publishers B. V.
- [8] Y. Kwok and I. Ahmad. Benchmarking and Comparison of the Task Graph Scheduling Algorithms. *Journal of Parallel and Distributed Computing*. Vol 59 number 3, December 1999. Pp. 38-422 Elsevier Science Publishers B. V.
- [9] Ch. Gogos, Ch. Valouxis, P. Alefragis, G. Goulas, N. Voros and E. Housos, Scheduling independent tasks on heterogeneous processors using heuristics and Column Pricing. *Future Generation Computer Systems*. Vol. 60. July 2016. Pp. 48-66. Elsevier Science Publishers B. V.
- [10] F. Xhafa and A. Abraham. Computational models and heuristic methods for Grid scheduling problems. *Future Generation Computer Systems*. Vol. 26 number 4. April 2010. Pp 608-621. doi 10.1016/j.future.2009.11.005 url <https://doi.org/10.1016/j.future.2009.11.005>, Elsevier Science Publishers B. V.
- [11] M. Akbari and H. Rashidi. A multi-objectives scheduling algorithm based on cuckoo optimization for task allocation problem at compile time in heterogeneous systems. *Expert Systems with Applications*. Vol 60 October 2016 Pp. 234-248 Elsevier Science Publishers B. V.
- [12] P. Erdős and A. Rényi. On random graphs I. *Publicationes Mathematicae (Debrecen)*. Vol 6. Debrecen 1956 Pp. 290-297
- [13] T. Tobita and H. Kasahara. A standard task graph set for fair evaluation of multiprocessor scheduling algorithms. *Journal of Scheduling*. Vol. 5 Number 5 September 2002 Pp. 379-394 Wiley Online Library
- [14] R. Dick, D. Rodes and W. Wolf. TGFF: Task Graphs For Free. In *Proceedings of the 6th International Workshop on Hardware/Software Codesign*. March 1998 Pp. 97-101 IEEE Computer Society. Washington, DC, USA
- [15] P. Winkler, Random orders. *Order. A Journal on the Theory of Ordered Sets and its Applications*. Vol 1. Number 4 December 1985. Pp. 317-331 Springer Netherlands
- [16] G. Melançon, and I. Dutour and M. Bousquet-Melou, Random Generation of Directed Acyclic Graphs. *Electronic Notes in Discrete Mathematics*. Vol. 10 November 2001. Pp. 202-207. Elsevier Science Publishers B. V.
- [17] S. Bressan, A. Cuzzocrea, P. Karras, X. Lu and S. Nobari. An Effective and efficient parallel approach for random graph generation over GPUs. *Journal of Parallel and Distributed Computing*. Vol 73 Number 3 March 2013. Pp. 303-316 Elsevier Science Publishers B. V.
- [18] P. Dutot T. N'Takpé, F. Suter and H. Casanova. Scheduling Parallel Task Graphs on (almost) Homogeneous Multiclustor Platforms. *IEEE Transactions on Parallel and Distributed System*. Vol. 20 Number 7 January 2009. Pp. 940-952. IEEE Xplore Digital Library
- [19] Y. Xu, K. Li, J. Ju and K. Li. A genetic algorithm for task scheduling on heterogeneous computing systems using multiple priority queues. *Information Sciences*. Vol 270. June 2014. Pp. 255-287 Elsevier Science Publishers B. V.
- [20] A. Velarde, E. Ponce de León, E. Diaz and A. Padilla. Planning and Allocation Tasks in a Multicomputer System as a Multi-objective Problem. *EVOLVE - A Bridge between Probability, Set Oriented Numerics, and Evolutionary Computation IV*. Vol 227. July 10-13, 2013. Springer, Heidelberg. Pp. 225-244
- [21] A. Velarde and E. Ponce de León. Planning And Allocation of Tasks in a Multiprocessor System as a Multi-Objective Problem and its Resolution Using Evolutionary Programming. *IJACSA*. Vol 7 Number 3. March 2016. Pp. 349-360 SAI United Kingdom

A Comprehensive IoT Attacks Survey based on a Building-blocked Reference Model

Hezam Akram Abdul-Ghani, Dimitri Konstantas
Geneva School of Economics and Management
Geneva University, Switzerland

Mohammed Mahyoub
King Fahd University of
Petroleum and Minerals, KSA

Abstract—Internet of Things (IoT) has not yet reached a distinctive definition. A generic understanding of IoT is that it offers numerous services in many domains, utilizing conventional internet infrastructure by enabling different communication patterns such as human-to-object, object-to-objects, and object-to-object. Integrating IoT objects into the standard Internet, however, has unlocked several security challenges, as most internet technologies and connectivity protocols have been specifically designed for unconstrained objects. Moreover, IoT objects have their own limitations in terms of computation power, memory and bandwidth. IoT vision, therefore, has suffered from unprecedented attacks targeting not only individuals but also enterprises, some examples of these attacks are loss of privacy, organized crime, mental suffering, and the probability of jeopardizing human lives. Hence, providing a comprehensive classification of IoT attacks and their available countermeasures is an indispensable requirement. In this paper, we propose a novel four-layered IoT reference model based on building blocks strategy, in which we develop a comprehensive IoT attack model composed of four key phases. First, we have proposed IoT asset-based attack surface, which consists of four main components: 1) physical objects, 2) protocols covering whole IoT stack, 3) data, and 4) software. Second, we describe a set of IoT security goals. Third, we identify IoT attack taxonomy for each asset. Finally, we show the relationship between each attack and its violated security goals, and identify a set of countermeasures to protect each asset as well. To the best of our knowledge, this is the first paper that attempts to provide a comprehensive IoT attacks model based on a building-blocked reference model.

Keywords—Internet of Things (IoT); building block; security and privacy; reference model

I. INTRODUCTION

Flooding a huge number of the physical objects into the Internet at an unprecedented scale is a consequence of the Internet of Things (IoT)[1], [2]. These physical objects include, but not limited to, temperature sensors, smart phones, air conditioning, medical equipment, light bulbs, smart grid, thermostats, and TVs. Being communicated directly without human intervention, physical objects are enabled not only to monitor their environments, but also to execute shared tasks and coordinate their decisions autonomously [3].

The importance of IoT systems in different aspects of our lives has been elucidating in many research studies [4], [5] associated with fetching a networked intelligence to the physical objects world-wide, allowing them to sense and collect environmental data. Furthermore, human lives seriously depend on transportation facilities traveling us every day, civil infrastructure systems such as electric power and

water, and critical healthcare infrastructure systems, all of them have created a proper environment around us. Being tightly coupled with human beings and their environment, a single vulnerability in such systems could lead to harmful consequences, ranging from loss of privacy, physical damage, financial losses, and the possibility of endangering humans' lives [6]. To this end, IoT security is the biggest concern, for citizens, consumers, organizations, and governments wanting to protect their objects from being hacked or compromised, and must be addressed with caution [7].

Protecting IoT objects necessitates a general security framework - which is a challenging task indeed - covering all IoT assets and their corresponding possible attacks in more details. Therefore, it is absolutely essential to identify all attacks against security or privacy of IoT assets, which is the first step towards developing such framework. Having said that, IoT ecosystem, without doubt, is very complex and confusing, especially when it comes to precisely defining its main assets. Literature, however, has shown several IoT threat models based on IoT assets, none of which has introduced a comprehensive IoT attack model along with compromised security goals for such a highly intricate system [8]. This paper has investigated all possible IoT security attacks and countermeasures in each IoT asset. More particularly, it:

- states a novel IoT reference model, comprising of four main layers and their corresponding building blocks. This kind of combination would play a crucial role in identifying IoT components or assets;
- approaches a great enhancement to IoT Reference Models (RMs) since the IoT RMs currently published have not addressed IoT attacks and threats, nor described required building blocks for each layer as this paper did;
- defines a set of IoT security goals, security attacks, and a secure object;
- proposes a comprehensive IoT attack model which consists of four main phases; Mainly, it could be used to support the creation of a secure IoT-related system. Application designers willing to develop secure IoT systems could integrate mitigation techniques explained in this paper with a list of common IoT attacks targeting each asset from the early stages of IoT development; and
- establishes what type of security goals has been violated for each addressed asset, such as privacy,

confidentiality, auditability, integrity, accountability, availability, trustworthiness, and non-repudiation;

As a summary, this comprehensive survey would be useful for academic and industry based researchers, who are engaged in design of secure IoT systems by examining which attacks have been investigated, how such attacks have been handled, and which attacks remain untouched.

The rest of the work has been organized as follows. The proposed IoT reference model is given in Section II. Section III shows the related work presented in the state-of-the-art. The proposed IoT attack model is discussed in details in Section IV, defining all possible attacks and their corresponding countermeasures on IoT physical objects, protocols, software, and data. Final remarks and future work conclude this paper are given in Section V.

II. IOT REFERENCE MODELS

The state-of-the-art has shown that there is a lack of standardized approaches for understating and modeling IoT vision in many aspects [12].

First, differentiating between an IoT system and a non-IoT system is not absolutely clear. It is worth noting that not every system is the IoT system. In fact, when data is created under the control of objects or entities and forwarded or sent across a network, it can be considered as the IoT system [11]. Second, identifying precisely IoT assets and its components is very confusing due to the complexity of IoT ecosystem, varying from physical objects placed in the environments until their data and applications resided in the cloud. As a result of this complexity, they are susceptible to many attacks and threats [13].

Third, IoT umbrella covers different applications, development stages or cycles, middleware, fog computing, software platform, protocols and hardware platforms. That said, it lacks a common ground to be understood by researchers or even IoT developers [14].

Motivated by above mentioned aspects, handful of papers have been proposed to establish a common ground of understanding IoT paradigm known as IoT reference models, the most dominant of which are the following:

1) The three-layer model as shown in Fig. 1 represents IoT system as an extension to wireless sensor networks (WSN) [9]. In other words, it can be considered as an integration of WSNs and cloud servers providing several services to the users.

2) The five-layer model as depicted in Fig. 2 is relatively more structured suggested to ease the communications among several components of IoT system by dividing the complex system into a well-defined part [15], compared to the previous one.

3) The seven-layer developed by Cisco as shown in Fig. 3 extends both the three-layer and the five-layer models, trying to create a comprehensive and agreeable IoT reference model[11]. Its capability of standardization makes it ideal for IoT system.

Despite the simplicity of RMs mentioned above which breaks down the complexity of IoT ecosystem into different

layers, they lack the required building blocks for their layers. An IoT building block is an essential unit or an enabler technology on which IoT system is constructed. In the context of IoT vision, building blocks are nowadays receiving more attention to provide a better understanding of IoT. Authors in [16] have described different building blocks. The most important ones are the identification, sensing, and communication.

To this end, we propose a four-layered reference model based on building blocks strategy as shown in Fig. 4, the main contributions of such model are the following:

First, the great contribution we intend to produce lies in merging each layer of IoT RMs with the required building blocks. This kind of combination would greatly help IoT stakeholders, paving the road for precisely identifying IoT components and assets. Second, we believe that building blocks would lead to a huge change in the mentality of security analysts who used to address security issues as a whole for each layer, making them address security issues of specific enablers technologies at each layer. Third, equipped with a set of building blocks at each layer, it introduces a new classification of IoT assets composed of four main components, hardware components, protocols, data at rest, and software including operating systems, firmware, and applications. These components will be used as a starting point in our attack model proposed in Section IV.

The proposed IoT reference model classifies building blocks broadly into three categories, protocols, hardware components, and software. In general, protocols fall under five building blocks in our model: connectivity, routing and networking, service discovery, communication, and web service and web servers protocols. Hardware components consists of two main building blocks: 1) sensing, which includes sensors, actuators, and RFID; and 2) hardware platforms or micro-controllers, which include different types of micro-controllers. Finally, software components are composed of four building blocks: operating systems, fog computing, middle-ware, and cloud solutions.

Despite the difference in the number of layers in both our model and Cisco reference models, they have the same IoT components. To validate that our reference model have covered the most important IoT components, we compare it with Cisco's reference model. Unlike Cisco's model, its first layer is specialized for physical devices, perception level in our model includes not only physical objects but also connectivity technologies represented in different layers in Cisco's model. By observing Fig. 3, it is obvious that layer 1 and layer 2 in Cisco's model have been merged into one layer in our reference model shown in Fig. 4. In contrast, the layer 3 in Cisco's model has been divided into two layers (2 and 3) in our proposed reference model. Finally, our last top layer, the cloud layer, includes four layers of Cisco model, starting from layer 4(Data accumulation) until the last one known as users and data centers.

It is worth noting that this paper is not meant to give a detailed explanation of the previous IoT reference models, because they are beyond the scope of this work. Each layer, in our model, is associated with specific tasks and functions and the data movement is often bidirectional, either from the cloud layer to the perception layer in the controlling mode or from

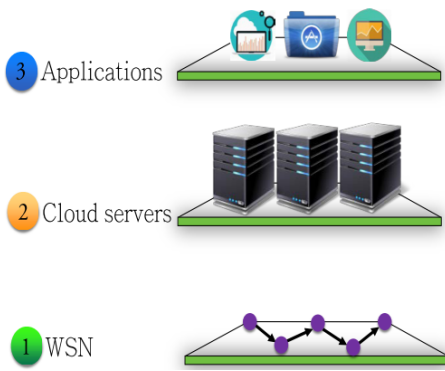


Fig. 1. Three-layer model [9].

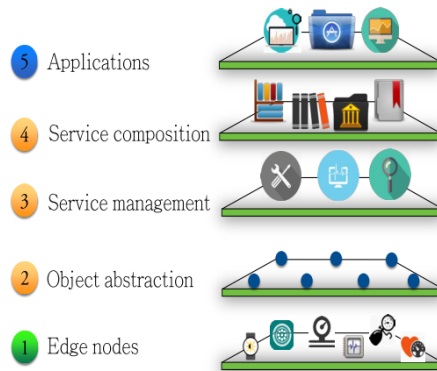


Fig. 2. Five-layer model [10].



Fig. 3. CISCO's seven-layer model [11].

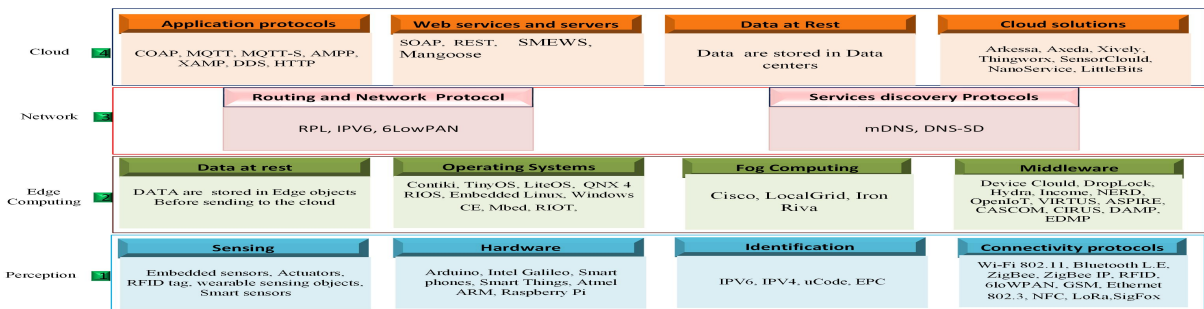


Fig. 4. An overview of the proposed IoT reference model and its building blocks.

the perception layer to the cloud in the monitoring mode.

III. RELATED WORK

The methodology followed to execute the conducted survey is illustrated here for the purpose of evaluating the research works that have been done in literature and to determine if the topic has been completely investigated. As IoT vision and its security is relatively new, our concentration was on the publications that were released in the period 2000-2017. These publications include books, journals, conferences, websites, white-papers, and reports. Fig. 5 provides the time period of this survey, and the number of published papers at each layer of the proposed reference model in that period. Perception, network, cloud, and edge computing layers are represented in Fig. 5 as a, b, c, and d bar charts, respectively.

According to Fig. 5, the key observation is that there has been an increase in the number of published papers addressing security attacks on all layers nearly from 2006 to 2015. This is, in our opinion, because of the rapid growth of IoT in a huge number of application domains such as critical infrastructure systems and the appearance of different attacks that threaten human lives and hamper the realization of IoT, which require a lot of research to be solved. As samples of our searching keywords, we have used “IoT security”, “IoT countermeasures”, “IoT security challenges”, “attacks on IoT”, “IoT security goals”, “IoT privacy”.

Although a huge number of research works have conducted to address security attacks of IoT systems in the state-of-the-art, handful of papers have attempted to investigate IoT attacks

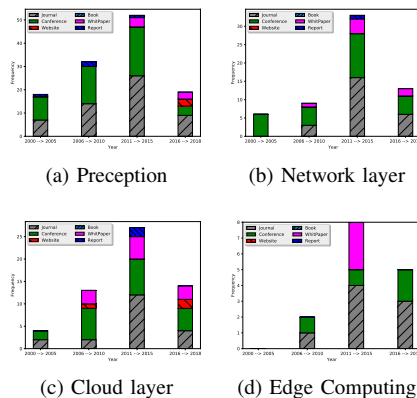


Fig. 5. Published paper frequency corresponding to different layers.

in a comprehensive approach, the most popular of which are the following:

In [17], authors have proposed a new approach of addressing IoT threats and attacks based on a four-layer model composed of objects, interfaces, storage, and transport. Although this paper described some attacks on these levels, it did not comprehend all possible attacks. For example, firmware tampering has only been discussed as an example of physical attacks against IoT objects.

In [8], edge nodes, edge computing, and communication have been investigated in details by identifying all possible threats and attacks on each level. Moreover, this paper has

introduced a set of countermeasures to mitigate such attacks. In spite of identifying possible attacks and their countermeasures in these levels, it untouched other important components in IoT systems. For example, attacks on data at rest either locally on IoT objects or remotely on the cloud have been completely uncovered.

In [18], IoT architecture has been divided into four layers: 1) application layer; 2) adaptation or support layer; 3) network layer; and 4) perception layer. Even though this approach described security threats in each layer, it lacks a comprehensive set of attacks of each layer. For example, it identified security attacks against IoT network in high level without analyzing the attacks against each network protocol. Furthermore, it uncovered the relationship between IoT attacks and their compromised security goals. IoT ecosystem presented in [19] has been divided into three levels, namely back-end system, network, and front-end sensors. The authors did not identify all attacks for each level. For example, only two types of attacks, management of the code and replacement of operator, have been identified in the network layer.

The authors in [20] divided IoT attack taxonomy into six categories, namely storage management, identity management, dynamic bidding, physical threats, communication threat, and embedded security. However, security attacks have been identified at high level in each category. Only three types of attacks on communication, denial of service, spoofing, and network injection, have been introduced.

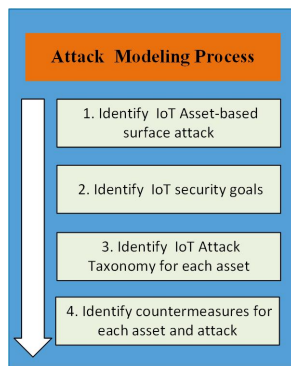


Fig. 6. An overview of the proposed attack model.

IV. OUR PROPOSED IoT ATTACK MODEL

In this section, we will explain the proposed methodology used to create a comprehensive IoT attack model for Internet of Things. The proposed methodology for developing IoT attack model consists of four main phases. An overview of the whole methodology is shown in Fig. 6, starting from phase one, which suggests a new IoT asset-based attack surface based on the proposed building-blocked reference model in section II, down to phase four, which identifies a set of countermeasures to protect each IoT asset. The main phases of the proposed approach are described in greater detail below:

A. Identify IoT Asset-based Attack Surface

By observing the proposed IoT reference model and its companion building blocks so far, we classify IoT asset according to its threats and attacks possibilities on its building

blocks into four categories: 1) physical objects; 2) protocols; 3) data; and 4) software. In other words, IoT attack surface, in the proposed IoT attack model, will be analyzed from a multi-layer perspective as shown in Fig. 7 and described as follows:

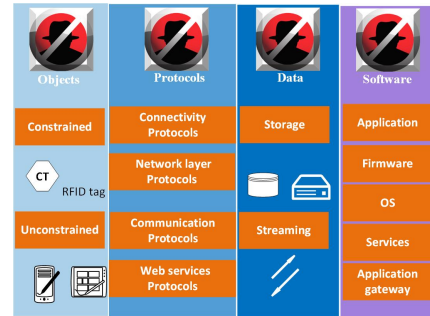


Fig. 7. IoT attack surface.

- 1) **Physical objects:** This category will focus on identifying all physical attacks targeting the hardware components of both constrained and unconstrained objects, resided in the perception and the edge computing layers, respectively. RFID tags, RFID readers, micro-controllers, actuators, and sensor nodes are examples of such components.
- 2) **Protocols:** This category is devoted to discover all potential attacks on IoT protocols. These protocols are connectivity, networking and routing, application and transport layers protocols known as communication protocols in the proposed reference model, and web services protocols. In other words, all possible attacks on IoT stack will be investigated.
- 3) **Data:** This category investigates the main attacks only on data at rest located either in IoT objects or in the cloud. This is because attacks on data in motion will be discussed on protocols' attacks as shown in Fig. 7.
- 4) **Software:** This category focuses on identifying all possible attacks on IoT software, including IoT applications located either in IoT objects or in cloud, firmware, operating systems, application gateway and services. [21].

B. Identify Security Goals and Security Attack

In this section, we will explain the two most common concepts used in IoT domain: a secure object and a security attack [8]. In order to define the secure object, it is mandatory to comprehend the security goals in which we can distinguish security. In the state-of-the-art, conventional security goals are divided into three key categories known as the CIA triad: confidentiality, integrity, and availability. Confidentiality is associated with a set of guidelines in which only authorized entities can get access to information. With the advent of Internet of things paradigm, it is important to ensure the confidentiality of IoT objects, since such objects may deal with sensitive data like medical records. Providing reliable services in the IoT requires integrity to ensure that IoT objects have received only legitimate commands and data. IoT availability ensures that IoT services are accessible only by authorized

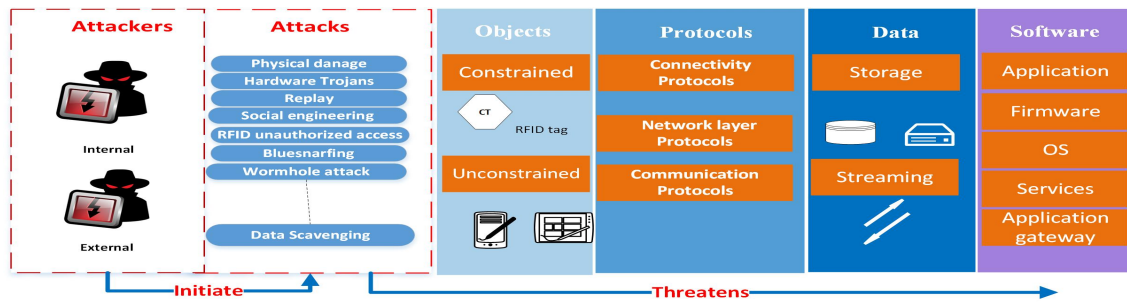


Fig. 8. IoT attack taxonomy.

TABLE I. IOT SECURITY REQUIREMENTS

Security Requirements	Definition	Abbreviations
Confidentiality	The process in which only authorized objects or users can get access to the data	C
Integrity	The process in which data completeness, and accuracy is preserved	I
Non-repudiation	The process in which an IoT system can validate the incident or non-incident of an event	NR
Availability	An ability of an IoT system to make sure its services are accessible, when demanded by authorized objects or users	A
Privacy	The process in which an IoT system follows privacy rules or policies and allowing users to control their sensitive data	P
Auditability	Ensuring the ability of an IoT system to perform firm monitoring on its actions	AU
Accountability	The process in which an IoT system holds users taking charge of their actions.	AC
Trustworthiness	Ensuring the ability of an IoT system to prove identity and confirm trust in third party	TW

users or objects. In spite of the popularity of CIA-triad, authors in [22] have proven that the CIA-triad fails in addressing novel threats, which emerge in a cooperating security environment. To fill this gap, they provide a comprehensive set of security goals known as an IAS-octave, referred to the Information Assurance and Security, by investigating a large number of information systems in terms of security and assurance. Table I outlines the security goals proposed by the IAS-octave, along with their definitions and abbreviations. Once the main security goals are identified, then the secure object and the security attacks can be defined as follows:

- Secure object is an object that matches or meets all the security goals shown in Table I.
- Security attack is an attack that compromises at least one of the security goals.

C. IoT Attack Taxonomy and Countermeasures for Each Asset

The proposed IoT attack taxonomy, as depicted in Fig. 8, shows different attacks launched either internally or externally, such as hardware trojans, viruses, and physical damage [21]; the list is almost endless. Such attacks target four asset categories mentioned in the asset-based attack surface. In other words, this attack taxonomy will be analyzed from multi-layer perspectives as follows:

1) **Physical-based attacks:** IoT software are subjected to so many attacks. Similarly, hardware components of IoT systems, such as controllers, RFID readers, sensors, and different types of RFID tags, are vulnerable to different physical attacks, [23]. In this section, the main attacks targeting the hardware components of IoT systems as depicted in Fig. 9 are described in greater detail below.

Object replication attacks: An attacker, in this type of attack, has a capability to add physically a new object to the network. For example, a malicious object could be added by replicating object’s identification. Such an attack, therefore, could cause a huge drop in the network performance. In addition to performance degradation, corrupting or misdirecting the received packets can easily be fulfilled by the malicious object, allowing the attacker to get access to sensitive data and extract the secret keys [24].

RF Interference on RFID: Sending a huge number of noise signals over radio frequencies, which are mainly used for RFID’ communication, is the main goal of this type of attack [34].

Hardware Trojan: A number of research works have shown that the main security issue in an integrated circuit is its vulnerability to a hardware trojan attack. The main purpose of such attack is to maliciously modify the integrated circuit to gain access to its sensitive data and firmware. Hardware trojan attack takes place at the design phase and remains dormant until receiving a trigger or an event from its designer [35].

Outage attacks: In some situations, a group of IoT objects placed in unattended environments may stop operating due to either turning off their power or using much power by an attacker.

Object jamming: In spite of the benefits of using wireless technology in IoT vision, its signals can easily be hindered using a jammer [36].

Physical damage: Being deployed in unattended environments, IoT objects are significantly susceptible to physical attacks, the easiest one of which is a direct harm of its components [36].

Camouflage: Physically inserting a counterfeit edge object to a network by an attacker, to be hidden among other objects so that it could be used as the normal object to process and redirect the packets, is the main idea behind this attack [37].

Malicious node injection: To gain an unauthorized access to an IoT network, the attacker could insert a malicious object

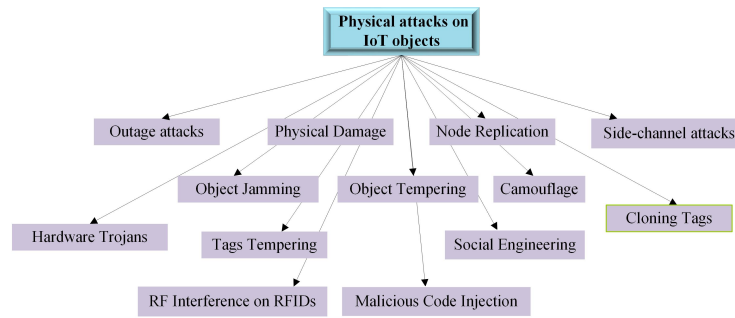


Fig. 9. Taxonomy of physical attacks against IoT objects.

TABLE II. PHYSICAL ATTACKS WITH COMPROMISED SECURITY GOALS AND COUNTERMEASURES

Physical attacks	Compromised security requirements	Countermeasures
Object tempering	ALL	Tamper proofing and self-destruction, minimizing information leakage [25] (adding randomized delay, intentionally-generated noise , balancing hamming weights , improving the cache architecture, shielding), integrating Physically Unclonable Function (PUF) into object [26]
Outage attack	A,AC,PAU,NP	Secure physical design [27]
Object replication	ALL	Encryption, Lightweight cartographic mechanisms, Hash-based techniques [8]
Camouflage	ALL	Securing firmware update, Encryption, hash-based schemes, authentication technique [8]
Side-channel attacks	C, AU, NR, P	Blocking, isolation, kill command, sleep Command, tamper proofing and self-destruction, mimimizing information leakage, obfuscating techniques [8]
Tag cloning	ALL	Encryption, hash-based schemes [28], authentication technique, kill sleep command, isolation, blocking, distance estimation. 8. Integrating PUFs into RFID tags [29]
Social engineering	ALL	Back up techniques, education of IoT users, tamper proofing and self-destruction [30]
Physical damage	ALL	Secure physical design, tamper proofing and self-destruction [8]
Malicious Code Injection	ALL	Tamper proofing and self-destruction, IDS [8]
Hardware Trojans	ALL	Side-channel signal analysis (based on path-delay fingerprint, based on symmetry breaking, based on thermal and power, based on machine learning), trojan activation [31]
Object jamming	ALL	Spread Spectrum, priority messages, lower duty cycle, region mapping, [32]
Tag Tempering	ALL	Integrating PUFs into RFID tags, encryption, hash-based schemes [28], tamper-release layer RFID, alarm Function for active Tags[33]

among legitimate ones in the network. As a result, he could gain access to any object, insert false data to hamper messages delivery, and perhaps control the entire network. [37].

Object tampering: The possibility of accessing IoT objects physically by attackers is very high due to the fact that some IoT objects may be deployed in unfriendly environments. Therefore, such objects are vulnerable to hardware attack, the most notable ones are the extraction of cryptography keys, the alteration of operating system or firmware, and the circuit modification. The replacement of the Nest thermostat with malicious one is an example of such attacks[38].

Social engineering: Authors in [36] show that a social engineering attack can be considered as a physical attack, since an attacker could physically modify the users of IoT system in order to get their sensitive data.

Side-channel attack: Most IoT objects, for security purpose, will be integrated with some of security mechanisms such as an encryption to protect their sensitive data. Side-channel attack, however, is intended to break such mechanisms by analyzing side channel information emitted by IoT objects. Power, and time analysis attacks are some examples of such attacks [8].

Malicious code injection: An adversary, in this type of attack, could insert physically a malicious code into an IoT object. The main goal of such injection is to gain a full control of IoT system [36].

Tag cloning: Due to the deployment of tags on different

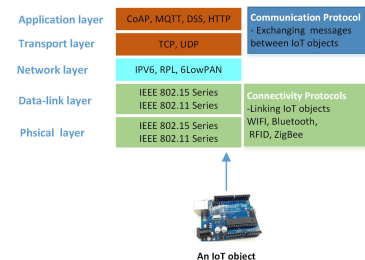


Fig. 10. The IoT stack.

objects, tags are vulnerable to physical attacks. An attacker could easily capture these tags and build a replica of them, which look like original ones to compromise a RFID system by deceiving even the RFID readers [8].

An overview of all attack against hardware components, their compromised security goals, and their available defense mechanisms is presented in Table II.

2) **Protocols-based attacks:** Unlike traditional internet stack designed for unconstrained objects, IoT system has its own stack, as described in Fig. 10. IoT stack requires lightweight protocols such as 6LoWPAN and IEEE 802.15.4 different from conventional internet protocols. For simplicity, we will classify IoT protocols into three groups known as connectivity protocols, communication protocols, and network protocols as shown in Fig. 10.

Connectivity protocols are used to link IoT objects with

TABLE III. CONNECTIVITY PROTOCOLS AND THEIR FEATURES

Connectivity protocols	Range	Data Rate	Power Con.	Topology	TCP/IP	Spectrum	Estimated node	Approx. Cost
Wi-Fi 802.11	100 M	<1Gbs	Varies	Mesh	√	2.4Ghs	100	<5 \$
Bluetooth	10 M	2to34 Mb	<30 mA	Piconet	p	2.4Ghs	7	<5 \$
Bluetooth L.E.	100 M	100 Kbps	>10 mA	Star	P	2.4Ghs		<2 \$
ZigBee	100 M	250 Kbps	<35 mA	Mesh	X	2.4Ghs	65536	<5 \$
ZigBee IP	100 M	250 Kbps	<35 mA	Mesh	√	2.4Ghs	65536	<5 \$
RFID	100 M	640 Kbps	Varies		X	860,960	< 100	<2 \$
6loWPAN	200 M	200 Kbps	<20 mA	Mesh	√	2.4Ghs	< 100	5-10
GSM	35 KM	150 Mbps	<200 mA	PTP	√	800-2100	< 100	<10 \$
NFC	10 cm	212 Kbps		PTP	X	13.56		<2 \$

each other, and implemented on data link and physical layers of IoT stack. Communication protocols are used to exchange messages between IoT objects, and implemented on application and transport layers of IoT stack.

2.1 Connectivity protocols-based attacks

IoT objects are armed with different connectivity protocols divided broadly into two main categories, wired and wireless protocols. The wired connection requires a physical medium between IoT objects, while wireless connection runs through radio waves. Both connectivity technologies have several key properties such as range, data rate, power consumption, spectrum, TCP/IP support, and topology. It is worth mentioning that this paper focuses only on wireless connectivity protocols, because most IoT objects are nowadays equipped with wireless connectivity protocols. Furthermore, attacks on wired connectivity protocols are adequately addressed in the context of traditional internet. An overview of the most popular wireless connectivity protocols and their properties is shown in Table III. In this section, the main attacks targeting the most common connectivity protocols as depicted in Fig. 11 are described in greater detail below.

2.1.1 RFID-based attacks: RFID technology facilitates automatic information exchange between tags and readers using radio waves. RFID uses the Automatic Identification and Data Capture (AIDC) technology. RFID tags, recently, have been utilized in many applications such as credit cards, assets tracking, and military [39]. However, RFID technology is vulnerable to many attacks, the most important of which are the following (Table V):

Replay: In this type of attacks, an attacker could use tags' responses to fake readers' challenges. In replay attacks, the transmitted signal between the reader and the tag is captured, documented, and repeated at a later time to the receiving object, resulting in counterfeiting the accessibility of the tag [39].

Spoofing: This type of attack happens when a malicious tag pretends to be a valid tag and obtains an unauthorized access. Spoofing attack used to eavesdrop the data coming from the valid tag, and copies the captured data to another one [39].

TABLE IV. COMMUNICATION PROTOCOLS AND THEIR PROPERTIES

Communication protocols	Publish/subscribe Request/ response	Transport protocol	Quality of service	Security support	Payload format	Node discovery	Centralized OP.	Header size	Decentralized Op.
COAP	√ √	UDP	√	DTLS	XML	√	X	4	√
MQTT	√ X	TCP	√	SSL	Binary	x	√	2	x
MQTT-S	√ X	TCP	√		Binary	x	√	2	x
AMPP	√ √	TCP	√	SSL	XML, <u>Json</u>		√	8	x
XAMP	√ x	TCP	x	SSL	Xml EXI	√	√	-	√
DDS	√ X	UDP	√	DTLS	User define	√	X	-	√
HTTP	X √	TCP	X	SSL	HTML...	√	√	-	X

Tracking: Tracking attack can be considered as a direct attack against an individual or a victim. Within the next few years, companies may place RFID tags on many household items. Tracking products using RFID tags could be used to threaten the privacy of human by tracking their movements, and generate an exact profile of their procurement [34].

Unauthorized access: Due to the lack of authentication in RFID system, tag could be vulnerable to an unauthorized attack. The main goal of such attack is to manipulate its sensitive data [40].

Virus: RFID system is not suitable environment for viruses as the tag has a small storage capacity of 128 bits. However, this situation has changed, as authors in [41] stated that RFID tags could be used as a medium to spread a computer virus. This paper also described how the RFID virus ran in supply chain products.

Eavesdropping: In RFID system, tags and readers are wirelessly connected and communicated without a human intervention. So, there is a possibility that their communication medium can be eavesdropped. In general, eavesdropping launches when an adversary captures data transmitted between tag and reader, since most RFID systems lack any encryption technique during transmission process due to the memory capacity. As a result, it is very easy for any attacker to obtain the sensitive data from RFID tags.

Man in the middle (MITM): MITM attack might be happened on RFID system during transmission of data between reader and tags. In this case, an attacker may intercept and modify the communication channel between the components of RFID system. This type of attack is considered as a real time attack, displaying and modifying the information before the legitimate object receiving it.

Killing Tag: Killing tag attack on RFID system could be launched to stop tags communication with their reader. Killing tags makes them impossible to be read, and therefore, it is absolutely essential to make sure that RFID tags are not killed by an illegal party. Kill command should be secured by a strong password as well[39].

2.1.2 NFC-based attacks: It uses in several payment

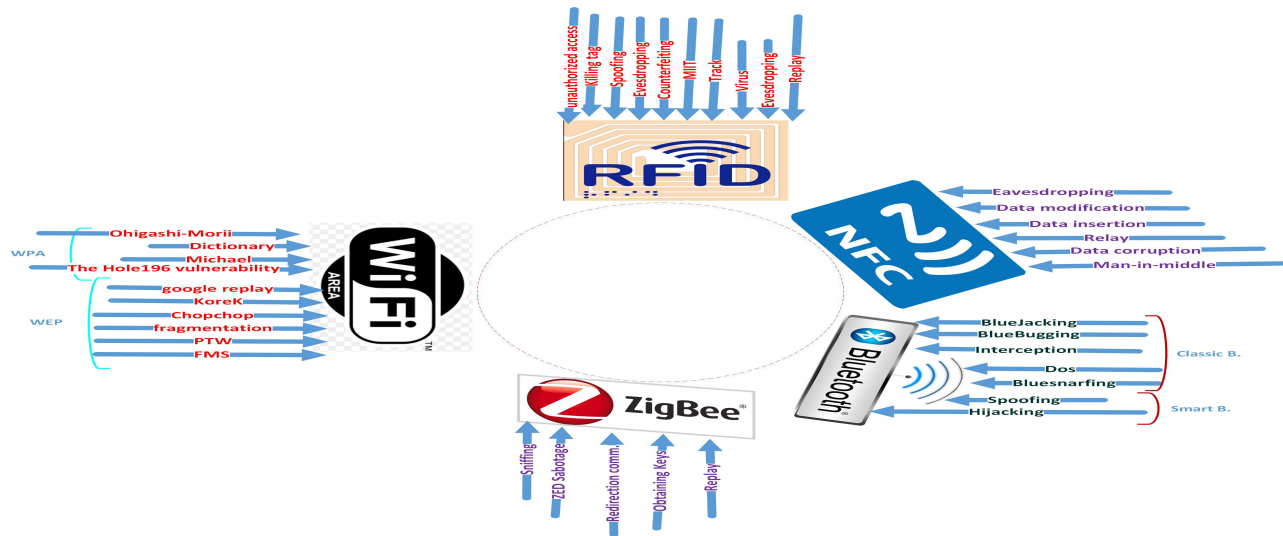


Fig. 11. Taxonomy of connectivity protocols attacks.

TABLE V. CONNECTIVITY PROTOCOLS AND THEIR SECURITY SUPPORTS

Connectivity Protocols	Security Modes	Reliability	Device type	Error Control
Wif-Fi 802.1X	WEP, WPA, WPA2 , Access Control List (ACL).	TCP/UDP others	Access point, devices	Frame Check Sequence (FCS)
Bluetooth	Three different security suites: null security 1, service level security 1, link level security 1	The acknowledge information (ACK or NAK bit)	Master and slave	1/3 rate FEC, 2/3 rate FEC, Automatic Repeat reQuest (ARQ)
ZigBee	Eight different security suites provided by IEEE 802.15.4 and key management	ACKS and control of duplicate packets	Coordinator and end device	Cyclic Redundancy Check (CRC)
Active RFID 802.15.4f	Eight different security suites provided by IEEE 802.15.4	TCP/UDP others	Tags and reader	CRC, ACKS optional
6LoWPAN	Eight different security suites provided by IEEE 802.15.4: null security 1, encryption only 1, authentication 3, authentication with encryption 3	TCP/UDP others	Edge router,mesh node(mesh under), router(route over), and host	CRC, ACKS optional

applications reaching almost 50 billions at the end of 2013. NFC was designed to allow different objects with the same technology to communicate securely with each other. However, this protocol suffers from several attacks [42]. The most important attacks are the following:

Eavesdropping: In NFC system, data exchange between two objects takes place in the close proximity. That said, such system is susceptible to an eavesdropping attack. Communication channel between two IoT objects equipped by NFC protocol is vulnerable to such attack, since NFC lacks any protection technique. An attacker could intercept the communication channel using a powerful antenna or be on close proximity of the communication range [43].

Relay attack: Performing this type of attacks relies heavily on the execution of the application protocol data unit instructions (ISO/IEC1443). Relay attack Forwards the request of victim’s reader to a malicious one and replays back its response as fast as possible [44].

Man-in-middle: Although NFC protocol requires a close proximity between communicated objects, these objects are theoretically vulnerable to man in the middle attacks. An attacker could intercept the data, modifying and relaying it to malicious objects. Besides the close proximity that makes these attacks are very difficult, encryption techniques also make them so hard to success if they implemented properly [45].

Data corruption: Data corruption launches when an at-

tacker has the capability to disturb communication channel between two objects by changing the transmitted data to an unreadable format, resulting in denial of services attack [46].

Data modification: Unlike data corruption, in which an attacker change only the format of transmitted data, data modification attack could alter the content of the data [47].

Data insertion: During the process of changing data transmitted between two bjects equipped with NFC protocol, an attacker could insert some data into this data only if the object requires a long time to reply. The successful insertion could only happen “if the inserted data can be transmitted, before the original device starts with the answer. If both data streams overlap, the data will be corrupted” [46].

2.1.3 Bluetooth-based attacks: In this section, we will identify the most popular attacks targeting Bluetooth protocol:

Bluesnarfing: The main goal of this attack is to get access illegally to Bluetooth devices so that the attacker could retrieve their information, and redirect the incoming calls to another [48].

BlueBugging: Bluetooth devices are vulnerable to many attacks, the most dangerous of which is bluedugging. In this type of attack, an adversary could be inside the victims device by exploiting some vulnerabilities in old devices firmware; hence, he could spy on phone calls, send and receive messages, and connect to the internet without legal users awareness [48].

bluejacking: Recently, the majority of Bluetooth devices have been designed to send a wireless business card. Consequently, a new attack has been designed to exploit this feature by sending an offensive card; however, such attack doesn't put information at risk. In this type of attack, the attacker should be very close-within 10meters- to the victim's device to establish this attack. To overcome such attack, it is recommended to put the devices armed with this protocol on nondiscoverable mode [48].

Denial of service (Dos): Repeatedly using his Bluetooth device to send a request pairing to the victim's device, an adversary could establish DOS attacks. Unlike a traditional Internet, where this kind of continuous request could shut down services, most of Bluetooth DoS attacks have been designed to create a nuisance because information in Bluetooth system can be transmitted without user's awareness. According to many research [49], performing DoS attacks is the simplest way to drain a device's battery.

Interception: Unencrypted transmission could be intercepted by a passive eavesdropper. Bluetooth interception does not require sophisticated nor expensive hardware. There are several affordable hardware options that help to accomplish this task, such as Ubetooth [50].

Hijacking: This type of attacks takes place when a configuration layer of the iBeacon has been compromised by an unauthorized third-part to control the beacon settings. DoS and spoofing might be happened as a consequence of such attack [51].

Spoofing: One of the most popular vulnerabilities in Bluetooth Low Energy is the spoofing, as the beacon is publicly broadcasted . A sniffing tool may be used to capture beacon's UUID by an attacker, imitate the beacon and break the rules made by the applications to verify the identity so that he could access to the services [51].

2.1.4 Wifi-based attacks: The development and the realization of IoT vision depends heavily on different enabler technologies. Wifi (IEEE 802.11) is one of such technologies . In this section, we identify possible attacks against the Wi-Fi.

FMS attack: This type of attack was released in 2001 by Fluhere, Shamir, and Mantin. The attackers have compromised the WEP protocol due to its vulnerabilities. It is a stream cipher attack in which attackers could recover the encryption key used to encrypt exchange by knowing Initialization vectors (IV). However, the possibility of this attack on RC4-based SSL(TLS) is very difficult as the key generation depends on a hash function [52].

Korek attack: Korek, an unknown participant on NetStumbler.org security forums, has discovered a new attack on Wired Equivalent Privacy (WEP) protocol [53]. Such attack depends on FMS-attack to find the key. Furthermore, he has released an A-neg attack through which the attackers could reduce the key generation possibilities to discover the key faster [54].

Chopchop attack: The Chopchop attack was developed by Korek. Instead of compromising a vulnerability in the RC4 algorithm, such attack focuses on the design defects in WEP protocol such as the vulnerability in CRC 32 check-sum and

the absence of replay protection. Chopchop attack allows an attacker to encrypt the exchange messages without knowing the key [53].

Fragmentation attack: A fragmentation attack has been discussed on the context of WEP protocol and the first implementation of such attack was published by Bittqu et al. [55]. To successfully perform this attack, eavesdropping a packet is required. All packets transmitted over 802.11 network have homogeneous headers and, which helps the attacker to guess the first 8 bytes of the headers by XORing these 8 bytes and 8 bytes of cipher text, to get 8 bytes from the IV [55], [53] .

PTW Attack: The Pyshkin Tews Weinmann (PTW) attack was released in 2007. This attack has introduced two new principals: 1) Jenkins relationship proposed to guess the key with less minimum attempts; and 2) multiple bytes prediction instead of guessing bytes individually [55].

Google Replay Attack: By setting Google.com as a home page, an attacker could simply discover a part of key stream using Google log downloaded every time the users open the Google website. The main difficulty of this attack is how to know exactly when users will download the Google log [53].

Michael Attacks: Michael's algorithm is used to generate a hash function. However, Reck and Tews in [53] discovered a method in which they could reverse this algorithm. Also, Beck in [73] found a method to execute attack based on Michael's flaws by exploiting its internal state to be reset when it reaching a particular point. In this case, an attacker could inject some code in a packet.

Ohigashi-Morii Attack: This type of attack was introduced as an extension to Beck-Tews attack on WPA-TKIP. In fact, this attack is effective for all modes of WPA. The time of injecting a malicious packet is minimized approximately from 15 to one minute in the best case [53].

The Hole196 Vulnerability: This vulnerability has been discovered by Sohail Ahmad in [74]. Ahmed found that there is a hole in standard 802.11 protocols exactly on the page 196. An attacker, who is an unauthorized user of the network, could send a fake ARP request with access point MAC address and other users will update their ARP tables upon the request. After updating their ARP tables, users will transmit their packets to attacker's MAC address instead of access point. The attacker, in this scenario, can get the packets decrypted by the access point, read them, and re-encrypt these packets with his own key [53].

Dictionary Attack: A dictionary attack is a technique in which an attacker could breach into a password-protected WiFi by guessing its passphrase by attempting millions or billions of possibilities, for instance words in a dictionary. [53].

2.1.5 ZigBee-based attacks

Sniffing: Because most ZigBee networks do not use any encryption technique, they might be vulnerable to sniffing attacks. The attacker can intercept some packets to perform malicious activities using KillerBess's zbdump tool [62].

Replay attack: Replay attack depends heavily on network traffic interception. Being able to intercept the packets, the attacker could re-transmit the intercepted data as if they sent

TABLE VI. CONNECTIVITY ATTACKS WITH COMPROMISED SECURITY GOALS AND COUNTERMEASURES

Connectivity attacks	Compromised security goals	Countermeasures
Killing Tag	ALL	Users or objects authentication [56]
Spoofing	ALL	RFID authentication and encryption techniques [51]
Man in the middle	C, I, P, NR	Encryption of the RFID communication channel [45], authentication techniques
Tracking	P, NR	Kill/sleep command, isolation, anonymous tag, blocking[57]
Virus	P, I, AU, TW, NR, C	Blocking strange bits from the tag using well-developed middleware, bounds checking and parameter [41]
Evesdropping	C, NR, P	Encryption techniques, shift data to the back end
Replay	C,I,AC,NR,P	A challenge and response mechanism, the time-based or counter- based scheme [41]
RFID unauthorized access	All	Network authentication [40]
NFC		
Eavesdropping	C, NR, P	Secure channel (authentication and encryption) [43]
Data modification	ALL	Changing the baud rate(use of 106k Baud), the continuous monitoring of RF field, secure channel[43]
data corruption	A, AC, AU, NR	The detection of RF fields during data transmission [43]
Relay attack	C, I, AC, NR, P	Timing(enforcing stricter timing restraints on responses) [58], distance Bounding (Round-Trip-Time (RTT) of cryptographic challenge-response pairs [59]
Data insertion	P, I, AU, TW, NR	Objects reply with no delay, a secure channel between the two objects [46]
Man-in-the middle	C, I, P, NR	A secure channel between the NFC objects
ZigBee		
Sniffing	C, NR, P	Implementing high security by preinstalling the network key on the ZigBee devices [60]
Replay attack	C,I,AC,NR,P	The implementation of freshness counter (a 32-bit frame counter), [61]
ZED Sabotage attack	All	The remote alerting system for warning about power failures of ZigBee objects, configure the legitimate ZEDs in a cyclic sleep mode [61]
Obtaining keys	P,I,AU,TW,NR	Out-of-band key loading method Using [62]
Redirecting Communication	C, I, AC, NR, P	Secure network admission control, preconfigure nodes with the Trust Center address [63].
Bluetooth		
Bluejacking	NR, AU, TW, AU	Putting objects on nondiscoverable mode, stay offline [48]
Bluebugging	All	Firmware and software update, use of RF signatures [64]
Interception	C,NR,P	Data/voice encryption, increasing user understanding of security issues, minimization of transmit powers,using only long PIN codes [64], pairing process in private settings [48]
DoS	A AC, AU, NR, P	Keeping a list of suspicious devices [65]
Bluesnarfing	All	Putting phones on nondiscoverable mode [48], stay offline[64], verify incoming transmission
Spoofing	P,I,AU, TW, NR	Secure UUID - Rotating UUIDw/ limited token scope, Private Mode with Rotating UUID, Secure Shuffling randomly rotating UUID [66]
Hijacking	All	Cloud-based token authentication,Secure Communications, Software Lock[66]
WiFi		
FMS	P, I, AU, TW, NR, C	The use of RC4-based SSL (TLS), the use of higher-level security mechanisms such as IPsec [67]
Korek, Chopchop, Fragmentation, PTW, Google replay	P, I, AU, TW, NR, C	The use of a very short rekeying time, disabling the sending of MIC failure report ,disabling TKIP and using a CCMP only network [68], the use of higher-level security mechanisms such as IPsec, DTLS, HTTP/TLS or CoAp/DTLS, DTLS for CoAp[69]
Michael	P, I, AU, TW, NR, C	Deactivating QoS or settingthe rekeying timeout to a low value[70], disable TKIP and switch to the more secure CCMP
Ohigashi-Morii	P, I, AU, TW, NR, C	Security protocols based on AES [71]
Dictionary Attack	P, I, AU, TW, NR, C	The use of salt technique [72]

by a legitimate user. The main consequence of such an attack relies on the content of the packets being re-transmitted [62].

Obtaining the key: What makes ZigBee protocol vulnerable to such an attack is that its keys need to be re- installed over the air if its objects are re-flashing [75].

Redirecting Communication: In the ZigBee network, an attacker could redirect and eavesdrop its packets. This attack attack could be used to launch a MITM attack, the main objective of this attack is intercepting and changing the transmitted data [76].

ZED sabotage attack: In [61], the authors have proposed a new attack against ZigBee protocol known as a ZigBee End-Device. The main goal of such attack is to vandalism the ZED by sending periodically a particular signal to wake up the object to drain its battery.

An overview of all attacks against wireless connectivity protocols, their compromised security goals, and their available defense mechanisms is presented in Table VI.

2.2 Network Protocols-based attacks

In this section, the main attacks targeting the network protocols as depicted in Fig. 12 are described in greater detail below.

2.2.1 RPL-based attacks

Routing Protocol for Low power and lossy network (RPL) has been designed to allow multiple-point to point, point to point, and point to multiple-point communication. Its topology depends heavily on the DODAG tree (Destination Orientation Directed Acyclic Graph) composed of one root known as a sink node [77]. The main attacks against RPL are the following:

Selective forward attack: Forwarding chosen packets by attacker to disturb routing paths is the main goal of this attack. Denial of service attacks may take place as a consequence of such attack. An attacker is capable of forwarding all RPL control packets and getting ride of the remaining traffic [78].

Sinkhole attack: In this attack, a malicious node may announce beneficial route or falsified path to attract so many nodes to redirect their packets through it. Despite not disruption the network, it could be dangerous if it is jointed with another attack [79].

Sybil attack: In this type of attack, a malicious object may use different identities in the same network. Such attack was designed to overcome the main goal of redundancy techniques in scattered data storage. Furthermore, it can be used to attack routing algorithms [80].

Wormhole attack: RPL is prone to the wormhole attack, which disturbs both network topology and traffic. This attack can be launched by creating private channel between two attackers in the network and forwarding the selective packets through it [78].

Blackhole attack: Like a hole, which absorbs everything, a blackhole attack has been designed to drop silently all data packets that are meant to it by maliciously advertising itself as the shortest path to the destination during the path-discovering mechanism [79].

Identity attack: In RPL network, identity attack is a combination of spoofing and sybil attacks. An attacker could illegally get access to packets intended to specific node by cloning its identity [78].

Hello flooding attack: Objects recently joining the network send broadcast packet known as a hello message. In this case, an attacker can represent himself as a neighbor object to several objects by broadcasting hello message with a high-powered antenna to deceive other objects to send their packet through it [80].

2.2.2 6LoWPAN-based attacks

IPv6 over Low-power Wireless Personal Area Network (6LoWPAN) enables the communication between resource constrained objects and IPv6 network. It performs as an adaptation layer between network and data link layers, offering many advantages such as encapsulation, header compression, fragmentation and reassembly mechanism. Despite the lack of security mechanisms in the 6LoWPAN, its security provide by the underlying layers such as IEEE 802.15.4. The main attacks against 6LoWPAN are the following:

Fragmentation Attack: Unlike IPv6, which has a minimum MTU of 1280 bytes, IoT object operated in IEEE 802.15.4 has Maximum Transmission Unit (MTU) of 127 bytes. Having designed with fragmentation mechanism, 6LoWPAN allows the transmission of IPv6 packets over IEEE 802.15.4. Being designed without any type of authentication, an attacker can insert his fragment among fragmentation chain [79].

Authentication Attack: Due to the lack of authentication in 6LoWPAN, any objects can join to the network and get an authorized access [79].

Confidentiality Attack: Due to the absence of encryption technique in 6LoWPAN, many attacks can be launched such as MITM, eavesdropping, and spoofing [79].

An overview of all attacks targeting RPL and 6LoWPAN, their compromised security goals, and their available defense mechanisms is presented in Table VII.

2.3 Communication protocols-based attacks

While connectivity protocols have been designed to link different IoT objects with each other, communication protocols

have been engineered to exchange messages between them by providing a standard way for naming, messaging, and controlling [92]. Standard naming refers to the process via which each IoT object will be reached, referred, and recognized. Standard messaging defines how each IoT message is structured so that all IoT objects can easily understand it. Standard controls allow IoT objects to manage communication flow. In this section, the main attacks targeting the communication protocols as depicted in Fig. 13 are described in greater detail below.

2.3.1 TCP-UDP-based attacks

Unlike application layer of IoT stack, which has different protocols to choose from such as HTTP, CoAP, MQTT, and DDS, transport layer has only two standardized protocols TCP and UDP. The most common attacks targeting these protocols are:

TCP-UDP Port scan: One of the most popular methods used by attackers to explore services to compromise them is a port scan attack. If used a port scan tool, an attacker can send a message to each port to test if the port is working to discover some weaknesses [93].

UDP flood: It is a kind of DoS attack in which an attacker sends a huge number of UDP packets randomly to different ports to force so many objects to send back ICMP packets which may make some object unreachable [94].

TCP Hijacking: The first step to achieve such an attack is to monitor a TCP session. In this case, an attacker can detect and guess the sequence numbers and check-sums of the communicated entities. Then, the attacker can inject a malicious TCP packet containing the check-sum and sequence numbers expected by the receiver, who lacks a mechanism to validate the packet source deeming it as a legitimate one [95].

TCP SYN flooding: According to [96], more than 90 percent of the DoS attacks target the TCP protocol, and the most popular of which is SYN flooding attack. This attack consists of a set of eavesdropped TCP SYN packets directed to victim's port. Web servers such as Mail servers, and FTP servers and the connected objects are vulnerable to such attack[94].

TCP-UDP fragmentation: In general fragmentation attacks in both TCP and UDP protocols cause a DoS attack. In UDP, the main objective of such attacks is to re-transmit malicious UDP packets of size bigger than the network's MTU to consume server's resources as it is difficult to resemble these packets [97].

2.3.2 Application layer protocols-based attacks

Application protocols play a major role in the IoT context. The most dominant protocols are MQTT and CoAP [98]. Table IV gives the summary of all IoT communication protocols and their main properties. A brief overview of attacks targeting IoT communication protocols is shown below:

Pre-shared key attack: Security mechanism in some IoT application such as a CoAP protocol depends on pre-shared keys. In some cases, these keys are hard-coded within the code. Therefore, the attacker can easily get access to them if he has access the library files. [99].

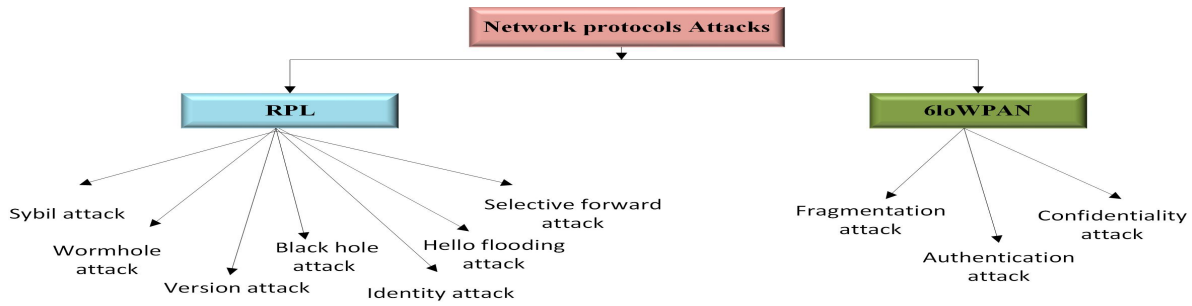


Fig. 12. Taxonomy of network attacks against IoT objects.

TABLE VII. NETWORK LAYER ATTACKS WITH ITS COMPROMISED SECURITY GOALS AND COUNTERMEASURES

Physical attacks	Compromised security goals	Countermeasures
Selective forward attack	C,I,AC,NR,P	Encryption technique , disjoint path or dynamic path between parent and children [79], heartbeat protocol, IDS solution.
Sniffing attack	C, NR, P	Encryption [81]
Sybil attack	C,I,AC,NR,P	Classification-based Sybil detection (BCSD) [82]
Wormhole attack	C,I,AC,NR,P	Markle tree authentication [82], binding geographic information [83]
Blackhole attack	C,I,AC,NR,P	The implementation of RPL in RIOT OS, Tiny OS, monitoring of counters [84], SEVELTE [85]
Identity attack	A, AC, I	Tracking number of instances of each identity, storing Identities of nodes in RPL, distributed hash table (DHT) [79]
Hello flood attack	C,I,AC,NR,P, A	link-layer metric as a parameter in the selection of the default route [86]
Version attack		Version Number and rank authentication, TRAIL [87]
Sinkhole attack	A, C, I	IDS solution [85], identity certificates, parent fail-over [88], and a rank authentication technique
Fragmentation attack	P,I,AU,TW,NR	Split buffer approach, content chaining approach [89], add new fields to the protocol fragmentation header
Authentication attack	C, I, P, NR	Authentication mechanism [90]
Confidentiality attack	C, I, P, NR	Moving Target IPv6 Defence in 6LoWPAN [91]

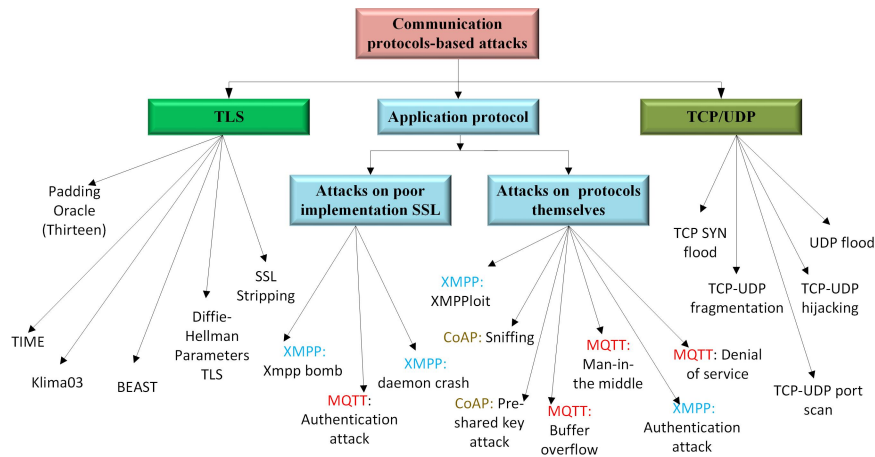


Fig. 13. Taxonomy of communication protocols attacks.

Sniffing attack: The use of sniffer applications may help sniffing or monitoring the network traffic to gain access to sensitive data especially if application protocols have been implemented without security mechanism such as CoAP with no-security mode [100].

SSL stripping: Secure Socket Layer (SSL) stripping was first developed by Moxie Marlinspike [101]. The main goal of such attack is to try to take out the use of SSL / Transport Layer Security (SSL/TLS) by manipulating unencrypted protocols to demand the use of TLS. More specifically, it manipulates both HTTP traffic and HTML pages while they are transmitted.

Beast: The beast attack depends heavily on exploiting the vulnerabilities in TLS 1.0, as it implements Cipher Block Chaining (CBC). Having used HTTP to run over TLS, the attacker can use the CBC to decrypt either parts of message

or HTTP cookies [102].

Diffie-Hellman Parameters: All TLS versions are vulnerable to some attacks known as cross-protocol attacks when Diffie-Helman and Elliptic Curve Diffie-Hellman parameters are used to exchange the pre-shared key [103].

Klima03: It is a kind of Certificate and RSA-related attacks on TLS. The process of deriving all session keys depends entirely on premaster-secret value. So, the entire captured SSL/TLS could be decrypted once an attacker get the premaster-secret value [114].

Time: It is a type of compression attacks using TLS with TLS-level compression, which may help an active adversary to decrypt the cipher-text, particularly cookies [113].

Padding oracle(Thirteen): This type of attack is intro-

TABLE VIII. COMMUNICATION PROTOCOLS ATTACKS WITH ITS COMPROMISED SECURITY GOALS AND COUNTERMEASURES

Physical attacks	Compromised security goals	Countermeasures
TCP SYN flood	A,AC,AU,NR,P	SYN Cache mechanism [94], SYN cookies, firewalls , switches and routers with rate-limiting and ACL capability [94]
UDP flood	A,AC,AU,NR,P	Firewalls, deep Packet Inspection [104]
TCP-UDP Port scan	A,AC,AU,NR,P	Network intrusion detection system(NIDS), external firewall[93]
TCP-UDP session hijacking	P,I,AU,TW,NR, C	Encrypted transport protocols[105] such as Secure Shell (SSH), Secure Socket Layers (SSL), and Internet Protocol Security (IPSec)
TCP-UDP Fragmentation	A,AC,AU,NR,P	Blacklisting/whitelisting mechanisms, a secure proxy [97]
XMPPlloit	P,I,AU,TW,NR	SSL
Sniffing	C, NR, P	DTLS [106]
Pre-shared key attack	P,I,AU,TW,NR, C	The use of the ephemeral keys as in ECDH key exchange guarantees PFS[99]
MITM	C, I, P, NR	Secure MQTT[107]
Buffer overflow	P,I,AU,TW,NR, C	Close the opening ports, awareness of security [40]
XMPP: Authentication attack	P,I,AU,TW,NR, C	Authentication mechanism [90]
Xmpp bomb	P,I,AU,TW,NR, C	Validating parsers using Document Type Definitions (DTD) and XML Schemas [108]
Daemon crash	P,I,AU,TW,NR, C	Good implementation of TLS
Padding oracle (Thirteen)	P,I,AU,TW,NR, C	The encryption-then-MAC instead of the TLS default of MAC-then-encryption [109].
Time	P,I,AU,TW,NR, C	Disabling TLS compression [110]
Klima03	P,I,AU,TW,NR, C	TLS 1.1, [111]
Beast	P,I,AU,TW,NR, C	Authenticated encryption algorithm like AES-GCM [109]
Diffie-Hellman parameters	P,I,AU,TW,NR, C	The of predefined DH groups [112]
SSL stripping	P,I,AU,TW,NR, C	HTTP Strict Transport Security (HSTS) [113]

duced as a result of using the MAC-then-encrypt in all TLS versions. A thirteen is a new type of such attack in which a timing side channel is utilizing to decrypt the ciphertext [115].

Xmpp bomb: This type of attack can be used to launch a DoS attack specially when the attacker sends a valid compressed request with lot of white spaces[116].

XMPPlloit: This attack depends heavily on XMPP weaknesses and the main goal of which is to act as a gateway between clients and server forcing clients to send their messages without encryption.

Man-in-the middle (MITM): Because MQTT has been designed to send its usernames and passwords without any encryption, it is vulnerable to the MITM attack[116].

Buffer overflow: The buffer overflow attack can be happened as a consequence of opening a port on MQTT protocol [117].

An overview of all communication protocol attacks, their compromised security goals, and their available defense mechanisms is presented in Table VIII.

3) **Data at rest-based attacks:** In this section, we will identify all potential threats and possible attacks targeting only IoT data at rest resided either locally in IoT objects or remotely in the cloud, as most of the attacks targeting data in motion have been implicitly discussed in protocols attacks. A brief description of all attacks targeting IoT data at rest is presented below and depicted in Fig. 14.

Data exposure: An IoT data is subjected to several attacks due to storing them remotely on the data centers with no supervision of their holders. The number of attacks will be increased, as the malicious objects can get access to these data once they are not properly protected due to the lack of encryption and key management [118]. Additionally, data may place in different data centers distributed at different geographical countries, and have a high power to access this data without permission of their holders [129].

Data loss: IoT objects and cloud providers should be equipped with data loss prevention to deal with high possi-

bility of losing data, causing harmful consequences such as a ransomware attack [130].

Account hijacking: Weak passwords and social engineering might be used to perform an account hijacking. An attacker may compromise, manipulate, and redirect the sensitive data [131]. In the cloud environment, application program interfaces such as SoAP, REST, and HTTP have been used to provides different services. However, many issues have been identified with such interfaces, and the most notable of which are week passwords, insufficient authorization inspections, and input data validation [132].

Data scavenging: Being recoverable, IoT data are vulnerable to many attacks if they are not properly destroyed or removed [133].

Data leakage The lack of the secure methods of processing, storing, and transmitting data is the main consequence of this attack, for example, storing unencrypted data either on the cloud or on IoT objects [134].

DoS: Making IoT data inaccessible by legitimate users is the main objective of such attack. Dos attack exploit the vulnerabilities of the application interface programs (API)[119], [132].

Data manipulation: Illegal manipulating of data at rest can be achieved in two ways: 1) exploiting different vulnerabilities in API like SQL injection, and cross site scripting; and 2) taking advantage of weak security mechanisms such as small passwords [134].

Virtual Machine (VM) Escape: VM escape exploits weaknesses of hyper-visor. The objective of such attack is to dominate the underlying infrastructure greedy for its configuration flexibility and code complexity, which matches companies needs [133].

VM Hopping: Due to the hyper-visor complexity, the unlimited resource allocation, and its configuration flexibility on the cloud, attackers may be able to attack one VM to gain access to another one [135].

Malicious VM creation: As many VM images are de-

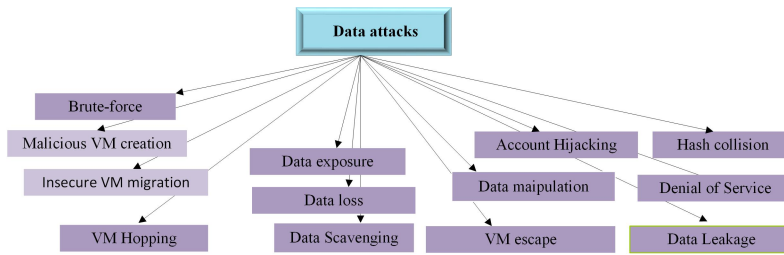


Fig. 14. Taxonomy of data at rest attacks.

TABLE IX. DATA AT REST ATTACKS WITH COMPROMISED SECURITY GOALS AND COUNTERMEASURES

Physical attacks	Compromised security goals	Countermeasures
DOS Exposure	C, I, PP	Strong encryption techniques, key management methods [118]
Data loss	ALL	Strong key generation, storage and management, and destruction practices [119], backup and retention strategies.
Data Scavenging	C, I, P	Symmetric key Cryptography [120]
VM Hopping	ALL	None [120]
Malicious VM Creation	ALL	Mirage [120]
Insecure VM Migration	All	Protection aegis for live migration of VMs(PALM) [121], VNSS offers protection through virtual machine live migration [122]
Account Hijacking	ALL	Identity and access management guidance, dynamic credentials [123]
Data Manipulation	ALL	Web application scanners (such as firewall) [124]
VM Escape	ALL	Trusted cloud computing platform, trusted Virtual Datacenter, hyperSafe, properly configuring the host/guest interaction [125] .
Data leakage	C, I	Digital Signature, fragmentation-redundancy-scattering (FRS) technique, homomorphic encryption [126], encryption [120]
Dos	P, A	Policies provided by providers [120]
Hash collision	C, I	Modern hashing algorithms like SHA-2, SHA-3, or bcrypt[127]
Brute-force	C, I	lockout mechanisms, IP address lock-out, detection tools, brute force site scanners[128]

ployed in unattended environments, an attacker could build legitimate VM account containing a malicious code like Trojan horse [134].

Insecure VM migration: An attacker could get access to data illegally during the immigration process of a VM to a malicious or a trusted host, which may expose its data to the network [136].

Brute-force attack: This type of attack depends on a trial and error method in order to get information such as user passwords or personal identification number (PIN). Brute force attack uses automated software to generate a huge number of sequential guesses to decrypt the the ciphertext [137].

Hash collision: The main objective of the collision attack is to discover two input strings of a hash function that gives the same hash value. Because hash functions have variable input lengths and a short fixed length output, there is a possibility that two different inputs generate the same output and this case is known as a collision [138].

An overview of all data at rest attacks, their compromised security goals, and their available defense mechanisms is presented in Table IX.

4) IoT Software-based Attacks: In IoT system, data security for IoT is not equivalent to software security. In some cases, even if the attacker hacks IoT application, he will not get an access to the data if it is well encrypted, but he might be able to do other harmful actions such as control the IoT object or sending spam to other IoT objects.

A brief description of all attacks targeting IoT data at rest as depicted in Fig. 15 is presented below.

4.1 Application-based attacks

Nowadays, IoT web application is rarely developed to operate in a stand-alone mode. Each application is connected to other applications that may inflict harm, making them vulnerable to many attacks. It is worth mentioning that most attacks on web applications often occur in unconstrained IoT objects resided in layer two or layer four in the proposed reference model. The most popular attacks targeting web applications are the following:

Exploitation of a misconfiguration: In some cases, several components such as operating systems, databases, and servers can be used to support running IoT applications. Thus, improper configuration of such components may lead to security issues in IoT application.

Malicious code injection: In this type of attack, an attacker injects a spiteful code into some packets to either steal or modify sensitive data[100].

Path-based DoS attack: The main objective of this attack is to inject malicious code into the packets or replay some packets to the network. It could destroy or destruct an IoT network by sending a huge number of legitimate packets to exhaust network resources along path to a base station. This attack, therefore, may prevent other objects from sending messages to the base [139].

Reprogram attack: Reprogramming the IoT objects remotely as done in some environments can be achieved using a network programming system. Once the programming process is not protected, the attacker could hijack this procedure to control a large part of the network [140].

Malware: The process of infection web applications with a malicious program is known as a malware. Recently, a

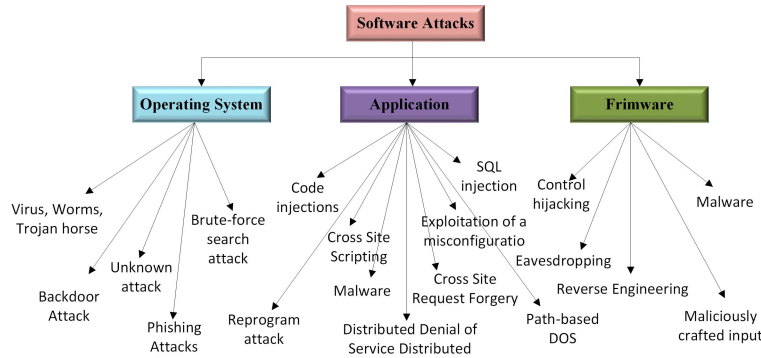


Fig. 15. Taxonomy of IoT software.

huge number of malware have been designed to attack IoT applications.

Distributed Denial of Service (DDoS): One of the main techniques that can be used to establish DDOS attack is a botnet. An example of this attack is the access prevention to a resource by flooding it with so many requests [141].

4.2 Operating system-based attacks

Phishing attack: It is one of the most common security challenges either to users or companies to keep their sensitive data secure. An attacker could get access to passwords, credit cards and other sensitive data via hacking an email, phones, or social media [142].

Backdoors: With the advent of IoT vision, many developers have proposed different IoT operating system like RTOS and Contik. Such operating systems may contain backdoor in which they could reprogram them to get access sensitive data anytime [143].

Virus, worm attack: Nowadays, many viruses and worms, like Mirai, Stuxnet, and Brickerbot, have been designed to attack some weaknesses such as lack of update mechanisms found in IoT objects [144].

Brute-force search attack: This type of attack has been designed to hack an IoT system by breaking its security mechanisms such as cryptography and authentication using different techniques [145].

Unknown attack: The authors in [146] stated that some common vulnerabilities and exposures (CVE) records have not provided with adequate information to define the preconditions of an attack, which classify as unknown attack.

4.3 Firmware-based attacks

Smart phones and computers systems have been designed to receive frequent updates to fix the future vulnerabilities or bugs. For example, companies such as Microsoft, Samsung, and Google have built in such a way that they update their vulnerabilities remotely when they are revealed. In contrast, IoT systems are rarely designed to receive regular updates as they are being created by offshore third parties. These third parties mostly don't have professional developers to secure these systems. Even worse, the majority of IoT devices lack any approach to be updated.

Control hijacking: The process of changing the normal flow control of the IoT object firmware by injecting a malicious code is known as a control hijacking attack [156], [146].

Reverse Engineering The main goal of this attack is to analyze the objects' firmware to get sensitive data such as credentials [146].

Eavesdropping: Unlike reverse engineering attacks, which is an active attack, eavesdropping is a passive attack. Eavesdropping attack monitors the packets transmitted between objects and servers during the firmware update process. The attacker could only get sensitive data if the packets are either weakly protected or not protected at all. Furthermore, the attacker could resend the packets to establish a replay attack [157].

Malware: Modifying the behavior of the IoT system after infecting its firmware with a malicious code is the main purpose of such an attack. Several malware have been found in the state-of-the-art such as BASHLITE, Hydra, and Darllzo [158].

An overview of all IoT software attacks, their compromised security goals, and their available defense mechanisms is presented in Table X.

V. CONCLUSION

The appearance of IoT paradigm in the last few years has unleashed so many threats and feasible attacks against security and privacy of IoT objects and individuals. These threats lead to hamper the realization of this paradigm if they have been left without proper countermeasures. Despite unprecedented number of security attacks generated on IoT domain, there is a lack of standard method to identify and address such attacks. This paper, therefore, makes a best effort to provide a comprehensive classification of IoT attacks based on a novel building-blocked reference model, along with proposed countermeasures to mitigate them. Given IoT developers and researchers, willing to develop a secure IoT system, a chance to investigate which attacks have been fired, how they have been mitigated, which attacks still stick around was the main objective of this paper. Moreover, if manufactures and academia have proactively and sharply targeted such attacks by leveraging their mitigation techniques from the ground up starting from the objects in the physical environment until the data centers in the cloud, the broad applicability of IoT will improve significantly.

TABLE X. IOT SOFTWARE ATTACKS WITH COMPROMISED SECURITY GOALS AND COUNTERMEASURES

Physical attacks	Compromised security requirements	Countermeasures
Virus, worms	All	Security updates, side-channel analysis, verify software integrity [147], control flow [148]), protective Software
Backdoor attack	ALL	Circuit design modification
Malicious Scripts	ALL	Firewalls [149]
Phishing Attacks	ALL	Cryptographic methods
Brute-force search attack	ALL	Securing firmware update, cryptography methods
SQL injection	ALL	Data validation, pretesting [150], network-based intrusion detection (IDS)
Cross Site Scripting	P,I,AU,TW,NR, C	Data validation [17]
Cross Site Request Forgery	P,I,AU,TW,NR, C	including a unique, disposable and random token [17]
Exploitation of a misconfiguration	All	A strong application architecture, perform scans and audits continuously [151]
DoS attack	A,AC,AU,NR,P	Access Control Lists[152]
Malware	All	Security updates, side-channel analysis, verify software integrity, control flow [148]), IoT Scanner [153]
Path-based DOS attack	A,AC,AU,NR,P	Combining packet authentication and anti replay protection [154]
Reprogram attack	P,I,AU,TW,NR, C	secure the reprogramming process [154]
Control hijacking	All	Use Safe programming languages , audit software, add runtime code [155]
Reverse Engineering	All	Tamper proofing and self-destruction(obfuscation)
Eavesdropping	C, NR, P	A secure channel

REFERENCES

[1] F. DaCosta, "Rethinking the Internet of Things: A scalable approach to connecting everything." *Apress Open*, p. 185, 2013.

[2] D. Konstantas, "An overview of wearable and implantable medical sensors." *Yearbook of medical informatics*, pp. 66–69, 2007.

[3] J. Pike, "Internet of Things - Standards for Things," 2014.

[4] E. Alsaadi and A. Tubaihat, "Internet of Things: Features, Challenges, and Vulnerabilities," *International Journal of Advanced Computer Science and Information Technology (IJACSIT)*, vol. 4, no. 1, pp. 1–13, 2015.

[5] S. Institute, "InfoSec Reading Room Securing the Internet of Things Survey," p. 22, 2014.

[6] E&Y, "Cybersecurity and the Internet of Things," *E&Y*, no. March, pp. 1–15, 2015.

[7] European Research Cluster on The Internet of Things (IERC), "Internet of Things: IoT Governance, Privacy and Security Issues." *European Research Cluster on the Internet of Things*, p. 128, 2015.

[8] A. Mohsen Nia and N. K. Jha, "A Comprehensive Study of Security of Internet-of-Things," *IEEE Transactions on Emerging Topics in Computing*, vol. PP, no. 99, p. d, 2016.

[9] J. Gubbi, R. Buyya, S. Marusic, and M. Palaniswami, "Internet of Things (IoT): A vision, architectural elements, and future directions," *Future Generation Computer Systems*, vol. 29, no. 7, pp. 1645–1660, 2013.

[10] L. Atzori, A. Iera and G. Morabito, "The Internet of Things: A survey," *Computer Networks*, vol. 54, no. 15, pp. 2787–2805, oct 2010.

[11] Cisco, "The Internet of Things Reference Model," *Internet of Things World Forum*, pp. 1–12, 2014.

[12] S. A. Al-Qaseemi, H. A. Almulhim, M. F. Almulhim, and S. R. Chaudhry, "IoT architecture challenges and issues: Lack of standardization," *FTC 2016 - Proceedings of Future Technologies Conference*, no. December, pp. 731–738, 2017.

[13] Z.-K. Zhang, M. C. Y. Cho, and S. Shieh, "Emerging Security Threats and Countermeasures in IoT," *Proceedings of the 10th ACM Symposium on Information, Computer and Communications Security - ASIA CCS '15*, pp. 1–6, 2015.

[14] Andreas Fink, *IoT: Lack of standards becoming a threat*.

[15] L. Atzori, A. Iera, and G. Morabito, "The Internet of Things: A survey," 2010.

[16] S. Agrawal, "Internet of Things: A Survey on Enabling Technologies, Protocols, and Applications," *Abakos*, vol. 1, no. 2, pp. 78–95, 2013.

[17] B. Dorsemaine, J. P. Gaulier, J. P. Wary, N. Kheir, and P. Urien, "A new approach to investigate IoT threats based on a four layer model," *IEEE Transactions on Emerging Topics in Computing*, no. Notere, 2016.

[18] D. Kajaree and R. Behera, "A Survey on IoT Security Threats and Solutions," *International Journal of Innovative Research in Computer and Communication Engineering*, vol. 5, no. 2, pp. 1302–1309, 2017.

[19] J. S. Kumar and D. R. Patel, "A Survey on Internet of Things : Security and Privacy Issues," *International Journal of Computer Applications*, vol. 90, no. 11, pp. 20–26, 2014.

[20] S. Babar, P. Mahalle, A. Stango, N. Prasad, and R. Prasad, "Proposed security model and threat taxonomy for the Internet of Things (IoT)," *International Conference on Network Security and Applications*, vol. 89 CCIS, pp. 420–429, 2010.

[21] J. Guo and I. R. Chen, "A Classification of Trust Computation Models for Service-Oriented Internet of Things Systems," *Proceedings - 2015 IEEE International Conference on Services Computing, SCC 2015*, pp. 324–331, 2015.

[22] Y. Cherdantseva and J. Hilton, "A Reference Model of Information Assurance & Security*."

[23] Symantec, "An Internet of Things Reference Architecture," 2016.

[24] J. Sen, "A Survey on Wireless Sensor Network Security," *International Journal of Communication Networks and Information Security (IJCNIS)*, vol. 1, no. 2, 2009.

[25] A. M. Nia, S. Member, S. Sur-kolay, and S. Member, "Physiological Information Leakage : A New Frontier in Health Information Security," vol. 4, no. 3, pp. 321–334, 2015.

[26] C. Wachsmann, "Physically Unclonable Functions (PUFs)," *Morgan & Claypool Publishers*, 2014.

[27] D. Puthal, S. Nepal, R. Ranjan, and J. Chen, "Threats to Networking Cloud and Edge Datacenters in the Internet of Things," *IEEE Cloud Computing*, vol. 3, no. 3, pp. 64–71, 2016.

[28] W. I. Khedr, "SRFID: A hash-based security scheme for low cost RFID systems," *elsevier*, 2013.

[29] H.-h. Huang, L.-y. Yeh, and W.-j. Tsaur, "Ultra-Lightweight Mutual Authentication and Ownership Transfer Protocol with PUF for Gen2 v2 RFID Systems," vol. II, pp. 16–19, 2016.

[30] Nate Lord, "Social Engineering Attacks: Common Techniques & How to Prevent an Attack — Digital Guardian."

[31] N. Lesperance, S. Kulkarni, and K.-t. T. Cheng, "Hardware Trojan Detection Using Exhaustive Testing of k-bit Subspaces," *IEEE Access*, pp. 755–760, 2015.

[32] A. Davis, "A Survey of Wireless Sensor Network Architectures," *International Journal of Computer Science & Engineering Survey*, vol. 3, no. 6, pp. 1–22, 2012.

[33] Q. Xiao, T. Gibbons, and H. Lebrun, "RFID technology, security vulnerabilities and countermeasures," *Supply Chain, The Way to Flat Organisation*, no. December, pp. 357–382, 2009.

[34] H. Li and Y. Chen, "The Survey of RFID Attacks and Defenses," *iee*, pp. 0–3, 2012.

[35] H. Salmani, "Hardware Trojan Attacks: Threat Analysis and Countermeasures," *iee*, pp. 247–276, 2014.

[36] J. Deogirikar, "Security Attacks inIoT : A Survey," *International conference on I-SMAC*, pp. 32–37, 2017.

- [37] Walters, "Security in distributed, grid, mobile, and pervasive computing," *ACM*, 2007.
- [38] G. Hernandez, O. Arias, D. Buentello, and Y. Jin, "Smart Nest Thermostat : A Smart Spy in Your Home," *Black Hat USA*, pp. 1–8, 2014.
- [39] M. Polytechnic and M. Polytechnic, "RFID Security Issues & Challenges," *ieee*, 2014.
- [40] M. M. Ahemd, M. A. Shah, and A. Wahid, "IoT security: A layered approach for attacks & defenses," *2017 International Conference on Communication Technologies (ComTech)*, pp. 104–110, 2017.
- [41] Q. Xiao, C. Boulet, and T. Gibbons, "RFID security issues in military supply chains," *Proceedings - Second International Conference on Availability, Reliability and Security, ARES 2007*, pp. 599–605, 2007.
- [42] A. Elbagoury, A. Mohsen, M. Ramadan, and M. Youssef, "Practical provably secure key sharing for near field communication devices," in *2013 International Conference on Computing, Networking and Communications (ICNC)*. IEEE, jan 2013, pp. 750–755.
- [43] N. B. Thorat and C. A. Lulkar, "Survey on Security Threats and Solutions for Near Field Communication," pp. 291–295, 2014.
- [44] M. Roland, J. Langer, and J. Scharinger, "Practical Attack Scenarios on Secure Element-Enabled Mobile Devices," in *2012 4th International Workshop on Near Field Communication*. IEEE, mar 2012, pp. 19–24.
- [45] A. Mitrokotsa, M. R. Rieback, and A. S. Tanenbaum, "Classifying RFID attacks and defenses," *springer*, vol. 12, no. 5, pp. 491–505, 2010.
- [46] E. Haselsteiner and K. Breitfuß, "Security in Near Near Field Communication (NFC) Strengths," *Semiconductors*, vol. 11, no. 71, p. 71, 2006.
- [47] C. H. Chen, I. C. Lin, and C. C. Yang, "NFC attacks analysis and survey," *Proceedings - 2014 8th International Conference on Innovative Mobile and Internet Services in Ubiquitous Computing, IMIS 2014*, pp. 458–462, 2014.
- [48] N. Be-Nazir, I. Minar, and M. Tarique, "BLUETOOTH SECURITY THREATS AND SOLUTIONS: A SURVEY," *International Journal of Distributed and Parallel Systems (IJDPSS)*, vol. 3, no. 1, 2012.
- [49] M. Tan, "An Investigation of Bluetooth Security Threats," *ieee*, 2011.
- [50] Ubetooth One, "Great Scott Gadgets - Ubetooth One."
- [51] H. Jun Tay, J. Tan, and P. Narasimhan, "A Survey of Security Vulnerabilities in Bluetooth Low Energy Beacons," 2016.
- [52] N. Chen, "Bluetooth Low Energy Based CoAP Communication in IoT CoAPNonIP: An Architecture Grants CoAP in Wireless Personal Area Network," 2016.
- [53] M. Caneill and J.-L. Gilis, "Attacks against the WiFi protocols WEP and WPA," 2010.
- [54] K., "Korek Attack," 2004.
- [55] A. Bittau, M. Handley, and J. Lackey, "The Final Nail in WEP's Coffin," 2006.
- [56] I. R. Adeyemi Norafida Bt Ithnin, "Users Authentication and Privacy control of RFID Card," 2012.
- [57] Gan Yong, He Lei, Li Na-na, and Zhang Tao, "An improved forward secure RFID privacy protection scheme," in *2010 2nd International Asia Conference on Informatics in Control, Automation and Robotics (CAR 2010)*. IEEE, mar 2010, pp. 273–276.
- [58] L. Francis, G. Hancke, K. Mayes, and K. Markantonakis, "Practical relay attack on contactless transactions by using NFC mobile phones," *Cryptology and Information Security Series*, vol. 8, pp. 21–32, 2012.
- [59] G. P. Hancke and M. G. Kuhn, "Attacks on time-of-flight distance bounding channels," *Proceedings of the first ACM conference on Wireless network security - WiSec '08*, pp. 194–202, 2008.
- [60] Cyber Security Community, "Different Attacks and Counter Measures Against ZigBee Networks — TCS Cyber Security Community."
- [61] N. Vidgren, K. Haataja, J. L. Patiño-Andres, J. J. Ramírez-Sanchis, and P. Toivanen, "Security threats in ZigBee-enabled systems: Vulnerability evaluation, practical experiments, countermeasures, and lessons learned," *Proceedings of the Annual Hawaii International Conference on System Sciences*, pp. 5132–5138, 2013.
- [62] X. Fan, F. Susan, W. Long, and S. Li, "Security Analysis of Zigbee," 2017.
- [63] K. Masica, "Recommended Practices Guide For Securing ZigBee Wireless Networks in Process Control System Environments," 2007.
- [64] K. HAATAJA, "Security Threats and Countermeasures in Bluetooth-Enabled Systems," 2009.
- [65] M. Keijo and H. Senior, "Bluetooth network vulnerability to Disclosure, Integrity and Denial-of- Service attacks," vol. 17, 2005.
- [66] Gofor, "Common attacks and how Kontakt.io can protect you."
- [67] A. Stubblefield, J. Ioannidis, and A. Rubin, "Using the Fluhrer, Mantin, and Shamir Attack to Break WEP," *Ndss*, no. Iv, 2002.
- [68] E. Tews and M. Beck, "Practical Attacks Against WEP and WPA," *Proceedings of the second ACM conference on Wireless network security*, pp. 79–85, 2009.
- [69] C. Schmitt, T. Kothmayr, W. Hu, and B. Stiller, "Two-Way Authentication for the Internet-of-Things," *springer*, vol. 25, pp. 27–57, 2017.
- [70] M. Beck, "Enhanced TKIP Michael Attacks," 2010.
- [71] T. Mekhaznia and A. Zidani, "Wi-Fi Security Analysis," *Procedia Computer Science*, vol. 73, no. Awict, pp. 172–178, 2015.
- [72] Wikipedia, "Dictionary attack - Wikipedia."
- [73] M. Beck, "Enhanced TKIP Michael Attacks," 2010.
- [74] M. S. Ahmad, "WPA Too!" *Defcon 18*, p. 7, 2010.
- [75] J. Wright, "KillerBee: Practical ZigBee Exploitation Framework or "Wireless Hacking and the Kinetic World"," 2009.
- [76] J. Markert, M. Massoth, K.-P. Fischer-Hellmann, S. Furnell, and C. Bolan, "Attack Vectors to Wireless ZigBee Network Communications - Analysis and Countermeasures," *Proceedings of the Seventh Collaborative Research Symposium on Security, E-learning, Internet and Networking (SEIN 2011), Furtwangen, Germany*, pp. 57–66, 2011.
- [77] M. Asim, "IoT Operating Systems and Security Challenges," vol. 14, no. 7, p. 5500, 2016.
- [78] A. Mayzaud, R. Badonnel, and I. Chrisment, "A taxonomy of attacks in RPL-based internet of things," *International Journal of Network Security*, vol. 18, no. 3, pp. 459–473, 2016.
- [79] P. Pongle and G. Chavan, "A survey: Attacks on RPL and 6LoWPAN in IoT," *2015 International Conference on Pervasive Computing: Advance Communication Technology and Application for Society, ICPC 2015*, vol. 00, no. c, pp. 0–5, 2015.
- [80] J. Sen, "Security in Wireless Sensor Networks."
- [81] T. Winter, P. Thubert, A. Brandt, J. Hui, R. Kelsey, P. Levis, K. Pister, R. Struik, J. Vasseur and R. Alexander, *RPL: IPv6 Routing Protocol for Low-Power and Lossy Networks*. Kenchiku Setsubi Iji Hozen Suishin Kyokai, 2004.
- [82] K. Zhang, X. Liang, R. Lu, and X. Shen, "Sybil attacks and their defenses in the internet of things," *IEEE Internet of Things Journal*, vol. 1, no. 5, pp. 372–383, 2014.
- [83] L. Lazos, R. Poovendran, C. Meadows, P. Syverson, and L. W. Chang, "Preventing Wormhole Attacks on Wireless Ad Hoc Networks: A Graph Theoretic Approach," *ieee*, 2005.
- [84] K. Chugh, A. Lasebae, and J. Loo, "Case Study of a Black Hole Attack on 6LoWPAN-RPL," *SECURWARE 2012, The Sixth International Conference on Emerging Security Information, Systems and Technologies*, no. c, pp. 157–162, 2012.
- [85] S. Raza, L. Wallgren, and T. Voigt, "SVELTE: Real-time intrusion detection in the Internet of Things," *Ad Hoc Networks*, vol. 11, pp. 2661–2674, 2013.
- [86] L. Wallgren, S. Raza, and T. Voigt, "Routing Attacks and Countermeasures in the RPL-Based Internet of Things," *International Journal of Distributed Sensor Networks*, vol. 794326, no. 11, 2013.
- [87] H. Perrey, M. Landsmann, O. Uguş, T. C. Schmidt, and M. Wählisch, "TRAIL: Topology Authentication in RPL," 2013.
- [88] K. Weekly and K. Pister, "Evaluating sinkhole defense techniques in RPL networks," *Proceedings - International Conference on Network Protocols, ICNP*, 2012.
- [89] R. Hummen, J. Hiller, H. Wirtz, M. Henze, H. Shafagh, and K. Wehrle, "6LoWPAN Fragmentation Attacks and Mitigation Mechanisms," 2013.
- [90] L. M. L. Oliveira, J. J. Rodrigues, A. F. De Sousa, and V. M. Denisov, "Network Admission Control Solution for 6LoWPAN Networks Based

- on Symmetric Key Mechanisms," *IEEE Transactions on Industrial Informatics*, vol. 12, no. 6, pp. 2186–2195, 2016.
- [91] M. Sherburne, R. Marchany, and J. Tront, "Implementing moving target IPv6 defense to secure 6LoWPAN in the internet of things and smart grid," in *Proceedings of the 9th Annual Cyber and Information Security Research Conference on - CISR '14*. New York, New York, USA: ACM Press, 2014, pp. 37–40.
- [92] Stéphane GARCIA, "Wireless Security and the IEEE 802.11 Standards," 2004.
- [93] McMaster University, "The Five-Layer TCP/IP Model: Description/Attacks/Defense - Computing and Software Wiki," 2008.
- [94] S. Kumarasamy and G. A. Shankar, "An Active Defense Mechanism for TCP SYN flooding attacks," *arXiv.org*, pp. 1–6, 2012.
- [95] O. Zheng, J. Poon, and K. Beznosov, "Application-Based TCP Hijacking," 2009.
- [96] D. Moore, G. M. Voelker, and S. Savage, "Inferring Internet Denial-of-Service Activity," 2000.
- [97] Incapsula, "What is an IP Fragmentation Attack (Teardrop ICMP/UDP) — DDoS Attack Glossary — Incapsula."
- [98] Toby Jaffey, "MQTT and CoAP, IoT Protocols."
- [99] S. Jucker, "Master 's Thesis Securing the Constrained Application Protocol by Stefan Jucker," no. October, pp. 1–103, 2012.
- [100] S. N. Swamy, "Security Threats in the Application layer in IOT Applications," pp. 477–480, 2017.
- [101] Moxie Marlinspike, "SSLstrip."
- [102] T. D. Juliano Rizzo, "Browser Exploit Against SSL/TLS Packet Storm."
- [103] N. Mavrogiannopoulos, F. Vercauteren, V. Velichkov, and B. Preneel, "A cross-protocol attack on the TLS protocol," *{ACM} Conference on Computer and Communications Security*, pp. 62–72, 2012.
- [104] Incapsula, "What is a UDP Flood — DDoS Attack Glossary — Incapsula."
- [105] B. S. Kevin Lam, David LeBlanc, "Theft On The Web: Theft On The Web: Prevent Session Hijacking."
- [106] J. Granjal, E. Monteiro, and J. Sa Silva, "Security for the Internet of Things: A Survey of Existing Protocols and Open Research Issues," *IEEE Communications Surveys & Tutorials*, vol. 17, no. 3, pp. 1294–1312, 2015.
- [107] M. Singh, M. A. Rajan, V. L. Shivraj, and P. Balamuralidhar, "Secure MQTT for Internet of Things (IoT)," *Proceedings - 2015 5th International Conference on Communication Systems and Network Technologies, CSNT 2015*, pp. 746–751, 2015.
- [108] UsingXML, "White Space in XML Documents."
- [109] P. Gutmann and University, "Encrypt-then-MAC for Transport Layer Security (TLS) and Datagram Transport Layer Security (DTLS)," pp. 1–7, 2014.
- [110] T. Be'ery and A. Shulman, "A Perfect CRIME? Only TIME Will Tell," *BlackHat Europe 2013*, 2013.
- [111] A. Choudhury and D. McGrew, "AES Galois Counter Mode (GCM) Cipher Suites for TLS Status," pp. 1–8, 2008.
- [112] D. Gillmor, "Negotiated Finite Field Diffie-Hellman Ephemeral Parameters for Transport Layer Security (TLS)," pp. 1–29, 2016.
- [113] P. S.-A. Y. Sheffer, R. Holz, "Summarizing Known Attacks on Transport Layer Security (TLS) and Datagram TLS (DTLS)," pp. 1–13, 2015.
- [114] V. Klima, O. Pokorny, and T. Rosa, "Attacking RSA-based sessions in SSL/TLS," *Cryptographic Hardware and Embedded Systems Ches 2003, Proceedings*, vol. 2779, pp. 426–440, 2003.
- [115] N. J. AlFardan and K. G. Paterson, "Lucky thirteen: Breaking the TLS and DTLS record protocols," *Proceedings - IEEE Symposium on Security and Privacy*, pp. 526–540, 2013.
- [116] M. Wang, "Understanding security flaws of IoT protocols through honeypot technologies MengWang," 2013.
- [117] P. Du, "IoT Message Protocols: The Next Security Challenge for Service Providers? The State of IoT," pp. 2–4, 2017.
- [118] C. Rong, S. T. Nguyen, and M. G. Jaatun, "Beyond lightning: A survey on security challenges in cloud computing," *Computers & Electrical Engineering*, vol. 39, no. 1, pp. 47–54, jan 2013.
- [119] Cloud Security Alliance, "Cloud Security Alliance," 2010.
- [120] S. Chandna, R. Singh, and F. Akhtar, "Data scavenging threat in cloud computing," no. August, pp. 17–22, 2014.
- [121] Webopedia, "PALM."
- [122] G. Xiaopeng, W. Sumei, and C. Xianqin, "VNSS: A network security sandbox for virtual computing environment," *Proceedings - 2010 IEEE Youth Conference on Information, Computing and Telecommunications, YC-ICT 2010*, pp. 395–398, 2010.
- [123] SYBASE, "Dynamic credentia."
- [124] Tenable, "Tenable.io Web Application Scanning — Tenable."
- [125] Z. Wang and X. Jiang, "HyperSafe: A lightweight approach to provide lifetime hypervisor control-flow integrity," *Proceedings - IEEE Symposium on Security and Privacy*, pp. 380–395, 2010.
- [126] N. P. Smart and F. Vercauteren, "Fully Homomorphic Encryption with Relatively Small Key and Ciphertext Sizes," *springer*, pp. 420–443, 2010.
- [127] Eric Z Goodnight, "What Is SHattered? SHA-1 Collision Attacks, Explained."
- [128] ALIEN VAULT, "Brute Force Attack Mitigation: Methods & Best Practices — AlienVault," 2016.
- [129] N. Kaaniche and M. Laurent, "Data security and privacy preservation in cloud storage environments based on cryptographic mechanisms," *Computer Communications*, vol. 111, pp. 120–141, 2017.
- [130] Claudia Chandra, "Data Loss vs. Data Leakage Prevention: What's the Difference?" 2017.
- [131] Cloud Security Alliance, "Top Threats to Cloud Computing V1.0," 2010.
- [132] W. Dawoud, I. Takouna, and C. Meinel, "Infrastructure as a service security: Challenges and solutions," *Informatics and Systems (INFOS), 2010 The 7th International Conference on*, pp. 1–8, 2010.
- [133] W. A. Jansen, "Cloud hooks: Security and privacy issues in cloud computing," *Proceedings of the Annual Hawaii International Conference on System Sciences*, pp. 1–10, 2012.
- [134] B. Grobauer, T. Walloschek, and E. Stöcker, "Understanding cloud computing vulnerabilities," *IEEE Security and Privacy*, vol. 9, no. 2, pp. 50–57, 2011.
- [135] B. A. Sullivan, "Securing the cloud: Cloud computer security techniques and tactics," *Security Journal*, vol. 27, no. 3, pp. 338–340, jul 2014. [Online]. Available: <http://link.springer.com/10.1057/sj.2012.16>
- [136] J. Rittinghouse and J. Ransome, *Cloud computing\Implementation, Management, and Security*, 2010.
- [137] Kelly Jackson, "Hacker's Choice: Top Six Database Attacks."
- [138] M. Stevens, A. Lenstra, and B. de Weger, "Chosen-prefix Collisions for MD5 and Colliding X.509 Certificates for Dierent Identities," nov 2007.
- [139] R. Singh, J. Singh, and R. Singh, "ATTACKS IN WIRELESS SENSOR NETWORKS : A SURVEY," vol. 5, no. 5, pp. 10–16, 2016.
- [140] U. Sabeel and N. Chandra, "Categorized Security Threats in the Wireless Sensor Networks : Countermeasures and Security Management Schemes," vol. 64, no. 16, pp. 19–28, 2013.
- [141] J. Mirkovic and P. Reiher, "A taxonomy of DDoS attack and DDoS defense mechanisms," *ACM SIGCOMM Computer Communication Review*, vol. 34, no. 2, p. 39, apr 2004.
- [142] A. Tsow, "Phishing with Consumer Electronics: Malicious Home Routers," 2007.
- [143] SecurityWeek News, "IoT Devices Easily Hacked to be Backdoors: Experiment — SecurityWeek.Com," 2016.
- [144] The OWASP Foundation, "Owasp top 10 - 2013 the ten most critical web applications security risks," 2013.
- [145] J. S. SARA BODDY, "The Hunt for IoT: The Rise of Thingbots," 2017.
- [146] D. Papp, Z. Ma, and L. Buttyan, "Embedded Systems Security : Threats , Vulnerabilities , and Attack Taxonomy," *iee*, pp. 145–152, 2015.

- [147] M. Msgna, K. Markantonakis, D. Naccache, and K. Mayes, "Verifying Software Integrity in Embedded Systems: A Side Channel Approach." Springer, Cham, 2014, pp. 261–280.
- [148] M. Msgna, K. Markantonakis, and K. Mayes, "The B-Side of Side Channel Leakage: Control Flow Security in Embedded Systems," *springer*, pp. 288–304, 2013.
- [149] W. L. W. Michael K. Bugenhagen, "Pin-hole firewall for communicating data packets on a packet network," 2007.
- [150] The OWASP Foundation, "Owasp enterprise security api."
- [151] OWASP, "Top 10 2013-A5-Security Misconfiguration - OWASP."
- [152] M. Ongtang, S. Mclaughlin, W. Enck, and P. Mcdaniel, "Semantically Rich Application-Centric Security in Android," 2009.
- [153] Kaspersky, "The Kaspersky IoT Scanner app helps you secure your smart home Kaspersky Lab official blog."
- [154] S. V. Mahavidyalaya, "Wireless Sensor Networks: Security, Attacks and Challenges," 2010.
- [155] M. Backes and C. Hricu, "Practical Aspects of Security Control Hijacking Attacks," 2009.
- [156] G. Hoglund, G. McGraw, and A. Wesley, "Exploiting Software How to Break Code," 2004.
- [157] D. Miessler, "Securing the Internet of Things: Mapping Attack Surface Areas Using the OWASP IoT Top 10."
- [158] K. Angrishi, "Turning Internet of Things(IoT) into Internet of Vulnerabilities (IoV) : IoT Botnets," pp. 1–17, 2017.

Enhanced Detection and Elimination Mechanism from Cooperative Black Hole Threats in MANETs

Samiullah Khan*, Faqir Usman[†], Matiullah[‡], and Fahim Khan Khalil[§],

*[§]Institute of Business Management Sciences, The University of Agriculture Peshawar-Pakistan

[†]Department of Computer Science, Qurtuba University of Science and Information Technology-Pakistan

[‡]Department of Basic Sciences and Islamiat, University of Engineering and Technology, Peshawar-Pakistan

Abstract—Malicious node invasion as black hole attack is a burning issue in MANETs. Black hole attacks with a single malicious node is easy to detect and prevent. The collaborative attacks with multiple cooperative malicious node is a challenging issue in security of MANETs as it is difficult to figure out due to its complex and sophisticated mechanism. This study proposed a novel signature-based technique to detect and handle the cooperative black hole attack in MANETs. For this purpose, diverse type of simulation scenarios are used with increasing number of nodes. The parameters such as average throughput, average packet drop, average end to end delay, average processing time and malicious node detection rate are used to measure the impact of signature-based malicious node detection scheme. AODV is used as routing protocol in this study. This study revealed that the performance of MANETs degrades with an increase in a number of malicious nodes. The average throughput of MANETs decreases with increase in average end to end delay and average packet drop. Signature-based malicious nodes detection mechanism is used to counter the cooperative black hole attack. The signature-based technique has enhanced the detection and elimination of cooperative black hole attack in MANETs. This helps in comparatively an increase in average throughput and decrease in packet delay and packet drop.

Keywords—Mobile Ad-hoc Networks (MANETs); black hole attack; AODV; malicious node; cooperative attack

I. INTRODUCTION

In the recent years, wireless network gained much attention from the researchers due to its diverse application in various fields. Mobile Ad-hoc Networks (MANETs) are specific types of wireless network that have autonomous and decentralised structure [1]. MANETs are easy to be deployed and are dynamic. These features of MANETs enable its usage in a situation which has strict geographical constraints, such as in battlefields and disaster management. In MANET, nodes are free to move and connect with all other nodes in an ad-hoc way. A node in MANETs can act as a source or destination as well as forwarder (router) node to relay the packets to another destination node as shown in Fig. 1. Routing in MANETs is performed in three different ways that are: Proactive, Reactive and Hybrid [2].

MANETs are susceptible to security threats due to a number of reasons like; open communication environment, dynamic topology requirements, lack of central monitoring and management, cooperative algorithms and no clear defense mechanism [1]. These security threats in MANETs have also changed the battlefield situation. The challengeable task is to ensure the security of routing protocols in MANETs against the misbehaviour of malicious nodes. A MANETs is more prone

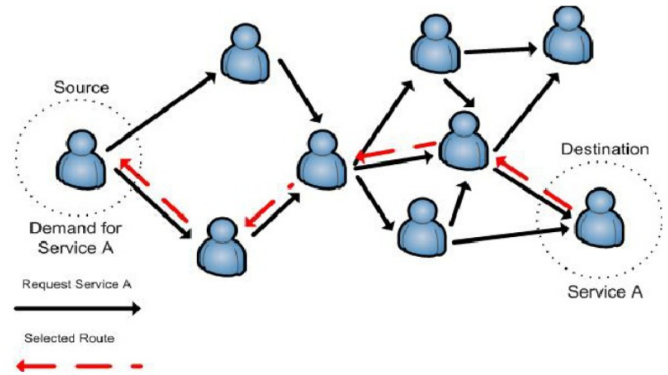


Fig. 1. Routing in MANETs [24].

to security attacks due to communication based on mutual trust between the nodes.

Some routing protocols such as Ad hoc On-Demand Distance Vector (AODV) [3], Dynamic Source Routing (DSR) Protocol [4], [27] and Destination-Sequenced Distance-Vector Routing (DSDV) [5] are developed to cope with routing in MANETs. AODV protocol is most widely used routing protocol for MANETs. Routing path selection in AODV routing protocol makes use of a sequence number to select most recent path to the destination [2]. In most of the discussed protocols, the routing decision relies on the cooperation and coordination between the nodes due to the lack of a centralised administration. Also, all of the nodes need to believe that each of them is trustworthy and well-behaved. Malicious nodes exploit these attributes of MANETs to launch attacks on the network. The wormhole attack, black hole attack, sybil attack, flooding attack, routing table overflow attack, Denial of Service (DoS), selfish node misbehaving and impersonation are possible active attacks on the routing protocols of MANETs [6]–[11].

In Black hole attack, the intermediate malicious nodes pretend to be the best forwarding nodes to the destination and ultimately drop the packets upon reception. Black hole attack can be categorised into two different attacks, based on the number of malicious nodes. The first one is termed as single Black hole attack where an individual node is acting as malicious nodes to perform the attack. Secondly, the multiple attackers synchronise their efforts to harm the network. This causes intense damage to the network and is called cooperative black hole attack [12], [13].

Black hole attacks that involve a single node are easy to figure out [14]. However, collaborative attacks are very complex, powerful and sophisticated in the mechanism. Thus, dealing with these types of attacks is comparatively more challenging. Some researchers have worked on techniques and protocols for detection and mitigation of the effects caused due to black hole attack [15], [16]. Most of them catered the problems in a very efficient way. However, in most of the presented solutions, there is a possibility of an increase in overhead and average end-to-end delay. The increase in overhead can lead to degradation in the overall performance of MANETs. This study intends to introduce a novel approach that will try to detect and eliminate cooperative malicious nodes in a path with minimum overhead and average end-to-end delay. The proposed approach will make use of the signature based mechanism for malicious node detection.

The rest of the research article is organised as follows: The background study of MANETs routing protocols and related work about the different types of attacks is presented in Section I. Literature survey of different approaches and protocols used for the detection of black hole (i.e. single and cooperative) attacks are presented in Section II. Section III discussed the proposed solution approach along with the working details. Result and discussion with detail of simulation scenarios and parameters are presented in Section IV. Finally, conclusion and future work are discussed in Section V.

A. Background of Study

In the last few years, wireless networks gained attention of industry as well as from the researchers due to its application in various fields. Example of currently used wireless networks includes Mobile Ad hoc Networks (MANETs), Vehicular Ad-hoc Networks (VANETs), Urban Mesh Networks (UMNs), and Wireless Sensor Networks (WSNs) [17], [18]. MANETs are self-organised wireless networks where nodes move freely around and interact with other nodes. Topology in MANETs is dynamic due to continuous movement of nodes in the vicinity. A node in the MANETs act as a source or destination or as a router at a time. Different routing schemes such as reactive, proactive and hybrid are employed to perform routing across the network as shown in Fig. 2. In reactive routing protocols, the source node initiates a request for the path towards the destination at a time when it has to send data to the destination [19]. Reactive routing protocols consume fewer resources and thus are efficient regarding memory as it does not need to maintain a routing table for all the routes. However, selection of the best path to the destination is a tough task in reactive protocols. Proactive routing protocols maintain a routing table and contain information about paths that lead to the destination [20]. Nodes that have a packet to send to any node can forward packet instantly, as routes to all nodes in the vicinity are listed in the routing. Even though proactive routing protocols can achieve good packet throughput, they have several disadvantages [47]:

- *Overhead of maintaining routing table .*
- *Slow convergence due to frequent path failures in MANETs due to having a dynamic topology.*

Hybrid protocols were introduced to combine the features of proactive and reactive routing protocols intelligently. Rout-

ing is performed in two different ways; use reactive approach for communication among neighbour nodes and use proactive routing strategy for communication among nodes that are located a distance of two or more hops from each other [21].

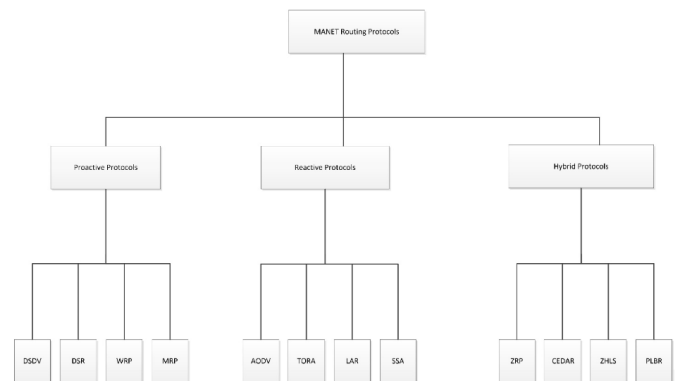


Fig. 2. Classification of routing protocols in MANETs.

1) *Ad hoc On-Demand Distance Vector (AODV):* AODV routing protocol is one of the important reactive routing protocols in MANETs that make use of sequence number to select a new path for the communication between the sender and destination nodes as shown in Fig. 3 [22]. To perform communication among nodes, AODV uses two different packets that are: Route request (RREQ) and Route Reply (RREP). RREQ contain information about the sending node whereas RREP is the response packet sent in a reply from intermediate nodes that have a new route to the destination node. A new route is a route whose sequence number is higher than the sequence number contained in the RREQ received at the intermediate nodes [23]. Since nodes in the MANETs communicate over the wireless medium, message security is indeed a major concern. The security of routing protocol in MANETs is vulnerable to jamming attack [24], worm hole attack [4], black hole attack and gray hole attack.

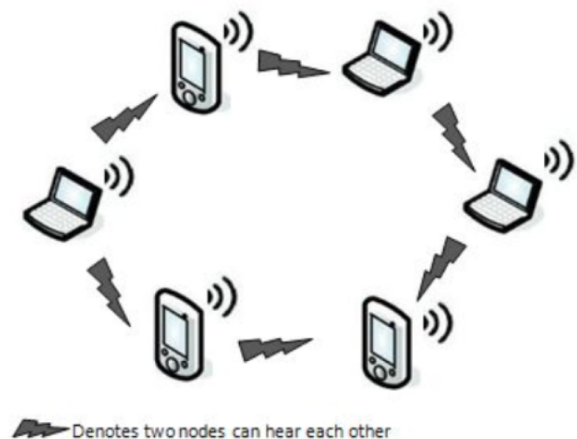


Fig. 3. Data communication among the nodes in MANETs.

2) *Black hole attacks in MANETs:* Blackhole attack is a type of attack which is launched by one or more of the intermediate nodes (called black hole nodes). These malicious nodes send a false RREP message to the source, claiming that it has the shortest path to the intended destination node [2], [25].

Black hole attack is considered as one of the most devastating attacks on the MANETs. The black hole node intercepts the packets, coming from the source nodes and silently drop. This will lead to immense loss of packets and cause an end-to-end delay to transfer the data packets through the network. Fig. 4 shows the example network topology where AODV protocol is used as a routing protocol. Suppose one of the nodes “S” has data that is to be sent to destination node “D”. The source node initiates route request by broadcasting RREQ packet to all the nodes in the neighbours. The malicious node “M” send a forged RREP reply message containing a spoofed destination address, less number of hops and smallest sequence number to deceive the source node. The source node selects the route contained in the forged RREP message for packet sending to the destination nodes. Packets that are received by the malicious nodes are dropped thereby not allowing communication between the sender and original destination.

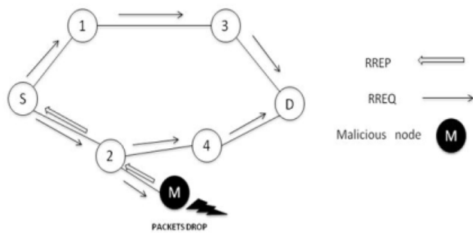


Fig. 4. Single black hole attack.

Another type of black hole attack is called Collaborative black hole attack that involves more than one node in launching the attack. The core idea behind this type of attack is to fabricate the RREP packet by all the malicious nodes with mutual understanding and cooperation [26]. Fig. 5 depicts the collaborative attack launched by malicious nodes “M1” and “M2”. The malicious nodes “M1” and “M2” intercept the RREQ message and reply back to the source node after a mutual consensus between “M1” and “M2”. Collaborative black hole attacks are more severe than single black hole attacks and can lead to huge packet loss.

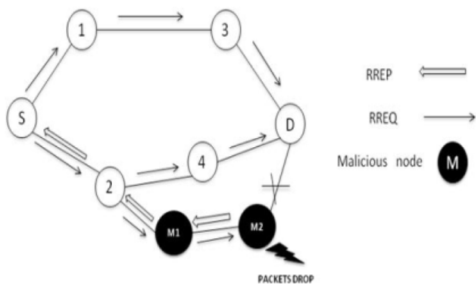


Fig. 5. Collaborative black hole attack.

B. Motivation

Collaborative attacks can lead to devastating impacts on a network causing huge packet loss in the MANETs. Securing routing against such destructive attacks in MANETs is a big challenge that has attracted many researchers. In [2], author proposed an approach which allows the source node to check the Next-Hop-Node (NHN) and Previous-Hop-Node (PHN) of

the Route Reply (RREP) of the intermediate nodes to ensure the authenticity of the route. In this research work, an enhanced attack detection and elimination technique are proposed that make use of a filtered based algorithm. The idea is to cope with collaborative black hole attack in a way that can lead to minimising overhead and average end-to-end delay.

C. Research Questions

This research work is going to answer the following research questions:

- Does the proposed filtered based approach is more accurate and less resource intensive as compared to the technique discussed in [2]?
- Does signature based malicious node detection technique is more efficient than the currently available approaches?

D. Research Objectives

The significant contributions of this research work are as follows:

- To analyse the effects of the single black hole and cooperative black hole attacks on AODV based MANETs.
- To mitigate the cooperative black hole attack on AODV routing protocol efficiently, while keeping packet overhead and network overhead as low as possible.
- To reduce the number of false positive nodes from being considered as malicious.
- Comparison of the proposed approach with the state of the art techniques.

E. Research Significance

Recently, wireless networks gained much attention from the researchers due to its diverse application in different fields. One of the most famous wireless networks is MANETs that has self-organised structure. Assuring data Integrity, confidentiality, and availability of wireless networks require all security concerns to be addressed. MANETs security is considered as essential concerns to assure normal functionality of the network. The lack of a centralised monitoring system and easy to access open wireless medium make MANETs more vulnerable to several attacks. Black hole attack is considered as one of the most disastrous attacks on the MANETs routing protocols. Malicious node deceives the source nodes convincing it to consider their route for sending a packet to the destination. Once the source node chooses the path containing the malicious nodes, the malicious nodes drop all the data packets received in the network [48].

The multiple attackers synchronise their efforts to harm the network cause intense damage to the network. Collaborative black hole attacks are very complex, powerful and sophisticated. Thus, dealing with these types of attacks is more challenging and exciting. Keeping in view the importance of security provisioning in MANETs, this research work introduces an enhanced approach to detect and mitigate collaborative black hole attack in an efficient way.

II. LITERATURE REVIEW

Wireless networks growth is observed in the last few years due to its applications in many fields. MANETs are one of the most famous wireless networks that attracted research community due to their versatile nature. MANETs have a high dynamic topology and self-organised. Their decentralised nature has led to the number of security concerns in their deployment. One of the most severe threat is the black hole attack. Some solutions are proposed by the researchers, which cope with the black hole attacks in the context of MANETs routing protocols (i.e. proactive, reactive and hybrid routing protocol). Few of the proposed approaches are discussed below.

Author in [29] introduced an approach that instructs all of the intermediate nodes to provide the information about next hop of its path that leads to the destination. Intermediate nodes incorporate the required information in its route reply (RREP) packet at the time of sending replies to the route request (RREQ) packet of the sender. The source nodes do not send packets immediately on the route specified by the intermediate. The source will try to send a special message FRq to the next hop node to ensure whether this node has a valid route to the destination [29]. The next hop node will reply with a special message FRp that contain the resultant information. At the sender side, if the next hop response regarding valid host is acknowledged with a positive reply, then route is constructed and chosen as the best path for transmission of data. However, if the response in FRp message contains negative acknowledgment then sender broadcast an alarm packet all other nodes to cope with this situation at their end. The proposed mechanism has good results regarding malicious node detection. However, extra overhead cost associated with the additional message sent to the next hop nodes for ensuring valid route. Secondly, the proposed solution is only feasible for single black hole detection and has no way to mitigate the cooperative black hole attacks [49].

Author in [30] has introduced a new approach to mitigating the issues related to cooperative black hole attacks in MANETs. The proposed mechanism makes use of an additional Data Routing Information (DRI) table that is used to detect the malicious nodes placed in the MANETs [30]. The idea is to get information about the next hop of all the neighbour nodes who claim to have a valid route to the destination. The neighbour nodes provide the required information in the RREP packet to the source that is placed in the source DRI table. Also, the source node requests the next hop node whether it has a valid route to the destination. Moreover, the next hop node is also required to provide information about its next hop node to the source node. The resulted information is helpful regarding cross-checking the validity of the node. However, this will lead to increase the average end-to-end delay. Author in [2] proposed an approach that allows the source node to check the Next Hop Nodes (NHN) and Previous Hop Nodes (PHN) of the Route Reply (RREP).

The packet is forwarded from the intermediate nodes to ensure the authenticity of the route [2]. The information regarding PHN and NHN is stored in a particular table called DRI. The proposed approach works in three different phases. In the first phase, the new path is to find out. Next step is to check the trustworthiness of the selected path, and lastly, the

malicious nodes are eliminated. The path that has the highest sequence number is selected as the best path for sending packets towards the destination. The algorithm detects all the attacking nodes that generate the false packets. One of the problems with the proposed technique is the overhead involved in processing the information regarding checking and storing NHN and PHN information in the DRI table.

Author in [31] proposed a table based approach to mitigate the cooperative black hole attack in the context of MANETs. The idea is to use data control packet to ensure the authenticity of all the nodes in the selected path. The concept of extended DRI table is used to detect and eliminate the malicious black hole nodes. The simulation result reveals improved overhead with no false positive records during the malicious nodes detection and elimination.

Enhanced Secure Trusted AODV (ESTA) protocol is proposed to mitigate the security issues related to the black hole attacks in MANETs [32]. The proposed approach makes use of an asymmetric key to assure security across the network. Also, a trust-based mechanism is used to select multiple paths for the delivery of packets across the network. The route selection involves two different tables namely "LINK-Table" to store information about the RREQ received from several neighbour nodes, and "Link-info" is a special control packet used by an intermediate node that is part of the selected path. The main drawback of the proposed approach is the overhead involved in storing information in two different tables [50].

Author in [33] introduced an approach to mitigate the black hole attacks in context of MANETs protocol. The proposed solution maintains a special table namely Collect Route Reply Table (CRRT) to prevent black hole attacks from occurring the MANETs. The main idea is to keep information about the sequence number and arrival time of the RREP packet from its neighbour nodes. The obtained information is used to calculate the timeout value about the RREP by first RREP arrival. Moreover, the source node looks for the repeated next hop nodes to ensure whether the route is safe or not. Repeated entry found the route and will be considered as safe. However, if no repeated next hop node found in the CRRT, any random path is chosen for the data delivery to the destination. One of the problems with this technique is that if no repeated next hop nodes are found in the CRRT. Then there is a fair chance of black hole attack at a time when the algorithm chooses a random path.

The concept of Fidelity Table is proposed to extend the approach to cope with the black hole (cooperative) attacks [34]. The table keeps information about all of the nodes of MANETs, by assigning every node a fidelity level. The fidelity level is used to find out the reliability of the intended nodes. The value of fidelity is calculated based on each nodes participation in routing convergence. The nodes fidelity status is checked after a certain interval of time and thus considered as malicious if its value dropped down to zero.

Author in [35] introduced Baited-Black hole DSR (BDSR) secure routing protocol that has the potential to mitigate the collaborative (black hole) attacks in the context of MANETs. The basic idea of the proposed approach is to allow the sending node to select one of the neighbour nodes to detect malicious nodes. The sender node makes use of that neighbour nodes

address for replying to the RREP message. Thus, black hole nodes can be detected and prevented by applying the concept of reverse tracing.

The idea of watchdog was proposed by [36] to tackle the problems related to black hole malicious in the context of MANETs. The basic idea is to use eavesdropping during the communication of the next hop node, to find out malicious activities, performed by the black hole nodes. The packet sent by the sending node is placed in the buffer and is compared with the overhead packet by the watchdog. If both of the packets found to be matching, the node is considered as legitimate, and thus packet is removed from the buffer. However, if there is a mismatch between the two packets, then the failure tally is incremented for the adjacent node. It may be the possibility that packet remained in the buffer for a certain period, which crosses the threshold value. Thus, a node will be considered as malicious if the value of tally crosses a certain threshold and the sending node is notified about the black hole node. Pathrater helps in finding the malicious free routes. Moreover, all the nodes keep track of the trustworthiness rating of every known node [36]. The shortest path is selected by the Pathrater in case if there are some routes leading to the intended destination node. One of the issue with the proposed technique is that it may not be possible to figure out malicious node if the transmission power is limited, partial packet drops or false behaviour [50]–[55].

Author in [37] proposed a novel technique namely REAct system to detect malicious black hole nodes in MANETs. The proposed approach is consist of three phases and are mentioned below:

- 1) Audit,
- 2) Search, and
- 3) Identification.

In the audit, each packet is verified before forwarded to the intended destination from the audit node. An audit node is selected by the sending node that makes use of bloom filter to generate a behavioural proof. Also, the sending node also makes use of bloom filter to generate a behavioural proof which is then compared with the proof produced by the audit node. The result of this comparison is used to identify the segment that has the black hole node. However, the proposed method can detect the malicious node only after an attack has already been launched by the malicious node.

Author in [38] introduced an approach for the detection of malicious (black hole) nodes in the context of MANETs that make use of the concept related to Merkle tree. The proposed solution can detect most of the malicious nodes at the cost of excessive computation overhead involved in the routing phase. Th proposed solution can detect and remove malicious black hole attacks in the context of MANETs. The basic theme of the research work is to make use of equal and small sized blocks of data and to observe the data packets during the transmission to detect cooperative malicious nodes. If the packets do not arrive at the intended destination, passing through a certain intermediate nodes, those nodes will be considered as malicious nodes. A major issue with the proposed solution is that it can lead to the increase in false positive records, which can consider some of the legitimate nodes as a malicious.

Author in [39] introduced an approach to mitigate the black hole attacks in MANETs routing protocols by making use of a certificate-based authentication method. Each node needs to have a certificate for authentication before they can start transmission over the network. The proposed solution performs the authentication of nodes in two distinct phases. First phase is related to the issuance of certificate whereas the second phase starts with the authentication of nodes over the MANETs. At the moment when the route is established between the source and destination, the nodes that are involved in the routing path enter into certification phase. The sending nodes send an authentication message to the destination node upon the reply of authentication and then the source node transmits the data to the destination. However, if the node is found to have incorrect information then this will lead to the revoking of the certificate, thereby considering the node as malicious.

Author in [40] came up with a novel approach namely Secure AODV (SAODV) to mitigate the problem of black hole attack in the context of MANETs. The proposed approach has led to cope with the security concerns inherent in the AODV and do avoid the black hole attacks. SAODV uses extra packets (i.e., for exchanging random numbers) to ensure the legitimacy of the destination node. Verification phase starts at a time when the RREP message is received by the sending node. The sender node then transmits verification (secure RREQ Packet) packets to the destination node that contains a random number generated at the sender side. The destination node then replies with a secure RREP packet that contains the random number generated. To obtain the best route, the source node waits until it gets two or more RREP (i.e., secure packets) along two different paths that have the same random number. Proposed algorithm will be unable to identify the black hole nodes in case of receiving only a single secure RREP packet. The overhead of maintaining information about the nodes and extra packets can lead to the processing overhead involved in the routing process. Moreover, the end-to-end delay is also increased because source node has to wait for the RREP packets from the receiver nodes that will be arriving through different paths towards the source.

Author in [41] extended the approach proposed in that make use of password-based approach during the routing process. All the nodes need to have a password at time of route selection process. Author in [42] introduced an approach namely DPRAODV, for the detection and isolation of black hole attacks in the context of MANETs. The basic theme behind the working of the proposed technique is that upon reception of RREP packet from the destination node, the sender node looks for the sequence number in its routing table and also try to find whether the sequence number is higher than a specified threshold value and is updated instantly. A node is considered as malicious RREP sequence has a higher value than the maximum threshold. The detected malicious node is blacklisted, and all of the nodes are sent an ALARM packet. The ALARM packet contains the black hole malicious node's address to alert the neighbour nodes. In this way, the nodes discard the RREP packet initiated from the black hole. However, one of the drawbacks of the proposed approach is the excessive overhead involved in maintaining the threshold value after a constant period.

Author in [43] proposed a novel security-based approach

for the detection of malicious black hole attacks in MANETs. The proposed approach is comprised of two parts that are detection and reaction. All the intermediate nodes maintain a special table called Black Identification Table (BIT) that contains the information about sending and receiving packets originating from the source node. A node is identified as malicious if there is a difference between the number of send and received packets. After malicious node identification, the next task is to isolate the black hole node and information is updated in a special table called Isolation Table (IT). Moreover, the ID of the black hole node is broadcasted across the whole network to prevent the malicious node from further participation in the routing operation. Higher packet delivery ratio is achieved, at the cost of small additional delay in the overall communication in the network.

The cluster-based technique is proposed in to cope with the issues related to black hole attacks in MANETs. The technique is also known as Black hole Attack Prevention System in Clustered MANETs (BHAPSC) that try to find out malicious nodes existence and its location at a specific time. The idea behind the proposed solution is to maintain a special table called Friendship (Table) that maintain the information about the cluster head and its neighbours within a certain cluster [44]. Based on the information of Friendship table, the conclusion are drawn about the node trustworthiness. The next hop node is said to be stranger if the table does not contain the record of the next hop. A special parameter called trust estimator is used to calculate the trust level, and thus table is updated with the value calculated at the trust level of a given next hop node. In the situation, where the node trust level (value) crosses the threshold value, that node's ID will be broadcasted as black hole node, to all the nodes in the network. The approach is costly regarding overhead in maintaining the trust information about all the nodes and processing involved in broadcasting information across the whole network for trust convergence.

Most of the proposed techniques were suffered from two different limitations. Firstly, the overhead required was too costly due to which the achieved throughput was very low. Second, the problem was the increase of end-to-end delay which causes performance degradation in most of the cases. Moreover, a significant problem with some of the proposed solution is the false positive records identification that leads to the performance degradation of the network. The resource constraints in MANETs require a malicious detection solution that is less costly regarding resources as well as efficient regarding the end-to-end delay. This work presents the solution that makes use of the signature-based scheme. The basic idea behind the proposed algorithm is to make use of the sequence number assigned to the nodes. In MANETs based networks, all the nodes are assigned a sequence number in a range of minimum to maximum.

Let Min-Seq-No be the minimum sequence number, Max-Seq-No be the maximum sequence number and Source-Seq-No is the sequence number of the node that can be either source or destination node. If the packet sends is an RREQ packet the Source-Seq-No represents the source sequence number. However, if the packet received is RREP, then the Source-Seq-No represents the sequence number of the destination node. Any node that sends or forwards an RREQ is accepted if

the value of the sequence number of that node is in between the minimum and maximum sequence number allowed in the MANETs (minimum and maximum are controlled in the proposed algorithm). However, if the sequence number is greater or less than the specified sequence numbers then the RREQ is rejected, and the node is considered as a malicious node. Similarly, the node that responds with an RREP packet is considered as a malicious node if its sequence number does not lie between the minimum and maximum sequence numbers specified. The collaborative attacks are handled in a way if all the nodes whose sequence numbers are higher than the specified maximum allowed sequence numbers and smaller than that of the sequence number allowed in the MANETs routing protocol. Table I presents the details about different approaches along with their limitations.

III. PROPOSED SIGNATURE BASED BLACK HOLE DETECTION MECHANISM

This work extends the work carried by [2] towards the mitigation of cooperative black hole attacks in AODV based MANETs routing protocol. The proposed algorithm makes use of the sequence number to identify the black hole nodes during the communication over the network. The pseudo-code of the algorithm is given as below:

Algorithm 1 Signature Based Black Hole Detection

Input: [Route Request (RREQ), Route Reply (RREP),
Min_Seq_No, Max_Seq_No, Destination (D)]
Output: [Accept RREQ/RREP, Reject RREQ/RREP]

A: Route Discovery Phase

Let route discovery phase is used by each node to search for ultimate destination D among all the neighbor nodes.

if next-hop != D && Loop free **then**

Source S broadcast the RREQ packet to all the neighboring nodes and continues till destination is not explored.

else

if Min_Seq_No \leq Node_Seq_No \leq Max_Seq_No **then**

Accept the RREQ

Destination D is reached

else

Reject the RREQ

end if

end if

B: Route Reply Phase

In the cache of the direct/intermediate nodes retrieve the routes from route caches.

Add these routes in the route record and then generate the route reply packets in that order.

if the route/s is/are found **then**

Maintain a list of all discovered routes as List of Routes (LR).

else

Destination node D is not reachable due to high mobility of nodes and network partitioning;

end if

The basic idea behind the proposed algorithm is to make use of the sequence number assigned to the nodes. In MANETs based networks, all the nodes are assigned a sequence number

TABLE I. SUMMARY OF PROPOSED APPROACHES FOR BLACK HOLE ATTACKS DETECTION

Authors	Summary	Single Black hole Detection	Cooperative Black hole Detection	Limitations
(Deng, Agrawal, 2002)	Use of intermediate node information about the next hop of its path that leads to the destination	Yes	No	Unable to detect cooperative black hole attacks [28]
(Ramaswamy et al., 2003)	Use DRI table detect the malicious nodes [29].	Yes	Yes	Overhead in maintain extra table
(Tamilselvan and Sankaranarayanan, 2007)	Use CRRT table to prevent black hole attacks from occurring the MANETs.	Yes	No	Overhead in maintain extra table
(Tamilselvan and Sankaranarayanan, 2008)	The fidelity level is used to find out the reliability of the intermediate nodes.	Yes	No	Overhead in maintain extra table
(Tsou et al., 2011)	Baited-Blackhole DSR secure routing protocol is proposed to mitigate the collaborative (black hole) attacks.	Yes	Yes	False negative records lead to detection of legitimate nodes as a black hole node
(Marti et al., 2000)	Use eavesdropping during the communication of the next hop node.	Yes	Yes	Overhead in maintain extra information and involve end-to-end delay
(Kozma and Lazos, 2009)	Comprised of three phases that are: 1) audit; 2) search 3) identification; that are used to detect black hole attacks	Yes	No	Can detect the malicious node only after an attack has already been launched by the malicious node.
(Anita and Vasudevan, 2010)	Use certificate based authentication method to mitigate black hole attacks	Yes	No	Lead to an increase in end-to-end delay.
(Nikdel, 2015)	Source node to checks the next hop nodes and previous hop nodes of the Route Reply packet forwarded from the intermediate nodes	Yes	Yes	An increase in overhead and end-to-end delay
(Ali, 2017)	Use data control packet to ensure the authenticity of the all the nodes in the selected path	Yes	Yes	Packet drop due to high end-to-end delay.

in a range of minimum to maximum. Let Min-Seq-No be the minimum sequence number, Max-Seq-No be the maximum sequence number and Source-Seq-No is the sequence number of the node that can be either source or destination node. If the packet sends are an RREQ packet the Source-Seq-No represents the source sequence number. However, if the packet received is RREP, then the Source-Seq-No represents the sequence number of the destination node. Any node that sends/forwards an RREQ is accepted if the value of the sequence number of that node is in between the minimum and maximum sequence number allowed in the MANETs (minimum and maximum are controlled in the proposed algorithm). However, if the sequence number is higher or less than the specified sequence numbers then the RREQ is rejected, and the node is considered as a malicious node. Similarly, the node that responds with an RREP packet is considered as a malicious node if its sequence number does not lie between the minimum and maximum sequence numbers specified. The collaborative attacks are handled in a way if all the nodes whose sequence numbers are higher than the specified maximum allowed sequence numbers and smaller than that of the sequence number allowed in the MANETs routing protocol.

A. Research Nature

The design of research methodology depends on the type of research, i.e., quantitative, qualitative and mixed approach. The qualitative approach is mostly used in research about social interaction, social settings, and social process [1]. On the other hand, quantitative-based research is used to find a numerical evaluation of the underlying research. The work in this study is evaluated using quantitative approach (i.e., simulation) in comparing the performance of the proposed algorithm with the work done in [2]. The simulation technique is a most common way of evaluating the performance of the developed systems. Some simulation tools (i.e., NS-2 [3], NS-3 [4], OMNeT++ [5], OPNET [6] and QualNet [7].) based on sequential/parallel Discrete Event Simulation (DES) kernel are

being employed by network researchers to verify their protocol designs. However, the selection of a network simulator depends on several important factors such as ease of configuration, learning curve of the programming language involved, type of scenario one may intend to simulate, provisioning of GUI environment, and support for scalability. This study considers OPNET modeler [6] as simulation tool.

B. Simulation Tool

Selection of relevant simulation tool is an important part of the performance evaluation. The selection of a network simulator depends on several important factors such as ease of configuration, learning curve of the programming language involved, type of scenario one may intend to simulate, provisioning of GUI environment, and support for scalability. OPNET modeler is selected to quantify the performance of the proposed algorithm. OPNET require the configuration of Visual C++ environment for the successful compilation and execution of the simulation. The implementation of simulation in OPNET required C language as a development platform to build the simulation application. The platform specification for simulation experiment about the proposed algorithm is shown in Table II:

TABLE II. PLATFORM SPECIFICATION

Simulation Tool	OPNET Modeler 14.5
Operating System	Windows
Memory	8 GB
Hardware	4
Number of Cores	Laptop core I-7

The simulation is sometimes conducted, to ensure the accuracy of the presented results. The same simulation is performed for the technique proposed in [2] and compared with the simulation of the proposed technique. The simulation is executed for 1000 seconds during each simulation run. The number of nodes chosen for the simulation is 45, and the number of malicious nodes is in the range of 1-18 nodes during different simulation execution. Random Way Point

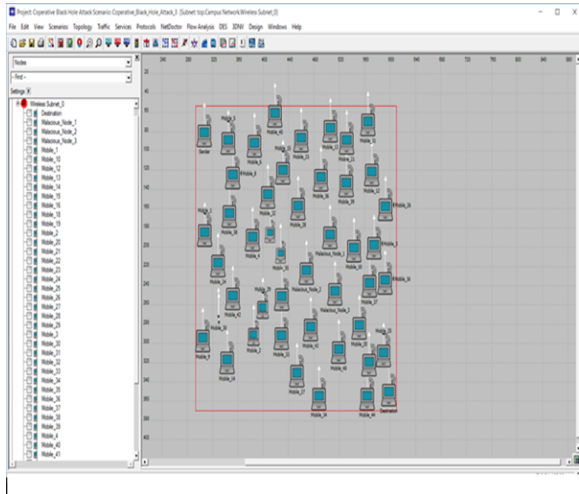


Fig. 6. Simulation environment of OPNET.

(RWP) mobility model is considered in this study [8] for nodes movement in the MANETs. All the nodes moved at the speed of 10 meters per second during the simulation execution. Fig. 6 shows the OPNET graphical view of the nodes used for the simulation experiments.

IV. RESULTS AND DISCUSSION

Four parameters, i.e. Average Throughput, Average Packet drop, Average Delay and Malicious Detection Rate are used to quantify the performance of the proposed signature-based approach. The overhead involved in malicious node detection may lead to the decrease in throughput. The packets will drop if the malicious node is not detected in due time. Packet Drop rate is used to compare the effectiveness of the proposed approach as compared to that of the existing techniques. End to end delay is defined as the time required for a packet to reach the intended destination. Malicious Detection Rate represents the success rate of detecting black hole attacking nodes, during the routing process in AODV. The proposed algorithm is implemented using OPNET and compared with the technique proposed in the base paper. The same simulation is run with four different combinations where a various number of malicious nodes (i.e., 1, 3, 6, 9, 12 and 18) are used. The results obtained from the simulation are discussed as below.

A. Average Throughput

Fig. 7 shows the average throughput of the signature-based scheme with a different number of nodes. Signature-based scheme achieves the high throughput of 40.4 Packets/Second. For single black hole attack, the average throughput is 39.2 Packets/Second. The minimum throughput value is observed when the cooperative black hole attack has three number of nodes. Results show an improved throughput by employing signature-based scheme as compared to the scenarios of cooperative black hole attack.

Average throughput is defined as average data packets received per unit time at the destination from a sender [45]. Fig. 7 presents the results regarding the achieved throughput for signature-based black hole detection technique and cooperative black hole attack with a various number of malicious

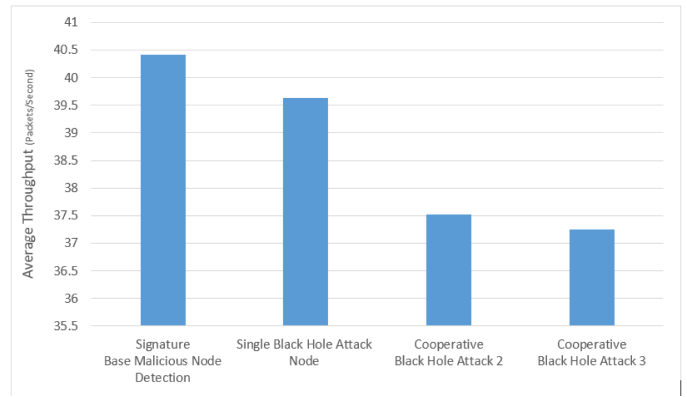


Fig. 7. Average throughput of signature-based malicious node detection.

nodes. A slight improvement (i.e., 2-5 %) in throughput is observed, when the number of black hole nodes was 1 and 3, during the first two simulations run. The proposed algorithm achieves better throughput (7-16%) with the increase in a number of malicious nodes as compared to that of state of the art technique. The presented results lead to the conclusion that with the increase in a number of a black hole, the proposed algorithm still able to achieve higher average throughput as compared to that of the technique used in [2] for cooperative black hole node detection. Moreover, both techniques reveal almost similar results with single black hole attack or when the number of black hole nodes is less than or equal to 3.

B. Average Packet Drop

Fig. 8 shows the results regarding some packets dropped when employing signature-based scheme with an increasing number of malicious nodes (i.e., 1, 2, and 3). Packets drop is reduced to zero with the implementation of the signature-based scheme for AODV based MANETs. The highest number of packets drops is observed when the number of cooperative-based malicious nodes are increased up to 3.

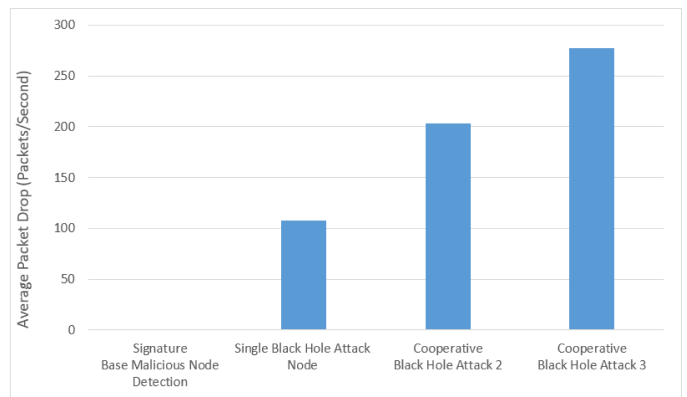


Fig. 8. Average packet drop (packets/second) of signature-based malicious node detections.

The results lead to the conclusion that signature base malicious node detection technique is efficient by having minimum average packet drop.

C. Average Delay

The average delay is defined as the average delay experienced by a packet to reach the intended destination [46]. The average delay is obtained by dividing the total delay by the total number of packets sent during the whole communication. The results presented in Fig. 9 corresponds to the average E2E delay, experienced by the network, for the signature-based algorithm. Results reveal better performance (regarding average end-to-end delay) for the proposed algorithm.

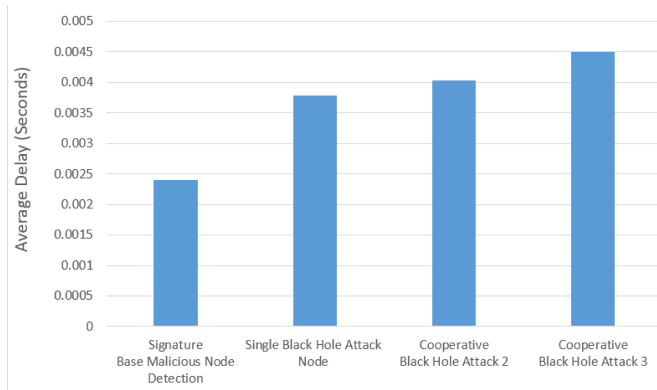


Fig. 9. Average delay of signature-based malicious node detection technique.

D. Average Processing Time

Fig. 10 shows the results of processing time taken on each of the techniques (i.e., proposed signature-based algorithm, and existing technique) for trusted route selection with varying number of malicious (cooperative black hole) nodes. The horizontal axis represent the number of black hole nodes, whereas the vertical axis represent the processing time (seconds) required to select the best suited route from source to the destination. The processing time for 1 and 3 number of black hole nodes on the proposed technique is almost equal to that of the base paper. Results shows an improvement of 10-22 % in processing time, for the route selection on our proposed algorithm as compared to that of the technique proposed in base paper. From the given results it can be concluded that the proposed algorithm can provide better connection rate as compared to that of the existing techniques. The proposed technique provides more scalable solution with a reasonable amount of processing time required for stable and trusted route selection from the sender to the destination nodes.

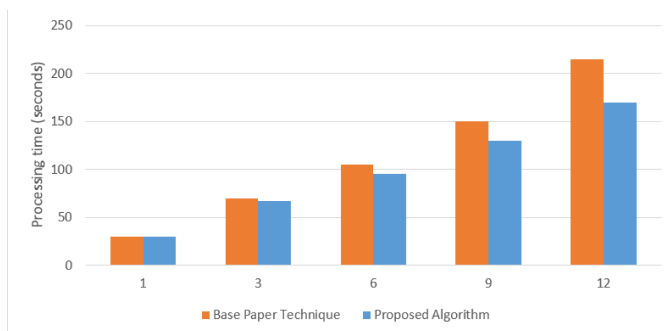


Fig. 10. Average processing time of signature-based malicious node detection technique.

E. Malicious Detection Rate

Fig. 11 presents the results of the black hole nodes detection rate on both the techniques (i.e., base paper and proposed technique). The simulation is configured for 45 mobile nodes and varying number (i.e. 6, 9, 12, 15 and 18) of black hole nodes. An equal detection rate is observed in both the techniques, i.e., proposed signature-based algorithm and base paper [2]. The results show an improvement of 11-17 %, as the number of black hole nodes is increased up to 6,9,12,15 and 18. The simulation results conclude that the proposed algorithm achieves better performance regarding malicious detection.

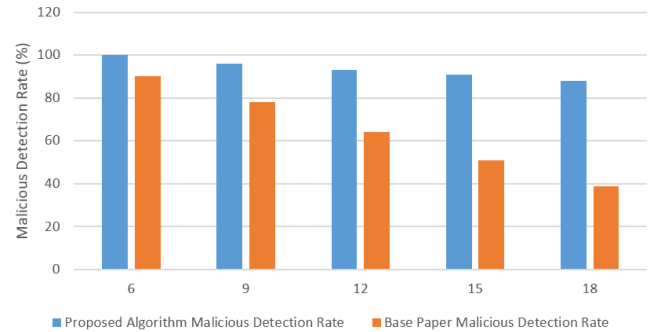


Fig. 11. Malicious detection rate of signature-based malicious node detection.

V. CONCLUSION AND FUTURE WORK

This research work presents an essential step towards an efficient detection of cooperative black hole attacks. The concept of signature-based detection in combination with the use of sequence number, lead to the implementation of an efficient approach for the detection of malicious attacks in AODV-based MANETs. The results obtained through simulation shows significant improvements regarding collaborative black hole detection. Results lead to the conclusion that with the increase in a number of malicious node in cooperative black hole attack, the proposed algorithm still able to achieve good throughput as compared to state of art techniques. Moreover, the proposed algorithm is efficient regarding detecting collaborative black hole attacks and can lead to efficient results regarding increased malicious attacks. Even though some techniques have been introduced to mitigate the black hole attacks in MANETs, many of the proposed solutions were capable of detecting single black hole attack and are unable to detect and avoid collaborative-based black hole attacks in the context of AODV based MANETs. The benefits of the proposed algorithm are mentioned below:

- 1) Better malicious detection rate for higher number of black hole nodes in the context of the cooperative black hole attacks.
- 2) Achieved less processing time regarding trusted path selection.
- 3) Good throughput and average delay.

In future, this research work will be extended by analysis of the proposed algorithm for Proactive routing (DSDV and DSR) protocols in MANETs. It is also recommended to increase the number of malicious nodes up to 100-150 and to the check the behavior of these routing protocols with the proposed technique.

REFERENCES

- [1] A.K. Jain, V. Tokekar, & S. Shrivastava. Security Enhancement in MANETs Using Fuzzy-Based Trust Computation Against Black Hole Attacks. In Information and Communication Technology, Springer, Singapore, pp. 39-47, 2018.
- [2] A. Dorri & H. Nikdel. A new approach for detecting and eliminating cooperative black hole nodes in MANET. In IEEE 7th Conference on Information and Knowledge Technology (IKT), Urmia, Iran, pp. 1-6, 2015.
- [3] C. Perkins, E. Belding-Royer, & S. Das. Ad hoc on-demand distance vector (AODV) routing (No. RFC 3561), 2003.
- [4] Johnson, B. David, A. David, Maltz, and J. Broch. DSR: The dynamic source routing protocol for multi-hop wireless ad hoc networks." Ad hoc networking Vol.5, pp. 139-172, 2001.
- [5] G. He. Destination-sequenced distance vector (DSDV) protocol. Networking Laboratory, Helsinki University of Technology, pp. 1-9, 2002.
- [6] N. Gupta, & S.N. Singh. Wormhole attacks in MANET. In Cloud System and Big Data Engineering (Confluence), Noida, India, pp. 236-239, 2016.
- [7] M.M. Singh, & J.K. Mandal. Effect of Black Hole Attack on MANET Reliability in DSR Routing Protocol. In Advanced Computing and Communication Technologies (pp. 275-283). Springer, Singapore. 2018.
- [8] A.K. Jain, V. Tokekar & S. Shrivastava. Security Enhancement in MANETs Using Fuzzy-Based Trust Computation Against Black Hole Attacks. In Information and Communication Technology (pp. 39-47). Springer, Singapore, 2018.
- [9] P.R. Muchintala, & L. Hash. Routing Protocols for MANETs, 2016.
- [10] R.H. Khokhar, M.A Ngadi & S. Mandala. A review of current routing attacks in mobile ad hoc networks. International Journal of Computer Science and Security, Vol. 2, No. 3, pp. 18-29, 2008.
- [11] Y.C. Hu, A. Perrig & D.B. Johnson. Rushing attacks and defense in wireless ad hoc network routing protocols. In Proceedings of the 2nd ACM workshop on Wireless security. pp. 30-40, 2003.
- [12] Routing in MANET, <https://goo.gl/LdjeVk>
- [13] D. Dave & P. Dave. An effective Black hole attack detection mechanism using Permutation Based Acknowledgement in MANET. In Advances in Computing, Communications and Informatics, pp. 1690-1696, 2014.
- [14] S. Sinha & A. Paul. FuNN-an Interactive Tool to Detect Sybil Attack in MANET. International Journal of Applied Research on Information Technology and Computing, Vol. 7, No.1, pp. 15-31, 2016.
- [15] A. Kalia & H. Bajaj. EDRI based approach with BERP for Detection & Elimination of Co-operative Black Hole in MANET. International Journal for Science, Management and Technology (IJSMT), Vol. 15, 2018.
- [16] A.K. Jain & V. Tokekar. Mitigating the effects of Black hole attacks on AODV routing protocol in mobile ad hoc networks. In Pervasive computing (ICPC), pp. 1-6, 2015.
- [17] K. Wehrle, M. Gnes & J. Gross. (Eds.). Modeling and tools for network simulation. Springer Science & Business Media, 2010.
- [18] M. Sharif & A. Sadeghi-Niaraki. Ubiquitous sensor network simulation and emulation environments: A survey. Journal of Network and Computer Applications, Vol. 93, pp.150-181, 2017.
- [19] K. G. R. Narayan, T.S. Rao, P.P. Raju & P. Sudhakar. A Study on Certificate-Based Trust in MANETs. In Proceedings of International Conference on Computational Intelligence and Data Engineering (pp. 41-54). Springer, Singapore, 2018.
- [20] Mbarushimana, C., & Shahrabi, A. Comparative study of reactive and proactive routing protocols performance in mobile ad hoc networks. In Advanced Information Networking and Applications Workshops, AINAW'07. Vol. 2, pp. 679-684, 2007
- [21] P. Nayak, & B. Vathasavai. Impact of Random Mobility Models for Reactive Routing Protocols over MANET. International Journal of Simulation-Systems, Science & Technology, Vol. 17, No. 34, 2016.
- [22] N. Marchang & R. Datta. Light-weight trust-based routing protocol for mobile ad hoc networks. IET information security, Vol. 6, No. 2, pp.77-83, 2012.
- [23] S. Kalwar. Introduction to reactive protocol. IEEE Potentials, Vol. 29, No. 2, pp. 34-35, 2010.
- [24] Routing in MANET, <https://goo.gl/LdjeVk>
- [25] A. S. K. Pathan. Security of self-organizing networks: MANET, WSN, WMN, VANET. CRC press, 2016.
- [26] [26] A. Rana, V. Rana & S. Gupta. EMAODV: Technique to Prevent Collaborative Attacks in MANETs. Procedia Computer Science, Vol. 70, pp. 137-145, 2015.
- [27] I. Woungang, S.K. Dhurandher, R.D. Peddi & I. Traore (2012, October). Mitigating collaborative blackhole attacks on dsr-based mobile ad hoc networks. In International Symposium on Foundations and Practice of Security. Springer, Berlin, Heidelberg, pp. 308-323, 2012.
- [28] H. Deng, W. Li & D.P. Agrawal. Routing security in wireless ad hoc networks. IEEE Communications magazine, Vol. 40, No.10, pp.70-75, 2002.
- [29] [29] S. Ramaswamy, H. Fu, M. Sreekantaradhya, J. Dixon & K.E. Nygard. Prevention of cooperative black hole attack in wireless ad hoc networks. In International conference on wireless networks, Vol. 2003, pp. 570-575, 2003.
- [30] L. Tamilselvan & V. Sankaranarayanan. Prevention of blackhole attack in MANET. In Wireless Broadband and Ultra Wideband Communications, 2007. AusWireless 2007. The 2nd International Conference on, pp. 21-21, 2007.
- [31] A. Dorri. An EDRI-based approach for detecting and eliminating cooperative black hole nodes in MANET. Wireless Networks, Vol. 23, No.6, pp. 1767-1778, 2017.
- [32] D. Singh & A. Singh. Enhanced Secure Trusted AODV (ESTA) Protocol to Mitigate Blackhole Attack in Mobile Ad Hoc Networks. future internet, Vol. 7, No.3, pp. 342-362, 2015.
- [33] L. Ta Tamilselvan & V. Sankaranarayanan. Prevention of co-operative black hole attack in MANET. JNW, Vol. 3, No. 5, pp.13-20, 2008.
- [34] P.C. Tsou, J.M. Chang, Y.H. Lin, H.C. Chao & J.L. Chen. Developing a BDRS scheme to avoid black hole attack based on proactive and reactive architecture in MANETs. In Advanced Communication Technology (ICACT), pp. 755-760, 2011.
- [35] S. Marti, T.J. Giuli, K. Lai & M. Baker. Mitigating routing misbehavior in mobile ad hoc networks. In Proceedings of the 6th annual international conference on Mobile computing and networking, pp. 255-265, 2000.
- [36] W. Kozma, & L. Lazos. REAct: resource-efficient accountability for nodemisbehavior in ad hoc networks based on random audits. In Proceedings of the second ACM conference on Wireless network security, pp. 103-110, 2009.
- [37] A. Baadache & A. Belmehdi. Avoiding black hole and cooperative black hole attacks in wireless ad hoc networks. arXiv preprint arXiv:1002.1681, 2002.
- [38] S. Jain, M. Jain & H. Kandwal. Advanced algorithm for detection and prevention of cooperative black and gray hole attacks in mobile ad hoc networks. International journal of computer Applications, Vol.1, No.7, pp.172-175, 2010.
- [39] D. Sathiyaa & B. Gomathy. Improved security and routing path learning in MANETs using BeerQuiche game theoretical model in cloud computing. Cluster Computing, pp.1-11, 2018.
- [40] S. Lu, L. Li, K.Y. Lam, & L. Jia . SAODV: a MANET routing protocol that can withstand black hole attack. In Computational Intelligence and Security, Vol. 2, pp. 421-425, 2009.
- [41] S. Deswal, & S. Singh. Implementation of routing security aspects in AODV. International Journal of Computer Theory and Engineering, Vol. 2, No. 1, pp. 135, 2010.
- [42] P.N. Raj & P.B. Swadas. Dpraodv: A dynamic learning system against blackhole attack in aodv based manet. arXiv preprint arXiv:0909.2371, 2009.
- [43] N. Jaisankar, R. Saravanan & K.D. Swamy. A novel security approach for detecting black hole attack in MANET. In Information processing and management, Springer, Berlin, Heidelberg, pp. 217-223, 2010.
- [44] D.B. Johnson & D.A. Maltz. Truly seamless wireless and mobile host networking. Protocols for adaptive wireless and mobile networking. IEEE Personal Communications, Vol. 3, No. 1, pp.34-42, 1996.
- [45] P. Manickam, T.G. Baskar, M. Girija & D.D. Manimegalai. Performance comparisons of routing protocols in mobile ad hoc networks. arXiv preprint arXiv:1103.0658, 2011.

- [46] S. Mylsamy & J. Premalatha. Performance amelioration of MANETs using cooperative routing with cross-layer design. *International Journal of Business Intelligence and Data Mining*, Vol. 13, No.3, pp. 15-25, 2018
- [47] S. Khan, M. A. Qadir, . Inter-path OOS packets differentiation based congestion control for simultaneous multipath transmission. *Int. Arab J. Inf. Technol.* Vol. 4, No. 6, pp.907-913, 2015.
- [48] S. Khan, M.A. Qadir, F.A. Khan and E. Rehman. Adaptive fast retransmission (AFR) with respect to receiver buffer (Rbuf) space in simultaneous multipath transmission (SMT) , *Malaysian Journal of Computer Science*, 2017.
- [49] S. Khan and M.A. Qadir. Deterministic Time Markov Chain Modelling of Simultaneous Multipath Transmission Schemes. *IEEE Access*, Vol. 5, pp.8536-8544, 2017
- [50] H. Ali, S. Khan and M. Quaid. Comparative analysis of controlled delay (CoDel) with Deficit Round Robin (DRR) to overcome bufferbloat problem in wired network. *International Journal of Current Engineering and Technology*, Vol. 5, No. 5, pp. 3378-3386, 2015.
- [51] F. Khan, S. Abbas and S. Khan. An Efficient and Reliable Core-Assisted Multicast Routing Protocol in Mobile Ad-Hoc Network. *International journal of advanced computer science and applications*, Vol. 7, No. 5, pp. 231-242, 2016.
- [52] S. Shakir, S. Khan, L. Hassain, Matiullah, QoS Based Evaluation of Multipath Routing Protocols in Manets, *Advances in Networks*. Vol. 5, No. 2, 2017, pp. 47-53. doi: 10.11648/j.net.20170502.13, 2017.
- [53] S. Khan, F. Faisal, M. Nawaz, F.Javed, F.A. Khan, R.M. Noor, Matiullah, Z. ullah, M. Shoaib and F.U. Masood, Effect of Increasing Number of Nodes on Performance of SMAC, CSMA/CA and TDMA in MANETs *International Journal of Advanced Computer Science and Applications (IJACSA)*, Vol.9 , No. 2, 2018. <http://dx.doi.org/10.14569/IJACSA.2018.090241>.
- [54] F.K. Khalil, S. Khan, F. Faisal, M. Nawaz, F. Javed, F.A. Khan, R.M. Noor, Matiullah, Z. ullah, M. Shoaib and F.U. Masood, Quality of Service Impact on Deficit Round Robin and Stochastic Fair Queuing Mechanism in Wired-cum-Wireless Network *International Journal of Advanced Computer Science and Applications (IJACSA)*, Vol. 9, No. 2, 2018. <http://dx.doi.org/10.14569/IJACSA.2018.090240> .
- [55] A. Rashid, F. Khan, T. Gul, Fakh-e-Alam, S. Ali, S. Khan and F.K. Khalil, Improving Energy Conservation in Wireless Sensor Network Using Energy Harvesting System *International Journal of Advanced Computer Science and Applications (IJACSA)*, Vol. 9, No.1, 2018. <http://dx.doi.org/10.14569/IJACSA.2018.090149> .

QTID: Quran Text Image Dataset

Mahmoud Badry
Faculty of Computers and Information
Fayoum University
Fayoum, Egypt

Hesham Hassan, Hanaa Bayomi
Faculty of Computers and Information
Cairo University
Cairo, Egypt

Hussien Oakasha
Faculty of Computers and Information
Fayoum University
Fayoum, Egypt

Abstract—Improving the accuracy of Arabic text recognition in imagery requires a big modern dataset as data is the fuel for many modern machine learning models. This paper proposes a new dataset, called QTID, for Quran Text Image Dataset, the first Arabic dataset that includes Arabic marks. It consists of 309,720 different 192x64 annotated Arabic word images that contain 2,494,428 characters in total, which were taken from the Holy Quran. These finely annotated images were randomly divided into 90%, 5%, 5% sets for training, validation, and testing, respectively. In order to analyze QTID, a different dataset statistics were shown. Experimental evaluation shows that current best Arabic text recognition engines like Tesseract and ABBYY FineReader cannot work well with word images from the proposed dataset.

Keywords—HDF5 dataset; Arabic script; Holy Quran text image; handwritten text recognition; Arabic OCR; text image datasets

I. INTRODUCTION

Optical character recognition (OCR) is the process of converting an image that contains text into a readable machine text. It has a lot of useful applications including document archiving and searching, automatic number plate recognition, and business card information extraction. It is also considered an assisting tool for blind and visually impaired people. Although OCR is an old problem, Arabic text recognition is still under development, especially in handwritten text [1], [2] due to many reasons including special Arabic language characteristics. Some of these characteristics are: A character may have up to four different shapes as depicted in Fig. 1, a character's width and height might change relative to its location within a word, the Arabic language is written from right to left, and some characters have the same shape except for the presence/location of dots above or below that shape. Another reason that Arabic text recognition is still under development is the lack of a standard robust comprehensive dataset [3].

This paper presents a new Arabic images dataset that can help machine learning models master the Arabic language text recognition. The dataset is generated from the Holy Quran, which contains a handwritten Arabic text including Arabic language marks. The Holy Quran is the book that Muslims believe is sent from Allah to Messenger Muhammad to guide all humans. It was written in Arabic which is the mother tongue of most of the Middle East. In fact, the Holy Quran consists of 114 Surah. Each Surah has a different number of Ayat. Moreover, an Ayah - singular of Ayat - consists of one or more Arabic words. There are 6,236 Ayat in the holy Quran, which form 77,430 Arabic words. The total number of unique words

Letter label	Isolate	Begin	Middle	End
ء	ء			
أ	أ	أ		
ؤ	ؤ	ؤ		
إ	إ	إ		
ئ	ئ	ئ	ئ	ئ

Fig. 1. Five different Arabic characters each has different shapes for different positions in an Arabic word.



Fig. 2. Two pairs of words with same characters shape but with different marks which give them different meanings.

is 18,994. The Holy Quran was chosen in this study due to three reasons: first, it is one of the sources of the Arabic language, second, it contains different words, characters, and marks from all over the Arabic language, third, the Mus'haf -the written work of Holy Quran- is written in Othmani font which is a handwritten text that has various shapes of characters.

The presented dataset contains a large set of handwritten characters and words with different shapes and sizes. As the data is the fuel for many machine learning models, creating a big modern dataset can help data-hungry machine learning models master the Arabic text recognition. In addition, it can be used as a benchmark to measure the current state of recognizing Arabic text. What makes this dataset different is that it is the first Arabic dataset to contain Arabic marks. In Arabic, two words with the same shape but with different marks may have different meanings as shown in Fig. 2.

The proposed dataset has 309,720 different word images that were collected from the Holy Quran words in four fonts. An example of a word in the four fonts is in Fig. 3. These images have been split into training, validation, and testing



Fig. 3. The same Arabic word with font sizes 22, 24, 26, and 28 pixels, respectively.

sets then saved in an HDF5 file, which is portable and can be used across operating systems.

This paper is organized as follows: Section 2 briefly discusses some Arabic Text datasets that have been created. Full steps to the creation of the dataset are described in Section 3. Section 4 analyzes the properties of the proposed dataset and gives some statistics about it. Experimental results and evaluations are shown in Section 5. Finally, the discussion and conclusions of this paper is presented in Section 6.

II. RELATED WORK

Through the years, Arabic text datasets have been created to help machines read Arabic text from images like any human being who knows how to read the Arabic language. These datasets played a great role in finding best methods to the mentioned goal. However, unlike English language, standard Arabic dataset is absence. Offline Arabic datasets like [4], [5], [6], [7] were made to help machine recognize text that has been scanned using a scanner or a camera and then stored digitally in an RGB or gray image. On the other hand, Online Arabic datasets like [8], [9], [10] helps machine understand text that was recorded using a digitizer as a time sequence of pen coordinates.

Datasets related to offline Arabic text recognition can be split into two groups: those that address printed text and the others that address handwritten text. This paper addresses each in turn.

Printed Arabic text recognition In this task, the purpose is recognizing Arabic characters, words, and paragraphs in which characters are typed using a printer and have a specific font. Additionally, the text is usually well structured. Many datasets have been created to solve this task. For example, a dataset with the goal of benchmarking open-vocabulary, multi-font, multi-size, and multi-style text recognition systems in Arabic, Arabic Printed Text Image (APTI) [5] was created in 2009. It contains 45,313,600 single word images that contain more than 250 million characters. This large dataset was generated using a lexicon of 113,284 words, 10 Arabic fonts, 10 font sizes, and 4-font styles. To focus on its goal each image has a clean white background with the annotation provided for each image in an XML file.

In 2015, the first public Arabic dataset ALIF [6] for recognizing Arabic text in videos was created. Creators of ALIF has extracted 6,532 text images from five famous Arabic TV channels that contain 18,041 words and 89,819 characters in total. These text images have different properties like fonts, sizes, color, backgrounds, and occlusions.

Handwritten Arabic text recognition In this task, the purpose is recognizing handwritten Arabic which was written by a human. Handwritten text recognition is harder than Printed text because the characters will have different appearances due to different writers and their styles besides one writer can produce the same character with different shapes in one sentence. Isolated Farsi/Arabic Handwritten Character Database (IFHCDB) [11] was made to help recognize Arabic isolated handwritten characters. It includes 52380 characters and 17740 numerals. The dataset is unbalanced which means that distribution of samples in each character is not uniform. Another dataset, IFN/ENIT contains 26,459 images that represent 937 names of cities and towns in Tunisia, written by 411 various writers. Each image is annotated by the ground truth text, position of word baseline, and information about each used character in a word.

A more recent dataset, KFUPM handwritten Arabic text (KHATT) [12] contains 2000 unique paragraph images, written by 1000 different writers, covering different topics like education, nature, arts, and technology. Moreover, each paragraph is segmented into lines and saved as individual images. The dataset has multiple research goals besides handwritten recognition like writer identification, noise removal techniques, binarization, and line segmentation.

Finally, A database that combines both printed and handwritten text named SmartATID [7], which stands for Smartphone Arabic Text Images Database has the purpose of recognizing Arabic text that has been captured by cell-phones cameras. The printed text version of this dataset includes 16472 document images, which are captured from 116 different paper documents with different capturing protocols like changing document layouts, cameras versions, light conditions, and position. With the similar capturing protocols, the handwritten text version of this dataset was created having 9088 images from 64 different handwritten documents.

The past pieces of work helped researchers in different Arabic OCR tasks, but none of them added the Arabic marks in their work although it is important as we have explained in the introduction section.

III. DATASET CREATION

The discussion will now move to how the dataset has been created starting from a words database and fonts, ending by training, validation, and testing HDF5 files.

A. Image Generation

The first task was to generate images that represent each word in the Holy Quran with different fonts as depicted in, Fig. 4. We made a query on a complete Holy Quran database¹ that selects each word and required font to render. Each word

¹Verified Holy Quran Database published on Github: <https://github.com/quran/quran.com-images>

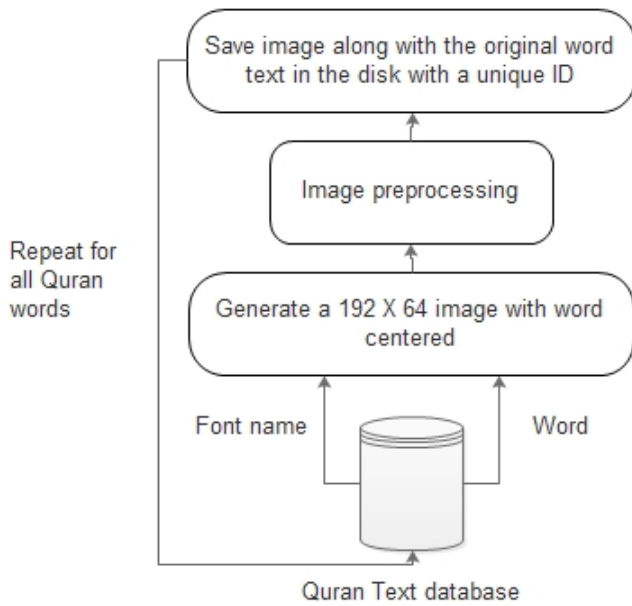


Fig. 4. Image generation steps.

is then rendered using the selected font in the middle of an image that has 192x64 dimensions. The 192x64 was selected as a dimension for the images of this study for three reasons: first, most machine learning models learn image of a fixed dimension; second, the biggest rendered word takes 180x61 dimensions; and third, the nearest numbers to 180 and 61 that can be vectorized through CPUs or GPUs are 192 and 64, respectively. The rendered images have a black background and a white text. Additionally, noise removal methods can be applied to each rendered image to make sure the images are clear. Finally, each image was given a unique id name and was saved in PNG image format on the disk along with a text file that represents the annotation of the image. The text file took the same id of the rendered image.

While reading words from the database, all the possible characters are recorded. After that, each character took a unique id to help generate one hot encoding representation of the images annotations. Ids range from 0 to 59 which represents 60 unique characters as shown in Fig. 5.

B. HDF5 files creation

The next task was to take all the generated images and then make training, validation, and testing sets which are then stored in HDF5 files as elaborated in Fig. 6. Initially, the process started by reading all the images paths into a big list. Before splitting up this list into training, validation, and testing lists, they were shuffled to make sure that random samples have been drawn for each of the lists. Afterwards, 90% of the paths list was taken for the training set, 5% for the validation set, and 5% for the testing set. The chosen percentage is based on the fact that our dataset is big enough and the trend is to take much smaller percentages for the validation and testing set as Andrew Ng² said on his notes³.

0	ء	1	أ	2	ؤ	3	إ	4	ئ	5	ا
6	ب	7	ة	8	ت	9	ث	10	ج	11	ح
12	خ	13	د	14	ذ	15	ر	16	ز	17	س
18	ش	19	ص	20	ض	21	ط	22	ظ	23	ع
24	غ	25	-	26	ف	27	ق	28	ك	29	ل
30	م	31	ن	32	هـ	33	و	34	ى	35	ي
36	ـ	37	ـ	38	ـ	39	ـ	40	ـ	41	ـ
42	ـ	43	ـ	44	ـ	45	ـ	46	ـ	47	أ
48	ـ	49	ـ	50	ـ	51	ـ	52	ـ	53	ـ
54	ـ	55	ـ	56	ـ	57	ـ	58	ـ	59	ـ

Fig. 5. Sixty Arabic characters each has a unique integer Id starting from zero.

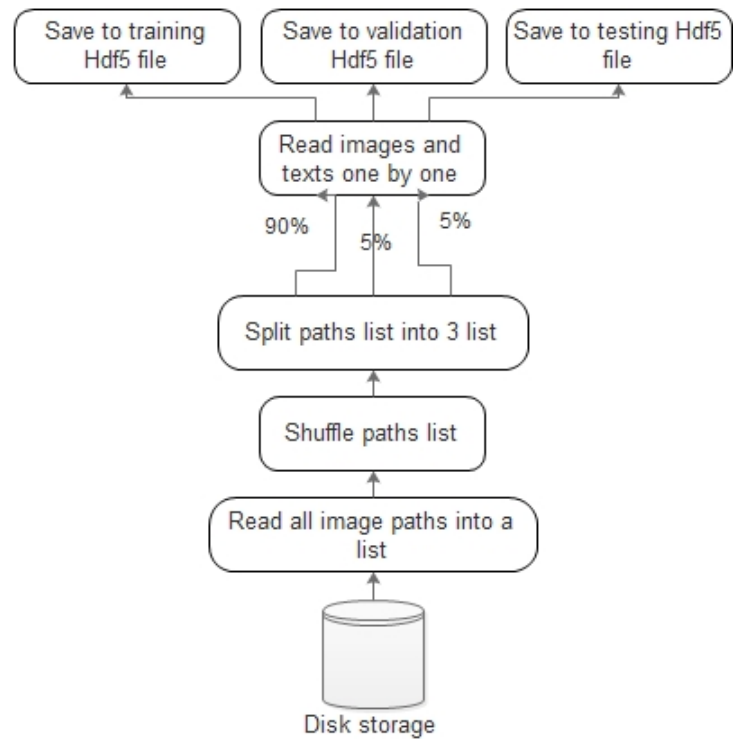


Fig. 6. HDF5 files creation steps.

Next, each image is read along with its text as they share the same unique id and then the image is converted into a 3-dimensional matrix. To make the dataset more flexible, the

²Andrew Ng one of the pioneers in machine learning
³<https://www.coursera.org/learn/deep-neural-network/lecture/cxG1s/train-dev-test-sets>

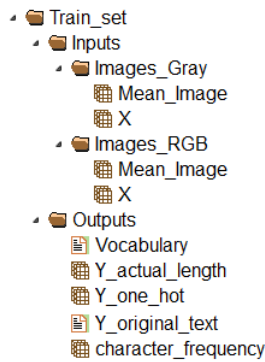


Fig. 7. Training HDF5 file architecture. Inputs consist of RGB and gray images matrices groups, while outputs contain corresponding original images annotations, text actual lengths, and one hot matrix, which corresponds to the input image matrices. Additional information includes vocabulary dictionary and character frequencies in the set.

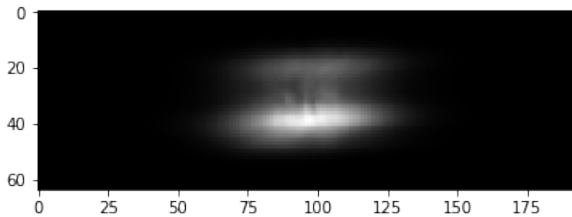


Fig. 8. Mean 192x64 gray image that can be used for normalization task.

3-dimensional matrix, which represents the RGB image, was converted into a 1-dimensional matrix that represents the gray image version of the same image. Then all the matrices are saved in an HDF5 file that has the architecture depicted in Fig. 7.

In addition to saving the text that represents each image, this text was converted into its one-hot encoding matrix using the extracted character ids, Fig. 5. To make the one-hot matrix clear, the characters ids were saved in a vocabulary list within the HDF5 files. The dataset is not balanced, that is why the characters frequencies were also saved along with the vocabulary so that each character can have its own weight in any further loss function. In addition, the lengths of these texts were saved for any further processing.

For the training set only, the mean images for the RGB and gray images have been calculated, converted to its corresponding matrices, and then saved in the training HDF5 file. Fig. 8 show the mean gray image.

IV. DATASET STATISTICS

Next, the properties of the Quran Text Image Dataset (QTID) were analyzed. The dataset consists of 309,720 different word image that contains 2,494,428 characters in total. Table I shows the detailed total quantity of word images and characters in the dataset. The 309,720 words were split over the training, validation, and testing sets as shown in the pie chart Fig. 9.

The number of instances per character for all the 60 characters is shown in Fig. 10. Additionally, the top 20 most

TABLE I. QUANTITY OF WORDS AND CHARACTERS IN THE DATASET

	Number of Words	Number of Characters
Unique words	18,994	188,918
Holy Quran	77,430	623,607
Total (Given 4 Fonts)	309,720	2,494,428

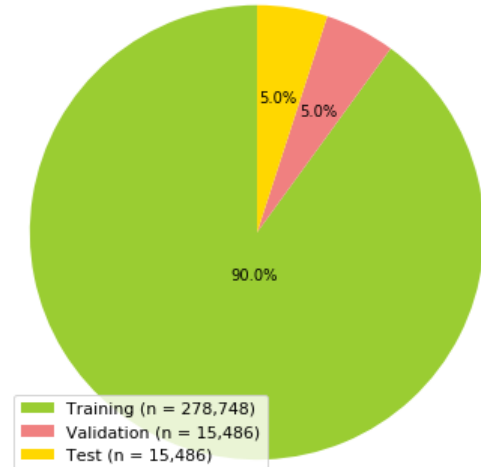


Fig. 9. Training, validation, and testing sets words distribution.

repeated words are in Fig. 11 and the max length of a word is 21 characters.

Finally, some benchmarks regarding the created HDF5 files are shown. To measure the reading time of the HDF5 file of the dataset, the testing dataset was split into 120 mini batches each consists of 128 images. Then some experiments was made to read all these mini batches 100 times. Then average of the reading time for every mini batch was calculated. The illustration is in Fig. 12.

V. EXPERIMENTAL EVALUATION

Two of the best Arabic character recognition engines were chosen to evaluate the dataset. The first one is Tesseract [13], an optical character recognition that was developed by Google and one of the most accurate open-source engines available. It can recognize many languages, which include the Arabic language. The second one is ABBYY FineReader⁴, also an optical character recognition that was developed by ABBYY for the commercial use. ABBYY team mentioned that it can recognize 190 different languages and that it has an accuracy of 99% for the Arabic language.

The dataset of this study has training, validation, and testing sets. The testing set has been evaluated only with the mentioned engines. The testing set consists of 15,486 Arabic word images, which contain 124,746 characters. In addition, it contains every possible character that is covered.

The recognition results have been evaluated using the five measures. The first one is character recognition rate (CRR) which is defined as follows:

$$CRR = \frac{\#characters - \sum LevenshteinDistance(RT, GT)}{\#characters}$$

⁴<http://finereader.abbyy.com/professional/>

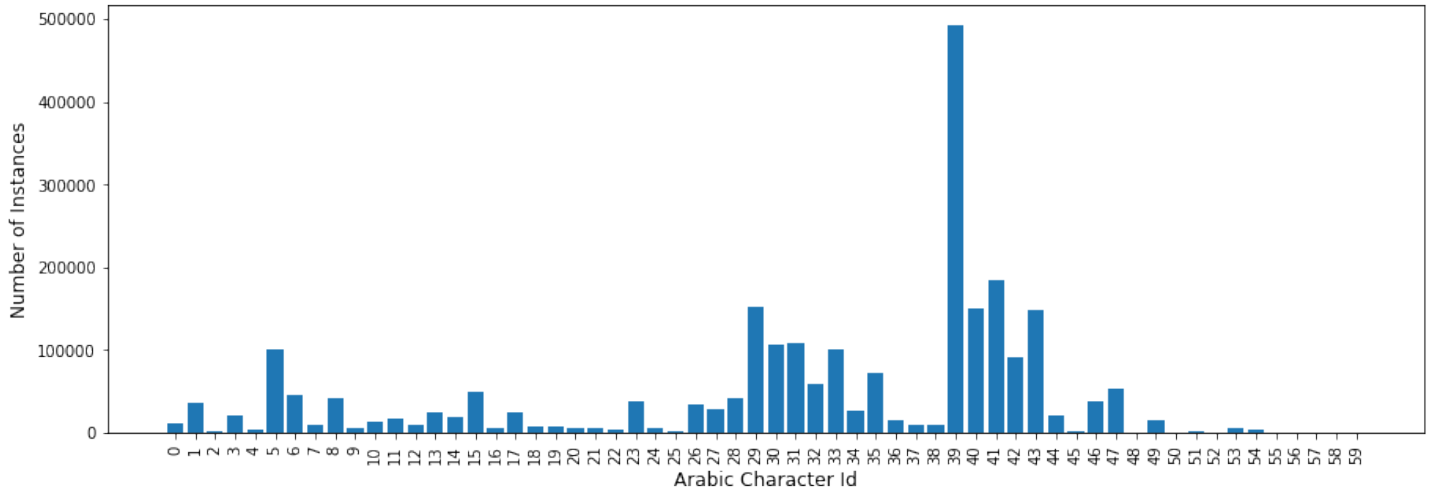


Fig. 10. Instances per character in the whole dataset.

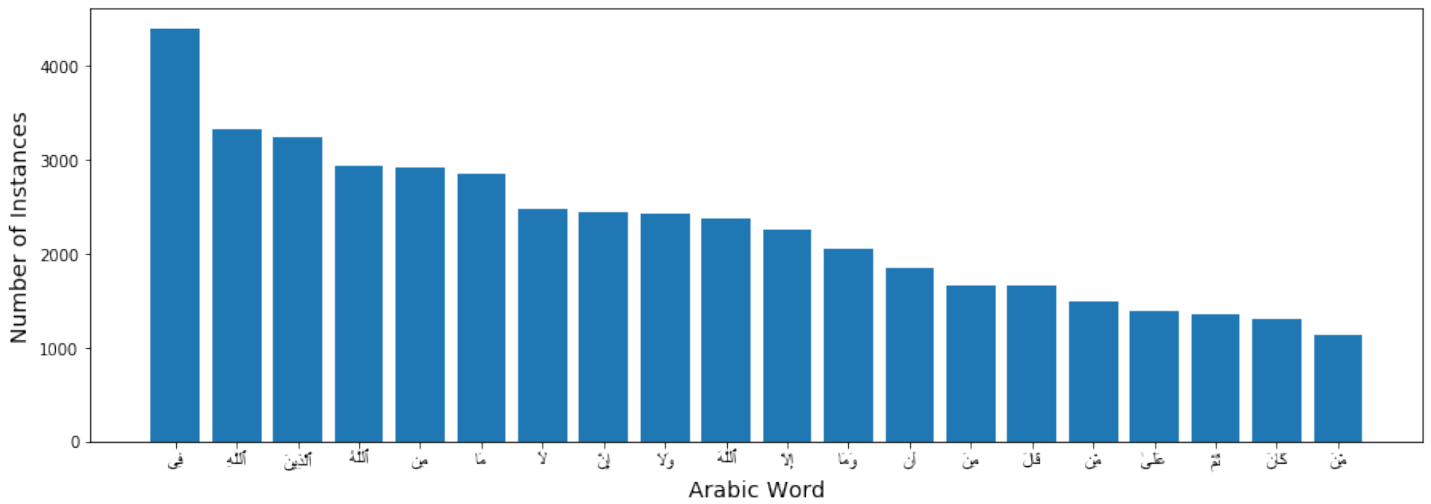


Fig. 11. Top 20 most repeated words in the whole dataset.

TABLE II. ACCURACY, PRECISION, RECALL, AND F1 RESULTS ON THE TEST SET

Engine	Accuracy (%)	Average Precision (%)	Average Recall (%)	Average F1 score (%)
Tesseract 4.0	10.67	56.73	18.44	27.83
ABBY finereader 12	2.32	34.37	4.06	7.27

Where (RT) is the recognized text and (GT) is the ground truth text. The results are in Table III. The other four measures are accuracy, average precision, average recall, and average F1 score which is defined as follows:

$$Accuracy = \frac{\#correctly\ recognized\ characters}{\#characters}$$

$$Precision_i = \frac{\#correctly\ recognized\ character\ i}{\#characters\ recognized\ as\ character\ i}$$

$$Recall_i = \frac{\#correctly\ recognized\ character\ i}{\#character\ appearances}$$

$$F1_i = \frac{2}{1/Precision_i + 1/Recall_i}$$

Before taking these measures, all the ground truth text was first aligned with the recognized text and then the confusion matrix for all the characters was calculated to easily extract the mentioned measures. Results are in Table II. The character with 3 as Id was Tesseract top precision character while the character with 33 as Id was the top for ABBYY FineReader. To know the character Ids refer to Fig. 5.

Finally, none of the used engines has recognized a complete word image with 100% accuracy.

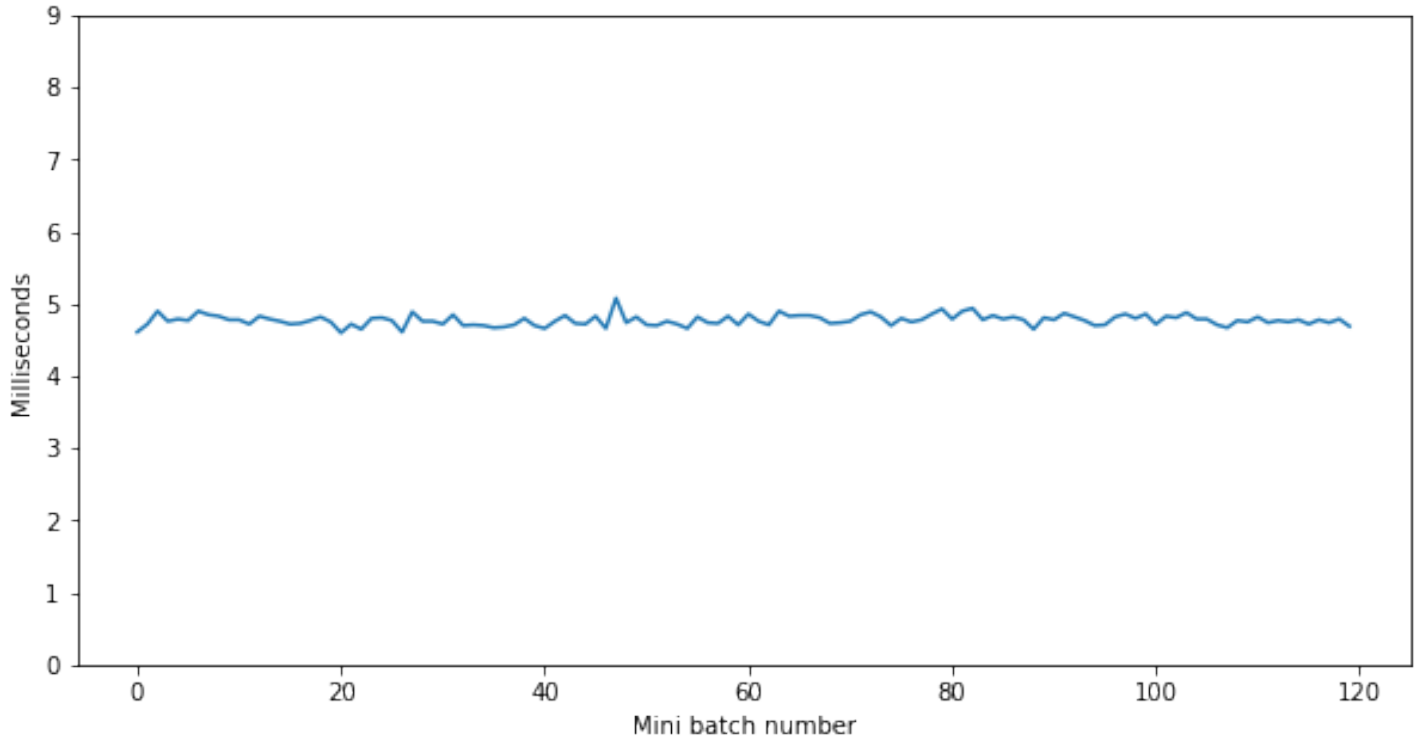


Fig. 12. HDF5 120 Mini batches reading benchmark. The experiment ran on a computer with these specifications: Intel i5 CPU, 8 DDR3 ram, and hard disk with rotation speed 7200 RPM.

TABLE III. CHARACTER RECOGNITION RATE RESULTS ON THE TEST SET

Engine	Character recognition rate (%)
Tesseract 4.0	11.4
ABBY finereader 12	6.15

VI. DISCUSSION AND CONCLUSIONS

Arabic text recognition accuracy is small compared to the accuracy of the Latin texts. In this paper, a new large dataset QTID that is made from the words of the Holy Quran was proposed in order to help machine learning models improve the accuracy of reading Arabic text from images. The dataset consists of training, validation, and testing sets that was split into 90%, 5%, and 5% respectively. It has been presented that the current best Arabic text recognition engines cannot work well with word images from the proposed dataset, which means that more work is needed to improve the Arabic text recognition task. Some of the limitations of the proposed dataset include: imbalanced characters instances, centered Arabic words images with black paddings, and dataset Arabic words do not cover the whole Arabic words dictionary. In the future, the dataset needs so improvements to the limitations by using data augmentation techniques and adding character segmentation support. In addition, the best model that can work with the proposed dataset hope to be found.

ACKNOWLEDGMENT

The authors would like to thank Alsherif Mostafa for his assistance while writing the paper, which greatly improved the

manuscript.

REFERENCES

- [1] T. Sobh, *Innovations and Advanced Techniques in Computer and Information Sciences and Engineering*. Springer, 2007. [Online]. Available: <http://www.springer.com/gp/book/9781402062674>
- [2] —, *Innovations and Advances in Computer Sciences and Engineering*. Springer, 2010. [Online]. Available: <http://www.springer.com/us/book/9789048136575>
- [3] N. Tagougui, M. Kherallah, and A. M. Alimi, "Online arabic handwriting recognition: a survey," *International Journal on Document Analysis and Recognition (IJDAR)*, vol. 16, no. 3, pp. 209–226, Sep 2013. [Online]. Available: <https://doi.org/10.1007/s10032-012-0186-8>
- [4] V. M. S. Mozaffari, K. Faez, "Strategies for large handwritten farsi/arabic lexicon reduction," *proceedings of the Ninth International Conference on Document Analysis and Recognition*, pp. 98–102, 2007. [Online]. Available: <http://ele.aut.ac.ir/image-proc/downloads/IFHCDB.htm>
- [5] F. Slimane, R. Ingold, S. Kanoun, A. M. Alimi, and J. Hennebert, "A new arabic printed text image database and evaluation protocols," in *2009 10th International Conference on Document Analysis and Recognition*, July 2009, pp. 946–950. [Online]. Available: <http://diuf.unifr.ch/diva/APTI/>
- [6] S. Yousfi, S. A. Berrani, and C. Garcia, "Alif: A dataset for arabic embedded text recognition in tv broadcast," in *2015 13th International Conference on Document Analysis and Recognition (ICDAR)*, Aug 2015, pp. 1221–1225.
- [7] F. Chabchoub, Y. Kessentini, S. Kanoun, V. Eglin, and F. Lebourgeois, "Smartatid: A mobile captured arabic text images dataset for multi-purpose recognition tasks," in *2016 15th International Conference on Frontiers in Handwriting Recognition (ICFHR)*, Oct 2016, pp. 120–125.
- [8] S. A. Azeem, M. El Meseery, and H. Ahmed, "Online arabic handwritten digits recognition," in *Frontiers in Handwriting Recognition (ICFHR), 2012 International Conference on*. IEEE, 2012, pp. 135–140.

- [9] M. W. F. Sherif Abdou, "Large vocabulary arabic handwritten online character recognition competition," http://www.altec-center.org/conference/?page_id=87, 2011. [Online]. Available: http://www.altec-center.org/conference/?page_id=87
- [10] H. El Abed, V. Märgner, M. Kherallah, and A. M. Alimi, "Icdar 2009 online arabic handwriting recognition competition," in *Document Analysis and Recognition, 2009. ICDAR'09. 10th International Conference on*. IEEE, 2009, pp. 1388–1392.
- [11] V. M. S. Mozaffari, K. Faez and H. El-Abed, "Strategies for large handwritten farsi/arabic lexicon reduction," *proceedings of the Ninth International Conference on Document Analysis and Recognition*, pp. 98–102, 2007. [Online]. Available: <http://ele.aut.ac.ir/imageproc/downloads/IFHCDB.htm>
- [12] S. A. Mahmoud, I. Ahmad, W. G. Al-Khatib, M. Alshayeb, M. T. Parvez, V. Märgner, and G. A. Fink, "Khatt: An open arabic offline handwritten text database," *Pattern Recognition*, vol. 47, no. 3, pp. 1096 – 1112, 2014, handwriting Recognition and other PR Applications. [Online]. Available: <http://www.sciencedirect.com/science/article/pii/S0031320313003300>
- [13] R. Smith, "An overview of the tesseract ocr engine," in *Document Analysis and Recognition, 2007. ICDAR 2007. Ninth International Conference on*, vol. 2. IEEE, 2007, pp. 629–633.

Analysis of Biometric Technology Adaption and Acceptance in Canada

Eesa Al Solami
University of Jeddah,
Saudi Arabia

Abstract—This study aimed at analyzing the analysis biometric technology adoption and acceptance in Canada. From the introduction, the paper reveals that biometrics technology has been in existence for many decades despite rising to popularity in the last two decades. Canada has highly advanced in information technology. It is observed that the three sectors for the adoption and acceptance of biometric technologies are: financial services, immigration, and law enforcement. The study uses judgment for sampling and questionnaires for the collection of data. Given the high rate of adoption and acceptance of biometric technologies in Canada, the paper concludes that the adoption of these technologies is at the adaptation state. Age and experience also influence the rate at which individuals accept biometric technologies with the most experienced participants showing the highest rate of approval.

Keywords—Adaption; biometric technology; organizational

I. INTRODUCTION

In the modern business environment, competition leaves organizations with no chance but use all the resources that are at their disposal to gain competitive advantage. One of the fronts where this kind of competition has been evident is technological. In most cases, the organizations that have innovative technologies carry the day. One of the most discussed technologies in business is the biometric technology. Biometric is the measure of the unique physical and behavioral traits. The use of biometrics for identification and security has become a common practice, especially in developed countries. The use of biometrics for authentication is one of the most secure and trusted options for user authentication. Various factors always influence the rate at which a technology such as biometric authentication is adopted in a country. This paper analyses biometric technology adoption and acceptance in Canada.

The paper is organized as follows. The next section highlights the Information technology investment in Canada. In Section 3, we present the literature review of the topic by explaining the mannerism of identification and use. Also, we show how the adoption of biometric security systems. In Section 4, we present the theoretical framework. Following this in Section 5, we explain the methodology of the work by defining the way of sampling, shows how is the data collection and also, the approach of data processing. In Section 6, we presents the data presentation and analysis and emphasis the regression analysis. Following this in Section 7, we show the discussion of results. The final section concludes the paper.

A. Contribution

In this paper, we analysed and studied biometric technology adoption and acceptance in Canada. The paper concluded that

three sectors in Canada where the adoption and acceptance of biometric technologies are financial services, immigration, and law enforcement. Furthermore, there are two main factors including age and experience influence the rate at which individuals accept biometric technologies with the most experienced participants showing the highest rate of approval.

II. INFORMATION TECHNOLOGY IN CANADA

Canada may not be a country that comes to the mind of any one with the mention of economic superstars, but it is one of the best-managed economies in the world. For many years, the government of Canada has put importance in the use of information technology for economic sustainability. The government of Canada Information Technology Strategic Plan 2016-2020 is one of the evidence of the extent to which the government has gone to make sure that the use of information technology in the country is complemented. This is according to a study that was done by [3]. Information technology has been of the most contribution to the growth of the main services sector in Canada. According to a report by The Information and Communications Technology Council (ICTC), aside from job creation and direct contribution to the GDP through the ICT sector that increased by \$2 billion in 2014, the contribution of ICT to the other sectors is beyond doubt. The proximity of the country to the US and their close business relationship has also contributed to the high rate of advancement of ICT in the country.

III. LITERATURE REVIEW

Despite biometric being on the verge of a breakthrough in human identification and security, it was not given much consideration as it is given in the modern society. Canadian stakeholders believe that there are benefits that come with the use of biometric technologies [5]. However, with all these advantages there are disadvantages such as age and occupational factors that may lead to difficulty in capturing physical attributes such as fingers. People in occupations such as construction are prone to such a disadvantage. The various biometric technologies can be judged in terms of universality, permanence, uniqueness, collectability, acceptability, performance, and circumvention. However, assert that none of these technologies is perfect. When they are reviewed in terms of the above-mentioned factors of judgment, there are some shortcomings that are noted for the use of biometrics as shown in Table I.

Table I reveals the imperfection of the biometrics that is used in Canada. Therefore, there is always a system that can be used in the evaluation of the performance of a biometric

system. The system has three criteria, which are: 1) False accept rate (FAR): the proportion of unauthorized users manage to get access. Such error is most likely to be as a result of a security breach. a) False reject rate (FRR): the proportion of authorized users that fail to get access. Such an error represents threats the rightful use of the system. b) Crossover error point (CEP): a scenario whereby the rate of false acceptances equals is equal to the rate of false rejections. Such an error implies optimal results to biometrics-based systems.

A. Mannerism of Identification and Use

Of the forms of biometrics that are used in various parts of the world, fingerprints have been used in Canada for the longest period. This technology has been particularly used in the finance sector in the identification of account holders for the sake of securing accounts from possible fraud [10]. In [9] asserts that there has been a significant decrease in the rate of fraud cases that relate to false acceptance. For the sake of security, some organization is fingerprint recognition that requires the use of all the ten fingers instead of just one because it enhances accuracy.

Another biometrics that is commonly used in Canada is facial recognition. This technology was initially manual with the administrators have to look at digital pictures for facial confirmation. However, with the advancement in technology in Canada, facial biometrics technology has been taken to a whole new level. A perfect example is the application of facial recognition at Canadian airports [13]. This is part of the program that was introduced by a traveler screening program by the Canadian Border Services Agency. This involves self-service border clearance kiosks that intend to make Canadian border points safer.

In [2] asserts that many people do not realize that Iris recognition is different from facial recognition. Iris is a muscle that performs the function of controlling the size of the pupil. The highly detailed texture makes it possible for Iris to be used for identification and authentication. Government agencies have been on the frontline in using Iris identification in Canada. An example of such a case is the partnership between IBM and ID Iris to provide iris recognition technology for NEXUS, a program under the Canadian Border Services Agency [8]. The private sector has also used this technology for authentication is some occasions.

Voice recognition technology has also been used by some organizations. This is an assertion that is true as far as the financial sector in Canada is concerned. RBC was the first Canadian company to successfully implement the voice recognition technology in 2015. However, that is not where the application of voice recognition technology ends. Soon, many other organizations were using this technology for recognition. The financial sector has been under pressure to use innovative technology in the recent past because of the changing expectations of their customers.

B. Adoption Biometric Security Systems

Despite many people not being opportunistic on the adoption of biometric technologies in Canada, the adoption rates have been relatively high as organizations strive to adapt to the expectations of their customers and international standards.

The government has also been under the equal pressure since of the advanced nature of security risks that the country may faces and the want to give assurance to people of the public that they are secure. As a technology that was considered by many members of the society as new three decades, the debate on the benefits and the shortcomings of these technologies were at the center of decisions that were made by the government agencies or organization on whether adopting biometrics technologies was a viable decision or not [4].

In Canada, the decisions to use biometric were guided by economic, operational, managerial, or, process related. According to most of the researches that were done on the adoption of biometric, these decisions were as a result of operational variables. This is further backed by the high costs that are included in the acquisition of such technologies [14]. Some managers, especially those managing small and medium-sized organizations know the security threats that their organizations face, and the benefits that they can get by adopting biometric identification and authentication but are limited by the lack of financial resources. It was also revealed that the research that informs to the ability formulation of implementation strategies might be a main factor that decreases the ability of some organizations to use biometric technologies. For most of the organizations and government agencies that adopted, security and better services were at the center of the decisions. Author in [6] argues that the money that is involved in the acquisition of this technology in Canada was not much as compared to the operational and process-related impact that it had.

C. Summary

Evidently, there is no single technology that will give absolute technology. Therefore, only the integration of various biometric identification options into a single application. This lead to different layered levels of security and that can lead to high layered levels of security as in the case for some of the organizations in the financial sector. The Canadian Border Services Agency has also been seen to use more than one biometrics identification technology. The use of biometric technology is advanced in Canada is more advanced than most parts of the world, especially the developing countries.

IV. THEORETICAL FRAMEWORK

Managerial, organizational, technological and environmental imperatives are all promoted by available theories on the use of technology [12]. Notably, the adoption of biometric technologies is not entirely a technological issue because of the high influence that cost has. Therefore, this study is going to assume that adoption has six phases, which are: initiation, adoption, adaptation, acceptance, re-utilization then infusion. As far as the available literature on the adoption of biometric technology in Canada is concerned, the country is at the adaptation stage of technology adoption. The model (Rogers, 1995) include the diffusion of innovation that is commonly used in understanding the diffusion of technologies is as seen in Fig. 1 below.

A. Usage

Biometric technologies in widely used by security agencies and financial organizations in Canada. However, not much has been seen in the other sector.

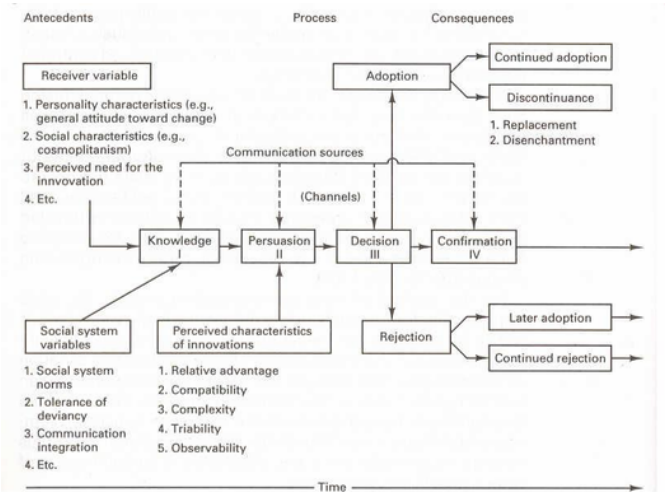


Fig. 1. Diffusion of innovation model. Source:(Rogers, 1995).

B. Variables of Receivers

The diffusion of innovation model uses organizational social characteristics, demographic characteristics, and perceived innovation need as essential variables that could have controlling impacts on the decision to adopt a technology by an organization or government agency. This study mainly focuses on organizational features such as type, size, age, and experience in IT as main factors that can affect the decision on whether or not to adopt the use of biometric technologies.

C. Perceived Innovation Characteristics

The diffusion of innovations theory asserts that the various dimensions of attitude toward an innovation are measurable using the five attributes, namely, compatibility, relative advantage, complexity, risk, and trialability. The perceived relative advantage of innovative technologies is directly proportional to the rate at which it is adopted [1]. Research also indicates that an innovative technology with substantial complexity needs more technical skills and needs greater implementation and operational efforts to increase its chances of adoption. Potential adopters of technology who are allowed to try an innovation will feel more comfortable with the technology and are likely to adopt it.

V. METHODOLOGY

A. Sampling

The sampling technique that was carried out in this study was a testing as opposed to random choosing. The study made use of three sets of samples which are financial institutions, immigration agencies, and law enforcement agencies. The choice of these sets of the sample was as a result of the high rate at which security measures and identification was of importance to these sectors. Participants were employees of the organization in the specialized IT department, especially those directly involved in the implementation of biometrics technologies. Although biometric not being a new trend in Canada, focusing on the IT specialists ensured that the data that was collected was of the maximum possible accuracy.

B. Data Collection

The data collection method that was used for this study was questionnaires. The selection of this method of data selection was directed by a high number of participants that the study willing to have and their variety in terms of age, the size of organizations in which they work, gender, and the roles that they play in these organizations [11]. The questionnaire used both open and closed questions with demographic details being of utmost importance. The questionnaires also had a section that focused on the variables concerning biometrics adoption. These variables included technology, ease of use, support of management, technological compatibility, and participant vulnerabilities and privacy needs [7]. We distributed the questionnaire to 10 organisations that have number of IT specialists. Therefore, we made up about one hundred questionnaires. One hundred thirty nine of them were filled and used for analysis and studies in this paper.

C. Processing

Exploratory factor analysis was used in the reduction of the number of variables into few factors that can influence the implementation of biometrics technology in an organization. The reduced factors were an improvement of service excellence, security, and productivity. Statistical Package for Social Sciences (SPSS) for Windows Version 14.0 was then used for factor analysis. The factors were also derived by principal axis factoring and rotating them by applying Promax with Kaiser Normalization method to increase the relationship between some of the factors and the variables. Multiple regression analysis was applied to test the hypotheses associated with the factors that influence implementation of biometric technologies.

VI. DATA ANALYSIS

The data that was collected from individuals from demographic perspective is as shown in Table II.

According to the data that was collected, the rate at which biometrics was adopted in the sectors that the study was based on. The findings according to the difference are presented in table three. The YY ratings imply that there was the adequate use of biometrics technologies. The Y ratings indicate that the use of biometrics was moderate while N rating implies that either were no cases of biometric adoption.

A. Regression Analysis

Regression analysis proved to be effective in the testing of the hypothesis. The regression analysis was based on the factors that determined the applicability and adoptability of biometrics technologies in Canada. It was from the relationship between the stated variable: technology, ease of use, support of management, technological compatibility, and participant vulnerability and privacy concerns and the state of biometric technology in the country.

VII. DISCUSSION OF FINDINGS

According to the results of the study reveal that ease of use, size and type of organization, and communication sufficiently influenced the adoption of biometric technology.

TABLE I. RESPONDENT CHARACTERISTICS

Characteristics	Number	Percent
Age		
25-34 years	45	35.71
35-44 years	49	38.89
45-55 years	18	14.29
55-65 years	9	7.14
More than 65 years	5	3.97
Gender		
Male	68	53.97
Female	58	46.03
Type of organization		
Financial institutions	43	34.13
Law enforcement	26	20.63
Immigration	29	23.02
Others	28	22.22
Position in organization		
Top level management	20	15.87
Middle management	22	17.46
Operational level management	30	23.81
Technical staff	27	21.43
Operational Staff	27	21.43
Size of organisation		
Very small	8	6.35
Smallmedium	15	11.90
Medium	19	15.08
Mediumlarge	22	17.46
Large	32	25.40
Age of organization		
Less than 5 years	7	5.56
5-9 years	15	11.90
10-19 years	9	7.14
20-29 years	29	23.02
30 years and above	28	22.22
IT experience		
Less than 5 years	24	19.05
5-9 years	26	20.63
10-19 years	32	25.40
20-29 years	21	16.67
30 years and above	23	18.25

TABLE II. ADAPTION RATES INDICATIONS

	Banking	Immigration	Law enforcement	others
Signature	YY	Y	YY	YY
Fingerprint	YY	YY	YY	YY
Voice	Y	Y	YY	Y
Face recognition	YY	YY	YY	Y
Iris	Y	Y	N	N
Hand and finger geometry	Y	Y	Y	Y
Gait	N	YY	YY	Y
DNA	N	Y	Y	Y
Keystroke	YY	Y	Y	Y
Retinal scanning	Y	N	Y	Y

Given that Canada is at the adaptation stage, there were very few participants still doubting the level of effectiveness of biometric technology in the enhancement of security. However, the participants were of the opinion that determination of the

right balance in terms of the technologies to be used and the nature of organization were the major challenges that were faced when it comes to the adoption of biometric technologies.

A. Expected Attributes of Biometric Technology

1) *Compatibility of the technology*: Though there is the significance of technological compatibility in the adoption of biometric technology, there has not been evidence that it is of high influence. As far as infrastructure that is used in the adaptation of this technology is concerned, most of the participants seem to think that the level of advancement of information technology in Canada is enough for any organization that intends to adopt biometric technologies.

2) *Use difficulty of use*: Majority of the respondents were of the opinion that the difficulty of use is no longer a determining factor on whether an organization adopts biometric technology. It used to be an important determinant in the past. However, with the level of advancement of information technology in Canada, it has become easier for organizations to adopt the biometric technology. This can be proved by the high number of organizations using biometric technologies in Canada. In most developing countries, older organizations tend to avoid innovative technologies because they are satisfied with the traditional techniques of identification and authentication. However, the situation in Canada is different because the older organizations are taking advantage of massive experience and access to capital that they can use in the adoption of biometric technology. This is an opinion that was held by 72.22% of the participants.

3) *Relative advantage*: Relative advantage proved to be of high influence on the adoption of biometric technology. Most of the participants were of the impression that their organizations opted for biometric technologies because of the fact that they provide identification and authentication advantages that none of the available alternatives could. Only 17.26% of the participants thought that potential relative advantage had no impact on the decision whether to adopt biometric technologies.

B. Variables of Social Systems

Suitable communication between information technology experts and users and organization managers is considered to be one of the principal factors that have contributed to the high level of adoption of biometric technology in Canada. 86% of the participants were adamant that lack of understanding of the technologies was a high contribution to the low rate at which these technologies were adopted in the past. Management support was also of significance because of the level to which management influence the strategies that are adopted and the extent to which they are adopted. This is a trend that proved to be persistent for participants who worked in government agencies.

C. Receiver Variables

As seen in the result, organizational demographic nature tends to have minimal influence its intention to use the biometric technology. There is no evidence from the collected data that can prove that the age of the organization had an influence on the decision to opt for biometric technology.

However, there was some difference when it comes to the size of the organization. The larger organizations in Canada appeared to adopt biometric technology at a higher rate as compared to the smaller ones. This difference can be attributed to the difference in access to resources.

VIII. CONCLUSION

Evidently, the use of biometric technologies in Canada has gotten to its adaptation stage. The level of understanding of the participants and the number of organizations that use these technologies is enough proof that the country is way past the infancy stage. However, it is clear that the nature of the organization and its goals in terms of identification and authentication was of high influence on the adoption of biometrics technology. This is the reason why the technologies are widely used in the banking, immigration, and law enforcement sectors. This proves the hypothesis that economic, operational, managerial, or, process factors determined the possibility of an organization adopting biometric technologies.

REFERENCES

- [1] Hossein Bidgoli. The introduction of biometrics security into organizations: A managerial perspective. *International Journal of Management*, 29(2):687, 2012.
- [2] Michael Colin Breward. Factors influencing consumer attitudes towards biometric identity authentication technology within the Canadian banking industry. PhD thesis, 2009.
- [3] Hyunbae Chun. Information technology and the demand for educated workers: disentangling the impacts of adoption versus use. *Information Technology*, 85(1), 2006.
- [4] Kathrin Cresswell and Aziz Sheikh. Organizational issues in the implementation and adoption of health information technology innovations: an interpretative review. *International journal of medical informatics*, 82(5):e73e86, 2013.
- [5] Ana Ortiz De Guinea and M Lynne Markus. Why break the habit of a lifetime? rethinking the roles of intention, habit, and emotion in continuing information technology use. *Mis Quarterly*, pages 433444, 2009.
- [6] Stephen J Elliott, Sarah A Massie, and Mathias J Sutton. The perception of biometric technology: A survey. In *Automatic Identification Advanced Technologies, 2007 IEEE Workshop on*, pages 259264. IEEE, 2007.
- [7] Inkingi Fred Gatali, Kyung Young Lee, Sang Un Park, and Juyoung Kang. A qualitative study on adoption of biometrics technologies: Canadian banking industry. In *Proceedings of the 18th Annual International Conference on Electronic Commerce: e-Commerce in Smart connected World*, page 20. ACM, 2016.
- [8] Rajeev Gupta and Ashok Kumar. Noisy iris recognition and its importance. *J. Ultra Sci. Phys. Sci*, 25(2):229234, 2013.
- [9] Kim Kristian Humborstad. How governments are creating the business case for biometrics. *Biometric Technology Today*, 2015(7):911, 2015.
- [10] Nancy Lewis. Expanding surveillance: Connecting biometric information systems to international police cooperation. *Global Surveillance and*
- [11] Shoshana Magnet. *When biometrics fail: Gender, race, and the technology of identity*. Duke University Press, 2011.
- [12] Jonathan I Mitchell, Marylne Gagn, Anne Beaudry, and Linda Dyer. The role of perceived organizational support, distributive justice and motivation in reactions to new information technology. *Computers in Human Behavior*, 28(2):729738, 2012.
- [13] Cristian Morosan. Biometric solutions for today's travel security problems. *Journal of Hospitality and Tourism Technology*, 3(3):176195, 2012.
- [14] G Premkumar and Anol Bhattacharjee. Explaining information technology usage: A test of competing models. *Omega*, 36(1):6475, 2008.

Enhancing Quality of Lossy Compressed Images using Minimum Decreasing Technique

Ahmed L. Alshami, Prof. Mohammed Otair
Amman Arab University
Faculty of Computer Science and Informatics
Amman, Jordan

Abstract—The acceleration in technology development came with the urgent need to use large amounts of information, and the way of storing or transferring the huge information via various digital networks became very important issues, particularly in terms of compressing size and quality preservation. The digital image usage has become widespread in many sectors; it become important to manipulate these images to use them in optimal form by maintaining the quality, especially during the compression process using the lossy techniques. This paper presents a new technique to enhance the quality of compressed images while preserving the compression ratio by adding some of pre-processing steps before implementing any existing lossy compression technique. The proposed technique depends on decreasing the minimum elements from the image pixels values in each: row, column, and 2×2 block, respectively. These steps minimize the required number of bits to represent each pixel in the compressed images. In order to prove the efficiency of the proposed technique, two lossy compression techniques (novel and classical) were implemented with the proposed. They implemented on wide range of well-known images with different dimensions, sizes, and types. The experimental results show that the quality of the decompressed images with the proposed technique were enhanced in terms of: MSE, MAE and PSNR as quality evaluation metrics.

Keywords—Image compression; lossy technique; lossless technique; image quality measurement; RIFD and JPEG

I. INTRODUCTION

The importance of the digital images and transmitting them along all networks either wired or wireless is increasing day-by-day. These images have very huge sizes in general and need to be compressed in order to accelerate transmitting process. As the digital image became widely used, image processing became a necessary field in many areas and for numerous reasons such as in medical imaging, social media, communications and security cameras. In the area of digital image processing the input for each process is an image, where the output can be an image or a certain attribute or information associated with the original or processed image that results after particular one or several processes applied on the original image [1].

Image compression is a field of image processes which means minimizing the size of the images file without effect on the quality of the image. Therefore, the aim of the compression is reducing the image size that allows the amount of disk or memory space to store more images. In addition, it reduces the time required for images to be sent or downloaded over the Internet [2].

The compression techniques are categorized into Lossless and Lossy. The first one has a good performance on the quality of the compressed images with no loss of any part of the images. However, when the researchers evaluate these techniques in terms of the compression ratio, they found that those techniques have very low performance comparing with the lossless techniques. On the other hand, lossy techniques have high distortion rates. So, most of the current researchers in this field try to find a good level of hashing both techniques, preserving or improving the compression ratio and reducing the distortion.

This paper tries to enhance the quality compressed images of the lossy compression techniques; it proposes a pre-processing lossless procedure prior to any lossy technique which produces a hybrid technique. In order to prove the achievability and efficiency of the proposed pre-processing technique, two lossy techniques were selected which are: the classic JPEG compression technique and the novel lossy technique RIFD [3]. The proposed technique can be applied generally on the digital images whether it is colored or gray scale with different bit-depth values (i.e. number of bits to represent the pixel values). It provides good compression ratio and lower distortion values, by taking the best features from the lossy and lossless techniques that has been used. Moreover, this paper aimed to reduce the bit-depth along with reducing the compression distortion and then improving the quality of the comparison process as a whole.

The rest of the paper is organized as follows: Section 2 introduces a general overview of the mostly related works. Section 3 describes the objective quality evaluation metrics that used in the experiments. The Proposed Technique which is called Minimizing Decreasing Technique (MDT) will be explained in Section 4. Section 5 discusses the experiments and the results of the paper. Finally, the paper is concluded in Section 6.

II. RELATED WORK

In the literature, the compression techniques can be mainly divided into two types: Lossy and Lossless, each one of them has its own positive characteristics. The priority of the lossy technique is the high compression ratio but with a percentage of distortion, while the lossless techniques compression produce a low rate of compression ratio without any distortion. This section presents some of the literature reviews that are related to the core subject of this study.

The researchers in [4] indicate that data can be compressed by decreasing the redundancy in the main data, but this makes

the data have further errors. In this study a novel method of an image compression depend on a different technique which has been formed for image compression which has been called Five Modulus Method (FMM). The new procedure consists of converting every pixel value in an 8×8 block into a several of 5 for every of the R, G and B arrays. Then the new values can be divided by 5 to have new 6-bit length pixel values, and it has lower storage area than the original image. This study offered a new compression order of the new values as a stream of bits, which improved the chance for storing the new compressed image easily. This study explains the potential of the FMM depend on image compression technique, the priority of this method is the high PSNR even though it has low compression ratio. This technique is appropriate for bi-level images, where the pixel is symbolize by one byte (8-bit). Because of the low compression ratio, this method cannot be used as a standalone technique, but it could add as scheme within other compression techniques.

Zhou et al. [5] proved a new image compression encryption hybrid algorithm based on compressive sensing and random pixel exchanging, where the compression and the encryption are completed simultaneously, where the key is easily distributed, stored or memorized. The image is divided into 4 blocks to compress and encrypt. Then random pixel exchanging is introduced to scramble the compressed and encrypted blocks. Compared with the methods adopting the whole measurement matrix as key, the proposed algorithm shortens the key greatly, which is of importance for a practical encryption algorithm. By utilizing the circulate matrix to construct the measurement matrix, in CS and controlling the original row vector of circulate matrix with chaos system, the proposed algorithm is secure. By introducing the random pixel exchanging and binding the random matrices with the measurement matrices, the security is enhanced further. The simulation results show that this image compression encryption hybrid algorithm can provide good security and nice compression performance.

Vijayvargiya et al. [6] explain the main goal of image compression is to exemplify an image in the smallest number of bits without losing the major information content within an original image Compression methods are being speedily improved for compress large data files like images, there are several algorithms which perform this compression in various ways; some of these compression methods are designed for the specific type of images, thus they will not be perfect for other kinds of images, this study addresses about different image compression method. In this study they look over various kinds of current procedure of image compression such as Inter Pixel Redundancy where about in image adjacent pixels are not statistically separate, it is according to the connection between the neighboring pixels of an image, this kind of redundancy is known as Inter-pixel redundancy, this kind of redundancy may also referred to as spatial redundancy, this redundancy may be examine in many ways, one of which is through expecting a pixel value depend on the values of its adjacent pixels. In order to do so, the original 2-D array of pixels is generally mapped into a various shape.

The JPEG has been suggested as a standard compression scheme for continuous-tone motionless images. It utilizes a $64 (8 \times 8)$ pixel-block discrete cosine transform (DCT) for gath-

ering the information into several transform coefficients, this block design takes advantage of the local spatial correlation property of images and also reduce the processing time. Yet, it is well known that this individual processing of each block will create visually disturbed blocking effects, especially when a high quantization parameter is used for high compression [7].

Otaïr and Shehadeh [4] proposed a novel lossy image compression technique called RIFD for compressing images. This scheme leans on increasing the redundancy and resemblance among the close pixels of images by rounding the pixels' intensities followed by the dividing process, which makes compression attainable, the main idea of the RIFD algorithm is based on two facts: 1) adjacent pixels are correlated or so identical; 2) the human sight can perceive a very limited number of intensities. So, if the intensity values of the adjacent pixels are rounding to the same value, then the redundancy will increase, and the updated intensity values will not be detectable by human sights. Raising the information redundancy supports the image to be more compressed. Therefore, finding a less correlated representation of the image is a significant thing. This technique can be implemented either individual or along with any lossless compression algorithm such as Huffman. The RIFD technique can be implemented via very simple steps as follow: 1) estimate image size; 2) rounding each pixel value to the nearest ten; 3) divide the rounded values by ten; and 4) apply Huffman Technique. This sequence aims to reduce the range of the intensities, as well as increasing intensities redundancy, which achieves better compression performance. A significant performance of RIFD technique remarked when it is followed by Huffman algorithm.

III. OBJECTIVE AND EVALUATION METRICS

Important image waste of information or property that may take place during the different image processing; Therefore, Image Quality Assessment (IQA) is deeply essential characteristic for evaluating image quality after been processed compared with the original image to ensure that any particular process is performing the required results, as in image compression it required to check the variation between the original and the processed Image [8]. IQA techniques could be: Objective or Subjective. Subjective evaluation is time-consuming, costly and resource-intensive, this type gets along with human visual system (HVS) [9]. Objective image feature metrics can be grouped according to the availability of an original (distortion-free) image, in which the distorted image is to be compared. The current measures that will be used in this paper includes [10], [11]: Mean Square Error (MSE), Peak Signal to Noise Ratio (PSNR), Mean Absolute Error (MAE).

A. Mean Square Error (MSE)

The cumulative difference between the compressed image and original image:

$$MSE = \frac{\sum_{m,n} [I_1(m,n) - I_2(m,n)]^2}{m \times n}$$

Where, M, N are pixel co-ordinate, I1: compressed image pixel, and I2: original image pixel.

B. Peak Signal to Noise Ratio (PSNR)

The rate within largest possible power and effective distorted noise on image impersonation:

$$PSNR = \frac{10 \times \log_{10} (Intensity_{(max)})^2}{MSE}$$

For 8-bit pixel gray scale, $Intensity_{(max)} = 255$,

$$PSNR = \frac{10 \times \log_{10} 255^2}{MSE}$$

C. Mean Absolute Error (MAE)

The metric represent the cumulative absolute value for the variance between the initial image and the refined one:

$$MAE = \frac{\sum_{m,n} |I_1(m,n) - I_2(m,n)|}{m \times n}$$

Where, M, N are pixel co-ordinate, I1: compressed image pixel, and I2: original image pixel.

IV. PROPOSED TECHNIQUE (MINIMIZING DECREASING TECHNIQUE (MDT))

This paper proposed a new lossless pre-processing technique that enhances the lossy techniques by producing a minimized distortion rates in the compressed. For this purpose two existing lossy techniques were selected as follow: the classical JPEG compression technique and new novel lossy technique called RIFD. The core idea of the proposed technique (which is called MDT) depends on minimizing the pixels values by decreasing/subtracting the minimum values from each row, column, and 2×2 block, respectively. The values of resulted pixels (after the decreasing steps were implemented) will be minimized and then could be represented by the minimum numbers of bits. MDT reduces the distortion and could enhance the compression ratio at the same time. The following steps are the detailed steps of the proposed compression phase:

- 1) Find the minimum pixel value for each row in the image(Store them into a one-dimensional array called *MinRowArray*).
- 2) Subtract every minimum value in MinRowArray from each pixel of its corresponding row.
- 3) Find the minimum pixel value for each column in the image (Store them into a one-dimensional array called *MinColArray*).
- 4) Subtract every minimum value in MinColArray from each pixel of its corresponding column.
- 5) Find the minimum value of the 2×2 block in the image (Store them into a two-dimensional array called *MinBlockArray*).
- 6) Subtract the minimum value in *MinBlockArray* from each pixel of its corresponding block.
- 7) Implement the compression phase of a Lossy technique.

The proposed technique tries to keep every bit value and by implementing a lossy technique a distortion will be minimized and it could improve the compression ratio in most images. These pre-process compression steps use four arrays: one for the compressed image and the three additional arrays to

preserve the minimum pixels values from rows, columns, and 2×2 blocks, respectively. Reversing the compression process in the correct sequence will be executed as follows:

- 1) Implement the decompression phase of the lossy technique.
- 2) Add the minimum value in *MinBlockArray* to each pixel of its corresponding block.
- 3) Add the minimum value in *MinColArray* to each pixel of its corresponding column.
- 4) Add the minimum value in *MinRowArray* to each pixel of its corresponding row.

A. How the Proposed Techniques MDT Does Work?

In order to explain how MDT does work, consider the following 10×10 block that taken from a well-known image 'Cameraman'(see Fig. 1).

154	195	44	11	10	148	229	188	134	152
153	189	58	15	18	201	229	215	90	150
37	46	29	22	27	91	68	63	42	121
12	12	13	16	17	37	26	11	20	109
13	12	11	13	15	25	25	11	13	74
20	12	9	9	9	8	8	8	8	28
17	11	10	9	8	8	9	8	9	12
15	11	9	9	9	9	9	8	10	10
15	12	10	14	39	32	18	9	9	10
12	17	11	79	186	178	87	15	14	17

Fig. 1. 10×10 block from Cameraman image.

Fig. 2 shows the result of the implementation the first four steps of MDT. The aim of these steps is to normalize pixels' values and increase the information redundancy which helps us to compress the image effectively (see Fig. 2).

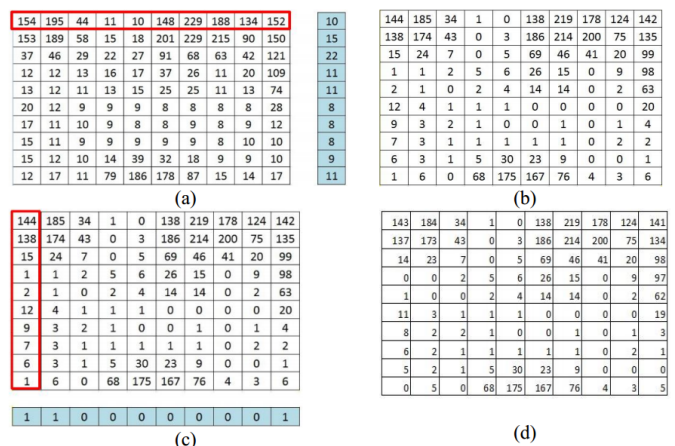


Fig. 2. (a) Find the minimum pixel value in every row, (b) Subtract the minimum row element from each pixel of its corresponding row, (c) Find the minimum pixel value in every column, (d) Subtract every minimum column element from each pixel of its corresponding column.

Fig. 3 shows the effect of implementing Steps 5 and 6 of MDT. The last two steps make the pixel values are ready to be compressed with any existing lossy compression technique

and preserve the quality compressed images at the same time (see Fig. 3).

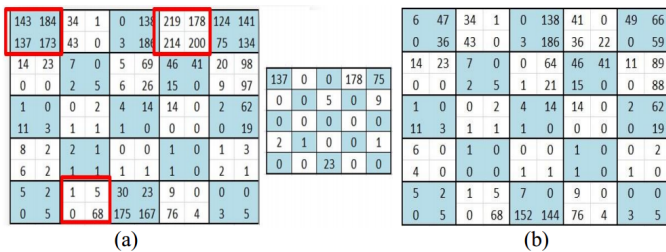


Fig. 3. (a) Find the minimum pixel value in every 2X2 block, (b) Subtract the minimum 2X2 block element from each pixel of its corresponding block.

Fig. 4 show the effect of implementing the RIFD steps on the last block from Fig. 3(b), which rounds every pixel to the nearest ten and then divide them by 10. Finally, the range of the pixels' values fall between 0 and 19 (as in Fig. 4(b)). Thus, every pixel could be represented by 5 bits rather than 8 bits.

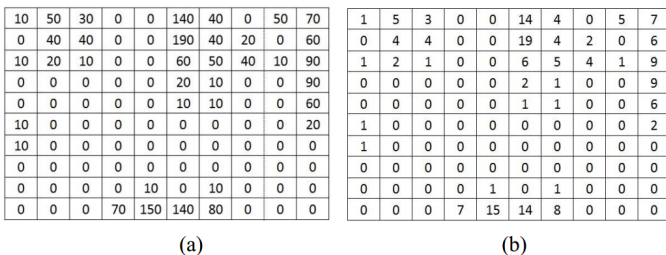


Fig. 4. (a) Rounding the Pixels' values to the nearest ten, (b) Dividing the Pixels' values by ten.

This scheme leans on increasing the redundancy and resemblance among the close pixels of images by rounding the pixels' intensities followed by the dividing process, which makes compression attainable.

V. EXPERIMENTS

In order to prove that MDT (the proposed pre-process compression steps) is suitable and efficient to be implemented before any lossy technique, two techniques were chosen as samples to achieve this purpose. The researchers of this paper chosen RIFD which is a simple and modern compression technique that depends on rounding and dividing steps (Hybrid: MDT-RIFD), and also the MDT was implemented with JPEG that performs complicated mathematical operations to compress the images (Hybrid: MDT-JPEG). All the techniques are written and implemented using Matlab2015a.

The researchers create an image set of 46 images: 30 gray-scale (14 images with 8-bit and 16 images with 16-bit depth) and 16 colored (RGB). These images are diverse in the types: GIF, TIF, PNG, and JPG. Moreover, they have different dimensions that varied from 120×120 to 1880×1200 . In the image compression field the lossy compression techniques are evaluated using: Subjective and Objective measures. The subjective evaluation is achieved by human observer who sentences the quality of the decompressed images.

A. Subjective Evaluation Experiments

The purpose of this subsection is prove efficiency of the proposed two hybrid techniques MDT-RIFD and MDT-JPEG from the subjective evaluation perspective. Fig. 5 shows the decompression process on two images from the image set of gray-scale 8-bit images. It is noticeable that the quality of the decompressed images using the two proposed techniques are very high and acceptable. Fig. 6 shows the decompression process on other two colored images from the image set. Once again, it is noticeable that the quality of the decompressed colored images using the two proposed techniques are very high and acceptable.

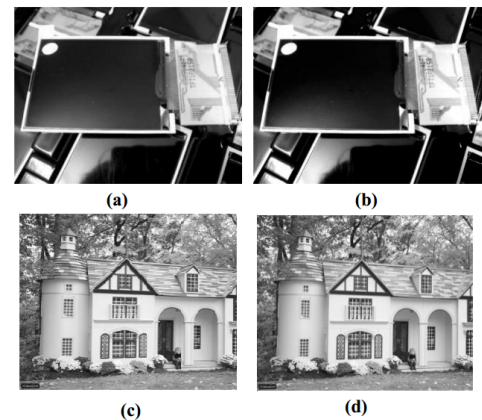


Fig. 5. Quality of Grayscale Image compression/Decompression using MDT-RIFD and MDT-JPEG: (a) Original Image-1, (b) De-compressed Image-1 using MDT-RIFD, (c) Original Image-2, (d) De-compressed Image-2 using MDT-JPEG.

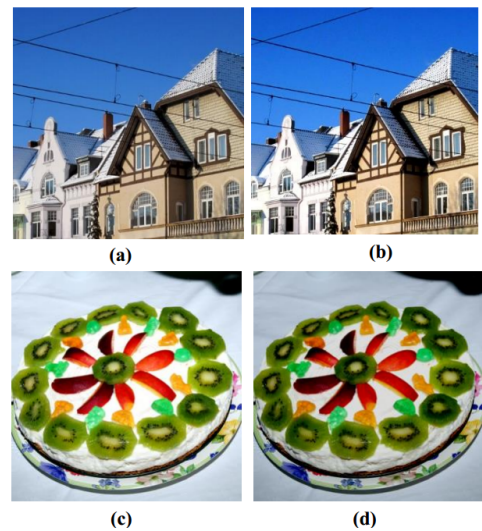


Fig. 6. Quality of Color(RGB) Image compression/Decompression using MDT-RIFD and MDT-JPEG: (a) Original Image-1, (b) De-compressed Image-1 using MDT-RIFD, (c) Original Image-2, (d) De-compressed Image-2 using MDT-JPEG.

B. Objective Evaluation Experiments

The objective evaluation measures (MSE, MAE, and PSNR as discussed in Section 3) were used in the objective experiments. The hybrid proposed techniques MDT-RIFD and MDT-

JPEG have been tested over all the image set, and then they were compared with the original RIFD and JPEG, respectively.

1) *Experiments on 8-bits images:* The purpose of the first part of the experiments is to test the hybrid proposed techniques MDT-RIFD and MDT-JPEG over the 8-bit images (labeled from g1 to g14). Table I compares RIFD and MDT-RIFD in terms of: MSE, MAE, PSNR, and Compression Ratio (CR). The compression ratio is computed using the following formula:

$$Cr = \frac{\text{compressed image size}}{\text{original image size}}$$

The results show the superiority of MDT-RIFD over the standard RIFD with all tested images based on the used measures and the compression ratio. The results of the used quality measures, MSE and MAE must be least as much as possible. At the other hand, PSNR is preferred to be larger. So, the hybrid MDT-RIFD achieved these goals with all tested images. The improvement percentage for each quality metric (MSE, MAE and PSNR) for each image will be computed based on the following formula:

$$\text{Enhancement} =$$

$$\frac{(MSE, MAE \text{ or } PSNR \text{ of } RIFD) - (MSE, MAE \text{ or } PSNR \text{ of } MDT - RIFD)}{(MSE, MAE, \text{ or } PSNR \text{ of } RIFD)}$$

Note: this formula was used to compare the achieved enhancement (in all experiments) using the proposed MDT-RIFD and MDT-JPEG with the classical ones in terms of MSE, MAE, and PSNR. For example the achieved enhancement of resulted MSE for image g3.png is computed as follows:

$$\text{Enhancement} =$$

$$\frac{(MSE \text{ using } RIFD) - (MSE \text{ using } MDT - RIFD)}{(MSE \text{ using } RIFD)}$$

$$\text{Enhancement for } (g3.png) = \frac{(8.34) - (6.39)}{(8.34)}$$

MSE Enhancement for g3.png = 0.23, which is the least achieved enhancement with all tested 8-bit images. At the other hand, the best achieved enhancement of MSE was with image g5.gif which is equal to 0.70. The remaining enhancement results for MAE and PSNR were as follows:

- MAE: from 21% (g10.tif) to 63% (g5.png)
- PSNR: from 3% (g3.png, g11.jpg, g14.jpg) to 14% (g5.png)

Fig. 7 is a graphical representation of Table I, which compares the results of RIFD and MDT-RIFD on 8-bit images. X-coordinate represents the image number, and Y-coordinate are: (a) MSE, (b) MAE, (c) PSNR, and (d) Compression Ratio results, respectively (X and Y coordinates in the rest figures are identical to Fig. 7). The experimental results show that MDT-RIFD enhances the quality of all decompressed 8-bit images. Moreover, it remains or enhances the compression ratio for 12 of 14 (of the tested images), which means that the proposed technique enhances the quality and the efficiency at the same time.

TABLE I. COMPARATIVE BETWEEN RIFD AND MDT-RIFD ON 8-BIT IMAGES

Image	MSE		MAE		PSNR		CR	
	RIFD	MDT-RIFD	RIFD	MDT-RIFD	RIFD	MDT-RIFD	RIFD	MDT-RIFD
g1.gif	9.93	4.35	3.1	1.33	38.19	41.78	0.48	0.46
g2.gif	8.53	6.52	2.63	1.9	38.86	40.02	0.54	0.51
g3.png	8.34	6.39	2.6	1.88	38.95	40.11	0.49	0.49
g4.gif	8.53	5.36	2.62	1.66	38.86	40.88	0.48	0.47
g5.png	11.87	3.61	3.21	1.18	37.42	42.59	0.49	0.41
g6.jpg	8.77	5.71	3.08	1.74	38.74	40.6	0.44	0.45
g7.tif	8.49	6.04	2.67	1.81	38.88	40.35	0.52	0.44
g8.png	7.76	5.23	2.63	1.57	39.27	40.98	0.43	0.46
g9.png	8.57	4.6	2.69	1.44	38.84	41.54	0.55	0.49
g10.tif	8.71	5.96	2.28	1.79	38.76	40.41	0.51	0.44
g11.jpg	8.45	6.3	3.24	1.86	38.89	40.17	0.55	0.53
g12.gif	8.43	6.02	3.24	1.81	38.9	40.37	0.53	0.51
g13.png	8.32	5.87	2.51	1.76	38.96	40.48	0.55	0.54
g14.jpg	8.41	6.5	2.53	1.9	38.92	40.04	0.58	0.53

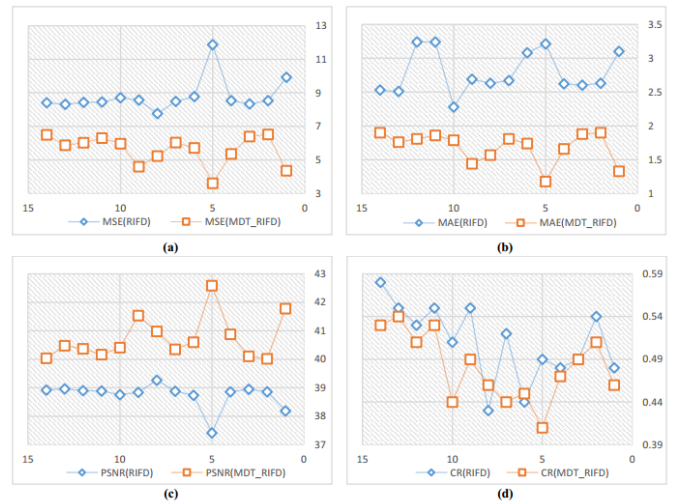


Fig. 7. Comparative between RIFD and MDT-RIFD on 8-bit Images:(a) MSE results, (b) MAE results, (c) PSNR results, (d) Compression Ratio Results.

Table II compares between JPEG and MDT-JPEG on the 8-bit image set. MDT-JPEG produced better results over the standard JPEG with all images according to the used measures and the compression ratio. The achieved enhancements were as follows:

- MSE: from 11% (g13.png) to 84% (g5.png)
- MAE: from 24% (g1.gif) to 97% (g10.tif)
- PSNR: from 1% (g11.jpg) to 24% (g5.png)

Fig. 8 is a graphical representation of Table II (it compares the results between JPEG and MDT-JPEG on 8-bit images). The curves show that MDT-JPEG enhances the quality of all decompressed 8-bit images. Moreover, it enhances the compression ratio with all images except a single image.

2) *Experiments on 16-bits images:* The purpose of the second part of the experiments is to test the hybrid proposed techniques MDT-RIFD and MDT-JPEG over the 16-bit images (numbered from 1 to 16). Table III compares RIFD and MDT-RIFD in terms of: MSE, MAE, PSNR, and Compression Ratio. MDT-RIFD gives better results in compare with the standard RIFD along all tested 16-bit images based on the used measures and the compression ratio. The achieved enhancements were as follows:

TABLE II. COMPARATIVE BETWEEN JPEG AND MDT-JPEG ON 8-BIT IMAGES

Image	MSE		MAE		PSNR		CR	
	JPEG	MDT-JPEG	JPEG	MDT-JPEG	JPEG	MDT-JPEG	JPEG	MDT-JPEG
g1.gif	82.24	60.48	12.12	9.21	29.01	30.35	0.33	0.38
g2.gif	255	86.06	143.73	6.04	24.1	28.82	0.36	0.42
g3.png	68.87	51.32	6.98	5.19	29.78	31.06	0.31	0.43
g4.gif	150.13	60.96	64.75	4.44	26.4	30.31	0.33	0.40
g5.png	186.57	30.76	33.11	2.89	25.46	33.28	0.25	0.29
g6.jpg	119.79	112.04	33.55	6.45	27.38	27.67	0.3	0.37
g7.tif	254.98	81.22	136	5.45	24.1	29.07	0.31	0.33
g8.png	254.43	114.38	164.69	6.92	24.11	27.58	0.37	0.39
g9.png	147.75	95.37	58.97	5.54	26.47	28.37	0.33	0.45
g10.tif	145.99	58.77	181.47	4.54	26.52	30.47	0.39	0.37
g11.jpg	103.53	97.19	29.24	6.68	28.01	28.29	0.39	0.43
g12.gif	117.24	93.46	13.14	6.32	27.47	28.46	0.40	0.48
g13.png	144.33	129.08	59.09	7.62	26.57	27.06	0.38	0.54
g14.jpg	116.31	101.33	37.28	8.88	27.51	28.11	0.34	0.51

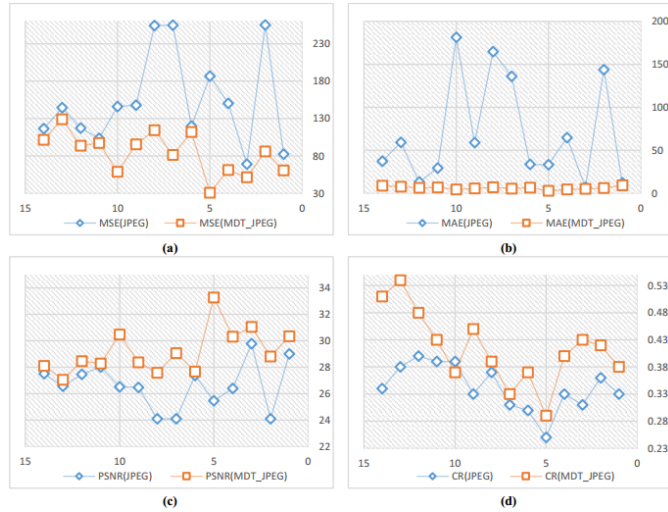


Fig. 8. Comparative between JPEG and MDT-JPEG on 8 bit Images: (a) MSE results, (b) MAE results, (c) PSNR results, (d) Compression Ratio Result.

- MSE: from 10% (15.png) to 43% (10.gif, 11.png, 13.tif, 14.tif)
- MAE: from 11% (15.png) to 69% (14.tif)
- PSNR: from 10% (15.png) to 43% (10.gif, 11.png, 13.tif, 14.tif)

Fig. 9 is a graphical representation of Table III (it compares the results of RIFD and MDT-RIFD on 16-bit images). The curves show that MDT-RIFD enhances the quality of all decompressed 16-bit images. Moreover, it enhances the compression ratio with all tested images.

TABLE III. COMPARATIVE BETWEEN RIFD AND MDT-RIFD ON 16-BIT IMAGES

Image	MSE		MAE		PSNR		CR	
	RIFD	MDT-RIFD	RIFD	MDT-RIFD	RIFD	MDT-RIFD	RIFD	MDT-RIFD
1.gif	21,869	18,065	125.96	103.17	47.64	53.76	0.35	0.41
2.gif	21,671	17,234	125.8	98.84	47.67	53.97	0.37	0.45
3.png	21,603	18,154	125.18	104.81	45.04	53.74	0.35	0.41
4.png	21,487	18,669	124.53	107.55	47.71	53.62	0.24	0.40
5.png	21,470	17,192	124.44	99.37	46.65	53.98	0.33	0.46
6.png	21,277	16,996	123.26	98.4	48.81	54.03	0.35	0.44
7.gif	21,053	16,457	122.15	95.29	45.13	54.17	0.35	0.42
8.png	21,859	17,876	126.43	103.9	37.05	53.81	0.31	0.39
9.png	21,490	18,997	124.85	109.35	45.06	53.54	0.31	0.38
10.gif	15,510	10,840	90.12	65.04	46.26	55.98	0.31	0.40
11.png	21,536	15,109	124.81	80.41	45.05	54.54	0.35	0.47
12.png	18,150	15,089	110.19	74.22	46.75	54.54	0.17	0.43
13.tif	20,678	14,447	117.69	72.78	45.2	54.73	0.35	0.44
14.tif	21,042	14,732	119.22	70.62	48.32	54.65	0.31	0.41
15.png	21,388	19,372	123.9	111.45	45.07	53.46	0.36	0.37
16.png	21,617	17,613	125.27	101.9	47.15	53.87	0.28	0.40

TABLE IV. COMPARATIVE BETWEEN JPEG AND MDT-JPEG ON 16-BIT IMAGES

Image	MSE		MAE		PSNR		CR	
	JPEG	MDT-JPEG	JPEG	MDT-JPEG	JPEG	MDT-JPEG	JPEG	MDT-JPEG
1.gif	32,193	22,404	18,819	680	51.25	52.83	0.25	0.40
2.gif	39,249	22,804	23,832	912	50.39	52.75	0.32	0.43
3.png	24,193	21,506	11,572	624	52.49	53	0.25	0.40
4.png	23,637	20,637	1261	592	52.59	53.18	0.29	0.43
5.png	32,696	26,696	3313	1391	51.18	52.07	0.35	0.46
6.png	28,447	23,447	6050	934	51.79	52.63	0.32	0.44
7.gif	39,181	32,179	7059	2306	50.4	51.25	0.41	0.34
8.png	21,480	19,480	3070	448	53.01	53.43	0.27	0.40
9.png	19,476	18,476	2875	364	53.43	53.66	0.27	0.40
10.gif	19,177	15,177	5577	716	53.5	54.52	0.28	0.40
11.png	27,717	23,717	11,604	1052	51.9	52.58	0.34	0.45
12.png	32,814	23,513	22,802	860	51.17	52.62	0.24	0.42
13.tif	30,882	23,882	6030	943	51.43	52.55	0.32	0.44
14.tif	25,024	21,024	3150	545	52.35	53.1	0.30	0.41
15.png	31,659	19,271	5610	379	51.32	53.48	0.26	0.40
16.png	27,698	21,698	1680	583	51.91	52.97	0.29	0.42

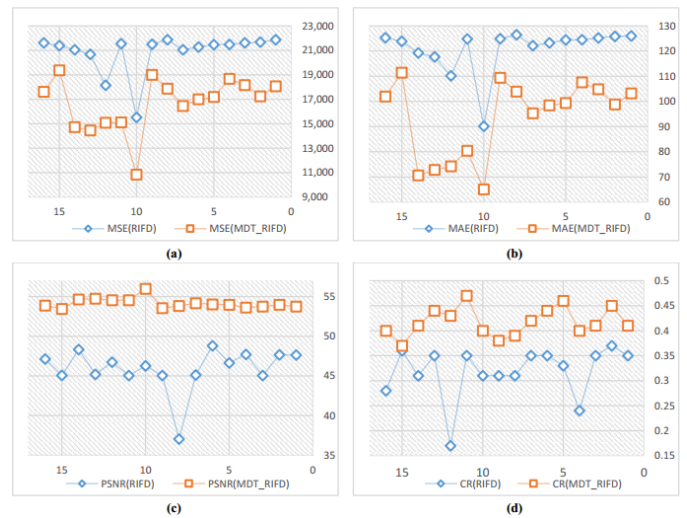


Fig. 9. Comparative between RIFD and MDT-RIFD on 16-bit Images: (a) MSE results, (b) MAE results, (c) PSNR results, (d) Compression Ratio Results.

Table IV compares JPEG and MDT-JPEG on the 16-bit image set in terms of: MSE, MAE, PSNR, and Compression Ratio. The results show the superiority of MDT-JPEG over the standard RIFD with all tested images based on the used measures and the compression ratio (except only one image). The achieved enhancements were as follows:

- MSE: from 11% (3.png) to 42% (2.gif)
- MAE: from 53% (4.png) to 96% (12.png)
- PSNR: from 1% (3.png, 4.png, 8.png, 11.png, 14.tif) to 5% (2.gif)

Fig. 10 is a graphical representation of Table IV, which compares the results of JPEG and MDT-JPEG on 16-bit images. The curves show that MDT-JPEG enhances the quality of all decompressed 16-bit images. Moreover, it enhances the compression ratio with all tested images except a single image.

3) Experiments on colored images: The purpose of the second part of the experiments is to test the hybrid proposed techniques MDT-RIFD and MDT-JPEG over the colored

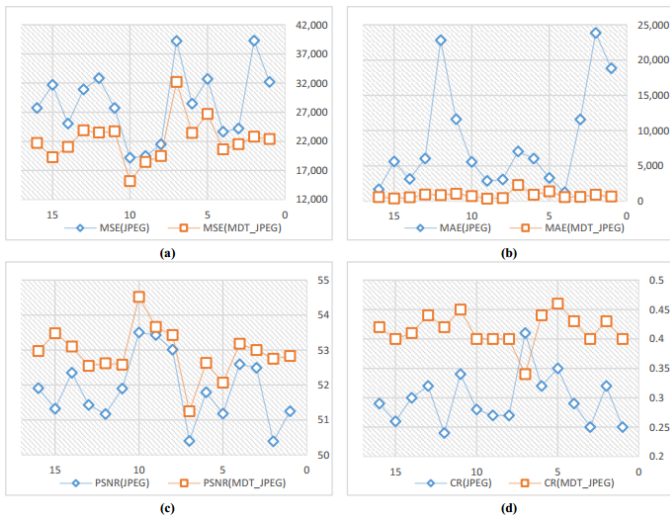


Fig. 10. Comparative between JPEG and MDT-JPEG on 16-bit Images: (a) MSE results, (b) MAE results, (c) PSNR results, (d) Compression Ratio Results.

TABLE V. COMPARATIVE BETWEEN RIFD AND MDT-RIFD ON COLOR (RGB) IMAGES

Image	MSE		MAE		PSNR		CR	
	RIFD	MDT-RIFD	RIFD	MDT-RIFD	RIFD	MDT-RIFD	RIFD	MDT-RIFD
c1.jpg	8.54	6.31	2.5	1.86	38.9	40.16	0.56	0.35
c2.png	8.95	3.95	2.62	1.33	38.7	42.2	0.45	0.26
c3.png	8.65	5.92	2.51	1.78	38.8	40.44	0.55	0.36
c4.jpg	8.32	2.79	2.46	1.1	39	43.7	0.43	0.23
c5.png	8.4	5.3	2.48	1.64	38.9	40.93	0.53	0.34
c6.jpg	8.56	5.51	2.51	1.68	38.8	40.75	0.53	0.33
c7.png	8.55	6.21	2.5	1.84	38.9	40.24	0.56	0.33
c8.jpg	8.39	5.65	2.48	1.73	39.9	40.65	0.52	0.29
c9.jpg	8.48	4.42	2.5	1.36	38.9	41.71	0.44	0.27
c10.tif	8.81	4.92	2.47	1.52	38.7	41.25	0.52	0.28
c11.png	8.46	6.34	2.48	1.86	38.9	40.15	0.58	0.44
c12.jpg	8.59	5.96	2.52	1.79	38.8	40.41	0.54	0.37
c13.tif	8.41	5.96	2.47	1.79	38.9	40.41	0.55	0.33
c14.png	8.4	6.22	2.45	1.85	38.9	40.23	0.38	0.25
c15.tif	9.14	3.73	2.59	1.31	38.6	42.45	0.48	0.24
c16.jpg	8.71	6.42	2.50	1.89	38.8	40.09	0.55	0.28

(RGB) images (labeled from c1 to c16). Table V compares RIFD and MDT-RIFD in terms of: MSE, MAE, PSNR, and Compression Ratio. The results show the superiority of MDT-RIFD over the standard RIFD with all tested colored (RGB) images based on the used measures and the compression ratio. The achieved enhancements were as follows:

- MSE: from 25% (c11.png) to 66% (c4.jpg)
- MAE: from 25% (c11.png) to 55% (c4.jpg)
- PSNR: from 3% (c1.jpg, c11.png, c14.png, c16.jpg) to 12% (c4.jpg)

Fig. 11 is a graphical representation of Table V, which compares the results of RIFD and MDT-RIFD on colored (RGB) images. The curves show significant quality enhancement of all decompressed colored (RGB) images using MDT-RIFD. Moreover, it enhances the compression ratio for all tested images. Table VI compares JPEG and MDT-JPEG on the colored (RGB) image set in terms of: MSE, MAE, PSNR, and Compression Ratio. The results show the superiority of MDT-JPEG over the standard JPEG with all tested images based on the used measures. The achieved enhancements were as follows:

TABLE VI. COMPARATIVE BETWEEN JPEG AND MDT-JPEG ON COLOR (RGB) IMAGES

Image	MSE		MAE		PSNR		CR	
	JPEG	MDT-JPEG	JPEG	MDT-JPEG	JPEG	MDT-JPEG	JPEG	MDT-JPEG
c1.jpg	119.53	9.66	8.64	1.26	27.39	38.32	0.3	0.26
c2.png	185.84	5.71	14.12	0.99	25.47	40.6	0.32	0.54
c3.png	120.98	9.98	7.21	1.21	27.34	38.17	0.22	0.14
c4.jpg	98.96	1.96	8.61	0.61	28.21	45.24	0.14	0.46
c5.png	172.56	9.56	14.98	1.22	25.8	38.36	0.49	0.46
c6.jpg	221.79	11.32	11.17	1.48	24.71	37.63	0.46	0.54
c7.png	144.24	14.24	12.46	1.81	26.57	36.63	0.57	0.33
c8.jpg	160.2	6.36	13.73	0.95	26.12	40.13	0.37	0.28
c9.jpg	290.66	4.25	15.41	0.75	23.53	41.88	0.27	0.35
c10.tif	91.88	8.88	7.29	1.29	28.53	36.68	0.38	0.84
c11.png	120.14	26.25	11.39	2.69	27.37	33.97	0.24	0.43
c12.jpg	120.5	10.12	8	1.42	27.35	38.11	0.44	0.49
c13.tif	95.38	9.55	8.99	1.21	28.37	38.36	0.55	0.15
c14.png	173.28	4.66	18.23	1.04	25.78	41.48	0.18	0.18
c15.tif	94.56	1.71	8.48	0.48	28.41	45.84	0.36	0.31
c16.jpg	274.04	8.85	13.55	1.34	23.79	38.7	0.39	0.31

- MSE: from 78% (c11.png) to 99% (c9.jpg)
- MAE: from 76% (c11.png) to 95% (c9.jpg)
- PSNR: from 24% (c11.png) to 78% (c9.jpg)

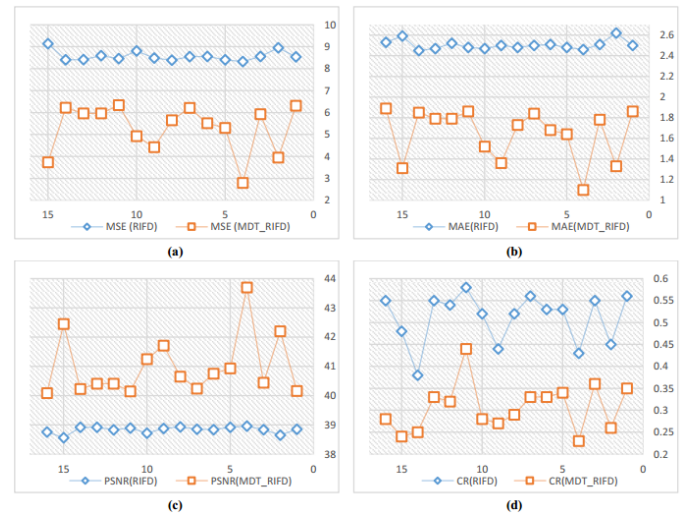


Fig. 11. Comparative between RIFD and MDT-RIFD on color(RGB) Images: (a) MSE results, (b) MAE results, (c) PSNR results, (d) Compression Ratio Results.

Fig. 12 is a graphical representation of Table VI, which compares the results of JPEG and MDT-JPEG on colored (RGB) images. The curves show that MDT-JPEG enhances the quality of all decompressed colored (RGB) images with significant percentage enhancement. However, it only enhances the compression ratio for 50% of the tested images.

VI. CONCLUSION

This paper presented lossless pre-processing steps that could be generalized to be implemented before any lossy technique and was performed on various images that varied in types, dimension, and bit-depth. Two distinct lossy techniques were chosen RIFD and JPEG to be implemented with the proposed technique. These lossy techniques are vary from each other since RIFD is a novel/new compression technique that uses simple steps of rounding and dividing the pixels while JPEG is a well-known and widely used as a lossy

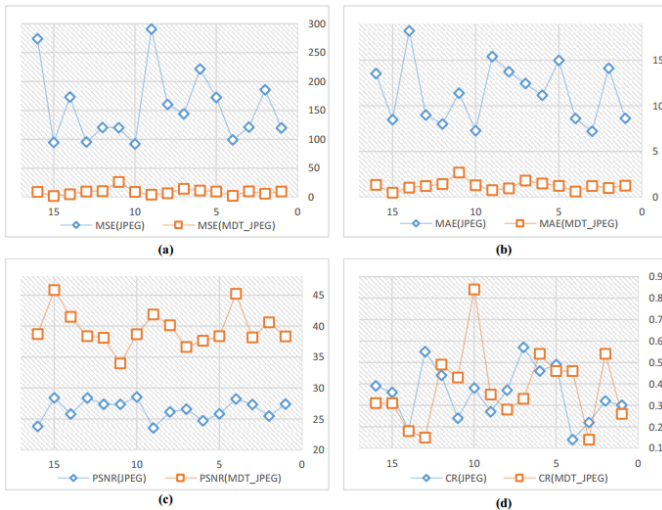


Fig. 12. Comparative between JPEG and MDT-JPEG on color (RGB) Images: (a) MSE results, (b) MAE results, (c) PSNR results, (d) Compression Ratio Results.

compression method which uses a complicated linear equations with discrete cosine transformation. The purpose of using these lossy techniques is to prove that the proposed technique can be applied along the most of the available and future lossy techniques. The results showed the superiority of MDT-RIFD and MDT-JPEG (over the standard RIFD and JPEG, respectively) in terms of the objective quality evaluation metrics such as: MSE, MAE, and PSNR. In the other hand, the hybrid techniques enhance the compression ratio with the

most images. The achieved enhancements were varied from one image to another regarding the image characteristics, and the used lossy technique.

REFERENCES

- [1] V. Hlavac, "Fundamentals of image processing," *Optical and Digital Image Processing: Fundamentals and Applications*, pp. 71–96, 2011.
- [2] I. T. Young, J. J. Gerbrands, and L. J. Van Vliet, *Fundamentals of image processing*. Delft University of Technology Delft, 1998.
- [3] M. M. H. Chowdhury and A. Khatun, "Image compression using discrete wavelet transform," *IJCSI International Journal of Computer Science Issues*, vol. 9, no. 4, pp. 327–330, 2012.
- [4] M. Otair and F. Shehadeh, "Research article lossy image compression by rounding the intensity followed by dividing (rifd)," 2016.
- [5] F. A. Jassim and H. E. Qassim, "Five modulus method for image compression," *arXiv preprint arXiv:1211.4591*, 2012.
- [6] G. Vijayvargiya, S. Silakari, and R. Pandey, "A survey: various techniques of image compression," *arXiv preprint arXiv:1311.6877*, 2013.
- [7] N. Zhou, A. Zhang, F. Zheng, and L. Gong, "Novel image compression-encryption hybrid algorithm based on key-controlled measurement matrix in compressive sensing," *Optics & Laser Technology*, vol. 62, pp. 152–160, 2014.
- [8] F. Huang, J. Huang, and Y.-Q. Shi, "New channel selection rule for jpeg steganography," *IEEE Transactions on Information Forensics and Security*, vol. 7, no. 4, pp. 1181–1191, 2012.
- [9] T. Samajdar and M. I. Quraishi, "Analysis and evaluation of image quality metrics," in *Information Systems Design and Intelligent Applications*. Springer, 2015, pp. 369–378.
- [10] M. Pedersen and J. Y. Hardeberg, "Full-reference image quality metrics: Classification and evaluation," *Foundations and Trends® in Computer Graphics and Vision*, vol. 7, no. 1, pp. 1–80, 2012.
- [11] P. Kaushik and Y. Sharma, "Comparison of different image enhancement techniques based upon psnr & mse," *International Journal of Applied Engineering Research*, vol. 7, no. 11, pp. 2010–2014, 2012.

The Impact of Quantum Computing on Present Cryptography

Vasileios Mavroeidis, Kamer Vishi, Mateusz D. Zych, Audun Jøsang
Department of Informatics, University of Oslo, Norway

Abstract—The aim of this paper is to elucidate the implications of quantum computing in present cryptography and to introduce the reader to basic post-quantum algorithms. In particular the reader can delve into the following subjects: present cryptographic schemes (symmetric and asymmetric), differences between quantum and classical computing, challenges in quantum computing, quantum algorithms (Shor's and Grover's), public key encryption schemes affected, symmetric schemes affected, the impact on hash functions, and post quantum cryptography. Specifically, the section of Post-Quantum Cryptography deals with different quantum key distribution methods and mathematical-based solutions, such as the BB84 protocol, lattice-based cryptography, multivariate-based cryptography, hash-based signatures and code-based cryptography.

Keywords—Quantum computers; post-quantum cryptography; Shor's algorithm; Grover's algorithm; asymmetric cryptography; symmetric cryptography

I. INTRODUCTION

There is no doubt that advancements in technology and particularly electronic communications have become one of the main technological pillars of the modern age. The need for confidentiality, integrity, authenticity, and non-repudiation in data transmission and data storage makes the science of cryptography one of the most important disciplines in information technology. Cryptography, etymologically derived from the Greek words hidden and writing, is the process of securing data in transit or stored by third party adversaries. There are two kinds of cryptosystems; symmetric and asymmetric.

Quantum computing theory firstly introduced as a concept in 1982 by Richard Feynman, has been researched extensively and is considered the destructor of the present modern asymmetric cryptography. In addition, it is a fact that symmetric cryptography can also be affected by specific quantum algorithms; however, its security can be increased with the use of larger key spaces. Furthermore, algorithms that can break the present asymmetric cryptoschemes whose security is based on the difficulty of factorizing large prime numbers and the discrete logarithm problem have been introduced. It appears that even elliptic curve cryptography which is considered presently the most secure and efficient scheme is weak against quantum computers. Consequently, a need for cryptographic algorithms robust to quantum computations arose.

The rest of the paper deals initially with the analysis of symmetric cryptography, asymmetric cryptography and hash functions. Specifically, an emphasis is given on algorithms that take advantage of the difficulty to factorize large prime numbers, as well as the discrete logarithm problem. We move on by giving an introduction to quantum mechanics and the challenge of building a true quantum computer. Furthermore,

we introduce two important quantum algorithms that can have a huge impact in asymmetric cryptography and less in symmetric, namely, Shor's algorithm and Grover's algorithm respectively. Finally, post-quantum cryptography is presented. Particularly, an emphasis is given on the analysis of quantum key distribution and some mathematical based solutions such as lattice-based cryptography, multivariate-based cryptography, hash-based signatures, and code-based cryptography.

II. PRESENT CRYPTOGRAPHY

In this chapter we explain briefly the role of symmetric algorithms, asymmetric algorithms and hash functions in modern cryptography. We analyze the difficulty of factorizing large numbers, as well as the discrete logarithm problem which is the basis of strong asymmetric ciphers.

A. Symmetric Cryptography

In symmetric cryptography, the sender and the receiver use the same secret key and the same cryptographic algorithm to encrypt and decrypt data. For example, Alice can encrypt a plaintext message using her shared secret key and Bob can decrypt the message using the same cryptographic algorithm Alice used and the same shared secret key. The key needs to be kept secret, meaning that only Alice and Bob should know it; therefore, an efficient way for exchanging secret keys over public networks is demanded. Asymmetric cryptography was introduced to solve the problem of key distribution in symmetric cryptography. Popular symmetric algorithms include the advanced encryption standard (AES) and the data encryption standard (3DES).

B. Asymmetric Cryptography

Asymmetric cryptography or public key cryptography (PKC) is a form of encryption where the keys come in pairs. Each party should have its own private and public key. For instance, if Bob wants to encrypt a message, Alice would send her public key to Bob and then Bob can encrypt the message with Alice's public key. Next, Bob would transmit the encrypted message to Alice who is able to decrypt the message with her private key. Thus, we encrypt the message with a public key and only the person who owns the private key can decrypt the message.

Asymmetric cryptography additionally is used for digital signatures. For example, Alice can sign a document digitally with her private key and Bob can verify the signature with Alice's known public key. The security of PKC rests on computational problems such as the difficulty of factorizing large prime numbers and the discrete logarithm problem. Such

kind of algorithms are called one-way functions because they are easy to compute in one direction but the inversion is difficult [1].

1) *Factorization Problem - RSA Cryptosystem*: One of the most important public-key schemes is RSA invented by Ronald Rivest, Adi Shamir, and Leonard Adleman in 1977. RSA exploits the difficulty of factorizing bi-prime numbers. According to Paar and Pelzl [2], RSA and in general asymmetric algorithms are not meant to replace symmetric algorithms because they are computationally costly. RSA is mainly used for secure key exchange between end nodes and often used together with symmetric algorithms such as AES, where the symmetric algorithm does the actual data encryption and decryption. Kirsch [3] stated that RSA is theoretically vulnerable if a fast factorizing algorithm is introduced or huge increase in computation power can exist. The latter can be achieved with the use of quantum mechanics on computers, known as quantum-computers.

2) *Discrete Logarithm Problem (DLP)*: Asymmetric cryptographic systems such as Diffie-Hellman (DH) and Elliptic Curve Cryptography (ECC) are based on DLP. The difficulty of breaking these cryptosystems is based on the difficulty in determining the integer r such that $g^r = x \pmod p$. The integer r is called the discrete logarithm problem of x to the base g , and we can write it as $r = \log_g x \pmod p$. The discrete logarithm problem is a very hard problem to compute if the parameters are large enough.

Diffie-Hellman is an asymmetric cipher that uses the aforementioned property to transmit keys securely over a public network. Recently, keys larger or equal to 2048 bits are recommended for secure key exchange. In addition, another family of public key algorithms known as Elliptic Curve Cryptography is extensively used. ECC provides the same level of security as RSA and DLP systems with shorter key operands which makes it convenient to be used by systems of low computational resources. ECC uses a pair (x, y) that fits into the equation $y^2 = x^3 + ax + b \pmod p$ together with an imaginary point Θ (theta) at infinity, where $a, b \in \mathbb{Z}_p$ and $4a^3 + 27b^2 \neq 0 \pmod p$ [2]. ECC needs a cyclic Group G and the primitive elements we use, or pair elements, to be of order G . ECC is considered the most secure and efficient asymmetric cryptosystem, but this tends to change with the introduction of quantum computers as it is explained in the next sections.

III. QUANTUM COMPUTING VS CLASSICAL COMPUTING

In 1982, Richard Feynman came up with the idea of *quantum computer*, a computer that uses the effects of quantum mechanics to its advantage. Quantum mechanics is related to microscopic physical phenomena and their strange behavior. In a traditional computer the fundamental blocks are called bits and can be observed only in two states; 0 and 1. Quantum computers instead use quantum bits also usually referred as *qubits* [4]. In a sense, qubits are particles that can exist not only in the 0 and 1 state but in both simultaneously, known as superposition. A particle collapses into one of these states when it is inspected. Quantum computers take advantage of this property mentioned to solve complex problems. An operation on a qubit in superposition acts on both values at the same time. Another physical phenomenon used in quantum computing is quantum

entanglement. When two qubits are entangled their quantum state can no longer be described independently of each other, but as a single object with four different states. In addition, if one of the two qubits state change the entangled qubit will change too regardless of the distance between them. This leads to true parallel processing power [5]. The combination of the aforementioned phenomena result in exponential increase in the number of values that can be processed in one operation, when the number of entanglement qubits increase. Therefore, a n -qubit quantum computer can process 2^n operations in parallel.

Two kinds of quantum computers exists; universal and non-universal. The main difference between the two is that universal quantum computers are developed to perform any given task, whereas non-universal quantum computers are developed for a given purpose (e.g., optimization of machine learning algorithms). Examples are, D-Wave's 2000+ qubits non-universal quantum computer [6] and IBM's 17 qubits universal quantum computer with proper error correction. IBM's quantum computer is currently the state of the art of universal quantum computers [7]. Both D-Wave and IBM have quantum computers accessible online for research purposes. Additionally, in October 2017, Intel in collaboration with QuTech announced their 17-qubits universal quantum computer [7].

Bone and Castro [8] stated that a quantum computer is completely different in design than a classical computer that uses the traditional transistors and diodes. Researchers have experimented with many different designs such as quantum dots which are basically electrons being in a superposition state, and computing liquids. Besides, they remarked that quantum computers can show their superiority over the classical computers only when used with algorithms that exploit the power of quantum parallelism. For example, a quantum computer would not be any faster than a traditional computer in multiplication.

A. Challenges in Quantum Computing

There are many challenges in quantum computing that many researchers are working on.

- Quantum algorithms are mainly probabilistic. This means that in one operation a quantum computer returns many solutions where only one is the correct. This trial and error for measuring and verifying the correct answer weakens the advantage of quantum computing speed [3].
- Qubits are susceptible to errors. They can be affected by heat, noise in the environment, as well as stray electromagnetic couplings. Classical computers are susceptible to bit-flips (a zero can become one and vice versa). Qubits suffer from bit-flips as well as phase errors. Direct inspection for errors should be avoided as it will cause the value to collapse, leaving its superposition state.
- Another challenge is the difficulty of coherence. Qubits can retain their quantum state for a short period of time. Researchers at the University of New South Wales in Australia have created two different types

of qubits (Phosphorous atom and an Artificial atom) and by putting them into a tiny silicon (*silicon 28*) they were able to eliminate the magnetic noise that makes them prone to errors. Additionally, they stated that the Phosphorous atom has 99.99% accuracy which accounts for 1 error every 10,000 quantum operations [9]. Their qubits can remain in superposition for a total of 35 seconds which is considered a world record [10]. Moreover, to achieve long coherence qubits need not only to be isolated from the external world but to be kept in temperatures reaching the absolute zero. However, this isolation makes it difficult to control them without contributing additional noise [3].

IBM in 2017, introduced the definition of *Quantum Volume*. Quantum volume is a metric to measure how powerful a quantum computer is based on how many qubits it has, how good is the error correction on these qubits, and the number of operations that can be done in parallel. Increase in the number of qubit does not improve a quantum computer if the error rate is high. However, improving the error rate would result in a more powerful quantum computer [11].

IV. CRYPTOSYSTEMS VULNERABLE TO QUANTUM ALGORITHMS

This section discusses the impact of quantum algorithms on present cryptography and gives an introduction to Shor's algorithm and Grover's algorithm. Note that Shor's algorithm explained in the following subsection makes the algorithms that rely on the difficulty of factorizing or computing discrete logarithms vulnerable.

Cryptography plays an important role in every electronic communication system today. For example the security of emails, passwords, financial transactions, or even electronic voting systems require the same security objectives such as confidentiality and integrity [12]. Cryptography makes sure that only parties that have exchanged keys can read the encrypted message (also called authentic parties). Quantum computers threaten the main goal of every secure and authentic communication because they are able to do computations that classical (conventional) computers cannot. Consequently, quantum computers can break the cryptographic keys quickly by calculating or searching exhaustively all secret keys, allowing an eavesdropper to intercept the communication channel between authentic parties (sender/receiver). This task is considered to be computational infeasible by a conventional computer [13].

According to NIST, quantum computers will bring the end of the current public key encryption schemes [14]. Table I adapted from NIST shows the impact of quantum computing on present cryptographic schemes.

A. Shor's Algorithm in Asymmetric Cryptography

In 1994, the mathematician Peter Shor in his paper "Algorithms for Quantum Computation: Discrete Logarithms and Factoring" [15], proved that factorizing large integers would change fundamentally with a quantum computer.

Shor's algorithm can make modern asymmetric cryptography collapse since it is based on large prime integer factorization or the discrete logarithm problem. To understand

how Shor's algorithm factorizes large prime numbers we use the following example. We want to find the prime factors of number 15. To do so, we need a 4-qubit register. We can visualize a 4-qubit register as a normal 4-bit register of a traditional computer. Number 15 in binary is 1111, so a 4-qubit register is enough to accommodate (calculate) the prime factorization of this number. According to Bone and Castro [8], a calculation performed on the register can be thought as computations done in parallel for every possible value that the register can take (0-15). This is also the only step needed to be performed on a quantum computer.

The algorithm does the following:

- $n = 15$, is the number we want to factorize
- $x =$ random number such as $1 < x < n - 1$
- x is raised to the power contained in the register (every possible state) and then divided by n
The remainder from this operation is stored in a second 4-qubit register. The second register now contains the superposition results. Let's assume that $x = 2$ which is larger than 1 and smaller than 14.
- If we raise x to the powers of the 4-qubit register which is a maximum of 15 and divide by 15, the remainders are shown in Table II.

What we observe in the results is a repeating sequence of 4 numbers (1,2,4,8). We can confidently say then that $f = 4$ which is the sequence when $x = 2$ and $n = 15$. The value f can be used to calculate a possible factor with the following equation:

$$\text{Possible factor: } P = x^{f/2} - 1$$

In case we get a result which is not a prime number we repeat the calculation with different f values.

Shor's algorithm can be used additionally for computing discrete logarithm problems. Vazirani [16] explored in detail the methodology of Shor's algorithm and showed that by starting from a random superposition state of two integers, and by performing a series of Fourier transformations, a new superposition can be set-up to give us with high probability two integers that satisfy an equation. By using this equation we can calculate the value r which is the unknown "exponent" in the DLP.

B. Grover's algorithm in Symmetric Cryptography

Lov Grover created an algorithm that uses quantum computers to search unsorted databases [17]. The algorithm can find a specific entry in an unsorted database of N entries in \sqrt{N} searches. In comparison, a conventional computer would need $N/2$ searches to find the same entry. Bone and Castro [8] remarked the impact of a possible application of Grover's algorithm to crack Data Encryption Standard (DES), which relies its security on a 56-bit key. The authors remarked that the algorithm needs only 185 searches to find the key.

Currently, to prevent password cracking we increase the number of key bits (larger key space); as a result, the number of searches needed to crack a password increases exponentially. Buchmann et al. [18] stated that Grover's algorithm have some applications to symmetric cryptosystems but it is not as fast as Shor's algorithm.

TABLE I. IMPACT ANALYSIS OF QUANTUM COMPUTING ON ENCRYPTION SCHEMES (ADAPTED FROM [14])

Cryptographic Algorithm	Type	Purpose	Impact From Quantum Computer
AES-256	Symmetric key	Encryption	Secure
SHA-256, SHA-3	–	Hash functions	Secure
RSA	Public key	Signatures, key establishment	No longer secure
ECDSA, ECDH (Elliptic Curve Cryptography)	Public key	Signatures, key exchange	No longer secure
DSA (Finite Field Cryptography)	Public key	Signatures, key exchange	No longer secure

TABLE II. 4-QUBIT REGISTERS WITH REMAINDERS

Register 1:	0	1	2	3	4	5	6	7	8	9	10	11	12	13	14	15
Register 2:	1	2	4	8	1	2	4	8	1	2	4	8	1	2	4	8

C. Asymmetric Encryption Schemes Affected

All public key algorithms used today are based on two mathematical problems, the aforementioned factorization of large numbers (e.g., RSA) and the calculation of discrete logarithms (e.g., DSA signatures and ElGamal encryption). Both have similar mathematical structure and can be broken with Shor’s algorithm rapidly. Recent algorithms based on elliptic curves (such as ECDSA) use a modification of the discrete logarithm problem that makes them equally weak against quantum computers. Kirsch and Chow [3] mentioned that a modified Shor’s algorithm can be used to decrypt data encrypted with ECC. In addition, they emphasized that the relatively small key space of ECC compared to RSA makes it easier to be broken by quantum computers. Furthermore, Proos and Zalka [19] explained that 160-bit elliptic curves could be broken by a 1000-qubit quantum computer, while factorizing 1024-bit RSA would require a 2000-qubit quantum computer. The number of qubits needed to break a cryptosystem is relative to the algorithm proposed. In addition, they show in some detail how to use Shor’s algorithm to break ECC over GF(p).

On the other hand, Grover’s algorithm is a threat only to some symmetric cryptographic schemes. NIST [14] points out that if the key sizes are sufficient, symmetric cryptographic schemes (specifically the Advanced Encryption Standard-AES) are resistant to quantum computers. Another aspect to be taken into consideration is the robustness of algorithms against quantum computing attacks also known as quantum cryptanalysis.

In Table III, a comparison of classical and quantum security levels for the most used cryptographic schemes is presented.

D. Symmetric Encryption Schemes Affected

For symmetric cryptography quantum computing is considered a minor threat. The only known threat is Grover’s algorithm that offers a square root speed-up over classical brute force algorithms. For example, for a n-bit cipher the quantum computer operates on $(\sqrt{2^n} = 2^{n/2})$. In practice, this means that a symmetric cipher with a key length of 128-bit (e.g., AES-128) would provide a security level of 64-bit. We recall here that security level of 80-bit is considered secure. The Advanced Encryption Standard (AES) is considered to be one of the cryptographic primitives that is resilient in quantum computations, but only when is used with key sizes of 192 or 256 bits. Another indicator of the security of AES in the post-quantum era is that NSA (The National Security Agency)

allows AES cipher to secure (protect) classified information for security levels, SECRET and TOP SECRET, but only with key sizes of 192 and 256 bits [20].

TABLE III. COMPARISON OF CLASSICAL AND QUANTUM SECURITY LEVELS FOR THE MOST USED CRYPTOGRAPHIC SCHEMES

Crypto Scheme	Key Size	Effective Key Strength/Security Level (in bits)	
		Classical Computing	Quantum Computing
RSA-1024	1024	80	0
RSA-2048	2048	112	0
ECC-256	256	128	0
ECC-384	384	256	0
AES-128	128	128	64
AES-256	256	256	128

E. Hash Functions

The family of hash functions suffer from a similar problem as symmetric ciphers since their security depends on a fixed output length. Grover’s algorithm can be utilized to find a collision in a hash function in square root steps of its original length (it is like searching an unsorted database). In addition, it has been proved that it is possible to combine Grover’s algorithm with the birthday paradox. Brassard et al. [21] described a quantum birthday attack. By creating a table of size $\sqrt[3]{N}$ and utilizing Grover’s algorithm to find a collision an attack is said to work effectively. This means that to provide a $b - bit$ security level against Grover’s quantum algorithm a hash function must provide at least a $3b - bit$ output. As a result, many of the present hash algorithms are disqualified for use in the quantum era. However, both SHA-2 and SHA-3 with longer outputs, remain quantum resistant.

V. POST-QUANTUM CRYPTOGRAPHY

The goal of post-quantum cryptography (also known as quantum-resistant cryptography) is to develop cryptographic systems that are secure against both quantum and conventional computers and can interoperate with existing communication protocols and networks [14]. Many post-quantum public key candidates are actively investigated the last years. In 2016, NIST announced a call for proposals of algorithms that are believed to be quantum resilient with a deadline in November 2017. In January 2018, NIST published the results of the first round. In total 82 algorithms were proposed from which 59 are encryption or key exchange schemes and 23 are signature schemes. After 3 to 5 years of analysis NIST will report the findings and prepare a draft of standards [22]. Furthermore, the National Security Agency (NSA) has already announced

plans to migrate their cryptographic standards to post-quantum cryptography [23].

The cryptographic algorithms presented in this section do not rely on the hidden subgroup problem (HSP) such as factorizing integers or computing discrete logarithms, but different complex mathematical problems.

A. Quantum Key Distribution

Quantum Key Distribution (QKD) addresses the challenge of securely exchanging a cryptographic key between two parties over an insecure channel. QKD relies on the fundamental characteristics of quantum mechanics which are invulnerable to increasing computational power, and may be performed by using the quantum properties of light, lasers, fibre-optics as well as free space transmission technology. QKD was first introduced in 1984 when Charles Bennett and Gilles Brassard developed their BB84 protocol [24, 25]. Research has led to the development of many new QKD protocols exploiting mainly two different properties that are described right below.

Prepare-and-measure (P&M) protocols use the Heisenberg Uncertainty principle [26] stating that the measuring act of a quantum state changes that state in some way. This makes it difficult for an attacker to eavesdrop on a communication channel without leaving any trace. In case of eavesdropping the legitimate exchange parties are able to discard the corrupted information as well as to calculate the amount of information that has been intercepted [27]. This property was exploited in BB84.

Entanglement based (EB) protocols use pairs of entangled objects which are shared between two parties. As explained in III, entanglement is a quantum physical phenomenon which links two or more objects together in such a way that afterwards they have to be considered as one object. Additionally, measuring one of the objects would affect the other as well. In practice when an entangled pair of objects is shared between two legitimate exchange parties anyone intercepting either object would alter the overall system. This would reveal the presence of an attacker along with the amount of information that the attacker retrieved. This property was exploited in E91 [28] protocol.

Both of the above-mentioned approaches are additionally divided into three families; discrete variable coding, continuous variable coding and distributed phase reference coding. The main difference between these families is the type of detecting system used. Both discrete variable coding and distributed phase reference coding use photon counting and post-select the events in which a detection has effectively taken place [29]. Continuous variable coding uses homodyne detection [29] which is a comparison of modulation of a single frequency of an oscillating signal with a standard oscillation.

A concise list of QKD protocols for the aforementioned families is presented below.

Discrete variable coding protocols:

- BB84 [24, 25] - the first QKD protocol that uses four non-orthogonal polarized single photon states or low-intensity light pulses. A detailed description of this protocol is given below.

- BBM [30] - is an entanglement based version of BB84.
- E91 [28] - is based on the *gedanken experiment* [31] and the generalized Bell's theorem [32]. In addition, it can be considered an extension of Bennett and Brassard's (authors of BB84) original idea.
- SARG04 [33, 34] - is similar to BB84 but instead of using the state to code the bits, the bases are used. SARG04 is more robust than BB84 against the photon number splitting (PNS) attack.
- Six state protocol [35–37] - is a version of BB84 that uses a six-state polarization scheme on three orthogonal bases.
- Six state version of the SARG04 coding [38].
- Singapore protocol [39] - is a tomographic protocol that is more efficient than the Six state protocol.
- B92 protocol [40] - two non-orthogonal quantum states using low-intensity coherent light pulses.

Continuous variable coding protocols:

- Gaussian protocols
 - Continuous variable version of BB84 [41]
 - Continuous variable using coherent states [42]
 - Coherent state QKD protocol [43] - based on simultaneous quadrature measurements.
 - Coherent state QKD protocol [44] - based on the generation and transmission of random distributions of coherent or squeezed states.
- Discrete-modulation protocols
 - First continuous variable protocol based on coherent states instead of squeezed states [45].

Distributed phase reference coding protocols:

- Differential Phase Shift (DPS) Quantum Key Distribution (QKD) protocol [46, 47] - uses a single photon in superposition state of three basis kets, where the phase difference between two sequential pulses carries bit information.
- Coherent One Way (COW) protocol [48, 49] - the key is obtained by a time-of-arrival measurement on the data line (raw key). Additionally, an interferometer is built on a monitoring line, allowing to monitor the presence of an intruder. A prototype was presented in 2008 [50].

Discrete variable coding protocols are the most widely implemented, whereas the continuous variable and distributed phase reference coding protocols are mainly concerned with overcoming practical limitations of experiments.

1) *BB84 protocol*: BB84 is the first quantum cryptographic protocol (QKD scheme) which is still in use today. According to Mayers [51] BB84 is *provable secure*, explaining that a secure key sequence can be generated whenever the channel bit error rate is less than about 7% [52]. BB84 exploits the polarization of light for creating random sequence of qubits (key) that are transmitted through a quantum channel.

BB84 uses two different bases, base 1 is polarized 0° (horizontal) or 90° (vertical) with 0° equal to 0 and 90° equal to 1. Base 2 is polarized 45° or 135° with 45° equal to 1 and 135° equal to 0. Alice begins by sending a photon in one of the two bases having a value of 0 or 1. Both the base and the value should be chosen randomly. Next, Bob selects the base 1 or 2 and measures a value without knowing which base Alice has used. The key exchange process continues until they have generated enough bits. Furthermore, Bob tells Alice the sequence of the bases he used but not the values he measured and Alice informs Bob whether the chosen bases were right or wrong. If the base is right, Alice and Bob have equal bits, whereas if it is wrong the bits are discarded. In addition, any bits that did not make it to the destination are discarded by Alice. Now Alice can use the key that they just exchanged to encode the message and send it to Bob. BB84 is illustrated visually in Fig. 1.

Worthy to mentioning is that this method of communication was broken by Lydersen et al. in 2010 [53]. Their experiment proved that although BB84 is *provable secure* the actual hardware implemented is not. The authors managed to inspect the secret key without the receiver noticing it by blinding the APD-based detector (avalanche photodiode).

Yuan et al. [54] proposed improvements to mitigate blinding attacks, such as monitoring the photocurrent for anomalously high values. Lydersen et al. [55] after taking into consideration the improvements of Yuan et al. [54] succeeded again to reveal the secret key without leaving any traces.

2) *Photon Number Splitting Attack*: The crucial issue in quantum key distribution is its security. In addition to noise in the quantum channel, the equipment is impractical to produce and detect single photons. Therefore, in practice, laser pulses are used. Producing multiple photons opens up a new attack known as Photon Number Splitting (PNS) attack. In PNS attack, an attacker (Eve) deterministically splits a photon off of the signal and stores it in a quantum memory which does not modify the polarisation of the photons. The remaining photons are allowed to pass and are transmitted to the receiver (Bob). Next, Bob measures the photons and the sender (Alice) has to reveal the encoding bases. Eve will then be able to measure all captured photons on a correct bases. Consequently, Eve will obtain information about the secret key from all signals containing more than one photon without being noticed [57].

Different solutions have been proposed for mitigating PNS attacks. The most promising solution developed by Lo et al. [58] uses decoy states to detect PNS attacks. This is achieved by sending randomly laser pulses with a lower average photon number. Thereafter, Eve cannot distinguish between decoyed signals and non-decoyed signals. This method works for both single and multi-photon pulses [59].

B. Mathematically-based Solutions

There are many alternative mathematical problems to those used in RSA, DH and ECDSA that have already been implemented as public key cryptographic schemes, and for which the Hidden Subgroup Problem (HSP) [60] does not apply; therefore, they appear to be quantum resistant.

The most researched mathematical-based implementations are the following:

- Lattice-based cryptography [61]
- Multivariate-based cryptography [62]
- Hash-based signatures [63]
- Code-based cryptography [64]

The existing alternatives and new schemes emerging from these areas of mathematics do not all necessarily satisfy the characteristics of an ideal scheme. In the following subsections we are going to give an overview of these cryptographic schemes.

1) *Lattice-based Cryptography*: This is a form of public-key cryptography that avoids the weaknesses of RSA. Rather than multiplying primes, lattice-based encryption schemes involve multiplying matrices. Furthermore, lattice-based cryptographic constructions are based on the presumed hardness of lattice problems, the most basic of which is the shortest vector problem (SVP) [61]. Here, we are given as input a lattice represented by an arbitrary basis and our goal is to output the shortest non-zero vector in it.

The Ajtai-Dwork (AD) [65], Goldreich-Goldwasser-Halevi (GGH) [66] and NTRU [67] encryption schemes that are explained below are lattice-based cryptosystems.

In 1997, Ajtai and Dwork[65] found the first connection between the worst and the average case complexity of the Shortest Vector Problem (SVP). They claimed that their cryptosystem is *provably secure*, but in 1998, Nguyen and Ster [68] refuted it. Furthermore, the AD public key is big and it causes message expansion making it an unrealistic public key candidate in post-quantum era.

The Goldreich-Goldwasser-Halevi (GGH) was published in 1997. GGH makes use of the Closest Vector Problem (CVP) which is known to be NP-hard. Despite the fact that GGH is more efficient than Ajtai-Dwork (AD), in 1999, Nguyen[69] proved that GGH has a major flaw; partial information on plaintexts can be recovered by solving CVP instances.

NTRU was published in 1996 by Hoffstein et al. [67]. It is used for both encryption (*NTRUEncrypt*) and digital signature (*NTRUSign*) schemes. NTRU relies on the difficulty of factorizing certain polynomials making it resistant against Shor's algorithm. To provide 128-bit post-quantum security level NTRU demands 12881-bit keys [70]. As of today there is not any known attack for NTRU.

In 2013, Damien Stehle and Ron Steinfeld developed a *provably secure* version of NTRU (SS-NTRU) [71].

In May 2016, Bernstein et al. [72] released a new version of NTRU called "NTRU Prime". NTRU Prime countermeasures the weaknesses of several lattice based cryptosystems, including NTRU, by using different more secure ring structures.

In conclusion, among all the lattice-based candidates mentioned above NTRU is the most efficient and secure algorithm making it a promising candidate for the post-quantum era.

2) *Multivariate-based Cryptography*: The security of this public key scheme relies on the difficulty of solving systems of multivariate polynomials over finite fields. Research has shown that development of an encryption algorithm based on

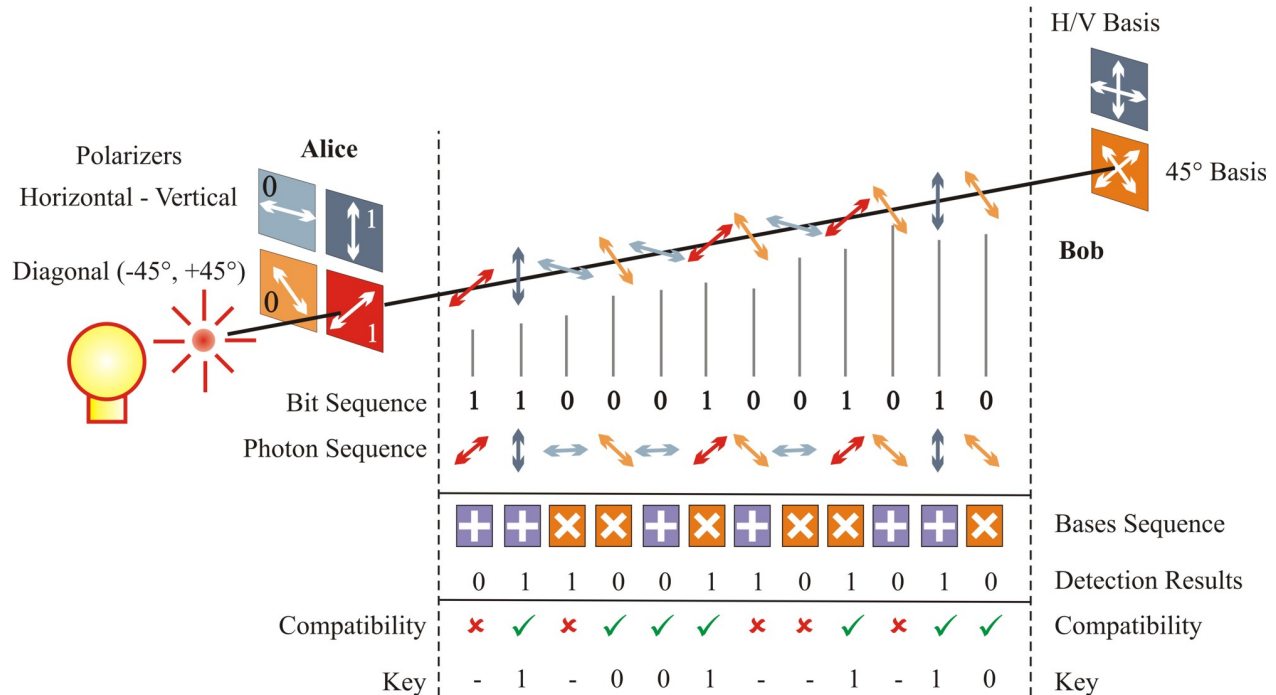


Fig. 1. Key exchange in the BB84 protocol implemented with polarization of photons (adapted from [56]).

Multivariate equations is difficult [13]. Multivariate cryptosystems can be used both for encryption and digital signatures. Tao et al. [73] explained that there have been several attempts to build asymmetric public key encryption schemes based on multivariate polynomials; however, most of them are insecure because of the fact that certain quadratic forms associated with their central maps have low rank. The authors [73] proposed a new efficient multivariate scheme, namely Simple Matrix (ABC), based on matrix multiplication that overcomes the aforementioned weakness. In addition, multivariate cryptosystems can be used for digital signatures. The most promising signature schemes include Unbalanced Oil and Vinegar (multivariate quadratic equations), and Rainbow. UOV has a large ratio between the number of variables and equations (3:1) making the signatures three times longer than the hash values. In addition, the public key sizes are large. On the other hand, Rainbow is more efficient by using smaller ratios which result in smaller digital signatures and key sizes [12].

3) *Hash-based Signatures*: In this subsection, we introduce the Lamport signature scheme invented in 1979 by Leslie Lamport. Buchmann et al. [18] introduced concisely the scheme. A parameter b defines the desired security level of our system. For 128-bit b security level we need a secure hash function that takes arbitrary length input and produces 256-bit length output; thus, SHA-256 is considered an optimal solution that can be fitted with our message m .

Private key: A random number generator is used to produce 256 pairs of random numbers. Each number is 256 bits. In total our generated numbers are $2 \times 256 \times 256 = 16$ KB. Therefore, we can precisely say that the private key consists of $8b^2$ bits.

Public key: All generated numbers (private key) are hashed

independently creating 512 different hashes (256 pairs) of 256-bit length each. Therefore, we can precisely say that the public key consists of $8b^2$ bits.

The next step is to sign the message. We have a hashed message m and then for each bit (depending on its value 0 or 1) of the message digest we choose one number from each pair that comprise the private key. As a result, we have a sequence of 256 numbers (relative to the bit sequence of the hashed message m). The sequence of numbers is the digital signature published along with the plaintext message. It is worth noting that the private key should never be used again and the remaining 256 numbers from the pairs should be destroyed (*Lamport one-time signature*).

The verification process is straightforward. The recipient calculates the hash of the message and then, for each bit of the hashed message we choose the corresponding hash from the public key (512 in number). In addition, the recipient hashes each number of the sender's private key which should correspond to the same sequence of hashed values with the recipient's correctly chosen public key values. The security of this system derives by the decision of using the private key only once. Consequently, an adversary can only retrieve 50 percent of the private key which makes it impossible to forge a new valid signature.

Buchmann et al. [18] explained that in case we want to sign more than one messages, chaining can be introduced. The signer includes in the signed message a newly generated public key that is used to verify the next message received.

Witernitz described a one time signature (WOTS) which is more efficient than Lamport's. Specifically, the signature size and the keys are smaller [74]. However, OTSs are not suitable for large-scale use because they can be used only once.

Merkle introduced a new approach that combines Winternitz's OTS with binary trees (Merkle Signature Scheme). A binary tree is made of nodes. In our case each node represents the hash value of the concatenation of the child nodes. Each of the leaf nodes (lowest nodes in the tree hierarchy) contains a Winternitz's OTS which is used for signing. The first node in the hierarchy of the tree known as root node is the actual public key that can verify the OTSs contained in the leaf nodes [74].

In 2013, A. Hulsing improved the WOTS algorithm by making it more efficient without affecting its security level even when hash functions without collision resistance are used [75].

Currently two hash-based signature schemes are under evaluation for standardization. Specifically, the eXtended Merkle Signature Scheme (XMSS) [76] which is a stateful signature scheme, and Stateless Practical Hash-based Incredibly Nice Collision-resilient Signatures (SPHINCS) [77] which is as the name indicates a stateless signature scheme.

4) *Code-based Cryptography*: Code-based cryptography refers to cryptosystems that make use of error correcting codes. The algorithms are based on the difficulty of decoding linear codes and are considered robust to quantum attacks when the key sizes are increased by the factor of 4. Furthermore, Buchmann et al. [18] state that the best way to solve the decoding problem is to transform it to a Low-Weight-Code-World Problem (LWCWP) but solving a LWCWP in large dimensions is considered infeasible. It would be easier to comprehend the process of this scheme by using Buchmann's [18] concise explanation of McEliece's original code-based public-key encryption system. We define b as the security of our system and it is a power of 2. $n = 4b \lg b$, $d = \lg n$, and $t = 0.5n/d$.

For example, if $b = 128$ then $n = 512 \log_2(128)$ which is equal to 3584. $d = 12$ and $t = 149$. The receiver's public key in this system is $d \times n$ matrix K with coefficients F_2 . Messages to be encrypted should have exactly t bits set to 1 and for the encryption the message m is multiplied by K . The receiver generates a public key with a hidden Goppa code structure (error-correction code) that allows to decode the message with Patterson's algorithm, or even by faster algorithms. The code's generator matrix K is perturbed by two invertible matrices which are used to decrypt the ciphertext to obtain the message m .

As for any other class of cryptosystems, the practice of code-based cryptography is a trade-off between efficiency and security. McEliece's cryptosystem encryption and decryption process are fast with very low complexity, but it makes use of large public keys (100 kilobytes to several megabytes).

VI. CONCLUSION

In today's world, where information play a particularly important role, the transmission and the storage of data must be maximally secure. Quantum computers pose a significant risk to both conventional public key algorithms (such as RSA, ElGamal, ECC and DSA) and symmetric key algorithms (3DES, AES). Year by year it seems that we are getting closer to create a fully operational universal quantum computer that

can utilize strong quantum algorithms such as Shor's algorithm and Grover's algorithm. The consequence of this technological advancement is the absolute collapse of the present public key algorithms that are considered secure, such as RSA and Elliptic Curve Cryptosystems. The answer on that threat is the introduction of cryptographic schemes resistant to quantum computing, such as quantum key distribution methods like the BB84 protocol, and mathematical-based solutions like lattice-based cryptography, hash-based signatures, and code-based cryptography.

ACKNOWLEDGMENT

This research is supported by the Research Council of Norway under the Grant No.: IKTPLUSS 247648 and 248030/O70 for Oslo Analytics and SWAN projects, respectively. This research is also part of the SecurityLab of the University of Oslo.

REFERENCES

- [1] M. Dušek, N. Lütkenhaus, and M. Hendrych, "Quantum cryptography," *Progress in Optics*, vol. 49, pp. 381–454, 2006.
- [2] C. Paar and J. Pelzl, "Introduction to Public-Key Cryptography," in *Understanding Cryptography*. Berlin, Heidelberg: Springer Berlin Heidelberg, 2010, pp. 149–171.
- [3] Z. Kirsch, "Quantum Computing: The Risk to Existing Encryption Methods," Ph.D. dissertation, Tufts University, Massachusetts, 2015, <http://www.cs.tufts.edu/comp/1116/archive/fall2015/zkirsch.pdf>.
- [4] M. A. Nielsen and I. L. Chuang, *Quantum Computation and Quantum Information: 10th Anniversary Edition*, 10th ed. New York, NY, USA: Cambridge University Press, 2011.
- [5] R. Jozsa, "Entanglement and Quantum Computation," in *Geometric Issues in the Foundations of Science*, S. Huggett, L. Mason, K. Tod, S. Tsou, and N. Woodhouse, Eds. Oxford University Press, July 1997.
- [6] W. Tichy, "Is quantum computing for real?: An interview with catherine mcgeoch of d-wave systems," *Ubiquity*, vol. 2017, no. July, pp. 2:1–2:20, Jul. 2017. [Online]. Available: <http://doi.acm.org/10.1145/3084688>
- [7] M. Soeken, T. Häner, and M. Roetteler, "Programming quantum computers using design automation," *arXiv preprint arXiv:1803.01022*, 2018.
- [8] S. Bone and M. Castro, "A Brief History of Quantum Computing," *Surveys and Presentations in Information Systems Engineering (SURPRISE)*, vol. 4, no. 3, pp. 20–45, 1997, http://www.doc.ic.ac.uk/~nd/surprise_97/journal/vol4/spb3/.
- [9] J. Muhonen and T. Dehollain, "Storing Quantum Information For 30 Seconds In a Nanoelectronic Device," *Nature Nanotechnology*, vol. 9, pp. 986–991, 2014.
- [10] D-Wave, "Quantum Computing: How D-Wave Systems Work," <http://www.dwavesys.com/our-company/meet-d-wave>.
- [11] L. S. Bishop, S. Bravyi, A. Cross, J. M. Gambetta, and J. Smolin, "Quantum volume," Technical report, 2017., Tech. Rep., 2017.
- [12] M. Campagna and C. Xing, "Quantum Safe Cryptography and Security: An Introduction, Benefits, Enablers and Challenges," ETSI, Tech. Rep. 8, 2015.
- [13] W. Buchanan and A. Woodward, "Will Quantum Computers be the End of Public Key Encryption?" *Journal of Cyber Security Technology*, vol. 1, no. 1, pp. 1–22, 2016.
- [14] L. Chen, S. Jordan, Y.-K. Liu, D. Moody, R. Peralta, R. Perlner, and D. Smith-Tone, "NIST: Report on Post-Quantum Cryptography," NIST, Tech. Rep., 2016.
- [15] P. W. Shor, "Algorithms for Quantum Computation: Discrete Logarithms and Factoring," in *Proceedings of the 35th Annual Symposium on Foundations of Computer Science*, ser. SFCS '94. Washington, DC, USA: IEEE Computer Society, 1994, pp. 124–134.

- [16] U. Vazirani, "On The Power of Quantum Computation," *Philosophical Transactions of the Royal Society of London A: Mathematical, Physical and Engineering Sciences*, vol. 356, no. 1743, pp. 1759–1768, 1998.
- [17] L. Grover, "A Fast Quantum Mechanical Algorithm For Database Search," Bell Labs, New Jersey, Tech. Rep., 1996.
- [18] D. Bernstein, E. Dahmen, and Buch, *Introduction to Post-Quantum Cryptography*. Springer-Verlag Berlin Heidelberg, 2010.
- [19] J. Proos and C. Zalka, "Shor's Discrete Logarithm Quantum Algorithm for Elliptic Curves," *Quantum Info. Comput.*, vol. 3, no. 4, pp. 317–344, 2003.
- [20] National Security Agency, "National Policy on the Use of the Advanced Encryption Standard (AES) to Protect National Security Systems and National Security Information," NSA, Tech. Rep., 2003.
- [21] G. Brassard, P. Høyer, and A. Tapp, *Quantum Cryptanalysis of Hash and Claw-Free Functions*. Berlin, Heidelberg: Springer Berlin Heidelberg, 1998, pp. 163–169.
- [22] D. Moody, "The ship has sailed: The nist post-quantum crypto competition." [Online]. Available: <https://csrc.nist.gov/CSRC/media/Projects/Post-Quantum-Cryptography/documents/asiacrypt-2017-moody-pqc.pdf>
- [23] N. Kobitz and A. Menezes, "A riddle wrapped in an enigma," *IEEE Security Privacy*, vol. 14, no. 6, pp. 34–42, Nov 2016.
- [24] C. H. Bennett and G. Brassard, "Quantum Cryptography: Public Key Distribution, and Coin-Tossing," in *Proc. 1984 IEEE International Conference on Computers, Systems, and Signal Processing*, no. 560, 1984, pp. 175–179.
- [25] C. H. Bennett, F. Bessette, G. Brassard, L. Salvail, and J. Smolin, "Experimental Quantum Cryptography," *Journal of Cryptology*, vol. 5, no. 1, pp. 3–28, 1992.
- [26] E. Panarella, "Heisenberg uncertainty principle," in *Annales de la Fondation Louis de Broglie*, vol. 12, no. 2, 1987, pp. 165–193.
- [27] H. Singh, D. Gupta, and A. Singh, "Quantum key distribution protocols: A review," *Journal of Computational Information Systems*, vol. 8, pp. 2839–2849, 2012.
- [28] A. K. Ekert, "Quantum cryptography based on bell's theorem," *Physical review letters*, vol. 67, no. 6, p. 661, 1991.
- [29] V. Scarani, H. Bechmann-Pasquinucci, N. J. Cerf, M. Dušek, N. Lütkenhaus, and M. Peev, "The security of practical quantum key distribution," *Reviews of modern physics*, vol. 81, no. 3, p. 1301, 2009.
- [30] C. H. Bennett, G. Brassard, and N. D. Mermin, "Quantum cryptography without bell's theorem," *Physical Review Letters*, vol. 68, no. 5, p. 557, 1992.
- [31] D. Bohm, *Quantum theory*. Courier Corporation, 1951.
- [32] J. F. Clauser, M. A. Horne, A. Shimony, and R. A. Holt, "Proposed experiment to test local hidden-variable theories," *Physical review letters*, vol. 23, no. 15, p. 880, 1969.
- [33] V. Scarani, A. Acin, G. Ribordy, and N. Gisin, "Quantum cryptography protocols robust against photon number splitting attacks for weak laser pulse implementations," *Physical review letters*, vol. 92, no. 5, p. 057901, 2004.
- [34] A. Acin, N. Gisin, and V. Scarani, "Coherent-pulse implementations of quantum cryptography protocols resistant to photon-number-splitting attacks," *Physical Review A*, vol. 69, no. 1, p. 012309, 2004.
- [35] C. Bennett and G. Brassard, "Quantum cryptography: Public key distribution and coin tossing," *Proceedings of IEEE International Conference on Computers, Systems and Signal Processing*, pp. 175–179, 1984.
- [36] D. Bruß, "Optimal eavesdropping in quantum cryptography with six states," *Physical Review Letters*, vol. 81, no. 14, p. 3018, 1998.
- [37] H. Bechmann-Pasquinucci and N. Gisin, "Incoherent and coherent eavesdropping in the six-state protocol of quantum cryptography," *Physical Review A*, vol. 59, no. 6, p. 4238, 1999.
- [38] K. Tamaki and H.-K. Lo, "Unconditionally secure key distillation from multiphotons," *Physical Review A*, vol. 73, no. 1, p. 010302, 2006.
- [39] B.-G. Englert, D. Kaszlikowski, H. K. Ng, W. K. Chua, J. Řeháček, and J. Anders, "Efficient and robust quantum key distribution with minimal state tomography," *arXiv preprint quant-ph/0412075*, 2004.
- [40] C. H. Bennett, "Quantum cryptography using any two nonorthogonal states," *Physical review letters*, vol. 68, no. 21, p. 3121, 1992.
- [41] N. J. Cerf, M. Levy, and G. Van Assche, "Quantum distribution of gaussian keys using squeezed states," *Physical Review A*, vol. 63, no. 5, p. 052311, 2001.
- [42] F. Grosshans and P. Grangier, "Continuous variable quantum cryptography using coherent states," *Physical review letters*, vol. 88, no. 5, p. 057902, 2002.
- [43] C. Weedbrook, A. M. Lance, W. P. Bowen, T. Symul, T. C. Ralph, and P. K. Lam, "Quantum cryptography without switching," *Physical review letters*, vol. 93, no. 17, p. 170504, 2004.
- [44] J. Lodewyck, M. Bloch, R. García-Patrón, S. Fossier, E. Karpov, E. Diamanti, T. Debuisschert, N. J. Cerf, R. Tualle-Brouiri, S. W. McLaughlin *et al.*, "Quantum key distribution over 25 km with an all-fiber continuous-variable system," *Physical Review A*, vol. 76, no. 4, p. 042305, 2007.
- [45] C. Silberhorn, T. C. Ralph, N. Lütkenhaus, and G. Leuchs, "Continuous variable quantum cryptography: Beating the 3 db loss limit," *Physical review letters*, vol. 89, no. 16, p. 167901, 2002.
- [46] K. Inoue, E. Waks, and Y. Yamamoto, "Differential phase shift quantum key distribution," *Physical Review Letters*, vol. 89, no. 3, p. 037902, 2002.
- [47] —, "Differential-phase-shift quantum key distribution using coherent light," *Physical Review A*, vol. 68, no. 2, p. 022317, 2003.
- [48] N. Gisin, G. Ribordy, H. Zbinden, D. Stucki, N. Brunner, and V. Scarani, "Towards practical and fast quantum cryptography," *arXiv preprint quant-ph/0411022*, 2004.
- [49] D. Stucki, N. Brunner, N. Gisin, V. Scarani, and H. Zbinden, "Fast and simple one-way quantum key distribution," *Applied Physics Letters*, vol. 87, no. 19, p. 194108, 2005.
- [50] D. Stucki, C. Barreiro, S. Fasel, J.-D. Gautier, O. Gay, N. Gisin, R. Thew, Y. Thoma, P. Trinkler, F. Vannel *et al.*, "Continuous high speed coherent one-way quantum key distribution," *Optics express*, vol. 17, no. 16, pp. 13 326–13 334, 2009.
- [51] D. Mayers, "Unconditional Security in Quantum Cryptography," *Journal of the ACM*, vol. 48, no. 3, pp. 351–406, 2001.
- [52] C. Branciard, N. Gisin, B. Kraus, and V. Scarani, "Security of Two Quantum Cryptography Protocols Using The Same Four Qubit States," *Physical Review A*, vol. 72, no. 3, p. 032301, sep 2005.
- [53] L. Lydersen, C. Wiechers, D. E. C. Wittmann, J. Skaar, and V. Makarov, "Hacking Commercial Quantum Cryptography Systems by Tailored Bright Illumination," *Nature Photonics*, pp. 686–689., October 2010.
- [54] Z. Yuan, J. Dynes, and A. Shields, "Avoiding the Blinding Attack in QKD," *Nature Photonics*, vol. 4, pp. 800–801, December 2010.
- [55] L. Lydersen, C. Wiechers, C. Wittmann, D. Elser, J. Skaar, and V. Makarov, "Avoiding the Blinding Attack in QKD," *Nature Photonics*, vol. 4, pp. 801–801, December 2010.
- [56] V. Makarov, "Quantum Cryptography and Quantum Cryptanalysis," Ph.D. dissertation, Norwegian University of Science and Technology Faculty of Information Technology, NTNU, 2007, <http://www.vad1.com/publications/phd-thesis-makarov-200703.pdf>.
- [57] G. Brassard, N. Lütkenhaus, T. Mor, and B. C. Sanders, "Security aspects of practical quantum cryptography," in *International conference on the theory and applications of cryptographic techniques*. Springer, 2000, pp. 289–299.
- [58] H.-K. Lo, X. Ma, and K. Chen, "Decoy state quantum key distribution," *Physical review letters*, vol. 94, no. 23, p. 230504, 2005.
- [59] M. Haitjema, "A survey of the prominent quantum key distribution protocols," 2007.
- [60] S. J. Lomonaco, J. Kauffman, and L. H., "Quantum Hidden Subgroup Problems: A Mathematical Perspective," *Quantum*, pp. 1–63., 2002.
- [61] D. Micciancio, "Lattice-Based Cryptography," in *Post-Quantum Cryptography*, 2009, no. 015848, pp. 147–192.
- [62] J. Ding and B.-Y. Yang, "Multivariate Public Key Cryptography," *Post-Quantum Cryptography*, pp. 193–241, 2009.
- [63] C. Dods, N. P. Smart, and M. Stam, "Hash Based Digital Signature Schemes," *Cryptography and Coding*, vol. 3796, pp. 96–115, 2005.
- [64] R. Overbeck and N. Sendrier, "Code-based Cryptography," in *Post-Quantum Cryptography*. Berlin, Heidelberg: Springer Berlin Heidelberg, 2009, pp. 95–145.

- [65] M. Ajtai and C. Dwork, "A Public-Key Cryptosystem With Worst-Case/Average-Case Equivalence," *Proceedings of The 29th Annual ACM Symposium on Theory of Computing - STOC '97*, pp. 284–293., 1997.
- [66] O. Goldreich, S. Goldwasser, and S. Halevi, "Public-Key Cryptosystems from Lattice Reduction Problems," *Advances in Cryptology - {CRYPTO} '97, 17th Annual International Cryptology Conference, Santa Barbara, California, USA, August 17-21, 1997, Proceedings*, vol. 1294, pp. 112–131, 1997.
- [67] J. Hoffstein, J. Pipher, and J. H. Silverman, "NTRU: A Ring-Based Public Key Cryptosystem," *Algorithmic number theory*, pp. 267–288, 1998.
- [68] P. Nguyen and J. Stern, *Cryptanalysis of the Ajtai-Dwork Cryptosystem*. Springer Berlin Heidelberg, 1998, pp. 223–242.
- [69] P. Nguyen, "Cryptanalysis of the Goldreich-Goldwasser-Halevi Cryptosystem," *Advances in Cryptology - CRYPTO*, vol. 1666, pp. 288–304, 1999.
- [70] P. S. Hirschhorn, J. Hoffstein, N. Howgrave-Graham, and W. Whyte, *Choosing NTRUEncrypt Parameters in Light of Combined Lattice Reduction and MITM Approaches*. Berlin, Heidelberg: Springer Berlin Heidelberg, 2009, pp. 437–455.
- [71] D. Stehle and R. Steinfeld, "Making NTRUEncrypt and NTRUSign as Secure as Standard Worst-Case Problems over Ideal Lattices," *Cryptology ePrint Archive*, Report 2013/004, 2013.
- [72] D. J. Bernstein, C. Chuengsatiansup, T. Lange, and C. van Vredendaal, "NTRU Prime," *IACR Cryptology ePrint Archive*, vol. 2016, p. 461, 2016.
- [73] C. Tao, A. Diene, S. Tang, and J. Ding, "Simple Matrix Scheme for Encryption," in *International Workshop on Post-Quantum Cryptography*. Springer, 2013, pp. 231–242.
- [74] R. C. Merkle, *A Certified Digital Signature*. New York, NY: Springer New York, 1990, pp. 218–238.
- [75] H. Andreas, *W-OTS+ –Shorter Signatures for Hash-Based Signature Schemes*. Berlin, Heidelberg: Springer Berlin Heidelberg, 2013, pp. 173–188.
- [76] J. Buchmann, E. Dahmen, and A. Hülsing, "XMSS-a Practical Forward Secure Signature Scheme Based on Minimal Security Assumptions," *Post-Quantum Cryptography*, pp. 117–129, 2011.
- [77] D. J. Bernstein, D. Hopwood, A. Hülsing, T. Lange, R. Niederhagen, L. Papachristodoulou, M. Schneider, P. Schwabe, and Z. Wilcox-O'Hearn, *SPHINCS: Practical Stateless Hash-Based Signatures*. Berlin, Heidelberg: Springer Berlin Heidelberg, 2015, pp. 368–397.

Media Content Access: Image-Based Filtering

Rehan Ullah Khan¹, Ali Alkhalifah²
Information Technology Department
Qassim University, Al-Qassim, KSA

Abstract—As the content on the internet contains sensitive adult material, filtering and blocking this content is essential for the social and ethical values of the many societies and organizations. In this paper, the content filtering is explored from still images' perspectives. Thus, this article investigates and analyses the content based filtering which can help in the flagging of the images as adult nature or safe images. As the proposed approach is based on the Chroma (colour) based skin segmentation and detection for detecting the objectionable content in images; therefore, the approach proceeds in the direction of the classical Machine Learning approaches and uses the two well-known classifiers: 1) The Random Forest; and 2) the Neural Network. Their fusion is also investigated. Skin colour is analyzed in the YCbCr colour space and in the form of blob analysis. With the “Adult vs. Safe” classification, an Accuracy of 0.88 and the low RMSE of 0.313 is achieved, indicating the usefulness of the detection model.

Keywords—Skin detection; content based filtering; content analysis; machine learning; random forest; neural network

I. INTRODUCTION

The most famous influential media platforms that allow the users to upload the recorded content (images and videos) are the Flickr, Facebook, Twitter, YouTube, and the DailyMotion. This is not limited to the social platforms. In fact, the internet itself is a gigantic and a general platform for digital media including images and videos resources. The content uploaded to platforms and the Internet itself is increasing rapidly as more and more people are finding access and enjoying the services provided by these providers. The negative side is that the media content; however, is becoming more and more liberal and one can easily access and see the partially/fully naked images on the internet. This opens risks in terms of many social factors. One of the major problems is the availability of these resources to the younger generation. The most feared element, however, nowadays is the availability of these media resources to the kids.

Therefore, in this paper, we analyze skin color based image content filter which can help in the flagging of the images as adult nature or safe images. As the proposed approach is based on color based skin segmentation and detection for detecting the objectionable content in images, therefore, we proceed in the direction of the classical Machine Learning approach and use the two well-known classifiers: The Random Forest and the Neural Network. For skin color analysis, we also investigate their fusion. We analyze skin color in the YCbCr color space and in the form of blob analysis. With the “Adult vs Safe” classification, we get an Accuracy of 0.88 and the low RMSE of 0.313, indicating the usefulness of our detection model. The success of this filter can have profound applications in media

filtering which will benefit not only the general society but also will be especially, useful for parental control over the media for the children and similar requirements. The basic filter developed can be further extended for videos and online streaming like YouTube and other resources.

Certain IP level porn and adult content blocking is possible, however, blocking the user's content on the IP level is always by-passable as there is certain Proxy bypassing tools available to bypass the restrictions and access the corresponding resources containing explicit content. Therefore, blocking and filtering the multimedia based on its content is of utmost importance.

There is interesting work available in the state-of-the-art regarding content based retrieval [1], [2], skin detection [3], [4], and content based filtering [5]. In [5], the authors propose a method combining evidence including video sequences, key shots, and key frames and evaluating performance with three the social networks. The work in [6] describes a sampling, based on the adaptive sampling analysis achieving an acceptable detection rates of 87%. The author in [7] use “bag of visual words approach” for filtering and blocking nude images using the associated voting scheme, analyzed and evaluated achieving 93.2 Accuracy. The work in [8] targets skin locus detection for content filtering using the 24 colors transformations in widely available images and videos. The framework of [9] produces an augmented classification model with independent of the access scenarios with the promising results. The authors in [10] combines the key-frame based approaches with a statistical MP4 motion vectors.

Generally, Image and Video Retrieval (IVR) paradigm is divided into two directions. One that uses media content directly by taking advantage of the visual information present in the images and videos. This type of approach is generally termed as the Content-Based Image and Video Retrieval (CBIVR). In CBIVR, the images and videos are retrieved and searched using the low-level features, for example, color, shape, texture and pixel relationships [11], [12]. Another approach that is nowadays advocated in conjunction with CBIVR is the Textual-Based Image and Video Retrieval (TBIVR). The textual analysis of images and videos uses mostly the tags assigned during the production of the media source. In order to overcome the limitations and drawbacks of the CBIVR, the TBIVR gracefully represent the visual information during the production or editing phase by users manually assigned keywords and or tags. The systems can also allow for later assignments of tags, however, this might introduce wrong tags and tags that are unnecessary. The TBIVR systems allow the users to type the information need as a text query.

In [13], the authors analyze content filtering for a Web-based P2P using the Machine learning to filter the explicit content and results show the feasibility of the approach. The work in [14] uses two visual features and are constructed from the video in question using decision variable based on the single frame and a group of frames. In [15], authors use the Hue-SIFT for nude and explicit content detection. In [16], authors propose visual motion analysis approach augmenting the visual motion features with the audio repetition in video. The [17] demonstrate a multimodal hierarchy based filtering for explicit content. The algorithm is made of 3 phases, i.e. Detecting initial video scene using the hashing signatures, real-time detection estimating the degree of explicit content, and finally, exploiting features from frame-group and thus achieving high detection rate. The authors in [18] uses optical flow for content filtering based on the selection of the frame as the key-frame. The work in [19] use similar approach of the motion estimation. In [20], authors present an objectionable (porn) video filtering approach using a fusion of audio features and video features. Training the Support Vector Machine (SVM) on the chromatic and texture cues of the SIFT key points for adult image frames integrated by the Bayes statistics for classification.

II. COLOR BASED SKIN DETECTION

For content filtering in still images, the basic feature for the detection starts with a reliable color based skin locus detection in images. We start with the experimental setup of the robust skin analysis using color features in the YCbCr color space. As the proposed approach is based on the Chroma (color) based skin segmentation and detection, therefore, we use the two well-known classifiers: The Random Forest and the Neural Network, selecting them due to the good classification performance in many related tasks.

III. CLASSIFICATION

As the proposed approach is based on the Chroma (colour) based skin segmentation and detection for detecting the objectionable content in images, therefore, we proceed in the direction of the classical Machine Learning approaches and use the two well-known classifiers: The Random Forest and the Neural Network. We also investigate their fusion in the Experiment section.

A. Random Forest

Recently, the tree based classifiers have gained considerable popularity. This popularity stems from the intuitive nature and the overall easy training paradigm. Classification trees, however, suffer from the classification and generalization accuracy. It is not possible to increase both the classification and generalization accuracy at the same time. Leo Breiman [21] introduced the Random Forest for addressing these issues. Random forest takes advantage of the combination of many trees from the same dataset. Random forest constructs a forest of trees such that each tree is

generated based on the random seed augmented on the data and assigns classes based on voting scheme from the trees.

B. Neural Network (ML)

From the neural network paradigm, we use the Multilayer Perceptron (MLP). A Multilayer perceptron is a Neural Network; a feed-forward Artificial Neural Network that functions by mapping the input variable of a dataset onto the output labels. Generally, it is significantly different than the linear perceptron in the way it takes advantage of the two or more layers of artificial neurons by integrating the non-linear activation functions. It can thus model linear and non-linear problems as well.

IV. FUSION

To achieve an effective and robust skin segmentation performance, the fusion of the two machine learning algorithms, i.e., the Random Forest and the Multilayer Perceptron is investigated. We believe that the fusion of the classifiers might report interesting results and increased classification performance. This fusion of the classification is investigated on the five parameters as follows:

- 1) *Average of probabilities*
- 2) *The product of probabilities*
- 3) *Majority voting*
- 4) *Minimum probability*
- 5) *Maximum probability*

V. SKIN BLOBS

By blob analysis, we mean the physical shapes the skin and non-skin regions/objects represent in an image. We believe that it may provide a good measure for prediction based on the shapes of skin regions. We use the 6 blob features for the skin non-skin regions analysis. These features are:

- Area
- Convex-Area
- Eccentricity
- Orientation
- Perimeter
- Solidity

VI. EXPERIMENTAL ANALYSIS

In this section, we discuss the datasets, the experimental setup and the results.

A. Dataset

The dataset for our experiments is a hybrid dataset containing images from [22] and our own additions. The total image patches present are 3242 skin and non-skin patches. This dataset contains two types of images, one is the original set of

images and the other is mask images as shown in Fig. 1. The dataset consists of images taken in different lighting conditions. It represents many types of skin ranging from white to black. Some images also have complex backgrounds similar to that of human skin color. We represent this dataset as DS_SKIN.

For adult content analysis, another dataset is also used for which contains an adult image, safe images and suspicious images (confusing the algorithm). This dataset contains 6000 images and most of them are extracted from the [23]. The dataset is represented as DS_ADULT and is used for the experimentation of differentiating between adult and non-adult content using skin features.



Fig. 1. Mask images from dataset.

B. Results and Evaluation

We discuss the experimental evaluation performed for different parameters discussed previously. First experiment consists of pixel based skin model generation in the YCbCr color space and analyzing its performance. The performance is then also analyzed in terms of the fusion of the two classifiers: The Random Forest and the MLP using different strategies.

Fig. 2 shows the evaluation of YCbCr color space using the Random Forest and the MLP and the five fusion strategies. The random forest reports an increased classification performance compared to the MLP.

The performance of the five fusion approaches of the Random Forest and the MLP shows that the average performance of the five fusion approaches is almost similar and has increased the performance of the MLP but has slightly decreased the performance of the Random Forest. In Fig. 2, the RMSE; however, shows variations with smallest RMSE for minimum probability and maximum for majority voting. This analysis shows that as of other fields, the Random Forest also shows increased classification performance in the pixel-based classification. The fusion though theoretically may increase performance; however, in practice, we did not find a big difference with the five strategies of fusion of classification. The minimum probability fusion reports a decreased RMSE in all the cases of the fusion strategies.

For blob analysis, a blob represents the physical shape of the skin and non-skin regions/objects present in an image. In blob analysis, we discuss the performance analysis using the six features of:

- 1) Area
- 2) Convex-Area
- 3) Eccentricity
- 4) Orientation
- 5) Perimeter
- 6) Solidity

Fig. 3 shows the performance analysis using blob analysis based on these six features. The random forest once again has comparatively higher performance than the MLP. The Random Forest has F-measure of 0.90, an accuracy of 0.90 and RMSE of 0.26. The MLP reports slightly decreased performance compared to the Random forest with an F-measure of 0.89, an accuracy of 0.89 and RMSE of 0.29. We get an approximately 1% of the increase in this case, which is not significant compared to the pixel analysis of Fig. 2.

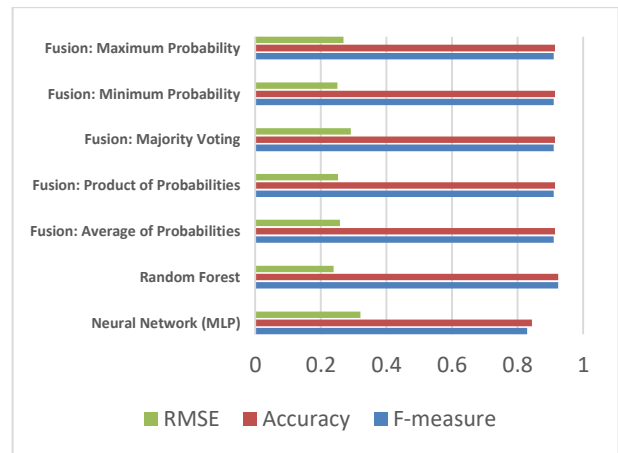


Fig. 2. Skin detection performance using YCbCr color space in the Random Forest and MLP setup and the fusion of classifiers.

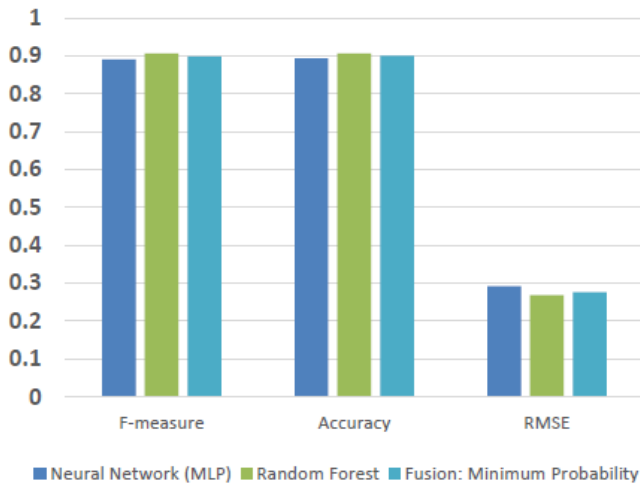


Fig. 3. Performance analysis of blobs of skin and non-skin regions.

For adult sensitive data classification, we use the dataset of images containing adult and non-adult content and is distributed into three classes:

- 1) Adult
- 2) Suspicious
- 3) Safe images

Adult images are sensitive images taken from porn movies. Suspicious images are purely not adult images but rather shots containing naked skin and naked people. It also consists of images with confusing backgrounds and having skin like color objects. Safe images are those with people and objects that are acceptable to most societies. This dataset contains almost 6000 images and most of them are extracted from [23]. The dataset is represented as DS_ADULT and is used for the experimentation of differentiating between adult and non-adult content using skin features. Fig. 4 shows the distribution of the images and their classes. The dataset consists of 2001 images of adult nature, 2001 suspicious images, and 2000 safe images.

Based on the over-all good performance in the previous experiments of skin and the state-of-the-art, compared to the MLP, we select the random forest for sensitive data classification. Fig. 5 shows the performance evaluation of the Random Forest within the four evaluation dimensions and the two parameters of the Accuracy and the F-measure. The four performance evaluation dimensions are:

- 1) Adult class vs. the suspicious class vs. the safe class
- 2) Suspicious vs. safe
- 3) Adult vs. suspicious
- 4) Adult vs. safe

From Fig. 5, it can be seen that the “Adult vs. suspicious vs. safe” gets an F-measure of 0.766, an accuracy of 0.766, and an RMSE of 0.356. Meaning that over-all, on average, out of 100 images, approximately, 76 are correctly identified as either “Adult”, “Suspicious” or “Safe”. The evaluation of “Suspicious vs. safe” images reports an increased classification compared to the previous class evaluation. With the “Suspicious vs. safe image”, we get an F-measure of 0.809, an Accuracy of 0.808, and an RMSE of 0.393. In Fig. 5, the “Adult vs. suspicious”

classification reports an increased classification of 0.859 (F-measure) and an Accuracy of 0.859 with low RMSE of 0.336. Our main interest is in the “Adult vs. the safe” classification. With the “Adult vs. safe” classification, we get an increased F-measure of 0.887, an increased Accuracy of 0.887 and low RMSE of 0.313. As the application of our research requires above 84% accurate model for adult vs. safe images, we get satisfactory results. Also since, suspicious images may be flagged as adult material; the latter can then manually be checked, thus satisfying our objectives.

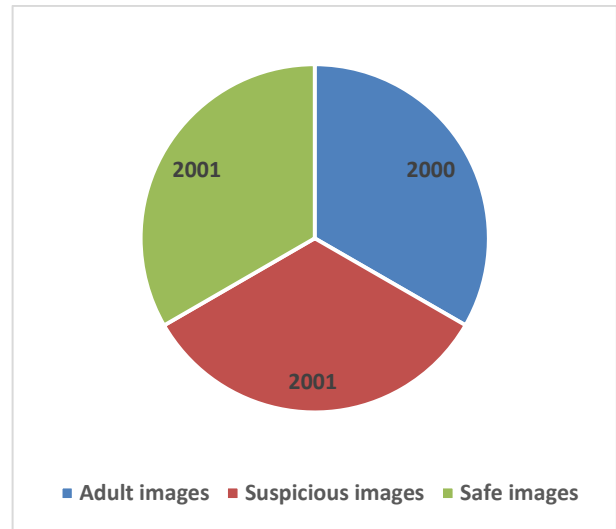


Fig. 4. Dataset distribution for image classification into three categories.



Fig. 5. Adult image classification performance.

VII. CONCLUSION

In this article, we explored the skin and content-based analysis of still images. As the proposed approach is based on the Chroma (color) based skin segmentation and detection for detecting the objectionable content in images; therefore, we walked in the direction of the classical Machine Learning approach and used the two well-known classifiers: The Random Forest and the Neural Network. This analysis showed that as of other fields, the Random Forest also shows increased classification performance in the pixel-based classification. Also, the fusion though theoretically may increase performance; however, in practice, we could not find a big

difference with the five strategies of fusion of classification. The Random Forest has increased classification performance in all the cases of three color spaces. The minimum probability fusion reports a decreased RMSE in all the cases of the fusion strategies. For the blob analysis, we got an increment of 1%, which is not significant compared to the pixel analysis. With the “Adult vs. safe” classification, we get an increased F-measure of 0.88, an increased Accuracy of 0.88 and low RMSE of 0.31. As the application of our research required above 84% accurate model for “adult vs. safe” images, we get satisfactory results. Also since, suspicious images may be flagged as adult material; the latter can then manually be checked.

ACKNOWLEDGMENT

The work in this article is funded in its entirety by the Dean of Scientific Research (SRD), Project number: 1335-coc-2016-1-12-S at the Qassim University, Kingdom of Saudi Arabia. We are thankful to Irfanullah of the Chongqing University for helping in experimental setup.

REFERENCES

- [1] S. H. Shirazi, A. I. Umar, S. Naz, N. A. Khan, M. I. Razzak, B. AlHaqbani, “Content-Based Image Retrieval Using Texture Color Shape and Region,” *International Journal of Advanced Computer Science and Applications (IJACSA)*, 7(1), 2016.
- [2] M. Alkhwilani, M. Elmogy and H. Elbakry, “Content-Based Image Retrieval using Local Features Descriptors and Bag-of-Visual Words,” *International Journal of Advanced Computer Science and Applications (IJACSA)*, 6(9), 2015.
- [3] S. A. S. Hani K. Al-Mohair, Junita Mohamad-Saleh, “Human skin color detection: A review on neural network perspective,” *Int. J. Innov. Comput. Inf. Control IJICIC*, vol. 8, no. 12, pp. 8115–8131, 2012.
- [4] K. Y. Md Foisal Hossain, Mousa Shamsi, Mohammad Reza Asharif, “Automatic facial skin detection using Gaussian Mixture Model under varying illumination,” *Int. J. Innov. Comput. Inf. Control IJICIC*, vol. 8, no. 2, pp. 1135–1144, 2012.
- [5] E. Valle, S. Avila, F. Souza, M. Coelho, and A. de A. Araujo, “Content-Based Filtering for Video Sharing Social Networks,” in *XII Simpósio Brasileiro em Segurança da Informação e de Sistemas Computacionais—SBSeg 2012*, 2011, p. 28.
- [6] P. Monteiro, S. Eleuterio, M. De, and C. Polastro, “An adaptive sampling strategy for automatic detection of child pornographic videos.”
- [7] A. P. B. Lopes, S. E. F. de Avila, A. N. A. Peixoto, R. S. Oliveira, M. de M. Coelho, and A. de A. Araújo, “Nude Detection in Video Using Bag-of-Visual-Features,” in *2009 XXII Brazilian Symposium on Computer Graphics and Image Processing*, 2009, pp. 224–231.
- [8] A. Abadpour and S. Kasaei, “Pixel-Based Skin Detection for Pornography Filtering,” *Iran. J. Electr. Electron. Eng.*, vol. 1, no. 3, pp. 21–41, 2005.
- [9] N. Agarwal, H. Liu, and J. Zhang, “Blocking objectionable web content by leveraging multiple information sources,” *ACM SIGKDD Explor. Newsl.*, vol. 8, no. 1, pp. 17–26, Jun. 2006.
- [10] C. Jansohn, A. Ulges, and T. M. Breuel, “Detecting pornographic video content by combining image features with motion information,” in *Proceedings of the seventeen ACM international conference on Multimedia - MM '09*, 2009, p. 601.
- [11] C. K. B. Dinakaran, J. Annapurna, “Interactive Image Retrieval Using Text and Image Content,” *Cybern. Inf. Technol.*, vol. 10, no. 3, pp. 20–30, 2010.
- [12] M. Y. M. Latha, B. C. Jinaga, and V. S. K. Reddy, “Content Based Color Image Retrieval via Wavelet Transforms,” *IJCSNS Int. J. Comput. Sci. Netw. Secur.*, vol. 7, no. 12, 2007.
- [13] J. H. Wang, H.-C. Chang, M.-J. Lee, and Y.-M. Shaw, “Classifying Peer-to-Peer File Transfers for Objectionable Content Filtering Using a Web-based Approach.”
- [14] H. Lee, S. Lee, and T. Nam, “Implementation of high performance objectionable video classification system,” in *2006 8th International Conference Advanced Communication Technology*, 2006, p. 4 pp.-pp.962.
- [15] A. P. B. Lopes, A. P. B. Lopes, R. E. F. De Avila, A. N. A. Peixoto, R. S. Oliveira, and A. De A. Araújo, “a bag-of-features approach based on hue-sift descriptor for nude detection.”
- [16] N. Rea, G. Lacey, R. Dahyot, and C. Lambe, “Multimodal periodicity analysis for illicit content detection in videos,” in *3rd European Conference on Visual Media Production (CVMP 2006)*. Part of the 2nd Multimedia Conference 2006, 2006, pp. 106–114.
- [17] S. Lee, W. Shim, and S. Kim, “Hierarchical system for objectionable video detection,” *IEEE Trans. Consum. Electron.*, vol. 55, no. 2, pp. 677–684, May 2009.
- [18] Y. S. L. Li, “Objectionable videos detection algorithm based on optical flow,” *Comput. Eng.*, vol. 12, p. 77, 2007.
- [19] Y. Qu, ZY; Liu, YM; Liu, Y; Jiu, K; Chen, “a method for reciprocating motion detection in porn video based on motion features,” in *IEEE International Conference on Broadband Network and Multimedia Technology*, 2009, pp. 183–187.
- [20] Z. ZHAO, “Combining SVM and CHMM classifiers for porno video recognition,” *J. China Univ. Posts Telecommun.*, vol. 19, no. 3, pp. 100–106, Jun. 2012.
- [21] L. Breiman, “Random Forests,” *Mach. Learn.*, vol. 45, no. 1, pp. 5–32, 2001.
- [22] Q. Zhu, C.-T. Wu, K.-T. Cheng, and Y.-L. Wu, “An adaptive skin model and its application to objectionable image filtering,” in *Proceedings of the 12th annual ACM international conference on Multimedia - MULTIMEDIA '04*, 2004, p. 56.
- [23] S. Avila, N. Thome, M. Cord, E. Valle, and A. de A. Araújo, “Pooling in image representation: The visual codeword point of view,” *Comput. Vis. Image Underst.*, vol. 117, no. 5, pp. 453–465, May 2013.

Half Mode Substrate Integrated Waveguide Cavity based RFID Chipless Tag

Soumaya Sakouhi¹, Hedi Ragad², Ali Gharsallah⁴
Dept. of Physics, Faculty of Sciences of Tunis
University of Tunis El Manar, 2092
Tunisia

Mohamed Latrach³
RF-EMC Research Group, ESEO-IETR
CS90717-49107 Angers Cedex 2
France

Abstract—This study presents the design of a compact Radio Frequency Identification chipless tag, with reduced size, important quality factor and improved results. The proposed prototype is based on Substrate Integrated Waveguide technology using the Half-Mode Substrate Integrated Waveguide technique to reduce the tag size by the half and preserve the same response. Further, the operating frequency band is from 5.5 to 8 GHz inside a compact surface of $1.3 \times 5.7 \text{ cm}^2$. The frequency domain approach is adopted based on the frequency shift coding technique.

Keywords—Radio frequency identification (RFID); chipless tag; substrate integrated waveguide (SIW); ultra wide band (UWB)

I. INTRODUCTION

Wireless RF components and systems have been studied widely in recent years, and are constantly growing. Microwave literature is full of numerous enhancement tests in order to design high performance RF components with lower losses, higher power capacity and improved quality factor [1]. Substrate Integrated Waveguide technology has been emerged as a promising tool for the last research decade [2]. It has become extensively investigated and applied; and still proving day after day that it makes difference and improves structure such as mixers [3], oscillators [4], and Amplifiers [5]. Hence, it is constructed by using two rows of metalized cylinders or slots integrated in the dielectric substrate that electrically connect the two metal plates (patch and ground) [6]. Also, it is characterized by different shapes as circular, rectangular, and triangular structure. Recently, various applications have been already suggested for SIW technology. Mainly, the RFID chipless tag, our study focus, which is a promising alternative to develop a technology of identification more efficient than barcode and cheaper than conventional RFID, that uses tags equipped with Application-Specific Integrated Circuit (ASICs) associated to an antenna. The manufacturing and association tasks of each ASIC and antenna is expensive. This is the main reason for the limited utilization of conventional RFID to military tracking and some common transport application. As a result, RFID chipless tag has appeared since 2005 as an RF barcode which consists of 5 metallic strips giving 5 resonant peaks [7]. Besides, research focuses on improving chipless technology. In [8], an important data density is presented using 35 spiral resonators associated with cross polarized antennas coding 35 data bits. A 24-bit RFID tag is designed in [9], the tag operates in the UWB, and the presence or absence of resonant peak is the adopted technique to obtain data bits. The

chipless tag in [10] uses three RF MEMS switch, giving 3-bit information over one period of the signal transmitted by an RFID reader. In [11], the tag encodes data using phase and frequency encoding technique. The proposed prototype in [12] is based on three split ring resonators, and it uses the geometrical angle relative to the reference ring resonator to encode data. SIW technology is applied in [13] using rectangular resonant cavity associated to an UWB antenna, as a chipless tag for space applications. Three tuning posts are used to shift frequency from 3.1 to 4.8 GHz.

From the research study, we can conclude that chipless technology is in intermediary phase, from the goal of improving the encoding capacity without being aware of the size and the application, towards a global reason which aims to combine the qualities of smart encoding technique, compact size, low losses, and reduced cost in industry. In this paper, a compact chipless tag based on SIW technology has an important quality factor is proposed. Its detailed behavior is presented theoretically and experimentally in Section 2. Also, it is tested and validated in Section 3.

II. PRESENTATION OF THE HALF MODE CAVITY BASED RFID CHIPLESS TAG BEHAVIOR

A. Half Mode Substrate Integrated Waveguide Cavity

The most important characteristics that merit to be studied when designing a chipless tag are mainly, the encoding technique that ensures the validity of numerous encoding states (ID), the compact size that allows its application flexibility in several fields and the response performances include the efficiency, the stability and the quality factor. As known, SIW technology has distinctive advantages, particularly for the reason of combination of waveguide and planar technology features. It is a promising technology, which has been investigated and developed in the last decade [14]. It ensures a reduced size, low losses and an important quality factor. The propagation of electromagnetic waves in SIW-based structures has an important resemblance to its propagation in rectangular waveguide [15]. For this reason, several formulas were built in order to obtain the equivalent rectangular waveguide width. Hence, a formula can be estimated according to the geometrical parameters illustrated in Fig. 1, and using (1) below:

$$a_{eq} = a_{SIW} - \frac{d^2}{0.95p} \quad (1)$$

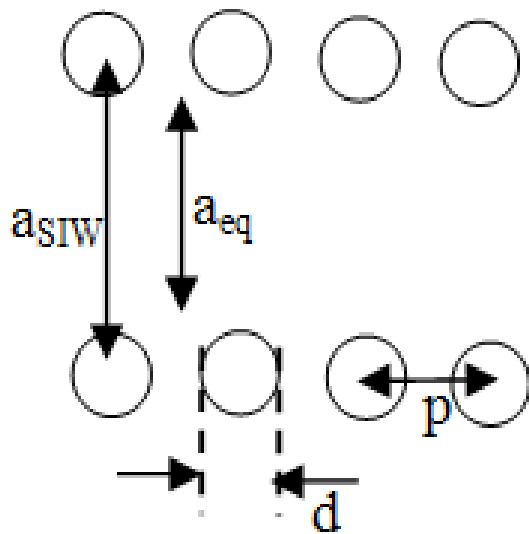


Fig. 1. Two metallic walls of metalized via in the SIW cavity.

Where, a_{eq} is the waveguide width, a_{SIW} is the distance between two rows of metalized vias, d is the diameter of each via, and p is the pitch which represents the spacing between two vias.

This section describes the use of SIW Technology aiming to develop chipless tag technology which consists of resonant cavity based on SIW technology associated to an UWB antenna characterized by an original shape and an UWB operation. Thus, the utilization of circular patch is chosen as an SIW cavity where a circular row of metalized via is drilled connecting the ground layer to the patch. The circular SIW cavity shape is studied. It has a width of 25 mm and a length of 30 mm, as shown in Fig. 2(b) and Fig. 4(a). It has a radius $R=10.75$ mm, the metalized via radius is of 0.8 mm, and a pitch of 1.89 mm. Moreover, a 50-Ohm microstrip is designed as a feeding line which allows the measurements of the circular SIW cavity and permits connecting the cavity to the antenna in order to form the complete chipless tag.

The simulation of the Circular SIW (CSIW) cavity is built using the FR4 substrate, with a thickness of 0.7 mm, a dielectric permittivity of 4.6 and loss tangent of 0.025. The maximum electric fields are concentrated inside the cavity limited by the metalized via and symmetric along the AB plane. The CSIW cavity is optimized, realized and measured. It operates in a sub band of the UWB from 5.5 to 8 GHz, giving a resonant peak at 5.825 GHz. The CSIW cavity prototype is shown in Fig. 2(b). Also, a good return loss characteristic is obtained at the operating frequency which exhibits a quality factor equal to 310. Therefore, the measurement is realized using the Agilent technology N5247A PNA-X network analyzer which covers the frequency range of 10 MHz to 67 GHz.

Fig. 3 shows the distribution of the E-field in the circular cavity. The maximum electric fields are concentrated inside the cavity limited by the metalized via and symmetric along the AB plane.

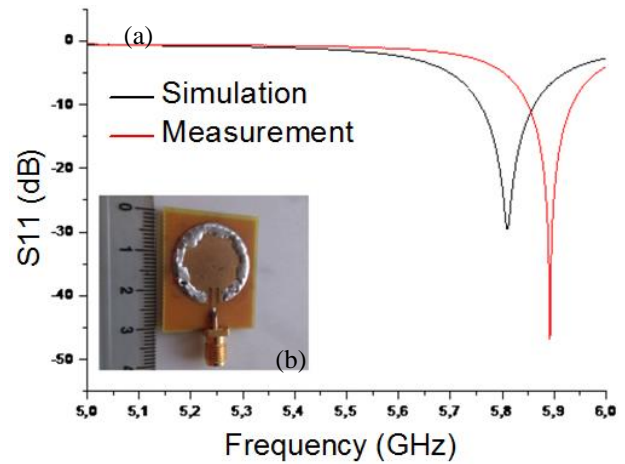


Fig. 2. (a) Simulated and measured $|S_{11}|$ of the Substrate Integrated Circular Cavity, (b) prototype photograph of circular SIW cavity.

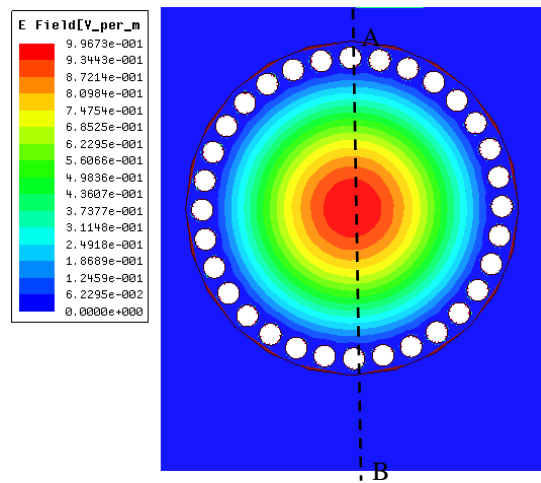


Fig. 3. Substrate integrated circular cavity.

The operating mode is the TM_{010} . The corresponding resonant frequency of TM_{010} is obtained using (2) below:

$$f_{010} = \frac{A_{010} c}{\pi R \sqrt{\epsilon_r \mu_r}} \quad (2)$$

Where c is the speed of light, A_{010} is the zero of the derivative of the Bessel function of TM_{010} , R is the radius of the circular cavity, ϵ_r is the relative permittivity and μ_r is the permeability of the substrate [16].

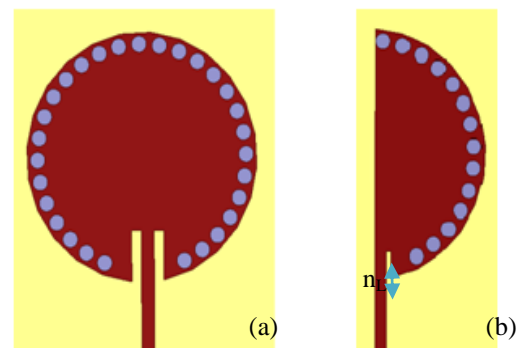


Fig. 4. The HMSIW technique: (a) the CSIW cavity, (b) the half-mode CSIW cavity.

Therefore, by dividing the circular cavity in two halves along the AB plane, two half-mode cavities with same field distribution as the original circular cavity are obtained (see Fig. 5). the half-mode CSIW cavity is shown in Fig. 4(b), characterized by a notch length $n_L = 2.2$ mm, and a notch width of 0.4 mm. The spacing between the tag edge and the Half-mode cavity patch is of 2 mm.

Fig. 6 above shows the Half-mode cavity responses of simulation and measurement. As already seen, the resonant peak of the configuration is the same of the whole structure at 5.825 GHz with a slight difference in the bandwidth. The prototype is also shown in the same figure which is characterized by a reduced size compared to the complete circular cavity. The measured $|S_{11}|$ is in good agreement with the simulated response giving a resonant peak at 5.825 GHz (see Fig. 6(a)), which validates the technique of miniaturization. The size of the Half-mode circular SIW cavity is then 1/2 of the circular SIW cavity with an identical resonant frequency which allows using the miniaturized half cavity as a main structure of our study.

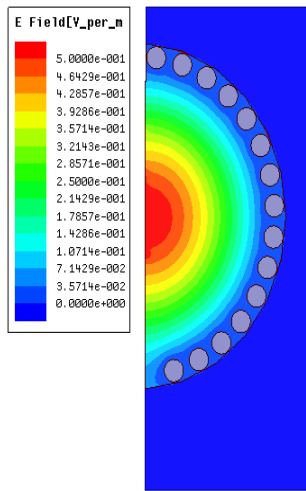


Fig. 5. The E-Field distribution in the HMSIW circular cavity.

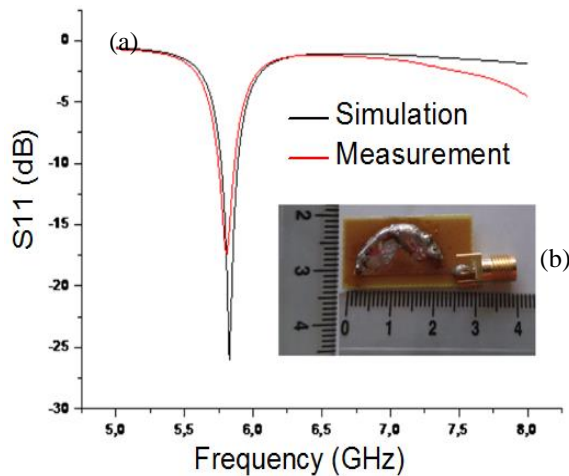


Fig. 6. (a) Simulated and measured $|S_{11}|$ of the half-mode CSIW Cavity, (b) Prototype photograph.

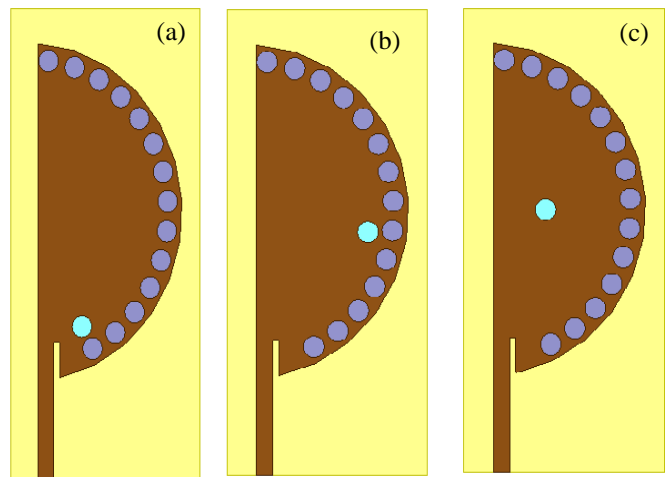


Fig. 7. The encoding technique using via holes and metalized via (a) first position, (b) second position, (c) third position.

Accordingly, the Half-Mode SIW circular cavity is the encoding area of our chipless tag. The frequency domain approach (FDA) is here adopted as an encoding approach using a simple frequency shifting technique which depends on the position and the nature of the via (air via or metalized via) inside the cavity substrate without influencing the tag size.

In fact, when an incident wave excites the Half-Mode cavity, it creates the fundamental resonant peak at 5.825 GHz. The concept in our actual study consists of demonstrate the encoding technique when adding via holes or metalized via in the substrate. Hence, the frequency domain approach is adopted using the frequency shifting technique. In Fig. 7, the manner of drilling via holes in the substrate is shown. It demonstrates that the first via hole drilled as given in Fig. 7(a), and respectively the second and the third position are shown in Fig. 7(b) and 7(c).

Hence, the via hole has a radius of 0.7 mm, and the HMSIW encoding surface proves that a frequency shift is realized after drilling only one via hole.

Thus, the addition of the via hole in the first position gives a frequency shift to lower value (compared to the original cavity response at 5.825 GHz) at 5.795 GHz as shown in Fig. 8. Changing to the second position ensures a new frequency value at 5.8 GHz. Further, changing to the third position gives a resonant frequency at 5.87 GHz. Consequently, the position changes of via holes shift the frequency to new values, mainly new encoding states. Each new position close to the maximum concentration of the E-field gives a maximum shift value that can be equal or greater than 45 MHz. This is explained by the electric field distribution which is concentrated at the superior edge of the Half-Mode SIW cavity as explained in Fig. 5. Also, each modification in the substrate parameters close to the maximum field concentration brings a high frequency shifts.

Besides, the addition of metalized via with same radius of 0.7 mm influences the frequency to be shifted to higher values from a position to another.

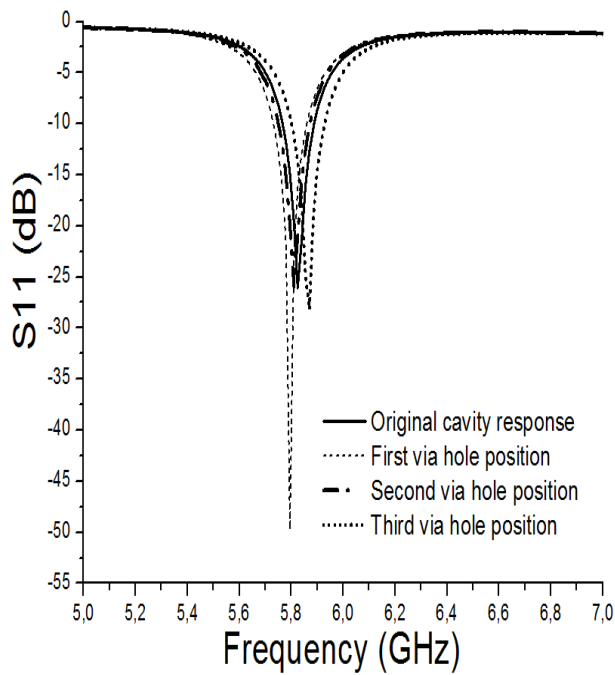


Fig. 8. Return loss responses of the HMSIW circular cavity after drilling via holes in three different positions.

Fig. 9 demonstrates the concept, and the metalized via placed at the first position gives a frequency shifts to 6.11 GHz, which is an important shift of 285 MHz. Besides, the second position of metalized via permits a shift towards 6 GHz. The third position of metalized via is placed in a maximum E-field distribution (see Fig. 7(c)) gives an important shift to a new value at 7.8 GHz. This lead us to conclude that the metalized via gives important shifted values compared to via holes.

Accordingly, drilling via holes or metalized via leads to new encoding states where each new position in the Half-Mode SIW cavity gives a new frequency value. Further, adding N via holes or N metal via one after one in the substrate guides to N shifted frequency, mainly N encoding states.

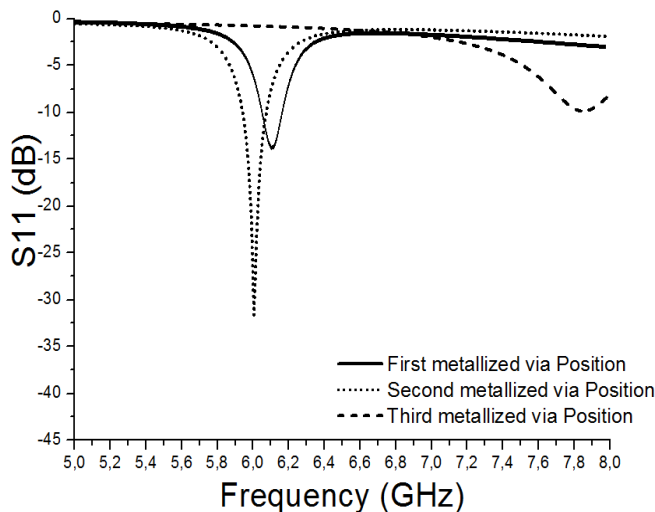


Fig. 9. The return loss responses of the HMSIW circular cavity after drilling metalized via in the substrate.

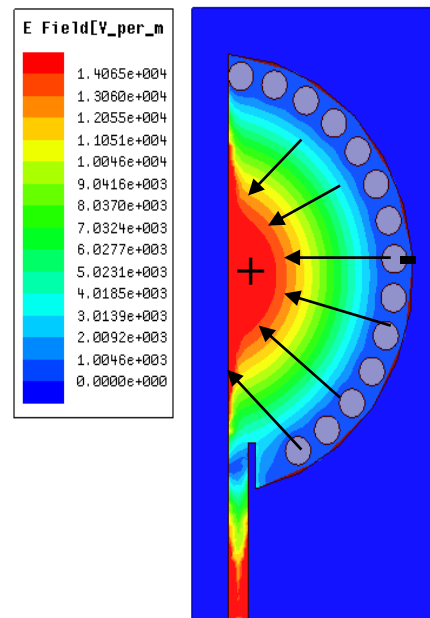


Fig. 10. The offset direction of the frequency values according to the E field distribution.

If we need to obtain close shifted values, we can drill via near to the EM wall created by the circular row of metalized via of the SIW technology. Also, we have the opportunity to obtain important shifts if metalized vias are drilled within the substrate in different positions. This shifts can reach and exceed 1 GHz if the via is placed in the middle of the cavity where the E field is maximum. Fig. 10 shows the direction of the concentration of E-field, and mainly the frequency values increase gradually in the cavity each time vias are drilled closer to the E- field concentration.

B. Ultra Wideband Crescent Shaped Antenna

The second designed component is an essential part of the RFID tag which is the chipless tag antenna. It is the crescent shaped antenna that ensures the wideband operation.

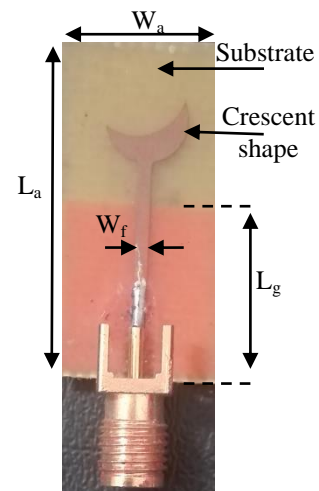


Fig. 11. Crescent UWB antenna.

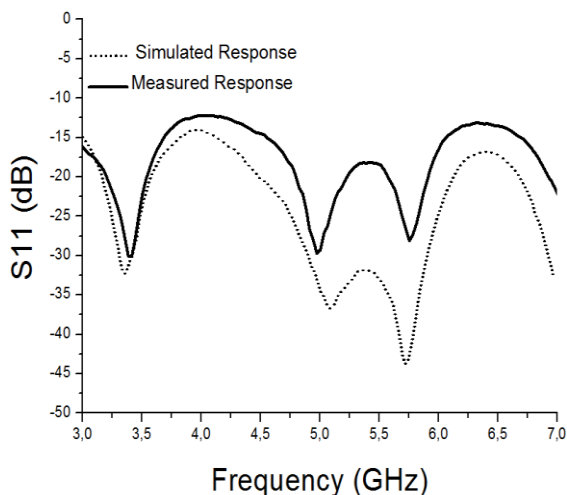


Fig. 12. Simulated and measured return loss of the crescent UWB antenna.

The crescent shaped antenna based chipless tag is characterized by a width of $W_a = 13.5$ mm, and a length $L_a = 27$ mm. The ground antenna cover the lower part of the antenna without covering the radiating crescent element, it has a length $L_g = 14$ mm. Fig. 11 shows the prototyped configuration.

The simulation results validates successfully the shape antenna choice and gives a gain of 1.3 dBi, and a well-adapted response from 3 to 7 GHz as shown the return loss response in Fig. 12.

III. CHIPLESS TAG ASSOCIATION

At this step, the two main components are ready to form the chipless tag based on SIW technology. Thus, the resonant Half-Mode SIW cavity is associated with the UWB crescent antenna as shown in Fig. 13. The chipless tag is characterized by a compact size of 1.3×5.7 cm².

The simulation setup imitates the real operating conditions. The metallic rectangular waveguide WR-159 (40.386×20.193 mm²) with a mono-modal band from 4.90 to 7.05 GHz was used as interrogator antenna to generate a broadband signal and to read the scattering radiation of the tag.

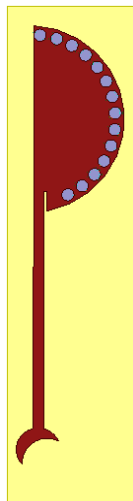


Fig. 13. The half-mode CSIW based tag.

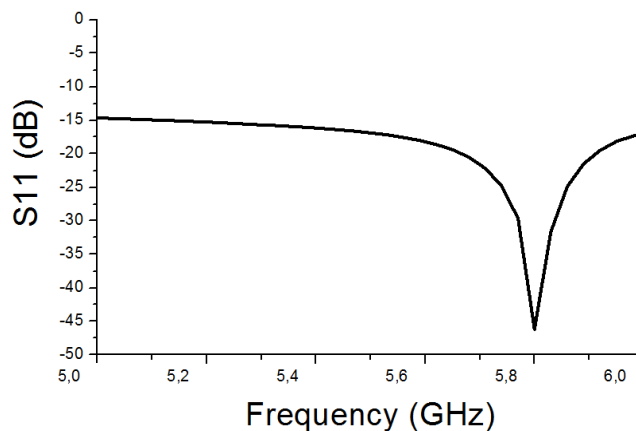


Fig. 14. Simulated tag response.

The chipless tag is placed under the waveguide separated by a distance of 1.5 cm, with the center of the UWB antenna aligned with the center of the rectangular waveguide. In particular, in the simulated chipless system, the configuration of the cavity is chosen in order to resonate at 5.825 GHz.

The simulated response of the tag is shown in Fig. 14. It is therefore clear that the notch appeared in the frequency response is the signature of the tag under test, which validates our proposed design.

As evaluation, our proposed design uses an efficient technique of size reduction. Its feasibility has been proved by both considering the experimental measurements and the system simulation. It is characterized by an improved size compared to the square shaped chipless tag based on SIW technology proposed in [13]. It offers a numerous encoding states in a reduced surface using the frequency shifting technique from 5.5 to 8 GHz.

Hence, a significant improvement will be initiated in order to improve the encoding capacity in the same frequency band and with the same encoding approach using some promising techniques of SIW technology. Also, the FR4 substrate should be transferred to green materials in order to be easily inserted in credit cards or personal ID cards using the same HMSIWC based chipless tag.

IV. CONCLUSION

A compact RFID chipless Tag based on SIW Technology has been designed in this paper using the technique of size reduction based on HMSIW technique. The HMSIW cavity and the UWB crescent shaped antenna based tag have theoretically and experimentally studied and validated on Ansoft HFSS. Using the frequency domain approach and referring to the modification of the effective permittivity of the substrate integrated resonator which gives a unique frequency signature. The tag can be easily modified by adding a via hole or metalized via in different position without touching the tag dimensions. The tag is able to obtain numerous encoding state, means high encoding efficiency using a reduced size cavity associated to a reduced size UWB antenna. The new tag has the advantage of having a high quality factor (310) as well as reduced size (1.3×5.7 cm²). Thus, a research should be initiated

to have the possibility to transfer the substrate to different types like paper, plastic and textile.

REFERENCES

- [1] K. Finkenzeller, "RFID Handbook," 2nd edition, John Wiley & Sons, 2003.
- [2] M. Bozzi, A. Georgiadis, K. Wu, "Review of substrate-integrated waveguide circuits and antennas", IET Microw. Antennas Propag., 2011, Vol. 5, Iss. 8, pp. 909–920. DOI: 10.1049/iet-map.2010.0463.
- [3] J.-X. Chen, W. Hong, Z.-C. Hao, H. Li, and K. Wu, "Development of a Low Cost Microwave Mixer Using a Broadband Substrate Integrated Waveguide (SIW) Coupler," IEEE Microwave and Wireless Components Letters, Vol. 16, No. 2, Feb. 2006. DOI: 10.1109/LMWC.2005.863199.
- [4] Y. Cassivi and K. Wu, "Low Cost Microwave Oscillator Using Substrate Integrated Waveguide Cavity," IEEE Microwave and Wireless Components Letters, Vol. 13, No. 2, pp. 48–50, Feb. 2003. DOI: 10.1109/LMWC.2003.808720.
- [5] K. W. Eccleston, "Corrugated Substrate Integrated Waveguide Distributed Amplifier", Proceedings of APMC 2012, Kaohsiung, Taiwan, Dec. 4-7, 2012. DOI: 10.1109/APMC.2012.6421604.
- [6] C. Jin, R. Li, A. Alphones, X. Bao, "Quarter-Mode Substrate Integrated Waveguide and Its Application to Antennas Design", IEEE Transactions On Antennas And Propagation, VOL. 61, NO. 6, JUNE 2013. DOI: 10.1109/TAP.2013.2250238.
- [7] I. Jalaly and I.D. Robertson, "RF barcodes using multiple frequency bands", in IEEE MTT-S Microwave Symp. Dig. Long Beach CA, June 2005, pp.139-141. DOI: 10.1109/MWSYM.2005.1516542.
- [8] S. Preradovic, I. Balbin, N. C. Karmakar, "Multiresonator based chipless RFID system for low-cost item tracking", IEEE Transactions on Microwave Theory and Techniques, vol. 57, no. 5, pp:1411-1419, May 2009.
- [9] R. Reza, M. Majid, "Complex-natural-resonance-based design of chipless RFID tag for high-density data", IEEE Trans. Antennas Propag., 2014, 62, pp. 653-656.
- [10] A. Attaran, R. Rashidzadeh, R. Muscedere, "Chipless RFID tag using RF MEMS switch". Electronics Letters, 2014, vol. 50, no. 23, p. 1720–1722. DOI: 10.1049/el.2014.3075.
- [11] A. Vena, E. Perret, S. Tedjini, "Chipless RFID tag using hybrid coding technique", IEEE Tran. Microw. Theory Tech., 2011, 59, pp. 3356-3364.
- [12] A. Vena, E. Perret, S. Tedjini, "A compact chipless RFID tag using polarization diversity for encoding and sensing", IEEE Int. Conf. on RFID 2012, Orlando, USA, April 2012, pp. 191-197.
- [13] S. Moscato, R. Moro, S. Sakouhi, M. Bozzi, et al. "Chipless RFID for space applications. In Proceedings of the IEEE International Conference on Wireless for Space and Extreme Environments WISEE 2014. Noordwijk (The Netherlands), October 2014. DOI: 10.1109/WiSEE.2014.6973075.
- [14] K. Wu, D. Deslandes, and Y. Cassivi, "The substrate integrated circuits—A new concept for high-frequency electronics and optoelectronics," in Proc. TELSIS, Oct. 2003, pp. 3–5.
- [15] M. Bozzi, A. Georgiadis, K. Wu, "Review of Substrate Integrated Waveguide (SIW) Circuits and Antennas," IET Microwaves, Antennas and Propagation, Vol. 5, No. 8, pp. 909-920, June 2011.
- [16] C. A. Balanis, Antenna Theory Analysis and Design, 3rd ed. New York, NY, USA: Wiley, 2005.